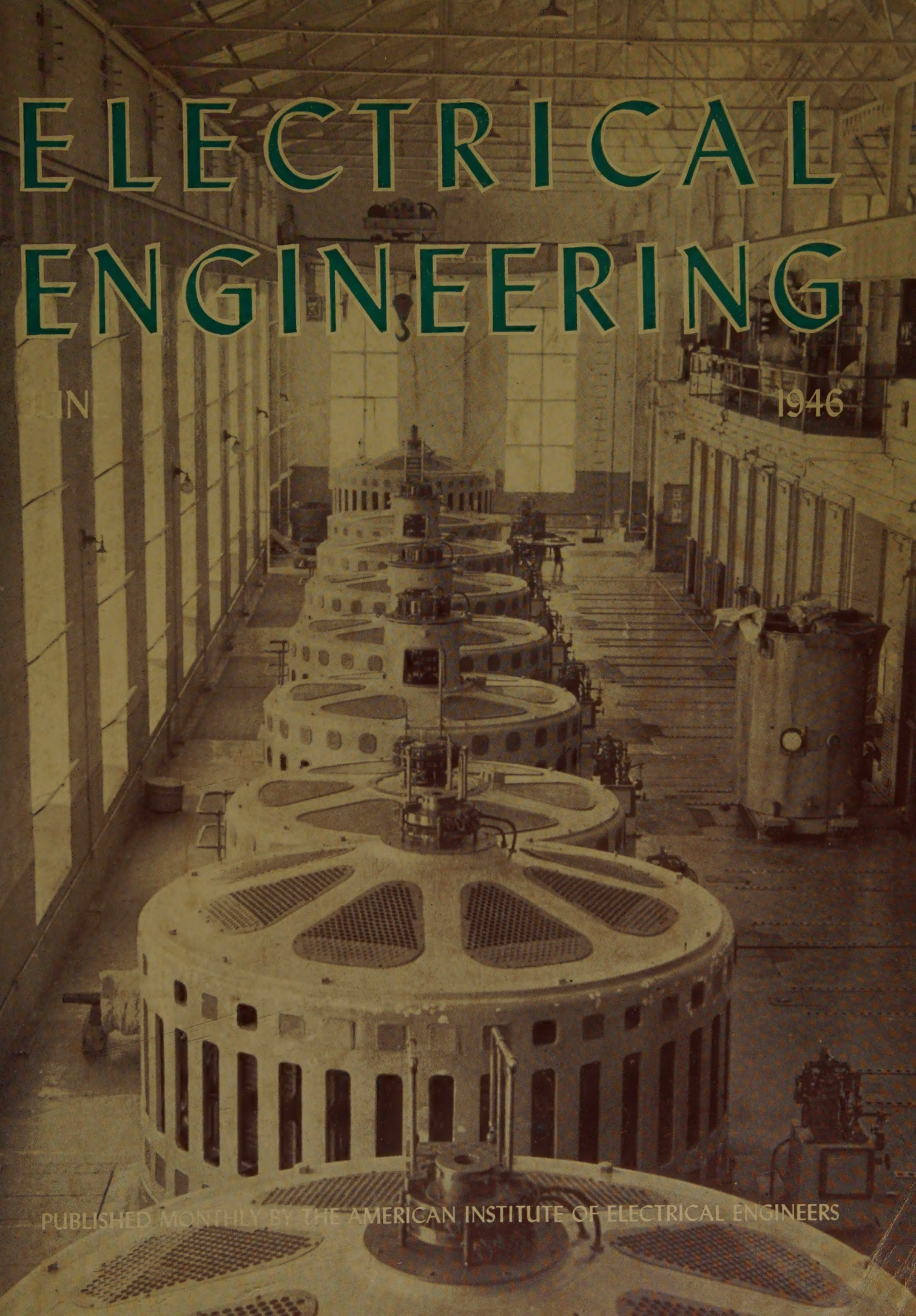
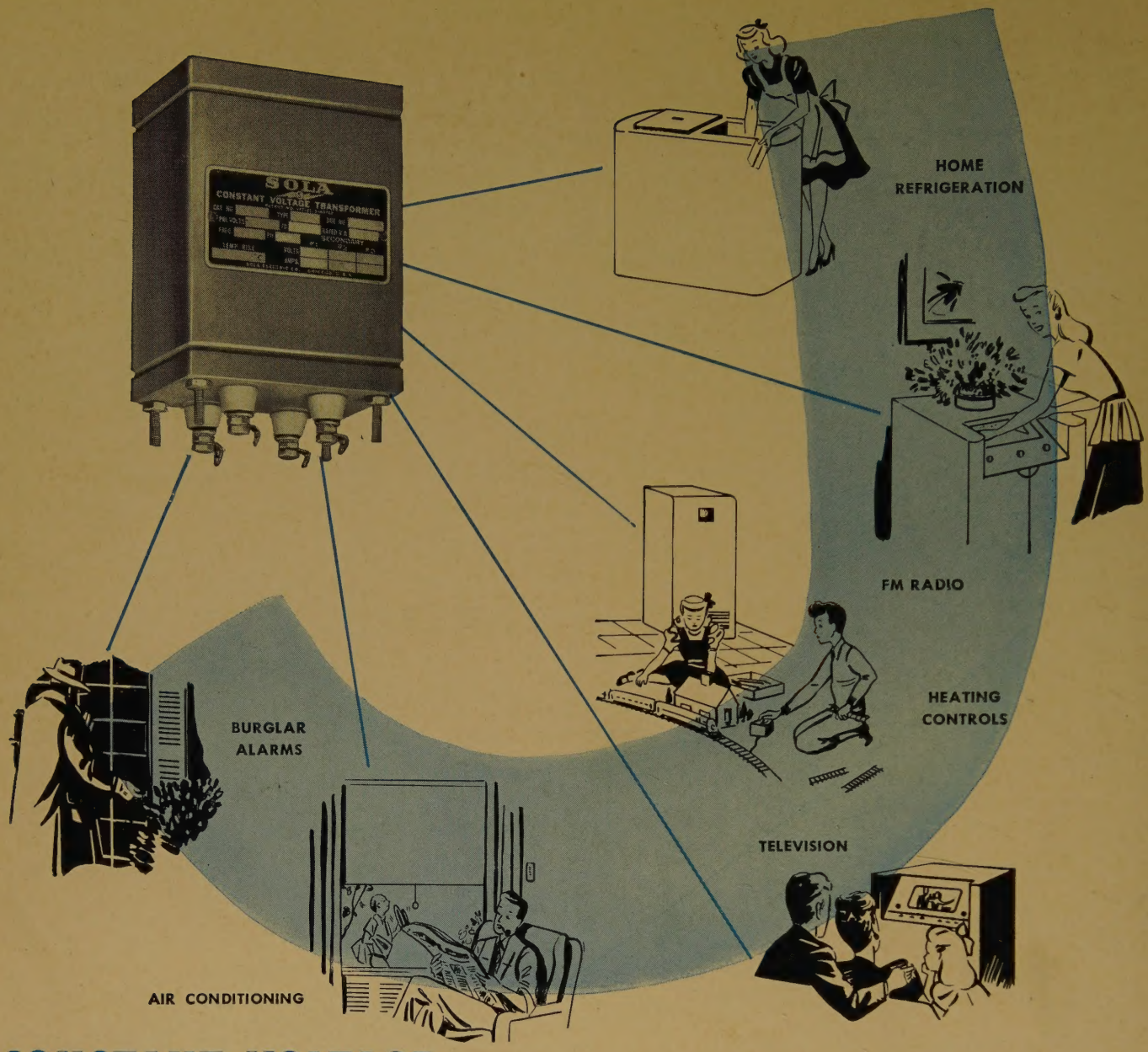
ELECTRICAL ENGINEERING

IN 1946



PUBLISHED MONTHLY BY THE AMERICAN INSTITUTE OF ELECTRICAL ENGINEERS



CONSTANT VOLTAGE for home equipment made possible by this low-cost transformer

With this transformer maintaining operating voltage within ±1% of rated requirements, regardless of supply line fluctuations as great as 30%, trouble-free operation of your equipment becomes a reality.

Here is what can be accomplished by building this SOLA Constant Voltage Transformer into your equipment.

1. *Increased efficiency.*
2. *Lowered cost to the user.*
3. *Reduced maintenance expense.*

This Type 11 SOLA Constant Voltage Transformer is designed specifically for such domestic applications as heating and ventilating controls, FM and television receivers, refrigeration and air conditioning controls and other similar products where stable voltages must be maintained. Like all SOLA Constant Voltage Transformers, regardless of size or capacity, it operates automatically, has no moving parts, and requires no supervision.

Type 11 is just one of 31 standard types in capacities ranging from 10VA to 10,000VA that are available to manufacturers of all types of electrically operated equipment. Special units can be built to your exact specifications. SOLA engineers are available for a discussion of your problems.

Write for new Handbook

A complete treatise on the subject of voltage stabilization. It provides the answer to a problem that confronts every manufacturer or user of electrically operated or electronic equipment.

Ask for Bulletin **ACV-102**

Constant Voltage Transformers SOLA

Transformers for: Constant Voltage • Cold Cathode Lighting • Mercury Lamps • Series Lighting • Fluorescent Lighting • X-Ray Equipment • Luminous Tube Signs Oil Burner Ignition • Radio • Power • Controls • Signal Systems • etc. **SOLA ELECTRIC COMPANY, 2525 Clybourn Avenue, Chicago 14, Illinois**

ELECTRICAL ENGINEERING

Registered United States Patent Office

JUNE
1946

The Cover. Necaxa hydroelectric plant in Mexico, with a static head of 1,453 feet, employs nine generators having a total capacity of 100,000 kw.

Mexican Light and Power Company, Limited, photo

Mexico's Electrification Program—II
Basil Nikiforoff, Alfonso F. del Busto, Alejandro Paez Urquidi, Oscar R. Enriquez 245

Realism in Engineering Education . . . A. S. Langsdorf . . . 251

Amortisseur Action of the Squirrel Cage . . . Edward Bretch . . . 255

Advances in Airport Lighting . . . W. A. Pennow . . . 259

Vertical Wind Tunnel . . . 265

Institute Activities . . . 267

Of Current Interest . . . 292

TRANSACTIONS SECTION

(Follows EE page 302; a preprint of pages 321–402 of the 1946 volume. Any discussion of these papers will appear in the June 1946 "Supplement to Electrical Engineering—Transactions Section" and in the 1946 volume.)

Speed Control Regulator . . . A. G. Conrad, F. E. Brooks, Jr., R. G. Fellers . . . 321

Inductance Formulas . . . Henry Peter Messinger, Thomas James Higgins . . . 328

Supervisory Control of Hydroelectric Plant . . . C. W. Bohner, A. P. Maness . . . 337

Signal and Noise Levels in Magnetic Tape Recording . . . D. E. Wooldridge . . . 343

The Mho Distance Relay . . . R. M. Hutchinson . . . 353

Metal-Clad Unit-Type Switchgear for 33-Kv Service . . . C. H. Kreger . . . 360

Induction Heating of Long Cylindrical Charges . . . Herbert F. Storm . . . 369

Ohm and Mho Principles and Protective Relays . . . A. R. van C. Warrington . . . 378

Magnetic-Type Power Circuit Breakers . . . L. J. Linde, B. W. Wyman . . . 386

Short-Circuit Characteristics of D-C Generators . . . G. E. Frost . . . 394

G. Ross Henninger
Editor

W. R. MacDonald, Jr.
Associate Editor

F. A. Norris
Business Manager

H. A. Johnston
Advertising Manager

Statements and opinions given in articles and papers appearing in *Electrical Engineering* are the expressions of contributors, for which the Institute assumes no responsibility. ¶ Correspondence is invited on all controversial matters.

Published Monthly by the

AMERICAN INSTITUTE OF ELECTRICAL ENGINEERS

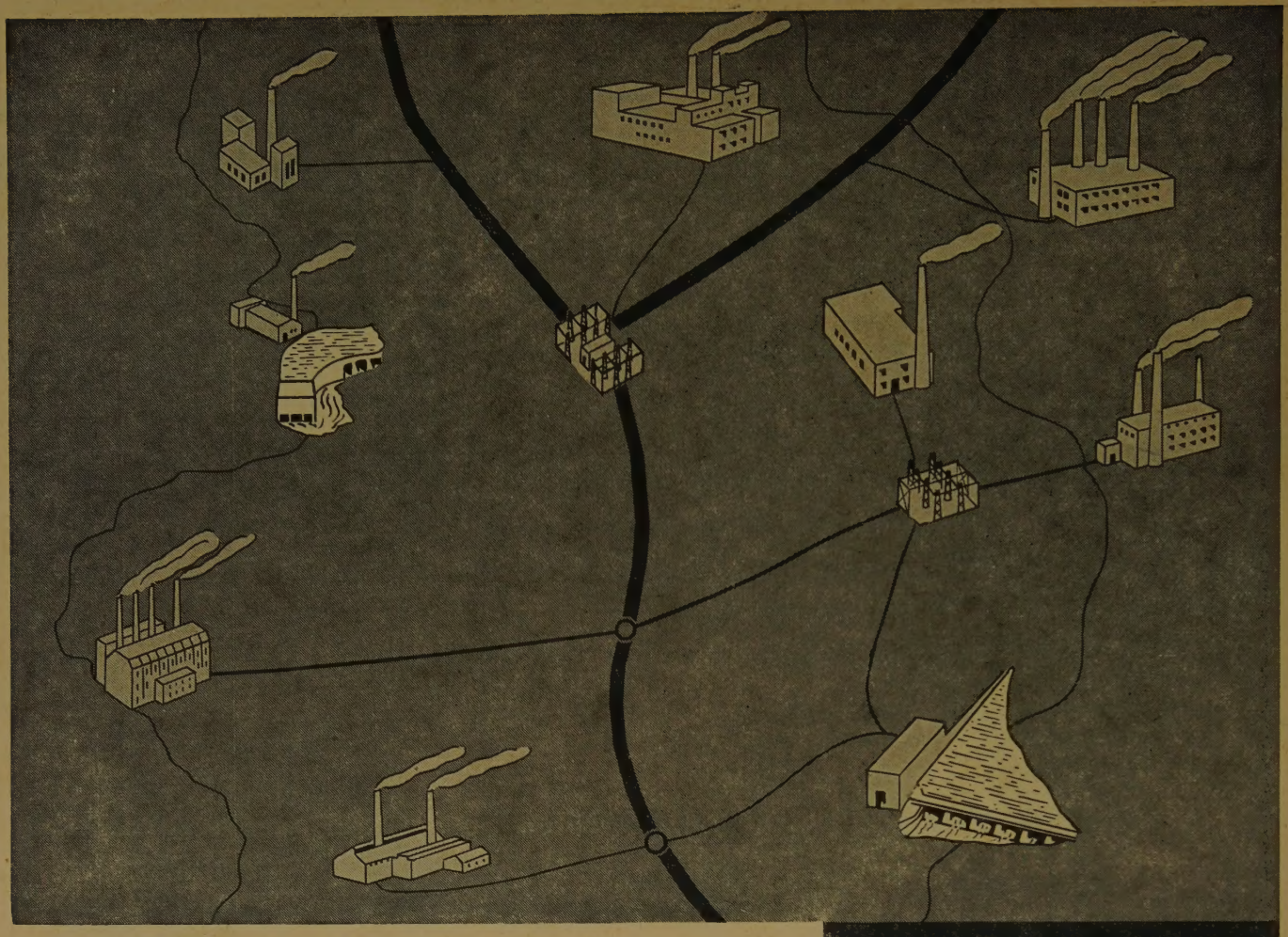
Founded 1884

VOLUME 65
NUMBER 6

WILLIAM E. WICKENDEN, President H. H. HENLINE, Secretary

PUBLICATION COMMITTEE: C. F. Wagner, *chairman* M. S. Coover H. H. Henline
B. M. Jones John Mills J. J. Orr H. H. Race G. A. Van Brunt

Electrical Engineering: Co pyright 1946 by the American Institute of Electrical Engineers; printed in the United States of America; indexed annually by the AIEE, weekly and monthly by *Engineering Index*, and monthly by *Industrial Arts Index;* abstracted monthly by *Science Abstracts* (London). Address changes must be received at AIEE headqu arters, 33 West 39th Street, New York 18, N. Y., by the 15th of the month to be effective with the succeeding issue. Copies undelivered because of incorrect ad dress cannot be replaced without charge.



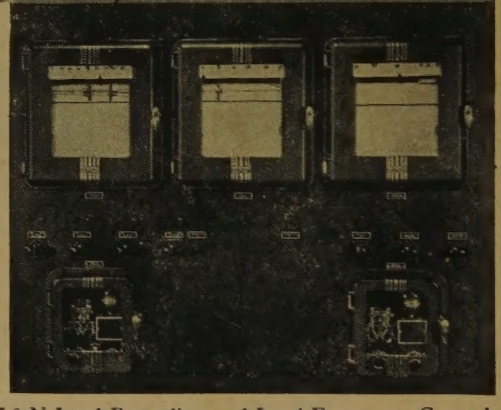
REALIZATION of a System's Potential Economy is Largely in the Dispatcher's Hands

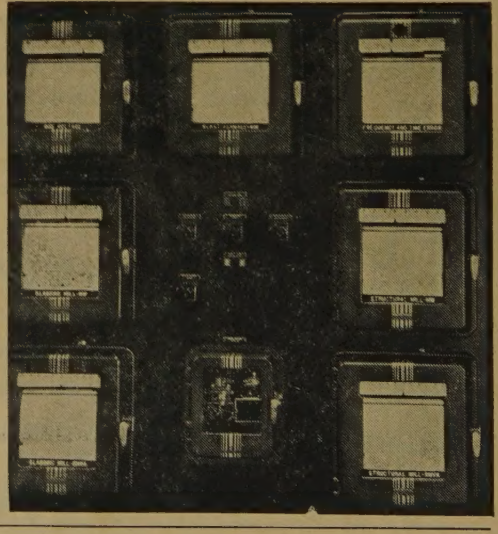
The system economy which a load dispatcher customarily maintains —and which is his regular responsibility—can be increased very substantially by giving him two automatic "tools" for his work.

One tool is a Micromax Load Recorder or Recorders to show load conditions promptly and continuously. The other tool is L&N Automatic Load-Frequency Control, to carry out the dispatcher's orders.

Approximately 1/100 of 1 per cent—or the order of twenty-five hundred dollars out of 25 million—of the total capital invested in a power system, will give its dispatchers this equipment. The installation is even more advisable when one recalls that the dispatchers are largely responsible for operation of the major equipment which represents a big share of the total investment.

This is just one reason why systems totaling more than 35,000,000 kw capacity now use these L&N instruments. At your request, an L&N engineer will be glad to sit down with you and explain, or to send Technical Publication N-56–161(1), as you may prefer.





L&N Load Recording and Load-Frequency Controlling Panels. Above—for a Public Utility; below—for a Steel Mill.

LEEDS & NORTHRUP COMPANY, 4962 STENTON AVE., PHILA., PA.

LEEDS & NORTHRUP

MEASURING INSTRUMENTS · TELEMETERS · AUTOMATIC CONTROLS · HEAT-TREATING FURNACES

Jrl. Ad N-50-161(4)

HIGHLIGHTS.....

North Eastern District Meeting. With 439 persons registered, the North Eastern District meeting held in Buffalo, N. Y., proved to be the best attended of the spring District meetings. Of the technical sessions, those on power systems, communication and war developments, and transmission and distribution were the most popular. Much interest was evinced also in a discussion of the nontechnical problems facing the engineering profession today. This discussion was the high point of a general luncheon meeting at which questionnaires, designed to ascertain the general attitude toward a proposed reorganization of the engineering societies, were distributed. The lighter side of life was not neglected and "a good time was had by all" at the various social events included in the program (*pages 274–5*).

Southern District Meeting. A lively interest by Student members highlighted the sixth annual meeting of the Southern District, held this year in Asheville, N. C., May 14–16, with representatives from 15 of the 18 Student Branches in the District participating in the Student conference. Another highlight of the meeting was a technical program which was devoted very largely to problems of particular interest to the industrial south. Worthy of note in the general field was an address by Past President Powel describing the present condition of Germany as based upon his observations during a recent 9-month tour of that country. Mr. Powel visited Germany as a member of the Allied Control Commission (*pages 267–8*).

New Institute Policies. Expansion of the AIEE headquarters staff with a corresponding increase in its responsibilities, separation of the publication of technical papers and discussions from the publication of articles and news of general interest, and revitalization of AIEE technical activities are the objectives of new policies considered by the AIEE board of directors during the Southern District meeting (*pages 269–70*).

Airport Lighting. During the war the necessity for adequate airport lighting to insure safety of landing and take-off was realized and provided for by the United States Armed Forces. In the face of the danger entailed by an ever-increasing volume of air traffic, it is imperative that commercial airports augment the usual insufficient prewar lighting budget in order to take advantage of war-fostered developments in lighted landing aids (*pages 259–65*).

Mexican Electrification. The fulfillment of Mexico's plans for industrialization, and, in general, for raising the standard of living of the Mexican people, will depend to a large extent upon her ability to develop her as yet practically unexploited natural resources. Cognizant of this fact, the Mexican government has made provision, through legislation, for strict regulation of Mexico's growing electrical industry. These points are brought out in the second and concluding part of an article prepared by members of the Mexico Section (*pages 245–51*).

Engineering Education. Again the old question arises as to the proper ratio of cultural and technical subjects in the education of an engineer. In view of the current need to renovate technical curricula in order to keep pace with growing technological demand, Dean Langsdorf, of Washington University's schools of engineering and architecture, takes a stand on the side of an improved, more intensive technical training. Because culture cannot be acquired through a few classroom lectures, he refers that aspect of the engineer's background to the national engineering societies (*pages 251–4*).

Statistical Quality Control Conference. Reports on methods and results of statistical quality control by five speakers with experience in that field attracted a large attendance at a conference held during the recent North Eastern District meeting in Buffalo. Professor M. A. Brumbagh, University of Buffalo, acted as chairman (*page 276*).

Vertical Wind Tunnel. The new structure on Wright Field's "Hurricane Hill," an 80-foot concrete tower, houses a vertical wind tunnel in which scale models of future United States Army airplanes are tested for design defects before the actual construction stage is reached. Many of these tests, such as that for airplane spin characteristics, cannot be performed in the average wind tunnel (*pages 265–6*).

Electrical Essay. In response to the electrical essay in the April issue, solutions—a number of them correct—were received from many members. Excerpts from those offering correct solutions, as well as the complete solution given by Mr. Leeds who submitted the essay, are presented (*pages 299–300*).

Metal-Clad Switchgear. According to a paper in this issue, after 17 years of operation by the Public Service Company of Northern Illinois, 33-kv metal-clad switchgear has proved itself safe, reliable, and, in a cost comparsion with switchgear of conventional open-type construction, economical as well. At present, development of this type of equipment has been allowed to lapse but, in the interest of reduced costs, its resumption would be advantageous (*Transactions pages 360–8*).

Inductance Formulas. Formulas have been derived for calculating the inductance of single-phase coaxial busses comprised of square tubular conductors. The general formula is obtained through use of geometric mean distance theory. A simple approximate formula, the conductors being considered as indefinitely thin, is epitomized in curves which yield values sufficiently accurate for most design work (*Transactions pages 328–36*).

Induction Heating of Cylindrical Charges. A new approach is offered for the analysis of the induction heating effect by using concepts commonly applied to a-c engineering and not involving differential equations. An analysis is provided which is valid for any size of the radius of the charge and the so-called depth of penetration (*Transactions pages 369–77*).

Correction. Three minor typographical errors appearing in the paper "Applications of Thin Permalloy Tape in Wide-Band Telephone and Pulse Transformers" by A. G. Ganz which was published in the AIEE *Transactions* for April 1946, pages 177–83, are corrected herein. On the lower right-hand corner of Figure 6, page 179, 2^{-7} should be corrected to 2. In column 3, paragraph 2, line 10, page 179, α should be changed to δ. On page 182, column 2, the second equation of the appendix should read $B_{avg} = \frac{15.5ET}{NA} 10^{+\delta}$.

Credit Where Due. Credit was not given, as it should have been, to the Douglas Aircraft Company, El Segundo, Calif., for the illustrated chart of flight and propulsion which appeared as Figure 4 of an article entitled "Power Plants for Airplanes" published in the April 1946 issue of *Electrical Engineering*, pages 160–3.

News 267

Submission of Lamme Medal Nominations.....270
Summer Convention Program.....271
Annual Meeting Announcement.....275
Standards.....276
Section Items.....277
Abstracts of Technical Papers.....278
Future Meetings
AIEE.....276
Other Societies.....297
Personal Items.....286
Membership.....290
Letters to the Editor.....298
New Books.....302
Pamphlets.....302

ELECTRICAL ENGINEERING. Published monthly by the American Institute of Electrical Engineers; publication office 20th & Northampton Streets, Easton, Pa. Editorial and advertising offices, 33 West 39th Street, New York 18, N. Y. Subscription $12 per year plus extra postage charge to all countries to which the second-class postage rate does not apply; single copy $1.50. Entered as second-class matter at the Post Office, Easton, Pa., under the Act of Congress of March 3, 1879. Accepted for mailing at special postage rates provided for in Section 538, P. L. & R. Act of February 28, 1925. June 1946, Vol. 65, No. 6. Number of copies of this issue 37,000.

NOW.. Simplified Instantaneous Recording of Transient Phenomena!

Brush Transient Recorder captures and graphically represents Transient Phenomena of 2/10 second or less



Brush Transient Recorder with oscilloscope. (Any good quality oscilloscope with low-frequency sweep may be used.)

This photo shows a typical transient produced by a condenser discharging into an inductance, as recorded by the Brush Transient Recorder.

Here is the instrument engineers have been waiting for! Electrical transients or any other transient phenomena capable of being converted into electrical impulses may be recorded and reproduced automatically. Such transients as vibrations, explosion waves, light flashes, welding cycles, etc. are but a few that can be recorded. Reproduction repeats continuously for visual analysis by a cathode ray oscilloscope. Signals may be photographed in entirety or expanded on the oscilloscope screen to show detail.

These results are accomplished by magnetically recording on a rapidly moving steel tape a frequency modulated high-frequency carrier. Reset button clears tape and prepares it for a new record.

One of the many and varied uses of the Brush Transient Recorder will undoubtedly meet your needs for accurate representation of transient phenomena. For complete details write today for technical bulletins.

THE BRUSH DEVELOPMENT CO.

3405 PERKINS AVE.
CLEVELAND 14, OHIO

Canadian Representatives:
A. C. Wickman, (Canada) Ltd., P. O. Box 9 Station N, Toronto 14

Mexico's Electrification Program

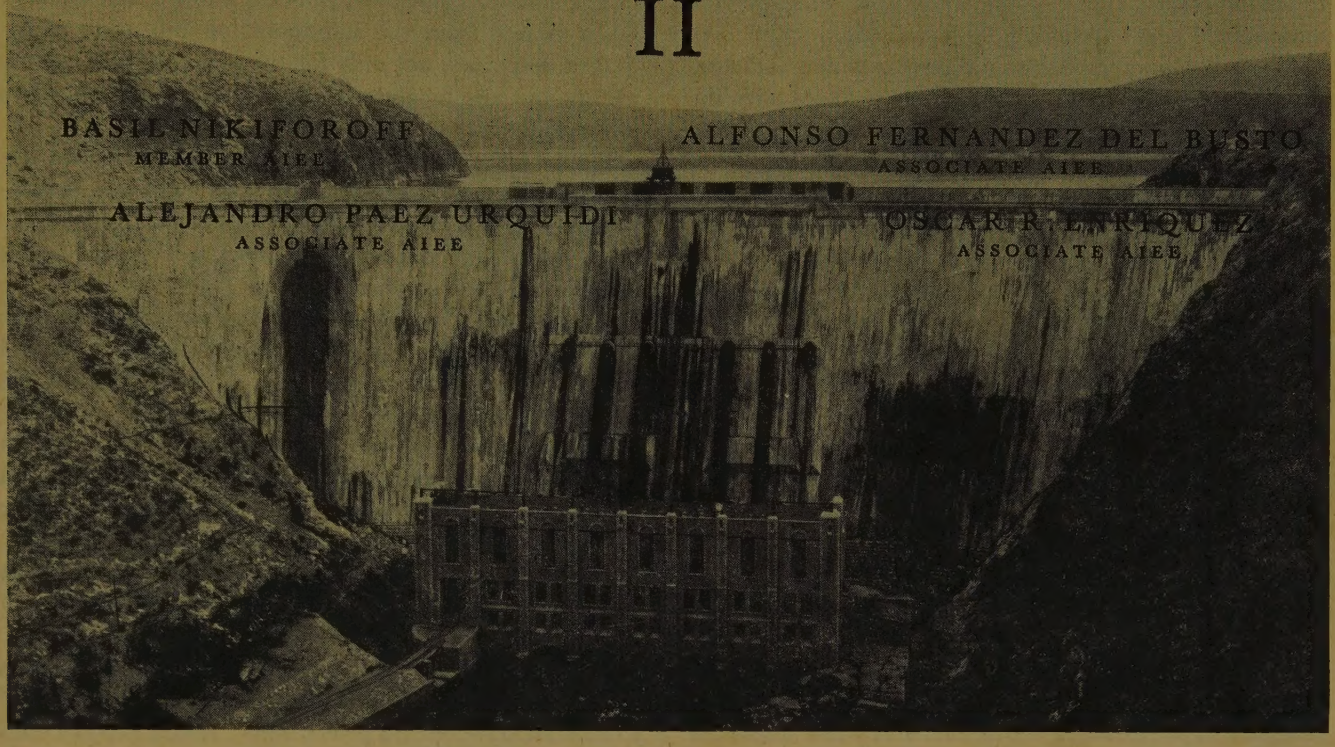
II

BASIL NIKIFOROFF
MEMBER AIEE

ALFONSO FERNANDEZ DEL BUSTO
ASSOCIATE AIEE

ALEJANDRO PAEZ URQUIDI
ASSOCIATE AIEE

OSCAR R. ENRIQUEZ
ASSOCIATE AIEE



Continuing a discussion of Mexican electrification which began in a preceding issue, part II evaluates the country's hydraulic, oil, and coal resources and comments on possibilities for future utilization in view of increased demand. The accessibility of these resources accents their importance in Mexico's growing industrialization, a trend which is being brought about through the co-operation of government and industry. The government's role is evident in comprehensive federal legislation which regulates all activities of the electrical industry from rate fixing to the establishment of standards for electric machinery.

IF POSSIBILITIES for the utilization of atomic energy are not taken into consideration, the natural resources in Mexico which could be used for the development of motive power may be listed as follows:

1. Harnessing the natural water power of the inland waterways.
2. The use, in thermoelectric plants, of the calorific power of available coal and oil deposits.
3. Utilization of the water derived from the melting of snow and ice covering high mountain peaks.
4. The use, in certain zones of the country, of the force of the wind.

The limited scope of this article does not permit the presentation of a detailed study of the natural resources that may be utilized for the production of motive power and, consequently, in the following considerations only the data corresponding to the natural resources mentioned in the first and second categories will be treated. Also, some ideas will be expressed advocating the coordinated use of natural resources which may be advantageous for electrification in Mexico and for the development of its economy.

HYDRAULIC RESOURCES

Mexico is, comparatively speaking, a country poor in hydraulic resources. Within the territory the rainfall varies from approximately 100 millimeters average per year in the northern part of the country to somewhat more than 2,000 millimeters in the southern tropical zones. Considering the large variation in rainfall as well as the factors affecting agricultural production, Mexican territory may be classified in three distinct zones; arid, intermediate, and humid. An arid zone is one in which no

Essential substance of a paper presented by the Mexico Section at the AIEE South West District meeting, San Antonio, Tex., April 16–18, 1946. Paper was prepared under the direction of Basil Nikiforoff.

Basil Nikiforoff is chief electrical engineer and **Alfonso Fernandez del Busto** is assistant superintendent of transmission and distribution, both of the Mexican Light and Power Company, Limited, Mexico, Federal District, Mexico. **Alejandro Paez Urquidi** is head of the rate and cost department, Cia. Impulsora de Empresas Electricas, Mexico, and **Oscar R. Enriquez** is head of the hydroelectric division, Comision Nàcional de Irrigacion, Mexico.

agriculture is feasible without adequate irrigation. The intermediate zone comprises the area where agricultural exploitation may be established, upon supplementing the natural rainfall by means of irrigation. A humid zone may be classified as one in which the natural rain precipitation is sufficient during the whole year to satisfy the agricultural needs without help of irrigation.

Figure 1 shows the hydraulic resources and indicates the division of Mexican territory in accordance with the classification of zones just mentioned. On the same map also is shown the division of watersheds located at different points throughout the territory as well as the regime of flow of some of the Mexican rivers. It may be observed that practically without exception the seasonal distribution of flow of these rivers is such as to require the establishment of storage reservoirs if the available water is to be used throughout the year and in an efficient way, thus necessitating the construction of dams.

In order to obtain an idea of the limitation of Mexico's hydraulic resources it may be mentioned that, at a total of 200 river-gauging and meteorological stations which have been maintained in service at the principal watersheds during a period that varies in some cases from 1890 to date, the flow registered in a total area of 530,000 square kilometers (204,600 square miles) has resulted in an average annual volume of 34,000,000,000 cubic meters (27,564,000 acre–feet). This volume corresponds approximately to that carried by the Colorado, Sacramento, and San Joaquin rivers in the United States up to the dam sites of Boulder, Shasta, and Friant, respectively.

Although the stream flow of a large number of important Mexican rivers, such as the Papaloapan, and the Uzumacinta, has not been studied properly, it has been estimated that hydraulic resources over the total extension of the country hardly reach an average annual amount of 125,000,000,000 cubic meters (approximately 100,000,000 acre–feet). The irregular orographic configuration of Mexico, with the great difference in levels between the high mountains in which the rivers originate and the Mexican Gulf and Pacific coasts where they discharge into the oceans, offers the possibility for hydroelectric developments of considerable magnitude, in spite of the comparatively low stream flow of the rivers themselves, and may be considered, in general, as favorable for such developments.

Studies made to determine the hydroelectric potentiality of Mexican streams indicate the possibility of developing approximately 6,300,000 horsepower. The water power already developed, or for which concessions have been granted, is only of the order of 800,000 horsepower, which means that only about $12^1/_2$ per cent of the hydraulic resources have been or are being developed.

It already has been mentioned that the character and distribution of population and the concentration of industries in a few localities handicaps the development of power supply systems; and the nature of the Mexican streams requiring, for their full utilization, extensive hydraulic works, frequently makes the cost of such development uneconomical when viewed from the standpoint of resulting cost of installation and energy.

The situation, however, presents a much better aspect when viewed from the standpoint of utilization of hydraulic resources, not only for the generation of electric energy, but also for purposes of irrigation and protection of the soil.

Figure 1 shows that a larger portion of Mexican territory lies in the arid zone where such combined utilization of water resources is of the greatest value, as the benefit to agriculture derived from irrigation alone justifies the high cost of such developments.

In zones with very little rainfall water constitutes the most important element for agricultural exploitation, and the supply of sufficient water for the cultivation of the fields justifies any expense and sacrifice.

This problem has been realized fully by Mexico with the resultant adoption of the present policy of irrigation works. This policy embraces the utilization of water for irrigation purposes in combination, whenever feasible, with hydroelectric generating plants. In this way it is expected to obtain maximum benefit for the economy of the country.

The utilization of the waters as described thus serves a double purpose; to encourage industrialization, and to increase agricultural production. Both purposes tend to raise the standard of living of the population and to provide the basic necessities of life. Therefore, no sacrifice or energy should be spared for the rapid development of the hydraulic resources of Mexico.

OIL RESOURCES

The Mexican Republic has been considered one of the countries with ample reserves of oil. In the opinion of geologic experts such as Wallace Pratt and Ezequiel Ordoñez, the undeveloped oil reserves of Mexico may be evaluated in something more than 24,000,000,000 barrels, and it is believed that in an area of approximately 160,000 square miles in which oil exploitation is feasible, a production totaling 27,000,000,000 barrels may be obtained. This represents approximately 75 per cent of expected oil production in the state of Texas. These amounts, if confirmed, indicate a very promising future for the exploitation of oil in Mexico.

It may be recalled that during the period from 1920 to 1922 Mexico occupied a most prominent place among oil producing countries, with an annual average produc-

Figure 1 (opposite). Map showing division of Mexico into arid, intermediate, and humid zones as well as location of watersheds

Graphs indicate representative average daily flow of various Mexican rivers (thousands of cubic meters per second)

UNITED STATES OF AMERICA
PACIFIC OCEAN
GULF OF MEXICO
DRY ZONE
INTERMEDIATE ZONE
RAINY ZONE
SCALE
KILOMETERS
MILES
1-COLORADO RIVER, USA
2-SONORA RIVER
3-YAQUI RIVER
4-BRAVO RIVER
5-CONCHOS RIVER
6-NAZAS RIVER
7-CULIACAN RIVER
8-SANTIAGO RIVER
9-LERMA RIVER
10-TEHUANTEPEC RIVER
11-GRIJALVA RIVER
12-GUAYALEJO RIVER
13-SAN JUAN RIVER
14-BRAVO RIVER
15-SABINAS RIVER
16-SAN JUAN RIVER
17-NADADORES RIVER
J F M A M J J A S O N D


MEXICALI
NOGALES
CIUDAD JUAREZ
U N I T E D S T A T E S O F A M E R I C A
HERMOSILLO
CHIHUAHUA
PIEDRAS NEGRAS
NUEVO LAREDO
G U L F
O F
M E X I C O
MONTERREY
MATAMOROS
TORREON
SALTILLO
CULIACAN
LA PAZ
DURANGO
C. VICTORIA
ZACATECAS
AGUASCALIENTES
S.L.POTOSI
TEPIC
GUANAJUATO
QUERETARO
GUADALAJARA
MORELIA
COLIMA
JALAPA
TOLUCA
CUERNAVACA
MERIDA
CAMPECHE
CHETUMAL
VILLAHERMOSA
CHILPANCINGO
OAXACA
TUXTLA
P A C I F I C
O C E A N
— LEGEND —
RAILROADS OF THE NATIONAL RAILROADS SYSTEM
RAILROADS OF OTHER SYSTEMS
FIRST CLASS PAVED ROADS
SECOND CLASS PAVED ROADS
FAVORABLE OIL PRODUCING ZONE (ACCORDING W. V. HOWARD)
LESS FAVORABLE OIL PRODUCING ZONE (ACCORDING W. V. HOWARD)
ZONE WHERE OIL PRODUCTION IS IMPROBABLE OR IMPOSSIBLE (ACCORDING W. V. HOWARD)
OIL PRODUCING ZONES ACCORDING MEXICAN GOVERNMENT SURVEYS
COAL PRODUCING ZONES
— SCALE —
KILOMETERS
0 100 200 400 600 800
0 100 200 300 400 500
MILES

tion of nearly 200,000,000 barrels. Since the beginning of 1924 production has decreased rapidly and at the present time the annual production is less than 50,000,000 barrels. During the last few years approximately 80 per cent of total oil production has been consumed within Mexico itself, and even if the demand for oil in Mexico is increased in the future to the extent of requiring a production of 200,000,000 barrels per year the reserves available should be sufficient for more than 100 years.

The utilization of natural gas should be given full consideration in addition to the use of oil. The volume of available gas resources has not been determined fully, although there is no doubt but that they constitute an important addition to the oil resources available for energy generation for many years to come.

Figure 2 shows the location of oil reserves throughout Mexico. The map was prepared from plans published by W. V. Howard (*Oil and Gas Journal*, December 1941) and from data obtained by actual explorations carried out by Mexican geologists. The coincidence in the results of these two studies may be noted. The abundance of these reserves suggests the possibility of using the oil for supplying energy to isolated sections of the country and for supplementing the production of hydroelectric systems as may be required for the expected demands of the growing industries.

COAL RESOURCES

The extent of Mexico's coal resources has not been defined as yet, even in the zone now being exploited. It is estimated that mineral coal reserves vary between 1.7 and 2 billion tons, with the annual production from 1890 to 1944 oscillating between 200,000 and 900,000 tons. Maximum production was 1,444,500 tons in 1925.

The principal zone of coal production in Mexico is located between the states of Coahuila and Nuevo Leon, and it is believed that this zone may extend to the state of Chihuahua although no studies have been made to determine its extent and volume. The discovery of coal resources in Mexico is of recent origin and the necessity for coal up to the present time has not been of sufficient importance to increase scientific exploration of other probable coal zones. During the past few years certain important anthracite deposits have been found in the state of Sonora and bituminous and lignite deposits are quite common in extensive zones of the territory, the potentiality of which is not known. Peat has been found in the vicinity of the city of Mexico where superficial geologic studies have been made. This fuel does not present any immediate interest due to its very low calorific power.

It may be said that even if the coal resources of Mexico have not been studied properly, the deposits of this combustible material are of sufficient importance to ensure the development of the iron and steel industries and, besides, to contribute to the production of thermoelectric power to complement hydroelectric generation.

Figure 2 (opposite). Map showing location of oil reserves in Mexico

A decisive factor in industrial development and in that of the generation of electricity from oil and coal is efficient distribution of available fuels. Such distribution requires adequate means of transportation which, in the case of oil, calls for a well-planned co-ordinated use of oil and gas pipe lines and of the railroads. In the case of coal it requires efficient transportation service by railroad and, to a certain extent, transportation over highways. Figure 2, in addition to indicating oil and coal resources, also shows principal railroads and Mexican highways.

MEXICAN LEGISLATION AND THE ELECTRICAL INDUSTRY

In Mexico all of the various activities related to the electrical industry, even those which do not involve commerce between two or more states, fall under the jurisdiction of the federal authorities and are subject to federal laws and regulations which, in turn, have their sources in the federal constitution of the country.

The generation of electric energy as well as its transformation, transmission, distribution, exportation, importation, sale, purchase, utilization, and consumption, are regulated by the Electric Industry Law of 1938 and by its regulations of 1945.

The use of federal waters or waters whose domain belongs to the nation, in the generation of electric energy, is subject to the provisions of the respective federal water laws that were in effect on the dates on which concessions were granted. New water developments are subject to the terms of the National Water Law of 1934, and its regulations of 1936.

Telegraphic, telephonic, and radio communications are subject to the Law of General Communications Facilities of 1940 and the regulations thereof issued on various subsequent dates.

Inasmuch as a detailed explanation of each one of the afore-mentioned laws and regulations would be much too lengthy to include in an article of this nature, it will be limited to a general idea of the most important dispositions contained in the Electric Industry Law and its regulations.

Article one of the Electric Industry Law gives a clear and concise idea of what the Mexican Federal Government intends to obtain through this law. The article reads as follows:

"The aims of this law are:

"I. To regulate the generation of electric energy, its transformation, transmission, distribution, exportation, importation, buying and selling, utilization and consumption, in order to obtain a better use of same for the benefit of the community.

"II. To encourage the development and betterment of the electrical industry in the country.

"III. To establish standards for the protection and safety of the life and property of persons, in matters pertaining to the electrical industry.

"IV. To fix the requirements for granting the necessary authorizations to carry out the activities related to the electrical industry.

"V. To determine which acts and omissions constitute violations to the law and to establish the corresponding penalties."

The regulatory function of the activities of the electrical industry mentioned in section one is exercised by the federal government through the Ministry of National Economy. This ministry is in charge of receiving, studying, and approving requests for concessions to carry out the activities mentioned therein, by private individuals or corporations, as well as by the state and municipal governments or by the Federal Commission of Electricity. The Ministry of National Economy is also the agency which receives, studies, and approves requests for permits to carry out the afore-mentioned activities when these activities do not involve the use of federal waters or public service activities, inasmuch as in these last two cases the law demands that said activities be subject to concessions and not just to permits.



Figure 3. "Los Morales" substation of the Mexican Light and Power Company, Limited, (20,000 kva, 85–6 kv) showing typical structure with steel-reinforced concrete poles

According to the Electric Industry Law, concessions can be granted only to Mexican individuals or to corporations organized under the Mexican laws. The duration of these concessions is for 50 years during which time the concessionaire is supposed to pay to the federal government a redemption tax equal to the value of the properties destined for public service, with exception of the value of the permanent hydraulic works. This tax payment is spread out over the 50 years of the concession at the rate of 2 per cent on the value of said properties. At the end of the 50-year period, the concessionnaire has the right to obtain a renewal of the concession for a period of time not to exceed another 50 years. During this second period the concessionnaire is not obliged to the 2 per cent payment and, on the other hand, can make annual accruals to amortize the value of the permanent hydraulic works. The money received by the federal government from the 2 per cent tax provides funds to enable the Federal Commission of Electricity to carry out its activities.

At the end of a concession, the concessionnaire may retire his installations and sell all property covered by the concession, with the exception of the permanent hydraulic works which revert to the nation without compensation. However, the federal government has the right to acquire installations and properties of the concessionnaire at the end of his concession, if it so desires, in which case the government must pay the price fixed by two experts named by both parties or by a third expert in cases of controversy.

In order to obtain a concession for activities of the electrical industry involving the use of federal waters, the solicitant previously must obtain a federal concession for the use of these waters. This concession must be requested and obtained in accordance with the requirements established by the National Water Law, the application and execution of which are in charge of the federal authorities through the Ministry of Agriculture and Development.

The rates that public service companies charge their customers for electrical service are regulated and fixed by the Ministry of National Economy through its General Electricity Bureau and Electric Tariff Commission.

The Electric Industry Law establishes the principle that electrical rates shall be fixed on the basis of allowing a fair return to the concessionnaire. The law contains rules for the determination of fair return, for the valuation of properties, and for determination of the rate of return.

The value of the properties of electrical public service concessionnaires, as represented by physical property in existence as of December 31, 1941, is determined by means of tables of unit values contained in the regulations of the law at present in effect. The investments in physical property made subsequent to December 31, 1941, are taken at cost in national currency on the date

they are made. To the value of the physical properties, determined as has been explained, should be added the value of the intangibles which in no case can exceed 15 per cent of the value of the physical property, and, in addition, an amount is added for working capital. The sum of these three elements constitutes the rate base on which the fair return is allowed.

The rate of return, according to the regulations of the Electric Industry Law, must be fixed with due consideration of the return made by other public service companies, and in general by other undertakings that are similar from the viewpoint of the risks, and of the amount and term of the investment. However, in no case should a rate of return be fixed at a lower figure than the highest rate of return corresponding to governmental bond issues, unless the concessionnaire requests and accepts a lower rate of return.

Naturally, the legislation also provides that the operating and maintenance expenses, taxes, except income tax which is not considered as an operating expense, insurance, and the retirement and replacement fund also should be taken into consideration in order to fix rates for a public service company.

Aside from the regulation exercised by the federal government on the activities of the electrical industry, there exists a control on the part of the federal authorities on installations for generation, transformation, transmission, distribution, and utilization of electric energy, from the standpoint of protection and safety to the life and property of persons. The Ministry of National Economy, through the General Electricity Bureau, watches, by means of previous approvals of plans and of inspections of installations, the proper observance of safety rules and specifications that must be fulfilled by all electrical installations according to the respective stipulations contained in the National Electric Code and subsequent rulings issued from time to time in line with new technical developments. The National Electric Code in general is modeled after that of the United States and contains the minimum safety requirements that electrical installations must fulfill.

All electric materials, devices, apparatus, or machinery used or sold in Mexico must fulfill certain essential characteristics of corresponding types approved by the Ministry of National Economy. Sales not complying with these essential specifications are subject to a fine.

The foregoing presents a general picture of the most important dispositions of the Electric Industry Law and its regulations. It is hoped that these rules will encourage the development and betterment of the electrical industry in Mexico, on the part of private industry as well as on the part of the federal government.

Realism in Engineering Education

A. S. LANGSDORF
FELLOW AIEE

Citing the cultural education of an engineer as a continuing process, Dean Langsdorf tosses the responsibility to the national engineering societies. He opposes further dilution of engineering curricula which already require streamlining and intensification if, in the face of expanding technology, they are to meet effectively their obligation of assuring their graduates the requisite fundamentals.

STANDING for the moment at the threshold of what we fondly hope may be a long era of world peace, it is appropriate to pause sufficiently to take stock of the trends that characterize our sector of the educational front, to the end that we may chart a course toward the goal we wish to reach. By definition we in education belong to a profession dedicated to the utilization of the forces and materials of nature for the benefit of mankind, and therefore it may be concluded that our objective is a peaceful world if it be granted that war is detrimental to human welfare. Somehow we must reconcile this conclusion with the fact that in the nearly 2,000 years of the Christian era there have been only 257 years of complete peace, and that in the 165 years of United States history from 1776 to 1941 the intervals between the country's major wars have averaged only slightly more than 25 years. We also must reconcile our conclusions with the fact that the art and science of engineering as it developed in civil life is a direct outgrowth of military engineering, and that in time of war such as we have experienced recently, the best scientific and tech-

Essential substance of an address presented at the South West District meeting, San Antonio, Tex., April 16–18, 1946.

A. S. Langsdorf is dean, schools of engineering and architecture, Washington University, St. Louis, Mo.

nical brains have been diverted to destructive ends. Does it not follow that the basic philosophy of engineers, and of physical scientists in general, henceforth must be so oriented as to contribute effectively to a world-wide pattern of social betterment?

ENGINEERS AND HUMAN RELATIONS

It is this consideration—that engineers and engineering are concerned with human relations, just as they obviously are concerned with impersonal forces, materials, and machines—that is the motivating idea of those educators who, within the recent past, have insisted upon a revision of engineering curricula to the end that approximately 20 per cent of the student's time be devoted to social and humanistic subjects. There can be no quarrel with the implication that engineering graduates must be something more than slide-rule pushers having no thought beyond the technicalities of their jobs; that they must be, in addition, responsible citizens willing and able to assume responsibility for the guidance of social, economic, and political affairs as these are affected by technology. But the 20 per cent dictum, when applied to the generally prevailing 4-year curriculum, means, in my opinion, that the remaining 80 per cent is grossly inadequate for a decent minimum of the basic sciences and technology. Without that minimum equipment of scientific training the graduate will cease to have the specialized mental equipment which alone entitles him to be listened to with respect on technical subjects. Insofar as this opinion is valid, it would seem to follow that there are only two alternatives: the lengthening of the curriculum to a minimum of five years, or some compulsion which will force the 4-year graduate to read and study on his own initiative after achieving a diploma. There is every reason to believe that within a relatively short time the 5-year curriculum is likely to supplant the presently prevailing 4-year arrangement. This lengthening of the course of study probably will come about eventually anyway, not because of the desirability of adding social and humanistic subjects, but because of the absolute necessity of incorporating in the training period an amount of the rapidly developing fundamental sciences that underlie their even more rapidly increasing applications sufficient to qualify the technical graduate to practice in his chosen field. More and more it will be necessary for technical schools to teach those fundamental subjects which are learned best under competent guidance, and to omit those subjects which can be mastered easily by a trained mind without special instruction and guidance. Why, for example, is it not entirely feasible to utilize the summer vacation periods for assigned reading in subjects such as general literature, history, biography, economics, or political science, in lieu of requiring a student to listen to lectures on these subjects at the rate of three, four, or five hourly doses per week? The lecture system of imparting information of this kind in any case is not so effective as independent reading. Someone once defined the lecture system as an educational device for transferring information from the notebook of the professor to the notebook of the student without the painful necessity of straining the material through the mind of either party.

THE TEACHER'S ROLE

I am convinced that the enlightenment of students concerning the social and economic aspects of modern industrial civilization can be secured as a by-product of instruction in science and technology provided the teachers of those subjects are enlightened and well-informed. This leads, of course, to the conclusion that teachers of engineering and science must be versed in the liberal arts at least as well as they want the young graduates to be. Not enough are. May it not be that some of the shortcomings of the average engineering graduate are attributable to the inadequacies of some of the teachers to whom he was exposed? There is no doubt but that the teaching profession is in great need of a larger percentage of vigorous and creative minds than it now possesses; teachers who by precept, and especially by example, have the power of stimulating the minds they presumably are molding. There is some bitter truth in George Bernard Shaw's salty mot: "Those who can, do; those who can't, teach." Part of the difficulty of securing and holding really first-class teachers is the limited income assigned to them by common consent. The monastic influence in education is still powerful; the notion that a teacher is set apart as a creature dedicated to poverty and obedience. Such circumstances are not attractive to vigorous and independent minds. Better salaries in the colleges would help to widen the field from which teachers might be recruited, and work must be done in that direction.

Tinkering with the curriculum is the great indoor sport of the educational world, and the effort to secure allocation of 20 per cent of the engineering curriculum to cultural instruction is merely the latest manifestation of what has been going on for a long time. Its ultimate objective is laudable—the desire to raise the intellectual level of the engineering profession because of widespread dissatisfaction with existing conditions. There are some who apparently believe that the inclusion of the 20 per cent of cultural subjects will of itself convert a young man of 22 or 23 into a sage capable of reforming the world by solving economic and social problems that have troubled mankind through all the ages. On the contrary, the acquisition of culture and wisdom is a life-long process. Education is not a kind of treatment that can be concentrated within school and college years; it is the end-product of a life of thoughtful study. If that fact is admitted, it must follow that the education of engineers is even more a function of the national engineering societies than it is that of the colleges. The colleges can and must serve as the preliminary training ground for the novitiates, but their subsequent mature

development must be the concern of the profession as a whole. For example, consider the case of the Association of Atomic Scientists, the men who staffed the laboratories at Clinton, at Los Alamos, and at the Metallurgical Laboratory in Chicago. They were professional physicists, chemists, and engineers who, for the most part, had not been exposed to the 80–20 per cent regime. Yet they had the wisdom and the foresight to see what disaster their work might bring upon mankind, and they took vigorous action in the interest of what they conceived to be the public welfare of the whole world. In my opinion, these scientists have set an example that all the engineering societies well may emulate; the dedication of their collective strength as a great moral force in the field of human relations.

Pedagogical Buck Passing

The College Teacher:
From stupid freshmen may I be spared,
The high schools send 'em up so unprepared.

The High School Teacher:
What results from us can you expect
When grade school teaching is so inept?

The Grade School Teacher:
If kindergarten teachers these kids would train,
They'd save us lots and lots of pain.

The Kindergarten Teacher:
Pity the homes from which these youngsters come,
Their parents must be extremely dumb.

The Mother:
Poor stupid child, you're not to blame,
Your father's folks were all the same.

Query:
Shall father in his own defense be heard?
No, let mother have the final word!

Lest these remarks would seem to indicate that I am opposed to the inclusion of a maximum amount of cultural studies in the engineering curriculum, I might add that more than 35 years ago my first act as a dean of engineering was to include in our curriculum a full year of instruction in economics. There was much objection to this requirement on the part of students who looked upon anything borrowed from the liberal-arts program as "sissy" stuff. It is amazing that even today so many high ranking technical schools are content with only one semester of economics. To my mind, the subject of economics is inseparable from a thorough understanding of the social effects of engineering. Unfortunately economics, long ago described as the dismal science, generally is not presented to college students in the stimulating manner in which it might be.

Since engineering is concerned so largely with the production of controlled energy, recent discoveries in the field of atomic physics are certain to play an important role in future engineering developments. The great plant at Hanford, Wash., on the Columbia River, even now is yielding by-product energy at the rate of nearly 1,500,000 kw which is going to waste in heating the water of the river. The time is bound to come when a method will be found to utilize that energy for industrial purposes. It even may be that the immense radioactivity incidental to the fission process may contain a promise of obtaining electric energy without the intervention of boilers, steam turbines, and generators. That is a consideration that will affect vitally many branches of engineering. It points to the conclusion that engineering education in the future must pay more attention to the new physics and the new chemistry inherent in the process. Already the term "nucleonic engineering" has been invented to forecast what lies ahead. It will provide more material for curriculum revision, but this time the emphasis undoubtedly will be placed on two or more years of graduate instruction, since there is no hope that the whole field can be compressed into the undergraduate period.

NEED FOR ANALYSIS

Since science will not remain stationary, but rather will grow in extent as time goes on, the need to include the fundamentals of expanding knowledge within a limited time is bound to force a critical examination of existing procedures. The problem faced by the teaching profession is not unlike that of a manufacturer who must increase the quantity and quality of his product without materially increasing his unit costs. Under such circumstances a wise management makes a critical job analysis in order to cut corners. That is the procedure that the educators must adopt. There is little doubt that present-day curricula contain much more than vestigial traces of ancient tradition, and that something akin to an appendectomy is necessary to remove a few accumulated appendages. Consider, for example, the customary college course in physics, which invariably begins with an elaborate treatment of statics and dynamics, moves on into the laws of heat, caroms lightly into acoustics, then advances upon optics, electricity, and magnetism. In many institutions instruction in statics and dynamics is given concurrently with, or sometimes just before, another course covering the same principles, but taught by the department of applied mechanics. Quite commonly this double exposure is followed by another in connection with machine design or framed structures. It may be that multiple exposure of this sort serves a useful purpose in the case of students who possess obtuse minds, on the principle that constant dripping will wear away a stone, but it is likewise true that much useless duplication is the result of hidebound tradition. The excision of unnecessary repetition can do much to make room for new material that now is excluded because of lack of time.

One of the underlying reasons for dissatisfaction with existing engineering training, one that explains the desire for a broader type of training, is the circumstance that practically every engineering enterprise requires the active co-operation of many workers having a great diversity of interests. The average young graduate does not comprehend fully this interdependence of people, but tends to focus his attention upon materials and machines. It is particularly regrettable that the schools pay so little attention to the all-important subject of labor relations and labor legislation. Engineers as a class are hostile to labor unions, probably because they are harassed so frequently by the jurisdictional disputes and restrictions on productivity that characterize some union activity. Nevertheless it is a fact that labor problems are here to stay, and that engineers must learn to work in a world where these problems constantly must be met and solved. Not much prophetic ability is called for to predict that all schools soon will require that all graduates must have become acquainted with the major outlines of this vitally important subject.

THE "G. I." PROBLEM

At this time technical schools throughout the country are filled to the bursting point with returning veterans who are taking advantage of the "G.I. Bill of Rights." Some curious circumstances have resulted. Whereas the average age of current seniors, mainly 4F men who were not inducted into service, is about the normal 21 or 22, the average age of the swollen freshman classes is four to five years greater. What has happened is that the Bill has oversold the capacity of the colleges by a factor of about three to one. This situation is nearly as bad in one direction as the unwise Selective Service policy was in the other. In the name of democracy it cut off a 5-year supply of the trained young men upon whom the future of industry must depend. This was not selective service at all; it was indiscriminate, unselective service. If the United States ever again is faced with the emergency of war it is to be hoped that the engineering profession will find a tongue to protest against such a policy for the good of the nation.

The present swollen registration in engineering colleges demands that steps be taken promptly to insure much more selectivity in the admission of students than heretofore has prevailed. This is a subject which for some time has been under study by Engineers Council for Professional Development, but the existing pressure is so great that something must be done quickly. In Washington University priority is being given to former students who showed satisfactory ability when last in residence. New students with no more than high school training are accepted if their rank was in the upper third; if middle third, an aptitude test must be passed; if lowest third, admission is denied. Transfer students with a year or more of college credit must have had a freshman record averaging a C grade, and if they had more than freshman credit, their average grade must have been intermediate between C and B. Coupled with these requirements for admission are regulations for remaining. Freshmen who fall below a C average will be dropped, as well as sophomores who fail to reach an average between C and B. The principle is that no poor student should be given a place at the expense of a worthier applicant. These are emergency regulations designed to keep registration within the limits set by physical facilities. It is hoped that the same basic principle can be maintained when the crest of the present flood has passed.

THE FUTURE

The future policy of engineering colleges must take into account the reform of certain deplorable conditions that characterize primary and secondary education in the United States. The teaching of grammar virtually has disappeared from grammar schools. The English subjects taught in high schools pay little or no attention to spelling, punctuation, or composition. In many of the states, a student can graduate from high school with only one year of what is called general mathematics, but which in reality is merely arithmetic that leaves the pupils with a blissful disregard of the position of decimal points. It is almost inconceivable that in an industrial nation—dependent as it is to a high degree upon engineering and science, with all which that implies as to an understanding of quantitative relations—the educationists should have acquired such a stranglehold on the public schools. Standards are lamentably low, and by a perversion of democracy the doctrine has been established that one child is as good as another, so no one is allowed to fail. The result is a generation of undisciplined minds, in which the poor ones regard themselves as well trained, and the bright ones have no incentive to excel or to realize their full potentiality. If these statements are thought unduly pessimistic, recommended collateral reading is a book by John Tildsley, former assistant superintendent with the Board of Education of the city of New York, entitled "The Mounting Waste of Secondary Education in the United States."

Now another peril to engineering education looms on the horizon in the form of indiscriminate universal military training. Common sense would lead one to believe that, since any future war is bound to be even more technological than this last one, everything possible must be done to conserve the supply of trained engineers. If there must be universal military training, let it be so arranged that bona fide students of engineering and of medicine, dentistry, physics, and chemistry are left undisturbed except during vacation periods. If there must be Reserve Officers Training Corps units in the engineering colleges, let it be so arranged that no undue amount of time shall be diverted from fundamentals to highly specialized military subjects such as marching and counter-marching and manual of arms.

Amortisseur Action of the Squirrel Cage

EDWARD BRETCH
MEMBER AIEE

Single-phase motor theory is a somewhat controversial subject because two distinct single-phase motor theories, the rotary field and the cross flux theories, have prevailed for 50 years. The physical concepts of the actions taking place in the motor that are developed by these two theories are not altogether consistent with each other or with test results and so it seems that some action is in order to co-ordinate these two theories into a single one, with the elimination of the inconsistent elements of both. The proposition that the quadrature flux of the single-phase squirrel cage motor is developed by the amortisseur action of the squirrel cage is submitted as a suggestion along this line.

IN THE STATIONARY TRANSFORMER, electric energy, in a primary circuit, is transformed into electric energy in a secondary circuit through the medium of a mutual magnetic flux. For the purpose of this discussion, this action, whereby electric energy is transformed from the primary to the secondary circuit by purely electrical means without involving mechanical energy, is termed the transformer action.

In rotating electric machines, such as motors and generators, the main function is a transformation between mechanical and electric energy. This is accomplished by the mechanical motion of the conductors of the electric circuit across a magnetic field. The driving energy in a generator, or output in a motor, is mechanical energy. In this case where the transformation is between mechanical and electric energy, the action is termed the speed action. It is evident that in the squirrel cage motor both of these actions are involved, although the speed action, or the transformation of electric energy into mechanical energy, is the most important under running conditions.

When an electric circuit encloses a magnetic circuit, the electric and the magnetic circuits are tied together by strong mutual reactions. Any change in current in the electric circuit produces a magnetic flux change and the flux change in turn produces a counter electromotive force which tends to oppose the current change. Consequently, in such an inductive combination, the current does not follow the voltage instantly. Conversely, in a magnetic circuit that threads an electric circuit, any flux change induces a current in the electric circuit and this induced current produces a counter magnetomotive force opposing any flux change so that the flux does not instantly follow the mmf.

Edward Bretch is associated with the Century Electric Company, St. Louis, Mo.

Through these mutual reactions between the magnetic and electric circuits each exercises a damping effect on the other. The effect on the electric circuit produced by the reaction of its induced field is termed self-induction. The corresponding effect on the field produced by the reaction of the induced currents in the closed circuits through which it threads has not been named and is referred to here as the "amortisseur action." This amortisseur action affects the flux in the magnetic circuit in exactly the same way that self-induction affects the current in the electric circuit. With a constant mmf, the magnetic flux is determined by reluctance alone. When the mmf is varying or alternating and the flux threads closed circuits, reluctance is no longer the sole factor controlling the flux. The amortisseur or inductive action of the induced currents in the closed circuits through which the flux threads affects the magnetic flux in the same way that self-induction affects the current in the electric circuit.

An amortisseur winding is a system of low resistance electric circuits enclosing the magnetic flux utilizing this stabilizing principle to oppose rapid flux changes. It operates both by the speed action and the transformer action. When the flux strength remains constant and there is a relative motion between the conductors and the flux so that the conductors cut across the flux, an emf is generated in the electric circuit by speed action and the resulting currents oppose the motion of the conductors with respect to the flux.

When there is a change of flux strength without relative motion between the conductor and the flux, the currents induced in the electric circuit by transformer action oppose and retard any flux change. Both variations of flux strength and relative motion of the flux with respect to the conductors are opposed by this amortisseur action. Flux strength variations are opposed by the transformer

action and relative motion between the conductors and the flux by the speed action. These actions may operate either singly or simultaneously.

In a rotor, the speed and transformer actions operate in space quadrature with reference to each other and consequently do not react on each other. Thus, the two actions can operate simultaneously in the same rotor without interference. As all the conductors of a squirrel cage are short-circuited completely, the squirrel cage rotor presents a short circuit across any axis. It is, in fact, a magnetic core completely enveloped by an amortisseur winding. As all the rotor flux threads it, the flux of necessity must be subjected to the influence of the amortisseur or damping action of the closed squirrel cage circuits through which it threads. The induced amortisseur currents in the squirrel cage oppose any variation of flux strength by the transformer action as well as any change of position of the flux with reference to the rotor conductors by speed action.

In the polyphase squirrel cage motor, a unidirectional rotary mmf is set up by placing symmetrically spaced windings around the field structure excited by alternating currents that correspond in time phase with the space phase of the exciting windings. If the number of phases was infinite and the exciting waves truly sinusoidal and of constant frequency, a constant unidirectional mmf, rotating at a constant speed, would be produced. Under these ideal conditions, a squirrel cage rotor at synchronism would have no emf induced in it either by the speed or transformer action and a constant rotary field would be produced without the aid of the amortisseur action of the synchronous squirrel cage.

In practice, these ideal conditions are not fulfilled, and the amortisseur action of the synchronous squirrel cage tends to oppose and dampen out the variations from the ideal. In commercial motors the number of phases usually is confined to three phase, two phase, and single or one phase. Under these conditions, there are always variations between phase bands in the mmf impressed on the rotor and the exciting waves frequently do not approximate the sine form very closely. While a unidirectional mmf is impressed on the synchronous rotor, there are cyclic variations of strength and shape. These cyclic variations are opposed and suppressed substantially by the amortisseur action of the synchronous squirrel cage.

In the polyphase motor the individual phase actions generally are assumed to combine vectorially so as to produce a constant unidirectional mmf rotating at a constant speed without reference to the amortisseur action of the synchronous squirrel cage. This is only partially true, since the shape and strength of the primary mmf impressed on the rotor varies in the shift from one phase band to the next. At synchronism, these variations between phase band shifts are opposed and damped out by the amortisseur action of the synchronous squirrel cage which results in a substantially uniform rotating field, both as to shape and strength throughout the complete cycle, irrespective of these cyclic variations of the primary impressed mmf.

In a 2-phase motor, these phase band variations of

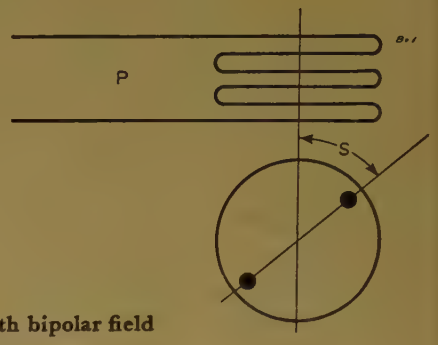


Figure 1. Rotor with bipolar field

the primary winding are quite prominent. At the instant the current in one phase is zero, the current in the other is at its crest and the total mmf is impressed by one phase alone. When the cycle has progressed 45 degrees, the mmf is impressed by both phases equally, but separated by 90 space degrees. It is evident that with the much broader combined span of both phases and the imperfections of wave form, the impressed mmfs are much different under the two conditions. These phase band mmf variations induce amortisseur currents in the synchronous squirrel cage that hold the field substantially constant throughout the cycle, both as to shape and strength even though there may be wide cyclic variations in the impressed mmf.

In a 3-phase motor, the phase band variations are less than in the 2-phase, while in the single-phase, they are at a maximum. This occurs because in the single-phase motor the impressed mmf goes through zero two times during each cycle while the synchronous squirrel cage amortisseur currents maintain the flux substantially constant during the complete cycle. As a cycle for the amortisseur currents that sustain and equalize the flux between phase bands is completed with each phase band passed by the rotor, at synchronism there is impressed on the rotor a phase band frequency six times the fundamental frequency in the 3-phase motor, four times in the 2-phase, and a double frequency in the single-phase motor.

As the phase band variations are most prominent in single-phase motors where the primary impressed mmf varies between zero and the maximum while the synchronous flux is sustained substantially constant throughout the cycle by the amortisseur action, and since the working range is limited to speeds near synchronism, the remainder of the article will be limited to the single-phase motor at and near synchronism.

Consider a bipolar field (Figure 1) with an exciting winding acting along the transformer axis across the space occupied by the rotor. The primary mmf along

this axis is proportional to the current flowing in the primary winding P. Also, consider two conductors of the squirrel cage spanning a diameter forming a rotor circuit or coil. The part of the primary mmf that is effective in this rotor circuit depends upon the sine of the space angle S it makes with the axis of magnetization. If this field is excited by a single-phase alternating current, since the current varies sinusoidally with respect to time, the mmf impressed on the field is $Ip \sin T$, where Ip represents the primary current and T the time angle of the exciting current. The mmf impressed on the secondary rotor circuit is then $Ip \sin T \sin S$.

At synchronism, $S = T$ and $\sin S = \sin T$. The synchronous mmf impressed on the rotor is $Ip \sin^2 S$, or $Ip \sin^2 T$. Mathematically, a quantity varying as the square of the sine is a quantity varying sinusoidally between zero and the positive limit at double frequency (Figure 2). The physical interpretation of this condition is not difficult. As the rotor rotates synchronously in the single-phase field, it moves from one pole to the next in the same time it takes the exciting current to reverse. Consequently it is subjected to a series of rotating unidirectional mmf impulses of double frequency varying from zero to a maximum instead of an approximately continuous unidirectional rotating mmf as in a polyphase motor. If the rotor had no closed circuits, which would eliminate any secondary mmf, the flux in the synchronous rotor would follow the impressed mmf, and vary unidirectionally between zero and the positive limit at double frequency.

This unidirectional mmf imposed on the synchronous rotor and varying sinusoidally between zero and the positive limit at double frequency can be resolved into two components (Figure 3). One of these is a positive constant component of one half the peak value of the unidirectional pulsating mmf and the other a double frequency alternating component varying between positive and negative limits of one half the peak value of the unidirectional pulsating mmf.

The effective fluxes set up by these mmf's must thread the synchronous squirrel cage. The amortisseur or choking action of the low resistance squirrel cage will oppose and choke out the double frequency flux component but will offer no opposition to the constant unidirectional component and no secondary emf will be produced by it. The extent to which the alternating component is suppressed depends upon the conductivity of the amortisseur or rotor circuit. If the rotor resistance could be reduced to zero, the alternating flux component would be eliminated entirely. While rotor resistance never can be zero, it is usually low enough so that the alternating component is eliminated substantially. This leaves a substantially constant rotor flux at synchronism.

When the squirrel cage operates at synchronism, this constant sustained rotor flux rotating at synchronism generates a counter emf in the primary winding by speed action in the same way that the rotating field of a synchronous generator does. It is a fundamental fact that a coil rotating in a constant flux generates the same emf that is produced by alternating the flux between the same limits at the same frequency. That is, the speed voltage and the transformer voltage are equal under like conditions. Therefore, to generate the same counter emf with the synchronous squirrel cage as with the open circuit rotor, the constant sustained rotor flux in the synchronous rotor must equal the peak single-phase flux with open circuit. Since, as is noted in Figure 3, the constant synchronous component is one half the peak impressed mmf, it follows that in order to generate the same counter emf with the synchronous squirrel cage rotor as with the open circuit rotor, the primary mmf required with the synchronous squirrel cage is double that required with the open circuit rotor. That is, the exciting current with the synchronous squirrel cage rotor producing a rotary field is double that required to produce the single-phase field with the secondary winding open-circuited.

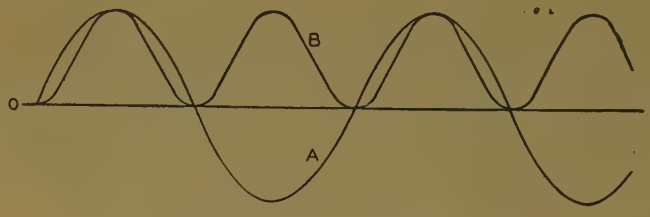


Figure 2. Magnetomotive waves

A = primary impressed mmf
B = double frequency synchronous unidirectional rotor mmf

The magnetic and electric conditions in the synchronous single-phase motor can be represented by stationary circuits as shown in Figure 4. As the alternating primary mmf is converted by synchronous rotation into a unidirectional double frequency pulsating mmf in the synchronous rotor, and this is the equivalent of a constant mmf superimposed on an alternating mmf, we may consider the excitation imposed on the synchronous rotor as produced by a direct current excitation I_c and an alternating excitation of double frequency I_a, the peak value of the alternating component being equal to the constant component. The secondary winding is separated from the primary winding by an air gap forming a magnetic circuit of relatively high reluctance. The secondary circuit in which the secondary current I_s flows is a low resistance short circuit representing the squirrel cage.

The flux due to I_c will pass through the low resistance secondary winding without opposition while that due to the double frequency component I_a will be opposed by the choking or amortisseur effect of the low resistance short-circuited secondary winding. In a transformer,

where the secondary load is entirely inductive, which is the case here, neglecting the secondary resistance, the primary current is the arithmetical sum of the exciting current plus the secondary current.

It has been shown that when circuit I_s is closed, the primary exciting current is doubled. As the exciting

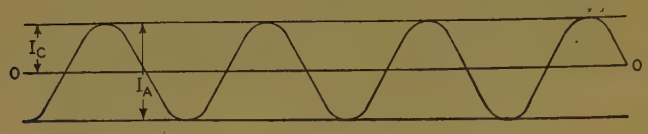


Figure 3. Components of magnetomotive waves

current is determined by open-circuit secondary conditions and the primary current is doubled by closing the secondary circuit, it follows that $I_s=1/2I_a$. That is, at synchronism there is a double frequency amortisseur current equal to one half the primary exciting current and also equal to the primary exciting current with open secondary winding.

While the primary exciting current and the synchronous double frequency rotor current are quite large because of the air gap in the magnetic circuit, the flux variations necessary to produce the comparatively large amortisseur currents in the rotor are not large if the secondary or rotor resistance is low. The amount of flux variation required depends on the secondary resistance.

Although the secondary resistance cannot be reduced to zero, in practice it is low enough so that the flux is held approximately constant throughout the cycle. This approximately constant flux, sustained throughout the cycle by the transformer action in the rotor and carried along with the synchronous rotor through the speed action during the interval the primary mmf is ineffective, produces a true rotary field.

The speed action of the squirrel cage rotor is understood well and need not be developed here. Each time a primary impulse is applied, or at each half cycle, the rotor flux will be pulled into synchronism and the near synchronous rotor will tend to follow it in exactly the same way as in a polyphase motor producing a torque. However, this torque is a series of double frequency impulses and drops to zero with each impulse.

It is also evident that the double frequency flux sustaining currents in the rotor that are due to the transformer action will become, as slip takes place, double frequency less slip. The slip current is due to the speed action and has a fundamental low slip frequency the same as in the polyphase motor with the impulse frequency superimposed. Thus, the resultant rotor current will comprise a low frequency slip component upon which is superimposed a double frequency component less slip.

As the speed and transformer actions operate in space quadrature in the rotor, the currents resulting from transformer action that level and sustain the flux are at a maximum 90 space degrees from the position of the maximum slip or torque currents that are due to speed action.

Such factors as reactance, resistance, slip, and iron losses prevent the sustained or cross flux from actually equalling the main flux or being displaced exactly 90 degrees, but it is not necessary to consider these factors in order to understand the fundamental principles as to how the amortisseur action operates through the transformer action to maintain the flux approximately constant throughout the cycle and through the speed action to produce a torque as the rotor tends to run in synchronism.

CONCLUSIONS

The synchronous or near synchronous squirrel cage in the single-phase motor operates as an amortisseur, opposing and suppressing sudden flux changes, either as to strength or position with relation to the rotor conductors.

The mmf impressed on the synchronous rotor is unidirectional and pulsating at double frequency between zero and a maximum.

The flux produced in the synchronous rotor by this pulsating unidirectional primary mmf is leveled off and

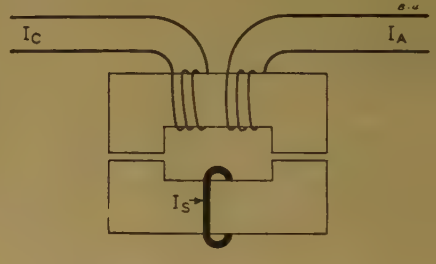


Figure 4. Representation of single-phase motor

maintained substantially constant throughout the cycle by the amortisseur action of the squirrel cage.

The induced amortisseur rotor currents, leveling and sustaining the flux constant throughout the cycle, are due to the transformer action, are of double frequency, and are equal to one half the primary exciting current. The synchronous mechanical rotation of this amortisseur sustained rotor flux produces the rotary field.

The speed action opposing relative motion between the flux and the rotor conductors, tending to pull the rotor into synchronism with the primary exciting impulses, produces a torque which pulsates at double frequency. This synchronously rotating and substantially constant rotating flux in its quadrature position is the so-called cross flux.

The speed action producing the torque and the transformer action sustaining the flux constant take place in space quadrature in the rotor and, as they do not react on each other, can operate either singly or simultaneously.

Advances in Airport Lighting

W. A. PENNOW

Developments in airport lighting for combat purposes initiated a trend toward much higher candlepower for contact lights and much more expensive lighting equipment generally for commercial airports. The new tendency is a welcome departure from the all-too-common prewar practice of allotting only one per cent or less of the airport's cost for lighted landing aids in spite of the failure of radio to provide adequate control in heavy air traffic. A combination of improved lighting with radio is offered as the only feasible method of affording the pilot the necessary margin of safety for landing or take-off.

AIRPORT LIGHTING developed for combat use differed very little basically from prewar peacetime practices, but the physical means of accomplishing those practices were, in many ways, vastly different from equipment that previously was used. As combat airports followed the flow of ground force action, equipment had to be extremely mobile; lightweight, so that it could be air-borne; simple in construction and operation, so that it could be serviced quickly and easily by semiskilled personnel; ruggedly made, so that it would stand the abuse of repeated assembly and disassembly; and most economical of electric power, as this had to come from portable air-borne gas-electric sets.

The system devised was unique in many respects. Marker and obstruction lights consisted of light stamped steel housings and plastic globes. The light used a prefocused bayonet base lamp and an automobile headlight-type socket, except that it had 120-volt insulation. The plastic globe was made in two types: symmetric and asymmetric horizontal distribution. With a clear asymmetric globe and a 40-watt T-8 bulb lamp, candlepowers over 500 were obtained in the useful zones. Mounted on a short length of fiber conduit and a stamped steel base, these were used as contact lights. Cable was supplied in 330-foot lengths and fitted with watertight push-type rubber connecting plugs. It was laid on top of the ground alongside the landing strip and the units were set on the ground and plugged together. Where a cable crossed another landing strip, it was buried two to four inches deep through the active area of the landing strip. It was possible for a three man crew and a jeep to lay both sides of a 5,000-foot runway in less than half an hour with this setup.

Asymmetric globes were supplied in clear, half clear–half yellow, and half green–half red colors. These made up a complete runway complement giving standard color sequence from either end—the pilot coming in over green, through clear, into yellow, toward red. The half green–half red units were set in lines of three or four units across the ends of the runway, green outermost. The last 1,500 feet, viewed from either end of the runway, were outlined in yellow.

Symmetric red globes were used as obstruction lights. Thirty-foot telescopic poles equipped with guy cables were standard, and could be set up easily by two men. The poles and guys could be combined for a maximum height of 60 feet, but in this case were difficult to set up with less than a four man crew, as intermediate guys carried the catenary during raising and had to be handled carefully to prevent buckling. A two man crew could set up and connect a 30-foot high obstruction light in less than ten minutes, while a four man crew could assemble, set up, and connect a 60-foot high obstruction light in about 15 minutes.

The gas-electric generator power supply was usually a 2-kva set, with a 5-horsepower 2-cylinder 2-cycle engine, with the control panel mounted as part of the set. These would handle up to 50 of the 40-watt lights, or handle one landing strip with obstruction lights and a beacon.

Additional equipment made the basic portable sets even more versatile. Small fiber cones mounted under the contact lights provided additional visibility for daytime marking. Special bases and longer lengths of fiber conduit provided an effective means of marking runways in deep snow, since the markers and cones were high enough to clear plowed banks.

Beacons were one of three types. The standard 24-inch airway beacon equipped with a special double beam lens was used in areas farthest from combat lines. A 500-millimeter Fresnel-lens-type beacon with a code flashing mechanism was used for certain operations. The most used beacon was the stroboscopic flashing type which employed the principles established by Doctor Edgerton of the Massachusetts Institute of Technology, Cambridge. This beacon consisted of a power-pack which included a step-up transformer, rectifier tubes, and capacitor bank; and a small light unit with a

Essential substance of an address delivered at the symposium on lighting during the AIEE winter convention, New York, N. Y., January 21–25, 1946.

W. A. Pennow is section engineer, lighting division, Westinghouse Electric Corporation, Cleveland, Ohio.

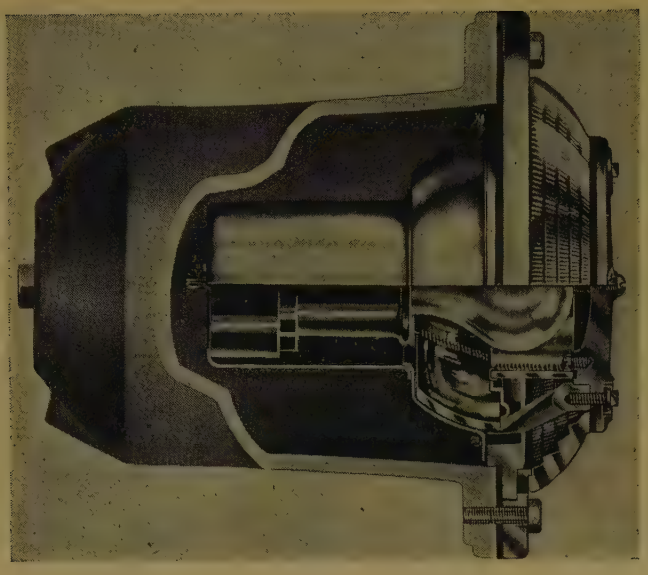


Figure 1. Airport contact lights with a dead load capacity of 100,000 pounds, an improvement over 18,000-pound dead load capacity prewar models

Fresnel-type globe and a tightly wound spiral of neon tubing with special electrodes. Alternating voltage of about 1,500 volts was rectified and fed to a capacitor bank. The rate of charge was governed by a small variable resistor. As the voltage across the capacitors built up, it reached a point where the neon tube broke into ionization and the capacitors then discharged into the tube, giving a very brilliant flash of light. Using discharges of 1,000 volts and about 350 amperes, candlepowers up to 30,000,000 were obtained. The flash duration was extremely short, something less than one microsecond. The effective light was about 25,000 candlepower seconds, compared to a little over 80,000 candlepower seconds for the 24-inch beacon which has a flash duration of about 1/12 second.

The stroboscopic beacon had a continuous energy consumption of about 200 watts and light emission of about 50 watts, for an over-all efficiency, including losses in the rectifier tubes, of 25 per cent. This was unusually high for this apparatus, normal being 18 to 20 per cent. The total weight of the assembly was less than 100 pounds and it could be set up on its 25-foot telescoping tripod tower in about ten minutes by a two man crew.

Combat hoods were supplied for all portable contact, marker, and obstruction lights and the stroboscopic beacon. These were designed to limit the visible angle of the lights to a very narrow angle, about ten degrees both vertical and horizontal, so that the entire lighting system absolutely blacked out in all directions except the actual approach. This feature was of great help in the African campaign and in the South Pacific, as it permitted night operations in areas that were under rather close enemy aerial surveillance.

About 1,500 airstrips and airports in combat areas were equipped with this type of apparatus, which in some cases was moved frequently to follow the combat lines. Complete lighting for an airstrip, with lights, cable, cable reels, poles, gas-electric set, spares, packing cases, and fuel for 24 hours operation, weighed 3,600 pounds and could be carried, with the entire crew, in a DC-3-type cargo airplane. Set-up crews usually consisted of eight men and the normal time allowance for setting up a complete airstrip was two hours. It has been said that one crew in the South Pacific, having had lots of practice hopping islands, made an amazing record of complete set up in 23 minutes from the time their cargo airplane stopped rolling. This included unloading the gear, unpacking the cases, loading the equipment into motor vehicles (which were on the job), and setting all units out, that is contact lights, obstruction lights, and beacon. This may or may not be the record for set up, but it does show the extreme usefulness of this purely combat equipment.

As the bases advanced and more men and materials were carried by air, semipermanent and permanent airports were constructed to serve as supply bases. Regular types of airport lighting equipment were used, making use of the development inspired by the rough service encountered on training fields. One of these developments was the contact light, which before the war had a dead load carrying capacity of 18,000 pounds. This had to be increased to 100,000 pounds to stand up under training operations, and under service conditions involving heavy bombers and cargo airplanes. These were used on all new construction, a total of over 75,000 of these contact lights being installed in all parts of the world, enough for 700 normal sized airports.

Two new developments were made for these airports. One was a high intensity contact and approach light. This unit looked like an inverted street lighting fixture and consisted of a spun steel body, a Fresnel-type inner lens, a blown glass color screen, and an asymmetric outer globe. Sector-type reflectors were used to aid correct distribution. The unit employed a 200-watt lamp, either series or multiple, and produced a sharply controlled beam of about 35,000 maximum candlepower as compared with about 1,000 candlepower on the regular contact lights. These units, with brightness control, permitted operation under much worse weather conditions than was possible with regular equipment. About 50 airports, particularly in Alaska and the Aleutians, were equipped with these units, and their record was quite good.

The other unit was a "mobile floodlight assembly," consisting of a 15-kva 115/230-volt generator and four 3-kw landing area floodlights on a $1^1/_2$-ton truck. The generator was driven by the truck engine through a power take-off. The control arrangement, by engine governor and variable voltage, was such that frequency and voltage were held to plus or minus one per cent automatically. A switchboard permitted part or all

of the generator capacity to be diverted to outside lines for powering portable electric tools or other uses. Four 3-kva step-down transformers, 230 to 32 volts, were used, one for each floodlight.

An adjustable pedestal, mounted at the rear of the truck bed, supported the four drum-type floodlights in such manner that each floodlight was adjustable through a 30-degree arc, vertical and horizontal, and the assembly of four also could be rotated or elevated as a unit and raised from 7 feet high over-all to 12 feet. The lenses on the floodlights were one each of plain, 10-degree, 30-degree, and 80-degree spread, providing 1/4-footcandle minimum intensity on a landing strip 400 feet wide by 4,000 feet long.

One hundred and fifteen of these assemblies were built and gave excellent service on all fronts.

A companion development to the contact lights took place in the auxiliary equipment. Most notable of these was the swing from the old standard moving coil constant current regulator to the static, or monocyclic square, regulator. The principle of this regulator was known quite well but not much attention had been paid to it. As power supplies on many of these new airports were limited, the need for improved power factor on partly loaded regulators caused engineers to take another long look at the monocyclic square. Much had been learned about the behavior of the square in its application to constant voltage transformers, and by applying that knowledge to the constant current unit, a much improved combination resulted. The new regulator was much more compact and maintained power factors of 90 per cent and higher under all load conditions. Further development enabled brightness control, whereby regulator output was such that light intensity of 100, 30, 10, 3, or 1 per cent was obtained, to be built into the regulator. This was accomplished by adding taps to the output transformer on the square and using relays mounted in the regulator case. This development thus condensed the constant current regulator, brightness control transformer, five high voltage relays, and a protective circuit relay into one compact unit and raised the lowest power factor condition from less than 20 per cent to more than 90 per cent.

Another development of auxiliary equipment was the "runway selector cabinet." Previously it was necessary to use up to four high-voltage series short-circuiting relays, and four heavy-duty high-voltage series absolute cutouts, mounted on a pipe rack, to connect the regulator output to the proper runway circuit and provide protection for maintenance personnel when the lights were being serviced. Wiring of this equipment was done on the job, and the installed cost varied from $500 to $750, depending on local conditions. The space requirement was about 75 cubic feet, 5 by 5 by 3. The runway selector cabinet combined all this equipment, plus line and load terminals, in one compact unit. Installed cost was cut in half and the space requirement was reduced to nine cubic feet, 3 by 3 by 1.

Many developments of airport and airway lighting for commercial use are now under way. For airway lighting, a new high intensity obstruction light to give better identification to radio towers or other major obstructions is nearing completion. Using only one 500-watt lamp, this new unit will have a candlepower of 40,000 in red compared with less than 5,000 in red from the present marker which uses two 500-watt lamps. Instead of flashing the lamps, which often causes troublesome radio interference, the new unit has a rotating semaphore lens system under a red glass dome. A standby lamp provides a safety factor not available on present equipment.

Also nearing the final test stage is a new intermediate airway beacon for use in areas where spacings of five miles, or less, must be used, due to terrain. This new beacon has light characteristics identical with the larger airway beacons, and has a maximum candlepower of 100,000, compared to about 10,000 candlepower from the present intermediate beacon. The new beacon is enclosed completely, making it impervious to wind, rain, snow, or sleet.

In airport lighting, the most notable tendency is toward much higher candlepower on contact lights, and much more expensive equipment generally. The wails of the airport lighting engineer are being heeded at last. The common practice of building magnificent airports, then using what money is left over, if any, for lighting must be changed. There is too much at stake. The idea of limiting lighted landing aids to a cost of one per cent, or less, of the airport cost can be classed as little less than criminal negligence. As an example, an airport with a

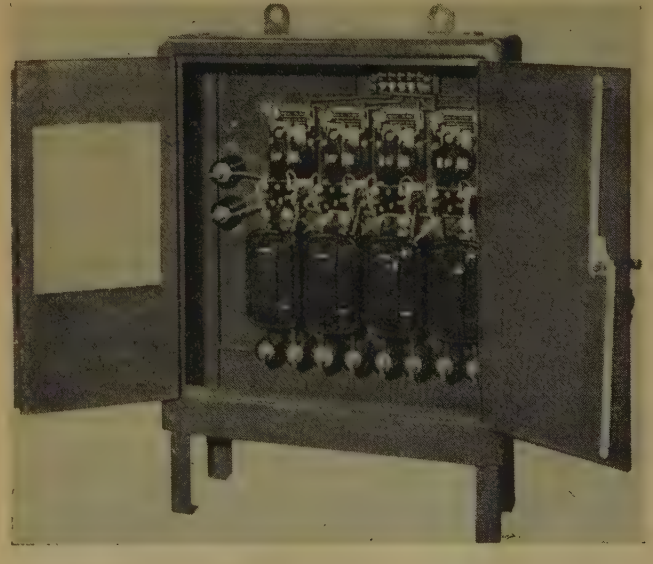


Figure 2. New runway selector cabinet which combines short-circuiting relays, series absolute cutouts, and brightness control equipment

Over-all size is approximately 3 feet by 3 feet by 1 foot

published cost of nearly $40,000,000 has field lighting equipment that costs under $100,000, or one fourth of one per cent of the total cost. Another example is an airport which costs well over $2,000,000, but the lighting equipment costs only a little over $10,000, or one half of one per cent. And these are supposedly *modern* airports.

Recently there were two airline accidents with the loss of two transport aircraft and the life of one passenger. One of these accidents occurred when a pilot tried to land the airplane during a blinding rain squall; the other

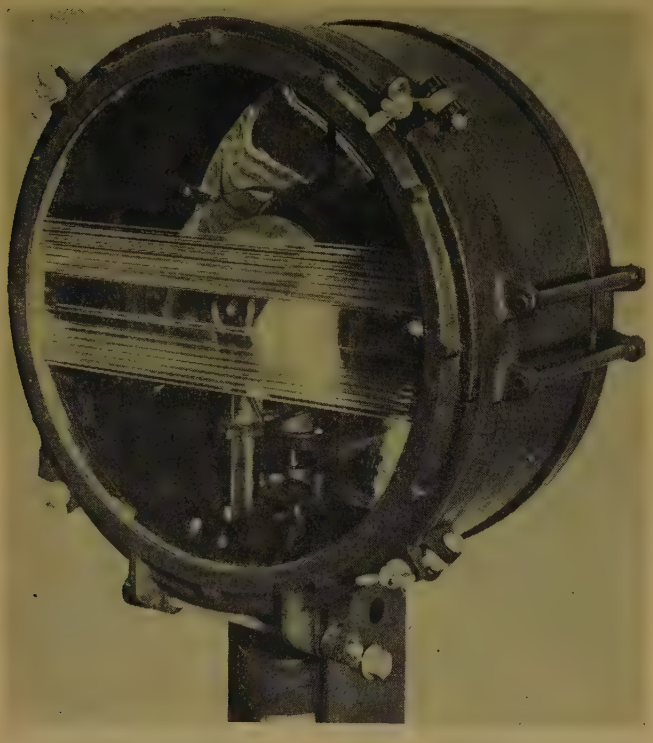


Figure 3. Projector-type approach lights which reach peaks of over one million candlepower

These lights are serviceable in daytime weather of heavy haze, or light snow or rain; or in night weather of medium fog, rain, or snow

was blamed on an attempt to land the airplane in what is described as "murky weather." Both accidents occurred at large airports on the airlines' regular schedules, and both were due to overshooting the runway.

These are not the first accidents of their kind, nor will they be the last.

Simple economics long have demanded that there must be no strings on the purse when safety is involved. These airplanes cost as much as all the lighting aids on the airports, and who will venture placing a cash value on human life? Newer, larger airplanes cost more than $1,000,000 each. One such airplane, with its load of humans, makes almost any airport lighting system seem insignificant.

But what are the engineers doing? New contact lights with candlepowers up to 100,000 are in production. These are a hundred times as powerful as those now in use.

New traffic control equipment, consisting of giant crosses and arrows made up of gaseous tube elements, have been tested thoroughly and are ready for use. These designate the runway to be used and give positive location at the end of the runway when crossed by an aircraft on an instrument approach.

Greatest engineering strides have been made on approach light systems, designed to work with so-called "blind landing" methods. Several years ago the Civil Aeronautics Administration devised the so-called "neon ladder" approach light system, which consisted of 5-foot long neon tubes in linear parabolic reflectors, mounted 100 feet apart in a row 1,500 feet long extending from the runway covered by a leg of the radio range. This system has been satisfactory in hazy daytime or light fog; or in light fog, light rain, or light snow at night; but it is useless under worse weather conditions, and is too bright on clear nights. A more recent CAA system uses projector-type equipment to supplement the ladder. These units have peaks of over 1,000,000 candlepower and are serviceable in daytime weather of quite heavy haze, light rain, or snow; and night weather of medium fog, medium rain, or medium snow.

Recently the United States Army Air Corps, the Bureau of Aeronautics of the Navy, and the Air Transport Command have been testing variations of these systems. One, called a "neon blanket," is an enlarged version of the old neon ladder. Each unit consists of 11 4-foot neon tubes. While spectacular in clear weather, it is little more effective than the neon ladder in daytime or adverse night conditions. On clear nights it is very glaring. A newer variation, with brightness control, appears much more effective.

Another unit is a variation of the projector unit, but employs an Edgerton-type flash lamp, similar to that used in the stroboscopic beacon. Sufficient data have been accumulated on this unit to prove that higher candlepower is the answer to lighting in really bad weather, and that a system with complete control of brightness is the answer to an all-weather system of approach lighting.

Such a system has been designed, and now is undergoing laboratory tests preparatory to a full scale installation. Test data at present indicate that this system will reach through any kind of weather, from clear to absolute zero-zero plus heavy snow or rain. As an indication of the power packed into this all-weather system, the candlepower range for each unit is from 100 candlepower to over *five billion.* A total of 72 units is required for each end of each runway, for a total candlepower of over 360 billion on each approach. For the first time candlepower can be talked about as glibly as is the "National Debt," with the candles at a dollar a throw.



Figure 4. Giant traffic control arrows which indicate whether the runway is clear or blocked

What about costs? Staggering, when compared with past ideas of airport lighting costs. But a complete installation at each end of three runways on an airport will total less than the cost of one Lockheed Constellation! Truly, a small price for insurance against a repetition of the two recent airline tragedies.

Airport lighting for commercial use is growing up, fast! Twenty years ago, a $2,500 allocation for lighting on a million dollar airport was a lot. It has grown to a quarter million dollar allocation on a 25 million dollar airport. Perhaps the not too distant future will see an allocation of $2^1/_2$ million dollars on a 75 million dollar project. And airport lighting in this article means equipment costs, not including cable, conduit, or installation. The percentage growth up to now has been from one quarter per cent to one per cent. Three per cent appears to be an absolute minimum.

Other developments are under way for commercial and private use. One of these, now nearing the production stage, is the "approach angle indicator." It is expected that this will be a *must* supplement at all airports, regardless of size or scope. Dubbed the "missing link" by pilots who have watched it work, it unerringly indicates the correct altitude for incoming planes. It is the first piece of equipment to give elevation information that has enough candlepower to match contact light systems. The indicator projects a three-color sandwich toward the incoming plane, showing red if too low, yellow if too high, and green if at correct elevation. To avoid confusion with other lights, a mechanical shutter obscures the light for 1/2 second 40 times per minute.

On airports with contact lights, the indicator replaces contact lights located 500 feet from the end of the runway, one on each side.

On small airports it guards against overshooting or undershooting the available landing area. When used for training purposes, the time needed to teach a student good landing technique is reduced by as much as 20 per cent in some cases, as no other means teaches the feel of proper rate of descent nearly as well as this unit.

Excellent accuracy of color separation is achieved; the area of color mix, vertically, is about four feet at a mile. Two sizes of lamps are proposed: a 100-watt lamp for private airports, giving nearly 500-candlepower average across the three colors; and a 240-watt lamp for commercial airports, giving over 1,000-candlepower average. Private airports usually are not confronted with high landing speeds, and the lower candlepower is considered sufficient.

Particular emphasis is being placed on new, low cost equipment for small airports, class one and class two, by the CAA Office of Airports. New equipment soon available for these small airports includes a small double-end rotating beacon, essentially a miniature of the 36-inch airport beacon but costing about a fourth as much, and a small wind cone mounted on a 25-foot hinged pole, externally lighted and equipped with an obstruction light. Although only two thirds as long and half the

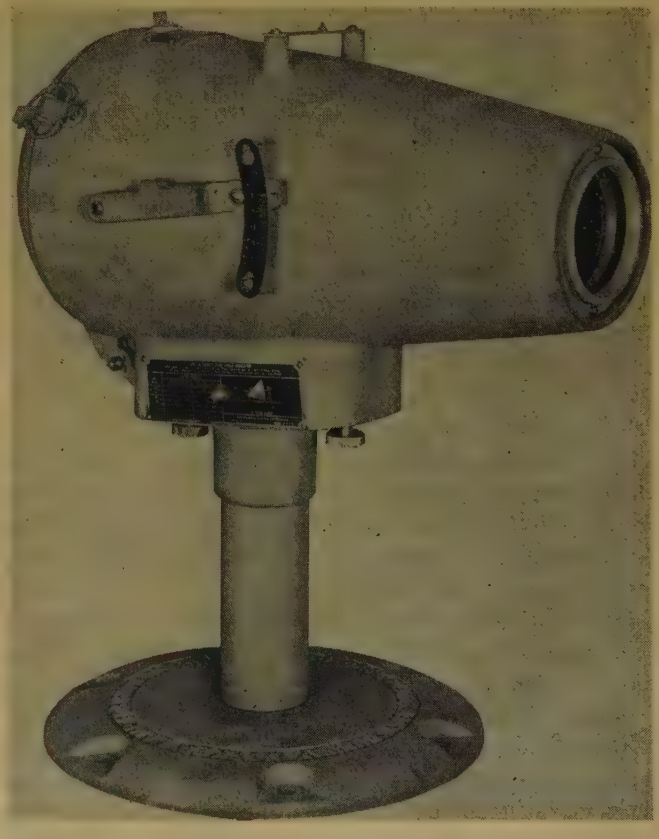


Figure 5. The approach angle indicator, sometimes referred to as the "missing link" of airport lighting

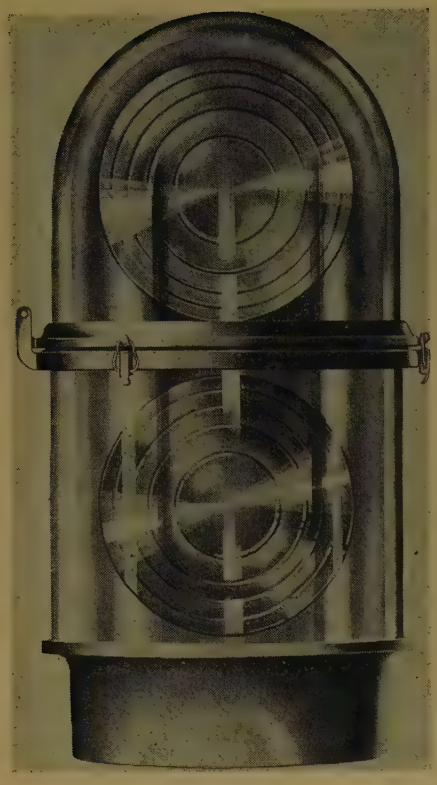


Figure 6. Small double and rotating beacon for small airports

This beacon costs only about a fourth as much as the standard 36-inch airport beacon

diameter, this cone has all the features of the standard wind cone, with an indicating range of one mile. It costs about as much with the pole as the standard wind cone itself.

Other items nearing the production stage are a new, low cost line of marker and obstruction lights, having most of the features of standard AN types, but using standard screw base lamps. There is a new low cost surface mounting contact light that bolts directly to the surface near the edge of a concrete or macadam runway. This unit has an integral junction box with watertight cable entrance bushings that projects over the edge of the runway into the earth fill. Cable is laid alongside the runway in regular trenches, breaking up to enter the contact light.

In the testing stage is a new asymmetric globe for either AN-type or the new low cost type marker lights. This will be used in place of contact lights on unpaved landing strips, on range lights, and on box lights at the ends of paved runways. This new globe also will be used on contact light extensions in snow country, giving essentially the same light distribution, and mounted on supports from 2 to 10 feet high to clear drifts or banks.

Airport lighting design engineers are busier than ever with two major problems facing them. The first, and most important, is to provide complete, all-weather lighted landing aids for commercial use to insure safety as far as possible. Do not be confused by all the loose statements that robot landings are just ahead. "Blind landing" equipment was on test in 1938; blind landings still are not made as a matter of course. Improvements in radio, loran, and radar must and will be made and they must be utilized to the fullest extent by airlines and airports. This still is not enough. Lighted landing aids must and will be used to provide that last ounce of prevention that means the difference between safe and something less than safe transportation.

The second, and most lucrative problem, is to provide complete, low cost, sturdy airport lighting equipment for small airports. This problem challenges the ingenuity of the designers in that performance and quality must be kept high while costs must be much lower than customary for this equipment. Volume production of the apparatus will not be high enough to justify the kind of tooling that brings costs down, so designs must take advantage of every bit of "know-how" and every production short cut.

As to what the future holds, there will be five general classes of airports, each with its own specific problems. The small privately owned airport, whether operated individually, by a flying club, or by a small community, either will be an all-way field having no runways or stabilized surface, or will have stabilized surface landing strips. Lighting equipment will include a small rotating beacon, a small wind cone, and either low cost boundary and obstruction lights to outline an all-way landing area, or asymmetric strip lights and approach angle indicators for stabilized surface landing strips. If activity and finances permit, a mobile lighting unit will be used as an all-purpose floodlighting system.

The small municipal airport in communities up to about 25,000 population generally will have two or three runways of stabilized soil. Lighting must be sufficient for private and feeder line aircraft, and will include a small rotating beacon, one or more small wind cones, asymmetric strip lights or low cost contact lights, obstruction lights, approach angle indicators at each end of each runway, and either a permanent floodlight system or a mobile floodlight unit.

Larger communities, up to 100,000 population, will have good sized airports with at least three paved runways, and these must be equipped to handle all types of aircraft, under some adverse weather conditions. Lighting facilities will have to be quite extensive, and should include a large rotating beacon, large wind cone or wind tee, contact lights with brightness and runway selector control, approach angle indicators, and landing area floodlights at each end of each runway, obstruction lights, and a low visibility approach lighting system consisting of neon ladder and projector approach lights at the end of at least one runway. This will be on the runway aligned with one leg of the radio range or equipped with a radio approach system.

Communities of over 100,000 population will have large airports designed primarily for commercial and feeder operations. Lighting equipment for these large airports will include a large rotating beacon, an auxiliary beacon to flash the code letters identifying the airport,

a ceiling projector for continuous check on ceiling height, a portable traffic signal for emergency control, and contact lights with brightness and selector control. At each end of each runway range lights with asymmetric globes, runway traffic control lights, approach angle indicators, landing area floodlights, a smoke wind indicator, cross and arrow runway designators, and projector-type approach lights with brightness control will be needed. Radio approach systems will be needed for one or more landing directions. Obstruction lights and taxi guidance lights also will be used.

Super airports, serving communities with over 1,000,000 population, will have at least three pairs of parallel runways, and complete all-weather lighting to insure safety of operation as far as possible.

Lighted aids for the super airport will include the large rotating beacon, auxiliary code beacon, ceiling projector, portable traffic signal, and wind cone or wind tee, or both. All runways will have high intensity contact lights with brightness control and each end of each runway will have asymmetric range lights, runway traffic control lights, landing area floodlights, cross and arrow runways designators, smoke wind indicators, and approach angle indicators. Each end of each runway normally used for landings will have an all-weather approach light system with complete intensity control. These approach lights will extend at least a half mile beyond the end of the runway.

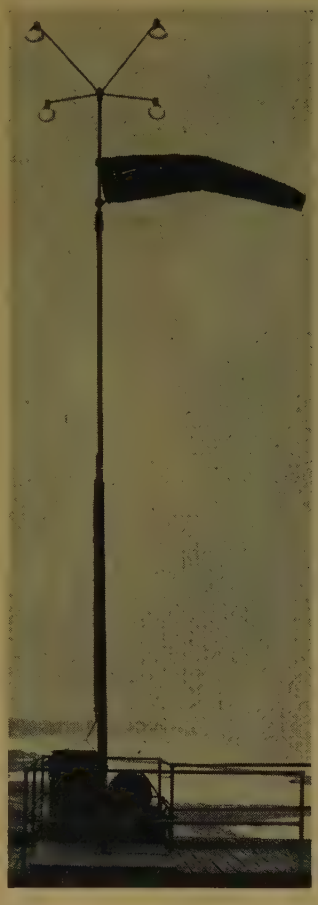


Figure 7. Illuminated wind cone for smaller airports

Taxi guidance lights will be on a block system of control, interlocked with the runway traffic control lights, cross and arrow runway designators, and approach lights so that a taxiing plane cannot be authorized to move across any runway when the runway signals indicate clear for landing or take-off. This system of control must have two stages of brightness, one for day time, the other for night use, to give adequate signals for operation 24 hours a day.

This emphasis on lighting as the major control method at airports is the result of the almost complete failure of radio control in heavy air traffic. Radio must be used to contact the incoming airplane and give preliminary approach instructions, including weather conditions, wind direction and velocity, and assigning priority for landing. Mass operations must be on a "follow-the-leader" basis, and the radio is used to set up this part of the landing operation. Once a pilot receives his weather data and is assigned his approach priority, radio contact ceases and lighting takes over. Similarly, on take-offs, radio is used to give weather and wind data, designate the runway to be used, and the taxiing route to take-off position; lighting does the rest. Thus two control officers, one on radio and the other on lights, easily can handle any volume of air traffic up to one movement per minute or more. Only by combining radio and lighting can such volume of air traffic be handled safely.

That is a picture of minimum requirements for airport lighting as it appears at present. How soon these minimum requirements will be met, particularly on large and super airports, is not apparent. Safety demands no less, and demands it now!

Vertical Wind Tunnel

WITHIN THE 80-FOOT concrete tower of the recently completed vertical wind tunnel at Wright Field, Dayton, Ohio, aerodynamic tests which may save many dollars, working hours, and even the lives of pilots now are being conducted on future Army Air Forces airplanes which are still in the blueprint stage.

The Air Matériel Command's new free-flow open-throat vertical wind tunnel, the scene of previously impossible tests for airplane spin characteristics, terminal velocity studies, parachute research, and experiments with helicopter rotor blades, has been erected near the 20-foot-wide horizontal tunnel and the 750 mile per

Based on material prepared by the public relations office of the Air Matériel Command, Wright Field, Dayton, Ohio.



Air Matériel Command photo

Figure 1. Structure housing new 80-foot vertical wind tunnel at Wright Field

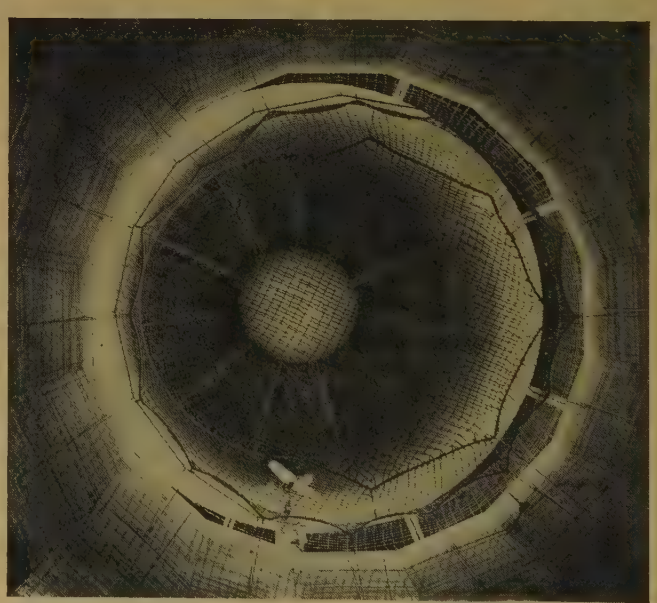
hour high-speed and high-altitude tunnel on Wright Field's "Hurricane Hill."

A 12-foot cylinder which runs up the center of the building serves as the test chamber and operational heart of the tunnel. An upward airstream is sucked through the test section and returned down an annular air passage between the inner cylinder and the outside concrete walls of the building by a 4-bladed wooden propeller, 16 feet in diameter. The fanlike propeller is turned by a 1,100-horsepower electric motor mounted above it at the top of the tunnel. Variations in airstream, ranging from almost zero to more than 100 miles per hour, are accomplished by means of a controllable pitch arrangement on the propeller, rather than by changes in the motor speed. Walls of the test section are faced with polished maple flooring to minimize airflow turbulence.

Tests are conducted from a recessed observation balcony which opens into the tunnel throat, halfway up the test section. Model airplanes, built to an extremely accurate scale from designer's specifications for new aircraft, literally are thrown from the balcony into the airflow which sweeps upward at a predetermined speed sufficient to sustain the miniature. As the model spins, dives, or climbs in the airstream, synchronized motion picture cameras located at the top and side of the test section record every motion and reaction of the plane. Subsequent study of these film records enables engineers to anticipate performance of a new ship, and to detect design errors before the full-size airplane enters the construction stage.

Wingspread on the model airplanes ranges from two to three feet, or approximately 1/30 that of a full-scale airplane. The miniatures are accurate to within 1/100 of an inch, and are balanced by weights to within 1/10 of a gram. Each free-flying model contains a complete set of controls, including ailerons, flaps, rudder, and elevators, which are operated by remote control with the precision of a pilot. The remote control mechanism, 12 half-inch solid copper cables banded together to circle the inner wall of the test chamber, magnetically activates the controls in the model airplane. As the power running through the copper rings is shut on or off, the position of the magnetized controls is changed and the flight pattern of the model is varied at the will of the operator on the observation balcony. When the test is completed the fanlike propeller is stopped, the airflow ceases, and the model falls into a nylon net stretched across the base of the test section.

As the Army continues its experimentation and development of the helicopter, the vertical tunnel will be utilized for research on rotor blades. Mounted on a streamlined hub at the base of the tunnel, model rotor blades can be tested for vibration and stress analysis while subject to simulated flight conditions created by the upsweeping airflow. Parachute models will be tested for "sway" in the airstream, and when attached from beneath to a force-recording mechanism, will be checked to determine the weight that the parachute can support safely in descent.



Air Matériel Command photo

Figure 2. Vertical wind tunnel as seen from its base

View shows, in order, polished maple surface of lower test chamber, nylon net into which models fall at completion of test, free-flying model airplane, and, at the top, vents through which a 16-foot propeller sucks winds at speeds greater than 100 miles per hour

INSTITUTE ACTIVITIES

Southern District Holds Sixth District Meeting in Asheville

With the South Carolina Section and the North Carolina Section collaborating as hosts, the sixth general conclave of the AIEE Southern District was held May 14–16 at the Grove Park Inn, Asheville, N. C. The dual features of the meeting were a very active student conference with representation from 15 of the 18 Student Branches in the District, and devotion of a large portion of the technical meetings program to the problems of especial interest to the industrial south. Total verified attendance was 373, in spite of last minute cancellation of nearly 50 advance registrations as the result of uncertainty over the railroad transportation situation. Registration statistics are given in accompanying tabulations.

The Southern District now includes 11 Sections, 4 Subsections, and 18 Student Branches. The Sections are: Alabama, East Tennessee, Florida, Georgia, Louisville, Memphis, Muscle Shoals, New Orleans, North Carolina, South Carolina, and Virginia. Subsections have become active at Little Rock, Ark., under the Memphis Section; at Charlotte, under North Carolina Section; and at Norfolk and Hampton Roads under the Virginia Section. Student Branches now are active at: Alabama Polytechnic Institute, Auburn; University of Alabama, University; Clemson Agricultural College, Clemson, S. C.; Duke University, Durham, N. C.; University of Florida, Gainesville; Georgia School of Technology, Atlanta; University of Kentucky, Lexington; Louisiana State University, Baton Rouge; University of Louisville, Louisville, Ky.; Mississippi State College, State College; North Carolina State College, Raleigh; University of South Carolina, Columbia; University of Tennessee, Knoxville; Tulane University, New Orleans, La.; Vanderbilt University, Nashville, Tenn.; Virginia Military Institute, Lexington; Virginia Polytechnic Institute, Blacksburg; University of Virginia, Charlottesville.

GENERAL SESSIONS

Presided over by AIEE Vice-President H. B. Wolf, the opening general session was given over to official welcome on behalf of the mayor of Asheville, introduction of President-Nominee J. E. Housley, and a general discussion on AIEE activities and engineering-society organization by AIEE Vice-President J. F. Fairman. Mr. Wolf called attention to the fact that the current total of 1,381 AIEE members of the Southern District represented some 22 per cent gross during the past 9 months. He paid special tribute to the individual[s] and southern industrial organizations whose contributions enabled his student activities committee substantially to underwrite the individual cost of student participation in the District meeting and student conference.

Speaking on behalf of the mayor of Asheville, Lee M. Bauer, president of the Engineers Club of Western North Carolina, presented the city's official welcome to those in attendance at the meeting. Indicating the interest of the south in the various aspects of electrical engineering incidental to the rapidly growing industrialization, Mr. Bauer stated that in 1944 southern industry used a billion kilowatt-hours more than in 1941, the total representing nearly one third of all industrial power requirements of the United States. With reference to engineering activities, and especially engineering education in the south, Mr. Bauer mentioned the program of the North Carolina Engineering Foundation which, with the object of providing the men and technique necessary for southern industrial growth, is very active in a program to "give qualified young men adequate technical training at home, and then to keep them at home in the south."

Vice-President J. F. Fairman (F '35) chairman of the AIEE committee on planning and co-ordination, then discussed Institute planning and was followed by several speakers who analyzed various aspects of the committee's program in more detail (see page 268 of this issue).

"Time" was the subject of an illustrated address given to the men, women, and students of the meeting assembled at an evening session by Commodore J. F. Hellweg (retired) of the United States Naval Observatory. Commodore Hellweg briefly traced the history of mankind's continuing attempts better to determine and report accurately the passage of time. He described and pictured early crude instruments, as well as the development of more precise instruments, including his own laboratory's development of equipment which automatically puts out radiobroadcast time signals accurate to 0.001 second.

Conditions existing in Germany since her military defeat a year ago were described by Past President C. A. Powel, recently returned from a 9-month tour of duty in Germany as chief of the electrical and radio branch of the Allied Control Commission. Mr. Powel expressed great concern over the fact that the Potsdam agreement calls for the reduction of German industry to that commensurate with a domestic economy of a level of no higher than that of surrounding countries, whereas the policy recommended jointly by the presidents of the major United States engineering societies (*EE, Nov '44, pp 393–4*) recommended the reduction of German industry to a level incapable of preparing for or supporting a war of agression, but sufficient to maintain German domestic economy at something like its prewar strength with reference to its neighboring countries. Mr. Powel contended that peace would be more secure with a commercially strong German industry. Many of his listeners agreed with him, but Commodore Hellweg who is intimately familiar with the German situation, past as well as present, strongly and unqualifiedly disagreed with him.

Southern District Meeting Attendance 1928–41

Date	Location	Attendance
1946—May 14–16	Asheville, N. C.	373
1943—Nov. 16–18	Roanoke, Va.	220
1941—Dec. 3–5	New Orleans, La.	384
1938—Nov. 28–30	Miami, Fla.	282
1930—Nov. 19–22	Louisville, Ky.	300
1928—Oct. 29–31	Atlanta, Ga.	400

BUSINESS MEETINGS

The AIEE board of directors held its May meeting, a double-header session, at Asheville during the Southern District meeting, at the invitation of and by prearrangement with Vice-President Wolf and the Southern District meeting committee. Other business meetings included an evening meeting of the District 4 executive committee, and the District 4 conference on student activities, and a business meeting of the North Carolina Section.

ENTERTAINMENT

Although there were no formal social activities with the exception of a brief luncheon for the women, special features arranged by the committee provided a nicely balanced program of diversion for both men and women. The Biltmore Industries on the grounds of the Grove Park Inn, devoted to jewelry making, famous homespun clothing fabrics, and various handicrafts, proved to be almost equally attractive to both men and women. The famous 12,000-acre Vanderbilt estate, Biltmore House, adjoining Asheville drew many informal groups of visitors during the course of the meetings. The huge castle-like "house" in the French Renaissance style, completely furnished in the original manner, now is operated as a public museum. A golf tournament for men was won by D. A. Quarles (F '41) of New York, with second prize to W. J. Waicman of Charlotte, N. C.; third prize to W. T. Johns (A '44) of Richmond, Va.; and fourth prize to L. A. Coone (A '39) of Charlotte.

Analysis of Registration at Asheville

Classification	North Carolina Section	District 4*	Other Districts	Total
Members	54	77	34	165
Student members	28	65		93
Men guests	18	49	5	72
Women guests	14	19	10	43
Totals	114	210	49	373

* Outside North Carolina Section.

Among the inspection trips, the trip to the Ecusta Paper Corporation in Pisgah Forest, N. C., about 35 miles from Asheville, took first place with a registration of 110. This plant is one of the largest and one of the very few in the world specializing in the production of cigarette paper. A close second in popularity was the trip to the American Enka Corporation about 12 miles from Asheville, for which the registration exceeded 90. This huge plant is the only producer of rayon in North Carolina. A total of 55 registered for two separate trips to the 30,000-kva Glenville hydroelectric plant of the Nantahala Power and Light Company about 70 miles from Asheville. This plant enjoys the distinction of being the highest head (1,150 feet) hydroelectric plant in the East. A total of 14 registered for two trips to the Cliffside steam plant of the Duke Power Company, also about 70 miles from Asheville. Features of this plant are two 40,000-kw 3,600-rpm units operating at 900 pounds and 900 degrees; work has been started on a 65,000-kw addition to operate at 1,250 pounds and 950 degrees.

STUDENT ACTIVITIES

The following résumé of student activities at Asheville was prepared by Miss Marie Foote, senior electrical engineering student at Duke University, and one of four women engineering students in attendance at Asheville. The others were: Miss Marie Kemper of the University of Kentucky, Lexington; Miss M. Theodorsen of Duke University, and Miss Betty C. Peters of the University of Kentucky, Lexington.

The Asheville student conference reestablished the normal status of these annual meetings of the Student Branches of the Southern District. The entire District meeting program was arranged to permit Student Members to attend most of the events, including all scheduled inspection trips and still attend their own conferences. Through the co-operation and financial support of industries located throughout the Southern District, a generous portion of the expenses of each Student Member in attendance was provided for by the general committee of the District meeting.

Fifteen of the 18 Student Branches of the District were represented by students and counselors. The remaining three Student Branches are active on their campuses, but were unable to be represented at this conference, principally because of conflicting examination schedules.

Student Branches represented, together with the Student Branch representative and counselors, are as follows:

University of Alabama: John P. Hynds, chairman; William J. Miller, counselor. Clemson Agricultural College: Thomas F. Dabney, Jr., chairman; F. T. Tingley, counselor. Duke University: Raymond M. Dunaiski, chairman; Otto Meier, Jr., counselor. University of Florida: no student delegate; E. F. Smith, counselor. Georgia School of Technology: Noel C. Turner, alternate; H. B. Duling, counselor. University of Kentucky: James M. Hisle, chairman; Brinkley Barnet, counselor. Louisiana State University: Julian S. Johnston, Jr., chairman; A. K. Ramsey, counselor. University of Louisville: Paul F. Wantland, chairman; M. G. Northrop, counselor. North Carolina State College: J. W. Chadwick, Jr., chairman; L. M. Keever, counselor. University of South Carolina: Claude E. Walston, chairman; Samuel Litman, counselor. University of Tennessee: Robert E. Ely, Jr., chairman; J. G. Tarboux, counselor. Tulane University of Louisiana: Lester L. Lenz, chairman; M. G. Zervigon, counselor. Virginia Military Institute: John W. Trumbo, chairman; J. S. Jamison, Jr., counselor. Virginia Polytechnic Institute: Frank L. Crow, alternate; Claudius Lee, counselor. University of Virginia: Theodore T. Patterson, Jr., alternate; L. R. Quarles, counselor.

Student Branches not represented were Alabama Polytechnic Institute, Mississippi State College, and Vanderbilt University.

The Student Branch of Duke University acted as host to the student conference. Professor Otto Meier, Jr., of Duke University, presided at the student conference as chairman of the committee on student activities of the Southern District. On Tuesday, May 14, the Duke Branch sponsored an informal gathering of all students, featuring a motion picture in colors of views of the Duke campus.

On Wednesday, May 15, 6 student papers were presented at the student papers session:

"A Study of Volume Expansion," Benjamin H. Carlisle, Jr., Duke University.

"Electrical Problems in the Drainage of New Orleans," Edwin G. Hays, Tulane University.

"Units and Dimensions," J. D. Tillman, Jr., University of Tennessee.

"Wave Analysis by the Wattmeter Method," Tommy H. Landrum, University of Tennessee.

"Design and Construction of a One-Kilowatt Frequency Modulation Transmitter," James M. Hisle, University of Kentucky.

"The Engineer and the Union," Howard D. Burns, University of Alabama.

The first prize of $15 was awarded to Benjamin H. Carlisle, Jr.; second prize of $10 was awarded to J. D. Tillman, Jr.; third prize of $5 was awarded to James M. Hisle. The presentation of the student prizes was made at a general session of the District meeting by E. W. O'Brien, chairman of the AIEE committee on Student Branches. The first prize student paper by Benjamin H. Carlisle, Jr., was presented a second time before a technical session of the District meeting on Thursday, May 16.

At the business meeting of the student conference held on Thursday, May 16, it was decided that the next annual Student Branch conference of the Southern District would be held at the University of Kentucky. Professor Brinkley Barnett, counselor of the University of Kentucky Student Branch, was elected unanimously as chairman of the committee on student activities of the Southern District for 1946–47 and was designated to represent the committee at the summer convention in June 1946 at Detroit, Mich.

The student conference voted to advise the board of directors that the Student Branches of the Southern District favor the establishment of an annual lecture tour providing for lectures by nationally prominent speakers at Student Branches. The conference also recommended that *Electrical Engineering* contain a student page for the purpose of recording outstanding activities of the Student Branches.

Institute Activities Given First Place on Southern District Meeting Program

The subject of the organization of the engineering profession as a whole, as well as possible changes in AIEE procedures, which has held the limelight at both the South West and Northeastern District meetings and at many recent Section meetings, through the efforts of the AIEE committee on planning and co-ordination, again was prominent at the Southern District meeting. The subject was introduced at the opening session of the meeting at 10 a.m., Tuesday, May 14, by Vice-President J. F. Fairman (F '35) chairman of the committee.

Vice-President Fairman outlined the work that has been done to date by the AIEE committee on planning and co-ordination toward the objective of its assignment last fall of the responsibility for a general study of AIEE activities with a view toward their improvement and vitalization. Acting for T. G. LeClair (F '40), chairman of the subcommittee on professional activities, Mr. Fairman reviewed the subcommittee report as published in the April issue of *Electrical Engineering*, covering the various possible plans of organizing or reorganizing the activities of the several engineering societies. To give specific point to the several proposals, Mr. Fairman called upon D. A. Quarles (F '41) of New York to discuss the contemplated advantages of plan A covering consolidation of the engineering societies in the electrical field; C. W. Evans (M '40) of Atlanta to discuss the qualities of plan B, which contemplates the maintenance of technical activities by the present technical societies and the concentration of the so-called professional or general public questions in a separate society devoted to that particular field, such as the National Society of Professional Engineers; and P. L. Alger (F '30) of Schenectady, N. Y., to discuss



Randall Wilson

Student members and counselors in attendance at the 1946 annual Southern District Student Branch conference at Asheville, N. C., May 14–16, 1946

the qualities inherent in plan C, the plan which calls for continuance of technical activities under the existing societies, with local councils for joint action on local matters of common interest and a federation at the national level to provide facility for joint action on national and international matters of common interest. There was insufficient time to provide for any general debate on the relative merits of the different ideas, but, for the guidance of his committee, Mr. Fairman circulated and collected questionnaires.

Discussing the technical activities of the Institute, M. D. Hooven (F '44) chairman of the AIEE technical program committee and also chairman of the technical activities subcommittee of the AIEE committee on planning and co-ordination, stated that, although there was plenty of room for more initiative in the promotion and development of technical activities, it was his opinion and that of his committee, that no major changes in Institute organization are required, and that none have been discovered that would be likely to contribute materially to more efficient operation in the technical field. He reported that his committee had surveyed the activities of some 50 technical organizations for purposes of comparison and was continuing its study of AIEE technical activities. A progress report covering a résumé of the activities of the subcommittee on technical activities was published on page 222 of *Electrical Engineering* for May 1946. Mr. Hooven called attention to the fact that his technical program committee was planning to begin its work earlier in the administrative year, by planning to hold a new national convention somewhere in the Midwest in the general vicinity of Chicago in the early fall of each year. He pointed out that this additional national convention not only would provide an outlet for additional technical papers, which would relieve somewhat the growing congestion of the present summer and winter conventions, but also would get the technical program committee and the technical committees busy developing technical papers earlier in the year than has been the case with the winter convention, the first major objective of the administrative year.

Directors Take Action to Broaden AIEE Activities

Actions taken by the AIEE board of directors at its May meeting calling for expansion and vitalization of AIEE technical activities, the broadening of the publications program, the better to serve the Institute's greatly increased membership, and calling for an expansion of the headquarters staff to enable it to take a more active part in the development and leadership of AIEE activities, are hailed by informed observers as marking the opening of a new era in AIEE affairs. The board held a double-header session at Asheville during the recent Southern District meeting, to provide adequate time for the normally heavy routine business of the May meeting and to provide the equivalent of a half-day session devoted entirely to the consideration of ways and means of extending and improving AIEE activities, providing for a greater flexibility in meeting the challenges of rapid developments and changing conditions in technological and other fields of direct concern to engineers, and of more effectively serving its individual members, all matters which have been under active study by the AIEE committee on planning and co-ordination in accordance with action taken by the Board at the beginning of the current administrative year.

After a preliminary discussion of key matters had indicated the general consensus of the board, P. L. Alger, R. T. Henry, and J. R. North were appointed to act with D. A. Quarles as chairmen of a special interim committee to function at an evening session between the two meetings of the board for the purpose of preparing specific statements of policy upon which definite action could be taken. Accordingly, at its second session, the board took action as indicated in detail in the following paragraphs.

HEADQUARTERS STAFF FUNCTIONS

Heretofore, it has been traditional that the headquarters staff function essentially in a passive capacity, carrying out the office and other routine operations incidental to the AIEE program, leaving the matter of active guidance and leadership entirely in the hands of the elected officers and appointed national committees. Desirous of establishing AIEE operating policy and procedure on a basis comparable with that successfully followed in industry,

with the staff taking a more active part akin to industrial management in the leadership and co-ordination of the various elements of the organization, acting on behalf of the board of directors and in correlation with the responsible leaders of the various AIEE activity groups to carry out the policy objectives established by the board, the board voted approval of the following statement of policy with reference to headquarters staff functions: "With the rapid growth of the Institute in numbers, in technical and geographical subdivisions, and in complexity of its technical field, it is the sense of the board of directors that means should be sought to increase the effectiveness of its management and administration. As one means to this end, the board proposes to strengthen the headquarters staff as may be required to render appropriate assistance to the various committees and agencies of the Institute. To take full advantage of this, the several committees are urged to seek the counsel and assistance of the secretary of the Institute and of the members of the headquarters staff. The secretary will consider the load on the staff resulting from this policy and recommend to this board such additions or changes as he may deem necessary to meet these requirements; and all members of the headquarters staff will be impressed with their duties and responsibilities in this connection, including the need for individual initiative in offering counsel and advice and in carrying out the policies and plans established by the responsible agencies and committees of the Institute."

TECHNICAL ACTIVITIES

To provide for broadening the scope of AIEE technical activities, and to provide for an increased flexibility in the pursuit of these activities which will make possible a more prompt response to the rapid changes characteristic of many of the varied fields of electrical engineering activity, the board adopted the following resolutions:

"Resolved, that it is the sense of the board of directors that the technical activities subcommittee of the committee on planning and co-ordination should be guided by the following principles: (1) that such additional technical committees should be organized as may be needed to cover the important items of electrical technology; (2) that these technical committees should be grouped in appropriate divisions or groups with a steering committee for each group fairly compact in numbers and reasonably concentrated geographically to promote effective action; (3) that the members of the steering committees be appointed by the president, and the members of the technical committees be appointed by their respective steering committees, all to serve for one year; (4) that each year the group steering committees, in addition to appointing their several technical committees, make recommendations to the president through the secretary on the membership and organization of their respective successor committees, including at least two alternates for each chairmanship; (5) that in such recommendations the steering committees provide for a turnover of at least 25 per cent of the steering committee personnel each year. Further, that it is the intent of this board that the responsible committees should proceed with such changes as they may determine to be necessary and proper to effectuate these principles unless the proposed changes are at variance with either the constitution or the bylaws, in which event they shall be referred back to this board."

PUBLICATIONS SERVICES

Recognizing the need for expanding the publication services of the Institute commensurate with its continuing substantial growth in membership and the greatly extended scope of subject matter currently of direct interest and importance to electrical engineers, the board took action on the following specific proposal:

1. Electrical Engineering. Recommended that the monthly publication be given latitude and flexibility to function more effectively as a general service periodical, the better to meet the needs of the membership as a whole; that it be planned and operated by its editorial staff under general policies established by the board; that material from various AIEE meetings and conventions be available for editorial selection preferably from the date of original submission, but certainly from the date of presentation; that other timely material be available for editorial selection regardless of source; to be distributed monthly to all members, Student members, and subscribers.

2. Proceedings. Recommended that an intermediate series of publications, to be called "Proceedings" or by other appropriate title, be established, in several separate sections corresponding to divisions or related groups of technical activities and interests; each section to be issued every two or three months in accordance with the amount of material available and other factors involved, the several sections to be spaced around the calendar year to equalize production load; the series of periodicals to contain full text of all currently available formal technical papers together with related discussions, and in addition thereto the full text or essential substance of virtually all other material presented at AIEE conferences, District meetings, and conventions, except that otherwise published in full in *Electrical Engineering* or in special form; any one section to be available for automatic distribution without charge, upon request, to any member in addition to *Electrical Engineering*, other sections to be available upon request at cost.

3. Special Publications. Recommended that special publications be encouraged, to be issued from time to time to accommodate the publication and appropriate distribution of material of especial value and importance in its field but of limited general interest or applicability; material highly technical or mathematical in content, or specialized in subject matter such as the "AIEE Lightning Reference Book," the AIEE joint subcommittee report "Telemetering, Supervisory Control, and Associated Circuits," the "Bibliography on Automatic Stations, 1930–1941," and other bibliographies; such publications to be available to members at cost; to others at higher prices.

4. Annual Transactions. Recommended that the content of the annual *Transactions* be drawn from the entire series of AIEE meetings, programs and other appropriate AIEE sources, but be limited to material critically selected and judged on basis of most important *new* contributions, or other material specifically selected on the basis of permanent record archival value, the whole content apportioned among subject fields appropriately in accordance with membership distribution in those fields; formal discussions to be included with the papers to which they apply; decisions and selections to be made by the publication committee at the close of each calendar year on the basis of original recommendations of qualified reviewers, observed membership reactions growing out of initial presentation or publication, relative merits of the several papers in any one subject field, and other factors significant from an archival record standpoint.

5. Annual Index. Recommended that a complete composite AIEE annual index be issued appropriately covering the content of *Electrical Engineering*, *Proceedings*, *Transactions*, and special publications; to be available for appropriate distribution without charge to members, Student members, and subscribers.

With specific reference to this proposal, as outlined by Secretary Henline, the board of directors voted that: "It is the sense of the directors that the underlying plan of Institute publications be reviewed, so as to provide for a journal of general interest to the membership and separate *Transactions* and special publications which will constitute a repository of original contributions to electrical science and its application; it is further the sense of the directors that the staff should be allowed broad latitude in the accomplishment of these purposes." Secretary Henline was requested by the board to submit the foregoing suggestions and actions to the publication committee. This was done, and in all probability will result in further action by the publication committee, during the summer convention in Detroit.

1946 Year Book Issued. The 1946 edition of the AIEE Year Book has been issued, in accordance with 1945–46 budget provisions. Addresses are corrected as of November 1, 1945. Copies have been distributed to all national, District, and Section officers, Student Branch counselors, and all members of national committees. Other members may obtain copies by writing to the AIEE, 33 West 39th Street, New York 18, N. Y. The Year Book is not available to nonmembers of the AIEE; nor is its use permitted for commercial, promotional, or other circularization purposes.

AIEE Summer Convention, Detroit, Mich., June 24-28, 1946

Monday, June 24

9:30 a.m. Conference on Automatic or Supervisory Control of Air Switches

46-147—ACO.* Operating Experience With Single Pole Switching. **I. T. Knight,** Kansas City Power and Light Company

9:30 a.m. Conference on Temperature Measurements and Standards

9:30 a.m. Instruments and Measurements

46-155. Frequency Compensated A-C Ammeters and Voltmeters. **J. M. Whittenton, C. A. Wilkinson,** General Electric Company

46-133. Functional Analysis of Measurements. **I. F. Kinnard,** General Electric Company

46-135. A New Design for the A-C Network Analyzer. **J. D. Ryder, W. B. Boast,** Iowa State College

46-142. High-Vacuum Leak Testing With the Mass Spectrometer. **W. G. Worcester, E. G. Doughty,** General Electric Company

9:30 a.m. Conference on Electronics in the Electrical Engineering Curricula

9:30 a.m. Resistance Welding

46-156. Characteristics of Resistance Welding Transformers. **F. E. Murray, R. C. Jones,** The Taylor-Winfield Corporation

46-137. Influence of Magnetic Materials on the Welding Characteristics of Resistance Welding Machines. **J. J. Riley, C. E. Smith,** The Taylor Winfield Corporation

46-141. The Application of Series Capacitors to Flash Welders. **J. F. Deffenbaugh,** Federal Machine and Welder Company

CP.** Voltage Change Due to Resistance Welding Loads. **C. M. Rhoades, Jr., H. A. Peterson,** General Electric Company

2:00 p.m. Conference on Section Operation and Management

There will be three separate Conferences with parallel meetings, one for the larger Sections, one for the intermediate Sections, and one for the smaller Sections. Delegates are requested to attend the meeting to which their Section is assigned.

The conference will be conducted in an informal manner. Each delegate will benefit from these conferences in direct proportion to his participation. Each meeting will be developed by discussion and questions from the floor covering the following subjects:

Operating committees
Technical groups
Fellowship
Section prize paper competition

Ten Minute Intermission

Signature of travel vouchers by delegates

Liability of Sections for injuries at meetings

Subsections

Announcement of special conferences of interest to the delegates:

(*a*). Local councils of engineer and technical societies

● PAMPHLET reproductions of authors' manuscripts of the numbered papers listed in the program may be obtained as noted in the following paragraphs.

● ABSTRACTS of most papers appear on pages 278–86 of this issue and pages 130 of the March and 174 of the April 1946 issues.

● PRICES and instructions for procuring advance copies of these papers accompany the abstracts. Mail orders are advisable, particularly from out-of-town members, as an adequate supply of each paper at the meeting cannot be assured. Only numbered papers are available in pamphlet form.

● COUPON books in five-dollar denominations are available for those who may wish this convenient form of remittance.

● THE PAPERS regularly approved by the technical program committee ultimately will be published in "Transactions"; many will appear in "Electrical Engineering."

(*b*). Student activities

Other activities

2:00 p.m. Conference on Section Operation and Management—Larger Sections

A. C. Muir, presiding

2:00 p.m. Conference on Section Operation and Management—Intermediate Sections

R. M. Pfalzgraff, presiding

2:00 p.m. Conference on Section Operation and Management—Smaller Sections

G. W. Bower, presiding

2:00 p.m. Conference on Automatic Switching of Capacitor Banks

46-106. Automatic Control of Large Synchronous Condensers. **M. J. Brown,** Westinghouse Electric Corporation

2:00 p.m. Conference on Electronic Instruments

The subject of the conference on electronic instruments will be limited to electronic recording instruments for potentiometric or bridge-type measurements. A short history of the development of electronic recorders will be presented. Problems encountered in perfecting the recorders and latest improvements and developments in the instruments will be discussed.

CP.** Electronically Operated Instruments for Industrial Measurements. **A. J. Hornfeck,** Bailey Meter Company

CP.** D-C to A-C Conversion Systems. **W. P. Wills,** The Brown Instrument Company

CP.** The Input Transformer Problem. **A. J. Williams, Jr.,** Leeds and Northrup Company

CP.** A New High Speed Recording Potentiometer. **V. L. Parsegian,** C. J. Tagliabue Company

CP.** Process Variables Made Available by Electronic Methods for Industrial Measurements. **D. H. Fuller,** The Foxboro Company

CP.** Sweep Balance Recorders. **George Keinath, R. K. Hellmann,** Great American Industries, Inc.

2:00 p.m. Marine Transportation and Electric Machinery

46-149. Control Problems With Diesel-Electric Synchronous Motor Ship Drives Propulsion. **E. Frisch,** Westinghouse Electric Corporation

46-127. Design of D-C Auxiliary Controllers for Marine Service. **W. Schaelchlin,** Westinghouse Electric Corporation

46-136. Current and Torque of D-C Machines on Short Circuit. **T. M. Linville,** General Electric Company

46-157. Factors Affecting Insulation Resistance of Large D-C Machines. **J. S. Johnson, C. Weil,** Westinghouse Electric Corporation

2:00 p.m. Safety

46-112. Dangerous Electric Currents. **C. F. Dalziel,** University of California

46-159—ACO.* Silent Invisible Industrial Hazard. **S. R. Warren, Jr.,** University of Pennsylvania

CP.** Shock Hazards of Low Voltage. **M. M. Brandon,** Underwriters Laboratories, Inc.; **R. L. Lloyd,** National Bureau of Standards

Tuesday, June 25

9:30 a.m. Cables

46-103. Determination of Cable Temperatures by Means of Reduced Scale Models. **Andrew Gemant, Joseph Sticher,** The Detroit Edison Company

46-115. F-3 Lead Alloy—An Improved Cable Sheathing. **L. F. Hickernell, C. J. Snyder,** Anaconda Wire and Cable Company

46-118. Semiconducting Shielding for A-C Power Cable. **E. J. Merrell,** Phelps Dodge Copper Products Corporation

46-121. High-Voltage D-C Testing of Rubber-Insulated Wire. **W. N. Eddy, W. D. Fenn,** Simplex Wire and Cable Company

46-160. Moisture Equilibrium Between Gas Space and Fibrous Materials in Enclosed Electric Equipment. **J. D. Piper,** The Detroit Edison Company

9:30 a.m. Communication

46-161. Systems Development of Military Communications. **T. R. Putnam,** New York Telephone Company

46-162. Properties and Uses of Thermistors—Thermally Sensitive Resistors. **J. A. Becker, C. B. Green, G. L. Pearson,** Bell Telephone Laboratories, Inc.

(*Continued an next page*)

46-163. Transmission Rating of Telephone Systems. **W. A. Codd,** Stromberg-Carlson Company

46-151. Mica Capacitors for Carrier Telephone Systems. **A. J. Christopher, J. A. Kater,** Bell Telephone Laboratories, Inc.

9:30 a.m. Electric Machinery

46-164. Oscillations of a High-Voltage Secondary Winding. **A. Boyajian,** General Electric Company

46-165. Temperature Limits for Short-Time Overloads for Oil-Insulated Neutral Grounding Reactors and Transformers—Part II. **V. M. Montsinger, J. E. Clem,** General Electric Company

46-166. Some Aspects of Polyphase Motor Design—The Design and Properties of the Magnetic Circuit. **T. C. Lloyd, H. B. Stone,** Robbins and Myers, Inc.

46-116. Electromechanical Transient Performance of Induction Motors. **C. N. Weygandt, S. Charp,** University of Pennsylvania

46-167. Rotating Electric Machine Time Constants at Low Speeds. **C. Concordia,** General Electric Company

9:30 a.m. Industrial Power Applications

CP.** Progress Report on Industrial Voltage Requirements. Industrial voltage requirements subcommittee

CP.** Protective Devices in Industrial Plants. **L. C. Peterman,** Ford, Bacon and Davis, Inc.

46-122. Protection of Industrial Plants Against Insulation Breakdown and Consequential Damages. **H. R. Vaughan,** Westinghouse Electric Corporation

CP.** Modern Power Distribution Systems for Large Nonindustrial Buildings. **D. L. Beeman,** General Electric Company

2:00 p.m. Conference of Officers, Delegates, and Members

R. M. Pfalzgraff, presiding

Opening remarks by chairman

Observations on Institute Activities. **Doctor W. E. Wickenden,** president, AIEE

Opportunities for Section Activities in the Industrial Field. **J. Elmer Housley**

District and Section Activities. **H. H. Henline,** secretary, AIEE

Sections Committee Report and Forecast. **G. W. Bower,** chairman, Sections committee

Progress Report of Planning and Co-ordination Committee on the Study of Institute Activities. **J. F. Fairman,** chairman, planning and co-ordination committee

(*a*). Technical activities subcommittee. **M. D. Hooven,** chairman

(*b*). Professional activities subcommittee. **T. G. LeClair,** chairman

Ten Minute Intermission

Section Membership Activity and Its Relation to the Progress of the Institute. **L. F. Howard,** chairman, membership committee

Institute Finance and Its Relation to the Sections. **W. R. Smith,** chairman, finance committee

Reports of the First Year of Operation of the Two New Institute Sections

(*a*). Beaumont Section

(*b*). Illinois Valley Section

Educational Courses Conducted by the Sections. **H. W. Bibber,** chairman, committee on education

AIEE Publications Services. **G. Ross Henninger,** AIEE editor

Section History. **M. S. Coover,** vice-president, District 5

General Discussion

Wednesday, June 26

10:00 a.m. Annual Meeting

President W. E. Wickenden, presiding

Report of board of directors, **H. H. Henline,** secretary

Report of treasurer, **W. I. Slichter**

Reports of committee of tellers on votes for nominees for AIEE offices

Introduction of president-elect, and presentation of president's badge to **J. Elmer Housley;** response by Mr. Housley

Report on Institute prizes for papers, **M. D. Hooven,** chairman, committee on award of Institute prizes

Westinghouse centennial address, **J. K. B. Hare,** vice-president, Westinghouse Electric Corporation

Presentation of Lamme Medal to David C. Prince, vice-president, General Electric Company

Any other business that may be presented.

President's address: Doctor W. E. Wickenden

2:00 p.m. Conference on Section Activities in Connection With Local Councils of Engineering and Technical Societies

G. W. Bower, presiding

The purpose of this conference is to review the organization and operation of local councils, with particular emphasis on the part the AIEE Sections have taken in this work. The three general types of local council organizations also will be presented by selected speakers, and the activities of these councils in their local areas will be discussed. This information will be valuable in assisting Sections in expanding the activities of the councils in their local areas, and where such councils do not now exist, will assist the Sections in forming councils.

An open discussion will be featured after the presentation of each speaker.

2:00 p.m. Power Generation

46-144. Improvements in Performance of Hydroelectric Generating Units on the 2,000,000-Horsepower Saguenay System. **F. L. Lawton,** Aluminum Company of Canada, Ltd.

46-108. Tennessee Valley Authority Hydroelectric Stations—Electrical and Mechanical Design. **R. A. Hopkins, H. J. Petersen,** Tennessee Valley Authority

46-152. Modern Excitation Systems for Large Synchronous Machines. **J. B. McClure, S. I. Whittlesey, M. E. Hartman,** General Electric Company

46-154. The Development of Modern Excitation Systems for Synchronous Condensers and Generators. **F. M. Porter, J. H. Kinghorn,** American Gas and Electric Service Corporation

2:00 p.m. Relays

46-168. Low-Current Secondary Current Transformers. **An AIEE Subcommittee Report**

46-169. Protection of Powerhouse Auxiliaries. **An AIEE Committee Report**

46-109. Fault Location and Relay Performance Analysis by Automatic Oscillographs. **H. P. Dupuis, W. E. Jacobs,** The Commonwealth and Southern Corporation

46-83. Operating Experience With Distance Ground Relays. **W. A. Wolfe,** Kansas Gas and Electric Company

2:00 p.m. Conference on Arc Welding

CP.** Power Requirements for D-C Arc Welders. **R. F. Wyer, R. C. Freeman,** General Electric Company

CP.** Application of Limited Input Arc Welders to the Power Distribution System. **C. N. Clark,** Duquesne Light Company

CP.** Limited Input Arc Welders. **E. Steinart,** Westinghouse Electric Corporation

2:00 p.m. Servomechanisms

46-113. Electrical Accuracy of Selsyn Generator–Control Transformer System. **Harold Chestnut,** General Electric Company

46-114. The Frequency Response of Automatic Control Systems. **Herbert Harris, Jr.** Sperry Gyroscope Company, Inc.

46-107. Parallel Circuits in Servomechanisms. **H. T. Marcy,** Massachusetts Institute of Technology

46-150. Dimensionless Analysis Servomechanisms by Electrical Analogy. **S. W. Herwald, G. D. McCann,** Westinghouse Electric Corporation

Thursday, June 27

9:30 a.m. Protective Devices

46-134. Application Ratings of Indoor Power Circuit Breakers. **O. B. Vikoren,** Philadelphia Electric Company

46-170. Performance Criteria for Current Limiting Power Fuses—I. **C. L. Schuck,** General Electric Company

46-171. Performance Criteria for Current Limiting Power Fuses—II. **E. W. Boehne,** General Electric Company

46-172. Philosophy of Relaying. **E. W. Knapp, B. C. Hicks,** The Shawinigan Water and Power Company

46-173. Simplicity in Protective Relaying. **L. F. Hunt,** Southern California Edison Company, Ltd.

9:30 a.m. Electronic Power Conversion

46-105. Inductive Co-ordination Aspects of Rectifier Installations. **An AIEE Subcommittee Report**

Standard Report 6. Proposed Standards for Pool-Cathode Mercury-Arc Power Converters. **An AIEE Subcommittee Report**

1.000 Section. Definitions. Presentation by **H. Winograd**

2.000 Section. Standards. Presentation by **C. C. Herskind**

3.000 Section. Test Code. Presentation by **J. H. Cox**

4.000 Section. Recommended Practice and Operating Guide. Presentation by **R. C. Marcum**

5.000 Section. Rectifier Transformers. Presentation by **E. V. DeBlieux**

Discussion of "Proposed Standards Pool-Cathode Mercury-Arc Power Converter." **I. R. Smith** representing the subcommittee on metallic rectifiers, **D. E. Marshall** representing the Institute of Radio Engineers. Discussion by other groups or individuals will be welcomed.

9:30 a.m. Industrial Control Devices

46-130. Dynamic Braking Control of D-C Series Motors—Calculation of Stability Limit. **G. W. Heumann, W. P. Smith,** General Electric Company

46-104. Silicone-Resin-Treated Magnet Coils. **G. L. Moses,** Westinghouse Electric Corporation; **J. J. Torok,** Corning Glass Works

46-126. Fundamental Properties of the Vacuum Switch. **R. Koller,** University of California

46-125. An Electronic Drive for Windup Reels. **K. P. Puchlowski,** Westinghouse Electric Corporation

9:30 a.m. Basic Sciences

46-110. The Influence of the Concentration and Mobility of Ions on Dielectric Loss of Insulating Oils. **B. P. Kang,** E. I. duPont de Nemours and Company

46-120. Negative Resistance Effects in Saturable Reactor Circuits. **J. M. Manley, E. Peterson,** Bell Telephone Laboratories, Inc.

46-128. A New Approach to Probability Problems in Electrical Engineering. **H. A. Adler,** Commonwealth Edison Company; **K. W. Miller,** Armour Research Foundation

46-119. Formulas for Calculating the Inductance of Channels Located Back to Back. **W. G. Schwantz,** Commonwealth Edison Company; **T. J. Higgins,** Illinois Institute of Technology

46-111. A Fractional Termination for Ladder Networks. **W. R. LePage,** Stromberg Carlson Company. Presentation by title

9:30 a.m. Industrial Power Applications

46-153. Low-Reactance Flexible Cable for Induction Heating. **Myron Zucker,** Mackworth G. Rees, Inc.

46-124. Design of Induction-Heating Coils for Cylindrical Magnetic Loads. **J. T. Vaughan, J. W. Williamson,** The Ohio Crankshaft Company

46-132. Electronic Register Control for Multicolor Printing. **W. D. Cockrell,** General Electric Company

CP.** Applications in the Rubber Industry. **J. Z. Linsenmeyer,** Westinghouse Electric Corporation

10:00 a.m. Conference on Student Activities

E. W. O'Brien, presiding

This conference will deal with Student Branch problems, particularly as related to the postwar problems in connection with the resumption of normal activity by the Branches.

2:00 p.m. Conference on Section–Branch Co-operation

A joint activity of the committee on Student Branches and the Sections committee

Professor V. P. Hessler, presiding

Opening remarks by the chairman

Basic Opportunities of Section–Branch Co-operation. **E. W. O'Brien,** chairman, committee on Student Branches

The Plan of Section–Branch Co-operation. **G. W. Bower,** chairman, Sections committee

Presentation by selected speakers of typical examples of Section–Branch co-operation

A Look Into the Future As a Result of Section–Branch Co-operation. **Everett S. Lee,** chairman, Engineers Council for Professional Development

An open discussion after each presentation will be a feature of this conference

In addition to the Section delegates, chairmen of the District committees on Student activities, counselors, Student Branch officers, and all other members interested in student activities are invited to attend and participate in the discussion

Friday, June 28

9:30 a.m. Power Transmission

46-175. Co-ordination of Insulation and Spacing of Transmission-Line Conductors. **W. W. Lewis,** General Electric Company

46-117. The Electrical Performance of Ceramic Dielectrics at Elevated Temperatures. **H. A. Frey, J. A. Jesatko,** Locke Insulator Corporation

46-123. The Preservative Treatment of Various Species Proposed for Poles and Crossarms. **J. D. MacLean,** Forest Service, United States Department of Agriculture

46-174. Carrier Supervisory Control of Pumping Station Over Power Cable. **W. A. Derr, W. A. Keller,** Westinghouse Electric Corporation; **H. A. W. Hedke,** United States Sugar Corporation

46-176. Six-Years' Experience With Factory-Built Unit Type Substations. **E. F. Miller, R. B. Miller,** Iowa–Illinois Gas and Electric Company

9:30 a.m. Electronic Tubes and Basic Circuits

46-139. Rectifier Capacity. **C. C. Herskind, H. C. Steiner,** General Electric Company

46-143. Nonlinear Commutating Reactors for Rectifiers. **A. Schmidt, Jr.,** General Electric Company

46-146. Circuit Cushioning of Gas-Filled Grid-Control Rectifiers. **D. V. Edwards, E. K. Smith,** Electrons, Inc.

46-138. Excitation, Control, and Cooling of Ignitron Tubes. **C. C. Herskind, E. J. Remscheid,** General Electric Company

46-140. A 400-Ampere Sealed Ignitron. **H. C. Steiner, H. N. Price,** General Electric Company

9:30 a.m. Air Transportation

46-131. Investigation of Porcelain Insulators at High Altitudes. **C. V. Fields, C. L. Cadwell,** Westinghouse Electric Corporation

46-145. Short-Time Current Ratings for Aircraft Wire and Cable. **B. W. Jones, J. A. Scott,** General Electric Company

46-148. A Unique Engine Synchronism Indicator for Aircraft. **D. B. Pearson,** General Electric Company

46-129. Electronic Control of Frequency Converter Sets for Testing Aircraft Models. **G. W. Heumann, W. F. Strong,** General Electric Company

46-85. Electric Equipment for Cornell Variable-Density Wind Tunnel. **C. C. Clymer, M. A. deFerranti,** General Electric Company. Presentation by title

46-87. Radiotelemetering for Testing Aircraft in Flight. **C. L. Frederick,** Cornell Aeronautical Laboratory. Presentation by title

9:30 a.m. Conference on Management and Quality Control

This conference is sponsored by the subcommittee on applications of statistical methods of the Standards committee. Several papers will be presented dealing with plant organization for quality control and methods of presenting results to management. Several outstanding executives also will discuss quality control from the point of view of management.

CP.** Statistical Quality Control—A Tool of Management. **T. D. Foy,** General Electric Company

*ACO: Advance copies only available; not intended for publication in *Transactions*.

**CP: Conference paper; no advance copies are available; not intended for publication in *Transactions*



Interior view of the Edison Museum, Detroit, Mich., showing locomotive exhibit

Power Systems and Communications Chief Drawing Cards at Buffalo Meeting

As might have been expected from that populous District, the three-day meeting of the North Eastern District held at the Hotel Statler, in Buffalo, N. Y., April 24–26, 1946, developed into the best-attended of the spring District meetings. However, the total registration of 439 was by no means the highest attained at a North Eastern meeting, as is evident from the table comparing registrations of former years.

Nine technical sessions, including a student session, important luncheon and committee meetings, a banquet, preceded by a social hour, and a smoker were held. Alternative inspection trips were taken to nearby industries, including a visit to the Westinghouse Motor Works or the Cornell Wind Tunnel and the hot strip mill of the Bethlehem Steel Company, where "flying shear" takes place. Another trip was to the C. R. Huntley Steam Generating Station and the Bell Aircraft Plant at Niagara Falls Airport, where several members were taken up in a helicopter. A principal event for the women who attended the meeting was a trip to Niagara Falls, which included visits to scenic spots along the frontier and a social hour and dinner, after which the illumination of the falls was viewed.

TECHNICAL SESSIONS

Most popular among the nine technical sessions were those on power systems, communication and war developments, and transmission and distribution, in the order named. Attendance at the opening session on power systems reached 200. The service record of a 1,000-kva mobile substation, electrical–mechanical features of the Jennison steam station, southeast emergency and power pooling in 1941, and automatic control of large synchronous condensers were the subjects of papers presented and discussed. R. T. Henry (F '33) vice-president of the North Eastern District, and W. S. Hill (M '35) chairman of the technical program committee presided.

A technical session on aircraft naturally aroused a great deal of interest in Buffalo, the home of several large aircraft manufacturers. The session was opened by presiding officer, D. R. Shoults (M '42) vice-president of sales, the Bell Aircraft Corporation, who introduced the first speaker, Doctor C. C. Furness, director of the Cornell Aeronautical Laboratory. Doctor Furness briefly outlined the organization and objectives of the laboratory which came into being January 1, 1946, with the gift by the Curtiss-Wright Corporation of the physical facilities of its airplane division research laboratory at Buffalo to Cornell University. Generous contributions to a working capital fund which assures the sound and continuing operation of the laboratory also were received from the Aviation Corporation, Bell Aircraft Corporation, Fairchild Engine and Airplane Corporation, Grumman Aircraft Engineering Corporation, Ranger Aircraft Engine Corporation, Republic Aviation Corporation, and the United Aircraft Corporation.

The Cornell Graduate School of Aeronautics regards the laboratory as the training ground for its advanced students in research and specialized instruction, Doctor Furness said. He explained that a realistic approach to airplane research requires a relatively large organization. "Not only must there be research and development on the airplane and its functioning as a whole," according to Doctor Furness, "but there must be continuing parallel work on the individual components, materials, and auxiliary devices. The research and development work of the Cornell laboratory is carried on by eight departments. Five of these: aerodynamics, structures, flight research, materials, and physics are the research division. The other three departments: development engineering, armament, and manufacturing constitute the development division. Thus the facilities and programs are such that a project can be carried from the basic research phase, through the stage of the first working prototype in the research division, and then on through the pilot-manufacturing stage in the development division shop. The results of the laboratory's research are to be made generally available to the public except where national security demands secrecy for some Government projects. Similarly, projects which are being supported directly by a company or groups of companies are kept confidential.

After Doctor Furness' address, papers were presented which described the electric equipment of the wind tunnel, the modern six-component wind tunnel balance system, and radio telemetering for testing aircraft in flight. The last paper presented dealt with dive testing aircraft by radio control. By courtesy of the Bell Aircraft Corporation a restricted colored motion picture of the equipment and flight of a jet-propelled plane directed by robot control for testing was shown. The telemetering equipment was designed by Princeton University and the National Defense Research Council.

Other sessions were held during the meeting on the subjects of transmission and distribution, electronics, industrial applications, aircraft and transportation, lighting, quality control, and communication and war developments. In the latter session a radar demonstration was given by E. F. Herzog of the General Electric Company.

GENERAL LUNCHEON

Nontechnical problems facing not only the AIEE but other engineering societies were the focal point of the general luncheon meeting held at noon on Thursday with R. T. Henry presiding. The question of whether the engineering profession is now organized to respond quickly to either technical or social changes was raised. Evidence that many engineering men are groping for an integrating force which will promote professional unity among the 90 engineering societies and 200,000 members was presented, and it was noted that the National Labor Relations Act likewise has introduced new problems, particularly as they affect the younger members of the profession. The degree of leadership which the AIEE should exercise in technical fields represented another debatable question.

The recent work of the AIEE committee on planning and co-ordination which is concerned with these problems was summarized by W. S. Hill, representing the committee. In his presentation of the subject Mr. Hill called attention to the greatly expanded operations of the AIEE with their accompanying new problems, and it was evident that reanalysis of the over-all operations is desirable in view of the changing character of industrial operations since the early days of the Institute. Mr. Hill outlined the technical activities subcommittee work which had been done under M. D. Hooven (F '44) and advanced the committee's proposals for improving the technical presentations, for obtaining wider publication of technical data, and for improving technical committee work. Reprints of the professional activities subcommittee's report (*EE, Apr '46, pp 169–73*) were distributed as well as a questionnaire on the four plans contained therein. Those at the luncheon were requested to give the problem careful study and return them to the committee. Representatives of many local Sections throughout the District and of adjacent Districts who were present were urged to initiate local discussions of the problem and were given additional copies of the report and questionnaire for distribution.

President W. E. Wickenden, in giving his

North Eastern District Meeting Attendance 1936–46

Date	Location	Attendance
1946—Apr. 24–26	Buffalo, N. Y.	439
1944—Apr. 19–20	Boston, Mass.	630
1943—Apr. 8–9	Pittsfield, Mass.	319
1942—Apr. 29–May 1	Schenectady, N. Y.	481
1941—Apr. 30–May 2	Rochester, N. Y.	355
1939—May 3–5	Springfield, Mass.	439
1938—May 18–20	Lenox, Mass.	417
1937—May 5–7	Buffalo, N. Y.	352
1936—May 6–8	New Haven, Conn.	310

Analysis of Registration at Buffalo

Classification	Niagara Frontier Section	District 1*	Other Districts	Totals
Members	98	113	82	293
Student Members	1	9	6	16
Men guests	58	39	17	114
Women guests	7	4	5	16
Totals	164	165	110	439

* Outside Buffalo.

views, remarked upon the interest in engineering circles which had been awakened through the activities of the planning and co-ordination committee and similar individual efforts in the other societies. He expressed the belief that there is real vigor behind this general movement and that the participation in it by engineers in other branches of the profession indicates equal interest. Because engineers generally have a collective capacity for moulding an important portion of the economic order, he is of the opinion that engineers, chemists, metallurgists, and other professional men ought to recognize their social responsibility and become a powerful collective influence in the professional and intellectual life of the country.

He spoke of the most successful technical work which the AIEE has done and is continuing to do, and the success of the AIEE in creating fellowship among engineers. He looked with concern on the increasing fragmentation occurring in all engineering societies and on the disordered confusion which frequently is apparent when the profession as a whole tries to express its views on professional matters.

Doctor Wickenden also mentioned briefly the work of the Engineers Joint Council which has taken a definite stand on several matters of national interest, particularly with reference to future military security and the demilitarization of German and Japanese industry.

DISTRICT EXECUTIVE COMMITTEE LUNCHEON

Reports of Branch and Section activity were made to the District executive committee luncheon at noon on Monday, and preliminary plans for next spring's meeting in Worcester, Mass., and for holding a summer convention in the District, possibly in 1950, were formulated. R. T. Henry presided at the luncheon.

The Ithaca Section has devised a plan for holding meetings successively in three centers of membership, Ithaca, Elmira, and Binghamton. The Niagara Frontier Section in co-operation with the Toronto Section has successfully promoted Subsection meetings with attendance from both the United States and Canada. Courses in electronics at a fee of $5 to members and $10 to nonmembers also have been offered by this Section. The Boston Section reported a negative response to its efforts to establish a Subsection in that part of New Hampshire falling within its jurisdiction. The New Hampshire members preferred the advantages of meetings in Boston. Of the 14 Student Branches in the District 14 are holding regular meetings, and all but one are organized to resume activity.

After some discussion of the subject it was agreed that local membership was both necessary and desirable in order to serve men of every caliber with interests in AIEE, and also to assist the financial program. Several Sections declared that this was a prime source for national members. The plan followed by the Boston Section is to limit local membership to three years, after which a man either must become a national member or must enter the Engineering Society of New England as a member-at-large.

The Massachusetts Sections have been reminding their members that the "grandfather clause" of the Engineering Registration Law expires January 9, 1947, and that engineers whose needs eventually will require licensing should apply soon.

Present at the luncheon were Victor Siegfried (M '38) secretary of District 1; H. H. Henline, AIEE secretary, and C. L. Dawes (F '35) representing R. G. Porter of the committee on student activities. Representatives of the various Sections were as follows: Boston—F. S. Bacon, Jr., T. S. Gray; Connecticut—V. J. Hayes, E. G. Horton; Ithaca—E. M. Strong, W. H. Erickson; Lynn—C. B. Fontaine, M. A. Princi; Niagara Frontier—J. M. Geiger, J. D. Hershey; Pittsfield—J. C. Russ; Providence—C. H. Parker; Rochester—W. Criley; Schenectady—P. H. Light, B. H. Caldwell, R. V. Shepherd; Syracuse—C. E. H. von Sothen, L. J. Audlin; Worcester—A. L. Duna.

Annual Meeting

The annual meeting of the American Institute of Electrical Engineers will be held at the Hotel Statler, Detroit, Mich., at 10 a.m. Wednesday, June 26, 1946.

At this meeting, the annual report of the board of directors and the report of the committee of tellers on the ballot cast for the election of officers will be presented. The Lamme Medal will be presented to David C. Prince (F '26), and awards of Institute prizes will be announced.

Such other business, if any, as properly may come before the annual meeting may be considered.

(*Signed*) H. H. HENLINE
Secretary

STUDENT CONFERENCE

Presentation of two prize-winning papers and an address on "Development Within the Profession," by Everett S. Lee (F '30) General Electric Company, Schenectady, N. Y., made up the program of Friday's student conference and technical meeting.

First prize of $15 for a student paper was awarded Thomas M. McCaw of Worcester Polytechnic Institute for his paper, "An Exposure–Color Temperature Meter." The meter, developed by Mr. McCaw to enable the color photographer to correct for the color temperature of light sources, depends on the interaction of two photoelectric cells, one red sensitive and the other blue sensitive. When exposed to light with a given color temperature, each will show a response, and the response of red to blue can be expressed as a ratio. The meter, however, has not been reduced to a physical size comparable with existing photoelectric exposure meters.

Second prize of $10 went to Henry Harper and Thomas E. Talpey of Cornell University for their paper, "Representation of Vectors on a Cathode-Ray Screen." The paper was presented by Mr. Talpey who described a method whereby a vector can be represented on a cathode-ray screen, its length proportional to the magnitude of the current or voltage it expresses, and its inclination to the horizontal proportional to the phase difference between it and some reference voltage of the same frequency. The method obviates the considerable amount of data and computations involved in plotting of the locus of a vector.

An interesting discussion among the approximately 40 students attending the conference followed each paper. Among the chairmen of Student Branches who attended were: R. W. Carpenter, Brown University; A. D. Sutherland, Cornell University; Richard Harris, Northeastern University; Aubrey Mitchell, Rensselaer Polytechnic Institute; J. W. Vorndran, Union College; and G. D. Keppert, Worcester Polytechnic Institute.

In his address to the students, Mr. Lee stressed the importance of affiliation with a national engineering society to an engineer who wished to extract the fullest benefits and chance for development from his professional life. Association with societies with more specific technical interests should and probably would come later in their careers, Mr. Lee told the students. In the same way he assigned affiliation with societies concerned with the engineer's relationship to society as a whole to a necessary but later stage in the career of the young engineer. He urged the students to set about planning to become registered engineers as soon as their state laws will allow. He advised them as citizens to become acquainted with their representatives in local, state, and federal bodies. As it is a problem with which they would be confronted upon entering industry, he also advised that the students study the material that has been collected and published on collective bargaining by the technical societies.

Professor R. G. Porter (F '44) of Northeastern University, chairman of the District committee on student activities, presided at the session.

SOCIAL EVENTS

An informal banquet preceded by a cocktail hour was held on Wednesday evening in the ballroom of the Hotel Statler. The principal speaker was the Honorable Orlo M. Brees, member of the New York State Legislature, whose subject was "The Secret of Happiness." R. R. McLeod, vice-president of the Buffalo Niagara Electric Corporation, was toast-master.

On Thursday evening a dinner and smoker was held in the Niagara Room. President Wickenden greeted the assemblage and commented on the good fellowship at the gathering, as well as that which exists between the 25,000 members of the Institute. Entertainment in the form of card tricks was provided by Mitchell MacDougall. Ted Rust gave a number of interesting ventriloquist demonstrations. G. M. Pollard (M '34) acted as toastmaster.

Conference Hears Advantages of Statistical Quality Control

A well-attended conference, held April 25 at the North Eastern District meeting, at which five speakers presented methods and results of statistical quality control is reported by P. L. Alger (F '30) of the General Electric Company, whose long-standing interest in the subject has been reflected in his efforts at promoting conferences and providing material for *Electrical Engineering*.

In opening the conference the chairman, Professor M. A. Brumbaugh of the University of Buffalo, cited the growing importance of statistical methods throughout industry and recommended the series of educational articles currently appearing in *Electrical Engineering* as a good introduction to the subject.

Joseph Manuele (M '44) of Westinghouse Electric Corporation, outlined the procedure for initiating the use of modern quality control methods in quantity production. He explained the value of using a scientific sampling procedure, with careful measurement of each piece in the sample lot, to supplement or replace the old-fashioned 100 per cent inspection methods. In this way the average quality of inspected lots can be maintained at the desired level, and the risk of any given lot containing a greater than normal number of defectives always is known. Supplementing these sampling procedures by control charts at critical points in the production process, and backing them up by corrective action of engineers and planners, yield large dividends in reduced inspection costs and time saved, as well as in a higher quality.

He stated further that the production incentives of piece work rates can be supplemented by incentives to quality maintenance, if operators are provided with adequate gauges and devices for checking their own work. Allowance in the piece rates for this inspection time should be made, and operators then should be required to replace defective parts on their own time. In this way a single inspector who makes first piece inspections, checks samples from time to time, and gives help when needed, has maintained good quality in a section with as many as 67 production workers.

A. V. Feigenbaum, General Electric Company, described the separate steps of organizing a quality control program, and assuring co-operation of inspection, testing, and planning, as well as engineering and manufacturing heads. He stressed the need of teamwork in obtaining the desired quality in the most economical way. As examples of successful work, he described the methods used in producing aircraft voltage regulators and reverse current relays, where manufacturing losses and inspection costs were both reduced by one third in a four-month period, with even greater reductions in field troubles.

D. C. Stewart (M '35) Buffalo Niagara Electric Corporation, presented a statistical analysis of safety records in the light and power industry, showing that significant differences in company methods of accident prevention are indicated when the accidents of a particular company depart from the industry average by more than twice the standard deviation. He showed curves of total accidents, time lost, and fatalities plotted against millions of man-hours worked, which showed that better records generally were achieved by large companies with well-organized safety procedures.

E. H. Schneider (A '43) and J. M. Jesatko (A '41), Locke Insulator Corporation, cited a 40 per cent reduction in rework and an over-all saving of $6 per man hour spent on statistical quality control secured by application of these methods in insulator manufacture. Control charts of materials obtained from different vendors are maintained, as well as for critical factory processes; and field complaints have been greatly reduced.

A. J. Winterhalter, Colonial Radio Corporation, compared the performance in manufacture of a certain radio receiver before and after use of statistical quality control methods. Production was well stabilized on an apparently satisfactory basis, using the old inspection methods, in October 1943. At that time statistical methods were introduced. By January 1, 1944, the defects had been reduced 16 per cent, by June they were down 43 per cent, and by December 1944, they were 53 per cent lower than at the start. A recent attack on the particularly troublesome problem of soldered joints lowered the rework level in the past six months from 33 per cent to 13 per cent, with the sharp downward trend still continuing. Mr. Winterhalter also cited tests indicating that the average inspector on 100 per cent inspection work finds only 60 to 70 per cent of the defects, and many find even less; whereas with the more careful attention given to samples and the aid of statistical methods, a very much higher fraction of the defects is discovered.

In the discussion several speakers gave figures showing that 100 per cent inspection cannot be relied upon to eliminate defects, and that modern sampling methods with adequate first piece and process inspection are far superior. It was pointed out that statistical measures of the performance of individual operators, inspectors, and machines are proving very valuable in training and selection programs for workers, as well as in maintenance and replacement programs for equipment.

Future AIEE Meetings

Pacific Coast Convention
Seattle, Wash., August 27–30, 1946

Great Lakes District Meeting
Fort Wayne, Ind., September 25–27, 1946

STANDARDS • • •

Sixth Report Submitted on AIEE Aeronautical Standards

The progress made in aeronautical electrical standards work since the fifth progress report (*EE, Apr '46, pp 173–4*) and the status of AIEE participation as of April 24, 1946, are summarized herewith.

Aircraft Electrical Systems Subcommittee (Chairman, R. H. Kaufmann [M '41]). An additional section of the proposed report on "Aircraft Electrical Systems" has been completed in preliminary form, and every effort is being made to complete the other sections as soon as practicable.

Aircraft Electric Rotating Machinery Subcommittee (Chairman, M. L. Schmidt [M '43]). A comprehensive draft of a "Test Code for D-C Machines" has been edited and distributed to subcommittee members for review. This subcommittee expects to have a report ready for submission to the air transportation committee in June.

Aircraft Electric Control and Protective Devices Subcommittee (Chairman, R. A. Millermaster [M '34]). This group is maintaining contact with various developments in the field of aircraft electric control and protective devices. It expects to hold a meeting when the work of certain other groups makes such feasible.

Aircraft Wire and Cable Subcommittee (Chairman, W. S. Hay). The paper "Short Time Current Ratings for Aircraft Wire and Cable" by J. A. Scott (M '34) and B. W. Jones (M '43) has been scheduled for presentation and discussion at the AIEE summer convention in Detroit. The effect of groupings of cables, proximity to other equipment, high altitudes, and so forth will need to be studied to carry the analysis of wire and cable application on to a full conclusion.

Aircraft Carbon Brush Subcommittee (Chairman, V. P. Hessler [F '43]). Subcommittee members are preparing material and recommendations concerning specific items of the "Proposed Test Code for Aircraft Carbon Brushes," and a meeting is to be held in June to discuss a revision of the Summers–Stauffer report and to prepare a draft of the proposed test code for general distribution.

Subcommittee for Basic Principles of Altitude Rating (Chairman, W. E. Pakala [M '45]). The air transportation committee has set up a new subcommittee under the chairmanship of W. E. Pakala, Westinghouse Electric Corporation, East Pittsburgh, Pa., to develop an AIEE Standard covering the basic principles of altitude rating of aircraft electric machinery. Mr. Pakala is anxious to learn of persons who can contribute information or experience and to know of facilities that can be made available for experimental work. AIEE Standards coordinating committee 1 (P. L. Bellasch

(F '40) Westinghouse Electric Corporation, Sharon, Pa., chairman) is concerned with the general subject of altitude ratings.

Electric Equipment Safety. It has been decided not to form an air transportation subcommittee on this subject. It is understood that the Civil Aeronautics Administration is starting an extensive investigation of airplane fire control methods and related matters.

Aircraft D-C Apparatus Voltage Ratings (AIEE 700). This report on a proposed Standard has been on a trial basis for over one year and soon will be circulated by the AIEE air transportation committee for review as a possible full Standard.

NASC—Standard Method of Electrical Load Analysis for Aircraft (Chairman, K. R. Smythe [M '44]). Comments concerning the "Standard Method of Electrical Load Analysis for Aircraft" have been summarized and circulated to various interested persons. The Army Air Forces is now preparing tentative AN "Specification for A-C Load Analysis." WCAB is now preparing AN "Specification for D-C Load Analysis."

SAE Committee A-2, Aircraft Electric Equipment (Chairman, Edmund Thelan). The work of this committee was very ably piloted by C. C. Shangraw during the war period. He has found it necessary to resign the chairmanship because of the press of other work and Edmund Thelan, Eclipse-Pioneer Division, Bendix Aviation Corporation, Teterboro, N. J., has accepted the responsibility. This committee plans to reconsider present aircraft electrical standards in the light of new peacetime applications and to introduce new specifications where necessary.

Standard Corrected. The following errata are to be noted in AIEE Standard 45, "Recommended Practice for Electric Installations on Shipboard." Under "Third" in Sections 18.65, 18.67, 18.69, 18.81, 18.83, 18.85, change 0.136 inch to 0.115 inch. Errata sheets for insertion in the 1945 edition of the Standard can be obtained by writing to AIEE headquarters, 33 West 39th Street, New York 18, N. Y.

Telemetering Subcommittee Prepares Questionnaires

The joint subcommittee on telemetering, in connection with its assignment to revise the 1941 AIEE report, "Telemetering, Supervisory Control, and Association Circuits," has prepared a questionnaire on telemetering apparatus and systems. This questionnaire, designed to obtain the basic data necessary to make an authoritative revision, has been mailed to the industry with as broad a distribution as the knowledge of the committee permitted. It is requested urgently that any manufacturer or distributor of such apparatus who has not received this questionnaire apply to AIEE headquarters, 33 West 39th Street, New York 18, N. Y., for copies.

A similar questionnaire on supervisory control systems is in the course of preparation and will be mailed in the near future. At present the committee has only a limited list of manufacturers or distributors of this equipment and so requests that all companies sponsoring such systems, which are not represented in the 1941 report, so advise the chairman, G. S. Lunge, General Electric Company, 1 River Road, Schenectady 5, N. Y., so that they may receive copies of the questionnnaire.

SECTION

Loran Navigation Is Topic At Final Philadelphia Meeting

The last of its meetings for the 1945–46 season was held by the Philadelphia Section, Monday, May 13, in the Engineers Club in Philadelphia, Pa., with an attendance of 145.

A review of the year's high lights in Section activities was given by C. T. Pearce (M '40) retiring chairman. These included the passing of the 1,000th member milestone, which represented a growth in membership in excess of 10 per cent during the year; the establishment of a basic science discussion group; the total of 42 meetings in all activities of the Section; and the establishment of additional committees on suggestions, section history, and Princeton–Trenton meetings. The efforts of the Wilmington Subsection and of the communications discussion group were given special mention.

Officials elected for the 1946–47 season were:

H. A. Dambly (F '42) *chairman;* E. W. Boehne (F '43) *vice-chairman;* W. R. Clark (M '44) *secretary;* and C. S. Schifreen (M '43) *treasurer.*

Following the short business session, J. A. Pierce of the Cruft Laboratory, Harvard University, spoke on "Loran—Long Range Navigation." The Loran system has been extended to cover three-tenths of the earth's surface, according to Doctor Pierce who gave the history of the development and outlined the fundamental concepts of hyperbolic navigation. Details of equipment in service and of future trends and potential uses were given. A film showing the routine methods of calculating position from oscillograph readings followed the talk.

As the final one of the season, the meeting closed with the usual award of attendance prizes by the fellowship and attendance committee, headed by J. E. Johnson (M '45). Numerous appropriate gifts had been presented to the committee for the occasion. As a method of awarding these prizes, a judge and a sergeant-at-arms were chosen by drawing. After these officials were suitably costumed, they supervised the drawing of names by lot from a mixing drum. Each winner had to prove his worthiness to receive a gift by some special stunt on the merit of which the judge and sergeant-at-arms were final authority.

New York Section Closes Extremely Active Year

As part of its accounting at the close of its administrative year, the New York Section recently assembled an impressive set of figures on meetings and attendance.

A total of 262 meetings attracting an attendance approximating 28,000 were sponsored by the Section in an 8-month period. Thirty regular Section meetings were arranged by various technical groups and program committees, and 232 were connected with the 21 courses conducted by the Section in special fields of current interest and in review of fundamentals as preparation for engineers' licenses. Attendance at the regular meetings totaled 6,900 and at the others, 21,000. This gives an average of 1.5 meetings for every weekday during the period covered by the tabulation. In addition, 26 conferences were held to give counsel to returning veterans, with an attendance of almost 700.

Fairman Addresses Lynn Annual Dinner Meeting

As guest speaker at the annual dinner of the Lynn Section held April 30, at the Thomson Club, Nahant, Mass., J. F. Fairman, AIEE vice-president, considered the topic, "Organization of the Engineering Profession."

Mr. Fairman discussed the recent report of the AIEE subcommittee on professional activities (*EE, Apr '46, pp 169–73*) and distributed a questionnaire prepared by the subcommittee. Following his address discussion continued for nearly an hour, and the Section membership expressed a strong interest in and enthusiasm for the work being done by the committee on planning and co-ordination through its subcommittees.

Approximately 200 members and guests attended the dinner.

Meetings of New Subsection of Lancaster–York Well Attended

The Lancaster–York Subsection of the Maryland Section was organized early in 1945 to relieve Section members living in Lancaster, York, and Adam Counties of Pennsylvania from the necessity of making the 60-mile trip to Baltimore under wartime difficulties.

A preliminary meeting was held in Lancaster, July 12, 1945, when tentative plans were made and a functioning committee organized. This committee called a meeting for September 13, when the final

organization of the Subsection was completed with 23 members present. The following officers were elected: R. W. Larsen, *chairman;* H. J. Stewart, (A '38) *vice-chairman;* J. L. Stauffer (A '24) *secretary–treasurer.* Since this meeting the membership has grown to 172. Six meetings have been held, four at Lancaster and two at York, with an average attendance of 112. It is evident that this Subsection is filling a real need.

Michigan Arc Display Draws Large Audience

A display of arcs, mainly at utilization voltages, was featured on the program of two evening meetings of the AIEE Michigan Section held in the laboratory of the Bull Dog Electric Products Company, Detroit, April 24 and 25.

Sponsored by the industrial power group of the Michigan Section in co-operation with the Industrial Electrical Engineering Society, a Detroit organization of plant operating engineers, a two-hour program of 30 scheduled items, ranging from small sparks to explosive arcs and including the destruction of unprotected 440-volt devices, was presented.

Speaker at the meetings was Lawrence E. Fisher (M '38) director of research, for the Bull Dog Electric company, who presented technical data and necessary explanations on the tests performed. Tests included arcs on insulators and the spraying of salt water and iron dust on energized plug-in duct. Movies taken by an ultra-high speed camera and timing clock showed slow-motion detail of arc interruption by circuit breakers and the periodic fluctuation of a 60-cycle maintained arc.

Approximately 140 attended each meeting and were dinner guests of the Bull Dog Electric company preceding the demonstrations. D. D. Douglass (M '44) chairman of the industrial power group headed the committee which arranged the meetings.

Philadelphia Announces Awards in Prize Paper Contest

In its 1945–46 prize paper competition the Philadelphia Section recently awarded three best paper prizes, one for each of its geographical divisions, Philadelphia, Delaware, and New Jersey. Prizes also were awarded for the best initial paper and honorable mention was given two papers.

Authors names and titles of the winning papers follow:

First Prize

Philadelphia division: "Application of the Ohm and Mho Principles to Protective Relays" by A. R. van C. Warrington (M '43).

Delaware Subsection: "Electrical Construction—Material and Time-Saving Methods" by R. G. Rudrow (M '41).

New Jersey division: "Salesmanship in Engineering" by R. T. King (M '37).

Best Initial Paper

"Coincidence Factor Relationship of Electric-Service-Load Characteristics" by Constantine Bary (M '43).

Honorable Mention

"Research on Aids for the Blind" by Thomas A. Benham (A '39).

"The Development, Design and Performance of Magnetic-Type Power Circuit Breakers" by B. W. Wyman (A '40), and L. J. Linde (M '45).

Illinois Valley Section Reports First Year's Activities

A total of 11 formal meetings held during the Illinois Valley Section's first year of operation is reported by Professor F. E. Dace (M'43), Section chairman. These were interspersed by technical groups meetings, attendance at which sometimes outnumbered that at regular Section meetings, according to Professor Dace.

Two of the Section meetings were held in Springfield, two in Pekin, and others in Peoria. The Section also has taken an active part in the Peoria Engineering Council, which represents 19 engineering organizations.

The Section's annual meeting, held May 4, was addressed by AIEE President W. E. Wickenden. The April 4 meeting was held on the campus of Bradley Polytechnic Institute, and the speaker for the evening and the members of the executive committee were guests of the college at dinner.



Joint meeting of the AIEE Michigan Section and the IEES in the electrical laboratory of the Bull Dog Electric Products Company, Detroit, April 24, 1946

ABSTRACTS• • • •

TECHNICAL PAPERS previewed in this section will be presented at the AIEE summer convention, Detroit, Mich., June 24-28, 1946 and will be distributed in advance pamphlet form as soon as they become available. Copies may be obtained by mail from the AIEE order department 33 West 39th Street, New York 18, N.Y., at prices indicated with the abstract; or at five cents less per copy if purchased at AIEE headquarters or at the convention registration desk.

Mail orders will be filled

AS PAMPHLETS BECOME AVAILABLE

Air Transportation

46-129—Electronic Control of Frequency Converter Sets for Testing Aircraft Models; *G. W. Heumann (A '44), W. F. Strong (A '41). 25 cents.* The paper describes the 65- to 400-cycle variable frequency a-c power system used for testing aircraft models in the United Aircraft Corporation wind tunnel at East Hartford, Conn. Induction type frequency converters, driven by d-c shunt motors with armature voltage control, supply variable frequency power. Electronic exciters energize the various d-c fields, and electronic regulators are described in detail for control of speed, current limit, volts per cycle, and load division during parallel operation of two converter sets. Antihunt circuits insure stable operation. The power system is used for speed control, by frequency control, of high-speed induction motors driving propellers. Aerodynamic performance is determined by precision measurement of speed and electric input into the model motors which, from motor calibration data, permit computing the mechanical input into the propeller. The electric controls enable the operator to obtain any test point within the range of the equipment.

46-131—Investigation of Porcelain Insulators at High Altitudes; *C. V. Fields (A '41), C. L. Cadwell. 15 cents.* The use of high voltage apparatus in military aircraft made it necessary to obtain flashover data on capacitor bushings at altitudes up to 50,000 feet. Some of the more pertinent data are presented in this paper which gives a-c and d-c flashover voltages for porcelain bushings having spacings of 5/8 inch to 2 7/8 inches from cap to ring. The tests were made at both normal atmospheric and reduced pressures, but no attempt was made to simulate the frosting conditions as encountered in flying. Correlations are shown between bushing spacings and the effect of pressure change. A single correction curve for pressure changes cannot be used, but a family of curves is required for various spacings of insulators

and electrostatic field configuration. This paper shows that the practical use of porcelain insulators is limited to altitudes and voltages well below maximum values proposed for aircraft use. It is recommended that solid insulation be used in such a manner as to obtain the benefit of its puncture strength rather than its flashover at the more extreme conditions of altitude and voltage.

46-145—Short-Time Current Ratings for Aircraft Wire and Cable; *B. W. Jones (M '43), J. A. Scott (M '34). 15 cents.* This paper gives the results of a series of tests on two sizes (AN-16 and AN-8) of insulated aircraft wires and cables which were made to determine their permissible short-time current carrying capacities. The times under consideration ranged from 0.01 to 1,000 seconds. A description is given of a very simple but adequate electrical test, together with an accompanying insulation test, to determine what are considered permissible transient temperatures. Tentative recommendations of short-time current carrying capacity for aircraft cable sizes AN-22 to AN-00 are made.

46-148—A Unique Engine Synchronism Indicator for Aircraft; *D. B. Pearson (A '41). 15 cents.* Greater passenger and crew comfort, improved flight efficiency, and minimized vibrational stresses are obtained by exact synchronism between the engines of multiengine aircraft. Much closer synchronism than is attainable with engine tachometers alone can be provided by using suitable synchronism indicators. The limited panel space available has dictated a very compact construction for synchronism indicators without sacrifice of accuracy or dependability. This has been accomplished by designing an indicator mechanism which utilizes a principle similar to that of electric-power-circuit synchroscopes, but which is much smaller in size. The construction and operating characteristics of this unique aircraft engine synchronism indicator are described.

Automatic Stations

46-106—Automatic Control of Large Synchronous Condensers; *M. J. Brown (M '44). 30 cents.* The considerations involved in the design of an automatic synchronous condenser control are discussed in this paper with an aim toward helping the designer and user of synchronous condenser equipment obtain modern and complete facilities in his design. A typical push button operated control for a large synchronous condenser is described, and the diagrams involved are shown. The description includes a detailed résumé of starting sequence, protective device operation, and automatic control of voltage and load. Emphasis is put on the adaptability of push button control to full automatic operation or remote operation by direct or supervisory control.

46-147-ACO—Operating Experience With Single Pole Switching; *I. T. Knight (M '42). 15 cents.* Single pole and two pole switching provide greater transient stability of interconnected systems. During swings, power is transferred through the grounded neutrals and over the phases remaining closed, alleviating stresses in generator equipment. The selection of the tripping circuits, together with the high speed carrier distance relaying and 20-cycle reclosing, necessarily complicates the control. However, complications are justified when it is considered that the purpose of the interconnection is to supplement generator capacity. Oscillograms and tables show the performance during testing with mimic power faults and load conditions.

46-174—Carrier Supervisory Control of Pumping Station Over Power Cable; *W. A. Derr (A '43), W. A. Keller, H. A. W. Hedke (A '34). 20 cents.* A recent installation of power-line carrier supervisory control provides for unattended operation of a pumping station in Lake Okeechobee. The pumping station provides the necessary water for a new starch plant of the United States Sugar Corporation. In addition to providing for the remote control of apparatus units, the supervisory control also provides selective telemetering and communication over the same single-frequency carrier channel. The carrier equipment operates over 4,000-volt power cable, part of which is rubber jacketed and part of which is armored submarine cable. The paper presents field test data on the attenuation values of the cable. The use of low-voltage capacitors similar to standard power factor correction capacitors instead of standard carrier coupling capacitors is described. The incorporation of the carrier and supervisory control equipment in a metal-clad switchgear assembly also is described.

Basic Sciences

46-110—The Influence of the Concentration and Mobility of Ions on Dielectric Loss of Insulating Oils; *B. P. Kang (A '40). 20 cents.* The purpose of this study is to help in clarifying one phase of the picture on the nature and mechanism of dielectric loss in insulating oils. It deals with the relations of dielectric loss on one hand and the concentration and mobility of the free ions on the other. To vary the concentration and mobility of ions, different percentages of a highly deteriorated oil were added to two highly refined oils of different viscosities. It was found that the dielectric loss varied inversely as a function of the viscosity logarithmically. If mobility of the ions is kept constant, the dielectric loss will be a linear function of the content of free ions in the oil. On the other hand, an increase in the concentration of ions in an oil may result in an actual decrease in dielectric loss, if the viscosity is increased to the point where the mobility of the ions is decreased relatively more than the ion concentration is increased.

46-111—A Fractional Termination for Ladder Networks; *Wilbur R. LePage (M '44). 20 cents.* By use of a uniform ladder network to simulate a smooth transmission line of sufficiently small electrical length, a termination intermediate between the ordinary mid-series and mid-shunt types is derived which is superior to the latter types. The superiority lies in a reduction of the errors of the four-terminal-network parameters, as compared with those for the smooth line, and in the reduction of the distinction between the mid-shunt and mid-series terminations. The new termination may have use when simulating lines shorter than a quarter wavelength. Formulas for the new terminations, and estimates of the errors of the parameters, are given for networks of any number of sections, but the results are of most practical value when there are few sections. It is found that no improvement is possible by modifying the next-to-the-terminal elements of the uniform network.

46-119—Formulas for Calculating the Inductance of Channels Located Back to Back; *W. G. Schwantz (Student), T. J. Higgins (A '40). 25 cents.* Formulas are derived for calculating the inductance of a bus comprised of two identical channels located back to back. It is assumed that the conductors are nonmagnetic, are of such length that end effects are negligible, are right cornered, are uniformly thick, and carry currents distributed uniformly over their cross sections. On these bases a general formula is obtained through use of geometric mean distance theory. An approximate formula, suitable for preliminary computation, stems from considering conductors infinitely thin rather than uniformly thick. Once these formulas are derived, their use is illustrated by calculation of several typical problems. Additional problems illustrate precautions to be observed in using the approximate formula.

46-120—Negative Resistance Effects in Saturable Reactor Circuits; *J. M. Manley, E. Peterson (M '26). 30 cents.* Sustained oscillations exhibiting many of the properties of free oscillations are found in saturable reactor circuits under appropriate conditions. The frequencies of such oscillations are classified in relation to that of the driving source as

1. Incommensurable.
2. Subharmonic and multiples thereof.
3. Harmonic.

General properties of the oscillations classified are elucidated by reference to an analysis of R. V. L. Hartley's dating back to 1917. In part I a comparatively simple form of analysis is used to demonstrate the development of negative resistance by what is essentially a modulation process. Applications then are made to the three classes of oscillations just listed. Some of the simplifying assumptions of part I are removed in part II to approximate practical conditions more closely for the evaluation of a specific product: the third subharmonic. Quantities evaluated over

wide ranges of the variables involved include the impedance of the nonlinear coil to the subharmonic, the subharmonic amplitude, its stability, and the conditions required for starting and maintaining the oscillation. Experimental data are found in general agreement with the results of computation.

46-128—A New Approach to Probability Problems in Electrical Engineering; *H. A. Adler (M '44), K. W. Miller (M '29). 15 cents.* In many electrical engineering problems the probable durations of simultaneous events and the probable intervals between such simultaneous occurrences are of great importance. The usual mathematical formulas and available methods determine only the probability or ratio of time occupied by simultaneous events, without specifying either their durations or intervals between recurrence. This paper presents formulas useful for determining average durations and intervals between simultaneous events for a variety of conditions encountered in engineering problems.

46-150—Dimensionless Analysis of Servomechanisms by Electrical Analogy; *S. W. Herwald (A '46), G. D. McCann (M '44). 15 cents.* This paper gives the results of a general study that has been made of standard forms of angular position servomechanisms. The rapidity with which complete transient solutions can be obtained on the mechanical transients analyzer has permitted the analysis for a wide range of servomechanism parameters. These data are plotted in dimensionless form, permitting the ready determination of the performance of a given servo system or the selection of parameters for optimum performance.

Communications

46-151—Mica Capacitors for Carrier Telephone Systems; *A. J. Christopher (A '28), J. A. Kater. 15 cents.* This paper discusses the types of mica capacitors used in carrier telephone systems in the Bell telephone plant. It covers the construction and some of the more important electrical characteristics of the silvered mica capacitors currently used in oscillators, networks, and other frequency determining circuits because of their inherently high capacitance stability with temperature changes and with age. Their use in place of the previous dry stack type, consisting of alternate layers of mica and foil clamped under high pressures, has made possible considerable manufacturing economies in addition to improving the transmission performance of carrier telephone circuits. The manufacturing economies are the result of relatively simple unit construction and ease of adjustment to the very close capacitance tolerance required.

46-161—Systems Development of Military Communications; *T. R. Putnam (M '45). 15 cents.* The broad phases of the problems involved in developing the land line network of signal communications required for extensive land and land-based air operations into a theater-wide system are discussed. The basic nature of both tactical and rear area communications are described and compared with commercial systems from an operating standpoint. The aspects reviewed are those concerned with unification of control of the over-all network under the handicap of War Department signal communication doctrine. The solution to the problem of developing the theater-wide network into a unified system in the North African theater of operations is given, together with some operating results.

46-162—Properties and Uses of Thermistors—Thermally Sensitive Resistors; *J. A. Becker (F '43), C. B. Green, G. L. Pearson. 30 cents.* A new circuit element and control device, the thermistor or thermally sensitive resistor, is made of solid semiconducting materials, the resistance of which decreases about four per cent per centigrade degree. The thermistor presents interesting opportunities to the designer and engineer in many fields of technology for accomplishing tasks more simply, economically, and better than with available devices. Part I discusses the conduction mechanism in semiconductors and the criteria for usefulness of circuit elements made from them. The fundamental physical properties of thermistors, their construction, their static and dynamic characteristics, and general principles of operation are treated. Part II of this paper deals with the applications of thermistors. These include: sensitive thermometers and temperature control elements, simple temperature compensators, ultrahigh frequency power meters, automatic gain controls for transmission systems, voltage regulators, speech volume limiters, compressors and expanders, gas pressure gauges and flowmeters, meters for thermal conductivity determination of liquids, and contactless time delay devices. Thermistors with short time constants have been used as sensitive bolometers and show promise as simple compact audio frequency oscillators, modulators, and amplifiers.

46-163—Transmission Rating of Telephone Systems; *W. A. Codd. 15 cents.* The problem of rating the transmission performance of telephone connections is considered, including a review in considerable detail of a method proposed by J. R. Hughes for "The Comprehensive Assessment of Telephone Communication Efficiency." A modification of Hughes' technique is presented with indications of certain attendant advantages.

Electric Machinery

46-116—Electromechanical Transient Performance of Induction Motors; *C. N. Weygandt (A '37), S. Charp (A '42). 30 cents.* Two phase induction motors commonly are used as servo motors because they can be reversed and controlled readily. Although they are extensively employed, such utilization is mainly on an "it works" basis. This paper is the result of a differential analyzer study of their starting and reversing characteristics, based upon solutions to the induction motor equations formulated by H. C. Stanley in 1938. These performance equations are solved, and summary curves based upon the conclusions reached are presented in a form useful to the motor designer. A comparison of the theoretical results with experimental data of an actual motor is made. No published data of the type presented in this paper have come to the attention of the authors.

46-136—Current and Torque of D-C Machines on Short Circuit; *T. M. Linville (M '34). 30 cents.* An analysis of d-c machines under short circuit is made, and formulas are derived for the armature current, field current, and torque. The formulas are applied to several machines and the calculated results compared with test data. The terms of the formulas can be evaluated easily, and in many cases, particularly with large machines having bar windings, approximate calculations can be made without need of manufacturer's data. The paper is useful in problems concerning the protection of machines and circuits against the abnormal currents and forces produced by short circuit. Important features of the paper are:

1. The expression for the relation between electromotive force, armature amperes, and field amperes.

2. An expression for the resistance to current flow created by the reactance voltage of the alternating current in the armature winding.

3. A formula for estimating the time constant of the armature circuit using an average coefficient of inductance.

46-157—Factors Affecting Insulation Resistance of Large D-C Machines; *J. S. Johnson (M '45), Conrad Weil (A '44). 25 cents.* Insulation resistance data of 1,100 new d-c machines in the range of 1,000 to 7,000 horsepower are analyzed. Estimates are made from a statistical study of the data and known machine design proportions of the relative magnitudes of the principal factors which affect the insulation resistance of new d-c machines. In addition to previously recognized factors, such as material resistivity, insulation temperature, and machine size, the absolute humidity of the surrounding air is shown to affect significantly the insulation resistance of commutator type machines. Based on this study, a simple linear insulation resistance formula for new d-c machines is developed which includes corrections for the effects machine size and the absolute humidity of the surrounding air at the time of test. Since the voltage range of large d-c machines is small, the rated machine voltage has been omitted in the suggested formula.

46-164—Oscillations of a High-Voltage Secondary Winding; *A. Boyajian (F '26). 30 cents.* Rational design of transformer insulation requires knowledge of the distribution of stresses under abnormal conditions. This problem has been analyzed fairly completely for the case in which the

disturbance is applied directly to the terminals of a winding. However, there is a need for a more complete analysis for the case when the disturbance is induced in a winding acting as a secondary winding. This paper presents a novel theory and outlines the method of analysis. A feature of the theory is that the natural mode of the oscillations of such a circuit are not quarter waves or half waves and their multiples, but intermediate fractions of waves. The paper gives methods of estimating the overvoltages as functions of such harmonics and explains how to determine the characteristics of the transformer for use in the calculations.

46-165—Temperature Limits for Short-Time Overloads for Oil-Insulated Neutral Grounding Reactors and Transformers—II; *V. M. Montsinger (F'29), J. E. Clem (F'38). 25 cents.* In part I, published in 1938, the principal question considered was the effect of ventilating coils on temperature limits for ground faults greater than one minute, for which it was assumed that 160 degrees centigrade based on all heat stored in copper only, was the correct limit. Since 1938 considerable new data have been obtained. This paper presents the new data and shows that:

1. For heating periods of one minute or less, practically all aging of insulation occurs during the cooling period. It is shown that temperature limits can be based on the "rate of cooling," rather than on the heating period.

2. In the heating period of one minute or less 25 to 45 per cent of the loss is dissipated from the copper to the insulation and oil. Formulas are developed for calculating the temperatures during the heating and cooling periods.

3. Temperature limits above 160 degrees centigrade for one minute are permissible for both nonventilated and ventilated coils, being approximately 200 degrees centigrade for windings which cool sufficiently rapidly.

46-166—Some Aspects of Polyphase Motor Design—The Design and Properties of the Magnetic Circuits; *T. C. Lloyd (M'46), H. B. Stone. 30 cents.* By comparing a great number of laminations used successfully for a number of years in polyphase induction motors, and taking into account various theoretical factors, rules are formulated for determining dimensions of a series of laminations. The theoretical determination of a best lamination involves a fixed number of poles; the method shown indicates means of obtaining average laminations for a range of usefulness, as well as designs for various poles. The maximum torque of a given lamination designed for a number of poles is indicated, as well as the inherent volt-ampere capacity. A liberal number of examples is used to illustrate the influence of lamination proportions on motor performance.

46-167—Rotating Electric Machine Time Constants at Low Speeds; *C. Concordia (M'37). 20 cents.* This paper presents the results of a study of the variation of the several time constants of electric machines with rotor speed. Previously, formulas for machine time constants at rated speed and at standstill have been used. As these time constants are quite different at these two speeds, it becomes important to show the way in which they vary continuously as the speed increases from standstill, and to determine proper values for use at very low speeds.

Electric Welding

46-137—Influence of Magnetic Materials on the Welding Characteristics of Resistance Welding Machines; *J. J. Riley, C. E. Smith (M'44). 25 cents.* The insertion of magnetic materials, such as steel sheets, into the throat of a resistance welder causes a reduction in the welding current. The degree of reduction and simple mathematical tools for estimating it are derived. The effect on welding current of thickness of sheets, of inserted length, of position in the welder throat, of width of sheets, and of magnitude of welding current were investigated. The change in welding current was evaluated by measuring the reactive and resistive voltage components caused by the steel sheets in the welder throat and summarizing them in nomogram form. This chart in combination with the short-circuit impedance constants of the welder provide the working tools. The effect of welding steel sheet independent of steel inserted in the throat also was investigated to complete the analysis of determining welding current changes in terms of circuit variables.

46-141—The Application of Series Capacitors to Flash Welders; *J. F. Deffenbaugh (A'42). 15 cents.* The application of series capacitors to spot, projection, and seam welders no longer presents any difficult problems, and such capacitors have been used successfully with these types of welders for several years. Essentially, enough capacitive reactance is placed in the primary circuit of the welder transformer to neutralize the inductive reactance of the welder. This theoretically produces unity power factor and reduces the kilovolt-ampere demand to the level of the kilowatt demand. Since the voltage across the capacitor units is directly proportional to the current flowing through them, units must be selected with a voltage rating high enough so that this rating is not exceeded, unless they are protected by an overvoltage device. The flash welder, however, presents an entirely different problem, as the welding operation is composed of two phases which differ widely in both power factor and kilovolt-ampere demand.

46-156—Characteristics of Resistance Welding Transformers; *F. E. Murray, R. C. Jones. 15 cents.* This paper deals with the practical design of resistance welding transformers. It is the authors' desire to convey to the readers the general characteristics and problems encountered in design. The material covered has been presented with the thought in mind that it will enable users of resistance welders to understand better this vital part of their equipment. A portion of the paper covers a sample design of a resistance welding transformer. This section contains a general picture of the design constants used in determining core and copper sections.

Electronics

46-105—Inductive Co-ordination Aspects of Rectifier Installations; *An AIEE Committee Report. 30 cents.* This report presents methods of classifying proposed installations from the inductive co-ordination standpoint, simple approximate methods of estimating harmonics in a-c systems associated with the operation of rectifier installations, and other information dealing with the inductive co-ordination aspects of rectifier installations.

46-126—Fundamental Properties of the Vacuum Switch; *R. Koller (A'43). 25 cents.* A study has been undertaken of the basic mechanism affecting the interruption of currents in high vacuum. The interruption starts as an ordinary vapor arc which is quickly deionized by a fast radial gaseous diffusion in the evacuated space. This first arc is followed by a series of short periods of extinction interspersed with arc bursts of microsecond duration. Cold emission restrikes and magnetic self-focusing are also active. The cathode loses material by sputtering. The main factors affecting this loss are: the current, the recovery voltage, the electrode material, the shape of the cathode, and the opening speed. The switch operates below 10^{-4} millimeter of mercury pressure. The sputtering acts to reduce the pressure due to gases and vapors evolved from the electrodes, by a combination of getter action and diffusion-pump-like action. A constant working pressure thus can be established.

46-138—Excitation, Control, and Cooling of Ignitron Tubes; *C. C. Herskind (M'40), E. J. Remscheid (M'40). 15 cents.* A description of the excitation, control, and temperature characteristics, limitations, and requirements of typical ignitron tubes is presented. Oscillographic tests show the grid action throughout the cycle. The control characteristics provided by the grid depend upon these arc processes. The procedure for specifying the limitations and requirements of the tubes as regards excitation, control, and cooling is outlined.

46-139—Rectifier Capacity; *C. C. Herskind (M'40), H. C. Steiner (M'44). 15 cents.* The application of mercury pool tubes to a variety of rectifier units having different circuits and ratings requires a knowledge of both the circuit duty and the rectifier capacity. The procedure for the determination of rectifier capacity and the application of rectifier tubes on the basis of such data is described. The relation between voltage, current, phase control, reactance, and rectifier capacity are shown. Tests and experience indicate that phase control is an important factor affecting rec-

tifier capacity. Curves showing the capacity characteristics of two typical ignitron tubes are presented.

46-140—A 400-Ampere Sealed Ignitron; *H. C. Steiner (M '44), H. N. Price. 20 cents.* As rectifier capacity is increased, it becomes desirable to use larger capacity rectifying elements. The choice of rectifying element size requires careful consideration in order to provide a complete range with a minimum number of units. The sizes of industrial ignitron tubes for welding control and for rectifier service have been chosen on a preferred number scale, providing a proportionate increase at each increment. The development of a 400-ampere ignitron for rectifier service was undertaken to provide the next larger size tube in the series. Development work disclosed that design problems become more complex as the physical size of the tube is increased. However, none of the factors involved have indicated an upper limit in size but rather a need for a more exact understanding of the phenomena involved.

46-143—Nonlinear Commutating Reactors for Rectifiers; *A. Schmidt, Jr. (M '45). 15 cents.* The factors involved in rectifier duty are discussed, and it is shown that increased reactance results in decreased rectifier duty. The same result may be obtained from suitable presaturated nonlinear reactors with less accompanying regulation as compared with linear reactors. The design of nonlinear reactors is discussed, and the circuit action of typical reactors is indicated. An example is given of the increase in rectifier rating which may result from the use of commutating reactors under severe duty conditions.

46-146—Circuit Cushioning of Gas-Filled Grid-Control Rectifiers; *D. V. Edwards (A '31), E. K. Smith. 15 cents.* In certain common rectifier and inverter circuits, gas-filled rectifier tubes, supplying highly inductive loads with firing delayed by grid control, are subjected to the application of high rates of rise of initial inverse voltage. This phenomenon results in short tube life because of the sputtering of anode material by the impact of residual ions attracted to the negative anode with consequent gas cleanup. The paper describes a method of slowing down or "cushioning" the rate of rise of initial inverse voltage. A small resistance and capacitance circuit connected between cathode and anode delays the voltage rise the few microseconds necessary to eliminate sputtering. Life test data and practical applications are cited which confirm the elimination of gas cleanup.

Induction and Dielectric Heating

46-124—Design of Induction-Heating Coils for Cylindrical Magnetic Loads; *J. T. Vaughan (A '44), J. W. Williamson (A '43). 20 cents.* Equations are presented by means of which the authors' previous paper "Design of Induction-Heating Coils for Cylindrical Nonmagnetic Loads" is extended to the design of coils for heating magnetic loads, where the load remains in a fixed position relative to the coil during the heat. In heating magnetic materials there is considerable variation in impedance of the coil circuit as the load temperature changes. The present paper first develops certain general principles by means of which a variable impedance circuit may be designed to absorb a predetermined maximum power, on the basis of constants determining the maximum and minimum impedance. Methods then are given by means of which these constants may be calculated for carbon steel loads of types SAE 1015-SAE 1045 or equivalent. In practice these methods apply to most through-heating and some surface-heating applications. The accuracy of calculations is substantiated experimentally.

46-153—Low-Reactance Flexible Cable for Induction Heating; *Myron Zucker (M '36). 15 cents.* A flexible water-cooled cable, designed primarily for portable spot welders, has been used for supplying power to induction heating coils at about 1,000 and 10,000 cycles. The increased voltage drops and power losses at the higher frequencies are especially important because of the relatively small current transmitted. Therefore, tests and calculations were made to determine the electrical characteristics. These are affected by the amount of copper in the cable and the number of parts into which the copper is divided. Inductive reactance, which is the most important factor, is computed and checked with reasonable accuracy. Approximations are available for other electrical characteristics. Formulas are obtained by which cable performance can be anticipated. These will be used where there is a demand for the flexible cable to supply power in the low-voltage kilocycle-frequency range.

Industrial Control Devices

46-104—Silicone-Resin-Treated Magnet Coils; *G. L. Moses (M '44), J. J. Torok (M '35). 20 cents.* Silicone insulation was investigated on magnet coils to parallel similar tests on motors. Laboratory tests are reported with standard coils. These tests covered the range between 200 and 275 degrees centigrade. These were aimed to determine the life-temperature characteristics and to evaluate the design advantages.

46-113—Electrical Accuracy of Selsyn Generator–Control Transformer System; *Harold Chestnut (A '41). 30 cents.* The military requirements for high accuracy position control systems have resulted in the development of the Selsyn generator-control transformer system which indicates electrically a mechanical shaft position. This signal source is dependable, capable of continuous rotation, and has a high inherent accuracy, although it is not completely error free. To determine the cause of inaccuracies in electric transmission, the system was studied

(*a*). Under static operation.
(*b*). Operating at constant velocity.

The effect on errors of such factors as unbalanced resistance or reactance, salient pole construction, and velocity has been determined. The dominant effect of unbalance resistance in a stator phase or in the lines between machines is to introduce an out-of-phase component of "error" voltage. However, reactance unbalance in the stator phases or certain harmonics of mutual reactance between rotor and stator produce a position error. Operation of the system at constant velocities comparable with the synchronous speed for excitation frequency employed produces an appreciable out-of-phase error voltage. However, at lower speeds of operation the error is primarily a position error in transmission, amounting to about 1 degree for 320 rpm.

46-125—An Electronic Drive for Windup Reels; *K. P. Puchlowski (A '43). 20 cents.* This paper gives a description of an electronic system which automatically controls the speed of the takeup reel motor in such a manner as to provide an essentially constant strip speed during the reeling operation. The system also provides means for selection of the strip speed within a wide range. The power supplied from an a-c line is rectified and controlled by the electronic system, and then is supplied to a conventional d-c shunt wound motor which drives the windup reel. With the exception of a small tachometer generator which indicates the speed of the strip, the main driving motor is the only rotating machine used in this drive. The paper also includes a general discussion of the operating principles of servo systems and emphasizes these principles in the description of the drive.

46-130—Dynamic Braking Control of D-C Series Motors—Calculation of Stability Limit; *G. W. Heumann (A '44), W. P. Smith. 15 cents.* This paper presents an extension of the conventional method of calculating speed-torque curves for d-c series motors used with dynamic braking controllers. By means of test data, it is shown that torque per armature current and electromotive force per speed are a function of both field and armature current. With low field currents, armature reaction limits the maximum braking torque the motor is able to deliver. A per unit method is given to calculate stability limit. It is shown that the stability limit can be increased by the use of external series resistance.

46-132—Electronic Register Control for Multicolor Printing; *W. D. Cockrell (M '43). 20 cents.* The popular illustrated magazines of today are printed on high speed rotogravure color presses. For acceptable pictures, the colors must be superimposed on one another, or registered, to a tolerance of a few thousandths of an inch in spite of paper stretch and shrinkage due

to tension changes and the necessary drying of each color between impressions. The two requirements of accurate register and high speed operation are met by an all-electronic register control system. In this paper a system is described in which electronic tubes perform all functions. Photoelectric tubes compare the relative positions of the printing cylinders and the incoming web. Pliotrons comprise the amplifier, comparison, and control circuits, and thyratron circuits supply the armature power to the reversing motor used to correct the position of the printing cylinder or compensating roll.

Industrial Power Applications

46-122—Protection of Industrial Plants Against Insulation Breakdown and Consequential Damages; *H. R. Vaughan (M '41). 15 cents.* Experience has shown that several electrical failures may occur simultaneously in an industrial plant as the result of a breakdown of insulation, causing high transient voltages. Available methods of surge protection to guard against insulation breakdown and neutral grounding to prevent high transient voltages are presented. Consideration is given to the merits and limitations of these methods when applied to industrial plants.

Instruments and Measurements

46-107—Parallel Circuits in Servomechanisms; *H. T. Marcy (A '42). 30 cents.* In a process controlled by a servomechanism, measurements are made of desired and of controlled quantities. Analytical techniques heretofore described by various authors become awkward to use

1. When the measurement of the error between desired and actual quantities is not very fast compared with the speed of response of the remaining system.

2. When there are components in the control system which employ feed-back circuits.

This paper describes the application to these problems of an analysis which uses the reciprocal of the usual system function. The reciprocal system function is defined as an operational expression of a nondimensional ratio of component input to component output.

46-114—The Frequency Response of Automatic Control Systems; *Herbert Harris, Jr. 30 cents.* This paper illustrates the advantages of the frequency response approach to the analysis of automatic control systems as contrasted to the analytic solution of transient response. At the same time the equivalence of information available from the two approaches is demonstrated. A numerical example is given based upon a torque amplifier using a motor-generator type control.

46-133—Functional Analysis of Measurements; *I. F. Kinnard (F '43). 30 cents.* This article shows the need for a practical method of systematically analyzing all types of measurement apparatus, and outlines such method actually in use. Specific new terms and definitions are suggested for various functional parts of measurement devices or systems, and other terms commonly used are defined carefully. A number of measurements performed by apparatus using electrical means are analyzed and illustrated, using the methods described. Statistical data on functional parts of measurement equipment are shown. The benefits that can be obtained from the application and general use of the proposed functional analysis and classification method are discussed.

46-135—A New Design for the A-C Network Analyzer; *J. D. Ryder (A '40), W. B. Boast (M '43). 20 cents.* In line with the increased interest in a-c network analyzers, the Iowa State College has been active in developing and constructing an analyzer for use by utilities of the Midwest area. A pilot model of the analyzer, to employ an operating frequency of 10,000 cycles per second, has been built and tested. Advantages obtained by the use of a high operating frequency are reduced instrument burden, reduced power levels, and the opportunity to avoid the use of iron cores in the reactor units. The latter feature provides a major improvement in accuracy. Lowered cost is shown as possible through the use of techniques and apparatus common to the electronic and radio fields.

46-142—High-Vacuum Leak Testing With the Mass Spectrometer; *W. G. Worcester (A '42), E. G. Doughty. 30 cents.* A simple mass spectrometer which will detect extremely small quantities of helium provides an excellent method for the detection and accurate location of leaks in vacuum systems. The instrument described offers high sensitivity and quick response and is capable of detecting a small leak in the presence of a large leak. Large or small systems of metal, glass, or other materials can be tested. Since the response is not affected by outgassing, it is not necessary to produce a high vacuum in the test piece. Testing time is short, and the system lends itself to production tests. The paper includes a discussion of the theory and design requirements of the leak detector, a description of the instrument, and a discussion of the applications of the method to large and small systems.

46-155—Frequency Compensated A-C Ammeters and Voltmeters; *J. M. Whittenton (A '37), C. A. Wilkinson. 15 cents.* A comprehensive discussion of the factors causing frequency errors in uncompensated type a-c moving-iron ammeters and voltmeters is covered in this paper. A general discussion is given to the practical methods of compensation which can be applied to standard instruments to reduce errors in calibration to negligible values when instruments are calibrated at one frequency and used over a range of 25 to 3,000 cycles. Results are tabulated to show the reduction of frequency errors in ammeters by the use of high permeability materials in proper combination in the magnetic circuit to reduce eddy current losses. The effectiveness of these improvements in combination with the proper shunting of a portion of the series resistors of the voltmeters with required values of capacitance to correct also for changes in inductive reactance is described, and the reduction in frequency errors is given.

Marine Transportation

46-127—Design of D-C Auxiliary Controllers for Marine Service; *W. Schaelchlin (M '46). 20 cents.* This paper briefly discusses the various problems involved in the design of control equipment for shipboard service. The effect the number of starting steps has on current surges, and the advantages and disadvantages of various means of automatic acceleration are described. Overload protection of continuously and intermittently rated motors is discussed in detail, and particular reference is made to the problem of protecting intermittent motors. Resistors for starting and speed regulating duty are considered an important controller component, and discussion of them includes a table with recommended resistor classes for the various applications. A number of points must be considered in the design of enclosures for dripproof or waterproof controllers. Strength, ventilation, condensation, and other such details are covered. The paper concludes with a discussion of various types of controller assemblies for deck and underdeck applications and contains illustrations of typical equipment.

46-149—Propulsion Control Problems With Diesel-Electric Synchronous Motor Ship Drives; *E. Frisch. 20 cents.* Although the many obvious advantages of ship propulsion drives with synchronous motors and generators and with power supplied by Diesel electric engines have been realized for some time, no actual installations were made in the United States until a few years ago. At that time a trial installation was completed on a 12,000 horsepower twin-screw vessel. Experience thus gained has established its superiority in many respects, and indications are that it may find extensive use on future vessels. The paper discusses control problems associated with the drive and describes methods of control and types of control equipment which have been found best suited for the drive.

Power Generation

46-108—Tennessee Valley Authority Hydroelectric Stations—Electrical and Mechanical Design; *R. A. Hopkins (F '43), H. J. Petersen. 25 cents.* Design policies have been developed and established during the building and operating of 14 major hydroelectric generating stations since 1934. Turbines, governors, generators, transformers, switchgear, and other major equipment have been selected generally in accordance with normal manufacturers' designs, except in specific cases where operating experience has indicated a definite

need for improvement. Many of the improvements have become standardized by the manufacturers. Switching, bussing, control, relaying, wiring, piping, auxiliary equipment, and other station features have been developed by the Authority, using manufacturers' standard components as far as possible. The bases for selection of equipment and for development of station designs undoubtedly are applicable to other hydro projects.

46-144—Improvements in Performance of Hydroelectric Generating Units on the 2,000,000-Horsepower Saguenay System; *F. L. Lawton (M '36). 25 cents.* The large number of high-capacity hydroelectric generating units in power plants of the Saguenay System, well-organized operating records, thorough engineering studies and experimentation, and foresighted management have made feasible important advances in efficiency and reliability of such units. Improved methods of operation have resulted in maximum energy output from storage water. Important criteria affecting rate of wastage of waterwheel-runner metal by pitting, and costs of repairs, are discussed. The significance of operating waterwheels at best gate, and means of accomplishing this by gate-position indicators, are noted. The effect of dirt on generator stator-winding temperature rise is developed. Improved generator performance from better application of stator-winding insulation, superior stranding and transposition of stator-winding coils, high-silicon stator iron, and better ventilation systems are discussed. Enhancement in waterwheel capacity and efficiency, effected through model and prototype performance tests, is noted.

46-152—Modern Excitation Systems for Large Synchronous Machines; *J. B. McClure (A '29), S. I. Whittlesey (A '45), M. E. Hartman. 20 cents.* This paper reviews the types of modern excitation systems that are now available for large synchronous machines. It includes a brief description of the complete excitation systems followed by a discussion of the modern types of exciters and regulators. The application guides indicate the present trends of excitation systems for the different types of synchronous machines. Co-ordinated excitation systems are now available for all types of application requirements, including existing installations. The automatic control features provided by modern voltage regulators make it possible to obtain improved system operation, to operate existing equipment at higher loadings, and to design more economical system extensions. Special motor-driven exciters may be used successfully in place of large high-speed shaft-driven exciters. Shaft-driven hydrogen-cooled exciters are available for moderate-speed synchronous machines.

46-154—The Development of Modern Excitation Systems for Synchronous Condensers and Generators; *F. M. Porter (M '45), J. H. Kinghorn (M '46). 25 cents.* This paper describes a development program for excitation systems of synchronous condensers and generators ranging in size from 5,000 to 36,000 kva. This improvement plan has been carried on over the past 15 years and includes 15 exciter applications which are located on the systems of the American Gas and Electric Company. Installations involving 5 electronic pilot exciters, 4 electronic main exciters, 14 electronic regulators, and 6 direct connected exciters with amplidyne control are covered. Descriptions of several typical arrangements with photographs and connection diagrams are given. Operating experience with this equipment is presented and discussed. Tables, including operating time and tube life for the nine electronic exciters, are given. The fine performance of the various excitation schemes is recounted and demonstrated. Definite conclusions are drawn by the authors as a result of many machine years of satisfactory performance obtained with these numerous modern excitation systems.

Power Transmission and Distribution

46-103—Determination of Cable Temperatures by Means of Reduced Scale Models; *Andrew Gemant, Joseph Sticher (M '39). 25 cents.* A method, using reduced-scale model installations, is developed for the laboratory determination of cable temperatures obtaining in the field. The theory of the method is given, followed by the description of three sets of experiments conducted to show the feasibility of the method. One set of experiments is concerned with a single-conductor cable buried directly in the soil of the model setup, and temperatures obtained are compared with computed values. Another set is concerned with a single-conductor cable in a model duct bank, and sheath and duct temperatures obtained are compared with those of field determinations in an actual field installation. The third set is concerned with a model three-conductor cable in a duct bank, and conductor-sheath temperature differentials are compared with field data. All tests show that the accuracy of the method is sufficient for practical purposes.

46-115—F-3 Lead Alloy—An Improved Cable Sheathing; *L. F. Hickernell (F '34), C. J. Snyder. 20 cents.* Operating requirements for the lead sheath of modern impregnated-paper insulated power cable are outlined. The properties of present sheathing materials are reviewed, and the deficiencies pointed out. To meet present requirements, an extensive development program was undertaken and the material evaluated by a large utility. The best results were obtained with a new sheathing material composed of small amounts of arsenic, tin and bismuth, and remainder lead, known as F-3 alloy. Tests have shown that this material has unusual endurance or fatigue resistance under both dynamic and static loading. Outstanding properties are its resistance to bending fatigue, creep, and cracking under long-time static loading. It will not harden with age. F-3 alloy can be applied to cables by available manufacturing equipment. Also, it can be used for joint sleeves. Commercial lengths have been produced and installed on utility systems.

46-117—The Electrical Performance of Ceramic Dielectrics at Elevated Temperatures; *H. A. Frey (M '43), J. A. Jesatko (A '41). 30 cents.* Some recent developments have emphasized the need for information concerning the temperature at which dielectrics can be operated without electrical breakdown. This paper deals primarily with porcelain, but some data are included on the performance of steatite, glass, and zircon compositions. Data are presented on the variation in resistivity of the materials with varying temperature and also with varying voltage gradient. From the temperature-resistivity curves a method is developed for approximating the combination of temperature and voltage gradient which will result in electrical failure. Supporting data in the form of breakdown tests made at various temperatures are included. These tests include practical insulator forms as well as prepared test specimens.

46-118—Semiconducting Shielding for A-C Power Cable; *E. J. Merrell (A '41). 15 cents.* Graphs showing the electrical properties of semiconducting shields for a-c power cable are presented, together with background theory, illustrative problems, and experimental verification. The theory is based upon an adaptation of the exact hyperbolic formulas for a-c transmission lines to the circuit conditions represented by a cable dielectric and its semiconducting covering. Formulas and co-ordinates have been expressed in conventional electrical engineering terms, so that the theory and graphs may find ready application to cable measurements and design. All probable cable constants are covered by the graphs, specific solutions being obtainable by interpolation.

46-121—High-Voltage D-C Testing of Rubber-Insulated Wire; *W. N. Eddy (F '40), W. D. Fenn (M '44). 15 cents.* At different stages in the manufacture of insulated wire and cable, various electrical and physical tests are made to ensure the quality and serviceability of the completed cable. One of the most important of these tests is the high voltage test—alternating or direct current. It may be applied to short sections of the insulated conductor as it passes through electrodes of various types, dry or wet, or to full factory lengths of the insulated wire, dry or wet. The scope of this paper is limited to the results of an experimental study made on the voltage limits suitable for the high voltage d-c testing of factory lengths of plain insulated wire immersed in water. In addition to many sample tests, the study included tests on more than 5,500 different factory lengths of submarine cable conductor, insulated with natural rubber, synthetic rubber, or polyethylene. Such factors as testing volt-

age, type of fault, and immersion time were varied over a wide range. From these data test voltage limits are suggested; the lowest test voltage that will indicate serious defects, and the highest test voltage that can be used without causing damage to sound insulation, from either the d-c test voltage itself or from impulse voltages incidental to the testing.

46-123—The Preservative Treatment of Various Species Proposed for Poles and Crossarms; *J. D. MacLean. 15 cents.* The unprecedented drain on the nation's supply of poles imposed by the war needs and the backlog of pole requirements that has been built up, coupled with the reduced supply of creosote, have resulted in an acute shortage of treated poles and crossarms. The results of research by the Forest Products Laboratory during the past three decades have been reviewed, and recommendations are made in this paper for the use of alternate species, including spruce, Eastern white pine, Douglas fir, and 11 other species. Although creosote is recognized as the leading preservative, the chlorinated phenols and the creosote solutions provide suitable protection when necessary penetrations are obtained. The pressure method of treatment is the most satisfactory because it affords a means of controlling the absorptions, but nonpressure methods may be used successfully. Minimum net retentions of 4 to 8 pounds per cubic foot are specified for the pressure treatment of poles. The treating conditions and specifications for pressure treatment are given for the 14 alternate species for poles and crossarms.

46-160—Moisture Equilibrium Between Gas Space and Fibrous Materials in Enclosed Electric Equipment; *J. D. Piper. 20 cents.* In enclosed equipment, such as gas-filled transformers, the moisture concentration in the gas space reaches equilibrium with that in any fibrous materials present. The resulting vapor pressure is a function of the constitution, moisture concentration, and temperature of the fibers, but, at least for paraffin-impregnated cotton, is independent of whether or not the fibers are impregnated. A chart, prepared from published literature, shows the equilibrium vapor pressures for cotton having moisture concentrations from 0.01 to 10 per cent by weight for temperatures from 10 to 110 degrees centigrade. By multiplying the moisture concentrations by 1.7, the same chart is approximately applicable for kraft paper. Agreement between the chart and experimental data for paraffin-impregnated cotton is shown. Practical uses of the chart include nondestructive estimation of moisture concentrations in fibrous materials from the temperature of the fibers and the dew point of the gas.

46-175—Co-ordination of Insulation and Spacing of Transmission-Line Conductors; *W. W. Lewis (F'38). 15 cents.* The following criteria are suggested as a basis for the selection of minimum line insulation: The 60-cycle wet flashover must equal or exceed the voltages expected from faults and switching surges; the impulse flashover should equal or exceed the standard basic impulse insulation level for the terminal equipment. With each level of insulation there is a proper spacing between conductors and to the steel structure to develop the full strength of the insulator string selected. It is proposed that the minimum spacing A to the steel structure have an impulse flashover ten per cent greater than the flashover of the insulator string. Then the horizontal spacing from conductor to tower when conductor is hanging vertical will be $1.5A$, spacing between conductors in vertical arrangement will be $2A$ and in horizontal arrangement $3A$, and height of ground wires above top conductors will be $2A$.

46-176—Six-Years' Experience With Factory-Built Unit Type Substations; *E. F. Miller (M'44), R. B. Miller (A'36). 15 cents.* This paper outlines six years of operating experience with factory-built unit type substations and their application in a 4-kv primary network. The results obtained with the use of bus regulation, where it has been substituted for individual induction feeder voltage regulators, are outlined, as are also operating and maintenance experience with this type of equipment. History of the distribution system in which these substations are used is outlined, and reasons for the selection of the primary network type of distribution system and the selection of factory-built unit type substations are given.

Protective Devices

46-109—Fault Location and Relay Performance Analysis by Automatic Oscillographs; *H. P. Dupuis (A'41), W. E. Jacobs (A'44). 15 cents.* The method for determining the location of ground faults described in this paper is independent of generation, fault resistance, or the type of ground fault. This method applies particularly to faults in a network of two or more parallel lines and is based on a comparison of the magnitude and direction of ground currents in the faulted and unfaulted circuits. The paper describes the procedure in making ground current and ratio curves, and illustrates their application in locating faults and in determining critical conditions for relay selectivity. The summary classifies the type and cause of 256 line faults analyzed over a period of 5 years.

46-134—Application Ratings of Indoor Power Circuit Breakers; *O. B. Vikoren (M'43). 20 cents.* Increased cost involved in serving electric power to customers and the aim to lower rates have accelerated the need for most efficient utilization of existing generating and distribution equipment. This paper describes a method for loading power circuit breakers on a temperature basis for the purpose of taking advantage of their inherent current carrying ability. Several years of practical application of the basic theory have proved entirely satisfactory on various types of electric equipment and have in many cases established considerable savings on new investments. While these savings are less applicable to circuit breakers than to other major power equipment, their application in accordance with temperature, rather than name plate rating, has put the use of new and existing facilities on an equally sound engineering basis.

46-168—Low-Current Secondary Current Transformers; *AIEE subcommittee report. 15 cents.* This paper is a report of a working group of the relay subcommittee, covering the use of current transformers having secondary current ratings less than the generally accepted 5-ampere standard. Applications requiring low secondary current ratings are considered along with the advantages and disadvantages resulting from the use of such transformers. Consideration has been given to the availability of equipment, such as meters, instruments, and relays, suitable for use with low-current secondary currents, as well as some of the problems involved in designing equipment for this service. Where applications require the use of low secondary currents, solutions are suggested using standard meters, instruments, or relays employing auxiliary current transformers.

46-169—Protection of Powerhouse Auxiliaries; *AIEE subcommittee report. 20 cents.* The AIEE relay subcommittee has reviewed the protection of generating station auxiliary power motors to obtain information on auxiliary power systems now in use and the protective methods being applied, and to make recommendations on preferred practices. The paper includes a number of answers to a questionnaire covering data on supply systems used, various forms of protection applied, and a summary of the experience obtained with these systems. The practices and experiences of several major companies are summarized, and preferred practices are recommended based on this experience.

46-170—Performance Criteria for Current Limiting Power Fuses—I; *C. L. Schuck (A'39). 20 cents.* This paper describes empirical results of changes in test circuit variables on the interrupting performance of current limiting power fuses. The influence of generated voltage, available current, fault starting angle, fuse operating time, frequency, power factor, and the number of phases, are appraised for their effect on the severity of test conditions. Reference is made to Part II of the paper, in which the analytical framework is developed, for the necessary generalizations and extensions of the empirical data. Oscillograms of fuse interruption tests made in a short-circuit testing laboratory are presented to illustrate differences in test severity. Based on these observations, recommendations are made for test procedures and conditions for establishing the interrupting ratings of current limiting power fuses.

46-171—Performance Criteria for Current Limiting Power Fuses—II; *E. W. Boehne (F '43). 30 cents.* This paper presents a graphical, analytical study of the effect of the circuit variables upon the performance of power fuses. The magnitude of the arc voltages and the time of their introduction following the short circuit are chosen to favor the performance characteristic of power fuses of the current limiting type. The analytical methods employed, however, as well as the general equations of arc energy and conductor heating presented in the paper, are applicable to the general fuse problem, but particularly adapted to the analysis of fuse performance operating in low power factor single-phase circuits. Some of the more interesting results of this work are confirmed by oscillograms which are discussed in paper 170. It is shown, for example, that maximum energy liberated by the power fuse is dependent upon the fault starting angle and is not associated necessarily with the maximum interrupting rating of the fuse. The effect of circuit frequency upon the fuse performance is particularly interesting.

46-172—Philosophy of Relaying; *E. W. Knapp (M '44), Ben C. Hicks (M '45). 20 cents.* Philosophically the electric power system exists to serve certain human needs, and it must serve them better and more economically than they could be served by other methods, or it would not be able to continue to exist or to grow. The rendering of service of the required degree of excellence, within economic limitations, is not an inherent attribute of the electric power system but is the result of sustained and carefully co-ordinated effort on the part of all concerned in the rendering of the service, including:

1. Precautions taken in the design of equipment to make it trouble free and reliable.

2. Precautions taken in system layout and connections to enable service to be rendered continuously under adverse as well as under favorable conditions.

3. Precautions taken in the operation and maintenance of the system to avoid unnecessary interruptions to service.

46-173—Simplicity in Protective Relaying; *L. F. Hunt (F '38). 20 cents.* Simplicity relay circuits and the importance of ground relaying are pointed out in this paper. Protection engineers have outgrown the small job of studying the behavior of relays. Their major task is to give customers of electric energy good continued service from an over-all system viewpoint by seeing that the least amount of equipment be tripped to isolate faulty sections. It is their duty to assist in over-all station and system designs that can be adapted for the ultimate of service with structures having the smallest hazards to faults. Many of the relay systems for transmission, distribution, and equipment are described that have given almost perfect operation on the entire system of the Southern California Edison Company, Ltd.

Safety

46-112—Dangerous Electric Currents; *C. F. Dalziel (M '39). 20 cents.* This paper discusses lethal electric currents and their accompanying physiological effects, and interprets the data of a former AIEE paper, "Effect of Electric Shock on the Heart," by L. P. Ferris, B. G. King, P. W. Spence, and H. B. Williams, in accordance with an original method of analysis found useful by the author in his own investigations of "let-go" currents. The present analysis concerns itself with threshold currents likely to produce instantaneous electrocution in one half per cent of a large group of normal men. Although the conclusions are derived from tests made on animals, it is believed that the results may be indicative of what might be expected to occur in man. The majority of the work is based on experiments made at 60 cycles with shock durations of 0.03 to 3.0 seconds. Predictions of lethal currents for both direct current and condenser discharges, while more speculative due to the limited data available, are included because of their importance due to the greatly increased use of d-c and electronic equipment. Dangerous effects at high frequencies also are mentioned.

46-159-ACO—Silent, Invisible Industrial Hazard; *S. Reid Warren, Jr. (M '41). 20 cents.* The use of X rays or gamma rays in industry is increasing. Adequate protection of personnel from harmful effects of these radiations is of paramount importance, particularly because these effects may not be evident until several months or years after exposure to radiation. This paper describes briefly some of the properties of X rays and gamma rays, the harmful effects that they may produce in human beings, and the principles upon which the design of adequate protection depends.

PERSONAL ....

L. R. Brown (M '24) formerly manager of the transformer division, General Electric Company, Pittsfield, Mass., has been advanced to the staff of the manager of the company's central station divisions. Mr. Brown was graduated from the University of Wisconsin in 1903 and that year entered the employ of the company. Mr. Brown was made manager of distribution transformer sales in 1910 and manager of the entire transformer division in 1923. **H. F. McRell** (A '25) formerly assistant manager of the distribution transformer division, General Electric Company, Pittsfield, Mass., has become division manager. Mr. McRell joined the company in 1910 in Schenectady and in 1913 was transferred to Pittsfield to the transformer division. He has been senior transformer engineer in New York, St. Louis, Mo., and Chicago, Ill. In 1924 he was made sales manager of the distribution transformer section and in 1942 assistant manager of the transformer division. **P. M. Staehle** (A '17) formerly sales manager of the specialty transformer section, General Electric Company, Fort Wayne, Ind., becomes manager of the newly formed specialty transformer division. A graduate of the University of Wisconsin, Mr. Staehle entered the employ of the company in 1912 in Schenectady. In 1913 he was transferred to the transformer engineering department at Pittsfield and to Fort Wayne in 1916. After a period, from 1924 to 1929, as Mr. McRell's assistant, he returned to Fort Wayne as manager of sales.

William McClellan (A '04, F '12) chairman of the board, Union Electric Company, St. Louis, Mo., has retired. Doctor McClellan, a past president of AIEE, holds the degrees of bachelor of science (1900), doctor of philosophy (1903), and electrical engineer (1914) from the University of Pennsylvania. Before 1907 he was associated with the Philadelphia (Pa.) Rapid Transit Company and Westinghouse, Church, Kerr and Company, New York, N. Y. Throughout his career he was partner in a number of engineering firms—Campion, McClelland Company, 1907–15; Paine, McClelland, and Campion, 1915–20; McClelland and Junkersfeld, 1922–29; William McClelland and Company, Ltd., 1930–33. Executive for many firms he was vice-president of the Cleveland Illuminating Company from 1919 to 1921 and of Stone and Webster Engineering Corporation from 1929 to 1933, and president of the Potomac Electric Power Company from 1933 to 1939, of the Washington Railway and Electric Company and from 1935 to 1940, and of the Union Electric Company since 1939. He has served as director to other public utility firms. He is a member of the American Society of Mechanical Engineers, the Newcomen Society, the American Association for the Advancement of Science, and the American Academy of Political and Social Science. He also is a member of Phi Beta Kappa and Sigma Xi.

O. L. LeFever (A '10, F '44) formerly general superintendent, Northwestern Electric Company, Portland, Oreg., has been appointed chief engineer of the company. Mr. LeFever was graduated from Iowa State College in 1906 and spent one year with each of the following companies: the Minneapolis (Minn.) General Electric Company; the Twin City Rapid Transit Company, St. Paul, Minn.; the Northwestern Bell Telephone Company, Minneapolis; the Western Electric Company, Chicago, Ill.; and the Portland Railway, Light and Power Company. In 1913 he joined the Northwestern Electric Company as general foreman of underground construction. He successively became superintendent of steam distribution and general superintendent. **Tom Perry** (A '21) formerly assistant general superintendent of the plant department succeeds Mr. LeFever as general superintendent. Mr. Perry joined the Northwestern company as assistant superintendent of Portland stations in 1919.

A. L. Samuel (M'34) formerly electronic research engineer, Bell Telephone Laboratories, Inc., New York, N. Y., has been appointed professor of electrical engineering at the University of Illinois, Urbana. Doctor Samuel received the degree of bachelor of arts from the College of Emporia in 1923, and the bachelor of science degree in 1925 and master of science degree in 1926 from Massachusetts Institute of Technology. Recently he was awarded the honorary degree of doctor of science by the College of Emporia. After two years, from 1925 to 1927, as instructor of electrical engineering at Massachusetts Institute of Technology, Cambridge, Doctor Samuel became a member of the technical staff of Bell Laboratories. He has been active in the development of gas rectifiers, thyratrons, and vacuum tubes for use at ultrahigh frequencies and has many technical papers and patents to his credit. He is a member of the American Physical Society, the American Association for the Advancement of Science, and the Institute of Radio Engineers.

Theodore Braaten (A '22, M '31) formerly lieutenant colonel, United States Army, has been appointed general manager of the Gas and Electric Department of Norwich, Conn. After his graduation from the Massachusetts Institute of Technology, Cambridge, in 1920, Mr. Braaten taught there for one year and then spent a year investigating hydroelectric facilities in Norway. Later he was connected with the Public Service Company of Northern Illinois, the Westinghouse Electric Corporation, East Pittsburgh, Pa., and Boston Mass., and the Boston Edison Company. Having served as a lieutenant of field artillery in World War I, he entered the Army in 1942 as a captain. Overseas he was assigned to Supreme Headquarters of the Allied Expeditionary Forces and was responsible for restoration of public utilities in Holland and Germany. Later he was titled chief of public utilities, SHAEF Mission, Norway.

Bernard Hague (M'30) formerly lecturer on electrical engineering, University of Glasgow, Scotland, has been appointed to the James Watt Chair of Electrical Engineering at the University of Glasgow. Doctor Hague holds the degrees of bachelor of science (1913), master of science (1919) and doctor of science (1927) from the University of London and the doctor of philosophy degree (1926) from the University of Glasgow. In 1916 he became a technical assistant in the physics research department of the Royal Aircraft Establishment, Farnborough, and relinquished this position to become a lecturer at the City and Guilds College, London, in 1920. He joined the faculty of the University of Glasgow in 1923 as lecturer in electrical engineering. In 1929 and 1930 he was visiting professor at the Polytechnic Institute of Brooklyn, New York, N. Y. Doctor Hague has published a number of books and many technical articles.

J. W. Sheffer (A'10, M'13) formerly general electrical engineer, improvement department, American Car and Foundry Company, New York, N. Y., has been appointed general improvement engineer. Mr. Sheffer holds the degrees of mechanical engineer (1907) from Cornell University and master of arts (1933) from Columbia University. He joined the company in 1908 at Berwick, Pa., where he successively was electrical engineer and assistant to the general superintendent and plant engineer. In 1926 he was transferred to New York where he has been occupied with improvement and development problems. He is a member of the American Welding Society and the Association of Iron and Steel Engineers. **H. F. Schwarting** (A'16, M'21) formerly field engineer, improvement department, has been appointed general electrical engineer with headquarters in St. Louis, Mo.

J. F. Calvert (A'27, F'45) chairman of electrical engineering department, Northwestern Technological Institute, Evanston, Ill., has received a letter of commendation from the United States Navy for planning and directing construction of the Pearl Harbor demagnetization station at which warships were treated electrically for protection against mines. The letter praised Professor Calvert as follows: "Through your devotion to duty, tireless effort, and acceptance of personal risk during and following the attack on Pearl Harbor, this station was completed by the summer of 1942, and remains the finest in all of the Pacific ocean areas. May it continue to serve . . . . as a constant testimonial to your exceptional engineering accomplishments."

H. L. Rusch (A'24) formerly executive vice-president, A. C. Nielsen Company, Chicago, Ill., now is associated with the Public Opinion Index for Industry, a division of the Opinion Research Corporation, Princeton, N. J. Mr. Rusch was graduated from the University of Wisconsin in 1923 and, after a four-year association with the Nielsen company, joined the Johns-Manville Corporation, New York, N. Y., in 1928 as supervisor of its technical data and performance report section. In 1933 he was made vice-president and Eastern manager of the Northern Pump Company, New York, N. Y. He rejoined the Nielsen company in 1937 and in 1938 was elected vice-president.

A. W. Ray (A'19, M'45) manager of the service department, Reliance Electric and Engineering Company, Cleveland, Ohio, has retired. Mr. Ray was born in Rockport, Ohio, and attended Ohio State University. The second employee to be hired by the Reliance company when it was organized in 1905, Mr. Ray has been design draftsman, chief draftsman, acting chief engineer, and senior design engineer. He was appointed manager of the service department in 1923.

G. E. Sangster (A'43) recently lieutenant in the United States Naval Reserve, has been appointed sales development engineer by Sangamo Electric Company. He is a graduate of both Benjamin Franklin University and George Washington University and previously was valuation engineer with the Potomac Electric Power Company, Washington, D. C.

F. B. Powers (M'37) overseas traction manager, Westinghouse Electric International Company, New York, N. Y., has resigned to become vice-president in charge of operations and engineering of all divisions of Great American Industries. Mr. Powers will supervise production activities of the Connecticut Telephone and Electric division, Meriden, Conn.; Virginia Rubatex division, Bedford, Va.; the Rex division, New Rochelle, N. Y.; the War LaFrance division, Elmira, N. Y.; and the Rutland, Vt., division.

Albert Preisman (M'41) formerly director of engineering texts and consulting engineer, Capitol Radio Engineering Institute, Washington, D. C., has been appointed vice-president in charge of engineering. Mr. Preisman, who holds the bachelor of arts and electrical engineering degrees from Columbia University, has been with the Radio Engineering institute since 1943. Previously he was senior engineer with Federal Telephone and Radio Corporation.

W. R. Hutchins (A'42) who for the past several years has been associated with Major Edwin H. Armstrong in research and development work on frequency modulation and radar at Columbia University, New York, N. Y., and in Alpine, N. J., has been appointed manager of frequency modulation broadcasting activities of E. Anthony and Sons, New Bedford, Mass.

I. C. Eppley (A'43) formerly supervisor of electrical engineering, Dayton (Ohio) Power and Light Company, has been made assistant manager of the electrical engineering division. Mr. Eppley joined the company in 1924 as assistant electrical engineer. **H. E. Deardorff** (A'37) formerly supervisor, system planning engineering, is now manager of the electrical planning department.

F. E. Baker (A'40) formerly section engineer in the distribution transformer engineering division, Westinghouse Electric Corporation, Sharon, Pa., has been appointed section engineering manager in the newly created specialty transformer department at Sharon. Mr. Baker joined the Westinghouse corporation as design engineer after his graduation from Bucknell University in 1925. He became section engineer in 1940.

E. M. Haacke (A'45) formerly associate editor of *Electrical News and Engineering*, Toronto, Ontario, Canada, has been appointed editor. Mr. Haacke was graduated

from Queens University in 1942, and from 1942 to 1944 served as navigator and radar officer in the Royal Canadian Air Force. He joined the staff of *Electrical News* in 1945.

M. W. Locke (M '44) chief engineer of the Powerton station of the Commonwealth Edison Company, Chicago, Ill., has been appointed superintendent of the superpower department. He will continue in his present position and in addition have charge of the transmission and construction division of the superpower department.

J. W. Pomazal (A '40) formerly engineer in the engineering department, Kurz and Root Company, Appleton, Wis., has been named sales engineer in charge of all sales activities. Mr. Pomazal, who joined the company in 1945, previously was associated with Louis-Allis Company, Milwaukee, Wis. He is a member of the Engineers Society of Milwaukee.

R. H. Porterfield (A '44) resident field engineer, Allis-Chalmers Electrical Manufacturing Company, Providence, R. I., has been appointed manager of a new branch office of the company in Providence. Mr. Porterfield, who has been with the Allis-Chalmers company since 1939, is a graduate of the University of Nebraska.

Joseph Slepian (A '17, F '27) associate director of research, research laboratories, Westinghouse Electric Corporation, East Pittsburgh, Pa., recently received a 1945 fellow award of the Institute of Radio Engineers "in recognition of his contributions as scientist, engineer, and inventer to the field of electronics."

C. W. Hansell (A '23, M '44) research supervisor, transmission, RCA Laboratories, Radio Corporation of America, Rocky Point, N. Y., recently received a 1945 fellow award of the Institute of Radio Engineers "for his pioneer work in the development and application of equipment for the ever higher frequencies employed for radio communication."

A. L. Samuel (A '34) electronic research engineer, Bell Telephone Laboratories, Inc., New York, N. Y., recently received a 1945 fellow award of the Institute of Radio Engineers "for his fundamental work in the field of electronic reesarch and for development of electronic devices of particular value at very high frequencies."

F. J. Given (A '28) engineer, apparatus development department, Bell Telephone Laboratories, Inc., New York, N. Y., has assumed the additional duties of transmission apparatus engineer and as such will have charge of work on transmission transformers and power apparatus.

J. D. Lawrence (A '25) formerly district manager, Logan, W. Va., has been appointed assistant division manager of the Roanoke division of the Appalachian Electric Power Company, Roanoke, Va. Mr. Lawrence, who has been with the company since 1923, has been district manager at Logan since 1943.

J. J. Conners (A '40) formerly general sales manager, Irvington (N. J.) Varnish and Insulator Company, has been appointed vice-president and sales manager of the Bishop Gutta Percha Company, New York, N. Y., and the Peters Manufacturing Company, Wollaston, Mass.

R. W. Raine (A '42) formerly manager of the electrical design department, Robert and Company, Eglin Field, Fla., has joined the firm of Edward D. de Luca and Associates, consulting engineers, Jacksonville, Fla., as head of the electrical design department.

L. E. Hildebrand (M '21) formerly electrical engineer, General Electric Company, Lynn, Mass., has been appointed assistant designing engineer of the motor engineering division. Mr. Hildebrand has been with the company at Pittsfield and Lynn, Mass., since 1913. He is a graduate of Oklahoma Agricultural and Mechanical College.

J. M. Evans (A '20, M '28) electrical engineer with the United States Army Engineers, San Francisco, Calif., has been named supervising electrical and mechanical engineer for the Navy Bureau of Yards and Docks and as such will have supervision over installations in the 11th and 12th Districts which comprise California, Nevada, and Utah.

H. E. Hill (A '31) formerly lieutenant colonel, United States Army, has returned to Bell Telephone Laboratories, Inc., New York, N. Y. Colonel Hill at various times was stationed in Aberdeen, Md., Fort Bliss, Tex., Hawaii, and at the headquarters of the Central Pacific Base Command.

A. C. Schwager (A '24, F '44) formerly vice-president and chief engineer of the Pacific Electric Manufacturing Corporation, San Francisco, Calif., has accepted the position of president of the Schwager-Wood Corporation, Portland, Oreg., specializing in the manufacture of high voltage airbreak switches.

A. B. Paterson (M '22) president, New Orleans (La.) Public Service Company, has been awarded the New Orleans Times-Picayune loving cup "in recognition of his 15-year record of civic services" to his community.

L. B. Potter (A '45) formerly field engineer, The Detroit (Mich.) Edison Company, has been appointed utilization equipment and primary supply engineer of system engineering. Mr. Potter entered the employ of the company in 1928.

R. P. Lapsley (A '38, M '45) lieutenant colonel, United States Army Engineers, has been presented with the Legion of Merit for his outstanding performance of services as chief, Electrical and Utilities Service Section, Engineering Division, of the South Atlantic Division.

James Bisset (A '28) assistant superintendent of the meter bureau, Consolidated Edison Company of New York, Inc., Flushing, N. Y., has retired. Mr. Bisset had been with the company since 1910.

N. B. Phillips (M '34) formerly superintendent of the testing laboratory and services, Buffalo (N. Y.), Niagara Electric Corporation, has been appointed superintendent of the meter department. Mr. Phillips joined the company in 1909.

W. R. Le Page (A '34, M '44) formerly assistant director, radiation laboratory, Johns Hopkins University, Baltimore, Md., is now senior research engineer, Stromberg-Carlson Company, Rochester, N. Y.

C. G. Suits (M '41) vice-president and director of research laboratory, General Electric Company, Schenectady, N. Y., has been elected a member of the National Academy of Sciences.

W. J. Gilson (A '26, M '38) general manager, Eastern Power Devices, Ltd., Toronto, Ontario, Canada, has been appointed vice-chairman of the Canadian Council of Professional Engineers and Scientists.

W. R. Harmer (A '37, M '44) supervising industrial engineer, sales promotion department, Hydro-Electric Power Commission of Ontario, Toronto, Canada, has been elected secretary of the Association of Municipal Electrical Utilities.

H. G. Sherlock (A '39) formerly equipment engineer, Mountain States Telephone and Telegraph Company, Denver, Colo., has been appointed equipment and building engineer. Mr. Sherlock joined the company in 1926.

J. E. Lawson (A '22) vice-president and general manager, executive department, Canadian Niagara Power Company, Ltd., Niagara Falls, Ontario, has been elected a director of the company.

G. R. Mezger (A '37) formerly commander in the United States Navy, has rejoined the Allen B. DuMont Laboratories, Inc., Passaic, N. J., as manager of instrument sales. He entered the Navy in 1941 as lieutenant, junior grade.

R. G. McCurdy (A '16, F '34) director of electric apparatus development, Bell Telephone Laboratories, Inc., New York, N. Y., has added the supervision of groups on electrical measurements and magnetic studies and applications to his duties.

K. T. Compton (F '31) president, Massachusetts Institute of Technology, Cambridge, recently was awarded the Medal of Merit "for outstanding services to his country" in the development of microwave radar.

F. D. Newbury (A '07, F '21) vice-president of Westinghouse Electric Corporation, Pittsburgh, Pa., has been elected a member of the board of directors of the company.

F. E. Terman (A '23, F '45) dean of engineering, Stanford University, Stanford University, Calif., recently was elected to the National Academy of Sciences.

G. C. Hyde (A '11) president, Louisiana Public Utilities Company, Inc., Dallas, Tex., has been elected president of the Gulf Public Service Company, Inc., New Iberia, La.

N. R. Gibson (M '32) vice-president, Buffalo (N. Y.), Niagara, and Eastern Power Corporation, has been elected a director of the Canadian Niagara Power Company, Ltd.

Hugh Jack (A '21) chief of the a-c engineering department, British Thomson-Houston Company, Ltd., Rugby, England, has become a director of the company.

Vannevar Bush (A '15, HM '45) director of the Office of Scientific Research and Development, and president of the Carnegie Institution, Washington, D. C., recently was awarded the Public Welfare Medal of the National Academy of Sciences.

A. A. Schuhler (A '19, M '27) formerly commercial engineer, Federal Telephone and Radio Corporation, Newark, N. J., has been appointed New York (N. Y.) branch manager, Stanley and Patterson division, Faraday Electric Corporation.

F. D. Newbury (A '07, F '21) vice-president, Westinghouse Electric Corporation, Pittsburgh, Pa., has been elected a member of the company's board of directors.

F. E. Harrell (A '26, F '40) general works manager, The Reliance Electric and Engineering Company, Cleveland, Ohio, has been elected a member of the board of directors of the company.

A. C. Streamer (A '10, M '41) vice-president, Westinghouse Electric Corporation, Pittsburgh, Pa., recently was awarded the honorary degree of doctor of engineering, by the University of Colorado from which he was graduated in 1907.

Rufus Moses (A '28, M '42) formerly division manager of the Pennsylvania Power Company, Sharon, is now Youngstown division manager for the Ohio Edison Company. Mr. Moses had been with the Pennsylvania company since 1926.

F. M. Oglee (A '41) formerly Philadelphia (Pa.) district manager, Trumbull Electric Manufacturing Company, has been appointed manager of sales in the company's Norwood, Ohio, plant. Mr. Oglee has been with the company since 1929.

B. F. Campbell (A '30) recently lieutenant commander in the United States Navy, has returned to the Philadelphia (Pa.) office of the Rumsey Electric Company as substation and transmission engineer.

C. S. Redding (A '12, M '41) president, Leeds and Northrup Company, Philadelphia, Pa., has been elected a director of the Philadelphia Electric Company. He is also president of the Franklin Institute.

H. B. Bryans (M '17, F '18) executive vice-president of the Philadelphia (Pa.) Electric Company, recently was elected president of the Electrical Association of Philadelphia.

J. F. Gogins (A '40) manager, apparatus department, General Electric Company, Spokane, Wash., has been elected to the executive committee of the Spokane Chamber of Commerce.

E. W. Loomis (A '19) district manager, Westinghouse Electric Corporation, Philadelphia, Pa., has been elected vice-president of the Philadelphia Electric Association.

W. K. Scott (A '42, M '44) formerly assistant chief electrician, Columbia Steel Company, Pittsburg, Calif., has been appointed electrical supervisor of new construction.

F. A. Lewis (M '35) vice-president, Hooton Chocolate Company, Newark, N. J., has been elected a director of the company.

S. R. Inch (A '04, F '38) formerly president of Ebasco Services, Inc., New York, N. Y., is now vice-chairman of the company.

J. I. West (A '26) district manager, Litchfield (Conn.) Electric Light and Power Company, since 1923, has resigned.

OBITUARY • • • •

Frank Alfred Wolff (A '99, M '34) retired principal telephone engineer, National Bureau of Standards, Washington, D. C., died March 28, 1946. Doctor Wolff, who was born April 8, 1871, in Baltimore, Md., received the degrees of bachelor of arts in 1890 and doctor of philosophy in 1893 from Johns Hopkins University. Following that he spent a year studying at the University of Leipzig in Germany. In 1894 he joined the Bureau of Soils of the Department of Agriculture in Washington as expert physicist. He first became associated with the Office of Standard Weights and Measures, later the Bureau of Standards, in 1897 as a verifier. From 1894 to 1898 he also was professor of physics and electrical engineering at Columbia University. Doctor Wolff successively was associate physicist, physicist, and senior physicist, and in 1915 became chief of the telephone section. In 1938 he was titled principal telephone engineer, and in 1941 he retired. He was concerned particularly with the establishment of the present system of international electrical units and published many technical papers. He was detailed to the Federal Communications Commission from 1935 to 1937. Doctor Wolff was an expert on valuation of currency and in this connection appeared several times as a witness in Senate hearings. He was a member of the AIEE committee on communication from 1918 to 1941.

Walter C. Dixon (M '36) of the engineering department of the Central New York Power Corporation, Syracuse, died February 28, 1946. Mr. Dixon was born in Warner, N. Y., June 24, 1887, and was graduated from Syracuse University in 1909. His first position was that of draftsman for the Gould Coupler Company, Depew, N. Y. Except for a period in 1914 and 1915 during which he was employed by the Duquesne Light Company, Pittsburgh, Pa., on the design of substations, he was associated with the Westinghouse Electric and Manufacturing Company, East Pittsburgh, Pa., from 1912 to 1934. He was in the switchboard engineering department until in 1922 he was transferred to the general engineering department. In 1926 he was stationed in St. Louis, Mo., as general engineer for the company. He became utilities engineer in the Department of Public Utilities of the City of Memphis, Tenn., in 1934 and was transferred to the Memphis Light and Water Division in 1936. Mr. Dixon entered the engineering department of the Central New York Corporation in 1937.

Byron W. St. Clair (A '17, M '24) president and treasurer, Mico Instrument Company, Cambridge, Mass., died April 4, 1946. Mr. St. Clair was born March 14, 1892, and commenced his career in the meter department of the Louisville (Ky.) Gas and Electric Company in 1911. He changed position in 1912 to become tester and laboratory assistant with the General Electric Company, West Lynn, Mass., remaining there until he was commissioned ensign in the United States Naval Reserve in 1918. Upon his return to the General Electric Company in 1919 he was made engineer in charge of the standardizing laboratory and held this position until 1937. He was appointed president of the Mico Instrument Company in 1937 and treasurer in 1944. He formerly served on the AIEE committee on instruments and measurements.

Samuel Charles Margolin (A '32) assistant electrical engineer, Board of Transportation, City of New York, N. Y., died January 3, 1946. Born February 5, 1903, in Russia, Mr. Margolin was graduated from the College of the City of New York with the degree of bachelor of science in 1923. In 1924 he received the degree of electrical engineer from the Polytechnic Institute of Brooklyn. After a year as laboratory assistant for the Freed-Eismann Corporation, New York, he became junior draftsman with the Board of Transportation in 1926. He was made junior electrical engineer in 1927 and assistant electrical engineer in 1930.

Harry Lee Thomson (A '21) meter and appliance engineer, Hartford (Conn.) Electric Light Company, died March 24, 1946. Mr. Thomson was born February 17,

1887, in Thomson, N. Y. He finished a special electrical course at Rensselaer Polytechnic Institute in 1907 and the college course at the General Electric Company, Lynn, Mass., in 1910. He became assistant to the superintendent of lighting for the Hartford company in 1910 and superintendent of lighting in 1918. In 1933 he was appointed meter and appliance engineer. He was active on technical committees of the Edison Electric Institute and the Association of Edison Illuminating Companies, and on the AIEE committee on instruments and measurements from 1931 to 1942.

Mathias W. F. Zimmermann (M '43) electrical designer, Calco Chemical Division, American Cyanamid Company, Bound Brook, N. J., died March 23, 1946. Mr. Zimmermann, who was born June 17, 1910, in Weehawken, N. J., studied at Rutgers University. He was electrical draftsman in the plant engineering department of the General Cable Corporation, New York, N. Y., from 1928 to 1935. In 1935 he joined the American Cyanamid Company as electrical designer.

MEMBERSHIP...

Recommended for Transfer

The board of examiners, at its meeting of May 16, 1946, recommended the following members for transfer to the grade of membership indicated. Any objections to these transfers should be filed at once with the secretary of the Institute.

To Grade of Fellow

Bettannier, E. L., gen. mgr. & chief engr., Municipal Lt. & Pr. Dept., Pasadena, Calif.
Eastman, A. V., prof. of elec. engg., Univ. of Washington, Seattle, Wash.
Krupy, A. J., sr. engr., Commonwealth Edison Co., Chicago, Ill.
Lomax, C. E., dev. engr., Automatic Elec. Co., Chicago, Ill.
Parker, R. D., telegraph dev. director, Bell Telephone Labs., Inc., New York, N. Y.
Starr, J. H., dev. & mfgr. of elec. equip., 345 N. Spring Ave., LaGrange, Ill.
Winograd, H., engr. in charge, rectifier div., Allis-Chalmers Mfg. Co., Milwaukee, Wis.

7 to grade of Fellow

To Grade of Member

Atwood, A. W., Jr., elec. engr., Southern Calif. Edison Co., Los Angeles, Calif.
Berry, M. D., chief engr., Leland Electric Can., Ltd., Guelph, Ont., Can.
Cowgill, H. A., vice-pres. & div. mgr., Ohio Public Service Co., Port Clinton, Ohio
Dunlop, C. E., elec. supt., Perron Gold Mines, Ltd., Perron, Que., Can.
Ehret, E. L., dist. engr., Westinghouse Lamp Div., St. Louis, Mo.
Erwin, R. A., elec. engg. assoc., Dept. of Water & Pr., Los Angeles, Calif.
Ewald, E., traveling dist. engr., Northern States Pr. Co., Minneapolis, Minn.
Feist, D. N., asst. chief engr., Warner Elevator Mfg. Co., Cincinnati, Ohio
Groncki, J. J., design engr., General Elec. Co., Lynn, Mass.
Hale, K. M., test engr., Gas Turbine Lab., U. S. Naval Engg. Experiment Station, Annapolis, Md.
Halloran, J. J., production engr., Electro Engg. Works, Oakland, Calif.
Hunt, R. M., requisition engr., General Elec. Co., Pittsfield, Mass.
Kaufmann, H. A., elec. insp. & layout, National Cash Register Co., Dayton, Ohio
Koch, C. R., cons. elec. engr., 2690 Marty Way, Sacramento, Calif.
Lott, H. A., operating engr., Southern Calif. Edison Co., Ltd., Los Angeles, Calif.
Macintyre, J. R., dev. engr., General Elec. Co., Lynn, Mass.
Macphearson, J. F., proposition engr., General Elec. Co., Lynn, Mass.
Maloney, F. V., production engr., Texas Co., Los Angeles, Calif.
Matthews, N. W., engr., head, control systems subsection, U. S. Naval Lab., Washington, D. C.
Mead, M. S., Jr., asst. div. engr., general engg. & cons. lab., General Elec. Co., Schenectady, N. Y.
Miller, C. R., supt., water & elec. dept., Village of Winnetka, Winnetka, Ill.
Milner, M. L., Jr., asst. elec. engr., Illinois Pr. Co., Decatur, Ill.
Mitchell, J. E. M., elec. engr., Porcelain Products, Inc., Parkersburg, W. Va.
Moody, W. S., elec. engr., General Elec. Co., Los Angeles, Calif.
Phillips, G. H., engr., elec. conductor div., Aluminum Co. of America, Pittsburgh, Pa.
Rives, G. S., mgr., H. A. Kuljian & Co., Engrs., Los Angeles, Calif.
Sandlin, D. S., elec. engr., Dow Chemical Co., Freeport, Tex.
Sickel, E. C., substation elec. engr., Northern States Pr. Co., St. Paul, Minn.
Speer, P. B., elec. engr., engg. dept., Northern States Pr. Co., Minneapolis, Minn.
Stehlik, R. F., chief engr., Automatique Electrique, S. A., Antwerp, Belgium
Tandberg, L. G., branch mgr., Wagner Elec. Corp., Los Angeles, Calif.
Wages, R. W., div. ind. pr. engr., Georgia Pr. Co., Columbus, Ga.
Weinstein, H. L., elec. designer, A. Yarus & Sons, Inc., Philadelphia, Pa.
Whittenton, J. M., asst. design engr., elec. instrument div., General Elec. Co., Lynn, Mass.
Winchester, L. V., engr., Bucyrus-Erie Co., So. Milwaukee, Wis.
Worthen, P. A., General Elec. Co., cent. sta. engg., Salt Lake City, Utah

36 to grade of Member

Applications for Election

Applications have been received at headquarters from the following candidates for election to membership in the Institute. Any member objecting to the election of any of these candidates should so inform the secretary before July 15, 1946, or September 15, 1946, if the applicant resides outside of the United States or Canada.

To Grade of Fellow

Grosch, H., Norges Elektriske Materiellkontroll, Oslo, Norway

1 to grade of Fellow

To Grade of Member

Alvarez S., S., Empresa Nacional Calvo Sotelo, Madrid, Spain
Ames, F. H., Jr., General Elec. Co., Schenectady, N. Y.
Ayre, J., Naval Ordnance Depot, York, Pa.
Bennett, G. L., General Elec. Co., Schenectady, N. Y.
Braisted, L., Braisted and Bair, Detroit, Mich.
Bullwinkle, R., Texas Utilities Company, Dallas, Tex.
Burdette, L. W., J. E. Sirrine & Co., Greenville, S. C.
Carter, G. W., University of Oxford, Oxford, England
Davis, H. U., American Tel. and Tel. Co., Philadelphia, Pa.
Dillon, J. P., Public Service Co. of Ind., Inc., Indianapolis, Ind.
Dresser, D. S., Chicopee Mfg. Corp. of N. H., Manchester, N. H.
Duvander, B. H., Clyde E. Bentley, Oakland, Calif.
Eichmann, A. W., Glenn L. Martin Co., Baltimore, Md.
Eason, W. H., General Elec. Co., Pittsfield, Mass.
Gay, H. M., Oklahoma Gas and Elec. Co., Oklahoma City, Okla.
Goodison, A. M., Jr., Westinghouse Elec. Corp., E. Pittsburgh, Pa.
Halsey, T. R., Halsey & Royer, San Antonio, Tex.
Hamm, H. F., New York Naval Shipyard, Brooklyn, N. Y.
Hayward, D. W., Orlando Power Station, Johannesburg, South Africa
Hedgecock, W. A., Consumers Power Co., Flint, Mich.
Hills, D. A., The Austin Co., New York, N. Y.
Hollaway, R. B., The B. F. Goodrich Co., Borger, Tex.
Hotchkiss, C., Perfex Corp., Milwaukee, Wis.
Howard, R. V., The Associated Broadcasters, Inc., and Universal Research Labs., San Francisco, Calif.
Hutton, J. G., General Elec. Co., Schenectady, N. Y.
Kelley, H. W., Rural Electrification Administration, Washington, D. C.
Lightfoot, J. R., Naval Ordnance Lab., Washington, D. C.
Longmire, H. E., General Elec. Co., Detroit, Mich.
Lundberg, O. C., Capitol Elec. Co., San Diego, Calif.
Luttropp, E. S., 18 Lincoln Blvd., Hempstead, N. Y.
Mac Donald, M., Crane Co., Chicago, Ill.
Mackenzie, A. E., E. A. Schmidt & Co., St. Louis, Mo.
McBain, K. W., British Thomson-Houston Co. Ltd., Rugby, England
Mc Brayer, W. R., Westinghouse Elec. Corp., Louisville, Ky.
McKeel, Q. G., National Carbon Co., Inc., Cleveland, Ohio
Patton, J. H., Sangamo Elec. Co., Springfield, Ill.
Platt, E. R., Foster Transformers and Switchgear, Ltd., South Wimbledon, London, England
Prag, E. R., Carson Machine and Supply Company, Oklahoma City, Okla.
Reisinger, E. J., 9 Laurel Place, W. Caldwell, N. J.
Ryan, R. E., Office of Supervisor of Shipbuilding, Camden, N. J.
Rystedt, S. E., New Jersey Power and Light Co., Dover, N. J.
Schehl, C. A., General Elec. Co., Philadelphia, Pa.
Smith, R. J., Transcontinental and Western Air, Inc., Kansas City, Mo.
Sparke, H., Kirklee's Ltd., Tottington, Bury, Lanc's, England
Staples, J. M., Westinghouse Elec. Corp., Atlanta, Ga.
Stone, R. G., Sr., Tennessee Eastman Corp., Knoxville, Tenn.
Swannell, H. C., J. E. Sirrine & Co., Greenville, S. C.
Schwedes, W. F., Oliver Iron Mining Co., Duluth, Minn.
Tung, Y.-S., Calif. Inst. of Tech., Pasadena, Calif.
Vose, R. S., Bendix Aviation Corp., Philadelphia, Pa.
Ward, J. E., Consumers Power Co., Flint, Mich.
Watson, J. G., British Admiralty Delegation, Washington, D. C.
Weathers, L. C., Vickers, Inc., Detroit, Mich.
Werthmann, F. J., Werthmann Radio Company, Seattle, Wash.
Williamson, J. A., Hydro-Elec. Comm. of Niagara Falls, Niagara Falls, Ont., Can.
Withey, R. B., Consumers Power Co., Flint, Mich.
Wilson, J. M., Minneapolis Honeywell Reg. Co., Minneapolis, Minn.
Wood, E. K., Westinghouse Elec. Corp., E. Pittsburgh, Pa.
Zeh, G. J., U. S. Navy Department, Portland, Oreg.
Zobel, J. A., The Commonwealth and Southern Corp., Birmingham, Ala.

60 to grade of Member

To Grade of Associate

United States and Canada

1. North Eastern

Akeley, L. T., General Elec. Co., West Lynn, Mass.
Alspach, P. H., General Elec. Co., Schenectady, N. Y.
Andrews, G. M., General Elec. Co., Schenectady, N. Y.
Barnhart, S. S., Jr., General Elec. Co., Schenectady, N. Y.
Bartlett, G., General Elec. Co., Schenectady, N. Y.
Battista, L. M. (Re-election), Children's Village, Hartford, Conn.
Bishop, H. M., Raytheon Mfg. Co., Waltham, Mass.
Briggs, R. H., Eastman Kodak Co., Rochester, N. Y.
Chang, N., General Elec. Co., Schenectady, N. Y.
Clark, R. F., Westinghouse Elec. Corp., Boston, Mass.
Crenshaw, R. M., General Elec. Co., Schenectady, N. Y.
Dimond, H. M., General Elec. Co., Schenectady, N. Y.
Egnor, W. D., General Elec. Co., Schenectady, N. Y.
Fomenko, J. C., General Elec. Co., Schenectady, N. Y.
Harrington, D. B., General Elec. Co., Schenectady, N. Y.
Hart, W. E., Westinghouse Elec. Corp., Boston, Mass.
Henderson, S. D., Westinghouse Elec. Corp., Boston, Mass.
Horton, F. M., Buffalo Niagara Elec. Corp., Buffalo, N. Y.
Johnston, D., Jr., Sunshine Laundry Co., Hartford, Conn.
Leonard, E. H., Jr., Simplex Wire and Cable Co., Cambridge, Mass.
Lundberg, J. E., General Elec. Co., W. Lynn, Mass.
Luraschi, C. D., Buffalo Niagara Electric Corp., Buffalo, N. Y.
Martz, S. G., General Elec. Co., Schenectady, N. Y.
Metz, E., Bryant Elec. Co., Bridgeport, Conn.
Miller, E. H. (Re-election), W. P. Creager, Consulting Engr., Buffalo, N. Y.
Mitropoulos, T. N., Simplex Wire and Cable Co., Cambridge, Mass.
Morgan, J. M., Jr., General Elec. Co., Schenectady, N. Y.
Olson, S. E., Mass. Inst. of Tech., Cambridge, Mass.
Phillips, C. H., Eastman Kodak Co., Rochester, N. Y.
Pierce, J. L., Harvard University, Cambridge, Mass.
Pitts, L. E., Buffalo Niagara Elec. Corp., Buffalo, N. Y.
Prentice, W. H., General Elec. Co., Boston, Mass.
Rogers, P. R., General Elec. Co., Schenectady, N. Y.
Russell, W. E., Naval Shipyard, Boston, Mass.
Sheets, J., General Elec. Co., Schenectady, N. Y.
Spencer, L. B., Cornell University, Ithaca, N. Y.
Stomski, W. J., General Elec. Co., Schenectady, N. Y.
Stone, D. W. (Re-election), Boston Naval Shipyard, Boston, Mass.
Tulloh, C. A., Jr., General Elec. Co., Schenectady, N. Y.
Wade, R. W., Central Hudson Gas & Elec. Corp., Newburgh, N. Y.
Whitehead, H. S., General Elec. Co., West Lynn, Mass.
Wilson, R. M., Jr., General Elec. Co., Schenectady, N. Y.

2. Middle Eastern

Ackroyd, P. H., 34 Lewis St., Phillipsburg, N. J.
Ashdown, K. T., General Elec. Co., Philadelphia, Pa.

Bishop, C. K., Crise Manufacturing Co., Columbus, Ohio
Bramble, J. H., Westinghouse Elec. Corp., Sharon, Pa.
Buckhold, J. F., Clark Controller Co., Cleveland, Ohio
Bundry, O. M., The Clark Controller Company, Cleveland, Ohio
Carleton, J. T., Westinghouse Elec. Corp., E. Pittsburgh, Pa.
Clark, W. H., Naval Research Laboratory, Washington, D. C.
Davis, R. T., Plate Ice Co. & Corbett Package Co., Wilmington, N. C.
Dickason, R. J., The General Elec. Co., Erie, Pa.
Frost, H. J., Ohio Bell Tel. Co., Cleveland, Ohio
Guarino, L. S., Naval Air Experiment Station, Philadelphia, Pa.
Henson, R. J., General Elec. Co., Philadelphia, Pa.
Hernick, P. W., Westinghouse Elec. Corp., E. Pittsburgh, Pa.
Hunt, W. A., Philadelphia Elec. Co., Philadelphia, Pa.
Hurd, T. J., Rural Electrification Administration, Washington, D. C.
Jarrett, E. L., Duquesne Light Co., Pittsburgh, Pa.
Johnson, E. C., Chesapeake and Potomac Tel. Co., Charleston, W. Va.
Johnson, W. H., Phila. Elec. Co., Philadelphia, Pa.
Kelly, R. E., Westinghouse Elec. Corp., East Pittsburgh, Pa.
Kline, R. H., Westinghouse Elec. Corp., E. Pittsburgh, Pa.
Lee, C. K., 701 Shafor Blvd., Dayton 9, Ohio
Lindley, L. E., Jr., Sylvania Elec. Products, Inc., Emporium, Pa.
Middleton, W. W., Capt., 511 East Pitt St., Bedford, Pa.
Moore, H. D., General Elec. Co., Philadelphia, Pa.
Pink, J. F., E. I. Du Pont & Co., Wilmington, Del.
Piotrowski, E. T., Pennsylvania Transformer Co., Pittsburgh, Pa.
Pitcher, W. J., Dayton Power & Light Co., Dayton, Ohio
Reese, H. N., Baltimore Transit Co., Baltimore, Md.
Roberts, C. A., Jr., United Engrs. & Const., Inc., Philadelphia, Pa.
Robertson, H. E., Westinghouse Elec. Corp., Baltimore, Md.
Roylston, T. A., RCA Victor, Camden, N. J.
Schafrik, E. M., Clark Controller Co., Cleveland, Ohio
Schultz, V. W., Firestone Tire & Rubber Co., Akron, Ohio
Smitheman, E. W., Philadelphia Naval Shipbuilding Yard, Philadelphia, Pa.
Snider, R. T., Virginian Elec. Inc., Charleston, W. Va.
Tittermary, J. R., Philadelphia Elec. Co., Philadelphia, Pa.
Weller, R., Locke Insulator Corp., Baltimore, Md.
Wendling, L. W., Navy Dept., Bureau of Ships, Washington, D. C.
Wilson, H. T. (Re-election), Appalachian Elec. Power Co., Bluefield, W. Va.
Wittenberg, H. H., RCA Victor Division, Lancaster, Pa.

3. New York City

Bonahur, A. A., S. J. O'Brien, Inc., New York, N. Y.
Brosche, M. F., New York Tel. Co., New York, N. Y.
Brownman, H. L., Polytechnic Institute of Brooklyn, Brooklyn, N. Y.
Derman, J., Watson Labs., Air Technical Service Command, Red Bank, N. J.
Gezon, L. B., General Elec. Co., New York, N. Y.
Howard, J. J., Watson-Flagg Eng. Co., Inc., New York, N. Y.
Kline, A., Garod Radio Corp., Brooklyn, N. Y.
Melillo, V., Voorhees Walker Foley & Smith, New York, N. Y.
Miller, T. W., The Teleregister Corp., New York, N. Y.
Oxhandler, R., Board of Transportation, New York, N. Y.
Renton, V. S., Public Service Elec. & Gas Co., Newark, N. J.
Small, C. S., Baker and Spencer, Inc., New York, N. Y.
Tapley, J. G., Crocker-Wheeler Elec. Co., Ampere, N. J.
Thoma, H. G., The Linde Air Products Co., New York, N. Y.
Tobin, M., Syska & Hennessey, New York, N. Y.
Vitrogan, D., Brooklyn Polytechnic Institute, Brooklyn, N. Y.

4. Southern

Ellis, W. B., Duke Power Co., Greenville, S. C.
Farrell, J. M., Carolina Elec. Supply Co., Charlotte, N. C.
Halpern, W., U. S. Navy, Porstmouth, Va.
Henning, A. F., Jr., Geo. M. Meriwether, Industrial Equipment, Birmingham, Ala.
Kaluk, N. S., Tennessee Valley Authority, Memphis, Tenn.
Keithler, G. K., Jr., Lt., The Engineer School, Ft. Belvoir, Va.
Johnson, F. L., Southwestern Gas and Elec. Co., Shreveport, La.
Mc Iver, A. B., Southwestern Gas and Elec. Co., Shreveport, La.
Noland, J. H., Jr., University of S. C., Columbia, S. C.
Sander, W. A., Jr., U. S. Naval Shipyard, Charleston, S. C.
Walker, H. K., Tennessee Valley Authority, Wilson Dam, Ala.
Webb, J. F., Jr., Alabama Power Co., Birmingham, Ala.

5. Great Lakes

Bachman, R. H., Caterpillar Tractor Co., East Peoria, Ill.
Binek, E., 13751 Conley Ave., Detroit, Mich.
Black, K. G., Square D Co., Milwaukee, Wis.
Blackman, C. H., Burroughs Adding Machine Co., Detroit, Mich.
Bloch, W. C., General Elec. Co., Fort Wayne, Ind.
Bremner, W. C., Commonwealth Edison Co., Chicago, Ill.
Burnham, G. C., Allen-Bradley Co., Milwaukee, Wis.
Crampton, H. E., Michigan Bell Tel. Co., Detroit, Mich.
Dichman, E. W., (re-election). Northwestern Aero Corp., St. Paul, Minn.
Fenton, E. L., Veterans Administration, Minneapolis, Minn.
Fischer, P. M., Cutler-Hammer Corp., Milwaukee, Wis.
Gellatly, J. S., Western Elec. Co., Inc., Chicago, Ill.
Grant, J. W., Armour Research Foundation, Chicago, Ill.
Karl, D. R., 2616 South Adams St., Peoria, Ill.
Klein, B., Sargent & Lundy, Chicago, Ill.
Knapp, T. F., Lear, Inc., Grand Rapids, Mich.
Kochevar, J. S., Minnesota Power & Light Co., Duluth, Minn.
Kuester, A. J., Vern E. Alden Co., Chicago, Ill.
La Rose, A. P., Electra-Voice Corp., Chicago, Ill.
Lofquist, B. H., Caterpillar Tractor Co., E. Peoria, Ill.
Mactague, H. K., Guardian Elec. Manufacturing Co., Chicago, Ill.
McCauley, W. B., General Elec. Co., Fort Wayne, Ind.
Meyer, I., Appleton Elec. Co., Chicago, Ill.
Nemetz, V. W., Public Service Comm. of Wis., Madison, Wis.
Newman, E. N., Reynolds Metals Co., McCook, Ill.
O'Hare, E. F., Western Elec. Co., Chicago, Ill.
Parrott, J. R., Commonwealth Edison Co., Chicago, Ill.
Rehm, F. J., Commonwealth Edison Co., Chicago, Ill.
Roasa, H. L., Commonwealth Edison Co., Chicago, Ill.
Rosenkranz, H. G., Allen-Bradley Co., Milwaukee, Wis.
Sayles, H. W., 1219 Knoxville Ave., Peoria, Ill.
Schaudenecker, A. F., Western Elec. Co., Chicago, Ill.
Schneider, R. C., Illinois Power Co., Belleville, Ill.
Sherman, R. E., 411 Ludington Ave., Menominee, Mich.
Stearns, F. V., Western Elec. Co., Cicero, Ill.
Stratton, M. L., A.C. Spark Plug Division of General Motors, Flint, Mich.
Teasdale, R. D., Ill. Inst. of Tech., Chicago, Ill.
Thornberry, H. C., Allen-Bradley Co., Milwaukee, Wis.
Van Camp, F. E., Commonwealth and Southern Corp., Jackson, Mich.
Vinci, C. F., Rockford Machine Tool Co., Rockford, Ill.
Weinberger, S. M., Allis-Chalmers Mfg. Co., Milwaukee, Wis.

6. North Central

Ericksen, H. N., Nebraska Public Power System, Columbus, Nebr.
Weber, J. D., Mountain States Tel. & Tel. Co., Denver, Colo.

7. South West

Baird, J. W., Gulf States Utilities Co., Beaumont, Tex.
Beck, C. W., Aluminum Company of America, Dallas, Tex.
Boise, D. R., Allis-Chalmers Mfg. Co., San Antonio, Tex.
Bridler, F. W., El Paso Elec. Co., El Paso, Tex.
Bukovatz, J. E., Fairbanks-Morse & Co., Kansas City, Mo.
Coxe, W. D., Dow Chemical Co., Freeport, Tex.
Henderson, G. W., Dallas Power & Light Co., Dallas, Tex.
Hutto, R. L., U. S. Engineer Office, Little Rock, Ark.
Leach, C. C., Syndicate Trust & Century Bldgs., St. Louis, Mo.
Robertson, O. L., The Elec. Storage Battery Co., Dallas, Tex.
Smith, F. K., Westinghouse Elec. Corp., Houston, Tex.
Zimmer, H. I., Jr., El Paso Elec. Co., El Paso, Tex.

8. Pacific

Allen, M., United Aircraft Products, Inc., Los Angeles, Calif.
Anderson, S. C., Pacific Gas & Elec. Co., San Francisco, Calif.
Arnerich, P. F., Douglas Aircraft Co., Santa Monica, Calif.
Baker, L. S., Consolidated Vultee Aircraft Corp., San Diego, Calif.
Bullock, H. H., General Elec. Co., Phoenix, Ariz.
Clack, J. F., Arizona Edison Co., Bisbee, Ariz.
Dusterberry, J. C., Nat'l Advisory Comm. for Aeronautics, Moffett Field, Calif.
Erickson, T. W., Pacific Gas and Elec. Co., Oakland, Calif.
Estes, B. E., U. S. Naval Air Station, Alameda, Calif.
Gilcrest, G. B., General Elec. Co., San Francisco, Calif.
Glaser, W. D., General Elec. Co., San Francisco, Calif.
Hawley, P. F., Consolidated Engg. Corp., Pasadena, Calif.
Huska, P., Douglas Aircraft Co., El Segundo, Calif.
Marshall, W. C., USNR, F.P.O., San Francisco, Calif.
Mayfield, F. E., Standard Oil of Calif., Richmond, Calif.
McDermitt, G. S., Arizona Light & Power Co., Phoenix, Ariz.
Neiswander, R. S., Calif. Inst. of Tech., Pasadena, Calif.
Peterman, H. A., Hyperion Project, Los Angeles, Calif.
Phelps, A. H., Westinghouse Elec. Corp., Sacramento, Calif.
Pridemore, F. W., George Young Co., Los Angeles, Calif.
Sibley, S. L., Pacific Gas and Elec. Co., San Francisco, Calif.
Taylor, G. W., 1955-A Jackson St., San Francisco, Calif.
Wortman, J. W., Ens., USNR, Ames Aeronautical Lab., Moffett Field, Calif.

9. North West

Alexander, A. I., Westinghouse Elec. Corp., Portland, Oreg.
Anderson, R. W., Lt. (jg) USNR, Tacoma Group, Nineteenth Fleet, Tacoma, Wash.
Bredemeier, G. E., Portland General Elec. Co., Portland, Oreg.
Burns, T. W., Commercial Iron Works, Portland, Oreg.
Dillow, J. C., Westinghouse Elec. Co., Portland, Oreg.
Estberg, N. L., Bonneville Power Administration, Portland, Oreg.
Fromm, F. W., 13th Naval District, Headquarters, Seattle, Wash.
Jarrett, C. W., Portland General Elec. Co., Portland, Oreg.
Jower, J. W., Commercial Iron Works, Portland, Oreg.
Kall, W. I., Bonneville Power Administration, Portland, Oreg.
Lawrence, S. E., Abernathy Road, Oregon City, Oreg.
Lester, H. D., U. S. Navy (Civil), Portland, Oreg.
Lundquist, A. H., Bonneville Power Administration, Vancouver, Wash.
Lundquist, L. E., U. S. Navy, Portland, Oreg.
Miller, D. R., Portland General Elec. Co., Portland, Oreg.
Moreland, W. J., Westinghouse Supply, Portland, Oreg.
Nicholson, W. I., General Elec. Co., Portland, Oreg.
Osipovich, A. A., Bonneville Power Administration, Portland, Oreg.
Porter, J. D., Bonneville Power Administration, Vancouver, Wash.
Seymour, R. S., Bonneville Power Administration, Portland, Oreg.
Strand, L. E., Commercial Iron Works, Portland, Oreg.
Swarner, J. H. (Re-election), Bonneville Power Administration, Portland, Oreg.
Tatiz, R., Bonneville Power Administration, Portland, Oreg.
Udy, G. W., The Pacific Tel. & Tel. Co., Portland, Oreg.
Wagenknecht, M. A., Portland General Elec. Co., Portland, Oreg.

10. Canada

Coxon, P. A., Hydro Electric Power Comm. of Ont., Toronto, Ontario, Canada
Fraser, W. J. S., Dept. of Trade & Commerce, Dominion Govt., Vancouver, B. C., Can.
Karkheck, H., Mercury Mills, Hamilton, Ontario, Canada
Louie, J., Cemco Electrical Manufacturing Company, Ltd., Vancouver, B. C., Canada
Piirainen, G. O., Sudbury Hydro Electric Commission, Sudbury, Ontario, Canada

Elsewhere

Dahlberg, R. S., Jr., Creole Petroleum Corporation, Caracas, Venezuela, S. A.
de Amarante, E., Escola Nacional de Engenharia da Universidade do Brasil, Rio de Janeiro, Brasil, S. A.
Eliopoulos, E. T., The Sun Engineering Company, Cairo, Egypt
Garciatorres T., A., Mexican Light and Power Company, Ltd., Mexico D. F., Mexico
Gutierrez Gro., R., Mexican Light and Power Co., Mexico D. F., Mexico
Lowe, I., Wellington Technical College, Wellington, New Zealand
Ofverholm, H., A.S.E.A., Vasteras, Sweden
Perez, C. P., International Standard Electric, Buenos Aires, Argentina
Powell, J. E., State Hydro-Elec. Dept., Auckland, New Zealand
Qadri, N. H., The British Institute of Engg. Tech., London, England
Rabie, M. M., Ministry of Public Works, Cairo, Egypt
Rolfe, E., Capt., Royal Elect. & Mech. Engrs., War Office, London, England
Rouse, F. W. D., Admiralty Signal Establishment, Glossop, Derbys., England
Tidd, J. L., Helemano Receiver Site, Oahu, T. of Hawaii

Total to grade of Associate
United States and Canada, 219
Elsewhere, 14

OF CURRENT INTEREST

Improved Facsimile Systems Demonstrated for the Press

Two facsimile systems showing many advances over prewar models recently were demonstrated for the press in New York, N. Y. The Finch Telefax was on view at the American Newspapers Publishers meeting in the Waldorf Astoria, and the Hogan Faximile System was demonstrated in the laboratory of Radio Inventions, Inc. J. V. L. Hogan (M'20) is president of the firm manufacturing the latter equipment, and W. G. H. Finch (M'26) is president of Finch Telecommunications, manufacturer of the Telefax.

Both sets are capable of reproducing and transmitting any black and white copy—photographs, diagrams, printed or handwritten material, or tabular matter—with greater speed, clearer definition, and larger page size than models used either before the war or during the war in Government operations.

However, the Finch company concentrated on facsimile as a new means of communication specially useful to police, railroads, interplant and interoffice transmission, mining and other industries with remote installations, forestry services, aviation, department stores, and shipping. The Hogan demonstration was concerned mainly with its possibilities as a broadcasting medium for use in conjunction with radio.

Speeds of from 15 square inches per minute to 48 square inches per minute have been attained by the Finch machine for which deliveries to the general public are expected for the early fall of 1946. The over-all size of the combined sending and receiving unit is about that of a standard typewriter.

The wide diversity of copy presented at the Hogan demonstration, ranged from news pictures, matter to accompany household programs such as recipes and sample menus, weather maps, comments on musical numbers and pictures and life stories of composers, cartoons, crossword puzzles, instruction texts and reference reading for educational programs, and special bulletin newspapers, made up in half pages tabloid size. The programs included pages designed for association with sound programs as a means of amplifying their entertainment or educational values.

Copy comes out of the home recorder with type matter of newsmagazine size appearing much faster than it can be read. During the usual 15-minute broadcast, four pages of illustrated reference copy can be transmitted by frequency modulation radio and reproduced in the home, thus permitting a 15-minute newscaster on an amplitude modulation station, for example, to accompany his spoken word on an associated frequency modulation station with 4,000 words of printed text or four pages of maps, diagrams, and photographs. The format was selected to permit four column layouts of standard newspaper size.

All of this is accomplished by a simple mechanism for converting the received picture broadcasting signal to a black line proportionate to the intensity of the shading of the picture being transmitted. These lines are drawn transversely on a continuous roll of recording paper and blend into an accurate reproduction of any kind of written, printed, drawn or photographic information.

The recording paper turns black to a degree controlled by the moment-to-moment intensity of the picture signal being received. The Hogan system uses an electrochemical process for attaining the black which eliminates all photographic finishing, the use of ink, or paper surface burning often associated with facsimile operation.

At the broadcasting station the copy to be transmitted is progressively scanned by an electric eye through a lens system at the rate of 105 lines per inch with a horizontal definition equivalent to over 100 lines per inch. The copy at the transmitter is mounted on a cylindrical drum for submission to the optical system which scans or analyzes 28.1 square inches of copy per minute. The electric eye varies the intensity of the current as the changes in the light intensity submitted from the subject matter. The frequency of the picture signal thus produced varies from 7,000 to 13,000 cycles, suiting it to radiation by any frequency modulation broadcasting station. This is the maximum speed obtainable by reason of band-width limitations of frequency modulation broadcast frequency allocations, but it will be entirely adequate for home purposes, since 16 pages of copy can be reproduced each hour.

The home recorder is loaded with 400 linear feet of the specially treated paper, enough for 24 continuous hours of reception or two to four weeks of home service. Reloading the paper supply is comparable with loading a simple camera.

The received picture signal is delivered to the home recorder from any frequency modulation receiver capable of receiving regular frequency modulation sound broadcast. The recorder includes a small amplifier for bringing the signal up to the necessary levels to pass it through the recording paper.

The Faximile recorder which prints in the radio set owner's home is a little larger than a portable typewriter. It may be manufactured for mounting in its own cabinet to be attached to a radio set already in the home, or it may be built into a radio console by the manufacturer.

There are no rapid reciprocating mechanical motions in the mechanism; the electrical contact for passing the received picture signal through the paper is made from a printer blade over the paper to a wire helix mounted on a drum which rotates at the slow rate of 360 rpm, which it is claimed will prolong the life of the apparatus. All the user need do is to tune in the station desired, turn on the recorder, and adjust the volume control.

One model of the home type recorder shown at the demonstration was equipped with an automatic synchronizer which makes it unnecessary for transmitting scanner and recorder to rely on the same power system, a problem encountered in some cities having partly d-c power supply or competing a-c power systems. It is expected that this device will not be incorporated in all recorders manufactured, as it is unnecessary in 80 per cent of the United States.

It is possible to install scanners in mobile units together with photographic equipment for finishing and broadcasting photographs taken at spot news and sporting events. When mass production of recorders for sale to the general public will begin is a matter of conjecture. However, no one familiar with the situation at the demonstration would predict that recorders would appear for general sale in less than a year.

At the present time, it appears that facsimile schedules may begin in about 15 leading cities within the next six months, primarily with a view to developing presentation techniques and determining public reaction to them. Apparatus will be manufactured by the General Electric Company, and the first program explorations to determine public reaction are expected to begin early in the winter of 1946.

British Cable Plans Include One Global Rate

Complete public ownership of Cable and Wireless, Ltd., British communications monopoly, and a standard world ceiling rate for cable or wireless communications were included in plans for the future development of the communication industries recently made public by the British Government.

The Government will purchase all shares, of which it already owns eight per cent,

of the Cable and Wireless company. The company's assets also include substantial holdings in the Dominion and the Indian companies. With Parliamentary approval, a Commonwealth Communications Board will be established to replace the Commonwealth Communication Council set up in 1945, following the London Communications Conference.

A standard world ceiling rate of 30 cents a word for cable and wireless messages has been set as one of the Government's goals, in accordance with the Bermuda agreement of December 1945.

German and British War Lighting Topic for U. S. Committee of ICI

Reports on lighting practice and developments in England and Germany during the war were made to the first postwar annual meeting of the United States National Committee of the International Commission on Illumination, November 1, 1945. Observations made on trips through England and Western Europe in the summer of 1945 were presented by Samuel G. Hibben (M '45) director of applied lighting, lamp division, Westinghouse Electric Corporation, Bloomfield, N. J.; and J. L. Kilpatrick (A '09) New York, N. Y.

Predictions of an expansion of fluorescent lighting in England stimulated by the necessity of fuel conservation and the urge to modernize the lighting of industry were made. High intensity mercury lighting also seems destined for considerable expansion, according to the reports. This was given a prewar tryout in both Germany and England, and a noticeable growth of mercury street and highway lighting has occurred in the British Isles. A wider variety of wattage sizes than are now standard in the United States have been used. High mounting, prismatic glassware control, and some serious problems of glare are involved in the installations.

Among the wartime casualties were tinted incandescent lamps, except those used for blackout purposes, and sodium and mercury installations which were discontinued in Germany and neighboring countries subject to bombing because of their peculiar color.

Applications of interior treatments to benefit lighting, such as hand painting machine tools and the use of colors designed to facilitate safe handling, still appear to be lacking in Western Europe.

Wartime automobile lighting in Germany concentrated upon the use of one driving headlamp mounted in the center or on the mudguard at the left side at the height of the regular headlamp. Statistics in England indicate that street traffic accidents increased because of dimout, in spite of curtailed vehicular traffic. A slight increase in illumination tended to increase the number of pedestrians and therefore the number of accidents.

By August 1945 most of England's street lighting was back to prewar conditions and functioning on regular schedules. In June most of the suburban and residential areas of German cities were supplied electric service for homes and residence lighting was in good shape, with reduced wattages of bulbs but with fittings comparable in quality and illumination supplied to those of the average middle class American home.

Street lighting in Germany conformed to international practice, but close spacing, high mounting, and sharp cutoff provided easier seeing conditions than those usually found in the United States.

Most of the technical high schools (colleges) in Germany conducted courses in illumination and awarded degrees in that study.

Both observers emphasized that in Germany all lighting standards and practice deteriorated progressively with the increase in bombing activity, until by the end of the war, local lighting from adjustable reflectors was most prevalent for industrial operations and bare incandescent lamps and exposed wiring were used for the little general illumination in operation.

In general, there was very little progress in the field of illumination in Germany during the war. Lighting research was primarily for blackout purposes and improvement of searchlights. In Mr. Kilpatrick's opinion the greatest obstacle to gleaning any data of real import lay in the fact that Berlin was the fountainhead of lighting knowledge in Germany and all worth-while equipment and personnel in all branches of industry were removed by the Russians prior to occupancy by British–American forces. Considerable work had been done in the infrared field in connection with radar development. There was a reported development of a 15-kw air-cooled mercury vapor lamp, but this was one of the Berlin items which had been removed.

Other matters discussed at the ICI meeting pertained to action needed to re-establish the smooth working of the international organization disrupted by the war. It was decided to propose to the central bureau of the ICI that of the Secretariats assigned to Germany in 1939 the United States National Committee take over the responsibility for colorimetry, lighting education, and the lighting of motion picture houses. It was thought that Great Britain would wish to take over the subject of natural daylight.

It was reported that organization is under way of the International Standards Co-ordinating Association, first meeting of which was held in London, England, May 27, 1946. As standardization is only a minor activity of the ICI, the United States committee agreed that there is no reason for the ICI to be dissolved and become a section of the new association, as has been suggested. The ICI will participate in the work of the association, however.

Distribution of copies of the unofficial version of the 1939 *Proceedings* of the ICI was considered, and it was voted to mail two copies to each national committee.

It also was decided to recommend that in future ICI *Proceedings* English be adopted as the official language.

It was learned that the Germans had issued two volumes of *Proceedings* of the 1939 sessions, copies of which are in the hands of some delegates to the last ICI meeting. None of these has reached the United States committee.

Preston S. Millar (M '13) president of the committee, presided and Doctor N. A. Halbertsma, of Holland who was elected president of the ICI in 1939, addressed the meeting on conditions in Europe and what the United States committee might do to assist in the revival of international lighting activities.

Others present at the meeting were:

D. W. Atwater (A '34), A. A. Brainerd, F. C. Breckenridge, A. D. Cameron, C. B. Conway (A '44), E. C. Crittenden, Hawthorne Deming, C. D. Fawcett (M '20), W. F. Forsythe, Ward Harrison (F '36), B. J. Hensen, W. C. Kalb (F '40), G. H. Stickney (F '24), F. V. Westermaier.

Silver Supply for Industry Nears Vanishing Point

The estimated production of silver for 1946 will be 44 per cent below the prewar level, which represents less than one quarter of that needed by American industries, according to a recent statement by the Silver Users Emergency Committee advocating Senate action on bills authorizing treasury sale of some surplus metal to industry.

The supply of the metal available to the silver using industries generally this year has varied from around 30 per cent of the volume needed in January to less than five per cent of requirements for some industries in April, the committee states. This worsening situation is attributed to the efforts of Senators from the silver-producing states to block consideration of the bills passed by the House of Representatives which would release some of the Treasury's stock of free silver for purchase by industry.

The silver bloc in the Senate meanwhile has been crusading to force the price of silver, whether for industrial or monetary use, to $1.29 an ounce. The present ceiling price is 71 cents, and the prewar level was about 35 cents.

Electric equipment industries will need 10 million ounces of silver in 1946. The cost of the year's supply at the present ceiling would be $7,100,000, and the proposed increase in price would add $5,800,000 to this bill.

No relief can be expected from foreign sources while Senate action is pending, as foreign owners are hoarding available supplies in the hope of a price advance.

CIGRE Resumes Sessions in Paris June 27 to July 6

The first plenary session since 1939 of the International Conference on Large Electric High-Voltage Systems (Conference Internationale des Grands Réseaux Electriques à Haute Tension) will be held in Paris, France, as is customary, from June 27 to July 6. Of the 100 technical papers to be presented, 10 are expected from United States authors. This is a better representation than at the 1939 session when only 5 of the 117 papers were of United States authorship.

Established in 1921 as a permanent international association, the Conference provides an international exchange of engineering information relating to the design, construction, and operation of large high-voltage electric systems. Biennial sessions are held in Paris, headquarters of the organization, at which delegates from all participating countries present and discuss technical papers and at which the international technical committees appointed by the CIGRE submit reports on results of interim studies. Anyone who complies with the conditions of membership may participate in these meetings subject to the permission of the national committee for his country.

Though not all the problems discussed are new in the United States, the extension of higher voltages and large interconnected systems in all parts of the world has developed operating experiences which are of value to American engineers engaged in the design and operation of similar systems. United States engineers engaged in the design of apparatus, equipment, and devices entering into these systems also are afforded a broad view of trends in engineering design throughout the world and the opportunity to disclose the merits of their own design and practice.

Also, since the proceedings, discussions and findings of CIGRE are submitted to the International Electrotechnical Commission for its consideration in the establishment of international electrical standards, the CIGRE sessions offer a valuable opportunity to American engineers and agencies interested in standards to take part in the preliminary and formative discussions incident to the CIGRE sessions.

The continuity of the work of the Conference between sessions is ensured by international technical committees. The 14 at present in existence are:

A-c transmission at extra high voltage, chairman, Philip Sporn (F '30); d-c transmission, chairman, Mr. Borgquist of Sweden; insulation materials; underground cables, chairman, Mr. Bakker of Holland; insulation oils, chairman, Mr. Weiss of France; circuit breakers, chairman, Mr. Juilard of Switzerland; improvement of power factor; surges, chairman, Mr. de Binuesa of Spain; insulators, chairman, Mr. Van Cauwenberghe of Belgium; co-operation with international telephone consulting committee, chairman, Mr. Charpentier of France; overhead conductors, chairman, Mr. Jacobsen of Norway; towers and foundations, chairman, Mr. Lavanchy of Belgium; mechanical calculations of lines, chairman, Mr. List of Czechoslovakia; and telephone and radio interference.

CIGRE also maintains national committees of the countries participating in its activities. These enroll memberships, assign and review technical papers for the sessions, and appoint members of the technical committees. The United States National Committee follows:

Frederic Attwood (M '27), J. C. Parker (F '12), I. W. Gross (F '45), Philip Sporn, W. W. Lewis (F '38). J. B. Whitehead (F '12), W. S. Peterson (M '29), P. L. Bellaschi (F '40), E. L. Moreland (F '21), M. S. Oldacre (M '42), Stanley Stokes (F '29), L. N. McClellan (F '38), S. H. Mortensen (F '20), Walker L. Cisler (M '35), William E. Wickenden (F '39) *ex-officio*, H. J. Scholz (M '39), H. L. Melvin (F '31), T. J. Little (M '45), Gano Dunn (HM '45).

Memberships in the United States may be individual or collective. In the first category regular members pay annual dues of $10 and associate members pay $5. Collective memberships may be sustaining, regular, or associate. For industrial, manufacturing, and consulting engineering companies, financial companies, public agencies of commercial character, universities and other institutes of learning or research, and all other noncommercial collective bodies the annual dues are $500, $100, and $50, respectively for the three grades of membership. Government and other public administrations and agencies and technical associations pay $1,000, $200, or $100 annually.

All individual members receive advance copies in English of all technical papers presented at the biennial sessions. All collective members receive copies of the bound proceedings in English.

Formal recognition of the CIGRE association and its biennial sessions is given by the State Department through the appointment of an official delegation to represent the United States Government, selected from the United States delegates attending the biennial sessions.

Registration by Endorsement Provided by National Bureau

The procedure and purpose of the registration service rendered engineers by the National Bureau of Engineering Registration is described in a recent information pamphlet issued by the Bureau. The Bureau was established primarily to minimize the effort and expense of engineers desiring to secure registration or license in more than one state.

Operated by the National Council of State Boards of Engineering Examiners, the Bureau is under the direction of a standing committee of the Council with an advisory board of representatives from national engineering societies. A secondary purpose of the Bureau is to act as a clearing house for state registration authorities, employers, societies, and others, acting as a reliable source of verified information regarding the professional records of engineers.

Endorsement by the National Council as well as by a state board usually means that an application for registration in various states will be expedited and promptly approved. To obtain such endorsement an

Classroom Mural to Inspire Freshmen



This representative engineering student surrounded by typical end products of his training is depicted in a four by eight foot photographic mural recently hung on the wall of the engineering drawing classroom at Cooper Union, New York, N. Y.

engineer files an application for a certificate of qualification with the National Bureau of Engineering Registration which will secure the endorsement of the state board of registration of his home state and, after verifying the professional record of the applicant will affix its endorsement, and the seal of the National Council.

The bylaws of the National Council and the registration laws or regulations of most states specifically provide for recognition of certificates of qualification issued by the Bureau, and all member boards of the Council accept certification by the Bureau, with endorsement by a state board as competent evidence of qualification for registration. However, all state boards reserve the right to take whatever action they deem necessary to conform with the requirements of their laws and regulations in connection with any application for registration in their state.

Any registered engineer desiring a certificate of qualification must submit to the Bureau on its prescribed form his complete record, including education, engineering experience, legal registration, technical examinations, membership in professional or scientific societies, and character and professional references.

This application then is submitted by the Bureau to the registration board in the state of which the applicant is a resident or in which he is practicing. The Board may require the applicant to furnish additional information or to pass an examination to establish his competency. Once this is established, the Board endorses the certificate of qualification to the effect that the applicant is entitled to be recommended to other state boards for registration. At this point the Bureau makes an independent investigation of each item in the applicant's record, verifying them or giving reasons for not doing so.

After this, the Bureau evaluates the professional record of the applicant and issues a certificate of qualification, if he meets the requirements of one of the following sections.

Graduation Plus Experience. Graduation from an engineering curriculum accredited by the Engineers' Council for Professional Development, and a specific record of eight years or more of experience in engineering work of a character satisfactory to the Bureau. Where the evidence presented does not appear to the Bureau conclusive, the applicant may be required to present further evidence for the Bureau and to pass examination (given by the registration board in his home state).

Examination Plus Experience. Successfully passing an examination (given by the registration board in his home state) designed to show knowledge and skill approximating that attained through graduation from an accredited engineering curriculum; and a specific record of eight years or more of experience in engineering work of a character satisfactory to the Bureau.

Long Established Practice. A specific record of 15 years or more of lawful practice in engineering work of a character satisfactory to the Bureau, provided the applicant is not less than 35 years of age.

Demonstration of applicants' competency will be based less on length of experience (provided the minimum is met in each case) than on the breadth, quality, and importance of pertinent experience, degree of progression, evidence shown of ability to accept increasing responsibilities, and of the possession of personal qualifications required for successful engineering work.

The fee for investigation, verification, and certification, including one photostatic copy of completed verified professional record, certificate of qualification, and state board endorsement is $20. Additional copies are $2 each. These fees represent actual cost of the work involved, as the Bureau is a nonprofit agency.

Engineers desiring legal registration or license in any state must communicate directly with the state board in question and secure its application form and regulations. Applications for registration by endorsement must be accompanied by photostatic copies, issued by the Registration Bureau, of certificates of qualification.

Members of the committee on National Bureau of Engineering Registration are:

L. M. Martin, chairman, representing the committee on qualifications for registration; C. C. Knipmeyer, (M '35), Indiana, representing the committee on Engineers Council for Professional Development; Roy M. Green, Nebraska, representing central zone; Joseph Weil (F '36), Florida, representing southern zone; A. G. Christie, Maryland, representing northeast zone; Daniel B. Jett, New Mexico, representing western zone; T. Keith Legaré, South Carolina, executive secretary, National Council of State Boards of Engineering Examiners.

Members of the advisory board are: American Society of Civil Engineers, Allen P. Richmond, Jr.; American Society of Mechanical Engineers, William G. Christy; AIEE, C. R. Beardsley (F '30); American Institute of Chemical Engineers, J. M. Weiss; National Society of Professional Engineers, Arthur V. Sheridan; Society for the Promotion of Engineering Education, Paul Cloke (F '38); American Association of Engineers, C. J. Ullrich; American Railway Engineering Association, R. E. Warden.

Army Used Infrared Radiation to Detect in Total Darkness

The use of infrared radiation for observation in total darkness by the United States Armed Forces, another of World War II's secret weapons, was revealed recently by the United States Army upon information that the Germans had utilized similar, though inferior and less effective, equipment.

The device is available in two models, a "sniperscope" mounted on a 30 caliber carbine and a "snooperscope," a hand model used for observation and signaling. The equipment employs a light source which, through filters, cuts out the "visible light" of the spectrum and transmits infrared radiation. The reflected infrared radiation is picked up by the objective lens of a telescope and focused on a photoelectric image tube. When the infrared rays strike this tube, electrons are released in direct proportion to the intensity of the radiation and, as all electrons possess a negative charge, the released electrons are attracted by the positive plates. These electrons are accelerated as they pass through the tube to bombard a fluorescent screen and thus produce a visible image corresponding to the infrared image on the front screen.

The device is operated by focusing it in the desired direction and moving it back and forth until the object is picked up by the invisible radiation. The visible image can be seen in the telescope by the operator who then may sight his gun.

Power packs for the device were manufactured by Electronics Laboratories, Inc., Indianapolis, Ind.; photoelectric tubes by Farnsworth Television and Radio Corporation, Fort Wayne; and telescope lenses by Bell and Howell Company, Chicago, Ill.

U. S. Engineers Resume Work on Southwest Flood Control

Temporarily suspended by the war emergency, flood control projects in the Southwest are again under construction, the office of the Southwestern Division Engineer, of the United States Corps of Engineers recently announced.

The first project upon which work has been resumed is the Canton Dam project, a $5,192,623 undertaking, on the North Canadian River above Oklahoma City, Okla. Work on Canton Dam was 25 per cent completed when it was placed in a stand-by status at the beginning of the war. When completed, the dam will create a reservoir with a total storage capacity of 390,000 acre-feet of water and will cover an approximate area of 15,500 acres. The dam will be 14,300 feet long, 32 feet wide at the crest, and 68 feet above the valley floor.

In addition to the Canton Dam the projects include: Wister Dam and reservoir on the Poteau River near the Oklahoma–Arkansas state boundary; the Fort Gibson Dam and reservoir on the Grand (Neosho) River near Muskogee, Okla.; the Hulah Dam and reservoir on the Caney River near the Oklahoma–Kansas state boundary; completion of the existing John Martin Dam and reservoir on the Arkansas River near Las Animas, Colo., by the installation of spillway gates; the Blue Mountain Dam and reservoir on the Petit Jean River west of Little Rock, Ark.; the Bull Shoals Dam and reservoir on the White River near the Arkansas–Missouri state boundary; the Clearwater Dam and reservoir on the Black River in southeast Missouri; the Fall River Dam and reservoir on a major tributary of the Verdigris River in Kansas; the Addicks Dam on Buffalo Bayou in Texas; and the completion of riprap protection to the existing Denison Dam near Denison, Tex.

Each of the projects is a unit in the comprehensive plan for development of flood control on major watersheds in the Southwestern Division. Although primarily designed for flood control, many of the works are planned for multiple purposes such as production of hydroelectric power, navigation, irrigation, abatement of pollution, industrial and domestic water supply, recreation, and conservation of wildlife. The Fort Gibson project, for flood

control and hydroelectric power production, consists of a concrete dam 2,850 feet long with its crest 110 feet above the stream bed. At elevation 582 feet above sea level, top of the flood-control pool, the reservoir will have a total storage capacity of 1,287,000 acre-feet. This capacity will be divided into 922,000 acre-feet for flood control and 365,000 acre-feet for power storage.

For both flood control and hydroelectric power, the Bull Shoals Dam will provide a large reservoir for recreation and wildlife as well as benefits to navigation. The dam will be a concrete structure, an overflow spillway will be located on the right side of the flood plain, and the nonoverflow section on the left. Flows will be regulated by radial crest gates.

War Department Seeks Aid in German Industry Surveys

The United States War Department is seeking the co-operation of American industry in its investigations of German industry. The Department wishes assistance in selecting and microfilming in Germany data that may be valuable to American science and industry. Suggestions about specific information which American companies would like to have from Germany, about where valuable information might be found, and about what industries in Germany might possess information not now available are wanted.

Help also is needed in recruiting personnel for the work of searching German files. Qualified American technicians are indispensable for the job of supervision and selection. Technical men are needed in the following fields: chemicals, aeronautics, automotive, machine tools, general industrial equipment, fuels and lubricants, metals and minerals, communications equipment, scientific instruments, shipbuilding, and textiles.

A knowledge of German is essential. Appointments are subject to Civil Service approval and are made for a minimum of six months. Any industry or scientific group interested in specific German industrial methods and able to assign personnel to visit Germany should write John C. Green, executive secretary, Office of the Publication Board, Department of Commerce, Washington 25, D. C.

Arthur B. Berresford, Engineer–Doctor, Dies

Arthur Beattys Berresford, former engineer and member of AIEE, who had been practicing as a physician since 1936, died April 16, 1946, in New York, N. Y. Doctor Berresford was 42 years of age and a resident of Ithaca, N. Y. He was the son of the late AIEE Past President A. W. Berresford.

When he finished his internship in the Waterbury (Conn.) Hospital in 1936, Doctor Berresford became a general practitioner in Ithaca. From 1942 to 1944 he was a research fellow in the department of allergy of the Roosevelt Hospital, New York, N. Y. He wrote several articles on allergy and was coauthor with A. B. Sperling of the book, "Know Your Hay Fever." His article, "Musings of an Engineer–Doctor," was published in *Electrical Engineering*, June 1945, pages 212–14. Doctor Berresford held the degrees of bachelor of arts and electrical engineer, as well as his medical degree.

Electrical Engineers Needed by Army Security Agency

The Army Security Agency, Arlington, Va., reports an urgent need for graduate electrical engineers, including electronic specialists, to undertake vital research and development work. The openings have been created by demobilization of military personnel. Base pay, depending on education and engineering experience, ranges from $2,650 to above $5,000 per annum. These are Federal Civil Service appointments, with a 40-hour work week, 26 days annual leave, and 12 days sick leave.

Arlington, Va., is a suburb of Washington, D. C. Room in a private home will be reserved in advance for employees. Application should be made only by American citizens on Federal Employment Form 57 (available at all Post Offices) and forwarded to: Chief, Personnel and Training Branch, WDGSS-61, Army Security Agency, The Pentagon, Washington 25, D. C.

Veterans Request Catalogues. The Veterans Administration Construction Service, 900 North Lombardy Street, Richmond, Va., desires to receive catalogues of materials and equipment from manufacturers and jobbers, covering general building construction, electric heating, ventilating, plumbing, refrigeration, air conditioning, outside utilities, waterworks, and sewerages.

JOINT ACTIVITIES

Doctor Craver Receives Certificate. At a dinner given in his honor May 22, 1946, Doctor Harrison W. Craver, retiring director of the Engineering Societies Library, New York, N. Y., received a certificate of appreciation of his services signed by the presidents of the Founder Societies. The certificate reads:

Harrison Warwick Craver has served as director of the Engineering Societies Library from 1917 to 1946. One of his first tasks was to consolidate into a single collection the libraries of the Founder Societies which had been maintained as separate collections up to that time. He also undertook and completed over a period of years a card catalog of these combined libraries. Through the institution of translation, abstracting, photostatic, and loan services, he gave the library national scope.

His skill as a librarian, his knowledge of applied science and engineering, his sound judgment, his zeal for his work, and his unfailing courtesy have combined to provide an unequalled library service for the engineers of the nation.

In token of its appreciation, the governing body of each of the Founder Societies, whose combined libraries constitute the Engineering Societies Library, has entered this minute on its official records.

Cleveland Council Guides High School Students

For the second successive year, the Cleveland Technical Societies Council recently devoted two evening sessions to counseling high school students, with the AIEE Cleveland Section a prominent participant.

Junior and senior high school students from public, private, suburban, and parochial schools in the Cleveland area were invited to attend a meeting covering the engineering and associated professions in a general way. Later the students were divided into smaller groups which dealt with the specific fields of their interest.

The general meetings were addressed by A. T. Colwell, vice-president, Thompson Products, Inc., Cleveland, on "The Application of Fundamentals in Practical Engineering." The electrical engineering group was led by D. E. Inman (M'45) engineering and service manager in the Cleveland district for the Westinghouse Electric Corporation. The panel of counselors for the electrical group was composed of:

L. T. Blaisdell (F '39) commercial vice-president, General Electric Company; W. H. Chase (M '42) chief engineer, Ohio Bell Telephone Company; C. C. Dash (M '39) president, Hertner Electric Company; W. C. Davis (A '35) professor of electrical engineering, Fenn College; W. R. Hough (M '41) chief engineer, Reliance Electric Company; J. R. Martin (A '35) associate professor of electrical communication, Case School of Applied Science; C. N. Rakestraw (M '21) supervisor, employees training, Cleveland Electric Illuminating Company; H. P. Sherer (M '45) chief engineer, Hertner Electric Company.

Before the meetings pamphlets briefly defining the engineering profession and its various branches were distributed to the high schools. Students planning to attend were asked to fill in cards indicating the branch of engineering in which they were specially interested, the points they would like discussed, and the name of any adult who would accompany them.

In addition to the one on electrical engineering, the following discussion groups were provided: architecture, chemical engineering, chemistry, civil engineering, mechanical engineering, metallurgy, and physics. The Cleveland Council has a membership of 35 organizations.

OTHER SOCIETIES

Quality Control Society Founded. The American Society for Quality Control was established at a meeting held February 16, 1946, in New York, N. Y., as a national society for those interested in industrial quality control. Representatives of 17 local societies organized during the war in various parts of the United States attended

Future Meetings of Other Societies

American Chemical Society. National Chemical Exposition, September 10–14, 1946, Chicago, Ill.

American Society for Testing Materials. Annual meeting, June 24–28, 1946, Buffalo, N. Y.

American Society of Mechanical Engineers. Annual meeting, June 17–20, 1946, Detroit, Mich.

American Welding Society. Annual meeting, November 17–22, 1946, Atlantic City, N. J.

Canadian Electrical Association. Annual meeting, June 26–28, 1946, Banff, Alberta, Canada.

Illuminating Engineering Society. National convention, September 18–21, 1946, Quebec, Quebec, Canada.

Instrument Society of America. Exhibit and conference, September 16–20, 1946, Pittsburgh, Pa.

International Conference on Large High-Voltage Networks. June 27–July 6, 1946, Paris, France.

National Electrical Manufacturers Association. June 17–19, 1946, Hot Springs, Va.

National Electrical Contractors Association. Annual meeting, October 14–18, 1946, Atlantic City, N. J.

National Electronics Conference. October 3–5, 1946, Chicago, Ill.

Refrigeration Equipment Manufacturers Association. Fourth refrigeration and air conditioning exposition, Cleveland, Ohio, October 29–November 1, 1946.

Television Broadcasters Association, Inc. Second conference and exhibition, New York, N. Y., October 10–11, 1946.

the first meeting. Purpose of the society will be the advancement and diffusion of knowledge of the science of quality control and its application to industrial progress. A magazine, *Industrial Quality Control*, originally published by the Buffalo, N. Y., society will be issued bimonthly. Professor Martin A. Brumbaugh of the University of Buffalo will be chairman of the editorial board. The first officers elected by the new society are:

President: George D. Edwards (M '26) director of quality assurance, Bell Telephone Laboratories, Inc., New York.

Vice-president: Andrew I. Peterson (A '23) manager of quality control, RCA Victor Division, Radio Corporation of America, Harrison, N. J.

Executive secretary: Ralph E. Wareham, manager, new products division, National Photocolor Corporation.

Treasurer: Alfred L. Davis, Rochester (N. Y.) Institute of Technology.

Valor Awards Re-established by EEI. Announcement of the reinstatement of its annual Claude L. Matthews Valor Awards, suspended during the war, has been made by the Edison Electric Institute. The awards honor "acts of devotion to duty wherein extraordinary courage has been exercised in efforts to maintain or restore important electric service in the shortest possible time." Any employee of a public utility, either publicly or privately owned, is eligible for the first postwar award, provided his deed of valor was performed during the calendar year of 1946. This is a departure from prewar practice as previously only employees of privately owned companies were considered. Recommendations for the awards must be made by the chief executive of a company and must be forwarded to the secretary of the Edison Electric Institute not later than April 1, 1947. Three cash awards of $150 are made, and an appropriate lapel emblem and citation accompanies each.

Fire Protection Association Observes 50th Anniversary

With its annual meeting in Boston, Mass., June 3–7, 1946, the National Fire Protection Association celebrates 50 years as international clearing house for authoritative information on the subject of fire protection and fire prevention. The association, which was established in Boston in 1896 as a noncommercial, nonprofitmaking organization, today includes more than 150 national organizations and 10,000 individuals in 37 countries in its membership. Although the majority of its members are recruited from industry, membership is open to any individual or organization interested in the protection of life or property from fire.

During the 50 years of its existence, a prime function of the NFPA has been to provide nearly 150 technical standards and other popular and technical literature in the field of fire waste control. Since 1923 the association has maintained a field service to make direct contact with states, provinces, and cities throughout the United States and Canada. The work of NFPA engineers is recognized as an influential factor in the establishment of techniques and practices which have reduced loss of life and destruction of property by fire. Among the most important developments in NFPA history was the establishment, in 1933, of the *Volunteer Firemen Magazine* (now *Firemen*) in an effort to reach the many small communities which are protected by volunteer fire departments.

One of the most recent and significant services rendered by the NFPA was occasioned by World War II. This war, unlike any previous war, was marked by the extensive use of fire as a devastating weapon, and thus the association, through its experience and knowledge of fire, was able to contribute much to the development of weapons for offensive warfare by the United States.

ASTM Moves to New Headquarters. The American Society for Testing Materials has moved its headquarters from 260 South Broad Street, Philadelphia, Pa., to its permanent headquarters building at 1916 Race Street, Philadelphia 3. The new building, which was purchased and remodeled through contributions made by many of the companies and individuals active in the society's work, provides additional space required by the expansion of the society's staff.

Howes and Gilson Appointed By Canadian Engineers' Council

Appointment of Doctor F. S. Howes as chairman and W. J. Gilson (M '38) as vice-chairman has been announced by the Canadian Council of Professional Engineers and Scientists, which was formed in 1945.

The Council is composed of the presidents or their alternates of 11 national scientific professional engineering societies in Canada and is the result of four or five years of discussions among interested groups. As it is organized as a Canadian District, the AIEE has been included in the Council. The Council deals on a national scale with such matters of general interest to engineers and scientists as economic status, postwar planning projects, and matters connected with the development of Canadian resources. After one year of operation the Council reports a considerable measure of success in its dealings with the Dominion Government.

Doctor Howes is a consulting radio engineer and an assistant professor of electrical engineering at McGill University, Montreal, Quebec, from which he was graduated with honors in 1924. His graduate studies were completed at the University of London and the University of California. He is member of the Institute of Radio Engineers and the Corporation of Engineers of Quebec. A biography of Mr. Gilson who is a former vice-president of AIEE may be found on page 129 of the March 1943 issue of *Electrical Engineering*.

Besides AIEE, the bodies represented in the Council are: the Dominion Council of Professional Engineers, the Canadian Institute of Mining and Metallurgy, the Chemical Institute of Canada, the Royal Architectural Institute of Canada, the Canadian Society of Forest Engineers, the Agricultural Institute of Canada, the Dominion Council of Federated Professional Employees, the Canadian Institute of Surveying, the Canadian Association of Professional Physicists, and the Canadian Council of the Institute of Radio Engineers.

Conference on Insulation Plans Meeting for November

The conference on electrical insulation of the National Research Council, after five years of relative inactivity, has announced that preparations are being made for a three-day meeting at the Johns Hopkins University, Baltimore, Md., November 7–9, 1946.

The last meeting of the conference, its 14th annual meeting, was held in 1941, and at that time Ward F. Davidson (F '26) director of research, Consolidated Edison Company of New York, Inc., was appointed to continue as conference chairman. Mr. Davidson had been chairman since 1939. Other members of the executive committee of the conference are:

S. O. Morgan, *vice-chairman;* Thorstein Larsen (A '34) *secretary;* C. L. Dawes (F '35); W. A. Del Mar

(F '20); R. N. Evans; C. F. Hill (F '39); F. L. Miller; H. H. Race (F '39); Arthur von Hippel (M '37); and John B. Whitehead (F '12).

Those desiring to receive copies of the detailed program and other notices are requested to send their names and addresses to Mr. Davidson.

EDUCATION

Yale Electrical Engineering Fellowship. An annual fellowship, to be known as the Westinghouse Fellowship in Electrical Engineering has been established at Yale University, New Haven, Conn. The fellowship will be open to all candidates holding a bachelor of science degree in electrical engineering from a college or university in the United States. The recipient will be chosen by the faculty of the Yale University department of electrical engineering. The first fellowship has been awarded to James A. M. Kelly who was graduated from Yale University in 1942 and who for the past three years has been doing research in the United States Naval Research Laboratory, Washington, D. C.

Westinghouse Fellowship at Illinois. Announcement of the establishment of a graduate fellowship in power systems engineering at the Illinois Institute of Technology by the Westinghouse Educational Foundation, has been made by Doctor Louis T. Rader (M '43) chairman of the institute's department of electrical engineering. The fellowship has been established on a yearly basis for five years. Final decision on the 1946 applicant will be made by June 16 by a joint committee representing both the foundation and the institute. In the case of veterans receiving Government allotments, the committee reserves the right to divide the fellowship between two candidates, while the Government would pay tuition fees. Ordinarily the fellowship provides a stipend of $1,500 with all tuition fees paid for 12 months of study leading to a degree of master of science in electrical engineering. The successful candidate will devote full time to the program's study of the technical problems of power generation, transmission, and distribution.

INDUSTRY

New Materials for Permanent Magnets Announced

Five new permanent-magnet materials, known as cunico, cunife, vectolite, alnico 12, and silmanal, have been announced by the General Electric Company. These new materials have many applications in the manufacture of aircraft instruments and products for which small lightweight magnets formed in intricate shapes are required.

Cunico is an alloy of copper, nickel, and cobalt. Magnets made from it are furnished only in their final shapes, because they are age-hardened in the manufacturing process. Cunico is malleable, ductile, and machinable.

Cunife is a copper-nickel-iron alloy which has all the physical properties of cunico, differing in that it has directional properties and must be magnetized only along the direction in which the material has been cold-worked, to obtain highest magnetic quality.

Vectolite is the first nonmetallic, nonconducting magnet material ever made. It is a hardened sintered combination of iron rust and cobalt oxide, mixed when still in powder form. Vectolite magnets are extremely light, being nonmetallic, and their nonconductive properties prevent electrical losses caused by conduction of current. In addition, they have a high resistance to demagnetizing forces.

Alnico 12 is made up of aluminum, nickel, cobalt, iron, and titanium. Magnets made from this material can be used in such applications as tachometer generators and electronic devices.

Silmanal has a high intrinsic coercive force, which makes magnets made from it useful in instruments where service in strong electric fields is required. Silmanal is ductile and malleable.

Electronic Heat Seals Many Consumer Products

The wartime promise that plastic fabrics would be sealed electronically in the manufacture of civilian goods now is being realized, Wiley D. Wenger, engineer of the Radio Corporation of America, recently stated at the annual spring meeting of the Society of the Plastics Industry.

Industry now is using electronic power in the fabrication of dress shields, bathing caps, raincoats, shower curtains, and many other thermoplastic products, he revealed.

A major advantage of electronic techniques, Mr. Wenger said, is that the high-frequency electric energy employed is not converted into heat until after it enters the work material. The metal electrodes used to apply the energy remain cool, while the heat generated is concentrated at the interface of two pieces of material, where it is wanted, and the degree and interval of heating can be closely controlled.

Since the electrodes themselves can be used to apply pressure, the three essentials of heat sealing—uniform heating of the surfaces to be joined, uniform pressure, and uniform cooling—can be accomplished simultaneously with a single operation.

A number of electronic heat-sealing installations saw service during the war in the production of such vital military requirements as solar stills, Wenger said, and the use of electronic equipment and techniques in this field has increased rapidly. The products involved range from ping pong balls and beach play balls to belts, button hole reinforcements, bibs, and baby pants.

A long-electrode bar sealer can be used either to produce a single seam as long as 48 inches at one shot for large articles, such as raincoats or shower curtains, or to seal several smaller objects, such as tobacco pouches. Another machine employs roller electrodes, which apply power and feed material through the machine at the same time, making a continuous seam of any length or contour.

LETTERS TO THE EDITOR

INSTITUTE members and subscribers are invited to contribute to these columns expressions of opinion dealing with published articles, technical papers, or other subjects of general professional interest. While endeavoring to publish as many letters as possible, Electrical Engineering reserves the right to publish them in whole or in part or to reject them entirely. Statements in letters are expressly understood to be made by the writers. Publication here in no wise constitutes endorsement or recognition by the AIEE. All letters submitted for publication should be typewritten, double-spaced, not carbon copies. Any illustrations should be submitted in duplicate, one copy an inked drawing without lettering, the other lettered. Captions should be supplied for all illustrations.

Glass and Marble Measuring Instrument

To the Editor:

The picture of the "original a-c–d-c instrument" which appeared on page 80 of the February issue of *Electrical Engineering*, interested me especially, as I had the picture taken, having found it among the old laboratory junk, while I was in charge of instrument development at the Westinghouse company.

The caption is not quite correct, as this type of instrument was never used for alternating current, having been acquired by George Westinghouse in connection with his purchase of the Waterhouse arc lighting system in order to get into the electric lighting business on a competitive basis. When he introduced the a-c system in connection with the Gaulard and Gibbs system of transformers, Phillip Lange, Doctor C. F. Scott, and others developed what they called the "glass and marble" instrument line which comprised a long bunched wire solenoid, mounted in a glass show case type of cover, on a marble base (Figure 1). This was in the year 1888—a year also famous for the introduction of the Shallenberger meter for a-c ampere-hours, and the great blizzard.

Both indicating instruments mentioned

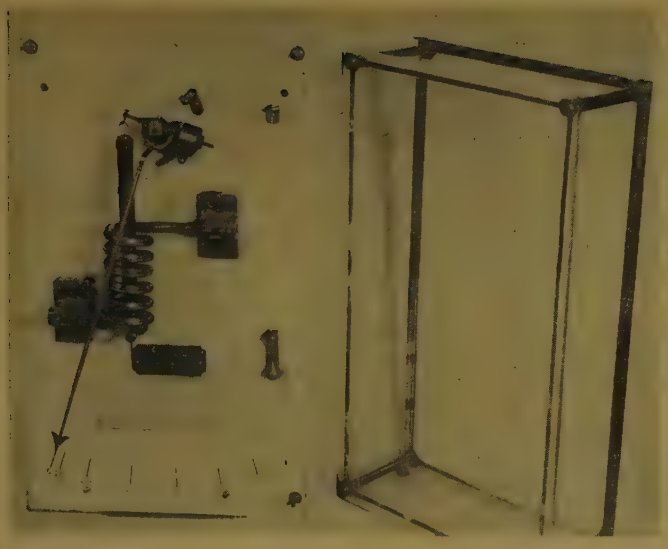


Figure 1.

operated with gravity control. Though the Waterhouse type would work after a fashion on alternating current, its inductance and the eddy current effects were too much for successful a-c operation.

It is interesting to note that in those days most designers did not think that either springs or permanent magnets were sufficiently reliable for measuring work—at least until Weston brought out his first d-c moving coil instrument—also in 1888.

PAUL MacGAHAN (F '42)

(Consulting electrical engineer, Woodstock, N. Y.)

Engineering Terminology

To the Editor:

Paul MacGahan's letter in the February issue of *Electrical Engineering*, objecting to the proposed use of the word "icon" to designate an insulated conductor, meets with my hearty approval. Apart, however, from mentioning its possible confusion with "iconoscope," a more or less legitimate application of the generic term, I have no desire to enter this controversy and shall let the contestants settle it between themselves.

I hope Mr. MacGahan's luck is better than mine in the protest against preemption of terms already recognized in other fields. My voice was raised against adoption of the term "oscilloscope" to designate the stabilized cathode-ray oscillograph, when the word already had been applied in British practice to an entirely different instrument. (Discussion by P. A. Borden of "The Oscilloscope," Frederick Bedell, Herbert J. Reich. AIEE *Transactions*, 1927, volume 46, page 550.) My appeal fell upon deaf ears; and the word now has its place in the "Standard Definitions of Electrical Terms."

Again, my protest against abuse of the noun "potentiometer" to designate a certain type of rheostat has been insistent and unremitting; and, while this example of technical slang does not yet seem to have appeared in recognized electrical standards, it is creeping into the dictionaries, and is rapidly finding a place in electrical literature—especially in the field of electronics—and in patents. So I suppose it will be but a matter of time until we reactionaries must bow to the inevitable and recognize this further short cut in the use of technical English.

PERRY A. BORDEN (F'44)

(Patent engineer, The Bristol Company, Waterbury, Conn.)

Electrical Essays

To the Editor:

With respect to my electrical essay on page 159 of the April 1946 issue of *Electrical Engineering* discussing the sudden paralleling of a capacitor C charged to a voltage E with another equal but uncharged capacitor, it is evidently incorrect to assume that a final rest condition can be reached without loss of energy. In order to analyze this problem, either the resistance or the inductance may be neglected but not both.

Qualitatively the situation is seen most clearly if the resistance is neglected, but a definite amount of series inductance is assumed to be present, in which case the charge will oscillate from one capacitor to the other indefinitely. Decreasing the inductance to a smaller value merely increases the frequency of oscillation.

At a particular instant when the charge is equally divided between the capacitors, there will be an amount of energy stored in the inductance exactly equal to that stored in the capacitors. To attain equilibrium there must be a means of losing energy, such as a resistance which will serve to damp out the oscillation and absorb the excess energy over the steady-state condition.

A quantitative solution is obtained rather easily by assuming a definite series resistance R in the circuit and neglecting the inductance. The equation for the current flow at any time is the well-known exponential:

$$i = \frac{E}{R}\epsilon^{-\frac{2t}{Rc}}$$

remembering that the combined capacitance of the two capacitors in series is $C/2$.

The total energy loss in the resistance is calculated as follows:

$$W_r = \int_0^\infty Ri^2 dt = \frac{E^2}{R}\int_0^\infty \epsilon^{-\frac{4t}{Rc}} dt = {}^1/_4 CE^2$$

Thus, it turns out that this loss is independent of the value of the resistance. It may be seen that as the resistance is decreased toward zero, the initial value E/R of the transient current becomes extremely high. In the more complicated case of a damped oscillation with inductance present, the resistance loss must be the same.

W. M. LEEDS (M '38)

(Manager, circuit breaker development section, Westinghouse Electric Corporation, East Pittsburgh, Pa.)

To the Editor:

The electrical essay for April illustrates the danger of setting up a "theoretical" problem without considering whether the conditions are theoretically justifiable. The fallacies in the problem as stated lie in assuming (1) the inductance of the circuit may be neglected, (2) a condition of static equilibrium will be attained.

NORTON SAVAGE (A '41)

(Engineering assistant, Federal Telephone and Radio Corporation, Clifton, N. J.)

To the Editor:

Referring to the electrical essay in the April issue, my practical comment is: Why assume the impossible? However, if the assumption of the impossible is permissible, why not consider what happens when a capacitor discharges through a circuit of negligible inductance and resistance? In this case the entire energy stored in the capacitor disappears, not one half.

The only realistic way to consider a situation of this sort is to treat it as a limiting case of vanishingly small resistance and inductance. This method explains the result correctly. As is done in the essay, I use circuit theory, not field theory, which is not entirely correct.

WALDO V. LYON (F '33)

(Professor of electrical machinery, Massachusetts Institute of Technology, Cambridge, Mass.)

To the Editor:

Referring to the electrical essay in the April issue, the fallacy in the statement of the problem resides in the assumption that, if the resistance in circuit between the two capacitors is negligible, the energy dissipated in that resistance will be negligible. The expression for the rate of dissipation of energy in a resistance across which is impressed a given potential is E^2/R which varies inversely with the resistance.

J. LESTER WOODBRIDGE (F '21)

(Patent department, Electric Storage Battery Company, Philadelphia, Pa.)

To the Editor:

I read with interest your electrical essay in the April issue. I would like to propose a corollary. Since the resistance and induction are negligibly small, the circuit will oscillate at infinite frequency for an infinite time. This will make a good perpetual motion radar set.

OTTO J. M. SMITH (A '42)

(Research Laboratory, Scranton Record Company, Scranton, Pa.)

To the Editor:

The electrical essays which appear from time to time in *Electrical Engineering* teach a strong lesson against the complete reliance on intuition in the solution of engineering problems. It is hoped that this department will be continued, not only for the recreation that it offers, but for its educational value in electrical fundamentals.

W. B. CONOVER (A '42)

(Works laboratory, General Electric Company, Pittsfield, Mass.)

To the Editor:

The law of conservation of energy always holds—even in the case of the electrical essay published in April 1946—as long as all the circuit parameters are included.

The resistance of the circuit is never so negligibly small that considerations of energy lost, especially in a transient circuit, may be tossed out the window.

No fair, gentlemen—include the resistance, put the heat back on, and let the energy dissipate as it ought to.

STANLEY C. MARSHALL (A '44)

(Editor of technical publications, Sauerman Brothers, Inc., Chicago, Ill.)

System of Graphing Capacities and Inductances

To the Editor:

A letter to the editor in the December 1945 issue of *Electrical Engineering*, page 469, brings to mind a simple precise system of graphing capacities and inductances, at the same time indicating impedance, as shown in Figure 1. Used in conjunction with Keuffel and Esser Company sheet number 359–47, values of all inductances and capacities with their impedances are obtained easily and precisely.

A. S. RUNCIMAN (M '35)

(Superintendent, Shawinigan Water and Power Company, Montreal, Quebec, Canada)

An Analysis of Electromagnetic Forces

To the Editor:

In the October 1945 issue of *Electrical Engineering* you published an article by W. A. Tripp titled "An Analysis of Electromagnetic Forces."

In this article the author criticizes the concept of the attraction of two parallel currents of equal direction, because two streams of electrons in parallel motion of equal velocity (which represent two parallel currents) cannot attract each other due to their velocity, as they have no relative motion. He then postulates new laws of nature governing electromagnetic phenomena and cites the observed constrictions of molten metals in which current flows as proof of these theories.

However, the attraction of two streams of electrons in parallel motion can be derived from electrostatics using the formulas of special relativity. Proof of this also will contain the answer to the author's question: "If parallel currents attract each other, why was the attraction of parallel electron streams never observed"? It also will explain the constriction of molten metals by passing direct currents.

Let us consider a co-ordinate system *S*

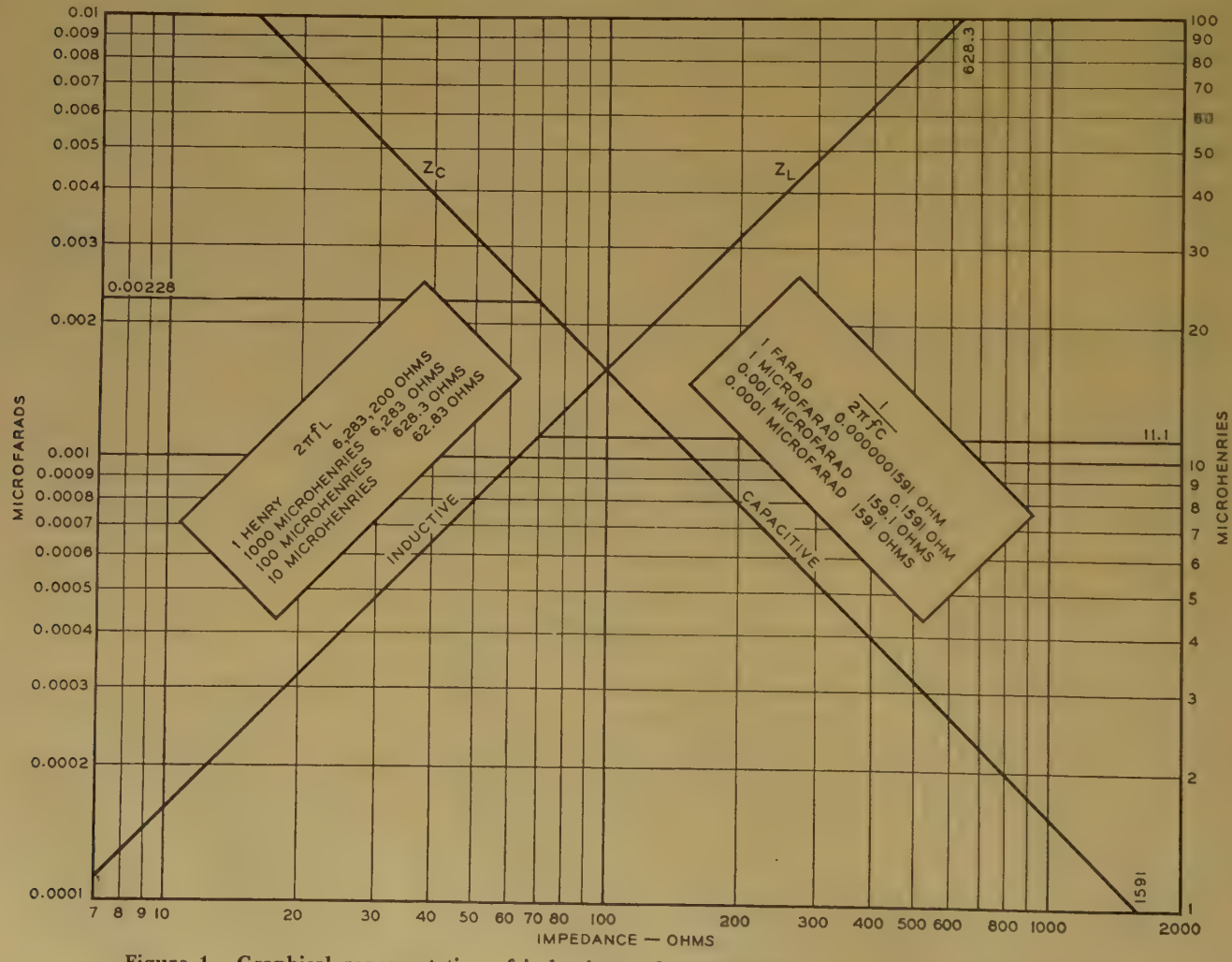


Figure 1. Graphical representation of inductive and capacitive impedance for F = 1,000 kilocycles

$y = \infty \ldots \alpha = \infty$
$y = -\infty \ldots \alpha = -\infty$

I hope that the foregoing lines, although they bring no material not previously known, will clarify the nature of electromagnetic attraction of currents to those to whom this concept is not entirely clear.

ALFRED GRONNER

(Montevideo, Uruguay)

NEW BOOKS

"Extinguishing and Alarm Equipment (National Fire Codes, volume 4, 1946 edition)." This edition of the National Fire Codes increases to 47 the standards dealing with automatic sprinklers and water supply, fire extinguishers, municipal and rural fire apparatus, watchman service, and other related features of supervision and maintenance. Suggesting measures providing reasonable safety without undue expense or inconvenience, in general these standards specify the methods of installation but do not attempt to rule as to the conditions under which the several kinds of protection should be provided. This volume supersedes the edition of 1943. All the codes are in the form of suggested ordnances, standards, or recommended good practice requirements and are recognized as authoritative guides to the best practices. The National Fire Protection Association, Boston 10, Mass., 1946. 735 pages, cloth, $3.

The following new books are among those recently received at the Engineering Societies Library. Unless otherwise specified, books listed have been presented by the publishers. The Institute assumes no responsibility for statements made in the following summaries, information for which is taken from the prefaces of the books in question.

SYMPOSIUM ON MAGNETIC PARTICLE TESTING. American Society for Testing Materials, 260 South Broad St., Philadelphia, Pa., 1945. 122 pages, illustrated, 9 by 6 inches, paper, $1.25. Eight papers by authorities and two tentative methods for testing are contained in this symposium. Topics covered by the articles include the equipment, specifications, and procedure for magnetic particle inspection; the application of the method to the testing of aircraft parts; and the inspection of castings and forgings.

VORLESUNGEN ÜBER DIFFERENTIAL GEOMETRIE UND GEOMETRISCHE GRUNDLAGEN VON EINSTEINS RELATIVITÄTSTHEORIE. Volume I, Elementare Differentialgeometrie. By W. Blaschke. Third edition, prepared by G. Thomsen, published by Dover Publications, New York, N. Y., 1945. 322 pages, illustrated, 8 3/4 by 5 1/2 inches, cloth, $3.50. Essentially a textbook of differential geometry in a Euclidean space of three dimensions, this volume provides also an introduction to original research in the field. The following is a partial table of contents: Introduction-vectors; theory of curves; elements of the theory of surfaces; invariant derivatives on a surface; geometry on a surface; problems of surface theory in the large; extremal properties of curves and surfaces; line geometry. Particular emphasis is placed on the relations between differential geometry and the calculus of variations.

RELAY ENGINEERING. By C. A. Packard. Struthers-Dunn, Philadelphia, Pa., 1945. 640 pages, illustrated, 7 by 4 1/2 inches, fabrikoid, $3. Following an introductory and historical opening chapter are 50 pages devoted to definitions of terms and illustrations with code designations of some 100 magnetic structures manufactured by the company issuing the manual. Succeeding chapters deal with description of relays and auxiliary equipment, applications and circuits, the selection of relays for specific tasks, installation and service work, and standards. A bibliography and an appendix of technical data are provided.

POLAR MOLECULES. By P. Debye. Dover Publications, New York, N. Y., 1945. 172 pages, illustrated, 8 3/4 by 5 1/2 inches, cloth, $3.50. A survey is presented of the questions which arise in connection with the conception of polar molecules as systems having a distribution of electric charges which can be characterized by a permanent electric moment. The treatment is comprehensive, and the introduction of quantum theory makes it possible to develop in detail the connection between polarity and the phenomena of dispersion and absorption, especially in the infrared.

DEVELOPMENT OF MATHEMATICS. By E. T. Bell. McGraw-Hill Book Company, Inc., New York, N. Y., and London, England, 1945. 637 pages, 9 by 5 3/4 inches, cloth, $5. Although this book covers the evolution of mathematics from about 4000 B.C. to the present day, it is not strictly a history. The author's intent is rather to indicate main trends over this period, presenting them only through typical major episodes in each. Chief principles, methods, and theories are considered in both pure and applied mathematics. The author clearly shows how seemingly unimportant phases have been developed into useful lines of endeavor.

AUTOBIOGRAPHY OF SCIENCE. Edited by F. R. Moulton and J. J. Schifferes. Doubleday, Doran and Company, Inc., Garden City, N. Y., 1945. 666 pages, tables, 8 1/8 by 5 1/4 inches, cloth, $4. From the time of the earliest records to the 20th century, the great triumphs of science in all fields are recorded in this volume in the original words of those who achieved them. The introductory notes by the authors immediately preceding the separate items provide brief information about the lives, activities, and achievements of the men whose writings are presented. This unusual collection will be of interest to those who like their information firsthand, allowing for the necessity of translation from foreign languages.

AUFGABEN UND LEHRSATZE AUS DER ANALYSIS. Volume I. Reihen, Integralrechnung Funktionentheorie. 342 pages. Volume 2. Funktionentheorie, Nullstellen, Polynome, Determinanten Zahlentheorie. 412 pages. By G. Polya and G. Szego. Dover Publications, New York, N. Y., 1945. Tables, 8 3/4 by 5 1/2 inches, cloth, $3.50 each volume. The purpose of this text is to present not merely a collection of problems but an arrangment of the problems in such order and grouping as will cultivate good habits in the mathematical thinking of the student. Accordingly the two volumes cover the following topics in the field of mathematical analysis as follows: Volume I, infinite series and sequences; integral calculus; functions of a complex variable-general part. Volume II, functions of a complex variable-special part; location of zeros; polynomials; determinants and quadratic forms; number theory.

ART OF PLAIN TALK. By R. Flesch, foreword by L. Bryson. Harper and Brothers, New York, N. Y., and London, England, 1946. 210 pages, tables, 8 1/4 by 5 inches, cloth, $2.50. Two years ago Mr. Flesch published his doctor of philosophy dissertation, "Marks of Readable Style." This book is a less formal presentation of the subject matter. It is not a book on basic English. Scientific studies of readability have produced a formula based on sentence length, and on the number of affixes and personal references included. The main feature of this book is this formula which is intended only as a yardstick. However, readers are warned not to allow the rules and computations to obscure the principles of plain English. Examples of difficult material rewritten in simple English are included.

BUILDING AN ENGINEERING CAREER. By C. C. Williams. Second edition, revised. McGraw-Hill Book Company, New York, N. Y., and London, England, 1946. 309 pages, illustrated, 8 1/4 by 5 1/2 inches, cloth, $2.50. An orientation course for freshmen engineers. The author discusses what engineering is and how to study it, gives something of its historical background, and calls attention to modern achievements.

PAMPHLETS

The following recently issued pamphlets may be of interest to readers of "Electrical Engineering." All inquiries should be addressed to the issuers.

Movies Go to Work. Bell and Howell Company, 7100 McCormick Road, Chicago 45, Ill., 23 pages.

Public Domain. A new weekly digest of expiring patents published by the Scientific Development Corporation, 614 West 49th Street, New York 19, N. Y. Charter subscriptions for one year, $45; for six months, $25; for ten weeks, $10; 250 pages.

A Dynamic Equipment Policy for America. Machinery and Allied Products Institute, 221 North La Salle Street, Chicago, Ill. Single copies, 25 cents; 5 to 24 copies, 15 cents each; 25 copies or over, 10 cents each; 26 pages.

How to Buy Surplus Machine Tools. National Machine Tool Builders' Association, 10525 Carnegie Avenue, Cleveland 6, Ohio, 21 pages.

The Foreman and the Veteran. By Ted Handelman. National Foreman's Institute, Inc., Deep River, Conn., 32 pages, 25 cents, subject to quantity discount.

What's Ahead for the Veteran. By Ted Handelman. National Foremen's Institute, Inc., Deep River, Conn., 22 pages, 15 cents, subject to quantity discount.

Publicity for the Small Company. By James W. Corey. National Electrical Manufacturers Association, 155 East 44th Street, New York 17, N. Y. Copies may be obtained at cost.

Airport Electrical Equipment. Westinghouse Electric Corporation, P. O. Box 868, Pittsburgh 30, Pa.

Protection of Electric Circuits and Machines. By C. F. Hedlund, A. L. Brown. Associated Factory Mutual Fire Insurance Companies, Inspection Department, 184 High Street, Boston 10, Mass., 72 pages, $2.

Production Moves Ahead. By the Director of War Mobilization and Reconversion. Bureau of Special Services, Bureau of the Budget, 1400 Pennsylvania Avenue N. W., Washington, D. C., 56 pages.

The Tin Research Institute 1942–1944. A report of the work of the Institute, its current researches, and their bearing on future developments. Fraser Road, Greenford, Middlesex, England. Represented in the United States by: Battelle Memorial Institute, 505 King Avenue, Columbus, Ohio, 32 pages.

Vickers, Rockwell, and Brinnell Hardness Values for Various Materials and Alloys. A chart. Prepared by J. T. Agnew. Engineering Experiment Station, Purdue University, Lafayette, Ind.

TRANSACTIONS SECTION

Preprint of Corresponding Pages From the Current Annual AIEE Transactions Volume

All-Electric Gun Charging

WILLIAM C. ROHN
NONMEMBER AIEE

GUN-CHARGING DEVICES are used to actuate the mechanism of automatic machine guns and cannon. This is required initially in order to prepare the weapon for automatic operation, or when misfire, misfeed, or any such malfunction renders the gun inoperative. It should be noted that automatic guns depend upon the force of recoil, gas pressure generated by the exploding cartridge, or both, to perform the task of extracting and ejecting the spent cartridge and delivering a live round into the chamber. The operation of charging consists of retracting the breech block for a stroke of from seven to ten inches, depending upon the caliber of gun, and then releasing it to return unimpeded to battery* under the force of the block-driving spring. Extraction, ejection, feeding, and cocking occur by means of cams, pawls, and levers actuated by movement of the breech block as in normal firing.

When guns on pursuit airplanes were mounted in the fuselage or in manually operated turrets, it was possible for the pilot or gunner to charge them by hand. As more guns were added, they were often mounted in remote positions in the wings. This and the advent of the remote-controlled turret made manual chargers impractical.

Various types of automatic, semiautomatic, and manually controlled power chargers have been introduced. These devices are hydraulically, pneumatically, or electrically powered and either manually or electrically controlled.

Both the hydraulic and pneumatic types of chargers are piston devices. A cylinder is placed parallel to the motion of the breech block, and a projection on the piston engages the block and actuates the mechanism of the gun. The driving force in the case of the hydraulic charger is oil pressure, tapped usually from the hydraulic system on the aircraft but occasionally from individual electrically driven units. The pneumatic charger almost without exception requires a separate source of compressed air, as few fighter craft have pneumatic systems. Cylinders of compressed air or carbon dioxide are the usual provision, either with one tank supplying all of the chargers or with individual containers for each gun. Separate electrically driven compressor units have also been introduced.

Either a hydraulic or pneumatic system necessitates piping and valving which are both bulky and vulnerable. Leakage of the fluid, especially at the charging cylinder or at rotating glands in turret installation, has always been a serious problem. It was only natural then that thought was directed toward the development of an all-electric charger.

When the charger to be described was first contemplated, the following points were considered prerequisites of a good design that would overcome most of the known difficulties of electric chargers in existence.

1. Adjustment should not be critical, and any charger should be readily transferable to any gun of similar type and model without readjustment.

2. The unit should be adaptable to more than one type of gun with only minor changes.

3. As much of the working parts of the charger should be detached from the gun as possible in order that these parts are not subjected to the high-acceleration loads that are normal to automatic weapons at a high rate of fire.

4. Any attachments on the gun should project as little as possible into the area immediately around the gun, as this space is often limited in wing and turret installations.

5. A means should be provided to apply repeated charging efforts to a gun which does not respond to the initial force exerted on the breech block.

6. Means should be incorporated in the charger to "safety" the gun. This requires holding the breech block out of battery, which is a positive assurance that the weapon cannot fire. The principal uses of this feature are to stop a gun which has become

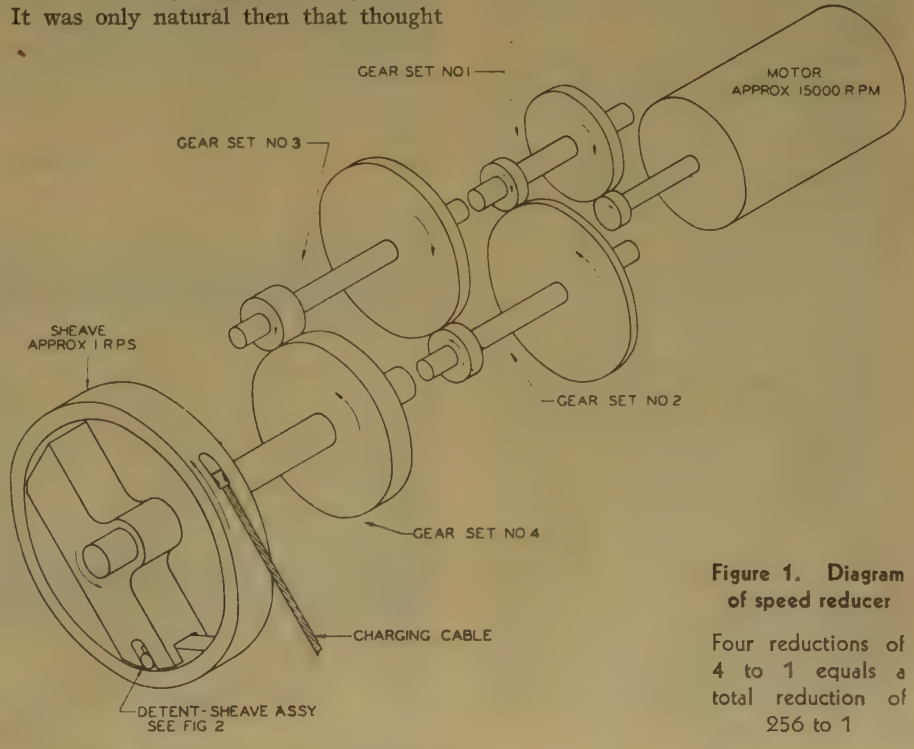


Figure 1. Diagram of speed reducer

Four reductions of 4 to 1 equals a total reduction of 256 to 1

Paper 46-1, recommended by the AIEE committee on air transportation for presentation at the AIEE winter convention, New York, N. Y., January 21–25, 1946. Manuscript submitted June 11, 1945; made available for printing October 9, 1945.

WILLIAM C. ROHN was project engineer, aircraft armament department, Bendix Products Division, South Bend, Ind., at the time this manuscript was prepared. He is at present assistant chief engineer, Allied Control Valve Company, Inc., South Norwalk, Conn.

The author acknowledges the assistance of G. A. Goepfrich and J. M. Boshka.

*A gun is in "battery" when the breech is closed and in firing position.

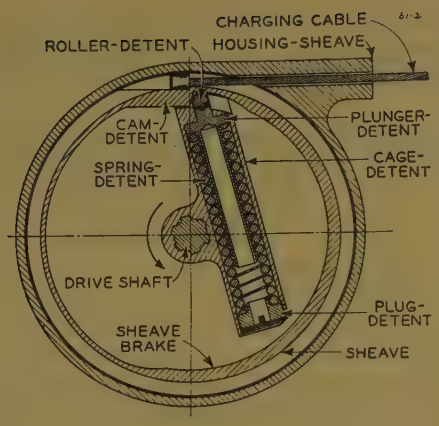


Figure 2. Diagram of detent and sheave assembly

overheated and is "cooking-off"† ammunition out of control and also to prevent accidental discharge due to the impact of carrier landings.

The resulting design consists of three basic units:

1. An electric-motor-driven speed reducer coupled to a torque-limiting detent.

2. An attachment to the body of the gun consisting of a sliding member which engages the breech block, and a guide for this member. Also two switches, one actuated by the sliding member of the charger and the other by the breech block of the gun.

3. A control box, mounted for convenience on the motor.

The motor is series wound, 24 volts direct current, developing approximately one-third horsepower at 15,000 rpm. This drives a four-stage spur-gear train (Figure 1) having a total reduction of 256 to 1. The last stage of the speed reducer is coupled by a spline shaft to the torque-limiting detent (Figure 2). This mechanism consists of a cage driven by the splined drive shaft. The detent plunger and spring are supported and guided by this member. The sheave or grooved drum upon which the charging cable winds straddles the detent cage and is supported by bearings in the sheave housing on either side. The detent cage is driven in the direction indicated and when the roller arrives at the position shown against the face of the internal cam in the sheave it forces the sheave to rotate with the cage. The cable being attached to the sheave therefore winds on its periphery, resulting in a linear pull. The magnitude of this pull is determined by the torque transmitted to the sheave, and this in turn is a function of the spring force and the angle of the face of the detent cam which the roller is forced to climb. The desired cable pull is translated in terms of torque, and the detent mechanism is adjusted to this figure. In operation then the roller engages the cam and rotates the sheave drawing in the cable. The other end of the cable is fixed to the sliding member of the attachment on the gun which engages the breech block (see Figure 3). The breech block is thereby forced rearward until its entire stroke is consumed and further movement is impossible. At this point, the torque transmitted to the sheave increases until it exceeds the setting of the detent mechanism and the roller is forced over the cam. The sheave is now free to rotate in the opposite direction urged by both the breech-block-driving spring and charger-return spring acting through the charger cable. The motor is stopped by dynamic braking, and the ratio of the charging stroke to the circumference of the sheave is arranged so that the cam comes to rest in a relationship to the detent roller convenient for the successive charging operation. The roller is in contact with the sheave brake surface during a portion of the return stroke to absorb the kinetic energy stored in the sheave mass.

The flexible cable transmitting the charging force from the power unit to the sliding member of the attachment on the gun passes through a sheath that is flexible, but rigid in compression.

The compressive load necessary to balance the tension in the cable is taken through this sheath and thereby allows practically universal position relationship between the gun and the charger power unit (Figures 4 and 5). In order to increase further the versatility of positioning, the sheave housing mounts symmetrically on the speed-reducer housing to provide eight directions of cable orientation (Figures 6 and 7).

† Ammunition is said to "cook off" when it is discharged by contact with an overheated firing chamber instead of being ignited by the primer.



Figure 3. Attachment to gun, including guide, slide, gun switch, and charger switch



Figure 4. Fully automatic 50-caliber electric charger installation, total weight, nine pounds

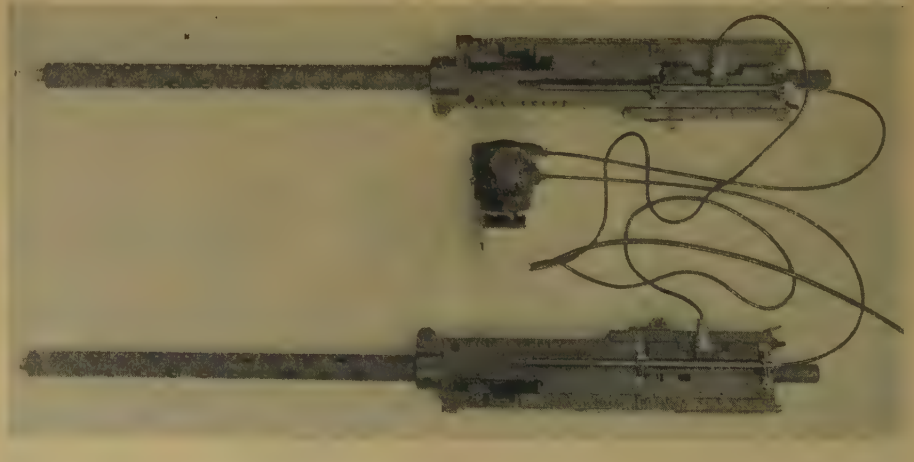


Figure 5. Two-gun 50-caliber semiautomatic electric charger installation, total weight, 11.5 pounds

The attachment on the gun consists of a bracket which supports the tube, serving as a guide for the member that engages the breech—block stud, and acts as a housing for the charging switch and the gun switch. The slide is also of steel tube construction (Figure 3), and is indexed by a slot in the guide tube so that the projecting lug will engage the breech-block charging stud. The interior of the slide houses and pilots the charger-return spring. The switching arrangement is best seen in the diagram, Figure 8. The charging switch is actuated by the lug on the slide only, and the gun switch on the other hand is actuated by the charging stud of the breech block. The charging switch normally is closed, but is held open by the charger lug in its normal position under the influence of the charger-return spring. The gun switch is normally open and is closed by the breech-block stud at its extreme rear position which occurs during a normal firing or a charging cycle.

The entire control apparatus is housed in a sheet-metal box supported on the motor. It may be mounted either above as shown or on the under side, depending upon the space characteristics of the installation. Three relays, a capacitor, and a thermal circuit breaker constitute the control elements for a single-gun fully automatic installation.

A brief description of the sequence of events in a fully automatic charging operation is as follows:

Refer to diagram, Figure 6, and consider first a normal charging cycle. With the control switch in the battery position and the circuit breaker closed, depress the trigger. This energizes the initiating relay, opens its normally closed contacts and removes from the capacitor and the time-delay relay one of the sources of positive potential. Continued firing of the gun now will maintain the other source intermittently through the gun

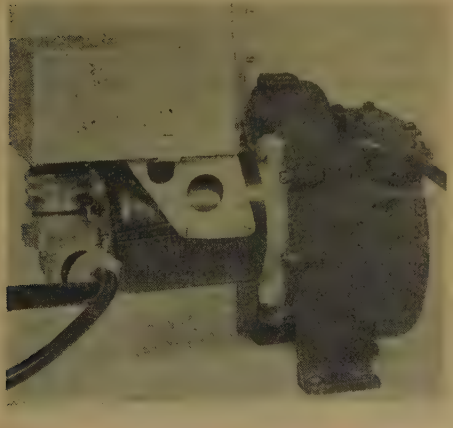


Figure 6. Speed reducer, motor, and control-box assembly

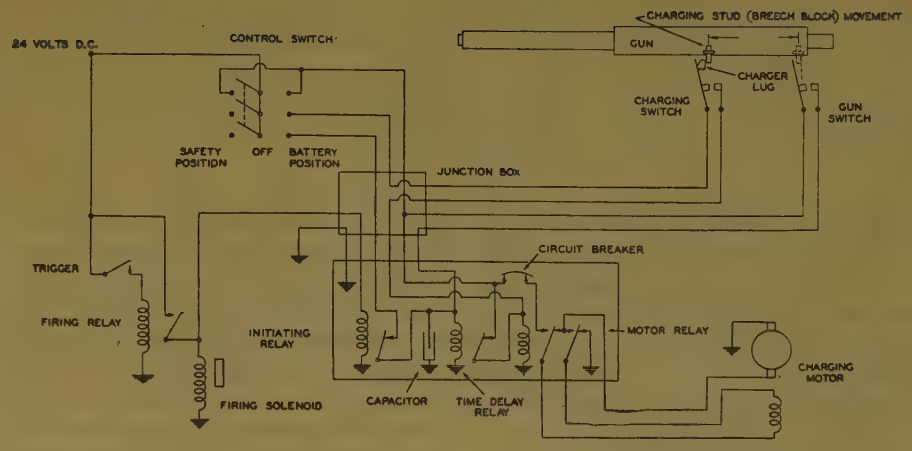


Figure 8. Schematic electric circuit, fully automatic charger

switch actuated by the breech-block charging stud. Should the gun jam‡ or fail to fire, the gun switch will remain open, thus allowing the voltage across the capacitor and time-delay relay to fall as the capacitor slowly discharges through the relay. In about one third of a second this voltage will be low enough to cause

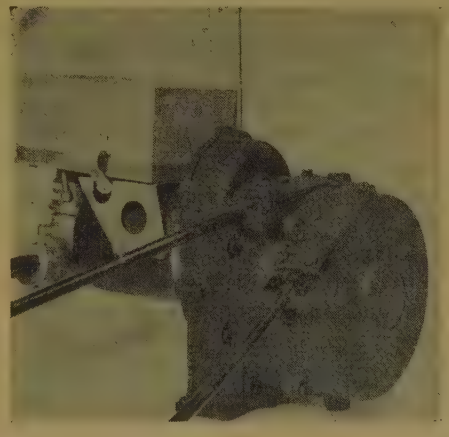


Figure 7. Speed reducer, motor, and control-box assembly for two-gun installation

the time-delay relay to close its contacts energizing the motor relay which starts the motor. The motor now will run until the breech-block stud actuates the gun switch which energizes the time-delay relay, opening the circuit to the motor relay. At this point the motor will stop unless some other means is provided to keep the motor relay energized until the charging cycle has been completed. Such means is provided by the action of the charging switch which closes a circuit to the motor relay as soon as the motor has drawn the charging lug slightly rearward. At the end of the charging cycle, the lug has returned to its forward position, opening the charging switch contacts and de-energizing the motor relay. The normally closed contacts of the motor relay

‡ A gun "jam" includes any malfunction which prevents normal operation.

provide a circuit for dynamically braking the charging mechanism to eliminate overtravel and position the detent properly for the next charging cycle. It can readily be seen that, if the rearward movement of the breech block is impeded at any point by malfunction of the gun, the torque-limiting detent will trip as in normal charging. This returns the slide and lug to the forward position, and another charge will ensue. Thus, repeated impacts will be delivered to the breech block, assuring a maximum possibility of correcting the malfunction and restoring proper operation of the weapon. The thermal circuit breaker is set to allow between six and ten charges before tripping and disconnecting the unit.

In order to "safety" (design item 6) the gun, it is only necessary to initiate a charging cycle and then stop the operation when the breech-block stud actuates the gun switch. By placing the control switch in the safety position, this is accomplished by the following sequence: Opening the circuit to the initiating relay contacts allows the capacitor to discharge, releasing the time-delay relay. This initiates a charging cycle the same as the normal one previously described. The control switch, however, also opens the circuit to the charging switch which allows the motor relay to drop out as soon as the gun switch energizes the time-delay relay, opening its contacts. The control switch may now be moved to the "off" position and the gun and charger left in the safety position with all power disconnected. The gear train is prevented from running in reverse with this imposed load by a spring-type ratchet clutch in the speed reducer. Returning the control switch to battery position completes the circuit through the closed charging-switch contacts to the motor-relay coil. The motor

A Carbon-Pile Speed Governor

C. T. BUTTON
ASSOCIATE AIEE

THE GOVERNOR described herein was designed for application on aircraft inverters, to hold the speed and, consequently, the output frequency substantially constant. While such a governor may be used on a variety of d-c motors, the discussion is confined to the operation of controlling the speed of a d-c motor which drives an a-c generator.

Comparison With Carbon-Pile Voltage Regulator

The problem of governing the speed of a d-c motor is not unlike that of controlling the voltage of an a-c generator—both involve sensitive variation of excitation of a d-c field in response to variation of the controlled quantity. By sensitive variation is meant a rapid or large change in excitation coincident with a small change in the controlled quantity. For example a two-per-cent change in either voltage or frequency of the generator output should produce perhaps 50-per-cent change in excitation of generator or motor field, respectively. Such a device may be regarded broadly as a rate-of-change amplifier with a high amplification ratio around the control point.

A contact-making regulator is the simplest form of such a device and has been used widely for both voltage and speed regulation. The limitations of a contact-making regulator are well known; and the advantages of a carbon pile for frequency regulation are exactly the same as for voltage control. Briefly, the functional advantage of the carbon pile is that it varies field excitation by infinitesimal steps so as to achieve a point of stability on a smooth curve for any given condition. A contact-making device on the other hand causes a more or less rapid fluctuation of field current by finite steps and thereby creates a modulation in output voltage. In the case of a speed governor this modulation is minimized not only by field inductance but also by rotor inertia; yet this modulation still exists in some degree. Practical disadvantages of the contact-making devices are that contact-point deterioration may affect performance; and such devices may contribute to radio interference. The ordinary carbon-pile voltage regulator when viewed as an amplifier may be compared with a triode amplifying tube by drawing an analogy between carbon-pile resistance and cathode-to-plate impedance; and between solenoid voltage and grid voltage.

The carbon-pile voltage regulator easily may be used to control speed by introducing either an inductance or a tuned circuit in series combination with the solenoid of the carbon pile so that it will be sensitive to frequency change. It may be mentioned incidentally that carbon-pile operation for a voltage regulator is opposite to that of a speed regulator in that increasing voltage requires a drop in generator field excitation, whereas increasing frequency requires an increase in motor field current.

While there are many ways of producing varying pressure on a carbon pile in response to change in frequency or speed, it may be stated without the burden of argument that probably the most direct and efficient way is to utilize thrust resulting from centrifugal force on rotating weights supported by springs. In this arrangement the spring is the basic reference for control just as it is in the voltage regulator. Incidentally it is interesting to note that centrifugal force varies as the square of the speed; and the force acting on the armature of a voltage regulator for a constant gap varies as the square of the solenoid voltage.

In the case of an armature moving in response to magnetic pull from a solenoid, ordinary simple construction results in this pull varying as a square function of the armature position. However, when weights move as a result of centrifugal force, the force varies only directly as the radius. Hence it is not necessary to provide special spring forms to prevent instability in the speed regulator.

Relatively large values of thrust are obtained easily with small weights at the speeds characteristic of aircraft inverters. No expenditure of energy is involved ex-

Paper 46-4, recommended by the AIEE committee on air transportation for presentation at the AIEE winter convention, New York, N. Y., January 21–25, 1946. Manuscript submitted September 10, 1945; made available for printing October 16, 1945.

C. T. Button is sales manager, aircraft and electrical controls division, The Master Electric Company, Dayton, Ohio.

---

then will run until the return of the charging lug opens the charging switch, de-energizing the motor relay.

Several units may be linked to the same trigger and control switch. It is only necessary to connect corresponding leads in parallel at a suitable junction box in such times.

Variations of this circuit adapt the charger to different automatic weapons having approximately the same breech-block stroke. Another modification is the semiautomatic system which requires the charging operation be initiated by the gunner pressing a button and is then carried to completion automatically. With this system two guns may be charged simultaneously by one power unit containing two detent assemblies, provided the force required to retract the breech block does not exceed 250 pounds per gun (Figure 7).

The charging cycle, when operating a 50-caliber machine gun, is approximately one second, and the current drain is eight to nine amperes. Two 50-caliber guns require approximately 15 amperes and charge in about $1^1/_2$ seconds. These figures pertain to room-temperature operation. The unit, however, will operate satisfactorily at 65 degrees Fahrenheit, at approximately twice the normal charging time. The unit will handle one weapon of 50-caliber or 20-millimeter size with fully automatic operation at a total apparatus weight of nine pounds. Two weapons of either size may be served semiautomatically at a total weight of $11^1/_2$ pounds.

Weight and dependability are the most important considerations in selecting the type of gun charger to use in an installation. If, for instance, an airplane has a hydraulic system of proper characteristics, a hydraulically powered charger electrically controlled may be the simplest and lightest type of installation. When an airplane has no hydraulic system and a considerable number of guns are to be used, a pneumatic charging system could have an advantage in weight since the weight of the compressor per gun may be comparatively small.

In an installation where guns are few or difficulties are encountered in sealing hydraulic or pneumatic fluids, such as in turrets that require rotating glands or releasable package-gun containers, an all-electric gun charging system has definite advantages.

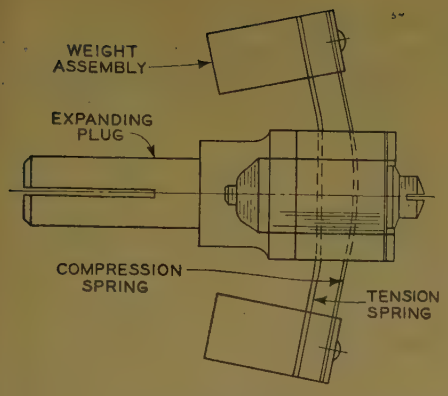


Figure 1. Rotating unit, side view of weight and spring assembly

cept a minute amount of windage and friction in transmitting a light force from the rotating assembly to the carbon pile.

While the centrifugal force varies as the square of the speed, the pressure on the carbon pile varies at a much higher rate. Just as in the case of the voltage regulator, the primary force is resisted by a spring, and the pressure on the carbon pile is a differential and may be referred to as a secondary force. Thus we may have a 10-pound thrust created by centrifugal force resisted by 9 pounds and 15 ounces from the spring and one ounce from the carbon pile. If the speed is increased one per cent, then the primary force becomes nearly 10 pounds $3^1/_4$ ounces. If constant spring tension is assumed, this means that the force applied to the carbon pile increases from 1 ounce to $4^1/_4$ ounces for a one-per-cent speed change.

For an inverter designed to operate at 8,000 rpm, for example, the governor carbon pile preferably should be subjected to not more than a light constant pressure to prevent sparking between disks until the speed is around 7,500 rpm. The pressure on the pile, as stated previously, should have its maximum rate of change at very close to the desired operating speed. In order to provide some shunt field for starting and accelerating, the carbon pile may have a light initial pressure provided by a spring, or have a fixed resistor connected in parallel with it, or both.

Description of Rotating Assembly

The physical construction of the governor may be explained in orderly manner by starting with the part which attaches to the motor shaft and proceeding outward. At the left in Figure 1 is seen a split expanding plug which is placed in a hole in the motor shaft. There is a screw which enters a tapered thread in the plug for tightening. In order to make this screw accessible, the rotating yoke separates from the plug by removing two screws. When in place, the yoke is held in concentric position by a pilot which enters a counterbore in the head of the plug.

The yoke carries a flat tension spring which lies substantially in a plane perpendicular to the axis. This spring carries a weight at each end in the position shown by Figure 1. The weights are riveted not only to the tension spring but also to the ends of a compression or arch spring. The latter is parallel to the tension spring and spaced from it by small separator blocks through which the weight rivets pass. The centers of gravity of the weights are on the inboard or plug side of the tension spring. The centrifugal force created by the rotating weights combines with a centripetal force in the tension spring to form a couple. This couple is balanced by a radial force in the arch spring acting as a column plus an additional component of force in the tension

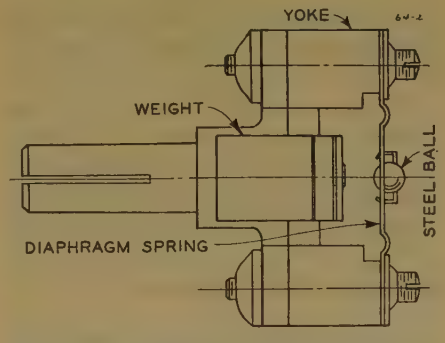


Figure 2. Rotating unit, rotated 90 degrees from view of Figure 1

spring. This simple balancing of radial forces is approximate only, as it is complicated by bending of the tension spring and the additional couples developed by the bending of the restrained ends of the arch spring.

As the centrifugal force increases, the compressive force on the arch spring becomes larger, so that the latter buckles and its center moves outward. The centrifugal force actually increases more rapidly than the square of the speed, since the centers of gravity of the weights are at an increasing radius. The force which a column will support is not linear with respect to displacement of its ends. As a matter of fact it is disclosed in the appendix that after a flat spring acting as a column starts to buckle, the force is substantially constant over a wide range of deflection. Also lateral displacement of the center of a column is not linear with respect to displacement of its ends. The net result is that the curve of displacement of the center of the arch spring plotted against speed with the latter on the horizontal axis is concave upward for a considerable distance. (dy/dS increases rapidly with S where y and S are the two quantities just mentioned.) As speed continues to increase, the arch spring comes in contact with the steel ball, which in turn presses against the stationary carbon-pile assembly. Thus there is a more or less abrupt stop to the change in configuration of the rotating weight and spring assembly resulting from increasing speed.

Also mounted on the rotating yoke is a third thin spring in a plane parallel to the tension spring but with its length at right angles to it (Figure 2). For convenience this may be called a diaphragm spring. It is attached rigidly to the yoke at its ends by eyelet rivets.

This diaphragm spring has two transverse corrugations near its ends so that it can stretch in length. Its center is required to move only a few thousandths of an inch, and it is made to be as flexible as possible consistent with maintaining concentricity of the small hardened steel ball which it carries in its center. This ball is held in a hole in the diaphragm which is cut after the diaphragm spring is assembled on the yoke and while the latter is rotating. This procedure provides the maximum assurance that the hole for the ball will be on the center line of rotation.

Figure 3 is a view of the rotating unit from the end having the steel ball.

The final operation in manufacturing the rotating unit is to drill a small hole in each weight as needed, more or less like a balancing operation, to insure that the arch spring will make contact with the ball at a speed just slightly below the operating point. The steel ball rotates without slip and transmits axial thrust from the arch spring to the contact button

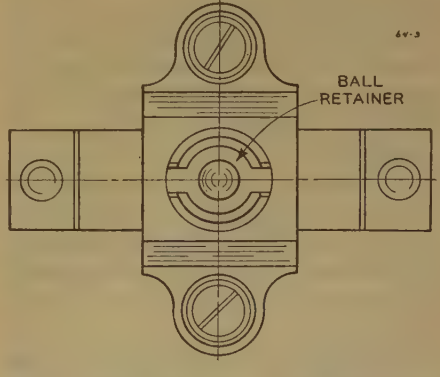


Figure 3. Rotating unit, view from outboard end

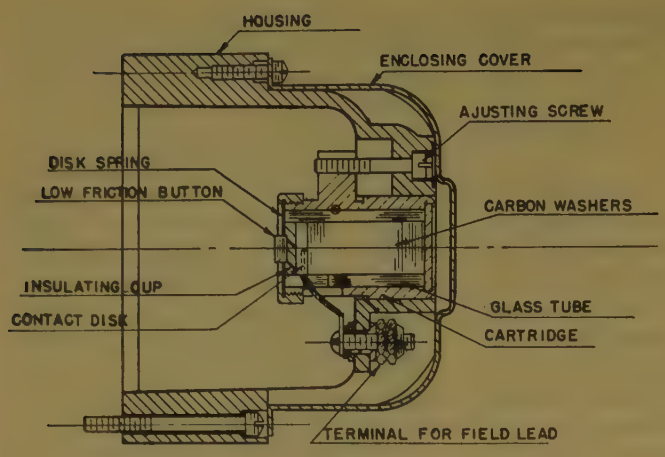


Figure 4. Stationary unit assembly, in section

of the carbon pile. This construction makes it possible to preset the governor quite closely by bringing the stationary unit up to a point where it is just touching the ball.

Description of Stationary Assembly

Proceeding from the inboard end outwardly as before, there is a small button of low-friction self-lubricating material (Figure 4) with which the rotating ball makes contact. The contact surface initially is flat and perpendicular to the axis so that no particular care in alignment is necessary. This low-friction contact button is not of hard material, and a small dimple appears from operation, since point contact is not possible in transmitting thrust.

The contact button is held by a cup made of insulating material capable of withstanding high temperature. Back of this cup is a contact disk to which is fastened a flexible pigtail attaching to a terminal for connection of the motor field lead.

The contact disk is held lightly against the pile of carbon washers by a small radial fingered disk spring, bearing against the insulating cup. A stack of carbon washers approximately one inch long is held in place by a glass tube placed inside a metal cartridge.

The cartridge has an ear on one side, with a tapped hole parallel to the axis. A screw held by the supporting housing enters this hole for adjustment of the longitudinal position of the carbon-pile assembly.

The inboard end of the cartridge is threaded on the outside. A flange screws on at this point, for holding and adjusting the disk finger spring, which determines the maximum resistance of the carbon pile.

The cylindrical hole for the cartridge in the supporting housing has a radial slot or split with transverse screw for clamping, after the longitudinal position of the carbon-pile cartridge assembly is set.

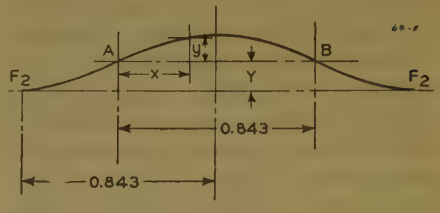


Figure 5. Curve assumed by arch spring in compression

The electric circuit of the carbon pile is from pigtail to contact disk, and through the pile to the inside of the closed outboard end of the cartridge which is grounded through the supporting housing.

Operation of the Governor

Typical resistance versus speed characteristic is shown by the curve of Figure 6. In normal operation the resistance range is from one to 30 ohms.

The permissible voltage across the pile is about 20 volts maximum.

Maximum watt dissipation is of the order of 25 watts, but this figure is subject to modification, depending upon the individual application requirements, ambient conditions, and ventilation provided. Limiting ratings have not been definitely fixed at this time inasmuch as life-test data under a variety of conditions have not been accumulated.

Appendix. Calculations for the Rotating Weight–Spring Assembly

Centrifugal force is given by

$$F_1 = M(2\pi N)^2 R$$

where

M = weight in pounds divided by 32.16
N = revolutions per second
R = radius in feet

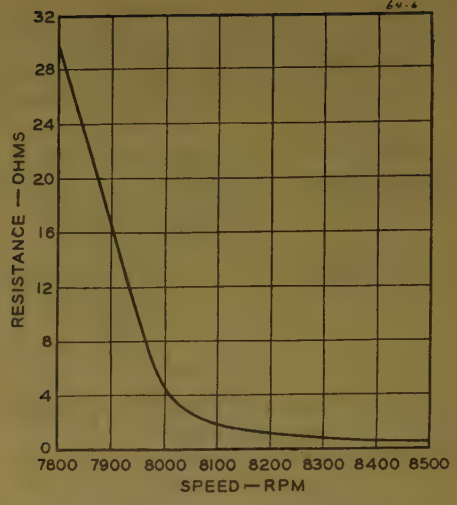


Figure 6. Typical curve of governor characteristic showing resistance versus speed, for one adjustment and a particular set of carbon rings

The total weight at each end of the spring assembly is 0.0356 pound. The center of gravity is at a radius of 0.843 inch from the center of rotation. At 7,500 rpm where the arch spring just starts to push the steel ball, the centrifugal force will be

$$F_1 = \frac{0.0356}{32.16}\left(2\pi\frac{7{,}500}{60}\right)^2\frac{0.843}{12} = 48 \text{ pounds}$$

The center of gravity of the weight assembly is at a distance of 0.162 inch from the center line of the tension spring. Thus the couple about the latter due to centifugal force is

$48 \times 0.162 = 7.75$ pound-inches

This is balanced by the couple due to compressive force in the arch spring F_2 with a lever arm of 0.137 inch (center-to-center distance between the two springs) plus the couple due to the bending at the ends of the arch spring.

In order to determine the bending moment in the arch spring, the curve of Figure 5 is referred to. A and B are points of counterflexure, with zero bending moment. The moment at the ends and the middle is F_2Y where $2Y$ is total deflection.

$F_2Y + 0.137F_2 = 7.75$ pound-inches

whence

$$F_2 = \frac{7.75}{Y + 0.137} \qquad (1)$$

The curve from A to B is a sine curve, and is the same as that of a column with ends free to turn, having length AB and supporting the load F_2. Incidentally, each half of the total curve is symmetrical so that the part from A to the center if rotated 180 degrees about A would coincide with the part from A to the left end.

Euler's formula for a column of length L and with free ends indicates that the column will fail if the load is

$$F_2 = \frac{\pi^2 EI}{L^2} \qquad (2)$$

For a steel spring having dimensions of 0.010 by 0.5 by 0.843 inch, the moment of inertia I would be

$$\frac{0.5}{12}0.01^3=\frac{10^{-6}}{24}$$

If E is 30×10^6, then EI would be 1.25, and the limiting load would be about $17^1/_2$ pounds. Actual test on a steel spring of these dimensions resulted in a measured force of 21 pounds maximum, which was substantially constant over a wide range of deflection and up to the point where the spring took a permanent set.

In Euler's derivation of maximum loading for a column the shape of the curve formed by a column with free ends is given as

$$y=C_1 \sin x\sqrt{\frac{F_2}{EI}} \qquad (3)$$

where x and y are co-ordinates of the curve with x measured along the length of the column.

From equation 2, this is found to be equivalent to

$$y=C_1 \sin \frac{x}{L}\pi \qquad (4)$$

The constant C_1 is the maximum deflection Y; and, as indicated, this is indeterminate inasmuch as the force F_2 is practically constant for a wide range of deflection.

It is interesting to note in passing that an oil-burner pump has been developed and patented utilizing the "Euler-column" spring acting on a piston. The oil pressure resulting is substantially constant for a considerable piston travel, eliminating the need for a by-pass pressure regulator.

An approximation of column deflection may be obtained by using the formula for maximum deflection of a simple beam supported at the two ends and with load in the center.

$$Y=\frac{WL^3}{48\,EI} \qquad (5)$$

It will be assumed that the beam has the same dimensions as the column, and that the bending moment at the center of each is the same.

The bending moment at the center of the arch spring is F_2Y. The bending moment at the center of a beam with center load W, length L, and with supports at the free ends, is $1/4\ WL$. Equating these two moments, the beam load is found to be

$$W=\frac{4F_2Y}{L} \qquad (6)$$

If L is 0.843 inch, this results in

$$W=4.75F_2Y \qquad (7)$$

From equations 5 and 7,

$$Y=\frac{4.75F_2Y\ 0.843^3}{48\,EI} \qquad (8)$$

Formula 8 reveals two things:

1. Since the deflection of a simple beam is directly proportional to the load W, which in turn was assumed proportional to the existing bending moment and a direct function of the deflection, F_2 is again shown to be a constant.

2. This formula indicates F_2 to be about 21 pounds, which checks the experimental result more closely than does Euler.

Formula 8 can be rewritten as

$$F_2=\frac{12EI}{L^2} \qquad (9)$$

This gives a larger value for F_2 than the Euler formula by the ratio of 12 to π^2. Thus there is the choice of the Euler formula which is theoretically more accurate, and the simple beam formula which more closely checks experimental observation, at least for the actual spring used in the governor in question.

If F_2 is taken as 21 pounds, and substituted in formula 1, the total deflection $2Y$ is seen to be 0.466 inch, at 7,500 rpm. This is more than permitted by the physical construction of the rotating unit before the arch spring touches the steel ball. In production, the weights are drilled until the desired deflection is obtained. In other words, the initial construction provides for overtravel, so that the units can be adjusted individually by removing weight.

In operation, the resisting pressure from the carbon pile acting through the contact button and the steel ball limits the deflection of the arch spring after contact is made. Thus the compression-spring column action is effective at low speeds, but, as speed increases above the point where contact is made with the carbon pile, the further deflection of the arch spring is a matter of a few thousandths of an inch. It may be assumed that at operating speeds differentials in centrifugal force will be reflected solely in change in carbon-pile pressure as all other forces or moments are substantially constant.

Recapitulation of Symbols Used

F_1 = centrifugal force
F_2 = compressive force on arch spring
M = mass of weight assembly on one side of rotating unit, in pounds divided by 32.16
N = revolutions per second
S = revolutions per minute
R = radius from center of rotation to center of gravity of weight assembly
x = distance measured along arch spring, from point A to point B, Figure 5
y = deflection of arch spring at any point x
Y = maximum deflection, measured from center of line AB
E = modulus of elasticity
I = moment of inertia
L = length of column, in this case = AB
W = load in center of beam, in pounds

The Measurement of Large Varying Currents

A. C. JOHNSON
ASSOCIATE AIEE

IN OSCILLOGRAPHIC STUDIES where it is necessary to measure current in the range of from 5 to 100 kiloamperes, one must often resort to the use of shunts, because

1. Addition of a current transformer may materially change the impedance of the circuit.
2. Current transformers for large currents are unwieldy.
3. The current may be pulsating direct current which would saturate a current transformer and render it useless.

It is extremely important that the shunts used be carefully designed and so connected into the circuit that the measuring-circuit current is proportional to and in phase with the shunt current. There follows an analysis and a basis for the design of shunts for measuring these currents, so that there will be no voltage induced in the measuring circuit for any of the frequencies or harmonic components normally encountered in the measuring of currents of these magnitudes. Consequently, the measuring-circuit current will be a function only of a shunt current and the ratio of the resistance of the shunt to that of the measuring circuit.

Physical Arrangement

The shunts discussed herein are cylindrical in shape because of the resultant simplification of the mathematical analysis and the relative ease of fabrication which that geometry affords. It is generally desirable that the shunt be hollow so that the wall thickness can be made less than the skin depth at the rates of change of currents involved. Since it may be desirable to water-cool the shunts, there is an additional advantage in using a hollow cylinder.

The current which flows in the measuring circuit is a function, not only of the points of connection to the shunt, but also of the geometry of the leads from the point of connection to the indicating or recording instrument.

There are four limiting geometries of measuring-circuit leads which are possible. These are shown in Figure 1. For the purpose of calculation in this paper, the shunt is assumed to consist of part of a long straight conductor, and the return conductor is assumed to be sufficiently far away as not to affect the field of the shunt current. Thus, the current produces a symmetrical field about the shunt. If this is not the case, the actual flux distribution and the voltage induced in the leads can be calculated, but the process will be somewhat laborious. With the best arrangement (this will be shown later to be that illustrated in Figure 1D), the error resulting from the false assumption that the shunt is part of an infinitely long straight conductor is negligible. If the leads are connected as in Figure 1A, that is, parallel to each other and perpendicular to the axis of the shunt for sufficient distance so as to be effectively out of its field, the voltage across the measuring circuit will be the actual voltage between the planes perpendicular to the axis of the shunt at the points of connection of the measuring circuit.

Figure 1B is another case of Figure 1A where the distance s is considerably smaller (in practice this would be as small as physical limitations would permit). For both of these arrangements, the measuring-circuit current is shown in the appendix to be

$$i_m = i_s \frac{R_s}{R_m} - \frac{3.19l}{2\pi R_m 10^8} \frac{di_s}{dt}\left[\frac{1-3b^2}{4(1-b^2)} + \frac{b^4}{(1-b^2)^2} \ln\frac{1}{b} + \ln\frac{1}{c}\right] \quad (1)$$

where

i_m = the measuring circuit current in amperes
i_s = shunt current in amperes
l = effective length of shunt between potential connections in inches
R_s = effective resistance of shunt in ohms
R_m = resistance of measuring circuit in ohms
$c = s/r_1$
s = distance from the axis of the shunt to the point where measuring-circuit wire is parallel to the axis of the shunt
r_1 = outside radius of the shunt
r_0 = inside radius of the shunt
$b = r_0/r_1$

If we let

$$q_\phi = \frac{1-3b^2}{4(1-b^2)} + \frac{b^4}{(1-b^2)^2} \ln\frac{1}{b} + \ln\frac{1}{c} \quad (2)$$

$q\phi$ is a function only of ratios s/r_1 and r_0/r_1 and has been plotted as a function of these ratios in Figure 2.

The measuring-circuit current then becomes

$$i_m = i_s \frac{R_s}{R_m} - \frac{3.19l}{2\pi 10^8 R_m} \frac{di_s}{dt} q_\phi \quad (3)$$

If measuring-circuit leads are connected as in Figure 1C, the net voltage induced in the measuring circuit is the difference between the voltage induced in a wire in the center of the shunt and the voltage induced in the shunt itself.

The current in the measuring circuit is shown in the appendix to be

$$i_m = i_s \frac{R_s}{R_m} + \frac{3.19l}{2\pi 10^8 R_m} \frac{di_s}{dt}\left[\frac{1}{2} - \frac{b^2}{1-b^2} \ln\frac{1}{b} - \frac{1-3b^2}{4(1-b^2)} - \frac{b^4}{(1-b^2)^2} \ln\frac{1}{b}\right] \quad (4)$$

or

$$i_m = i_s \frac{R_s}{R_m} + \frac{3.19}{2\pi R_m 10^8} \frac{di_s}{dt} q_\phi \quad (5)$$

where

$$q_\phi = \left[\frac{1}{2} - \frac{b^2}{1-b^2} \ln\frac{1}{b} - \frac{1-3b^2}{4(1-b^2)} - \frac{b^4}{(1-b^2)^2} \ln\frac{1}{b}\right] \quad (6)$$

$q\phi$ is a function only of b and is also plotted in Figure 2.

Figure 3 is an oscillographic illustration of an exaggerated case of type of shunt connection in Figures 1A, B, and C. The measurements were made using a hollow copper pipe as a shunt and the shunt measurement compared to the current as measured by a current transformer. It is obvious that, with the geometry of the measuring circuit as in Figures 1A and B, the measuring-circuit current lags behind the main current. If the shunt connection in Figure 1C is used, the measuring-circuit current leads the main current. This is also apparent from equations 1 and 4. It is evident that by using some intermediate geometry the number of flux linkages can be so controlled as to result in no net induced voltage in the whole measuring circuit (including the shunt as part of the measuring circuit). Consequently, the only voltage is that due to

Paper 46-2, recommended by the AIEE committee on instruments and measurements for presentation at the AIEE winter convention, New York, N. Y., January 21–25, 1946. Manuscript submitted September 7, 1945; made available for printing October 9, 1945.

A. C. JOHNSON is electrical engineer with the Edward G. Budd Manufacturing Company, Philadelphia, Pa.

The author expresses his appreciation for the guidance and co-operation given by C. A. Adams, the assistance of H. D. VanSciver, and the sponsorship of the E. G. Budd Manufacturing Company.

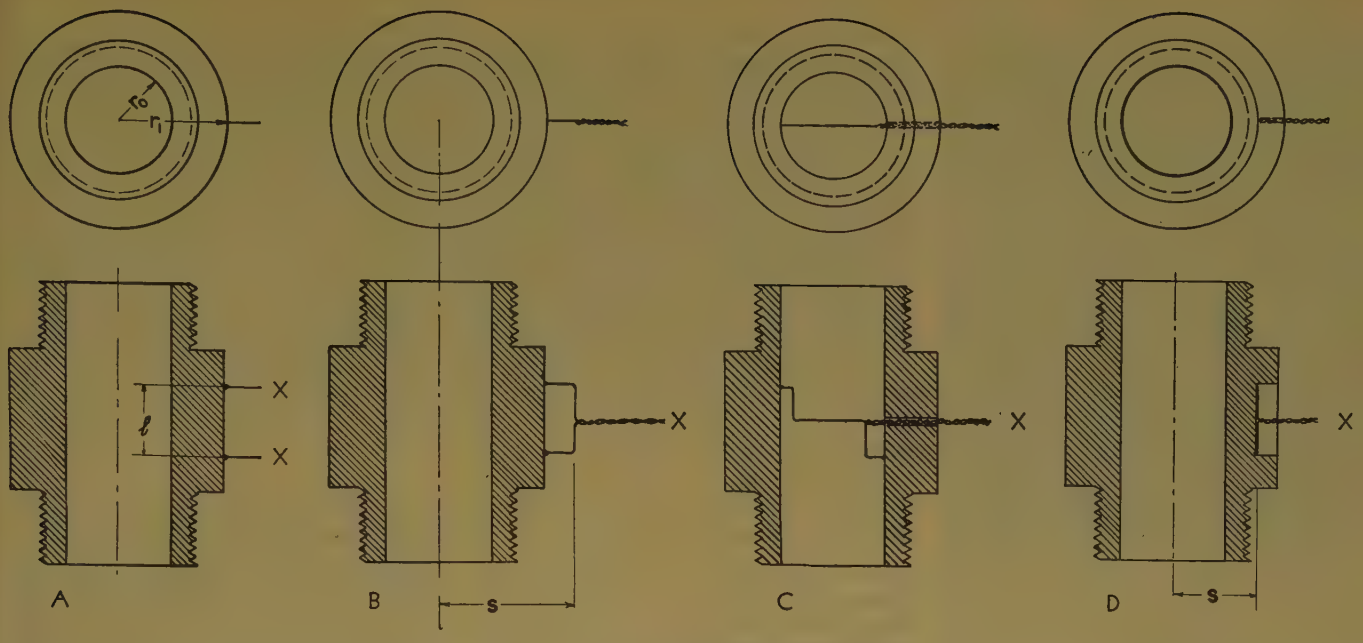


Figure 1. Various arrangements of measuring-circuit leads

By properly locating the leads the measuring-circuit current can be made to be proportional to the shunt resistance voltage at every instant

X—To measuring circuit

the *IR* drop in the shunt. The measuring-circuit current will therefore be proportional to the shunt current at every instant, for all rates of change of current for which the current density can be assumed to be approximately uniform.

If the measuring circuit is arranged as in Figure 1D, the measuring circuit current is

$$i_m = i_s \frac{R_s}{R_m} - \frac{3.19l}{2\pi 10^8 R_m}\frac{di_s}{dt}\left[\frac{1-3b^2}{4(1-b^2)} + \frac{b^4}{(1-b^2)^2}\ln\frac{1}{b} - \frac{a^2-b^2}{2a^2(1-b^2)} + \frac{b^2}{1-b^2}\ln\frac{a}{b}\right] \quad (7)$$

By setting equal to zero that part of equation 7 which emanates from induced voltage, it is possible to obtain a geometry in terms of the ratios r_0/r_1 and s/r_1 which will result in a balance of flux linkages so that the induced voltages are canceled. The relationships between the ratios a, b, and c and the magnitude of the permeance factors are shown in Figure 4. The values of these ratios necessary to make the permeance factors and hence the induced voltages equal to zero are given in Figures 5 and 6.

For these geometries for which there is no net induced voltage, the measuring-circuit current obviously will be proportional to the shunt current. It is well to keep in mind that these equations are based on the assumption of a uniform current density across the section of the shunt. This assumption is valid only if the wall thickness is less than the skin depth at the greatest rate of change to be encountered. For rates of change for which this is not true, the tendency will be for more of the flux to link with the measuring-circuit wire embedded in the shunt, and the shunt will approach the condition of Figure 1C. This arrangement itself is reasonably good and produces an almost negligible error insofar as induced voltage is concerned, as is shown by the oscillograms in Figure 7. Under these conditions, the effective resistance of the shunt will not be constant. It is advisable, however, to locate the measuring-circuit wires as near as possible to the ideal position, since this will result in the most accurate shunt and also does not require that the measuring wires enter the hollow center of the shunt with the consequential difficulty of getting the wires out and keeping the water in.

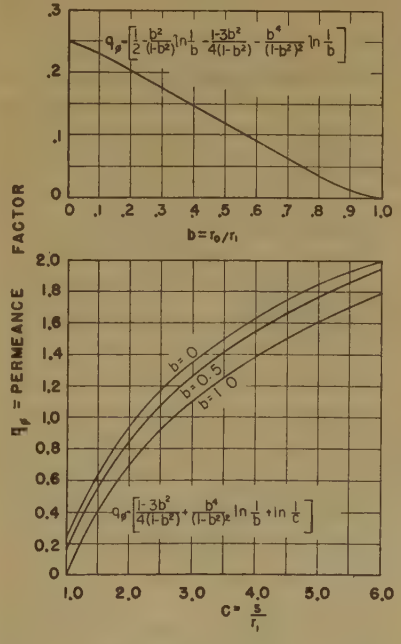


Figure 2. Permeance factors for shunts *A* and *B*

See equations 1 and 6

Thermal Considerations

It is generally advisable to water-cool shunts of the type described herein. Such shunts are usually used on low-voltage circuits, and the only precaution necessary is that rubber hose be used for the water connections to the shunt. The heat generated in the shunt is $60I^2R/1{,}055$ Btu per minute where R is not the effective resistance of the shunt between potential connections, but the entire terminal to terminal resistance. The heat removed will be 8.35 Btu per gallon per degree Fahrenheit water temperature rise. The dissipation to air and to the connected conductors can be neglected. If the shunt is to be used for the measurements of impulses, as for example for the measurement of spot-welding currents, it may not be necessary to water-cool it, unless it is part of a production set up. If t is the duration of the impulse (seconds), the heat generated will be $I^2Rt/1{,}055$ Btu. If we assume that no heat is dissipated, the temperature rise will be

$$\Delta\theta = \frac{I^2Rt}{1{,}055wc} \quad (8)$$

where

w = weight of the shunt in pounds

c = thermal capacity of shunt material in British thermal units per pound per degree Fahrenheit

If the shunt is to be air cooled and used continuously, the rate of heat dissipation to the surrounding air can be safely assumed to be approximately 0.005 watt per *OC* per square inch of exposed surface.

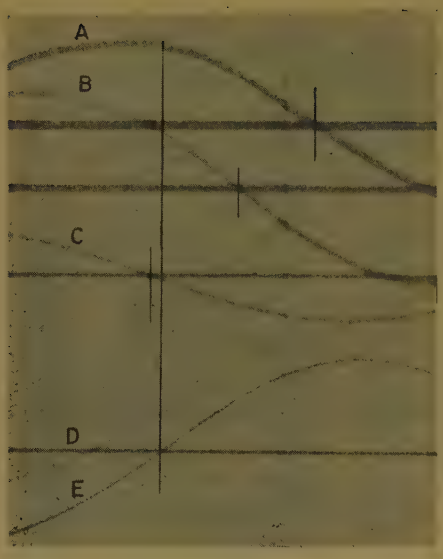


Figure 3. Oscillogram of measuring-circuit currents for different arrangements of potential leads

Traces *D* and *E* are current-transformer secondary currents. Trace *C* corresponds to shunt type *C* and leads the shunt current. Traces *A* and *B* correspond to shunt type *A* and *B* and lag the shunt current

Figure 5. Geometries for which permeance factor in equation 7 is zero

For the geometries corresponding to these ratios the measuring-circuit current is proportional to the shunt current at each instant

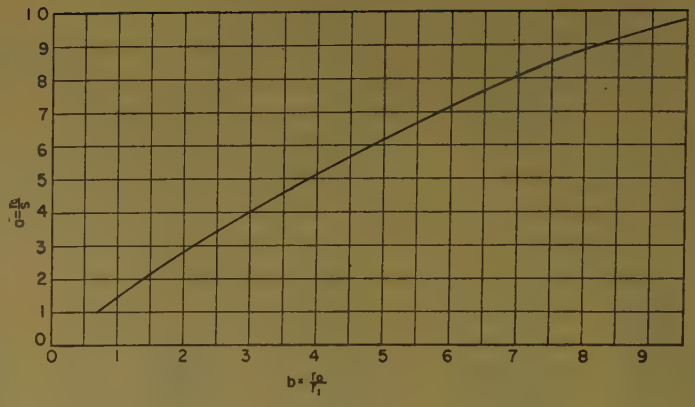
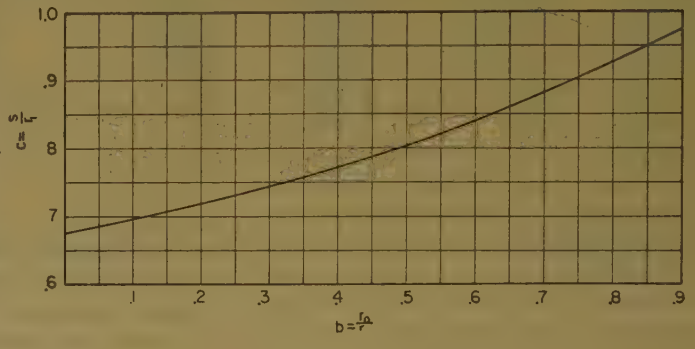


Figure 6. Geometries for which permeance factor in equation 7 is zero

For the geometries corresponding to these ratios the measuring-circuit current is proportional to the shunt current at each instant



Conclusions

It is theoretically and practically possible to construct shunts for the measurement of large varying currents, so that measuring-circuit current is proportional to the shunt current at each instant. The author has successfully used such shunts for measurement where rates of change of the order of 2×10^8 amperes per second were involved.

The simplest form for these shunts is that of a hollow cylinder which may or may not be water cooled depending upon the type of service to which it is to be put.

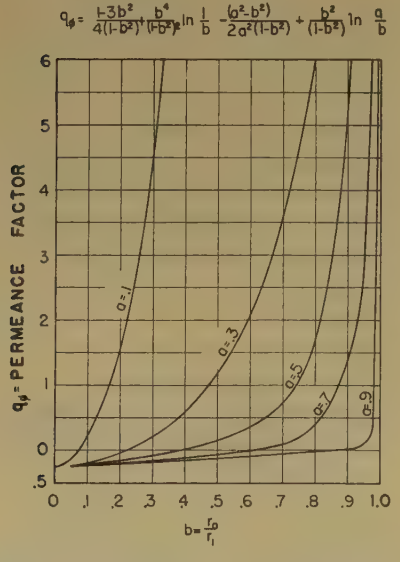


Figure 4. Permeance factor for equation 7 as a function of the ratios a, b, and c, corresponding to shunt D

Appendix

Calculation of Measuring-Circuit Current for Shunts A and B

The shunt is assumed to be part of a long straight conductor. The total voltage induced in the shunt per inch length is (see Figure 1B)

$$e_s'' = -L_1''\frac{di_s}{dt} - L_2''\frac{di_s}{dt} - L_3''\frac{di_s}{dt} - L_4''\frac{di_s}{dt} \qquad (9)$$

where

L_1'' = that part of the inductance of the shunt due to the linkage of flux within the radius r_1, with the shunt current i_s

L_2'' = that part of the inductance due to the linkage of flux between $r=r_1$ and $r=s$, with the shunt current

L_3'' = that part of the inductance due to the linkage of flux outside of $r=s$

L_4'' = that part of the inductance due to the linkage of flux produced by the current I_s in the return conductor, with the current in the shunt

The voltage $L_3''(di_s/dt)$ is induced in both the shunt and the measuring-circuit wire, and cancels when voltages are added around the measuring circuit.

If d is large, the voltage $L_4''(di_s/dt)$ also is induced in the shunt and measuring-circuit wire, and hence also cancels.

$L_1'' = \psi''/10^8$ where ψ'' is the flux linkage per ampere-inch.

The flux $d\phi_1$ in an increment, dr in thickness, at a radius r inside the radius r_1 is

$$d\phi'' = \frac{3.19}{2\pi} i_s \int_{r_0}^{r_1} i_1 \frac{dr}{r} \qquad (10)$$

where i_1 is the ratio of the current inside the radius r, to the total current i_s, the flux per ampere is

$$\frac{d\phi''}{i_s} = \frac{3.19}{2\pi}\int^{r_1} i_1 \frac{dr}{r} \qquad (11)$$

and the flux linkage per ampere is

$$i_1\frac{d\phi''}{i_s} = d\psi'' = \frac{3.19}{2\pi}\int i_1^2 \frac{dr}{r} \qquad (12)$$

If we assume that the current density is uniform throughout the conductor cross section,

$$i_1 = \frac{r^2 - r_0^2}{r_1^2 - r_0^2}$$

then

$$\psi'' = \frac{3.19}{2\pi}\left[\frac{1-3b^2}{4(1-b)^2} + \frac{b^4}{(1-b^2)^2}\ln\frac{1}{b}\right] \qquad (13)$$

where

$$b = r_0/r_1$$

since

$$L_1'' = \frac{\psi_1''}{10^8}$$

therefore

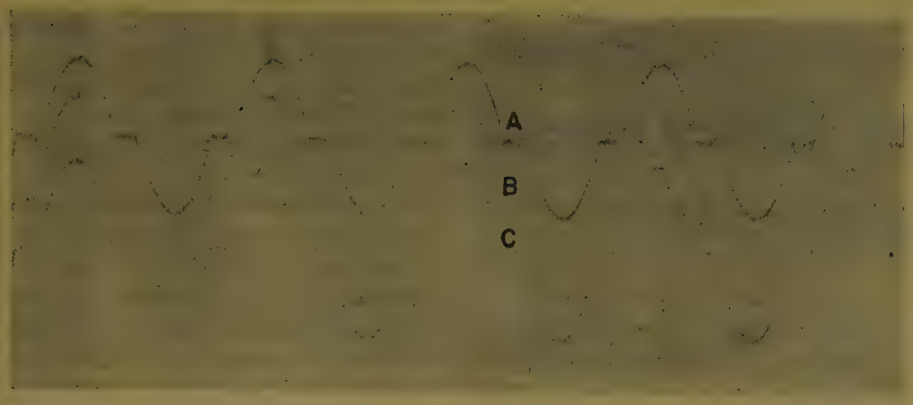
$$L_1'' = \frac{3.19}{2\pi 10^8}\left[\frac{1-3b^2}{4(1-b^2)} + \frac{b^4}{(1-b^2)^2}\ln\frac{1}{b}\right] \text{henrys} \qquad (14)$$

The same analysis will yield L_2. Since all of the current produces and is linked by the flux, $i_2 = 1$, hence

$$\psi_2'' = \frac{3.19}{2\pi}\int_{r_1}^{s}\frac{dr}{r} = \frac{3.19}{2\pi}\ln\frac{s}{r_1} \qquad (15)$$

and

$$L_2'' = \frac{3.19}{2\pi 10^8}\ln c \qquad (16)$$



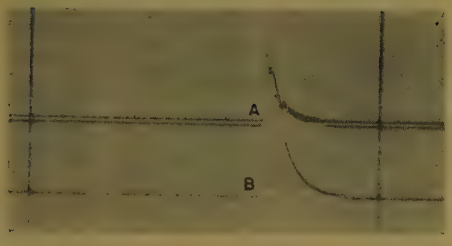


Figure 7. Oscillograms of the same current

Traces *A* show currents in measuring circuit of shunt *B*. Traces *B* show currents in measuring circuit of shunt *D*. Trace *C* is current-transformer secondary current. The capacitor discharge current reached a peak value of 40,000 amperes in 0.002 second

where

$c = s/r_1$

The voltage induced in the measuring-circuit wire per inch length is

$$e_w'' = -L_s'' \frac{di_s}{dt} - L_4'' \frac{di_s}{dt} \tag{17}$$

if the field of the measuring-circuit current is neglected. The sum of the voltage drops in the measuring circuit is

$$-i_s R_s - e_s + e_w + i_m R_m = 0$$

$$i_m = i_s \frac{R_s}{R_m} + \frac{e_s - e_w}{R_m} = i_s \frac{R_s}{R_m} \left[L_1 \frac{di_s}{dt} + L_2 \frac{di_s}{dt} \right]$$

$$i_m = i_s \frac{R_s}{R_m} - \frac{3.19l}{2\pi R_m 10^8} \frac{di_s}{dt} \times \left[\frac{1-3b^2}{4(1-b^2)} + \frac{b^4}{(1-b^2)^2} \ln \frac{1}{b} + \ln \frac{1}{c} \right] \tag{18}$$

Calculation of Measuring-Circuit Current for Shunt C

In this case, all of the flux outside of r_1 links with the shunt and with the measuring-circuit wire. The voltages thus induced by this flux cancel when voltages are added around the measuring circuit. If those terms which ultimately cancel are omitted

$$e_s'' = -L_1'' \frac{di_s}{dt} \tag{19}$$

and

$$e_w = -10^{-8} \frac{d\phi^4}{dt}$$

where L_1 has the same meaning as for shunt *A* and ϕ_1, is the total flux surrounding the measuring-circuit wire, and inside of r_1. Hence

$$e_s = lL'' \frac{di_s}{dt} = \frac{3.19l''}{2\pi 10^8} \frac{di_s}{dt} \times \left[\frac{1-3b^2}{4(1-b^2)} + \frac{b^4}{(1-b^2)^2} \ln \frac{1}{b} \right]$$

$$\phi_1'' = \frac{3.19}{2\pi} i_s \int_{r_0}^{r_1} i_1 \frac{dr}{r} = \frac{3.19}{2\pi} i_s \int_{r_0}^{r_1} \frac{r^2 - r_0^2}{r_1^2 - r_0^2} \frac{dr}{r}$$

$$= 3.19 i_s \left[\frac{1}{2} - \frac{r_0^2}{r_1^2 - r_0^2} \ln \frac{r_1}{r_0} \right] = \frac{3.19}{2\pi} i_s \times \left[\frac{1}{2} - \frac{b^2}{1-b^2} \ln \frac{1}{b} \right]$$

$$e_w'' = -\frac{1}{10^8} \frac{d\phi''}{dt} = -\frac{3.19}{2\pi 10^8} \frac{di_s}{dt} \left[\frac{1}{2} - \frac{b^2}{1-b^2} \ln \frac{1}{b} \right] \tag{20}$$

If the voltage drops are added around the measuring circuit,

$$i_s R_s + i_m R_m - e_s + e_w = 0$$

$$i_m = i_s \frac{R_s}{R_m} + \frac{3.19l}{2\pi 10^8 R_m} \frac{di_s}{dt} \times \left[\frac{1}{2} - \frac{b^2}{1-b^2} \ln \frac{1}{b} - \frac{1-3b^2}{4(1-b^2)} - \frac{b^4}{(1-b^2)^2} \ln \frac{1}{b} \right] \tag{21}$$

Calculation of Measuring-Circuit Current for Shunt D

The correction factors for induced voltage in the final equations for i_m for shunts *A*, *B*, and *C* have been arranged so that the absolute value of the correction is positive. Since these correction factors appear in the two equations with opposite signs, it is reasonable to expect that for some intermediate geometry the correction factor will be zero. Hence, if the measuring-circuit wire is placed in a slot in the wall of the shunt, the depth of the slot can be determined by finding the equation for the measuring-circuit current, and setting the correction factor equal to zero. As before, if we omit those terms which produce canceling voltages:

$$e_s'' = -\frac{3.19}{2\pi R_m 10^8} \frac{di_s}{dt} \left[\frac{1-3b^2}{4(1-b^2)} + \frac{b^4}{(1-b^2)^2} \ln \frac{1}{b} \right]$$

The voltage e_w induced in the measuring-circuit wire is due to the flux between *s* and r_1.

The flux $d\phi_2$ in the increment *r* is produced by all of the current inside radius *s* plus that current between *s* and *r:* that is, by all of the current inside radius *r*. This current is $i_s i_1$ where $i_1 = (r^2 - r_0^2)(r_1^2 - r_0^2)$

$$\phi'' = \frac{3.19}{2\pi} i_s \int_s^{r_1} i_1 \frac{dr}{r}$$

$$= \frac{3.19}{2\pi} i_s \int_s^{r_1} \frac{r^2 - s_0^2}{r_1^2 - r_0^2} \frac{dr}{r}$$

$$= \frac{3.19}{2\pi} i_s \left[\left(\frac{r_1^2 - s^2}{r_1^2 - r_0^2} \right) \frac{1}{2} - \frac{r_0^2}{r_1^2 - r_0^2} \ln \frac{r_1}{s} \right] \tag{22}$$

If we let $r_0/r_1 = b$ and $r_0/s = a$,

$$\phi'' = \frac{3.19}{2\pi} i_s \left[\frac{1}{2} \left(\frac{a^2 - b^2}{1-b^2} \right) \frac{1}{a^2} - \frac{b^2}{1-b^2} \ln \frac{a}{b} \right]$$

$$e_w' = -\frac{1}{10^8} \frac{d\phi}{dt} = -\frac{3.19l}{2\pi 10^8} \frac{di_s}{dt} \times \left[\frac{a^2 - b^2}{2a^2(1-b^2)} - \frac{b^2}{1-b^2} \ln \frac{a}{b} \right]$$

$$i_m = i_s \frac{R_s}{R_m} - \frac{3.19l}{2\pi 10^8} \frac{di_s}{dt} \times \left[\frac{1-3b^2}{4(1-b^2)} + \frac{b^4}{(1-b^2)^2} \ln \frac{1}{b} - \frac{a^2 - b^2}{2a^2(1-b^2)} + \frac{b^2}{1-b^2} \ln \frac{a}{b} \right] \tag{23}$$

In order to find the correct position of the measuring-circuit wire, set

$$\left[\frac{1-3b^2}{4(1-b^2)} + \frac{b^4}{(1-b^2)} \ln \frac{1}{b} - \frac{a^2 - b^2}{2a^2(1-b^2)} + \frac{b^2}{1-b^2} \ln \frac{a}{b} \right] = 0 \tag{24}$$

Since this equation is not analytically soluble the permeance factor

$$\left[\frac{1-3b^2}{4(1-b^2)} + \frac{b^4}{(1-b^2)} \ln \frac{1}{b} - \frac{a^2 - b^2}{2a^2(1-b^2)} + \frac{b^2}{1-b^2} \ln \frac{a}{b} \right] \tag{25}$$

has been plotted in Figure 4 against *b* for different values of *a*. As expected, there is a value of *b* for each value of *a* which makes the expression and hence the induced voltage equal to zero. The values of *a* or *c* which will result in zero correction are plotted in Figures 5 and 6 against *b*.

Hence, for ratios as determined from these two curves,

$$i_m = i_s \frac{R_s}{R_m} \tag{26}$$

which is the desired relationship for any shunt. This relationship is independent of frequency so long as the wall thickness is less than the skin depth. As the frequency is increased, this shunt will approach that shown in Figure 1C. Even this latter type has been used without appreciable error for measurements involving rates of change of currents of 1.8×10^8 amperes per second.

Basic Design Principles for A-C Electric-Power Systems in Large Military Aircraft

C. K. CHAPPUIS
MEMBER AIEE

LEONARD M. OLMSTED
MEMBER AIEE

THE ELECTRIC LOADS of early aircraft were small and the electric systems resembled those commonly used in automobiles. As the design of aircraft progressed, however, additional demands upon the electric system exceeded the capacity of the 14-volt d-c system, and a 28-volt d-c system was developed. Continued increases in electrical demands were met by increased generator ratings and parallel operation of generators at 28 volts direct current. As loads and aircraft sizes increased, the 28-volt d-c system became increasingly heavy to the point where it was obvious that a more economical generating and distributing system would be required.

Two methods of attaining increased electrical capacity were selected as having promise. The 115-volt d-c system was proposed and incorporated into a large cargo airplane. Owing to the limited development personnel available, there has not been sufficient work on this system to obtain complete information on its potentialities. However, it would appear that the anticipated difficulties of commutation and switching of higher direct voltages at high altitudes may not be so serious as anticipated and that switching may actually be somewhat improved. The second method was based on the fact that a similar distribution problem had been solved many years ago by the utilities with the 115/200-volt three-phase system and it seemed reasonable to consider a similar system for several large aircraft.[1,2]

The commercial frequency of 60 cycles proved undesirable, because it limited three-phase motor speeds to 3,600 rpm and required excessive weight in the rotating equipment. Motor speeds up to 10,000 rpm already had proved desirable and analyses indicated the optimum frequency for motor designs to be at least 250 cycles. Similar analyses of electronic equipment indicated an optimum frequency of approximately 800 cycles. The selection of 400 cycles for aircraft is a compromise between these considerations, giving a choice of 6,000, 8,000, 12,000, and 24,000 rpm for motor speeds and falling between the optimum values for motor design and electronic-equipment design.

The use of single-phase and three-phase variable-frequency alternating current has been proposed for power supply to certain electronic equipment, and some installations have been made. Frequency varying over the range involved in main-engine-driven alternators cannot be considered satisfactory for motor operation, however, unless accompanied by a compensating change in voltage which cannot be tolerated by the constant-voltage electronic equipment. Likewise, it does not satisfy the requirement of certain navigation and servo devices for fixed frequency. The principle reason for considering variable-frequency alternating current has been the difficulties in developing satisfactory constant-speed drives at minimum weight.

Certain radio, navigation, radar, radar countermeasure, and similar equipment already in service operates on 115-volt single-phase 400-cycle power supply. This power is supplied on present d-c aircraft by use of inverters, which are heavy and extremely inefficient with over-all weight of 50 to 60 pounds per kilovolt-ampere of 400-cycle output. The proposed 115/200-volt system permits this type of load to be supplied single phase, from the three-phase system, without conversion, or such equipment can be redesigned to operate three phase, within certain limitations, at lesser weights or increased performance.

A review of the electric systems in use or proposed for military aircraft includes the following:

1. 14-volt direct current.
2. 28-volt direct current.
3. 115-volt direct current.
4. 115/200-volt three-phase 400-cycle alternating current.
5. 115/200-volt three-phase variable-frequency alternating current.
6. 115-volt single-phase variable-frequency alternating current.
7. 115-volt single-phase 400-cycle alternating current.

Certain of these systems are not complete in themselves but must be used in combination with others. This paper applies specifically to the design of 115/200-volt three-phase 400-cycle systems for large aircraft, although some portions may be applicable to several of the other systems.

Basic A-C System Design Requirements

The electric system must provide the utmost possible reliability in order that the aircraft may retain maximum effectiveness on its missions as well as the ability to return to its base in spite of damage. The reliability for the conditions of aircraft operation must compare favorably with the reliability of public power systems, with the exception that the expected life for aircraft equipment is 500 to 1,000 hours, instead of 15 to 25 years as in utility requirements. All of this must be accomplished with a minimum of weight. The generating and distribution system must retain its ability to supply satisfactory power to the using equipment as long as that equipment is capable of operation. From this it is apparent that such equipment as motors must remain on the line until the motor has reached a temperature beyond which immediate and permanent damage will occur. In order to supply power to all equipment until this point is reached, it is necessary to insure that the distribution and circuit protection system shall not fail earlier. This requires temperature-actuated protective devices built into the using equipment and system protection co-ordinated to avoid cutting off power to any load still in operating condition.

It is considered necessary to have at least one alternator and preferably two, as stand-by power. This is due not only to possible failure of an alternator but also to expected incidence of engine failures on long flights. The most effective use of the system requires parallel operation for best voltage and frequency regulation, which also makes available the maximum stand-by power with the least attention from the flight personnel. Since the equipment developed for three-phase 400-cycle aircraft electric systems is untried and had to be designed, built, and tested in a comparatively short period

Paper 46-3, recommended by the AIEE committee on air transportation for presentation at the AIEE winter convention, New York, N. Y., January 21–25, 1946. Manuscript submitted August 27, 1945; made available for printing October 16, 1945.

C. K. CHAPPUIS is a major with the Matériel Division, Office of Assistant Chief of Air Staff, United States Army Air Forces, Washington, D. C. LEONARD M. OLMSTED is special consultant, Air Technical Service Command, Wright Field, Dayton, Ohio.

The authors acknowledge the assistance of officers and personnel of the Army Air Force, Air Technical Service Command Engineering Division, equipment laboratory, in securing factual data, and the co-operation of aircraft and electric-equipment manufacturers in determining operating characteristics of equipment.

of time, it is felt that parallel operation cannot be guaranteed. Certainly during combat conditions it is impossible to insure that battle damage will not prevent parallel operation of alternators. Therefore, the system must be so designed that isolated operation is feasible even though not the desired operating condition. The main-power panel is somewhat complicated by this requirement, as circuit breakers are necessary to sectionalize the ring bus and load-transfer switches may be required to balance the loads for satisfactory isolated operation.

Good voltage control is essential, as many of the load devices require substantially normal voltage for satisfactory operation and life. Voltage control is accomplished at present by use of a conventional aircraft carbon-pile regulator actuated by rectified a-c system voltage and controlling the exciter field. The alternator is rated 120/208 volts and with the regulator is capable of regulation within ±2 per cent at its terminals. The excitation of the alternator will go from no load to ceiling current in approximately 0.1 second including regulator time. The system is normally considered as a 115/200-volt system inasmuch as this is approximately the normal full-load voltage at the main-power panel; the motors are designed for this voltage ±10 per cent. Design calculations indicate that with 75 per cent of the transmission capacity available and with the largest motor in locked-rotor condition, the voltage will not drop below 115/200 volts on the main-power panel and 90 per cent of this value at the most distant load bus. Thus it is apparent that the system regulation is satisfactory for motor operation. Electronic equipment, which includes radio and radar, is in a different classification as to voltage regulation requirements. Most radio equipment within the medium-, high-, and very high-frequency bands will operate satisfactorily with ±5 per cent voltage regulation. However, present radar equipment requires ±2 per cent regulation for satisfactory operation, and this problem is now being thoroughly investigated so that the characteristics of radar requirements and power supply can be reconciled.

It was necessary to develop new meters[14] inasmuch as no aircraft systems of this type were in use and consequently no suitable meters were available which were sufficiently light in weight and sufficiently reliable for the conditions of temperature and altitude encountered in aircraft operation. Wattmeters presented a design problem, but this has been solved satisfactorily, and the same meter is used to measure vars by means of a selector switch. Hermetically sealed meters would be a great improvement.

The distribution system serving this equipment likewise required extensive design effort in order that it might meet the difficult requirements of reliability, light weight, and voltage regulation. Commercial 120/208-volt systems are largely of the network type, with numerous feeding transformers located adjacent to the more concentrated loads to convert from the high-voltage primary system to utilization voltage. This type of system definitely requires parallel operation of power sources with strong ties to control the sharing of the load. It was obvious that such a system could not be used until successful parallel operation of alternators had been accomplished; attention was directed to developing an alternative type of system which would retain as many of the advantages as possible and still permit sectionalized operation from power sources out of parallel.

Operation of the system must require a minimum of attention by the flight crew. Many functions may be made automatic or partially so, and these portions of the system which are installed in multiple can be arranged to protect themselves. Every effort must be exercised to provide a system which will require the least possible specialized training for crew personnel.

Maintenance requirements must be simple enough to be handled with a minimum of special equipment and without excessive specialized training of personnel. Replacements must be convenient and require the smallest possible number of new stock items.

Power Source

Two common means are available for generating the a-c power, namely:

1. Auxiliary power plant.
2. Main-engine-driven alternators.

The first method involves electrical problems generally similar to central-station practice in that the electric system determines the size and speed of the prime mover and has sufficient capacity to assist in maintaining synchronism among several such auxiliary power units operating in parallel. The second method, while complicated by the fact that the size and speed of the prime movers are regulated by aircraft propulsion requirements, had definite advantages in savings of weight and useful space, over-all fuel economy, and availability of full-power output at all altitudes from the supercharged main engines. The main engines have been selected as the preferable power source, requiring that a power take-off be provided which converts engine speeds of 700 to 3,000 rpm to a constant speed for the alternator shaft drive. Since 400-cycle alternating current will be required to start the main engines, however, an auxiliary power unit must be provided either as a ground power source or as a supplement to the aircraft electric system.

The alternators[3] are designed for high speed and forced-air cooling to secure maximum output with minimum weight. Exciters are built into the alternator frames and directly connected to the alternator field, thereby assuring excitation to the alternator, regardless of disturbances on the a-c system. Adequate

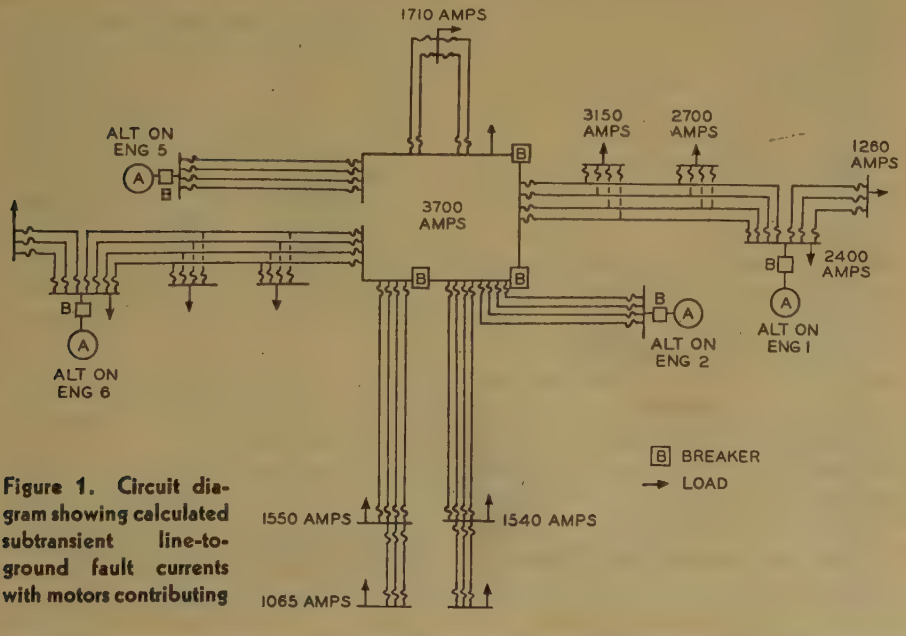


Figure 1. Circuit diagram showing calculated subtransient line-to-ground fault currents with motors contributing

capacity is provided for short overloads up to 200 per cent of rated output for five seconds without appreciable drop in terminal voltage, to facilitate the starting of large motors and the clearing of system faults. Typical characteristics of such an alternator are as follows:

Rating: 40 kva at 75-per-cent power factor, 120/208 volts, three phase
Speed: 6,000 rpm
Weight with exciter: Approximately 80 pounds

Substransient reactance $X_d'' = 0.136$ per unit
Transient reactance $X_d' = 0.191$ per unit
Synchronous reactance $X_d = 1.350$ per unit
Negative-sequence reactance $X_2 = 0.136$ per unit
Zero-sequence reactance $X_0 = 0.087$ per unit
Armature resistance (25 C) $r_a = 0.0215$ per unit
Field resistance (25 C) $r_f = 0.328$ ohm
Short-circuit time constant $T_d' = 0.01$ second
Substransient time constant $T_d'' = 0.0022$ second
D-c-component time constant $T_a = 0.002$ second
No-load rated voltage excitation = 17.6 amperes
No-load air-gap excitation = 15.6 amperes
Rated load, rated voltage excitation = 41.0 amperes
150-per-cent load, rated voltage excitation = 55.0 amperes
200-per-cent load, 203 volts excitation = 68.0 amperes
$R_1 = R_2 = R_0 = R_a$

Voltage is regulated by means of a solenoid-actuated carbon pile in the shunt field circuit of the exciter. The solenoid is connected to the 120/208-volt alternator terminals through transformers and rectifiers to measure the average of the three-phase voltages. The regulator circuit includes temperature compensation, back feed from the exciter terminals to provide antihunting features, and a connection to bias the solenoid current with reactive current.

Frequency is controlled by means of a governor in the constant-speed-drive system. This governor is actuated by alternator drive-shaft speed, biased by the electric-power output of the alternator to give a slight droop in speed at full load.[4] This characteristic permits a heavily loaded alternator momentarily to drop frequency slightly, thereby assuming an electrical angle somewhat behind other alternators carrying less load.

Parallel operation of alternators[5] requires identical shaft speeds with proper sharing of power output and reactive current. The governor itself holds reasonably uniform shaft speed, and the kilowatt sensing function of the governor control circuit tends to correct small differences in speed by introducing a slight droop in speed as load is applied to the alternator. Kilowatt division and shaft speed thus are controlled by the governor and constant-speed drive. Reactive-current division between alternators operating in parallel is controlled by the excitation; an overexcited alternator tends to supply excessive reactive current with but slight increase in system voltage, whereas an underexcited alternator shirks reactive current. Differentially connected current transformers on the alternator leads isolate the differences in distribution of reactive current, which are used to bias the voltage regulators and thereby to shift the excitation as required to correct the distribution of reactive current.

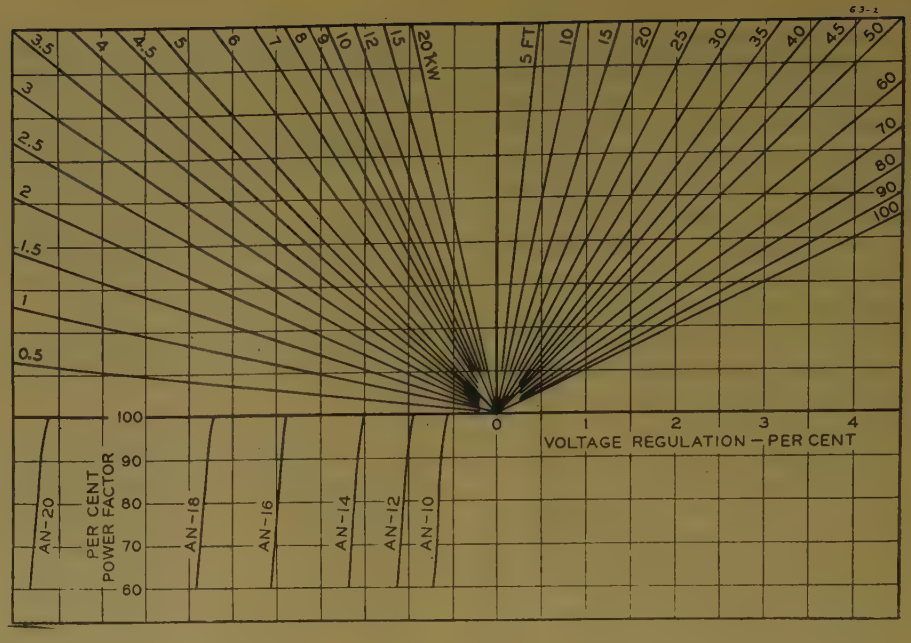


Figure 2. Voltage regulation chart—120/208 volts, 400 cycles, three phase, wires tied in close configuration

Protection in the power source is designed to isolate the power source and cut off its excitation for any of three abnormal conditions, namely:

1. Excitation at ceiling current for more than five seconds.
2. Frequency below 360 cycles.
3. Faults in the alternator armature winding or connections.

The first protects the exciter and alternator field against overheating but serves indirectly as protection for the power source against sustained heavy overload or failure to clear a fault on the system. The second protects magnetic devices on the system against excessive magnetizing currents permitted by low frequency at normal voltage. The third removes a damaged alternator from the system before the distribution system is impaired by fuse operations. This protection is accomplished by means of a ceiling-field relay actuated by the exciter field current, a frequency relay actuated by the alternator terminal voltage, and a differential relay actuated by unbalanced current in the alternator phase leads. All three relays energize the trip coil of the alternator circuit breaker which has an auxiliary contact to open the exciter field circuit. Tripping power is supplied from either rectified a-c terminal voltage or exciter armature voltage, one or the other of which can be expected to provide sufficient voltage under all normal and abnormal conditions.

Power-Distribution System

Although d-c power systems have been used on aircraft for many years, few if any data from these systems have value in a-c system design. D-c networks proposed for certain very heavy bombers have been analyzed on calculating boards, but the difference in characteristics due to the d-c generators and storage batteries makes these data inapplicable. A conference of engineers, called to discuss design requirements of the 115/200-volt three-phase 400-cycle a-c system, agreed upon the following design objectives:

1. Provide multiple power paths to all important loads as a means of protection against faulted conductors.
2. Design a system which will clear at least one fault in any section of a feeder without interruption of power to any load, unless the fault is on a load bus. The fuses adjacent to the fault shall clear the faulted section in such time that no other fuses shall lose their

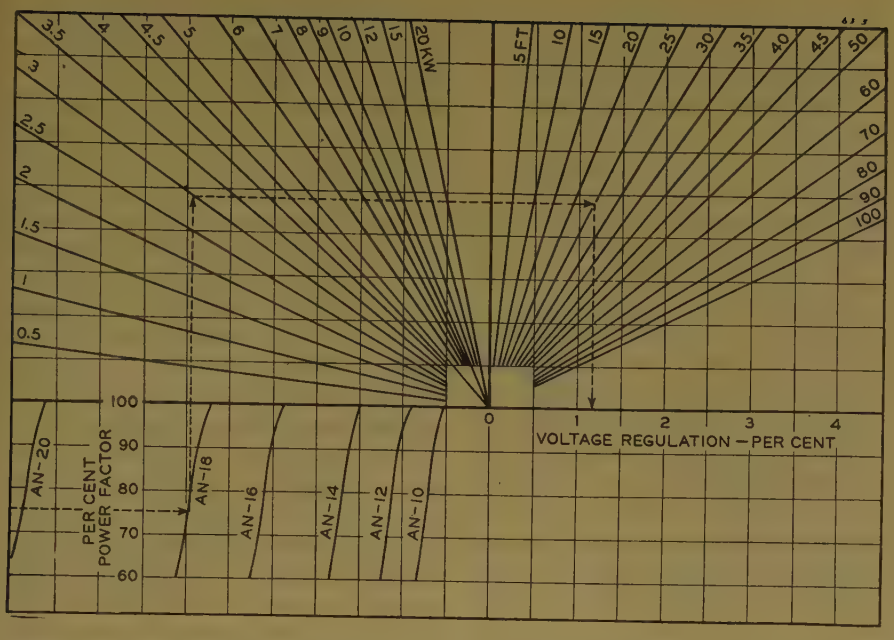


Figure 3. Voltage regulation chart—120/208 volts, 400 cycles, three phase, wires at 0.5 inch flat spacing

original ability to carry current or fail to co-ordinate in accordance with their design characteristics.

3. Be able to clear a second feeder fault in any designated load area without loss of power to the load. Damage to adjacent fuses in this case is undesirable but may be tolerated; co-ordination is essential.

4. Faults on load busses should be recognized as a secondary possibility, owing to the small area of conductor involved. Load lost should be limited to the load on the faulted bus.

5. The system should be designed to provide rapid clearing (maximum 0.1 second) to prevent motor stalling during faults with two or more alternators in parallel. Such clearing time is desirable, of course, with isolated operation but may be unattainable.

6. Any circuit must carry locked-rotor current for at least 30 seconds without damage to fuses, after the first fault has been cleared in any feeder. An exception may be necessary for motor-generator sets and hydropump motors.

7. Motors shall be able to start after a second fault in any feeder has been cleared.

8. Faults on the alternator terminals or the main bus should be recognized as a secondary possibility, and some means found to limit the portion of the circuit affected. Design of busses should provide mechanical features to minimize damage by gunfire.

9. The total number of fuses and range of sizes of fuses should be held as low as possible, consistent with good design.

10. The current distribution in each section, for load or fault conditions, must be balanced.

11. The system should be designed to operate in parallel or isolated. However, if the system operates isolated, the requirements of fast clearing must be somewhat relaxed.

The argument as to whether single or multiple circuits should be used depends for an answer upon the following: degree of reliability required, decrease in weight due to better cooling of smaller conductors, type of protection to be used and its weight, and characteristics of load. In general, it is found that more current can be carried in four wires than in one wire of similar weight without exceeding the maximum allowable operating temperature. Since maximum reliability is one of the prime requirements, it is necessary to provide alternate paths, so that remaining parallel circuits will operate at full efficiency after damage which isolates any one. In public power systems such reliability is obtained by a combination of loops, networks, complicated switching and protective devices, and continuous maintenance. The use of alternate paths for aircraft is feasible, provided a reliable lightweight method of insuring the continued operation of these circuits is available. It is obvious that complicated switching and protective systems, requiring balanced current, pilot wire, directional current, and similar methods of relaying which are very satisfactory for transmission lines, are in general too heavy and too complicated for aircraft. Such equipment probably would increase the vulnerability of the aircraft electric system. The use of properly balanced multiple circuits allows one of two methods to be used to clear faults. The first method is to take advantage of the small wires, allowing them to burn off and thus clear the fault. Much argument has been encountered on this method, but it appears to be rather uncertain, particularly where clearing time and co-ordination are important. The alternative is to use an accurate lightweight overcurrent device on each circuit at each bus to remove that portion of the circuit which is faulted. The most logical device of this type appears to be a small accurate high-speed fuse using a high-temperature fusing element.[6]

Radial, network, and loop circuits were examined for their applicability to large aircraft. It was found that none of these provided the most reliable, lowest weight, and best operating system. The final type of design, as shown in Figure 1, is a multiple-circuit radial system with alternators feeding to the main-power panel and also feeding loads located in the vicinity of the alternator. Thus the alternator leads to the main-power panel also serve as load feeders, and the alternator busses also serve as load busses. The output of the alternators is utilized in such a way that isolated operation is satisfactory whenever such operation is necessary. It is essential that all multiple paths between busses be equal in length, as otherwise the currents become unbalanced and make fuse co-ordination extremely difficult. One of the unbalanced loop conditions which was examined had an unbalanced current, under some fault conditions, of approximately 200 per cent which was reflected in the fuse co-ordination as an effect of 400 per cent in clearing time, owing to the I^2R effect on the fuse link. The use of combination load circuits and feeders made it mandatory to keep each alternator bus in service even though the alternator failed. The solution of this problem depends upon differential protection and high-speed breakers to remove a faulted alternator from the bus.

Three wire configurations were considered: three wires laced together, flat with one-half-inch spacing between centers, and flat with two-inch spacing between centers. The impedance of these three types was discussed by the authors in "Impedance of 400-Cycle Three-Phase Power Circuits on Large Aircraft and Its Application to Fault Current Calculations."[7] In general the impedance decreases with the decrease in separation. The ease of installation probably is increased when three wires can be placed together, but the vulnerability to gunfire and the difficulty of clearing trouble are greater. Where the wiring is easily accessible, the flat arrangement is the most satisfactory with use of one-half-inch spacing to keep the reactance low. The final decision as to wire configuration must depend upon the space available for

the installation. Voltage regulation charts are shown in Figures 2, 3, and 4.

Conductor sizes are determined by the allowable current-carrying capacities under specification *AN-J-C*-48 for a maximum ambient temperature of 160 degrees Fahrenheit. Under temperature and pressures encountered at higher altitudes, it is anticipated that wire temperatures will not exceed 100 degrees centigrade when operating at full load on the circuit and with one of the multiple paths out of service. The maximum wire size used on multiple circuits will usually be number 12 or smaller in present systems. The smallest sizes used will not be less than number 18 or number 20, owing to the mechanical weakness of smaller size.

Protection of this electric system depends upon the following: fuses, breakers, armor, and material protection. The ideal fuse characteristic for these circuits appears to be as shown by Figure 5. This is a high-speed fuse using a high-temperature link such as silver or copper to minimize the effect of differences in temperature. Owing to close co-ordination requirements the fuse must be extremely accurate, and it must also be explosion-proof with very short arcing time. The differential relays and circuit breakers used to remove any faulted alternator from the system must be extremely fast, clearing the maximum alternator bus fault in 0.02 second or less, to leave the fuses at the alternator bus intact for operation of the load circuits. In addition to this the breaker must be able to interrupt fault currents up to 4,000 rms amperes and perform all normal switching operations, up to 120 amperes, incident to operation of the aircraft. All of these operations must be performed under temperatures and altitudes required by Army Air Force specifications. Inasmuch as the requirements over wide ranges of altitude and temperature are so exacting, it is possible that development of sealed breakers may prove necessary.

Protection of the fuses, breakers, and busses can be accomplished only by mechanical means. The inherent protection of engines and heavy structural parts of the airplane can be used for part of the protection, and armor strips placed to protect vulnerable angles. The busses are so located that much natural protection is available and can be so designed structurally to minimize the possibility of battle damage by use of hollow sections of high-strength material for bus conductors.

The co-ordination of fuses and breakers is determined by the maximum fault currents, and the maximum clearing time is determined by the minimum fault current. Much research and many calculations were required to secure information on zero-sequence impedance for use in calculating line-to-ground fault currents.[7] The maximum fault currents occur from line to ground with the four alternators in parallel, and the minimum fault currents occur with three-phase faults and isolated operation. The requirement of parallel normal operation but emergency isolated operation greatly complicates the protection problem by causing a tremendous spread between maximum and minimum fault currents. The circuit arrangement and fault currents on one of these systems are shown in Figure 1. Under minimum fault-current conditions the maximum clearing time must be sufficiently small so that the rotating equipment will not stop or slow down to a point which will cause excessive reaccelerating current. The wide range of fault currents, with rigid requirements for co-ordination and fault clearing, made it necessary to design a new fuse for system protection.[6]

The alternator circuit breakers are required to co-ordinate with fuses only for failure of the alternator winding or leads; under this condition, however, co-ordination requires extremely fast differential-relay and breaker operation in order that the alternator bus fuses may remain undamaged to carry the electric load connected to that bus.[9] The same breaker, arranged for remote or manual operation, is suitable for the tie breakers on the main power bus.

The main power-panel bus is arranged as a ring bus of four sections tied with the same type of breaker as used for the alternators. By proper distribution of the load on the bus sections, it is possible to provide satisfactory load distribution for isolated operation with four alternators. By the use of two or three transfer switches, it is possible to provide acceptable load distribution for isolated operation with three alternators. Operation with two alternators whether isolated or parallel requires disconnection of some of the combat load. The load busses are so designed that the protective system can remove them from the system, in case of bus faults, without disturbance to the system. Loss of the main bus must be considered vital but sections can be lost without loss of the entire system.

Selection of the 115/200-volt three-phase 400-cycle a-c system for large aircraft permitted the use of three-phase induction motors.[10-12] Brushes and commutator problems thus were eliminated, and the motors became substantially constant-speed devices capable of reliable operation through a wide range of conditions. Momentary high torque loads can be handled by methods already established in commercial design practice. Such motors are contemplated in sizes ranging from one-eighth to 16 horsepower and speeds of 6,000 to 12,000 rpm. The few drives requiring variable speed are equipped with d-c motors supplied through motor generator sets or transformer–rectifiers. All motors are star-connected to permit emergency operation with reduced torque output after power supply to any one phase has failed, and the protective equipment must permit such operation.

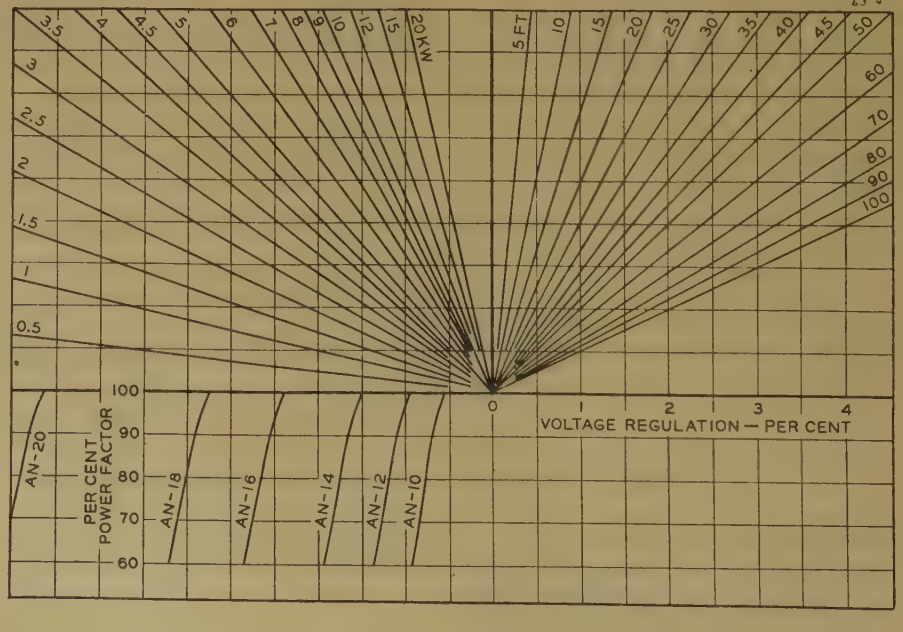


Figure 4. Voltage regulation chart—120/208 volts, 400 cycles, three phase, wires at 2.0 inches equivalent delta spacing

Provision for D-C Loads

While the major portion of the electric devices is suited to operation by a-c motors or transformers, a number of smaller devices, such as contactors and relays, solenoids, and certain instruments, still require d-c power. The connected load of these d-c devices is approximately 20 per cent of the total connected electric load of the aircraft, but many of the devices operate extremely infrequently with such diversity that their combined load probably is less than ten per cent of the total diversified load of the a-c power system. The need for this small amount of direct current adds complication to the a-c system, and there has been continuous effort to replace d-c devices with alternating current, with the ultimate objective of complete elimination of direct current from the aircraft. Under these conditions, it is expedient to install conversion equipment at the d-c load center and supply this load from the a-c system.

Both motor generator sets and transformer–rectifier sets have been built to convert the 115/200-volt three-phase alternating current to 28-volt direct current. The transformer–rectifier is quiet in operation, lighter, and somewhat more efficient than the motor generator. It has the further advantage, particularly in small ratings, of supplying acceptable voltage to relatively steady loads without the use of a voltage regulator, and thereby becomes attractive as a means of supplying the d-c load at several isolated small load centers rather than the center of the combined load.

Storage batteries appear to have little value on an electric system of this type and size. It is not practical to provide sufficient battery and conversion equipment to serve as reserve capacity for the a-c system supplying the major loads, and there is little advantage in backing up only the d-c system serving secondary loads.

Very few of the d-c loads draw enough power to require multiple circuits for carrying capacity or voltage regulation. The method is still applicable, however, to those circuits where vulnerability to damage because of length or exposure indicates the need for more than a single circuit to serve any particular device.

Future Trends

There is a continuous trend to larger electrical requirements on aircraft, and the trend is most pronounced in combat aircraft. Hydraulic lines are particularly susceptible to battle damage, inasmuch as damage to almost any part of the system may cause loss of pressure on the entire hydraulic system. Electric power for cabin supercharging would reduce air-duct requirements and weight and simplify installation of equipment. The use of electricity for propeller deicing and electric blowers to distribute heated air through small ducts at high velocities for wing and cabin deicing would reduce weight and simplify installations as well as provide positive air flow as required. Aircraft armament is increasing in size of guns and number of turrets; as flying speeds are increased, the demand for higher turret speeds and accurate split-second remote fire control is becoming more insistent; all of these add to the power requirements. With greater flying ranges and more complex tactical operations, the demand for additional communication equipment also is becoming greater. Radar and allied equipment are essential if aircraft operations are to be consistently effective in all weather conditions. Ten to 15 kva of electric power are required for radar and countermeasures equipment for special installations and are anticipated for future aircraft. Static dischargers requiring electric power are under development. The use of television to transmit information to the pilot is a distinct possibility. The all-electric airplane using electric motors to drive the propellers is within the realm of possibility. All of the "Buck Rogers" items for aircraft, control of aircraft, or against which aircraft must be defended require electric power.

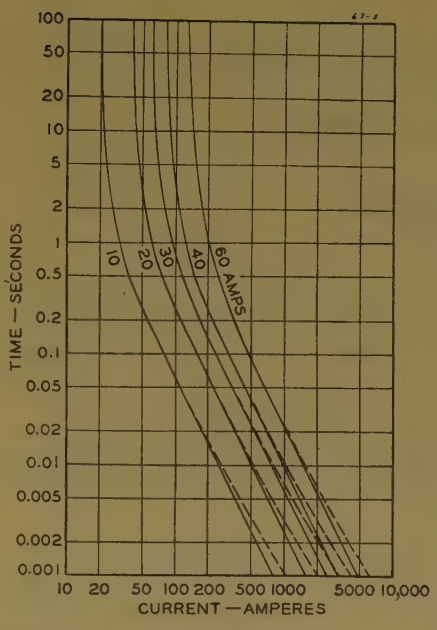


Figure 5. Time–current curve for 400-cycle 120/208-volt aircraft fuses

Solid lines—Average melting
Dashed lines—Average clearing

Any attempt to restrict the amount of electric power available to combat aircraft for these uses places the designers at a severe disadvantage. This is particularly true of electronic equipment, much of which is comparatively new. The demand for radar and countermeasure equipment is often so insistent and immediate that engineers do not have time to design it for best performance with small amounts of power. Several aircraft now under design have 120 kw of generating capacity. This capacity may be compared with public power systems, where 120 kw normally would be adequate for 100 to 125 miles of rural distribution line.

References

1. Why Tomorrow's Planes Will Have A-C Electrical Systems, T. B. Holliday. *Electrical Manufacturing*, July 1943, page 88.

2. Basic Considerations in Selection of Electric Systems for Large Aircraft, W. K. Boice, L. G. Levoy, Jr. AIEE Transactions, volume 63, 1944, June section, pages 279–87.

3. A 40-Kva 400-Cycle Aircraft Alternator, H. E. Keneipp, C. G. Veinott. AIEE Transactions, volume 63, 1944, November section, pages 816–21.

4. Governor Requirements for Aircraft Alternator Drives, W. K. Boice, L. G. Levoy, Jr. AIEE Transactions, volume 64, 1945, July section, pages 534–40.

5. Parallel Operation of Airplane Alternators, D. W. Exner. AIEE Transactions, volume 62, 1943, December section, pages 755–60.

6. A Current-Limiting Fuse for Aircraft Applications, A. H. Powell. AIEE Transactions, volume 64, 1945, July section, pages 541–5.

7. Impedance of 400-Cycle Three-Phase Power Circuits on Large Aircraft and Its Application to Fault-Current Calculations, C. K. Chappuis, L. M. Olmsted. AIEE Transactions, volume 63, 1944, pages 1213–20.

8. Army–Navy Aeronautical Specification—Cable; Electric, Low-Tension, Aircraft.

9. A 208/120-Volt 120-Ampere Three-Pole 400-Cycle Electrically-Operated Aircraft Circuit Breaker, C. H. Titus, P. J. Reifschneider. AIEE Transactions, volume 64, 1945, August section, pages 551–5.

10. Design Characteristics of 400-Cycle Aircraft Motors, M. B. Sawyer, Sr. AIEE Transactions, volume 63, 1944, December section, pages 877–9.

11. 400-Cycle Aircraft Motor, G. O. Schwandt. AIEE Transactions, volume 64, 1945, July section, pages 508–12.

12. Some Aspects of the Application of Induction Motors to Aircraft, H. J. Braun. AIEE Transactions, volume 63, 1944, October section, pages 769–72.

13. Alternating-Current Electrical System for Large Aircraft, Westinghouse engineers. Pamphlet *R*-1064, October 1943, Westinghouse Electric Corporation, East Pittsburgh, Pa.

14. Instrumentation of 400-Cycle Aircraft Electric Systems, A. J. Corson, A. G. Stimson, W. A. Soley. AIEE Transactions, volume 63, 1944, November section, pages 830–5.

Temperature Rise of Water-Cooled Power Transformers

J. R. MEADOR
MEMBER AIEE

Synopsis: This paper contains an analysis of the oil temperature rise of water-cooled power transformers. It is shown that by factoring the effect of viscosity oil temperatures can be calculated more accurately for a variety of conditions. Equations and curves are given with supporting test data for determining the temperature rise for different loads, ingoing water temperatures, and rates of water flow. The variations in temperature rise with load, water rate, and water temperature are appreciably different from published data on the subject. A discussion of winding hot-spot temperature is included, although no new test data are given.

WATER-COOLED transformers have cooling coils located in the upper portion of the tank usually adjacent to the tank wall. Water flow through these coils carries away the heat generated in the core and windings. The top-oil temperature depends on the amount of cooling coil, the transformer losses, the water rate, and the ingoing water temperature.

As the flow of oil through the windings of a water-cooled transformer is very similar to that in a self-cooled transformer having external cooling radiators, the same general equations for winding rise over oil can be used.

The purpose of this paper is to show how the transformer-top-oil temperature varies when the load, water rate, and ingoing water temperature are changed and to give curves for estimating the effect on the winding hot-spot temperature.

General Conclusions

1. Oil temperature rise over ingoing water is not a simple function of the loss dissipated. However, oil rise varies approximately as $(\text{loss})^{0.85}$ (see Figures 4 and 5).

2. When the water rate is changed, the oil temperature rise varies 40 per cent as much as the change in water temperature rise (see Figure 5).

3. When the water temperature is lowered, the oil temperature rise over ingoing water increases 0.75 per cent for each degree the ingoing water temperature is below 25 degrees centigrade (see Figure 4).

4. In a typical transformer the load can be increased 0.8 per cent for each degree the ingoing water temperature is below 25 degrees centigrade (see Figure 8).

In these general conclusions it is assumed that the radiation and convection losses from the tank surface are negligible. In a specific case the tank loss can be properly evaluated.

Components of Oil Temperature Rise

The heat generated in the windings and core of a water-cooled transformer is dissipated to the oil by free convection. The heated oil becomes less dense and flows upward to the top of the tank. The cooling coils in the upper portion of the tank receive heat from the oil by free convection. As the oil is cooled, it becomes more dense and flows downward and into the windings again. (A small percentage, usually 10 per cent to 20 per cent of the heat is dissipated from the tank surface.) The water flowing through the cooling coils removes the heat by forced convection and, in the process, the temperature of the water is raised. If the water temperature rise is measured carefully and the rate of flow is known, the watts loss carried away by the water can be calculated from the equation:

Watts loss = 264 × water rise, degrees centigrade × gallons per minute.

This thermal circuit is the basis for an equation of the following general form:

Top-oil temperature = ingoing water temperature
+ ½ water temperature rise
+ water-film drop (water to tube)
+ oil-film drop (tube to oil)
+ top-oil increment (1)

Each of these components is known or can be determined by test.

The top-oil increment is the difference in temperature between the top oil and the average oil surrounding the cooling coils (which is also approximately the average oil temperature in the windings). Experience has shown that in most water-cooled power transformers the top-oil increment is approximately two degrees centigrade over a wide range of conditions.

The oil-film drop, which is the local temperature difference between the cooling-tube wall and the adjacent oil, can be expressed with good accuracy by an equation of the following form:

$$\text{Oil-film drop, degrees centigrade} = K W_s^x \mu_f^y$$

where

W_s = watts per square inch outside surface of cooling coil.

μ_f = viscosity of oil, in centipoise, at average temperature of oil film. (Average film temperature is tube temperature plus one half of oil-film drop)

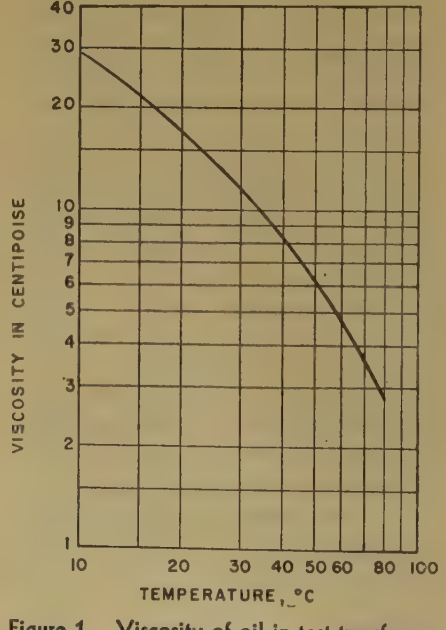


Figure 1. Viscosity of oil in test transformer

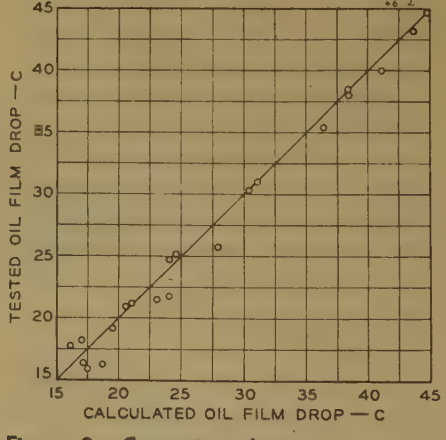


Figure 2. Comparison between calculated and tested oil-film drop

Paper 46-6, recommended by the AIEE committee on electric machinery for presentation at the AIEE winter convention, New York, N. Y., January 21–25, 1946. Manuscript submitted September 26, 1945; made available for printing October 30, 1945.

J. R. MEADOR is research engineer in the power transformer engineering division of the General Electric Company, Pittsfield, Mass.

The author acknowledges the assistance of L. Wetherill and Miss J. E. Shipton, both of the Pittsfield works of the General Electric Company in the preparation of this paper.

K = a constant
x, y = exponents to be determined

The water-film drop is the local temperature difference between the cooling-tube wall and the adjacent water flowing through the cooling coil and can be expressed with sufficient accuracy by the following equation:

$$\text{Water-film drop, degrees centigrade} = \frac{K_1 W_i^{1.0}}{V^{0.8}}$$

where

W_i = watts per square inch inside surface of cooling coil
V = water velocity in feet per second
K_1 = a constant

The water-film drop is comparatively small and can be expressed simply by $(0.37 W_s^{1.0})$ in a normal power transformer.

The water temperature change enters into the equation for oil rise as water temperature rise/2. Though this is not theoretically exact, it is sufficiently accurate when the water rise is appreciably less than the oil rise. The error becomes appreciable at small loads and very low water rates.

Thus equation 1 can be written:

$$\text{Top oil temperature degrees centigrade} = \text{ingoing water temperature degrees centigrade} + {}^1/_2 \text{ water temperature rise, degrees centigrade} + 0.37 W_s^{1.0} + K W_s^x \mu_f^y + 2 \text{ degrees centigrade} \quad (2)$$

The only unknowns in equation 2 are K, x, and y. These are determined from the tests given below.

Test Data

Table I contains heat-run results on a 6,000-kva water-cooled transformer with $1^3/_8$-inch-outside-diameter copper-cooling coils. The tabulated net watts loss dissipated by the cooling coils is the total loss held minus the estimated tank dissipation. This loss was varied from 21,740 watts to 75,600 watts, the water rate from four gallons per minute to 35.3 gallons per minute and the ingoing water temperature from 6.6 degrees centigrade to 40.5 degrees centigrade.

All tests were run until the top-oil rise over ingoing water was constant.

Commercial test facilities were used throughout for these heat runs with no special precautions taken to obtain laboratory accuracy.

Table I shows the calculated as well as the tested water temperature rises. The agreement is fair, usually within two degrees centigrade. In analyzing the data averages of the calculated and tested values were used.

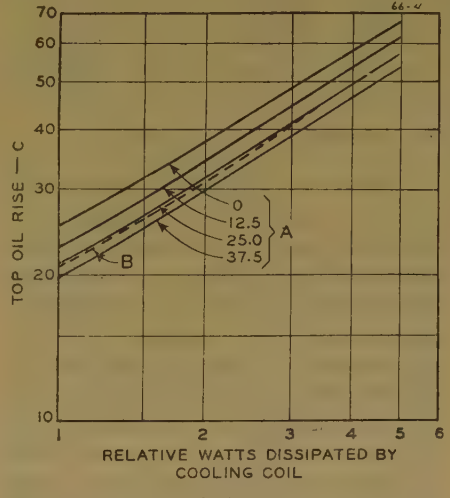


Figure 4. Effect of changing ingoing water temperature, holding ten degrees water rise

A—Ingoing water temperature, degrees centigrade
B—Design curve used since 1938 for 25-degree-centigrade ingoing water and ten-degree-centigrade water rise

Analysis of Test Data

By substituting these heat-run results into equation 2, a value of oil-film drop (tube to oil) is found for each test. By analyzing these tests the unknowns K, x, and y in the oil-film-drop equation are determined. The oil in this transformer has a viscosity–temperature relationship as shown in Figure 1. Its thermal properties are essentially the same as other transformer oils used throughout the industry.

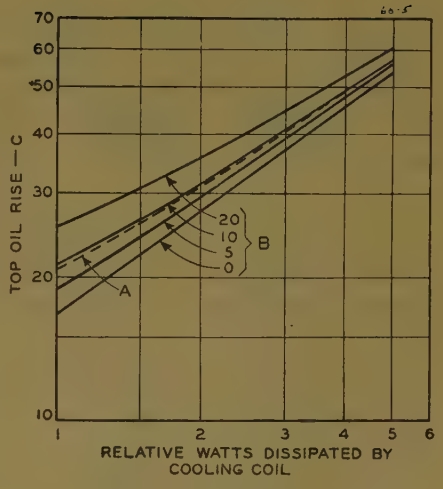


Figure 5. Effect of changing water temperature rise, holding 25 degrees ingoing water

A—Design curve used since 1938 for 25-degree-centigrade ingoing water and ten-degree-centigrade water rise
B—Water rise, degrees centigrade

$$\text{Oil film drop, degrees centigrade} = 7.4 W_s^{0.88} \mu_f^{0.28} \quad (3)$$

To show that these determinations are accurate, the test values are compared with those calculated from equation 3 in Figure 2. Equation 3 is in good agreement with published data[1] on free convection in the range used in this paper.

With this factor determined the final equation for oil temperature becomes:

$$\text{Top-oil temperature, degrees centigrade} = \text{ingoing water temperature degrees centigrade} + {}^1/_2 \text{ water temperature rise, degrees centigrade} + 0.37 W_s^{1.0} + 7.4 W_s^{0.88} \mu_f^{0.28} + 2 \text{ degrees centigrade} \quad (4)$$

The heat-run results in Table I are

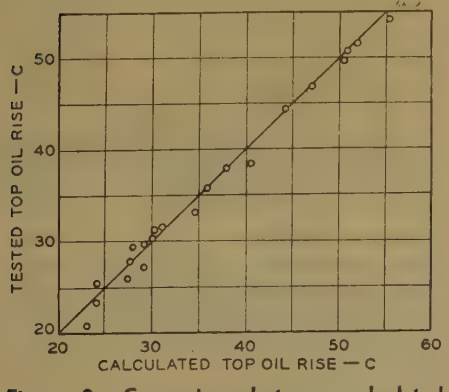


Figure 3. Comparison between calculated and tested top-oil rise over ingoing water

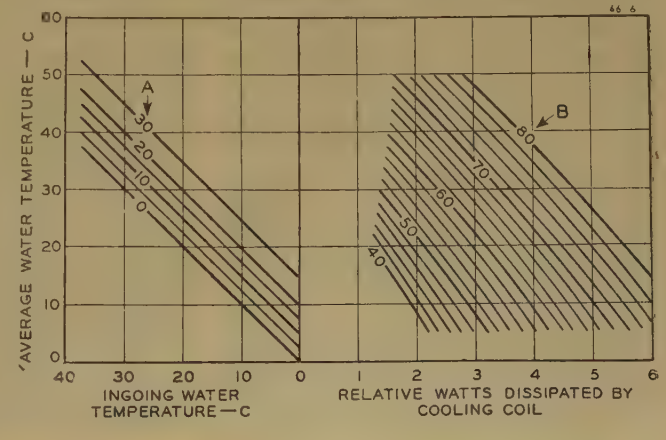


Figure 6. Effect of changing ingoing water temperature and water temperature rise on top-oil temperature

A—Water rise, degrees centigrade
B—Top-oil temperature, degrees centigrade
Water rise, degrees centigrade = watts ÷ (264 × gallons per minute)

Table I. Heat Runs on 6,000-Kva Water-Cooled Transformer

Test	Watts Dissipated by Cooling Coil	Ingoing Water Temperature, Degrees Centigrade	Water Rate, Gallons per Minute	Top-Oil Temperature, Degrees Centigrade	Water Rise, Degrees Centigrade	
					Test	Calculated*
1	59,800	24.4	35	68.7	6.5	6.5
2	61,000	24.3	20.0	71.0	10.7	11.6
3	59,800	24.8	10.0	74.4	19.5	22.6
4	62,000	6.6	35.3	57.3	6.0	6.6
5	62,000	7.5	22.5	59.0	8.8	10.4
6	60,700	7.8	10.5	61.9	19.0	21.9
7	38,000	8.1	30	43.8	3.8	4.8
8	37,900	8.1	15	46.0	9.0	9.6
9	36,200	9.6	7	48.0	17.0	19.6
10	34,500	37.0	30.0	62.9	3.9	4.4
11	31,600	37.5	15.0	65.3	8.4	8.0
12	32,100	37.7	7.5	69.2	14.0	16.1
13	30,900	40.5	7.5	70.8	14.7	15.6
14	34,000	25.0	30	54.7	4.3	4.3
15	33,300	25.5	15	56.7	6.9	8.4
16	33,500	25.0	7	58.1	14.5	18.1
17	20,300	12.0	30	32.8	0.5	2.6
18	18,800	10.8	8	34.1	8.1	8.8
19	18,900	11.1	8	36.5	8.7	8.9
20	20,100	10.8	4	37.9	14.3	19.0
21	18,800	11.6	4	40.9	16.8	17.6

*Calculated water rise = watts/(264 × gallons per minute).
The air temperature ranged from 17 degrees centigrade to 27 degrees centigrade during these tests.

compared with calculations using equation 4 in Figure 3.

Curves for Top-Oil Temperature Rise

From equation 4 curves of top-oil temperature rise versus loss are plotted in Figure 4 for ingoing water temperatures from 0 degrees centigrade to 37.5 degrees centigrade, holding a constant water temperature rise of 10 degrees centigrade.

On Figure 5 similar curves are shown for water temperature rises from 0 degrees centigrade to 20 degrees centigrade, holding a constant ingoing water temperature of 25 degrees centigrade.

On both Figure 4 and Figure 5, a dotted line for 25 degrees centigrade ingoing water temperature and 10 degrees centigrade water temperature rise is plotted. This curve was derived by the author in 1938 for design use, and acceptance heat runs on dozens of transformers have shown it to be quite accurate.

In order to make these heating curves more usable by the transformer operator, the double family of curves on Figure 6 has been prepared. With these curves, if the transformer-oil temperature rise is known for any one condition of loss, water rate, and ingoing water temperature, then the temperature can be determined for any other set of conditions. As an example, for any known load and water temperature, the water rate can be predetermined to hold a specified oil temperature.

If a high degree of accuracy is required, the tank dissipation should be estimated. For each square foot of tank surface allow one watt for each degree centigrade the oil temperature is above the air temperature. For example, if the tank surface is 500 square feet and the expected oil temperature is 30 degrees centigrade above the air, the tank dissipation will be 15,000 watts. In a normal water-cooled power transformer the error in this simple calculation will affect temperature-rise calculations by less than one degree centigrade.

Winding Hot-Spot Temperature

This paper contains no new test data on winding hot-spot temperatures. It appears, however, that published information on self-cooled transformers can be used to estimate the hot-spot temperature in water-cooled transformers.

There is a wealth of information on hot-spot temperatures in self-cooled transformers in reference paper.[3] The data have to be analyzed in a somewhat different manner, however, to be used in this paper.

Reference paper 2 states that when the top-oil increment is relatively small, the winding hot-spot temperature rise over top oil varies as $(\text{loss})^{0.8}$. An examination of the tests shows this to be true if the increases in load are accompanied by an increase in oil temperature. In making normal short-time overload calculations, this relation between hot-spot rise and loss is reasonably accurate, because an increase in loss increases the oil temperature. To use these data for other conditions of top-oil temperature variation, the hot-spot temperature rise must be given a viscosity correction. Since

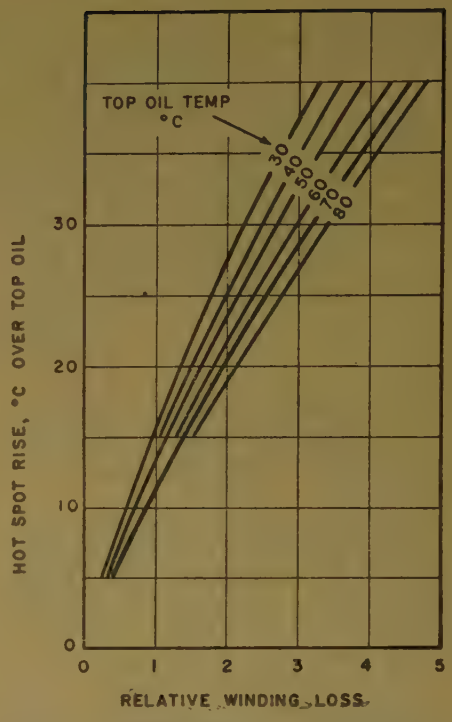


Figure 7. Winding hot-spot temperature rise over top oil as a function of winding loss and oil temperature

the hot-spot rise over top oil is largely an oil-film drop, such a correction should be legitimate.

After analyzing the test data in reference paper 2 and other data on oil-film drop, the writer has come to the conclusion that hot-spot rise over top oil can be

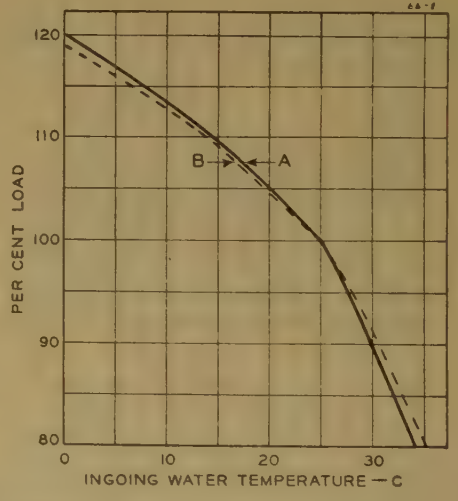


Figure 8. Effect of ingoing water temperature on permissible load, keeping constant hot-spot temperature

At 100 per cent load:
Water temperature = 25 degrees centigrade
Water rise = 10 degrees centigrade
Top-oil temperature = 69 degrees centigrade
Hot-spot temperature = 90 degrees centigrade
Loss ratio = 2:1
A—For constant water rise
B—For constant water rate

expressed approximately by the following equation:

$$\text{Hot spot over top oil, degrees centigrade} = K_2 L^{0.9} \mu_f^{0.3} \quad (5)$$

where

K_2 = a constant depending on the winding dimensions
L = winding loss in watts
μ_f = oil viscosity at film temperature in centipoise

The data supporting this conclusion are as follows.

1. The oil-film drop on the water-cooling coil was found to vary as $(\text{loss})^{0.88}$ and $(\text{viscosity})^{0.28}$.

2. Plate-to-oil tests shown in reference paper 3 can be correlated accurately by assuming the oil-film drop to vary as $(\text{loss})^{0.8}$ and $(\text{viscosity})^{0.4}$.

3. The hot-spot data from the three transformers tested in reference paper 2 can be correlated in a similar fashion. Taking only those conditions having a relatively low top-oil increment and assuming the hot-spot rise to be an oil film drop gives the following relations:

Transformer	Oil-Film-Drop Correlation
H-60-2,000 kva	$(L)^{0.9}(\mu_f)^{0.12}$
H-60-2,500 kva	$(L)^{0.9}(\mu_f)^{0.46}$
OAP-60-3,125 kva	$(L)^{0.9}(\mu_f)^{0.25}$

When all of the foregoing was taken into consideration, the use of $(\text{loss})^{0.9}$ and $(\text{viscosity})^{0.3}$ seemed to be the best average to use until more reliable data are available. From study of other unpublished data the author believes the use of these exponents for overload calculations will give conservative results.

This viscosity effect is particularly important for calculating permissible continuous overloads at reduced ambient temperatures. Under this condition as the load goes up the oil temperature comes down. Thus, on overloads the oil viscosity is higher than at normal load in standard ambient. The effect is to increase the hot-spot over top oil as approximately $(\text{loss})^{1.0}$. This is fortunate since turn insulation and other solid insulation temperature drops also increase as $(\text{loss})^{1.0}$.

To facilitate calculation, a family of curves has been plotted on Figure 7 showing hot-spot variation with winding loss and oil temperature as plotted from equation 5.

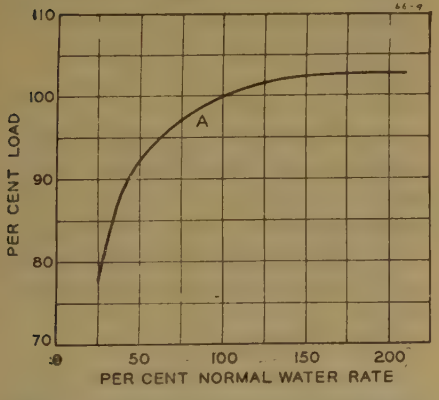


Figure 9. Effect of water rate on permissible load, keeping constant hot-spot temperature

At 100 per cent load:
Water temperature = 25 degrees centigrade
Water rise = 10 degrees centigrade
Top-oil temperature = 69 degrees centigrade
Hot-spot temperature = 90 degrees centigrade
Loss ratio = 2:1
A—For 25-degree-centigrade ingoing water temperature

Permissible Loading When Water Temperature and Water Rate Are Changed

By the use of the curves in this paper, the effect of changing the water rate and the ingoing water temperature on a typical water-cooled transformer can be calculated. Assume that a transformer has the following characteristics at 100 per cent load:

Ingoing water temperature = 25 degrees centigrade
Water temperature rise = 10 degrees centigrade
Hot-spot temperature = 90 degrees centigrade
Top-oil temperature = 69 degrees centigrade
Loss ratio = 2:1

By using Figure 6 and Figure 7 the permissible loads that can be carried by this transformer with other ingoing water temperatures are shown on Figure 8. One curve is for a constant water rate, and the other applies if the water rate is changed with load to maintain ten degrees centigrade water rise at all times. It is interesting to note that very little is gained by increasing the water rate at the higher loads. For either condition the load can be increased approximately 0.8 per cent for each degree centigrade the water temperature is under 25 degrees centigrade and should be reduced approximately two per cent for each degree centigrade the water temperature is above 25 degrees centigrade.

Similarly, Figure 9 shows how the load can be varied, if the water rate is changed, holding constant ingoing water temperatures.

Figures 8 and 9 are drawn on the basis of maintaining a constant winding hot-spot temperature except for loads less than 100 per cent, where the top oil temperature is kept constant on account of the core temperature being the limiting factor.

Discussion

Incrustations in the cooling coil will increase the temperature difference between the water and the cooling coil by adding a scale temperature drop and consequently will increase the oil temperature.

It is apparent from the foregoing that the viscosity of the oil is a very important factor in water-cooled transformer calculations. If the oil in a transformer does not have a viscosity–temperature relation similar to that shown in Figure 1, the curves given in this paper will not apply. In general, however, an appreciable difference will be noted only when the ingoing water temperature is low.

Additional test data must be obtained to permit a more precise calculation of winding hot-spot temperatures in water-cooled transformers. However, with the small difference in temperature between top oil and average oil that exists in most water-cooled transformers, hot-spot temperatures are usually not a problem to the designer. This is in contrast to some self-cooled transformers that have top-oil increments of as much as ten degrees centigrade, or even more where the average winding rise must be reduced to meet the hot-spot limit.

Even in a water-cooled transformer, where the oil encounters very little friction in its path of flow, the top-oil increment may be five degrees centigrade or six degrees centigrade instead of two degrees centigrade, if the oil level is only a small distance above the core and coils or if the cooling coil extends down too far along the core and coils. For these cases the curves in this paper still can be used with little error to estimate the effect of changing load, water temperature, and water rate. (The designer must know how much the oil temperature will increase to be sure that the hot-spot-temperature limit is not exceeded.)

References

1. The Basic Laws and Data of Heat Transmission, W. J. King. *Mechanical Engineering*, March–August 1932.

2. Emergency Overloading of Air-Cooled Oil-Immersed Power Transformers by Hot-Spot Temperatures, V. M. Montsinger, P. M. Ketchum. AIEE Transactions, volume 61, 1942, pages 906–16.

3. Transformer Engineering (book), L. F. Blume, A. Boyajian, G. Camilli, and V. M. Montsinger. John Wiley and Sons, Inc., New York. N. Y., 1938. Page 314.

Formulas for Conductor Size According to Cost of Resistance Loss

HERBERT B. DWIGHT
FELLOW AIEE

IN DESIGNING an electric-power line the choice of conductor depends on several factors such as mechanical strength, corona loss, reactance, and resistance. In the early years of electric-power transmission and distribution, a size of conductor was chosen which was considered the best in view of all the requirements. At present so many different types of line conductors are available that each feature can be provided for almost independently. Thus, a core of steel or bronze may be specified to provide the required mechanical strength; a hollow conductor may be chosen to avoid corona and to reduce the reactance; and the resistance, that is the current density, may be chosen according to the cost of resistance loss or according to temperature rise.

In this paper are described formulas by which the conductor size, usually expressed by the number of circular mils, can be computed conveniently according to the cost of resistance losses.

The effect of the cost of resistance loss is such that in most cases where one is choosing a conductor for a power circuit that is to be built there is a certain current density at peak load that should not be exceeded.

The cases are divided into two classes which are markedly different. Where the conductors are owned by the company which generates the power, conditions at peak load are predominant. On the other hand, where the losses in the conductor are paid for by the kilowatt-hour, a careful determination must be made of the ratio of the yearly average resistance loss to the maximum. This ratio may be very low on some branch circuits which may go practically unused for extended periods. In spite of the difference between the two classes, the same formulas may be used for both.

Where the conductors are owned by the power company, the problem depends almost entirely on conditions at peak load, and the work of choosing a conductor size becomes comparatively simple. After the maximum advisable current density has been determined for a given location, it can be applied quickly for almost any case that might arise, and the length of line, voltage, and so forth, need not affect directly the choice of conductor cross section. After the maximum current density for uninsulated conductors has been determined, it is a simple rule to state that in specifying new conductors of that type at any voltage, this current density should not be exceeded unless there is an exceptional case.

The simplest case will be taken up first, and details arising from various items will be added later.

Let

C = circular mils of a bare overhead copper conductor

Cubic inches of copper per 1,000 feet $= \frac{\pi}{4} C \times 10^{-6} \times 12{,}000$

Cost of copper at v dollars per pound, installed, and 0.321 pound per cubic inch is

$$0.321 \times \frac{\pi}{4} 10^{-6} \times 12{,}000\, Cv = 0.00303\, Cv \text{ dollars per 1,000 feet}$$

Annual fixed charge at m_1 per cent $= 0.0000303\, Cvm_1$ per year

Resistance at 0.692×10^{-6} ohm per inch cube at 25 degrees centigrade $= 0.692 \times 10^{-6} \times 12{,}000 \times \frac{4}{\pi C} \times 10^{6} = \frac{10{,}600}{C}$ ohms per 1,000 feet

Resistance loss at I amperes $= 10.6 \frac{I^2}{C}$ kilowatts per 1,000 feet (1)

The numerical coefficients would be different for aluminum conductors as shown by equations 13 and 14.

Let power be supplied by a water-power station and an intervening power circuit whose first cost is s dollars per kilowatt and whose annual fixed charge is m_2 per cent. Let the station be enlarged enough to supply the resistance loss. Let I be the current in the conductor at the time of peak load on the station. The fixed charge for this enlargement of the station for 1,000 feet of conductor is

$$0.106 \frac{I^2 s m_2}{C} \text{ dollars per year}$$

Total annual charge for the copper and its resistance loss is

$$M = 0.0000303\, Cvm_1 + 0.106 \frac{I^2 s m_2}{C} \text{ dollars per 1,000 feet of conductor} \quad (2)$$

The rate of change of M for a given current I, as C varies, is

$$\frac{dM}{dC} = 0.0000303\, vm_1 - 0.106 \frac{I^2 s m_2}{C^2} \quad (3)$$

As long as this is negative, it pays to increase C. The most economical size is when $dM/dC = 0$. Then

$$\frac{C^2}{I^2} = \frac{0.106}{0.0000303} \frac{sm_2}{vm_1}$$

$$\frac{C}{I} = 59 \sqrt{\frac{sm_2}{vm_1}} \text{ circular mils per ampere} \quad (4)$$

Section of conductor is

$$A = \frac{\pi}{4} C 10^{-6} \text{ square inch}$$

Most economical current density is

$$\frac{I}{A} = \frac{4 \times 10^6}{59\pi} \sqrt{\frac{vm_1}{sm_2}} = 21{,}500 \sqrt{\frac{vm_1}{sm_2}} \text{ amperes per square inch} \quad (5)$$

Thus, let

$v = 0.25$ dollar per pound, installed
$s = 150$ dollars per kilowatt
$m_1 = m_2 = 12$ per cent
temperature of conductor = 25 degrees centigrade

$$\frac{sm_2}{vm_1} = \frac{150}{0.25} = 600$$

Circular mils per ampere $= 59 \sqrt{600} = 1{,}450$ by equation 4.

Fuel Cost

Let the ratio of average resistance loss to its value at the time of peak load on the generating station be b. This is less than the load factor.

The kilowatt-hours of resistance loss per 1,000 feet of conductor per year are

$$8{,}760 \times 10.6 \frac{bI^2}{C} = 93{,}000 \frac{bI^2}{C}$$

Let the fuel cost per kilowatt-hour be g dollars.

$$\text{Annual fuel cost} = 93{,}000 \frac{bgI^2}{C}$$

Annual fixed charge on a portion of the generating station to supply the line losses $= 0.106 \frac{I^2 s m_2}{C}$ where s and m_2 have the meanings already described.

Paper 46-8, recommended by the AIEE committee on power transmission and distribution for presentation at the AIEE winter convention, New York, N. Y., January 21–25, 1946. Manuscript submitted September 15, 1945; made available for printing November 1, 1945.

HERBERT B. DWIGHT is professor of electrical machinery, Massachusetts Institute of Technology, Cambridge, Mass.

Annual charge for the conductor and its loss is

$$M=0.0000303Cvm_1+\frac{I^2}{C}(0.106sm_2+93{,}000bg) \quad (6)$$

$$\frac{dM}{dC}=0.0000303vm_1-\frac{I^2}{C^2}(0.106sm_2+93{,}000\,bg)$$

For the most economical current density, including fuel cost,

$$\frac{C^2}{I^2}=\frac{0.106sm_2+93{,}000bg}{0.0000303vm_1}$$

$$\frac{C}{I}=182\sqrt{\frac{0.106sm_2+93{,}000bg}{vm_1}} \quad (7)$$

at 25 degrees centigrade.

The cost of copper, v dollars per pound, should include the cost per pound for installation and also the cost of any part of the supports whose cost varies directly with the weight of copper.

If the energy is purchased at a certain amount per kilowatt-hour, this amount is to be taken as the value of g, and in such a case s is to be taken as zero unless there is a further charge proportional to the peak or demand. In computing the saving from reduced resistance losses where a step rate is used, the lowest step should be taken as the value of g. In case of payment by the kilowatt-hour, I is to be the peak current in the conductor, and b is to be computed for peak load on the conductor instead of on the generating system.

Varying Cost Per Pound of Insulated Copper

When the cost per 1,000 feet of a given type of insulated conductor is plotted, it is found that the conductor cost does not increase so fast as the weight of copper. The insulation tends to be a rather constant part of the complete conductor.

Let the rate of increase of conductor cost be h times the rate of increase of copper. An average value of h may be about 0.75, but it may be much less for small wire sizes. It usually may be taken as one for bare transmission-line conductors.

In order to find the value of h, the cost of various sizes of insulated conductor in dollars per 1,000 feet may be plotted against the number of circular mils of copper and a smooth curve drawn through the points. This curve usually is fairly straight. Suppose, for example, that two points which give the slope of the curve at a desired part of the range are \$150 per 1,000 feet for 100,000 circular mils and \$210 per 1,000 feet for 150,000 circular mils. The percentage increase in cost is $60/150 \times 100 = 40$ per cent, and the percentage increase in the copper is 50 per cent. Then $h=40/50=0.8$ for this example.

Since equation 3 gives the rate of increase in cost with change of copper section, the factor h applies to the first term of equation 3 but not to the second. Thus equation 4 becomes

$$\frac{C}{I}=59\sqrt{\frac{sm_2}{hvm_1}} \quad (8)$$

and equation 5 becomes

$$\frac{I}{A}=21{,}500\sqrt{\frac{hvm_1}{sm_2}} \quad (9)$$

for water-power systems.

Similarly, for insulated copper conductors, equation 7 becomes

$$\frac{C}{I}=182\sqrt{\frac{0.106sm_2+93{,}000bg}{hvm_1}}$$

circular mils per ampere (10)

The current density is given by

$$\frac{I}{A}=7{,}000\sqrt{\frac{hvm_1}{0.106sm_2+93{,}000bg}}$$

amperes per square inch (11)

Formulas 6, 10, and 11 are the only ones that need to be put on record for copper conductors, as with bare conductors h may be put equal to one and in appropriate cases g, the fuel cost, may be put equal to zero. Where energy is purchased by the kilowatt-hour the quantity s may be put equal to zero.

The change in resistance due to temperature or other cause is easily taken into account. For instance, where the temperature of the conductor at peak load is to be taken as 75 degrees centigrade instead of 25 degrees centigrade, the resistance will be 19 per cent higher. An inspection of the derivation shows that the numbers 0.106 and 93,000 are proportional to the resistance and will be 19 per cent higher for 75 degrees centigrade. The most economical value of C^2/I^2 will be 19 per cent larger, and that of C/I will be 9 per cent larger than given by the formulas. Similarly, if the conductors are hard drawn, the resistance will be about 2 per cent higher, and the most economical value of C/I will be 1 per cent larger.

Formulas for Aluminum Conductors

If the derivation of equation 1 is repeated for aluminum instead of for copper, the cost of aluminum at v dollars per pound installed and 0.098 pound per cubic inch is

$$0.098(\pi/4)10^{-6}\times 12{,}000\,Cv=0.00092\,Cv$$

Cv dollars per 1,000 feet

Resistance at 1.135×10^{-6} ohm per inch cube at 25 degrees centigrade is

$$\frac{17{,}300}{C}$$ ohms per 1,000 feet

Resistance loss at I amperes $=17.3(I^2/C)$ kilowatts per 1,000 feet

The kilowatt-hours of resistance loss per year are

$$8{,}760\times17.3\frac{bI^2}{C}=152{,}000\frac{bI^2}{C}$$

The annual charge for the aluminum conductor and its resistance loss is

$$M_{(a)}=0.0000092Cvm_1+\frac{I^2}{C}(0.173sm_2+152{,}000bg) \quad (12)$$

For the most economical current density

$$\frac{C^2}{I^2}=\frac{0.173sm_2+152{,}000bg}{0.0000092\,hvm_1}$$

$$\frac{C}{I}=330\sqrt{\frac{0.173\,sm_2+152{,}000\,bg}{hvm_1}}$$

circular mils per ampere (13)

and

$$\frac{I}{A}=3{,}900\sqrt{\frac{hvm_1}{0.173\,sm_2+152{,}000\,bg}}$$

amperes per square inch (14)

for aluminum conductors.

The steel core scarcely needs to be considered, as it may be taken to be similar to an equal weight of insulation, so far as this computation is concerned.

In cases where the generating system is not fully loaded and has no prospect of being so for some years (the ownership of the conductors being the same as that of the generating system), then the equations described in this paper should not be used, but the smallest possible conductors should be specified.

The question of how heavily a conductor should be loaded with current after it has been installed is not discussed in this paper. It is an entirely different question from that of choosing the size of a conductor that is not yet installed. After a line is built, it may be advisable to load it to a higher current density than the value for greatest economy used in an original design.

The determination of conductor size according to cost of resistance loss is particularly appropriate for overhead conductors, as the heating limit is seldom approached and there is a considerable range of resistances that can be chosen without much effect on the reactance or mechanical strength. The calculation of the most economical conductor size is simple and definite, especially where it

depends mainly on the peak value of current rather than on the kilowatt-hours of resistance loss.

List of Symbols

A = area of conductor section in square inches
b = ratio of average resistance loss to its value at the time of peak load
C = area of conductor section in circular mils
g = fuel cost in dollars per kilowatt-hour
h = ratio of increase in conductor cost to increase in conductor section
I = current in the conductor at time of peak load
M = total annual charge for a copper conductor and its resistance loss
M_a = total annual charge for an aluminum conductor and its resistance loss
m_1 = per cent, annual fixed charge on conductor
m_2 = per cent, annual fixed charge on generating system
s = first cost of generating system, dollars per kilowatt
v = cost, dollars per pound of copper or aluminum

Example 1

An example that shows clearly how losses in conductors can be balanced directly against a proportionate part of the cost of the entire generating system is that of the leads from the terminals of a water-wheel generator whose rating in amperes is 1,800 amperes. Take the following values (see list of symbols):

I = 1,800 amperes
$g = o$
$h = 1$
$m_1 = m_2 = 15$
s = \$160 per kilowatt
v = 0.20 dollar per pound

temperature of the annealed copper = 40 degrees centigrade at rated load current

$$hvm_1 = 0.20 \times 15 = 3.0$$

$$\frac{R_{40}}{R_{25}} = \frac{235+40}{235+25} = 1.058$$

$$1.058 \times 0.106\, sm_2 = 1.058 \times 0.106 \times 160 \times 15 = 269$$

By formula 11

$$\frac{I}{A} = 7{,}000\sqrt{\frac{3.0}{269}} = \frac{7{,}000}{\sqrt{89.7}} = \frac{7{,}000}{9.5}$$

= 740 amperes per square inch

$$A = \frac{1{,}800}{740} = 2.43 \text{ square inch, that is, a section of 0.4 by 6 inches may be used.}$$

It is seen that in this example one kilowatt of extra loss in the leads, whether they are long or short, would mean a reduction by one kilowatt in the rated output of the generator and of the complete water-power plant. It is worth \$160 to eliminate one kilowatt of loss in the generator leads. Even if the leads are only 20 feet long, it is right that they should have, at least, a cross section of $A = 2.43$ square inches.

A comparison is of interest with the design that might commonly be used based on current-carrying capacity and temperature-rise limit.

A single copper strap, one-fourth by six inches, has a current-carrying capacity of 1,800 amperes at about 35 degrees centigrade rise. This is 63 per cent as much copper as the 0.4-by-6-inch size.

The annual charge per 1,000 feet of conductor is given by equation 6.

The circular mils of conductor of 2.43 square inch section are

$$C = 2.43 \times \frac{4}{\pi} \times 10^6 = 3{,}090{,}000 \text{ circular mils}$$

$$M = 0.0000303 \times 3{,}090{,}000 \times 0.20 \times 15 + \frac{1{,}800^2}{3{,}090{,}000} \times 1.058 \times 0.106 \times 160 \times 15$$

= 281 + 281 = \$562 per year

Note that the two terms are equal, for minimum annual charge, when $h = 1$.

The circular mils of 1/4 by 6-inch conductor are

$$\frac{1}{4} \times 6 \times \frac{4}{\pi} \times 10^6 = 1{,}910{,}000 \text{ circular mils}$$

$$M = 0.0000303 \times 1{,}910{,}000 \times 0.20 \times 15 + \frac{1{,}800^2}{1{,}910{,}000} \times 1.058 \times 0.106 \times 160 \times 15$$

= 174 + 456 = \$630 per year

This is 12 per cent greater than the minimum, \$562. Besides saving 12 per cent in annual charges, the heavy size of copper has the advantages of lower temperature and less reactance.

As in other cases of this application of Kelvin's law, to specify heavier conductors at improved economy does not necessarily mean a larger investment by power companies which have plant extensions in prospect. The matter is a choice in engineering design, whether a certain fraction of the investment be made in conductors or in generator-station capacity. See reference 1.

Example 2

A 70,000-kva hydroelectric station and a 35-mile 115-kv transmission line with 350,000-circular-mil copper conductors were designed and built at the same time. The line carries the output of the station to a city, where the voltage is regulated by synchronous condensers. The cost data are taken to be the same as in example 1.

The transmission line of 350,000-circular-mil conductors has 3.1-per-cent resistance drop and 14-per-cent reactance drop. The circular mils per ampere are 1,000 rated current being 350 amperes.

By equation 10 the most economical value of circular mils per ampere is

$$\frac{C}{I} = 182\sqrt{\frac{269}{3.0}} = 1{,}730 \text{ circular mils per ampere}$$

$$C = 1{,}730 \times 350 = 600{,}000 \text{ circular mils}$$

By equation 6 the annual charges for 1,000 feet of 600,000-circular-mil conductor are

$$M = 0.0000303 \times 600{,}000 \times 0.20 \times 15 + \frac{350^2}{600{,}000} \times 1.058 \times 0.106 \times 160 \times 15$$

= 55 + 55 = \$110 per year

The annual charges for 1,000 feet of 350,000-circular-mil conductor are

$$M = 32 + 94 = \$126$$

which is 15-per cent greater than the minimum value, \$110.

Note that with usual types of conductors, to change from 350,000 circular mils to 400,000 circular mils reduces the resistance by 12 per cent, but the 60-cycle reactance at ten-feet effective spacing is reduced only one per cent. With hollow conductors the change might be made by keeping the same diameter and increasing the thickness, in which case the reactance would be changed practically not at all.

Example 3

Although the formulas in this paper are chiefly applicable to bare overhead conductors, occasionally a case occurs in which the current density in an insulated wire or cable at its maximum permissible temperature is greater than the most economical current density, and so it pays to specify a larger conductor than one ordinarily would.

A conductor insulated with asbestos and varnished cambric is used in wiring in a long run in a dry location in free air, the temperature of the copper being 75 degrees centigrade. The peak current is 600 amperes. The conductor is owned by the same company that owns the steam station supplying the power. Take

$b = 0.25$
$g = 0.002$ dollar per kilowatt-hour
$h = 0.7$
$m_1 = m_2 = 15$
s = \$110 per kilowatt
$v = 0.55$ dollar per pound of copper at 700,000 circular mils

$0.106\, sm_2 = 0.106 \times 110 \times 15 = 175$
$93{,}000\, bg = 93{,}000 \times 0.25 \times 0.002 = 46$
Total 221

$hvm_1 = 0.7 \times 0.55 \times 15 = 5.78$

By equation 10, with the correction factor 1.193 inserted for 75 degrees centigrade, the most economical value of circular mils is

$$600\times182\times\sqrt{\frac{1.193\times221}{5.78}}=737{,}000 \text{ circular mils}$$

for which 700,000 circular mils might be chosen. The code size for 600 amperes for the conditions described is 350,000 circular mils.

To show the effect of the factor b, let the computation be repeated with $b=0.15$

$$93{,}000\,bg=93{,}000\times0.15\times0.002=28$$
$$28+175=203$$

The most economical value of circular mils is

$$600\times182\sqrt{\frac{1.193\times203}{5.78}}=706{,}000 \text{ circular mils}$$

for which the size 700,000 again would be chosen. The difference in the two computed results is four per cent.

Again, putting $b=0$, the most economical value is

$$600\times182\sqrt{\frac{1.193\times175}{5.78}}=650{,}000 \text{ circular mils}$$

Though this is a slightly smaller size than 700,000 circular mils, it is much larger than the size given by heating considerations alone. Although the factor b for a conductor which is being specified is not always easy to estimate, the precise value of b is not of very great importance in cases where the conductor is owned by the power company, as in the case of most transmission and distribution lines.

The percentage increase in size from 350,000 to 700,000 circular mils is 100 per cent. Then the ratio in the cost per 1,000 feet of the two sizes is

$$1+1.00\times0.7=1.7$$

For 350,000 circular mils, the cost per pound of copper is

$$0.55\times\frac{2.0}{1.7}=0.65 \text{ dollar}$$

The annual charge for 1,000 feet of the 700,000-circular-mil conductor is by equation 6, taking $b=0.25$,

$$M=0.0000303\times700{,}000\times0.55\times15+\frac{600^2}{700{,}000}\times221=175+114=\$289$$

For 1,000 feet of 350,000-circular-mil conductor,

$$M=0.0000303\times350{,}000\times0.65\times15+\frac{600^2}{350{,}000}\times221=103+227=\$330$$

which is 14 per cent greater than $289, the minimum value.

In this example, even if the load factor were almost zero, a heavy conductor could be specified at a saving in annual cost, with the additional advantages of lower temperature, longer insulation life, less voltage drop from reactance, and greater overload capacity.

Example 4

The corridors of an apartment building are wired with number-10 wire in iron conduit. The main electrical load is the lighting fixtures which are turned on for an average of 15 hours a day throughout the year. The current in the wires of the lighting circuits is 22 amperes, diminishing uniformly toward the end of the branch circuits, plus three amperes taken for short times from the outlets. This gives a maximum current in the wire of 25 amperes, for which the code size of wire is number 10.

Because of the current's tapering off uniformly along the wire, its resistance loss is one-third of what it would be with full current in all parts. Then

$$b=\frac{1}{3}\times\frac{15}{24}=0.208$$

Take $g=0.016$ dollar per kilowatt-hour, in lieu of fuel cost, $h=0.65$, $m_1=14$, $s=0$, $v=\$2$ per pound of copper installed, including cost of conduit and insulation, for number-8 wire.

$$93{,}000\,bg=93{,}000\times0.208\times0.016=310$$
$$hvm_1=0.65\times2.00\times14=18.2$$
$$\frac{C}{I}=182\sqrt{\frac{310}{18.2}}=750$$

where $I=22$ amperes, the current which flows 15 hours each day.

The most economical section of wire is

$$C=750\times22=16{,}500 \text{ circular mils}$$

that is, number-8 wire.

The percentage increase in size from 10,400 circular mils to 16,500 circular mils is 59 per cent. Then the ratio in the cost per 1,000 feet of the two sizes is

$$1+0.59\times0.65=1.38$$

For number-10 wire, the cost per pound of copper is

$$2.00\times(1.59/1.38)=\$2.30$$

The annual charge for 1,000 feet of number-8 wire is, by equation 6,

$$M=0.0000303\times16{,}500\times2.00\times14+\frac{22^2}{16{,}500}\times93{,}000\times0.208\times0.016$$
$$=14.0+9.1=\$23.1$$

For 1,000 feet of number-10 wire,

$$M=0.0000303\times10{,}400\times2.30\times14+\frac{22^2}{10{,}400}\times93{,}000\times0.208\times0.016$$
$$=10.1+14.4=\$24.5$$

which is six per cent greater than 23.1, the minimum value.

Example 5

Groups of lighting fixtures are supplied by number-10 wire, the conditions being the same as in example 4, except that the wiring is owned by the company which owns the steam station.

$g=0.002$ dollar per kilowatt-hour
$m_2=14$
$s=125$ dollars per kilowatt
$0.106\,sm_2=0.106\times125\times14=186$
$93{,}000\,bg=93{,}000\times0.208\times0.002=39$
Total 225
$hvm_1=0.65\times2.00\times14=18.2$

By equation 10

$$\frac{C}{I}=182\sqrt{\frac{225}{18.2}}=640$$

where $I=22$ amperes, the current which flows 15 hours per day.

If one wire size is to be chosen for this entire part of the wiring, the most economical section is

$$C=640\times22=14{,}000 \text{ circular mils}$$

For the wires leading to the groups of fixtures, the current has full value and

$$b=\frac{15}{24}=0.625$$

$$93{,}000\,bg=93{,}000\times0.625\times0.002=116$$
$$186+116=302$$
$$\frac{C}{I}=182\sqrt{\frac{302}{18.2}}=740$$

$C=740\times22=16{,}300$ circular mils, or number-8 size

Thus, if the current density is watched for each part of the wiring, larger than code sizes may be specified free of extra cost for the more heavily loaded parts. If the slight complication of changing wire sizes is considered worth while, the advantages of reduction in voltage drop, longer insulation life, and greater overload capacity may be obtained. This applies to the same extent to example 4.

Reference

1. Resistance Loss and Conductor Size Herbert B. Dwight. *General Electric Review*, November 1938.

Measurement and Effect of Contact Resistance in Spot Welding

ROBERT A. WYANT
NONMEMBER AIEE

SPOT WELDING consists essentially of clamping two pieces of sheet metal between two copper electrodes and passing through the pieces an electric current of sufficient strength to fuse them together at the spot where the current is most concentrated. Spot welding is the simplest of the electric resistance-welding processes which depend upon the Joule effect, $H=I^2RT$, for the generation of heat. The total resistance, R, in spot welding consists of the body resistance of the metal between the electrodes plus the sum of the sheet-to-sheet and electrode-to-sheet contact resistances. The purpose of this paper is to report to the electrical-engineering profession on recent investigations of the electrical resistance of these contacts and the importance of these resistances in the spot-welding process.

Contact resistance is believed to be extremely important in the spot welding of all metals. Knowledge of the subject, however, is very limited in spite of extensive use of the spot-welding process. Doctor F. J. Studer at Union College and Doctor W. B. Kouwenhoven at Johns Hopkins University have made a good start in studying contact resistance from the point of view of spot welding, but much remains to be done.[1,2] In England R. F. Tylecote has done much to advance knowledge of the subject.[3] During the past few years much has been learned about contact resistance and the spot welding of aluminum alloys.[4] This has been largely the result of the aircraft spot-welding research program at the welding laboratory of the Rensselaer Polytechnic Institute. The work was sponsored by the National Advisory Committee for Aeronautics, the Army Air Forces, and the Navy Bureau of Aeronautics. Prior to the latter work some observations of contact resistance were made at the same laboratory in connection with research on the spot welding of steels.[5] This work was sponsored by the Welding Research Council of the Engineering Foundation, of which the AIEE is a cosponsor with the American Welding Society.

Paper 46-9, recommended by the AIEE committee on electric welding for presentation at the AIEE winter convention, New York, N. Y., January 21–25, 1946. Manuscript submitted October 2, 1945; made available for printing November 5, 1945.

ROBERT A. WYANT is assistant professor, department of metallurgical engineering, Rensselaer Polytechnic Institute, Troy, N. Y.

Methods of Measuring Contact Resistance

The contacts in spot welding do not have constant values of resistance. Before the welding current starts to flow the resistance of the contacts depends primarily upon the surface condition of the contacting metals. Factors of less importance are the kinds of metal in contact, the electrode force, and the size and shape of the electrode tips. As soon as the welding current starts to flow, the resistance of each contact quickly decreases as more intimate contact is made between the two metals. In studying these contacts two types of resistance measurements are necessary: a measurement under static conditions to determine the initial contact resistance and an oscillographic measurement to follow the change in resistance while the weld is forming. The latter measurement necessarily must be made with the specimens clamped between the electrodes of an actual spot-welding machine. The initial contact resistance may be measured with the specimens clamped between the electrodes of either a spot-welding machine or a small press built especially for the purpose. The small press usually is employed when contact resistance measurements are used to evaluate the surface condition of the metals to be welded.

Attention must be called to the fact that the resistances measured in this work are not simple contact resistances. The sheet-to-sheet resistance includes the contact resistance plus the resistance of one sheet of material. Likewise, the electrode-to-sheet resistance includes the contact resistance plus the resistance of one-half sheet of material. This point is illustrated by Figure 1. At the start of the weld the body resistance of the material is usually negligible in comparison with the contact resistance. As the formation of the weld progresses, the body resistance of the material accounts for an increasingly greater part of the measured resistance.

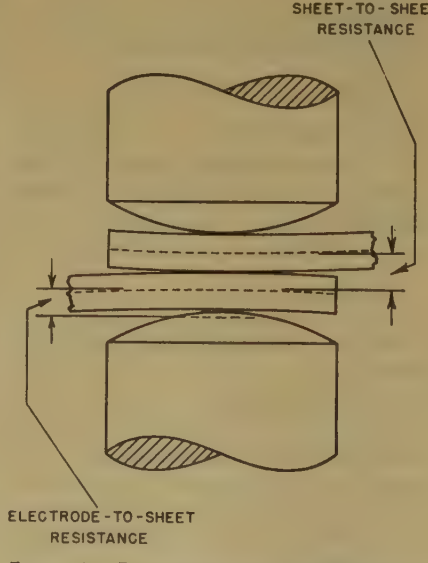


Figure 1. Diagram showing planes between which sheet-to-sheet and electrode-to-sheet resistances are measured

Static Measurements

Though there are several different methods of measuring contact resistance, they all require a small press for clamping a pair of specimens in contact with each other. A typical press is shown in Figure 2. The essential features of this press are the copper electrodes and the hydraulic jack and calibrated spring for applying a force of known magnitude to the electrodes.

The electrodes are made of one of the copper alloys which are commonly used for spot-welding electrodes. In fact the press should be designed to take a pair of standard electrode tips. One electrode has to be insulated electrically from the press in order to direct the current through the specimens. The contour of the electrode faces should be spherical with a radius of curvature of three or four

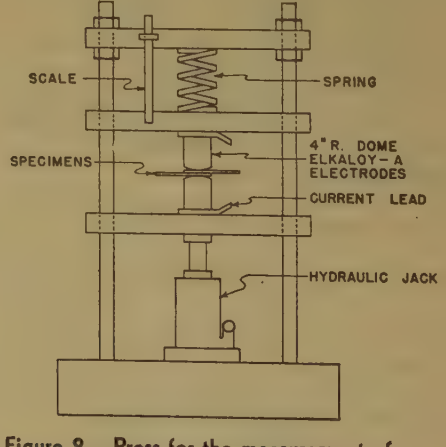


Figure 2. Press for the measurement of contact resistance

inches. This is an important point, because erratic measurements may result from using electrodes with flat faces. It is difficult to keep flat faces parallel, and as a result the distribution of pressure over the contact area may be inconsistent. When the electrode contour is spherical, the specimens tend to adjust themselves to that contour, as indicated by Figure 1 in which the effect is greatly exaggerated. This naturally tends to produce a more consistent area of contact and distribution of pressure over that area. Another factor, which may affect the consistency of the results, is play or freedom of movement of the electrodes with respect to their intended axis of alignment. The construction of the press must be such as to keep the electrodes rigidly in alignment and yet to permit their easy movement along the alignment axis. An electrode force of 1,000 pounds is employed with electrodes having a contour four inches in radius. Satisfactory results also may be obtained by using an electrode force of 500 pounds with electrodes having a contour three inches in radius.

At least three different circuits have been successfully employed for measuring contact resistance. At this laboratory a modified Kelvin double-bridge circuit is used, as shown in Figure 3. The current through the contact is limited to within 20–100 amperes by means of R_b. Within this range the actual magnitude of the current has no appreciable effect on the resistance of the contact, but it must be high enough to make the circuit sufficiently sensitive. In this circuit R_s is a standard resistance of 100 microhms. Each of the R_1 and R_3 resistance arms consists of two decade units in series (10 and 100 ohm steps). Each of the R_2 and R_4 resistance arms consists of a fixed resistor of the plug-in type (10, 100, or 1,000 ohms). Thus by changing R_2 and R_4 three ranges of R_x can be covered: 100 to 10,000, 10 to 1,000, and 1 to 100, all in microhms. In operating the bridge, R_1 is always kept equal to R_3, and R_2 is kept equal to R_4. The circuit is direct reading in the sense that, when it is balanced, the value of R_x in microhms is obtained simply by multiplying the reading of R_1 by a multiple of ten. Although the precision of the circuit is not great, it is ample for the requirements of this work. For more details on this circuit the reader is referred to previous papers.[6,7]

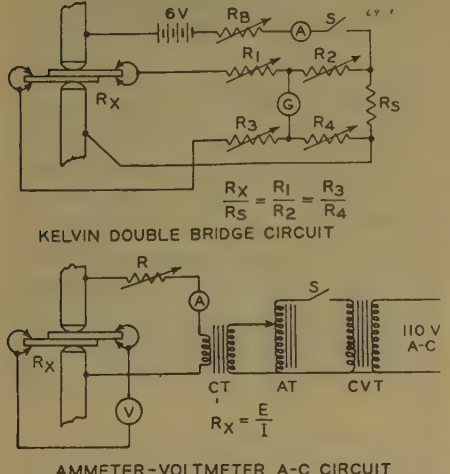


Figure 3. Circuits for measuring contact resistance

Contact-resistance measurements at some laboratories are made by the voltmeter–ammeter method using alternating current, as shown in Figure 3.[8] This circuit requires the use of a sensitive vacuum-tube voltmeter for measuring the voltage drop across the contact. Current and voltage readings have to be taken simultaneously, and, therefore, to avoid errors due to fluctuations in line voltage, a constant-voltage transformer usually is employed. The magnitude of the current in this circuit also is limited to a range from about 20 to 100 amperes. This circuit is somewhat faster in operation than the bridge circuit just described.

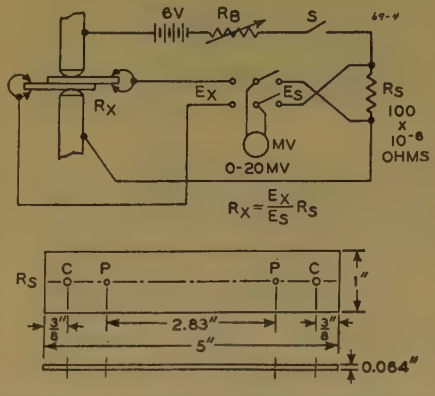


Figure 4. Circuit and standard resistance for measuring contact resistance by means of millivoltmeter

Material for R_s—Bare 24S-T aluminum alloy
C—Points for current connections
P—Points for potential connections

The circuit shown in Figure 4 is recommended for plants where there is a lack of electric equipment and where contact-resistance measurements are to be made at a minimum of expense. In this circuit the unknown contact resistance is compared with a standard resistance, R_s, of 100 microhms. The most important element in the circuit is the millivoltmeter, which should have a range of from 0 to 20 millivolts for measuring resistances below 1,000 microhms. The resistance, R_b, is used to keep the current within a range from 20 to 100 amperes. The actual magnitude of the current is not important, but it should not vary while the voltage drops across the contact and the standard resistances are being measured. A standard resistance of 100 microhms and of sufficient accuracy for this work can be easily made from a piece of 24S-T aluminum-alloy sheet as shown in Figure 4. The precision of this circuit depends upon the accuracy of the millivoltmeter and the standard resistance. Therefore, it is recommended that the resistance of the standard be checked by some means and adjusted to within at least plus or minus five per cent of its intended value. The resistance of such a standard does not change appreciably, because of the heating effect of the current while measurements are being made. The alignment chart, shown in Figure 5, is provided for obtaining the resistance of the contact from the millivoltmeter readings without making calculations.

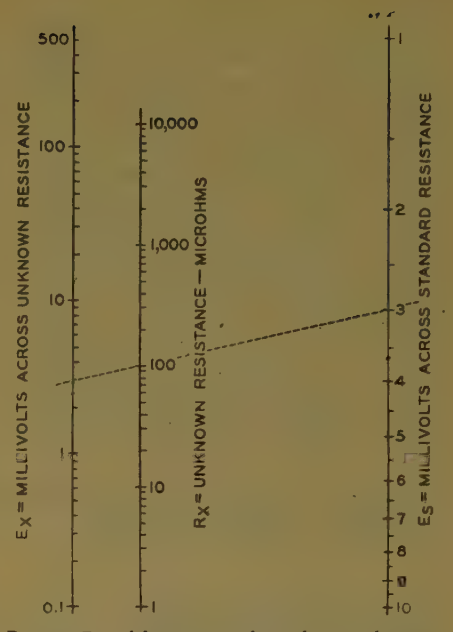


Figure 5. Alignment chart for evaluating measurements made with circuit shown in Figure 4

$$R_x=\frac{E_x}{E_s}R_s$$

R_s = 100 microhms

Dynamic Measurements

Contact resistance is measured during welding by means of an electromagnetic oscillograph, as shown in Figure 6. A shunt, consisting of a piece of manganin (R_s), is installed in the lower electrode holder for the purpose of obtaining a voltage drop which is an accurate measure of the welding current. Suitable potential connections are made to the shunt,

electrode tips, and specimens. The leads for these connections have to be twisted carefully and arranged to avoid inductive effects. With this arrangement a complete record of the four important voltage drops is obtained when a weld is made. The oscillograph circuits are calibrated in terms of volts per inch deflection, and the desired values of resistance are obtained by measuring the oscillograms and making the necessary calculations. This is done for each contact, and the results are plotted as a function of time. It is usually desirable to superimpose a plot of the welding current on the resistance curves.

Contact Resistance and the Spot Welding of Aluminum Alloys

The surfaces of aluminum alloys are characterized by the presence of an oxide film which must be removed or otherwise operated upon before these alloys can be satisfactorily spot-welded. The surfaces of these alloys can be prepared for spot welding by either mechanical or chemical methods. By the mechanical methods the original oxide film is removed from the surface of the metal by means of a wire brush, steel wool, or abrasive cloth. The chemical methods consist of immersing the metal in a chemical solution which removes the original oxide film or transforms it in such a way as to make the surface suitable for spot welding. Chemical methods have many advantages over mechanical methods, and during the past few years the trend in industry has been toward chemical methods.

Original Experiment

An experiment was devised in which a pair of specimens could be clamped between the electrodes of a spot-welding machine, and the contact resistance measured both before and during welding.[4] The circuit by which this was accomplished is shown in Figure 7. In the experiment specimens of Alclad 24*S*-*T* sheet were treated in a solution of hydrofluoric acid, which was recommended for the purpose at that time (1941). After treatment each pair of specimens was clamped between the electrodes and the initial contact resistance measured by means of the Kelvin double-bridge circuit shown in Figure 7. Without disturbing the specimens in any way the welding current next was passed, and the change in contact resistance was followed oscillographically by means of the connections that are also shown in Figure 7. The results of the initial bridge measurements are plotted in Figure 8. It will be noted that the contact resistance was a critical

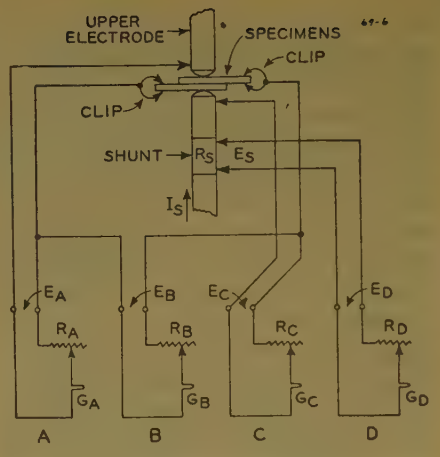


Figure 6. Oscillograph connections for measurement of voltage drops in secondary circuit of spot welder

A—Upper electrode to sheet
B—Sheet to sheet
C—Lower electrode to sheet
D—Secondary current

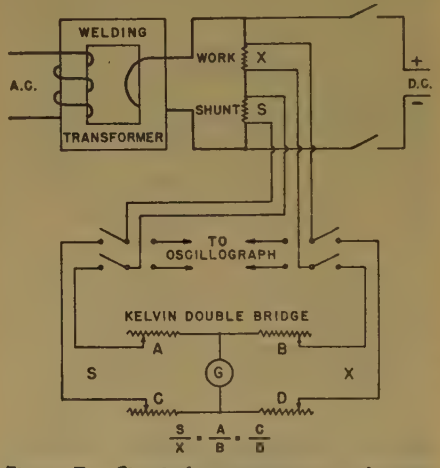


Figure 7. Circuit for measurement of resistances in original investigation of the surface preparation of aluminum alloys for spot welding

function of the time of immersion in the hydrofluoric acid. The contact resistance fell from an average of 608 microhms at zero time to 226 microhms at five seconds, and it reached a minimum of 20 microhms at ten seconds. As the treating time was increased, the contact resistance increased to 49 microhms at 15 seconds, and it reached a value of 586 microhms at 30 seconds. The welds which were made immediately following these measurements were carefully examined. It was found that the best welds, with respect to uniform shape of the fused zone, were obtained at treating times of 10 and 15 seconds where the contact resistance was low. Photomicrographs of typical sections through the welds are also shown in Figure 8. These welds indicated that, when the contact resistance was low, the welding current was distributed uniformly over the contact area, and therefore the fusion occurred uniformly across the weld zone in all directions. When the contact resistance was high, the welding current tended to concentrate at the points of least resistance on the contact area, and therefore the distribution of heat was not uniform throughout the weld zone. This was the origin of the concept that a low contact resistance is desirable for spot welding the aluminum alloys. Some typical results of the oscillographic measurements are shown in Figure 9. The values of contact resistance at zero time were the result of the initial bridge measurements, and the values at the other intervals after the start of the weld were obtained by analysis of the oscillograms. The correlation between the initial and oscillographic measurements indicated that the contact resistance measured under static conditions was essentially the same as the prevailing contact resistance at the instant when the welding current started to flow. Following this experience, the static method of measuring contact resistance in a small press was adopted to facilitate further research on the surface preparation of aluminum alloys for spot welding.

Untreated and Mechanically Prepared Sheet

Contact resistance measurements were applied to untreated and wire-brushed specimens at an early date.[4] The resistance between untreated specimens is consistently high and usually greater than

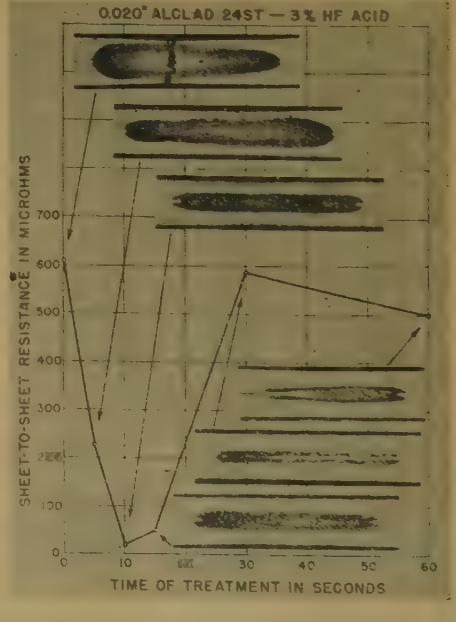


Figure 8. Surface-treating characteristic and photomicrographs showing relation between sheet-to-sheet resistance and distribution of fusion in weld zone

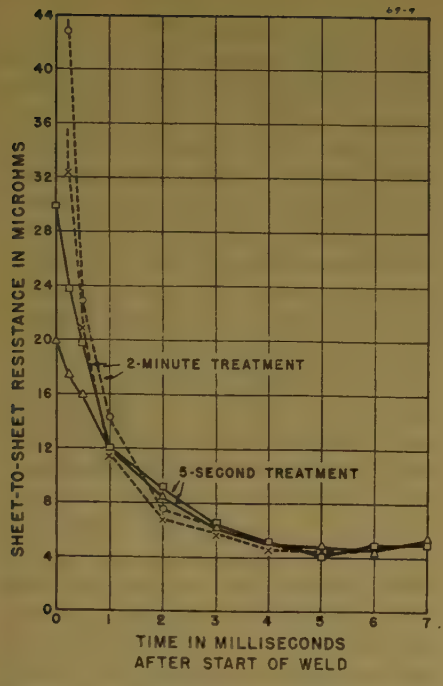


Figure 9. Sheet-to-sheet resistance during formation of spot weld in an aluminum alloy

Six per cent hydrofluoric acid, 0.040-inch Alclad 24*S-T*, four-inch dome tips
Electrode pressure—1,000 pounds
At $T=0$, $R_0=221$, $R_z=244$

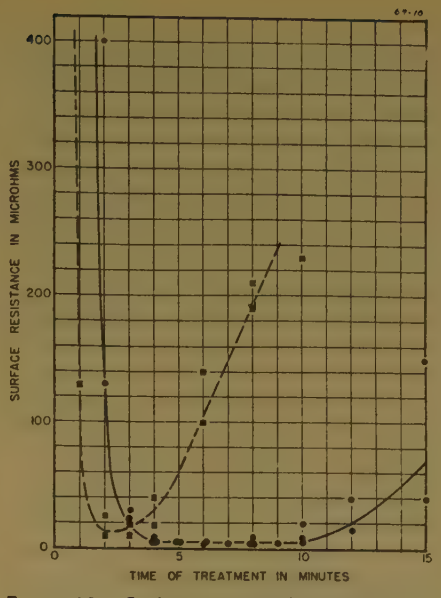


Figure 10. Surface-treating characteristics for the aluminum alloy, Alclad 24*S-T*, in hydrofluosilicic-acid solution at 75 degrees Fahrenheit

Three-per-cent H_2SiF_6 solution, 0.020-inch alloy
—●—Nitrate heat treated
—■—Air heat treated

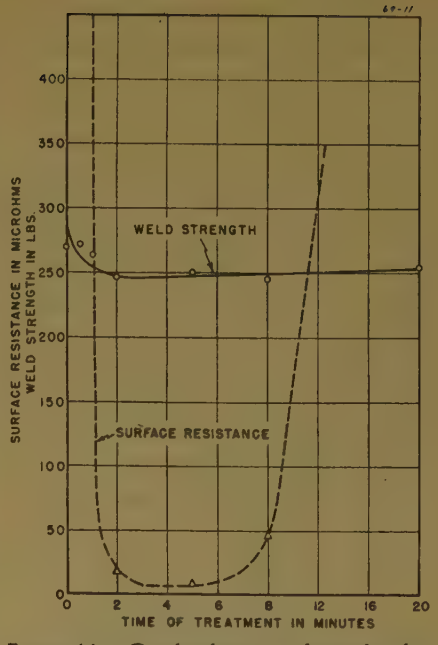


Figure 11. Graphs showing relationship between initial sheet-to-sheet resistance and weld shear strength

Three-per-cent H_2SiF_6 solution, 75 degrees Fahrenheit, 0.020-inch Alclad 24*S-T*, nitrate heat treated, capacitor-discharge welder, rapidly rising current, 25,000-ampere peak

1,000 microhms. Between wire-brushed specimens the resistance is consistently low and of the order of 5 to 25 microhms, provided that the surface preparation has been thorough. Untreated sheet cannot, of course, be satisfactorily spot-welded. Very good welds can be made in wire-brushed material, but this method of surface preparation has been largely displaced by chemical methods.

Development of Chemical Methods of Surface Treatment

At the time of the original experiment with hydrofluoric acid, proprietary solutions were just beginning to appear on the market for the surface treatment of aluminum alloys for spot welding. No time was lost in applying contact-resistance measurements in an investigation of those proprietary solutions and a number of purely experimental solutions.[6] All of the effective solutions gave characteristics similar to that shown in Figure 8 for hydrofluoric acid, except for the fact that they were all less critical with respect to time. Furthermore, very good welds always were obtained when the contact resistance was low, regardless of what treating solution was used. The fact soon became well established that the contact resistance between chemically prepared specimens is primarily a function of the time of immersion in the treating solution. Other factors which may affect the resistance are the initial surface condition and composition of the alloy being treated, and the composition, strength, and temperature of the treating solution. For any chemical solution that is effective for treating a given alloy, there is usually a range in immersion time over which the contact resistance is consistently low and frequently of the order of five to ten microhms. Outside this range the resistance is usually much higher.

A typical characteristic is shown in Figure 10 for the chemical surface treatment of Alclad 24*S-T* sheet in one of the newer solutions which has proved to be very satisfactory and economical, both in the laboratory and in production. This solution is a result of a research program in which contact-resistance measurements were employed extensively at this laboratory.[7] It consists of three per cent by volume of 28 per cent hydrofluosilicic acid, H_2SiF_6, plus 0.1 per cent by weight of the wetting agent, Nacconol NR, in water. This solution has many desirable characteristics. For example, no heating units are required as it operates at room temperature. The solution is very simple in composition. The time of treatment is not critical, there being an ample range of treating time with little danger of overtreatment. The acid is available in ample quantities and at low cost. There is no health hazard in the use of this solution, as there are practically no vapors evolved, and the solution is not ordinarily irritating to the skin. A bright smooth finish is obtained on Alclad material. The strength of the solution may be determined by a simple titration. This is an outstanding advantage of the solution, since it permits rapid and precise control. The solution is effective for treating nearly all of the aluminum-alloy sheet materials with the possible exception of the bare 24*S* and 61*S* alloys.

Many other laboratories have adopted contact-resistance measurements to facilitate the investigation, development, and control of surface-treating solutions since the original work was reported. Many improved solutions now are in use as a result. Contact-resistance measurements are employed at many aircraft plants to control the surface-treating operations in production. Furthermore, the latest Navy spot-welding specification calls for contact-resistance measurements.

Effects of Contact Resistance

In spot-welding aluminum alloys the relationships between contact resistance and the following factors are of considerable interest:

1. Size and strength of spot welds.
2. Consistency with respect to strength.
3. Uniformity with respect to shape.
4. Electrode-tip life.

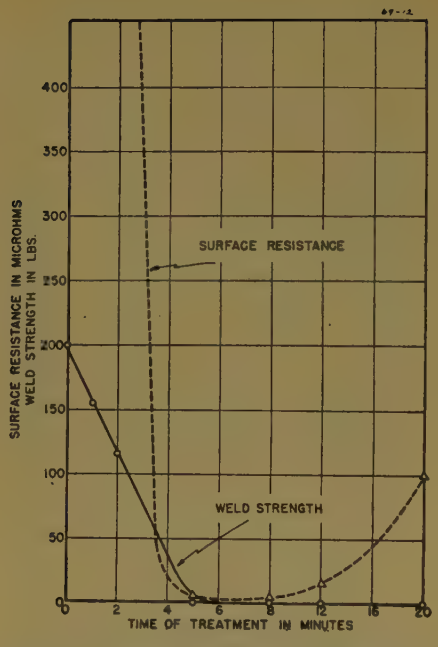


Figure 12. Graphs showing relationship between initial sheet-to-sheet resistance and weld shear strength

0.020-inch Alclad 24*S-T*, nitrate heat treated, capacitor-discharge welder, rapidly rising current, 25,000-ampere peak

The relationship between spot-weld strength and contact resistance frequently is misunderstood. The evidence at the Rensselaer laboratory indicates that there is no general relationship. This is shown by the typical curves in Figure 11 which were obtained by keeping all welding conditions constant except treating time. At short treating times, which are not long enough to obtain the minimum contact resistance, the weld strength tends to be proportional to the contact resistance. At longer treating times the weld strength tends to be constant and independent of contact resistance. In other words there does not seem to be a sound basis for the common idea that the magnitude of the welding current can be adjusted to compensate for changes in contact resistance. In Figure 11 the welding conditions were selected so as to obtain a 250-pound weld at the minimum value of contact resistance. Similar curves are shown in Figure 12 for conditions which produced a 200-pound weld between untreated specimens and a dud weld at the minimum value of contact resistance. Comparison of the latter two figures suggests that at the short treating times the effect of contact resistance on weld strength depends upon the average size of the welds produced.

The effect of contact resistance on the consistency of spot-weld strength cannot be discussed fully without reference to a characteristic of weld strength as a function of the welding current. A typical characteristic is shown in Figure 13 for the 52*S*-1/2*H* aluminum alloy. The best consistency is obtained at points toward the upper end of the curve. This is primarily caused by the fact that at low values of current the curve is steep, and small variations in current produce large changes in weld strength. It is also at the lower values of current where variations in contact resistance are most likely to affect the weld strength. The symbols used for plotting the curve in Figure 13 indicate that consistent and sound welds were obtained between 35 and 40 kiloamperes. Below 33 kiloamperes the welds were very inconsistent. Above 42 kiloamperes the welds were consistent, but expulsion of molten metal and excessive sheet separation were observed. It may be said, therefore, that the point of operation on the strength–current characteristic is a much more important factor than contact resistance in determining the consistency of spot welds with respect to strength. Surprisingly good consistency can be obtained by welding specimens with untreated faying surfaces, provided that this principle is observed

The effect of contact resistance on the shape of the spot welds was the only effect observed in the original experiment described. This effect has been confirmed many times in later work. The welds are always round and uniform in shape when the contact resistance is near its minimum value. The welds become very irregular in shape when the contact resistance is high as a result of too short a treating time. The effect of a high contact resistance as a result of too long a treating time depends upon the nature of the treating solution. There is a tendency for the welds to become irregular in shape with all solutions under this condition, but the effect is much more pronounced with some solutions than with others. This effect is illustrated by the spot-weld fractures shown in Figure 14. For another example the reader is referred back to Figure 8 and the discussion

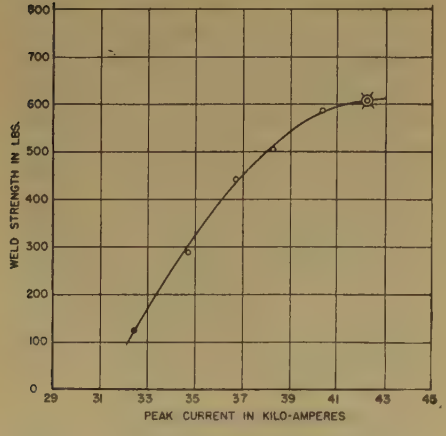


Figure 13. Typical strength-current characteristic for spot welds in the aluminum alloy, 52S-1/2H

0.040-inch alloy
Electrode tips—Four-inch *R* domes
Electrode force—1,200 pounds (weld), 2,400 pounds forge
Forge timing—34 milliseconds
Average rate of current rise—3,300 amperes per millisecond

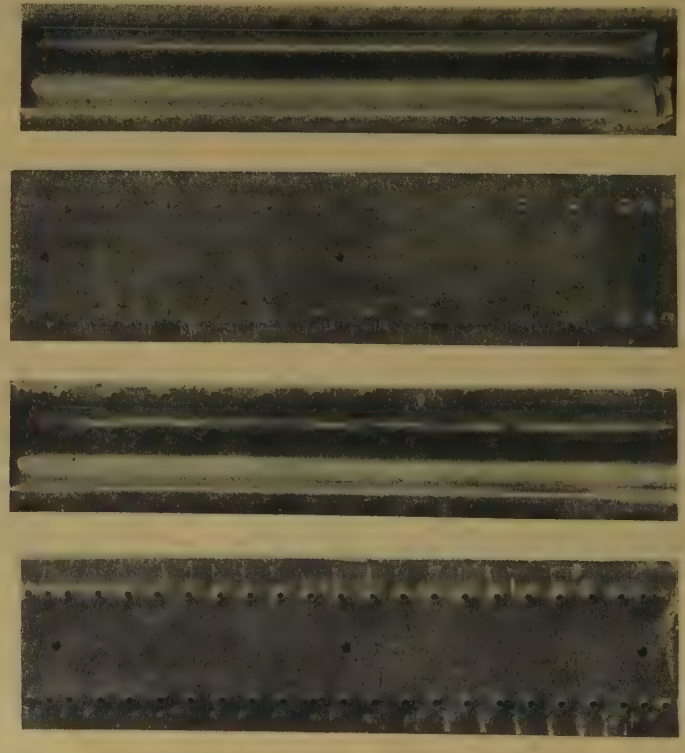


Figure 14A. Irregularities in weld shape when sheet-to-sheet resistance is high and inconsistent

Figure 14B. Uniformity of weld shape when sheet-to-sheet resistance is consistently low

thereof. It should be pointed out that the actual shape of spot welds in aluminum alloys may have little effect on their shear strength and their consistency with respect to shear strength. It is only when variations in surface condition influence the size of the weld that the shear strength is affected.

The spot welding of aluminum alloys is characterized by comparatively rapid fouling of the electrode tips with aluminum and the necessity for frequent cleaning of the tips. Perhaps the most important effect of contact resistance is on electrode-tip life or the number of welds which can be made per cleaning. It is difficult to obtain conclusive and quantitative data on this relationship, because there are so many variables which affect tip life. However, there are many indications that the best tip life is obtained when the contact resistance is near the minimum value for the material being welded. The effect of any variable on tip life is best observed under actual production conditions. Unfortunately, it is under such conditions that the effect of the variable under observation may be obscured by the effects of other variables which may not be controlled adequately or even recognized.

Contact Resistance Between Electrodes and Sheet

The emphasis in the work at the Rensselaer laboratory has been on the sheet-to-sheet resistance. This has been a result of the fact that in the original work the sheet-to-sheet resistance was found to be more sensitive than the electrode-to-sheet resistance with respect to changes in surface condition of the specimens. The electrode-to-sheet resistance deserves further study. A British investigator has gone so far as to say that the electrode-to-sheet resistance must not exceed a specified value if rapid fouling of the electrode tips is to be avoided.[9]

Measurements of Instantaneous Power

The oscillograms which are used for determining the dynamic resistance characteristics also may be analyzed in terms of instantaneous power at the sheet-to-sheet and electrode-to-sheet contacts. A plot of the resistance, power, and current characteristics of two spot welds in Alclad 24*S*-*T* is shown in Figure 15. The oscillograms for these two particular welds were chosen for complete analysis, because one weld exhibited a shear strength of 505 pounds, whereas the other weld, made under identical conditions, exhibited a strength of only 140 pounds. It will be noted that the resistance characteristics and current wave forms for the two welds were practically identical. The only difference is in the peak power at the sheet-to-sheet contact. Whether this was responsible for the extreme difference in strength is questionable. A similar plot is shown in Figure 16 for two welds which started with different values of sheet-to-sheet resistance and ended up by exhibiting a marked difference in shear strength. It should be noted that the weld which started with the higher initial sheet-to-sheet resistance produced the lower strength, in spite of the fact that the welding current and other recognized conditions were identical for the two welds. This is contrary to what might have been predicted and is further evidence that there is no sound basis for adjusting the magnitude of the current to compensate for differences in initial contact resistance. The phase relation of the power curves for the sheet-to-sheet contact should be noted in Figure 16. This difference in phase is believed to have been a result of the difference in initial contact resistance and to have been responsible for the difference in weld strengths. These cases are presented to illustrate the complex nature of the relationship between contact resistance and weld strength in working with the aluminum alloys.

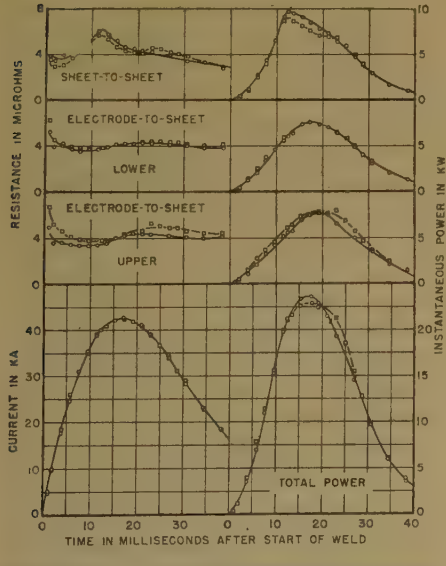


Figure 15. Dynamic resistance and instantaneous power characteristics of two spot welds made under identical conditions but exhibiting widely different shear strengths

0.040-inch Alclad 24*S*-*T*
-O- $S = 505$ pounds, R_o = five microhms
-□- $S = 140$ pounds, R_o = four microhms

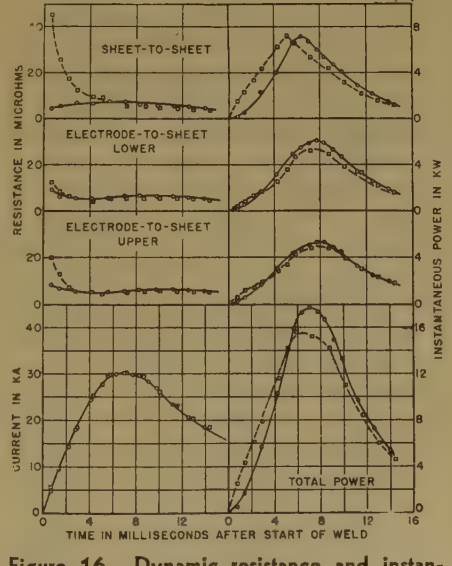


Figure 16. Dynamic resistance and instantaneous power characteristics of two spot welds illustrating an inverse relationship between initial sheet-to-sheet resistance and weld shear strength

0.020-inch Alclad 24*S*-*T*
-O- Nitrate treated, $S = 240$ pounds, $R_o = 6$
-□- Air treated, $S = 160$ pounds, $R_o = 90$

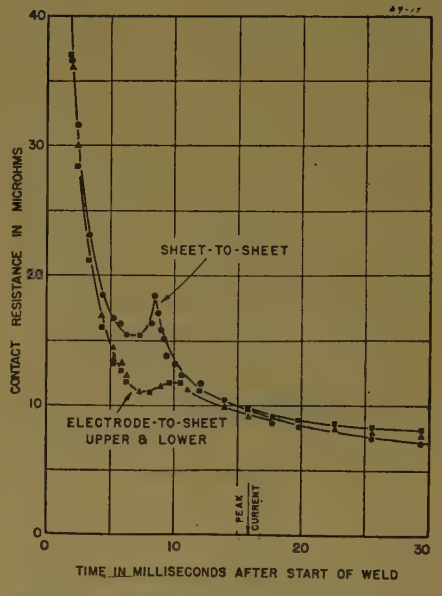


Figure 17. Dynamic resistance characteristics illustrating effect of method of drying chemically treated specimens of the aluminum alloy, *R*-301-*T* (compare with Figure 18)

0.064-inch alloy, three-per-cent H_2SiF_6 solution, wiped dry

Unusual Contact Phenomena

Several very interesting contact phenomena have been observed in this work. For example, the method of drying aluminum-alloy specimens following their chemical surface preparation affects the sheet-to-sheet resistance. This was first observed in spot-welding the new aluminum alloy, *R*-301-*T*. A typical dynamic resistance characteristic is shown in Figure 17 for specimens which were dried by

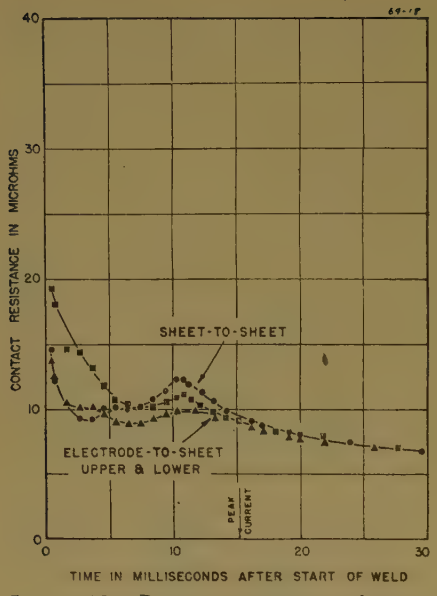


Figure 18. Dynamic resistance characteristics illustrating effect of method of drying chemically treated specimens of the aluminum alloy, *R*-301-*T* (compare with Figure 17)

0.064-inch alloy, three-per-cent H_2SiF_6 solution, air dried

wiping with a clean cloth. The irregularity in the sheet-to-sheet resistance curve should be noted. When the specimens were allowed to dry in clean air, the corresponding characteristics assumed quite a different shape, as shown in Figure 18. It should be noted also that the initial resistance was considerably lower when the specimens were dried in air. The effect of method of drying on the contact resistance of Alclad 24*S*-*T* sheet was next investigated. The results are illustrated by the surface-treating characteristics shown in Figure 19. Wiping raised the general level of the treating characteristic, and it tended to make the measurements erratic. This effect is not too important in production, because at most plants air drying is employed. The phenomenon is mentioned here, because it illustrates the great importance of details in the technique of preparing specimens for contact-resistance measurements.

Another interesting phenomenon is that of the effect of direction of current flow in determining which electrode will tend to become fouled with aluminum. In some spot welders of the condenser-discharge type the welding current always passes in the same direction. In these machines there is a definite tendency for aluminum to adhere to the electrode which is positive with respect to the work, provided that the welding conditions are all reasonably good. The same tendency has also been observed in a-c spot welding with equipment in which the first half cycle of current always passes in the same direction. In this case the aluminum tends to adhere to the electrode, which is positive during the first half cycle. It was thought that the cause of this might be revealed by comparing dynamic resistance characteristics for the positive electrode-to-sheet contact with similar characteristics for the negative electrode-to-sheet contact. However, nothing has been apparent in the experimental results to date, as shown by the resistance curves in Figures 15 and 16. The effect is much more pronounced in spot-welding the magnesium alloys, as will be shown later.

Contact Resistance and the Spot Welding of Other Metals

Magnesium Alloys

The magnesium alloys are very similar to the aluminum alloys with respect to their surface preparation for spot welding. Up to recent times no chemical methods were available for the surface treatment of magnesium alloys for this purpose. Contact-resistance measurements have played an extremely important part in the recent development of chemical solutions for this purpose. In several respects contact resistance is even more important in spot-welding the magnesium alloys than in spot-welding the aluminum alloys. For example, there is much more positive evidence that fouling of the electrode tips with magnesium is accelerated greatly when the contact resistance is high. This fact has been confirmed recently by several investigators.[10,11,12] The effect of the direction of current flow on the fouling of the electrodes is also much more pronounced. Furthermore, it is evident in the dynamic resistance characteristics for the electrode-to-sheet contacts. A set of typical characteristics is shown in Figure 20. The irregularity in the curve for the positive or upper electrode-to-sheet contact should be noted. The effect of this irregularity in terms of power is shown in Figure 21. It is evident that much more heat is developed at the positive electrode-to-sheet contact than at the negative contact. This is responsible for the rapid fouling of the positive electrode and the displacement of the weld in the sheets toward that electrode. When the flow of welding current is reversed, the same irregularity occurs in the characteristic for the positive or lower electrode-to-sheet contact.

Steel

In spot-welding steel it is usually taken for granted that the metal must be clean and free from oxide scale if high quality welds are to be obtained. This is essentially a matter of contact resistance, but it has seldom been treated as such. Steel was the chief material used in the first investigations of contact resistance in spot

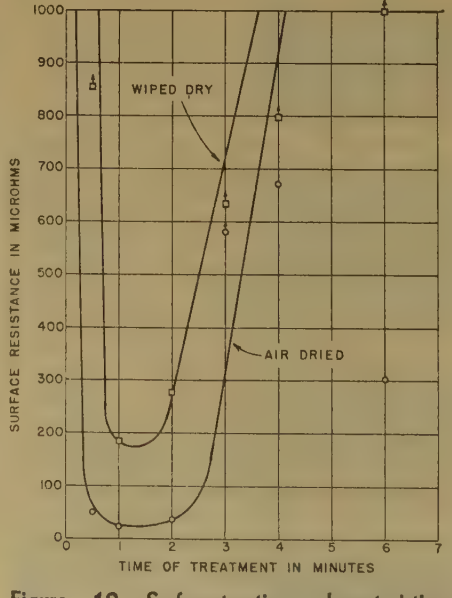


Figure 19. Surface-treating characteristics illustrating effect of method of drying chemically treated specimens of the aluminum alloy, Alclad 24*S*-*T*

0.020-inch alloy, air heat treated, three-per-cent H_2SiF_6 solution at 70 degrees Fahrenheit

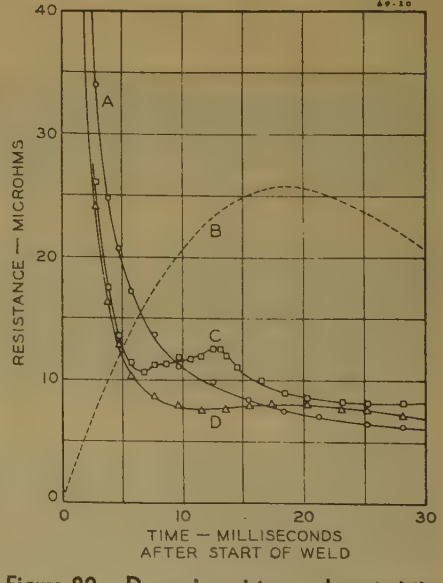


Figure 20. Dynamic resistance characteristics illustrating effect of direction of current flow in spot-welding the magnesium alloy, AM3S-O

0.040-inch alloy, chemically cleaned, tip condition clean

A—Sheet to sheet
B—Current
C—Upper electrode to sheet (positive)
D—Lower electrode to sheet (negative)

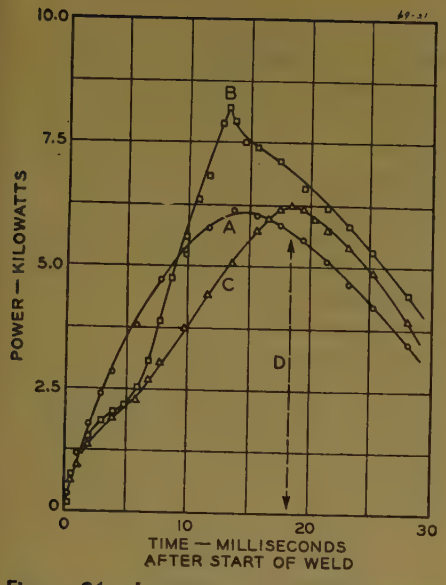


Figure 21. Instantaneous power characteristics illustrating effect of direction of current flow in spot-welding the magnesium alloy, AM3S-O

0.040-inch alloy, chemically cleaned, tip condition clean

A—Sheet to sheet
B—Upper electrode to sheet (positive)
C—Lower electrode to sheet (negative)
D—Time to peak current

welding. A good start was made in those investigations, but even yet very little is known about the fundamental importance of contact resistance in the formation of the weld. It is evident, however, that the body resistance of the metal is a more important factor in the spot welding of steel than in the spot welding of the light metals. In a number of instances trouble has been experienced in spot-welding certain steels which have been identical in composition and structure to other steels which have been easily spot-welded. The trouble is believed to have arisen from a difference in surface condition which could have been detected by contact-resistance measurements.

Copper Alloys

Practically nothing is known about contact resistance and the spot welding of the copper alloys. However, much trouble has been experienced due to contact phenomena in spot-welding a brass with a high zinc content. The zinc tends to migrate rapidly from the work into the copper electrodes. As a result the resistivity of the electrodes is increased, and the amount of heat generated at the electrode-to-sheet contacts increases with each successive weld. These phenomena may or may not be related to the surface condition of the sheet. The effect would certainly be aggravated by a surface condition that is characterized by a high contact resistance. Thus, it appears desirable to apply contact-resistance measurements in any future investigations of the spot welding of the copper alloys.

Nickel Alloys

Nickel-alloy sheet can be obtained with a surface condition that is very well suited to spot welding. However, there are instances where trouble is experienced because of the migration of nickel into the copper electrodes. Contact-resistance measurements might show that this effect is related to a surface condition that might be improved. Such measurements should not be overlooked whenever there is any evidence that surface condition is causing trouble in spot-welding these alloys.

Research Problems

There are many opportunities for further research in this field. For example, the fundamental relationship between contact resistance and the surface condition of the metals in contact should be investigated. Electron-diffraction studies should be employed to determine the presence and identification of surface films. Surface profilometers should be employed to evaluate the degree of surface roughness. Surface hardness should be determined by suitable instruments. The ultimate objective of the work would be to learn how contact resistance is affected by these three factors: surface films, surface profile, and surface hardness. Contacts between both similar and dissimilar metals should be studied.

In spot-welding a number of alloys there is a strong tendency for the electrodes to pick up or become fouled with metal from the work. A fundamental investigation is needed of the transfer of metal across contacts between dissimilar metals under the conditions imposed by spot welding. The objective of the work would be to learn how the transfer of metal is affected by such factors as composition and structure of the copper-alloy electrodes, surface condition of the metals in contact, current density, electrode force, and temperature at the contact. The contact problem in spot welding differs from other electric contact problems with respect to current density, nature of metals in contact, and the fact that the circuit is always dead when the contact is made or broken. The current density may easily reach a value of the order of 5,000,000 amperes per square inch. The contact combinations include copper to aluminum, copper to magnesium, copper to zinc, and sometimes copper to nickel. The contact never is required to conduct current unless the pressure density is within the range from about 5,000 to 50,000 pounds per square inch.

Knowledge of the fundamental part that contact resistance plays in the formation of a spot weld in any material, still is too limited. The investigations of this subject, which were interrupted by the war, should be revived as soon as circumstances permit. Contact-resistance measurements have proved to be of great value in investigations of the spot welding of the light metals. The use of such measurements should be extended to investigations of the spot welding of steels, copper alloys, and nickel alloys.

References

1. Contact Resistance in Spot Welding, F. J. Studer. *Welding Journal* (Research Supplement), volume 18, October 1939, pages 374-s–80-s.

2. Measurement of Contact Resistance, W. B. Kouwenhoven, J. Tampico. *Welding Journal* (Research Supplement), volume 19, October 1940, pages 408-s–13-s.

3. The Function of Contact Resistance in Spot Welding, R. F. Tylecote. *Transactions* (London, England), Institute of Welding, volume 4, July 1941, pages 154–65.

4. An Investigation of the Surface Treatment of Alclad 24S-T in Preparation for Spot Welding, W. F. Hess, R. A. Wyant, B. L. Averbach. *Welding Journal* (Research Supplement), volume 21, June 1942, pages 257-s–65-s.

5. Further Studies of The Spot Welding of Low Carbon and Stainless Steels, W. F. Hess, R. A. Wyant. *Welding Journal* (Research Supplement), volume 18, October 1939, pages 348-s–54-s.

6. The Surface Treatment of Alclad 24S-T Prior to Spot Welding, W. F. Hess, R. A. Wyant. B. L. Averbach. *Welding Journal* (Research Supplement), volume 23, August 1944, pages 402-s–13-s.

7. The Surface Treatment at Room Temperature of Aluminum Alloys for Spot Welding, W. F. Hess, R. A. Wyant, B. L. Averbach. *Welding Journal* (Research Supplement), volume 23, September 1944, pages 417-s–35-s.

8. Contact Resistance Measurements as Control for Preweld Cleaning of Aluminum Alloys, G. W. Scott, Jr., E. B. Charles. *Welding Journal* (Research Supplement), volume 23, January 1944, pages 1-s–7-s.

9. Spot Welding of Light Alloys—Trends in Recent Progress, R. F. Tylecote. *Welding*, volume 12, March 1944, pages 142–4.

10. Cleaning of Magnesium Surfaces for Satisfactory Spot Welds, F. Linville, M. Disotell. *Product Engineering*, volume 15, December 1944, pages 811–12.

11. Cleaning of Magnesium Alloy Sheet for Spot Welding, K. E. Dorcas, N. H. Simpson. *Aero Digest*, volume 48, January 15, 1945, pages 107, 212.

12. Spot Welding of Magnesium Alloys, K. E. Dorcas, N. H. Simpson. *Iron Age*, volume 155, April 5, 1945, pages 50–3, April 12, 1945, pages 68–73.

13. The Use of Statistical Control in Corrosion and Contact Resistance Studies, W. E. Campbell. *Transactions*, Electrochemical Society, volume 81, 1942, pages 377–90.

14. Die Technische Physik der Elektrischen Kontakte, R. Holm. Springer, Berlin, Germany, 1941; Edwards Brothers, Ann Arbor, Mich., 1944.

15. Factory Preweld Cleaning of 24S-T Alclad and 61S-W Aluminum Alloys With Hydrofluosilicic Acid Solution, G. W. Scott, Jr., R. V. Ingram, A. A. Burr. *Welding Journal*

Electronic Regeneration of Teleprinter Signals

H. F. WILDER
MEMBER AIEE

Synopsis: On asynchronous or start–stop telegraph circuits of extended length it frequently becomes necessary to insert at repeater points signal regenerative devices to reduce the cumulative effects of fortuitous distortion. Regeneration is a process of signal scanning by a succession of accurately timed impulses whose phase is as nearly as possible independent of the phase variations of the signal impulses. In one form of a mechanical regenerator, reception of a start signal transition permits the engagement of a brush arm with a continuously rotating constant-speed shaft. The signal polarity then is determined at the instant of contact of the brush with commutator segments that are short in comparison with the signal period. Following retransmission of the signal the brush arm is disengaged from the shaft and held on a stop to await the arrival of the start transition of a second character. Mechanical regenerators have been developed to a high level of performance, accompanied by some complexity and the need for skillful maintenance. This paper describes an electric signal regenerator utilizing the time of delay of a recurrent filter network to generate the scanning impulses, which together with the electrical equivalents of the start and stop functions provide a regenerative repeater without mechanism. The composition of an illustrative teleprinter signal character and its peculiar susceptibility to interfering line currents is discussed. The development and the electric characteristics of the delay network are described, and an explanation of the regeneration of the signal character by the device is given.

AN UNDERSTANDING of the operation of the electronic signal regenerator will be facilitated by a review of the principles of start–stop signaling and of one electromechanical device now used to decrease the fortuitous distortion on long circuits. Start–stop signals are semisynchronous; sufficiently good exactness of phase between the sending and receiving machines is maintained only for the time of duration of a single character after which a rest period must be provided to permit the entire system to come to a stop in preparation for the next character. Teleprinter signaling is thus differentiated from the synchronous systems, such as the multiplex, where each signal transition contributes to the continuous maintenance of exact phase.

The code containing the intelligence to be transmitted is common to both systems and consists of the various combinations of five unit length impulses of either spacing or marking polarity of the sending battery. In a synchronous system these arrive without interruption and are separated into groups of five units by a synchronized commutator. In an asynchronous system it is insufficient to transmit the five unit groups in isolated bursts followed by a rest period, for in some characters the first intelligence impulse is of the same polarity as the rest interval. The additional impulse required to initiate operation of the receiving device is created by a signal transition from the rest condition potential to the opposite pole and precedes the five intelligence impulses. Neither the rest nor this start impulse can be made shorter than unit length, if transmission on long lines is not to be impaired.

Though the start or synchronizing transition of the polar teleprinter signal is not inherently susceptible to the influence of random interfering line currents, phase shift of this transition is doubly damaging on a teleprinter circuit, as the selecting mechanism of the receiving printer is set in motion by the start signal and not by the phase of the average signal as in the synchronous systems. A transient disturbing current that advances the start-signal transition in time may well have its counterpart appear in the intelligence group and there delay a signal impulse by an equal amount to cause selection to be made close to the edge of the impulse. Therefore, when the interference level is the limiting factor in circuit operation, the teleprinter system requires just as careful engineering attention as a synchronous system of twice the transmission speed.

If fortuitous distortion is present in each of the separate lines of a long teleprinter circuit, the effects are accumulative when the lines are coupled by simple relays. Before the shifting in time of the signal transitions becomes sufficient to impair accuracy of service, signal regenerators are inserted at one or more of the repeater points. The basis of regeneration is a process of signal scanning by accurately timed impulses that are independent of the variations in arrival time of the signal impulses. From these observations made in the vicinity of the center of each impulse a new signal is created and retransmitted free of fortuitous distortion.

Mechanical Regeneration

The theory of a mechanical start–stop signal regenerator is shown in Figure 1. The system is at rest having completed the regeneration of the letter *F*. When released by their latches, the brush arms are rotated by the friction drives *CC* on the continuously rotating constant-speed shafts. Upon reception of a start-signal transition, the receiving-relay armature moves to the spacing contact *S*, energizing the start magnet *SM*-1 through the outer pair of brushes and releasing the brush arm on the receiving commutator shaft. As this arm moves counterclockwise, the signal polarity appearing on the tongue of the receiving relay is set up periodically on the selecting relay through connection to the shorter pickup segments. Immediately following signal selection the longer segments successively connect the selecting relay armature to the coils of the five storing relays. These relays firmly bank in the selected position. Only the intelligence impulses are scanned. If the speed of rotation of the brush arm is approximately that of the distant trans-

Paper 46-7, recommended by the AIEE committees on communications and electronics for presentation at the AIEE winter convention, New York, N. Y., January 21–25, 1946. Manuscript submitted August 9, 1945; made available for printing November 1, 1945.

H. F. WILDER is with the Western Union Telegraph Company, New York, N. Y.

(Research Supplement), volume 23, September 1944, pages 443-s–54-s.

16. SPOT WELDING—PART III—CONTACT RESISTANCE, **R. F. Tylecote.** *Welding Journal* (Research Supplement), volume 20, December 1941, pages 591-s–602-s.

17. THE PICKLING OF ALCLAD D.T.D. 390 AND B.S.S. 5L3 PRIOR TO SPOT WELDING, **R. F. Tylecote.** Institute of Welding, *Transactions* (London, England), volume 7, November 1944, pages 129–36.

18. ELECTRICAL CONTACTS, **G. Windred.** Macmillan and Company, London, England, 1940.

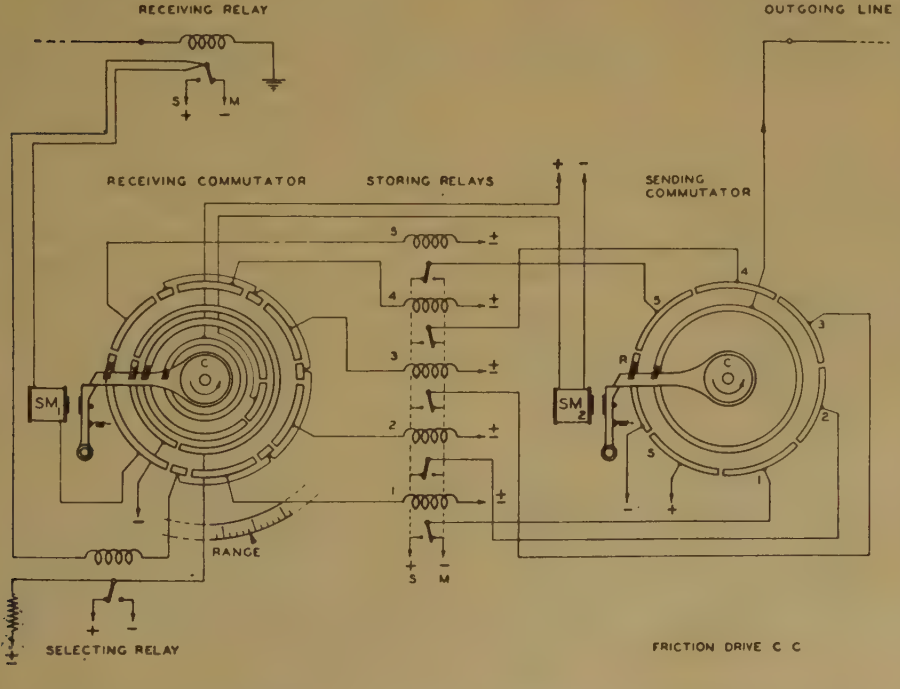
19. ELECTRIC CONTACT RESISTANCE, **G. Windred.** *Journal* of the Franklin Institute, number 231 June 1941, pages 547–85.

20. INVESTIGATION OF THE FINAL RINSING OPERATION IN THE CHEMICAL SURFACE PREPARATION OF ALCLAD 24S-T FOR SPOT WELDING, **R. A. Wyant, D. J. Ashcraft, T. B. Cameron.** *Welding Journal* (Research Supplement), volume 24, July 1945, pages 361-s–9-s.

mitter, the receiving relay will be on its marking contact, corresponding to the rest polarity, when the arm reaches the latch at the end of one revolution, and it will again come to rest.

At some time before the brush arm completes its revolution, a second pair of brushes is arranged to complete the energizing circuit of the unlatching magnet *SM*-2 to release the sending commutator brush arm. The latter continues to send the rest polarity momentarily until it passes over the segment *S* permanently connected to spacing telegraph battery to inject the start-signal impulse that must always precede the intelligence group. Further rotation of the arm connects the storing relays to the outgoing line in correct sequence and time of duration and entirely removed from the influence of the receiving relay. In circuit regulating a teleprinter is connected to the output of the sending commutator while a prearranged test signal is being received and the receiving commutator oriented until limits on the range scale are found within which the retransmitted signals are correct. The center of this angle or range is the center of the average of all the intelligence impulses; correct signal selection is most probable with this angular position of the scanning segments. This adjustment also compensates for the time interval required to accelerate the brush to shaft speed and for any change in clutch operation that may have previously occurred.

Figure 1. Theory of the mechanical teleprinter signal regenerator



The Timing Network

Perhaps the most interesting problem in the development of the electronic regenerator was the choice of a scanning-impulse generator. Two rather incompatible requirements are presented. To insure good signal quality it is desirable that the timing of these impulses be of such an order that the last scanning impulse in any train shall not deviate from a standard time taken with the start-signal transition as the origin by more than one half of one per cent. Following the production of a single train of impulses, the generator must come to rest immediately if a retardation in the generation of a second train is not to result. And, being part of a start–stop system, the generator always must come up to speed, as it were, regardless of the time that it may have been at rest. Simple oscillators of the specified frequency stability do not lend themselves to this purpose because of the transients which cushion the change from rest to steady state and vice versa. However, the resonance phenomena that give the oscillator frequency stability may be retained in certain reactive filter networks, and in particular the uniform recurrent ladder structure, without the troublesome transient effects. With correct configuration these structures will provide time of delay between the mesh junctions dependent upon the choice of the network parameters, and, if a connection is effected between the junctions and electronic relays arranged to scan the received signal impulses, the rate of transmission of the regenerated signal will be a function of these time intervals.

For this application the network should not exhibit frequency discrimination. It should pass all frequency components in the driving force with a constant time of delay. Then the arrival curve will possess infinite slope (zero time of build up), and the triggering of the vacuum-tube relays connected to the network junctions will occur precisely at times determined only by the reactive components of the network and independent of the regulation of the power-supply voltage.

In general the attenuation and time of delay of reactive networks are not invariant with frequency. The mid-shunt or pi section of the familiar low-pass filter composed of a series inductance and shunt capacities will discriminate somewhat against frequencies even below cutoff, and the phase characteristic is so concave that frequencies near the cutoff are delayed considerably more than components approaching zero. Either frequency or delay distortion in the filter will act to decrease the slope of the transient response or arrival curve, and experiment soon confirmed the necessity for correcting the natural behavior of the network. Equalization with additional network components was objectionable because of the increased cost and space requirements, so attention was given to improving the inherent frequency characteristics of the delay-network sections. The steps leading to a section having a satisfactory transient response are shown in Figure 2.

The actual coils had ferromagnetic cores and a Q of 20 at 45 cycles per second. With this Q the effects of dissipation are not excessive, and the output voltage at the terminating resistance is more than half that of the driving force. For comparison the total inductance and total capacity in each of the four cases calculated were held constant. The loci of the short- and open-circuit reactances were first computed and the square root of their product, the characteristic impedance Z_0 plotted immediately below. In the determination of the frequency response only one section of each type was considered. The section was assumed to be driven by a harmonic generator having an internal resistance equal in ohms to the nominal value of the characteristic impedance of the network and to be similarly terminated. This is the situation in the regenerator, except that several sections are in cascade. The frequency response Y is the locus of the IR drop across the terminating resistance versus frequency and is an admittance function. The time of delay has been plotted directly below the transfer admittance, and at the origin this time in seconds is the

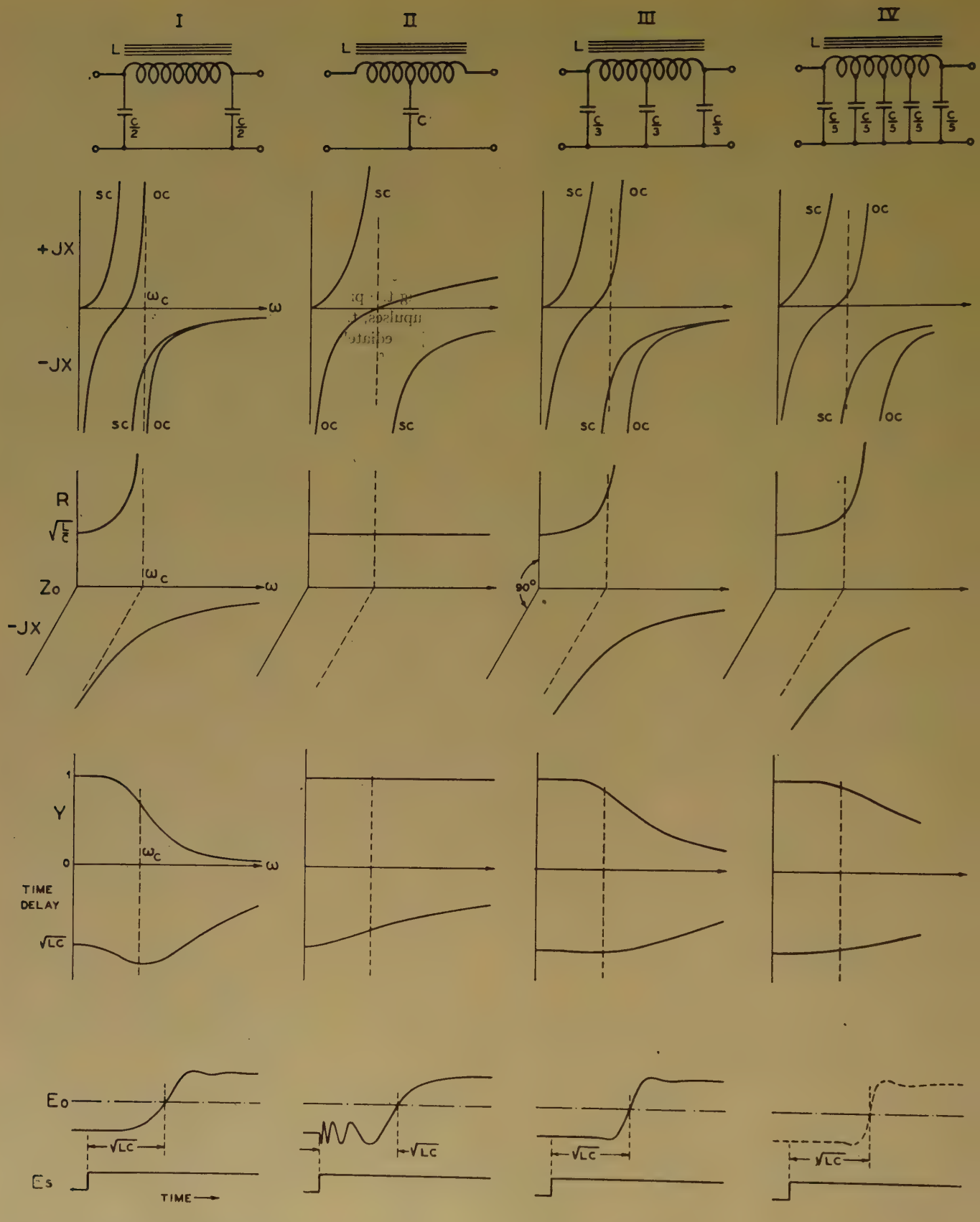


Figure 2. Frequency characteristics of delay network sections

square root of the oscillation constant, LC. With each increase in frequency the delay was obtained as the quotient of the angle of current lag in radians and the angular frequency ω. In all the loci having the angular frequency as abscissas the ordinate ω_c, the theoretical cutoff frequency of section I has been drawn in for reference.

The transient response at the resistive termination of a cascade of six sections is shown at the bottom of Figure 2. These are reproductions of oscillograms. The rectangular driving voltage is E_s. There has been no opportunity to confirm experimentally the transient response of section IV, and the dotted curve is only a prediction of its form.

Returning to the first filter studied, section I, an inspection shows that as long as the short- and open-circuit reactances are of opposite sign, the characteristic impedance, the impedance that would be seen looking into an infinite number of such sections in cascade, is a pure real quantity and has the appearance of a rapidly increasing resistance with frequency up to the cutoff point. In this range the network will absorb power from the generator and transfer this power to the resistance termination. Beyond the cutoff frequency the reactances are of like sign, the impedance becomes an imaginary quantity decreasing with frequency, and the power transmitted by the filter falls off rapidly. In the transmission range between zero and the cutoff frequency where the attenuation is low, the delay distortion is of particular interest, for in this region it has the major effect on the transient response. As the frequency of the driving force is increased, the delay is not constant but increases to a maximum at the cutoff frequency. In a section having a nominal time of delay of 22 milliseconds, for example, the cutoff frequency is 14.3 cycles, and components in this vicinity will be so delayed as to arrive nearly 180 degrees out of phase with respect to the components of the wave near zero. Beyond the cutoff frequency the delay time is of less interest, for the components beyond this point are so attenuated as to contribute very little to the slope of the arrival curve anyway. Because of this variation in transmission time the slope of the transient response continuously changes, being initially low as the low-frequency groups arrive first and only attaining maximum steepness after crossing the zero axis as the frequencies in the vicinity of cutoff finally make their appearance. This form of response is not ideal for the operation of devices responsive to the magnitude of the driving voltage, and it was recognized as similar to the arrival curve of a loaded submarine telegraph cable. Here in the receiving network a mid-series or T section with mutual coupling between the coil arms is used as a distortion equalizer, and so similar sections as in section II at first were alternated with the pi sections with considerable success.

Because the characteristic impedance of section II is real and constant, the filter transmits power without discrimination at all frequencies from zero to infinity. Its phase characteristic, however, is convex and opposite to the concave characteristic of its alternate, the pi section. The slope of the phase characteristic, the delay time, is a decreasing function of frequency. A network composed of these sections alone is just as unsatisfactory as the mid-shunt section, because now the low frequencies are the last to contribute to the arrival curve, and the higher frequencies arrive early, with those approaching infinity having no delay at all. Alternation of the two types doubled the number of coils in the complete delay network.

If a center tap on the coil of the pi section is connected to a portion of the total shunt capacity, the new filter, section III, will be found to have a response equivalent to the alternate arrangement of sections I and II. From an inspection of the characteristics we find that the pole of the characteristic impedance has moved to a somewhat higher frequency and that the impedance locus is more nearly constant over a wider range of frequencies prior to the cutoff frequency. Consequently there is less loss in the transmission range because of increased coincidence with the terminating resistances. Of equal importance is the less rapid decline in the transfer admittance beyond the cutoff frequency of the pi section. The improvement in the locus of time delay is most prominent. Up to the new critical frequency the delay is constant, as the opposite characteristics of the combined filters mutually compensate, and the ultimate decrease is at a lower rate than either alone. This region beyond the cutoff is now of real importance, as the less attenuated higher frequencies are present in the transient response in more nearly correct phase with the lows and can contribute to its steepness. The transient response is the result of the synthesis of a wider band of frequencies of nearly simultaneous arrival time, so that its time of build up is a minimum, and it is symmetrically located about the zero-voltage axis. This is the configuration used in the timing network of the electronic regenerator.

The network contains a minimum number of coils, and the timing of the individual sections may be adjusted easily in a step-by-step refinement of the nominal capacity values without disturbing the timing of the preceding sections. With trigger tubes that will operate on a voltage swing one third that available at the terminating resistance, the variation in their operating time is well within the prescribed limits for a ten-per-cent change in the power-supply voltage and the ambient-temperature range ordinarily encountered. The precision of operation is comparable to that of a well-machined commutator with a synchronous motor-driven brush arm. The actual network consisted of six sections, each having a coil of 72 henrys and a total shunt capacity of 6.7 microfarads, preceded by a seventh section of half the delay. The time of delay of each larger section is 22 milliseconds; very closely the time length of a single teleprinter signal impulse. As measured at the terminating resistance, the time of build up was 40 milliseconds, which becomes less at junctions nearer the input terminals. The network occupies a space of approximately one cubic foot.

One might theorize as to the response of a section similar to III in which the total shunt capacity is still further subdivided into a not impractical number of paths. Improvement would be evidenced by an increase in the steepness of the transient response. To confirm this speculation the frequency characteristics of such a filter, section IV, in Figure 2, were calculated. In the locus of the characteristic impedance Z_0 the critical frequency has moved still farther to the right, and the real part of the impedance is more flat for a wider range of frequencies. Consequently both frequency characteristics are improved. Although the time of delay is somewhat more constant than that of section III the greater improvement appears in the frequency response, Y, which is noticeably more constant.

In this paper the time of build up of the transient response has been assumed to be the time interval between the intersection of the timing wave with a prolongation of the steady-state levels before and after its occurrence. In filter sections having nearly constant time of delay, so that all components arrive in correct phase, the time of build up will be inversely proportional to the band width. Neither section III, nor particularly section IV, can be said to have definite frequencies of cutoff limiting the band width. However, when it is recalled that after all the low frequencies furnish the bulk of the wave, it is interesting to establish arbitrarily such a limit for the three sections at a frequency 2.5 times the cutoff frequency of section I and to then compare the relation between the areas under the admittance loci and the times of build up. The inverse ratio of the areas of section III and section I is 0.74, a rather close agreement with the experimentally determined times of build up of 40 and 55 milliseconds respectively for timing net works composed of such sections alone. In like manner the inverse ratio of the areas under the Y loci of sections IV and III is 0.85, so that the predicted time of build up for section IV becomes 85 per cent of 40, or 34 milliseconds.

It seems, therefore, that continued subdivision of the shunt capacity will not increase the steepness of the timing wave reversal sufficiently to justify more numerous coil taps and capacitors. For timing purposes section IV is an adequate approach to the ideal section of constant attenuation and constant time of delay.

The Electronic Regenerator

The theory of the electronic teleprinter signal regenerator with a timing network of type-III delay sections is shown in Figure 3. The relays and regenerative circuits are in the rest condition. A series of voltages occurring in the system for the regeneration of the letter *F* is shown in the lower part of the figure. While the times t_0, t_1, and so on, represent instants of signal transition in the absence of distortion, the existence of extraneous line currents has been assumed, and the signal transitions have been delayed or advanced to an extent not greatly different from that actually encountered in operation. In any event the theoretical limit is one fourth the period of a single impulse.

In the regenerator twin-triode vacuum tubes are arranged in symmetrical push–pull circuits to eliminate polarity distortion. Pair 2 and their external plate resistors form a bridge circuit the diagonal of which is the impedance presented by the input terminals of the timing network. The plate circuits of the other low-power tube, pair 4, are the differentially wound coils of the sending relay. Telegraph battery potential is connected to the contacts of this relay, and from its armature the regenerated signal is applied to the apex of the duplexed east line. The remaining tubes are characterized by relatively low transfer conductance and high amplification factor. The pickup and latch tubes are simply electronic switches. Dependent upon the polarity of the control-grid voltage, these tubes present either an extremely high plate–cathode resistance or a resistance comparable to the impedance of the circuits to which they are transformer coupled. The remaining nine tube pairs are connected in a balanced Eccles–Jordan trigger or flip-flop circuit. This circuit displays negative resistance between plate elements over a portion of the characteristic between the stable states, and, if a momentary displacement of the grid voltage occurs, the potential from plate to plate will instantly reverse. This relay characteristic will convert any general input wave form in the grid circuit above a definite minimum to a rectangular output wave of constant amplitude.

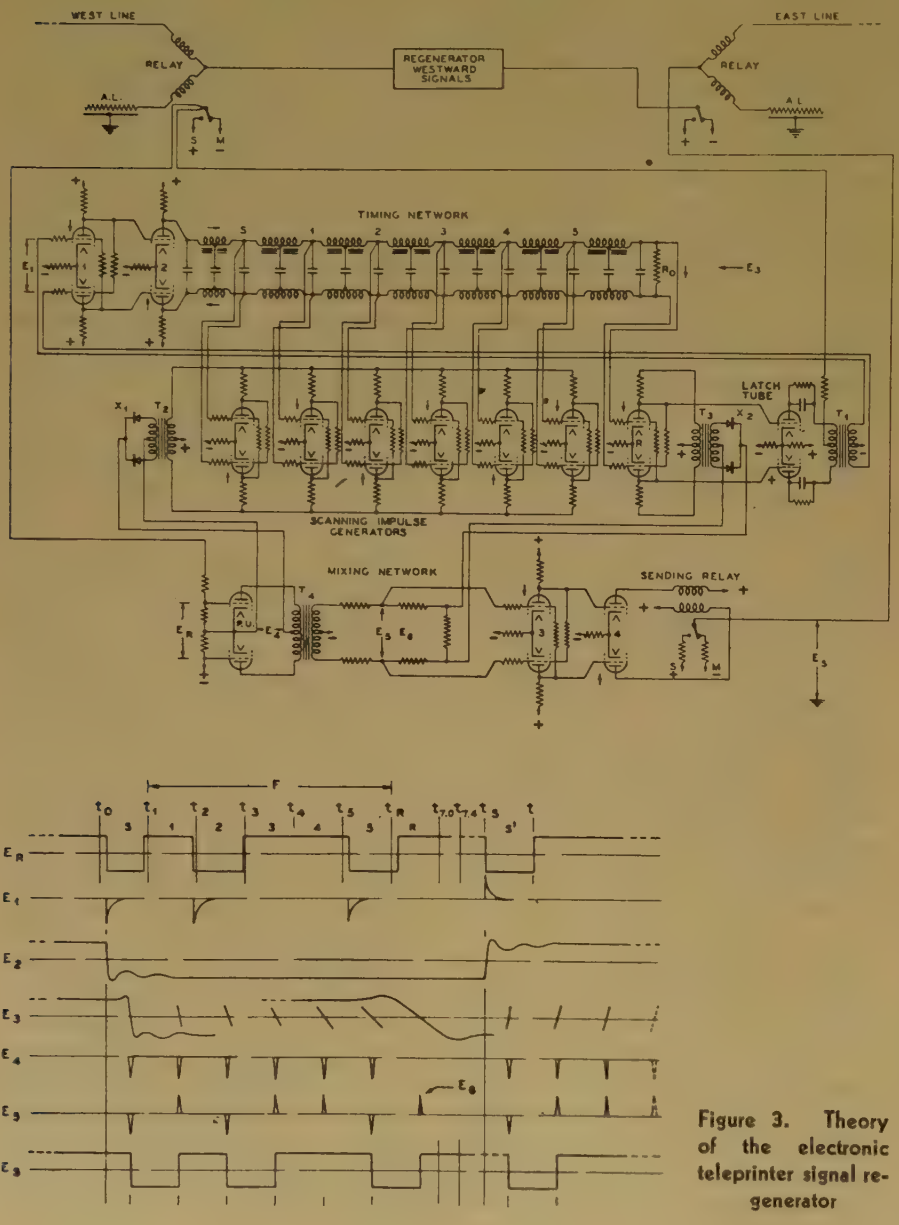


Figure 3. Theory of the electronic teleprinter signal regenerator

The nominal characteristic impedance of the timing network is equal to the resistance looking back into the bridge circuit of tube 2. Except for the first section of the network, which has half the delay of any one of the following six, each section has a time delay ($t_d = \sqrt{LC}$) equal to the time of duration of an undistorted signal impulse, or 21.98 milliseconds. Each inductor consists of two identical windings on a single silicon steel core so disposed that the cathode returns of the six scanning-impulse generators and the rest-interpolating tube are equipotential with a horizontal plane bisecting the network. A reversal of the network input potential appears across the junction *S* eleven milliseconds later and at the termination R_o in a total elapsed time of 143 milliseconds.

Regeneration is begun by movement of the receiving-relay armature to the relay-spacing contact in response to the start impulse of a teleprinter character. As directed by the latch tube, a single reversal of potential is applied to the timing network by its driving tubes. With progression of the timing wave from junction to junction a series of six pickup impulses are generated successively activating the pickup tube scanning the incoming signal. The observed polarity of each signal impulse is at once transferred to the sending-relay drive tubes through the mixing network. Twenty-two milliseconds after the selection of the fifth intelligence impulse the timing-wave reversal appears across the resistance termination and triggers the *R* tube to interpolate an impulse

of the rest polarity in the mixing network and simultaneously to make the latch tube again receptive to any future start signal.

A more detailed description must begin with an examination of the circuit conditions with the regenerator at rest. Now the receiving-relay armature is held on its negative contact by the marking line current received, and negative battery is applied to the center tap of the transformer T-1. A second circuit from the receiving-relay armature develops the incoming-signal voltage E_r in the grid circuit of the deenergized pickup tubes. As indicated by the small arrows adjacent to the tube elements, all trigger tubes are banked in the direction last operated; a condition that will be reversed after the regeneration of a complete character.

A constant current from positive battery flows through the external plate resistor associated with the upper tube of the driving pair to the right and along the upper windings of the inductors to the terminating resistance R_o. This current returns to negative battery through the lower windings and the lower and conducting drive tube. By reversing every other pair of wires connecting the scanning-impulse generators to the network junctions, these tubes are banked in alternate directions, and the sum of their plate currents entering the center tap of the primary of T-2 is divided equally between the winding halves. Consequently as the scanning-impulse generators are triggered successively, the differential primary current never exceeds unit amplitude, and hysteresis effects in the core material are minimized.

Just as a similarity will be recognized in the function of the latch tube and the brush-arm release mechanism of the mechanical distributor, so are the R-tube functions equivalent to the R segment on the sending commutator and the two paired segments on the outer rings of the receiving commutator which permit the start magnet circuit to be energized only after a complete revolution of the brush arm. If the upper R tube is conductive, the plate of the nonconducting lower tube will be at a very high positive potential and will by direct connection correspondingly elevate the grid of the lower latch tube. Upon reception of a teleprinter signal the center tap of T-1 is at once made positive as the receiving-relay armature contacts its spacing stop. Under the conditions established, however, a charging current to only the lower-resistance shunted condenser flows in the lower half of the primary winding of T-1. The transient secondary voltage is E_1. In the course of reception of the incoming signals negative potential is at times applied to the center of T-1, and in these intervals the condenser charge is dissipated in the shunting resistance. If correctly poled the transient E_1 causes tube 1 to trigger, reversing tube 2 and the potential across the timing network. Subsequent impulses of like polarity in E_1 may occur in the reception, two more are present in the letter F, but the initial impulse alone is of importance.

Although the continuity of the description perhaps is interrupted, an interesting operating condition now may be described. This occurs when either the west line is opened or, if in circuit, regulating, the west transmitter sends steady spacing battery. In either case the marking battery applied to the apex of the west duplex line at the regenerator station causes a current to flow in the artificial line winding of the receiving relay, which holds the armature on the spacing contact and so applies positive battery to the midpoint of T-1. Now upon the arrival of the first timing wave at R_o the conductivity of the latch tubes is interchanged while their plate circuits are energized positively and a starting impulse of local origin is created in E_1. A second timing wave is set up, and the process becomes continuous. A characteristic recurrent signal of six-unit length impulses of spacing polarity followed by a half-unit length marking impulse is transmitted to the east line; a signal that is easily interpreted by the distant east receiver as an open line west of a regenerative repeater.

Returning to the description, the R tube is also the circuit element that restores the sending relay to its marking contact after the transmission of the intelligence impulses. A reversal of the R tube in either direction produces a transient voltage in the secondary of T-3. These are introduced at the right of the mixing network after being made unidirectional by the rectifier X_2. The solid triangular impulse E_6 in the time diagram is of this origin. Consequently the regenerator cannot fail to send a rest signal.

The wave form of the timing-wave reversal across the network input terminals is shown in E_2. Until this reversal has reached the termination R_o and operated the R tube, another reversal cannot occur, and then only with reception of a second character of which S' is the start impulse. Although a gradual decrease in slope of the wave is apparent as successive meshes attenuate the higher-frequency components, symmetry is retained as depicted in E_3. The scanning-impulse generators are triggered at intervals of at first 11, and then 22 milliseconds. The sum of their plate currents in the differentially connected primary windings of T-2 is either zero or unit amplitude, depending upon whether an even or odd number of impulse generators are at any instant banked in like electrical position, and a change in net primary current occurs six times with the passage of a single timing wave. The resultant series of six alternately poled derived impulses of extremely short duration in the transformer secondary is rectified by X-1 and introduced, as E_4, between the cathode and plates of the pickup tubes.

Any one of these scanning impulses can produce current flow only in that half of the primary of T-4 associated with a pickup tube whose grid is positively displaced with respect to the common cathode connection. The polarity of the transformer secondary voltage is therefore dependent upon the polarity of the incoming signal E_r at the instant of scanning. A proportion of the polarized pickup voltage appears as E_5 at the midpoints of the mixing network to position the sending-relay drive tubes and the sending relay. E_s is a plot of the telegraph battery potential transmitted by the sending relay to the east line. It is a reproduction of the perfect signal originally transmitted, being composed of unit length impulses as determined by the timing network and independent of variation in received-signal transition time.

If signals are transmitted from a slowly operated keyboard, the rest impulse is considerably longer than unit length. Frequently, however, intelligence groups contained in a perforated tape are passed through a transmitter that automatically inserts a rest-and-start impulse between groups. In this case the rest impulse may be considerably shortened, if, under the most adverse effect of signal distortion, the preceding start impulse suffered delay in arrival and the start transition of the following character is advanced in time. Then the rest signal is not regenerated but must absorb the total phase shift of the two start impulses. In some systems a 42-per-cent extension in length of all rest impulses is made to absorb these phase shifts, but a reduction in the number of letters per minute transmitted must be accepted if the same maximum line frequency is retained.

Performance

To measure the telegraphic efficiency of the regenerator a chemically recording transmission testing machine was used. Transmission was continuous from a pre-

pared tape, unless to simulate keyboard sending the transmitter was sporadically autostopped. To permit the time relation between any regenerated signal impulse of a character and its start impulse to be observed, the sending ring could be rotated through increments of one segment.

With this arrangement the timing of the network sections was adjusted successively until the maximum departure from normal of any regenerated impulse was less than two per cent. By moving the segment sending the start impulse with respect to the segments sending the intelligence group, the minimum time of duration of an impulse required to insure correct selection by the pickup tubes was found to be 0.5 millisecond. The response of the latch tubes to the start signal was instantaneous, irrespective of how long the regenerator had been at rest.

Physical Aspects

The electronic regenerator has been developed as an adjunct to direct-point repeaters. Any one of a group of rack-mounted unidirectional units may be inserted quickly in a teleprinter circuit at a repeater station. Experience has shown that the regenerator will operate continuously for six months without attention.

Correction for Paper 45-167

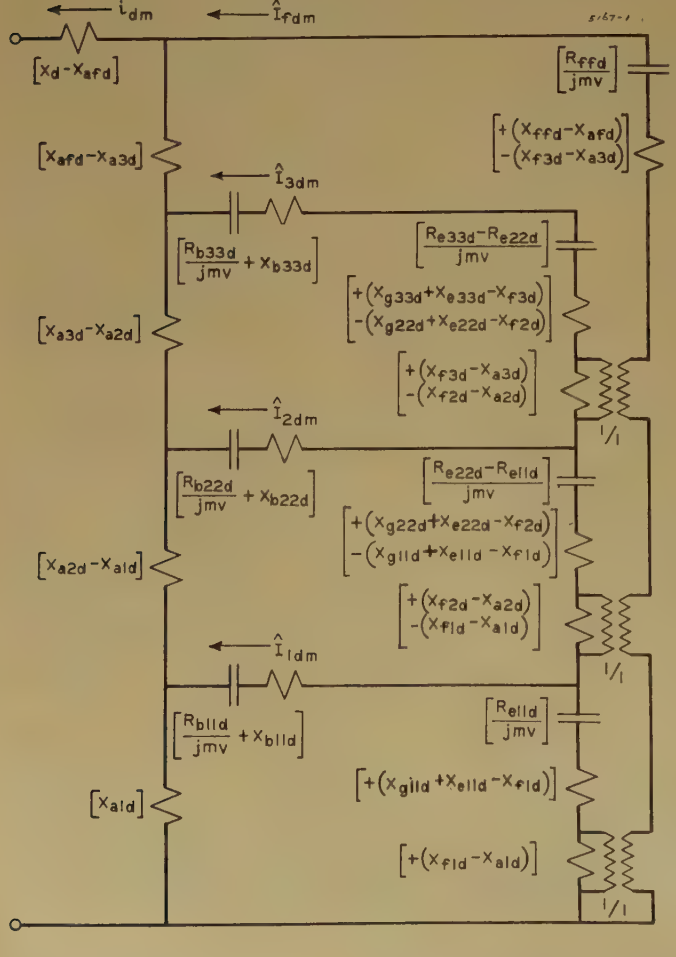


Figure 1. Direct-axis complete equivalent circuit for five or six bars per pole, $x_d(jmv)$

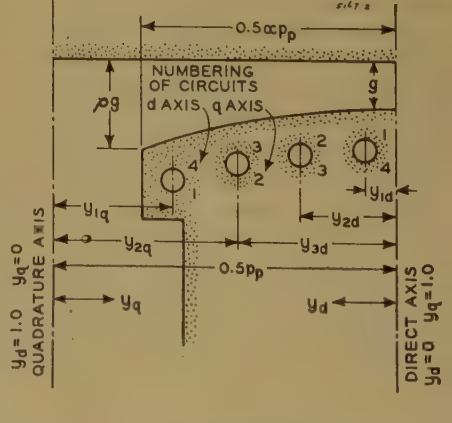
$\frac{R}{jmv}$ = capacitive reactance

x = resistance

The quadrature-axis complete equivalent circuit is obtained from this circuit by substituting q for d

Figure 2 (right). Pole and damper-bar dimensions and numbering of damper-winding circuits

Y_d and Y_q are measured in per unit of half the pole pitch ($0.5P_p$). Y_{nd} and Y_{nq} are the values of Y_d and Y_q, respectively, to circuit n, measured from and numbered from the corresponding (d or q) axis



As published on pages 862 and 864 of the Transactions section of the December 1945 issue of ELECTRICAL ENGINEERING, Figures 1 and 2 of the paper, "The Direct- and Quadrature-Axis Equivalent Circuits of the Synchronous Machine," by A. W. Rankin contained drafting errors. Corrected versions of the figures are printed here.

TRANSACTIONS SECTION

Preprint of Corresponding Pages From the Current Annual AIEE Transactions Volume

A New Submersible Network Protector of Higher Rating

G. G. GRISSINGER
MEMBER AIEE

F. D. JOHNSON
ASSOCIATE AIEE

DURING THE DEVELOPMENT of the original low-voltage a-c-network distribution system, preliminary studies indicated that the use of a relatively large number of medium-sized distribution transformers would provide the most flexible and most economical arrangement. Furthermore, very satisfactory operating experience with network systems of this type gave considerable justification for their use.

Obviously the network protectors required were also of relatively small size, since the continuous ampere rating and the interrupting rating were influenced by the size of the distribution transformers used. This meant that the majority of the protectors had continuous ampere ratings of 250 and 500 amperes at 60 cycles and interrupting ratings of 15,000 to 20,000 amperes at 220 volts.

However, the rapid growth of the a-c low-voltage-network distribution system, together with its adoption in many different types of application, soon developed the need for network protectors of considerably higher ampere ratings. The first expansion extended the continuous ampere ratings to 800 and 1,200 amperes. Subsequently the range was increased further to include 1,600- and 2,000-ampere ratings.

During this period the interrupting ratings remained at 20,000 amperes. But operating experience with systems having greater power concentrations, together with calculations of possible short-circuit currents, eventually led to the development of network protectors having interrupting ratings up to and including 40,000 amperes.

The need for the higher interrupting ratings also resulted from the use of spot networks requiring large concentrations of power and involving a number of large distribution transformers. In addition to having high interrupting ratings the network protectors for these applications required continuous ampere ratings as high as 3,000 amperes 60 cycles.

Most of the original network protectors were located in building or basement vaults not subject to flood conditions. This meant that the protectors could be mounted in the open air or in ventilated enclosures. Heat losses generated in the protectors therefore were dissipated readily, and it was not a difficult matter to provide reasonably compact units for any of the required ampere ratings.

Extension of the secondary network distribution system soon showed the desirability of installing network units in subway vaults either under the street or under the sidewalk. Installations of this type were of course subject to flood conditions, and both transformers and network protectors had to be made submersion proof. In the case of the network protectors, which were essentially automatic air circuit breakers, the enclosures had to be watertight, in fact airtight. Dissipation of heat from an airtight enclosure, with air inside the enclosure as the transfer medium, could occur only by straight conduction, convection, and radiation, with very little benefit from air flow.

This problem obviously becomes more difficult as the continuous ampere rating increases due to the greater heat losses developed. It is believed therefore that the problems involved and the methods used to produce a 3,000-ampere a-c submersible network protector of reasonable dimensions will be of interest.

General Description

The 3,000-ampere submersible network protector for 120–208-volt three-phase 60-cycle service is the latest development for application to secondary networks having highly concentrated load areas. The interrupting rating of this protector is 40,000 amperes. The accepted practice for network protectors requires that the circuit breaker withstand an initial instantaneous peak of $2^1/_4$ times the rms current which is to be interrupted, in this case a peak of 90,000 amperes, and requires that it carry the short-circuit current for 60 cycles before the current is interrupted.

The submersible network protector, as the term implies, is enclosed in a heavy steel housing suitably constructed to withstand submersion in water up to a depth of at least 15 feet and is in addition so constructed as to be readily accessible for maintenance. Figure 1 shows such a network protector completely closed as it is in service. The only electrical connections are those to the main circuit by means of the solid copper studs through porcelain bushings. The cover of the housing is a separate fabrication which is hinged, gasketed, and clamped to the tank body in such manner as to be readily

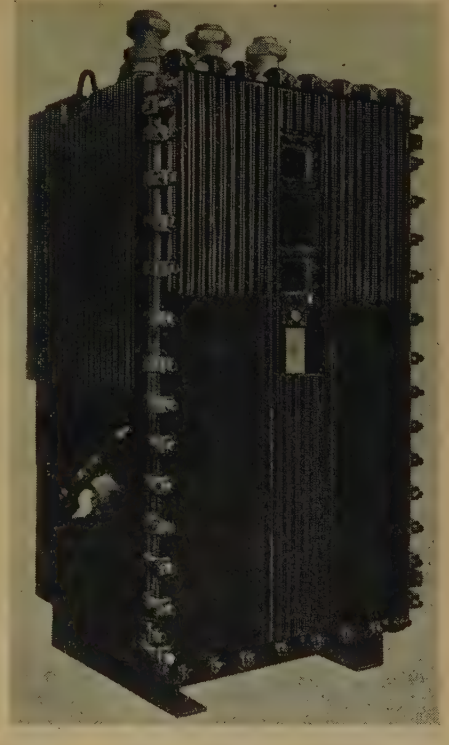


Figure 1. Submersible-type 3,000-ampere network protector for transformer mounting showing exterior cooling fins

Paper 46-11, recommended by the AIEE committee on protective devices for presentation at the AIEE winter convention, New York, N. Y., January 21–25, 1946. Manuscript submitted October 3, 1945; made available for printing November 14, 1945.

G. G. GRISSINGER and F. D. JOHNSON are in the switchgear control engineering department, Westinghouse Electric Corporation, East Pittsburgh, Pa.

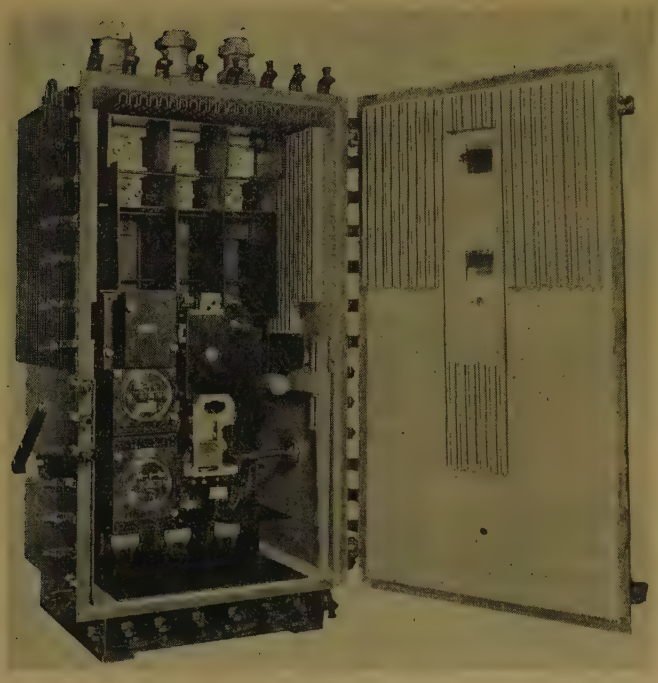


Figure 2. Submersible-type 3,000-ampere network protector for transformer mounting showing interior cooling fins

opened for access. The protector proper is a unit assembly which can be disconnected readily at top and bottom from the power circuit and rolled forward on collapsible tracks mounted within the housing. Briefly described, this protector unit consists of a three-pole motor-operated circuit breaker, three fuses, a master network relay, a phasing relay, and a desensitizing relay. See Figure 2.

Reduction of Copper and Iron Losses

It is well known that for solid copper conductors of a size suitable for carrying 3,000 amperes at 60 cycles there is considerable "skin effect" and also that there is considerable power loss in magnetic members in proximity to such conductors. Both of these factors are comparable to an increase in resistance of the conductor, and, as such, it is evident that the power loss within the protector varies directly as the square of the current carried. This is roughly a measure of the difficulty encountered in increasing the current-carrying capacity of the network protector without at the same time drastically increasing its operating temperature. It is impractical to increase the carrying capacity without some increase in total losses, and the dissipation of these additional losses through the housing to the outside air further complicates the heat problem. A network protector, like most electric equipment, must be made as compact as is consistent with good design; this mechanical requirement is in direct opposition to the tendency of higher currents to result in larger conductor sizes, higher magnetic forces on contacts, and, hence, larger mechanisms. It was the judicious balancing of these factors with certain improved arrangements which made the present development possible.

The phenomenon of skin effect is well known, and in general its effect is quite readily calculated.[1] However, in the case of a compact multiple-pole circuit breaker with its irregular current paths, proximity of adjacent phases, and proximity of magnetic materials the problem is complicated by proximity effect,[2,3] by iron losses, and by contact losses. Because of the indeterminate nature of the combined losses it was decided early to study the losses experimentally by measuring the actual a-c resistance of the circuit breaker and its parts. The loss in relay potential and current coils is a small part of the total, and hence the problem is entirely one of current losses, except for consideration of the temperature rise of the coils themselves. A search of the literature on the subject did not disclose a previously available method of readily and directly measuring the 60-cycle resistance of such heavy copper circuits. The method employed is described in the appendix.

Conductors of a size to carry 3,000 amperes at 60 cycles are most efficient when made in a tubular form, preferably of circular section, with a wall thickness of approximately 0.5 inch but specifically related to the actual diameter.[3] Because of practical considerations in arranging contacts and connections in limited space a hollow conductor of square section has been used for current-carrying parts wherever practical. Since these hollow conductors are open at each end and since they are mounted vertically, natural convection is effective for cooling inside as well as outside surfaces. (For a comparison of some typical conductors, see Table I.)

The movable contact or bridging member of the circuit breaker cannot readily take the form of a hollow conductor, especially in the limited space available in a network protector, and hence an alternate type of conductor had to be used here. The conductor used takes the form of six copper blades per pole in parallel, these being hinged at their lower end similar to the blade of a knife switch, and engaging stationary jaws at their upper end. The copper blades are arranged in pairs with three such pairs making up a bridging member for each pole. In each pair the blades are placed with the flat faces of one parallel to those of the other. The next pair is in a similar position but spaced approximately one inch away. This configuration of six flat bars in parallel if extended in length would have a current distribution over its cross section no better than would a solid conductor of the same outside dimensions. However, in this case each of the six conductors is only several inches in length and at each end there is a contact, the resistance of which is appreciable compared with that of each bar itself. The effect of these contacts is to equalize the current flowing through the six bars, and therefore the current distribution over the cross section

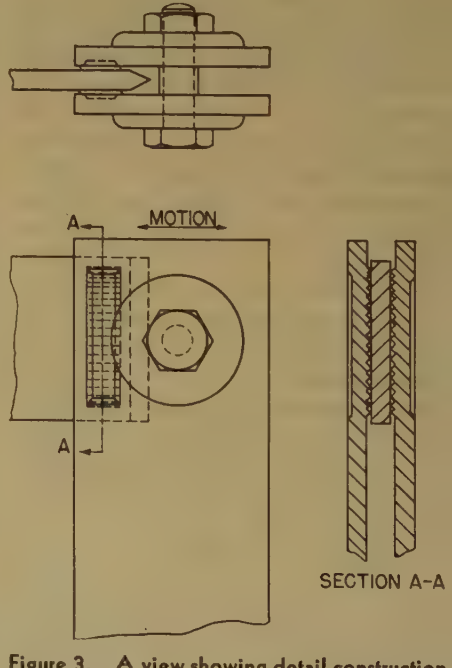


Figure 3. A view showing detail construction of the multiple silver-plated line contact at the break end of the bridging- or moving-contact members

of each bar is comparable with that which would flow in a single isolated bar, and all six bars carry current effectively.

At the hinge joint of each pair of bars the contact is a hard silver plate of substantial thickness on both the moving bars and on the stationary jaw which is placed between them. Pressure is applied to these contacts by means of a through bolt and cup-washer springs.

At the break end of the bridging members the stationary jaw is similarly silver plated and is tapered at its engaging edge to facilitate engagement with the moving bars. The bars, however, engage this jaw only for a portion of their width in order to conserve travel. The portion of a bar which engages the jaw at this point is silver-plated and then by high pressure dies is embossed into a series of parallel, raised, and hardened silver lines each with its axis in the direction of the sliding action of the contact. Figure 3 shows the arrangement of the embossed-silver multiple-line contact. Pressure on the break contact just described is secured in the same manner as at the hinge joint, that is, by means of a transverse bolt through the two bars and a cup-washer spring on either side. Figure 4 shows the construction of the circuit breaker.

Each pole of the protector is fitted with a fuse, usually on the network side, to serve as standby protection in case of apparatus failure or to open the circuit in case of a bad nonclearing fault on the network side close to the protector. These fuses are designed to operate at an unusually low temperature in order not to add unduly to the heat problems of the protector. Low operating temperature is obtained by constructing the fuse with a fusing member from a small section of low-melting-point eutectic alloy; the balance of the fuse body is heavy copper.

Network protectors commonly are enclosed in steel housings, and, because they are made as compact as practical, it is obvious that at some point the conductors will approach this steel enclosure or actually pass through it, resulting in hysteresis and eddy-current losses in the steel. These losses actually may equal or exceed the copper losses, unless preventive measures are taken. The method of measuring a-c losses which is described in the appendix was especially useful in tracing and eliminating these iron losses. It was found necessary to make the top plates where the main bushings pass through, and the rear plate of nonmagnetic steel. Also, mechanism brackets, levers and frames, and circuit breaker mechanical parts had to be nonmagnetic.

Heat Dissipation

When the circuit breaker has been developed to generate the minimum practical amount of copper and iron loss there still remains the problem of dissipating this heat through the steel housing or enclosure at the relatively small temperature differential which is available. The usual air circuit breaker has only copper loss to be dissipated and dissipates this by conduction, radiation, and convection directly to the surroundings; the usual oil circuit breaker by conduction to the oil and then by conduction, radiation, and convection to surroundings. The temperature differential available for the dissipation of heat is 85 degrees centigrade for class-*B* insulation.

The radiation of copper losses takes place in the network protector in three stages, namely, in one temperature drop from the copper to its barriers and immediate surroundings, in a second temperature drop from these surroundings to the inside of the enclosing housing, and in a third temperature drop from the housing exterior to surrounding objects. Similarly, in the dissipation of copper losses by convection it is found that there are three temperature drops in series, namely, first from the copper to the surrounding air, second from this heated air to the housing structure, and third from the housing to the exterior air. By conduction some heat is transmitted directly to immediate surroundings of the conductor and from there is taken by radiation and convection to the housing and to the outside; but the amount of copper loss which may be conducted directly to the housing structure is very small. Conduction through air to the housing walls accounts for a very small portion of the heat loss. Fortunately the iron losses which are allowed to remain are generated directly in the housing itself.

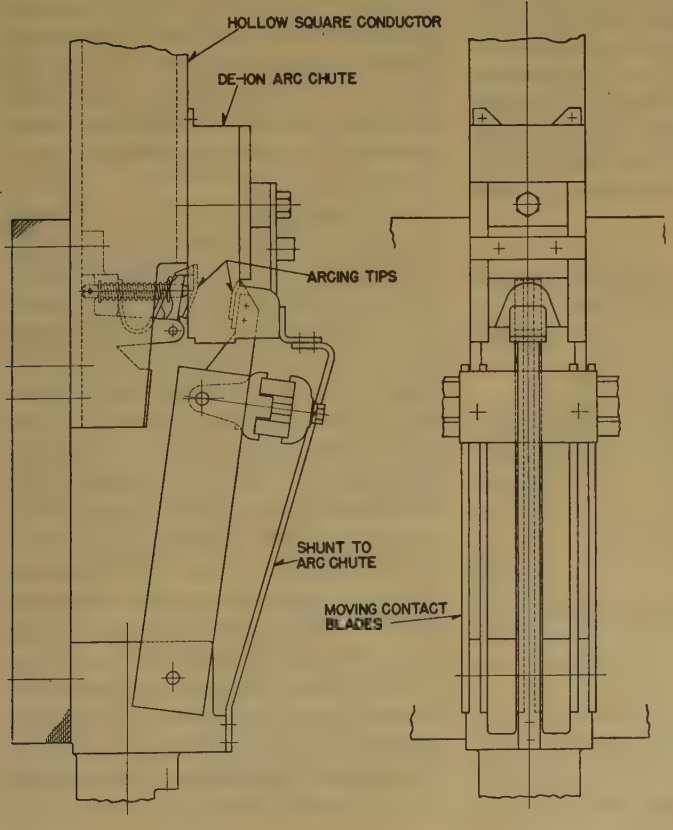


Figure 4 (left). A view showing the arrangement of circuit-breaker contacts and deion arc chute

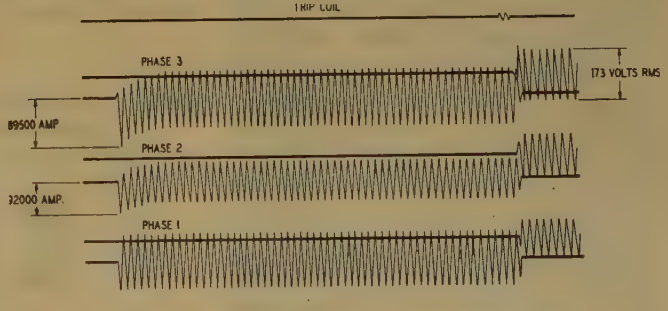


Figure 5. Oscillogram of a short circuit of 40,000 amperes at 300 volts, 60 cycles

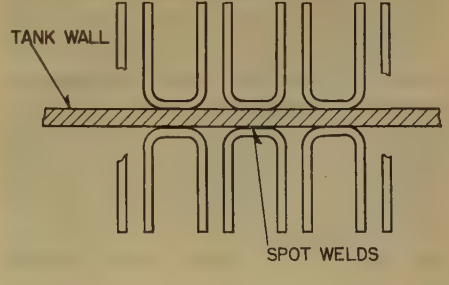


Figure 6 (right). Cross section showing arrangement of cooling fins

As radiation and convection are the chief factors in the dissipation of the copper losses, it is proper that all possible factors should be introduced into the design favoring the dissipation of the heat by these means.

The dissipation of heat by radiation is given by the Stefan–Boltzman law:

$$Q = 5.7 \times 10^{-12}(T_1^4 - T_2^4)e$$

where

Q = energy radiated, in watts per square centimeter
T_1 = absolute temperature of radiating body in degrees Kelvin
T_2 = absolute temperature of surrounding surfaces in degrees Kelvin
e = total emissivity of surfaces

Since this quantity is proportional to the difference of the fourth power of the two absolute temperatures, it is evident that dissipation by radiation can be very useful even for small temperature differentials, provided the values of e are as high as are practically obtainable. To this end the copper conductors are given an oxidized copper finish the emissivity of which is 56.8 per cent[5] as compared with unoxidized or unfinished metal surfaces which have an emissivity of four per cent or less. The housing surfaces, both interior and exterior, are finished with pigmented paints having even greater values of emissivity.

The convection factor for the removal of heat from the conductors is enhanced by taking advantage of the chimney effect of the vertical hollow conductors and by the bridging member of the circuit breaker being a number of thin conductors in parallel. The return bus bars at the rear of transformer-mounted network protectors are mounted on insulating members to the rear plate of the housing, which plate is nonmagnetic steel, with nonmagnetic steel cooling fins extending from the plate forward between the bus bar members and at each side of them. These fins, in this interleaving manner, both by radiation and by convection, extract heat from the bus bar members for their full length.

It is just as necessary to favor the heat transmission through the housing as it is to favor getting it out of the conductors. The housing is painted inside and out, giving these surfaces an emissivity of around 89 per cent, so that for radiated heat the walls are a good transmission means. However, by conduction the conductors heat the air within the housing, and it immediately rises to the upper portion of the housing, where it tends to stagnate. The conductors occupy the full height of the housing and generate

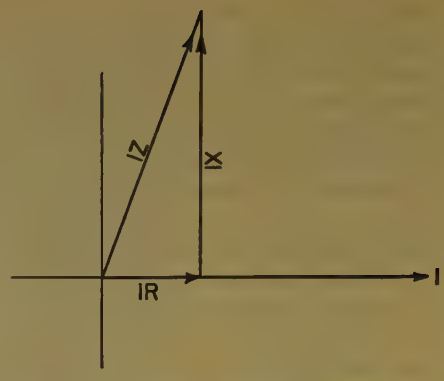


Figure 7. Diagram showing balancing of voltage components in the bridge circuit

I = test current
IR = inphase test voltage
IX = 90-degree test voltage
IZ = voltage drop of test specimen

heat for their entire length, so that the heated air tends to circulate upward past the conductors, and they get the benefit of true convection cooling. However, the heated air moving upward stagnates in the top of the housing and is cooled mainly by conduction through the housing walls. To cool this air and establish a full circulating system it is necessary to add greatly to the exposed surface of the housing, both internally and externally, in the hot region. This is done by adding cooling fins to both the inside and the outside surfaces as shown in detail in Figure 6, this being necessary only for approximately the upper one half of the housing. For each one square inch of base or radiating area, either inside or outside, there is an exposed area including fins of 5.1 square inches. The fin arrangement shown is a practical means of construction devised to get the necessary heat through the available wall area without increasing housing dimensions prohibitively; it is not theoretically correct in proportions, either in efficiency of a given amount of base surface or in the amount of metal used. Radiation alone is not sufficient to cool the conductors and housing, and it is not practical to load the conductors with cooling fins; therefore, it has been necessary to allow a relatively large temperature differential from the conductors to the air in the housing and to work toward smaller temperature drops from this air to the housing wall and from the wall to the outside air by heavily loading the housing walls with fins.[4,6,7]

Table I. Comparison of Typical Copper Conductors at 60 Cycles

	Gross Section, Square Inches	Surface, Square Inches Per Inch	A-C Resistance, Microhms Per Inch	$\frac{R_{a-c}}{R_{d-c}}$
1¼x4	5.00	10.5	0.327	2.07
Solid bus[4]				
4-inch hollow square ⅛-inch wall	5.24	27.3	0.193	1.22
3-inch hollow square ¼-inch wall	4.57	17.4	0.245	1.35
3-inch outside diameter of tube ½-inch wall	3.93	15.7	0.224	1.30
4-inch outside diameter of tube ½-inch wall	5.50	22.0	0.162	1.31

Mechanical Features

Working in opposition to the requirements for low loss and low temperature rise, as well as the requirements for high interrupting ability and high short-time current rating, is the ever present need for minimum physical size. The methods used to accomplish the required temperature results have been described. The mechanical features whereby the stresses of interruption and of high currents are held under control now will be discussed.

The current values encountered in short-circuit interruption by network protectors are high and must be held under control until interruption is accomplished. The 3,000-ampere network protector is required to interrupt a short circuit, the initial crest of which reaches an instantaneous value of 90,000 amperes or more, followed by a decreasing current for 60 cycles, at which time the circuit breaker opens and interruption is accomplished at 40,000 amperes or more rms. During this time it is necessary that the large magnetic forces do not blow any of the contacts open, with the resulting burning of contacts.

The magnetic forces of short-circuit currents act in three ways, all tending to force open the contacts or bridging member of the circuit breaker. The design is such as to minimize or nullify all three of these factors. First, there is the largest of the three magnetic forces, that due to the return-current path in the bus bar to the rear of the circuit breaker. Its effect is minimized by one end of the bridging member being hinged (see Figure 4), so that 50 per cent of this force is expended at the hinge pin. The 50 per cent of the force at the contact or break end is expended, not against springs, but rather against the rigid members of the mechanism. The second component of magnetic force which is commonly encountered on bridging members of circuit breakers of this general configuration is that caused by the bridging member not forming one

straight conductor with the upper and lower conductors.[8,9] This component is minimized and controlled in the same manner as the first component and also is minimized further by the bridging member being closely in line with its terminal conductors. The third component of magnetic force tending to blow the contacts open is that due to the current converging to a small cross section and high density at points of contact. At any given point of contact this force will vary as the square of the current. This factor in the present circuit breaker arrangement is minimized by the current being divided into six contact paths (one for each of the six blades) and further into the multiplicity of line contacts at each embossed contact; the force at each detail contact will vary as the square of the current through it, but the sum of the squares of the individual currents is a value less than the square of the sum of the currents, which would be the case if the total current passed through a single contact. The effect is minimized further by the fact that the forces are in a direction 90 degrees to the main motion of the bridging member and further are more than counteracted by the cup-washer springs and by the magnetic forces of the parallel currents in each pair of blades tending to pull the blades together.

When the circuit breaker opens, the two side pairs of blades open first and transfer all of the current of one pole to the center pair which opens slightly later and in turn transfers the total current to be interrupted to the butt type of arcing contacts with tungsten-alloy arcing tips. The hinging of and flexible connection to this arcing contact are arranged so that the nonuniform magnetic field resulting holds these tips in contact until the motion of the circuit breaker and mechanism opens the contact. When the contact does open, the current is transferred to the deion arc chute for interruption. Once transferred the current is carried to the deion chute through a separate conductor for the purpose and no longer is carried by any of the circuit-breaker contacts. The general arrangement of the circuit-breaker and arc chute is shown in Figure 4.[10] Figure 5 is a typical oscillogram of an interruption.[10]

From the foregoing it is noted that the mechanism need only be large enough to close the circuit breaker against frictional forces and the forces of opening or accelerating springs. It is not required to deflect contact springs which (as commonly used in circuit breakers) are sufficiently strong to withstand directly the magnetic forces of short-circuit currents.

Appendix. Measurement of A-C Resistances at Low Frequencies in Heavy Conductors

In the case of commercial power frequencies the a-c resistance of heavy-current conductors, or the wattage of power resulting therefrom, normally is arrived at by calculation rather than by measurement. When the conductor is irregular in size and arrangement, or when return phases by proximity become factors, or when there is magnetic steel in the vicinity, calculations become tedious and often questionable. Frequently the conductors are so short that the voltage drop in their length is a matter of millivolts, even with several thousand amperes flowing, and normally the power factor through the conductor is very low. With these circumstances the problem does not lend itself to the use of the conventional wattmeter. Further complications arise from induced voltages in the potential circuits by reason of the proximity of the heavy-current circuits.

The method of measuring wattage loss developed in conjunction with high-current network protectors is based on the use of a bridge circuit wherein the voltage drop across the test specimen is balanced by a voltage made up of two components, both variable in magnitude, one component known to be inphase with the test current and the other known to be 90 degrees out of phase with the test current. See Figure 7. By calibration of the source of the inphase component the effective resistance of the specimen is determined.

The test circuit is shown in Figure 8 in diagram form. The source of test energy is a transformer of the required frequency capable of circulating several hundred amperes through the test specimen; the current value is not critical, nor is it necessary that it be constant. The test current from terminals *A–A* is circulated through a current transformer *C*, through the test specimen *B–B*, and through a section of concentric conductor *D* (shown in section), the latter being heavily shielded magnetically. All test circuits other than the source of heavy current are of the concentric shielded type. The secondary of the current transformer is connected to a potentiometer type of resistor having a double-contact type of slide *SH* and designed to have very low reactance and very low skin effect at the frequency used.[11] This potentiometer is the source of a voltage, adjustable in magnitude, which is closely inphase with the current in the primary of the current transformer, and hence is closely inphase with the *IR* component of the voltage drop through the test specimen. The position of the double-contact slide is calibrated in terms of the d-c resistance of the section of conductor which is included between the two contacts. When a balance is established (described later), the a-c resistance of the test specimen is known to be the d-c resistance of the potentiometer at the particular setting divided by the ratio of the current transformer. From the foregoing it is evident that

1. The potentiometer must have no appreciable skin effect.
2. The current transformer must have very little phase-angle error.
3. The ratio of the current transformer under load must be accurately known.

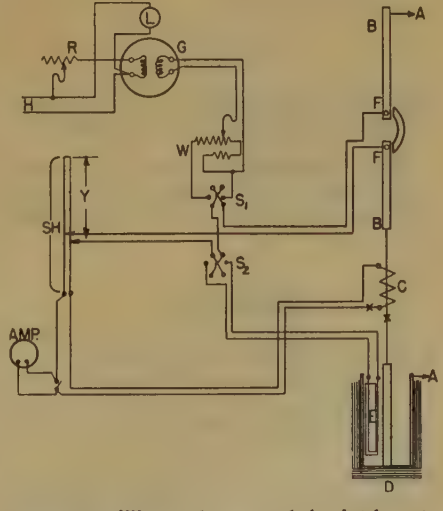


Figure 8. Wiring diagram of the bridge circuit used for measuring a-c resistance of large copper conductors

In order completely to balance the voltage drop appearing at *FF* across the test specimen it is necessary to obtain a voltage which is variable in magnitude and which is known to be accurately 90 degrees inphase position relative to the test current. This is obtained by induction from coil *E* which is mounted pivotally in the annular space between the inner and the outer conductors of the concentric conductor *D*. The 90-degree relation is known to obtain, because the magnetic flux in the annular space is of necessity inphase with the current in the central conductor, and the voltage induced in coil *E* leads this flux by 90 degrees. These phase-angle relations hold accurately for conditions of balance, for then there is no current flow in the galvanometer circuit which could upset the angular relations. The coil *E* is wound upon an entirely nonmetallic structure and is wound of very fine wire in order not to distort the phase-angle relation of voltage induced with respect to test current. The magnitude of voltage to secure a balance is obtained by adjusting the plane of coil *E* with respect to a plane described by a radius of the concentric conductor and the axis of the same conductor.

By means of shielded cable, voltages from *SH* and from *E* are connected in the same circuit with the voltage from test specimen *FF* and with vibration galvanometer *G*. Double-throw switches *S*1 and *S*2 permit of reversal of test connections and thereby eliminate some minute effects of stray fields upon the test specimen. Rheostat *W* controls the sensitivity of the vibration galvanometer. The galvanometer is tuned to the test frequency by means of the field rheostat *R*. The vibration type of galvanometer is preferred as an indicator of balance because of its fine sensitivity and because of its freedom from the effects of harmonics in the test current. *H* is the d-c source of field excitation for the galvanometer, and *W* is the lamp used for mirror and light-beam registration. The galvanometer is magnetically shielded.

The Solution of Transmission-Line Problems in the Case of Attenuating Transmission Line

GEORGE GLINSKI
ASSOCIATE AIEE

COAXIAL LINES with solid dielectric often are used as feeders. Such lines have appreciable attenuation (of the order of 1.5 decibels per 100 feet at 100 megacycles per second). Application of standing-wave method of finding the receiving-end impedance, as based on the assumption of lossless transmission line, would introduce an appreciable error, increasing with the length of the line used. The purpose of this paper is to show how by the application of the standard transmission-line theory the standing-wave method of measuring impedance can be extended to the case of transmission lines with attenuation, if the appropriate corrections are introduced. As seen from this point of view, the paper brings together and somewhat systematizes information available in the existing technical literature.[1,2]

Voltage Distribution Along the Line

The total complex voltage $\boldsymbol{V}$ at any given point of the transmission line is the sum of the incident complex voltage $\boldsymbol{V_i}$ and the reflected complex voltage $\boldsymbol{V_r}$. As we go along the attenuating transmission line from its receiving toward its sending end, the amplitude of the incident vector voltage increases. This is taken into account by the multiplication of the reference magnitude V_i by $e^{\alpha x}$. Hence, at the point x from the receiving end the incident voltage has the magnitude $V_i e^{\alpha x}$ (Figure 1). The factor α is called the attenuation constant of the line.

Also, if we go along the attenuating transmission line from the receiving toward the transmitting end, the phase of the incident complex voltage changes. This is again taken into account by the multiplication of the reference magnitude by $e^{j\beta x}$. Hence, at the point x from the receiving end the incident complex voltage is $V_i e^{\alpha x} e^{j\beta x}$ (Figure 2).

The factor β is called the phase constant of the line. As we see, the simultaneous attenuation and phase shift can be taken into account by multiplying the reference magnitude V_i by $e^{\gamma x}$ (Figure 3) where $\gamma = \alpha + j\beta$. The factor γ is called the propagation constant of the line. Hence the general expression of the incident voltage at point x from the receiving end of the line is $V_i e^{\gamma x}$.

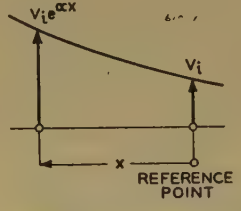


Figure 1 (left). Effect of attenuation

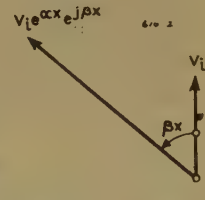


Figure 2 (right). Effect of phase shift

Similarly the reflected complex voltage at the point x from the receiving end of the line can be represented by $V_r e^{-\gamma x + j\psi_o}$, where V_r is the magnitude of reflected voltage at the receiving end of the line and ψ_o its phase difference in relation to the incident voltage at the receiving end (Figure 4).

Hence the total complex voltage at the point x from the receiving end of the line is

$$\boldsymbol{V} = \boldsymbol{V_i} + \boldsymbol{V_r} = V_i e^{\gamma x} + V_r e^{-\gamma x + j\psi_o} \qquad (1)$$

The ratio of the reflected complex voltage at the receiving end to the incident complex voltage at the same point is called the voltage complex reflection coefficient $\boldsymbol{K_R}$:

$$\boldsymbol{K_R} = K_R e^{j\psi_o} = \frac{V_r}{V_i} e^{j\psi_o} \qquad (2)$$

Introducing this into equation 1 we obtain

$$\boldsymbol{V} = V_i(e^{\gamma x} + \boldsymbol{K_R} e^{-\gamma x}) = V_i e^{\gamma x}(1 + K_R e^{j\psi_o} e^{-2\gamma x}) \qquad (3)$$

Voltage Distribution Near the Receiving End

Let us assume, as a first approximation, that, although the line is attenuating, the

Paper 46-10, recommended by the AIEE committee on communication for presentation at the AIEE winter convention, New York, N. Y., January 21–25, 1946. Manuscript submitted May 2, 1945; made available for printing November 9, 1945.

GEORGE GLINSKI is special studies engineer in the electronics division of the Northern Electric Company, Montreal, Quebec, Canada.

In the use of this test circuit the current is adjusted to any suitable value at the desired frequency, and balance is obtained by adjustment of *SH* and *E* until zero response is obtained on galvanometer *G*. Rough balance is made first with *W* large and then the sensitivity gradually increased as closer and closer balance is achieved. When balance is reached the a-c resistance of the test specimen is the d-c resistance of section *Y* of the potentiometer divided by the ratio of the current transformer.

Although the test arrangement described was used on appreciably heavier conductors, actual comparison with values calculated for a ten-inch length of seven-eighths-diameter copper bar was made as follows:

D-c resistance of ten-inch length, ohms	1.315×10^{-5}
Ratio of a-c–d-c resistance	1.0668
Calculated a-c resistance, ohms	1.40×10^{-5}
Measured a-c resistance, ohms	1.45×10^{-5}

With a galvanometer having an impedance better matched to the problem at hand even greater sensitivities should be obtainable.

References

1. SKIN EFFECT OF A RETURN CIRCUIT OF TWO ADJACENT STRAP CONDUCTORS, H. B. Dwight. *The Electric Journal*, volume 13, 1916, page 157.

2. SKIN EFFECT IN TUBULAR AND FLAT CONDUCTORS, H. B. Dwight. AIEE TRANSACTIONS, volume 37, 1918, part 2, pages 1379–1400.

3. SKIN EFFECT AND PROXIMITY EFFECT IN TUBULAR CONDUCTORS, H. B. Dwight. AIEE TRANSACTIONS, volume 41, 1922, pages 189–98.

4. FREE CONVECTION OF HEAT IN GASES AND LIQUIDS—II, Chester W. Rice. AIEE TRANSACTIONS, volume 43, 1924, page 131.

5. INTERNATIONAL CRITICAL TABLES, volume 5. Page 242.

6. HEAT TRANSMISSION, Wm. H. McAdams McGraw-Hill Book Company, Inc., 1933.

7. TEMPERATURE RISE OF ELECTRICAL APPARATUS AS AFFECTED BY RADIATION, G. W. Penney. AIEE TRANSACTIONS, volume 59, 1940, page 338.

8. CALCULATION OF MAGNETIC FORCE ON DISCONNECTING SWITCHES, H. B. Dwight. AIEE TRANSACTIONS, volume 39, 1920, part 2, pages 1337–50.

9. ELECTROMAGNETIC INDUCTION, W. F. Dunton. *The Electrician* (London, England), volume 105, November 28, 1930, page 681.

10. EXTINCTION OF AN A-C ARC, J. Slepian. AIEE TRANSACTIONS, volume 47, 1928, page 1398. THEORY OF THE DEION CIRCUIT BREAKER, J. Slepian. AIEE TRANSACTIONS, volume 48, 1929, page 523.

11. RESEARCH PAPER 133, United States Bureau of Standards.

attenuation of the line of a length of about $\lambda/2$ is negligible. Let us find the voltage distribution along the first half wave length of line from the receiving end. According to our assumption for this length $e^{\alpha x} \longrightarrow 1$ and from equation 3 we obtain

$$\boldsymbol{V} = V_i e^{j\beta x}(1 + K_R e^{j\psi_0} e^{-j2\beta x}) \qquad (4)$$

This is a well-known[3] equation of the voltage distribution along the lossless line. The expression in the brackets on the right side of the last equation is the vector sum of the unit vector ***OA*** (Figure 5a) drawn along the real axis and the vector $\boldsymbol{AB} = K_R e^{j(\psi_0 - 2\beta x)}$ drawn from the point (1.0) as shown on the same figure. The vector $\boldsymbol{K}_R e^{j(\psi_0 - 2\beta x)}$ rotates, with increasing x, in the clockwise direction and completes one revolution when $x = \lambda/2$ (since the phase constant $\beta = 2\pi/\lambda$).

To find the magnitude of this vector sum in the brackets for a given length of line x, we must rotate the vector $\boldsymbol{K}_R$ through the angle $2\beta x$ from its original position and in the clockwise direction. Let us assume that x is such that the vector takes the position ***AB*** in Figure 5a Then the segment OB gives us the magnitude of the vector sum. Moreover, this magnitude is proportional to the magnitude V of total complex voltage at the point x, of the line, since the factor $e^{j\beta x}$ before the brackets changes only the phase angle.

In Figure 5b the magnitude of the vector sum in the brackets versus the length x of the line is plotted. According to what has just been said, this also gives the distribution of the magnitudes of the total voltage along the line.

Voltage Distribution Far From the Receiving End

Let us suppose that the line under consideration is terminated in such a load that the receiving-end-voltage reflection coefficient and voltage distribution are as shown in Figures 5a and b.

Let us find the voltage distribution on the line starting at some distance $x_2 = n(\lambda/2)$ where $n \gg 1$. Since, according to our previous assumption, the attenuation though existing is constant along the considered $\lambda/2$ section of the line, the equation 3 yields

$$\boldsymbol{V} = V_i e^{\alpha x_2 + j\beta x}(1 + K_R e^{j\psi_0} e^{-2\alpha x_2} e^{-j2\beta x}) \qquad (5)$$

We shall use again the graphical construction. On the real axis (Figure 6a) we shall plot the unit vector ***OA***. Then, using point A as a center, we shall draw the circle of the radius $K_R e^{-2\alpha x_2}$. The

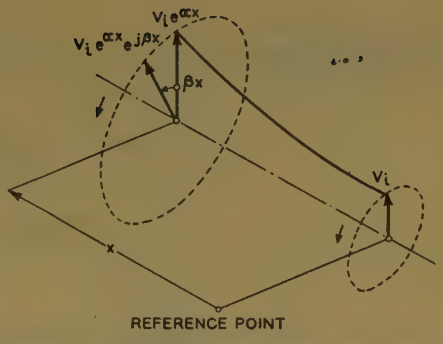


Figure 3. Effect of attenuation and phase shift

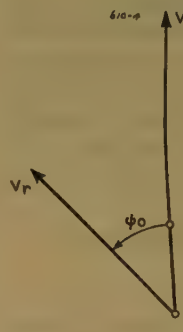


Figure 4. Incident and reflected voltages at the receiving end of the line

vector ***AC*** will be equal to $K_R e^{-2\alpha x_2} e^{j\psi_0}$ The magnitude of the vector ***OC*** is proportional to the magnitude of the total voltage at the point x_2 of the line. By rotating the vector ***AC*** in the clockwise direction and in the way just explained, we obtain again the voltage distribution on the section of line considered. This voltage distribution is plotted in Figure 6b

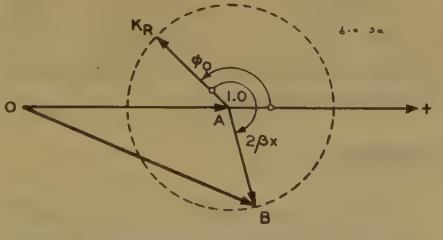


Figure 5a. Graphical construction for voltage distribution near receiving end

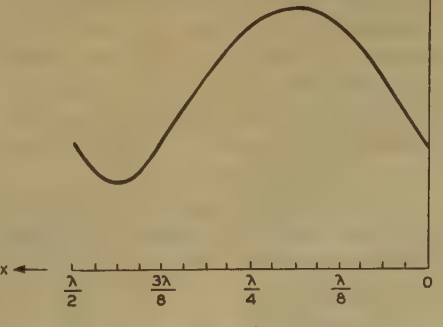


Figure 5b. Voltage distribution near receiving end

versus the distance along the line. Comparing the Figures 5b and 6b (when plotted to the same scale), we see that the voltage distribution farther from the receiving end of the line differs from that at the receiving end in two respects:

1. Farther from the receiving end the standing-wave ratio q, that is, the ratio of maximum to minimum voltage, decreases. In other words the attenuation of the line decreases the standing-wave ratio q.

2. The space average magnitude of the voltage is higher farther from the receiving end.

Attenuating Line as an Impedance-Measuring Device

For the voltage distribution starting at the point x_2 of the line (far from the receiving end), the maximum magnitude is

$$V_{max} = V_i e^{\alpha x_2}(1 + K_R e^{-2\alpha x_2}) \qquad (6)$$

and the minimum magnitude is

$$V_{min} = V_i e^{\alpha x_2}(1 - K_R e^{-2\alpha x_2}) \qquad (7)$$

Hence the standing-wave ratio in the vicinity of the point x_2 is

$$q_2 = \frac{V_{max}}{V_{min}} = \frac{1 + K_R e^{-2\alpha x_2}}{1 - K_R e^{-2\alpha x_2}} \qquad (8)$$

Solving the foregoing for K_R yields

$$K_R = e^{2\alpha x_2} \frac{q_2 - 1}{q_2 + 1} \qquad (9)$$

The last equation gives us the magnitude K_R of the receiving-end-voltage reflection coefficient. This can be used now to find from the known formula[3] the standing-wave ratio q_R near the receiving end of the line:

$$q_R = \frac{1 + K_R}{1 - K_R} \qquad (10)$$

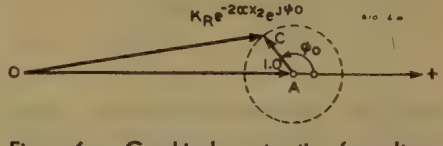


Figure 6a. Graphical construction for voltage distribution far from receiving end

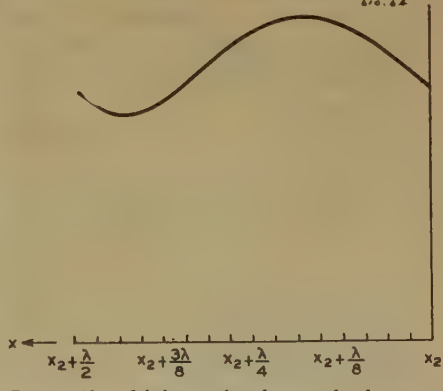


Figure 6b. Voltage distribution far from receiving end

This standing-wave ratio, together with relative shift of the voltage minimum in relation to the point x_2, can be used in the standard way[1] to find Z_R/Z_o from the appropriate chart (Z_R equals the receiving-end (load) impedance; Z_o equals the characteristic impedance of the line).

If we prefer the graphical construction, we can proceed as follows: Suppose that the vector ***OB*** in Figure 7a is proportional to the first minimum voltage encountered along the line when going from the point x_2 toward the sending end, whereas the vector ***OD*** is proportional to the maximum voltage. The circle with center A midway between the points B and D and going through these points is the locus of the reflected voltage near the point x_2 of the line. If the first minimum of the voltage is shifted a distance x_3 from the point x_2 (Figure 7b), then the corresponding angle is $2\beta x_3$. We shall rotate the vector ***AB*** counterclockwise through this angle $2\beta x_3$; this yields the vector $K_R e^{-2\alpha x_2} \times e^{j\psi_o}$ proportional to the reflected voltage at the point x_2 of the line. Its magnitude is given by $K_R e^{-2\alpha x_2}$. Let us suppose that the attenuation constant α and the distance x_2 are known, then the factor $e^{2\alpha x_2}$ can be calculated. The multiplication of the magnitude $K_R e^{-2\alpha x_2}$ by the factor $e^{2\alpha x_2}$ gives obviously K_R.

Let us draw the circle of the radius K_R with a point A as a center. Then the vector ***AF*** gives us the reflection coefficient at

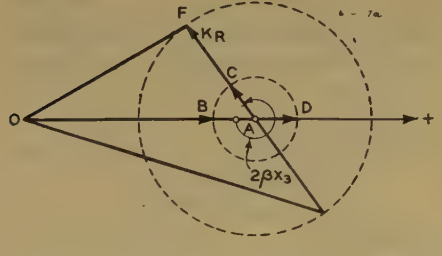


Figure 7a. Graphical construction for finding Z_R/Z_o from the voltage distribution curve far from receiving end

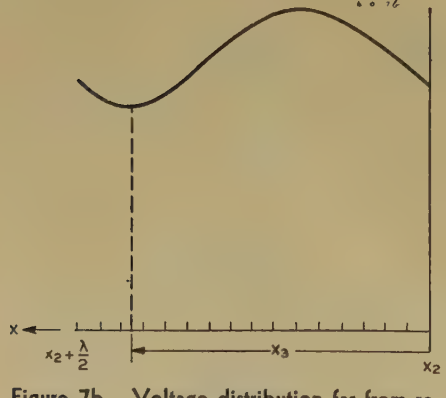
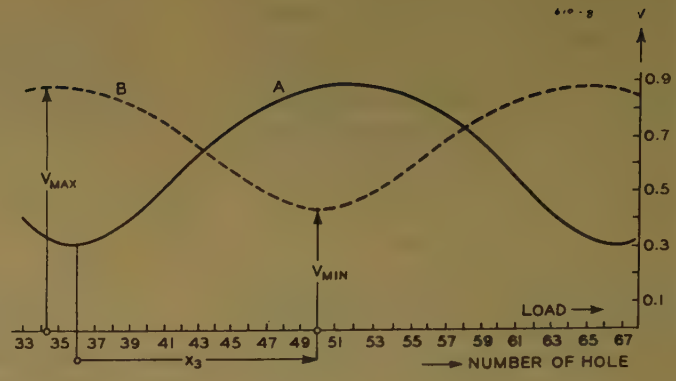


Figure 7b. Voltage distribution far from receiving end

Figure 8. Short-circuit and load voltage distributions



the receiving end of the line. As it is known, the ratio of segments OF and OG (the point G being diametrically opposite to the point F) gives us the magnitude of Z_R/Z_o. The phase of Z_R/Z_o is given by the angle GOF. This phase is positive (Z_R inductive), if ***OF*** leads ***OG***; it is negative (Z_R capacitive), if ***OF*** lags ***OG***.

Determination of Transmission-Line Attenuation

From the previous discussion it follows that the measurement of the receiving-end impedance Z_R requires among other things a knowledge of the attenuation constant α of the line.

The constant α can be determined readily from the measurement of the voltage distribution on the line when short-circuited at the receiving end. In this case, as we know, the magnitude K_R of the voltage reflection coefficient is equal to one and equation 9 yields

$$e^{2\alpha x_2} = \frac{q_{sh.c}+1}{q_{sh.c}-1} \qquad (11)$$

Note that $q_{sh.c}$ is measured in the vicinity of the point x_2 of the line, that is far from the receiving end.

Example

Let us assume that the coaxial measuring section of transmission line is connected through a long coaxial line to the unknown receiving-end impedance Z_R. When the line is short-circuited at the receiving end the measured voltage distribution is as shown by curve A in Figure 8. Curve B on the same figure represents the voltage distribution with the receiving-end impedance Z_R connected. The frequency of applied signal is 96.3 megacycles per second.

The total attenuation of the line can be found from the formula 11. The standing-wave ratio in the case of the short circuit is

$$q_{sh.c} = \frac{0.905}{0.32} = 2.83$$

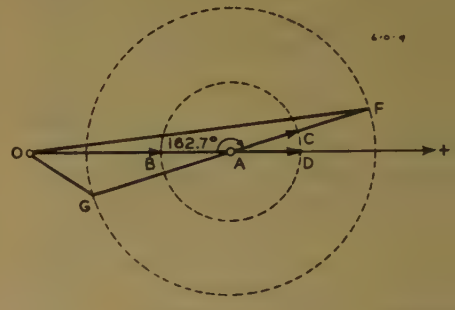


Figure 9. Graphical construction for finding Z_R/Z_o

Hence

$$e^{2\alpha x_2} = \frac{2.83+1}{2.83-1} = 2.1$$

That is, the total attenuation $\alpha x_2 = 0.37$ *nep* or 3.2 decibels.

In the case of the load connected the measured standing wave ratio is

$$q_2 = \frac{0.90}{0.445} = 2.02$$

The standing-wave ratio at the receiving end can be found from the known formula [1] using formula 9 as

$$q_R = \frac{1+2.1\,\dfrac{2.02-1}{2.02+1}}{1-2.1\,\dfrac{2.02-1}{2.02+1}} = 5.9$$

This example was chosen intentionally to show how important the correction of standing-wave ratio for the attenuation on the line between the measuring section and the receiving end can be.

The shift of the minimum when the line is loaded as referred to the minimum when the same line is short-circuited is $x_3 = 14$ holes, Figure 8, (Coaxial measuring section is provided with equidistant holes for the purpose of measuring voltage distribution. These holes are numbered and distances along the measuring section are measured conveniently in number of holes), or 0.226λ (since $\lambda = 64$ holes, as can be found from the curve B on Figure 8) toward the load. Hence the load is inductive.

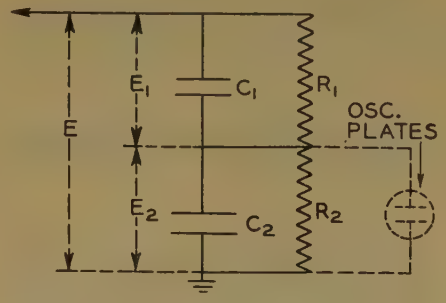
Electrical Measurements on Aircraft-Engine Ignition Circuits

WM. E. BERKEY
MEMBER AIEE

Synopsis: A method of measuring ignition voltages with a cathode-ray oscillograph is described. Magneto and spark-plug voltage oscillograms covering several consecutive firing pulses were taken on a complete aircraft magneto ignition system under several engine operating conditions. Oscillograms taken with spark plugs firing in air show differences when compared with engine tests. An improved electronic oscillograph has been developed which is well adapted for ignition measurements.

THE spark ignition system is recognized as the greatest single source of trouble in an aircraft engine.[1] New ignition problems have been created, and old ignition troubles intensified in modern engine developments. The ignition system on the high-power engines of today must function under higher output per cylinder, higher temperatures, greater numbers of firing sparks per second, higher altitude operation, and more stringent radio-interference requirements. The fact that large numbers of high-power aircraft engines are in operation today reflects great credit to the ignition engineers who have succeeded in solving their major problems.

A magneto ignition system generates and distributes a series of timed transient electric discharges. The magneto output voltage is created by a sudden disturbance in two coupled circuits each simply oscillatory, and, therefore, may be regarded as the resultant of two normal modes of different amplitudes, frequencies, and damping. A distributor alternately connects the different length spark-plug circuits with the magneto through a short air gap. The current which flows in the circuit then is complicated by the magneto characteristics, the variable circuit parameters, and the spark-dis-



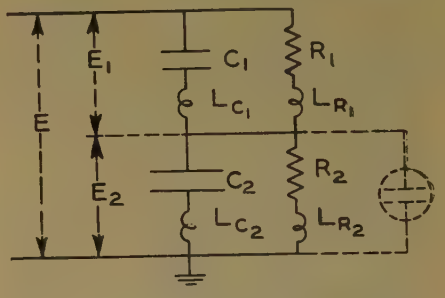
A—Simple resistor-capacitor divider

$$\frac{E_1}{E_2}=\frac{R_1}{R_2}=\frac{\frac{1}{\omega C_1}}{\frac{1}{\omega C_2}}=\frac{C_2}{C_1}$$

$$R_1C_1=R_2C_2$$

$$\frac{E}{E_2}=\frac{E_1+E_2}{E_2}=\frac{R_1+R_2}{R_2}=\frac{\frac{1}{C}+\frac{1}{C_2}}{\frac{1}{C_2}}=\frac{C_1+C_2}{C_1}$$

C_2 includes capacitance in plate circuit



B—Resistor-capacitor compensated divider

$$\frac{L_{R_1}}{R_1}=\frac{L_{R_2}}{R_2}$$

$$C_1L_{C_1}=C_2L_{C_2}$$

$$\frac{L_{C_1}}{R_1}=\frac{L_{C_2}}{R_2}$$

$$R_1C_1=R_2C_2$$

Figure 1. Parallel capacitor-resistor type voltage divider

Paper 46-14, recommended by the AIEE committee on air transportation for presentation at the AIEE winter convention, New York, N. Y., January 21–25, 1946. Manuscript submitted June 15, 1944; made available for printing November 21, 1945.

WM. E. BERKEY is research engineer in the research laboratories of the Westinghouse Electric Corporation, East Pittsburgh, Pa.

The engine tests described in this paper were made at the Pratt and Whitney Aircraft Division, United Aircraft Corporation plant, East Hartford, Conn. The co-operation of Val Cronstedt, executive engineer, E. K. von Mertens, project engineer, and the entire ignition group is gratefully acknowledged.

Using the transmission-line calculator,[4] we shall find that the resistive component R_R and reactive component X_R of the receiving end impedance Z_R are $R_R/Z_o=3.3$, $X_R/Z_o=2.9$.

The graphical construction for this case is shown in Figure 9. It consists of the following steps:

1. Draw OB proportional to V_{min} from Figure 8, curve B.
2. Draw OD proportional to V_{max} from Figure 8, curve B.
3. Draw the circle on BD as a diameter (point A is its center).
4. Translate the shift of the minimum x_3 into the angle $2\beta x_3$. In the case considered, since x_3 is shifted toward the load, the vector BA should be rotated clockwise. The angle of rotation is equal to $4\pi x_3/\lambda$. In the case considered it is 2.84 radians or 162.7 degrees.
5. The vector $\boldsymbol{AC}$ is proportional to $K_R e^{-2\alpha x_2} e^{j\psi_0}$.
6. Find $e^{2\alpha x_3}$ from formula 11.
7. Multiply the magnitude of vector AC by $e^{2\alpha x_3}$ and draw the circle of the radius K_R with point A as a center. The vector $\boldsymbol{AF}$ is proportional to the reflection coefficient $\boldsymbol{K}_R$ at the receiving end of the line.
8. The ratio of the segments OF/OG gives us the magnitude of Z_R/Z_o.
9. The angle GOF gives us phase of Z_R/Z_o

$$\frac{Z_R}{Z_o}=4.36$$

$$\angle\frac{Z_R}{Z_o}=42 \text{ degrees}$$

or

$$\frac{R_R}{Z_o}=3.22$$

$$\frac{X_R}{Z_o}=2.92$$

As we see, these figures agree fairly well with those obtained when using the transmission-line calculator.

Conclusion

As it is seen, the existence of attenuation in the transmission line does not change the method of determining the load impedance; with appropriate connection the same method can be used.

References

1. GRAPHICAL SOLUTION OF VOLTAGE AND CURRENT DISTRIBUTION AND IMPEDANCE OF TRANSMISSION LINES, R. C. Paine. *Proceedings* of the Institute of Radio Engineers, volume 32, 1944 number 11, pages 686–95.

2. AN ANALYSIS OF R-F TRANSMISSION LINES, G. B. Hoadley. *Communications*, volume 23, 1943, number 2, pages 22, 24–6, 28, 50, 52.

3. THE CONDUCTION OF HIGH-FREQUENCY OSCILLATORY ENERGY, H. O. Roosenstein. *Proceedings* of the Institute of Radio Engineers, volume 16, 1931, number 10, pages 1849–83.

4. TRANSMISSION-LINE CALCULATOR, P. H. Smith. *Electronics*, volume 12, January 1939, page 29.



Figure 2. Pratt and Whitney aircraft ignition test assembly

M—Magneto; *D*—Distributor; *P*—Plug mount

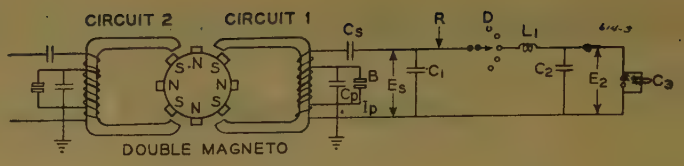


Figure 3. Magneto-ignition circuit constants

C_S = 2,000-micromicrofarad series capacitor
C_P = 0.35-microfarad primary capacitor
C_1 = 150-micromicrofarad capacitance of secondary to ground at distributor
C_2 = 100- to 300-micromicrofarad capacitance in harness and plug lead
C_3 = 35-micromicrofarad capacitance of spark plug
E_S = 25,000 volts maximum secondary open circuit volts
E_P = 85 volts maximum primary volts
L_P = 2.65 to 4.3 × 10 $^{-3}$ henrys primary inductance in coil
L_S = 30 to 42 henrys secondary inductance in coil
L_1 = 0.004 microhenry per centimeter in concentric cable (calculated)
I_P = six amperes crest
F_S = 2,000 approximate natural frequency with *D* open and *B* open
F_P = 6,000 approximate natural frequency with *D* open and *B* closed
F_1 = 10^7 cycles per second approximate frequency of $C_1L_1C_2$ (calculated)
R_S = 6,800 ohms
R_P = 0.25 ohms

charge characteristics in both the distributor and spark plug. Calculation of an ignition circuit is thus at present not possible. Measurements of voltage and current in an ignition system are not easy, because high voltages, high frequencies, and low total energies are involved. Ignition voltages of 15 kv commonly are encountered at the magneto. Ignition currents from frequency of firing to hundreds of megacycles are detected by wave meters. A magneto ignition spark may release only 50 millijoules in the spark gap.[2]

The object of this paper is to describe some recent measurements made on a modern aircraft-engine ignition system with the hope that further investigation will be stimulated.

Combined Capacitance-Resistance Voltage Divider

In an oscillographic study of ignition-circuit voltages it is necessary to reduce the ignition voltage to values suitable for the oscillograph deflection plates. The construction of a divider, which will not change the ignition voltage being measured and will reproduce faithfully the ignition wave on the film, constitutes a major problem. A noninductive resistance divider of ten megohms total resistance gave frequency distortion due to the oscillograph plate capacitance of 25 micromicrofarads. Capacitance dividers were found to be unsatisfactory for low-frequency measurements due to unequal leakage around the capacitors. In ignition circuits both high- and low-frequency voltages are known to be present; therefore, a combined capacitance-resistance divider was built.

The simple capacitance-resistance divider is sketched in Figure 1A. When the time constants for each divider step are made equal, the frequency of the voltage being measured has no effect upon the ratio of the divider if the lead inductance is neglected. The effect of lead

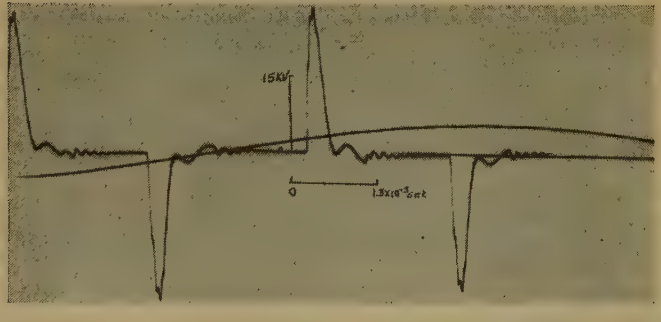




Figure 4. Open-circuit magneto voltages

A (left)—Open-circuit secondary voltage
B—Open-circuit secondary voltage with primary-circuit open

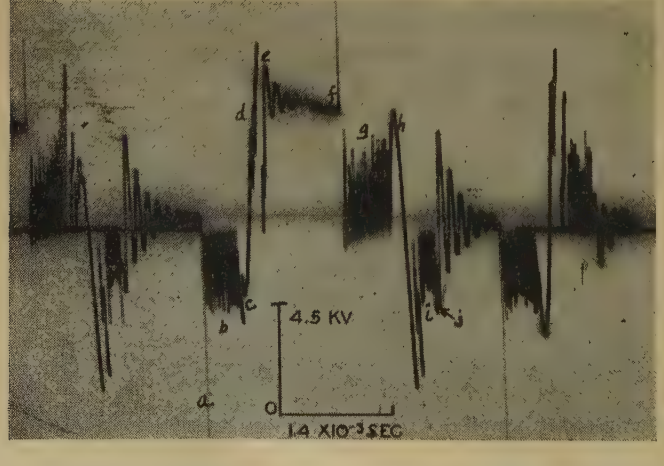
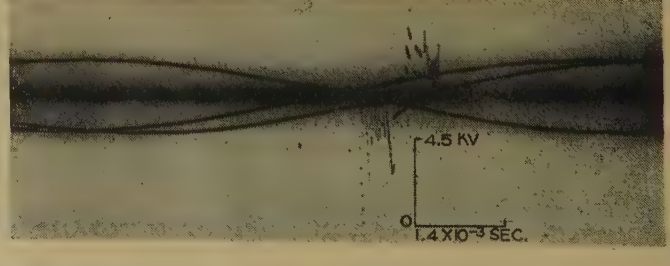


Figure 5. Distributor and plug voltage characteristics

A (left)—Distributor voltage to ground
B—Spark-plug voltage to ground



inductance is considered in the compensated divider of Figure 1B. With complete compensation it is possible to make a divider with constant ratio for direct current and high frequency.[3]

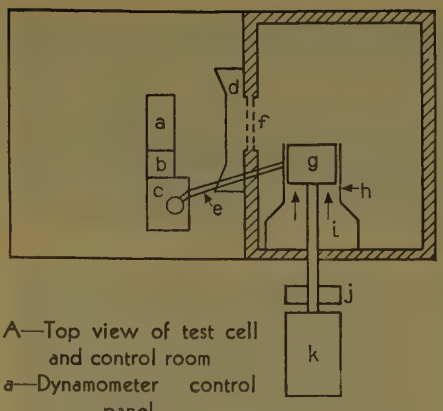
In the experimental investigation, the simple capacitance-resistance divider was found satisfactory. The constants of one divider were

$R_1 = 11.2 \times 10^6$ ohms $\quad C_1 = 25 \times 10^{-12} F$
$R_2 = 0.8 \times 10^6$ ohms $\quad C_2 = 350 \times 10^{-12} F$

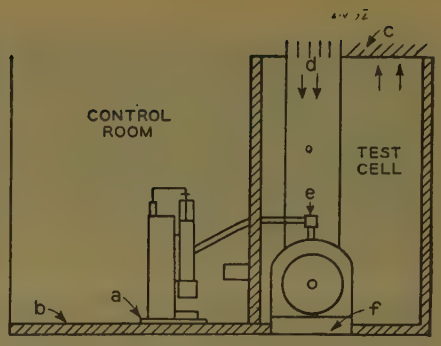
It is necessary to keep the stray ground capacitance of R_1C_1 step low and to locate the divider as closely as possible to the point of voltage measurement.

Ignition Assembly Tests

The ignition system investigated was that used on the Pratt and Whitney *R*-2800 18-cylinder engine. It consists of a double magneto, which generates simultaneous ignition pulses for two circuits of 18 plugs each through the two separated distributors. Initial tests were made with this ignition system mounted upon an engine nose section with plugs firing in air as shown in Figure 2. The standard magneto and distributor gears were driven by an electric motor mounted in the rear. The magneto was an eight-pole rotating-magnet type with two coils and breaker structures. The magneto rotor was geared to rotate at $1^1/_8$ times crankshaft speed. The breaker cam had 18 lobes ground for compensated timing and rotated at one-half crankshaft speed. A series capacitor of 2,000 micromicrofarads in the coil secondary, located in the magneto housing, enables the magneto to deliver more than 1,350 rpm×18= 24,300 firing discharges per minute through each circuit. The voltage divider was attached to a spare high-voltage terminal provided in the magneto housing. A schematic circuit of this ignition system is drawn in Figure 3. The circuit constants measured and calculated for this circuit are listed below the circuit diagram.



A—Top view of test cell and control room
a—Dynamometer control panel
b—High-voltage d-c rectifier
c—Oscillograph and control panel
d—Engine-control panel
e—Transmission line
f—Double window
g—Test engine
h—Shroud
i—Air blower
j—Water brake
k—Dynamometer



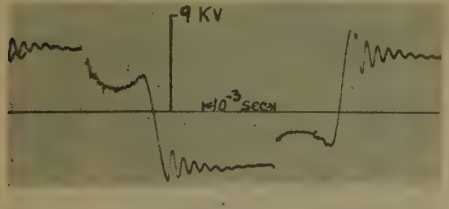
B—Side view of test cell and control room
a—Shock mount
b—Concrete floor
c—Roof vents
d—Air
e—Potentiometer
f—Bed plates

Figure 7. General layout for engine test

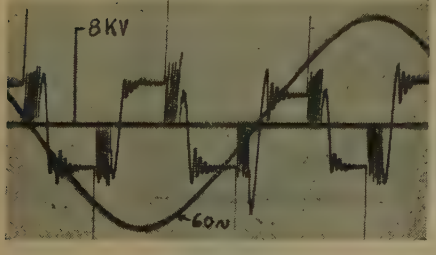
The rotating-film cathode-ray oscillograph[4] recorded the magneto and spark-plug voltage transients. The low-voltage side of the divider led directly to the deflection plates. The time scale was provided by rotation of the film. An exposure was made by unblocking the beam relay for a predetermined time with a voltage applied and removed by mechanical contactors.

The open-circuit voltage obtained on the magneto with the divider connected directly to the high-voltage side of the coil secondary is shown in Figure 4A. The open-circuit voltage rises to 28-kv crest with an initial rate of rise of about 400 volts per microsecond. The two frequency components of 2,000 and 6,000 cycles are visible in this oscillogram. Figure 4B shows the open-circuit voltage record obtained with the circuit breaker blocked open and the divider connected directly to the magneto.

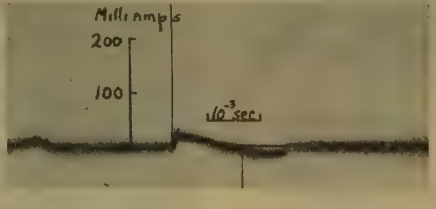
The distributor voltage to ground obtained with the complete ignition circuit, but with the spark plugs firing in air, is shown in Figure 5A. The voltage rise at point *a* occurs when the primary circuit breakers open and the value of this crest voltage is determined by the breakdown voltage of the distributor gaps. The electric charge stored in the magneto secondary circuit up to the distributor then is shared with the spark-plug circuit on a high-frequency transient. The resultant voltage is usually high enough to break down the spark plug and discharge the secondary on a high-frequency damped-current oscillation. The air gaps then partially recover some dielectric strength, and the secondary circuit rises again, but now the voltage required to break down the distributor gaps is less than the initial breakdown, probably due to residual ionization in the gap. This action is repeated many times at *b* until finally at *c* the generated secondary voltage is no longer able to break down the gaps. The voltage reverses as a result of the buildup of reverse flux through the magneto coil, and at *d* several breakdowns occur. At *e* the primary circuit breaker closes, and the distributor spark goes out, leaving the high-voltage lead with a trapped charge because of the secondary series capacitor.



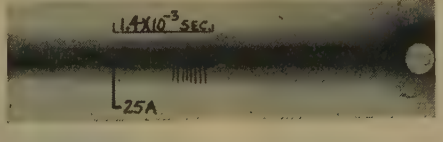
A—Type-*A* discharge voltage



B—Type-*B* discharge voltage



C—Type-*A* discharge current at plug; restrike on flux reversal



D—Type-*B* discharge current at plug

Figure 6. Voltage and current oscillograms of two types of ignition discharges

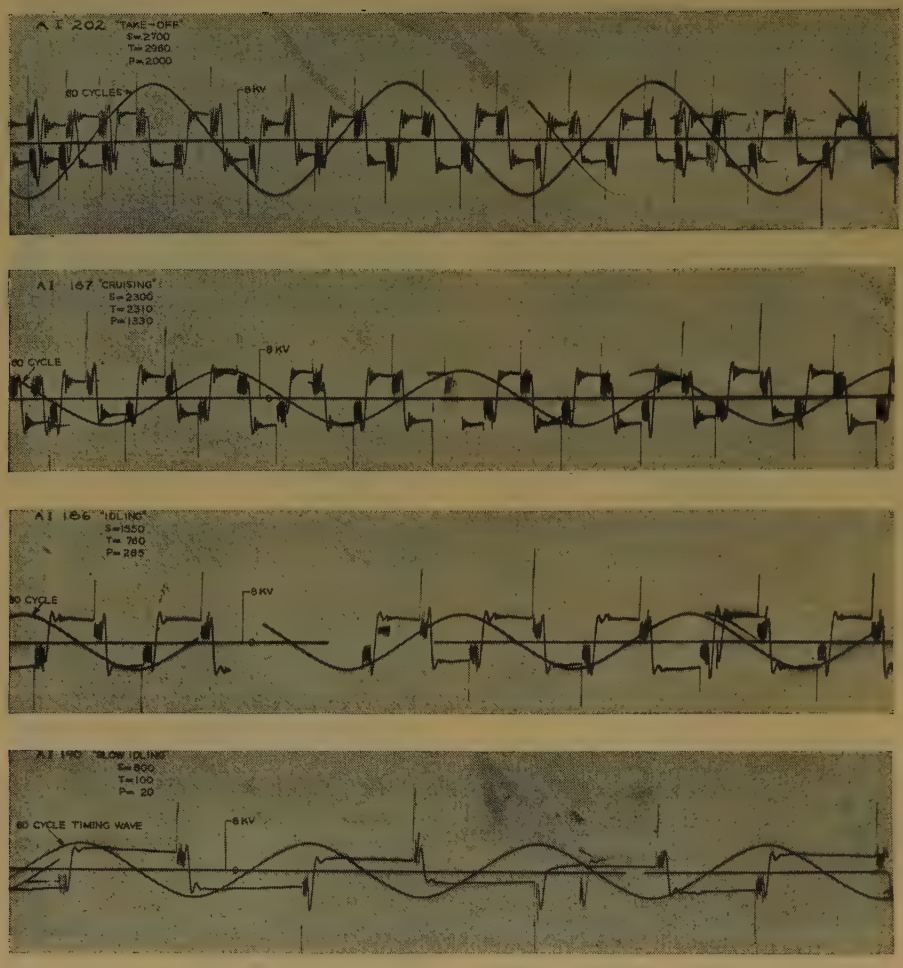
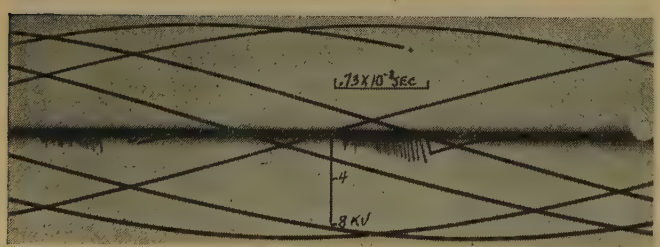


Figure 8. Magneto voltage with different engine-operation conditions

S—Speed, rpm
T—Indicated torque
P—Brake horsepower



A (above)—Typical oscillogram
AI-217 number-1 front plug
S—1,500 rpm idling

B—Effect of 15,000-ohm resistor in high-voltage lead at distributor
AI-268, number 1 rear plug take-off
S—2,700, *T*—2,900, *P*—2,000
R_S = 15,000 ohms at distributor



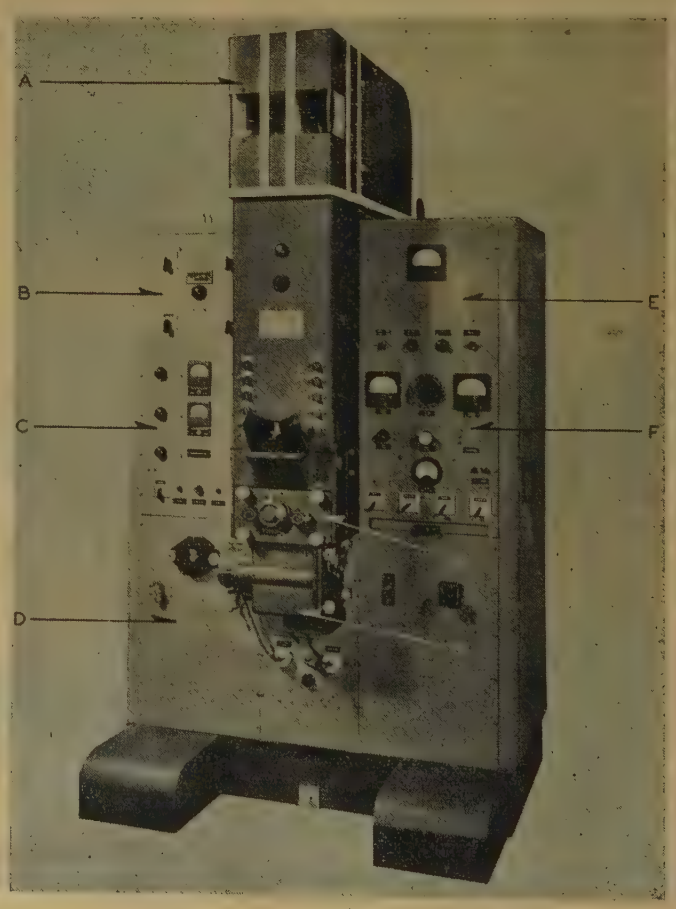
Figure 9. Spark-plug voltage records obtained during engine tests

Secondary voltage oscillations attributed to primary-current short-circuit transients are superimposed upon the residual direct voltage of this line section. At *f* the next pulse occurs on opposite polarity with the rotating distributor finger now adjacent to the next spark-plug circuit terminal. Repeated voltage rises and breakdown occur at *g*, the secondary magneto voltage reverses at *h*, and a second breakdown period is found at *i*, followed by the primary circuit breaker closing at *j*. This time the magneto–distributor lead was left at almost zero direct potential, although the a-c oscillations are relatively large.

An oscillogram of the spark-plug voltage is shown in Figure 5B. Two ignition discharges of opposite polarity taken on the same plug are recorded. Repeated charging- and breakdown-voltage varia-

Figure 10 (below). Westinghouse electronic oscillograph

A—Cathode housing, 50 kv, d-c maximum
B—Sweep and timing circuits
C—Focusing and bias control
D—Vacuum pumps
E—Calibrating and film-drum exposure control
F—Main control panel
G—Stationary film
H—Rotating film



tions are observed on the film. Also complicated reflection and extinction effects are indicated in this oscillogram.

Two types of magneto firing-voltage records were recorded on the assembled ignition system with spark plugs firing in air. Figures 6A and C illustrate typical voltage–time and current–time oscillograms associated with the steady type-A discharges. Figures 6B and D show oscillograms of voltage and current associated with the intermittent type-B discharges. Other investigators[5,6] have called these discharge types "inductive" and "capacitive" sparks. The steady sparks appear reddish and diffuse, whereas the intermittent sparks appear bright bluish and concentrated.

Ignition Tests on Engine

The layout of the test cell and control room is sketched in Figure 7. The test engine was loaded with a dynamometer and a water-wheel brake. A cathode-ray oscillograph was set up in the control room with a two-wire transmission line connecting the deflection plates to the voltage divider located over the engine. The length of the line was 12 feet. The test engine was operated under several fixed conditions, and records made of the magneto firing voltage and the spark-plug voltage to ground. In Figure 8 typical records of the magneto high-voltage lead voltage to ground are shown. A 60-cycle voltage was recorded to provide calibration of each oscillogram. An external mechanical relay used in these tests to trigger the beam frequently bounced to cause apparently unconnected short portions of the trace.

The intermittent-type discharge-voltage characteristic was found in all oscillograms taken with the ignition system firing the engine. The magneto firing-voltage records obtained do not differ greatly for different engine test conditions. No significant differences in the breakdown voltages are observed in Figure 8. The restriking voltages which follow the breakdown are observed to be higher at higher speeds and greater engine power output.

A spark-plug voltage record is reproduced in Figure 9A. In this record the initial breakdown is not visible due to the extremely fast rise and fall. When a 15,000-ohm carbon resistor was installed in the high-voltage lead at the distributor, the breakdown voltage was observed as shown in Figure 9B. In this record the initial breakdown of the spark plug is clearly visible. The resistor serves to decrease the rate of rise of voltage on the spark plug.

Electronic Oscillograph

Oscillograms described in this report were obtained with an oscillograph of older design. A newly designed cathode-ray oscillograph[7] with complete operating accessories is pictured in Figure 10. New features which make it particularly valuable for ignition studies are

1. Provision for either stationary or rotating film recording.
2. Photoelectric means for exposing the rotating film for exactly one revolution, independent of speed of film rotation.
3. Enclosed and shielded electric circuits in removable panels with safety features.
4. Sweep circuit selector switches which enable a quick setting of sweeps from one microsecond to 20,000 microseconds.

The different operating circuits are built into the cabinet on removable panel assemblies. The high d-c beam voltage is supplied by a transformer and rectifier tubes with capacitor filter all built into the main cabinet. The combination of high writing speed with either short- or long-time recording makes this a useful instrument for studying ignition circuits.

Conclusions

Ignition currents and voltages are measured with a cathode-ray oscillograph. Typical oscillograms are shown which explain the operation of an ignition system used on a high-power aircraft engine. The importance of complete radio shielding and adequate electrical insulation becomes apparent with increased knowledge of ignition voltages and currents. Future ignition studies will be facilitated with a newly developed high-voltage cathode-ray oscillograph.

References

1. Shortcomings of Mica Insulation for Aviation Spark Plugs, **Val Cronstedt.** Society of Automotive Engineers *Journal*, volume 46, 1940, page 223.

2. Method of Measuring Heat Energy of Ignition Sparks, **F. B. Silsbee, L. B. Loeb, E. I. Fonseca.** National Advisory Committee on Aeronautics Technical Report 56, page 175.

3. Frequenzunabhaengige Kapazitiv-Ohmsche Spannungsteiler für Messzwecke, **O. Zinke.** Elektrotechnische Zeitschrift (Berlin, Germany), volume 60, August 1939, pages 927–31.

4. Arc-Extinction Phenomena in High-Voltage Circuit Breakers Studied With a Cathode-Ray Oscillograph, **R. C. Van Sickle, W. E. Berkey.** AIEE Transactions, volume 52, 1933, pages 850–7.

5. Principles of Ignition (book), **J. D. Morgan.** Pitman and Sons, Ltd., London, England, 1942. Pages 1–2.

6. Some Factors Controlling the Development of Electrical Ignition of Aero Engines, **G. E. Bairsto.** Royal Aeronautical Society *Journal* (London, England), volume 44, number 350, 1940, pages 119–62.

7. Electronic Oscillograph—Time Microscope, **O. Ackermann, E. Beck.** *Westinghouse Engineer*, volume 4, November 1944, page 169.

Capacitor Stabilization of Arc-Welding Transformers

J. H. BLANKENBUEHLER
MEMBER AIEE

R. V. LESTER
NONMEMBER AIEE

SINCE THE PROCESS of metallic arc welding was discovered, some of this welding has been done with alternating current. The fact that a transformer, with no moving parts and its resultant simplicity, could be used always has made the use of alternating current for welding desirable. When only bare welding electrodes were available, it was necessary to have a welding transformer with the secondary voltage so high as to be dangerous to the operator. Even with this high open-circuit voltage, the arc with the bare electrode was so unstable that it was very difficult to maintain. Consequently, the transformer was never popular as a power source for welding until the bare welding electrodes had been replaced by the modern coated electrode.

Seven or eight years ago, the standard secondary voltage for welding transformers was approximately 110 volts. Improvements in the coatings of the electrodes used for a-c welding since have enabled us to reduce the standard open-circuit voltage of these welding transformers to between 70 and 80 volts. Some transformers which are expected to be used with a limited variety of electrodes have secondary voltages as low as 50 volts.

During this period of growth, the users of the a-c equipment for welding naturally have become aware of its advantages as a power source in comparison with the rotating machinery generally used as the d-c power source, but always have been somewhat dubious about the relative safety of the two systems. Experts in both types of welding can argue at great length on this subject, but experience seems to bear out the fact that lower open-circuit voltages must be used with the a-c systems if they are to have safety equivalent to the d-c system.

During these last few years, most of the companies manufacturing a-c welding transformers have supplied as an optional feature a no-load voltage-reducing apparatus consisting of the necessary contactors and relays to change the voltage at the electrode holder from the usual no-load value of 70 to 80 volts to a lower value of 25 to 35 volts. Of course there are those who properly might contend that even these voltages are not safe, and probably one must agree that the only safe voltage is zero.

One method of arriving at a desirable voltage for the a-c welding system would be to assume that the present-day d-c welding systems are safe, because very few accidents are reported on these d-c operations. Many of these d-c welding sets have maximum no-load voltages of 90 to 100 volts. It might be reasonable, therefore, to assume that any a-c system which had a peak voltage on the a-c sine wave no higher than the voltage of the d-c welding system would be equally safe. Using this reasoning, we can assume that a transformer with a secondary voltage of 70 volts is equivalent in safety to a d-c welder with a no-load voltage of 99 volts, and a transformer with 65 volts corresponds in safety to a d-c welder of 92 volts. This logic is not easily proved to be correct, and the writers do not contend that it is; but on the basis of this logic an attempt was made to develop a transformer for general purpose welding with a secondary voltage of 65 volts which would perform satisfactorily with all makes and varieties of a-c welding electrodes.

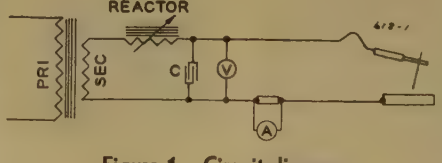


Figure 1. Circuit diagram

Investigation of the a-c welding arc with the magnetic and cathode-ray oscillograph indicated that capacitance in parallel with the arc produced a stabilizing effect because of the possible higher restriking voltages at current zero and because of the extra energy delivered to the arc immediately after restriking. Practical welding tests with capacitors connected as shown in Figure 1 bore out the results indicated by the oscillograph tests. It was then necessary to develop some means of determining the actual value of a particular amount of capacitance in reducing the required no-load voltage of the transformer. Our electrode development engineer, E. H. Turnock, suggested that welding tests with different transformer no-load voltages would indicate the degree of arc stability by the number of times the arc extinguished itself per electrode used. Tests therefore were conducted in which a number of electrodes were used at each of a number of transformer no-load voltages. The number of arc outages per electrode was recorded. These tests gave a reasonably smooth curve, indicating a definite relationship between the number of the arc outages and the transformer voltage. By extending these curves to the zero axis of the arc outage scale, one can assume that with this particular kind of electrode and welding setup, the voltage indicated by the curve to give no arc outages will be the minimum stable open-circuit voltage.

By running a series of such curves with various types and sizes of electrodes, one could determine the minimum open-circuit voltage which could be used for that variety of electrode. Similar curves also were taken with various values of capacitance connected across the transformer output terminals as shown in

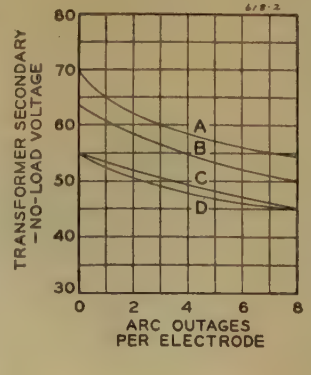
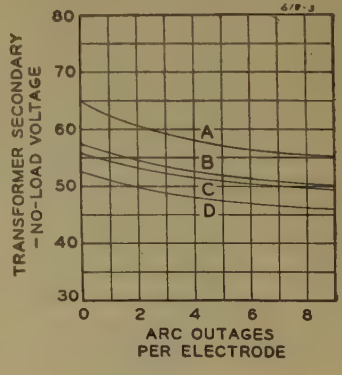


Figure 2(left). Stability curves for 3/16-by-18-inch class 6020 electrode

60 cycles, 180 amperes

Figure 3(right). Stability curves for 1/8-by-14-inch class 6011 electrode

60 cycles, 105 ampere



Figures 2 and 3: *A*—No capacitor, *B*—60 microfarad, *C*—120 mircofarad, *D*—180 microfarad

Paper 46-18, recommended by the AIEE committee on electric welding for presentation at the AIEE winter convention, New York, N. Y., January 21–25, 1946. Manuscript submitted November 13, 1945; made available for printing November 27, 1945.

J. H. BLANKENBUEHLER and R. V. LESTER are with the Westinghouse Electric Corporation, East Pittsburgh, Pa.

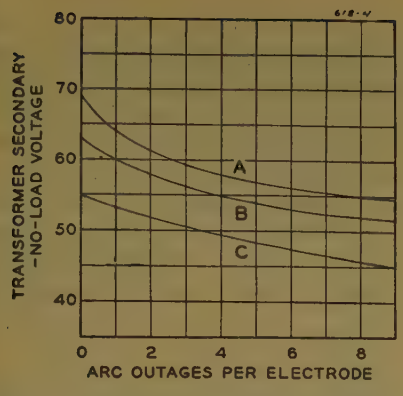


Figure 4. Stability curves showing effect of high lead reactance

$^3/_{16}$-by-18-inch class 6020 electrode, 60 cycles, 180 amperes

A—No capacitor
B—120-microfarad long leads
C—120-microfarad short leads

Figure 1. Figure 2 shows that for a given electrode, the addition of a 60-microfarad capacitor reduced the required secondary voltage from 70 volts to 63 volts, and a 120-microfarad capacitor allowed a reduction of the transformer secondary voltage to 55 volts. Figure 3 shows the results of similar tests on a different type of welding electrode.

another test, were arranged in coils on a steel floor. The latter arrangement proved to have twice as much reactance as the former, and the center curve in Figure 4 indicates the result of such a lead arrangement in reducing the stabilizing effect of the capacitor. This combination of 200-foot leads in coils gave a higher lead reactance than ever has been reported in actual practice, and this is considered to be an extreme condition.

In planning a line of welding transformers using this method of stabilization, the designer must compare the additional cost of the capacitor and its mounting with the reduced size of the transformer itself as well as the more abstract, but nevertheless desirable, improvement in safety. He also must allow sufficient margin in the use of the curves obtained by such tests to care for a reasonable length of welding leads and for a low primary voltage. The amount of margin included to care for these points is empirical and must be based on the designer's experience with these factors. One could assume, however, that a 120-microfarad capacitor and 65-volt transformer would give a reasonable margin of stability as indicated by the afore-mentioned curves.

Figure 5 shows a typical oscillograph record of the welding current and arc voltage with such a transformer–capacitor combination. Figure 6 shows a similar record without the capacitor. Visual observation of the cathode-ray oscillograph screen during welding with this capacitor stabilization indicated that the capacitor gave energy to the arc not only at the current zero point, but also occasionally within the half cycle of current flow when some arc disturbance seemed to require such energy.

The capacitor during any half cycle is charged with a certain amount of energy. When the voltage drops to zero, the capacitor tends to discharge. Figure 1 indicates that there are two possible paths for discharge of this stored energy. One of these paths is through the secondary winding of the welding transformer in series with the adjustable reactor. This combination offers a very high impedance in the form of reactance to the discharge of the capacitor energy. The other possible path is through the welding arc which is presumably an air gap at the time of current zero and therefore also offers high impedance in the form of resistance to the discharge of the capacitor. This causes the potential of the capacitor to build up very rapidly until it reaches a value that will break down the air gap. This reestablishes the welding arc at a lower transformer secondary voltage than would be the case without the high initial potential of the capacitor discharge. As current flows across the arc, the capacitor discharges. If the arc opens, the capacitor potential rises again, and the arc is re-

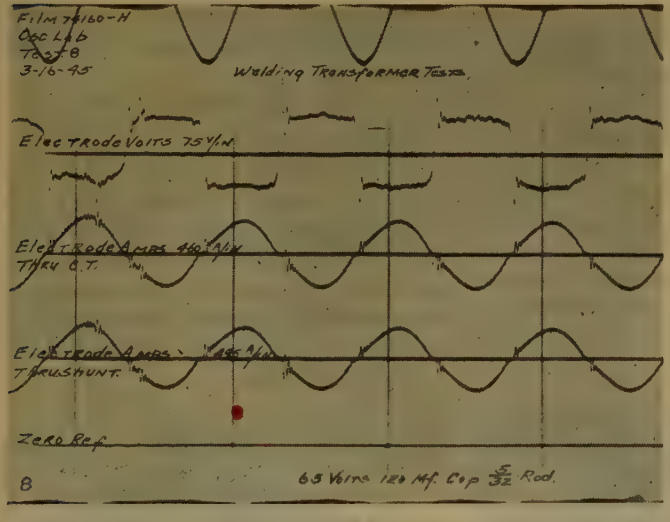


Figure 5 (left). Oscillogram of welding current and arc voltage with capacitor stabilization

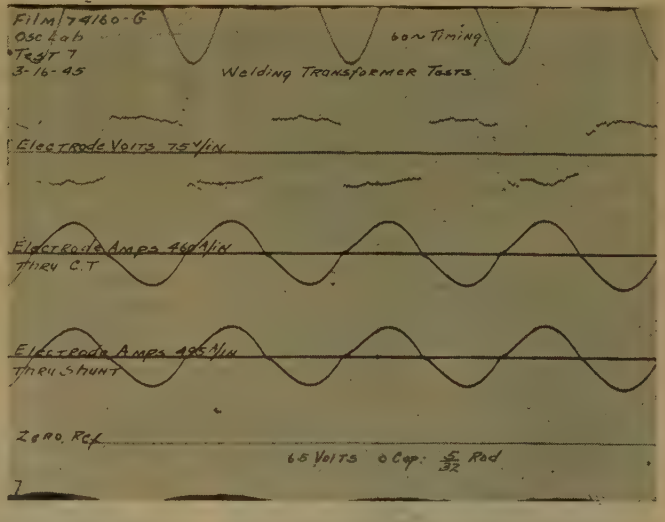


Figure 6. Oscillogram of welding current and arc voltage without capacitor stabilization

It was expected that the long leads sometimes used for welding would introduce a considerable reactance in the welding circuit between the arc and the capacitor and reduce the effectiveness of the capacitor as a stabilizer. In order properly to determine the effect of such leads, tests were conducted with the same transformer and capacitor arrangement with 200 feet of single conductor welding cable from each terminal to the welding position. These 200-foot leads were in one test laid out on a steel floor and, in

ignited. Figure 5 shows that the discharge of the capacitor is oscillatory and shows that this discharge may occur at other times than the zero current point.

The net result is that a stable welding arc can be maintained at a lower transformer secondary open-circuit voltage with a capacitor across the arc than without the capacitor. It is the authors' opinion that capacitor stabilization can be used economically to improve simultaneously the performance and safety of welding transformers.

Shutdown Versus Hot-Spot Temperatures in Polyphase Induction Motors

C. P. POTTER
FELLOW AIEE

A. E. FROHARDT
ASSOCIATE AIEE

THE "Test Code for Polyphase Induction Machines," AIEE Standard 500, paragraphs 50 to 58 inclusive, contains complete instructions for making temperature tests and reads in part as follows:

"The temperatures indicated by the thermometers placed on the motor at the start of the test usually rise when the motor is stopped: These values . . . . must be recorded. . . . . The highest temperature . . . . recorded will be taken as the actual temperature attained during the test."

The test code, therefore, requires that the temperature rise of a motor taken either while running, or at any time after shutdown, must not exceed the value stamped on the nameplate.

Readings are taken after shutdown in order to disclose abnormal temperatures which may not be detected by thermometers on the windings or core or by the resistance method. There seems to be no doubt that shutdown readings are desirable and necessary, but there may be some doubt whether the shutdown temperatures always should be restricted to the same values as the running temperatures. It is the writers' purpose to report the results of certain tests which were made to investigate this point and to recommend desirable changes in the test code and in ASA Standards.

Paper 46-58, recommended by the AIEE committee on electric machinery for presentation at the AIEE winter convention, New York, N. Y., January 21–25, 1946. Manuscript submitted October 15, 1945; made available for printing December 4, 1945.

C. P. Potter and A. E. Frohardt are with the Wagner Electric Corporation, St. Louis, Mo.

Scope of Tests

Temperature tests were made at various loads and frequencies on a motor having a protected frame; with openings cut in the frame to make it of the open type; and with very large openings giving practically unrestricted ventilation. Tests also were made with most of the openings closed to imitate a totally enclosed machine. Several rotors were tested having different resistances and load losses. The temperature rise of the stator windings was measured by three methods:

1. Surface thermocouples on the hottest accessible part of the winding.
2. Resistance.
3. Embedded thermocouples (using enough to locate the hot spot).

Description of Motor Tested

The motor tested was a 50-horsepower 405-frame 1,750-rpm 3-phase 60-cycle 440-volt machine having a semienclosed slot stator wound with heavy formvar covered round wire. The windings were of the double-layer diamond type, and the free ends were completely taped. The assembled windings were given two dipped and baked coats of varnish. There were no ventilating ducts in either the stator or rotor, and the various rotors tested all were of cast aluminum construction. Figure 1 shows the motor as originally built; Figure 2 as altered to make it of the open type; Figure 3 as altered to have practically unrestricted ventilation.

Location of Temperature Indicators

Sixteen thermocouples were located inside of the windings as shown in Figure 4. Thermocouples 17, 18, 19, and 20 were silk taped inside the loops of the coils just inside the tape which covered the free ends. Thermocouples 6, 8, 10, 12, 14, and 16 were silk taped to the coils inside the slot next to the 0.025-inch insulation separating the winding from the wooden wedge. Thermocouples 5, 7, 9, 11, 13, and 15 were silk taped to coil sides which lie in the bottom of the slot, just below the 0.060-inch insulation separating the coil sides. Thermocouples 1, 2, 3, 4, 21, and 22 were on the outside of the tape on the free ends, embedded in crevices in the windings, and covered with a small amount of sealing compound. Thermocouples 0, 23, and 24 were located on the outside surface of the stator core and were covered with a small amount of sealing compound.

Test Procedure

Several temperature tests were made with various conditions of load, distribution of losses, types of enclosure, and so forth, and each run was continued until the temperatures became constant. Readings of all thermocouples were taken while



Figure 1. Protected type squirrel-cage motor



Figure 2. Normal open type squirrel-cage motor

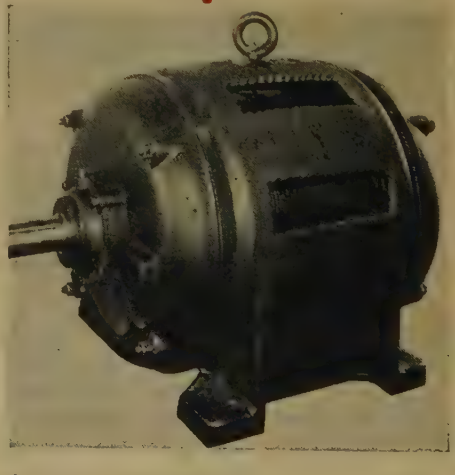


Figure 3. Exaggerated open type squirrel-cage motor

the motor was running. Readings of all thermocouples, resistance, and rotor temperatures were taken at frequent intervals after the motor was shut down to determine how the heat was redistributed. These readings were continued until well after all of them had reached their maximum.

Results

Fifteen sets of observations were made to determine the behavior of the temperatures of various parts after shutdown, and five of them are plotted in Figures 5, 6, 7, 8, and 9. The conditions of test are given in Table I.

These graphs show the behavior of the temperatures after shutdown at the hottest part of the core and the copper available to surface thermocouples, the hot spot as located by embedded thermocouple, and the rotor. The temperature rise by resistance also is plotted.

Table I. Test Conditions

Figure	Frame	Rotor
5	Totally enclosed	Low resistance
6	Protected	High resistance
7	Protected	Low resistance
8	Normal open	Low resistance
9	Exaggerated open	Low resistance

Table II. Hot-Spot and Maximum Shutdown Temperatures

Figure	Frame	Temperature Rise		Shutdown in Per Cent of Hot-Spot Temperature Rise*
		Shutdown	Hot Spot	
5	Totally enclosed	50	50.6	98.8
6	Protected	61.9	69.7	88.8
7	Protected	47.5	54.5	87.2
8	Normal open	39.0	46.4	84.0
9	Exaggerated open	38.5	48.6	79.2

* The shutdown figures are the maximum values taken by thermocouples located on the hottest part of the windings or core accessible to thermocouples.

Table III. Temperature Data for Open-Type A-C Motors

Horsepower	Table	Number of Tests	Shutdown in Per Cent of Hot-Spot Temperature Rise*
Integral	II	5	88 to 91
		1	77
Integral	IV	4	91.1 to 95.5
Fractional	I	2	92 to 95
Fractional	II	10	86.5 to 95.3
Fractional	IV	8	89 to 98
Fractional	VI	6	94 to 97
Fractional	VII	16	92 to 102

* The shutdown figures are the maximum values taken by thermocouples located on the hottest part of the windings or core accessible to thermocouples.

The hot-spot temperatures and maximum shutdown temperatures taken from these graphs are given in Table II.

Two papers published in 1945[1,2] contain data taken from temperature tests made by ten different observers, and the

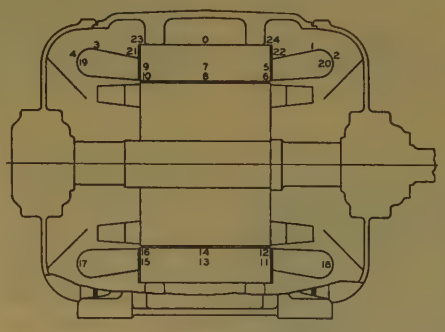


Figure 4. Location of thermocouples

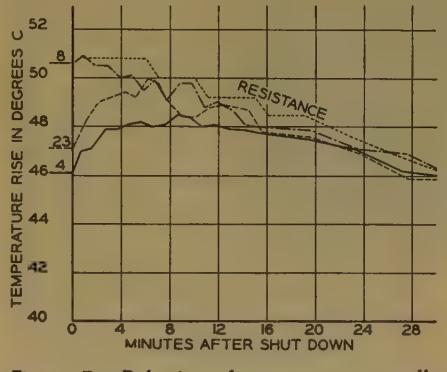


Figure 5. Behavior of temperatures, totally enclosed squirrel-cage motor

Line 8—Hot spot
Line 23—Core
Line 4—Winding surface

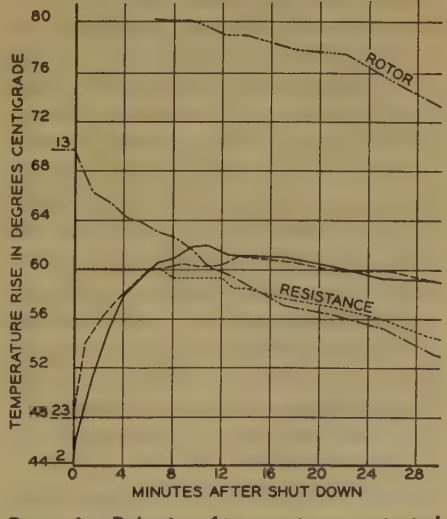


Figure 6. Behavior of temperatures, protected type squirrel-cage motor

Line 13—Hot spot
Line 23—Core
Line 2—Winding surface

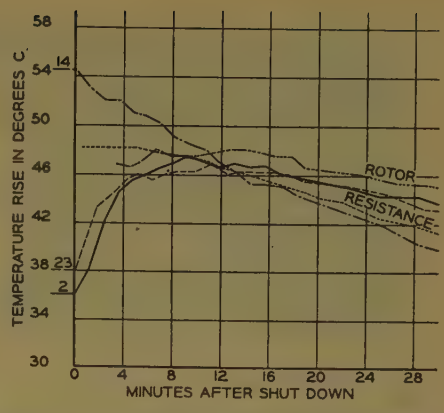


Figure 7. Behavior of temperatures, protected type squirrel-cage motor

Line 14—Hot spot
Line 23—Core
Line 2—Winding surface

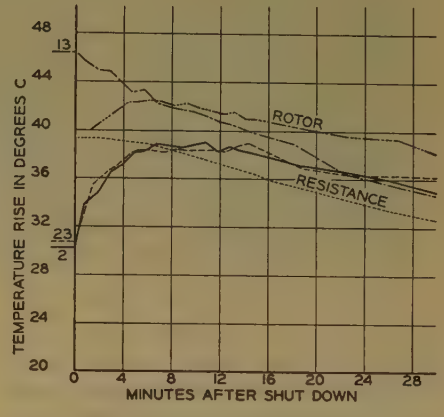


Figure 8. Behavior of temperatures, normal open type squirrel-cage motor

Line 13—Hot spot
Line 23—Core
Line 2—Winding surface

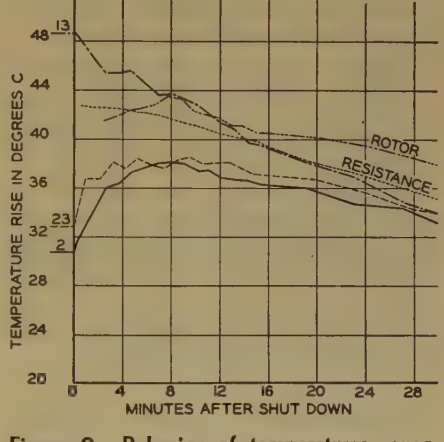


Figure 9. Behavior of temperatures, exaggerated open type squirrel-cage motor

Line 13—Hot spot
Line 23—Core
Line 2—Winding surface

Pressure-Arc-Interruption Circuit Breakers for 400-Cycle Aircraft Electric-Power System

B. O. AUSTIN
MEMBER AIEE

A THOROUGHLY TESTED lightweight circuit breaker for the 208Y–120-volt 3-phase 400-cycle a-c system for large aircraft is now a reality. The circuit breaker is electrically operated, remotely controlled, with latched-in main contacts. The design is suitable for paralleling generators and busses, circuit interruption, manual or automatic synchronization, and interlocks are provided for use in various control circuits. Operating solenoids are designed for low current requirements and for wide ranges of voltages and ambient temperatures. Size and weight have been kept to a minimum.

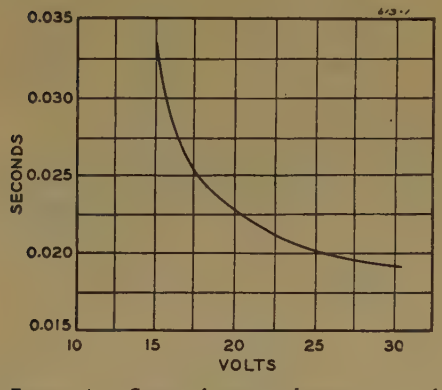


Figure 1. Curve showing closing time of 400-cycle 208–120-volt 120-ampere aircraft circuit breaker at various applied voltages

General Considerations

The Army Air Forces has become very much interested in a high-voltage high-frequency 3-phase a-c system for large aircraft. Reasons for the use of such a system in very large aircraft are many and varied and have been covered thoroughly elsewhere. ("Why Tomorrow's Planes Will Have A-C Systems," T. B. Holliday. *Electrical Manufacturing*, volume 32, July 1943, page 88.)

Paper 46-13, recommended by the AIEE committee on air transportation for presentation at the AIEE winter convention, New York, N. Y., January 21–25, 1946. Manuscript submitted November 8, 1945; made available for printing November 27, 1945.

B. O. AUSTIN is section engineer, aviation control, Westinghouse Electric Corporation, Lima, Ohio.

Circuit breakers for this system must perform under extreme variations in environment. Satisfactory performance has been proved in altitude chambers up to and including 55,000 feet, the limitations being in test equipment and not in the circuit breaker. It operates satisfactorily from −70 degrees centigrade to +60 degrees centigrade. The circuit breaker continues to function properly after being subjected to a relative humidity of 95 to 100 per cent at a temperature of approximately +40 degrees centigrade for a period of 30 days. Vibration encountered in aircraft does not affect the operation of the circuit breaker. One vibration test passed by this circuit breaker consisted of subjection to vibration for a period of more than three hours in each of the three planes of operation; the vibration consists of a simple harmonic motion having a total excursion of 1/16 inch and a frequency varied uniformly between 10 and 55 cycles per second. The circuit breaker

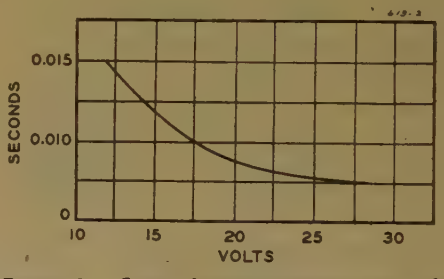


Figure 2. Curve showing opening time of 400-cycle 208–120-volt 120-ampere aircraft circuit breaker at various applied voltages

Table IV. Temperature Data on Plain Enclosed Type A-C Motors

Horsepower	Table	Number of Tests	Shutdown in Per Cent of Hot-Spot Temperature Rise*
Integral	I	2	93 to 95
Integral	II	3	95 to 98
Integral	IV	5	92.3 to 95.9
Fractional	I	2	92 to 98.5
Fractional	III	8	91.2 to 98.2
Fractional	IV	8	95 to 100
Fractional	VI	6	95 to 98
Fractional	VII	8	96 to 101

* The shutdown figures are the maximum values taken by thermocouples located on the hottest part of the windings or core accessible to thermocouples.

tests on the a-c motors may be summarized as in Tables III and IV.

Conclusions

From these tests it may be concluded that the relation between hot-spot temperature rise and the temperature rise after shutdown (taken by thermocouples which are located on the hottest part of the windings or core accessible to thermocouples) is a function of the motor ventilation. In the case of a totally enclosed motor the hot-spot temperature rise and the temperature rise after shutdown are almost equal. In the case of a motor which has a minimum amount of enclosure the ratio between the temperature rise after shutdown and the hot spot is 0.792, or when the hot-spot temperature rise is 50 degrees centigrade, the temperature rise after shutdown is 39.6 degrees centigrade. The "Test Code for Polyphase Induction Machines" was written prior to 1934 and probably was based on experience with motors having a minimum amount of enclosure and unrestricted ventilation. Squirrel-cage motors as built today are fairly well protected, and it would seem perfectly fair to conclude that the shutdown temperature rise in these motors is about 90 per cent of the hot-spot temperature rise, which would allow a shutdown temperature rise of 45 degrees centigrade instead of the 40 degrees centigrade figure now required.

Recommendations

In view of the fact that the trend is toward protected motors, it is recommended that the "Test Code for Polyphase Induction Machines AIEE 500" and the "American Standard Rotating Electrical Machinery C-50" be modified to allow a temperature rise after shutdown of 45 degrees centigrade on protected type motors having a nameplate temperature rating of 40 degrees centigrade.

References

1. INVESTIGATION OF HOT-SPOT TEMPERATURES IN INTEGRAL-HORSEPOWER MOTORS, L. E. Hildebrand, B. M. Cain, F. D. Phillips, W. R. Hough, J. G. Rosswog, C. P. Potter. AIEE TRANSACTIONS, volume 64, 1945, March section, pages 124–8.

2. INVESTIGATION OF HOT-SPOT TEMPERATURES IN FRACTIONAL-HORSEPOWER MOTORS, L. H. Hirsch, R. F. Munier, M. L. Schmidt, L. W. Wightman, F. S. Himebrook, T. C. Lloyd, O. G. Coffman, C. P. Potter. AIEE TRANSACTIONS, volume 64, 1945, March section, pages 128–36.

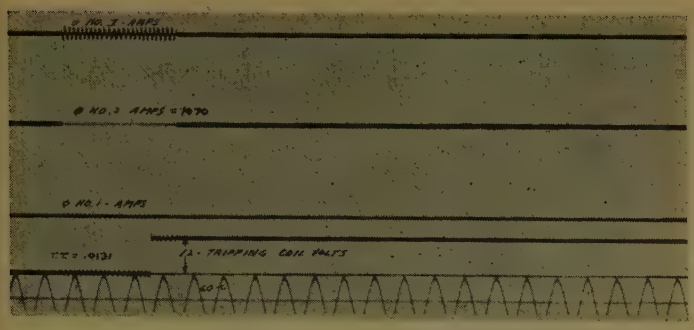


Figure 3. Oscillogram of a short circuit to neutral of a 3-phase system showing interrupting test phase number 2 at 400 cycles, 208 volts, pressure and temperature equivalent to 55,000-feet altitude (—40 degrees centigrade)



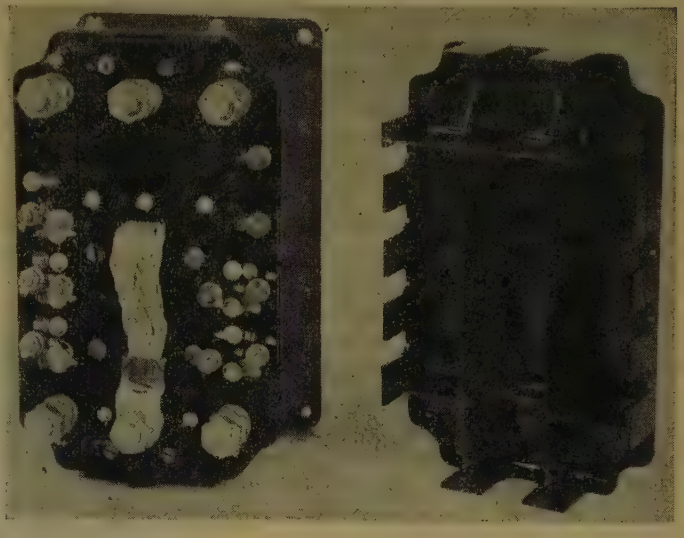
withstood a sand-laden air stream test for a period of five hours.

Obviously the most important single function a circuit breaker must perform is satisfactory interruption of current under all conditions of operation. High voltages at high altitudes are more difficult to handle when arc rupturing is involved. This is due to the decreased atmospheric pressure surrounding the arc when it is established. An effective method of controlling this difficulty is to design arc interrupters which are not subject to altitude conditions.

Figure 4(upperright) View of complete 208Y–120-volt 120-ampere 3-phase 400-cycle remote electrically operated aircraft a-c circuit breaker

Figure 5. View of circuit breaker showing terminal cover removed

Note straps for changing interlock combinations at the control terminals; also note that the main leads enter at one end and leave at the opposite end



Pressurized Arc Interruption

The basic design problem in producing such a circuit breaker was the devising of a suitable structure which would deionize effectively the arc gases and thus interrupt high current and high voltages at altitude without damage. Several well-known means commonly are employed to cool and deionize the gases of the arc column, thereby producing an instability of the arc which results in its disappearance. They are

1. Lengthening of the arc column.
2. Air or gas blasts.
3. Surface deionization.
4. High gas pressure or vacuum.
5. Fluid action.
6. Multiple arc gaps.

One or more of these principles is employed in all circuit breakers.

This circuit breaker uses high gas pressure, surface deionization, and multiple arc gaps. The design is such that the circuit breaker has several operating advantages. With a self-pressurized arcing chamber the circuit breaker is independent of altitude conditions. Confinement of the arc to the self-pressurized chambers eliminates exposed flame which may contribute to fire. The simplicity of the arc-rupturing mechanism and the chambers makes possible a compact and light structure. Each of the 3-phase circuits are opened and closed by actuating the contact bridges located in the arc chambers. Each bridge bar is equipped with contacts which engage or disengage two stationary contacts. In this manner double or multiple air gaps are provided. Pressurizing the arc to extinguish it quickly also makes possible having the contact mechanism operate through a short distance, thereby making possible higher magnetic forces in a small lightweight closing magnet and high opening speed.

Arcing compartments of the circuit breaker are designed with a minimum of volumetric space. In other words the mass of the moving and stationary contacts occupies more than 50 per cent of the volume of arcing compartments. The side walls and contact parts also cool the arc, aiding in its disappearance. The circuit is broken rapidly as shown in Figure 3. Pressure which is built up in the semi-sealed-off compartments is generated by the arc, and this pressure is adequate to extinguish the arc at 55,000 feet or higher. It has not been found necessary to seal hermetically the arc compartment, and the pressure disappears fairly rapidly.

Construction

The contact mechanism is of the simple bridge type having two breaks per phase. Contact design is similar to that used on thousands of d-c contactors and has been tested thoroughly in aircraft service. Contact materials used are of the sintered type, using a mixture of silver and cadmium oxide which resist high vaporization thus limiting support to the continuity of the arc. Contact life exceeds 5,000 cycles of operation under rated load at 75 per cent power factor.

The latched mechanism used to hold the circuit breaker closed has the advantage of keeping the circuit energized, even though there is a temporary or permanent failure of the direct current which is used to control the circuit breaker. Springs with forces powerful in proportion to the masses to be accelerated are used to obtain high-speed contact separation. This reduces total operating time, reduces heating time, and, therefore, minimizes arcing and wear of contacts. Closing of the circuit breaker is accomplished by the use of a powerful solenoid which produces very high forces in proportion to the weight of masses to be accelerated. Manual operation is not provided. The small travel incident to use of pressurization permits a small magnet to develop the necessary high forces.

Six snap-action interlocks, vibration tested, are provided for use in the manual or automatic synchronizing control circuits, or in other control circuits where

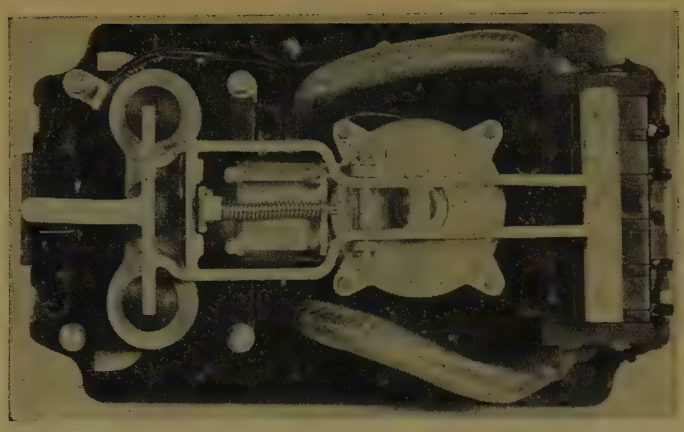




Figure 6. Plan view of circuit breaker showing closing tripping-magnet assemblies, also interlock and main contact operating lever

Figure 7 (above right). Elevation view of circuit breaker showing arrangement of internal parts



Figure 9. Exploded view of closing magnet assembly showing the component parts



Figure 8. Exploded view of arc rupturing compartments showing contact assemblies



Figure 10. View of moving-contact assembly showing springs and contact chambers

their use is necessary for the proper functioning of the controls. Individual interlocks can be made, either normally open or normally closed, simply by changing the position of the external links, thus providing the ultimate in flexibility.

One interlock operated by the main circuit breaker mechanism is in series with the operating coil and interrupts the closing coil circuit as soon as the circuit breaker is latched closed. Thus the coil is excited only during operation, and it is possible to make the solenoid assembly smaller than it would be if continuously rated. The latch mechanism is released by means of a d-c-operated solenoid.

The circuit breaker mechanism is enclosed with a seal which is sufficient to exclude dirt, water, or other foreign materials to a degree insuring operation under the most unfavorable conditions likely to be encountered.

Four mounting holes are provided, and the circuit breaker mechanism may be removed readily without disturbing the mounting or enclosure. Three main leads enter one end of this circuit breaker and leave the opposite end of the circuit breaker providing straight-through wiring. The control circuits enter from each side of the circuit breaker and at the same level as the main leads. Main and control terminals both are protected against accidental contact.

Operating Results

Speed of closing the main contacts of the circuit breaker from the time voltage is applied until the circuit is closed is very rapid. Figure 1 shows a voltage–time curve which gives actual operating speeds on closing as measured by oscillograph. The tripping or opening speed of the circuit breaker is shown in Figure 2. Operating speeds are well within the specifications of the Army Air Forces and assure proper functioning of the system under normal and fault operating conditions.

Closing coil and tripping coil are operated from the 28-volt d-c system which also is provided on the a-c-powered airplane, so that undesired operation will not occur during momentary faults.

Conclusions

This circuit breaker functions much the same as circuit breakers for industrial systems but weighs only a very small percentage of what a comparable industrial circuit breaker would.

Pressurized arc interruption is well adapted to circuit breaker performance under altitude conditions.

Effective sealing of the arc reduces the fire hazard present with open arcs.

Unusual high speed action during the closing and tripping periods has been obtained.

That operation is satisfactory under conditions of humidity, sand, dust, vibration, altitude, and acceleration normal to aircraft has been thoroughly proved.

It is handy for installation because the main lead arrangement is straight through and the control leads also are straight through at right angles to the main leads.

Lead terminals, both control and main, are shielded against accidental contact when this device is mounted in position.

Space requirements are small, and the device weighs only five pounds.

Design and test experience with this type of circuit breaker indicate that the same fundamental principles can be used for breakers having much higher ratings.

Transients in A-C Motors and Generators

GEORGE S. SMITH
MEMBER AIEE

IN THE PAST, few electrical-engineering curricula have offered the undergraduate student more than the rudiments in the study of electric transients. Even today many engineering schools offer such courses only as graduate work. The result is that most engineering graduates confronted with such problems in connection with their work must acquire such information by self study and experience.

Many engineers in charge of the design, maintenance, or operation of large power systems of today are confronted with such problems as the choice, settings, or proper operation of such apparatus as circuit breakers, relays, and other protective equipment. Such equipment must operate adequately to protect the apparatus effectively and yet not cause undue interruption of service. Many such problems involve the conditions occurring during the transient period. Thus a clear conception of the nature of the changes during such periods is of great importance.

A great amount of valuable research work has been done in such studies, and a great deal of information is available.[1–8] Some of this material is in the nature of explanation or suggested methods of procedure, while some is in usable mathematical form, but most of the literature on such studies involves a great amount of detail and too often is written for those who already have a clear conception of the principles involved.

This paper proposes no mathematical study but does attempt to give a simple and clear conception of the variations that take place in the electric and magnetic circuits of a-c motors and generators and reactions between the armature and field, as well as reflected reactions between them during changes in operation. The analysis will be based upon well-known fundamental principles, and in some cases the results will be compared with mathematically derived results found in other papers as well as with actual oscillograms. This method of arriving at a physical conception of such transient conditions has been used quite successfully in introducing undergraduate students to the more advanced information available.

Paper 46-5, recommended by the AIEE committee on electric machinery for presentation at the AIEE winter convention, New York, N. Y., January 21–25, 1946. Manuscript submitted June 21, 1945; made available for printing October 25, 1945.

GEORGE S. SMITH is a professor in the department of electrical engineering, University of Washington, Seattle, Wash.

Method of Analysis

In order to acquaint the reader with the method used in this analysis and also present a very brief review of a few rudiments of the study of electric transients for those who have not recently pursued such studies, a couple of simple transient cases will be analyzed.

First consider the sudden application of a direct voltage, E, to a simple series circuit consisting of a resistance, R, and inductance, L. Using Kirchhoff's voltage law, the algebraic summation of all the voltages involved in the closed loop must be equal to zero, which may be expressed thus:

$$Ri+Ldi/dt=E \qquad (1)$$

Solving this differential equation for the current flowing at any time after closing the switch, gives the result,

$$i=E/R-(E/R)\epsilon^{-Rt/L} \qquad (2)$$

In Figure 1, the oscillograph trace i shows this value at any time after the application of the voltage. If a horizontal line, I, is constructed at a distance above the zero line, equal to a current value of E/R to the same scale as the current i, it will be tangent to the oscillograph trace at a time when i attains its final steady-state value. Also let another curve, i', be constructed equal to $-(E/R)\epsilon^{-Rt/L}$ for the various values of t after closing the switch. The dashed decrement curve below the zero line will result. The sum of the ordinates of the two constructed curves at any time, t, always will give the ordinate of the oscillograph curve, i, for that time. This agrees with equation 2 which states that the actual current flowing in the circuit at any time after closing the switch is the sum of the final steady-state current and a hypothetical transient value.

Next consider that an alternating voltage of $E \sin(\omega t+\gamma)$ is applied to the same series circuit of resistance and inductance instead of the direct voltage E. Now the differential equation is

$$Ri+Ldi/dt=E\sin(\omega t+\gamma) \qquad (3)$$

and the solution for the instantaneous current, i, at any time, t, is

$$i=(E/Z)\sin(\omega t+\gamma-\theta)-(E/Z)\epsilon^{-Rt/L}\sin(\gamma-\theta) \qquad (4)$$

In Figure 2 the oscillograph trace, i, shows the actual current flowing at each instant. The constructed current wave, I, is equal to $E/Z \sin(\omega t+\gamma-\theta)$ or the current which would have been flowing in the circuit during the interval shown, had the switch been closed many cycles earlier. This coincides with i after steady-state conditions in the circuit are attained. The decrement curve, i', is a plot of $-(E/Z)\epsilon^{-Rt/L}\sin(\gamma-\theta)$. Here again equation 4, as well as the summation of the ordinates of the constructed curves, show that the actual current can be considered the final steady-state value plus the transient value.

The decaying transient value in each of these circuits varies as the logarithmic function of ϵ^{-x} where x in the cases mentioned was a function of time t. In Figure 3 a plot of ϵ^{-x} for varying values of x is shown and appears as a decimal factor, the value of which is unity at $x=0$ and drops to zero when x reaches infinity. It might be termed one of nature's laws of change which, in simple terms, says that the amount of decrease taking place at any time is always proportional to the magnitude at that time of the quantity changing. If the amount of change were at each instant added to the quantity changing, as in continually compounded interest, the logarithmic factor would be ϵ^{x} and

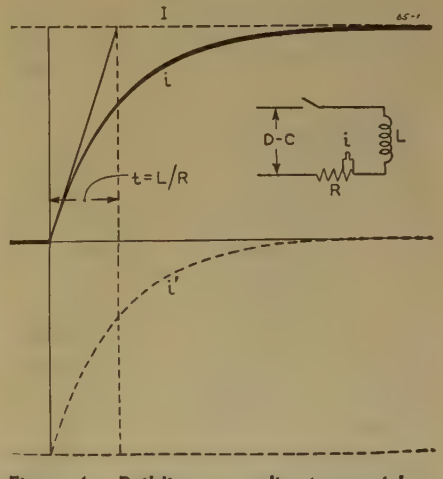


Figure 1. Building up a direct current in a circuit of resistance and inductance in series

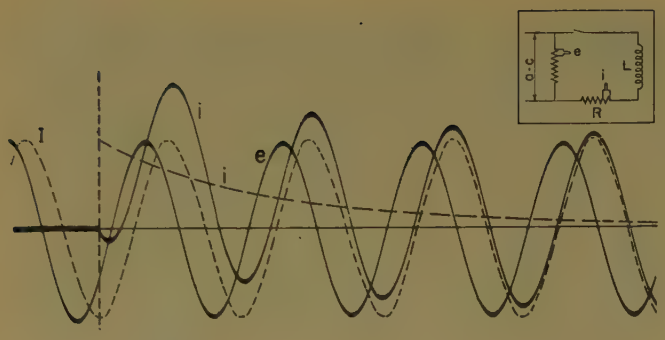


Figure 2. Building up an alternating current in a circuit of resistance and inductance in series

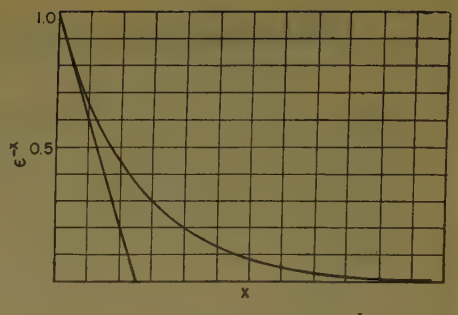


Figure 3. Decaying transient decrement curve

would start at unity when x is equal to zero and approach infinity as x approaches infinity. Other intermediate types of change factors might be such as $(\epsilon^{x}+\epsilon^{-x})\div 2$ or cosh x, or $(\epsilon^{jx}-\epsilon^{-jx})\div 2j$, or sin x, and so on.

The method of adding known components, illustrated by the two oscillograms, often proves to be a rather simple and fairly accurate method of arriving at the desired results and has been used quite extensively by Kurtz and Corcoran in their text on transient studies as one method of analyzing the transient conditions considered.

In the cases of the illustrations given, the circuit parameters were assumed constant. However, in electric machinery where magnetic materials are involved and in some circuits where the resistance or capacitance might vary for some possible reason, a mathematical determination of the components or the results in any other way is not easy. Such components or results sometimes can be determined by mathematical means, provided the law of the change involved is known; they may sometimes be determined by a series of very small but finite increments using relations known from experimental information; or they may be isolated from experimental determinations by the elimination of known components.

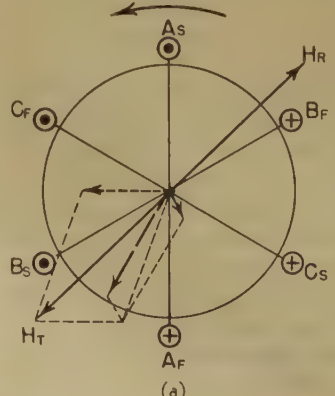
A final word of explanation in the use of vectors in this analysis seems also desirable. In the study of the effects of armature reaction in electric machinery, especially motors and generators, the final value and distribution of the magnetic flux is given by the resultant of all of the magnetomotive forces acting on the reluctance of the magnetic-flux path. Such magnetomotive-force components wound on the circular peripheries of the machine cannot be combined by assuming each to be a vector quantity, except as a very rough approximation. However, the resulting magnetic field-intensity along a given path resulting from each magnetomotive force can be considered more correctly a vector value. The magnetic flux caused by such a field intensity vector also can be considered a vector in the same direction, though not always proportional to the field intensity unless the permeability of the magnetic path remains constant.

Since the simplicity of this analysis depends to a large extent upon the use of vectors and since the method is not intended to be mathematically correct, the magnetomotive forces will be assumed to produce vector field intensities, and these in turn will be assumed to produce corresponding magnetic-flux vectors, which vectors will be combined in the usual manner. Where a change of permeability of importance must be taken into consideration, a gradual change in the length of the vector, according to the known law of change, will be assumed. Such assumptions will be pointed out at the time they are used.

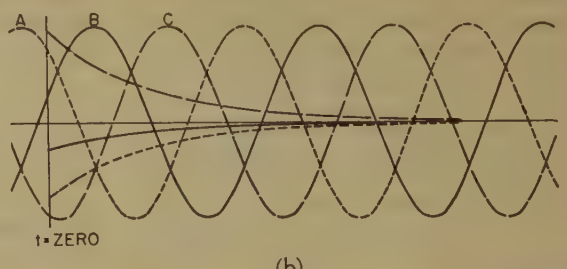
Building Up the Rotating Magnetic Field of a Three-Phase Induction Motor

A three-phase induction motor stator (for simplicity assume a two-pole winding) connected to a suitable three-phase voltage supply has, after steady-state conditions have been attained, a single nonvarying rotating magnetic field produced by the varying combinations of magnetomotive forces of the three phases carrying the respective phase currents. In Figure 4a the three-phase windings $A_S A_F$, $B_S B_F$, $C_S C_F$, each is represented by a single turn in the proper angular position with respect to the polarity of the voltage applied or the direction of the current flowing in the coil at some definite instant of time. The subscript S indicates start and F finish of coil. Assume the phase currents shown in Figure 4b are flowing in the respective coils. The directions of the currents in the coils at a time indicated by the ordinate at t = zero time are identified by the usual plus and dot signs in the conductors. The resulting magnetomotive force of each phase will produce vector values of field intensities (not indicated) which would combine to produce the resultant field intensity H_R. For any time later H_R can be proved to remain constant in value but to rotate counterclockwise in synchronism with the supply. This vector will be called the final steady-state field intensity and will produce the final steady-state magnetic field ϕ_R shown in Figure 5a. This field flux also rotates at synchronous speed in the same direction.

Thus far the assumption has been made that the voltage had been applied at some earlier time. Now assume that the switch is closed at the time indicated by the ordinate t = zero. Since the circuit is inductive, all currents must start at zero, and similar to the case in Figure 2, the starting current in each phase will be the sum of the steady-state current in that phase plus a unidirectional decaying transient current. Both components are indicated in Figure 4b while the actual starting currents would appear

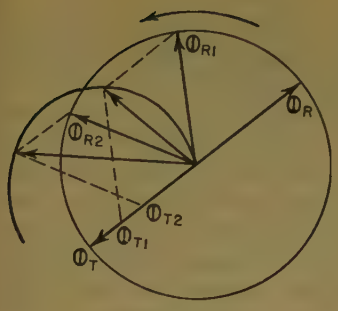


(a)

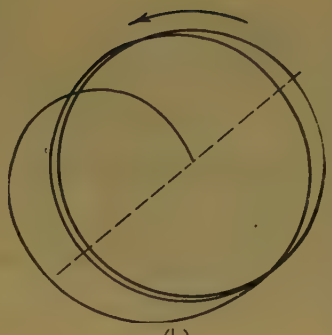


(b)

Figure 4(a) and (b). Components of field intensities and the three-phase steady and transient currents producing them



(a)



(b)

Figure 5(a) and (b). Components of magnetic fluxes and vector combinations to give instantaneous values

similar to the starting currents shown in Figure 7.

Likewise the magnetic field must start from zero and also can be assumed to be made up of the steady-state value ϕ_R, already explained, plus a component due to the combination of the magnetomotive forces set up by the transient currents in their respective coils.

In Figure 4a the corresponding instantaneous vector intensity for each of these transient currents at t=zero is shown in its proper directions and magnitudes, and their vector sum is H_T, which is equal in magnitude but reversed in direction to the rotating vector H_R. In Figure 5a the corresponding vector ϕ_T is indicated. The sum of ϕ_T and ϕ_R is zero at time t=zero, as it should be. Unlike the vectors H_R and ϕ_R which rotate, the transient vector H_T and corresponding flux ϕ_T remain stationary in space, since they are produced by unidirectional currents flowing in stationary coils. However, they decrease toward zero as time goes on in accordance with the decrement currents which cause them.

At any time after t=zero the actual magnetic field ϕ can be found by adding ϕ_R, which is in a new angular position, to the remaining value of ϕ_T. Such vector additions are shown in Figure 5a for angular positions of ϕ_R at 45 degrees and 90 degrees from the starting position.

By carrying out such vector additions at small angular increments for a few cycles of the alternating current, the value of ϕ becomes alternately greater and less than the final steady-state value but rapidly approaches a steady value as time goes on. The envelope thus derived is shown in Figure 5b, and the same values of ϕ plotted against time are shown in rectangular co-ordinates in Figure 6.

Figure 7 is an oscillogram of the actual currents flowing in the three phases of the induction-motor stator when first excited. These should correspond quite closely to curves obtained by adding the steady-state and transient values for each phase current in Figure 4b. However, in Figure 7 the permeability changes in the iron probably have introduced some distortions not assumed in Figure 4a, and the resulting magnetic-field variations also would be slightly altered from those shown in Figure 5b and Figure 6.

Three-Phase Alternator or Synchronous-Motor Load Changes

Closely related to the changes just described for the three-phase induction motor are those occurring when some sudden alteration in load takes place in the operation of a three-phase alternator or synchronous motor. Such an alteration may be from no load or part load to a much greater load or even short circuit, or it may be the reverse from a high load to a lower one or to no load. Were the machine an alternator the type of load might be resistive, inductive, or capacitive. In all cases the inductive nature of the machine's internal impedance always must be present.

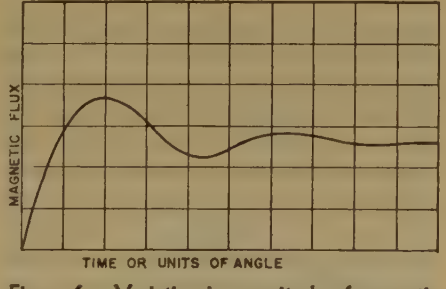


Figure 6. Variation in magnitude of magnetic field in rectangular co-ordinates

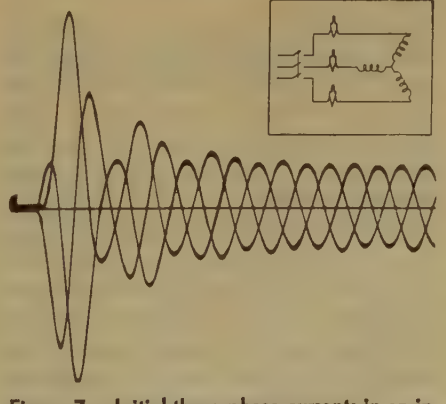


Figure 7. Initial three-phase currents in an induction-motor stator

To illustrate the method of analysis, an alternator operating at no load suddenly will have a near short-circuit load applied to its terminals. For a clear conception of all the changes occurring the reader must rely on his knowledge of armature reaction in alternators, of the effects of the load power factor, and the effects of changes in the permeability in the magnetic circuit.

A two-pole three-phase alternator stator shown in Figure 8a, identical to the one used in discussing the induction motor, will be assumed. The only addition will be a two-pole d-c-excited rotor operating at some given speed. Again the three-phase steady-state currents are shown in Figure 8b. If the load switch had been closed at the time indicated as t=0, the transient component shown for each phase is also necessary. At this point, however, a radical difference from the previous case occurs. The alternator, rotating at a constant speed and with its d-c-excited field, is generating a rather high no-load voltage, while the final sustained current shown is caused by a greatly reduced voltage in comparison, since armature reaction and permeability changes have greatly reduced the magnetic flux of the field. Thus the so-called steady-state component of current flowing in each phase at the instant of closing the switch is somewhat greater than the final sustained value, and these components would be more in the order of those shown only as tips of waves in Figure 8b. As armature reaction reduces the field flux, these currents also will drop off to the final steady-state current values.

In each phase the final sustained value of current is assumed as one component, as was done in the case of the induction motor. A second is the usual unidirectional decaying current with an initial value equal to the value of the sustained current at the instant the switch was closed but reversed in sign. The decay of this must depend upon the resistance and inductance of the armature circuit. Since the sum of these two will not account for the unusually high values at the time the switch was closed, a third component must be present. Evidently this must be the difference between the final sustained current and the so-called steady-state value indicated by only the wave tips. This component will be a full-frequency oscillating current, decaying with time and with a decay factor depending upon the rate of change in the field flux, thus is controlled by the re-

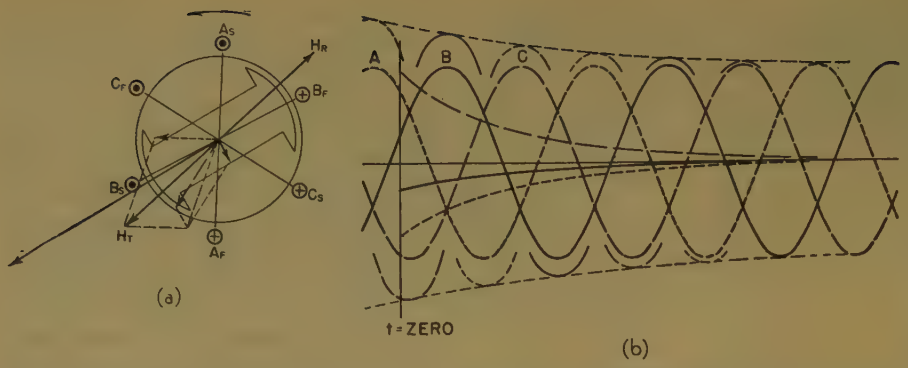


Figure 8(a) and (b). Components of field intensities and the three-phase steady and transient currents producing them

sistance and inductance of the field circuit. This has not been shown as an isolated component in the drawing.

The field-intensity components are shown in Figure 8a. The d-c field current at no load produces a field intensity of H_o. The final rotating field intensity, H_R, is the armature reaction arising from the sustained currents in the three phases. The transient intensity, H_T is due to the unidirectional currents of the three phases. As there is still another component in each phase of the armature which must have an armature reaction effect upon the field, it will rotate with the field similar to H_R but will decay to zero as the sustained armature currents are approached. This component will be accounted for by a decrease in the value of the flux generated primarily by the d-c field current.

Figure 9 is a typical equivalent single-phase vector diagram for the alternator showing the armature current and all the various voltages and voltage loss components, as well as the no-load field flux ϕ_o proportional to H_o, ϕ_R proportional to H_R, and ϕ_T proportional to H_T. The no-load voltage E_o is generated by ϕ_o. As explained in the discussion on the field-intensity components, a portion of the ϕ_0 is lost because of the high initial armature currents and the resulting excess armature reaction. Reducing ϕ_o by the amount of this loss leaves ϕ_F the final steady-state flux due to the d-c excitation. This combines with the armature reaction flux ϕ_R to leave ϕ_G as the remaining flux to generate the internal generated voltage E_g, a part of which is lost in the winding impedance to leave E_T at the terminals. The final steady-state current is I which must be in phase with ϕ_R and the near short-circuit power-factor angle is θ.

To explain further the lost component of field flux, refer to the typical partial hysteresis loop, Figure 10, showing both increasing and decreasing field-excitation values. Assume the no-load condition to be at the maximum point with H_0 excitation due to the d-c field resulting in ϕ_o as the total flux. The initial armature current reduces the excitation by the amount of H_1 with the flux following the upper saturation curve. As the armature current drops in magnitude to its final steady-state value, the armature reaction reduces to H_R, and the flux value increases on the dashed curve to the final value of ϕ_G. Had this reversal not occurred, the saturation would have remained on the upper curve and would have been greater by the component of ϕ_L. Thus the flux ϕ_L equal to $\phi_o - \phi_F$ was lost due to the changes in permeability.

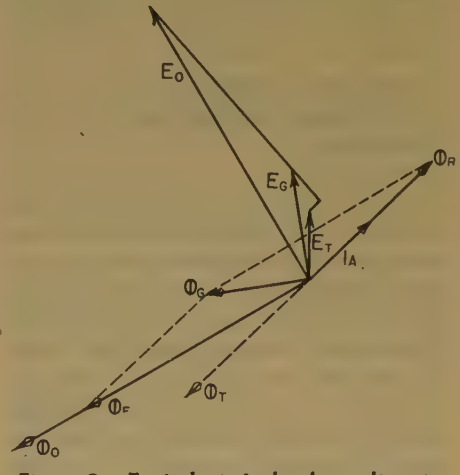


Figure 9. Equivalent single-phase alternator vector diagram

In Figure 11a the flux due to the no-load d-c excitation is shown as ϕ_o, the steady-state armature reaction at the instant of t=zero is shown as ϕ_{R0}, and the transient of the armature reaction values as ϕ_T. The vector sum of these three is evidently ϕ_o, as it should be. After ϕ_R has rotated through 45 degrees to ϕ_{R1}, the d-c excited field has rotated to ϕ_1. Notice that ϕ_1 is less than ϕ_o by a fraction of ϕ_L indicated on the field decrement curve of Figure 12 for the time angle of 45 degrees. Also ϕ_T, though stationary, has decreased to T_1 by an amount indicated on the armature decrement curve of Figure 12 for the same time angle. The sum of these three vectors gives the actual flux value ϕ_{S1} at that instant. A second step is shown after 90-degrees rotation, giving the sum of ϕ_{R2}, ϕ_2, and T_2 as the instantaneous value of flux ϕ_{S2}.

By carrying out such vector summations for small increments over a few cycles, the polar diagram envelope of the flux variations is shown in Figure 11b. The flux value starts to decrease rapidly but pulsates for a short interval, finally reducing to a steady rotating value of ϕ_G.

This varying flux is replotted in rectangular components in the graph A of Figure 13. In the graph B the various voltages acting in the d-c field coils are shown. Before the load is thrown on the alternator the direct voltage alone causes field current to flow. Just after throwing the load on, armature reaction causes a rapid decrease in the field flux ϕ_o, which change in flux induces a considerable voltage in the field coil. Because the flux value alternates, the induced voltage also alternates. The voltage is maximum when the flux is changing most rapidly and is zero when the flux is at a high or low point and not changing. The inductive nature of the field circuit will not allow the field current to change instantly, thus a transient component of voltage also must be present. This must have an initial value equal to the initial induced voltage but of the reverse polarity. The decrement factor of this transient voltage will depend upon the d-c field coil inductance and resistance.

When the ordinates of all of the components of voltage at each instant of time are added, the resulting curve is the actual voltage acting in the field circuit to cause current to flow. Thus the field

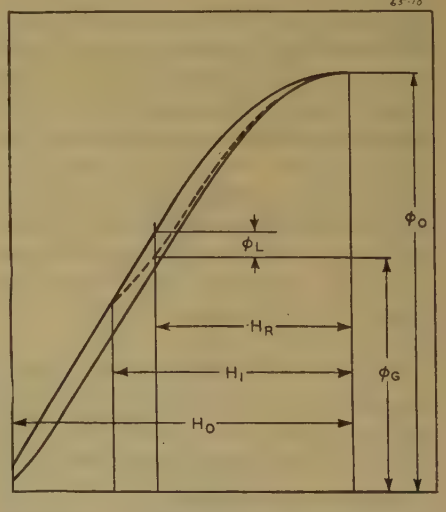
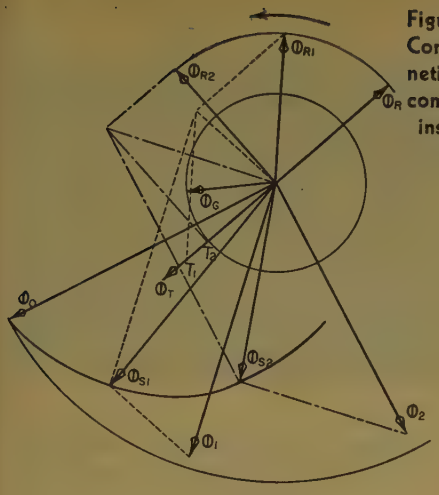
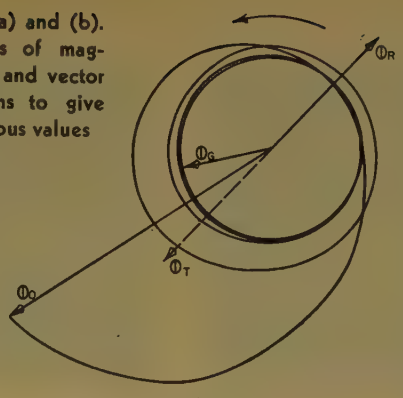


Figure 10. Typical partial hysteresis loop for alternator



(a)



(b)

Figure 11(a) and (b). Components of magnetic fluxes and vector combinations to give instantaneous values

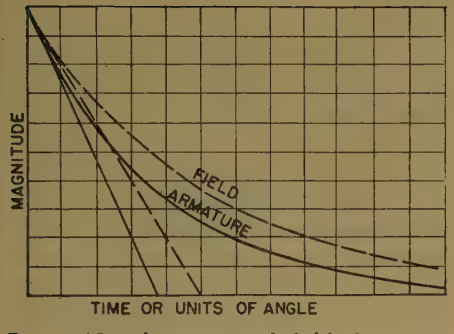


Figure 12. Armature and field decrement curves

current would be a similar curve, but lagging the voltage by some amount. A comparison of this constructed field-voltage curve with the field-current waves of oscillograms shown in Figures 14 and 15 shows the same characteristics.

The oscillogram in Figure 14 shows the voltage across one phase, the three-phase currents, the d-c field current, and the air-gap flux on a rotating-field type of alternator. Figure 15 shows the same values taken on a machine with stationary field poles and a rotating armature. This machine has a rather strong 11th harmonic due to armature slots.

The lower trace in all alternator oscillograms shows the actual value of the air-gap magnetic flux recorded by means of a bismuth-bridge type of magnetic-flux meter.[14-15] Using this with a stationary-pole type of alternator as in Figure 15 shows the rapid decrease of the flux due to armature reaction at the center of the pole face. On the leading tip the decrease is even more rapid, while on the trailing tip the flux often rises above the no-load value before it decreases, indicating flux distortion. In Figure 14 the increase in flux just after load is thrown on is caused by the position of the probe under a trailing pole tip at that instant.

Many attempts have been made to express mathematically the armature and field currents during such transient periods. Doherty and Nickle[6] give the following equations for the armature currents in phases A, B, and C:

$$i_A = \frac{e_0}{x_d}\cos(\omega t-\alpha)+e_0\frac{x_d-x_d'}{x_d\,x_d'}\times \epsilon^{-\sigma_f t}\cos(\omega t-\alpha)-e_0\frac{x_d'+x_q}{2x_d'\,x_q}\epsilon^{-\sigma_a t}\times \cos\alpha+e_0\frac{x_d'-x_q}{2x'_d\,x_g}\epsilon^{-\sigma_a t}\cos(2\omega t-\alpha) \quad (5)$$

i_B = same as phase A except for the use of $(\alpha+2\pi/3)$ instead of α (6)

i_C = same as phase A except for the use of $(\alpha+4\pi/3)$ instead of α (7)

Each phase current is made up of the algebraic sum of the four components shown. The first is the sustained value of current and corresponds to the sustained value of current in Figure 8b. The second is a full-frequency decaying current caused largely by the high no-load voltage, and decays as the armature reaction reduces the field flux to its final steady-state value. The coefficient of its decay factor σ_f depends upon the field-circuit constants. This component was accounted for by the loss of flux ϕ_L. The third factor is the unidirectional decrement corresponding to the decrement curves in Figure 8b. Its initial magnitude is equal to, but of the opposite polarity to, the instantaneous value of the sustained current corresponding to the point on the voltage wave at which the load switch was closed. The coefficient of its decay factor σ_a depends upon the circuit constants of the armature circuit. The fourth factor, which is usually not very large and is absent or nearly so in some types of generators is a double-frequency component, the decay of which depends upon the armature constants. No attempt was made to indicate this in Figure 8b. This component often appears in salient-pole types of machines which have no damper windings. There are possible sources for many small-scale variations other than those mentioned, as changes produced in the field by armature reaction will in turn cause altered generated voltages and currents in the armature. These in turn will further alter the field. There is no limit to the reflected effects back and forth between armature and field, but fortunately each succeeding reflection rapidly decreases toward zero.

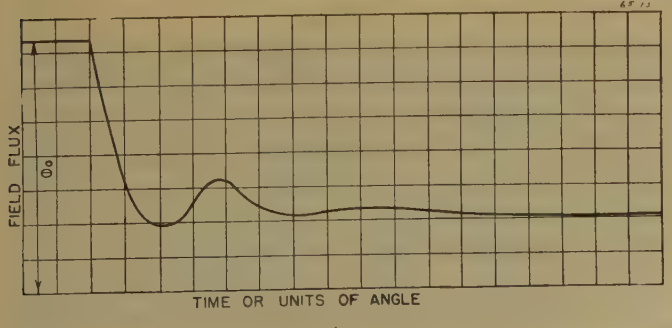
The same authors give the field-current equations as

$$i_f = e_0+e_0\frac{x_d-x_d'}{x_d'}\epsilon^{-\sigma_f t}-e_0\frac{x_d-x_d'}{x_d'}\epsilon^{-\sigma_a t}\cos\omega t \quad (8)$$

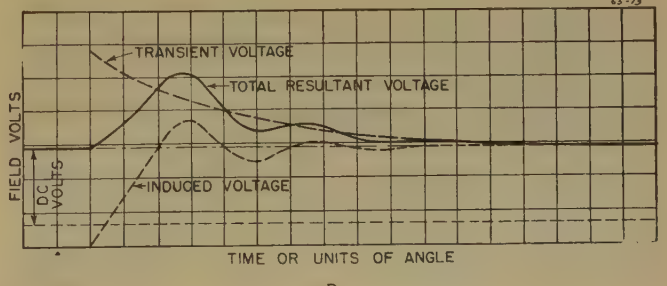
This equation might be altered thus

$$i_f = I_0+KI_0\epsilon^{-\sigma_f t}-KI_0\epsilon^{-\sigma_a t}\cos\omega t \quad (9)$$

where K is a constant depending upon the reactances involved. Here the three components are shown similar to the three components of voltage in Figure 13. The first is the current due to the direct voltage, the second is the unidirectional decaying component, the decay of which depends upon the field-circuit constants,



A



B

Figure 13. Magnetic-field variations and voltage components in field winding

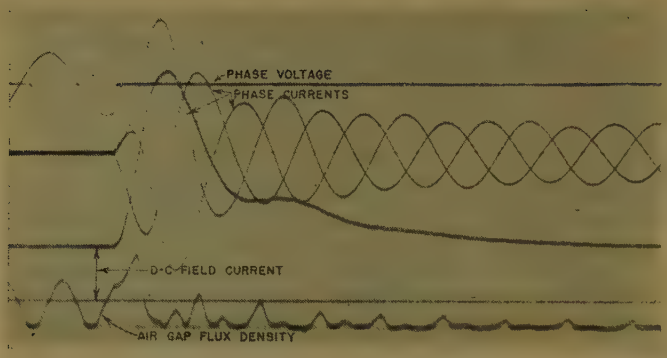


Figure 14 (left). Oscillogram of transients in an alternator with rotating field poles

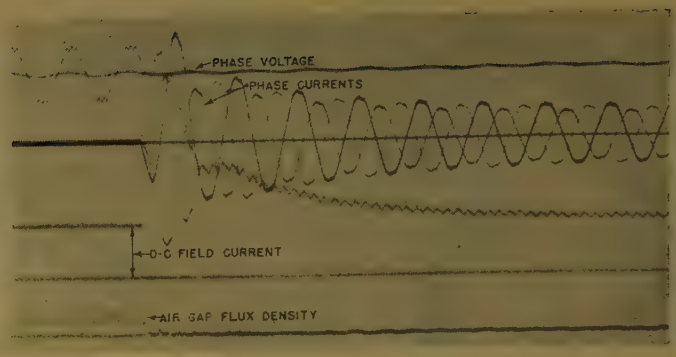


Figure 15. Oscillogram of transients in an alternator with stationary field poles

the third is the component due to the full-frequency alternating induced voltage, the decay of which depends upon the armature circuit constants.

Doherty and Nickle express all initial current components in terms of the no-load voltage e_o, assuming no saturation, and a percentage factor derived from the reactance acting, as the resistance of an alternator is usually so low its effect may be neglected in such factors. Thus the final steady-state current is the ideal no-load voltage e_o divided by the direct-axis component of synchronous reactance x_d.

A brief comment on the various reactances used in such mathematical studies might be of value here. In any circuit the current for a given voltage is limited by the impedance of the circuit. Each component of the impedance will absorb a proportional component of the total voltage, and the countervoltage of each reactance through which the current flows will just balance a corresponding component of the voltage applied. The reactance is then the ratio of that component of voltage to the current.

Referring to the armature current tracings in oscillograms such as Figures 7, 15, or 16, the impedance, or reactance if resistance is neglected, must continually vary from instant the switch is closed to the time when final steady-state conditions prevail, if the generated voltage is to be assumed constant. Since constant values of reactances are desired, certain limiting values are used. Further subdivisions of the reactances also are used. For example, synchronous reactance is a function of the armature current magnetomotive force, largely acting as armature reaction. At any given power factor of the load the armature magnetomotive force, which has been assumed to produce flux ϕ_R in Figure 9, might be considered as the resultant of two components, one acting on the axis of the main field, producing a demagnetizing action, the equivalent reactance of which is termed direct-axis synchronous reactance x_d, and the other acting at right angles to the main field, causing flux distortion of the main field, the equivalent reactance of which is termed quadrature-axis synchronous reactance x_q.

Thus the direct-axis synchronous reactance x_d for the balanced steady-state conditions might be defined as the ratio of the fundamental component of the reactive armature voltage, due to the fundamental direct-axis component of armature current, to this component of armature current, at rated frequency. The quadrature-axis synchronous reactance is defined in a very similar manner.

The reactance during the first several cycles after short circuit must be lower than the steady-state value, as the current is higher, which gives rise to the term transient reactance x'. This might be defined as the ratio of the fundamental component of reactive armature voltage due to the fundamental component of the armature current to this initial component of current at the time short circuit occurs, providing such current follows the normal decrement curve of the decreasing current. This initial value of current must be obtained by projecting the normal current transient back to the time of closing the switch. For most machines, and especially for those having damper windings on the rotor, the first two or three cycles do not follow the normal decrement curve but are abnormally high, though they decay rapidly down to the normal decrement values. For this portion of operation the reactance is still less and is accounted for by a subtransient reactance x''. This is the ratio of the generated voltage to the highest initial value of current which was produced at the instant of closing the switch. Such initial values are only the average of all three phases.

In practice both of these again are divided into the direct, x_d' and x_d'', and quadrature, x_q' and x_q'', values. All of these terms are defined in the AIEE "Standard Definitions of Electrical Terms" and may be determined by tests

Figure 16 (left). Oscillogram of transients in an alternator suddenly loaded with three-phase inductive load

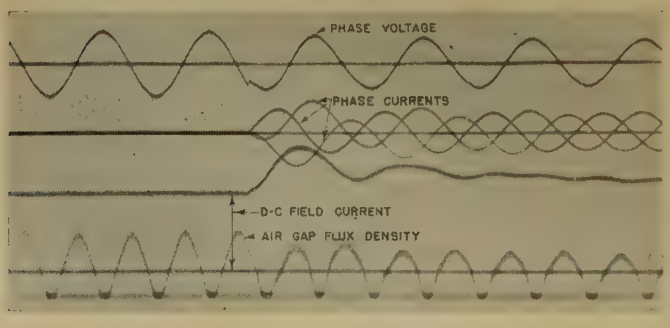
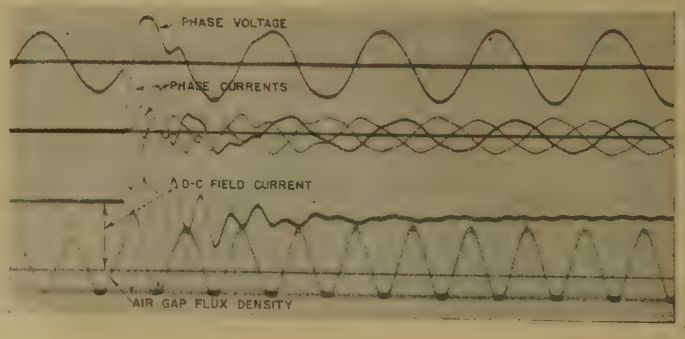


Figure 17. Oscillogram of transients in alternator suddenly loaded with a three-phase capacitive load



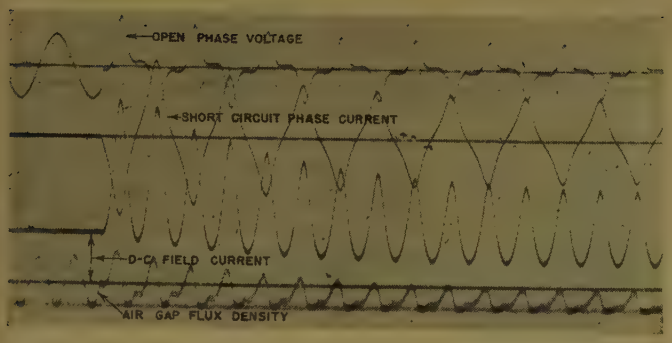


Figure 18. Single-phase short circuit on a three-phase alternator with rotating field poles, symmetrical type

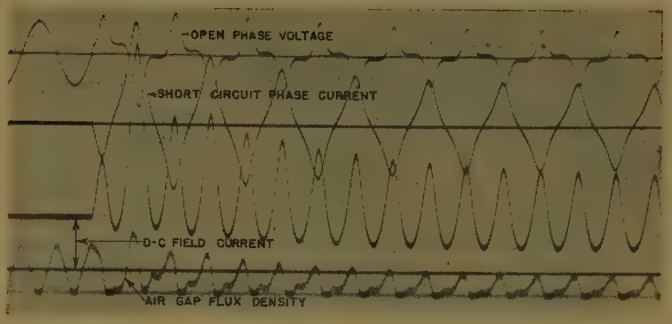


Figure 20. Single-phase short circuit on a three-phase alternator with rotating field poles asymmetrical type

or calculation, as proposed by various authors.[9–12]

Closely related to the reactance values in their importance during the transient period, are the decrement factors or their reciprocals, termed time constants T. In equation 2 the decrement factor is R/L, while the time constant is L/R and is a factor which gives an indication of the time required for the decreasing term to approach zero. In modern a-c machinery the reactance x which is a function of the inductance L purposely is made large either in the design of the machine or by introducing reactance in some part of the circuit, in order to limit the currents under short-circuit conditions. This can be done since the voltage regulator will maintain a constant voltage under steady conditions. The resulting large time constant causes the transient condition to persist for a considerable period after such changes, up to several seconds. The persistence of such high currents often may require higher settings on protective equipment than otherwise would be desired.

Many other transient conditions in alternators or synchronous motors might be analyzed in a similar manner. Two other oscillograms of such conditions are shown. Figure 16 shows the voltage, armature currents, field, and air-gap flux for the same alternator used for Figure 14, except that it is suddenly loaded with a highly inductive air-core inductance load. Here the inductance requires energy from the generator for a portion of the cycle and returns the energy the next half cycle. The resulting armature reaction in reducing the field, both during the transient period and after, is less than for the near short circuit. Figure 17 again is the same machine suddenly loaded with a capacity load. Here the capacity causes the current to lead the voltage, which gives a decided increase in the air-gap flux due to armature reaction.

Load Changes in a Single-Phase Alternator

The single-phase alternator proves quite interesting as a study of interrelated electric and magnetic fields, both under transient conditions as well as steady-state conditions. The theory is also important since faults often result in single-phase operation for their duration. The usual distortions in the voltage and current waves when using one phase of a three-phase alternator for careful tests may introduce considerable error in the results. The same is true for any single-phase alternator, unless it is specially designed to give a fair sine wave at all loads.

Such an alternator has the usual d-c excited field but has only one armature winding which usually does not use the whole periphery of the armature core. As the field rotates 180 electrical degrees for each half cycle, the armature reaction on the field always acts in the same direction, causing a continuous double-frequency pulsation in the field flux. When the load on such an alternator suddenly is changed or the alternator is short-circuited, two possible types of transient relations are possible. In the first, or symmetrical case, fairly perfect examples of which are shown by the oscillograms in Figures 18 and 19, the load switch was closed at a point on the voltage cycle at which, under steady-state conditions, the current value would have been zero, and the second, of which Figure 20 is a typical example, where the switch was thrown at a point on the voltage cycle where the steady-state current would not have been zero. This will be termed the asymmetrical case.

In making an analysis of these single-phase cases, certain assumptions again will be made which would alter the final general results only slightly. First the current waves will be assumed to be sine wave in shape, and second the effects of iron saturation will only be approximated.

Symmetrical Case

If the switch of a series resistance and inductance circuit is closed at a point on the voltage cycle when, under steady-state conditions, the current would have been zero, the usual inductive type of transient as in Figure 2 will not be present; the current will start at zero and continue at its final steady-state value. However, in the case of the single-phase alternator, as in the three-phase case, the no-load field flux and generated voltage are much higher than after the armature reaction has been able to reduce the strength of the field. Because the voltage is high at this first instant, the current also will be high but will drop as the armature reaction becomes effective in reducing the field. There then will be a decay of the armature current value but an equivalent decay will occur on both the positive and negative halves of the wave, and the resulting current will be symmetrical with respect to the zero.

Such a decaying alternating current in

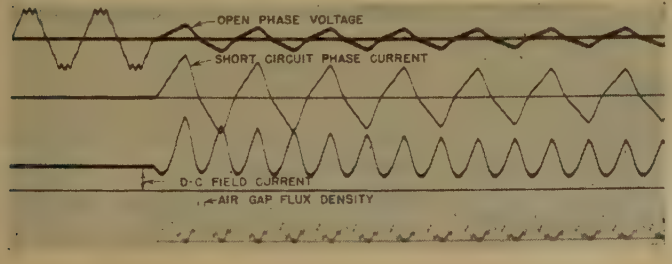


Figure 19. Single-phase short circuit on a three-phase alternator with stationary field poles, symmetrical type

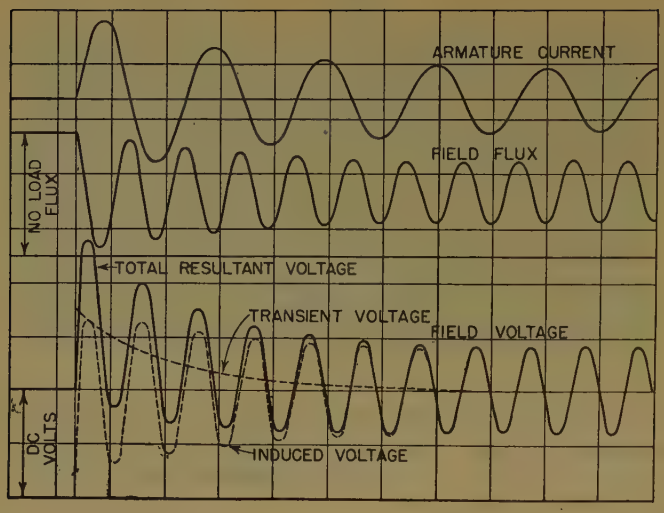


Figure 21. Armature and field components and their phase relations in a symmetrical single-phase alternator short circuit

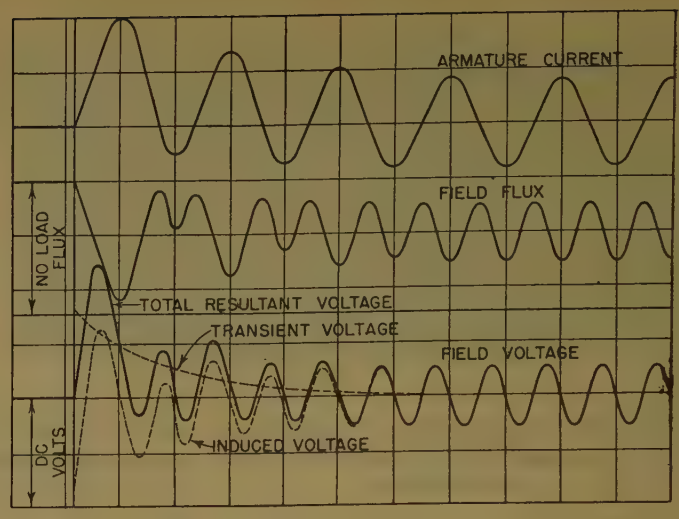


Figure 22. Armature and field components and their phase relations in an asymmetrical single-phase alternator short circuit

a single-phase alternator is shown as the top constructed curve in Figure 21. Since the d-c excited field, because of its rotation is always in a position to receive the same armature reaction effect for both polarities of the armature current, the magnitude of the flux will have two pulsations per cycle. If the usual short-circuit conditions are assumed the reaction will be to cause the flux to decrease most when the current is maximum, and the resulting field flux curve construction will be as shown by the second curve.

The variations in the field flux will generate a voltage in the d-c field winding of the same frequency and of a corresponding magnitude. This pulsating voltage is indicated as a dash curve in the lower set of curves. Since the field current and thus the field voltage must start at the no-load value and cannot jump instantly, the usual unidirectional decrement voltage, shown as a dash line, also must be present. The sum of the d-c, the pulsating, and unidirectional decrement components of voltage will give the actual voltage acting on the field circuit as shown by the full-line oscillation. This corresponds very well with the actual field current in oscillograms, Figures 18 and 19.

Asymmetrical Case

If the load switch is closed at a point on the voltage wave when, under steady-state conditions the current would not have been zero, then the type of transient shown in Figure 2 will be present. However, the effect of the high no-load voltage will amplify the magnitude of the current peaks, both positive and negative, just after closing the switch, but this excess current will die away to the final steady-state current after armature reaction has reduced the field flux to its final steady pulsating value. The upper curve in Figure 22 shows such an armature current curve. The second constructed curve is that of the resulting field flux because of armature reaction. In the lower set of field-circuit voltage curves, the pulsating induced voltage component due to the field-flux pulsations, and also the unidirectional decrement component, are shown in dash lines. Again the sum of these components, together with the direct voltage, gives the full-line curve as the actual voltage acting in the field circuit which corresponds well with the field current in oscillogram, Figure 20.

The induced voltage in the field circuit, as well as the current component resulting from this voltage, could have been further subdivided into a sustained pulsation at double-frequency component and a full armature-frequency pulsating component which decays with a decrement factor, depending upon the armature circuit constants.

Again Doherty and Nickle[5] have worked out quite complete and reasonably accurate equations for the armature field currents, as well as for the open-circuit voltage where a three-phase generator is supplying a single-phase load. For the armature current in the symmetrical case they give

$$i = 2ke_o \frac{K}{J} \sin \omega t + 2ke_o \frac{P}{J} \epsilon^{-\sigma_f t} \sin \omega t \quad (10)$$

and for the asymmetrical case

$$i = 2ke_o \frac{1}{H} \epsilon^{-\sigma_a t} \cos \alpha - 2ke_o \frac{K}{H} \times \cos(\omega t + \alpha) - 2ke_o \frac{P}{H} \epsilon^{-\sigma_f t} \cos(\omega t + \alpha) \quad (11)$$

In the symmetrical case, equation 10, the current is made up of the alternating sustained value plus an alternating value at the same frequency but decaying with a decrement factor depending upon the field-circuit constants. This second component is due to the high no-load field causing a high armature voltage and current at the instant of closing the load switch but dies away as armature reaction reduces the field. In the asymmetrical case, equation 11, the last two terms are components similar to those of equation 10. The additional first term is a unidirectional decaying component with a decrement factor depending upon the armature-circuit constants, with the initial magnitude depending upon the point on the voltage wave at which the load switch was closed. These components correspond very closely to the components necessary to give the armature currents assumed in Figures 21 and 22 respectively.

For the symmetrical case they give the field current as

$$i_f = e_o \frac{CK}{J} + e_o \frac{FP}{J} \epsilon^{-\sigma_f t} - e_o \frac{FK}{J} \times \cos 2\omega t - e_o \frac{FP}{J} \epsilon^{-\sigma_f t} \cos 2\omega t \quad (12)$$

and for the asymmetrical case

$$i_f = e_o \frac{CK}{H} + e_o \frac{CP}{H} \epsilon^{-\sigma_f t} + e_o \frac{FK}{H} \times \cos(2\omega t + 2\alpha) + e_o \frac{FP}{H} \epsilon^{-\sigma_f t} \cos(2\omega t + 2\alpha) - e_o \frac{G}{H} \epsilon^{-\sigma_a t} \cos(\omega t + \alpha) \cos \alpha \quad (13)$$

Thus the actual field current of equation 12, similar to the field voltage shown in Figure 21, is made up of a steady d-c component, plus the usual decrement

component, where a change in direct current takes place, plus a sustained double-armature-frequency pulsating component caused by armature reaction of the sustained armature current, plus a similar double-frequency component which decays with a decrement factor depending upon the field circuit constants. This component is the result of the decreasing armature current as it reduces to the final sustained value.

The field current of equation 13 similar to the field voltage of Figure 22 consists of four similar components plus a fifth decaying component, the decay of which depends upon the point on the voltage wave at which the load switch was closed. Notice that this is the full-frequency component before mentioned. All of the components in the equation are not shown as definitely separate components in Figures 21 and 22.

The constants in equations 10 to 13 are all rather involved factors made up of the various reactances of the machine and can be found in the original article; thus they will not be given here.

One additional observation might be mentioned. The voltage across the open-circuit phase in Figures 18, 19, and 20 are very distorted, and the phase current likewise is distorted. This is characteristic of single-phase loads on alternators not specially designed. The generated voltage is a function of the magnitude of the field flux and speed of rotation. If the magnetic flux is constant, the constant speed will generate a good sine wave shape of voltage. However, when the field flux is pulsating because of the single-phase armature reaction, at one instant the rate at which armature conductors are cutting flux is increased above that due to rotation by the increase in flux value and will generate a high peak of voltage, while at the next quarter cycle the flux is decreasing, which tends to decrease the total flux cutting action with the result that little or no voltage is generated at this time. Rather high voltage peaks may be the result, especially at the instant just after the load switch was closed.

Conclusion

No claim is made in offering more than a very approximate method of arriving at definite values in transient conditions of this nature. Other workers have covered quite adequately the more accurate mathematical phases. However, the analysis does attempt to offer a simple means of visualizing what to expect in such cases and of comparing the component parts thus visualized to the mathematical components derived by others. In short, the author has attempted first to offer a reasonably simple means of interpreting and visualizing the changes which result in such cases for the station operator or engineer who has little interest in knowing the magnitude of results and, second, to help acquaint the engineer who must deal with such magnitudes with the aid at his disposal, as well as to offer him a simple means of visualizing the components and reasons for components involved.

Nomenclature

R = total series resistance of the circuit in ohms
L = total inductance in circuit in henrys
e_o = no-load voltage generated by the alternator, assuming no saturation
x_d = three-phase line-to-neutral synchronous reactance on the direct axis
x_d' = three-phase line-to-neutral transient reactance on the direct axis
x_q = three-phase line-to-neutral synchronous reactance on the quadrature axis
x_q' = three-phase line-to-neutral transient reactance on the quadrature axis
$\omega = 2\pi f$, where f is normal frequency
ωt = angle in radians at time t
α = displacement angle between armature winding axis and axis of field pole at time of closing the switch
γ = angle between time of zero voltage and time of closing switch
θ = phase angle between current and voltage
i_A = current in phase A of alternator
i_B = current in phase B of alternator
i_C = current in phase C of alternator
i_f = current in d-c excited field winding of alternator
σ_a = decrement factor of armature circuit, a function of armature resistance and inductance
σ_f = decrement factor of field circuit, a function of field resistance and inductance

Other constants are explained in text.

References

1. Transient Electric Phenomena and Oscillations, C. P. Steinmetz. McGraw-Hill Book Company, Inc., New York, N. Y. Chapter 14.

2. A Simplified Method of Analyzing Short-Circuit Problems, R. E. Doherty. AIEE Transactions, volume 42, 1923, pages 841–9.

3. Transient Conditions in Electric Machinery, W. V. Lyon. AIEE Transactions, volume 42, 1923, pages 157–79.

4. Synchronous Machines, R. E. Doherty, C. A. Nickle. Part I. An Extension of Blondel's Two-Reaction Theory. Part II. Steady-State Power-Angle Characteristics. AIEE Transactions, volume 45, 1926, pages 912–47. Part III. Torque-Angle Characteristics Under Power Conditions. AIEE Transactions, volume 46, 1927, pages 1–18.

5. Synchronous Machines—Part IV. Single-Phase Alternator Operation. AIEE Transactions, volume 47, 1928, pages 457–92.

6. Synchronous Machines—Part V. Three-Phase Short-Circuit Synchronous Machines. AIEE Transactions, volume 49, 1930, pages 700–14.

7. Transient Analysis of A-C Machinery Ho H. Ku. AIEE Transactions, volume 48, 1929, pages 707–15.

8. Two-Reaction Theory of Synchronous Machines, R. H. Park. AIEE Transactions, volume 48, 1929, pages 716–30.

9. The Reactances of Synchronous Machines, R. H. Park, B. L. Robertson. AIEE Transactions, volume 47, 1928, pages 514–36.

10. Calculation of the Armature Reactance of Synchronous Machines, P. L. Alger. AIEE Transactions, volume 47, 1928, pages 493–513.

11. Determination of Synchronous-Machine Constants by Test Reactances, Resistances, and Time Constants, Sherwin Wright. AIEE Transactions, volume 50, 1931, pages 1331–50.

12. Measurement of the Subtransient Impedances of Synchronous Machines, Gordon F. Tracy, W. F. Tice. AIEE Transactions, volume 64, 1945, February section, pages 70–5.

13. Test Code for Synchronous Machines. Preliminary Report. AIEE Standards, January 1937.

14. A New Magnetic-Flux Meter, G. S. Smith. AIEE Transactions, volume 56, 1937, April section, pages 441–5.

15. Use of Bismuth-Bridge Magnetic-Flux Meter for A-C Fields, G. S. Smith. AIEE Transactions, volume 58, 1939, February section, pages 52–5.

Lightning Performance of 220-Kv Transmission Lines—II

AN AIEE COMMITTEE REPORT

THE LIGHTNING performance of high-voltage transmission lines in the nominal 220-kv class was presented in a paper[1] before the Institute in 1935. That report presented data on the construction of these lines as well as their operating performance from a lightning viewpoint. There were then only ten companies operating transmission lines in the 220-kv class, and the significant data on all these companies' lines were reported.

The collection of data at one time and presentation in one place on the performance of these lines were of such interest and value in the transmission field that the committee recently was requested to bring the record up to date. Complying with this request, the committee is presenting this present paper. To obtain the data on which the present record is based, questionnaires were sent to 13 companies which were known to have lines built for operation in the 220-kv range, and replies were received from all 13 companies. The questionnaire, which was set up carefully by the lightning and insulator working group, comprised a total of 36 questions dealing with line construction, lightning outages, features used to improve lightning performance, and other features of the lines believed significant in studying and evaluating the lightning performance of the lines.

Purpose and Scope

The purpose of this report is, as just mentioned, to bring up to date the record of the lightning performance of lines in the 220-kv class. In presenting the data the lightning outage record, which was given on transmission lines reported in the previous paper,[1] has been continued to 1944 inclusive, and in one or two cases the major part of the record for 1945 is included. The record includes data from all companies in the United States and Canada known to be operating lines in the 220-kv class.

The plan of this paper is to present most of the data which are considered pertinent to the lightning record of the line and to comment on and compare in some cases the relative benefits of various factors which are known from experience and believed by theory to be conducive to better performing lines.

Another feature of value which it was expected would appear in replies to the questionnaire was any unusual means taken to improve lightning line performance and the benefits actually obtained. In addition to giving the outage record of the lines involved, the discussion presented herein gives the committee's evaluation of the effectiveness of different features of line construction. However, it is recognized that with so many variables influencing the lightning performance of lines of this type, opinion may differ as to the relative merits of different remedial measures which have been taken in actual line construction. Therefore, practically all of the data received from the contributors have been presented, so that anyone who chooses may study and analyze them in his own way.

Presentation of Data

Practically all the data which are considered pertinent to the subject at hand are included in Table I. In all cases the data are presented practically as submitted by the separate companies involved but may differ in minor features where the questions asked or the replies received were not wholly clear. Although the lines in this table are referred to as nominal 220-kv class, it should be pointed out that one (reference 2) operates at 190 kv and two (references 14 and 15) at 287.5 kv.

Paper 46-16, recommended by the AIEE committee on power transmission and distribution for presentation at the AIEE winter convention, New York, N. Y., January 21–25, 1946. Manuscript submitted November 16, 1945; made available for printing November 21, 1945.

This report was prepared by the lightning and insulator working group of the AIEE committee on power transmission and distribution. The personnel of the working group comprised: I. W. Gross, American Gas and Electric Service Corporation, New York, N. Y., *chairman;* H. A. Frey, Locke Insulator Corporation, Baltimore, Md.; W. W. Lewis, General Electric Company, Schenectady, N. Y.; J. T. Lusignan, Jr., Ohio Brass Company, Mansfield, Ohio; G. D. McCann, Westinghouse Electric Corporation, East Pittsburgh, Pa.; F. W. Packer, Pennsylvania Power and Light Company, Allentown, Pa.; Philip Sporn American Gas and Electric Service Corporation, New York, N. Y.; S. K. Waldorf, Pennsylvania Water and Power Company, Baltimore, Md.; E. R. Whitehead, Duquesne Light Company, Pittsburgh, Pa.

The committee expresses its appreciation to all 13 electric power companies for their prompt cooperation in supplying the records on which this paper is based, and also to G. D. Lippert for his efforts in compiling the data for analysis.

The extent of the 220-kv systems covered is shown in Table II, wherein it is shown that 13 companies are operating 35 lines totaling approximately 3,988 miles of line (right of way) and 6,601 miles of 3-phase circuit.

Discussion of Data

A brief summary and discussion of the outstanding features of line construction and line performance are presented. For convenience of analysis, however, some of the various factors which influence lightning performance have been segregated and discussed separately. It is realized that the effect of any one of these factors is so interlaced with that of the others, that it is not possible to evaluate definitely its influence from the insufficient data available.

Structural and Related Features

Location of Lines

The lines reported on are located in lightning territory which ranges from very light to heavy, the isokeraunic levels ranging from 5 in California to 45 in Illinois, but none being in the 70 to 90 range of the extreme southeastern section of the country. The isokeraunic levels shown in column 25 of Table I were taken from the United States Weather Bureau isokeraunic map.[3] The lightning severity, reported by each company is in column 24.

The average elevation of each line above sea level is given in column 21. These values range from 68 feet in California to 3,020 feet also in California. These figures are not considered particularly significant: first, because elevation above sea level in this range is not believed to have any appreciable influence on lightning frequency and severity; and secondly, because lines shown located in low average terrain may, and in some cases do, have part of their length in high-elevation country.

The types of country traversed by the lines (column 22) range from flat to rolling, hilly, and even mountainous. Most of the lines are in rolling to hilly country.

The average height of top conductor above ground (column 37) varies from 37 feet to 122 feet, the higher figure being on a 2-circuit line where right-of-way difficulties controlled. The more general range of top conductor elevation is from about 55 to 85 feet.

Towers, Conductors, and Overhead Ground Wires

Towers. The towers may be classified in three general types, as illustrated

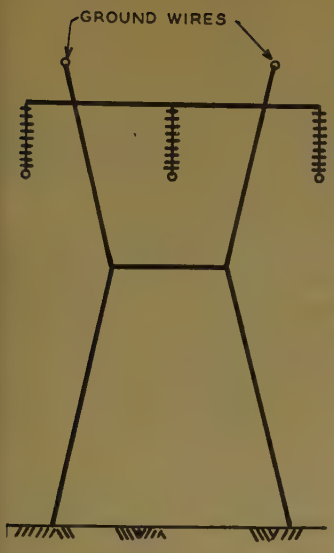


Figure 1 (left). Typical 220-kv single-circuit tower

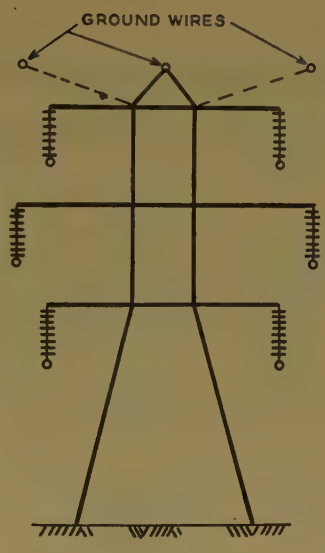


Figure 2. Typical 220-kv double-circuit tower

in Figures 1, 2, and 3. Figure 1 is a single-circuit line with conductors horizontally arranged. About 73 per cent of all the lines reported have this arrangement. Figure 2 is a double circuit structure with conductors vertically arranged. About 26 per cent of the lines have this arrangement. A part of only one line was arranged as in Figure 3, or about 1 per cent of the lines reported.

Line Conductors. The line conductors vary from 500,000 circular mils to 1,034,000 circular mils, with one line 1.4 inch in diameter. About 85 per cent of the lines have aluminum conductor steel reinforced conductors, and 15 per cent copper.

Overhead Ground Wires. About 14 per cent of the lines reported have no overhead ground wires, except that two lines have wires extending out one mile from the terminals. About 19 per cent have one overhead ground wire, and about 67 per cent have two overhead ground wires. The material is steel, aluminum conductor steel reinforced, Copperweld, and copper in the proportion of about 63 per cent, 16 per cent, 11 per cent, and 10 per cent respectively of the lines with overhead ground wires. The sizes vary for the steel wires from 3/8- to 3/4-inch diameter, for the aluminum conductor steel reinforced from 184,000 to 203,000 circular mils, for the Copperweld from 3/8- to 1/2-inch diameter, and for the copper from 2/0 to 4/0.

Insulation

Insulator Strings. In columns 12 and 13 of Table I are given the number of insulator disks and spacings between disks. The spacings vary from $4^3/_4$ to $6^1/_2$ inches. In order to place these on a comparable basis, so that published flashover data may be used, the suspension strings are reduced to equivalent number of units spaced $5^3/_4$ inches apart (column 59). It will be noted that these vary through a wide range, from approximately 10.6 to 18.4 units for lines operated at 220 to 240 kv, 8.4 to 12.3 units for lines operated at 190 to 200 kv, and 21 units for the 287-kv lines.

The critical flashover values of the insulator string[2] based on the 1.5x40 positive impulse wave are given in column 60.

Clearance to Structure. In column 57 is given the clearance to the tower with the conductor swung from the vertical to the angle given in column 58. These angles are 30 degrees, except in one case in which the angle is given as 45 degrees.

In column 61 are given the critical flashover values based on the 1.5x40 positive wave, assuming that the conductors are swung to the angle given in column 58. The rod gap values[2] are used to obtain the flashover values.

It is believed that under the wind and loading conditions prevailing in the lightning months, a 30-degree swing is ample to cover practically all cases.

Average Span

Average span lengths range from 590 feet to 1,320 feet or 9 to 4 towers per mile. The general average for all lines reported is in the order of 1,000 to 1,100 feet, or about 5 towers per mile.

Grading and Arcing Devices

The practice varies in the use of devices to grade the voltage on the insulator string or to take the arc on flashover. Some companies report using grading rings (column 26) or rings and horns, and others report horns only. In the light lightning severity territory of California, horns, or rings and horns, are used even for the early lines built between the years 1914 and 1923.

A number of companies report not using any grading or arcing devices, particularly where lines have been built in the last 15 years or so. It is suggested that the reason for the omission of these devices may be the high immunity from insulator and conductor damage experienced in service. This in turn possibly may be the result of faster clearing of faults over the insulator strings by high-speed circuit breakers or shortened relay time. It seems from the record that the use of grading shields and arcing devices on the newer lines generally is being abandoned.

Analysis of Lightning Performance

The three most important features of line construction that correlate most closely with actual lightning performance, although not necessarily in their order of importance, are thought to be:

1. **Use and location of overhead ground wires.**
2. **Insulation.**
3. **Tower footing resistance.**

Line Outages

The actual line outages are shown in column 54 for all lines. These have been reduced to a 100-mile-per-year basis in column 55 and to an isokeraunic level of 50 in column 56. On the 100-mile-per-year basis, actual outages vary from a high of 11.5 to a low of 0, with an average of about 2.30. The high figure of 11.5, references 7 and 7A, comprises the record of a line which initially was built and operated without ground wires and was located in a heavy lightning territory. It is interesting to note that this line, since protective features such as ground wires, counterpoises, and so forth, were installed, has a record for the past four years of 1.2 outages per 100 miles of line per year.

In case of 2-circuit lines, the single-line outages only usually are considerably

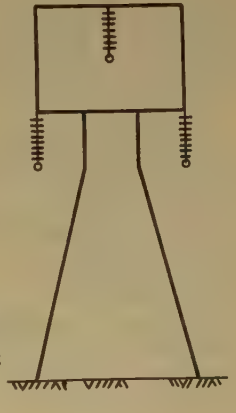


Figure 3. Special 220-kv single-circuit tower

Table I. Lightning Performance and Design Features of 220-Kv Lines

REF	NAME OF CO REPORTING	LINE DESIGNATION	DATE FIRST IN SERVICE	LENGTH OF LINE IN MILES	NO OF CIRCUITS	CIRCUITS PER STRUCTURE	OPERATING KV PHASE TO PHASE	TOWERS			INSULATORS		CONDUCTORS					WIRE SAG		AVG. ELEV. ABOVE SEA LEVEL (FT.)	TYPE OF COUNTRY	NATURE OF SOIL	LIGHTNING SEVERITY	ISOCERAUNIC LEVEL	INSUL. ARCING DEVICES	
								NO. PER LINE	TYPE (FIG. NO.)	AVG. SPAN (FEET)	NO. PER STRING SUSP./D.E.	SPACING (2) (INCHES	LINE SIZE (MCM)	LINE MATERIAL	GR WIRE NUMBER	GR WIRE SIZE (IN. OR MCM)	GR WIRE MATERIAL	GW. ON AVG. SPAN (FEET)	COND. ON AVG. SPAN (FEET)						TYPE	ARC DIST. (INCHES)
1	2	3	4	5	6	7	8	9	10	11	12	13	14	15	16	17	18	19	20	21	22	23	24	25	26	27
1	NEW ENGLAND PWR SERV CO	FIFTEEN MILE FALLS - TEWKSBURY	9/30/30	126 4	2	1	231	1127	1	590	15/17	5 3/4	795	ACSR	2	1/2"	S	12	16	800	MOUNTAINS AND HILLS	ROCK CLAY SAND	—	24	RINGS	79 5
2	SHAWINIGAN WATER AND POWER CO.	NO 25-26	8/6/27	135 3	2	2	190	796	2	910	10/12 (1)	4 3/4 / 5 3/4	397	ACSR	2	7/16"	S	17	20	1000	HILLS ROLLING	GRAVEL	MODERATE	15	(3) HORNS	(4) 47 5
3	"	NO 31	11-/38	108 1	1	1	240	538	1	1060	16/16	5 / 5 3/4	795	ACSR	2	7/16"	S	24	29	600	HILLS ROLLING FLAT	ROCK SAND	MODERATE	15	NONE	—
4	"	NO 35	11/-/40	74 3	1	1	200	388	1	1010	14/14	5 / 5 3/4	605	ACSR	2	7/16"	S	25	25	200	ROLLING FLAT	ROCK CLAY SAND	MODERATE	15	NONE	—
5	PHILADELPHIA ELECTRIC CO	CONOWINGO-PLYMOUTH-MEETING	3/5/28	57 7	2	1	220	261	1	1170	16/18	5 3/4	795	ACSR	2	184	ACSR	29 2	34 8	360	ROLLING	ROCK CLAY	MODERATE	35	RINGS	83 3
6	"	PLYMOUTH MEETING-SIEGFRIED	2/18/28	99	1	1	220	57	1	916	16/18	5 3/4	795	ACSR	2	184	ACSR	18 4	21 9	300	ROLLING	ROCK CLAY	MODERATE	35	NONE	—
6A	PENNSYLVANIA PWR & LIGHT CO	"	2/18/28	38 8	1	1	220	186	1	1100	16/18	5 3/4	795	ACSR	2	184	ACSR	29.0	43 0	500	FLAT ROLLING	ROCK CLAY	SEVERE MODERATE	35	RINGS	82 3
7	"	SIEGFRIED-WALLENPAUPACK TAP ROSELAND	4/11/26	66 2	1	1	220	317	1	1100	14-16/16	5 3/4	795	ACSR	(21) 2	184 7/16"	ACSR CW	18 5	31 5	1000	MOUNTAINS ROLLING	ROCK CLAY SAND	SEVERE	35	RINGS & HORNS	72 0
7A	PUBLIC SERV ELEC. & GAS CO.	SIEGFRIED-ROSELAND.	4/8/32	45 8	1	1	220	211	1	1150	16-18/18-20	5 3/4	795	ACSR	2	203	ACSR	32.9	35 8	700	MOUNTAINS HILLS	ROCK CLAY	MODERATE	35	RINGS	83 3
8	"	PLYMOUTH MEETING-ROSELAND	8/31/30	46 2	1	1	220	235	1	1040	16/18	6	795	ACSR	2	203	ACSR	27 0	29 4	205	ROLLING FLAT	CLAY SAND	MODERATE	33	RINGS	85 3
8A	PHILADELPHIA ELECTRIC CO	"	8/31/30	29 6	1	1	220	145	1	1080	16/18	5 3/4	795	ACSR	2	203	ACSR	26 0	29 4	335	ROLLING	ROCK GRADE CLAY	MODERATE	35	SHIELD	83 3
9	PENNSYLVANIA WATER & PWR CO	SAFE HARBOR-RIVERSIDE	11/1/37	50 0	1	1	220	281	1	940	20/20	5 1/4 / 5 3/4	795	ACSR	2	3/8"	CW	17.1	26 5	330	ROLLING	ROCK CLAY SAND	SEVERE	36	NONE	—
10	"	SAFE HARBOR-TAKOMA TAP-WESTPORT.	12/6/31	92 0	1	1	220	477	1	1020	20/20	5 1/4 / 5 3/4	795	ACSR	2	203	ACSR	21 5	26.5	475	ROLLING	ROCK CLAY SAND	SEVERE	36	NONE	—
11	COMMONWEALTH EDISON CO	POWERTON-CHICAGO.	9/28/40	147 0	2	1 & 2	240	761 (6)	1 & 2	1020	18/20	5 3/4	900	ACSR	2	1/2"	CW	92 (18A) / 268	116 6 (12A) / 386	650	ROLLING FLAT	MOSTLY LOAM	—	45	NONE	—
12	BONNEVILLE PWR ADMINISTRATION	COVINGTON-COULEE NO 1	7/16/42	183 0	1	1	230	850	1	1140	16/18 (8)	5 3/4	795	ACSR	(7)	—	—	—	34	2500	MOUNTAINS TO FLAT	ROCK CLAY SAND	MODERATE	8	—	—
13	"	COULEE-SPOKANE 3 & 4.	3/15/43	82 8	2	2	230	422	2	1035	16/18	5 3/4	795	ACSR	(7)	—	—	33 5	51 5	2800	HILLY TO FLAT	ROCK CLAY SAND	MODERATE	8	(9)	60
14	CITY OF LOS ANGELES	BOULDER DAM-LOS ANGELES 1 & 2.	10/-/36	263 5	2	1 & 2 (10)	287 5	2693	1 & 2	790/970	24/22	5/6	1.4"	CU	2	7/16"	CW	378/158	458/236	2400	MOUNTAINS TO FLAT	ROCK CLAY SAND	MODERATE LIGHT	15	HORNS	110
15	"	BOULDER DAM-LOS ANGELES 3.	5/-/40	263 5	1	1	287 5	1428	1	970	24/22	5/6	1.4"	CU	2	1/2"	S	378	458	2400	MOUNTAINS TO FLAT	ROCK CLAY SAND	MODERATE LIGHT	15	HORNS	110
16	PACIFIC GAS & ELECTRIC CO	PITT LINES NO. 1 & 2. HORIZ CONFIG SECT	1923 (11)	83	2	1	230	-	1	720 (13)	13/12	5	518	ACSR	0	—	—	—	17	2000	HILLS	VARIOUS	LIGHT	5	HORNS	71
16A	"	PITT LINES NO 1 & 2 VERT CONFIG SECT	11/-/23 (12)	214	2 (14)	2 (14)	230	-	2	-	13/12	5/5½	500	CU	0	—	—	—	24	200	ROLLING TO FLAT	CLAY	LIGHT	5	HORN OR SHIELD	71
17	"	TIGER CREEK-NEWARK HORIZ CONFIG SECT	6/-/31	16	2	1	230	-	1	790 (13)	13/13	5½	518	ACSR	0	—	—	—	17	2500	MOUNTAINS	VARIOUS	LIGHT	5	DISC SHIELD	71 5
17A	"	TIGER CREEK-NEWARK. VERT CONFIG SECT	6/-/31	93	2	2	230	—	2	—	13/13	5½	500	CU	0	—	—	—	24	500	HILLS TO FLAT	ROCK CLAY	LIGHT	5	DISC SHIELD	71 5
18	"	BUCKS CREEK-BELLOTA BUCKS CREEK-OROVILLE SECT	(23) 1926	33	1	1	230	-	3	—	14/16	5 3/4	795	ACSR	0	—	—	—	17 5	1000	MOUNTAINS	ROCK VARIOUS	LIGHT	5	DISC SHIELD	80 5
18A	"	BUCKS CREEK-BELLOTA OROVILLE-BELLOTA SECT	11-/44	110	1	1	230	-	2	—	14/16	5 3/4 / 5½	795	ACSR	0	—	—	—	24	150	ROLLING TO FLAT	VARIOUS	LIGHT	5	DISC SHIELD	77
18B	"	BUCKS CREEK-BELLOTA BELLOTA-HERNDON 1 & 2	6/-/31	102	2	2	230	-	2	—	14/16	5 3/4 / 5½	500 CU / 795	ACSR	0	—	—	—	24	150	ROLLING TO FLAT	VARIOUS	LIGHT	5	DISC SHIELD	77
19	METROPOLITAN WATER DIST OF SO CAL	BOULDER	11/1/38	237	1	1	230	945	1	1320	13/15	5 3/4	795	ACSR	2 (20)	1/2"	S	24	35	2000	HILLS TO FLAT	MOSTLY CLAY	MODERATE	15	NONE	—
20	HYDRO-ELECTRIC PWR COMMISSION OF ONTARIO	PAUGAN-CHATS FALLS-LEASIDE HASTINGS-LEASIDE SECT	10/1/28	110.7	3	1	220	1666	1	1050	18/18	5 / 5 3/4	795	ACSR	2	3/8"	S	32	36	600	HILLS	ROCK CLAY SAND	—	25	NONE	-
20A	"	PAUGAN-CHATS FALLS-LEASIDE, PAUGAN-CHATS FALLS-HASTINGS SECT.	10/15/31	117 3	(24) 2&3	1	220	1631	1	1050	18/18	5 / 5 3/4	795	ACSR	2	3/8"	S	32	36	800	HILLS	ROCK CLAY SAND	—	25	NONE	-
21	"	BEAUHARNOIS-MASSON-CHATS FALLS	7/1/33	128 2	1	1	220	516	1	1310	18/18	5 / 5 3/4	795	ACSR	2	3/4"	S	32	36 5	250	FLAT	MOSTLY CLAY	—	25	NONE	—
22	"	LEASIDE-BURLINGTON	8/-/41	44 8	2	2	220	273	2	870	18/18	5 / 5 3/4	500	CU	1	3/8"	S	25 3	34	550	ROLLING	CLAY	—	25	NONE	-
23	"	BEAUHARNOIS-LEASIDE	4/9/41	300.5	1	1	220	1404	1	1125	18/18	5 / 5 3/4	795	ACSR	2	3/8"	S	32	36	250	HILLS ROLLING FLAT	—	—	25	NONE	-
24	SO CAL EDISON CO LTD.	NORTH & SOUTH LIGHTHIPE-LAFRESA	2/27/30	97	2	2	220	57	2	900	13/15	—	667	ACSR	1	2/0	CU	12	13	—	FLAT	SAND	—	5	RING & HORN	—
25	"	BIG CREEK 2-2A-3	7/15/28	5.9	1	1	220	29	1	1080	13/15	6¼	667	ACSR	2	3/0	CU	31	39	2950	MOUNTAINS	ROCK	LIGHT	5	RING & HORN	—
26	"	EAST & WEST EAGLE-BELL	1923	268	2	1	220	(132 (27) / 128	1	1090	13/15	5¾ / 6½	667	ACSR	1&2	1/2"	S	19	23	1490	MOUNTAINS TO FLAT	ROCK CLAY SAND	LIGHT	5	RING & HORN	—
27	"	BIG CREEK 3 MAGUNDEN	1/29/28	12.8	1	1	220	457	1	1480	13/15	6¼	1034	ACSR	2	1/2" / 9/16	S	33	34	2638	MOUNTAINS TO FLAT	ROCK CLAY SAND	LIGHT	5	RING & HORN	—
28	"	MAGUNDEN-EAGLE ROCK	11/14/26	102 6	1	1	220	470	1	1150	13/15	6¼	1034	ACSR	2 (28)	1/2 / 9/16	S	30	31	3020	MOUNTAINS TO FLAT	ROCK CLAY SAND	SEVERE	5	RING & HORN	—
29	"	CHINO-BARRE	9/20/39	26	2	(29) 1&2	220	116	1&2	1190	15/16	5 3/4	605	ACSR	(30) 1&2	1/2"	S	21	28	905	HILLS TO FLAT	CLAY SAND	—	5	HORNS	—
30	"	CHINO-LAGUNA BELL	1/29/42	33 4	1	1	220	132	1	1340	15/15	5¾ (31) / 6½	605	ACSR	1&2	2"	S	17	23	830	HILLS TO FLAT	CLAY SAND	—	5	RING & HORN	—
31	"	EAST & WEST LIGHTHIPE-LAGUNA-BELL	10/30/27	7.0	2	1	220	68	1	1090	14/15	6¼	1034	ACSR	1	1/2"	S	14	16	80	FLAT	SAND	—	5	RING & HORN	—
32	"	BARRE-LIGHTHIPE	8/10/41	15 8	1	1	220	91	2	920	14/15	6½	605	ACSR	1	1/2"	S	12 5	15	68	FLAT	SAND	LIGHT	5	HORNS	—
33	"	EAST & WEST BIG CREEK	4/14/14	243 7	2	1	(32) 220	3448	1	700	11/13	5¾	667	ACSR	2	1/2"	S	8	11	2870	MOUNTAINS TO FLAT	ROCK CLAY SAND	LIGHT	5	RING & HORN	-
34	"	EAST & WEST LONG BEACH-LIGHTHIPE	6/16/28	9.8	2	2	220	55	2	945	15/15	6½	650	CU	1	4/0	CU	27	24	—	FLAT	SAND	—	5	—	—
35	"	NORTH & SOUTH BOULDER-CHINO	(33) 11/15/41	233 7	2	1	220	1652	1	750	15/16	5 3/4	605	ACSR	2	1/2"	S	18	31	2870	MOUNTAINS TO FLAT	ROCK CLAY SAND	LIGHT	15	HORNS	—

1. Suspension assemblies: 12 units after 1943–44.
2. First value suspension; second value dead end.
3. Armor rods on 25 per cent of line.
4. 57 inches after 1943–44.

4A. 4.8 after 1943–44.

5. 10.5 after 1943–44.
6. 637 towers: 1 circuit per tower. 124 towers: 2 circuits per tower.
7. 1 mile of ground wire at terminals only.
8. 20 per cent porcelain, 80 per cent glass.

8A. Apparently now being added.

9. Experimental devices on 25 per cent of line (not described).
10. 222.65 miles: 1 circuit per tower. 40.85 miles: 2 circuits per tower.
11. 60 miles in 1923, 9 miles added in 1925, 14 miles added in January 1944.
12. 142 miles: 2 circuits in 1923. 43 miles: 1 circuit added in March 1944. 29 miles: 2 circuits added in April 1944.
13. Data from 1935: 220-kv paper.
14. Except 43 miles of single circuit.
15. See note 23.
16. Estimated.
17. To August 1, 1945.

Table I. Lightning Performance and Design Feature of 220-Kv Lines (Continued)

TOWER FOOTING RES. (OHMS) BEFORE AUX. GROUNDING			AFTER AUX. GROUNDING			AUXILIARY GROUNDING	LIGHTNING PROT. OTHER THAN G.W. AND LOW GR. RES.	LTN. IMPROVE. BEING CONSIDERED	TOP COND. ABOVE GROUND (FT.)	WIRE SPACING AT TOWER (FEET-MIN) COND. HORIZ.	COND. VERT	GR. WIRE HORIZ	GR. WIRE VERT	LIGHTNING OUTAGES ONE CIRCUIT / TWO CIRCUIT 1934	1935	1936	1937	1938	1939	1940	1941	1942	1943	1944	1945	AVG PER YEAR	AVG. PER 100 MI. PER YEAR ACTUAL	50 (26) LEVEL	LINE CLEARANCE TO STRUCTURE AT COND. SWING OF (DEG.) FT.	MIN NO INSULATORS EQUIV. 5¾ IN. UNITS	1½X40 μSEC CRITICAL POS. IMPULSE KV. INSULATORS	AIR CLEARANCE AT 30° SWING	MAX SHIELDING ANGLE (DEGREES) (25)	REF
MAX	MIN	AVG	MAX	MIN	AVG	34	35	36	37	38	39	40	41	42	43	44	45	46	47	48	49	50	51	52	53	54	55	56	57	58	59	60	61	62	63
28	29	30	31	32	33																														
—	—	—	—	—	—	NO	NO	NO	44.2	235	—	250	148	3	1	10	9	10	4	9	4	6	8	11	—	6.8	5.4	11.3	72	45	15	1345	(AT 45°) 1340	37/40	1
—	—	150	—	—	LOW	2 CONT CP.	NO	NO	73.5	235 33.5	12	335	98 (5)	11/11	1/3	0/3	3/5	1/7	4/0	0/3	0/2	0/2	0/2	1/0	—	19/35	14/2.6	47/8.7	(44) 4	30	8.43	820	780	27	2
200	10	150	45	—	—	CP & GR (8A)	NO	YES ADD 2 CP.	63.3	253	—	265	12.8	—	—	—	—	5	2	0	2	1	1	1	—	1.7	1.6	5.3	65	30	14 48	1310	1220	43/46	3
300	5	50	—	—	—	2 CONT CP+CP	NO	NO	62.2	26 5	—	37.0	22.5	—	—	—	—	—	—	—	0	0	0	0	—	0	0	0	55	30	12 30	11 30	10 40	20/39	4
—	—	—	—	—	242	MISC CP	NO	NO	62.0	255	—	255	16.1	0	1	2	3	1	0	2	4	1	1	0	—	1.4	2.4	3.4	6.0	30	16	1425	1125	38	5
—	—	—	—	—	—	ONE 600'CP	NO	NO	62 0	255	—	255	16.1	0	0	2	2	1	1	0	2	0	0	0					80	30	16	1425	1475	38	6
61	47	15	—	—	—	NO	NO	NO	65 9	26.3	—	238	13 6	0	0	2	2	1	1	0	0	0	0	0	2 (17)	0 83	1 7	2 4	7.8	30	16	1425	1445	47/41	6A
330	5	75	40	1	5	CP	NO	NO	66 0	22 5	—	23.1	10.1	12	14	28	29	18	18	16	(20)	0	1	2	3 (17)				70	30	14	1265	1300	47	7
300	1	64	27	1	18	CP	NO	NO	62 5	28 5	—	285	14.8	0	1	1	1	0	0	(18)	(18)	(18)	(18)	(18)	—	12 9	11 5	17 0	76	30	16	1425	1405	44	7A
105	0	6	-	—	—	NO	NO	NO	62 5	28 5	—	285	14 8	0	1	0	0	1	1	(18)	(18)	(18)	(18)	(18)	—				76	30	16 65	1480	1405	44	8
28	18	10	—	—	—	ONE 650'CP	NO	NO	62 7	25 5	-	43 0	16 2	0	1	0	0	1	1	1	2	0	0	2	-	0 73	0 96	1 45	73	30	16	1425	1360	14/53	8A
150	1	67	19	1	10	CP	NO	NO	58.3	28 3	—	42.3	25.7	—	—	—	—	0	0	0	1	1	1	0	—	0 43	0.86	1 20	90	30	18 35	1615	1655	15/39	9
130	1	74	32	1	12	CP & GR	NO	NO	58.3	28.3	—	42.3	25 7	0	0	0	0	0	0	0	0	0	1	0	—	0.091	0.099	0.137	90	30	18 35	1615	16 55	15/39	10
—	—	—	5	-	18	CP & GR.	NO	NO	100 (18A) 65 2	40 (18A) 33 3	20 6	48 (18A) 46 3	23 (18A) 29	-	-	—	—	—	—	0	0	0	0	0	—	0	0	0	93	30	18	1585	1710	19/39	11
—	—	—	850	13	—	GR.	(9)	(9)	37	27	—	37 (7)	23 (7)	—	-	-	—	—	—	—	—	5	1	8	—	47	2 6	16 2	50	30	16	1425	945	—	12
—	—	—	350	12	—	GR	(9)	(9)	376	38/31	20 3	—	22 4 (7)	—	—	—	—	—	—	—	—	7/1	6/2	3/1 (18)	5.3/1 3	64/1 6	40/10	50	30	16	1425	945	—	13
50	-	1	7 6	0.4	0 8	2-CP	NO	NO	112 / 77 1	40 5 / 32 5	24 5 / —	401 / 50	32	—	—	0/0	0/0	0/0	1/0	0/0	0/0	0/0	1/0	0/0	—	0 22/0	0 08/0	0 27/0	90	38	21	1825	1655	13/38	14
50	-	1	7 6	0 4	0 8	2-CP	NO	NO	77 1	32 5	-	50	32	-	-	-	-	-	—										90	30	21	1825	1655	13/38	15
	-	-	500 (16)	2 (16)	3 (16)	2' SQ PLATE	NO	YES GW.	441	19 5	—	—	—	2	1	3	2	1	2	2	0	2	0	2	-	15	19	19 0	45	30	10 57	1000	865	—	16
-	-	—	11 (16)	0.8 (16)	4 (16)	2' SQ PLATE	NO	YES GW.	84 9	24	15	-	—	4/0	8/0	1/0	0/0	4/0	10/0	1/0	1/0	5/0	1/0	1/0	(19) 0/0	38/0	25/0	25/0	5	30	11 05	1030	945	—	16A
—	—	—	100 (16)	2 (16)	15 (16)	GR	NO	NO	46 7	20	—	—	—	0/1	0/0	0/0	0/0	0/0	0/0	0/0	0/0	0/0	0/0	0/0	-	0/0 09	0/0 56	0/5 6	45	30	12 46	1145	865	-	17
—	—	—	100 (16)	2 (16)	15 (16)	GR	NO	NO	85 3	28	15	—	—	0/0	2/0	3/0	4/0	0/0	7/0	0/0	4/1	1/0	1/0	0/2	1/0 (19)	19/0 25	2.0/0 27	20/2 7	43	30	12 46	1145	825	—	17A
(16) 00	(16) 2	(16) 15	—	—	—	NO	NO	NO	—	27	—	—	—	—	—	—	—	—	—	—	—	—	—	0	3 (19)	15	45	45	55	30	14	1265	1040	—	18
(16) 00	(16) 2	(16) 15	—	—	—	NO	NO	NO	87	27 3	16	-	—												7/0 (19)	15/0 08	0 71/0 08	71/0 8	57	30	14	1265	1080	-	18A
(16) 00	(16) 2	(16) 15	—	—	—	NO	NO	NO	87	27.3	16	-	—	0/0	1/0	0/0	0/0	1/0	1/0	3/0	2/0	1/0	1/0	1/1					57	30	14	1265	1080	-	18B
31	1	11 5	—	—	—	NO	NO	NO	70.5	22 3	—	31 9	16 5	—	—	—	—	—	37	22	26	33	1 (20)	0	-	19 8	8 4	28	51	30	13	1185	960	21/44	19
200	3	25	—	—	—	NO	NO	NO	54 7	25 3	-	26 8	13 3	1	2	1	4	3	0	0	2	2	2	2	-	1 7	1 55	2 10	8	30	15 78	1415	1475	41/45	20
150	2	250	1550	2	250	CP (22)	NO	NO	54 7	25 3	-	26 8	13 3	10	4	6	4	9	12	4	17	6	18	16	-	9.64	8 24	16 48	8	30	15 78	1415	1475	41/45	20A
200	2	25	—	—	—	NO	NO	NO	54 7	25 3	—	26 8	13 3	1	2	1	0	0	2	0	1	0	1	1	-	0 82	0 64	1 28	8	30	15 78	1415	1475	41/45	21
14	1	3 7	-	—	—	NO	NO	NO	—	34/54	20	—	—	—	—	—	—	—	—	—	—	1	3	0	-	1 3	2 97	5 94	8	30	15 78	1415	1475	—	22
200	1	47	25	1	65	CP	NO	NO	54 7	25 3	—	21 3	26 9	—	—	—	—	—	—	—	3	0	4	1	-	2 0	0 67	1 34	8	30	15 78	1415	1475	29/32	23
—	—	—	—	—	—	NO	NO	NO	121 1	31 0	20 0	—	17 6	—	—	—	—	—	—	—	—	—	—	—	—	—	—	—	—	—	—	—	—	41	24
—	—	—	—	—	—	NO	NO	NO	51 9	22 2	—	24 0	12 7	0	0	0	0	0	0	0	0	0	0	0	—	0	0	0	—	—	14 05	1270	—	39/44	25
—	—	—	—	—	—	NO	NO	NO	52 5	22 2	-	24 0	12 5	0	0	0	1	0	0	0	2	0	1	1	-	0 46	1 72	17 2	-	-	13	1185	—	39/44	26
—	—	—	—	—	—	NO	NO	NO	55 3	22 2	—	24 0	12 7	0	0	0	0	0	2	0	1	0	0	2	—	0 45	0 35	3 5	6	30	14 05	1270	1125	39/44	27
—	—	—	—	—	—	NO	NO	NO	55 3	22 2	—	24 0	12 7	1	3	1	0	12	7	3	4	1	4	3	-	(18) 3.54	3.45	34 5	6	30	14 05	1270	1125	39/44	28
—	—	—	—	—	—	NO	NO	NO	227 / 638 (18A)	165 (18A) / 23	20 / - (18A)	— / (18A) 24	16 / (18A) 11 7	—	—	—	—	—	0	0	0	0	0	0	-	0	0	0	45	30	15	1345	865	43/46	29
—	—	—	—	—	—	NO	NO	NO	70 8	23.0	—	24.0	11.7	—	—	—	—	—	—	—	0	0	0	0	-	0	0	0	45	30	15	1345	865	43/46	30
—	—	—	—	—	—	NO	NO	NO	51 4	22 2	—	—	13 2	—												—	—	—	—	—	15 15	1360	—	59/0	31
—	—	—	—	—	—	NO	NO	NO	122 7	33 0	20	—	16	—	—	—	—	—	—	—	0	0	0	0	—	0	0	0	—	—	15 68	1405	—	46	32
—	—	—	—	—	—	NO	NO	NO	35 7	17 2	—	18	10 8	1/0	0/0	0/0	1/0	2/0	4/0	2/0	1/0	0/0	1/0	2/0	-	1.27/0	0 52/0	5 2/0	-	—	11	1025	—	37/40	33
—	—	—	—	—	—	NO	NO	NO	110	33	20	—	17	—	—	—	—	—	—	—	—	—	—	—	—	—	—	—	—	—	16 85	1510	—	44	34
00	0.5	-	70	0.5	18	TOWER CP.	NO	NO	70.6	23	—	24	11.7	—	—	—	—	—	0	3	0	1/0	1/0	0/0	—	0 83/0	0 36/0	1.2/0	45	30	15	1345	865	43/46	35

18. Data not reported.

18A. First value for 2-circuit towers. Second value for 1-circuit towers.

19. To September 1, 1945.

20. Ground wire installed 1943.

21. Line completely equipped with ground wire 1941.

22. Counterpoise as required to reduce resistance to 25 ohms. First 10 miles from Chats Falls only.

23. Operating at 165 kv to January 1944.

24. 88.5 miles is 3 circuit. 28.8 miles is 2 circuit.

25. First number for outer conductor. Second number for middle conductor.

26. On basis of 50 isokeraunic level.

27. First figure for east line. Second figure for west line.

28. No ground wire for 64 miles of line due to severe sleet loading.

29. 17 miles: 1-circuit towers. 9 miles: 2-circuit towers.

30. 17 miles: 2-ground wires. 9 miles: 1-ground wire.

31. Also some 12 and 14 units of fog type in suspension.

32. Originally designed for 150 kv.

33. North line June 22, 1939.

Table II. Extent of 220-Kv[1] Lines

13 Companies, 35 Lines

		Approximate Miles
Single circuit	Right of way	1,838
Two circuit on single towers	Right of way	717
Two circuit on separate towers	Right of way	970
Three circuit on separate towers	Right of way	463
Total miles	Right of way	3,988[2]
Total circuit miles of 3-phase line		6,601[2]

1. 135.3 miles of right of way operated at 190 kv and 263.5 miles operated at 287 kv.

2. Not including 550 miles of right of way for company references 12 and 13 (Table I) which were mentioned but not reported on.

Table III. Average Lightning Outages[1] on 220-Kv Lines

	Right of Way, Miles	Outages Per Year Actual	Outages Per 100 Miles of Line Per Year on Basis of 50 Storms Per Year
All lines	3,988.5	92.83	9.97
Lines without ground wires	916.8	21.92	19.30
Lines with ground wires	3,071.7	70.91	7.19
With ground wires[2]	349.0	32.70	24.20
With 1 ground wire	87.1	1.3	4.3
With 2 ground wires	2,446.8	32.91	3.8
With 1 and 2 ground wires[3]	86.2	0.46	0.53
With ground wire on part of line only	102.6	3.54	34.5

1. Based on actual outages and actual miles (not average of columns 55 and 56, Table I).

2. Lines having ground wire added during period of outage record 1934–45.

3. Lines having 1 ground wire on part of line, balance 2 ground wires.

higher than 2-line outages, as would be expected. The one exception is the case of line reference 2, where the single-circuit outages on a 100-mile-per-year basis is 1.4, and double-circuit outages 2.6, or nearly double.

The outage record seems to indicate clearly that, even with the highest insulation used in 220-kv lines, the insulation alone does not render the line lightning-proof without the aid of other remedial measures, such as ground wires and low tower-footing resistances.

Overhead Ground Wires

Benefit of Use. A summary of lightning outages for all lines and for lines with and without ground wires is given in Table III. Of the nearly 4,000 miles of line (right of way) covered by this report, the outages on a 100-miles-of-line-per-year basis at a 50 isokeraunic level is 9.97. Twenty-three per cent of the line mileage does not have ground wire, and its outage record is 19.3 per 100 miles of line per year. Of the line mileage 63.5 per cent has either one or two ground wires over the entire line, and its outage record is 3.8 to 4.3 outages on the above basis, the lower figure being for two-ground-wire lines, and the higher for the single-ground-wire groups.

In Figure 4 a further breakdown of the outage data on nonground-wire and ground wire lines where tower footing resistances were reported is shown. Based on a 50 isokeraunic level, the average outages per 100 miles of line per year is 27.5 for lines without ground wires, and 4.5 for ground wire lines. Ground wire lines of over 25 ohms average footing resistance have 15.4 outages, and lines with 25 ohms or less 1.94 outages.

The foregoing record clearly demonstrates the value of overhead ground wires and low footing resistance in reducing lightning outages.

Height and Spacing. Column 40 gives the horizontal spacing between the overhead ground wires where there are two ground wires. These spacings vary from 21 to 48 feet for the lines in the 190- to 240-kv class and from 40 to 50 feet for the 287-kv lines. The height of the ground wire plane above the plane of the conductors at the towers is given in column 41. This varies from approximately 10 to 29 feet for the 190- to 240-kv class lines and is 32 feet for the 287-kv lines. In Figure 5 is plotted the height of ground wires above conductors from column 40 against outages per 100 miles per year at isokeraunic level 50 from column 56. In cases where two ground-wire heights are given in the length of the line, the average height is plotted.

There does not appear to be any consistent relation between height of ground wires and outages experienced. A number of lines with heights ranging from 22.5 to 32 feet show outages from zero to 1.34 per 100 miles per year (column 56), but other lines with heights from 11.7 to 16.2 feet show outages in the same range. For example, two lines, 21 and 23, with the same impulse insulation level, 1,415 kv, show practically the same outage performance (1.28 and 1.34 per 100 miles per year,, although one has the ground wires 13.3 feet and the other 26.9 feet above the conductors.

Shielding Angle. In column 62 is given the angle between a vertical line through the ground wire and the slanting line between the ground wire and line conductor, or the so-called shielding angle. This angle varies widely, from a minimum of 13 degrees to a maximum of 47 degrees for the outside conductors of horizontally arranged lines and for the top conductor of vertically arranged lines. For the middle conductors of horizontal lines the angle is in one case as much as 53 degrees. In Figure 6 are plotted shielding angles from column 62 against tripouts per 100 miles per year at isokeraunic level 50 from column 56. Where the angle for middle conductor is different from the angle for outside conductor, the angle for the outside conductor is used.

The relationship between shielding angle and outages does not follow a consistent pattern. There is a zone of low outages with shielding angles ranging from 13 to 44 degrees (zero to 1.5 outages per 100 miles per year). Low footing resistance seems to be more important than small shielding angle.

Insulation Values

The flashover strength of the line is the lower of the values given in columns 60 or 61, that is, the insulator string flashover or the flashover from conductor to tower when the conductor is in the swung position.

In Figure 4 are plotted the impulse flashover strengths of the various lines (taking the value from column 60 or 61, whichever is lower), against the number of outages reduced to a common isokeraunic level of 50. The points are pretty well scattered, as a result of the masking effect of ground wires and tower footing resistance already discussed.

It will be noted, on comparing columns 60 and 61, that in many cases the flashover strength in column 61 is less than the insulator flashover in column 60. That is, the clearance from conductor to tower is not sufficient to develop the full strength of the insulator strings.

Mid-Span Flashovers

The possibility of getting mid-span flashovers long has been an unanswered question. If such occur to any extent, they are always difficult to detect, as the evidence, such as burned conductor at mid-span, is almost impossible to locate with certainty in the field.

A study of this feature from the data of Table I shows that mid-span clearances between ground wires and conductors have been increased by all companies. The vertical separation between ground wire and top conductor varies from 9.8

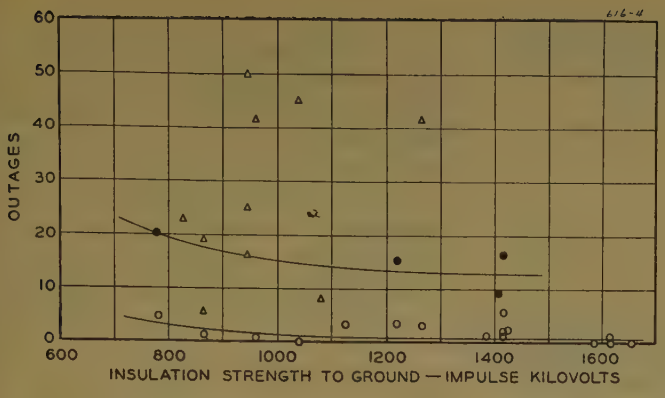


Figure 4. Insulation strength to ground versus outages per 100 miles of line per year at isokeraunic level of 50

△—No overhead ground wire
•—Over-25-ohms footing resistance
○—25-ohms footing resistance

to 32 feet at the tower (column 41) with an increase of minus 3 feet to 18 feet at mid-span (columns 19 and 20) with a general range of 10 to 15 feet increase on the lines of newer design where this feature apparently was given consideration. Whether this increase in ground-wire-to-conductor spacing was predicated on lightning performance only or, in some cases, on sleet considerations, the records at hand do not show.

Taking the rough average height of ground wire above conductor at the tower as 15 feet, the increase in mid-span as 15 feet, and an average shielding angle of 30 degrees, there results an average ground-wire-to-line-wire separation of about 35 feet. At 180 kv per foot spark-over in air, this spacing would have a 1.5x40-microsecond positive wave critical flashover of about 6,300 kv and, of course, much higher on a steep-front short-tail lightning voltage wave. Comparing these values with the insulation flashover at the tower, which range from about 800 to 1,600 kv, there does not seem much likelihood of mid-span flashover in general, even with waves of extremely rapid rate of rise.

Tower Footing Resistance

The data given on tower-footing resistance are rather meager in many instances (columns 28 to 33 inclusive) but do indicate extremely wide variations between maximum and minimum on particular lines, for example, 2 to 1,550 ohms on line 20*A*.

In some cases a marked decrease may be noted after counterpoises or ground rods have been used. As an example, the maximum footing resistance of line 3 came down from 700 to 45 ohms.

Means for Reducing Footing Resistances. In about 68 per cent of the lines reported, means have been taken to reduce the tower footing resistances. These means consist of various arrangements of counterpoises, driven rods, and buried plates, the percentages of the cases where

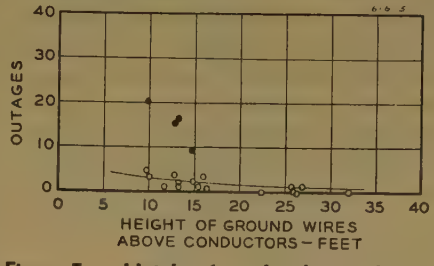


Figure 5. Height of overhead ground wires versus outages per 100 miles of line per year at isokeraunic level of 50

•—Over 25-ohms footing resistance
○—25-ohms-or less footing resistance

improvements have been made being about 62, 28, and 10 per cent respectively.

Effect on Outages. In Figures 4, 5, and 6 are plotted line outages against insulation strength, height of ground wire, and shielding angle, for two different ranges of footing resistance, that is, over 25 ohms and 25 ohms or less. In some instances a change was made in the shielding or in the footing resistance during the period covered, and these data were prorated for the figures. The benefit of low footing resistance is apparent from these figures.

Line Damage

Although a definite attempt was made by specific questions in the questionnaire to obtain information on line damage including damage to insulators, broken strings, and damaged conductors, replies

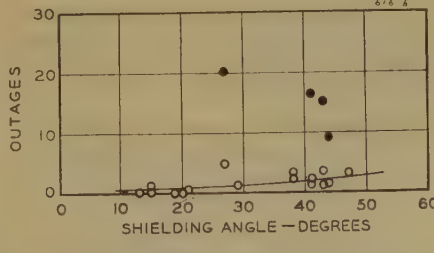


Figure 6. Shielding angle of ground wire versus outages per 100 miles of line per year at isokeraunic level of 50

○—25-ohms-or-less footing resistance

indicated that these are so extremely rare as not to present a real problem. Only two companies reported damage of any kind to hardware or conductors. One reported two cases where an insulator string was severed, and the other reported shattered insulators.

Likewise, duration of line tripouts of lines in this voltage class does not appear, from the replies received, to be of great concern. In one of the cases mentioned the line was out for ten hours. The second company reported merely "long outages" without giving the time involved.

Improved Lightning Performance Being Considered

Only three companies report that they are giving any consideration to making further changes in their line construction to improve its lightning performance. One (reference 3) is adding two counterpoises. The second company (references 12 and 13) is experimenting with devices not described in an attempt to better the line performance. Still a third company (references 16 and 16*A*) reports that it is considering installing ground wires because of the increase in lightning outages reported during the past year. This improvement apparently is being considered on only one line of the company. It should be noted in this connection that this line is in an area where the isokeraunic level is indicated as 5.

Summary and Conclusions

The lightning outage records of 35 transmission lines in the 220-kv class (operating at 190 to 287 kv) have been presented and discussed. Data also are given on some of the design features of these lines which are believed to be factors in their lightning performance.

If equal lightning intensities are assumed, theory and experience have shown that certain factors have a predominating influence on flashovers and outages, namely:

1. Overhead ground wires.
2. Insulation strength.
3. Tower footing resistance.

In the data disclosed by the present survey, it is difficult to separate definitely these influences and to place relative values upon them. However, the following conclusions seem to be justified:

1. The beneficial effects of overhead ground wires clearly is indicated in reducing lightning outages. Nonground-wire lines have a yearly outage record per 100 miles of line per year of 19.3 against 7.19 for lines now

Combined Light and Power Systems for Industrial Plants

D. L. BEEMAN
MEMBER AIEE

THE upward trend in illumination levels in industrial plants has resulted in an increased power demand of the lighting load. Illumination levels of 50 foot-candles are in general considered good practice at the present time, with some thinking of illumination levels as high as 100 foot-candles. The lighting load is a sizable portion of the total plant load. In many average manufacturing plants the lighting load will represent 2 to 4 volt-amperes per square foot, and the power load 8 to 10 volt-amperes per square foot. The same technique that has been applied in distributing power to machine tools and other power loads will pay dividends in distributing power to the lighting load.

For incandescent lamps 120-volt systems have been used almost universally. Higher-voltage incandescent lamps are fragile and generally not satisfactory.

With the introduction of fluorescent lamps the 120-volt restriction no longer applies. All fluorescent lamps have ballasts in series with them. By combining a slight transformer action with the ballast, the fluorescent lamp ballast can be supplied at any voltage from 120 to 260 volts. The industry, however, has standardized on the following ballast ratings: 118, 208, 230, and 260 volts. The introduction of higher-voltage fluorescent lamp ballasts has opened new avenues for using higher-voltage lighting circuits, thereby reducing the cost of the power system which supplies the lighting load. The trend toward load center power distribution systems also has enabled the use of combined light and power systems for industrial plants. This paper outlines the economy of combined light and power systems and higher-voltage lighting circuits.

Paper 46-52, recommended by the AIEE committee on industrial power applications for presentation at the AIEE winter convention, New York, N. Y., January 21–25, 1946. Manuscript submitted November 23, 1945; made available for printing December 4, 1945.

D. L. BEEMAN is in the industrial engineering divisions, General Electric Company, Schenectady, N. Y.

Conclusions

1. Combined light and power systems are less expensive than systems using separate substations for light and power.

2. High-voltage lighting circuits are generally most economical when using 260-volt 2-lamp 100-watt fluorescent lamp ballasts, so that the lighting load may be operated directly off the 480–277-volt substation

Table I. Cost Per Kilovolt-Ampere of Transformers, Panel Boards, and Wiring as a Function of Ballast Voltage

Line	Ballast Voltage	Transformer Rating	*Transformer Cost, Installed	**Panel Board Cost, Installed	Branch Wiring Cost (See Figure 8)	Total Cost
1	118	3 phase, 480–208Y–120 volt	12.50	5.60	6.40	$24.50
2	208	3 phase, 480–208Y–120 volt	12.50	5.60	3.80	21.90
3	120	1 phase, 480–240–120 volt	11.50	5.60	6.40	23.50
4	230	1 phase, 480–240–120 volt	11.50	5.25	3.00	19.75
5	260	1 phase, 480–265–132.5 volt	11.50	4.85	2.50	18.85

* Installation included at $2.50 per kilovolt-ampere.

** Installation included at $1.85 per kilovolt-ampere.

having ground wires (Table III). For lines having ground wires throughout the ten years covered by this report, the corresponding outage figures are 4.3 for one-ground-wire lines and 3.8 for two-ground-wire lines. One outstanding case of the benefits of ground wires is shown on line reference 7, where the observed outages averaged 19.2 for 7 years before the line had ground wires and 1 per year for 4 years after 2 ground wires were installed.

2. The sag of ground wires ranges from 11 to 45 feet, averaging 25 to 30 feet. Vertical separations between ground wire and line wire at mid-span are greater than at the tower by a range from minus 3 to 18 feet, with a general average of about 15 feet.

3. The shielding angles of ground wires vary from 13 to 59 degrees with a trend indicated that the smaller shielding angles reduce line outages.

4. Regarding overhead ground-wire location, in general these are placed from 9.8 to 32 feet above the horizontal plane of the top conductors at the towers. The general average of elevation of the ground wire, however, is about 15 feet above the top conductor.

5. Insulation supplied by a practical length of insulator string, or by a similar air clearance from conductor to tower, is not sufficient in the 220-kv class to prevent lightning flashover of the line. Flashovers have been experienced on the lines reported with impulse strengths as high as 1,600 kv.

6. Where reduction of tower footing resistances has been made, the final average values range in the general order of 1 to 20 ohms. The data submitted show definite benefits derived from the lowering of ground resistance. Reduction of ground resistances to 10 ohms or less reduces outage rates to the order of 1 per 100 miles of line per year, assuming shielding of the type reported herein, and an isokeraunic level of 50.

7. The reduction of tower footing resistances has been accomplished largely by ground rods and counterpoises, with the use of counterpoises predominant.

8. Average span lengths range from 590 to 1,480 feet with the majority of lines having a span of approximately 1,100 feet. There are insufficient data to indicate the effect of these practical span lengths on the lightning outage record of the lines.

9. Arcing devices on insulator strings, which were prevalent in the earlier designed lines, are being omitted on later built lines, with no adverse operating experience reported.

10. Damage to lines, caused by lightning, appears in general to be very infrequent and of minor concern to the service performance of the lines. Only two companies report prolonged outages; these involved shattered or broken insulators. Both cases were on lines not equipped with ground wires.

References

1. LIGHTNING PERFORMANCE OF 220-KV LINES, AIEE Lightning and Insulator Subcommittee. AIEE TRANSACTIONS, volume 53, 1934, November section, pages 1443–7; AIEE Lightning Reference Book, pages 1272–6. Discussion, AIEE TRANSACTIONS, volume 54, 1935, July section, pages 780–1.

2. FLASHOVER CHARACTERISTICS OF ROD GAPS AND INSULATORS, Edison Electric Institute-National Electrical Manufacturers Association Subcommittee on Correlation of Laboratory Data. AIEE TRANSACTIONS, volume 56, 1937, June section, pages 712–14.

3. THE DISTRIBUTION OF THUNDERSTORMS IN THE UNITED STATES, W. H. Alexander. *Monthly Weather Review*, July 1924.

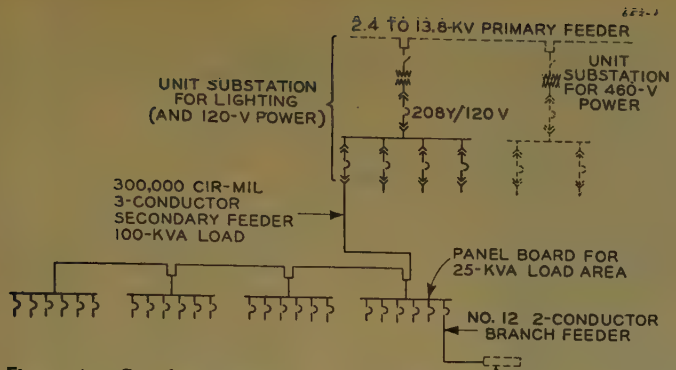


Figure 1. One-line diagram of system with separate substations for power and light services—system *A*

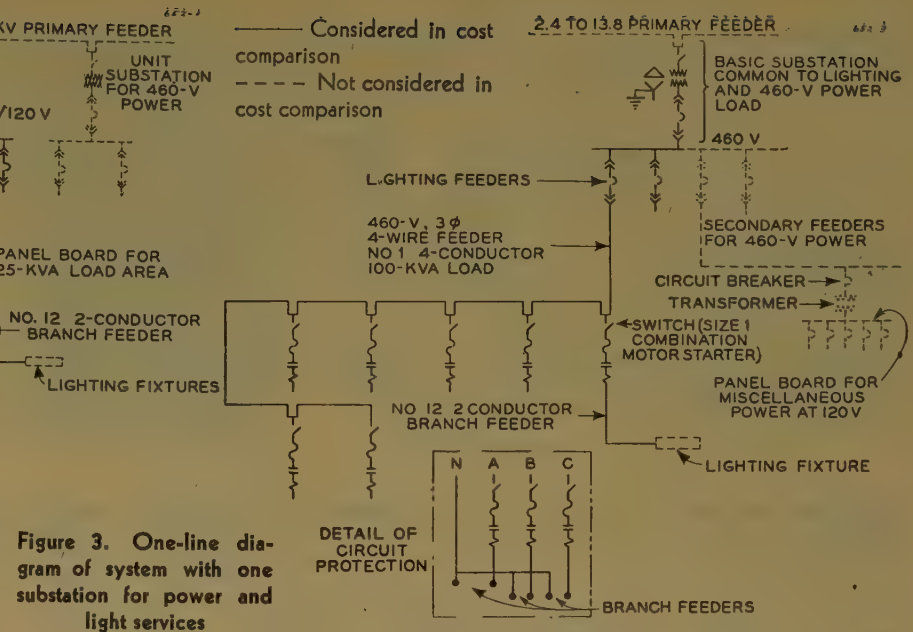


Figure 3. One-line diagram of system with one substation for power and light services

260-volt fluorescent lights supplied from 460-volt feeders—system C

without intervening transformation. Generally 120 volts are most economical overall for 40-watt fluorescent lamp installations.

3. With the modern load center power system, the objectionable flicker from welders practically can be eliminated by using separate transformers for resistance welders or by serving the lights from one transformer and the resistance welders from another in a secondary selective system, Figure 17.

Combinations Studied

Three basic combinations of power supply for lighting systems are considered in this paper. These are:

1. A 208Y–120-volt 3-phase 4-wire power system for lighting load, with separate substations for 460-volt power for motors, and the like, Figure 1.

2. Combined substations for power and light, that is, one 480-volt substation serving motors directly and the lighting load through step-down dry-type transformers located at strategic points through the factory, Figure 2.

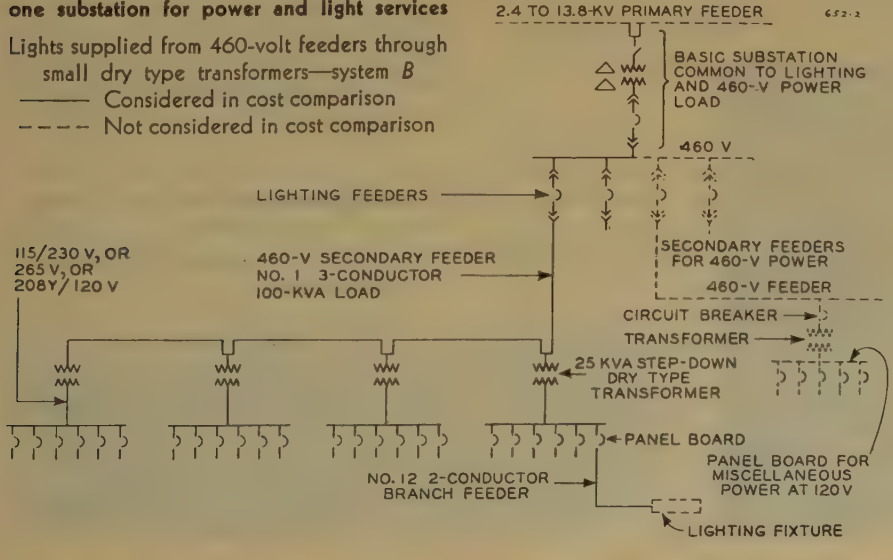
3. A 460Y–265-volt combined power and lighting system in which the motors are operated at 3 phase, 460 volts and fluorescent lights from phase to neutral at 265 volts, from the same substation, Figure 3.

Figure 2. One-line diagram of system with one substation for power and light services

Lights supplied from 460-volt feeders through small dry type transformers—system *B*

——— Considered in cost comparison

– – – – Not considered in cost comparison



Items Included in Study

It is assumed that the primary feeder system is the same, regardless of which of the three afore-mentioned systems are selected. Therefore, the items considered are the step-down substations, secondary feeder circuit breakers, secondary feeders, dry-type transformers, panel boards, and branch wiring, as illustrated by the solid lines in Figures 1, 2, and 3.

The type of unit substation considered throughout this study is shown in Figure 4. To allow for diversity it is assumed that 1 kva of transformer capacity in the substation would have 1.25 kva of lighting load connected to it. Hence, the secondary feeder circuit breakers and cable have a capacity of 1.25 times the transformer kilovolt-ampere rating of the unit substation.

Installation cost of the substations is considered at 20 per cent of the substation price. These values—that is, 20 per cent for installation and 1.25 allowance for diversity—will be used throughout this study. The cost of substations as a function of kilovolt-ampere capacity is shown in Figure 6.

All secondary feeders are assumed to be varnished-cambric-insulated interlocked-armor cable, Figure 5.

The branch wiring from the panel board or control switch to the trough of the fluorescent lighting fixtures is included, but the wiring within the fixtures is not. The branch circuits have been limited to number 12 BX wire, with a current carrying capacity of 20 amperes, because it is believed that a 20-ampere fuse or circuit breaker is the largest which will give reasonable short-circuit protection to the ballasts. In most cases the load current per circuit is about 16 or 17 amperes. Branch circuit wiring costs are assumed to be 25 cents per foot of 2-conductor number 12 BX. To approximate the amount of branch circuit wiring for the various voltages, typical layouts were made—Figure 8.

System A—Separate Substations for Light and Power, Figure 1

This type of system may operate at either 208Y–120 volts, 3 phase, 4 wire, or 230–115 volts, single phase, 3 wire. In line with modern practice the 208Y–120-volt system will be used in the comparison.

A 208Y–120-volt system will care for the general area fluorescent lights, as well

Table II. Summary of System Comparisons

Type of System	First Cost, Per Kilovolt-Ampere	Safety					Where Most Adaptable
		Voltage to Ground	Voltage on Fluorescent Lamps and Starters	Short-Circuit Current	Flicker Caused by 460-Volt Power Load	Ground on Power System	
A—Separate lighting and power substations, Figure 1, 208Y–120 volt	$45	Less than 150	Same for all systems	High (more than 5,000 amperes)	None	Not required	Where all 460-volt busses have too great fluctuations in voltage, due to resistance welders; and where the total 120-volt load is over 50 per cent of the total load at 600 volts or less
B—Combined power and lighting substations, step-down lighting transformers, Figure 2	39.95	Less than 150	Same for all systems	Low (less than 5,000 amperes)	Possible (due to resistance welders)	Not required	Plants now having 460- or 575-volt delta systems. Where total lighting and miscellaneous load is less than about 50 per cent of the total load at 600 volts or less. Adaptable for incandescent, fluorescent, or any other kind of lighting
C—Combined power and lighting substations, 3 phase, 4 wire, 480Y–277 volt, Figure 3	22.95	265	Same for all systems	*Low (less than 3,000 amperes)	Possible (due to resistance welders)	Yes	In new factories, or in old factories where new 460-volt power systems are installed. Adaptable only for fluorescent or mercury-vapor lighting. Not adaptable to 575-volt power systems

* Using size 1 fused combination motor starters for controlling lighting circuits.

as the miscellaneous 120-volt power and lights. The system is laid out on the basis of $4\frac{1}{2}$ volt-amperes load per square foot to evaluate that part of the substation and secondary feeder cost which must be charged to the general area lighting system.

The minimum installed cost of the 208Y–120-volt substation and secondary feeders is $28.75 per kilovolt-ampere of substation rating when using 500-kva substations, the most economical size—top curve, Figure 6. A deviation from this size will increase the cost per kilovolt-ampere as shown by the curves.

The load per secondary feeder has been assumed to be 100 kva. The 4-conductor 300,000 - circular - mil secondary - feeder cable has an installed cost of $2 per foot. Each feeder will supply four circuit breaker panel boards of the type shown in Figure 7, with 25 kva of lighting load per panel board. The total cost of panel boards is estimated at $5.60 per kilovolt-ampere installed and wired (installation $1.85 per kilovolt-ampere).

It is realized that the circuit breakers in these panel boards do not have sufficient interrupting rating (only 5,000 amperes) for this service. However, there are no available devices which meet the space requirements for this service and which have adequate interrupting rating for the short-circuit current duty imposed on them.

The total cost of system *A* is

$28.75...Substations and secondary feeders
5.60...Panel boards
6.40...Branch wiring at 120 volts

$40.75

per kilovolt-ampere of lighting demand.

In general lighting substations as large as 500 kva (the most economical size from Figure 6) are not used. The substations often are laid out with a larger power and a smaller lighting substation at the same location. Where these small lighting units, that is, 150 kva, are used, the cost of the substation is increased. Using the cost from the top curve on Figure 6 for 150-kva substations, the total cost of system *A* is increased to

$33.00...Substation and secondary feeders
5.60...Panel boards
6.40...Branch wiring at 120 volts

$45.00

per kilovolt-ampere of lighting demand.

The cost may be increased even further if a primary protective device is required on the small lighting substation transformer. Hence, the cost of system *A* may go as high as $75 per kilovolt-ampere of lighting demand. Therefore, it is believed that $45 per kilovolt-ampere is a fair average to use in the general comparison with other systems.

System A With 208-Volt Ballast

The figures of $40.75 and $45 per kilovolt-ampere mentioned will be reduced to $38.15 and $42.40 per kilovolt-ampere, if 208-volt ballasts are used for the general area fluorescent lamps instead of 118-volt

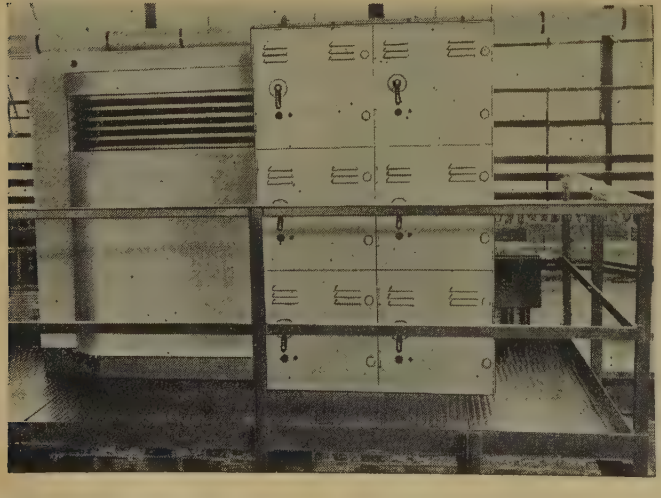
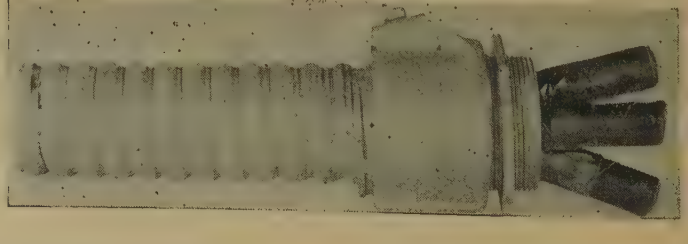


Figure 4 (left). Typical unit substation considered in cost analysis

Figure 5. Interlocked-armor type of secondary feeder cable considered in cost comparison



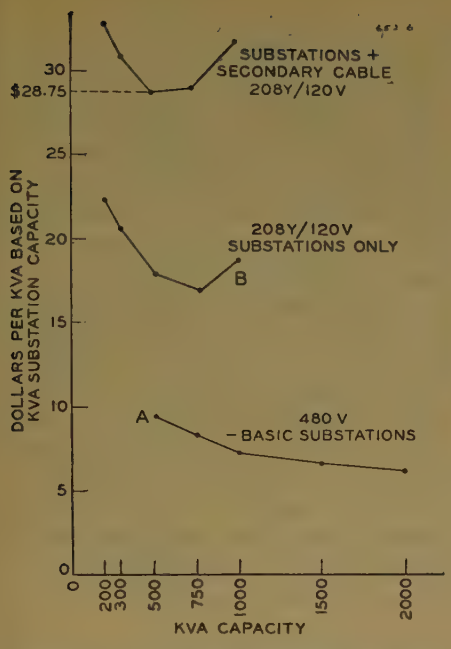


Figure 6. Cost of unit substations and secondary feeders as a function of unit substation size

20 per cent for installation
Feeder capacity is 125 per cent of substation capacity



Figure 7 (left). Typical circuit breaker panel board for branch feeder protection

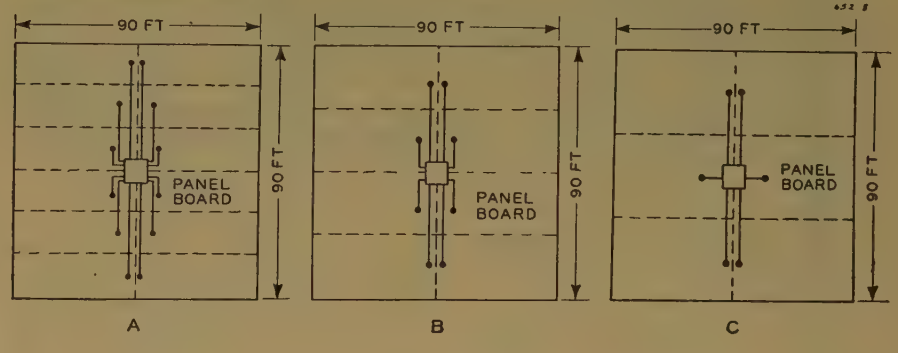
Figure 8. Diagrams used for determining branch circuit length

All branch circuits are number 12 2-conductor BX wire. 25-kva of lighting demand per load area

A—120-volt 1-phase branch circuits; total length 510 feet, including 240 feet for vertical runs

B—208-volt 1-phase branch circuits; total length 7/8 of 510 feet to adjust for 7 circuits; length of 7 circuits 300 feet, including 140 feet for vertical runs

C—230-volt 1-phase branch circuits; total length 240 feet, including 120 feet vertical runs



ballasts considered in the foregoing tabulations. The saving is made in branch circuit wiring only because the system is 3 phase, 208Y–120 volt up to that point. Since detail circuit arrangements may alter materially the branch circuit wiring costs, it is felt that the saving from using 208-volt ballasts rather than 118-volt ballasts may not be as great as shown. For the sake of uniformity of ballasts throughout a plant, many operators would use 118-volt rating for all ballasts if they elected to use system *A*.

System B—Combined Light and Power Substation, Figure 2

It is assumed that the same 480-volt substation will supply power to the 460-volt power feeders and to the 460-volt feeders which supply step-down transformers for the lighting load. The only portion of the step-down substation common to both the lighting and the power system is the primary switch, transformer, and main secondary circuit breaker. This is referred to as the basic substation, the installed cost of which is shown in curve *A*, Figure 6. Since other studies have shown the most economical size substation to be 750 to 1,000 kva, an average figure of $7.50 per kilovolt-ampere has been selected from curve *A* to represent the basic substation cost for the combined light and power system.

The 460-volt secondary feeder circuit breakers for the lighting system have been chosen with 25,000-ampere interrupting rating (large enough for 1,500-kva 480-volt 5.5 per cent impedance transformers). The load per feeder is maintained at 100 kva. On this basis the assumed installed cost of the secondary feeder circuit breakers is $5.40 per kilovolt-ampere.

The secondary feeder layout of Figure 9 is used to determine the length of cable for a 100-kva circuit. The 3-conductor number 1 interlocked-armor cable has an assumed installed cost of 90 cents per foot or $3.55 per kilovolt-ampere. Each secondary feeder connects directly to four step-down dry type transformers.

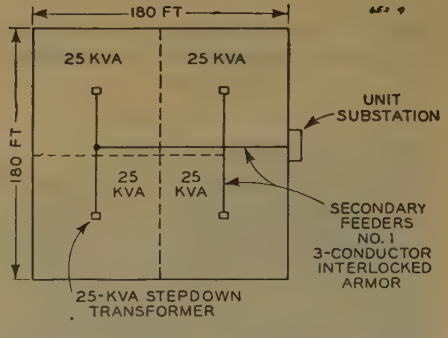


Figure 9. Diagram for determining length of secondary feeder serving 425-kva load areas—system *B*

Total length of secondary feeder cable approximately 315 feet

Use of Small Dry Type Transformers

Because they are the largest single-phase 480–240-120-volt transformer of standard design which can be used and the secondary short-circuit currents kept within 5,000 amperes, the interrupting rating of the circuit breakers in the panel boards, 25-kva transformers were chosen. Taps may be used in the 480-volt winding of these transformers to compensate for transformer voltage drop when necessary.

Separate 460-volt feeders are assumed to be used for serving lighting load only. There are many more outages on power feeders than on lighting feeders because of the greater number of changes made in power feeders. Furthermore, the power feeders may have more voltage drop due to fluctuating loads. Hence, separate lighting feeders often are used for greater reliability and to reduce voltage drop.

A typical outline of an installation of a dry type transformer and a panel board is shown in Figure 10. The installation view in Figure 11 shows two small dry type transformers and panel boards, one for the general area lights and one for miscellaneous 120-volt power.

Switches or circuit breakers are not used ahead of the dry type transformers on the lighting feeder, because the secondary feeder circuit breaker at the unit substation will provide adequate short-circuit

protection for these transformers. Since the lighting load is constant, it is assumed that overload protection is not required. However, should these transformers be connected to heavy power feeders, individual air circuit breakers should be used ahead of each transformer for protecting the transformer under short-circuit conditions and due to overload. The main circuit breaker at the unit substation will afford practically no protection for a small dry type transformer connected to a heavy power feeder.

There is a negligible difference in the cost of dry type step-down transformers and panel boards for various single-phase and 3-phase combinations of transformers and various ballast voltages—that is, 118, 208 volts, and so forth. Therefore, the selection between single-phase and 3-phase banks of small dry type step-down transformers is dependent upon local conditions.

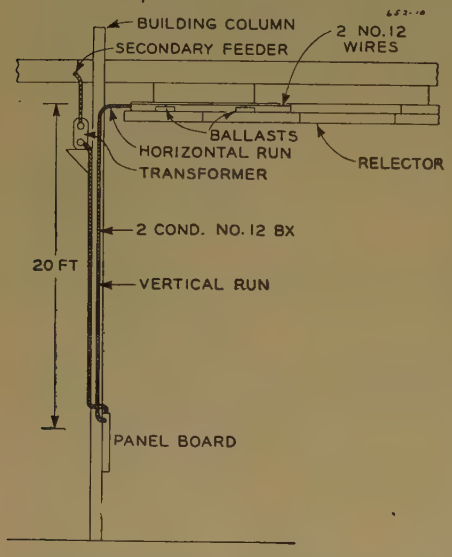


Figure 10. Arrangement of branch feeder panel board and small dry type transformer installations

Selection of Ballast Voltage for System B

The elements of system *B* considered thus far have the same cost regardless of ballast voltage. There are several different ballast voltages which may be selected—namely, 118, 208, 230, or 260 volts. To simplify the selection of ballast voltage, the cost of the items which are affected by ballast voltage are summarized in Table I. There is a slight saving in branch wiring for the higher voltages, but, as pointed out previously, the saving may largely disappear, depending upon local conditions. Hence, to have uniform ballast rating throughout the plant when using system *B*, many operators will use 120 volts, even though there is slightly higher branch circuit wiring cost for that voltage. However, the cost of branch wiring should be studied on each particular job to see if there is any substantial economic benefit to be gained from ballast voltages higher than 118 volts.

The total cost of system *B* is

$ 7.50	Basic substation
5.40	Secondary circuit breakers
3.55	Secondary cable
23.50	Step-down transformers, panel boards, branch circuit wiring, line 3, Table I
$39.95	

per kilovolt-ampere of lighting demand.

Using 230-volt ballast instead of 118-volt ballast would, according to the figures of Table I, reduce the cost of system *B* to

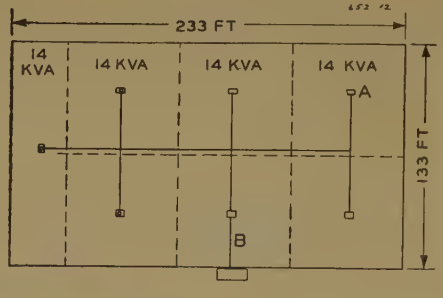


Figure 12 (above). Diagram for determining length of second feeders to serve 7 14-kva load areas, 260-volt fluorescent lamp ballasts —system C

Total length of secondary feeder cable approximately 417 feet

A — Motor starter used as switch for lighting circuit

B—Secondary feeder number 1 3-conductor and neutral interlocked armor cable

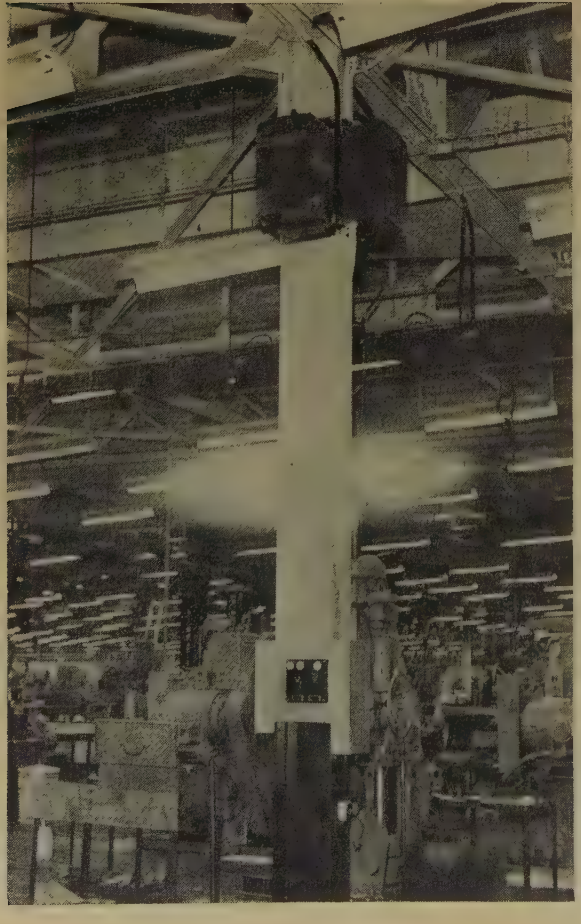


Figure 11 (left). Installation view of two panel boards and two small dry type transformers on a building column

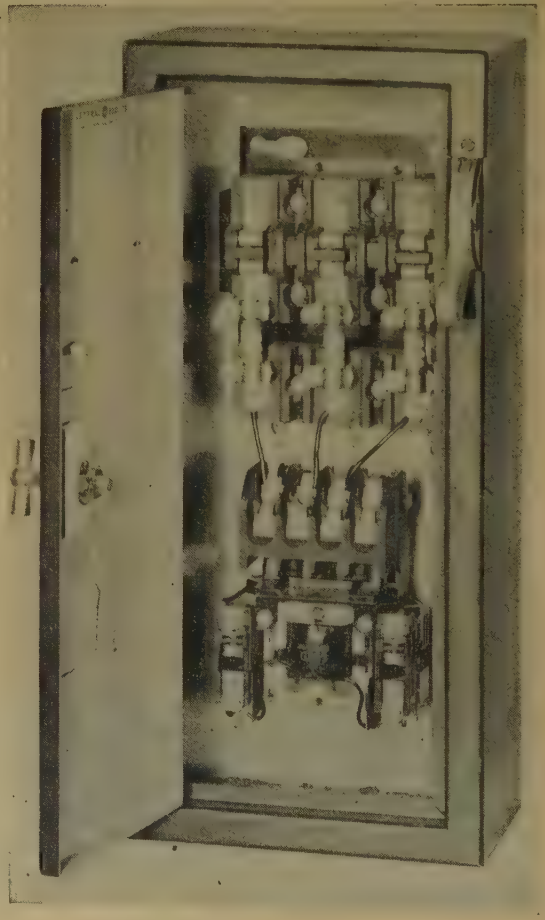


Figure 13. Typical fused combination motor starter used for switching 265-volt fluorescent light circuits—system C

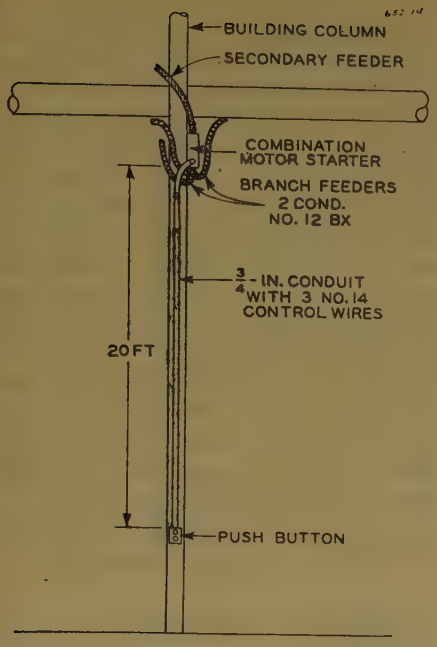


Figure 14. Typical mounting arrangement of fused combination motor starter for switching 265-volt fluorescent light circuits—system C

$36.20 per kilovolt-ampere of lighting demand.

System C—Combined Light and Power Substation, Figure 3

This system is similar to system *B*, Figure 2, except that the fluorescent lamp ballasts are rated 260 volt, and the power system substation is rated 480Y–277 volt, 3 phase with grounded neutral. Several large aircraft assembly plants built at the start of the war used this system for supplying fluorescent lighting loads for general area illumination. It also has been used in many other types of plants since that time. The reason for using this system in the aircraft plants was to save material and not to save money. However, the economic considerations now are more important than material considerations; hence, that system is being reevaluated on the basis of economics.

The substation and secondary feeder circuit breaker costs are the same as for the system *B*, that is, $7.50 and $5.40 per kilovolt-ampere, respectively.

The secondary feeder cost is higher than for system *B*, because a greater length is required to reach the smaller load areas, Figure 12, and because 4-conductor cable is used for the lighting feeders (3-conductor cable for the power feeders). The secondary cable cost is assumed at $1 per foot or $5.20 per kilovolt-ampere.

The branch circuits for the lighting load may be controlled by a 3-pole size 1 fused combination motor starter (for application on circuits with 50,000-ampere available short-circuit current) with three thermal overload elements, Figure 13. Three branch circuits at 265 volts phase to neutral are taken from each motor starter. Since these circuits are limited to about 20 amperes, the lighting load per motor starter is limited to about 14 kva. A typical method of installing a motor starter for this service is shown in Figure 14, where the motor starter is mounted up on the column at the same level as the lights, so that the branch circuits do not have to be run up and down the column. The push button may be located at any convenient spot. The motor starters and push buttons are assumed to cost $3.85 per kilovolt-ampere installed and wired (installation $1 per kilovolt-ampere).

The branch circuit wiring cost, Figure 15, is assumed at $1 per kilovolt-ampere.

The total cost of system *C* as described is

$ 7.50	Basic substation
5.40	Secondary feeder circuit breaker
5.20	Secondary feeder cable
3.85	Controller
1.00	Branch wiring
$22.95	

per kilovolt-ampere of lighting demand.

In some plants now using 260-volt fluorescent ballasts panel boards have been used instead of combination fused motor starters for switching lighting circuits. That substitution reduces the secondary feeder cable required and increases the expense for panel boards and branch wiring. If panel boards with 25 kva of load per board are used, the cost of system *C* is

$ 7.50	Basic substation
5.40	Secondary feeder circuit breakers
3.95	Secondary cable
4.85	Panel boards
2.50	Branch wiring
$24.20	

per kilovolt-ampere of lighting demand.

Short-Circuit Currents

Some operators have objected to system *C* at first glance because of the high short-circuit currents of the power system being available on the lighting circuits. The short-circuit currents on the lighting system are actually very low when the fused combination motor starter is used for controlling the light circuits. The fuses in the motor starter are decidedly current limiting in their action. The three thermal overload elements have a very high impedance and limit the current to even lower values than the fuses would without the thermal elements. The combined effect is to allow not more than about 3,000-ampere peak short-circuit current to flow for a fault in the lighting system, even though the available short-circuit current on the 460-volt power system may be as high as 50,000 rms amperes. To get proper performance of the fused combination motor starter, it is necessary to use not larger than 20-ampere fuses and to have the three thermal overload elements in place in the starter.

The panel board circuit breakers have no current-limiting action; therefore, they allow larger short-circuit currents to appear on the lighting system. However, the application of panel board circuit breakers may allow no higher short-circuit currents to flow in this system than in system *A*, which also is supplied directly from larger transformers. Panel board circuit breakers have the same limitations for application in system *C* as application in system *A* relative to their short-circuit rating.

Other Than General Area Lighting

In systems *A* and *B* 120 volts are available for general area lighting, as well as for miscellaneous 120-volt power and lighting. Therefore, all load other than the 460-volt load can be taken off the same circuits in those two systems.

With system *C* 260-volt ballasts should be used only in fixtures for general factory area lighting. These fixtures must be more than 8 feet from the floor and must not have individual switches mounted in the fixtures. The National Electric Code requires that all lighting for offices, individual benches, machines, and so forth should be operated at 120 volts. Since there is always some load of this nature around any plant, it is necessary to obtain the power for that load from the 460-

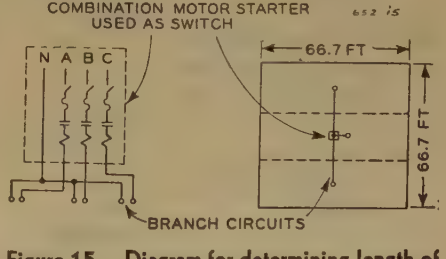


Figure 15. Diagram for determining length of branch circuits for 14-kva load area for system C

Branch circuits are number 12 2-conductor BX wire
Total length of branch circuit 45 feet



Figure 16. A fluorescent lighting installation for general area illumination

volt feeders of system *C*. This can be obtained just as in the case of system *B* with small step-down, dry type transformers as shown to the right of Figure 3. If these transformers are connected to heavy 480-volt feeders, the same precautions should be used in protecting the small transformers as outlined under system *B*.

It is believed that no sacrifice in safety is made with the higher-voltage fluorescent ballasts for the general area fluorescent lighting system, because the lamps and starter voltages are essentially the same, regardless of the voltage rating of the ballast. When the ballasts are changed, the circuit to which the ballasts are connected should be de-energized regardless of the circuit voltage.

Summary of Economic Comparison

Representative first costs of systems *A*, *B*, and *C* are

A..Separate light and power substation, 208Y–120 volt—Figure 1.....	$45 per kilovolt-ampere
B..Combined substations (step-down lighting transformers)—Figure 2.....	39.95 per kilovolt-ampere
C..Combined substations (460Y–265 volt)—Figure 3.....	22.95 per kilovolt-ampere

On the basis of system *A* being 100 per cent, system *B* costs only 89 per cent as much, and system *C* only 51 per cent as much. The savings of the combined light and power system will justify the selection of this system where the total 120-volt load is as high as 50 per cent of the total load at 600 volts or less.

This general comparison also will hold true where incandescent lamps are used throughout, or where other types of gaseous discharge lamps are employed. The ballast for certain types of mercury vapor lamps may be operated from 460-volt circuits.

Although cost comparisons of fluorescent lighting systems are beyond the scope of this paper, it is well to point out that the afore-mentioned figures must be considered in relation to the specific fluorescent lamp layout. The first cost of the power system is small compared with the first cost of the lighting fixtures. The carrying charges on the capital investment of the power system is small compared with the operating cost of the lighting system. Taking all those factors into account, some general guides as to over-all costs of power systems and the lighting fixture system are given in Table III.

Table III shows that even in over-all system cost, combined power and light systems are less expensive than system *A* using separate substations. System *A* does not appear once in the tabulation.

The choice between system *B* and system *C* depends, if one looks at the over-all picture, upon the type of fluorescent lighting fixture used.

For general illumination of very large areas, such as the general working area of a factory, many operators prefer the 100-watt lamp, because it takes fewer lamps and fewer fixtures to light a given area. When this combination is used, system *C*, using 260-volt ballasts, is the least expensive, either from the power system standpoint or from the over-all cost picture. In other cases the 3–40-watt lamp type of fixture is used for general area lighting, and in these cases system *B*, using 208-volt or 118-volt lamp ballast, is the least expensive when the over-all operating costs are considered.

These figures refer only to general area lighting systems, Figure 16, for, as pointed out previously, all fixtures less than 8 feet from the floor in factory areas, or all fixtures in offices or other places readily accessible to factory personnel should be operated from 120-volt systems.

Grounding of 460-Volt Power Systems

The 460Y–265-volt system must have the neutral grounded to accommodate 260-volt lighting fixtures. While some operators who have not had experience with 460-volt grounded Y systems may object to grounding, there are many advantages to having the system neutral grounded, even though 260-volt lighting fixtures may not be used. The biggest single advantage of grounding any power system is immediate isolation of a ground fault before it develops into a double line to ground fault, tripping out a considerable portion of the load.

Grounding of the 460-volt system neutral does not necessitate three thermal overload elements (1940 National Electric Code) in the motor starter for motor circuits. The thermal overload elements are for protection of the motor against overloading and not for short-circuit protection. It does require that all three

Table III

Type of Fixture	*Ballast Voltage	**Type of System With Lowest Cost: First Cost	Operating Cost	Annual Cost
3–40 watt	208	*B*	*B*	*B*
3–40 watt	118	*B*	*B*	*B*
3–40 watt	260	*C*	*C*	*C*
2–40 watt	260	*C*	*C*	*C*
2–40 watt	208	*B*	*B*	*B*
2–40 watt	118	*B*	*B*	*B*
2–100 watt	260	*C*	*C*	*C*
2–100 watt	118	*B*	*B*	*B*
2–100 watt	208	*B*	*B*	*B*

* Voltages are in order of cost, the top representing the least expensive combination and the bottom the most expensive combination for each particular type fixture.

** Includes capital investment in power system, lighting fixtures, cleaning and maintenance, energy cost, and so forth.

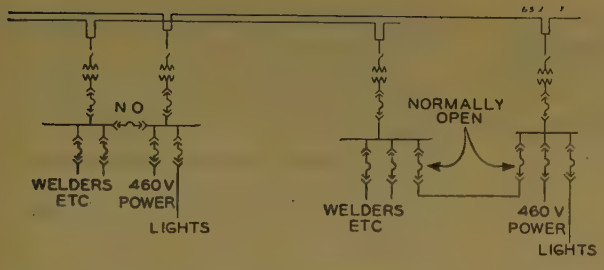


Figure 17. Secondary selective arrangement of load center power distribution system with resistance welders on one 460-volt bus and lights on the companion 460-volt bus

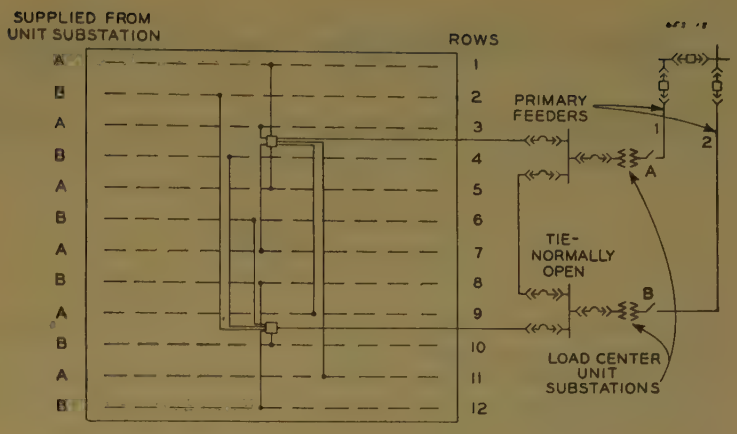


Figure 18. Secondary selective arrangement of load center power distribution system with overlapping areas of lights supplied for different substation busses to prevent complete loss of light should one bus be de-energized

phase branch circuit breakers have three overcurrent elements or three fuses.

Voltage Flicker of Combined Light and Power System

Voltage flicker due to fluctuating power loads will not cause objectionable light flicker in the average factory. Large resistance welders, or large motors which start frequently, should not be connected to the 460-volt bus that serves the plant lighting. Resistance welders are being used in increasing quantities in manufacturing plants, particularly in those that fabricate metal products. In many larger plants employing load center power distribution systems, the welders are connected to a separate transformer which supplies nothing but welding load. In these plants there is no problem of lamp flicker due to resistance welders, unless the plant is supplied by a very weak primary system, in which case the flicker problem will be essentially the same whether or not combined light and power systems are used.

In manufacturing plants where the total resistance welder load is not sufficient to justify separate welding transformers or where there are no exceptionally large welders, the secondary selective arrangement of the load center distribution system may be used, with one of the two substations (Figure 17) for general power load and resistance welders and the other for combined light and power. During normal operation the two substation busses are not in parallel, and the flicker on the bus to which the welders are connected will not affect the lights connected to the other bus. When during an emergency one of the primary feeders or one of the transformers is out of service, the busses may be paralleled, and during that emergency period the flicker may be noticeable. In general there has been no difficulty with combined light and power systems where the principles mentioned have been followed.

Increased Reliability of Lighting Circuits

With any of the systems discussed in this paper, consideration should be given to overlapping the area fed by one substation, so that an outage on that substation will not cause complete outage of lamps in any one area. One method of accomplishing increased reliability economically with the secondary selective load center power system is shown in Figure 18.

Small plants with demands of 500 to 1,500 kva usually require only one substation. It has been common practice to install a power transformer bank and a lighting transformer bank. The welders and power load are connected to the larger bank, and the lights to the smaller one. By using the arrangement shown in Figure 18 with two transformers equivalent in total kilovolt-amperes to the lighting plus the power demand, considerable increase in service reliability can be obtained without incurring objectionable flicker from the welders. With two transformers of equal size, both stepping down to 460 volts, the plant may be kept in at least partial operation with lights and major power apparatus in service with one transformer de-energized. Where separate lighting and power banks are used, this cannot be done. Increased service reliability for the same reason can be obtained in larger plants by using the secondary selective system with substations in pairs, both stepping down to 460 volts, instead of individual light and power substations scattered through the working area.

Effect of Altitude on Ventilation and Rating of Aircraft Electric Machines

CYRIL G. VEINOTT
MEMBER AIEE

Synopsis: Fundamental problems involved in the cooling and rating of aircraft electric machinery at medium and high altitudes are discussed in this paper, primarily to assist users in the application of such equipment, and to assist builders in designing equipment to meet the requirements. In addition flight tests are reported which confirm in part the blast-tube theory developed in a previous paper. For blast-cooled generators, an equation has been developed to show the maximum permissible output in terms of entering-air temperature and density, ramming-head pressure, and winding temperature. For motors curves of total winding temperature at rated load have been plotted as a function of altitude; these curves were plotted for selected values of sea-level temperature rise. Specific conclusions are drawn as to:

1. Permissible generator output as a function of altitude and sea-level rise.
2. Limiting sea-level temperature rises for motors on the basis of constant or reduced life at altitude.

This paper presents a qualitative method of analysis rather than a definitive solution of the problems involved.

ONE of the first steps to be taken when applying a blast-cooled generator to any given airplane is to determine the amount of pressure head available for each significant flight condition. By comparing this head with the pressure on which the machine's rating is based, the application engineer can determine approximately what output can be obtained without danger of overheating the generator. One object of this paper is to demonstrate a method for readily determining the available pressure head without as many flight tests as now commonly taken. A knowledge of this pressure head under more conditions makes it possible to apply generators more accurately and to obtain more representative altitude-chamber data.

Altitude rating of generators is approached from the standpoint of determining the load required at all altitudes to give the same total winding temperature. This approach leads to the permissible output of the generator for constant insulation life at all altitudes.

Altitude rating of motors has been approached from a somewhat different angle. Load and speed are assumed constant, and relationships are established between sea-level rise and total winding temperature at altitude. By assuming that insulation life halves with each 10-degree-centigrade increase in temperature, the effect of sea-level temperature rise on the altitude life of insulation was determined and plotted in Figure 1, which was derived from Figure 8.

It must be emphasized, however, that generator outputs above full load well may be limited by commutation or by excitation power. This paper is concerned only with the influence of temperature on rating and starts with a study of blast-cooling phenomena.

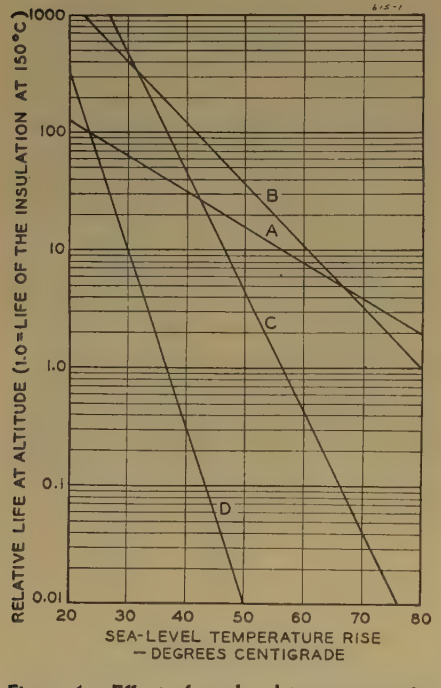


Figure 1. Effect of sea-level temperature rise of fan-cooled motors, open or enclosed, upon the insulation life at different altitudes (derived from Figure 8)

A—At sea level +60 degrees centigrade ambient temperature
B—At 20,000 feet +10 degrees centigrade ambient temperature
C—At 40,000 feet −40 degrees centigrade ambient temperature
D—At 50,000 feet −40 degrees centigrade ambient temperature

Summary and Conclusions

A. A theory of blast-tube cooling has been developed and confirmed in part by actual flight tests.

B. Application of this theory appears to offer the following advantages:

1. Reduction in number of flight tests required.
2. More accurate information on ram-head pressures available for specific generators in specific airplanes.
3. More accurate information in applying generators.
4. More accurate information for altitude-chamber tests.

C. Salient features of this blast-tube theory are:

1. Air flow is measured in terms of velocity head.
2. Blast-tube characteristics can be represented by two factors:

(*a*). Closed-end pressure, analogous to open-circuit voltage of a battery.

(*b*). Air-flow resistance, analogous to internal resistance of a battery.

3. A generator without a fan has air-flow resistance only.
4. A generator with internal fan has air-flow resistance plus internal pressure.
5. Calculations of air flow (in terms of velocity head) are analogous to, and as simple as, the application of Ohm's law.
6. Closed-end pressure of a blast tube is independent of altitude, but for any given airplane is approximately proportional to the square of the indicated air speed.
7. Air-flow resistance of the blast tube, or generator, is independent of altitude, and independent of the indicated air speed.
8. Total pressure head on a blast-cooled generator, at any given indicated air speed, is substantially independent of altitude, unless the generator has an internal fan.

D. Generally speaking, the permissible output of a blast-cooled generator varies with the ramming-head pressure: above full load, the output tends to vary as the fourth root of the pressure; below full load, the output tends to vary as the square root of the pressure.

E. Altitude adversely affects the rating of the following classes of machines in the order given:

1. Fan-cooled machines (open or enclosed)—most affected.
2. Blast-cooled machines.
3. Totally-enclosed machines (not fan-cooled)—least affected.

F. Increase in altitude has its greatest effect on the rating of all classes of electric equipment in the isothermal stratosphere which begins, according to Army maximum standards, at 40,000 feet.

G. As a rule the higher the sea-level temperature rise, the more the output is affected adversely by increase in altitude. Conversely, the higher the specified maximum altitude, the lower must be the sea-level rise.

H. Since apparatus with a high sea-level temperature rise is affected more adversely by altitude than apparatus with a low sea-

---

Paper 46-15, recommended by the AIEE committee on air transportation for presentation at the AIEE winter convention, New York, N. Y., January 21–25, 1946. Manuscript submitted June 12, 1945; made available for printing November 23, 1945.

CYRIL G. VEINOTT is section engineer with the Westinghouse Electric Corporation, Lima, Ohio.

This paper is based on a talk made before the AIEE Dayton Section in January 1945.

The author acknowledges the assistance of Captains W. M. Green and C. A. Maple of the United States Army Air Forces and J. B. Crockford of the Westinghouse Electric Corporation in obtaining flight-test data. He also thanks H. J. Braun for permission to use Figures 8 and 10, G. G. Setterlund for permission to use Figure 7, and D. S. Pearson and J. C. Cunningham for assistance.

level rise, it follows that the use of high-temperature insulation offers less promise of weight reduction as the specified maximum altitude is raised.

I. Blast-cooled generators with class *A* insulation should be able to deliver full output up to 49,000 feet, provided the entering-air temperature does not exceed the Army maximum specification. If class *B* insulation is used, and if the sea-level rise is increased accordingly, full output should be expected only up to 40,000 feet.

J. Fan-cooled generators generally are not practicable for altitudes above 20,000 feet.

K. Fan-cooled motors which are expected to deliver full rated output with full life expectancy at 40,000 feet should have a sea-level temperature rise not exceeding:

1. 50 degrees centigrade if class *A* insulation is used.
2. 56 degrees centigrade if class *B* insulation is used.

These figures are based on an ambient temperature per Army maximum specification and full life expectancy at altitude. Considerable reduction in life expectancy at altitude does not increase the permissible sea-level rise so much as might be supposed. See Figure 1.

L. Fan-cooled motors which are expected to deliver full rated output with full life expectancy at 50,000 feet should have a sea-level temperature rise not exceeding:

1. 33 degrees centigrade if class *A* insulation is used.
2. 37 degrees centigrade if class *B* insulation is used.

These figures are likewise based on an ambient temperature per Army maximum specification and full life at altitude. Reduction of altitude life for changes in sea-level rise is shown in Figure 1.

M. Fan-cooled motors designed for a maximum altitude of 50,000 feet may be as much as 20 per cent heavier than comparable motors designed for 40,000 feet, unless the life at top altitude is considerably reduced.

N. Enclosed motors, and static apparatus cooled by radiation and free convection, can be permitted a sea-level rise of 70 degrees centigrade for class *A* insulation, or 90 degrees centigrade for class *B* insulation; such apparatus should be satisfactory for all altitudes up to 50,000 feet, provided the ambient temperature does not exceed the Army maximum value.

Air-Flow Mechanics of Blast-Tube Cooling

Heretofore the only method available for determining the total pressure head available for a particular blast-cooled generator has been by an actual flight test. This method has the advantage of being simple and direct. But it has the important disadvantage of requiring a flight test for every generator–airplane combination to be studied. Because this procedure would require too many flight tests, there is an unfortunate tendency to take a mere guess at the pressure. A somewhat different approach to this problem was presented to AIEE in 1944.[1] Since then some flight tests have been made which tend to confirm the practicability of this approach. The method therein presented is summarized in the following paragraphs, together with flight-test data.

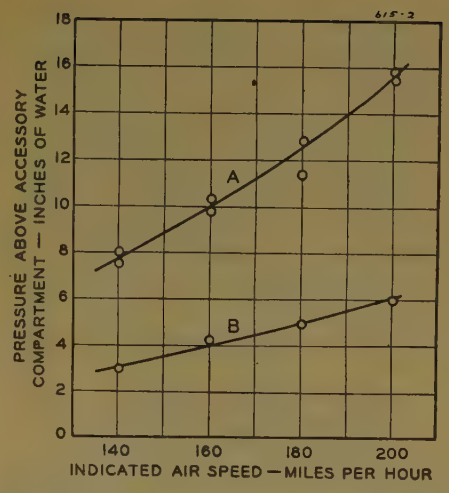


Figure 2. Flight-test measurements of the total pressure head available at the generator end of the blast tube with no generator

Four-engine bomber, number 2 nacelle
A—Closed-end readings
B—Open-end readings
Altitude: 5,000 feet

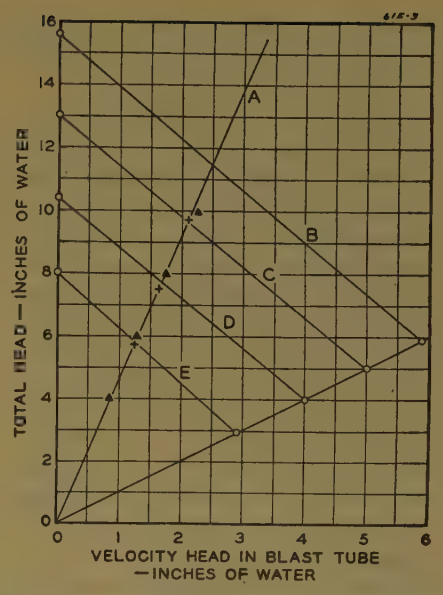
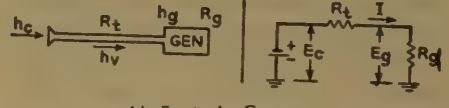


Figure 3. Pressure-flow curves of blast tubes and aircraft generators

Two-inch-diameter blast tube
O Blast-tube pressure-flow curves determined by flight tests without generators
Δ Generator pressure-flow curve determined by laboratory tests
\+ Generator pressures measured on flight test
A—Pressure-flow curve of a representative generator
B—Blast-tube pressure-flow curves at 200-miles-per-hour indicated air speed
C—At 180-miles-per-hour indicated air speed
D—At 160-miles-per-hour indicated air speed
E—At 140-miles-per-hour indicated air speed

The underlying philosophy of this method is to measure, by means of a flight test, the pressure-flow curve of the blast tube itself; that is, a curve of total pressure head available versus the quantity of air taken from the tube. Similarly, by means of a laboratory test the pressure-flow curve of the generator under consideration is determined by measuring the pressure required to force different amounts of air through the generator. When these two pressure-flow curves are plotted on the same curve sheet, the point of intersection automatically gives the pressure across the generator as well as the amount of air flow. Likewise, the pressure-flow curve for any other generator then can be determined and plotted in order to determine the pressure and amount of air available for that particular generator *without an additional flight test.* But the pressure and amount of air can be computed even more easily by making use of the equations of Figure 4 which have been arranged in the form of simple electric-circuit equations; use of these equations is explained more fully later.

Extremely significant to this method is the factor selected as an indication of "quantity of air," namely, velocity head. Because of its importance the significance

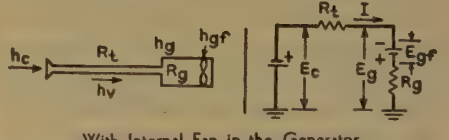


No Fan in the Generator

Closed-end head = h_c
Blast-tube resistance = R_t
Velocity head of flow = h_v
Generator resistance = R_g
E_c = open-circuit volts
R_t = line resistance
I = current
R_g = load resistance

$$h_v = \frac{h_c}{R_t + R_g} \qquad I = \frac{E_c}{R_t + R_g}$$

$$h_g = h_v R_g = \frac{R_g h_c}{R_t + R_g} \qquad E_g = IR_g = \frac{R_g E_c}{R_t + R_g}$$



With Internal Fan in the Generator

$$h_v = \frac{h_c + h_{gf}}{R_t + R_g} \qquad I = \frac{E_c + E_{gf}}{R_t + R_g}$$

$$h_g = h_v R_g - h_{gf} = \frac{R_g h_c - R_t h_{gf}}{R_t + R_g} \qquad E_g = IR_g - E_{gf} = \frac{R_g E_c - R_t E_{gf}}{R_g + R_t}$$

Note: If h_g is −, generator fan helps overcome R_t as well as R_g, and more air would flow through generator if blast tube were removed from generator.

Note: If E_g is −, E_{gf} helps overcome R_t as well as R_g, and more current would flow if terminals E_g were short-circuited.

Figure 4. Electric circuit analogue

of the use of velocity head as an indication of flow merits some discussion.

Velocity Head as an Indication of Air Flow

Air flow through the blast-tube might be measured in any number of ways: cubic feet per minute, pounds per minute, linear velocity, or velocity head. Of these, velocity head is by far the most useful for a number of important reasons. One reason is that, when flow is expressed in terms of velocity head, the pressure-flow curve of the blast tube, as well as the pressure-flow curve of the generator, *is substantially independant of air density and, therefore, substantially independent of altitude.* A second, and very important advantage of the use of velocity head, is that the pressure-flow curves of both blast tubes and generators alike become straight lines. Now, since the pressure-flow curve of a blast tube is a straight line, it is necessary to measure only two points on it. (For a generator pressure-flow curve, only a single point is needed.) These two points can be determined most conveniently by measuring the open-end and closed-end pressures, as pointed out in a previous paper.[1]

Flight Tests to Check Basic Theory of Blast-Tube Cooling

Flight tests were made at Vandalia, Ohio, with the co-operation of the Army Air Forces, for the purpose of verifying the principle and for obtaining specific data on at least one particular airplane. For purposes of these tests, a 4-engine bomber was selected. The generator was removed from number 2 nacelle, and in its place a 24-inch length of straight tubing 2 inches in inside diameter was used. Near the end of this straight tube a conventional pitot tube was installed. For the first flight test the end was capped and the airplane flown at various indicated air speeds at various altitudes. Total pressures at the end of the blast tube above accessory compartment were measured and recorded. A second flight test was made with the end of the blast tube open and with the tube discharging freely into the accessory compartment. It was found, as expected, that the total pressure above the accessory compartment, whether the end was closed or open, depended upon the indicated air speed but was substantially independent of the altitude. The open- and closed-end readings which were taken at an altitude of 5,000 feet have been plotted in Figure 2. Two additional similar curves were taken flying at altitudes of 10,000 and 15,000 feet, respectively; the resulting data

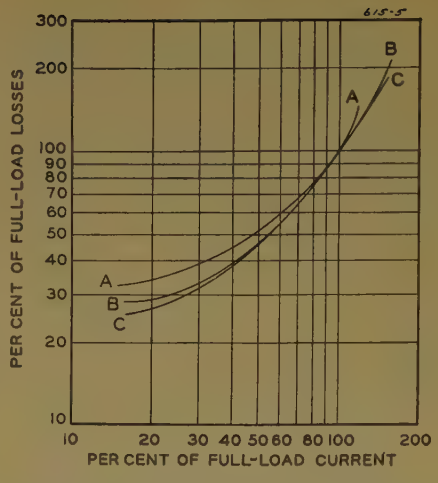


Figure 5. Variation of total losses of an aircraft generator as a function of output amperes and rpm

A—At 4,000 rpm
B—At 6,000 rpm
C—At 8,000 rpm

Generator rating: 9 kw, 30 volts, 300 amperes, 4,400–8,000 rpm

were nearly identical with those of Figure 2.

From the open- and closed-end readings taken on the flight tests, pressure-flow curves of the blast tube were plotted for different indicated air speeds; these curves are given in Figure 3. (In Figure 3 each point is the average of several readings taken at three different altitudes.) Next the generator was set up in the laboratory, and total pressure heads of 4, 6, 8, and 10 inches, respectively, were impressed on the generator. Temperature of the entering air was held at various values from −5 degrees centigrade to +20 degrees centigrade, and the pressure altitude of the incoming air was varied from 5,000 to 15,000 feet. Velocity heads of the entering air were measured and averaged for each different applied pressure. In Figure 3 velocity head in the blast tube has been plotted against total pressure head applied, obtaining the pressure-flow curve of this particular generator. (Ordinarily it is sufficient to measure the flow for a given pressure at ground-level conditions; entering-air temperature and atmospheric pressure have relatively little effect in this measurement, because velocity head is used as the measure of flow.)

Points of intersection of the pressure-flow curve of the generator with the respective pressure-flow curves of the blast tube give the pressures to be expected upon that generator in flight; these intersection points also give the velocity heads of air flowing through the blast tube and generator. As a check, this generator was installed and flight tested; observed values of generator head are indicated by crosses on the curve. The agreement is remarkable and demonstrates that the theory is workable.

Electric-Circuit Analogue an Aid to Blast-Tube Calculations

Instead of actually plotting pressure-flow curves and determining the point of intersection, it is much simpler to calculate the point of intersection. For this purpose one concept needs to be introduced—that of air-flow resistance—which is defined as the ratio of the lost head to the velocity head. This concept makes air-flow resistance comparable to ohmic resistance in an electric circuit, which is the ratio of the voltage drop to the current. In a blast tube, however, a note of caution must be given: in any given blast-tube system, all velocity heads must be referred to the same diameter of tube. Air-flow resistance of the blast tube is

$$R_t = \frac{h_c - h_o}{h_o} \qquad (1)$$

Air-flow resistance of a generator without a fan is

$$R_g = \frac{h_g}{h_{vg}} \qquad (2)$$

A tube resistance, R_t, of 4.0 means that the head loss in the tube is equal to 4.0 velocity heads. Thus, air-flow resistance, as defined and used herein, does have a definite physical significance.

Just as the characteristics of a battery can be expressed in terms of open-circuit voltage and internal resistance, so can the pressure-flow curve of a blast tube be ex-

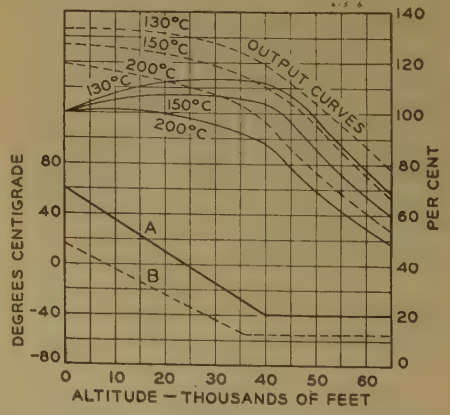


Figure 6. Influence of altitude on the permissible continuous outputs of blast-cooled generators

Calculations are based on the constant winding temperatures shown on the respective curves
—— Output based on Army maximum ambient temperatures
– – Output based on NACA ambient temperatures

A—Army maximum ambient temperature
B—NACA ambient temperature

pressed in terms of closed-end pressure and tube resistance. The blast-tube pressure-flow curves of Figure 3 are represented in Table I. It will be noted that the open-end pressures are given; these were used in calculating the tube resistance. It is particularly gratifying to note that the tube resistance does not vary with altitude, nor does it vary to any significant extent with indicated air speed. There is no particular reason why it should vary with altitude or with air speed, and the slight discrepancies noted may be due to test errors.

Equations for calculating the pressure head available for any generator of known air-flow resistance are given in Figure 4, where they are compared with exactly analogous equations for a simple d-c series circuit. The analogy is of great assistance in remembering the equations. Extension of this theory to include generators with an internal fan was a natural development of the electric-circuit analogue.

Generators With Internal Fan

Internal fans alone usually do not provide enough ventilation to make generators satisfactory above 20,000 feet. However, use of an internal fan does provide some ground power capacity and, when used in conjunction with blast cooling, has the general effect of increasing the air flow. Let the pressure of the internal fan be denoted by h_{gf}. This pressure is proportional to the square of the speed and to the first power of the air density; it can be represented by the equation

$$h_{gf}=F_p\times\left(\frac{N}{1{,}000}\right)^2\times\frac{\rho_A}{\rho_o} \qquad (3)$$

where F_p is an empirical constant. Physically, F_p is the pressure developed by the fan at sea-level air density at 1,000 revolutions per minute. This constant F_p might be measured by blocking either the inlet or the outlet and measuring the pressure at the blocked end of the generator; readings should be taken at different speeds and the constant F_p determined from equation 3.

Air-flow resistance of a fan-cooled generator can be determined by applying a known pressure head h_g and measuring the velocity head h_{vg} of the entering air. The air-flow resistance is then

$$R_g=\frac{h_g+h_{gf}}{h_{vg}} \qquad (4)$$

Velocity head of the air flowing into a fan-cooled generator and pressure head across it can be computed by using the equations of Figure 4. It is to be noted that the same constants of the blast tube apply whether the generator has an internal fan or not. However, since the pressure of the generator fan does vary with altitude, the pressure drop across the generator also will vary with altitude. If there is no internal fan in the generator, the pressure across the generator will not vary with altitude. If there is an internal fan, the general effect of altitude will be to reduce the velocity-head flow and to increase the pressure across the generator.

Of interest is the case of the blast-cooled generator with internal fan operating on the ground with no ram-head pressure applied. From the equations of Figure 4, the air flow through the generator and blast-tube combination and the pressure across the generator (necessarily negative) readily can be computed. The cooling effect, of course, is determined by the weight of air flowing, rather than by the pressure head.

Table I. Blast-Tube Characteristics Obtained From Flight Tests

Indicated Air Speed	Open-End Pressure, h_o	Closed-End Pressure, h_c	Tube Resistance, R_t
140	2.9	8.0	1.76
160	4.0	10.4	1.60
180	5.0	13.0	1.60
200	5.9	15.6	1.64

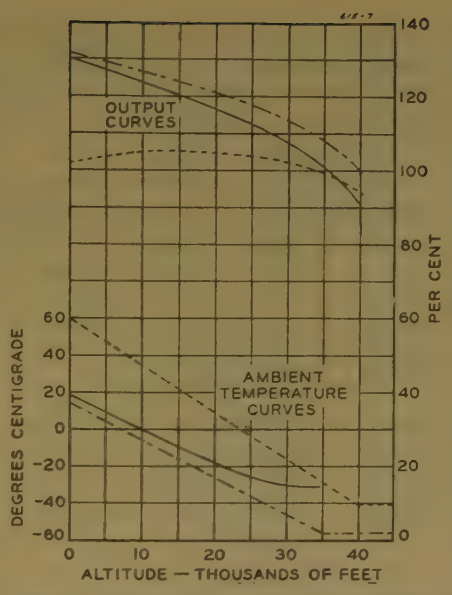


Figure 7. Influence of ambient temperatures on the permissible continuous output of a blast-cooled generator at various altitudes

Generator rating: 9 kw, 300 amperes, 30 volts

Winding temperature: 150 degrees centigrade

– – – NACA temperature

——— Actual ambient temperatures used in laboratory tests

- - - - - Army maximum temperatures

Factors That Determine the Permissible Output of a Generator

In a blast-cooled generator the total watts taken away by the cooling air can be assumed to be approximately proportional to the total weight flow of the cooling air and also to the temperature rise of the windings above the entering-air temperature. In other words

$$P_1\propto W(T_s-T_a) \qquad (5)^*$$

but, for the general case,

$$W\propto\sqrt{\rho h_g} \qquad (6)$$

for blast-cooled generators with no internal fan

$$h_v\propto h_g$$

so that we may assume

$$W\propto\sqrt{\rho h_g} \qquad (6a)$$

therefore,

$$P_1=C_1\sqrt{\rho h_g}(T_s-T_a) \qquad (7)$$

Equation 7 is of inestimable value in evaluating altitude performance. It shows how the heat-dissipating capacity of the cooling air depends upon:

1. Air density.
2. Pressure head across the generator.
3. Winding temperature.
4. Ambient temperature.

Of even greater interest to the user of generators, however, is a knowledge of how the permissible output, rather than permissible loss, depends upon these same factors. For this purpose, it is necessary to know how the total losses in the machine vary with the output.

There is no single fixed relationship between output and losses which holds for all aircraft electric machines. Generally speaking the losses may be divided into two broad classes:

1. Constant losses.
2. Variable losses which generally vary as the square of the current.

Maximum efficiency of the generator is obtained when the constant losses are equal to the variable losses, and, at this point, the efficiency curve is usually quite flat. An efficiency curve flat over a range means that the losses are directly proportional to the output over the same range. Below the maximum-efficiency point they decrease more slowly than the output. How these total losses vary with the current has been plotted in Figure 5 for a typical 9-kw d-c aircraft generator.

* More accurately, W should have an exponent slightly less than 1.0, but for the purposes of this paper the gain in accuracy in using a decimal exponent here is hardly justifiable.

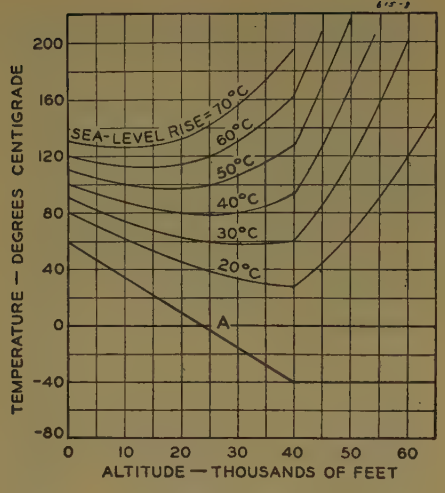


Figure 8. Fan-cooled motors, open or enclosed, effect of altitude on the winding temperature for different values of sea-level rise

Output, losses, and rpm assumed constant
A—Ambient temperature (Army maximum)

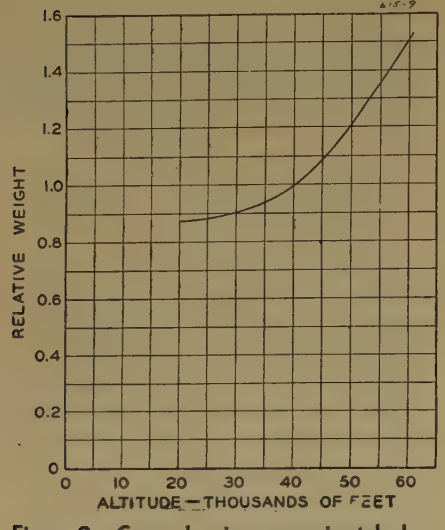


Figure 9. Curve showing approximately how the weight of an open fan-cooled motor is affected by the maximum altitude for which it is designed

Based on Army maximum ambient temperature curve and a motor designed for 40,000-foot altitude as unit weight

It will be noted that the variation of losses with current also is affected by the generator's operating speed, which changes the distribution between the constant and variable losses. It will be observed on this curve that, the higher the load, the faster the losses increase with increase in current. It would be convenient if we could express the losses as a simple function of the load current, such as

$$P_1 = C_2 I^{\beta} \qquad (8)$$

Unfortunately the value of β, which is the slope of the curve, is not constant throughout the load range. However, it is sufficiently accurate and generally safe to take β equal to 2.0 for outputs above full load and to assume it equal to 1.0 for loads from full load down to half load.

Variation of the output with the ram-head pressure, h_g, on the generator now can be expressed. Equation 7 can be rewritten, first, in terms of permissible loss, as follows:

$$\frac{P_{1A}}{P_{1o}} = \sqrt{\left(\frac{\rho_A}{\rho_o}\right)\left(\frac{h_{gA}}{h_{go}}\right)}\left(\frac{T_{SA}-T_{aA}}{T_{So}-T_{ao}}\right) \qquad (9)$$

Subscript A denotes any altitude, and subscript o denotes sea level. This equation shows how the losses that can be dissipated vary with altitude conditions, and with ramming-head pressure. It will be noted that the permissible watts vary as the square root of this ramming-head pressure. This relationship then can be interpreted in terms of current output as follows:

$$\frac{I_A}{I_o} = \left[\sqrt{\left(\frac{\rho_A}{\rho_o}\right)\left(\frac{h_{gA}}{h_{go}}\right)}\left(\frac{T_{SA}-T_{aA}}{T_{So}-T_{ao}}\right)\right]^{1/\beta} \qquad (10)$$

When the expression in brackets is greater than unity, β may be taken equal to 2.0. When the expression in brackets is less than unity, β may be taken equal to 1.0. In other words, if the pressure available is less than the rated pressure, the generator should be derated proportionally to the square root of the applied pressure; if the pressure is more than the specified value, the generator could be uprated, so far as overheating is concerned, as the fourth root of the pressure. However, it must be borne in mind that commutation, field excitation, or some limit other than temperature rise may limit the uprating of the generator.

Equation 10 was developed for the most common case of a generator without a fan. To take into account the effect of an internal fan, equation 10 can be written as follows:

$$\frac{I_A}{I_o} = \left[\sqrt{\left(\frac{\rho_A}{\rho_o}\right)\left(\frac{h_{vA}}{h_{vo}}\right)}\left(\frac{T_{SA}-T_{aA}}{T_{So}-T_{ao}}\right)\right]^{1/\beta} \qquad (10a)$$

In this equation, h_{vo} represents the velocity head of the air entering the generator at sea level with rated pressure applied. Theoretically, this equation should be applicable when no ram head is applied; practically, the equation is of rather doubtful value when extended so far because:

1. The β exponent does not hold so well for low values of load, for instance, below 30 per cent.

2. The effect of the rotation of the armature, which is more important under these conditions, is not fully taken into account.

Effect of High Altitude on Output of Blast-Cooled Generators

Factors affecting the rating of a generator at altitude, from the standpoint of winding temperature, are:

1. Density of the cooling air. (See Table II.)

2. Ram-head pressure or h_g; for a blast-cooled generator, this does not vary with altitude.

3. Ambient temperature. In the following analysis this generally was assumed to be as specified by the Army maximum curve (see Figure 6, and Table II), but this may not always be so. Test data are needed on entering-air temperatures of blast-cooled generators.

4. Permissible or assumed temperature of the windings.

5. β, that is, how much the losses vary with the current output.

A general relationship between the foregoing factors is shown in equation 10. In Figure 6 are plotted some curves calculated from this equation. In all of these curves the total winding temperature has been assumed constant at all altitudes. These curves show the influence of altitude on the permissible continuous output of blast-cooled generators. Three different machines were taken for this analysis, having assumed winding temperatures of 130 degrees centigrade, 150 degrees centigrade, and 200 degrees centigrade respectively. This would correspond approximately to class *A* insulation, class *B* insulation, and special high-temperature insulation. It further was assumed that the temperature of the entering air was at Army maximum value, as shown in Figure 6 and Table II, and that the machine had rated temperature rise at sea level. Also, the permis-

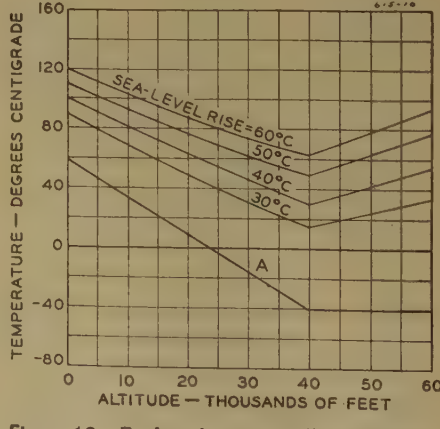


Figure 10. Enclosed motors, effect of altitude on the frame temperature for different values of sea-level rise

Output and losses assumed constant
A—Ambient temperature (Army maximum)

sible outputs of these same machines were computed on the basis of entering-air temperatures equal to National Advisory Committee on Aeronautics ambient temperatures; these temperatures are also shown in Figure 6 and Table II. Some interesting conclusions are deducible from the curves in Figure 6.

If the sea-level temperature rise is not over 70 degrees centigrade, full output rating can be obtained up to 49,000 feet. However, if the machine is designed for a higher sea-level temperature rise, such as 90 degrees centigrade, full rated output can be maintained only up to 42,000 feet. If extra-high-temperature insulation is used that permits the machine to have a sea-level rise of 140 degrees centigrade, full rating can be maintained only up to 20,000 feet. Any given machine can develop more output without overheating in an NACA standard atmosphere than in an Army maximum standard atmosphere, because the former has lower temperatures. This effect is shown in Figure 6 for the three hypothetical machines by plotting the permissible output for both ambient-temperature curves. The difference in output decreases with altitude, especially above 40,000 feet.

Curves shown in Figure 6 should be fairly representative of blast-cooled generators. For purposes of comparison, similar curves, except that they are based on actual tests on a typical aircraft generator, are given in Figure 7. These curves are based on altitude-chamber tests on a 9-kw d-c generator. Actual temperature rises were measured at different altitudes in the chamber, and the three output curves at the top of the sheet were corrected by calculation to correspond to the three different ambient temperature curves shown at the bottom. In making these corrections, it was assumed that temperature rise was directly proportional to watts loss. Permissible watts loss was converted to current output by making use of Figure 5, which applies to the particular generator that was altitude-tested. In general these curves agree with the 150 degrees centigrade curve of Figure 6 with a reasonable degree of accuracy. However, they tend to show that there is some loss in permissible output above 34,000 feet, whereas the theoretical curve of Figure 6 shows full output being maintained up to 42,000 feet.

Effect of Altitude on Aircraft Motors

Permissible loss in an aircraft motor varies with speed as well as with permissible temperature rise and air density. Hence, it is difficult to express the output as a function of altitude because of the variation in speed, particularly in the case of a series motor. Furthermore, for many applications the load imposed on the motor does not vary with altitude, so that the motor has to carry the same load at all altitudes. Therefore a new and somewhat different approach has been used. This approach involves investigating the actual temperatures encountered by the windings at different altitudes, assuming a constant load and a constant speed. However, in some applications, notably fan, the load falls off at altitude, and the speed will increase if a series motor is being used. For the present, however, the following discussion is confined to motors operating at a constant load and a constant speed.

There are two types of motors to be considered: fan-cooled, open or enclosed; and enclosed.

Table II. Standard Temperatures and Densities of Air for Both National Advisory Committee on Aeronautics and Army Maximum Standards

Altitude, Feet	NACA Standard Conditions: Pressure, Inches H_g	Pressure, Centimeters H_g	Temperature, Degrees Centigrade	Pounds Per Foot, ρ	ρ / 0.07651	$\sqrt{\rho / 0.07651}$	Army Maximum Conditions: Temperature, Degrees Centigrade	Pounds Per Foot, ρ	ρ / 0.06617	$\sqrt{\rho / 0.06617}$
0	29.921	76.00	15	0.07651	1.0000	1.0000	60	0.06617	1.0000	1.0000
5,000	24.89	63.23	5.1	0.06591	0.8615	0.9282	47.5	0.05719	0.8643	0.9297
10,000	20.58	52.26	−4.8	0.05651	0.7386	0.8594	35.0	0.04921	0.7437	0.8624
15,000	16.88	42.88	−14.7	0.04813	0.6291	0.7932	22.5	0.04207	0.6358	0.7974
20,000	13.75	34.91	−24.6	0.04076	0.5327	0.7299	10.0	0.03578	0.5407	0.7353
25,000	11.10	28.19	−34.5	0.03427	0.4479	0.6693	− 2.5	0.03022	0.4567	0.6758
30,000	8.880	22.56	−44.4	0.02861	0.3739	0.6115	−15.0	0.02535	0.3831	0.6190
35,000	7.036	17.87	−54.3	0.02369	0.3096	0.5564	−37.5	0.02200	0.3325	0.5766
40,000	5.541	14.07	−55.0	0.01872	0.2447	0.4947	−40.0	0.017513	0.2647	0.5144
45,000	4.364	11.08	−55.0	0.01474	0.1927	0.4390	−40.0	0.013793	0.2084	0.4565
50,000	3.436	8.730	−55.0	0.011607	0.15171	0.3895	−40.0	0.01086	0.16412	0.4051
55,000	2.707	6.876	−55.0	0.009143	0.11950	0.3457	−40.0	0.008556	0.1293	0.3596
60,000	2.132	5.415	−55.0	0.007201	0.09412	0.3068	−40.0	0.006738	0.10182	0.3191
65,000	1.679	4.265	−55.0	0.005671	0.07412	0.2723	−40.0	0.005307	0.08020	0.2832

Fan-Cooled Motors (Open or Enclosed)

Temperature-rise tests taken in an altitude chamber on a number of aircraft motors under different conditions showed that the temperature rise was approximately inversely proportional to the density raised to the 0.9 power. By use of this empirical fact, the winding temperature of open fan-cooled aircraft motors has been calculated and plotted in Figure 8 as a function of altitude with sea-level rise as parameter. From these curves a number of interesting conclusions can be deduced:

1. Winding temperatures start to increase sharply above 40,000 feet. For satisfactory performance at high altitude, a comparatively low sea-level temperature rise is essential.

2. Use of high-temperature insulation is not particularly helpful, either in increasing the maximum altitude rating or in reducing the weight by increasing the permissible sea-level rise.

3. For a maximum altitude rating of 40,000 feet, at a maximum ambient temperature of −40 degrees centigrade, the maximum permissible sea-level rise is: for class *A* insulation, 50 degrees centigrade; for class *B* insulation, 56 degrees centigrade.

4. For a maximum altitude rating of 50,000 feet, at a maximum ambient temperature of −40 degrees centigrade, the maximum sea-level rise would be: for class *A* insulation, 33 degrees centigrade; for class *B* insulation, 37 degrees centigrade. Use of a high-temperature insulation which would permit a temperature rise of 140 degrees centigrade (total temperature of 200 degrees centigrade) still would require the motor to have a sea-level rise as low as 46 degrees centigrade.

These conclusions are somewhat pessimistic for motors smaller than 4 inches in diameter, and optimistic for motors larger than this.

Weight is always a matter of primary concern, and it would be interesting to know how the weight of a motor is affected by the maximum altitude at which the motor is intended to operate. Curves in Figure 8 show what the sea-level rise has to be in order not to exceed safe temperatures at any given altitude, but it is not so easy to determine how the weight of the motor is affected by the sea-level temperature rise for which it is designed. However, since it frequently is assumed that weight is proportional to the square root of the output, it seems fairly reasonable to assume that the weight would vary inversely as the square root of the specified sea-level temperature rise. On this assumption, Figure 9 was plotted to show how the weight of an open fan-cooled aircraft motor is affected by the maximum altitude for which the motor is designed. This curve shows that a motor actually designed for 50,000 feet

might be as much as 20 per cent heavier than similar motors designed for a maximum altitude of but 40,000 feet.

Enclosed Motors (Not Fan Cooled)

The dissipating capacity of an enclosed motor does not fall off with increase in altitude so fast as that of a fan-cooled motor, primarily because:

1. Watts loss dissipated by radiation is independent of the air density.

2. Watts loss dissipated by natural convection is proportional to the square root of the density. (With forced convection, as in blast-cooled or fan-cooled machines, the watts dissipated are proportional to the first power of density.)

Using a combination of empirical and theoretical data, the frame temperature of a totally enclosed motor has been calculated as a function of altitude, with sea-level temperature rise of the frame as parameter. These curves are given in Figure 10. (It must be borne in mind that the temperature of the winding will be somewhat higher than the frame temperature.) Comparing these curves with those of Figure 8, it readily is concluded that the rating of enclosed motors is not reduced so much at altitude as those of fan-cooled motors. In fact, if a totally enclosed motor is designed for a sea-level rise of 70 degrees centigrade, it should give satisfactory performance at all altitudes from sea level up to well above 60,000 feet. It also appears likely that a motor designed for class B insulation with a 90-degree-centigrade temperature rise at sea level would be satisfactory at all altitudes from sea-level up to 50,000 or 60,000 feet.

Summary of Effect of Altitude on Heat Transfer

Generally speaking, the heat generated in an aircraft electric machine may be dissipated in a number of different ways. How altitude conditions affect the amount of heat lost by each of the different components of heat transfer are summarized in the following equations.

Forced convection, blast cooling, without internal fan:*

$$\frac{P_{1A}}{P_{1o}}=\sqrt{\left(\frac{\rho_A}{\rho_o}\right)\left(\frac{h_{gA}}{h_{go}}\right)}\left(\frac{T_{SA}-T_{aA}}{T_{So}-T_{ao}}\right) \tag{11}$$

Forced convection, fan cooling:

$$\frac{P_{1A}}{P_{1o}}=\frac{\rho_A}{\rho_o}\times\frac{RPM_A}{RPM_o}\times\frac{T_{SA}-T_{aA}}{T_{So}-T_{ao}} \tag{12}$$

Free convection:

$$\frac{P_{1A}}{P_{1o}}=\sqrt{\left(\frac{\rho_A}{\rho_o}\right)}\left(\frac{T_{SA}-T_{aA}}{T_{So}-T_{ao}}\right)^{1.25} \tag{13}$$

Radiation:

$$\frac{P_{1A}}{P_{1o}}=\frac{(T_{SA}+273)^4-(T_{aA}+273)^4}{(T_{So}+273)^4-(T_{ao}+273)^4} \tag{14}$$

Symbols

A = subscript A denotes "at altitude." May be added to any of the following symbols

o = subscript o denotes "at sea level." May be added to any of the following symbols

h_c = closed-end pressure of a blast tube above accessory compartment, inches of water

h_o = open-end pressure of a blast tube above accessory compartment, inches of water

h_g = total head across the generator, inches of water

h_v = velocity head of air flowing through blast tube, inches of water

h_{vg} = velocity head of air entering generator, inches of water (equation 4)

h_{gf} = pressure head developed by an internal fan, inches of water

F_p = pressure developed by an internal fan at 1,000 rpm at sea-level air density

N = revolutions per minute

T_o = temperature of exit air, degrees centigrade

T_s = temperature of stator windings, degrees centigrade

T_a = temperature of ambient air or of air entering generator

P_1 = total watts loss carried away by cooling air

W = weight flow of cooling air, pounds per minute

ρ = specific weight of air, pounds per cubic foot

$C_1, C_2, \ldots$ = proportionality constants

β = exponent in equation 8

I_o = current rating of generator at sea-level, amperes

I_A = permissible current output (thermal basis only) at altitude, amperes

References

1. Blast-Tube Cooling for Aircraft Generators, Cyril G. Veinott. AIEE Transactions, volume 63, 1944, July section, pages 520–5.

2. Altitude Rating of Electric Apparatus, Paul Lebenbaum, Jr. AIEE Transactions, volume 63, 1944, December section, pages 955–60.

* If an internal fan is used, substitute h_{vA} and h_{vo} for h_{gA} and h_{go}, respectively.

Electrical Analogy Methods Applied to Servomechanism Problems

G. D. McCANN
MEMBER AIEE

S. W. HERWALD
NONMEMBER AIEE

H. S. KIRSCHBAUM
ASSOCIATE AIEE

Synopsis: This paper describes the application of the transient analyzer to the solution of servomechanism problems by the electrical-mechanical analogy method. The analogies for angular position servomechanisms are developed in detail together with the fundamental concepts by which the systems can be defined in terms of dimensionless parameters. This permits the results to be given in dimensionless form suitable for general application. Typical solutions of representative systems are given in the form of transient response curves. These show the response characteristics for suddenly applied constant velocity and sinusoidal motion. Also shown are the effects of varying the controlling parameters of the system including the stiffness constant, one, two, and three time delays, and methods of producing system stability including negative RC feedback and anticipatory control. A method is developed for setting up the analogy for a specific system on the transient analyzer by a suitable change in time and impedance bases.

WITH THE RAPID INCREASE in the use of accurate servomechanisms it has become desirable to provide a practical means of quickly and accurately analyzing in detail their performance under various operating conditions. The complexity of most servo systems makes it impractical to calculate transient response in any detail by conventional mathematical methods. Although it is usually possible to determine natural frequencies and damping rates, sufficient calculations to determine actual response for an optimum design is quite laborious and time consuming. The method of electrical analogy now has been applied to this type of system. Additional facilities in the form of special amplifier circuits have been developed to be used in conjunction with the mechanical-transients analyzer[1,2] for setting up the electrical analogue of many of the basic types of servo systems. With this equipment an analogous electric circuit is set up; the desired transient or steady-state condition to which the servo system must regulate is generated as an electrical excitation function; and the complete solution for its response is viewed or recorded on the screen of a cathode-ray oscilloscope. This paper treats the application of the transient analyzer to angular position servomechanisms, a fundamental analysis of which is given in reference 3.

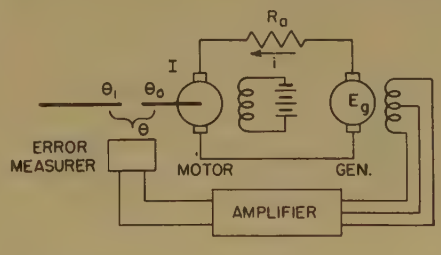
Paper 46-17, recommended by the AIEE committee on instruments and measurements for presentation at the AIEE winter convention, New York, N. Y., January 21–25, 1946. Manuscript submitted November 8, 1945; made available for printing November 27, 1945.

G. D. McCANN, S. W. HERWALD, and H. S. KIRSCHBAUM all are with the Westinghouse Electric Corporation, East Pittsburgh, Pa.

Electrical Analogies for Angular Position Servomechanisms

For most systems involving mechanical motion there are several practical electrical analogies.[2] Thus several completely electric circuits can be used to represent an electromechanical system. The one used here for angular position servomechanisms is illustrated in Figures 1 and 3. Figure 1 shows the case of a simple error-control system with no electric time delays. A single differential equation (equation 1) can be formed expressing the mechanical motion of the system in terms of both mechanical and electrical parameters. The inertia is represented by an inductance and the motor-generator armature circuit losses by a resistor. The analogue for the error measurer is the capacitor C_0 of Figure 1. The voltage across it is proportional to the charge that is analogous to angular displacement $\theta_1 - \theta_0$ when the circuit for simulating the motion θ_1 to be followed by the servo system is connected as shown. A wide variation in the character of the motion θ_1 can be simulated with the excitation circuits of the mechanical-transients analyzer.[2] With these a voltage is produced proportional to the assumed velocity of the device to be followed. This feeds current into C_0 through a relatively high resistor, so that the voltage across C_0 is negligible during the period in which the solution is obtained. The capacitor voltage (which is the error voltage) also must be very small compared to the voltages across L and R of the servo analogy so as not to distort its motion. This requires a fairly large value of capacitance for C_0. The amplifier of Figure 1 completes the analogous circuit. Its output voltage E_0 is analogous to the controller torque M_c, giving the simple relationship of equation 2 (Figure 1) for the stiffness constant K.

General solutions[3] of this simple system can be expressed readily in dimensionless form as shown in Figure 2. This is of considerable value, as it greatly increases the usefulness of the solutions. As will be shown later, solutions for the more com-



A—Mechanical system
Equation for armature circuit:

$$E_g = R_a i + g\frac{d\theta_0}{dt}$$

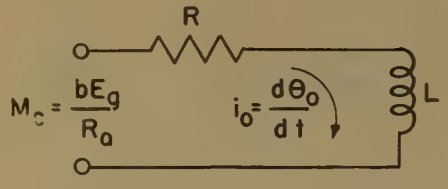
Equation for motor torque:

$$bi = I\frac{d^2\theta_0}{dt^2}$$

Combining in a single torque equation:

$$\frac{bE_g}{R_a} = I\frac{d^2\theta_0}{dt^2} + \frac{bg}{R_a}\frac{d\theta_0}{dt} = M_c = K(\theta_1 - \theta_0) \qquad (1)$$

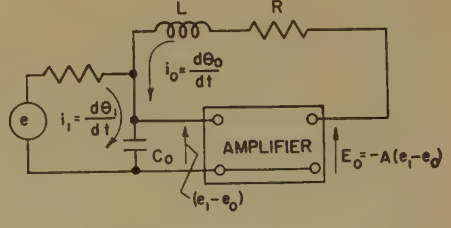
Figure 1. Electrical analogy used for simple error-control servomechanisms with no electric time delays



B—Analogous circuit for torque equation

$$R \equiv c = \frac{bg}{R_a}$$

$$L \equiv I$$

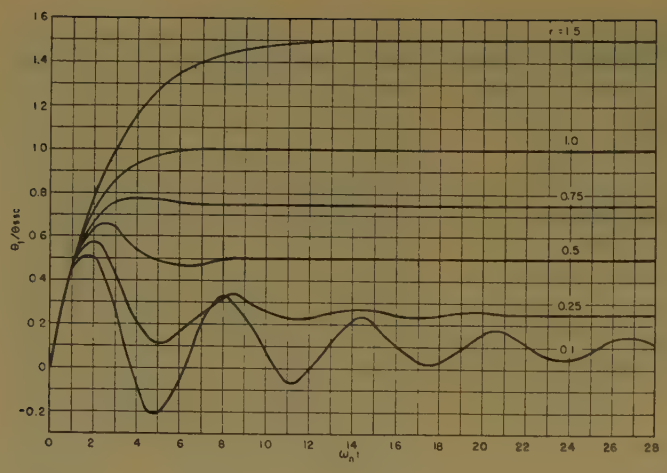


C—Complete analogous circuit

$$M_c = K(\theta_1 - \theta_0) \equiv A(e_1 - e_0)$$

$$(e_1 - e_0) \equiv \frac{\theta_1 - \theta_0}{C_0}$$

$$K = \frac{A}{C_0} \qquad (2)$$



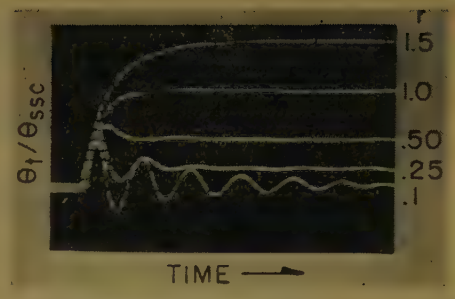


Figure 2 (left and right). Response curves of simple error servomechanisms to constant velocity

$\theta(t)$ = error angle as function of time
θ_{ssc} = steady-state error angle for critically damped systems

$$\theta_{ssc} = 2\frac{\omega_1}{\omega_n}$$

ω_1 = magnitude of applied constant velocity

$\omega_n = \sqrt{\frac{K}{I}}$ = undamped natural frequency

K = stiffness constant
I = total system inertia

$r = \frac{c}{2\sqrt{IK}}$ = ratio of actual to critical damping

c = actual damping

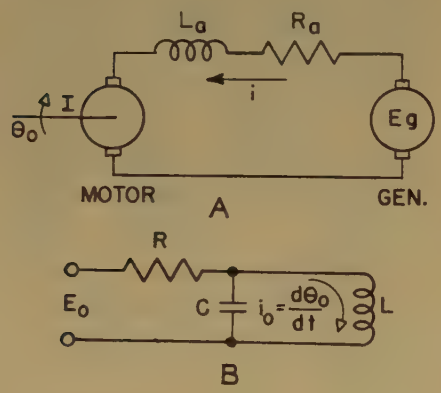
plex practical servomechanisms also can be put in this same dimensionless form. It is this characteristic that allows the use of a calculating board device (with a limited range of variation in its circuit constants) for the general solution of such problems. Thus for convenience in setting up a given system on the analyzer the time base and the impedance base can be changed arbitrarily to form a new system from which either the actual numerical solution for the given system or a dimensionless solution readily can be obtained. The conversion formulas for making these changes are given in Table I. These are understood readily from consideration of the equations at the bottom of the table. Since the ratios of the angular motion θ to the system torques are reduced by the factor a in the simulated system, its stiffness constant K'' must be greater than the actual stiffness K by the same ratio. The application of this table to the solution of an actual problem will be illustrated later.

Effect of Additional Time Delays

The analogous circuit for cases where the motor generator armature circuit inductance is taken into account is developed in Figure 3a. This inductance has its analogy in a capacitance C_1, resulting in an RC time delay T_1. Other time delays, such as that in the generator field, can be represented by RC circuits placed between stages of the amplifier as shown in Figure 3b. It is necessary, however, that each delay circuit be isolated by a stage of amplification. Such time constants must be changed, when the time base is changed, as shown in Table I. When defining them for a general solution in dimensionless form they must be multiplied by ω_n.

Stabilization With RC Feedback

For servomechanisms of this type system stability frequently is obtained by



a. Representation of armature circuit inductance

A—Mechanical system
B—Analogous all-electric circuit

$$E_g = R_a i + L_a\frac{di}{dt} + g\frac{d\theta_0}{dt}$$

$$bi = I\frac{d^2\theta_0}{dt^2}$$

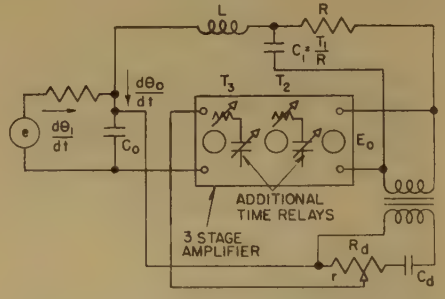
giving

$$M_c = \frac{bE_g}{Ra} = \frac{L_a I}{Ra}\frac{d^3\theta_0}{dt^3} + I\frac{d^2\theta_0}{dt^2} + \frac{bg}{Ra}\frac{d\theta_0}{dt}$$

Electric circuit equation:

$$E_0 = RCL\frac{d^2 i_0}{dt^2} + L\frac{di_0}{dt} + Ri_0$$

where, $R \equiv \frac{bg}{Ra}$, $L \equiv I$, $C \equiv \frac{La}{bg} \equiv \frac{T_1}{R}$



b. Analogous circuits for time delays and negative RC feedback

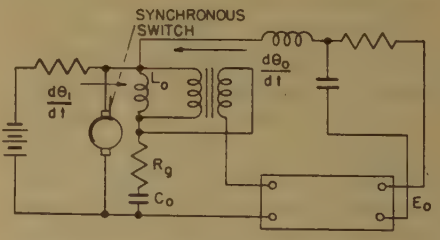
Equation for feedback voltage:

$$e_d = \frac{-rC_d p}{(1+pt_1)}(E_0 \equiv M_c)$$

$$p = \frac{d}{dt},\ t_1 = R_d C_d,\ n = \frac{r}{R_d}$$

$$e_d = \frac{-npt_1}{(1+pt_1)}(E_0 \equiv M_c)$$

Figure 3. Electrical analogies used for various elements of angular position servomechanisms



c. Analogous circuit for error-plus-error rates control

For actual system:

$$M_c = K(\theta_1 - \theta_0) + KT_a p(\theta_1 - \theta_0) + K(T_L)^2 p^2(\theta_1 - \theta_0)$$

In analogous circuit:

$$E_0 \propto M_c$$

$$E_0 = \frac{A}{C_0}(\theta_1 - \theta_0) + AR_g p(\theta_1 - \theta_0) + AL_0 p^2(\theta_1 - \theta_0)$$

$$K = \frac{A}{C_0},\ T_a = \frac{AR_g}{K},\ (T_L)^2 = \frac{AL_0}{K}$$

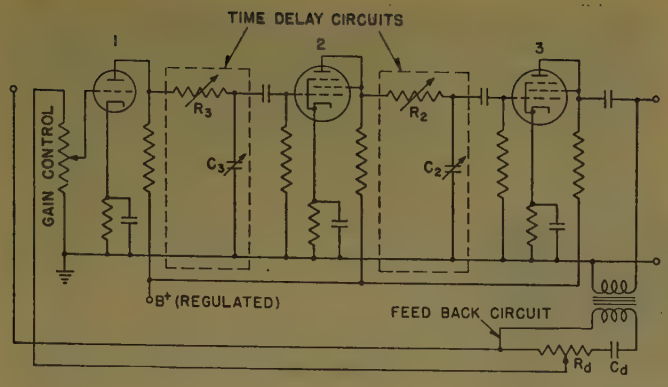


Figure 4. Circuit elements of amplifier used for servomechanism analogies

using a resistance-capacitor network connected across some voltage that is proportional to the controller torque M_c. The equation for the feed-back voltage from this type of circuit is shown in Figure 3b. It is put in general form by expressing it in terms of a dimensionless ratio n and a time constant t_1. For dimensionless solutions t_1 must be multiplied by ω_n.

Error-Plus-Error Rates Control

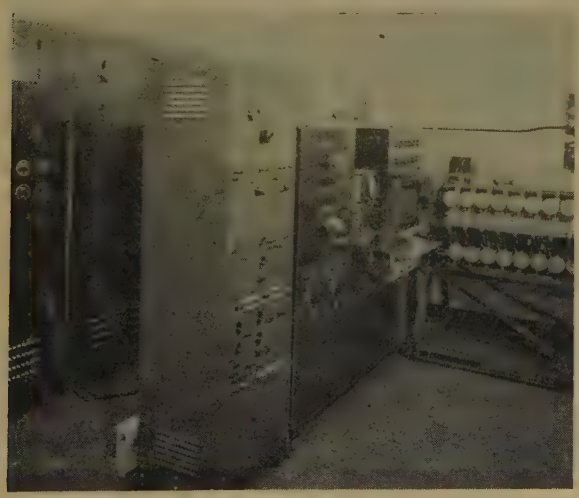
Other forms of system stability consist of providing an additional control torque term proportional to the first derivative of the error angle $\theta_1-\theta_0$ and possibly a negative term proportional to the second derivative of the error angle. The forms for these control functions together with their electrical analogy are given in Figure 3c. These functions are expressed in terms of the stiffness constant K and time constants, so that they can be defined readily in dimensionless form. In actual systems the control term proportional to the rate of change of the error angle (commonly called anticipatory control) usually must be produced by a mechanism having its own time delays. This is sometimes a gyroscopic mechanism. The method of representing these additional terms is shown in an example to be discussed later (see Figure 11).

Description of the Servomechanism Analyzer

Suitable amplifiers and associated circuits have been developed to be used in conjunction with the mechanical-transients analyzer to provide facilities for the rapid analysis of such servomechanisms as have been described above. The amplifier, typical elements of which are illustrated in Figure 4, is of the conventional resistance coupled type, designed to have a frequency response that is flat down to 10 cycles per second, that being the frequency at which the transient forcing functions usually are repeated on the analyzer.[1,2] This response is achieved by using large coupling and by-pass capacitors and by using a regulated power supply which prevents regeneration at low frequencies. Although the amplifiers must be linear, the added complication involved in using push-pull resistance coupled amplifiers was not justified, and single-ended triode amplifiers were found to be satisfactory. The maximum harmonic distortion in the last stage is about 5 per cent; the distortion in the previous stages is entirely negligible. Power amplifiers are used for all but the first stage, so that various damping and time delay circuits connected to the outputs of the various stages do not affect the amplification.

Time delay, such as that arising from the field of an exciter, is represented by a circuit such as R_2, C_2 of Figure 4. The voltage developed at the grid of the third tube will lag behind the plate voltage of the second tube in exactly the same way that an exciter armature voltage will lag behind the voltage applied to its field terminals. The time constant which describes this delay is R_2C_2 in seconds. Additional time delays can be introduced as shown at the input to the second stage. Resistance-capacitance feed-back damping voltages from the amplifier output are fed back to the input by using an isolating transformer. This transformer has very good frequency response down to 10 cycles per second, thus reproducing accurately the voltage which appears at the output of the amplifier. These transformers also may be used as damping transformers when simulating voltage regulating systems.[4] Flexibility in the general application of the amplifier is obtained by making the amplifier stages, the time delay circuits, the isolating transformers, and the RC feed-back circuit each a separate entity.

Figure 5 shows the laboratory equipment. To the right are the synchronous switches which repeat the transient 10 times per second. Next to the switches is the central control desk from which the operator can measure on the oscilloscopes any voltage across or any current flowing in the various circuit elements. This desk also contains generators for producing various types of arbitrary forcing functions. To the left is the servomechanism analyzer cabinet, which contains the amplifiers and associated circuits described in the accompanying paragraph. Low-loss inductances and capacitors for representing mechanical systems are contained in the cabinets arranged behind the control desk and servomechanism analyzer cabinet.



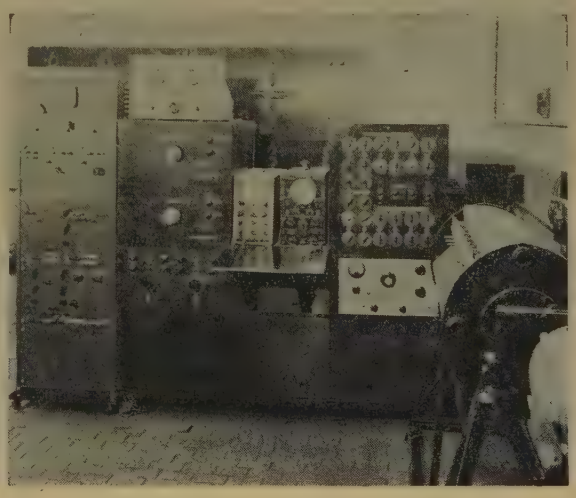


Figure 5. Setup in transients analyzer laboratory for the solution of servomechanism problems

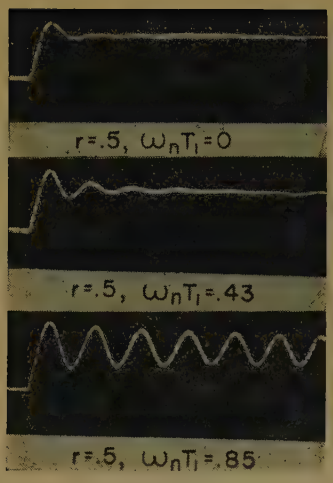


Figure 6. Response curves of error servomechanism, with one time delay, to constant velocity

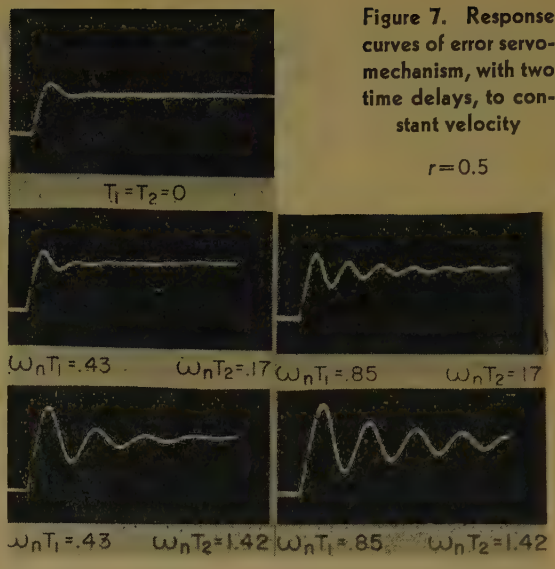


Figure 7. Response curves of error servomechanism, with two time delays, to constant velocity

$r=0.5$

Typical Solutions

In Figure 2 oscillograms are shown of general solutions for the response of the simple error control system to a constant velocity for comparison with calculated curves. The value of this method of analogy can be appreciated when it is considered that such a set of oscillograms can be obtained in a matter of minutes. Figures 6, 7, and 8 show the effect of time delays on the response of the typical angular position servomechanism to a suddenly applied constant velocity. Figure 6 shows the effect of varying the magnitude of a single time delay. The magnitudes of the time delays are given in the dimensionless form, $\omega_n T$, so that the results have general application. The results with $\omega_n T_1$ constant and a second time delay, $\omega_n T_2$, varied are given in Figure 7. Similarly, Figure 8 shows the effect of varying $\omega_n T_3$ with $\omega_n T_1$ and $\omega_n T_2$ constant. In a practical case the three time delays could represent armature, generator field, and exciter field time delays, respectively. The range of parameters used represents practical control systems.

Obtaining system stability by negative *RC* feedback is probably the most common method in use today. Figure 9 shows two cases of stability obtained by negative *RC* feedback. The time constant of the *RC* circuit, $\omega_n t_1$, as well as the system damping and time delays, all are given in dimensionless form. The large initial overshoot and the considerable reduction in system frequency which is always characteristic of negative *RC* feedback is quite apparent in each of the two examples shown in Figure 9. The *RC* time constants are large, when compared with the system time delays, and are in the optimum range for best results.

The response of any servomechanism to a sinusoidal forcing function is usually of great interest in design. Figure 10 shows the response of an angular position servomechanism to a suddenly applied sinusoidal motion of varying frequency, ω_1.

Figure 8. Response curves of error servomechanism with three time delays, to constant velocity

$r=0.5$

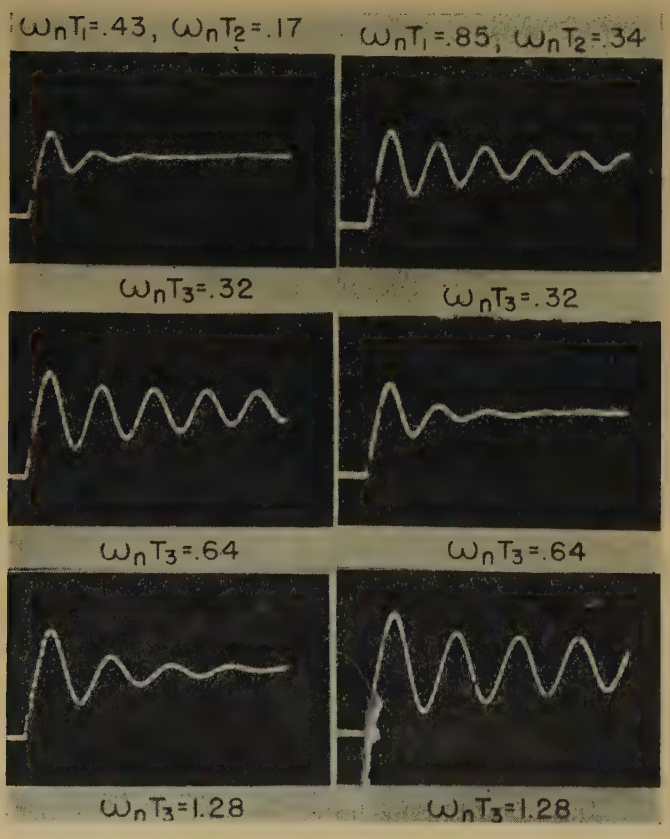
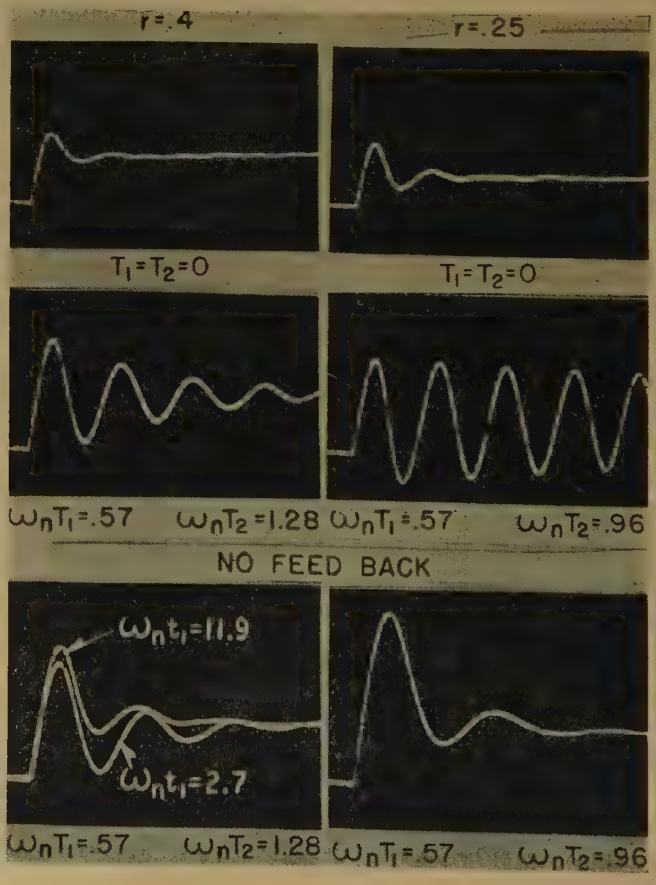


Figure 9. Response curves of error plus negative *RC* feedback servomechanism with two time delays to constant velocity



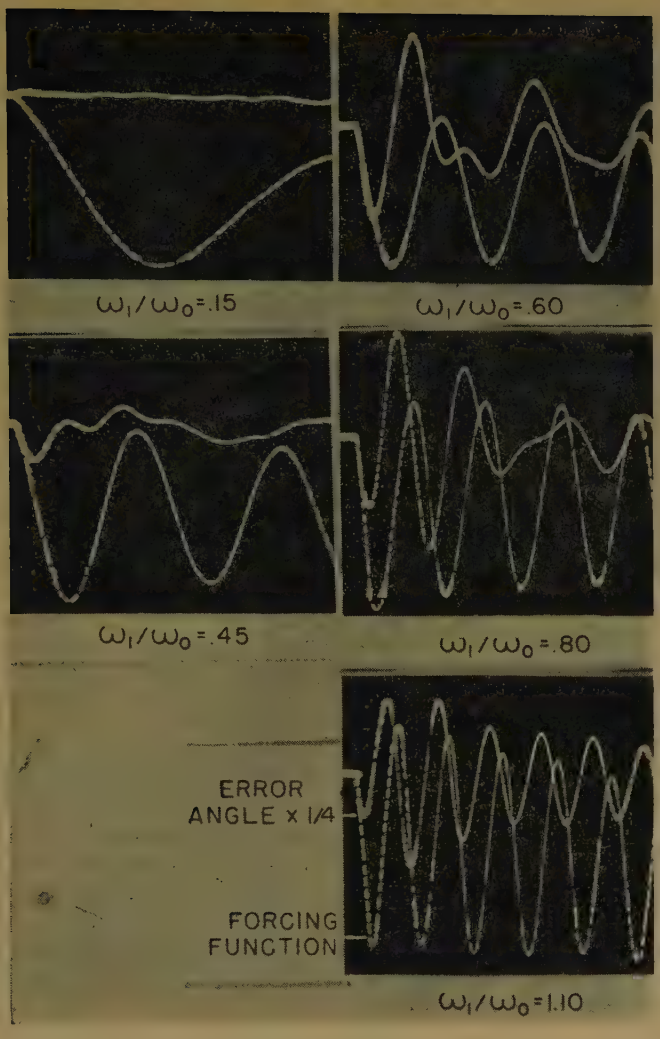


Figure 10. Response curves of error servomechanism to sinusoidal motion

r=0.17

The response at frequencies well below the system frequency, ω_0 is quite good with hardly any error appearing. However, as the frequency is increased, the response becomes poorer with large following errors. When ω_1 is very close to ω_0, such as the case $\omega_1/\omega_0=1.10$, the error actually becomes larger than the applied disturbance θ_1. The steady-state response to sinusoidal motion also can be obtained quite easily when an oscillator is used as the excitation function for θ_1.

Tank Turret Traverse Servo System

The following example serves to further illustrate the application of the electrical analogies and the conversion formula of Table I to the solution of a specific system. This problem is that of an electric drive that had been designed for the traverse movement of a tank turret.[5] The schematic of the mechanical system, its equation of motion, the analogous electric circuit, and the units for both the actual system and the electrical analogy are given in Figure 11a. The gyroscope in the actual system serves as the means for obtaining system stability. If the gyroscope is rotated proportional to $\theta=(\theta_1-\theta_0)$ and is also capable of restrained rotation about an axis 90 degrees from the θ axis; any point of the gyroscope not on either axis has a motion proportional to $\theta+p\theta$. This motion is used to operate a silverstat in the generator field circuit. This is anticipating control and is a phase advance that tends to compensate for the system time delays. The rate component of gyroscope movement is caused by the gyroscope torque, exerted about the 90-degree axis, that is proportional to the speed of rotation about the θ axis. There is spring restraint, inertia, and critical damping about the 90-degree axis, so that instead of a rotation instantaneously proportional to $p\theta$ (as shown in Figure 3b) it is delayed and appears as the term

$$\frac{KT_a p(\theta_1-\theta_0)}{(1+t_1 p)^2}$$

of the mechanical system equation shown in Figure 11a. T_a is the ratio of torque per unit velocity error, $p\theta$, to torque per unit displacement error, θ.

With the constants shown in Figure 11a, the calculated turret frequency was 1.4 cycles per second and the damping decay 78.1 per cent per cycle.[5] The oscilloscope record of Figure 11b with delayed anticipation represents the same calculation and checks to within 5 per cent or better. The remaining oscillographs of Figure 11b show the system as it would hunt without any means of obtaining system stability; what could be done with negative *RC* feedback, with undelayed anticipation, and what could be done by a combination of negative *RC* feedback and delayed anticipation. The two disadvantages of negative *RC* feedback compared with anticipating control are quite apparent in Figure 11b. The initial overshoot is much greater, and the system frequency has been considerably reduced. The combination of anticipation and some *RC* feedback gives the best response for this particular example. It is to be noted, however, that the improvement over anticipation alone is not too

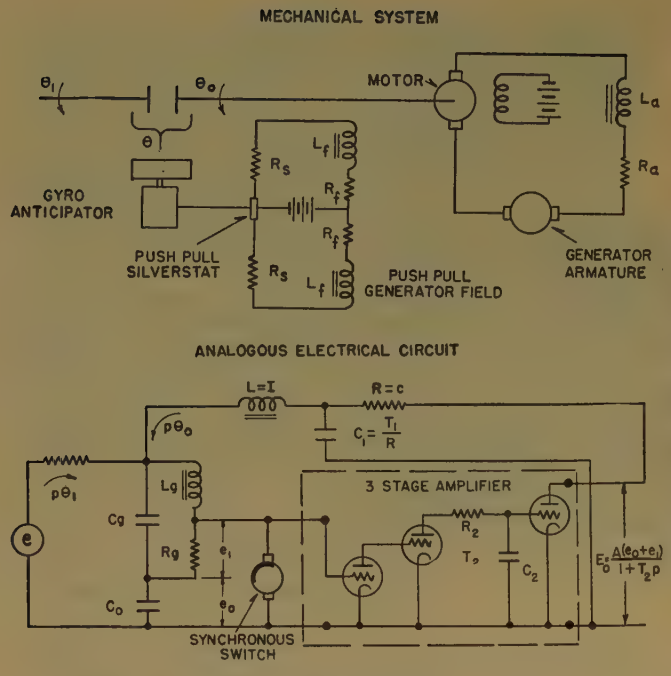
Table I. Conversion Formula for Changing Time and Impedance Bases in Setting Up Analogy for Servomechanisms

Actual System	Time Base Changed to $t'=t/n$	Impedances Multiplied by Constant a
L (henrys) $=l$ (pounds-inch-seconds^2)	$L'=L/n^2$	$L''=aL/n$
R (ohms) $=c=\frac{bg}{R_a}$ (inch-pounds/radians per second)	$R'=R/n$	$R''=aR/n$
E_0 (volts) M_c (inch-pounds)	$E_0'=E_0$	$E_0''=E_0$
i_1, i_0 (amperes) $\alpha \frac{d}{dt}(\theta_1, \theta_0)$ radians per second	$\theta'=\theta$	$\theta''=\theta/a$
$\omega_n=2\pi\times$undamped natural frequency	$\omega_n'=n\omega_n$	$\omega_n''=n\omega_n$
$K=\omega_n^2 I$	$K'=K$	$K''=aK''$
$K=M_c/(\theta_1-\theta_0)$	in analogous electric circuit	$K''=A/C_0$
Time delays T (seconds)	$T'=T/n$	$T''=T/n$

Equation for simple error servomechanism: $M_c=K(\theta_1-\theta_0)=\frac{bEg}{R_a}=L\frac{d^2\theta_0}{dt^2}+R\frac{d\theta_0}{dt}$

Transformation to time base $t'=t/n$: $Mc'=L/n^2\frac{d^2\theta_0'}{dt'^2}+\frac{R}{n}\frac{d\theta_0'}{dt'}$

Multiplying impedances by a: $M_c''=\frac{aL}{n^2}\frac{d^2\theta_0''}{dt''^2}+\frac{aR}{n}\frac{d\theta_0''}{dt''}$



11a. Analogous circuit and system constants

Equation for mechanical system:

$$Ip^2\theta_0+\frac{cp\theta_0}{1+T_1p}=\frac{K\left(1+\frac{T_ap}{(1+t_1p)^2}\right)\theta}{(1+T_1p)(1+T_2p)}$$

Units

Actual mechanical system:

$I=7.78\times10^{-2}$ pound-inch seconds^2
$c=0.33$ inch-pound per radian per second
$T_1=0.02$ second
$T_2=0.1$ second
$K=4$ inch-pounds per radian
$T_a=0.15$ second
$t_1=0.01$ second

Converted electric system with $n=200$ and $a=3.1\times10^6$

$$L''=\frac{aI}{n^2}=6.02 \text{ henrys}$$

$$R''=\frac{ac}{n}=5{,}130 \text{ ohms}$$

$$T_1''=\frac{T_1}{n}=10^{-4} \text{ seconds}$$

$$T_2''=\frac{T_2}{n}=5\times10^{-4} \text{ seconds}$$

$K''=aK=12.2\times10^6$
$C_0''=14\times10^{-6}$ farads
$A''=K''C_0=171$

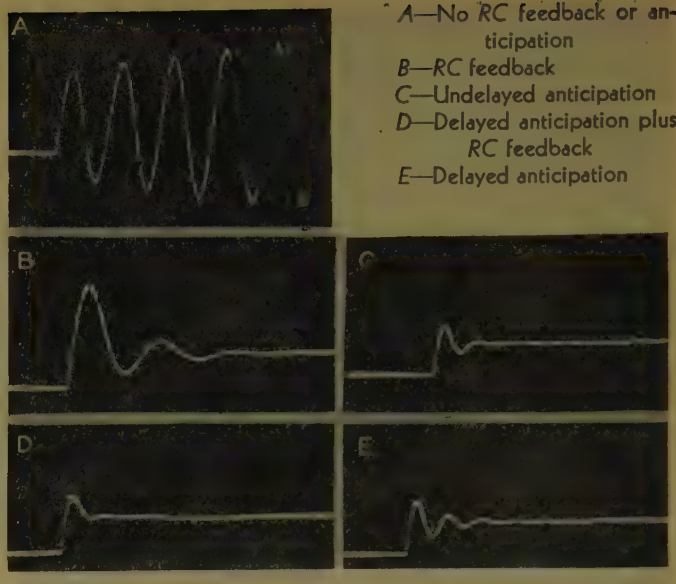
$$T_a''=T_a/n=7.5\times10^{-1}$$

$$R_1''=\frac{K''T_a''}{A''}=54 \text{ ohms}$$

$$t_1''=t_1/n=5\times10^{-5} \text{ seconds}$$

$$C_1''=\frac{2t_1''}{R}=1.86\times10^{-6} \text{ farads}$$

$$L_1''=\frac{R_1''t_1''}{2}=1.35\times10^{-3} \text{ henrys}$$



A—No RC feedback or anticipation
B—RC feedback
C—Undelayed anticipation
D—Delayed anticipation plus RC feedback
E—Delayed anticipation

11b. Response curves to constant velocity

Figure 11 (left and above). Tank turret traverse servomechanism

great and would not warrant the use of much extra equipment.

Conclusions

From the examples shown it can be seen that the transients analyzer offers an excellent method for solving fundamental servomechanism problems. The ease with which the response of systems involving high order differential equations can be obtained points the way toward many useful solutions not only of particular systems but also in dimensionless form for general application. The accuracy of the method has been demonstrated by close checks with previously calculated cases. It therefore provides a reliable and practical method for the general analysis of certain basic types of servomechanisms and of specific systems too complex for adequate study by conventional mathematics.

References

1. System Recovery Voltage Determination by Analytical and A-C Calculating Board Methods, R. D. Evans, A. C. Monteith. AIEE Transactions, volume 56, 1937, June section, pages 695–705.

2. A New Device for the Solution of Transient Vibration Problems by the Method of Electrical-Mechanical Analogy, H. E. Criner, G. D. McCann, C. E. Warren. *Journal of Applied Mechanics*, September 1945, volume 12, number 3, page 135.

3. Considerations in Servomechanism Design, S. W. Herwald. AIEE Transactions, volume 63, 1944, December section, pages 871–6.

4. Recent Developments in Generator Voltage Regulation, C. R. Hanna, K. A. Oplinger, C. E. Valentine. AIEE Transactions, volume 59, 1940, pages 692–700.

5. Electric Turret Traversing Mechanism for the M-4 Tank, S. J. Mikina, Jr. *Applied Mechanics*, December 1945, page 334.

TRANSACTIONS SECTION

Preprint of Corresponding Pages From the Current Annual AIEE Transactions Volume

Investigation of Arc Starting Characteristics of D-C Welders With Reference to Electrode Freezing

JOSEPH M. TYRNER
ASSOCIATE AIEE

Synopsis: A method for investigating the starting characteristics of an arc in d-c arc welding was developed and equipment was designed and built to simulate the behavior of an operator in starting such an arc. This testing equipment was used to compare the arc striking ability and the arc freezing tendency of an electrode when used with various types of welding generators. It was found that the determining factor is the electrode contact duration, that is, the time during which the operator leaves electrode and work in contact when he attempts to start an arc. Generators, to be satisfactory, should permit at least 40 milliseconds contact duration. Where the permissible contact duration between work and electrode is less than 40 milliseconds, only experienced welders are able to start an arc. Less trained men freeze the electrode to the work piece in a large percentage of their attempts. Five generators of different design were tested with the apparatus. Oscillograms of the current surge during the contact period were taken and the freezing point marked on the curves. It was found that the location of the freezing point depends on the shape of the current surge. Characteristics of a welding generator as developed in these tests which yield good striking and nonfreezing results are not contradictory to good general welding characteristics.

SUCCESS IN STARTING an arc using power from a d-c welding generator does not depend on the electric circuit alone, but also to a great extent on the skill of the operator. An experienced man has fewer failures than an untrained one. If we want to design an apparatus with something like "adjustable operator skill" we have to analyze the skill of a welder. We find that operators when striking an arc may differ in the contact pressure they exert, and also in the time they leave the electrode in contact with the work.

As far as the contact pressure is concerned, it is reasonable to assume that every operator tries to keep the contact pressure as low as possible in order to avoid freezing.

On the other hand, the aptitude of the man determines the duration of the contact between electrode and work piece. Therefore, it seems justified to accept this contact duration as the predominant characteristic of his skill.

With the foregoing in view, an apparatus was built which makes contact between the electrode and work for an adjustable and measurable duration. Figures 1 to 3 show various views of the apparatus. Figure 4 is a diagrammatic picture of it.

The apparatus consists of three parts as shown in Figure 4 numbered 1, 2, and 3. These three parts may move independently around the common axis *A–A*. Part 1 is a pendulum, on the upper extension of which an adjustable bracket (5) together with a chuck (6) is provided. The test electrode (7) is clamped in this chuck (6). The pendulum is kept in a raised position as long as the electromagnet (8) is excited to hold the armature (9). If the circuit of the coil (10) is opened, the magnet (8) releases the armature and the pendulum is free to swing.

Part 2 is the support of the work piece (11), which is used for the freezing test with the electrode (7). The weight (12) on part 2 tends to turn it counterclockwise, but part 2 is held in approximately horizontal position by the bracket (13), which rests on part 3.

The position of part 3 may be adjusted by the stop (15), against which it is held by the weight (14). In this way, the stop (15) establishes not only the position of part 3, but by means of the bracket (13), the position of part 2 as well.

When the pendulum (1) swings in a clockwise direction, the electrode (7) eventually reaches the test piece (11) and makes contact. The impact of the electrode (7), striking against the test piece (11), moves part 2 clockwise, lifting the bracket (13) from part 2. Electrode and test piece stay in contact until, on the return swing, the bracket (13) touches part 3 again. This stops part 2 and electrode and test piece become separated. In this way, the position of part 3, adjusted by the stop (15), determines the length of the contact duration. If the electrode (7) freezes to the test piece (11), the support (2) must follow, even after the bracket (13) reaches part 3. In this case, part 3 is pushed from the stop (15) and the weight (14) is lifted.

It is obvious that one weight (12) controls the contact pressure of electrode and test piece while the force which tends to separate electrode and test piece is determined by the other weight (14).

Contact pressure and breakaway force were not varied during the experiments. They were adjusted to conditions comparable to actual welding as performed by an experienced operator.

The contact duration is measured by the cycle counter (16). If the switch is in its "up" position, an a-c circuit through the cycle counter is closed as long as electrode and test piece are in contact. Swings of the pendulum with the switch in its upper position are used to adjust the contact time by setting the stop (15). The operator is protected from electric shock by the limit switch (18), which keeps the alternating voltage from the electrode-test piece gap, as long as the pendulum is held by the electromagnet (8).

The actual freezing test is made by putting one switch (17) into its down position. This removes the alternating voltage from the electrode-test piece gap and applies it to the holding coil (19) of contactor (20), which connects the genera-

Paper 46-12, recommended by the AIEE committee on electric welding for presentation at the AIEE winter convention, New York, N. Y., January 21–25, 1946. Manuscript submitted September 13, 1945; made available for printing December 11, 1945.

JOSEPH M. TYRNER is in the apparatus research department, Air Reduction Sales Company, New York, N. Y.

The author acknowledges and appreciates the cooperation given by J. J. Crowe, assistant vice-president, and E. E. Tisza of the apparatus research department, and the assistance of E. H. Cushman who built the apparatus and ran the tests covered by this paper. Acknowledgment is made also of the encouragement given to the investigation by C. I. MacGuffie, R. F. Wyer, and R. C. Freeman.

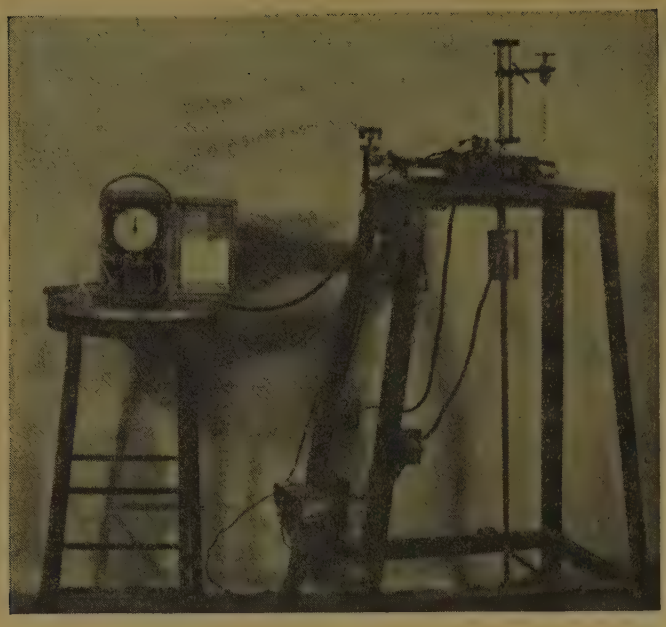


Figure 1. Apparatus with cycle counter

tor being investigated to the apparatus. Another switch (18), in this case, prevents energization of the coil as long as the pendulum is held by the solenoid. Thus, the operator is protected against an accidental flash. The circuit of the holding coil contains a second limit switch (25), which is opened by the movement of part 3 in case of freezing. This terminates the flow of welding current through the short circuit of electrode and test piece. If the electrode does not freeze, the lengthening of the arc drawn by the electrode breaks the circuit automatically and no switch is necessary.

Tests are initiated with the push button (24) which breaks the circuit of the coil (10) of the electromagnet (8).

The coil (10) of the electromagnet (8) is energized by direct current from the welding generator. It was found that the slight vibrations caused by an a-c magnet at that place falsify the test results.

The contact duration during the freezing test can be checked by taking an oscillogram as shown in Figure 5.

Procedure of Test

The operator clamps an electrode in the chuck (6) and provides a proper test piece (11). He adjusts the electrode roughly by moving the sleeve of the bracket (5) on the pendulum. The switch (17) is put into its "up" position. The button (24) is pressed and the pendulum released. The contact time is observed on the cycle counter. Then the stop (15) is adjusted to bring the contact time nearer to the desired value and the test repeated. After several trials, the apparatus is ready for test. To increase accuracy three timing swings are made without resetting the counter to zero. The reading thus becomes the sum of three contact times and one third of this value is considered to be the average contact time for the actual striking test. After the apparatus is adjusted to the desired contact time, switch (17) is put into its "down" position for the application of welding power. The next swing produces either a flash or the electrode freezes to the test piece.

A series of tests for different contact durations is run with a fairly large number of tests for each setting. For each setting, a number of freezings and a number of flashes are obtained. The frequency of freezings is calculated and plotted as a function of the contact duration. A curve thus is obtained which moves from a low percentage of freezings, at short durations, to a high percentage at long durations. The change from the low percentage to the high percentage is sudden. The contact duration yielding an equal number of freezings and flashes is called arbitrarily the "freezing time" of the generator.

Influence of Circuit Setting, Electrode Size, and Electrode Coating

It can be shown theoretically that the curve of the surge does not change much with different current settings. Therefore, the freezing time also does not change. The electrode size has no influence because the contact in the testing apparatus is a point contact only, and it

Figure 2. Front view of apparatus



Figure 3. Rear view of apparatus



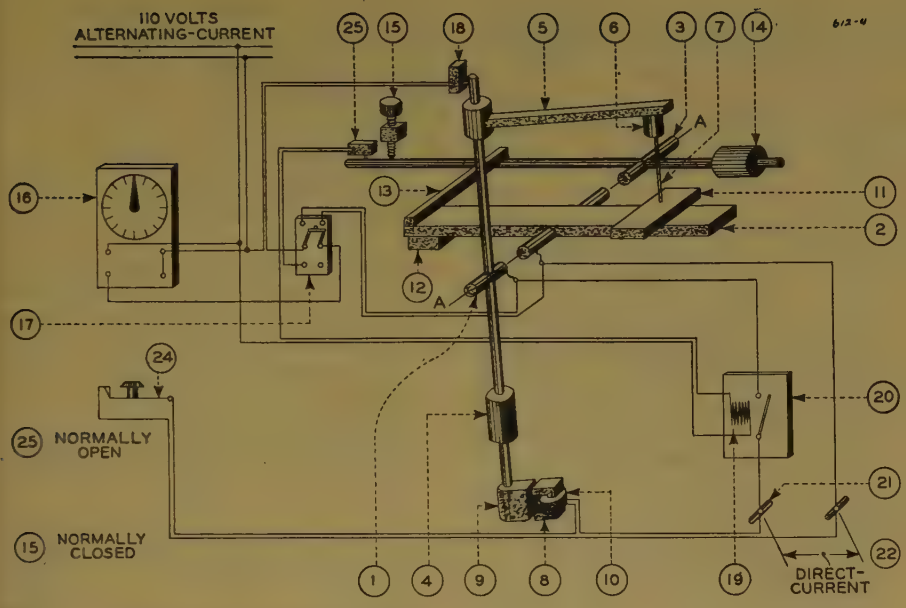


Figure 4. Diagrammatic picture of apparatus

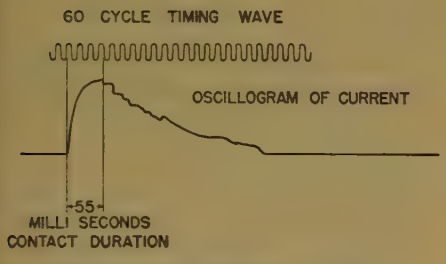


Figure 5. Oscillogram of current

does not matter whether the contact-making point is on a 1/16-inch diameter or on a 1/8-inch diameter electrode.

The coating has no influence provided the coating is kept away from the point of contact.

Consequently, it was decided to make all tests with bare electrodes of 3/32-inch diameter with generator settings of about 70 amperes welding current.

A few tests were made with other settings and with electrodes of other sizes and with different coatings. They confirmed these conclusions.

In order to eliminate the influence of scale, electrodes were ground square and test pieces cleaned thoroughly.

Generator Tests

Four commercial and one experimental generator with different circuits, but all of the same rating, were tested. All generators were set for the same welding output. The test results are shown in Table I.

Table I

Generator Tested	Critical Contact Time in Milliseconds
A	70
B	40
C (Generator *B* without external reactor)	25
D	50
E (Experimental)	1,000

In order to correlate these tests with the properties of the different electric circuits, open circuit short circuit transients of the five generators were determined by taking oscillograms. The freezing times are marked on the current curves shown in Figure 6. These curves show that freezing occurs some time after the highest point of the surge. The explanation may be that, during the decline of the surge, not enough heat is furnished to keep in a molten state the metal which melted at the height of the surge. The conclusion would be that the generator should reach its maximum current as late as possible. This is corroborated by the curve of generator *E* which approaches the maximum short circuit extremely slowly. Tests show that this generator practically never freezes.

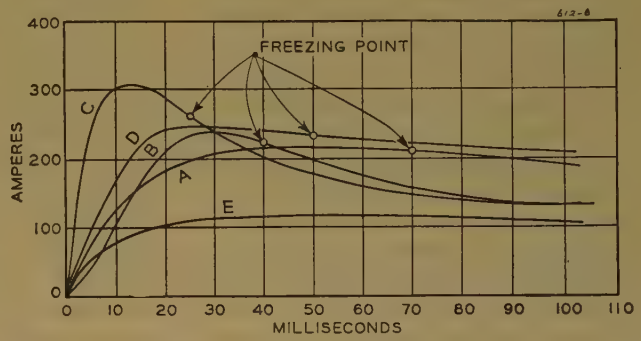


Figure 6. Threshold values of contact time

Freezing of electrodes

Operator Requirements

The requirements of the operator were determined by watching the reaction of different men to the generators which had been tested.

It was found that the average operator is satisfied with a generator which does not freeze during the first 40 milliseconds. Generators with contact times as long as 70 milliseconds are very good. Everything beyond that is excellent.

Simplified Tests

An apparatus of the kind described here usually is not available and it would be advantageous to be able to use standard equipment to judge a generator for its starting properties. Fortunately, an oscillogram of an open circuit short circuit test yields sufficient information. The curves of Figure 6 show that the critical time is approximately twice the time the generator needs to reach the crest of the surge. If we accept this without trying to find any reason for it, we may say that a generator should take at least 20 milliseconds to reach the crest of the surge. If it takes less, the generator is difficult to handle. On the other hand, a longer time indicates a generator with improved starting properties.

Stress Measurement by Electrical Means

ROBERT E. KERN
ASSOCIATE AIEE

SIDNEY B. WILLIAMS
ASSOCIATE AIEE

THE ADVENT of electric strain gauges[1] suitable for the measurement of mechanical performance on a strength basis not only has widened the field of the electrical engineer with regard to equipment and techniques but gradually has imposed upon him a responsibility to the aeronautical or mechanical engineer in his role as interpreter. For if the designer turns to electric strain gauges (and by this is meant herein the bonded wire gauge,[2] unless otherwise stated) for verification of his work, it is only natural for him eventually to leave the whole problem of gauge operation and data analysis to the electrical engineer. It is essential that both the man who measures and the man to whom the measurements are reported clearly understand the scope of their separate responsibilities. Otherwise there may exist a gap which will destroy the accuracy necessary to the honest affirmation or negation of the design. Accordingly, the authors here endeavor to present the strength evaluation problem broadly enough for one working in a relatively narrow element of it to appreciate the requirements of the whole, while emphasizing the electrical aspects primarily and keeping always in sharp focus the prime requisite, accuracy.

The Mechanical Problem

Design

As Sir Charles Darwin explained in his illuminating James Forrest lecture[3] entitled "The Extreme Properties of Matter" there is more opportunity for improvement in the strength of materials than in the refinement of almost any other property of materials. The theoretical ultimate shear strength of steel as given by Darwin is the shear modulus of elasticity divided by 2π. Depending on the grade of steel, this represents a possible improvement of 10 to 50 times, which values well might be assumed to be applicable to steel strength in general. These are figures to conjure with, but their ultimate realization probably will stand for years as the goal of physicists and metallurgists. A more realizable goal is the safe reduction of safety factors—or ignorance factors—relating the actual strength to the necessary strength. These are smaller in magnitude than the figures just quoted, lying perhaps in the range of 2 to 20, but represent possible weight and dimension savings in every industry large enough to guarantee a broad and lasting activity in strength analysis and strength measurement.

This, then, is the beginning of the problem. The optimum design stems from an accurate knowledge of the loads to be imposed. The quiescent and dynamic loads, their interrelation, the expected life and the relative importance of an occasional failure, make this problem complex. And it is complicated many-fold by that imponderable, the proper theory of failure.[4] Suffice it to say that there exist at least five theories of failure, but most test data have been reported and analyzed in terms of stress, rather than strain, energy, or other parameters. As most loading in combined stress studies appears to have been performed in terms of stress, it is reasonable to evaluate strength in terms of stress. The available literature tends to indicate that there is not enough evidence to substantiate any one general theory of failure, although certain theories appear to be more applicable than others depending upon the particular materials and loading encountered. The designer's problems, then, are the first source of error, and it is the designer's responsibility to the measurer to acquaint the latter with enough of the theory so that the proper measurements can be made. This may be as simple as a statement to the effect that the results are to be reported in terms of stress, or of strain. The nature of the available types of measurement is such that it often is not possible to correct data from one type to another after the gauge installation has been made.

Stress-Strain Relations for Plane Stress

The relations existing between the three mutually orthogonal stresses σ_x, σ_y and σ_z in the x, y, and z directions respectively and the three corresponding strains ϵ_x, ϵ_y, and ϵ_z may be found in many texts.[5] For any work involving surface measurements, however, σ_z (the stress normal to the surface) is zero, whereupon the plane stress equations on the surface may be reduced[6] to

$$\left(\sigma_x - \frac{\sigma_p + \sigma_q}{2}\right)^2 + \tau_{xy}^2 = \left(\frac{\sigma_p - \sigma_q}{2}\right)^2 \qquad (1)$$

where

σ_x = normal stress on x plane (in x direction)
σ_y = normal stress on y plane (in y direction) (this does not occur in the foregoing equation but represents a normal stress acting perpendicularly to σ_x)
σ_p = maximum principal stress
σ_q = minimum principal stress
τ_{xy} = shearing stress on x plane (in y direction)

Correspondingly, the strain equations for plane stress may be used to derive a similar equation:

$$\left(\epsilon_x - \frac{\epsilon_p + \epsilon_q}{2}\right)^2 + \left(\frac{\gamma_{xy}}{2}\right)^2 = \left(\frac{\epsilon_p - \epsilon_q}{2}\right)^2 \qquad (2)$$

where

ϵ_x = normal strain on x plane (in x direction)
ϵ_y = normal strain on y plane (in y direction) This bears the same relation to ϵ_x as σ_y does to σ_x. See equation 1
ϵ_p = maximum principal strain
ϵ_q = minimum principal strain
γ_{xy} = shearing strain on x plane (in y direction)

It will be appreciated that equation 1 and equation 2 both define circles, and it will be observed that each circle equation is of the form

$$(x-h)^2 + y^2 = r^2 \qquad (3)$$

where h represents the circle center and r the circle radius. Constructing these two circles, known as the Mohr circles of stress and of strain respectively, will show why individual stress measurements cannot be converted directly to strain measurements, unless enough data (three stress or three strain vector measurements at a point) are taken to draw the circles of stress and of strain. This is understood better when it is appreciated that any given measurement represents the projection on an axis of some point on the circle circumference. Normal stresses and strains are projected as points on the N axis while shear stresses and strains appear as points on the S axis. These two circles may be drawn concentrically,[6] as shown in Figure 1, provided that the scales are chosen so that the ratio of stress units to strain units is as $E_Y/(1-\mu)$ where E_Y is the modulus of elasticity in tension or compression, and μ is Poisson's ratio. When the circles are drawn in this manner it will be found that the stress circle radius is smaller than the strain

Paper 46-60, recommended by the AIEE committee on instruments and measurements for presentation at the AIEE winter convention, New York, N. Y., January 21–25, 1946. Manuscript submitted July 14, 1945; made available for printing December 11, 1945.

Robert E. Kern and Sidney B. Williams, assistant project engineer, are both in the propeller division, Curtiss-Wright Corporation, Caldwell, N. J.

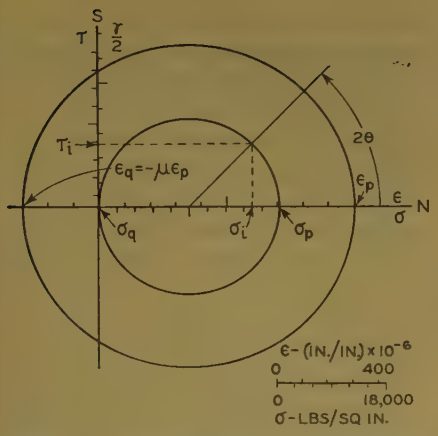


Figure 1. The Mohr circles of stress and strain for a simple axial stress of +30,000 pounds per square inch

Young's modulus is taken to be 30×10^6 pounds per square inch and Poisson's ratio to be 0.3

circle radius in the ratio of $(1 - \mu)/(1 + \mu)$ and the angular position of the point (σ, τ) on the Mohr diagram is twice that of the physical direction of measurement, so that if a measurement be made in the direction θ (with respect to the direction of principal stress) the corresponding direction on the circle diagram makes an angle of 2θ with the N axis. This is reasonable because a complete revolution around the Mohr circle must represent a 180-degree rotation of the measuring device. The concept of the two Mohr circles is not appreciated by many workers in the field, and it is perhaps for this reason that difficulty with the stress–strain relation is prevalent. It is because of the Poisson or lateral contraction exhibited by a stressed member that the ratio of stress to strain is not constant even while operating in the elastic state. For example, the ratio of stress to strain in the direction of the load (σ_p/ϵ_p) for a simple tension test is by definition equal to the modulus of elasticity, E_γ, but the ratio of stress to strain in a direction perpendicular to the load is zero. The load has no component in this direction $(\sigma_q = 0)$ but the lateral strain $(\epsilon_q = -\mu\epsilon_p)$ is finite and opposite in sign. Further examination of Figure 1 will show that the simple tension case is represented with σ_p (+30,000 pounds per square inch) positive and σ_q zero. It can be seen that $\epsilon_q = -\mu\epsilon_p$ and particularly that the ratio $\sigma_\theta/\epsilon_\theta$ is not constant as the radius is rotated, and were the center of the circles displaced somewhat $(\sigma_q \neq 0)$ even the ratio $\sigma_p/\epsilon_p = E_Y$ would not hold.

Thus far, only *normal* stresses and strains have been discussed. *Shear* stresses and strains cannot be detected as a change in length, but can be calculated from two stress or strain measurements, the difference between two mutually orthogonal normal stresses or strains being proportional to the shear stress measured on the plane whose direction bisects that of the two orthogonal measurements. In fact, this leads to the solution of the Mohr circle diagrams from three normal strains separated in direction by increments of 45 degrees:

As the first and third strains are orthogonal they must lie on extremities of some diameter of the circle, and consequently their arithmetic mean must coincide with the circle center. Now, the difference of the first and third (orthogonal) normal strains is equal to the shearing strain associated with the second normal strain, since the direction of the latter bisects that of the first and third strains. As dictated by the second term of equation 2, half of this value is plotted as an ordinate at the abscissa corresponding to the second strain, thus locating the point $(\epsilon_2, \gamma_2/2)$ on the circumference, and the radius drawn from the center to this point just found must be perpendicular to the diameter determining the points corresponding to the first and third measurements as the 45-degree increments on the specimen must exist as right angles on the strain circle diagram. The solution is completed by constructing the stress circle with its smaller radius, $(1-\mu)/(1+\mu)$ as large as the strain circle radius, whereupon the various points (σ_t, τ_t) can be obtained, although the most pertinent information usually consists of the extremes of the circle dimensions and the angle 2θ (measured counterclockwise from the direction of the first strain to the N or normal axis). The method is checked by projecting the three solution points located on the strain (or stress) circle circumference to the N axis; if the construction has been made correctly the projections will coincide with the three measured strains (or stresses). The word "stresses" is used advisedly because, with the proper gauges, stresses can be measured directly.

Electrical Measurements: The Bonded Wire Gauge

Strength measurements can be obtained from numerous types of gauges[7] but the principles controlling the use of the bonded wire resistance gauge will apply generally to other methods, except that the resistance-type units are characterized by lower mechanical inertia and lower voltage output than most. The bonded wire gauge, commonly referred to as the wire strain gauge, has for its principle of operation the variation in resistance of a fine metallic filament bonded to the surface whose deformations are to be measured. In order to make its installation practical the filament first is cemented to a paper "carrier" which, in turn, is cemented to the specimen. This carrier is in no way necessary to the operation of the gauge. In fact its elimination

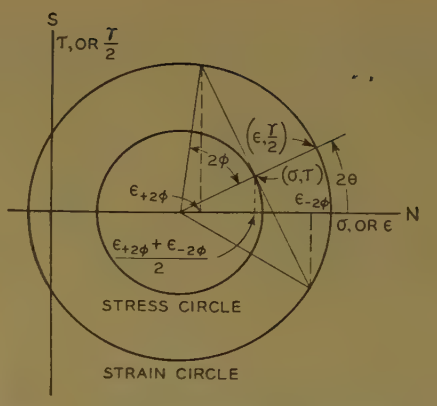


Figure 2. The Mohr circles of stress and of strain on which is shown graphically the manner whereby the Vee type of gauge can be made to yield a result proportional to the stress in the direction of its axis

would be desirable so that the filament might be closer to the specimen, while also allaying the danger of improper transfer of the "mechanical signal" to the active element of fine wire. Actually, the wire first is wound in the form of a grid to which wire leads are joined, after which the grid and leads are placed against the paper carrier for cementing. After the gauge (filament plus cement plus carrier) is cemented to the specimen the assembly acts as if it were part of the specimen in that it accepts uniformly the dimensional changes, both positive and negative, of the deformed surface, while offering negligible restraint in so doing because of its small mass and low effective moduli of elasticity. This action is possible because the dimensions of the wire filament are defined by the matrix of cement in which it is embedded, and it is essential that in the design of such a gauge the wire diameter be small enough so that this effect is achieved. Otherwise compressive strains might result in buckling of the wire with resultant destruction of the bond. This situation is somewhat comparable to the reinforcing rods in a concrete beam, wherein the concrete transmits the tension to the rods, and prevents the rods from buckling in compression (assuming that compressive loads might be placed on such a part of the beam). This transmission of the mechanical signal to the wire results in a permissible amplitude, with linear resistance-versus-strain response, in excess of the proportional limit of the filament material. This amplitude is represented by the manufacturer to approximate one per cent with negligible change in unstrained resistance, and to attain values of two to three per cent for linear operation without complete zero return. The gauge change of resistance is linear and consistent, but not explainable in terms

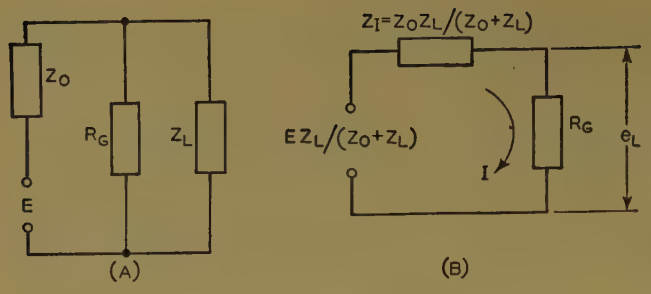


Figure 3. Fundamental gauge circuit (*A*) and its equivalent (*B*)

of the known properties of the filament material in larger sizes. Were the volume resistivity of the wire to be constant with respect to elastic strains it would be reasonable to expect the unit relative change in resistance (dR/R) for unit relative change in length (unit strain, ϵ) to be $(1 + 2\mu)$, where μ = Poisson's ratio. This ratio $dR/R\epsilon$ is defined as S, the gauge sensitivity, and because Poisson's ratio has a theoretical maximum of 0.5, the sensitivity should not exceed 2.0. Actually, certain gauges (made of "Advance" alloy) have such a sensitivity but many gauges are made with sensitivities lying in the range of -5 to $+3.5$, a fact which either contradicts the 0.5 maximum for Poisson's ratio or sheds some interesting light on the volume resistivity of fine wire materials as a function of stress. To date this anomaly is unsolved but may yield to electron microscopy (for use in determining Poisson's ratio for the strained filament). As a matter of interest the operating current density in the usual gauge wire is of the order of 25,000–50,000 amperes per square inch.

Bonded wire gauges are manufactured to meet a demand which requires both thermal stability and sensitivity. Currently these are conflicting requirements because the most sensitive materials (of which the invar, "Iso-elastic," an alloy originally developed for constant modulus of elasticity versus temperature, is representative) are very sensitive to temperature changes. Thermal stability implies that the sum of the effect of differential coefficient of expansion between the filament and the strained surface and the effect of filament temperature coefficient of resistance approaches zero, obviously a function dependent upon the characteristics of the material upon which the gauge is mounted. It is not surprising, therefore, that Advance wire gauges are thermally quite stable on steel, not as stable on aluminum, and not at all stable when suspended in air and subject to the erratic behavior of the unmounted paper carrier, the latter condition representing an academic case. Currently available are the thermally stable Advance gauges with a sensitivity of approximately 2.0 and suitable for all types of deformation measurement, and the Iso-elastic gauges with a sensitivity of 3.5 but suitable only for dynamic work. The latter type are inherently of a higher resistance, permitting generally a higher voltage drop, which condition may be interpreted as a further increase in sensitivity when the load is effectively an open circuit, such as a vacuum tube.

Gauges are available in a wide variety of dimensions and resistances ranging from units 1/16 inch square with 60 ohms resistance to others six inches long (300 ohms) and again some approximately 1/2 inch square with a resistance of 2,000 ohms. Still others, termed rosettes, are arranged in groups of two, three, or four units mounted close together, but oriented in different directions, for the measurement of the complete state of stress by means of the Mohr circle diagram.

The Stress Gauge

In a biaxial stress field the measurement of stress can be simplified greatly by the use of a gauge which responds both to strains parallel and strains perpendicular to the gauge axis[6]. Provided that the gauge specific transverse sensitivity (the ratio of the lateral to the axial response of the gauge) is equal to Poisson's ratio, the gauge output is continuously proportional to the stress in the direction of the gauge axis. This is in accordance[5] with equation 4:

$$\sigma_x = \frac{E_Y}{1-\mu^2}(\epsilon_x + \mu\epsilon_y) \qquad (4)$$

The proof of the stress response characteristic of the gauge is shown conveniently for a particular geometric pattern actually used in commercial gauges. This pattern has the wire arranged in a V, the angle between the wires being selected so that the average of the strains from each arm of the V yields an output proportional to the stress.

The measurement of stress in the direction θ with respect to the direction of the principal axis, requires that the projection of the point (σ, τ) in Figure 2 be determined. A tangent to the stress circle drawn at the point (σ, τ), will intersect the strain circle at points whose projections on the N axis have an average value proportional to the desired quantity. Thus to measure the stress in the θ direction, the gauge V arms will have directions of $(\theta + \phi)$ and $(\theta - \phi)$ respectively.

The general output expression for a gauge of this type when written as a function of the included angle 2ϕ becomes

$$\tfrac{1}{2}(\epsilon_{+2\phi} + \epsilon_{-2\phi}) = (\cos^2\phi)(\epsilon_x + \epsilon_y \tan^2\phi) \qquad (5)$$

where ϵ_x is oriented in the θ direction. The included angle of the gauge V, 2ϕ, is chosen so that $\tan^2\phi$ equals Poisson's ratio for the tested material. Then the right-hand member of equation 5 reduces to $\sigma_x/[E_Y/(1-\mu)]$. Steel, for example, with a Poisson's ratio of 0.28, requires an angle of about 55 degrees, the exact angle being determined by methods of manufacture. This type of stress gauge is used extensively in the testing of hollow steel aircraft propeller blades.

For the stress gauge, the expression which relates the relative change in gauge resistance to the stress producing it is

$$dR_G/R_G = F\epsilon' \qquad (6)$$

where R_G is the gauge resistance and ϵ' is the ratio of stress along the gauge axis to Young's modulus for the material upon which the gauge is mounted. The stress gauge factor F has the following relationship with S, the strain gauge factor:

$$F = (1-\mu)S \qquad (7)$$

It can be shown from equation 5 that the ratio of the output of a stress gauge to the output of a strain gauge of equivalent wire length and resistance and under uniaxial stress is $(1 - \mu)$.

The use of stress gauges can reduce materially the effort required to determine stresses. The direct indication of stress is of particular importance when complex vibratory stresses are measured; under such conditions two strain records separately recorded would have to be converted to stress through a point-by-point conversion if the instantaneous stresses could not be indicated directly.

Errors of Location and Installation

Before proceeding to a discussion of the electric circuits of resistance wire gauges it is appropriate to discuss the theoretical and mechanical considerations which may contribute to inaccuracy in the final conclusions. These may be called the errors of location and installation. That is, the output of the gauges must be indicative of the most critical stress in the part, the stress at the points where failure will occur

if it is to occur. Presumably this will be on the surface at the geometrical center of one of the gauges, though many failures do not start at the surface. On a test specimen such as a hollow steel propeller blade an error of a fraction of an inch in location can produce a change in output of 100 per cent or more, and since any one gauge will cover less than one-tenth per cent of the total area, the location of a few dozen gauges or less over the whole propeller must be chosen with great care. Moreover, if only one gauge is to be located at any one point, the gauge axis orientation is also important, as can be judged by Mohr circle theory. Fortunately, some knowledge of critical areas and stress direction is often available from photoeleastic[5,8] and brittle lacquer[9] ("Stresscoat") studies, discussions of which are beyond the scope of this article. The former method is not convenient for vibratory work and both tend to be laboratory procedures so that it is not always possible to simulate field loadings. Having chosen the proper location it will not always be possible to place gauges where desired due either to inaccessibility or to the physical size of the gauge, which may be so large as to cause an error by integrating the stress or strain over the gauge length when the stress gradient is such as to be masked by the use of too large a gauge length. The availability of shorter gauges has improved this latter situation but sometimes the minimum size of gauge is dictated by electric circuit background noise, the higher resistance gauges being required to produce sufficient signal to result in an acceptable signal-to-noise ratio. This difficulty is probably peculiar to tests on rotating objects such as aircraft propellers, which exhibit accessibility problems also, since flight measurements commonly are made inside the hollow blades, even near the tip, and some work has been done within the hub itself. (Flight stress measurements are made on nearly every propeller–engine–aircraft combination before final acceptance of the design by the customer.) One of the most common sources of gauge error lies in the neutral-axis correction, which is applicable to any survey involving bending stresses. The classical bending-beam theory shows that the stress is proportional to the distance from the beam neutral axis (plane of zero stress); in consequence, bending-stress measurements made at any distance from the neutral axis but that of the surface will be incorrect in direct proportion to this distance. Since the gauge acts as a part of the tested material, accurate bending-stress measurements must correct for the effective gauge elevation above the surface. The diameter of the wire filament is about 0.001 inch and its centerline is perhaps 0.003 inch above the tested surface due primarily to the thickness of the paper carrier. That this is not negligible may be appreciated from a consideration of measurements on a 0.060-inch plate in bending, where the 0.003-inch elevation will cause an exaggeration of ten per cent if the neutral axis is in the central plane of the plate (pure bending). When bending is combined with tension or compression neutral axis error sometimes can be avoided by mounting identical gauges on opposite faces of the plate; their sum eliminates the bending component to yield the tension or compression while their difference eliminates the tension or compression and thermal components, though the resultant bending measurement still is subject to neutral axis error. Returning to the problem of installation, or mounting, it hardly should be necessary to state that the proper bonding of the gauge to the tested surface is of extreme importance to a successful technique. Conservative instructions are supplied by the manufacturer, and occasionally the time allowed for curing or drying of the adhesive may be shortened, but in all cases care should be taken to insure proper preparation of the tested surface (preferably roughening with fine sandpaper plus cleaning with acetone) and adequate application of the adhesive. In the interest of quick drying there is a tendency to apply the adhesive sparingly, which may result in an incomplete bond. Poor surface preparation sometimes is evidenced by the flaking off of a gauge after the test has been completed and the tested parts are no longer available for retest. Where practical the installed gauges may be checked by a calibration with a known load, or another type of gauge, such as the Tuckerman optical strain gauge, may be placed over the installed gauge and the specimen loaded to produce a given strain. The Tuckerman gauge is relatively small and light, and often may be applied with no more force than its own weight, but it is distinctly a laboratory instrument (more often used as a standard).

Other sources of error contributing uncertainty and which pertain more directly to the tested material itself include "locked-in" or residual stresses, the deviation of the remainder of the "universe" from the sample tested, the elastic modulus (if stresses are to be computed), and "creep."[10] Unless the material is in a "dead-soft" or perfectly annealed condition there usually will be certain unrelieved or locked-in stresses remaining. Residual stresses will not affect greatly the readings obtained but will determine somewhat the interpretation read from the data by the designer, as they contribute to or inhibit failure. The actual measurement of locked-in stresses by bonded wire gauges is not possible unless the gauge can be installed prior to the manufacturing operation producing such stresses, or as now is being done to an increasing extent,[11] the gauge is installed while the residual stress is present, after which most of the restraining material is removed carefully and the local stress under the gauge relieved. The indicated stress pattern is then a "negative" of the locked-in pattern.

Young's modulus, E_Y, occurs in the equation relating stress and strain. For the two-dimensional (biaxial) case this is in accordance with equation 4. But the stress–strain relationship for many engineering materials is distinctly nonlinear (aside from the fact that E_Y at zero load is subject to a degree of uncertainty) so that an indicated vibration stress of $\pm 10{,}000$ pounds per square inch, when no steady load existed, might differ from the indicated value when a steady load of 50,000 pounds per square inch was applied simultaneously. Such considerations might be affected differently for steady locked-in or surface stress than for uniformly-distributed steady stress. Modulus correction of this nature is not known to the authors but would have to be considered in evaluating closely the probable error. Creep is the phenomenon of gradual continued deformation at constant load and is ordinarily negligible in steel at low temperatures (below 200 degrees Fahrenheit) but may be appreciable in some other materials such as lead, plastics, and gauge bonding agents when large deformations are involved. It may prevent a return to a zero-stress reading, even when the gauge itself is operating properly. It may be obscured by or confused with drift due to poor temperature compensation or the chang-

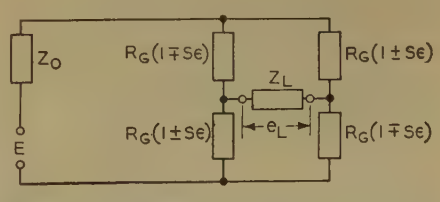


Figure 4. Equiarm strain gauge bridge circuit

Parenthetical term of R_G indicates direction and magnitude of resistance change in each gauge as a function of gauge factor and applied strain

ing leakage characteristics of the electrical insulation, as will be discussed later.

The Electrical Problem

Gauge Circuits

Two general circuits which may be used for the conversion of strain to electrical signal are shown in Figures 3*A* and 4. The simpler circuit of Figure 3*A* often may be used when a knowledge of only transient or vibratory stress or strain is desired, while the bridge circuit of Figure 4 is employed when the steady component with or without the vibratory component is to be determined or when protection from excitation circuit disturbances (as in slip-ring installations) is required.

When vibratory shear, or the difference in strain between two gauges at right angles, must be measured, the "matching" resistor, Z_O, in Figure 3*A* becomes one gauge while the active gauge, R_G, becomes the second of the two required orthogonal strain-sensitive elements. The bridge circuit can be arranged suitably to enable the measurement of total shear, since differential measurements are applicable for shear, torsion, and many bending problems.

Network theorems[12,13] are used conveniently to calculate the voltage which appears when the active circuit elements are strained. Thus the Thévenin equivalent of Figure 3*A*, shown in Figure 3*B*, yields current in the gauge of

$$I=\frac{EZ_L/(Z_O+Z_L)}{R_G+Z_OZ_L/(Z_O+Z_L)}=\frac{EZ_L}{Z_OZ_L+R_G(Z_O+Z_L)} \quad (8)$$

The change in load voltage dE_L due to a change dR_G associated with the strain ϵ is

$$dE_L=e_L=d(IR_G)=IdR_G+R_GdI \quad (9)$$

Evaluating dI (by means of the compensation theorem) and collecting terms,

$$e_L=I\left(\frac{dR_G}{R_G}\right)\frac{R_GZ_OZ_L/(Z_O+Z_L)}{R_G+Z_OZ_L/(Z_O+Z_L)} \quad (10)$$

The sensitivity S of a strain gauge has been defined previously as $dR/R = S\epsilon$. Using this relation together with the fact that the coefficient of $I(dR_G/R_G)$ is the parallel combination of R_G and Z_I, equation 10 is simply

$$e_L=ZIS\epsilon \quad (11a)$$

where $Z = R_GZ_I/(R_G + Z_I)$ evaluated at the strain frequency and I is evaluated from equation 8 at excitation frequency. For practical applications the impedances are entirely resistive, with the load impedance Z_L (usually amplifier input impedance) much greater than the gauge resistance, R_G. The greatest output voltage for a given value of E occurs when the product of ZI (or more commonly RI) is a maximum, that is, when Z_O equals R_G. When it is possible to measure two or four strains which are exactly equal but occur in conjugate pairs as shown in Figure 4, the bridge circuit increases the no-load voltage output above that of Figure 3*A* by two and four times respectively.

The voltage output equation for four active equal bridge arms is developed in a manner similar to that of equation 11a and is

$$e_L=ZIS\epsilon \quad (11b)$$

where Z, just as in equation 11a, is the impedance (at the strain frequency) measured across the terminals of the load impedance Z_L, when other voltage sources in the circuit are not generating but are replaced with their equivalent internal impedances. Expressed explicitly this impedance, Z, is $R_GZ_L/(R_G + Z_L)$. Note that when the load impedance Z_L is large with respect to the gauge resistance, the output voltage e_L is given by the expression $E\epsilon S$, and further, that I is the current of excitation frequency supplied the gauges, or $E/(R_G + Z_O)$.

The quantity $S\epsilon$ may be regarded as an average value determined by the number and characteristics of the gauges acting. If the output from a gauge (due either to its location in the bridge circuit or because of the sign of strain) tends to cancel the effects from another, the algebraic signs of the two quantities $S\epsilon$, associated with the respective gauges, may be regarded as opposite. Thus a bridge with only two active gauges (but these connected in one side of the bridge and subject to equal and opposite strains) will exhibit an output voltage of $e_L = (1/2)ZIS\epsilon$, since two of the four gauges have zero as their effective value of $S\epsilon$.

Output voltage equations 11a and 11b may be examined to ascertain the errors which may result from variation in the controllable parameters. It is immediately evident that errors in E, the excitation voltage, and errors in gauge sensitivity, S, contribute in direct proportion to the error in gauge output voltage. Excitation voltage may be monitored or controlled by the operator; the gauge sensitivity factor is supplied with commercial gauges and usually is guaranteed to plus or minus one per cent.

Since the nominal value of gauge resistance may be subject to as much as a two or three per cent manufacturing tolerance, particularly in those gauges supplied for dynamic work, it is necessary to examine the ZI term in equation 11a to evaluate the effect of changing the gauge resistance. Assuming that the impedances are essentially constant and resistive in the operating portion of the spectrum (a condition necessary for good amplitude-frequency response) and that Z_L is large with respect to Z_O, the relative change in output voltage is

$$de_L/e_L=d(ZIS\epsilon)/ZIS\epsilon=d(ZI)/ZI = -(dR_G/R_G)(R_G-Z_I)/(R_G+Z_I) \quad (12)$$

where Z_I is $Z_LZ_O/(Z_L + Z_O)$ and dR_G/R_G is the relative change in the nominal resistance and not $S\epsilon$, which here is considered constant. The condition R_G equal to Z_I suffices for zero error in calculated output voltage as a function of tolerance in gauge nominal resistance; moreover since Z_L is large in comparison to Z_O, it is possible to have the zero error condition coincide with the maximum output condition by setting Z_O equal to R_G.

As stated previously, measurements of steady strain require that gauge resistance be a function of strain only and be unaffected by temperature or variation in electrical leakage. Temperature effects are eliminated most nearly by using a compensating gauge mounted on material equivalent to the test specimen and subject to the same ambient temperature variations. The compensating gauge may be active or passive but is connected in the bridge arm adjacent to the compensated unit.

Using an unstrained specimen equipped with two nitrocellulose bonded gauges wound with Advance wire, temperature compensation to within two microinches per inch over a range from 70 to 170 degrees Fahrenheit has been attained in the laboratory. However, general practice indicates that two microinches per inch per degree Fahrenheit is a more practical estimate of realizable temperature compensation.

The measurement of vibratory stresses up to a temperature of about 180–200 degrees Fahrenheit is possible with nitrocellulose bonded gauges. A specific case for ±400 microinches per inch of strain showed at 230 degrees Fahrenheit a drop of 30 per cent from the value of apparent gauge factor at 200 degrees Fahrenheit, the difference due to softening of the cement. For elevated temperature operation up to 300 degrees Fahrenheit, resin-bonded gauges are used.

In order to prevent "zero" instability due to absorption of moisture by the gauge or associated leads, it is necessary to weatherproof the installation by first driving off all moisture and then coating or impregnating with a nonhygroscopic

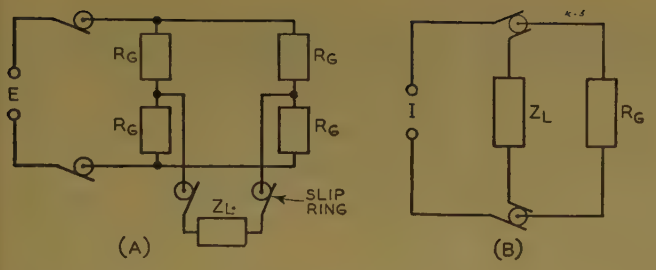


Figure 5. Location of slip rings and related components in a constant-voltage gauge circuit (*A*), and in a constant-current circuit (*B*)

material such as a hydrocarbon wax. A typical gauge, having a resistance of 120 ohms and a sensitivity of 2.0, will change in resistance by only 0.008 ohm when subjected to a stress of 1,000 pounds per square inch in steel (33 microinches per inch). This change also may be produced by a shunt resistance across the gauge of 1.8 megohms (very nearly $R_G/S\epsilon$) thus making evident the necessity for thorough moistureproofing. A value of 1,000 megohms is recommended by the gauge manufacturer. When many gauges are in a circuit possessing one or more common leads, it is often convenient to make provision for measuring the leakage to ground. Such an indication cannot be interpreted explicitly but serves as a warning of changing insulation conditions.

The nitrocellulose, and to a lesser extent the resin base, bonding agents both are subject to creep under prolonged strain and also exhibit slight apparent hysteresis over a stress–strain cycle. Proper application and curing helps reduce creep to a minimum and several preliminary loading cycles usually suffice to make hysteresis effects negligible. The possibility of errors from this source should not be overlooked if readings having a tolerance of five to ten microinches per inch must be obtained. Moreover it is only reasonable to assume that creep difficulties will increase with stress level and temperature.

Special Circuits

When the information as to the state of stress on a rotating member is to be obtained with the aid of sliding contacts, it usually will be necessary to minimize contact resistance effects by arranging a balanced bridge on the rotating element as in Figure 5*A*. Results free from slip-ring interference, especially at high surface speeds, are impossible of achievement if the slip rings are connected directly to make up part of the gauge resistance. Inspection of the current term in equation 11b shows why the bridge circuit of Figure 5*A* is relatively free from effects resulting from variation in resistance of the slip rings supplying the exciting current, and inspection of the impedance term will show how Z_L may be chosen to make the effect of output-circuit slip-ring resistance variation negligible. It is also essential that the slip rings located in the leads which supply the load do not introduce thermal electromotive forces. An alloy consisting of 97 per cent silver and 3 per cent platinum, the latter for hardness, used in conjunction with silver-graphite brushes, has proved very satisfactory under brush pressures of 40 pounds per square inch and surface speeds of about 4,000 feet per minute. Improvement in the strain signal-to-slip-ring noise ratio may be obtained by the use of a bridge-output transformer mounted on the rotating object, provided that the resultant phase and amplitude distortion versus frequency of the signal is negligible. Such a system is suited especially for use with carrier-current excitation.

Constant-current excitation sometimes is employed in slip-ring circuits to overcome the resistance variation in the transfer system. With this method, the output voltage is equal to IdR_G as the component $R_G dI$ no longer is present. The gauge output voltage for constant-current excitation is twice that obtained from constant voltage excitation when the average currents in both cases are equal. Referring to Figure 5*B*, it will be seen that the voltage drop across the slip-ring contact resistance need not be measured as two brushes, one for the excitation current and another for the signal voltage, may be used. It is still possible, however, for thermopotentials arising at the signal brush to mask out the strain voltage unless the proper materials, such as those described in the foregoing, are employed.

To find the stress in a material subject to biaxial stress, it is necessary to take the proper proportions of two orthogonal strains as explained in the discussion of the stress gauge. But if it is desired to measure two orthogonal stresses at a point the purpose perhaps can be served best by using a pair of orthogonal strain gauges with their electric circuits arranged so as to crosstalk mutually the correct lateral or transverse component each into the other (refer to equation 4) to produce the effect of two stress gauges. This arrangement requires a double installation compared to a single stress gauge but yields two stress measurements, which can be taken separately or simultaneously, just as if the strain gauge filaments had been arranged in the path of stress gauge grids and the mutual impedance removed. Both sections of such a

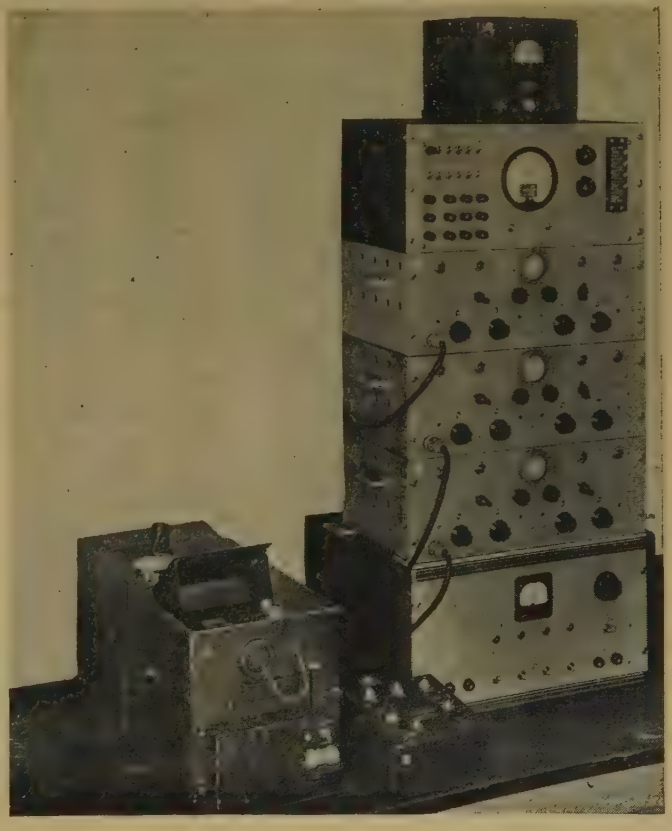


Figure 6. Twelve-channel amplifier-oscillograph equipment showing oscillograph, power supply, three banks of amplifiers, switching panel, and calibrator

circuit must be furnished excitation current, however, even if recorded at separate times. One such arrangement consists of connecting together two gauges, whose directions have the required rectangular relationship, with a common impedance Z_C joining the output or load terminals. If the two gauge circuits (composed entirely of resistive elements) have like components it can be shown that when Z_C is set equal to $R_I(1 + \beta)(1 - \mu)/(\mu - \beta)$ where R_I is $R_G R_O/(R_O + R_G)$, μ is Poisson's ratio and β is the gauge specific transverse sensitivity, then each gauge will have an output voltage proportional to the stress in the direction corresponding to the particular gauge orientation. When the gauge and matching resistor have values of 500 ohms each, Z_C becomes approximately equal to 700 ohms for representative conditions of μ and β equal to 0.28 and 0.02 respectively.

Instruments and Their Selection

As the signal is measured in terms of microinches per inch it will be readily apparent that the voltages available from low resistance gauge circuits must be small, usually less than 100 millivolts. A structure may be stressed at zero frequency, (static loading), or may be a resonant member vibrating at frequencies of several thousand cycles per second, or be subject to shock loading. Sensitive measuring equipment consequently must be selected, keeping in mind the frequencies to be encountered. Vacuum tube equipment usually is required although static and slowly varying strains are measured successfully with d-c microammeters and light-beam galvanometers. Generally, in a stress survey, a number of points must be examined and correlated with one another with respect to time or other variables. Multichannel amplifier recording oscillograph combinations prove most useful in obtaining and preserving this data for later analysis. Figure 6 shows a typical 12-channel oscillograph with 12 channels of amplifiers (three banks of four), a-c power supply, switching panel, and calibrator. For flight work the a-c power supply is replaced with a battery-powered unit.

The instruments can be chosen properly only by an honest evaluation of the response required. This implies the determination of the minimum acceptable gain and the choice of f_{min} and f_{max}, the extreme values of signal frequency which must be transmitted and between which the amplitude-frequency response must be "flat" within, say, $\pm p$ per cent. In general there will be other frequencies, f_1 and f_2, between which the phase distortion must not deviate from a linear function of frequency within some prescribed limit. Then there will be the decision upon indicating or recording instruments, and if recording, whether automatic or attended. If accuracy is very important, some null-balancing arrangement usually is indicated, though such equipment ordinarily will have but a very poor amplitude-frequency response, particularly if manual balancing is used. Generally it will be found that phase response can be improved at the expense of amplitude response and conversely. For instance, a galvanometer element with about 0.6 critical damping will exhibit a flat amplitude response to a higher frequency than it will for any other value of damping, but the phase-frequency characteristic will deviate from linearity at a lower frequency than when the damping is lower than 0.6 critical. This is a difficult choice, for phase relations in the complex stress wave are important if peak values are not to be distorted beyond the specified p per cent. To demand perfect phase and amplitude response (good square-wave characteristic) may mean using quite a different instrument. Once the response characteristics have been fixed—the least requirements for acceptable results—the size, weight, and cost of the equipment can be estimated. A very rough indication of the type of instrument required may be obtained by dividing the instruments into six classes, each one decade apart in the frequency spectrum, as shown in Table I.

Table I. Instruments Classed by Frequency Response

Nominal Frequency Spectrum (Cycles per Second)	Instruments
0–0.2	Indicating instruments and manually balanced null devices (manual recording)
0–2.0	Automatic null-balance recorders
0–20	Direct-coupled galvanometers (no amplification)
2–200	Amplifier-galvanometer combinations (magnetic damping of galvanometers, or piezo-crystal galvanometers)
2–2,000	Amplifier-galvanometer combinations (oil-damped galvanometers)
2–20,000	Amplifier-oscilloscope (cathode-ray) combinations

Static and dynamic strains may be recorded simultaneously by using carrier current excitation or d-c excitation to the bridge circuits and associated recording equipment. The former method is more complex in that it requires a high-frequency source and freedom from variational reactive components in the bridge (which in turn requires phase balancing and probably a phase-sensitive demodulator-filter arrangement). Excitation from a d-c source requires that those components of signal frequency not passed by the amplifier be recorded by some other means. A very satisfactory method which may be used with conventional amplifier-oscillograph equipment has been termed the "insertion" system,[14] whereby the signal is short-circuited cyclically. If the wave form and frequency of the switching action are chosen properly the recorder passes the zero signal pulses, thereby establishing the axis of zero signal on the recording medium. The pulse height is exactly equal to the instantaneous value of the signal, which fact sometimes is used in the exact reduction of the data. Such a system has been in use for over a year in the measurement of steady and transient strains in aircraft propellers.

The choice of instruments will be influenced by the required accuracy, particularly with respect to ambient conditions of temperature, pressure, humidity, mechanical vibration and noise, and power supply variation. Ordinarily, characteristics of the equipment may be specified so that these variables will be of little consequence but oftentimes it becomes desirable to use an instrument under conditions for which it was not intended. Variations in temperature affect the operation of oil and electrolytic capacitors, the response of oil-damped galvanometers, and the lubrication of moving parts in oscillographic equipment. Pressure and humidity affect the operation of slip ring brush combinations in oscillograph motors and transfer equipment (such as is required for aircraft propeller testing). Amplifiers often are subject to disturbance from noise or vibration or both. It even has been the experience of the authors that the severe vibration present on aircraft engine nose sections is sufficient to produce a signal comparable in wave form and amplitude to that of a stress signal, merely due to piezoelectric or electrostrictive effects on certain laminated plastic insulating materials used in the slip-ring assembly and brush rigging. This first was discovered during a check run with the excitation battery disconnected; it subsequently was eliminated by discontinuing the use of these laminated plastics as structural members in the transfer equipment and by other design changes.

When the records are analyzed there remain a few more sources of error and uncertainties. In a complex vibratory

Linear Couplers, Field Tests and Experience at York and Middletown, Pa.

E. L. HARDER
MEMBER AIEE

E. H. KLEMMER
ASSOCIATE AIEE

R. E. NEIDIG
ASSOCIATE AIEE

THE system of bus protection using linear couplers, or air-core mutual reactors, in place of current transformers was described before the Institute in January 1942.[1] By special design the mutual reactors were made astatic or insensitive to outside fields. Through the use of air core the troublesome problem of saturation of iron by the d-c transient component of short-circuit current was eliminated. At the same time adequate energy was derived for decisive relay operation. The coupler secondaries were connected in a series loop including the relay to form a bus protective system.

Several applications of this system have been made now, and it is the purpose of this paper to describe the field tests and subsequent performance of the pioneer applications at the York and Middletown Pa., stations of the Metropolitan Edison Company. Following an analysis of the field tests, which more firmly establish the operating limits of the system, the proposed field of application will be defined in relation to other bus protective systems.

The advantages of bus protection in clearing faults rapidly from a system are well recognized by the industry, and the provision of relay protection for major station busses has been standard practice for a number of years. The problems involved in such protection also are quite well known. One of the principal ones is the saturation of current transformers by the d-c transient component of the short-circuit current. In severe cases the d-c transient component may require 100 times as much flux capacity in the current transformer as is required by the a-c component to prevent saturation completely. The theory of this problem was presented before the Institute by Langguth and Marshall in 1929.[2]

Solutions

There were a number of successful solutions to the problem and it will be necessary to mention a few of these to illustrate the proper field of application of the linear coupler system in relation thereto.

First was the use of large current transformers which would not be saturated by the d-c component. These were used with low resistance leads to minimize the current transformer requirements in this respect. A formula was advanced specifying the requirement of iron cross-section, turns, and lead resistance for non-saturation, as a function of the fault current and the d-c transient time constant. This was a "bull-by-the-horns" solution and its size, weight, and cost could be afforded only in the most important installations. However, it provided the possibility of instantaneous tripping without any time delay.

A method[3] was developed for calculating, with reasonable engineering accuracy, the time to saturate with off-set currents, and the time and current settings required to prevent misoperation with time-delay overcurrent relays and usual current transformers. However, the time delays required were frequently so long as to point the need of a better solution.

Relays[4] also were developed which would not operate falsely even when used with normal sized current transformers which saturated due to the d-c component. These are multirestraint relays; however, their success is due also to exploitation of variable percentage

Paper 46-36, recommended by the AIEE committee on protective devices, power transmission and distribution for presentation at the AIEE winter convention, New York, N. Y., January 21–25, 1946. Manuscript submitted November 19, 1945; made available for printing December 17, 1945.

B. L. HARDER is central station engineer and E. H. KLEMMER is switchgear engineer, Westinghouse Electric Corporation, East Pittsburgh, Pa. R. E. NEIDIG is electrical engineer, Metropolitan Edison Company, Reading, Pa.

---

stress wave it should be proper to consider only those stress reversals which occur often enough to be considered dangerous in the life of the tested part, but this is a matter on which it is impossible to be exact.

Conclusions

The quantity and complexity of electrical stress measurements have grown to such an extent that a relatively small part of the whole stress problem may require the full time of one or more individuals. This trend toward specialization naturally reduces the possibility of any one person appreciating the problem as a whole, with the result that one or two aspects may be emphasized while another of equal importance may be neglected. This situation, as discussed in the paper, is exemplified by a precise electrical measurement of a stress which may be subject to appreciable uncertainty in itself (due, say, to neutral axis error) or may be unrepresentative (gauge location in error), so that the responsibility for the procurement of results which depend upon many variables is evident. Although it has been possible to touch but lightly on most of these phases of the measurement problem, it is hoped that the broader consideration of stress determination, as herein presented, will prove helpful to those presently engaged in or who will enter this field.

References

1. THE DEVELOPMENT OF ELECTRICAL STRAIN GAGES, A. V. deForest, H. Leaderman. National Advisory Committee for Aeronautics Technical Note 744, January 1940.

2. United States Patent 2,292,549, MATERIALS TESTING APPARATUS, Edward E. Simmons. August 11, 1942.

3. THE EXTREME PROPERTIES OF MATTER, Sir Charles Darwin. *Engineering*, volume 155, February 5, 12, 19, 1943, pages 105, 106, 136, 137, and 144.

4. MECHANICAL PROPERTIES OF MATERIALS AND DESIGN (book), Joseph Marin. McGraw-Hill Book Company, New York, N. Y., 1942. Chapters 1–4.

5. PHOTOELASTICITY (book), M. M. Frocht. John Wiley and Sons, Inc., New York, N. Y., 1941. Volume 1, chapter 1.

6. THE DYADIC GAGE, Sidney B. Williams. *Proceedings* of the Society for Experimental Stress Analysis, volume 1, number 2, 1944, pages 43–55.

7. ELECTRIC GAGING METHODS, H. C. Roberts. *Instruments*, volume 17, number 6, through volume 18, number 10, 1944–1945.

8. TREATISE ON PHOTOELASTICITY (book), E. G. Coker, L. N. G. Filon. Cambridge Press, 1930.

9. PRACTICAL STRAIN ANALYSIS BY USE OF BRITTLE COATINGS, Greer Ellis. *Proceedings* of the Society for Experimental Stress Analysis, volume 1, number 1, 1943, pages 46–53.

10. Reference 4, chapter 6.

11. Papers presented at Society for Experimental Stress Analysis symposium (May 1944) on residual stresses, C. S. Barrett and others. *Proceedings* of the Society for Experimental Stress Analysis, volume 2, number 1, 1944, pages 147–225.

12. ELECTROMECHANICAL TRANSDUCERS AND WAVE FILTERS (book), Warren P. Mason. D. Van Nostrand, New York, N. Y., 1942. Pages 13–20.

13. RADIO ENGINEER'S HANDBOOK (book), F. E. Terman. McGraw-Hill Book Company, New York, N. Y., 1945. Page 198.

14. MEASUREMENT OF STEADY AND VIBRATORY STRESSES IN AIRCRAFT PROPELLERS, E. F. Shelley. Institute of the Aeronautical Sciences, New York, N. Y., 1946.

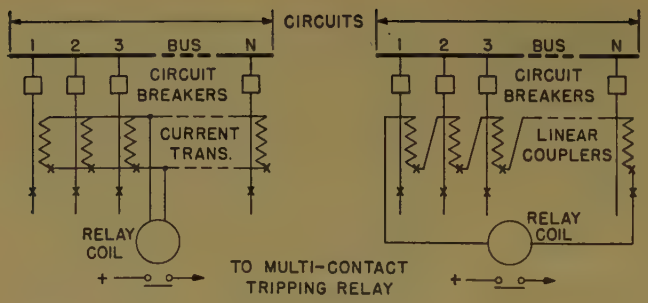


Figure 1. Schematic diagram of differential protection systems

characteristics and the tendency of the d-c component to brake, rather than drive, the induction disk. No small part of this development was the reduction of its operating limits to a few simple rules which insure safe application. This relay provides operation generally in from three to six cycles.

The linear coupler system combines the advantages of high speed and simplicity of the "bull-by-the-horns" method described first, with moderate size and weight of the multirestraint system, and some important advantages of its own. In principle it is the simplest possible system as will be noted (Figure 1b). It is the only system which can be tested at low currents to ascertain for a certainty what its performance will be at high current values. The coupling devices are no larger and often lighter than normal-sized current transformers. They can be mounted in the usual bushing current transformer compartments of circuit breakers. A single relay per phase is required irrespective of the number of circuits involved on the bus, a ground relay being used in addition if ground fault currents are relatively small. Figure 2 illustrates a typical coupler and relay.

The theory of the linear coupler system has been outlined in previous papers.[1,5] Consequently, only a sufficient résumé will be given here to show the significant factors which should be investigated in the field tests.

Résumé of Theory of Linear Couplers

As shown in Figure 1 linear couplers are connected normally in series whereas current transformers are connected in parallel to form a differential protection circuit. The current transformer is designed to produce in its secondary a current proportional to the primary current. As long as there is no bus fault the vector summation of currents in all circuits connected to the bus is equal to zero. Hence the summation of secondary currents, obtained by the parallel connection is likewise zero. In event of a bus fault the current in the relay is proportional to the fault current.

The linear coupler is a mutual reactor and consequently produces in its secondary a *voltage* proportional to the current in its primary. Usually this proportionality is 5 volts secondary per 1,000 amperes primary. If there is no fault on the bus the summation of primary currents is zero and consequently the summation of secondary voltages, obtained by the series connection, is likewise zero. If there is a bus fault the net voltage induced in the coupler-relay loop is proportional to the fault current, that is, 5 volts per 1,000 amperes of fault current in the usual design.

York and Middletown Installations

The first installations of the linear coupler scheme for bus differential protection were made on the Metropolitan Edison Company's system in the new 114-kv, outdoor substations at Middletown and York, each authorized for construction in 1942. Load growth in the York area necessitated conversion to 114 kv of the two 66-kv lines from Middletown to York. The Middletown station provides the interconnection between these two lines and the existing 114-kv circuit to Reading, as well as a principal outlet for the Middletown generation into the general transmission system. The York substation serves as the terminal for the 114-kv lines and the main source of supply into the York area, stepping down through 67,500 kva of transformers.

The Middletown substation is shown in Figure 3. Both substations are identical in basic design, utilizing a compact steel structure, protected by four overhead static wires spaced on 44-foot centers, "back-to-back" circuit bays, and main and transfer strain busses. Each circuit is provided with an oil circuit breaker having 1,500,000 kva interrupting capacity. Three coupling capacitor potential devices are connected to the main bus for relay and synchronizing potential. All secondary cables for control, current (including linear coupler secondaries), potential, power, andl ighting, as well as carrier current concentric cables, are buried directly in the earth in a common trench, between the control room and their respective terminal locations at the outdoor structure. The control and relay panels at Middletown are located about 350 feet distant from the nearest circuit breaker, whereas at York this distance is 200 feet.

A one-line diagram of the six-circuit station at Middletown is shown in Figure 4. An identical 114-kv bus diagram applies for the York station, excepting that there are five circuits instead of six.

The decision to install bus differential protection at these two important substations was made only after long deliberation, including careful analysis of the use of all known differential schemes. The calculated maximum and minimum

Figure 2

(a). Linear coupler
(b). LC-2 linear coupler relay





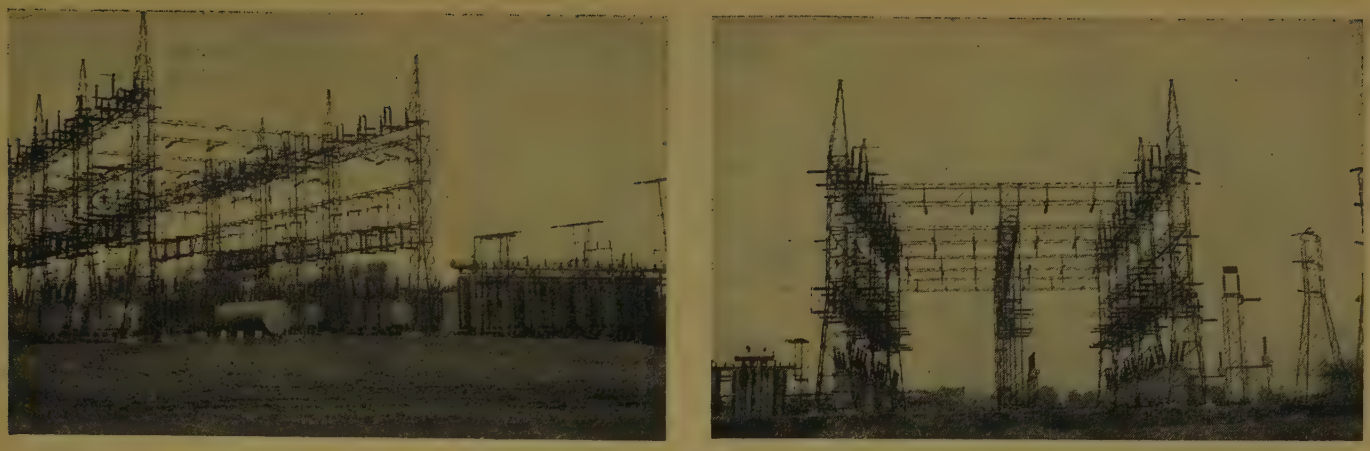


Figure 3. Views of Middletown substation

114-kv bus fault currents for which the relay systems must function were 6,250 and 1,400 amperes respectively at Middletown, and 4,500 and 1,050 amperes respectively at York. All 114-kv transformer banks on this system are wye connected with solidly grounded neutrals, resulting in bus interphase and ground fault currents of approximately equal magnitude. The calculated d-c time constant at Middletown was 0.12 second, and at York 0.06 second.

Conventional Methods Analyzed

Conventional methods, using standard bushing type current transformers in the 115-kv circuit breakers, with paralleled secondary connections, were given first consideration. The "bull-by-the-horns" method was, of course, economically impractical. The method using time delay overcurrent relays appeared unfavorable, as high-speed operation was necessarily sacrificed through provision of sufficient time delay to overcome the effects of d-c saturation in the current transformer. Calculations indicated that the intentional time delay required to permit offset transient recovery would result in relay times ranging from 7 to 60 cycles, under maximum to minimum fault currents, respectively. In addition to extending damage such times would adversely affect the co-ordination with transmission line protection.

The "multi-restraint relay" type of bus protection[4] was found applicable, and under the fault conditions previously stated would result in relay times ranging from 3 to 5 cycles. The number of circuits involved, however, required that two relays per phase be installed at each station. The current transformer connections and relay wiring would be arranged so as to maintain restraint on at least one relay per phase under all through-fault conditions. Since in general two relays per phase provide protection for up to seven source circuits per bus, the addition of main circuits at Middletown might have presented a problem.

A safe application of either of the foregoing systems requires consideration of maximum and minimum fault currents and their distribution, relay and lead burden, ratios and iron cross sections of current transformers, number of generating sources, and d-c time constant, together with other pertinent operating conditions. Since the total burden on the current transformers is an important factor in the successful application of the previously described methods, it follows that the size of conductor used in the secondary cable from the current transformer to the relay may have to be increased as the distance between them is increased.

Linear Couplers Selected

Laboratory tests of the linear coupler scheme previously described offered conclusive evidence that a simple, high-speed bus differential relay system had been developed which was free from all of the inherent problems associated with conventional current-transformer methods. While the linear coupler relay is of necessity a low energy device, any fear that unwanted operations might occur from induced potentials in the secondary cable was believed groundless. Calculations had indicated that such potentials would be very small compared with operating voltages if a continuous secondary loop circuit was provided for each phase, with the outgoing and incoming conductors in a common spiraled cable throughout. Thus, any tendency for induced potentials to appear in the coupler loop would be cancelled. This was proved in field tests at York, to be described later.

Linear coupler bus protection was therefore installed at Middletown and York substations for the following reasons:

1. Simplicity. No calculations were required other than maximum and minimum bus fault curredts and the relay setting for the desired pick-up. Sound fundamental theory of operation had been substantiated by the manufacturer with exhaustive laboratory tests.

2. Linear characteristics of couplers for all values and types of fault current meant freedom from fear of saturation effects caused by offset transients.

3. Faster relay operation (1 to 2 cycles) would be obtained through complete range of fault currents, with only one comparatively simple relay per phase, regardless of the number of circuits connected to the bus. Thus, no complex relay and current transformer secondary connections, and less switchboard space would be required.

4. A complete system required only one secondary cable consisting of six, number 10 copper conductors, running from the relay panel to the first circuit breaker, thence to the second, third, and so on until the loop is completed in the last breaker (Figure 4). Actually, a smaller size conductor can be used, depending entirely upon the desired mechanical factor of safety. A considerable reduction in secondary cable was realized with the linear coupler scheme. For example, at Middletown a total of 2,800 feet of 4-conductor cable would have been required with the multi-restraint relay scheme. For the linear coupler installation a total of 775 feet of 6-conductor cable was installed. Therefore, for the installations under discussion, the latter scheme required approximately 41 per cent of the conductor-feet, that would have been required by the former.

5. If a cable duct system is used the amount of main duct run space saved with the linear coupler scheme is the total number of circuits involved, minus one. This also applies for future circuit additions, in which case the new circuit breaker is connected into the coupler loop by simply extending a 6-conductor cable from the nearest existing breaker, plus a few feet of wire on the relay panel to connect the added breaker

trip circuit to the multicontact tripping relay.

6. With the linear coupler scheme an open circuited secondary or relay coil renders that phase inoperative, whereas such conditions occurring with the conventional current transformer schemes may cause undesirable operation sooner or later. Either manual or automatic equipment is available to check the continuity of the relay-coupler loop if desired.

7. Cost of linear couplers and relays (not including savings in secondary cables) was competitive on new installations with the multirestraint scheme using bushing type current transformers.

It is of interest to note that the 6-conductor secondary cables for both installations were installed in the same trench with all other control and secondary cables leaving the relay panel, being buried directly in the earth over the greater part of the distance to the circuit breakers. Standard 600-volt, nonleaded, unshielded "mummy finish" spiral cable was used.

Field Tests

For a successful linear coupler system which will always trip when desired for internal faults and never trip when undesired as for external faults, the following requirement must be met.

The mutual reactance, or proportionality between secondary voltage and primary current must be the same for all couplers on a bus within certain limits. If the couplers on the circuits where current entered the bus produced voltages 1.5 per cent high and those where current left the bus produced voltages 1.5 per cent low, a through-fault current would produce 3 per cent as much voltage as an internal fault of the same magnitude. Thus a through fault of 33 times the relay setting would be just enough to cause faulty tripping. The tolerance can be reduced to any desired amount but the cost is increased in proportion because of the refinements required in manufacture and testing.

Analysis and measurement of samples had indicated that a tolerance of ±1.5 per cent could be held quite readily. This tolerance includes several sources of variation which will be discussed briefly.

Linear couplers are wound in the form of a toroid similar to a bushing current transformer with a uniformly distributed winding. The core is of course nonmagnetic. This form of coil has theoretically zero mutual reactance to any conductor not linking the toroid and a constant mutual to any conductor which does link it irrespective of its position within the opening. Also its mutual theoretically is unaffected by any external magnetic fields. There are, of course, minor variations due to irregularities of winding so that the mutual is slightly affected by positions of the center and return conductor, and the presence of neighboring iron. Further variations occur due to finite steps of adjustment of individual couplers to the standard coupler. These effects have been exhaustively studied and reported previously[1] and are all included in the ±1.5 per cent over-all tolerance.

In the case of the York and Middletown installations most of the couplers were supplied separate from the circuit breakers, and were mounted in the usual bushing current transformer housings of the breakers in the field. Polarities were checked by impulsing with a flashlight battery as for current transformers. However, the field tests provided an overall check of the tolerance as described above including position effects within the circuit breaker, effect of the iron cases, leads, and coupling with other phases if any. Provision of adequate energy for operation at the proposed relay setting had been demonstrated in the prior laboratory tests of the scheme and therefore merely was confirmed by the field tests.

Tests for accuracy and performance of a linear coupler differential are extremely simple because the d-c component in a

Figure 4 (below). One-line diagram of Middletown substation

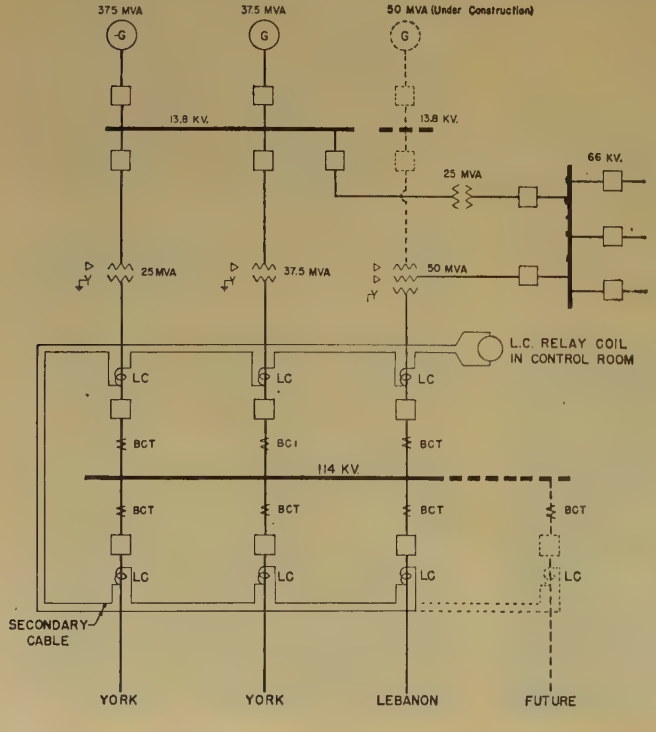


Figure 5 (right). Current–voltage relations in relay-coupler loop

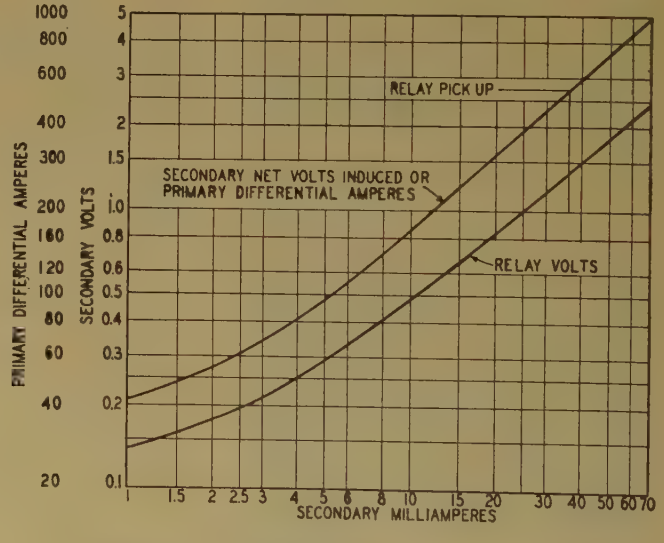
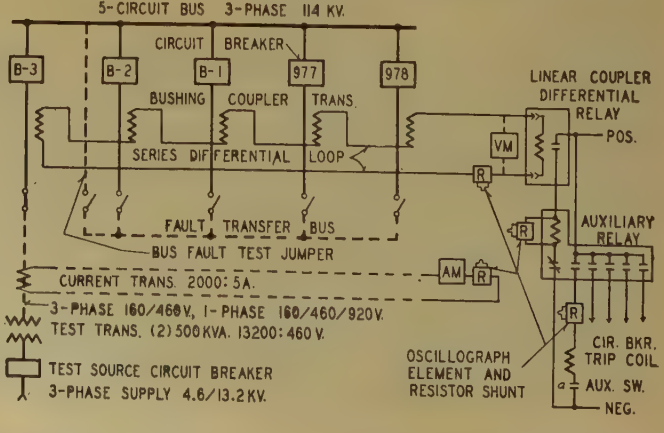


Figure 6 (lower right). Diagram of test connections



fault current has a negligible effect, and the secondary induced voltage is strictly linear with respect to the primary a-c component magnitude. Hence measurements may be made with primary currents just sufficient to give accurate readings on a secondary circuit voltmeter. An electronic voltmeter is ideally suited for reading these low voltages as it has very high impedance so as not to disturb the current flow in the differential circuit.

Methods of Measuring Differential Error

Measurements of differential error are made most directly by opening the series differential loop and measuring the net induced voltage for a through primary current passing into and from the bus. The per cent differential error is then 100 times the net induced volts divided by the secondary voltage of five volts per thousand amperes of through-fault current. Differential error also may be determined with the secondary circuit closed so as to permit normal relay operation by measuring either the voltage across the relay or the secondary current. Either of these measurements are readily translated to net induced volts by a curve (Figure 5). This curve is obtained by applying a voltage in the coupler-relay loop while all primary circuits are open, and reading total volts, relay volts, and secondary current. The operating point of the relay should be definitely noted and indicated on this curve. Tests of this type were made at both Middletown and York. In addition some oscillograms were taken at York for record purposes.

Test Facilities at York and Middletown

Test arrangements at York are shown schematically in Figure 6 and, those at Middletown were similar except that the bus has six circuits and only one 500-kva transformer was available as a test supply. The two test transformers at York permitted tests for all types of faults and a wider range of fault currents. For 3-phase faults the transformers were connected open delta. For heavy-current single-phase faults, phase-to-phase or phase-to-ground, the transformer primaries were connected in parallel and their secondaries in series. The regular high-voltage disconnect switches and transfer bus facilitated selection of the primary circuits to be used during a test. One high voltage circuit was considered the incoming circuit and each of the other circuits in turn were used as outgoing circuits to determine their percentage differential error and to check proper phasing and polarity.

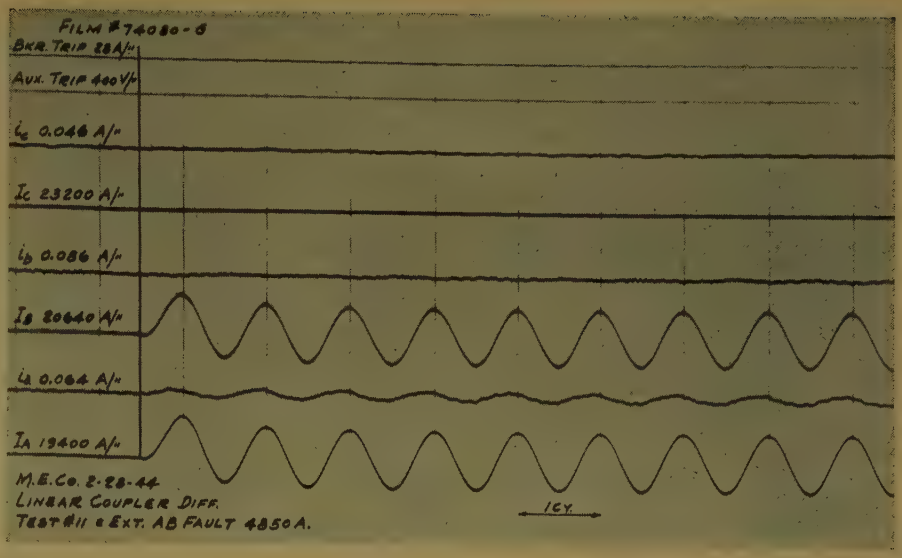


Figure 7. Oscillogram of an external phase-to-phase *AB* fault of 4,850 amperes using relay setting of 550 amperes

Reading from the bottom up the traces are:
I_A—Phase *A* primary current. It shows 4,850 amperes a-c component and a large rapidly decaying d-c transient
i_a—Phase *A* secondary differential error current. It shows 2.5 milliamperes representing 1.3 per cent error
I_B—Phase *B* primary current. It shows same as for phase *A*
i_b—Phase *B* secondary differential error current. It shows negligible error
I_C—Phase *C* primary current. It shows zero current
i_c—Phase *C* secondary differential error current. It shows no induction from the fault current
Aux. trip—Voltage across auxiliary tripping relay coil. It shows that the differential relays did not close their contacts
Bkr. trip—Current through *B*-3 circuit breaker trip coil. It shows that it was not tripped

Results of Tests

The highest differential error measured between any two couplers was found to be 2.1 per cent at York and 2.6 per cent at Middletown. The average of such differential errors was about 0.75 per cent. As maximum capacity through faults involve more than one incoming circuit and may involve more than one outgoing circuit, the actual differential error depends upon the fault current distribution through the various couplers and their individual errors. This would be less than the highest per cent differential error between any two couplers, but by assuming it to be the same an additional factor of safety is included against operation for through faults.

External Fault Oscillogram

Figure 7 shows an oscillogram for an external *AB* phase-to-phase fault of 4,850 amperes fed through circuit breakers *B*-3 and 977. The relays were set to pick up for a 550 ampere bus fault, or 11.3 per cent of this through fault current, and did not operate as the differential error was less than the relay setting. The oscillogram shows the fault currents I_A and I_B initially offset, negligible i_b differential current in the *B* phase loop, and 2.5 milliamperes i_a differential in the *A* phase loop. From Figure 5 this 2.5 milliamperes indicates 0.318 volt net was induced in the loop and this in turn represents 1.31 per cent differential error. During this test the *A* phase relay voltage was read as 0.15 volt indicating 1.27 per cent differential error, and the *B* phase relay voltage was read as 0.05 volt indicating 0.203 per cent differential error. A further check of these differential errors was obtained more precisely in a steady-state test for an external 3-phase fault of 1,075 amperes by reading the net induced voltages directly with the differential loops open; and it gave differential errors of 1.30 per cent for phase *A*, 0.208 per cent for phase *B*, and 0.524 per cent for phase *C*. With 1.3 per cent differential error and a relay set to pick up for a 550 ampere bus fault, a through fault current of over 42,000 amperes would be required to cause undesired tripping.

Internal Fault Oscillogram

Figure 8 shows an oscillogram for a 3-phase bus fault of 1,157 amperes repre-

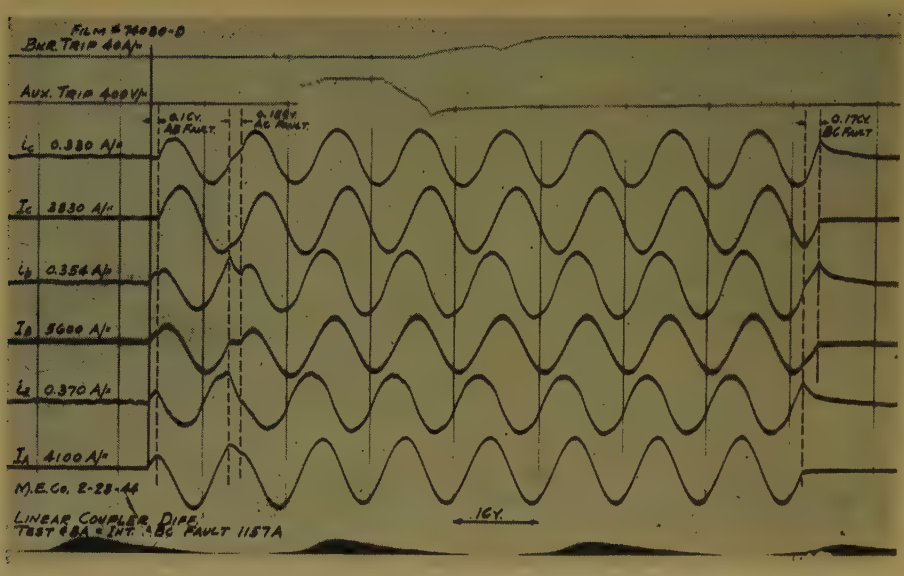


Figure 8. Oscillogram of an internal 3-phase fault of 1,157 amperes (average of 3 phases) using relay settings of 550 primary amperes, 36 milliamperes secondary current

Reading from the bottom up the traces are:

I_A—Phase *A* primary current. It shows 1,120 amperes

i_a—Phase *A* secondary differential current. It shows 87 milliamperes

I_B—Phase *B* primary current. It shows 1,310 amperes

i_b—Phase *B* secondary differential current. It shows 95 milliamperes

I_C—Phase *C* primary current. It shows 1,040 amperes

i_c—Phase *C* secondary differential current. It shows 76 milliamperes

Aux. Trip—Voltage across auxiliary tripping relay coil. It shows that the differential relays closed their contacts in 1.75 cycles

Bkr. Trip—Current through *B*-3 circuit breaker trip coil. It shows it was energized 3.13 cycles after inception of fault

senting 2.1 times the 550 ampere pick-up of the relays. It shows that the linear coupler relays energized the auxiliary trip relay in 1.75 cycles, the auxiliary trip relay energized the breaker trip coil at 3.13 cycles, and the fault was cleared at 8 cycles. This 3-phase fault was unusual in that it changed to different types of interphase faults because the test source voltage of 160 volts was not sufficient to establish or maintain arcs under oil with minute separation of the breaker contacts. The fault was successively an *AB* fault for 0.10 cycle, an *ABC* fault for about a cycle, an *AC* fault for 0.15 cycle, an *ABC* fault until the breaker started to interrupt and ended as a *BC* fault for the final 0.17 cycle. These fault transients did not interfere with operation of the relays as each showed a target, indicating all three relays closed their contacts within a 1/4 cycle period, required for the first trip circuit to be sealed. This test was a repeat of the previous test made without oscillograph and with the relay trip circuit disconnected so that the fault could be held long enough to read the three primary currents and the three relay voltages. These readings verified each other and the subsequent oscillographic record.

Summary of York Tests

These two oscillograms and their explanations are representative of the series of 19 fault tests made on the 114-kv circuits at York. They included 3-phase, phase-to-phase, and phase-to-ground faults both external and internal. The phase-to-ground faults were made through the structural steel and its multiple paths lowered the impedance to give fault currents up to 6,500 amperes. This current for a bus fault reduced the relay time to 1.33 cycles. The ground fault tests showed a neglible induction effect in the unfaulted phase loop circuits. In addition to the fault tests made on the 114-kv circuits, a ground fault was applied to a lighting circuit installed in the same trench as the bus differential leads to the structure and it was found that the 250 amperes that flowed out on the lighting circuit to return by way of ground induced quite negligible voltages, 0.012 volt, in the bus differential loops. This is less than half of one per cent of that necessary to operate the relays with the settings used.

Middletown Tests

The Middletown tests were similar but were made without oscillograph and with only one single-phase test transformer, which was able to deliver up to 4,800 amperes for a through fault. So as to demonstrate better the reliability of the linear coupler differential, the relay setting was deliberately lowered from the contemplated 700 ampere setting to 150 amperes, representing 3.1 per cent of the 4,800 ampere maximum through fault test. A complete round of 32 tests were made with this sensitive setting. The relays operated for all bus faults and did not operate for any external faults, even though differential errors up to 2.6 per cent were measured. After this the relays were returned to their normal 700 ampere pickup setting and then their complete tripping operation was demonstrated with bus faults of about 1,100 amperes.

Operating Experience

Field experience must be depended upon to show up any factors which may have been overlooked, and constancy of performance over a period of time, and to bring out any problems of maintenance or adjustment that may be involved.

Based on minimum fault current of 1,400 amperes and 1,050 amperes at Middletown and York, respectively, the linear coupler relays were set at a pick-up value of 700 amperes and 550 amperes, respectively. They have been in service approximately two years, and although during this period there have been no bus faults at either location to require operation, there have been a total of 8 faults on the Middletown-York circuits and 35 faults on the Middletown-Lebanon circuit, none of which caused incorrect operation.

A 66-kv ground fault on the 50,000 kva transformer bus structure at Middletown likewise did not cause operation of the linear coupler relays although the linear coupler secondary cable is buried in the earth in close proximity to the fault location.

Conclusions

In addition to providing assurance that the York and Middletown bus protection systems are in first class operating conditons, the tests have established the following facts of importance in general application of the system.

1. Linear couplers can be factory tested separately from the circuit breakers and then mounted in the breakers in the field, without any special adjustments.

2. The factory tolerances being maintained on the coupler mutual reactance results in over-all variations after mounting not over ±1.5 per cent.

3. With normal precautions of keeping the wires of the coupler-relay loop in a common

spiraled cable, induction from other circuits in the control ducts is negligible.

4. Field tests confirm that significant tests can be made at reduced primary currents. The system is linear and the percentage errors so determined apply equally well at higher currents. This facility is not enjoyed by any other system.

In many applications the choice lies between the multirestraint relay with current transformers and the linear-coupler system. If the current transformers already exist and are usable as they are or with rewinding, there may be an economic factor in favor of the multirestraint relay. However, this must be balanced against the lower cost of secondary cable installation with the linear couplers. Also, if partial differential feeder-backup protection is to be applied using the same current transformers, the corresponding equipment has not yet been developed for application with the couplers. The 3- to 6-cycle operating time of the multirestraint relay system has usually proved adequate from a stability standpoint.

On new installations or revamping projects where either current transformers or couplers will need to be procured, the linear coupler system offers instantaneous tripping in a very simple system which can be readily applied and tested. Its cost is competitive with the multirestraint relay system.

The multirestraint relay is applicable when the current range from maximum through fault to relay setting is up to 100 to 1. One relay per phase suffices with up to three major sources (generators, transformers, bus-ties) per bus sections; two per phase for up to seven major sources.

With the linear coupler system but one relay per phase is used irrespective of the number of circuits connected to the bus. However, energy requirements fix the lower limit of relay setting for positive action at approximately 300 amperes with six circuits per bus, plus 25 amperes per additional circuit. The range of currents from maximum through fault to relay setting has been limited purposely to 17 to 1. As demonstrated by these tests this limit is quite conservative in the case of the installations described. This range usually covers the required range for phase currents and also for ground currents on solidly grounded systems. Where ground currents are limited as by grounding resistors, making the over-all current range more than 17 to 1, a separate ground relay is required in the linear coupler system and is prevented from operating for other than single-line-to-ground faults by a ground detector relay described by Sonnemann.[6] The ground current setting cannot be below the 300 amperes for a 6-circuit bus plus 25 amperes per additional circuit.

Summarizing, local conditions will frequently dictate the proper application. Where high speed, simplicity and reliability are important, the linear coupler system should receive prime consideration.

References

1. Linear Couplers for Bus Protection, E. L. Harder, E. H. Klemmer, W. K. Sonnemann, and E. C. Wentz. AIEE Transactions, volume 61, 1942, May section, pages 241–8.

2. Current Transformer Excitation Under Transient Conditions, D. E. Marshall, P. O. Langguth. AIEE Transactions, volume 48, 1929, pages 1464–74.

3. Current Transformers and Relays for High Speed Differential Protection, With Particular Reference to Offset Transient Currents, E. C. Wentz, W. K. Sonnemann. AIEE Transactions, volume 59, 1940, August section, pages 481–8; discussion pages 1144–8.

4. Considerations in Applying Ratio Differential Relays for Bus Protection, R. M. Smith, W. K. Sonnemann, G. B. Dodds. AIEE Transactions, volume 58, 1939, June section, pages 243–52.

5. Air Core Couplers Simplify Bus Protection, E. L. Harder. *Westinghouse Engineer*, May 1942, page 43.

6. A New Single-Phase-to-Ground Fault-Detecting Relay, W. K. Sonnemann. AIEE Transactions, volume 61, 1942, September section, pages 677–80; discussion pages 995–6.

Long 60-Cycle Arcs in Air

A. P. STROM
MEMBER AIEE

Synopsis: Volt-ampere characteristics of 60-cycle arcs in still air with lengths and currents such as occur in power systems have been investigated under laboratory conditions. The arcs varied in peak current from 68 to 21,750 amperes and in length from 1/8 to 48 inches. Typical oscillograms and volt-ampere curves of these tests are presented. The voltage gradient in the arc is affected very little by current magnitude. Throughout the entire range all gradients remained between 21.5 and 50 volts per inch, with 35 per cent of all values in a 5 volt per inch interval having an average value of 34 volts per inch. The increase in apparent gradient due to voltage drop at the electrodes was found to be negligible where the arc length exceeds several feet. The decrease in short-circuit current of a power system through a series arc as compared with that for the same system with a metallic short circuit has been investigated. Data are presented showing the actual reductions observed for various conditions of circuit voltage and impedance.

SHORT CIRCUITS on transmission lines and at terminals of high voltage power apparatus practically always take place through long arcs in air. It is important, therefore, to know to what extent these arcs limit the short-circuit current and make it less than would occur with a metallic short circuit. The drop across the arc also affects the phase angle between voltage and current in directional types of relays. The data in the form presented here also can be used to indicate the current limiting effect of arcs on low voltage circuits. Although considerable data from field studies of transmission line flashovers are available,[1,2] the uncontrolled conditions do not permit any accurate determination of the arc characteristics of the arcs in the flashovers.

This investigation, therefore, has been carried out under laboratory conditions where better control of the variable factors is possible.

Testing Procedure and Apparatus

In order to cover a wide range of current values the 27,000-kva single-phase transformers in the Westinghouse high voltage laboratory at Trafford, Pa., were used to supply power for these tests. The current was limited by the impedance of the transformers and reactors connected in series.

Arcs varying in length from 1/8 to 48 inches and in peak current from 68 to 21,750 amperes were investigated. Most of these tests were made with brass electrodes at 48 inches separation. This large electrode separation was chosen so that the voltage drop adjacent to the electrodes would be negligibly small. However, owing to the limited capacity of the transformer bank, for currents in excess of 10,000 amperes the transformers had to be reconnected for smaller voltage. This voltage was insufficient to maintain the current in the 48-inch arc. For this reason these tests were made at 24-inch and 12-inch contact separations.

The arcs, which were initiated by means of fuse wires, were drawn in a vertical

Paper 46-22, recommended by the AIEE committee on protective devices and presented at the AIEE winter convention, New York, N. Y., January 21–25, 1946. Manuscript submitted November 20, 1945; made available for preprinting December 13, 1945.

A. P. Strom is with the research laboratories, Westinghouse Electric Corporation, East Pittsburgh, Pa.

Table I. Arc Volts Per Inch at Peak Current on Long 60-Cycle Arcs in Air

Test	Arc Length, Inches	Peak Arc Currents Each Half Cycle							Arc Volts Per Inch on Each Half Cycle						
		1	2	3	4	5	6	7	1	2	3	4	5	6	7
A	48	140	145	134	136	135	137	125	25	27	31	40	35	38	27
B	48	68.5	130	109					27	21.5	21.5				
C	48	260	238	236	192				25	30	30	30			
D	48	544	445	500	435	405			32	29	32	32	31		
E	48	396	322	337	330	300			26	31	38	40	36		
F	48	1,460	1,340	1,385	1,290	1,385	1,380	1,240	38	35	31.5	44	32	27	30
G	48	2,500	2,680	2,630	2,680	2,630	2,480	2,525	35.5	30	30	26	28	28	27
H	48	1,010	1,675	1,820	1,920	1,780	1,410		35	27	30	26	29	29	
I	48	708	870	1,535	2,060	3,780			35	37	33	31	30		
J	48	735	2,360	3,540	3,730	3,380			43	30	31	29	30		
K	48	1,135	812						41	36					
L	48	2,100	4,040	6,780	10,000	10,000			43	34	35	30	30		
M	48	8,230							35						
N	48	3,550							35						
O	48	7,750							35						
P	48	6,450	3,225	5,330	6,450	10,150	10,150		40	46	42	43	30	28	
Q	48	2,580	2,420	7,750	9,500	8,550	7,600		40	38	32	34	33	36	
R	48	5,200	7,150	6,660	7,070	6,750	6,660		35	36	36	35	30	28	
S	48	4,370	5,440	5,150	5,100	5,150	4,800		36	31	31	31	31	31	
T	48	4,370	5,400	5,150	5,250	5,250	4,910		34	31	31	27	27	26	
U	48	4,270	5,490	5,000	5,250	4,910			40	34	39	31	34		
V	48	5,400	5,150	5,250	5,250	5,150	4,910		54**	35	31	27	31	32	
W	24	10,000	14,200	11,900	12,250	11,900			35	34	40	38	50		†
X	24	2,010							48						†
Y	24	7,640							47						†
Z	12	6,840	20,500	17,500	18,500	17,700				54	59	59	56		†
AA	12	12,450	19,100	17,500	19,100	14,900			46.3	50.5	59	56	55		*
AB	12	11,700	21,750	21,150	20,000				45	41	41	40			‡
AC	12	10,900	15,100	14,500	14,000	12,500			45	43	39	41	39		‡
AD	12	6,900	8,670	7,950	8,070	7,370			41	34	36.5	40	39		‡
AE	12	7,330	8,200	8,320	7,720				52	47	36.5	42			‡
AF	12	6,990	8,125	7,800	7,650				37	39	38	38			‡
AG	12	7,150	7,970	7,650	7,650	7,550			42	42	43	44	50		‡
AH	12	6,570	8,125	7,800	7,650	7,230			38	43	38	39	43		‡
AI	12	4,770	5,680	5,180	5,180				37	37	37	43			‡
AJ	12	8,550	15,750	14,500	14,500				34	41	41	38			‡
AK	12	10,450	17,700	19,700	19,700				43	43	43	43			‡
AL	0.125	15,750	15,250	15,750	14,900	14,000			(34.8)	(42.6)	(45.2)	(45.2)	(44)		‡, #
AM	0.125	22,100	26,000	25,000	23,200				(42.6)	(64.5)	(86.5)	(90.4)			‡, #
AN	12	12,850	20,900	16,700	21,500	14,000			43	41	46	41	40		‡
AO	12	9,970	15,250	13,300	13,500	11,200			46	47	42	45	45		‡

† Probable bowing of arc.
* Photograph indicates bowing of arc to approximately 1.5 gap length.
‡ Leads to test rearranged. Photograph shows no bowing of arc on *AB*.
Figures give total arc volts on the 1/8-inch gap.
** Abnormally high voltage undoubtedly due to its occurrence immediately after fusing of large size fuse wire.

plane to prevent arc elongation by convection. To eliminate as far as possible any looping of the arc, the current leads to the terminals were placed along the longitudinal axis for a distance of 2 to 4 feet. Observations made through dark glasses and also by photography indicate that the arc is reasonably straight between the electrodes when these precautions are taken.

Magnetic oscillograms were taken of all tests, and measurements of current and arc voltage data were made from these records.

Variation of Voltage Gradient in the Arc With Current

Table I summarizes the data for all the arcing tests, giving the peak current and corresponding voltage gradient in the arc for each half cycle of arcing. No correction has been made for potential drop at the electrodes in this table.

Figure 1 shows graphically the variation of voltage gradient in the arc with current, using the data from Table I. A correction of 3 volts per inch was made for electrode drop in plotting the data for the 12-inch long arcs, as this is approximately the proper value indicated by tests which will be discussed further in a later paragraph. Tests *W* to *AA* inclusive were omitted from this curve, as it is believed that there was some arc elongation on these tests due to magnetic fields from the current supply leads.

This curve shows that practically all of the arc voltage gradients found in these tests fall between 25 and 50 volts per inch. The average of the gradients appears to remain constant at 31 to 33 volts per inch for all currents up to 5,000 amperes, rises slowly to 38 volts per inch at 10,000 amperes, and remains constant up to over 20,000 amperes.

The fact that the arc voltage gradients cover a rather wide band has not been entirely explained. It is believed, however, that at least a part of this variation can be accounted for by the effects of magnetic forces moving the arc about. If the

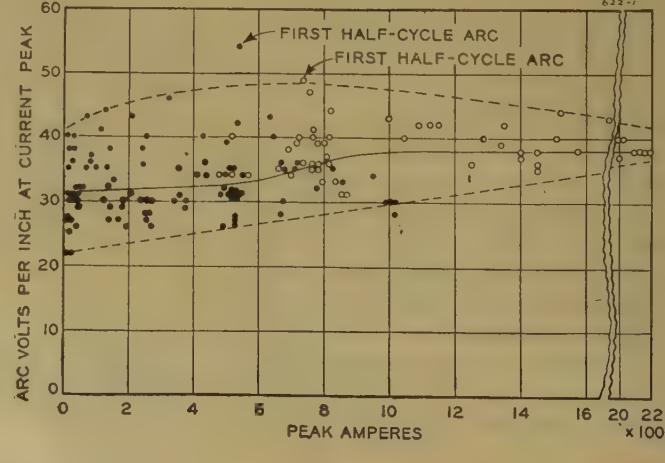


Figure 1. Voltage gradients at peak current on 60-cycle power arcs in air

● 48-inch arcs
○ 12-inch arcs

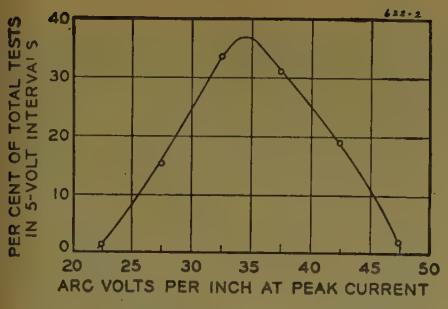


Figure 2. Distribution of voltage gradients at peak current on 153 half cycles of arcing

Peak current range from 68 to 21,750 amperes

arc terminals strike unsymmetrically, or if the axis of the arc moves away from the axis of the electrodes, magnetic forces act to accelerate such motion. This results in slight variations in arc path and relative motion of the arc and surrounding air. The effect of convection air currents and turbulence conditions at the arc boundary change and cause a more rapid loss of heat and ionization requiring higher arc voltage to maintain the current. The 3.7-ampere arc in Figure 11 shows variations in arc path of a substantially

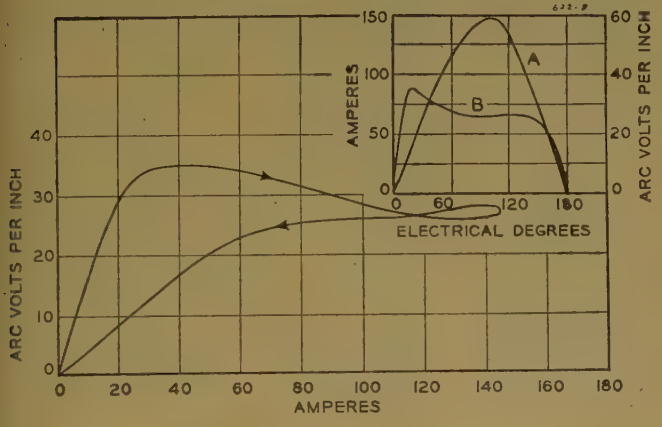


Figure 3. Volt-ampere characteristic for a 100 rms ampere arc

Test *A* of Table I.
Arc length 48 inches
A—Amperes
B—Volts

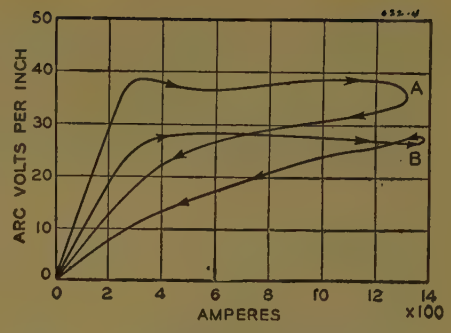


Figure 4. Volt-ampere characteristics of a 1,000 rms ampere arc

Second and sixth half cycles of test *F*, Table I.
Arc length 48 inches
A—Second half cycle
B—Sixth half cycle

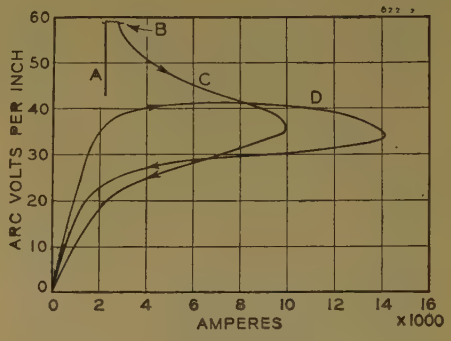


Figure 5. Volt-ampere characteristics of a 10,000 rms ampere arc

First and second half cycles of test *W*, Table I
Arc length 24 inches
A—Fusing current, 2,260 amperes
B—Arc volts at fusing, 178 volts per inch
C—First half cycle
D—Second half cycle

Table II. Current Limiting Effect of Series Arcs on Short-Circuit Currents

Test	No-Arc Short-Circuit Peak Current	Arc Length, Inches	Circuit Volts, Rms	First Half Cycle Arc Current, Per Cent of No-Arc Short-Circuit Current	Maximum Arc Current, Per Cent of No-Arc Short-Circuit Current
A	144	48	5,750	97	100
B	142	48	2,300	47.5	77
C	382	48	2,300	68	68
D	735	48	2,300	74	74
E	360	48	4,600	100	100
F	1,420	48	4,600	100	100
G	2,830	48	4,600	88	95
H	2,830	48	2,300	35	68
I	2,830	48	2,300	25	97
J	5,660	48	2,300	13	66
K	9,900	48	2,300	11.5	11.5*
L	16,600	48	2,300	12.7	60
M	16,600	48	2,300	50	50*
N	16,600	48	2,300	21.5	21.5*
O	16,600	48	2,300	48	48*
P	16,600	48	2,300	39	61
Q	16,600	48	2,300	15.6	57
R	8,150	48	4,600	64	88
S	5,630	48	6,900	77	97
T	5,500	48	6,900	80	98
U	5,450	48	6,900	78	100
V	5,450	48	6,900	99	99
W	16,300	24	2,300	61	87
X	27,300	24	1,150	7.4	7.4*
Y	27,300	24	1,150	28	28*
Z	33,400	12	1,150	20	61
AA	27,300	12	1,150	45	70
AB	27,300	12	1,150	43	80
AC	16,300	12	2,300	67	93
AD	8,100	12	4,600	85	100
AE	8,100	12	4,600	90	100
AF	8,100	12	4,600	86	100
AG	8,100	12	4,600	88	98
AH	8,100	12	4,600	81	100
AI	5,450	12	6,900	88	100
AJ	16,300	12	2,300	52	96
AK	27,300	12	1,150	38	72
AL	16,300	0.125	2,300	97	97
AM	27,300	0.125	1,150	80	95
AN	27,300	12	1,150	47	78
AO	16,300	12	2,300	61	93

* Arc extinguished itself in 1 or 2 half cycles.

straight arc which seem to agree with this explanation.

Two tests in Table I, *AL* and *AM*, were made on 1/8-inch long gaps in order to determine the approximate additional voltage due to drops at the electrodes. The maximum currents on the first half cycles of these tests were respectively 15,750 and 22,100 amperes, and the corresponding arc voltages 34.8 and 42.6 volts. Although a small part of this voltage can be attributed to positive column drop in the 1/8-inch long arc, the results indicate that approximately 30–40 volts can be attributed to drop at the electrodes. The positive column gradient expressed in volts per inch is, therefore, approximately, $(e_a - 35) \div l$, where e_a is total arc volts, and l is arc length in inches. This indicates that drop at the electrodes has a negligible effect on the apparent gradient if the arc length exceeds several feet.

The distribution of voltage gradient values for the entire series of tests from

68 to 21,750 peak amperes in 5 volt per inch intervals is shown graphically in Figure 2. This curve indicates that over 35 per cent of the gradients fall in a 5 volt per inch range having an average value of 34 volts per inch.

Volt-Ampere Characteristics

Figures 3, 4, 5, and 6 show volt-ampere characteristics of arcs varying in peak current from 145 to 21,750 amperes. The volt-ampere curves are similar for both high and low currents, but there is considerable variation from one half cycle to another. This is illustrated by the curves of Figure 4 showing two half cycles of a 1,000 rms ampere arc. Here the sixth half cycle is considerably lower in arc voltage than the second. This might suggest that arc voltage decreases as arcing progresses from one half cycle to another, but examination of the test data fails to show any definite trend in this direction.

Current Limiting Effect of Arcs

The current limiting effect of the arc at short-circuit currents was studied for a considerable number of the tests recorded in Table I, by first drawing an arc between a pair of electrodes and then taking the short-circuit current under the same conditions, except with the arc gap short-circuited with a heavy copper conductor.

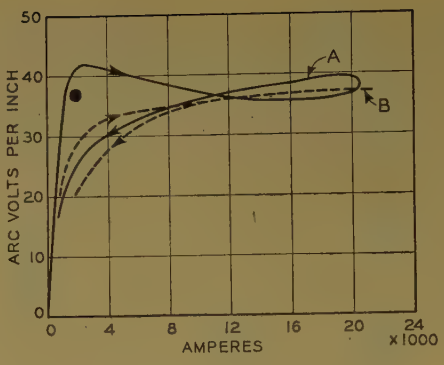


Figure 6. Volt-ampere characteristics of a 15,000 rms ampere arc

Second and fourth half cycles of test *AN*, Table I. Arc length 12 inches. Gradients corrected for drops at electrodes

A—Second half cycle

B—Fourth half cycle

In Table II the values of short-circuit current without a series arc for each test condition of Table I are given together with the percentage reduction in current observed when the same circuit is short-circuited through a series arc. Nominal values of the no-arc short-circuit currents are given for the tests in which these values were not experimentally observed.

Typical oscillograms are shown in Figures 7 and 8, illustrating the reduction in short-circuit current due to series arcs. These oscillograms show that a 48 inch long arc reduces the current very appreciably on a 4,000-ampere 2,300-volt circuit, but has much less effect at 6,900 volts with approximately the same current. This may be expected, as the arc voltage in the latter case is a much smaller part of the applied circuit volts. As a rough estimate the arc may be treated as a series resistance having a value equal to arc volts divided by normal rms short-circuit amperes. The approximate reduced value of current with a series arc then may be estimated as the quotient of rms volts and the impedance, in which the arc resistance is added vectorially to the normal circuit impedance.

Since the arc voltage, e_a, is nearly constant in value, a better estimate may be made by directly integrating the differential equation of the circuit but remembering that e_a changes sign when the current reverses. This requires a redetermination of the constant of integration at each current zero.

For example, to determine the steady state current for a circuit which consists of a pure inductance and a series arc, we may start with the equation,

$$A \cos wt + B \sin \omega t - L\frac{di}{dt} - e_a = 0 \qquad (1)$$

where

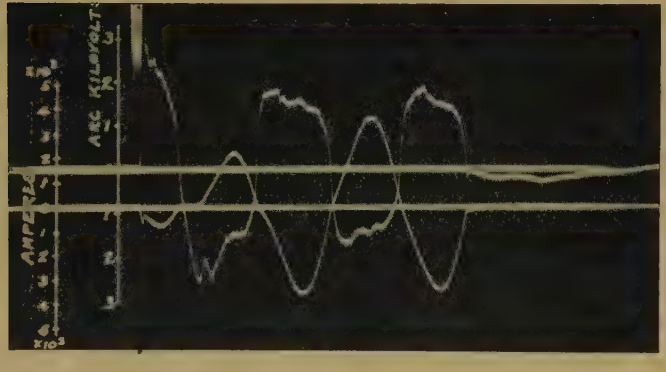


Figure 7 (above). Effect of a series arc in reducing short-circuit current in a 4,000 rms ampere 2,300 rms volt system

A. Current and arc voltage with a 48-inch series arc. Test *J*, Table I. Maximum peak current 3,730 amperes

B. Current in the same circuit without a series arc. Maximum peak current 5,660 amperes

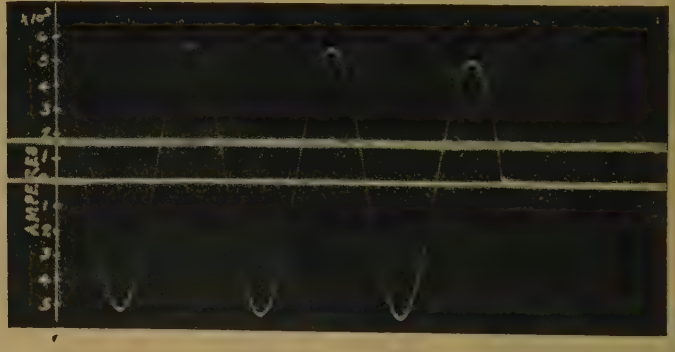
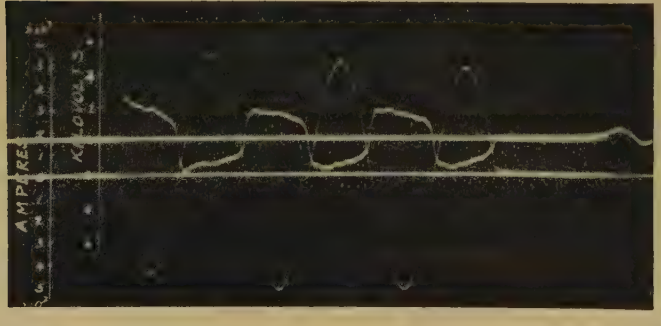
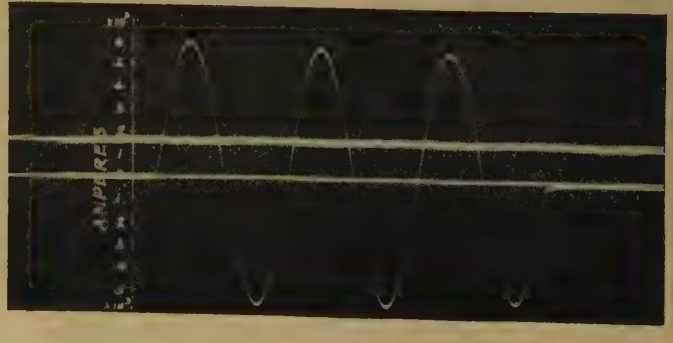


Figure 8 (below). Effect of a series arc in reducing short-circuit current on a 4,000 rms ampere 6,900-volt system

A. Current and arc voltage with a 48-inch series arc. Test *S*, Table I. Maximum peak current 5,440 amperes

B. Current in the same circuit without a series arc. Maximum peak current 5,630 amperes





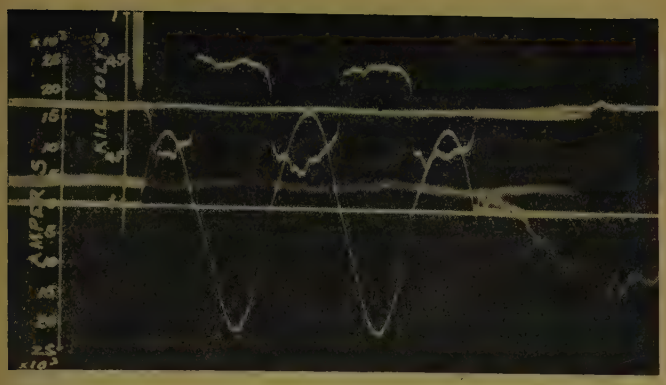


Figure 9 (above). Oscillogram of a short-circuit test on a 20,000 rms ampere, 1,150 rms volt circuit, with a 12-inch series arc

Test *AN*, Table I. Maximum peak current 21,500 amperes



Figure 11 (right). Photograph of a 48-inch 3.7 rms ampere arc showing variations in arc path of a substantially straight arc

$A \cos \omega t + B \sin \omega t$ = sinusoidal impressed voltage

$\sqrt{A^2+B^2} = E_m$ = maximum value of impressed voltage

L = inductance in henrys

e_a = arc voltage (assumed of constant value)

Integrating equation 1 gives

$$i = \frac{A}{\omega L} \sin \omega t - \frac{B}{\omega L} \cos \omega t - \frac{e_a}{L} t + K \qquad (2)$$

Figure 10. Photographs of 12-inch high current arcs showing the effect of the magnetic field due to the supply leads on the shape of the arc

A (below, left). Substantially straight arc when current supply leads are brought in along the axis of the arc. Test *AK*, Table I. Maximum peak current 19,700 amperes

B (below, right). Bowing of the arc when the supply leads are not located along the axis of the arc. Test *AA*, Table I. Maximum peak current 19,100 amperes

The supply leads have been retouched to show their locations more clearly





as long as the current and with it e_a does not change sign.

We now assume that i is initially zero when t is zero and passes through zero again at uniform half cycle intervals. Then the constants K, B, and A may be evaluated as follows:

When $t=0$, $i=0$; substituting these values in equation 2 gives

$$K = \frac{B}{L\omega}$$

When $t=1/2$ cycle or π/ω, $i=0$; substituting these values in equation 2 gives

$$B = \frac{e_a \pi}{2}$$

$$A = \sqrt{E_m^2 - B^2} = \sqrt{E_m^2 - \left(\frac{e_a \pi}{2}\right)^2}$$

Using these values for A, B, and K in equation 2 gives the solution for the current in terms of known constants as follows:

$$i = \frac{\sqrt{E_m^2 - \left(\frac{e_a \pi}{2}\right)^2}}{\omega L} \sin \omega t - \frac{e_a \pi}{2\omega L} \times \cos \omega t - \frac{e_a}{L} t + \frac{e_a \pi}{2\omega L} \qquad (3)$$

The ratio of this current at peak value to that without the series arc is very nearly

$$\frac{\sqrt{E_m^2 - \left(\frac{e_a \pi}{2}\right)^2}}{E_m} = \sqrt{1 - \left(\frac{e_a \pi}{2E_m}\right)^2}$$

It also may be shown from equation 1 that the current lags the voltage by an angle,

$$\theta = \cos^{-1} \frac{B}{\sqrt{A^2+B^2}} = \cos^{-1} \frac{e_a \pi}{2E_m}$$

In actual faults the arc length usually increases by bowing or looping, and the arc voltage gradient also may rise slightly as a result of air currents. Estimates of current reduction in which the values for arc voltage gradient presented in this paper are used, therefore, should give conservative, that is slightly too high, current values.

Conclusions

1. The average voltage gradients at current peak for 60-cycle arcs in air lie between 31 and 38 volts per inch for currents over the entire range from less than 100 to over 20,000 peak amperes.

2. The arc voltage varies considerably from one half cycle to another. The extreme range of this variation was from 21.5 to 50 volts per inch. Arc voltages on low currents vary over a wider range than on high currents.

3. While the variability of arc voltage has not been explained satisfactorily, it is believed that it is due at least in part to the magnetic forces acting on the arc which tend to shift the arc core into new arc paths that are less highly ionized and require higher arc voltage to maintain the current.

4. The average arc voltage gradient at current peak appears to rise from about 31 volts per inch at currents below 5,000 peak amperes to 38 volts per inch in the 10,000 to 20,000 ampere range.

5. For the complete range of currents from 68.5 to 21,750 peak amperes, 35 per cent of all the arc voltages fall within a 5 volt per inch interval having an average value of 34 volts per inch.

6. The current limiting action of arcs on short-circuit currents depends on the relative value of the total arc voltage to the circuit voltage. Approximations by calculation or graphical means of current reduction resulting from a series arc should be possible

Industrial Application of Rototrol Regulators

W. R. HARRIS
MEMBER AIEE

Synopsis: The Rototrol has been applied in considerable numbers to a wide variety of industrial applications. It has met adequately the need for a simple and reliable regulator which is capable of withstanding the rigors of general industrial usage and which is sufficiently elemental in operation that it can be understood by nontechnical maintenance personnel. It has been accepted enthusiastically by industry, and applications in both existing and new fields are increasing rapidly. This paper discusses the fundamental theory of the Rototrol, the application of the circuits most commonly used, and cites operating results for typical installations.

THE Rototrol is nothing more than a d-c generator similar in design and theory of operation to the standard d-c generator, but with a number of field windings which are designed and connected in various ways, depending on the regulating problem. The Rototrol functions entirely through the interaction of these fields, and has no moving parts or circuits which require delicate adjustment for proper operation or to compensate for wear. After initial adjustment during installation no further attention is required other than the routine maintenance associated with a d-c machine of similar size. The Rototrol is driven at constant speed either by a small squirrel-cage induction motor or as a part of the motor generator set or exciter set of the adjustable voltage drive which it serves.

The Rototrol, as shown in the functional diagram, Figure 1, is one of the most simple regulators yet devised. The principal elements are a self-energizing field (either in series or in parallel with the armature) and the separately excited control fields (usually two in number). One of the control fields commonly is referred to as the pattern field and is excited from a constant potential source. The other control field measures the quantity to be regulated and is referred to as the pilot field. The pattern and pilot fields usually are connected with their ampere turns in opposition, so that the pilot field measures the quantity to be regulated and compares it with the pattern field. Any net difference in these fields will cause the Rototrol to exert corrective forces to reduce the difference, so that the pattern and pilot fields balance out when the quantity under regulation is at the proper value.

Assume for the moment that the self-energizing field is short-circuited. Under this condition the ampere turns required to generate output voltage necessarily must come from the difference in excitation of the pattern and pilot fields. Precise regulation would be impossible, as a change in operating conditions would necessitate a greater or less difference in ampere turns, and the quantity under regulation would vary. From this it is concluded that for high accuracy the pattern and pilot fields must control the Rototrol output without supplying the ampere turns required to generate output voltage. The self-energizing field must perform this function so that the control fields are free for their regulating and forcing functions.

The self-energizing field is designed and tuned by a simple resistor adjustment, so that its resistance line is coincident with the air gap line of the no-load saturation curve. For instance, if 1 ampere in the self-energizing field generates 50 volts across the brushes, and the resistance of the self-energizing field circuit including the Rototrol armature, the self-energizing field, the field of equipment under control, and the tuning resistor is 50 ohms, 50 volts will cause 1 ampere to flow through the circuit. Following this further, if 2 amperes flow in the self-energizing field, 100 volts will be generated which will cause 2 amperes to flow through the tuned or self-energized circuit. With the self-energizing field so designed and adjusted, it is possible for the Rototrol to operate over the straight portion of its saturation curve without the control fields supplying the magnetomotive force necessary to generate voltage. Such a device then may be used as a simple and accurate regulator.

In order for the saturation curve to approximate closely the self-energizing field circuit resistance line, it is necessary to minimize hysteresis effects. By the use of special steels, or by special treatment of standard steels, hysteresis or residual magnetism can be reduced to the point where its effect is negligible. For example, a recent Rototrol on the basis of normal saturation for a d-c generator tested 0.4 per cent residual voltage. A comparable value for the usual d-c machine is 5.0 per cent.

Although the foregoing discussion describes a Rototrol with two control fields, it is possible to supply additional control fields to receive main or supplementary regulating intelligence. For instance, in certain speed control problems, it is desirable to limit the armature current which flows in the main machines to a definite value. An additional Rototrol control field is added and its circuit designed so that it takes control should the current exceed a definite value for either motoring or regenerative conditions. This field acts to hold the current within definite limits during acceleration or retardation and is particularly advantageous where the inertia of the mechanical

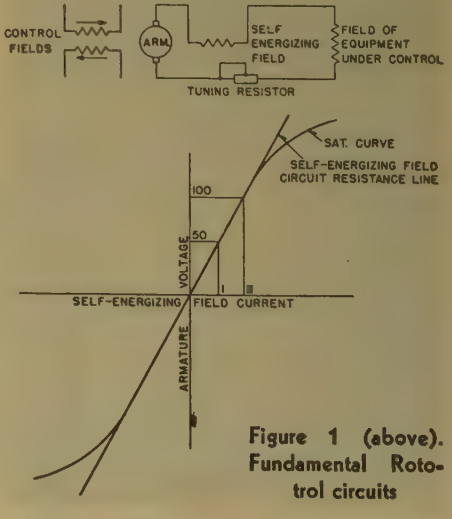


Figure 1 (above). Fundamental Rototrol circuits

Paper 46-57, recommended by the AIEE committee on industrial power applications and presented at the AIEE winter convention, New York, N. Y., January 21–25, 1946. Manuscript submitted November 23, 1945; made available for printing December 6, 1945.

W. R. HARRIS is in the industry engineering department, Westinghouse Electric Corporation, East Pittsburgh, Pa.

when arc voltages and circuit conditions are known.

References

1. A STUDY OF TRANSMISSION LINE POWER ARCS, Paul Ackerman. *Engineering Journal*, volume 11, May 1941, pages 309–23; 504

2. FREE BURNING HIGH CURRENT ARCS AT 100 KILOVOLTS A-C VOLTAGE, E. Gross. *Schweizer Archiv* (Solothurn, Switzerland), volume 7, July 1941, pages 196–201.

3. ELEKTRISCHE SCHALTVORGANGE (book), Reinhold Rüdenberg. Pages 204–15.

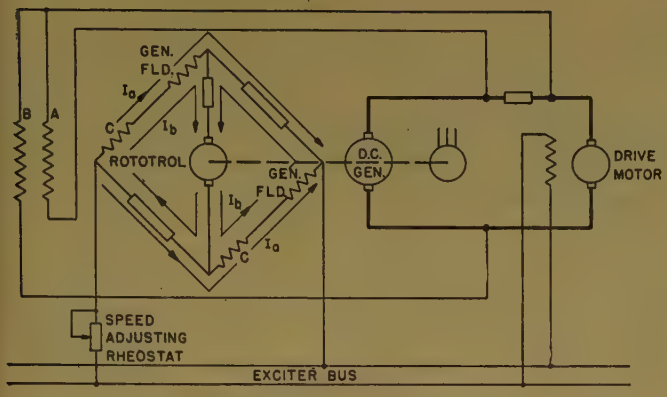


Figure 2. Elementary circuits of counterelectromotive force type speed regulator

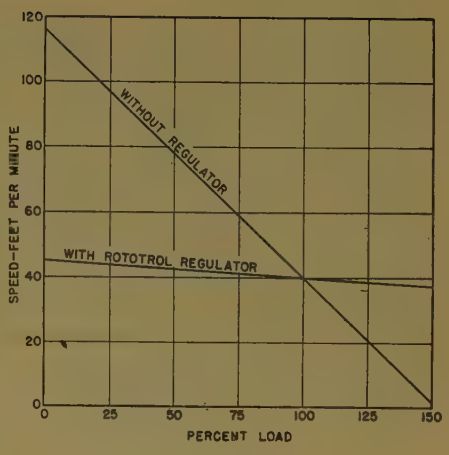


Figure 4 (right). Plot of test results at 1/30 speed for 150 horsepower supercalender drive with and without Rototrol counter electromotive force type regulator

system is large and a considerable period of time is required to accelerate from one speed to another.

The Rototrol is particularly well suited for application in closed cycle control systems. The criterion for a closed cycle system is that the deviation from the ideal performance be used to modify the flow of power to reduce the deviation. In such systems stability of operation must be carefully considered. A complete analysis of stability is beyond the scope of this paper, but a review of the factors that affect it is in order. The most important factors are the level of ampere turns in the control fields, the speed of response of the Rototrol system as determined by the time constants and mutual linkages of the various fields, series or parallel connection of the self-energizing field, and the electrical and mechanical inertias of the machines or system of machines under control. By proper evaluation of these various factors and care in the design of the system it has been possible to apply most Rototrols without the use of external stabilizing means. This makes the device well suited for industrial applications where simplicity of circuits and functions are desirable, both from the standpoint of operation and maintenance and of initial cost.

A few of the Rototrol circuits most commonly used with typical applications and operating results are described in the following paragraphs. These applications are chosen as indicative of the wide variety of functions which the device will perform.

Counterelectromotive Force Type Speed Regulator

The Rototrol counterelectromotive force type of speed regulator circuit is perhaps the most widely applied. Representative applications are feed drives for machine tools, adjustable voltage planer drives, high speed adjustable voltage elevator drives, skip hoist drives, and supercalender drives. It is applied where wide speed ranges are required with good speed regulation at all speeds, particularly at the minimum speeds. The circuit does not require a pilot generator to measure the motor speed, which results in a space saving about the machine and in a simplification of the electric equipment and circuits.

Figure 3. High speed supercalender equipped with Rototrol counterelectromotive force speed regulator

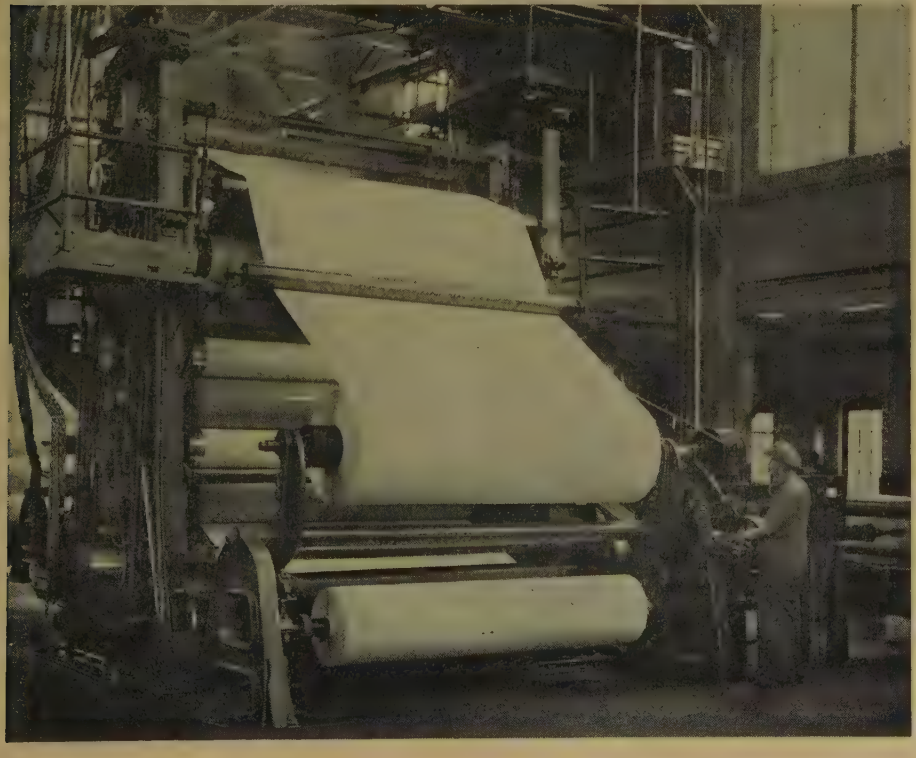


Figure 2 shows the elementary circuits of the Rototrol counterelectromotive force type of speed regulator. The speed of a d-c motor is given by the well-known formula,

$$S = \frac{V - (IaRa)}{K\phi}$$

in which S is the motor speed, Va, Ia, and Ra are armature circuit voltage, current, and resistance respectively, ϕ is the flux, and K is a constant depending on the motor design. If the motor is excited separately at constant potential, the flux may be assumed constant with small error. The motor speed is then proportional to the counterelectromotive force, which is the voltage across its armature minus the resistance drop in its armature circuit. Rototrol pilot field B measures the voltage across the armature, and pilot field A measures the armature current which is directly proportional to resistance drop. Field A is connected in opposition to field B, so that the net result of these two fields measures the motor counterelectromotive force, which is directly proportional to motor speed.

Rototrol fields C are connected in a bridge circuit with the generator field and perform the double duty of both pattern and self-energizing functions. All legs of the bridge are of the same resistance. The component of current Ia flowing from the exciter bus serves as pattern

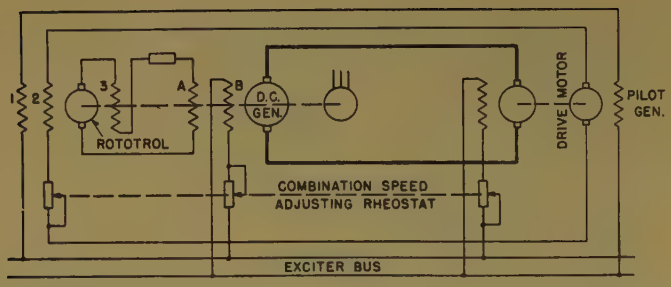


Figure 5. Elementary circuits of precision type speed regulator with pilot generator for measuring motor speed

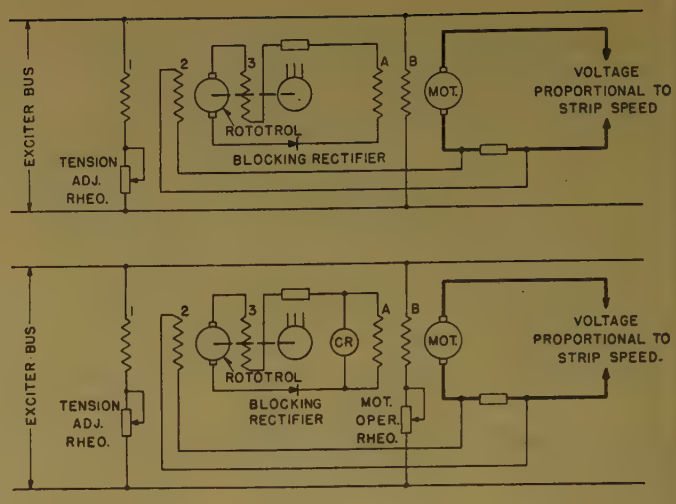


Figure 7 (right). Elementary circuits of tension control system for core type reels

a. Without speed limit feature
b. With speed limit feature

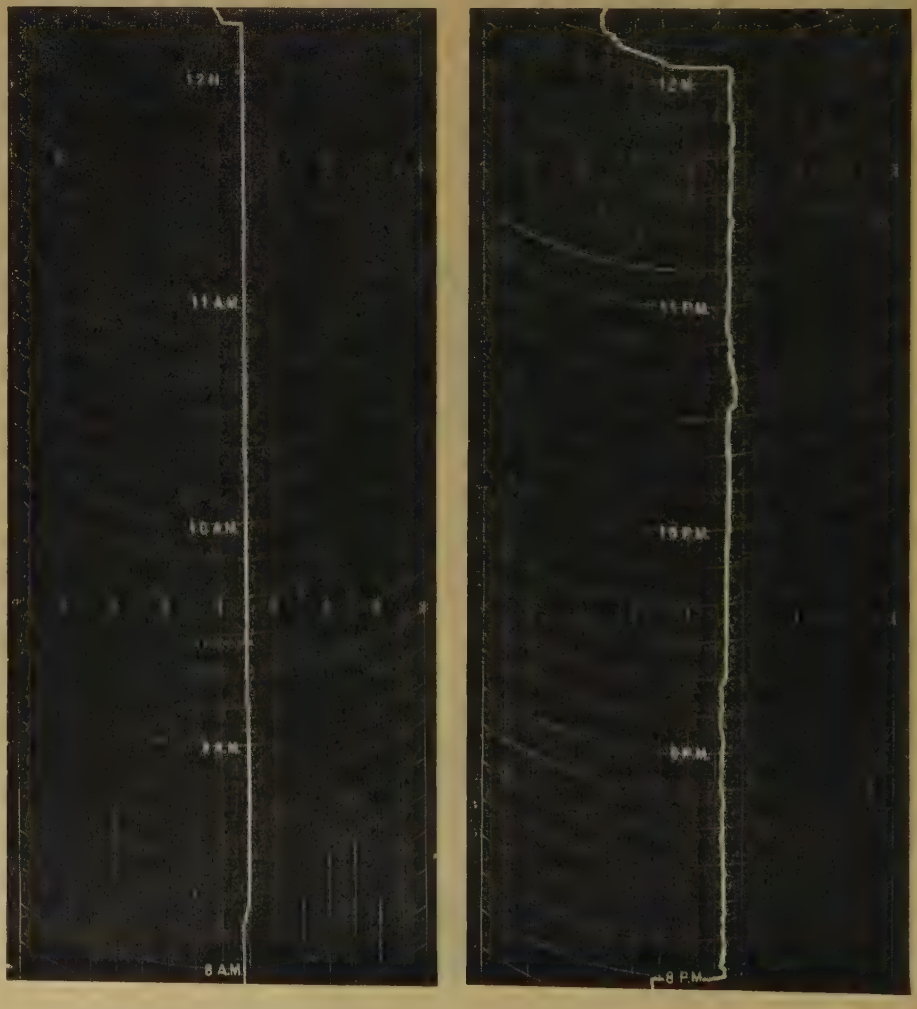
field current and in such a bridge will not cause a voltage drop across the Rototrol armature circuit. The component of current *Ib* flowing from the Rototrol armature through the bridge serves as the self-energizing component and conversely does not cause a drop across the terminals connected to the exciter bus. The circuits are arranged so that the pattern component of current through fields *C* is in opposition to the net effect of pilot fields *A* and *B*. Thus the pilot fields measure the motor speed and compare it with the pattern field component of current through fields *C*. If a difference exists, the Rototrol will compensate the generator field excitation and thus the motor speed until these fields again balance out.

A typical application of this circuit is to high speed adjustable voltage supercalender drives used in the paper industry. On supercalenders production speeds of from 1,200 to 2,000 feet per minute are becoming common, and the calender must be threaded at approximately 50 feet per minute, which results in an extremely wide speed range. Furthermore, the threading speed must be held constant for ease in threading and for safety to the operator. This requirement is complicated, because at threading speed the generator is operated near residual voltage, and a small change in residual voltage or in operating load means a relatively large speed change. Also as a result of threading the paper through the stack and the application of weighting, the load may vary 2 to 1 or more, which results in considerable speed variation with an unregulated drive.

In the past several methods of obtaining stable threading speed have been used. One method was to obtain part of the speed range by motor shunt field control which only partially eliminated the difficulty and was expensive because of the large frame size of the driving motor. Another method made use of a separate motor geared to drive the calender at threading speed to an overrunning clutch. This method gave stable threading speed but resulted in a complicated mechanical layout. The use of a Rototrol speed regulator obviates these disadvantages and is simple, as it requires only a small Rototrol set and a minor modification of the control circuits.

Figure 3 shows a view of a high speed supercalender driven by an adjustable voltage drive designed for a maximum speed of 1,200 feet per minute and a threading speed of 40 feet per minute. The entire range of 30 to 1 is obtained by armature voltage control. Figure 4 is a plot of test results at threading speed with and without the Rototrol regulator. Excellent regulation of threading speed is obtained as well as ample torque to break away the high static friction torques on the sleeve bearing stack.

Figure 6. Graphic speed charts taken on a 250-horsepower drive illustrating performance with (left) and without (right) Rototrol precision type regulator



Precision Type Speed Regulator

On applications where it is desirable to hold the speed of the driving motor within very close limits, a pilot generator for measuring motor speed directly is used in conjunction with the Rototrol. Typical applications of this type of speed regulator include drives for paper machines, wind tunnel propellers, and dynamometers.

The schematic diagram of a Rototrol regulator for precise speed regulation is shown in Figure 5. A pilot generator is used to measure the drive motor speed and excites the Rototrol pattern field 2. Pattern field 1 is excited from the exciter bus as is the pilot generator field. These fields are connected in series to minimize the effect of changes in exciter bus voltage and changes due to unequal field heating. The Rototrol excites generator field *A* and supplies only the regulating field power. Generator field *B* supplies the base excitation of the generator for any speed setting. To assure high sensitivity at all speeds, the speed adjusting rheostat is located in Rototrol field 2 which is served from the pilot generator so that a constant level of forcing excitation is obtained over the complete speed range.

When the drive motor speed is at the correct value, the control fields 1 and 2 balance out. If the motor speed departs from its correct value, the speed change is detected by the pilot generator and transmitted to the Rototrol pilot field 2. A difference then will exist between the pilot and the pattern fields, which causes the Rototrol to compensate the generator excitation to bring the motor speed back to the correct value.

Operating results with this type of Rototrol speed regulator have been excellent. Typical performance is shown by the graphic charts of Figure 6 showing speed regulation before and after application of the Rototrol regulator. The charts were taken on a 250-horsepower single-motor paper machine drive which was modernized by addition of the Rototrol speed regulator. The performance was obtained without the use and complication of supplementary amplifiers and demonstrates the high amplification and speed of response of the Rototrol.

Tension Regulator for Core Type Reels

In the steel, textile, paper, and rubber industries there are a large number of windup and unwind operations utilizing core type reels. A drive for such a reel must maintain constant tension in the strip and must change its speed continually and smoothly as the roll builds up from a small core to a full roll. A number of Rototrol controlled drives for this service have been applied. The Rototrol is used in conjunction with an adjustable-speed d-c motor which has a speed range by shunt field control equivalent to the ratio of the full roll diameter to the empty core diameter.

Figures 7a and 7b show schematically the circuits for a constant tension reel drive. The reel motor is supplied with a voltage proportional to strip speed, either from the adjustable voltage generator serving the main drive or from an auxiliary generator driven at machine speed. The Rototrol modifies the shunt field excitation of the motor to compensate for changes in roll diameter and to maintain uniform strip tension. This is accomplished by maintaining the motor armature current constant, and, as the supply voltage is uniform at any particular strip speed, the power output of the motor and the tension in the strip will be substantially constant.

In Figure 7a Rototrol pilot field 2 measures the motor armature current and compares it with pattern field 1. Any net difference of these two fields will cause the Rototrol to change the excitation of motor field A to hold the armature current constant. Field *B* is the speed limit field and is adjusted to give a motor speed proportional to empty core diameter. The blocking rectifier situated in motor field *A* prevents reversal of this field in the event of a break or end of the material being reeled. Under these conditions the power formerly taken by sheet tension acts to accelerate the motor toward higher speed, and the Rototrol gradually will weaken field *A* until it is at zero excitation, at which time the blocking rectifier prevents reversal. With this scheme the equipment will accelerate to empty core speed when a break or end occurs. This is desirable when a new roll is to be started but is undesirable when rethreading is necessary.

Figure 7b shows the equipment modified to obtain a speed limit feature on strip breaks. Motor field *B* is the main field and is adjusted by a motor-operated rheostat. Field *A* receives its excitation from the Rototrol. As the roll builds up, field *A* is strengthened gradually, and the voltage across relay *CR* increases until the relay picks up. The relay contacts energize the motor-operated rheostat in such a direction as to strengthen field *B*. Simultaneously the Rototrol will decrease the excitation of field *A* in accordance with the regulator requirement of constant current in the motor armature circuit. This action progresses until relay *CR* drops out and stops the motor-oper-

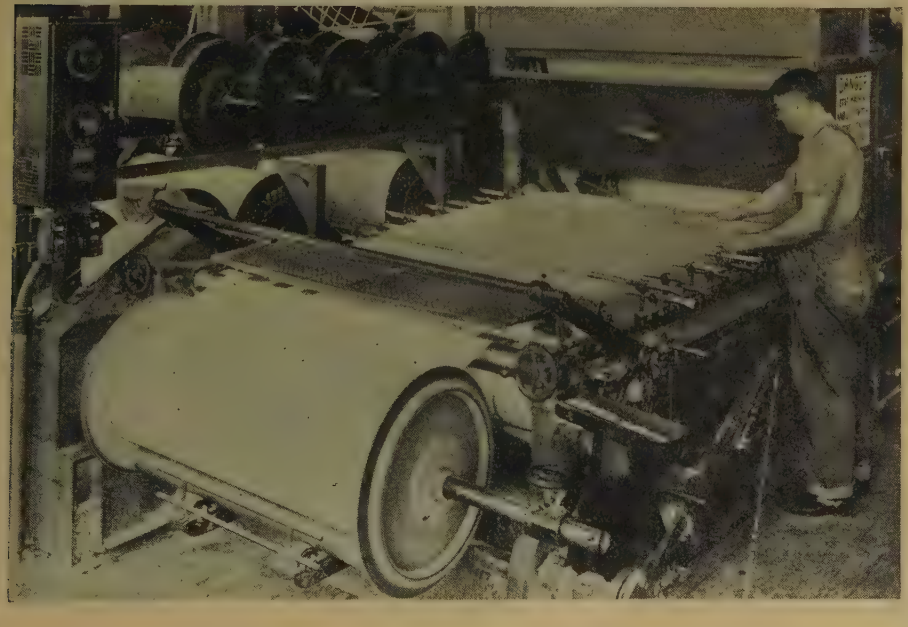


Figure 8. Core driven beam of a slasher in the textile industry using Rototrol control for speed and tension

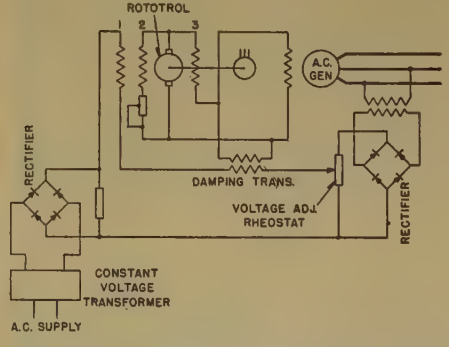


Figure 9. Schematic diagram of Rototrol voltage regulator applied to an a-c generator

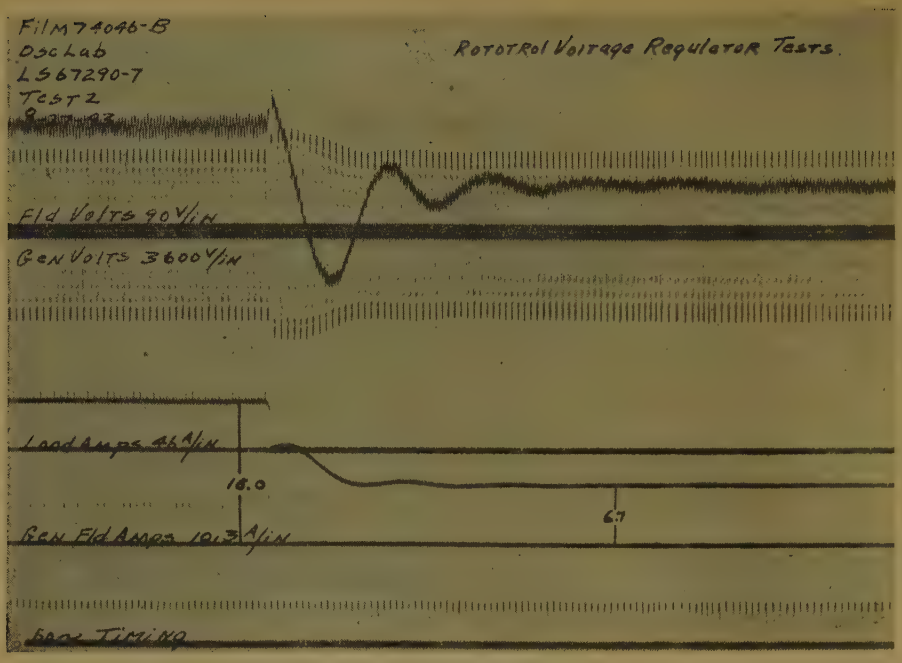


Figure 10. Oscillograph showing performance of Rototrol voltage regulator on release of 70 per cent power factor load on a-c generator

ated rheostat, and the cycle is restarted. A paper break under this condition will only speed the equipment up until field *A* is at zero excitation, as it cannot reverse because of the blocking rectifier. By proper relay selection this speed-up can be limited to between 10 and 20 per cent. Thus the roll is essentially at the proper speed, and rethreading is easily accomplished.

The strip tension is adjustable by means of a small manually operated rheostat located on the operator's panel. These adjustments may be observed readily on the motor ammeter which serves as a relative indication of tension and permits duplication of results to obtain the most satisfactory roll for any given weight and grade of material.

Essentially the same type of circuits are applied to unwind stands wherein the operation is reversed and the regenerative power fed back into the system.

Figure 8 illustrates the application of Rototrol tension control to the core driven beam of a slasher in the textile industry. Constant tension on the thread comprising the beam results in uniform beam diameter, a reduction in yarn breakage, and fewer stops for changes and adjustments, since more yardage can be wound on the beam. The more important advantages are increased efficiency in the subsequent weaving operation and improved quality of the finished cloth.

Voltage Regulation

A number of Rototrol exciters have been built for voltage regulation of a-c or d-c generators. Figure 9 illustrates the essential circuits of the regulator as applied to an a-c generator. The generator voltage is measured through a transformer and dry type rectifier and bucked against the rectified voltage of the constant voltage transformer. The difference controls the Rototrol excitation through field 1 to restore normal generator voltage. To obtain a high degree of stability, a damping transformer is used in the control field circuit. Where use of an a-c supply for the constant voltage transformer is not advisable, static "intersecting impedance" networks have been applied.[1]

To obtain high rates of response both parallel and series self-energizing fields are used. The circuit is tuned by adjustment of the resistor in field 2, so that fields 2 and 3 sustain the Rototrol output at any point on the straight portion of the saturation curve. This arrangement takes advantage of the almost instantaneous transient change in generator field current and provides extremely fast response of the Rototrol exciter.

Typical performance is shown by the oscillograph of Figure 10 which was taken during the sudden release of full load at 70 per cent power factor on a 150-kva 3-phase 60-cycle 2,400-volt generator controlled by a Rototrol voltage regulator. The voltage was returned to normal in 1/4 of a second with very little overswing. The oscillograph demonstrates excellent stability as well as very high speed of response of the Rototrol exciter.

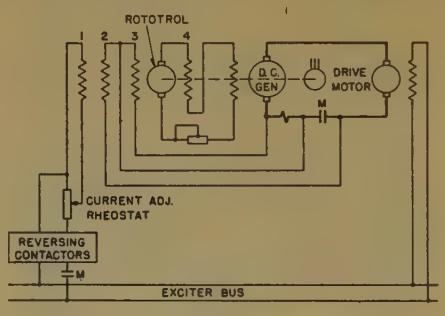


Figure 11 (above). Elementary diagram of Rototrol current regulator applied to a large tire testing machine



Figure 12. Tire testing machine using Rototrol acceleration control

Acceleration of High Inertia Loads

The Rototrol has been applied to many problems concerning acceleration and retardation of high inertia loads. For such problems it is desirable to accelerate at uniform torque from minimum to maximum speed, to reduce the current peaks and mechanical shock experienced with step type controllers, and to eliminate many of the relays and contactors associated with conventional magnetic control. The Rototrol is able to perform these various requirements with a surprising simplicity of the control circuits. Typical applications are bomb spinners, centrifugal casting machines, balancing machines, tire testing machines, and large mine hoists.

Figure 11 shows schematically the circuits of a Rototrol exciter as applied to a large tire testing machine drive. The machine consists of a flywheel which is accelerated to various speeds and then stopped by bringing the tire into contact with it. The huge flywheel has a WR^2 of 10,000,000 pound feet squared and requires an accelerating torque equivalent to 400 horsepower at 350 rpm to reach maximum speed in 30 minutes. The Rototrol is arranged to control the armature current and thus the torque of the separately excited drive motor. As the system gradually speeds up, the Rototrol increases the generator voltage to maintain uniform accelerating torque. The control is arranged to provide regenerative braking to standstill by simply reversing the pattern field 1 when such operation is necessary.

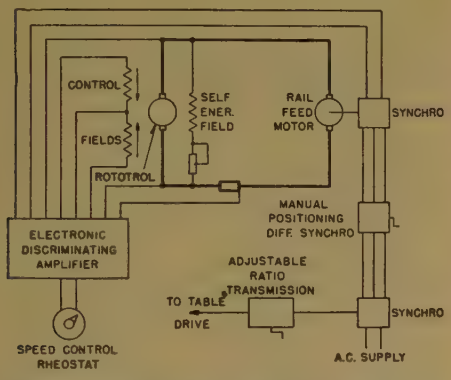


Figure 13. Simplified diagram of feed drive for large boring mill using a Rototrol in combination with an electronic discriminating amplifier

After the system is up to speed and the motor and generator disconnected, the generator voltage is matched automatically to the motor counterelectromotive force. This is desirable so that the circuits may be reclosed at any time for retardation or further acceleration. This function is accomplished by connecting Rototrol field 3 across the main circuit contactor M and de-energizing pattern field 1 when M is open. Any voltage difference will cause current to flow in field 3, which modifies the Rototrol and generator voltages to reduce the difference.

Helper Drive Torque Control

The circuit of Figure 11 with omission of field 3 has been used rather widely as a driving effort or torque regulator for helper drives operated in conjunction with a main drive. The system is applicable to either mechanically or electrically driven machines. Typical applications are the various auxiliary drives for the wet ends of paper machines and top roll drives for press rolls which are used in many industries. This arrangement assures constant helper motor torque over a wide speed range, regardless of speed variation of the main drive or changes in effective roll diameter due to change in nip pressure on soft rolls. Often a number of motors are served by a common generator. Here the total driving effort of the motors is determined by the Rototrol with the division of load secured by individual motor shunt field rheostats.

Speed Matching

Electronics often is used in combination with the Rototrol to solve difficult drive problems. An interesting application is the feed drive for a large vertical boring mill. The Rototrol is used with an electronic discriminating amplifier, and the circuits are arranged to provide either speed matching of the feed motion to the main table drive or straight speed control of the feed.

The elementary circuits are shown in Figure 14. For matching the speed of the feed screw motor to the speed of the table, small synchro units are driven from the feed screw motor and from the table drive. Angular displacement between the synchros will cause an error voltage which is fed into the electronic discriminating amplifier. The amplifier senses the direction of the error and changes the current through the Rototrol control fields to modify feed screw motor speed to reduce this angular difference. The system accurately matches the relative speeds of the feed and table over the complete range of table speed. Adjustment of relative speeds is obtained by the adjustable ratio transmission between the table and the synchro unit.

It is also desirable to operate the feed motor on straight speed control capable of adjustment over a wide range and with good speed regulation at all speeds. The discriminating amplifier is designed for this function and provided with a transfer switch to effect changeover. The motor counterelectromotive force is measured by means of armature current and voltage and balanced against a standard voltage in the discriminating amplifier. The difference controls the Rototrol excitation to maintain the proper motor speed.

This type of drive simplifies the mechanical parts of the machine by eliminating the many gear changes and the mechanical connection from the table to the feed screw on the rail. The large number of feed speeds, readily available, facilitates machine adjustment and results in increased production.

Conclusion

The large number of Rototrol applications have proved it to be an excellent and versatile regulator for industrial service. Operating experience has shown that it can be understood by nontechnical maintenance personnel, that its inherent reliability and stability assure trouble free operation with relatively little maintenance, and that it combines the necessary degrees of amplification and speed of response to meet the requirements of industrial problems. Existing applications cover a wide field, and the future holds considerable promise of broader utilization.

Reference

1. Static Voltage Regulator for Rototrol Exciter, E. L. Harder, C. E. Valentine. AIEE Transactions, volume 64, 1945, August section, pages 601–06.

Thermal-Demand-Meter Testing Techniques

E. E. LYNCH
MEMBER AIEE

M. E. DOUGLASS
NONMEMBER AIEE

THIS PAPER is written to encourage thinking and development on the subject of thermal-demand-meter testing procedures with specific reference to the development of shorter testing techniques. Conventional test methods in the past have involved relatively long periods of load holding to bring the meters under test to thermal equilibrium for the calibration check and adjustment. With the increasing use of thermal meters it is desirable to use some testing method which more nearly resembles tests on watt-hour meters. This paper outlines three general methods for shortening the test time and leaves to the reader the choice of the method, or modification of it, best suited to his requirements.

The principal problem in thermal-demand-meter testing is to determine the ultimate or final indication of the meter on constant load at thermal equilibrium. The response characteristic of the particular meter being tested will influence the available techniques for obtaining this information in short periods of time. This discussion is limited to meters having a simple logarithmic response, such as the meter shown in Figure 1, the characteristics of which have been covered in a previous article.[1] Appendix A gives an arbitrary definition and a mathematical description of this characteristic, and Appendix B demonstrates its importance in facilitating the establishment of a simple and sound short test method.

At the present time it is customary to return thermal demand meters to the laboratory for checking and calibration. The following or a similar step-by-step procedure usually is followed:

1. Connect meters in gangs, and apply potential to each for 2 to 24 hours.
2. Check the zero reading, and adjust if necessary.
3. Apply load to be checked, and hold constant for 45 minutes.
4. Check the meter indication against the load held, and adjust if necessary.

Paper 46-69, recommended by the AIEE committee on instruments and measurements and presented at the AIEE winter convention, New York, N. Y., January 21–25, 1946. Manuscript submitted November 23, 1945; made available for printing December 14, 1945.

E. E. Lynch and M. E. Douglass are with the General Electric Company, Lynn, Mass.

A short test method for checking thermal meters should be a distinct advantage to electric power companies, particularly as a means of checking the accuracy of these meters on the customers' premises in relatively short periods of time.

For a meter possessing the simple logarithmic response characteristic, mentioned previously, three general types of short test methods have been suggested and evaluated. Though other methods and modifications may be developed, particularly for meters having other than a simple logarithmic response, the three general types described herein provide an opportunity for large reductions in the testing time or man-hours for meters having this characteristic. The following terms have been coined to identify these three methods:

(*a*). "Two point method."
(*b*). "Double load method."
(*c*). "Thermal standard method."

The two point method is adaptable to testing on customers' premises. A graph or tabulation can be used to simplify the procedure. The double load method in one form is best adapted to testing single meters, whereas another form is more suitable for gang testing in the laboratory. The thermal standard method is usable on either gang or individual testing and is useful in its man-hour saving, although the elapsed time of test may not be shortened materially.

The Two Point Method

As the name denotes, the two point method involves obtaining sufficient readings of the meter indication at known intervals of time to predict the ultimate indication. The method is based on the solution of simultaneous equations, derived from equation 2 in Appendix A.

$$D = W(1 - e^{-kt})$$

where

D = instantaneous deflection
W = ultimate deflection
t = time
k = a constant
e = 2.72

An examination of this equation shows that there are two unknown quantities, namely k and W, when the quantities D and t are determined by simultaneous readings of the meter indicating pointer and a stop watch. Since there are two unknowns in the equation, two sets of values D and t must be determined to give two equations from which W and k can be found. To substitute the readings into the equation and perform the solution would be needlessly laborious for the meter tester, as the solution can be set up in the form of a graph. Two variations of the test are possible. In one, the pointer readings at two given times after constant test load application are used to indicate the ultimate reading. In the other, the time intervals that are required after constant load application for the meter to indicate two different scale points are used to compute the ultimate meter reading. Each of the two point methods is adapted to checking only one meter at a time, and is suitable for checking the calibration only, since at the end of the test period the meter reading still is increasing, and an adjustment under these conditions would be difficult at best. The methods have the advantage that the maximum demand pointer rather than the indicating pointer can be used for the check.

To describe briefly a step-by-step procedure to check a meter according to the first variation of the two point method, the following list is given:

1. Reverse potential with a load applied until indicating pointer reads zero.
2. Start stop watch and simultaneously apply a known load and hold constant.
3. At 3 minutes (or any other suitable time depending on the charts set up) after the load is applied, read the meter indication. Continue holding load.

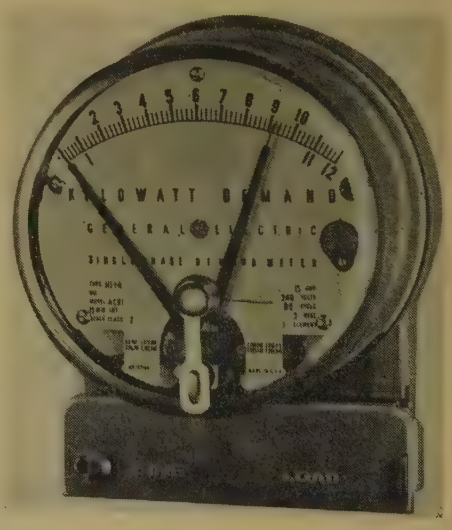


Figure 1. Thermal watt demand meter having a simple logarithmic response characteristic

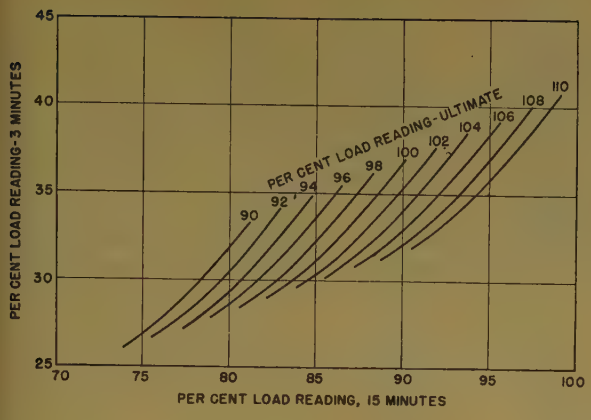


Figure 2. Chart to determine ultimate deflection when indication is read after a given time

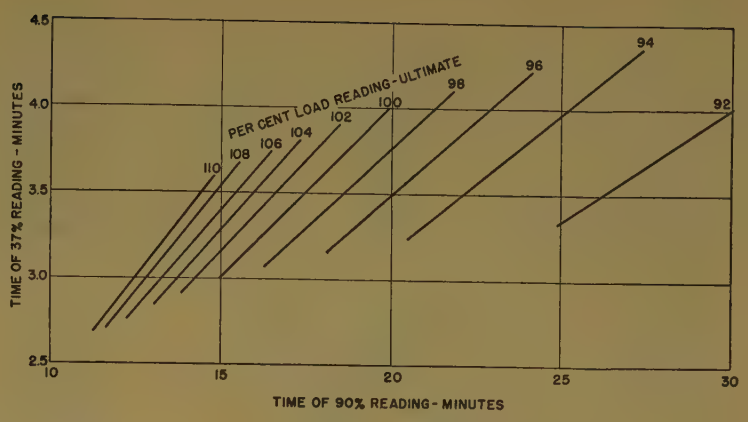


Figure 3. Chart to determine ultimate deflection when time is read for a given indication

4. At 15 minutes (or any other suitable time depending on the charts set up) after load is applied, read the meter indication.

5. Check the charts (Figure 2) to find the ultimate indication of the meter—compare this with what the ultimate indication should be from the load held.

The step-by-step procedure for using the second variation of the two point method is similar to the first, except that two stop watches are started simultaneously with the application of load in step 2, and one is stopped as the pointer reaches a predetermined point (37 per cent of the load applied); the other is stopped when the pointer reaches another predetermined point (90 per cent of the load applied). From the stop watch readings the ultimate deflection is determined from a chart (see Figure 3).

The Double Load Method

The double load method, as the name indicates, requires the application of double load to the meter under test for an interval of time, followed by a short period of holding the test load. Two variations in the general method are apparent: first, the double load may be held for a specified length of time; or second, the double load may be held until a definite indication on the meter is attained. An outline of step-by-step procedure for the first follows:

1. Reverse potential until meter reads zero indication. (Gang test meters will read zero at end of potential preheat.)
2. Apply double load for a specified time.
3. Cut load to test load, and hold constant for a specified time.
4. Read meter and compare it with the load value being held.
5. Make any adjustment necessary in the meter.

This procedure is adapted to gang testing of meters if desired, and the meter may be adjusted at the end of the test. The indicating pointer must be used during the test rather than the maximum demand pointer, as the indication at the end of the test may be lower than at the end of the double load period.

A step-by-step procedure for the second double load variation follows the first, except that the meter need not necessarily read zero at the start of the double load period, and the load should be reduced to the test load as soon as the meter reads the test load. Obviously this procedure is suitable for testing only one meter at a time. It does allow adjustment of the meter at the completion of the check.

The Thermal Standard Method

The thermal standard method requires the use of an accurately calibrated thermal meter of approximately the same response characteristics as the meter under test. Two variations of this method suggest themselves. The first is actually a combination of the double load and test standard methods. The second, which does not involve applying double load, conserves man-hours but does not reduce testing time appreciably.

Both variations of the thermal standard method are suitable for either single-meter or gang testing. Adjustments can be made on the meters at the conclusion of the test, since the test meters are at thermal equilibrium. The indicating pointer must be used rather than the maximum demand pointer, since load variation may cause a downward pointer movement during the test. The use of the accurately calibrated thermal meter as a standard eliminates the necessity for precise load holding, although reasonable limits must be maintained, so that differences in the response time of the test meter and the standard do not introduce errors.

The sequence of operations for the procedure using double load is as follows:

1. Reverse potential on test meter, and bring reading to zero.
2. Connect standard and test meter to same load.
3. Apply double load to both meters until the standard one indicates the value of the test load.
4. Drop to the test load and hold approximately correct load for a specified time.
5. Compare the reading of the standard meter under test.

The second procedure is simply to connect the accurate, standard meter and the meter under test to the same load and leave them for three or more demand intervals,[2] for example, 45 minutes for a meter used on 15-minute demand interval service. At the end of that time the deviation of the reading of the meter under test from the standard meter indicates the error of the meter under test.

In the descriptions of the various methods given, only a single point check of the meter has been considered. If the zero position of the indicating pointer is not correctly set on the scale zero, errors at points other than the one checked will be present. With a meter that does not overshoot on transient load, the following step-by-step procedure is suggested for checking the zero when desired:

1. Reverse potential, and apply load until indicating pointer reads zero.
2. Remove load, and reconnect potential.
3. With potential applied wait for one demand interval, and note the indication of the pointer. If no appreciable change has taken place, the meter is very close to correct zero. Any change that has taken place represents 90 per cent of the total deviation from zero at thermal equilibrium, and an adjustment can be made on this basis.

In connection with this brief description of some possible methods of shortening the test time a comparison of the accuracy of the various methods is given in Table I. The three test methods are listed across the top of the table, and the

Table I. Estimated Errors When Using Short Test Methods

Factors Influencing Errors	Two Point Method		Double Load Method		Thermal Standard Method	
	Indication at Given Time	Time for Given Indication	Held for a Definite Time	Held to a Definite Indication	Combined With Double Load	Thermal Standard Alone
1. Zero adjustment	No effect	No effect	No effect	No effect	No effect	No effect
2. Initial calibration	No effect	No effect	No effect	±5 per cent calibration error causes about ±0.5 per cent error in the ultimate indicated reading at end of one meter period	No effect	No effect
3. Time of response deviation	No effect	No effect	±1 minute deviation of response time from value for which test is devised gives about ±0.5 per cent ultimate indication error at end of one meter period	Insignificant effect	±1 minute deviation of response time from thermal standard causes about ∓0.5 per cent error in the ultimate indicated reading at end of one meter period	No effect if meter response times match*
4. Test timing	±seconds on 3-minute point gives about ∓2 per cent; ±5 seconds on 15-minute point gives about ±1/4 per cent	±5 seconds on 37 per cent point gives about ∓1 per cent; ±5 seconds on 90 per cent point gives about ±1/4 per cent (depends on calibration of meter)†	±20 seconds in time at which load is reduced to single value causes about ±0.2 per cent error	No reasonable variation in time of ultimate reading (±several minutes) will have any appreciable effect	No reasonable variation in time of ultimate reading (±several minutes) has any appreciable effect	No effect
5. Load holding accuracy	±1 per cent load error gives ±1 per cent error	±1 per cent load error gives ±1 per cent error	±1 per cent error in double load causes ±0.1 per cent error; ±1 per cent error in test load causes ±1 per cent error	Error in double load has no effect; ±1 per cent error in test load causes ±1 per cent error	No effect*	No effect*
6. Reading accuracy	±1 per cent on zero reading gives ±1 per cent error; ±1 per cent on 3-minute reading gives about ∓2 per cent error; ±1 per cent in 15-minute reading gives about ±2 per cent error	±1 per cent on the zero reading gives about ±1 per cent error; ±1 per cent on 37 per cent point gives about ∓1 per cent error; ±1 per cent on the 90 per cent point gives about ±1½ per cent error	±1 per cent in reading zero causes ±0.1 per cent error; ±1 per cent in reading ultimate causes ±1 per cent error	Error in reading zero does not produce any error; ±1 per cent in reading ultimate indication causes a ±1 per cent error	±1 per cent in reading zero causes about a ±0.1 per cent error or less. Reading error at the ultimate reading produces a corresponding error	Reading accuracies and calibration error of thermal standard are only errors of any appreciable magnitude in this method
7. Over-all accuracy (estimated)	±3 per cent	±2.5 per cent	±2 per cent	±2 per cent	±2 per cent	±2 per cent

* In the thermal standard methods load variation during the test will not produce any error in the ultimate deviation of test meter from thermal standard, provided that the response time of the two meters match. If response times are different on the test meter and the standard, load variations will cause indication differences. For reasonable load variations (±5 per cent) and reasonable response time differences (2 minutes) the errors in general from this source should be within ±½ per cent to ±1 per cent. †See Figure 3.

factors that contribute to errors are listed down the page on the left-hand side. At the bottom of the table are statistical estimates of the probable accuracies of each method of test. These are based on a combination of measured and estimated frequency distribution curves of the individual sources of errors involved and therefore represent only the order of magnitude of errors to be expected from these methods.

In the foregoing discussion of short test methods it has been assumed that the voltage has been applied to the meters for a sufficient length of time to produce complete change in the zero indication of the meter due to potential alone. In the case of periodic accuracy checks on customers' premises this undoubtedly would be the fact. In the case of gang testing in the shop time must be allowed for this item. In the methods where ultimate indication practically is reached, such as the double load or thermal standard methods, this potential preheating time may be overlapped with the time required to obtain final indication.

Conclusion

The purpose of this paper is to stimulate thought and experiment on short test methods and to indicate that such methods are possible. The procedures outlined are intended to show only the general steps in the various methods and are not to be considered detailed instructions for testing meters. Quite probably methods other than those suggested can be devised, and modifications and combinations of the methods discussed may be developed. Although it is possible that test methods can be found that will shorten materially the testing time of indirectly heated meters, nevertheless, this discussion has been limited entirely to testing meters with a simple logarithmic response characteristic that will not overshoot on transient load. This characteristic is realized on some thermal meters using direct (or internally) heated bimetallic spirals. Although actual test data are limited, nevertheless it indicates that short test methods are practicable when the greatest accuracy is not required.

Appendix A. The Meaning of a Simple Logarithmic Average

The simple logarithmic average is mentioned a number of times in the main portion of the paper. In this appendix an arbitrary definition of it will be given, and it will be expressed in mathematical symbols.

An understanding of the simple logarith-

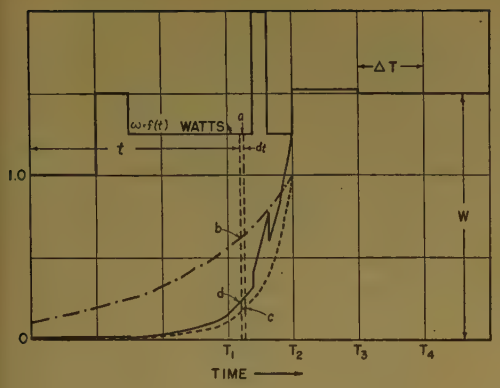


Figure 4 (left). Curve used to illustrate a definition of logarithmic average

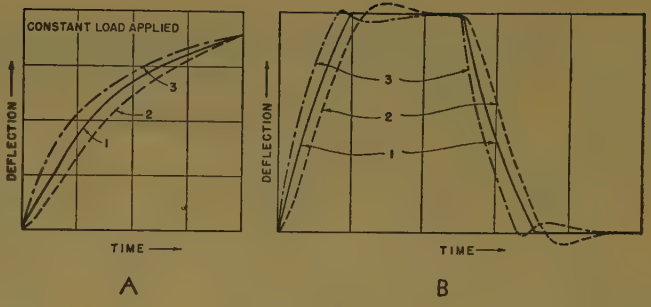


Figure 5 (right). Curves showing overshooting and dipping characteristics of typical thermal meters

mic average is obtained best by comparing it with the arithmetic average. In demand metering both averages are used, and each has been found satisfactory for assisting in obtaining information necessary for billing. In considering an average of watts such as curve a in Figure 4, the arithmetic average at time T_2 can be expressed by $1/(T_2-T_1)\times\left(\int_{T_1}^{T_2} w\,dt\right)$ where $w=f(t)$ and represents the watts and where T_1 and T_2 are the beginning and end of the time interval concerned. If the time interval is extremely short, T_2 nearly equals T_1, and the arithmetic average approximates the instantaneous value. If the time interval is extremely long, all past watt values are given equal importance. Because in many cases neither of these arithmetic averages gives exactly what is wanted for demand purposes, the average over a given period of time, such as 15 minutes, often is used. Most mechanical demand meters indicating this sort of average do not do so continuously but do their integrating continually over definite intervals, so that changed readings are available only at the end of definite time intervals. Thermal meters indicating a logarithmic average are expected to do so continuously.

The simple logarithmic average of the watts curve will be considered as the area under a weighted curve (d in Figure 4), which is made up of the product of all points a (on the watts curve) multiplied by corresponding points on a weighting curve c. The weighting curve follows the simple logarithmic form $e^{-k(T_2-t)}$ where T_2 is the time at which the average is expressed and t is the time at which the watts were a. Mathematically it is expressed:

The simple logarithmic average,

$$D=K_1\int_{-\infty}^{T_2}[f(t)]_1 e^{-k(T_2-t)}]dt$$

The proportionality factor K_1 is chosen such that for any constant load W the logarithmic average is numerically equal to the load W. It is therefore equal to the arithmetic average which is also W. That is,

$$D_{(\text{For constant load})}=K_1\int_{-\infty}^{T_2} We^{-k(T_2-t)}\times dt=W$$

This equation is satisfied only if $K_1=k$. Therefore

$$D=k\int_{-\infty}^{T_2}[f(t)][e^{-k(T_2-t)}]dt \qquad (1)$$

For constant load applied from zero indication this reduces to:

$$D_o=W(1-e^{-kt}) \qquad (2)$$

The choice of weighting curve determines the response characteristic of the meter, and for simple logarithmic weighting curves the value of k in the expression $e^{-k(T_2-t)}$ controls the relative effect of recent and remote loads. Figure 4 shows two weighting curves, curve c has k equal to 0.1535 corresponding to a 15-minute meter interval, while curve b has k equal to 0.0384 corresponding to a 60-minute meter interval.

The simple logarithmic average then is simply a value proportional to the arithmetic average of the weighted curve that is obtained when the watts curve is multiplied by a simple logarithmic weighting curve.

It has been shown previously[1] that, although the theoretical weighting curve of thermal watt demand meters is of the nature of a simple exponential curve, nevertheless the characteristics of many commercial meters differ appreciably from this ideal. However, it also has been shown that an internally heated bimetal type of meter as built does have this form of response, and it will be shown in Appendix B that such a meter will neither overshoot nor undershoot, nor will it have an indication dipping characteristic.

Appendix B. Why Simple Logarithmic Average Thermal Demand Meters Will Not Overshoot

In this paper it is disclosed that meters with certain response characteristics are well adapted to short testing methods. Meters having these characteristics measure a simple logarithmic average and, since they respond in this manner, they will neither overshoot nor dip. The proof of this will follow, but first it is necessary to understand what is meant by overshoot and dip.

Overshoot and Dip

If the pointer of a thermal meter is moving upscale owing to a relatively high load, and the load is reduced suddenly to a value close to the indication of the meter, a temporary dipping of the pointer below the instantaneous load is called dipping. If it continues temporarily to increase above the instantaneous load, it is said to overshoot. Neither condition is especially desirable when testing meters by a short method, but each characteristic can and does occur in some commercial thermal meters.

Proof That Simple Logarithmic Meters Will Not Overshoot

In order to prove that some meters cannot overshoot, a time will be taken (T_3 in Figure 4) at which the indication is a given value W. It then will be shown that, if a constant load W is held from this time on for some definite time interval (ΔT), the indication of the meter will not be changed. Since ΔT is chosen arbitrarily, it may be as long or as short as desired and even may be an an infinitesimally short time dt. Since the indication of the meter does not change for any of these conditions, it will have been proved that there is no tendency to overshoot, undershoot, or dip. The meter involved is assumed to measure a simple logarithmic average demand.

At the time T_3 the indication has arrived at a value W by any means whatever in its past history.

$$\text{Indication at } T_3=k\int_{-\infty}^{T_3}[f(t)]\times[e^{-k(T_3-t)}]dt=W \qquad (3)$$

At some later time (T_4) the indication is by definition:

$$\text{Indication at } T_4=k\int_{-\infty}^{T_4}[f(t)]\times[e^{-k(T_4-t)}]dt \qquad (4)$$

This indication (at T_4) can be separated into the integrals $\int_{-\infty}^{T_3}+\int_{T_3}^{T_4}$ as follows, since the load is constant from T_3 to T_4.

$$\text{Indication at } T_4=k\int_{-\infty}^{T_3}[f(t)]\times[e^{-k(T_3+\Delta T-t)}]dt+k\int_{T_3}^{T_4}We^{-k(T_4-t)}dt \qquad (5)$$

Since $e^{-k\Delta T}$ is a constant for a particular value of (ΔT) and since e^{-kT_4} is a constant for a particular value of T_4, they can be taken outside the first and second integrals respectively.

$$\text{Indication at } T_4=[e^{-k\Delta T}]\times\left[k\int_{-\infty}^{T_3}f(t)e^{-k(T_3-t)}dt\right]+[kWe^{-kT_4}]\left[\int_{T_3}^{T_4}e^{kt}dt\right] \qquad (6)$$

From equation 3 and a solution of the

Co-ordinated Electric Drive for a Rubber Calender Train

K. W. JOHN
MEMBER AIEE

G. W. KNAPP
ASSOCIATE AIEE

W. A. MOSTELLER
NONMEMBER AIEE

Synopsis: The continuous process of coating fabrics with rubber, such as is used in tire manufacturing, involves several individual machines that present operating problems not met successfully by mechanical drives. A new co-ordinated electric drive has been developed which does meet these requirements using amplidyne, and also electronic, control. It is expected that quality and production will be improved by this equipment. The means employed may be applied successfully to other industries.

IN THE MANUFACTURE of many rubber goods, textile fabrics are coated on both sides with rubber in a machine called a calender. Associated with the calender are auxiliary devices for handling the fabric before and after coating, making up a processing train.

Tire fabrics are one of the most important examples of this process in the rubber industry[1] and their production in a calender train, using a newly developed electric drive, will be discussed in this paper. The complete equipment now is installed in the Detroit, Mich., plant of the United States Rubber Company and parts of it are shown in Figures 1 and 2.

The calender itself, the train auxiliaries, and all of the electric equipment were manufactured from designs which were co-ordinated closely by the operating company, the machinery builders, and the electrical manufacturer. The importance of this procedure will be appreciated readily from the operating requirements.

Description of Process

A schematic diagram showing the mechanical arrangement of the processing train is shown in Figure 3.

Rolls of fabric are started at one of the entry letoffs. A maximum diameter of 42 inches can be accommodated. The fabric widths vary up to 60 inches.

The entry festoon forms a storage reserve of 80 feet of fabric so that the letoff can be stopped for changing rolls without shutting down the calender. The alternate letoff positions are provided to save time during this operation.

After drying, the fabric enters the calender rolls as shown. These rolls are 32 inches in diameter and 70 inches wide. Rubber from the top bank coats the upper side of the fabric, while that from the lower bank coats the under side.

The thickness or "gauge" of the rubber coating on either side of the fabric is determined by the opening between the rolls and also, to some extent, by the roll speed. Gauge is very important because a coating which is undersized produces an inferior tire and therefore must be rejected. On the other hand, if it is oversized, expensive rubber compound is being wasted.

While constant roll speed would have some favorable influence on gauge, there is another consideration for it which is even more important. To obtain maximum production, the calender rolls should run continuously at the maximum speed which certain processing limitations allow. This speed depends on the type of compound and fabric, and usually is established by considerations of plastic flow. If no means are provided for holding the calender speed at that maximum value, the average speed at the end of a day may be somewhat less. Even if this is only a small amount, a surprising amount of production can be lost.

The delivery festoon provides 64 feet of space for storing fabric when changing rolls at the windup. Finished rolls are wound on one of the fabric windups. The maximum diameter, as in the case of the letoff roll, is 42 inches. Alternate windup positions also are provided here. To keep layers of stock from sticking together, a separator or "liner" also is wound on the roll. This is supplied from a separate liner letoff for each fabric windup. Sometimes coated fabrics are run through the calender train a second time. For this purpose, liner windups also are provided at the entry letoffs.

Operating Requirements

The operating speed range of the train is from 7 to 70 yards per minute. A sepa-

Paper 46-56, recommended by the AIEE committee on industrial power applications for presentation at the AIEE winter convention, New York, N. Y., January 21–25, 1946. Manuscript submitted November 16, 1945; made available for printing December 5, 1945.

K. W. JOHN is an electrical engineer, United States Rubber Company, Detroit, Mich. G. W. KNAPP is in the industrial engineering division, General Electric Company, Schenectady, N. Y. W. A. MOSTELLER is in the engineering division, General Electric Company, Detroit.

---

second integral with respect to t:

$$\text{Indication at } T_4 = [e^{-k\Delta T}][W] + [kWe^{-kT_4}] \times \left[\frac{1}{k} e^{kt}\right]_{T_4}^{T_3}$$

$$= [e^{-k\Delta T}][W] + [We^{-kT_4}] \times [e^{kT_4} - e^{kT_3}]^{T_4}$$

$$= [e^{-k\Delta T}][W] + [W][1 - e^{-k(T_4 - T_3)}]$$

$$= We^{-k\Delta T} + W - We^{-k\Delta T} \quad (\text{since } T_4 - T_3 = \Delta T)$$

$$= W \qquad (7)$$

Thus the indication at T_4 is the same as that at T_3 (no matter what the time interval between T_3 and T_4), and therefore there has been no tendency to overshoot, undershoot, or dip.

Since the foregoing is based only on the indication of a meter whose response meets this definition of a simple logarithmic average, it is to be expected that some meters whose response differs from this average can overshoot or undershoot, or may have a tendency to dip. That this is true is shown in Figure 5, where A shows the response of three designs of commercial meters with different response characteristics when subjected to a constant load, starting from zero.

Figure 5B shows the response of these same meters when double load is applied until the pointers reach a given indication and then the load is changed to a constant load which ultimately will give this same indication. The loads are changed on the 3 meters at different times, since they arrive at the given indication at different times. All meters are correctly calibrated. The potential is reversed, and the meters run to zero. As each meter reaches zero its potential is returned to normal and its current reduced to zero. It can be seen that both meters 2 and 3 overshoot or undershoot considerably or have the characteristic of indication dipping.

When, therefore, it is desirable to eliminate overshooting or undershooting indication in order to save time during short tests or for any other reason, a meter whose response follows the simple logarithmic average should be chosen. It will neither overshoot nor undershoot, nor will it have the indication dipping characteristic.

References

1. THEORETICAL POSSIBILITIES IN AN INTERNALLY HEATED BIMETAL TYPE OF THERMAL WATT-DEMAND METER, E. E. Lynch. AIEE TRANSACTIONS, volume 61, 1942, October section, pages 764–70.

2. CODE FOR ELECTRICITY METERS. Edison Electric Institute.

rate threading speed of 7 yards per minute also is provided for running-in the fabric initially.

The calender itself should be able to operate over the speed range, independent of its train auxiliaries, for "warming up" operations when first starting. It also should be capable of reversing, with and without the central auxiliaries.

Jogging operation, forward or reverse, is required for all of the windups and let-offs. This is used either when starting or finishing up a roll that is not in train operation.

Emergency stopping is provided for the complete train from a number of control positions located throughout its length. This is an important requirement for the safety of operating personnel. There is a national code which specifies certain stopping performance that must be met.

In addition to the foregoing operating requirements, it is very desirable to maintain the tensions in the fabric, on either side of the calender, at constant values. These tensions are such that those before the calender exert a drag on it, while those after the calender are in the pull direction. The calender rolls, then, driven at constant speed, provide the necessary reactions for these tensions as a reference point. The benefits of constant tension to each part of the train have been tabulated at the bottom of Figure 3.

Past Practice, Mechanical Drive

In the past, calender trains have been driven by a single motor connected to the calender through a gear reducer. At some spot on the calender a mechanical takeoff was provided to drive a line shaft through gearing. The line shaft usually extended the length of the train and the auxiliaries were driven from it through right-angle gears, chain drives, and so forth.

Naturally, the electric drive with proper control equipment could be made to fulfill the operating requirements for the calender itself, but mechanically driven auxiliaries fall short of the mark.

To adjust tension, friction clutches and adjustable speed transmissions have been employed. These devices are not self-regulating and the operators must readjust them frequently. This is not practicable and, as a result, optimum adjustments seldom are obtained and production may suffer.

Furthermore, if good adjustments of tension have been made, there is no means for holding them there, nor can they be measured for future reproduction on other runs. There is another disadvantage in that maintenance is quite high on the friction clutches and the other mechanical component parts.

Electric Sectionalized Drive

With the electric drive, the entire train is sectionalized so that each auxiliary which ordinarily would have a mechanical drive is provided with its own motor. Co-ordinated control takes the place of the line shaft tie and, in addition, provides the proper tensions and speeds. Furthermore, once optimum adjustments have been established, the control holds them there. Electric instruments make it possible to take measurements and record the adjustments. Thus, if that same run is to be repeated in the future, the best operating conditions can be obtained very quickly.

The various pushbuttons and rheostat dials which are used for the adjustments are located remotely from the driven auxiliaries, in convenient groups. Each group consists of several interdependent and related adjustments, thus providing maximum convenience to the operator and also a more favorable opportunity to make correlated adjustments correctly.

Circuits

Power Circuits

The general arrangement of the power circuits for the various drives is shown in Figure 3.

The main drive for the calender is of the adjustable voltage (Ward-Leonard) type, providing ten to one speed range, of which five to one is by armature voltage control and two to one by motor field control.

The adjustable voltage scheme was selected because of the wide operating speed range and the advantage of being able to control the speed of the motor by adjusting its armature voltage. Furthermore, as has been pointed out by Cassidy and Mosteller,[1] the first cost is less.

The motor field range is used because at low operating speeds (below basic speed), substantially more than constant torque may be required by the calender.

The group of drives which is called the "central auxiliaries" always operates at the speed of the calender. They are not supplied, however, from the calender generator. This is done primarily for reasons of simplicity. For example, the auxiliary motors themselves are much smaller than the calender motor so that their IR drops are considerably higher. Thus, at one-tenth speed the terminal voltage that they require would be sub-

Figure 1. Calender and driving motor

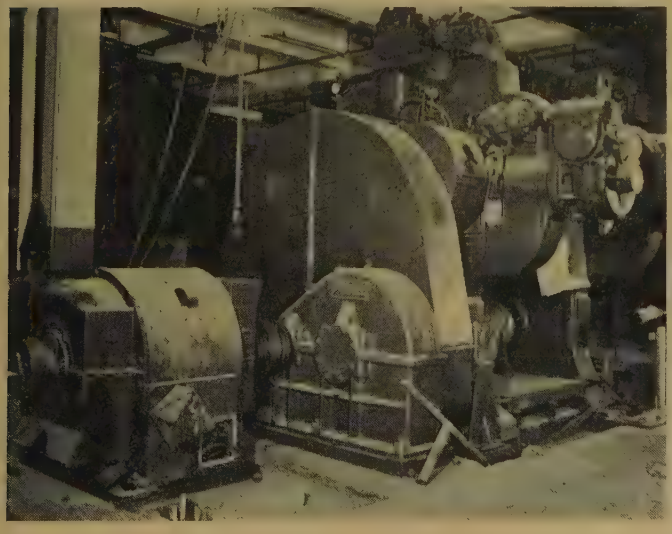
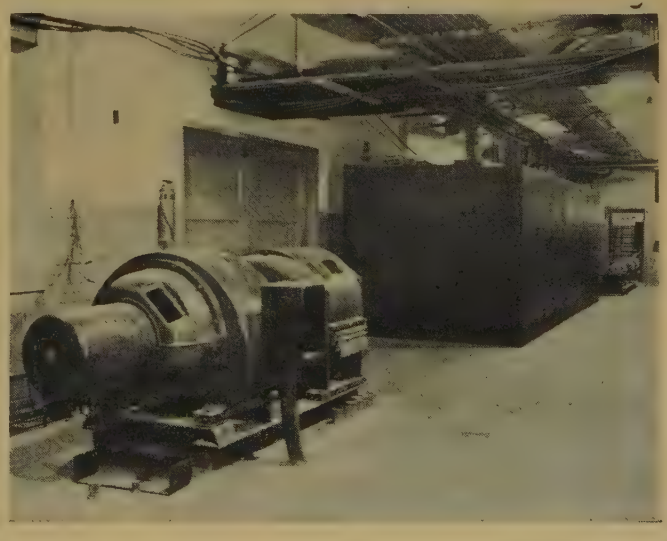


Figure 2. Calender motor-generator set and d-c control panels

One of the auxiliary motor-generator sets is in the background



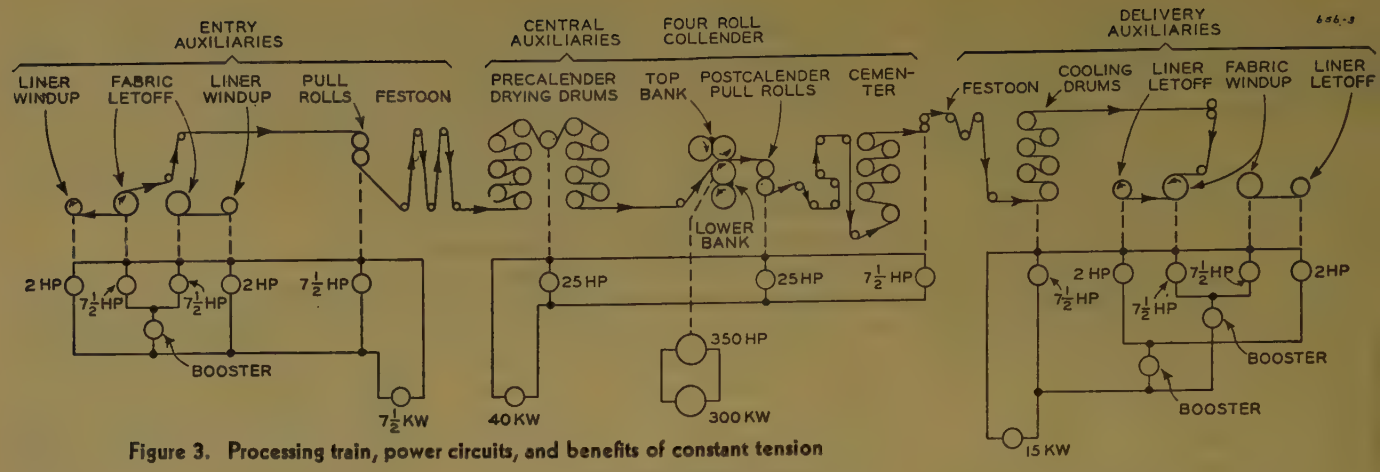


Figure 3. Processing train, power circuits, and benefits of constant tension

The Benefits of Constant Tension

Letoff	Drying Drums	Postcalender Pull Rolls	Cementer Pull Rolls	Windup
1. Compensation for elliptic or eccentric fabric rolls which produce tension variations that stretch fabric severely	1. Compensation for shrinkage or stretch 2. Elimination of loose wrinkles which would be cut by calender rolls	1. Compensation for shrinkage or stretch 2. Favorable influence on maintaining gauge	1. Compensation for shrinkage or stretch 2. Favorable influence on even distribution of cement	1. Elimination of loosely wound rolls which deform in storage 2. Elimination of tightly wound rolls where fabric sticks to liner in later operations

stantially more than what would be available from the main generator and a booster would have to be used to overcome this.

The power circuits for both the entry auxiliaries and the delivery auxiliaries are treated in the same manner. In either group the individual drives always operate together. They must be separated from the central auxiliaries and the calender because of the roll-changing requirements. They are stopped for roll changes while the calender is running, restarted, and then temporarily overspeeded to restore the amount of stock in the festoons to normal.

Calender Control

A simplified schematic diagram of the calender control circuit is shown in Figure 4. The electronic preamplifier makes use of vacuum tubes to provide excitation to the amplidyne that controls the generator field. This combination provides very accurate control of speed, preset speed, and what may be termed "timed acceleration."

So-called "timed acceleration" is simply a means for obtaining the kind of operation a motor-operated generator field rheostat furnishes but with more flexibility. It consists of a resistor–capacitor circuit in the electronic preamplifier arranged so that as the capacitor charges, the speed of the calender motor accelerates with it and as the capacitor discharges, the calender motor decelerates. The range of time provided is from 15 to 100 seconds and is readily adjustable by changing the amount of resistance. These time values represent total time from zero speed to the top speed of 70 yards per minute, or from the top speed down to zero speed. For speed changes of smaller value, such as threading speed to top speed, the time is proportionally less.

The timed acceleration circuit represents a very important operating feature in calender control as too rapid acceleration is quite undesirable. The auxiliaries associated with the calender train must follow whatever speed changes occur on

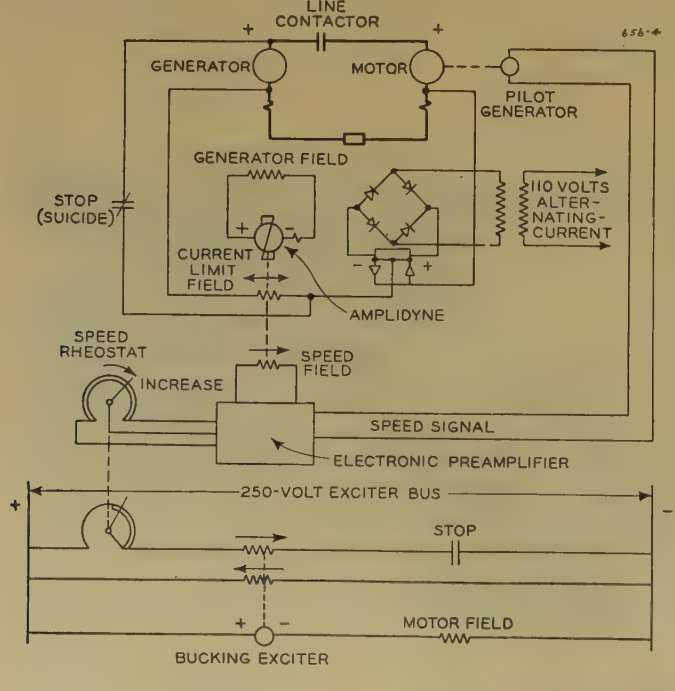


Figure 4 (left). Calender control circuit

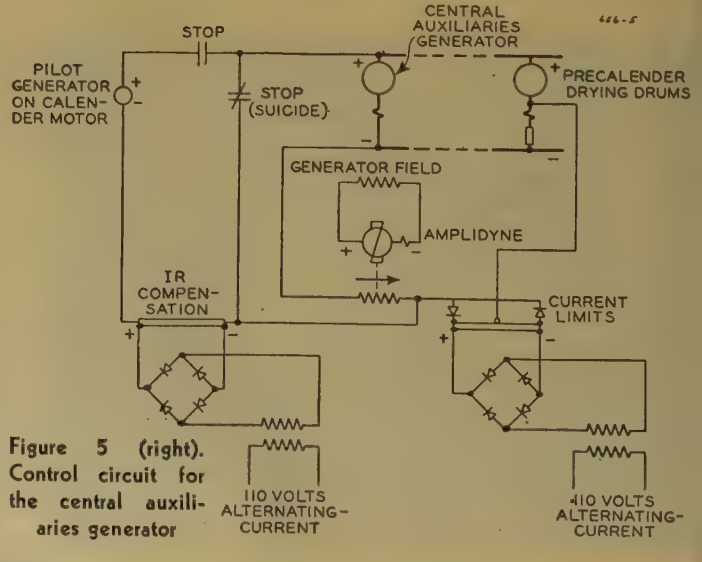


Figure 5 (right). Control circuit for the central auxiliaries generator

the calender itself. If these changes are rapid, excessive changes in tension are produced. Furthermore, the calender operators have no opportunity to adjust the calender roll screwdowns with rapid changes of speed to hold gauge.

In effect, this circuit provides an infinite number of speed points so that acceleration and deceleration are both very smooth.

The control also furnishes means for limiting both motoring and regenerative currents to values required either from the standpoint of performance or commutation. Under conditions of acceleration or normal deceleration, current limit is not necessary because of the timing circuit. It is provided only as a safety means. However, to meet the requirements of fast emergency stopping, regenerative current limit is an extremely important function.

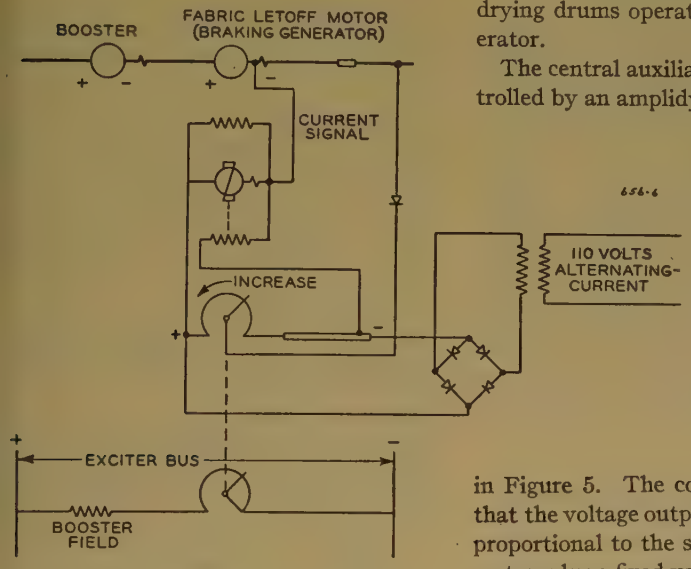


Figure 6. Control circuit for the fabric letoff motor and booster

When the stop button is pushed, the amplidyne exciting the generator is connected in a "suicide" circuit so that the generator voltage collapses rapidly. As the regenerative current from the motor to the generator reaches a value of approximately 200 per cent, the current limit circuit prevents the generator voltage from decaying at a rate faster than the decrease of the motor internal voltage with deceleration.

The regenerative current is held at the 200 per cent limit until the internal voltage of the motor, at about 5 per cent speed, no longer is able to overcome the *IR* drop of the armature loop circuit.

When stopping, full field is established in the motor as rapidly as possible. This is done to obtain maximum torque per ampere and a high rate of deceleration. The inductive lag of the motor field, which resists this change, is reduced materially by reversing the output of the bucking exciter and applying approximately twice normal voltage across the motor field.

Stopping performance is considerably better than that obtained by dynamic braking in conventional equipment operating from a constant potential d-c source. In contrast to a braking current of 200 per cent obtained by the amplidyne control with regenerative braking, the average current using dynamic braking is usually 30 or 40 per cent, with an initial peak of 200 per cent.

Control for Central Auxiliaries

In this group of auxiliaries, the motors on the post-tension rolls and the cementer pull rolls operate conventionally as motors, but the motor on the precalender drying drums operates as a braking generator.

The central auxiliaries generator is controlled by an amplidyne exciter, as shown in Figure 5. The control is arranged so that the voltage output of the generator is proportional to the speed of the calender motor, plus a fixed value for what we may call *IR* compensation. The speed-voltage component is established by taking a signal from the pilot generator on the calender motor. The motors on both the post-tension rolls and the cementer have substantially the same *IR* drop and the fixed voltage introduced for *IR* compensation is made equal to it. Hence, at any speed of the calender itself, the voltage available for these two motors will be very nearly equal to what they require for counterelectromotive force and full load current.

Each of the three motors has an amplidyne exciter. For the two machines which actually are motoring, the amplidyne control is arranged to hold constant armature current. Hence, at the voltage established by the speed of the fabric, constant current is equivalent to constant horsepower input to the motors. Neglecting their internal losses, this is substantially constant horsepower output, or constant torque at any given speed. As the friction torque required by these auxiliaries is low and does not change much, most of the motor output goes into tension, and this will be substantially constant.

As the speed of the fabric is changed, the voltage level is readjusted proportionately. The horsepower input to the motors therefore is changed accordingly, and with armature current unchanged, constant tension is maintained over the speed range.

The amplidyne control for the drying drums motor operates in a somewhat different manner. Since it is regenerating, its internal voltage not only must be sufficient to overcome its internal *IR* drop, but also the *IR* compensation voltage, which is a component of the generator voltage. This is done easily at top speeds where a very small increase in flux provides a large increase in internal voltage. However, at one-tenth speed, the flux must be increased substantially. The flux variation from top speed to bottom speed is about two to one.

For constant tension, it is necessary to hold a constant torque output from this machine at any speed within the operating range. Thus, as the flux is increased, the regenerative current must be reduced. The amplidyne control is arranged to do just that. At any particular speed, it maintains the current output constant. If the speed is increased, the current also is increased to compensate for the decrease of flux. The converse is true when the speed is decreased. At one-tenth speed, where the flux is twice the value at top speed, the control holds a current equal to only one-half the value established at top speed.

When the "stop" button is pushed, the amplidyne control of the generator is reconnected in a "suicide" circuit. Current limit control is provided, using a signal proportional to the armature current of the drying drums motor.

When stopping, there is no control over the regenerative currents from either the post-tension rolls motor or the cementer pull rolls motor, as they have lower inertias than the drying drums motor and can decelerate with it without difficulty.

Control for Entry Auxiliaries

The fabric letoff operates as a braking generator, with an amplidyne exciter holding constant current to obtain substantially constant drag tension on the fabric (Figure 6). The pull rolls motor provides the necessary reaction to overcome this tension and determines the speed at which the fabric is taken from the letoff. It is controlled by regulating the generator voltage in accordance with

the position of the bottom rolls of the festoon. The rolls adjust the air gap of a solenoid, which controls an amplidyne used to excite the generator. If the rolls drop from their normal position, the pull rolls motor is slowed down, and if they raise, the motor is speeded up.

The motor on the liner windup operates as a motor and is under constant tension control, with an amplidyne exciter regulating its armature current.

The influence of *IR* drop, particularly at the lower speeds, has a material influence on the circuit designs. If the fabric tension is increased by strengthening the regenerative current from the fabric letoff motor, the voltage level on all motors is increased because the tension reaction must come from the pull rolls machine. This makes it more difficult for the letoff motor to regenerate.

To overcome this, a booster generator is used in series with the armature of the letoff motor. The voltage from the booster is of such a magnitude and direction that it not only compensates for the internal *IR* drop of the letoff motor, but also the rise in generator voltage, when the stock tension is increased.

As the pull rolls motor and the liner windup motor both are supplied from the same generator, a booster on the windup motor is unnecessary. However, these machines must be designed so that their internal *IR* drops are the same.

Current limit control for acceleration and deceleration is employed, using a current signal from the armature circuit of the pull rolls motor.

When speed is changed in either direction, the tension being used between the letoff and pull rolls is sufficiently high so that only small changes occur. However, this is not the case for the liner windup and a circuit is used for inertia compensation. When accelerating, it increases the regulated value of current to supply an accelerating component, and conversely, decreases it under deceleration.

To replace the festoon storage after a shutdown to change rolls, the entry auxiliaries are overspeeded by a maximum of 20 per cent with respect to the speed at which the fabric is being taken away from the festoon. This is accomplished automatically by the solenoid control.

When a stop is to be made, the generator amplidyne is reconnected in a "suicide" circuit with current limit control from the pull rolls motor.

Instead of using regenerative braking, dynamic braking is used on both the fabric letoff and the liner windup. These motors have wide field control ranges. Thus, their inertias are determined by their base speed, or frame size. When operating at weak field speed, however, the torque is considerably less than full field would provide. Accordingly, if regenerative braking were used, at weak field, insufficient torque would be available.

In view of this, dynamic braking is employed. The circuit is arranged so that constant armature current is held over the field control range. Thus, when operating at weak field, as deceleration occurs and the motor slows down, the field is strengthened so that the internal voltage of the motor is kept at a constant value. Once base speed is attained, the dynamic braking current, of course, decays with speed.

Both the liner windup motor and the stock letoff motor are extremely difficult to stop and several times normal current must be used in the dynamic braking circuit.

Figure 7. Control board for the a-c accessory drives



Control for Delivery Auxiliaries

The delivery auxiliaries group is quite similar to the entry auxiliaries. The fabric windup, in this case, operates as a motor, with amplidyne control maintaining constant winding tension. The motor on the cooling drums provides the reaction to this winding tension and determines the speed at which fabric is taken from the festoon. As in the previous case, its speed is controlled by the position of the bottom rolls in the delivery festoon, using the same solenoid control scheme for generator voltage. If the rolls drop from their normal position, the cooling drums motor is speeded up; if the rolls raise, the motor is slowed down.

The motor on the liner letoff operates as a braking generator to hold a constant drag tension on the liner and is under amplidyne control.

For the delivery auxiliaries as well, the influence of *IR* drop affects the circuit design materially. As the fabric tension is increased, the voltage level is reduced to lower the torque output of the dry cans motor. As a matter of fact, at very high values of fabric tension, this machine actually must regenerate as there is insufficient festoon weight and friction load in the cooling drums to provide the tension.

The decrease in voltage level, however, makes it more difficult for the stock windup motor to obtain motoring current. A booster is used, therefore, with this machine. The voltage from the booster consists of a component to overcome the internal *IR* drop of the windup motor, and also an additional voltage equivalent to the reduction in generator voltage with increases in tension.

The liner letoff motor, which operates as a braking generator, is provided also with a booster which compensates for the *IR* drop of the letoff motor and changes in the voltage level.

For current limit control, when accelerating or decelerating, a signal is taken from the armature circuit of the dry cans motor. This control operates as it did for the entry auxiliaries, adjusting the gener-

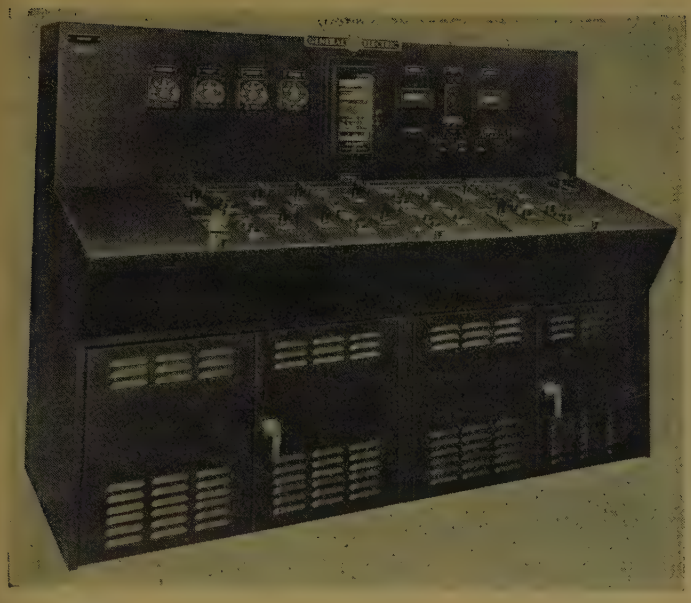


Figure 8. Main calender desk

ator voltage to hold either accelerating or decelerating current constant, as the case may be.

The fabric and liner tensions remain substantially constant when speed changes are made. However, in the case of the fabric windup, inertia compensation must be used, as explained previously for the liner windup on the entry auxiliaries.

Following the shutdown of the delivery auxiliaries for a roll change, the storage of fabric in the festoon must be removed. To do this, 20 per cent overspeed with respect to the speed at which fabric is being delivered to the festoon is available. The solenoid control does this automatically.

When a stop is to be made, the generator amplidyne is "suicided" and the current limit control from the cooling drums motor determines the rate of deceleration. Dynamic braking is used on both the fabric windup and the liner letoff for the same reasons that it was chosen for their counterparts in the entry group. Several times normal current must be used to stop these auxiliaries.

Co-ordination of A-C Accessory Drives

The driving motor of the large motor-generator set is a 450-horsepower unity power factor synchronous machine, supplied from a 2,300-volt source. A switchgear-type controller is furnished for this motor, suitably interlocked with the d-c control equipment in case of a loss of voltage, or an overcurrent indication.

There are also about 24 low voltage devices such as motors, solenoids, or valves, which operate from a 440-volt supply. These are controlled and interlocked with the d-c equipment. A load center type of control board, shown in Figure 7, is used.

The motors involved include those for ventilating fans in the cementer, cement pumps, calender lubricating pumps, water pumps for the cooling drums, feed conveyors for the rubber banks in the calender, and also the driving motors of the small motor-generator sets used for the train drive. Interlocking between these units and the d-c control is very important. For example, in case of a loss of lubrication, the calender must be shut down promptly. If ventilation is lost in the cementer, this also must be done.

Operation

To satisfy the operating requirements previously described, a substantial number of selector switches and pushbuttons is required. However, these are conveniently grouped in a main desk (Figure 8) located at the calender, an entry letoff desk, and a delivery windup desk. In addition, there is a small operator's panel located right next to the letoff and another at the windup. These contain the switches which are of immediate use to the operators when changing rolls. A considerable amount of precautionary interlocking is employed to avoid misoperation and mistakes on the part of the operators.

For normal running, once the calender train has been threaded, operation is actually simpler than with a conventional type of mechanical drive. The calender running speed, acceleration rate, and tensions are preadjusted, so that the operator only has to push a "Run" button and the entire train accelerates to the predetermined speed. This may be done only from one central point, the main desk.

On this desk also are located a recording and indicating tachometer calibrated in yards per minute, instruments for thickness gauge, and yardage counters which indicate the total yardage into and out of the train at the end of a day's operation. The master speed adjusting rheostat is also on this desk, but a speed limit rheostat which determines the maximum speed for any particular run is placed on the main control board so that it is accessible only to supervisors. Adjustment and indication of the current in both the drying drums motor and post-tension rolls motor are provided on the desk, so that the operator can control the precalender and postcalender tensions. Selector switches and pushbuttons for the roll screwdown motors and the necessary threading and jogging buttons are there as well.

The letoff and windup desks have the adjustments and instruments for the motors associated with them, as well as certain jogging and bypass buttons.

The entire train can be stopped from a number of places including several rope-operated safety switches. All stops are treated as emergency stops in order to bring the train down quickly, and give a constant check on stopping performance.

Changing Rolls at the Windup

When the operator observes from a yardage indicator on the windup desk that the fabric roll is nearly full, he places an operating switch in the "Change Rolls" position. This slows down all of the auxiliary drives associated with the delivery festoon to half speed. When the desired maximum roll diameter actually is reached, he moves the operating switch to the "Stop" position which quickly stops all of the delivery festoon auxiliaries. The calender in the meantime continues to run, filling the empty festoon.

As the delivery auxiliaries stop, a clamp roll, immediately above the windups, is set so that it holds the stock in place against the festoon weight when the operator cuts it. The cutting operation is done automatically by a "fly knife" which travels transversely across the stock.

After the cut has been made, the operator places a selector switch in position for the alternate windup. This windup previously had been operated by jogging so that a few turns of liner are wrapped around it from the liner letoff associated with it.

The operator then returns his operating switch to the "Change Rolls" position so that the alternate windup with the other delivery auxiliaries starts up. An air valve control device then actuates a small conveyor which transfers the leading end of the cut fabric from the first

windup to the one that now will be used. It puts it in such a position that it is caught automatically in the "bite" formed by the liner as it wraps around the roll.

After the stock has made several wraps around the roll with the liner, the operator puts his operating switch in the "Slack Takeup" position which automatically removes slack and establishes tension, with the delivery auxiliaries still operating at half speed. He then moves the operating switch to the "Normal" position and the delivery auxiliaries accelerate to a speed somewhat higher than that of the calender, depending upon how much storage must be removed from the festoon.

Changing Rolls at the Letoff

This operation is quite similar to that at the windup. The operating switch has the same positions. In the "Change Rolls" position the entry auxiliaries operate at half speed. In the "Stop" position a mechanical brake is set to hold the fabric against the weights of the festoon rolls when the fabric letoff no longer provides the necessary tension.

When the operator has spliced the trailing end of the stock going to the festoon to the leading end of the fabric from a new letoff roll, the "Slack Takeup" position automatically reverses the letoff and its associated liner windup to take up slack. This is very important because the splice is not strong and if slack were not eliminated, the resulting jerk at starting the entry auxiliaries might break the splice.

In the "Normal" position, the entry auxiliaries accelerate to some speed higher than that of the calender so that normal storage of fabric can be returned to the festoon.

Conclusion

It is expected that the automatic control, made possible by the use of individual electric drives, will result in a substantial improvement in the quality of the product. Regulated tensions should eliminate fabric that is stretched too much, or so slack that it wrinkles. This will reduce rejections and increase production.

The rubber industry deserves praise for pioneering this type of equipment and discarding the conventional. Processing techniques may benefit, not only in this industry but also in others, such as textiles, plastics, and photographic film where similar problems exist.

Reference

1. Continuous Processing for Automobile Tire Fabrics, G. E. Cassidy, W. A. Mosteller. AIEE Transactions, volume 58, 1939, May section, pages 218–23.

A New Crystal Channel Filter for Broad Band Carrier Systems

E. S. WILLIS
ASSOCIATE AIEE

Synopsis: A new crystal channel filter for use in broad band carrier telephone systems is described. It requires less than two-thirds as much mounting space as the earlier design and savings in materials and manufacturing effort are realized. These savings were made possible by assembling the four crystal units in one lattice-type filter section rather than two, resulting in a reduction in the number of component coils and capacitors.

CRYSTAL filters first were used commercially as channel selecting filters in a carrier system developed for use on cables.[1] Their use in that system permitted the placing of a large number of telephone channels close together in the frequency spectrum. The terminal equipment of the system was designed to provide a bank of 12 channels in a frequency band 48 kilocycles wide, suitable for any transmitting medium capable of providing this band width. Subsequent to its use on cable circuits, this 12-channel bank was applied to other new broad band carrier systems for use on open wire lines and on coaxial cables. The crystal filters used in this original bank were those described by C. E. Lane in 1938.[2]

As the demand for broad band carrier systems increased, a need developed for a channel filter which could be produced in relatively large quantities more economically than the original design. The type of design which seemed most promising was one which used a more compact configuration for the filter, thereby reducing the number of coils and capacitors required. However, this type of filter is critical of adjustment and the desired performance is realized only if the electrical characteristics of the component elements are maintained close to their theoretical values. This requires that the crystal units be adjusted precisely and that they retain their electrical characteristics accurately for variations in time and temperature.[3] As a step in this direction, the stability of performance of crystal units was improved by the development of the wire-supported mountings in place of the earlier clamp-type mountings, and the provision of hermetically sealed containers.[4] The use of this new type of crystal unit construction made it practical to provide the new filter design described in this paper. The four coils used in the old filter were replaced by two less expensive coils, and four of the capacitors were omitted in the new design. These changes and the resulting reduction in size made possible the saving of large quantities of materials and greatly reduced the required manufacturing effort.

A comparison of the size and internal appearance of this new filter (type 219) and the old filter (type 75) is shown in Figure 1. The new filter weighs less than half the old one and requires less than two-thirds as much mounting space. In order to utilize efficiently the size reduction of the filters they are assembled in a new design of terminal equipment. Figure 2 shows a typical office installation in which old and new type terminal equipments are mounted in adjacent bays. The 219-type filters appear in the equipment in the two bays on the right, whereas the 75-type are shown in the equipment on the left.

All 12 of these channel filters transmit the lower sidebands derived from the modulation of speech signals and carrier frequencies located 4 kilocycles apart in the range from 64 to 108 kilocycles. An insertion-loss frequency characteristic which applies to each of these filters is shown in Figure 3. This performance curve is very similar to that of the earlier channel filter, but the loss in the pass band is lower and the filter has sharper cutoffs than the earlier design.

Crystal filters usually are designed as lattice-type rather than ladder-type structures because of the greater flexibility afforded by the lattice design. For a lattice-type structure the functions for the propagation factor and characteristic impedance may be chosen independently as they involve only the quotient and product of the impedances or admittances of the series and diagonal branches.[5] The

Paper 46-26, recommended by the AIEE committee on communication for presentation at the AIEE winter convention, New York, N. Y., January 21–25, 1946. Manuscript submitted November 21, 1945; made available for printing December 1945.

E. S. Willis is with Bell Telephone Laboratories, Inc., New York, N. Y.

complexity of the branches of the lattice structure is dictated by the sharpness of the cutoff and the width of the pass band desired. The schematic circuit of the 219-type filter is shown in Figure 4. By relocating the shunt capacitances and series inductances as part of each lattice branch and replacing each crystal element by its equivalent network, an inductance and capacitance in series shunted by a second capacitance, the schematic of Figure 5 is obtained. The theoretical values of the elements shown in this schematic are derived from the following assumptions:

1. The location of the two cutoff frequencies.
2. The location of five frequencies of infinite attenuation.
3. The value of the impedance constant.
4. The coincidence between zeros and poles of the series and diagonal branches at the four critical frequencies occurring within the filter pass band.

Figure 6 shows the elements that comprise the filter. At the two ends are located the two air-core coils mounted in drawn copper cylinders. This coil is a duolateral type having a Q, that is, the ratio of reactance to effective resistance, of approximately 150 at the operating frequency. The same coil is used in each of the 12 filters. Because of the high coil impedance called for by the filter design, care is taken to make the parasitic capacitances between the windings and between the windings and the case as low as practicable. This is accomplished by winding the coil in four sections as shown in Figure 7. Such reduction in capacitances also results in improved stability of the coil and filter characteristics under service conditions.

Four resistances, two at each end of the filter, regulate the loss level in the pass band so that the band loss of each of the 12 filters is approximately the same. Fixed molded silvered mica and fixed and adjustable air capacitors are the remaining elements mounted on the upper side of the panel. The silvered mica capacitors and the two end adjustable air capacitors provide the shunt capacitances at the input and output of the lattice. The center adjustable capacitor is a differential air capacitor which, along with the two small fixed air capacitors, provides small capacitances across each of the four



Figure 2. The 219-type filters form a part of the 12-channel banks on the right, whereas the 75-type filters are utilized in those on the left

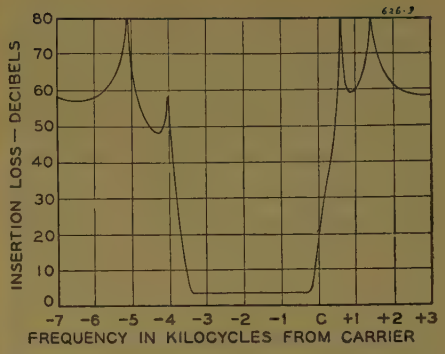


Figure 3. The insertion-loss frequency characteristics of the 12 filters are the same when plotted in cycles removed from the carrier frequencies

lattice branches. The four crystal plates, mounted in glass envelopes and assembled as a unit, form the basic structure of the lattice. Figure 8 shows one such group of four plates and illustrates how the 16 wires from the crystal units are connected to the terminals forming the four corners of the lattice. The main differences among the 12 channel filters are the differences in the dimensions of the crystal plates. The crystals are -18.5 degree X-cut longitudinal plates supported by fine wires located along their nodal lines. The mounting and fabrication of these crystal units has been covered very thoroughly in a recent paper by R. M. C. Greenidge.[6]

The length of a -18.5-degree plate in a quartz crystal unit is determined almost entirely by the frequency of resonance desired. The width and thickness are controlled mainly by the inductance. In addition to obtaining the desired resonant frequency and inductance it is essential that the strong secondary resonant frequency (this is an objectionable response) of each crystal unit be confined to a region that is not being used for the transmission of speech. There are such regions, each approximately 700 cycles wide, between the adjacent channel bands. The length, width, and thickness of the crystal plates then are determined discretely by the desired resonant frequency, inductance, and location of secondary response.

The equivalent inductances of the crystal units used in these 12 filters range in value from 38 henrys to 576 henrys. Even the four crystal units assembled in one filter cover a relatively wide range of inductance values. The ratio of the inductances of the two crystal units connected in parallel in the series branches o the lattice is five-to-one and in the diagonal branch crystal units is four-to-one. The crystal plates range in length from 1.66 inches for the lowest frequency unit

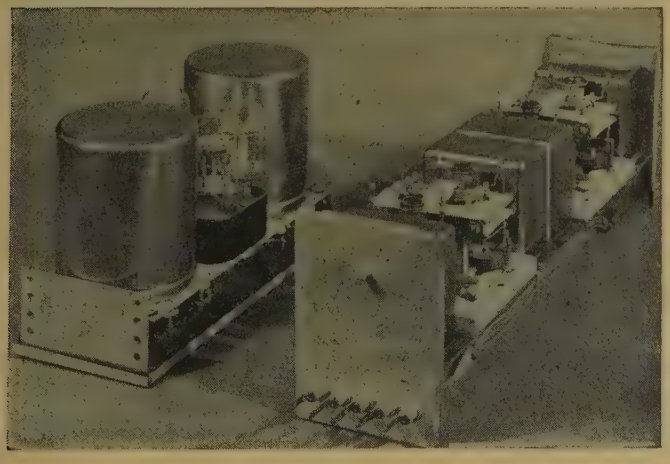


Figure 1. The 219-type filter requires less than two thirds of the mounting space and weighs less than half the 75-type filter

to 0.94 inch for the highest. The extremes in thickness are 0.019 and 0.085 inch. The ratios of the widths of the crystals to their lengths range from about one tenth to slightly less than one half. These crystal plates are narrower than the plates used in the earlier channel filters resulting in a saving in the amount of raw quartz required per system terminal.

The resonant frequency of the crystal unit is adjusted in an electric circuit to within seven to ten cycles of the desired frequency by grinding down the length of the plate. The inductance of the crystal unit is held to within three per cent of its nominal value by manufacturing tolerances on the fabrication of the plate. However, as shown later in the paper, this rather broad range of inductance values would permit a wide divergence in filter performance. In order to limit this range of performance the four crystal units used in any one filter are selected so as to have approximately equal departures in inductance from the nominal values. The magnitudes of their respective variations from a common percentage departure from nominal are plus or minus one half per cent for the two low inductance units and plus or minus one per cent for the two high inductance units.

In order to meet this close requirement on inductance grouping with the limited number of crystal units available, the inductances of a large percentage of the plates are adjusted in the manufacturing process. The inductances of all units are made to fall within one of two groups, each meeting the foregoing limits, one centered about the nominal value and the other two per cent above nominal. The inductance of a coated crystal plate may

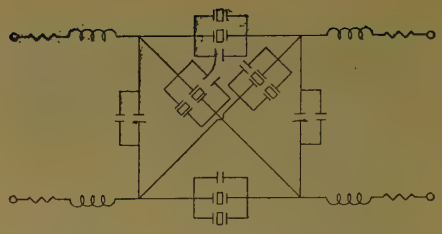


Figure 4. The schematic circuits of the 12 channel filters are the same

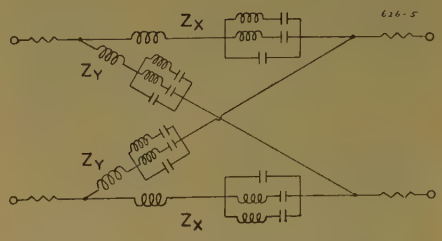


Figure 5. The schematic for design purposes has all of the elements within the lattice excepting the resistances which form a portion of the terminating impedances

be increased by isolating or effectively removing from the electric circuit a portion of the metallic coating. The procedure followed in the manufacture of the units is to divide the metallic coating on one surface of the plate by a transverse line located near one end of the plate thereby reducing the effective plated area by a small percentage. In manufacture this operation is done just prior to the assembly of the crystal plate in its cage.

These filters provide 50 to 60 decibels loss to all frequencies more than about 700 cycles from the edges of the pass band. To maintain this high loss in one lattice-type filter section necessitates a close impedance balance between the branches of the lattice. A plot of the reactance-frequency characteristics of the two branches of the lattice, Figure 9, helps to explain the transmission properties of the filter. Where the reactances Z_x and Z_y of the two branches are of opposite signs the filter is transmitting but where they are of like signs the filter attenuates. Figure 10 shows on an expanded scale the percentage difference between these two reactance curves in the attenuating region of the filter Where this difference is zero the attenuation is infinite, or, in other words, a peak of attenuation is located at this frequency. There are four peaks of attenuation located at finite frequencies as shown by the points at which this difference curve crosses zero and also a peak of attenuation located at infinite frequency where the two reactance curves meet.

To obtain discrimination of approximately 60 decibels and maintain it over the anticipated life of the filter requires precise adjustment of the filter elements and the stable performance of these elements in service. Certain elements have greater effect on filter performance than others and hence greater precision of adjustment and more stable performance is required of them. An examination of the function of each of the various elements in shaping the two reactance curves Z_x and Z_y will reveal the elements in which the greatest precision of adjustment is required. Any small change in an element which causes similar changes in the two reactance curves without changing their relation to each other will have very little effect on the attenuation curve. But, any change in an element which changes one reactance curve with respect to the other will alter the filter performance greatly. Thus changes in the elements which appear in the series branches and not in the diagonal branches or which appear in the diagonal branches and not in the series are the ones that cause relative movement of the two reactance

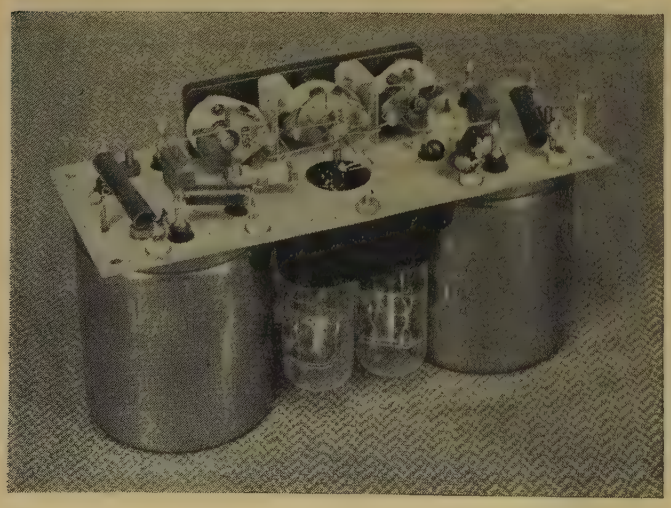


Figure 6. The elements are assembled on a panel in much the same position as they are shown in the filter schematic

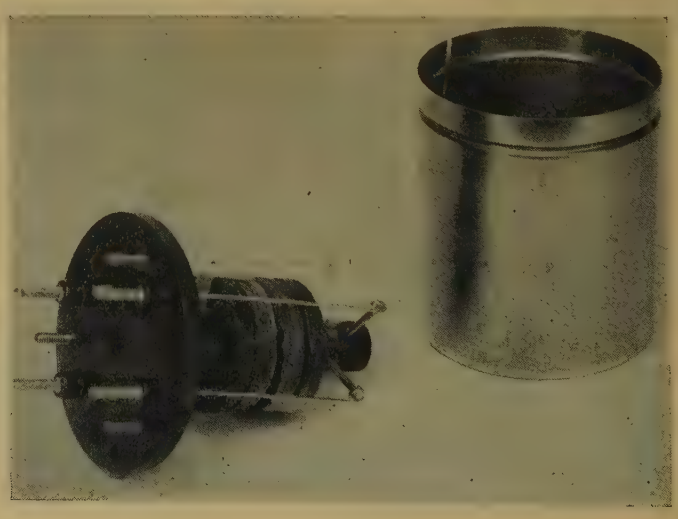


Figure 7. The coil winding is sectionalized to reduce the parasitic capacitances

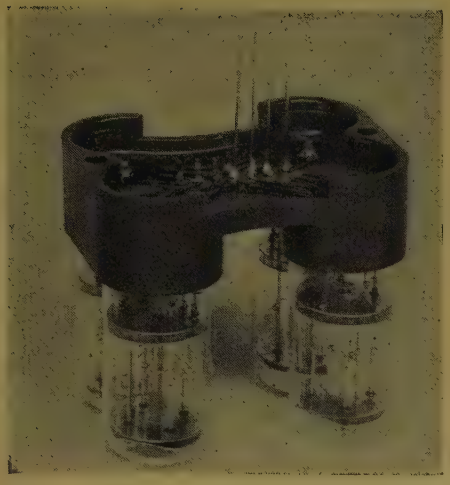


Figure 8. This crystal unit is a four-terminal lattice network comprised of four divided quartz plates and electrically providing two crystal elements in parallel in each branch of the lattice

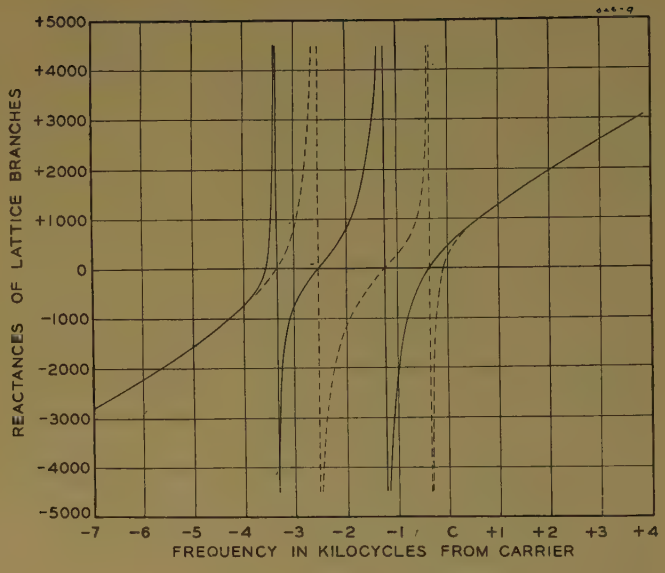


Figure 9. Where the reactances of the two branches of the lattice are of opposite signs the filter transmits and where they are of like signs the filter attenuates

curves. Hence it is the elements which appear within the lattice structure, that is, the four crystal units and the lattice of capacitances consisting of the differential air and fixed air capacitors, that require precise adjustment and stable performance.

In order to obtain uniform performance in the filters it is necessary to hold the resonant frequency and inductance of the crystal units within very narrow limits. For example, the solid curve of Figure 11 illustrates a normal transmission loss characteristic in which the elements are all at their nominal values. The two dotted curves illustrate the characteristics that result when the inductance values of the crystal units in either the series or diagonal branches depart from their nominal value by about one per cent. A negative departure in one pair of branches results in about the same effect in performance as a positive departure in the other pair. The two curves shown assume positive and negative departures for the inductances of one pair of branches. The selection and grouping of crystal units assembled in any one filter in relation to their inductance departures from nominal, as discussed earlier in this paper, restricts the variations in filter performance.

Departures of about ten cycles per second in the resonant frequencies of the crystal units of either series or diagonal branches will produce variations in discrimination of about the same type and magnitude as those illustrated in Figure 11 for departures in inductance. However, if all crystal units exhibit equal frequency departures, the entire transmission characteristic will be shifted by the frequency departure of the crystal units, and there will be little change in discrimination. For a 20-degree Fahrenheit change in temperature this frequency shift is approximately 0.03 per cent of the operating frequency.

The lattice of capacitances is balanced in the final adjustment of the filter by the tuning of the differential air capacitor. This adjustment moves one reactance curve with respect to the other to locate one of their crossings, and thus one peak frequency, at 600 cycles above the carrier frequency.

In the foregoing discussion the effect of dissipation in the elements forming the filter has been neglected. As there is some dissipation associated with each coil, capacitor, and crystal unit, the effect of each in turn will be considered. The dissipation associated with the coils may be considered as part of the terminating impedances and variation in this dissipation raises or lowers the loss level in the band of the filter without affecting the discrimination. Dissipation in the shunt capacitors at the input and output of the lattice produces similar effects on the filter. When these effects become too large, causing the loss in the pass band to fall outside the specified limit, the resistances at either end of the filter are changed in value to compensate for the change in dissipation.

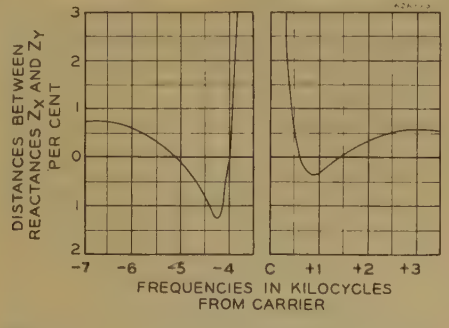


Figure 10. The two reactance curves cross at four frequencies which determine the location of the four attenuation peaks

The elements forming the branches of the lattice, that is, the crystal units and the capacitor lattice introduce very little dissipation. However, since unbalances in the dissipation associated with the lattice branches of the filter will degrade the filter performance to the same extent as reactance unbalances in these branches, extreme care must be exercised to keep the dissipation among these branches balanced. Instead of referring to the reactances of the branches of the lattice, Z_x and Z_y, it is more convenient in the following discussion to refer to their reciprocals, the susceptances B_x and B_y. Dissipation associated with these susceptances is expressed in terms of the conductances, G_x and G_y. To obtain a peak of attenuation in a lattice-type filter it is necessary to have a conductance balance as well as a susceptance balance of the series and diagonal branches of the lattice. Equal conductances across the series and diagonal branches of the lattice have the same effect as equal conductances across the input and output of the lattice. That is, they have the effect of raising the loss in the pass band of the filter slightly. However, an unbalance between the conductances of the series and diagonal branches of the lattice upsets the bridge balance at the filter peak frequencies. The effect of a slight unbalance is a reduction in the magnitude of the peak losses of the filter. As this unbalance is increased the filter peaks may disappear entirely even though there is a susceptance balance at the peak frequencies. This is illustrated by the curves in Figure 12. The solid line represents a normal transmission-loss characteristic of the 219AM filter, with carrier fre-

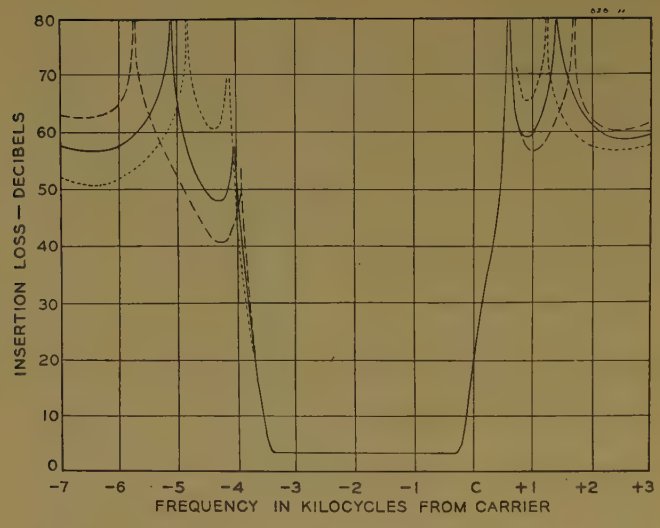


Figure 11. Precise cutting and adjustment of crystal units are required to obtain uniform filter performance

The foregoing effects were produced by inductance departures of one per cent from nominal of crystal units in either pair of lattice branches

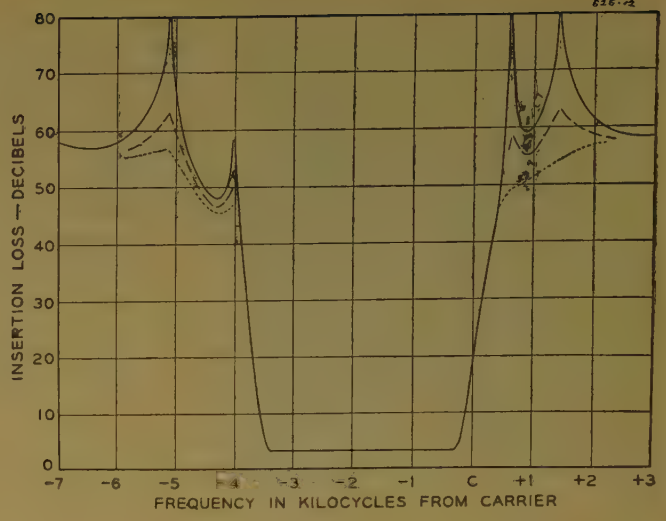


Figure 12. To obtain high peak loss in a lattice-type filter the conductances and susceptances of the series and diagonal branches must be equal

The effects of differences of 0.010 and 0.030 micromho conductance in these branches are shown, respectively, by the dashed and dotted curves

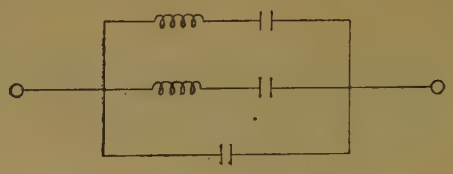


Figure 13. This two-terminal network is connected across the paralleled end of the filters to improve the transmission over the two end channels of the group of 12

quency at 108 kilocycles, in which there is a perfect balance of both the conductance and susceptance at the peak frequencies. The dashed and dotted lines show the effect of 0.010 and 0.030 micromho conductance unbalance, respectively. Greater amounts of conductance unbalance are required to produce these same effects in the lower frequency filters in inverse ratio to the square of the operating frequencies.

Even though the crystal plates are surrounded by dry air and enclosed in sealed glass containers it is still necessary to protect the filter against atmospheric conditions of high relative humidity. The dashed curve of Figure 12 shows the effect of 0.010 micromho conductance unbalance of the lattice. This unbalance is equivalent to 100 megohms insulation resistance. With clean parts and a relatively dry atmosphere insulation resistance many times as high as this can be maintained across the branches of the lattice. However, a trace of salt or other contamination across the terminals in the molded base of the crystal unit or across the ceramic in the air capacitors will make the insulation resistance highly sensitive to the moisture in the adjacent air. To guard against this condition of low insulation resistance, the following precautions are taken:

1. Where insulating materials are required within the lattice structure only homogeneous low-loss materials are used.

2. The insulating parts assembled in the filters are kept clean.

3. The filters are adjusted, tested, and sealed hermetically when surrounded by an atmosphere in which the relative humidity is not greater than 40 per cent.

In the construction of the filter the elements are mounted on the panel and wired as shown in Figure 6. This panel assembly with cover and end brackets attached is inserted in an adjusting shield through which the three capacitor adjustments are made. The resonant frequencies looking in either end of the filter are located where they should occur theoretically, by the adjustment of the two end air capacitors. The other adjustable air capacitor is used to locate a peak of attenuation at 600 cycles above the carrier frequency.

The function of the channel filters in service is to select the modulated electrical impulses from 12 subscribers' sets and combine them for transmission over the line, and at the receiving terminal to separate the various electrical impulses for transmission to the 12 subscribers' sets. Thus, in operation the 12 filters are paralleled on one end. Over the pass band frequencies of any one of the 12 filters the impedance paralleling this filter should be high so that by far the greater portion of the energy in this frequency range passes through the filter and is not dissipated in the paralleling filters. With the 12 filters connected in parallel this condition is satisfied over all channel bands excepting the two end channels. Good transmission is obtained over all channels by connecting a two terminal network, the schematic of which is shown in Figure 13, across the paralleled end of the filters.

The 219-type "Crystal Channel Filter" is the first commercial application of lattice-type filter circuits in which more than one crystal unit is used in each branch of the lattice. The use of this circuit reduces the number of component elements required in each filter and results in a saving in mounting space required. As these filters constitute a large portion of the broad band carrier terminal equipment this development has contributed to a considerable saving in office space. The labor required for producing these filters has been reduced by a third in comparison with that required for the earlier design. Also, substantial savings in the use of tin, nickel, molybdenum, brass, and raw quartz are realized.

References

1. Cable Carrier Telephone Terminals, R. W. Chestnut, L. M. Ilgenfritz, A. Kenner. AIEE Transactions, volume 57, 1938, May section, pages 237–44.

2. Crystal Channel Filters for the Cable Carrier System, C. E. Lane. AIEE Transactions, volume 57, 1938, May section, pages 245–9.

3. Effects of Manufacturing Deviations on Crystal Units for Filters, A. R. D'heedene. *Bell System Technical Journal*, volume 23, July 1944, page 260.

4. The Mounting and Fabrication of Plated-Quartz Crystal Units, R. M. C. Greenidge. *Bell System Technical Journal*, volume 23, July 1944, page 234.

5. Electromechanical Transducers and Wave Filters (book), W. P. Mason. D. Van Nostrand Company, New York, N. Y., 1942.

6. See reference 4.

Die Cast Rotor Testing by Test Stator Method

P. H. TRICKEY
MEMBER AIEE

FOR some years now, it has been a common practice to die cast the squirrel cages of induction motor rotors. The die cast rotor has many advantages of simplicity, ruggedness, and durability as well as low cost. One feature of die castings is the tendency for all castings to have a perfect outside surface even though the interior may contain voids, blow holes, or porosity. This feature is an advantage when the appearance of the die cast article is of primary importance. However, in an electric rotor, it is a disadvantage as no visual inspection methods will disclose a faulty interior which may affect the electrical performance.

Since the conductivity of the best electrical materials such as copper and aluminum are affected by small amounts of impurities, there is always the possibility of low conductivity being introduced at some stage between ingot and final cast rotor. This defect also cannot be detected by visual inspection.

It is necessary, therefore, to have some means other than inspection for testing die cast rotors. Of course, one way of testing such rotors is to build them into complete motors and make thorough tests on the motors. Obviously, this has the great disadvantage of performing many expensive and time consuming operations before it is known that a rotor is defective. Sometimes also other variations in the completed motor make it very difficult to lay positively the cause of poor performance to the die cast rotor.

There are, of course, an infinite number of ways in which a rotor can be defective such as wrong laminations, core stack, skew, and shaft hole, but in general, if the resistance is correct, all other defects can be caught by inspection and gauging. Once in a great while open bars may get by a resistance test but except for rare cases a measurement of the average rotor resistance can be used to select the satisfactory rotors.

There are two common methods of measuring the effective secondary or rotor resistance of a squirrel-cage motor. One method obtains the rotor resistance from readings of slip and secondary copper loss. This has certain definite usefulness for polyphase motors, but has the disadvantage of requiring the rotor to be finished completely and tested in a motor with bearings. The other method involves a measurement of the impedance of the motor with rotor held stationary. From this impedance, the rotor resistance is separated by calculation from the stator resistance and reactance. By taking full advantage of the locked impedance method which requires no rotation, bearings, or line up variations, a very satisfactory method of testing die cast rotors may be devised.

Paper 46-64, recommended by the AIEE committee on electric machinery and technical program for presentation at the AIEE winter convention, New York, N. Y., January 21–25, 1946. Manuscript submitted August 25, 1945; made available for printing December 11, 1945.

P. H. TRICKEY is chief engineer, Diehl Manufacturing Company, Finderne, N. J.

Test Stator for Testing Die Cast Rotors

It would be possible to use a normal stator and, without end covers or bearings, make an impedance test for rotor resistance of a die cast rotor. Special care would have to be taken in testing, as the stator being designed for normal operation at full speed would draw heavy currents and get very hot with rotor standing still. The rotor also would get hot. Correction of resistance measurements for temperature would be subject to error as the temperature not only would be high, but also changing rapidly.

To overcome these and other difficulties, stators for testing die cast rotors are made of special construction and proportions.

1. The stator slots are made much larger than normal, to give 8 to 10 times the normal winding area. This in itself reduces the stator temperature and the amount of primary resistance to be subtracted from the total resistance. It gives a stator much larger in diameter than normal, but the additional size and cost do no harm for a test device.

2. The number of effective turns are usually much greater than the normal stator to give about half the normal flux densities. This keeps the iron loss of the large stator down, and reduces the effect of saturation.

3. Since under locked impedance conditions the phases operate independently, only one phase is necessary for the stator winding.

4. The inside diameter usually is made slightly larger than normal, just big enough to admit rotor cores as they come from die casting before the outside diameter is turned to final size. If the stator has open or partially open slots and the mould allows aluminum to flow over the unfinished surface, it may be necessary to remove this excess aluminum to obtain accurate readings. If it is desired to test soldered or brazed copper or brass rotors in such a stator, it may be necessary to trim off the excess solder or brazing material in order to get the rotor into the stator. Otherwise, the air gap may have to be increased too much and errors are introduced.

5. In general, the width or stack of the test stator is made as narrow as the shortest rotor likely to be tested in quantity, and used for all rotors of that diameter. There is very little error introduced when the rotor is longer than the stator, but if the rotor is shorter, new calibration curves may have to be made because of the change in air gap area.

6. Stators usually are mounted vertically and the windings given thick protective coatings to minimize the damage of rotors continually striking against the stators during insertion. In spite of all precautions, the windings ultimately become short circuited or the laminations badly worn and hammered together at the air gap. If production testing is to be continuous and shutdowns for repair avoided, it is well to have spare stators available for immediate replacement. If it is expected that the windings of individual stators will vary in resistance, it may be desirable to add a rheostat to the circuit which may be adjusted as each new stator is installed thus keeping the same value of total resistance in the primary circuit and eliminating the necessity of new calibration curves for each new stator.

7. In general a single phase concentric winding is used with the turns distributed sinusoidally. A typical core lamination is shown in Figure 7.

Testing Circuit

The equivalent circuit of each phase of an induction motor under locked rotor condition is as shown in Figure 1. For

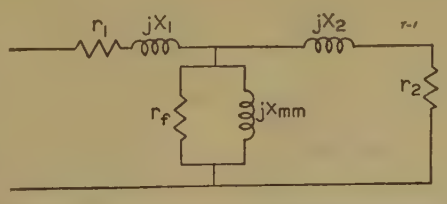


Figure 1. Equivalent circuit of induction motor with rotor locked

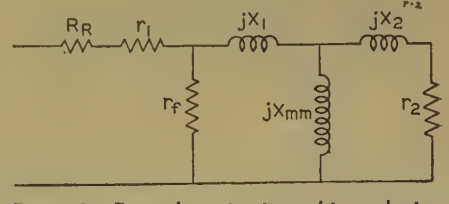


Figure 2. Equivalent circuit used in analyzing tests of die cast rotors

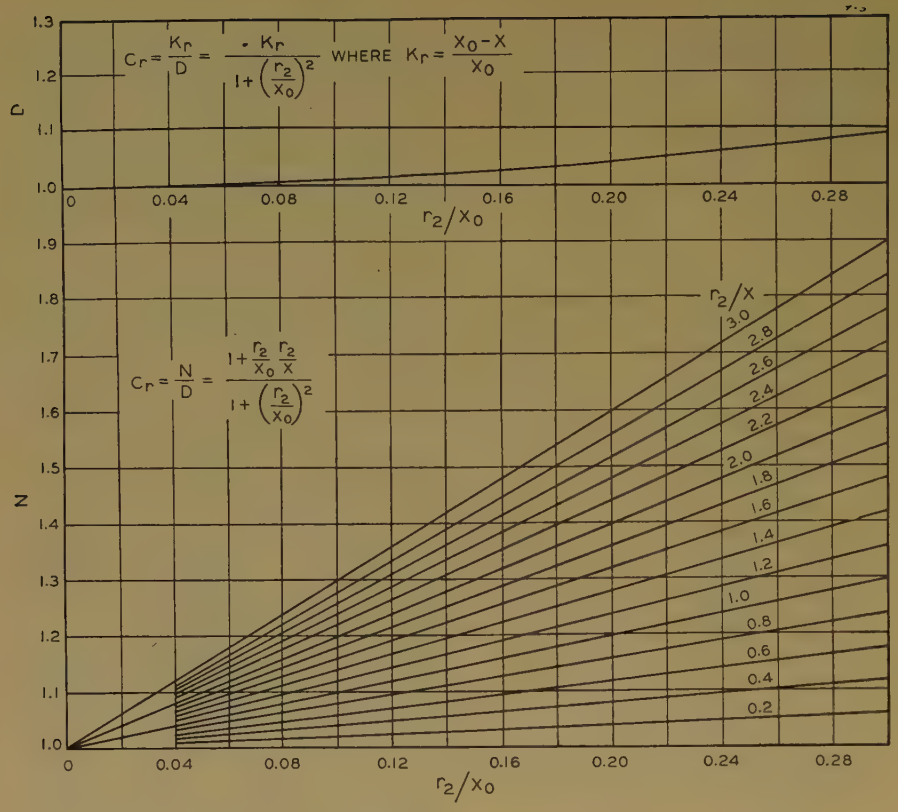


Figure 3 (left). Locked rotor impedance

Single-phase and polyphase induction motors

the purpose of rotor testing, it is satisfactory to assume the iron loss branch to be in shunt across the input as shown in Figure 2. The impedance of the network beyond the iron loss branch has been shown by C. G. Veinott to be:

$$Z_L = R_L + jX_L = (r_1 + r_2 C_r) + jXC_R$$

where

X = ideal short-circuit reactance

$$= x_1 + x_2 \frac{X_{mm}}{x_2 + X_{mm}}$$

$$C_r = \frac{X_{mm}^2}{(x_2 + X_{mm})^2 + r_2^2}$$

$$C_R = \frac{1 + \{(x_1 + X_{mm})/X\}\{r_2/(x_2 + X_{mm})\}^2}{1 + \{r_2/(x_2 + X_{mm})\}^2}$$

r_1 = primary resistance
r_2 = secondary resistance referred to primary
x_1 = primary leakage reactance
x_2 = secondary leakage reactance referred to primary
X_{mm} = mutual or magnetizing reactance

For the purpose of rotor testing, it is satisfactory to assume primary and secondary leakage reactances to be equal. With this assumption the correction factors become

$$C_r = \frac{K_r}{1 + (r_2/X_o)^2}$$

and

$$C_R = \frac{1 + (r_2/X)(r_2/X_o)}{1 + (r_2/X_o)^2}$$

I	2.5	2.5
r_2	10	50
r_2/X_0	0.0388	0.194
r_2/X	0.252	1.26
D (FIG. 3)	1.001	1.04
N (FIG. 3)	1.013	1.245
$C_R = N/D$	1.011	1.197
$X_L = X C_R$	40.2	47.5
$C_r = K_r/D$	0.845	0.815
$r_2 C_r$	8.45	40.7
r_1	2.10	2.10
R_R	0.10	0.10
$R_L = r_1 + R_R + r_2 C_r$	10.65	42.9
$Z_L = \sqrt{R_L^2 + X_L^2}$	41.5	64
$E = I Z_L$	103.9	160
IRON LOSS	7.1	16.9
$I^2 R_L$	66.5	268
WATTS INPUT = IRON LOSS + $I^2 R_L$	73.6	284.9

Figure 4. Calculation sheet for die cast rotor calibration curves

where

$X_o = X_{mm} + x_1 = X_{mm} + x_2$ = ideal short-circuit reactance

$$K_r = \left\{\frac{X_{mm}}{X_{mm} + x_1}\right\}^2 = \left\{\frac{X_{mm}}{X_{mm} + x_2}\right\}^2 = \left\{\frac{X_{mm}}{X_o}\right\}^2 = \frac{X_o - X}{X_o}$$

Figure 3 is sometimes a convenient aid in using these formulas.

Referring to Figure 2, if it is assumed that the current in the iron branch has negligible effect on the magnitude of the total line current, the following expressions may be used:

$E = IZ_L$ where $Z_L = \sqrt{R_L^2 + X_L^2}$, $X_L = XC_R$

and

$R_L = R_R + r_1 + r_2 C_r$ (R_R = rheostat resistance)
Watts input = $I^2 R_L$ + iron loss

A convenient calculation form is shown in Figure 4. It is customary to calculate a complete curve of watts versus r_2 and to use this curve in setting test limits for production test. Such a curve is shown in Figure 5.

Determination of Circuit Constants

In order to use the form shown in Figure 4, it is necessary to know the circuit constants r_1, X, X_o, and the iron loss.

r_1 can be measured easily by resistance bridge.

X can be obtained from a locked rotor reading using a typical rotor, preferably of low resistance. It is usually necessary to have tests with finished and unfinished rotors so that rotors can be tested later under either condition. Usually the same values of test constants can be used re-

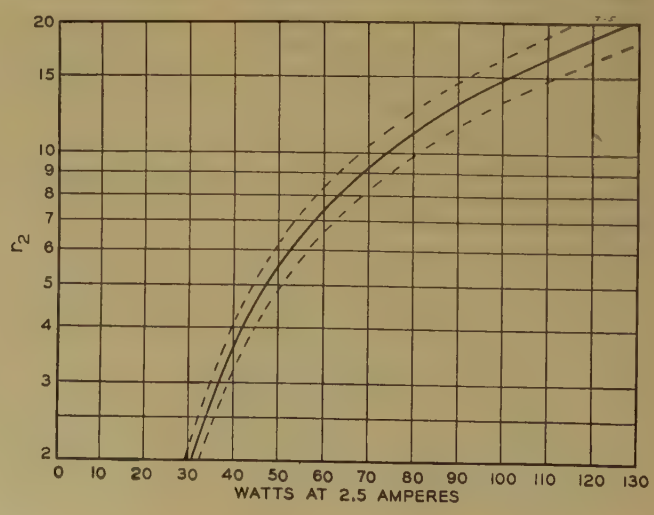


Figure 5. Typical calibration curve for test stator

Dotted curves indicate upper and lower watt limits

1	NO LOAD (DUMMY ROTOR) VOLTS	84
2	NO LOAD (DUMMY ROTOR) AMPS I_0	0.469
3	NO LOAD (DUMMY ROTOR) WATTS	5.458
4	PRIMARY RESISTANCE AFTER NO LOAD READING	2.08
5	$I_0^2 r_1 = (2)^2 (4)$	0.458
6	IRON LOSS = (3) − (5)	5.00
7	$X_0 = Z_0 = E/I_0 = (1)/(2)$	179
8	LOCKED ROTOR VOLTS	84
9	LOCKED ROTOR AMPERES	2.5
10	LOCKED ROTOR WATTS	63.5
11	IRON LOSS	5.0
12	NET WATTS	58.5
13	R = TOTAL EFFECTIVE RESISTANCE = $(12)/(9)^2$	9.35
14	PRIMARY RESISTANCE AFTER LOCKED READING	2.10
15	P = (13) − (14)	7.25
16	$Z_L = (8)/(9)$	33.6
17	$Q = \sqrt{(16)^2 - (13)^2}$	32.2
18	$X_0 - Q = (7) - (17)$	146.8
19	r_1 = PRIMARY RESISTANCE COLD (@ 25°C)	2.08
20	$r_2 = (15)\ (7)/(18)$	8.76
21	$r_2/X_0 = (20)/(7)$	0.049
22	$1+(r_2/X_0)^2 = 1+(21)^2$	1.024
23	$Q[1+(r_2/X_0)^2] = (17) \times (22)$	32.3
24	$r_2\ r_2/X_0 = (20) \times (21)$	0.43
25	X = (23) − (24)	31.9

Figure 6. Calculation sheet used for determining circuit constants

gardless of core stack, but it is well to try different stacks just to be sure. For the purpose of analyzing the locked rotor tests, we can assume the equivalent circuit of Figure 2. The locked impedance of the network beyond the iron loss branch has been shown to be

$Z_L = [r_1 + P] + jQ$
where $P = r_2 C_r$ and $Q = XC_R$

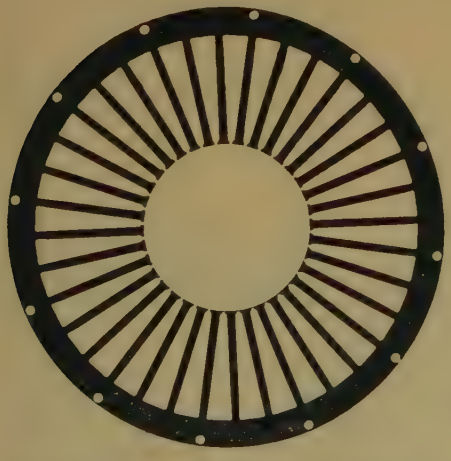
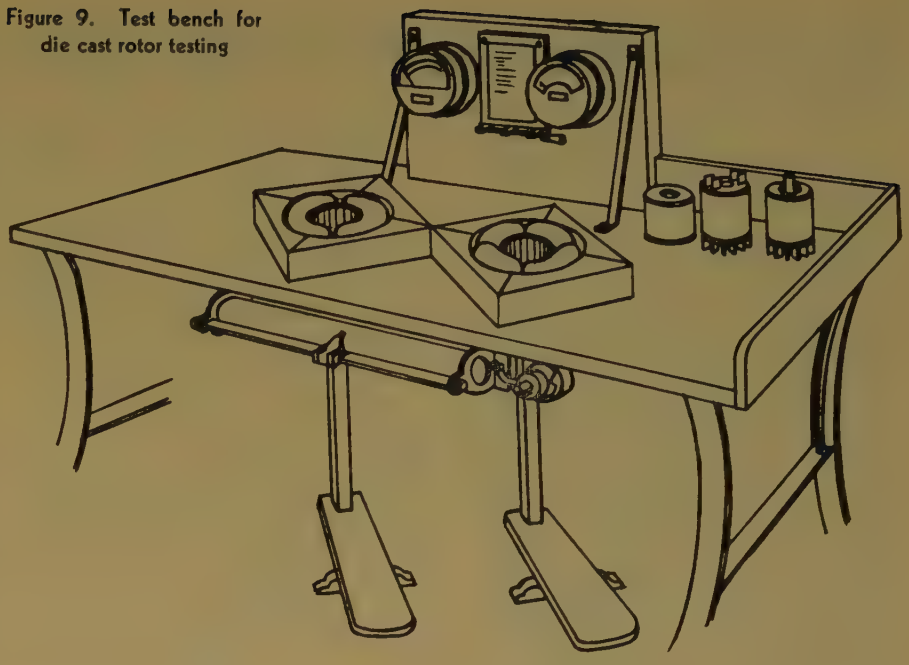


Figure 7. Typical test stator lamination for die cast rotor test

Figure 9. Test bench for die cast rotor testing



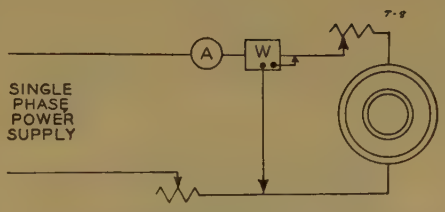


Figure 8. Wiring diagram for die cast rotor test circuit

Assuming that the current in the iron loss branch has a negligible effect on the magnitude of the total line current, we find

$Z_L = E/I_L$, $R_L = [\text{watts input} - \text{iron loss}]/I_L^2$

$P = R_L - r_1$ and $Q = \sqrt{Z_L^2 - R_L^2}$

Mr. Veinott has shown that

$$r_2 = \frac{PX_o}{X_o - Q}$$

where

$X_o = X_{mm} + x_1 =$ ideal open circuit reactance

He also has shown that

$$Q = XC_R = X\frac{1+(r_2/X)(r_2/X_o)}{1+(r_2/X_o)^2}$$

Transposing and solving for X

$$X[1+(r_2/X)(r_2/X_o)] = Q[1+(r_2/X_o)^2]$$
$$X + r_2(r_2/X_o) = Q[1+(r_2/X_o)^2]$$
$$X = Q[1+(r_2/X_o)^2] - r_2(r_2/X_o)$$

X_o and the iron loss for this type of test stator can be obtained from input readings using a rotor similar to a typical rotor except with no squirrel cage at all.

Under this condition, it can be assumed that

$X_o = Z_o = E/I_o$

and that the

Iron loss = input − copper loss

In this case also, it is usually desirable to have tests with both finished and unfinished rotor diameters. It is desirable to take the dummy rotor tests over a fairly wide range of voltages to be sure to cover any case of high or low rotor resistance in later tests. A convenient form for analyzing these tests is shown in Figure 6.

References

1. Segregation of Losses in Single-Phase Induction Motors, **C. G. Veinott.** AIEE Transactions, volume 54, 1935, pages 1032–6.

2. Discussion by **P. H. Trickey** and author's closure of Segregation of Losses in Single-Phase Induction Motors, **C. G. Veinott.**

3. Single-Phase Induction Motors, **W. J. Branson.** AIEE Transactions, volume 21, 1912, pages 1749–87.

4. Starting Windings for Single-Phase Induction Motors, **C. G. Veinott.** AIEE Transactions, volume 63, 1944, pages 288–94.

5. Induction Motor Resistance Ring Width, **P. H. Trickey.** AIEE Transactions, volume 55, 1936, pages 144–50.

New Series Capacitor Protective Device

R. E. MARBURY
MEMBER AIEE

J. B. OWENS
ASSOCIATE AIEE

Synopsis: A series capacitor is best protected from overvoltage during fault by a gap having low arc drop with no tendency to cut off. In this manner the capacitor is not subjected to repetitive voltage peaks during fault, and high current oscillations in the circuit formed by the capacitor and gap are minimized. A special design of graphite gap with self-centering arc characteristics is described. A new type of by-pass switch is also described for automatically by-passing the gap and series capacitor and removing the by-pass after the fault has cleared. The switch shown provides an inherent time delay on closing thus allowing time for the capacitor to discharge through the gap and avoid damage to the switch contacts. The switch also provides time delay on reopening thus eliminating the necessity for a holding means which has been a problem always with magnetic contactors in this application. The motive power for closing the switch is derived from a sealed bellows using high resistance metal and containing a volatile liquid. The passage of current through the bellows changes the vapor pressure and furnishes the forces required to operate the switch. A device of this type is not subject to damage by steep wave front surges associated with the discharge of the capacitor through the protective gap, nor is it damaged by intermittent line faults. The combination of this gap and switch has many advantages over a conventional gap and magnetic contactor and should permit a more general application of series capacitors to distribution circuits.

Paper 46-45, recommended by the AIEE committee on protective devices for presentation at the AIEE winter convention, New York, N. Y., January 21–25, 1946. Manuscript submitted October 29, 1945; made available for printing December 13, 1945.

R. E. Marbury and J. B. Owens, Westinghouse Electric Corporation, East Pittsburgh, Pa.

A CAPACITOR connected in series with an electric circuit improves its voltage regulation by inserting a negative reactance which in effect cancels all or part of the inductive reactance of the circuit. Such a capacitor is called a "series capacitor." A series capacitor installation consists of a bank of capacitors connected in series with each phase of a transmission or distribution line, each bank having the reactance necessary to cancel the desired portion of the phase reactance and designed to handle the maximum continuous and momentary line currents.

Capacitors may be subjected for brief periods to twice their rated voltage without damage to the dielectric; therefore, series capacitors may be allowed to handle momentary currents which are twice their continuous current rating. However, in most circuits to which series capacitors are applied the currents which flow during fault conditions are considerably more than twice the maximum working current. For this reason it is necessary either to use capacitors with a continuous current rating equal to one half the maximum current which may flow during a fault or to use a voltage limiting device.

For a given reactance the cost of capacitors increases approximately as the square of the rated voltage so that usually it is much more economical to use capacitors whose rating is based on the working current and limit the voltage which can appear across their terminals by means of auxiliary apparatus.

Protective Gaps

The device used to protect a series capacitor during fault conditions must not allow the capacitor voltage to rise above twice the rated value even for a short time. Thus, it must function to by-pass the capacitor during the first half cycle of fault current. A gap is the only device which meets this requirement effectively.

The fundamental protected series capacitor circuit consists of a series capacitor shunted with a gap. If, however, this is a metallic gap which has a high arc volt

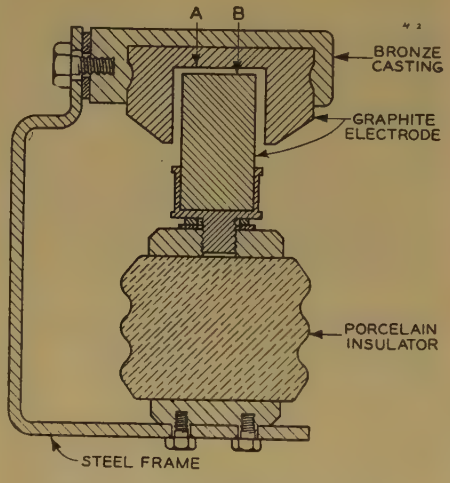


Figure 2. Cross section of new gap

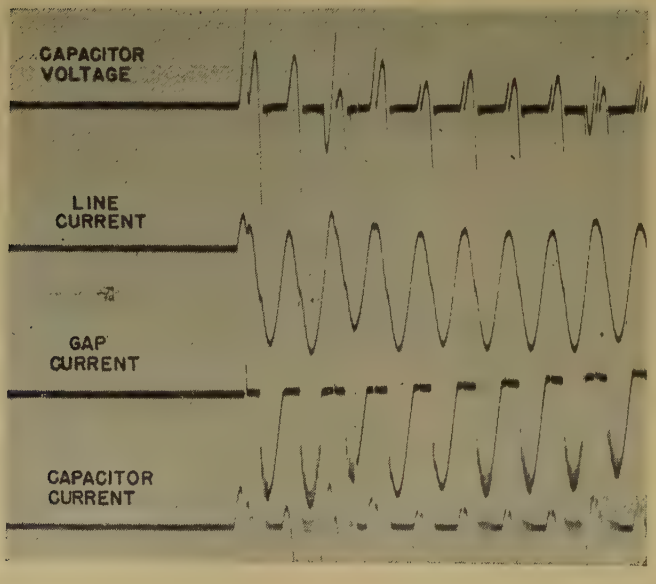


Figure 1. Oscillogram showing operation of a conventional gap protecting a 33-ohm, 60-cycle, 1,410-volt series capacitor on a 100-ampere fault

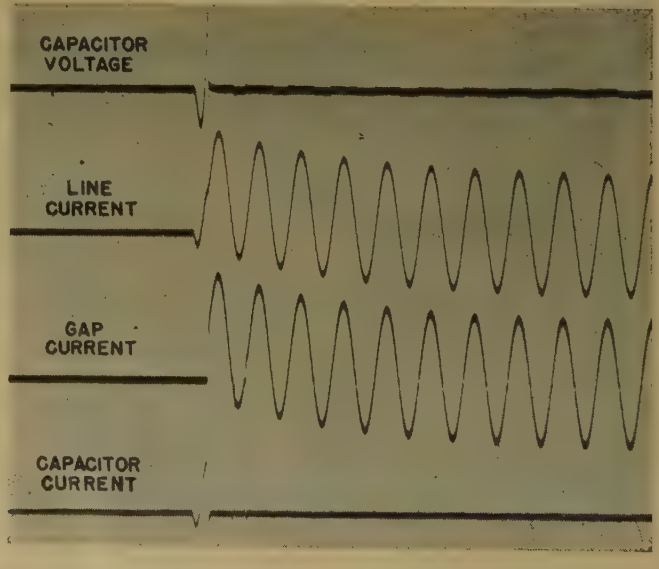


Figure 3. Oscillogram showing operation of new gap protecting a 33-ohm 60-cycle 1,410-volt series capacitor on a 100-ampere fault

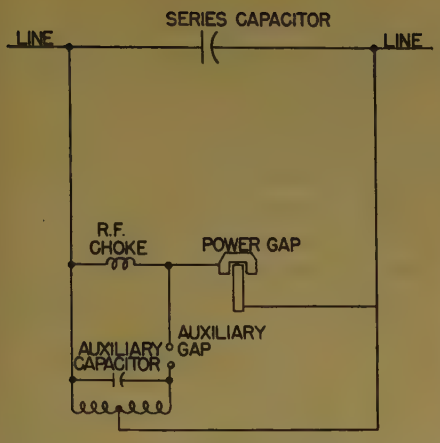


Figure 4. Series capacitor protective device for low voltage capacitors

age and a restriking arc, the series capacitor will be subjected to high currents while the arc exists in the gap. Figure 1 shows an oscillogram made of the current in a 33-ohm, 60-cycle series capacitor with a shunt gap set to break down at 3,000 volts. The gap electrodes were made of brass.. The normal current of 43 amperes was increased to 100 amperes. The oscillogram shows the presence of high currents in the capacitor after the gap breakdown occurred. Such high currents cause heating of the capacitor and may cause serious damage.

The use of a gap having special graphite electrodes gives a low arc voltage and limits the current flowing in the series capacitor leads to a low value. Even with graphite electrodes, however, the arc will be moved out of the space between the electrodes by magnetic forces, thermal air currents, and random air currents unless special precautions are taken in the gap design.

Figure 2 shows the cross section of a special type of gap the authors have developed to insure a stable arc with a low arc voltage. The arc occurs between the surfaces *A* and *B* and is shielded from air currents by the upper electrode. Magnetic forces produced by the current traveling radially through the upper electrode are in such a direction as to keep the arc in the gap. Gaps of this design have been tested at currents up to 5,000 amperes for one second and sustained no damage. The arc remained between the gap faces at all currents, and there was no tendency for the arc to wander down the sides of the lower electrode. Figure 3 shows the results of a test using this new gap on the same circuit as that used for Figure 1.

As the spacing of a gap is decreased, the variation in breakdown voltage on successive operations becomes greater. For dependable operation a gap should be adjusted to break down at not less than 3,000 volts. Since the gap must function dependably at no more than twice the rated capacitor voltage, it cannot be used to protect a capacitor rated at less than 1,500 volts unless an auxiliary means is provided to ionize the gap when the capacitor voltage reaches twice the rated value.

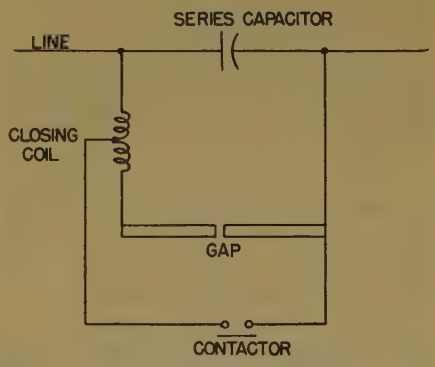


Figure 5. Series capacitor protective device with magnetic contactor to extinguish arc in the gap

Figure 4 shows a diagram of a gap-protected capacitor with a continuous voltage rating of less than 1,500 volts. A step-up autotransformer is used to increase a voltage obtained across the series capacitor to a level such that the auxiliary gap will break down when the voltage on the series capacitor is twice the rated value. The breakdown of the auxiliary gap allows the small auxiliary capacitor to discharge into a radio frequency choke which is in series with the main power gap. This discharge causes a high frequency voltage to appear across the choke. Since the series capacitor has a low impedance at this frequency, the voltage appears across the power gap causing it to break down and pass power current.

A simple gap-protected series capacitor is a satisfactory installation provided no fault is of sufficient duration that the heat generated by the arc will damage the gap, and provided the arc in the gap will go out when the line current drops to normal. Such conditions may exist on low voltage circuits. Usually, however, some special means must be employed to extinguish the arc in the gap.

Magnetic Contactors for By-Passing

Series capacitor protective devices made in the past have utilized gap current

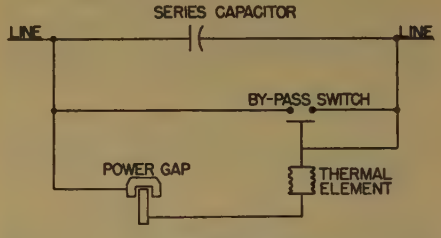
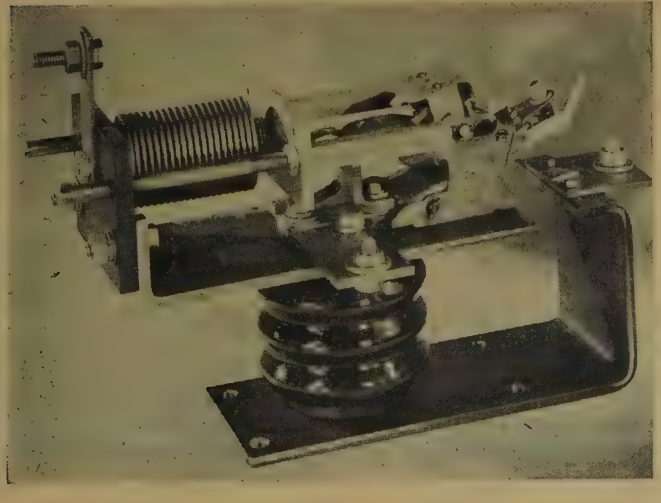
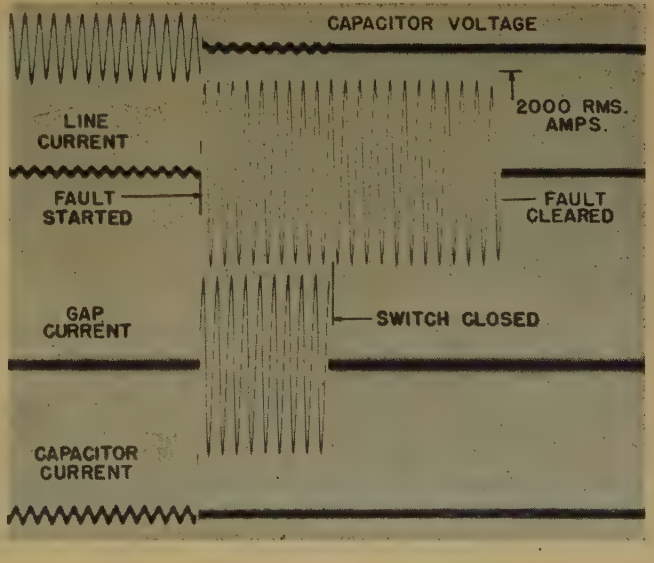


Figure 7. Series capacitor protective device using thermal switch

Figure 6 (below). Bellows operated toggle switch

Figure 8 (right). Operation of series capacitor protector using bellows operated switch





to initiate the closing of a magnetic contactor which by-passes the capacitor and gap to extinguish the arc. Such an arrangement is shown in Figure 5. The capacitor closing coil is placed in series with the gap so that when the gap breaks down the current flowing through the gap will cause the contactor to close. The contacts are connected to shunt the gap and all but a small portion of the closing coil. The number of turns remaining in the circuit is sufficient to cause the contacts to remain closed until the current in the line drops to normal. Thus, the arc exists in the gap only for the time required for the contactor to close, and the contactor shunts the capacitor for the duration of the fault.

The magnetic contactor provides adequate protection of the gap in a gap-protected series capacitor; however, a special and expensive contactor must be designed and built for each application. The size of the operating coil must be adjusted for each equipment so that the contactor will pick up at twice the rated capacitor current and drop out when the current drops to the rated value. The coil must be designed to withstand the steep wave front surge imposed upon it when the gap breaks down and the stored energy of the capacitor is discharged into the coil. In addition to stressing the coil, this surge also causes the contactor to accelerate very rapidly so that its contacts are closed while the capacitor discharge current is still high. This imposes severe duty on the contacts, and they must be carefully designed to prevent welding or excessive burning.

New By-Passing Switch

To overcome the difficulties encountered in the use of magnetic contactors, the authors set about to design a new type of by-pass switch to meet the following requirements:

1. It must close rapidly enough to protect the gap from overheating during any fault up to 2,500 amperes.

2. It should have sufficient time delay on closing in order that any capacitor bank up to 180 kva at 230 to 2,400 volts would be substantially discharged through the gap before the contacts engaged.

3. The motor element must not be damaged by the maximum combined fault current and capacitor discharge current.

4. It must have sufficient time delay on opening to allow a fault to be cleared by the line breakers so that no holding arrangement is required.

The switch shown in Figure 6 was developed for this purpose. It is a thermally actuated toggle switch which has quick-make and quick-break action and is connected as shown in Figure 7. The bellows is evacuated and charged with a small quantity of a liquid having a low vapor pressure at any ambient temperature which may be encountered in service. At such temperature the bellows remains collapsed because of external atmospheric pressure. When mounted in the switch, it is stretched to the normal length and exerts a pull more than sufficient to open the switch mechanism. When gap current passes through the walls of the bellows, heating occurs which changes the vapor pressure of the enclosed liquid. Continued heating causes the vapor to exert a pressure sufficient to actuate the toggle mechanism causing the switch to close. Figure 8 is an oscillogram showing the gap and switch operation in protecting a 16-ohm, 60-cycle series capacitor during a 2,000 ampere fault.

The closing of the switch by-passes the entire series capacitor and thus terminates the flow of gap current and allows the bellows to start cooling. Cooling causes the vapor to recondense, and the resulting differential pressure reopens the switch and restores the series capacitor to service

The gap may be allowed to reach a temperature of 250 degrees centigrade with no risk of damage. Figure 9 shows the time-current characteristics of the gap shown in Figure 2 based on an attained temperature of 250 degrees centigrade on the top casting and shows also the time required for the switch to close for the same currents. From this it is seen that the switch meets the first requirement of protecting the gap for all currents in the operating range. The tests from which these data were procured were made at an ambient of 25 degrees centigrade; however, the gap and switch combination is temperature compensating, and adequate protection is obtained throughout the operating temperature range. At high ambient temperatures the gap reaches the maximum permissible temperature in a shorter time, but the switch closes more rapidly. At low ambients the switch operates more slowly, but the gap requires longer to reach the temperature limit. Temperatures below the freezing point of the enclosed liquid do not damage the bellows because of its flexible nature and because the quantity of liquid is very

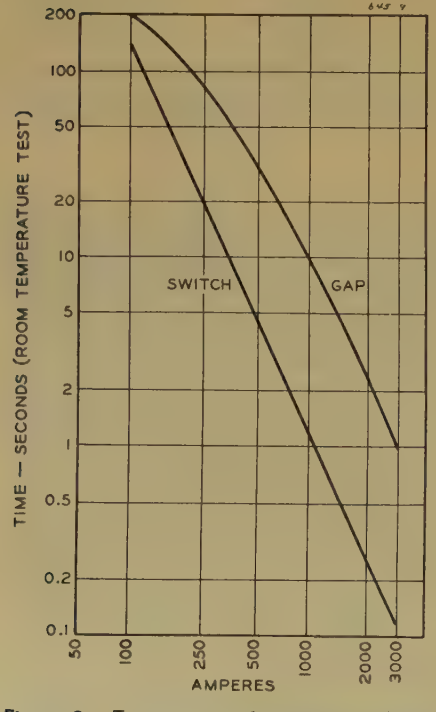


Figure 9. Time-current characteristic of gap and switch

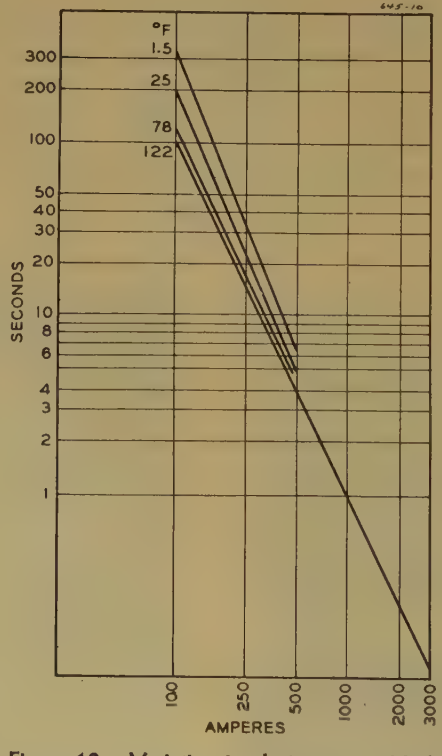


Figure 10. Variation in closing time of bellows operated switch with variations in ambient temperature

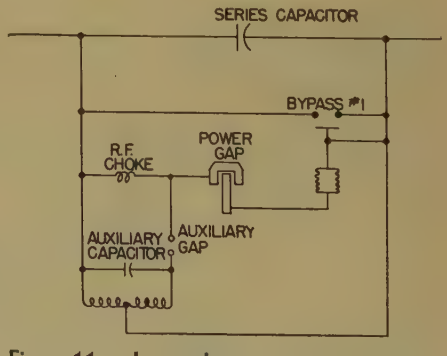


Figure 11. Low voltage series capacitor protective device

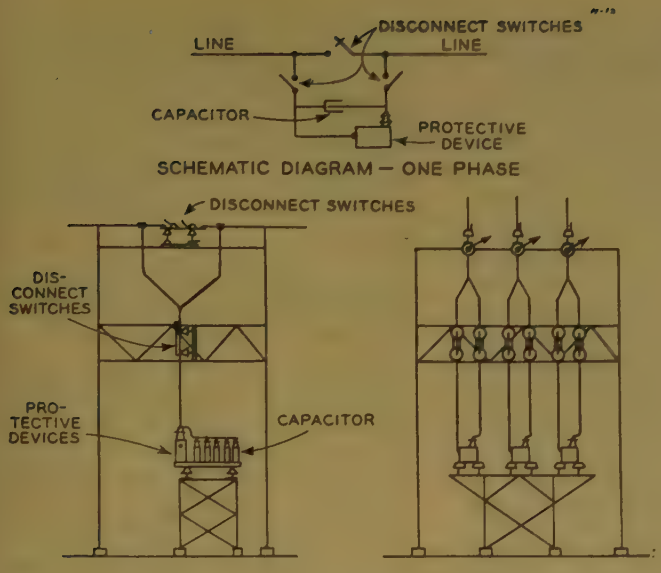


Figure 12 (left). Typical series capacitor installation

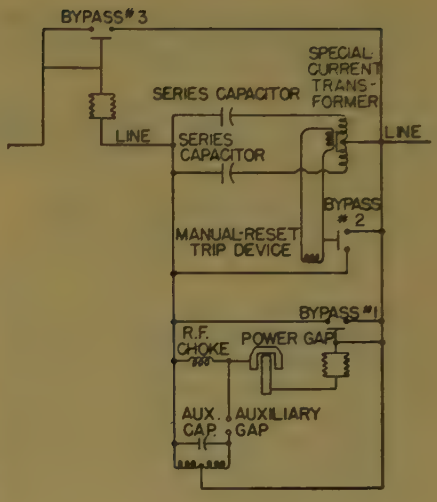


Figure 13 (right). Series capacitor with short circuit, overload, and dielectric failure protection

small. Operations at ambients below freezing do not take appreciably longer than those above freezing since the heat of fusion of the liquid is small compared to the total heat input required to raise the bellows to the operating temperature. The operating time of the switch for various ambients is shown in Figure 10.

The motor element in the new switch is essentially self-protecting since the switch operates to stop the current flow in the bellows when it reaches a certain temperature. High currents simply cause the switch to operate more quickly. The switch shown has been tested with fault currents of 2,500 amperes and capacitor discharge currents of 100,000 amperes and sustained no damage.

The opening time of the switch varies from two to five minutes over the ambient temperature range of −20 degrees centigrade to +50 degrees centigrade. Thus, any fault will be cleared by the line breaker before the switch opens to restore the capacitor to service. An arcing ground on the system cannot cause operation of the switch more often than once every two minutes so that heating in the capacitor caused by discharge through the gap cannot be cumulative and cause damage.

Method of Installation

Figure 7 is the diagram of a high voltage (above 1,500 volts) series capacitor with short circuit protection. Figure 11 shows the low voltage equipment. In either case the complete assembly of equipment for each phase is mounted on a platform which is insulated from ground for the line-to-ground voltage as shown in Figure 12. Outdoor type capacitor units are used, and the protective equipment is housed in a weatherproof steel housing with one entrance bushing. A stud on the housing serves as the other terminal. Disconnect switches are provided to bypass and isolate the capacitor for inspection and maintenance.

Operating Limits

During momentary overloads, such as might be caused by motor starting or the operation of a resistance-welding machine, the series capacitor rated current may be exceeded, and it is not intended that the short circuit protective device should operate at such times. The breakdown voltage of the protective gap is subject to variation with temperature, humidity, condition of electrode surfaces, and rate of rise of the applied voltage. To allow for these variations, the gap is set positively to break down at 200 per cent of the rated voltages and never to break down at 150 per cent of the rated voltage. Therefore, it is important that the momentary current peaks never exceed 150 per cent of the continuous current rating of the capacitor. In some cases the current peaks will exceed considerably the normal sustained current. In these cases it is necessary to use a capacitor with a sufficiently high current rating that it will never be exceeded by more than 50 per cent, even though the capacitor will run most of the time with less than rated current.

Other Types of Protection

A series capacitor will be damaged by continuous operation at more than 110 per cent of its rated current. The short-circuit protective device may not function at less than 200 per cent of rated current; therefore, it is sometimes desirable to provide overload as well as short-circuit protection. The overload protective device should have an inverse time-current characteristic which can be coordinated with that of the capacitor to allow momentary but not continuous overloads. The bellows operated switch is ideal for this purpose. It is necessary only to connect a bellows of the proper current rating in series with the capacitor and to connect the switch to shunt the capacitor and bellows.

Still another type of protection that is sometimes used for series capacitors is dielectric failure protection. This is a means of detecting a failure in the working insulation of a capacitor unit in a capacitor assembly. In an unfused capacitor bank a short-circuited capacitor unit may sustain an internal arc which will cause gas to be generated in the unit. Continued operation will cause the pressure to reach a value which will rupture the case and possibly cause damage to other units and equipment. If the units are equipped with individual fuses, a fuse operation to remove a faulty unit increases the reactance of the bank and continued operation at the rated current of the original bank will subject the remaining units to overvoltage. The by-pass switch used in a protective device for dielectric failure protection is spring biased to the closed position and latched in the open position. A magnetic device is used to trip the latch when the currents become unequal in two equal branches of the capacitor bank. Each phase of the series capacitor bank is divided into two equal branches and connected so that the two branch currents pass in opposite directions through one winding of a special current transformer. No voltage is induced in the secondary winding until the two currents become unequal as a result of a short circuit in one of the capacitor units or a removal of one or more units by operation of individual fuses.

Figure 13 shows the diagram of a series

A B–H Curve Tracer for Magnetic-Recording Wire

T. H. LONG
MEMBER AIEE

G. D. McMULLEN
NONMEMBER AIEE

Synopsis: The equipment described is able to show on the screen of an oscilloscope the cyclic hysteresis loop of a sample of magnetic-recording wire a little over one inch long and 0.004 inch in diameter. Results obtained with the equipment in studying recording wires are given. A discussion is included of the operation of the equipment, and of possible modifications.

IN EXPERIMENTAL study of the performance of any particular type of recording or playback head in relation to magnetic-wire recording it becomes evident that there are at least two variables. One of these, and frequently the most serious, is the condition of the head as influenced by accumulations of dirt. The dirt that accumulates in such a head is usually magnetic, but it is probable that any kind of dirt is almost equally bad on account of the separation it causes between the wire and the pole pieces. Magnetic dirt has the additional disadvantage of causing a shunting effect on the gap. The second variable is the magnetic character of the wire itself.

It is a matter of experience that with suitable recording and playback heads the performance of a wire recording system is stable to within about 0.5 decibel for short lengths of wire. For frequencies above 2,500 cycles the performance may be subject to variations as great as 15 decibels in playing through a 1 hour spool of wire at 2 feet per second. Performance at lower frequencies may be subject to roughly one-third as much change. These figures apply to 0.004-inch diameter stainless steel wire available early in 1945.

It is known further that a normal change in the condition of the head will account for only a small part of the change in low frequency performance but that it may account for all of the change observed at high frequencies. This situation makes it important to be able to separate the variables of head condition and wire magnetic characteristic in order to find out what actually is happening. This requires special equipment for expediently measuring the magnetic characteristics of the recording wire.

The characteristics obviously of interest in a recording wire that is to be used as a permanent magnet are retentivity and coercive force. Other magnetic characteristics that may be of interest are the shape of the normal magnetization curve, the erase noise level, and the so-called d-c saturation noise level. These last two items usually are studied on a record-and-playback setup and will not be discussed further here.

Paper 46-30, recommended by the AIEE committee on communication for presentation at the AIEE winter convention, New York, N. Y., January 21–25, 1946. Manuscript submitted November 8, 1945; made available for printing December 26, 1945.

T. H. LONG is senior research engineer and G. D. McMULLEN is research engineer with C. G. Conn, Ltd., Elkhart, Ind.

Requirements for Equipment for Magnetic Measurements

Perhaps the most important requirement for magnetic measurements is that they should be made at a sufficiently intense magnetization to insure saturation of the wire. Measurement at any arbitrarily selected lower level may not be proportional to saturated measurements and in extreme cases will give little idea of the actual magnetic property of the wire. It originally was estimated that 1,500 ampere turns per inch would be necessary for the saturation of any wire. Subsequent experience has indicated that this is satisfactory for any wire suitable for magnetic recording with present head designs but that wire can be produced that requires more than 2,500 ampere turns per inch for saturation.

A requirement of almost equal importance is that the equipment should be able to operate continuously and indicate continuously the magnetic retentivity and coercive force of the wire as it runs through the equipment at a speed comparable to recording speed. The resolving power of the equipment should correspond to something on the order of 0.1 second playing time. There seem to be no variations in performance of an undesirable nature or magnitude that are of shorter duration than perhaps one-half second. If there were shorter transients, they could be studied best by oscillographic methods on a record-and-playback system which has a resolving power of a few thousandths of one inch.

Considerations of magnetizing coil design suggest the desirability of operating at a low audio frequency, perhaps several hundred cycles. A secondary consideration pointing in the same direction is the possibility of winding the detector coil on a stainless steel (nonmagnetic) tube.

It occasionally may be desirable to make rather accurate measurements at very low inductions, such as 100 lines per square inch. In order to avoid compromising the design as far as more normal use at much higher flux densities is concerned, it may be desirable to provide for measurement in such cases on a small bundle of wires. An example of this use would be the getting of that part of the

capacitor having short circuit, overload, and dielectric failure protection. Actually, overload and dielectric failure protection are seldom needed on distribution circuit series capacitors. These capacitors are usually selected on the basis of the maximum expected line currents, and these currents are not likely to be continuously exceeded because other equipment such as transformers would be damaged. When the units are applied in this manner and are properly protected against damage from short circuits, they seldom fail in service.

Conclusions

A graphite gap designed to hold the arc in a relatively fixed position provides the most effective protection for a series capacitor because it does not permit recurring rises in voltage on the capacitor during a fault. It can be designed to handle the fault current without being damaged and without serious changes in the breakdown characteristics.

A thermally operated by-pass switch of the type described provides an economical and effective means of extinguishing the arc in a series capacitor protective gap. The bellows operating element has a negligible inductance and is not damaged by the steep wave front surge of the capacitor discharge. The time delay on closing relieves the contacts of handling capacitor discharge current. The time delay on opening eliminates the need for a holding mechanism.

The thermal switch has an inverse time-current characteristic which makes it ideal for overload protection of series capacitors.

normal magnetization curve that is near the origin.

Calibration should be simple and precise with independent adjustments for coercive force and retentivity and should be relatively stable. A permissible drift might be as much as 5 per cent per hour. An absolute calibration would be desirable.

The equipment should be adjustable to obtain full scale retentivity readings at several convenient values between 10,000 and 100,000 lines per square inch. Adjustment also should be provided for full scale ampere turns per inch from perhaps 100 to 3,000.

Theoretical Considerations

The practicability of the use of the oscilloscope in obtaining hysteresis loop information on small punched washers of magnetic material has been demonstrated by Adler.[1] It would seem that something of the same technique should be applicable to the present problem. It hardly would be practicable to form the recorder wire into a loop to apply Adler's technique directly. Such a loop would require several turns to minimize end effect; and very high magnetizing currents would be required since the recording wire is actually a very efficient permanent magnet material.

An alternative is to run a straight wire through a magnetizing coil. The magnetizing force near the axis of a magnetizing coil of practical proportions will not be constant but will increase toward the center of the coil. Most of the change will be near the ends, and, if only the central one-third of the magnetizing coil is occupied by the detector and balance coils, the variation actually encountered will amount to only a few per cent, and an average value may be satisfactorily used; this is subject to limitations imposed by end effect. If the end effect is spread out over a length of the order of 100 times the wire diameter, it should not affect the results appreciably, and this expectation has been realized.

It is clear that, since operation is required on the flux contained in one piece of 0.004-inch diameter wire, a great many turns will be required in the detector coil through which the wire will run. It is further evident that a very substantial part of the flux through this coil will be flux outside of the wire and in air. For instance, if the inside diameter of the winding is 0.312 inch and the radial thickness of the winding is neglected, the ratio of the areas of air and iron included by the coil will be about 6,000. It will be necessary to exclude the influence of this air flux from the measurements, since it would mask completely the flux being measured. This is reasonably simple to do with a balance coil having a product of turns times area slightly greater than the detector coil and located along side of the detector coil within the magnetizing coil. A potentiometer adjustment can be used for the adjusement of the final balance as one of the steps in calibrating the equipment.

A definite limitation is imposed on the equipment by the requirement of handling wire for which the maximum induction is as great as 100,000 lines per square inch, since the voltage from the balance and detector coil combination must not overload the amplifiers that precede the integrating circuit.

This voltage prior to the integrating circuit is a very peaked wave, so that a fairly wide range of frequency must be handled without appreciable distortion, and what is perhaps more important, without appreciable relative phase shift between the various harmonic components at any point in the circuit. This will require the use of unusually large capacitors on the screen grids, and the elimination of cathode by-pass capacitors with a corresponding material loss in amplifier gain.

An interesting theoretical question is an appropriate design for an air core magnetizing coil to provide 1,500 ampere turns per inch continuously at say a maximum frequency of 500 cycles. It is known[2] that for a coil wound from round or square wire, and having proportions suited to the present problem, if the eddy current loss increases the effective resistance by more than about 50 per cent, the total loss will be reduced by winding with smaller wire to the same total turns and axial coil length. This makes it ap-

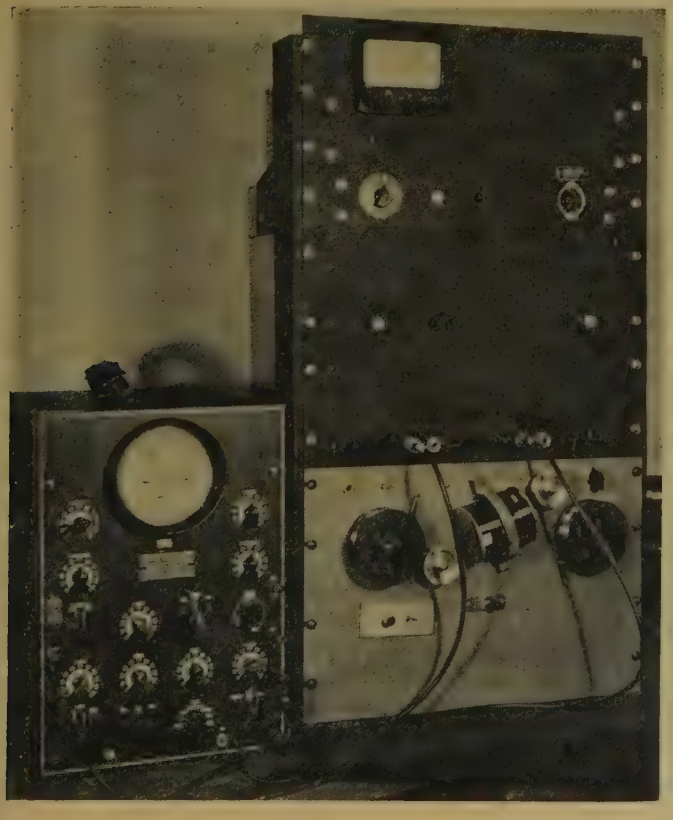
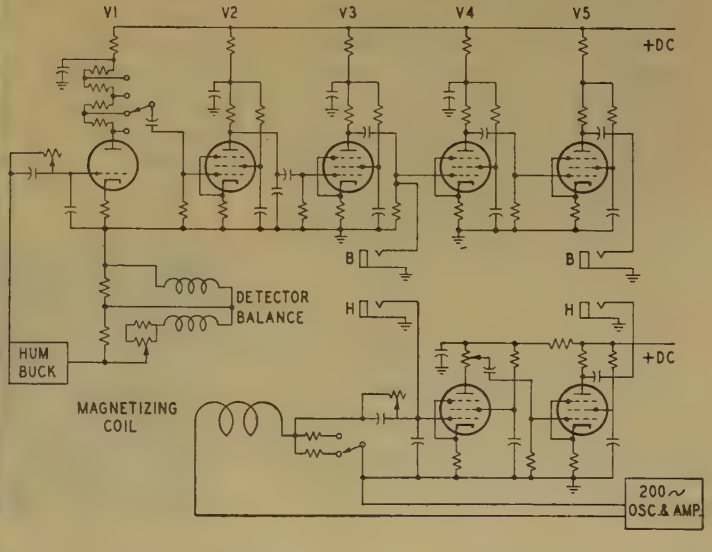
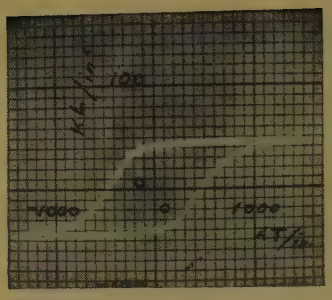


Figure 1 (left). Equipment for continuous magnetic measurements on magnetic-recorder wire

Figure 2 (below). Simplified schematic diagram of B–H curve tracer





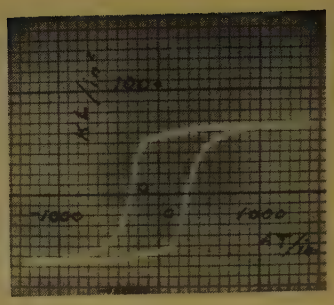


Figure 3. Saturation hysteresis loops for two samples of stainless steel recording wire

pear that for a radial winding depth of 1.25 inches the maximum practicable round wire size will be about 0.040 inch. The maximum practicable wire size will be roughly proportional to the reciprocal of the radial depth of the winding.

B–H Curve Tracer

The equipment as finally developed for the continuous measurement of retentivity and coercive force of moving or stationary samples of magnetic recording wire is shown in Figure 1. The lower section is occupied by the wire handling equipment and the magnetizing coil. Behind this unit on the relay rack is the power supply for the power amplifier that energizes the magnetizing coil at the finally selected frequency of 200 cycles. This power amplifier is at the top of the rack. In between there is a 200-cycle oscillator, an integrating circuit for the induction channel and associated amplifier, an amplifier for the magnetization channel, and the controls associated with these items. The equipment is self contained except for the oscilloscope and includes sufficient amplification for 20-volt output signals in both channels.

Figure 2 is a simplified schematic diagram in which certain standard items are designated simply by blocks. The resistance coupled amplifiers are modified from strictly conventional circuits to meet the special requirements of the present problem as just indicated. The omission of the cathode by-pass capacitors results in a reduction in the maximum practicable gain per stage to about one half of normal, or around 50 for a pentode stage. The required minimizing of phase distortion requires unusually large coupling capacitors. This results in an amplifier that has a very high gain even at a frequency of a few cycles. Transients in the 60-cycle supply come through a conventional filter sufficiently to cause substantial instability in the oscilloscope image, so a rather elaborate filter is necessary. This filter is a combination of two inductance–capacitance stages and four resistance–capacitance stages. The hum bucking circuit provides for the variation in phase and magnitude of a small inserted 60-cycle voltage and uses a capacitance–resistance phase split for the phase variation.

The afore-mentioned difficulties are increased by the necessity of using an integrating circuit in the induction channel of the amplifier, identified as *B* at the output jacks. This integrating circuit is, in effect, a resistance and capacitance in series that are so proportioned as to have a time constant on the order of 100 times the length of a half cycle. The resistance involved is the load resistance of amplifier *V*2 in parallel with the plate resistance of that amplifier, and the capacitance is connected from amplifier plate to ground.

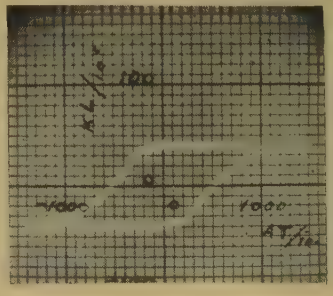
In spite of the various steps taken to minimize phase distortion, a prohibitive amount remains, and this has been corrected to a tolerable value by the use of the resistance–capacitance network shown at the input to each of the channels. The adjustment of the phase correction network in the induction channel varies the position of the nearly vertical lines of the hysteresis loop, and in the proper operating range of this adjustment there is no other pronounced change in the hysteresis loop seen on the screen of the oscilloscope. This fact seems to preclude the expedient arriving at what might be called an absolute calibration of the system. Calibration against standard samples that have been measured by a point by point method is an easy way out after the standard samples have been measured. In making point by point measurements on standard samples of stainless steel recording wire it is necessary to calculate the cross section of the bundle of wire used and the cross section of the detector coil and then correct for the air flux. This correction amounts to about 10 per cent of the coercive force, when measurements are made on a ring sample.

Results Obtained With the B–H Curve Tracer

The advantages of being able to arrive quickly at the magnetic characteristics of short samples are too obvious to require further comment. The fact that these measurements are subject to an absolute error that may be as large as 10 per cent is not a serious handicap. The relative error is substantially less and depends only on the accuracy to which the image on the oscilloscope screen can be measured, on the accuracy with which the wire diameter can be measured (this influences retentivity only), and on the linearity of the oscilloscope. Figure 3 shows saturation hysteresis loops for two different samples of stainless steel wire, and Figure 4 shows two hysteresis loops taken on a single sample of wire about a foot apart; the difference may be due to the second loop's being in a part of the wire that had been welded at an earlier stage in the drawing. The change between these two loops was fairly gradual, and several half-pound spools were run through to find such a case.

When this project was started it was believed that the most important use of the equipment would be continuous measurements to determine the uniformity of the magnetic characteristics of a recording wire from one end of the spool to the other. This indeed has been important, and Figure 5 shows the retentivity and coercive force plotted against winding time for a constant spool speed that gave a nominal wire speed of 5 feet per second. The variations are of sufficient magnitude to account for several decibels of variation in the low frequency playback, but they are definitely not sufficient to account for the magnitude of frequently encountered variations in high frequency performance. The variations shown seem to be typical of current production of stainless steel wire (as of November 1945).

In the earliest use of this equipment for continuous measurements on running



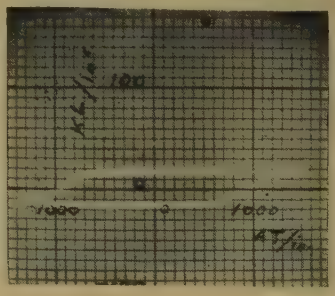


Figure 4. Hysteresis loops for two sections of a stainless steel recording wire about one foot apart

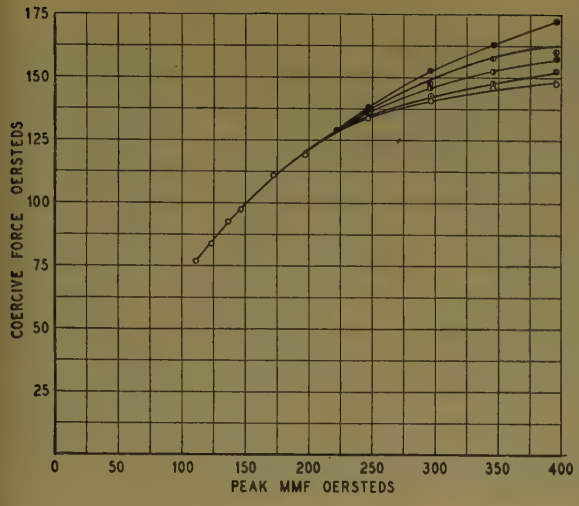
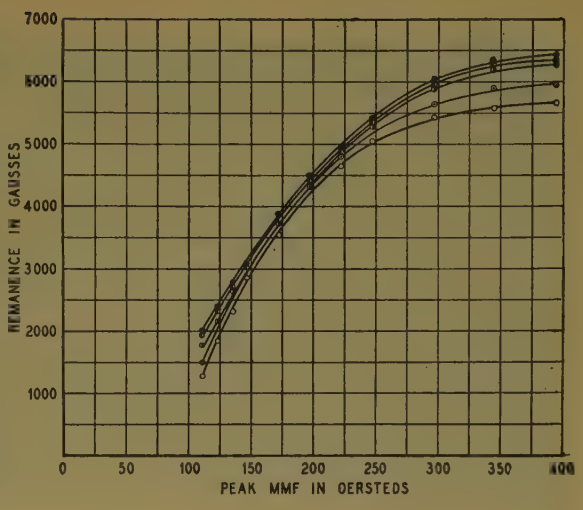


Figure 6A (left). Coercive force versus magnetization for several values of tension

Figure 6B (right). Retentivity versus magnetization for several values of tension

Both parts are for stainless steel wire of 0.004-inch diameter. Tension varied from 0 to 2 pounds in half-pound steps, maximum tension at top



wire, a small pulsation of the hysteresis loop on the oscilloscope screen was observed. This amounted to only a few per cent of the intercepts on the B and H axes but seemed to be associated with the motion of the wire. It was found that this was caused by something analogous to magnetostriction. Small variations in tension that accompany the motion of the wire influence the magnetic properties of the wire to an appreciable extent.

A study of this effect was made in various wires to find out what the magnitude might be and how it varied between samples. Figures 6A and 6B show characteristic results in which coercive force and retentivity are plotted against peak magnetizing force for various values of tension. In general an increase in tension always is accompanied by an increase of coercive force, and may be accompanied by either an increase or decrease in retentivity. The magnitude of the affect for a change in tension from zero to two pounds varies from 0 to 12 per cent for coercive force, and from 0 to 50 per cent for retentivity.

These stated values apply to the working range of magnetizations, and some wires do not exhibit either effect appreciably in this range, although it is evident above this range.

The B–H curve tracer, which might be more conveniently called a magnetoscope, also is useful in determining normal magnetization curves of recording wire. It seems necessary in this case to use a point by point procedure, and, to get good detail at the bottom of the curve where the induction is very low, it is expedient to use several wires (perhaps as many as 10), but such curves can be obtained in about 5 or 10 minutes after the equipment has been calibrated. It usually will be expedient to measure the magnetizing force on a voltmeter connected across a resistance in series with the magnetizing coil and to read the induction on the screen of the oscilloscope. Figure 8 is a sample of normal induction curves obtained in this manner.

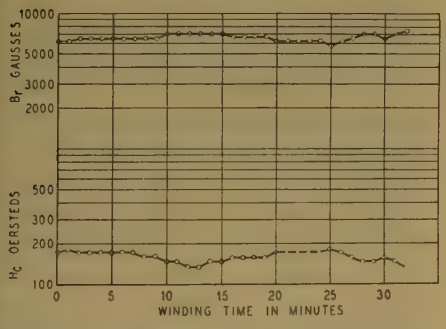


Figure 5. Retentivity and coercive force plotted against running time for a one-half pound spool of 0.004-inch diameter wire

Nominal running speed was 5 feet per second

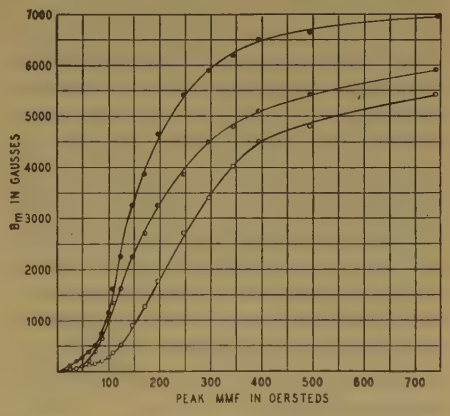


Figure 7. Normal induction curves for three samples of stainless steel wire

●—H_c 150, B_r 5,900
◐—H_c 185, B_r 5,400
○—H_c 250, B_r 4,800

Conclusions

The necessity and adequacy of the magnetoscope as a development tool in experimental work on wire recording have been demonstrated. It would seem that the magnetoscope would be equally useful in control work, if the advantages of stainless steel wire are to be fully realized.

The utility of the magnetoscope is by no means limited to the field that has been explored in some detail in this paper. For instance it might be possible to use the magnetostrictive characteristic of a magnetic material to get a direct and almost instantaneous measure of the tension in the material.

The account that has been given has been limited to a measuring device in which the end effect (or return magnetic circuit) could be safely neglected. This is not a limitation inherent in the device. In the present form of the equipment the detector coil is somewhat sensitive to magnetic material closely adjacent to the magnetizing coil. This is associated with the energy loss so caused and the consequent lag between flux and current. It is probable that an external magnetic return circuit can be employed in spite of this by energizing the magnetization channel from a search coil and integrating circuit. This would make it possible to use such equipment in measuring the magnetic characteristics of a single strip of transformer grade alloy. In such applications a detector coil of only a few turns would be required, and the balance coil would be unnecessary.

References

1. B–H Curve Tracer for Lamination Samples, Robert Adler. *Electronics*, November 1943, pages 128–31, 314, 316–17.

2. Eddy-Current Resistance of Multilayer Coils, T. H. Long. AIEE Transactions, 1945, volume 64, October section, pages 712–18.

An Automatic Oscillograph With a Memory

A. M. ZAREM
ASSOCIATE AIEE

Synopsis: The memory oscillograph described in this paper is used for obtaining photographic records of randomly occurring electric transients. This instrument differs from other oscillographs of the memory type[1,2] in that its operation is completely automatic. Forty sets of oscillograms can be recorded without the aid of an operator. Because of this feature, such an oscillograph may be used for monitoring electrical systems in which sporadic circuit disturbances are to be studied. The unit consists essentially of three cathode-ray tubes with associated power supply, a saw-tooth oscillator to provide the horizontal time axis, amplifiers for the vertical deflection circuits, a beam blanking circuit, and an automatic camera. When the memory oscillograph is in operation, the cathode ray tubes are continuously excited. The vertical deflection circuits of the tubes are connected to the voltages to be investigated, and each tube screen carries a cathode-ray pattern characteristic of the voltage applied to its vertical deflection plates. Upon the occurrence of a transient pulse, the camera shutter is released and the electronic beams of the cathode ray tubes are interrupted. The camera then records the persistence of fluorescence, which is characteristic of the material used on the tube screens. In this way a record is obtained of electric events that occurred previous to the opening of the shutter. To insure successful operation, the component parts of the automatic memory oscillograph must be electrically co-ordinated and controlled. The sequence of functions performed by a control circuit for this purpose is described. Photographic records of transients which may arise during the operation of a mercury-arc polyphase inverter are included.

IN CONNECTION WITH research and development work on mercury-arc power converters, it is frequently necessary to study electric transients which occur at irregular intervals. Particular attention has been directed to the investigation of factors which encourage faulty operation. Not all of these factors are known and those that are known are not understood entirely. It is not a simple matter to obtain information concerning the initiation of transients. The random character of backfire phenomena in rectifiers, for example, makes it difficult to study electrical conditions in rectifier circuits immediately preceding backfire. Yet such a study is of prime importance if we are to learn more about the manner in which such faults occur.

The cathode ray memory oscillograph is an ideal instrument for this purpose. It can be made to provide a record of electric conditions previous to the occurrence of a transient as well as of the transient itself. The heart of this instrument is the cathode ray tube.

The Cathode-Ray-Tube Screen

A very useful characteristic of the fluorescent materials used for coating cathode ray tubes is the persistence of their luminescence after the exciting cathode ray beam is extinguished. All other conditions being the same, the rate of decay of the afterglow depends upon the kind of fluorescent material used.

Generally speaking, these coatings fall into three classes, and the tubes in which they are used consequently are referred to as short, medium, or long persistence cathode ray tubes.

Figure 1 illustrates in a general way the relative brightness retained for three different types of cathode ray tubes as a function of time. Curve *A* is characteristic of the short-persistence type P5 tube. The screen material used for this tube is an efficient emitter of light, and fluoresces in the blue range. The relative brightness falls to ten per cent in approximately 10^{-8} second. This rapid decay of brightness limits the use of these tubes in a memory oscillograph. Screens of this type find an important application when moving film recording is to be done. Due to the very short persistence, fogging of the film is kept to a minimum.

The medium-persistence P1 tube has a screen characteristic like that given by curve *B*. The relative brightness of such a screen falls to ten per cent in about 20 milliseconds. Most of the radiant energy of the P1 screen occurs in the yellow-green region.

The long-persistence P2 screen has a brightness-time curve similar to curve *C*. At voltages below 5 kv, the photographic efficiency for this tube is much lower than that of the P5 or P1 tubes.[3]

After careful consideration of tube characteristics and the requirements imposed by the intended application, the type P1 medium-persistence tube generally will be preferred for ordinary memory oscillograph studies. With an accelerating anode potential of 3,750 volts, the P1 screen provides sufficient after glow to allow a memory time of approximately 100 milliseconds, or 6 cycles of a 60 cycle a-c wave. By increasing the anode potential to 4,500 volts the memory time may be elevated substantially. However, because the use of beams of very high intensity has a markedly adverse effect on screen life, and since a cathode ray pattern of one type or another is on the tube screen continually, it is a matter of economics to avoid the use of very high intensities when they really are not required. For this reason an anode accelerating potential of 3,750 volts is desirable for normal operation. In anticipation of occasions when greater memory time may be required, provision may be made to allow the use of a tube voltage of 4,500 volts. As a further aid to lengthening screen life, the horizontal sweep oscillator can be allowed to remain unsynchronized so that the cathode ray pattern drifts slowly across each screen. With these precautions taken, the instrument can be operated

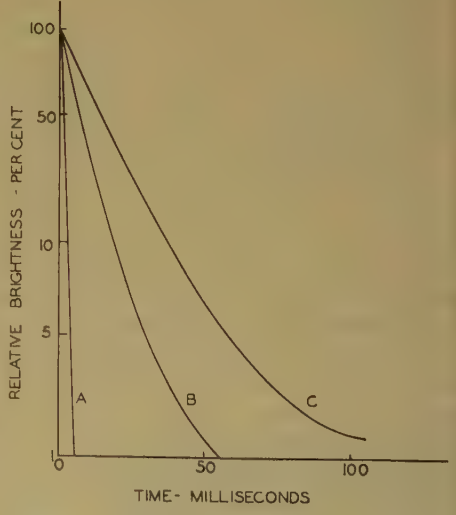


Figure 1. Curves illustrating typical variations in relative brightness as a function of time for three types of cathode-ray-tube screens

A—Short persistence
B—Medium persistence
C—Long persistence

Paper 46-67, recommended by the AIEE committee on instruments and measurements for presentation at the AIEE winter convention, New York, N. Y., January 21–25, 1946. Manuscript submitted October 29, 1945; made available for printing December 17, 1945.

A. M. Zarem is on the research staff of California Institute of Technology, Pasadena, Calif., while on leave of absence from the Allis-Chalmers Manufacturing Company, Milwaukee, Wis.

The author acknowledges the assistance of W. Richter and his associates at the Allis-Chalmers Manufacturing Company in the design of the instrument described here.



Figure 2. The automatic memory oscillograph

The automatic camera, the cathode-ray-tube unit, and the horizontal and vertical deflection control unit are shown

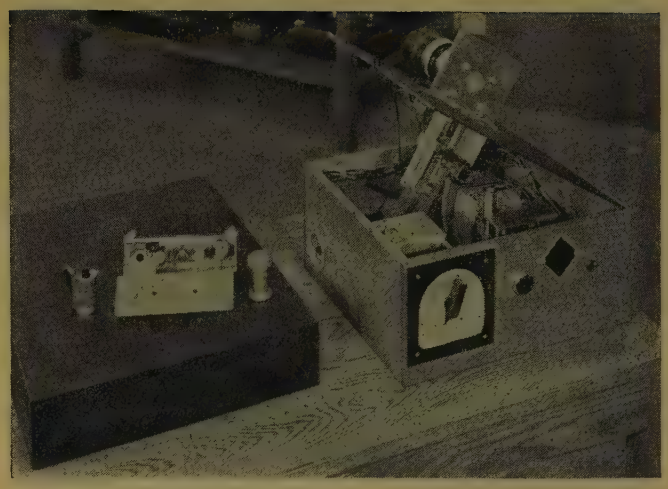


Figure 3. The automatic camera unit open to view

The camera and film loading cartridge are shown at the left

continuously 24 hours a day, with tube replacements required about once every five months. Tubes removed from the memory oscillograph, of course, will still be usable for ordinary cathode ray work.

Description of the Oscillograph Unit

Figure 2 is a picture of the automatic memory oscillograph. In normal operation a light-tight shield is placed between the camera lens and the cathode ray tubes. The lower tube unit shown in Figure 2 houses 3 5-inch cathode ray tubes with the necessary power supply and beam blanking equipment. Adjustments for focus, intensity, and accelerating potential are made by means of knobs on the front panel. Three values of accelerating tube voltage are available: 3,000 volts, 3,750 volts, and 4,500 volts.

Beam blanking may be accomplished in a variety of ways. If a trigger circuit[4] of the Eccles-Jordan[5] type is used, the output of this circuit is arranged so that the control grids of the cathode ray tubes will suddenly be made negative with respect to their cathodes when the circuit is tripped. Tripping may be accomplished by a voltage pulse of either positive or negative polarity. The pulse required is supplied by a control circuit which is actuated by the transient to be studied. Provision for adjusting the time delay between the opening of the shutter and the operation of the beam blanking circuit is contained in the control circuit. With such an arrangement, if the duration of the transient is not too great, it is possible to obtain a picture of the electrical conditions before, during, and after the occurrence of the transient. Information concerning conditions existing after the occurrence of a transient will be obtained at the expense of "memory time." However, situations may arise where such knowledge is desired.

The upper unit shown in Figure 2 contains the sweep oscillator for the horizontal timing wave and three sets of amplifiers for the vertical deflection plates of the cathode ray tubes. Each tube has its own 2-stage resistance-coupled amplifier. These amplifiers have a frequency response which is essentially flat up to 30,000 cycles per second.

The saw-tooth oscillator which provides the timing axis is common for all three cathode ray tubes. Simultaneous events therefore appear at the same relative location on all three tubes. Should the occasion demand it, the tubes may be operated with separate timing axes. This is done by means of convenient connections located on the rear panel of the tube unit. To aid in aligning electric events occurring at the same time, arrangement is made for simultaneously marking the traces on all three screens.

The usual means are provided for the adjustment of the vertical and horizontal gain as well as the vertical and horizontal positioning of the pattern for each tube. The saw-tooth oscillator may be interlocked with the frequency of the circuit being investigated, with a 60-cycle voltage, or with any outside alternating voltage.

The camera unit is shown in Figure 3. In addition to a lens and shutter, it contains a motor for automatically winding the photographic film and for closing the shutter after a picture has been taken. A step-type relay is included for the purpose of keeping count of the number of exposures made. By adjusting the knob of the relay, the unit may be preset to take a given number of pictures and then turn itself off. A maximum of 40 photographs can be taken with one loading of film. This number may be increased by changing the film loading cartridge and the step relay.

The shutter is of the focal plane type. It is kept in position against spring tension by a small movable latch placed

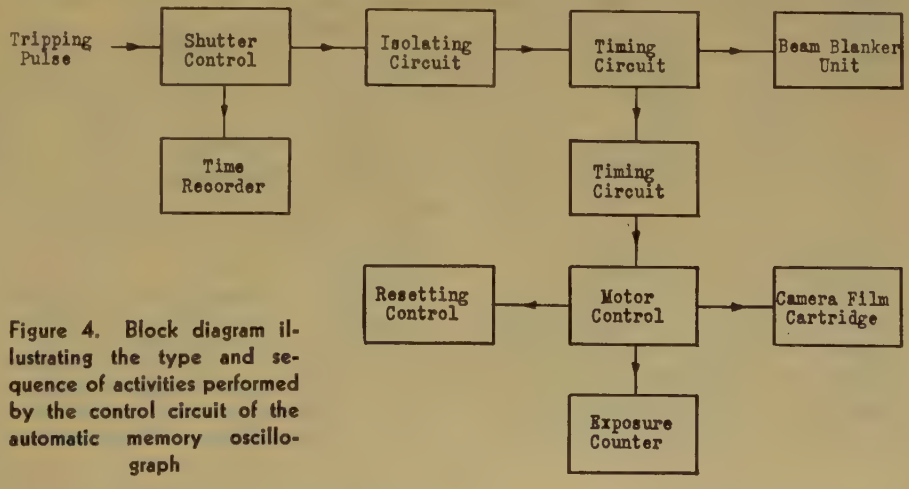


Figure 4. Block diagram illustrating the type and sequence of activities performed by the control circuit of the automatic memory oscillograph

close to the poles of an electromagnet. Release of the shutter is accomplished by exciting the current coil of the magnet.

The camera uses 35-millimeter film. Loading is accomplished by means of standard film cartridges. For photographing the green P1 medium-persistence screen, panchromatic-xx film gives excellent results. The lens has an opening of f1.5 and a focal length of three inches.

Control Circuit

Figure 4 is a block diagram illustrating the sequence of functions performed by the automatic memory oscillograph control circuit. The control is initiated by a voltage pulse applied to the grid of an electron tube. This pulse may be supplied by the transient voltage itself—or some other voltage pulse which occurs simultaneously with the transient to

Figure 7. Photographic record of oscillogram obtained with the automatic memory oscillograph connected as in Figure 6

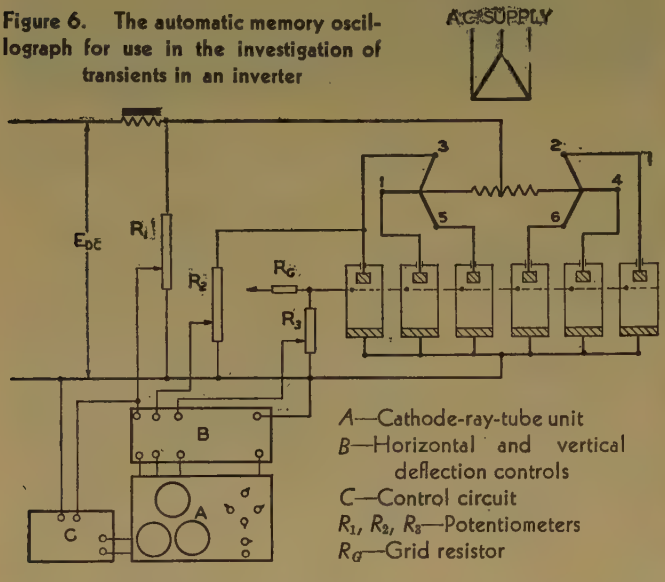
The camera shutter coil received its impulse at *A*. The cathode ray beam was blanked at *B*. The time at which the transient occurred is given by the clock *C*. Memory time preset at 50 milliseconds

e_{a-c}—Anode to cathode voltage for one anode of the inverter

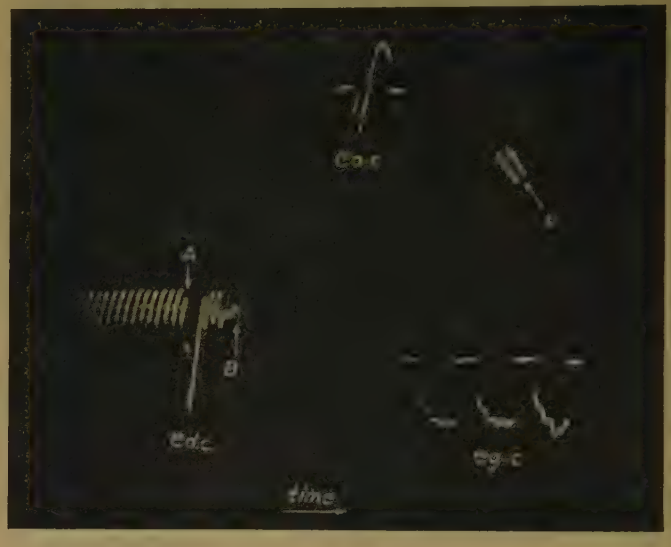
e_{d-c}—Main direct voltage of the inverter

e_{g-c}—Grid to cathode voltage

Figure 6. The automatic memory oscillograph for use in the investigation of transients in an inverter



A—Cathode-ray-tube unit
B—Horizontal and vertical deflection controls
C—Control circuit
R_1, R_2, R_3—Potentiometers
R_G—Grid resistor



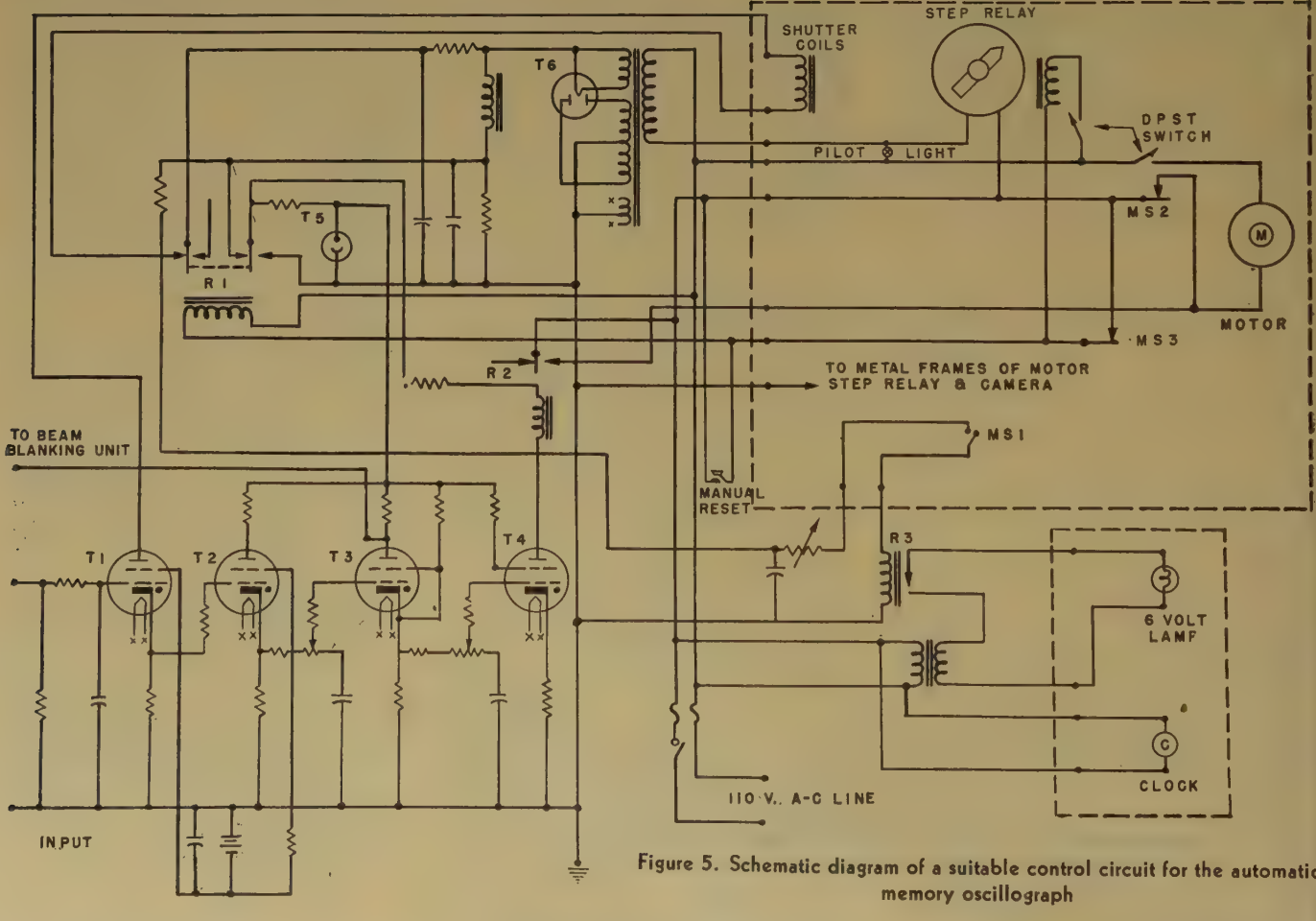


Figure 5. Schematic diagram of a suitable control circuit for the automatic memory oscillograph

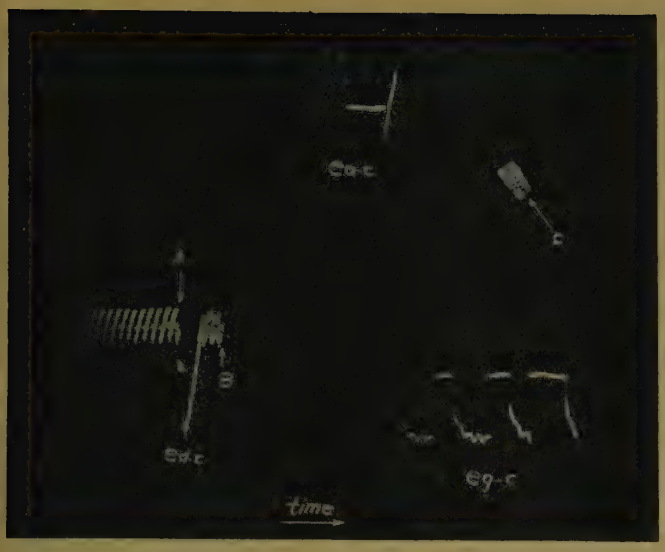


Figure 8. Record of an oscillogram obtained with the automatic memory oscillograph when the anode being monitored suffers preignition

The ability of the oscillograph to record electrical conditions preceding, during, and after the occurrence of a transient is clearly indicated. Memory time preset at 50 milliseconds



Figure 9. Photographic record of an oscillogram illustrating a backfire followed by an arc-through on a polyphase mercury arc rectifier

Memory time approximately 50 milliseconds

be studied. As the input impedance of the control circuit is quite high, very little current is required for its operation.

The first operation is a multiple one. The shutter is opened, a clock dial is momentarily illuminated, and an electric pulse is released to an isolating circuit. An adjustable time thereafter the beam blanking unit receives its impulse, and a second timing circuit is actuated. The latter operates the motor control unit which in turn resets the camera, excites the coil of the step-relay exposure counter, and places the entire control circuit in readiness for the next transient to be recorded. The timing circuits are included in order to allow the adjustment of both memory time and exposure time. The clock mechanism insures that every oscillogram record contains the time at which the initiating transient occurred.

Figure 5 is a schematic diagram of a control unit, which may be used successfully to perform the sequence of operations illustrated in the block diagram of Figure 4. $T1$, $T2$, $T3$, and $T4$ are gas-filled control tubes. $T6$ is a rectifier tube for the power supply of the unit, and $T5$ is a voltage regulator tube. $MS1$, $MS2$, and $MS3$ are microswitches.

When the circuit is ready for operation, the relay contacts, $R1$, $R2$, and $R3$ are in the positions shown and tubes $T1$, $T2$, $T3$, and $T4$ are in a nonconducting state. Tube $T1$ controls the opening of the camera shutter and applies a positive voltage pulse to the grid of $T2$ which serves as an isolating tube. A variable resistor determines the time interval between the firing of tubes $T2$ and $T3$. The voltage pulse for operating the beam blanking circuit[4] is taken from the plate of $T3$. Tube $T4$ which will become conducting an adjustable time after $T3$ is fired, controls the operation of the motor that resets the camera and places the entire control circuit in readiness for the next transient pulse. The amount of motor travel is determined by two microswitches $MS2$ and $MS3$ operated by a cam on the motor shaft. An additional microswitch $MS1$ is actuated by the shutter when it reaches the bottom of its travel. Operation of $MS1$ causes the momentary illumination of a synchronous clock mechanism located in the light-tight shield placed between the oscillograph unit and the camera.

A bell may be placed across the terminals of the motor to attract attention when a transient is recorded.

Performance of the Unit

During operation, the cathode ray tubes are continuously energized. The vertical deflection inputs are connected to the voltage sources being investigated. Screen patterns of the desired sizes and positions are obtained by adjustment of the control for the horizontal and vertical deflection plates of the various tubes. The cathode-ray-tube accelerating potential and beam intensity are set to meet the memory time requirements, and the camera is loaded with sufficient film for the number of exposures desired. The stepping relay is set for the number of photographs to be taken. After arrangement is made for the transient pulse to operate the control circuit, the equipment is ready for operation.

Upon the occurrence of a transient, the camera shutter, normally closed, immediately is triggered open and the clock dial in the light shield is illuminated momentarily. Depending upon a preset delay time, the cathode ray beams are then extinguished. The fluorescent material on the cathode ray tubes retains the images on the cathode ray screens for a time sufficiently long so that successful photographic recording is accomplished. After a fixed delay the camera motor operates, closing the shutter, winding the film to the next frame, and resetting the control circuit. This places the memory oscillograph in readiness to record the next transient disturbance.

The accuracy of reproduction and the excellent frequency response of the oscillograph amplifiers make this cathode ray instrument suitable for the study of switching transients and other disturbances of short duration. In many instances the transient voltages being investigated are of such magnitude that no amplifiers are required. For successfully recording transients of extremely high speed, cathode-ray-tube voltages higher than those used here must be employed.[3]

Results

The automatic memory oscillograph described here may be put to use in the study of randomly occurring transients in mercury arc converters. Figure 6 is an illustration showing the instrument connected for recording faults in a mercury arc polyphase converter. The con-

Design and Measurements of Capacitor Discharge Welding Transformers

T. W. DIETZ
NONMEMBER AIEE

G. M. STEIN
MEMBER AIEE

Synopsis: A method is presented to calculate the size of core and windings of a capacitor discharge welding transformer required to supply a given welding current. It is further shown how the resistance and inductance of a certain welder can be determined from oscillograms of the current and voltage. The mathematical derivation of the formulas used is included.

FOR THE SPOT WELDING processes, where high instantaneous or closely controlled welding currents are required, an energy storage system will be of advantage. For this purpose, the capacitor discharge system has been developed. One typical application for this type of welding is the light metals, like aluminum and magnesium alloys, which require a high instantaneous and also closely controlled welding current. Another example is found in stainless steel whose welding current has to be of very short duration if carbide precipitation is to be avoided.

A capacitor discharge welder fundamentally consists of a series *RLC* circuit, with the energy originally stored in the capacitor and then discharged through the *RL* portion of the circuit by means of some switching device.

The resistance and inductance of a typical aluminum welder are in the order of 50 microhms and 1 microhenry respectively. To quote a specific weld schedule for 0.102-inch 24 ST "alclad" aluminum, this impedance must be matched with 2,520 microfarads to give peak current 0.029 second after the start of the current wave. It is the function of the welding transformer to effect this impedance match.

A classical analysis of the circuit which has been worked out and expanded for the oscillating condition is included in the appendix.

Let us first study the design of the transformer. For this purpose we investigate a welder which has been built to make a given weld. The resistance and inductance of this welder can be obtained from 60-cycle measurements. The inductance so obtained will remain relatively constant over a wide variation of current wave lengths, so this value can be used without appreciable error, but the resistance may vary by 100 per cent or more due to skin effect as the wave length deviates from one-half of a 60-cycle wave. The curves in Figure 1 show the ratio of 60-cycle resistance to actual resistance under capacitor discharge conditions for various wave lengths of a standard "Hi-Wave" welder.

For determining the size of a transformer core of a new welder, the desired time T_m to the first peak current, the value I_{2a} of the first secondary peak current necessary to do the welding job in question must be known from previous welding experience, for they are the fundamental requirements to which the welder shall be designed.

Then, as shown in the appendix,

$$\phi_T = \frac{1}{N_2} I_{2a} L_2 \times 10^8 \lambda(\tau_0) \qquad (35)$$

Paper 46–41, recommended by the AIEE committee on electric welding for presentation at the AIEE winter convention, New York, N. Y., January 21–25, 1946. Manuscript submitted October 5, 1945; made available for printing December 7, 1945.

T. W. DIETZ is research engineer, The Taylor-Winfield Corporation, Warren, Ohio, and G. M. STEIN is transformer design engineer, Westinghouse Electric Corporation, Sharon, Pa.

---

trol impulse is taken from a potentiometer placed across the direct voltage. Faulty anode firing will cause changes in the direct voltage and these changes initiate the operation of the oscillograph.

Simultaneous oscillograms of the main direct potential e_{a-c}, the anode to cathode voltage e_{a-c} and the grid to cathode voltage e_{g-c} are obtained with a circuit similar to that shown in Figure 6. Figure 7 is an illustration of a photographic record of faults occurring in an inverter. The memory time for this oscillogram has a preset value of about 50 milliseconds. The reproduction does not show all of the "memory" present in the original film. The camera shutter coil received its impulse at *A*, and cathode ray beam blanking occurred at *B*. Time proceeds from left to right.

The anode to cathode potential in Figure 7 shows that the disturbance recorded is due to the preignition of one of the inverter anodes. The regularity of the grid to cathode voltage indicates that the grid of the specific anode under observation suffers no ill effect due to this transient. A study of the wave shapes shown reveals the phase in which the fault occurs and the moment of initiation. The time at which the oscillogram is taken is shown by the counter dial *C* in the figure.

Figure 8 is an example of loss of grid control on the anode being monitored, and Figure 9 is an illustration of a case in which a "backfire" and a subsequent "shoot-through" occur.

Concluding Remarks

The automatic memory oscillograph can serve successfully in studying transients of a random character. Oscillograms may be obtained which are of value in the investigation of faults in the operation of apparatus such as mercury arc converters. It is possible to obtain information concerning the type of fault, the moment of its occurrence, its duration, and its severity. These data are of value in stimulating research and development work on all types of electrical equipment. As a laboratory tool, the automatic memory oscillograph may far surpass the ordinary oscillograph in utility. Its application to the study of physical phenomena in all branches of engineering where random transients must be investigated is only a matter of time. The study of mechanical transients by converting them into electric pulses suggests itself. The advantages possessed by virtue of the fact that the operation of this oscillograph is completely automatic, are obvious.

References

1. A NEW HIGH-SPEED CATHODE-RAY OSCILLOGRAPH, H. P. Kuehni, S. Ramo. AIEE TRANSACTIONS, volume 56, 1937, June section, pages 721–8.

2. A MEMORY ATTACHMENT FOR OSCILLOSCOPES, W. E. Pakala. AIEE TRANSACTIONS, volume 57, 1938, December section, pages 682–4.

3. PHOTOGRAPHIC PATTERNS ON CATHODE RAY TUBES, Rudolph Feldt. *Electronics*, volume 17, February, 1944, pages 130–7.

4. A BEAM BLANKING CIRCUIT FOR OSCILLOSCOPES, Walther Richter. *Electronics*, volume 17, September, 1944, pages 128–30.

5. THEORY AND OPERATION OF ELECTRON TUBES (book), H. J. Reich. McGraw-Hill Book Company, New York, N. Y., page 206.

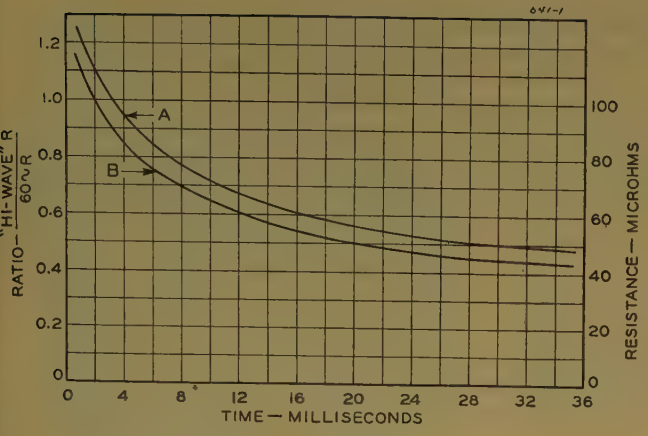


Figure 1. Variation of welder resistance as a function of wave shape

A—Ratio of actual resistance under capacitor discharge welding conditions, to 60∿ resistance, as a function of time to peak current

B—Total welder resistance referred to the secondary winding plotted against time to peak current

where

ϕ_T = maximum flux change
N_2 = secondary turns
R_2 = total resistance referred to secondary (ohms)
L_2 = total inductance referred to the secondary (henrys)
$\lambda(\tau_0)$ = a function of τ_0 (see Figure 2)

$$\tau_0 = \frac{T_0}{\pi}\frac{R_2}{2L_2}$$

T_0 = time to zero current (seconds)

The desired wave to make a given weld usually is expressed in terms of maximum current, and time to maximum current T_m; but T_0 is required to solve equation 35. Equation 28 shows the relationship of T_m and T_0, and can be solved for T_0 in the following way

Determine

$$g(\tau_0) = \frac{R_2}{2L_2} T_m$$

Obtain τ_0 from the curve $g(\tau_0)$ in Figure 2, and calculate $T_0 = \frac{2L_2}{R_2}\pi\tau_0$

Having evaluated τ_0, the amount of $\lambda(\tau_0)$ can be taken from the curve in Figure 2. The size of flux ϕ_T so obtained will be the total flux change. The first weld will leave the core magnetized with a residual flux which will vary with the type of core construction and the type of transformer steel used, but, in any case, it will be high enough to require a core of very large cross section unless it is compensated for. There are three ways to take care of this condition.

1. An air gap in the core for small transformers.

2. A magnetic flux bias by means of a direct current between welds.

3. Alternate reversal of the direction of the discharge through the welding transformer.

The third method will allow a simple economical design and therefore will be described in detail.

The residual flux for standard Hi-Wave transformers, when worked to maximum permissible flux density, is 42,000* lines per square inch and the core, which is made of special transformer steel, may be magnetized to 111,000 lines per square inch without measurable difference between primary and secondary ampere turns of the load current. This gives a maximum permissible flux density change per weld of 42,000 + 111,000 lines per square inch so that the net core area is total flux, as calculated by equation 35, divided by 153,000. Heating due to core loss need not be considered as even the highest welding speed possible at present would amount to only a very few cycles per second.

As can be seen from the problems just discussed, the accurate design of the core of a capacitor discharge welding transformer requires considerable experience, and measurements of similar setups, since most of the quantities which must be considered as known, vary with changing conditions of design, wave shape, and method of manufacture.

The next point for consideration is the copper.

Determination of effective current for the general circuit, that is for all combinations of L, R, and C, from the overdamped wave to a violently oscillating wave, is rather cumbersome from a mathematical approach.

A very large percentage of the total energy stored in the capacitor is lost in the welder and transformer so that we may assume, for design purposes, that the circuit must dissipate the total stored energy which may be expressed as

$$J = {}^1/_2 CE^2$$

joules per weld where

$$C = L_2\left[\frac{I_{2a}}{E}h(\tau_0)\right]^2 10^6 \text{ microfarad} \qquad (29)$$

C represents the capacity of the capacitor (microfarad). $h(\tau_0)$ can be taken from the curves in Figure 2.

The rate of energy dissipation or power will become

$$P = {}^1/_2 CE^2\frac{S}{60} \qquad (1)$$

Where J = energy in joules and S = average welding speed in spots per minute.

The power dissipated in the transformer will bear the same relation to the total power as its resistance referred to the secondary winding will bear to the total circuit resistance. It remains only to pick a desired efficiency η and, with welder resistance R_w known, to determine the corresponding total transformer resistance R_t referred to the secondary winding by the relationship $R_t = R_w\left(\frac{1}{\eta} - 1\right)$. With the resistance R_t determined, the copper sections can be calculated.

We now have iron cross section and copper cross section which furnish the physical size of the welding transformer. Having the loss and physical size, the temperature rise can be determined ac-

* The method of determining the residual flux will be presented later in this article.

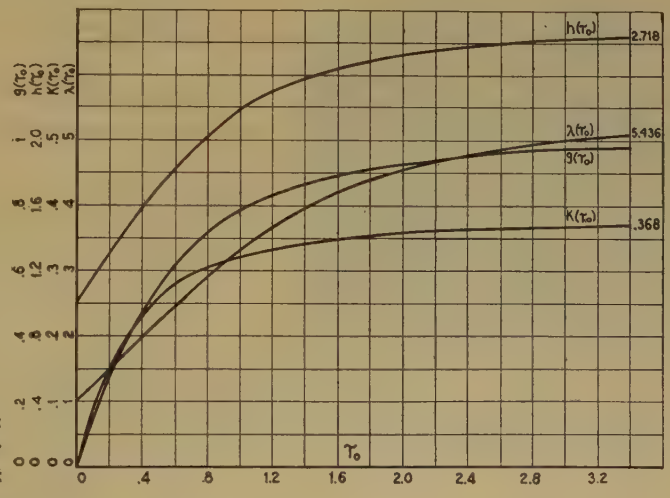


Figure 2. Characteristic functions of a capacitor discharge welding circuit

cording to standard transformer design practice which is outside the scope of this paper. The temperature rise may dictate water cooling which can be applied to the usually one turn secondary winding (see Figures 5 and 6), or it may require an increased copper section, or both.

The turns ratio remains to be fixed, and may be calculated from the expression

$$\frac{N_1}{N_2}=\frac{2Ek(\tau_0)}{I_{2a}R_2} \tag{30}$$

$K(\tau_0)$ can be taken from curves in Figure 2.

Measurements

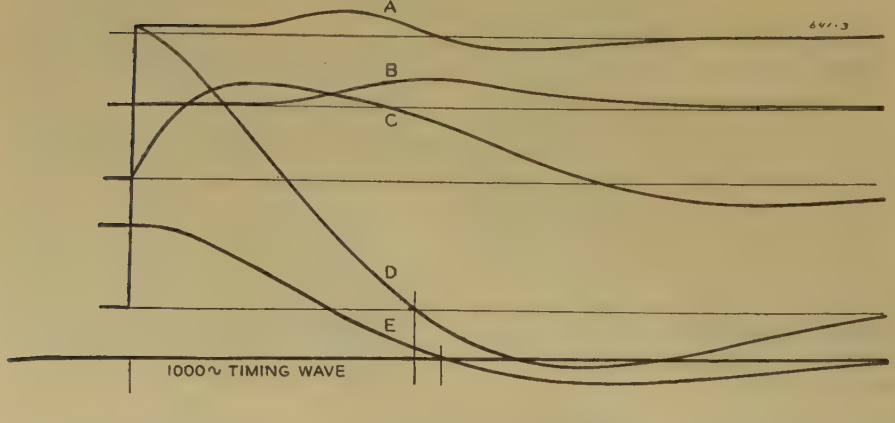
The accuracy of a design, such as we just have considered, will depend largely on the experience of the designer and can be relied upon only when a suitable safety factor is applied which would be the correct procedure for one-of-a-kind design. When the design is to be used for a standard-line, a pilot unit should be built and accurate measurements made in order that some of the original assumptions may become definitely known quantities.

As has been stated before, all the characteristics which are considered more or less constant in the average electric circuit vary as the turns ratio and capacity are varied. It is, therefore, necessary to make measurements under the desired conditions, or over a range of capacity and turns ratio so that curves can be drawn.

Oscillograms are to be made of the primary current, of the capacitor voltage, and of a timing wave, usually 1,000 cycles. (See Figure 3.) From this we can measure all characteristics of the wave necessary for determining primary resistance and inductance of the welder and transformer circuit.

Figure 3. Oscillogram taken in the primary circuit of a capacitor discharge welder

A—Magnetizing watts
B—Magnetizing current
C—Primary current
D—Induced voltage
E—Capacitor voltage



The inductance L_1 referred to the primary winding can be calculated according to equations 27 to 30, by substituting valves for g, h, and k, as

$$L_1=\frac{T_o^2\tan^2\pi\frac{T_m}{T_o}}{\pi^2C\left(1+\tan^2\pi\frac{T_m}{T_o}\right)}$$

The inductance L_2 referred to the secondary winding may be found from the relationship

$$L_2=\frac{L_1}{a^2}$$

where a = turns ratio.

The next step is the determination of the resistance of the circuit. From equation 31 we find

$$\frac{I_{1b}}{I_{1a}}=\epsilon^{-\pi\tau_0} \tag{31}$$

Where I_{1a} and I_{1b} are peak values of the primary current for the first and second half cycles respectively of the oscillating wave.

From equation 31 we find

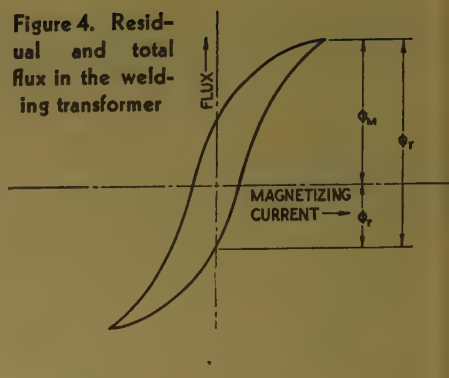
$$\tau_0=\frac{T_o}{\pi}\frac{R_1}{2L_1}=\frac{1}{\pi}\log_e\frac{I_{1a}}{I_{1b}}$$

and determine

$$R_1=\frac{4.61L_1}{T_o}\log_{10}\frac{I_{1a}}{I_{1b}} \tag{2}$$

Having obtained actual values of R, L, T_m, T_o, and I, it is possible to make a more accurate determination of total flux change, equation 35. In addition to this we will have to find the magnitude of the actual core flux. Furthermore, the entire mathematical analysis presupposes that applied voltage is equal to induced voltage, which is not strictly true, due to IR and IX drops in the transformer primary winding. The flux change, therefore, must be determined from induced voltage oscillograms.

Figure 4. Residual and total flux in the welding transformer



If the total flux change to produce a weld is ϕ_T, the residual flux is ϕ_r, and the maximum flux to which the iron actually is magnetized is ϕ_m (see Figure 4) then we may write

$$\phi_T=\phi_r+\phi_m \tag{3}$$

The unsymmetry of the hysteresis loop describing the reversal of the flux shall be neglected. Since we can test directly only ϕ_T, we must find a method to determine one of the other two quantities, ϕ_r or ϕ_m, in order to apply equation 3.

It was decided to measure the flux ϕ_m. As there are no pole manifestations on a transformer core, this could be done only by comparing the magnetizing current of a typical transformer with a d-c magnetization curve of the same transformer which had been prepared from 60-cycle oscillograms. To obtain the magnetizing current, it was necessary to connect the transformer primary winding in parallel with another identical transformer which had been installed in a welding machine in the normal manner. Both transformers had the same residual ϕ_r. The voltage wave form of the transformer under test was identical with that of the transformer which actually was welding, and as the test transformer's secondary winding was open, its primary winding carried only magnetizing current. After several previous discharges with the same energy, an oscillogram of the magnetizing current was taken, and its peak value was compared with the d-c magnetization curve to determine the flux ϕ_m. This value of ϕ_m is subject to the same error as that caused by considering capacitor voltage to be the same as transformer induced voltage, because the primary winding of the test transformer carries only magnetizing current, and hence the difference between induced voltage and applied voltage will be negligible. This means that the test transformer's induced voltage will be equal to the welding transformer's applied voltage. A correction factor for any one setting of capacity, voltage, and turns ratio can be established. If the total flux change is calcu-

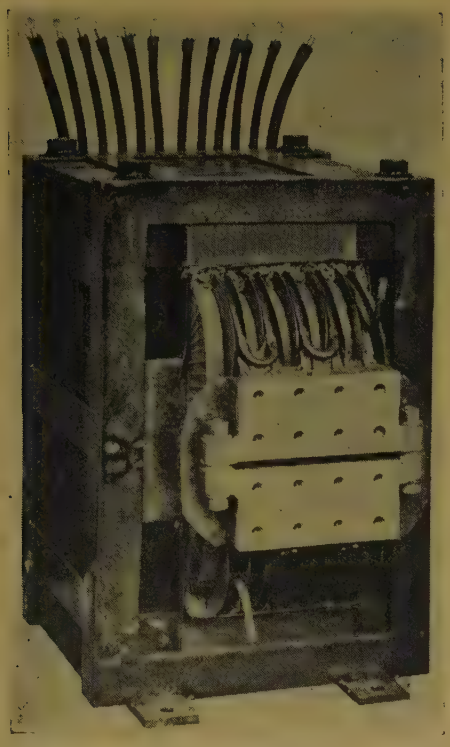


Figure 5. Standard "Hi-Wave" welding transformer

lated on the basis of capacitor voltage and called ϕ_{TC} and again is calculated on the basis of induced voltage and called ϕ_{TE}, then the actual flux to which the iron is excited may be stated as

$$\phi_m = \frac{\phi_{TE}}{\phi_{TC}} \phi_m \text{ (test)} \qquad (4)$$

if we assume the ratio of the corresponding residual fluxes ϕ_r is the same as that of the main fluxes ϕ_m and ϕ_m (test). It now remains to determine the total flux change accurately.

The fundamental voltage equation is

$$e = N\frac{d\phi}{dt} \times 10^{-8} \qquad (5)$$

where

N = number of turns
e = instantaneous voltage

From this we can write

$$\phi = \frac{10^8}{N} \int_{t_1}^{t_2} e dt \qquad (6)$$

where t_1 represents the time at the beginning of discharge and t_2 any time thereafter. Then $\int_{t_1}^{t_2} e dt$ represents the area under the voltage curve which equals

te (average) (7)

so that we may write total flux change

$$\phi_T = \frac{10^8 t}{N} e \text{ (average)} \qquad (8)$$

Inspection shows that this expression holds completely only for an oscillating condition where T_o is finite, since in a case where T_o is infinite, e will approach o and the expression becomes indeterminate. Equation 8 can be evaluated, however, for any portion of the wave so that we may evaluate from $t = o$ to a value of t where e (instantaneous) is practically equal to zero.

The value te (average) may be obtained from the area under the oscillogram of the voltage e by some graphical method.

In this way ϕ_{TC} can be determined from an oscillogram of the capacitor voltage. An induced voltage oscillogram will give the actual total flux change ϕ_{TE}.

The induced voltage can be measured by placing a search coil of several turns evenly distributed on the center core leg next to the iron.

To summarize:

1. Total flux change ϕ_{TE} can be determined by applying equation 8 to an induced voltage wave.

2. Maximum flux to which the core is excited is according to equations 4 and 8.

$$\phi_m = \frac{te \text{ (average) from induced voltage}}{te \text{ (average) from capacitor voltage}} \times \phi_m \text{ (test)} \qquad (9)$$

where ϕ_m (test) is read from a magnetization curve of the transformer in question, having measured its magnetizing current as described previously.

This method of determining maximum flux and flux change was developed to measure accurately the flux conditions of a previously designed line of transformers with a view of possible refinement of the design. Its usefulness lies in the fact that any piece of equipment whose induced voltage can be recorded on an oscillogram may be investigated, regardless of the complexity of the induced voltage wave.

Pictures of the assembly and of the secondary winding of a standard Hi-Wave CC1T capacitor discharge welding transformer are shown in Figures 5 and 6.

Appendix. Mathematical Analysis

Figure 7 shows a simplified capacitor discharge welding circuit for which we will use the following symbols:

e = voltage across capacitor (volts)
E = maximum or initial value of e (volts)
C = capacitance of capacitor (farads)
R_t; L_t = total resistance (ohms) and leakage inductance (henrys) of the welding transformer referred to the secondary side
R_w; L_w = total resistance (ohms) and inductance (henrys) of the external secondary welding circuit
R_C; L_C = total resistance (ohms) and inductance (henrys) of the external primary capacitor circuit
R_1; L_1 = resultant resistance (ohms) and inductance (henrys) referred to the primary side
R_2; L_2 = resultant resistance (ohms) and inductance (henrys) referred to the secondary side
N_1; N_2 = primary and secondary number of turns
$a = \frac{N_1}{N_2}$ = turns ratio
i_1; i_2 = primary and secondary currents (amperes)
I_1; I_2 = maximum values of i_1 and i_2 (amperes)
I_{1a}; I_{1b}; I_{2a}; I_{2b} = first and second maximum values of i_1 and i_2 for oscillating discharge (amperes)
kva_C = power rating of capacitor referred to 60-cycle excitation (kilovolt-amperes)
ϕ_T = maximum flux change of magnetic core flux of welding transformer (maxwells)
T = time (seconds) to any current peak $i_1 = I_1$ or $i_2 = I_2$
T_m = time (seconds) to first current peak
T_o = time (seconds) of half cycle of i_1 and i_2
T_C = time (seconds) to first zero e
n = number of current peaks up to time T

[Since R_c and L_c of the capacitor circuit may be neglected, we may write $R_2 = R_t + R_w$; $L_2 = L_t + L_w$]

The general circuit equations are

$$L_1\frac{d^2 i_1}{dt^2} + R_1\frac{di_1}{dt} + \frac{i_1}{C} = 0$$

$$i_1 = -C\frac{de}{dt}$$

Introducing

$$Z = \sqrt{\left(\frac{R_1}{2}\right)^2 - \frac{L_1}{C}} \qquad (10)$$

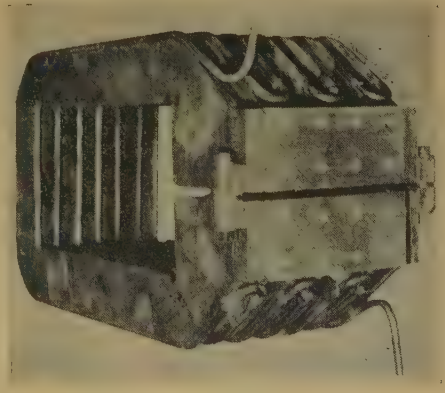


Figure 6. Standard "Hi-Wave" welding transformer secondary winding

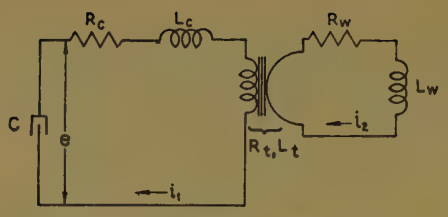


Figure 7. Simplified capacitor discharge welding circuit

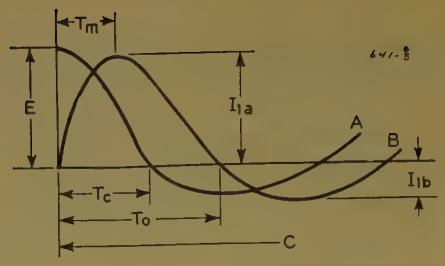


Figure 8. System of current and voltage oscillations of the primary capacitor circuit

A—Capacitor voltage e
B—Primary current i_1
C—Time t

The complete solution is

$$i_1 = A\epsilon^{-\frac{1}{L_1}\left(\frac{R_1}{2}-Z\right)t} + B\epsilon^{-\frac{1}{L_1}\left(\frac{R_1}{2}+Z\right)t}$$

$$e = A\left(\frac{L_1}{C}\right)\left(\frac{\epsilon^{-\frac{1}{L_1}\left(\frac{R_1}{2}-Z\right)t}}{\frac{R_1}{2}-Z}\right)+B\left(\frac{L_1}{c}\right)\times\left(\frac{\epsilon^{-\frac{1}{L_1}\left(\frac{R_1}{2}+Z\right)t}}{\frac{R_1}{2}+Z}\right)$$

where A and B are constants of integration. A and B are determined from the boundary conditions $t=O$; $i=O$; $e=E$ so that we obtain

$$i_1 = \frac{E}{Z}\epsilon^{-\frac{R_1}{2L_1}t}\sinh\frac{Z}{L_1}t \tag{11}$$

$$e = E\epsilon^{-\frac{R_1}{2L_1}t}\left[\frac{R_1}{2Z}\sinh\frac{Z}{L_1}t+\cosh\frac{Z}{L_1}t\right] \tag{12}$$

to get the maximum value I_1 of i_1 determine $\frac{di_1}{dt}$ from equation 11, equate to zero, solve for i_1, introduce $i_2=ai_1$; $a^2R_2=R_1$; $a^2L_2=L_1$, and obtain

$$T = \frac{L_1}{Z}\tanh^{-1}\frac{2Z}{R_1} \tag{13}$$

$$I_1 = E\sqrt{\frac{C}{L_1}}\epsilon^{-\frac{R_1}{2L_1}T};\quad I_2 = E\sqrt{\frac{C}{L_2}}\epsilon^{-\frac{R_2}{2L_2}T} \tag{14}$$

The foregoing solutions are general. For a numerical application the following three special cases should be considered.

Case 1. Aperiodic Discharge

$\left(\frac{R_1}{2}\right)^2 > \frac{L_1}{C}$; Z of equation 10 is real so that we may apply equations 10 to 14 directly. Since there is only one maximum $I_1=I_{1a}$ or $I_2=I_{2a}$ of the currents i_1 and i_2, we may write $T=T_m$ and obtain for

$$\text{kva}_C = \frac{1}{2}(2\pi 60)\frac{CE^2}{1{,}000}$$

the expression

$$\text{kva}_C = 0.1885 I_{2a}^2 L_2 \epsilon^{\frac{R_2}{L_2}T_m} \tag{15}$$

or

$$\text{kva}_C = > 1.4 I_{2a}^2 L_2$$

$$e = E\left(\frac{R_1}{2L_1}t+1\right)\epsilon^{-\frac{R_1}{2L_1}t} \tag{22}$$

$$T = T_m = \frac{2L_1}{R_1} \tag{23}$$

$$I_2 = 0.368\sqrt{\frac{C}{L_2}}E \tag{24}$$

$$\text{kva}_C = 1.4 I_{2a}^2 L_2 \tag{25}$$

In spite of the fact that equations 11, 17, and 21, for example, are of greatly different form, it can be seen from the reasoning in developing equation 21 from 17, and a similar process could be applied to develop equation 21 from equation 11, that for $\left(\frac{R_1}{2}\right)^2 \leqslant \frac{L_1}{C}$ the equations 21 to 25 could be used, without great error for either case 1 or 2.

For the purpose of machine design, equations 15 to 20 for the periodic discharge case 2 shall be transformed so that the desired machine constants may be determined for any specific wave form. In this analysis R_2 and L_2 are fixed with the selection of the size and form of the welding throat as well as of the efficiency and per cent impedance of the welding transformer. I_2 and T_m are determined by the desired welding effect, and E may be fixed if we standardize on a certain value of capacitor voltage.

If instead of T_m the time T_o of the first half current cycle is introduced, it will be possible to determine explicitly, all other values, like $a=\frac{N_1}{N_2}$; I_{1a}; E; ϕ_T; L_1 and R_1 as functions of the given circuit constants. T_o is obtained from equation 17 for $i=o$ by

$$\frac{Z}{L_1}T_o = \pi$$

or

$$T_o = \frac{L_1\pi}{Z};\quad Z = \sqrt{\frac{L_1}{C}-\left(\frac{R_1}{2}\right)^2} \tag{26}$$

This value of T_o is introduced into equations 15 to 20 by combining the functions

$$\left.\begin{aligned}\tau_o &= \frac{T_o}{\pi}\frac{R_2}{2L_2}\\ g(\tau_o) &= \tau_o\tan^{-1}\frac{1}{\tau_o}\\ h(\tau_o) &= \epsilon^{g(\tau_o)}\\ k(\tau_o) &= \frac{\tau_o}{\sqrt{1+\tau_o^2}}\frac{1}{h(\tau_o)}\\ \lambda(\tau_o) &= \frac{\tau_o}{\sqrt{1+\tau_o^2}}h(\tau_o)\left[\frac{-\pi\tau_o}{k(\tau_o)}+2\right]\end{aligned}\right\} \tag{27}$$

$g(\tau_o)$; $h(\tau_o)$; $k(\tau_o)$; $\lambda(\tau_o)$ are plotted against τ_o in Figure 2. Using the values taken from these curves, we may write instead of equations 15 to 20

$$T_m = \frac{2L_2}{R_2}g(\tau_o);\quad T = T_m+(n-1)T_o;\quad T_C = T_o - T_m \tag{28}$$

Case 2. Periodic Discharge

$\left(\frac{R_1}{2}\right)^2 < \frac{L_1}{C}$; Z of equation 10 is imaginary so that we transform

$$\sqrt{\left(\frac{R_1}{2}\right)^2-\frac{L_1}{C}} = j\sqrt{\frac{L_1}{C}-\left(\frac{R_1}{2}\right)^2}$$

By using a real

$$Z = \sqrt{\frac{L_1}{C}-\left(\frac{R_1}{2}\right)^2} \tag{16}$$

we may write instead of equations 11 to 14

$$i_1 = \frac{E\epsilon^{-\frac{R_1}{2L_1}t}}{Z}\sin\frac{Z}{L_1}t \tag{17}$$

$$e = E\epsilon^{-\frac{R_1}{2L_1}t}\left[\frac{R_1}{2Z}\sin\frac{Z}{L_1}t+\cos\frac{Z}{L_1}t\right] \tag{18}$$

$$T_m = \frac{L_1}{Z}\tan^{-1}\frac{2Z}{R_1};\quad T = T_m+(n-1)\pi\frac{L_1}{Z} \tag{19}$$

The expressions for I_1 and I_2 remain the same as in equation 14 while I_{1a} and I_{2a} are represented by

$$I_{1a} = E\sqrt{\frac{C}{L_1}}\epsilon^{-\frac{R_1}{2L_1}T_m};\quad I_{2a} = E\sqrt{\frac{C}{2L}}\epsilon^{-\frac{R_2}{2L_2}T_m} \tag{20}$$

Kva_c is given by equation 15 and lies between the limits

$$0.1885 I_{2a}^2 L_2 < \text{kva}_C < 1.4 I_{2a}^2 L_2.$$

Case 3. Limit of Aperiodic Discharge

$\left(\frac{R_1}{2}\right)^2 = \frac{L_1}{C}$; Z becomes zero. In substituting $Z=0$ in equations 17 to 19 we have to evaluate the expressions

$$\lim_{Z\to 0}\left(\frac{\sin\frac{Z}{L_1}t}{Z}\right) = \frac{t}{L_1};\quad \lim_{Z\to 0}\left(\frac{\tan^{-1}\frac{2Z}{R_1}}{Z/L_1}\right) = \frac{2L_1}{R_1}$$

and obtain, instead of equations 15 and 17 to 19

$$i_1 = \frac{E}{L_1}t\epsilon^{-\frac{R_1 t}{2L_1}} \tag{21}$$

Phonograph Reproducer Design

W. S. BACHMAN
NONMEMBER AIEE

PHONOGRAPH reproducers, which convert the mechanical motion of the stylus to a corresponding electric voltage, have been in commercial use for the past two decades. They have employed a wide variety of voltage generators such as carbon microphone buttons, variable reluctance magnetic circuits, moving coils in magnetic fields, and Rochelle salt crystals. Although excellent performance has been obtained with many of these types, there has been a continued effort to reduce the mass of the moving system and to simplify the mechanical construction, even to the extent of sacrificing output voltage.

While the carbon button type of reproducer was one of the first to appear, it was soon outmoded by subsequent types. The variable resistance principle, however, again is employed in one of the reproducers to be described in this paper. An important difference between it and the carbon button type is that the variable resistance element is a fine metallic wire the resistance of which changes in response to strain. These wires may be of the same material as is used in strain gauges, but in this case there is no need to determine the absolute value of the strain, since only the voltage resulting from the change in strain is utilized. This imposes the requirement of linearity, if distortion is to be avoided, which easily is met by most of the commonly used strain sensitive wires. Measurements have shown that the ratio of change of resistance to change of length is constant through and even beyond the elastic limit of the wire.[1]

One of the first successful designs employing a wire resistance strain element is shown in Figure 1. The stylus is carried in a small cantilever beam 9, and the strain element 14 is attached to it at a point about 1/3 of its length from the fixed end. The strain wire is held in tension sufficient to stress it about halfway to its elastic limit by the piano wire springs 15, and the Textolite pins 16 serve as snubbers to prevent the tension springs from following the motion of the cantilever. The circuit employed to polarize this reproducer is shown in Figure 2.

Since the voltage derived from the strain is proportional to the displacement, the output of this reproducer is proportional to the displacement of the stylus by the record. This makes it easy to check the frequency characteristic without knowing the actual displacements which are pressed on a frequency, or constant tone record. If the same band is driven at various speeds, the amplitude of the reproduced wave should be the same. This was found to be true from 10,000 cycles down to the low frequency resonance except for a wave form distortion at about 6,500 cycles, which was found later to be caused by the second mode of vibration of the cantilever which occurred at 13,000 cycles. This could be damped readily by placing a small block of a material such as Pyralin approximately at the loop of the second mode of vibration, at which point a negligible amount of loading would be reflected to the stylus tip for the fundamental mode of vibration. These modes of vibration are shown in Figure 3.

Although the output voltage was low, about −65 decibels below 6 milliwatts with a displacement of 0.0003 inch (Columbia WT-1, frequency record, 1,000 cycle band), the performance was very nearly ideal. In order to avoid variations in tension the design shown in Figure 4 was evolved. The strain wires were soldered to 1/16 inch diameter rods which were free to move axially in holes provided in the Textolite mounting block. The tension, as previously, was applied by means of piano wire springs, but instead of the snubbers the rods were lubricated with a viscous liquid which readily permitted them to move slowly in an axial direction to equalize variations in tension in the strain wire, but offered a high impedance to the motion resulting from the rapid strain variations due to the useful stimulation of the cantilever. In other words the strain wires were resistance terminated.

Another solution of the termination problem is shown in Figure 5. In this model use is made of the fact that an increase in strain on one side is accompanied by a decrease on the other. If both ends were terminated at the same point, the two forces would balance out. The tiny bell cranks 35 at the root of the cantilever serve to change the direction of the strain by approximately 90 degrees, and the ends of the strain element both are attached to the yoke 36, which applies the desired tension to them.

All of these designs require the use of the strain elements under tension, restricting their operating range to about half of their potential range. In order to make use of the compression as well as the tension range, the design in Figure 6 was developed. Although not shown in the

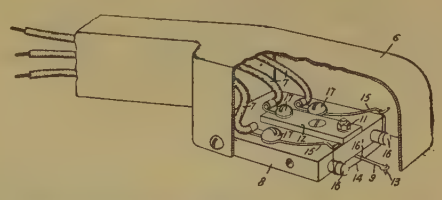


Figure 1. Early form of strained wire resistance reproducer

Paper 46-32, recommended by the AIEE committee on communication for presentation at the AIEE winter convention, New York, N. Y., January 21–25, 1946. Manuscript submitted November 19, 1945; made available for printing December 17, 1945.

W. S. BACHMAN is with the General Electric Company, Bridgeport, Conn.

$$C = L_2\left[\frac{I_{2a}}{E}h(\tau_0)\right]^2 10^6 \text{ microhms} \quad (29)$$

or

$$E = \sqrt{\frac{L_2}{C}}\, I_{2a} h(\tau_0) 10^3$$

$$\frac{N_1}{N_2} = \frac{E}{I_{2a}}\,\frac{2k(\tau_0)}{R_2} \quad (30)$$

or

$$I_{2a} = \frac{N_2}{N_1}\,\frac{2k(\tau_0)}{R_2}\,E$$

$$\frac{I_{2b}}{I_{2a}} = \frac{I_{1b}}{I_{1a}} = -\epsilon^{-\pi\tau_0} \quad (31)$$

$$\frac{i_2}{I_{2a}} = \frac{\tau_0}{k(\tau_0)}\,\epsilon^{-\tau_0\pi\frac{t}{T_0}} \sin \pi\frac{t}{T_0} \quad (32)$$

$$\frac{e}{E} = \epsilon^{-\tau_0\pi\frac{t}{T_0}}\left[\tau_0 \sin \pi\frac{t}{T_0} + \cos \pi\frac{t}{T_0}\right] \quad (33)$$

$$\text{kva}_C = 0.1885 L_2 [I_{2a} h(\tau_0)]^2 \quad (34)$$

Calculate also

$$\phi_T = \int_0^{T_0} \frac{e 10^8}{N_1}\, dt$$

and obtain

$$\phi_T = \frac{1}{N_2} I_{2a} L_2 10^8 \lambda(\tau_0) \quad (35)$$

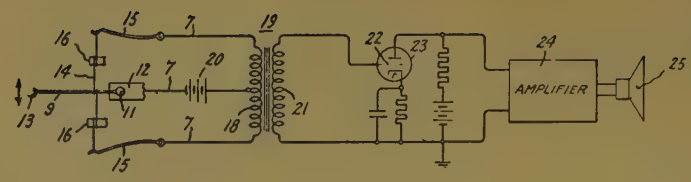


Figure 2. Circuit for polarizing variable resistance reproducer

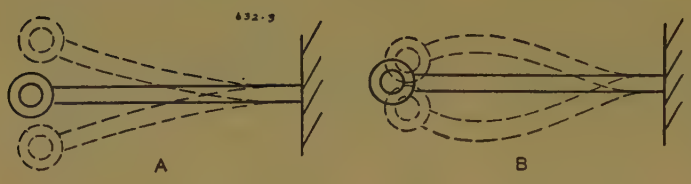


Figure 3

A—Normal mode of vibration of cantilever stylus support
B—Second mode of vibration

figure, the back end of the cantilever 55 is fastened to a stud which mounts rigidly to the tone arm. In it the strain wires were cemented to the cantilever itself to measure the strains in the outer fibers of the beam. Being attached in repose, they are subjected to both tension and compression. Although a strain element need be applied to only one side of the cantilever, it actually was applied to both, principally to permit balancing of the direct current in the primary winding of the input transformer. In this form the resistance reproducer lends itself readily to the application of a new technique for the damping of the resonance between the supporting arm mass and the suspension compliance.

It is usual, in most pickup designs to obtain damping of this resonance by introducing some dissipation in the pivots or bearings, such as by the use of rubber sleeves or blocks on the axis of oscillation. This imposes an additional load upon the record, as may be seen from a study of the electrical equivalent of the mechanical system, as shown in Figure 7.

Inspection of the equivalent electric circuit of such a reproducer, Figure 7B, shows that the presence of R is desirable to limit the impedance rise at the resonance frequency. In the useful audible range above the resonance the proper operation of the pickup depends upon the motion of M being negligible in response to signal stimulation. This requires that practically all of the applied motion be suffered by R and C (practically all of the current must travel through the path R, C). If R were omitted, the needle point impedance would decrease with frequency, but in the equivalent circuit it readily is seen that it can never drop below R as the frequency increases.

To give a quantitative illustration of the importance of this problem, consider a pickup and tone arm assembly having an effective arm mass (referred to the needle point) of 30 grams and a suspension compliance of 10^{-6} centimeter per dyne. For critical damping of the arm resonance it would require

$$R^2=\frac{4M}{C}=\frac{4\times 30}{10^{-6}}=120\times 10^6$$

$$R=10.9\times 10^3\ \frac{\text{dyne seconds}}{\text{centimeters}}$$

Under stimulation of 15 centimeters per second, a quite usual value of velocity, a lateral force of

$$F=RV-10.9\times 10^3\times 15=165\times 10^3 \text{ dynes or } 167 \text{ grams}$$

would be developed. Assuming 45-degree inclined groove walls, a bearing weight of 5.9 ounces would be necessary to keep the needle in contact with the groove.

Of course it is not necessary to provide critical damping of the tone arm resonance, but, if the damping is not sufficient, the reproducer will be very unstable when shock excited and even may tend to jump out of the grooves of a warped or uneven record. In many designs the bearing upon the record is made large for this reason alone.

Because of the extremely small size of the generator unit shown in Figure 6 and the fact that the output voltage is obtained as a result of the bending of the cantilever only, it became possible to apply a new arm resonance damping technique. The mechanical schematic of the system is shown in Figure 8A. The electrical equivalent of the system is shown in 8B. It is obvious in the circuit of 8B that the resonance may be damped critically without any increase in the mechanical impedance above resonance. Such a system is not mechanically stable, however, as is evident from inspection of Figure 8A. In this mechanical system there is no restoring force available to keep the needle point and the arm from wandering away from each other as energy is dissipated in R. In other words the resistor must be restricted from any except oscillatory motion. This is done by the system shown in 8C and 8D. If C_2 is made very large, the circuit of 8B approaches the performance of 8C, except that a new resonance, which would be damped only very lightly, appears at the frequency where the reactance of C_1 and C_2 in parallel is equal to the reactance of m. By proper choice of C_1 and C_2, R may be made effective for both resonance frequencies, as may be seen from the curve of mechanical impedance at the needle point versus frequency shown in Figure 9.

Figure 10 shows a design of the resistance pickup employing this new type of arm resonance damping. Corresponding to the element R in Figure 8 are the rubber sleeves bearings 72, and the Pyralin disc 74; all are in torsion. The compliance C_2 is that of the spring 80. This reproducer with only 15 grams of bearing weight on the record would not leave the groove even with quite violent shocks ap-

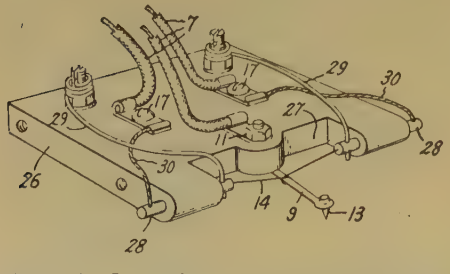


Figure 4. Strained wire resistance reproducer with means for maintaining uniform tension in resistance wire

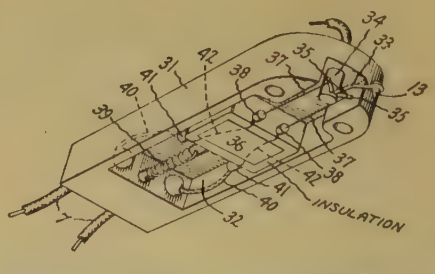


Figure 5. Alternate form of strained wire resistance reproducer in which opposing strains are balanced against each other

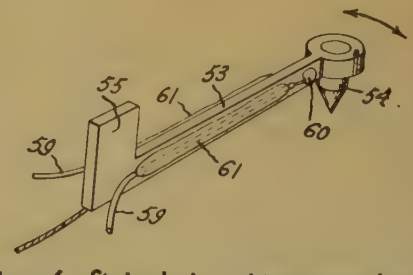


Figure 6. Strained wire resistance reproducer element having strain wires applied directly to the cantilever to measure strain in its outer fibers

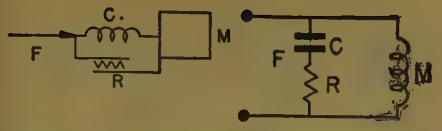


Figure 7A (above, left). Mechanical schematic diagram of a reproducer having damping material at its pivots

F = force exerted by needle upon record
C = compliance of suspension
R = mechanical resistance represented by the damping material
M = mass of cartridge and arm
Mass of needle is neglected being insignificant at low frequency

Figure 7B (above, right). Electrical equivalent of mechanical system shown in Figure 7A (motions of the mechanical elements are represented as currents in the electric network)

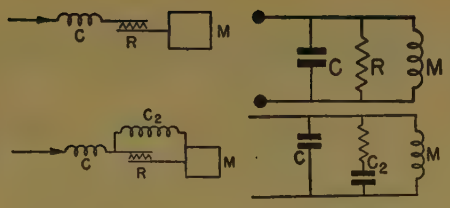


Figure 8A (above, upper left). Mechanical schematic diagram of a reproducer having a preferred form of low frequency resonance damping

Figure 8B (above, upper right). Electrical equivalent of system shown in Figure 8A

Figure 8C (above, lower left). Practical mechanical system retaining advantages of idealized system shown in Figure 8A

Figure 8D (above, lower right). Electrical equivalent of system shown in Figure 8C

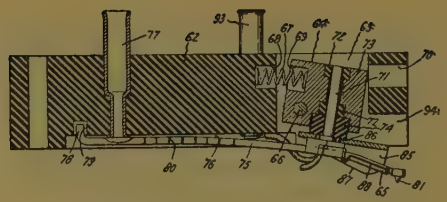


Figure 10. Design of strained wire resistance reproducer utilizing element of Figure 6 and having damping applied as shown schematically in Figure 8C

plied to the motor board and turntable. The effect of this damping system was observed by watching the displacement output of the reproducer on an oscilloscope while a tone band of a frequency record was allowed to coast down from rated speed to zero. The observed amplitude remained uniform until the resonant frequency, approximately 25 cycles, was nearly reached, below which the amplitude dropped smoothly. No rise before cutoff occurred.

While the strained wire resistance reproducer provides nearly ideal performance, the techniques acquired during its development are by no means limited to its type of generator element. The following is a description of a variable reluctance or magnetic type of reproducer embodying similar mechanical design considerations.

The fact that even a simple cantilever carrying the stylus at its free end required some damping to restrain its second mode of vibration, as mentioned in reference to Figure 3, made it very evident that no more complicated system could be relied upon to transmit the motion of the stylus tip to an armature or reed without introducing a frequency characteristic describing their relative motions. Accordingly a design was worked out in which the armature is right at the stylus, so that the motion of the armature is inseparably that of the stylus. Obviously this design could have no frequency characteristic as long as the stylus properly traces the groove, the output voltage being proportional to the stylus velocity.

The armature is a steel ribbon having a cross section of 0.010 inch by 0.030 inch. As may be seen from Figure 11, it has a 90 degree twist near the fixed end, which makes possible nearly as much compliance in the vertical direction as is provided laterally. This is desirable to permit the stylus to recede within the guard, provided by the two pole faces, when subjected to excessive downward forces such as in dropping. The small block of Pyralin just forward of the twist provides sufficient damping to restrain the second mode of vibration of the cantilever, which has already been discussed. At the free end the width of the armature is increased to receive the stylus. The dynamic mass of this stylus armature assembly is in the order of 8 milligrams. This mass is suspended on the spring, represented by the cantilever, the mechanical schematic of which is shown in Figure 12A. The electrical equivalent, Figure 12B, is a simple series circuit which expresses the mechanical impedance at the stylus tip. At low frequencies the system is stiffness controlled, and the impedance therefore decreases linearly with frequency until the resonance of M_1 and C is reached. The impedance at this resonance becomes very nearly zero, since very little mechanical resistance is reflected to the stylus tip from the Pyralin damping block attached near the fixed end of the cantilever. This, then, is the frequency at which practically no force is required to move the stylus, and with the values of

Figure 9. Low frequency needle point impedance and response of magnetic phonograph reproducer

⊙ Measured values

$\text{Response} = \frac{B_e}{Y}$

$C = 0.875 \times 10^{-6}$ centimeter per dyne
$C_2 = 3.54 \times 10^{-6}$ centimeters per dyne
$R = 6{,}000$ dyne seconds per centimeter

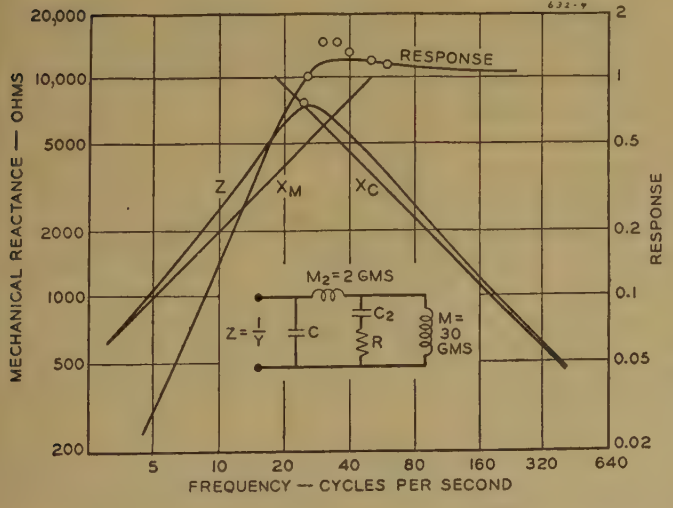
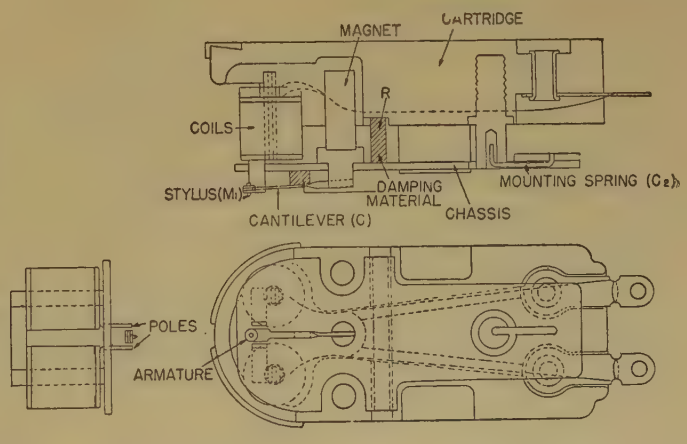


Figure 11. Magnetic or variable reluctance reproducer



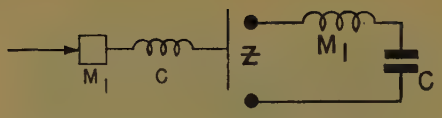


Figure 12A (left). Mechanical schematic of the stylus cantilever assembly. The fixed end of the cantilever is assumed to be rigid, which is very nearly so at high frequencies

M_1 is the dynamic mass of the stylus assembly
C is the compliance of the suspension

Figure 12B (above, right). Electrical equivalent of system shown in Figure 12A

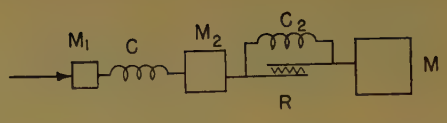


Figure 13A. Mechanical schematic of magnetic pickup

M_1 is the dynamic mass of the stylus assembly
C is the suspension compliance
M_2 is the mass of the coils, poles, and magnet assembly
R is the arm resonance damping
C_2 is the compliance which provides the operating point for R
M is the cartridge and arm mass

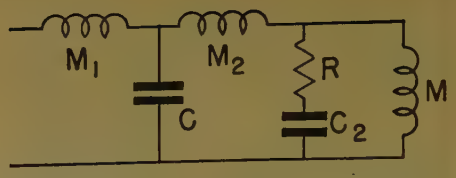


Figure 13B. Electrical equivalent of system of Figure 13A

dynamic mass and suspension compliance noted previously it occurs at approximately 2,300 cycles per second.

Above this resonance the system is mass controlled, the impedance rising linearly with frequency. Because the mass is so small, this system will remain in contact with both side walls of a 45 degree inclined side wall groove under acceleration of 2,000 g with a bearing weight upon the record of only 16 grams.

The mechanical system shown in Figure 12 accurately represents the needle point impedance except at the low frequency end of the range, where the dynamic mass of the arm and cartridge resonates with the compliance C. This condition was discussed with reference to Figure 8, and the same treatment for the control of this resonance is applied to this magnetic design. Again referring to Figure 11, the poles, coils, magnet, and armature all are mounted upon a chassis which is spring-mounted to the cartridge and arm assembly. Between the chassis and cartridge another block of Pyralin is inserted which provides the mechanical damping resistance, R. The mechanical system of the magnetic reproducer is shown in Figure 13A. It differs from that of Figure 8C in the presence of M_2. If this mass is too large, the resonance of M_2 with C and C_2 in series may be low enough so that R is not very effective, giving another frequency at which high impedance appears at the needle point. If M_2 is small enough to avoid this condition, it may be neglected. In this particular design the total weight of the magnet, coil, poles, and chassis assembly is approximately two grams. Figure 9 shows the calculated mechanical impedance, Z, of the magnetic reproducer, taking M_2 into account. The two asymptotes which the curve approaches correspond to the reactances of the suspension compliance C, and the total mass, M_1 and M. It is seen that the resonant rise is very slight.

The frequency response characteristic of this reproducer may be calculated by finding the ratio of the admittance of the path through C, referring to Figure 9, to the total admittance of the circuit. This is the same as the ratio of the motion of the cantilever to the motion imparted to the stylus tip, the open circuit voltage output of the reproducer being proportional to the velocity of motion of the cantilever. The network may be considered to be fed from a constant current source, the record groove being a stiff or high impedance source.

Also plotted in Figure 9 are measured values of response which were obtained by first measuring the output of the cartridge supported in an arm, and repeating the run with the cartridge clamped in a vise, the ratio of these values indicating the low frequency response. The source for these measurements was a crystal cutter head the exact mechanical impedance of which was not determined but which, because of the head's very evident stiffness, was regarded to be high. The agreement with the calculated response is reasonable considering this and also that the damping material is not a pure mechanical resistance. Similar technique was employed as mentioned previously in the case of the resistance pick-up for determining the response in the range above arm resonance, with the important difference that the electric output was integrated before being fed to an oscilloscope. Under these conditions no change in amplitude of the trace was observed, regardless of the rotational speed, below 78 rpm at which any tone band from 10,000 cycles down was driven. This indicates the absence of any frequency characteristic from 10,000 cycles down to the region in which the arm resonance occurs.

Reference

1. Characteristics and Aircraft Applications of Wire Resistance Strain Gauges, A. V. deForest, *Instruments*, volume 15, April 1942.

Technique of Electrical and Hydraulic Testing of Hydroelectric Units

G. D. FLOYD
MEMBER AIEE

J. J. TRAILL
NONMEMBER AIEE

Synopsis: The application of the AIEE Test Code for Synchronous Machines in field testing of hydroelectric generators is discussed, and the preferred method of making certain tests is indicated, together with reasons for its selection. Methods of making acceptance tests on turbines are outlined in sufficient detail to establish the fundamental theory, and the electrical measurements on the generator required to establish the generator input for the hydraulic test, are listed, with brief reference to the accuracy required, and to means of obtaining it. Rating and other hydraulic tests on hydroelectric units are also described.

ALTHOUGH commercial or acceptance testing of hydroelectric units has been the rule rather than the exception, very little has been written of the technique, especially of matters peculiar to field testing. The Test Code for Prime Movers of the American Society of Mechanical Engineers,[1] has been available for some years, and the AIEE Test Code for Synchronous Machines[2] was approved recently. The latter "provides in convenient reference form the more generally applicable and accepted methods of conducting and reporting tests of a commercial nature, which apply to the fulfillment of performance guarantees and to acceptance tests." This code serves a very useful purpose, permitting manufacturer and purchaser to agree on methods of conducting tests, and avoiding the necessity of specifying in detail how performance guarantees may be determined. It is the purpose of this paper to discuss:

1. The application of the Test Code for Synchronous Machines to field testing of hydroelectric generators, noting especially which methods given in the code can be used, and why alternative methods are unsuitable.

2. Certain aspects of field testing of hydraulic prime movers.

3. The frequent necessity for making electrical measurements on the generator when the primary test is on its associated turbine, and the method of measurement and accuracy required.

It is not the purpose of the paper to record methods of making either electrical or hydraulic tests where the technique is routine and straightforward, and presents no difficulties other than those usually present when tests are made on any generator or its prime mover.

Paper 46-70, recommended by the AIEE committee on power generation for presentation at the AIEE winter convention, technical meeting, New York, N. Y., January 21–25, 1946. Manuscript submitted November 26, 1945; made available for printing December 13, 1945.

G. D. FLOYD is electrical consultant, electrical engineering department, Hydro-Electric Power Commission of Ontario, Toronto, Ontario, Canada; J. J. TRAILL is with the same company.

Electrical Tests

General

In the great majority of cases, hydroelectric generators are erected on the site. The stator iron and complete stator winding in the larger units are often assembled in the field, and field poles mounted on the rotor spider or rim. Even when the above operations can be performed in the factory the assembly of the unit is of necessity a field job, and any tests on the completed generator must be performed at the site, after erection is completed. This situation produces the first peculiarity in testing under field conditions, in that the facilities for testing may be, and usually are, restricted greatly, compared to those usually available in the factory. Restrictions may be imposed by units already in routine operation in the plant, by construction, and because the generator is permanently connected to its bus, and in fact, may have been in commercial operation before certain of its acceptance tests are made. The site may be many miles from the factory, and from the utility's laboratory. It is, therefore, essential, before proceeding to the site to make the required tests, that the specification be carefully examined, the tests to be made listed, and the methods of making them discussed. It is of the utmost importance to list all portable instruments likely to be required, of such ranges as will accommodate the potential and current transformers associated with the generator. It is very seldom necessary to provide special potential or current transformers for routine acceptance tests. Where tests of a special nature are included, it may be necessary to devise special equipment to obtain the desired measurements. All this work should be done, if possible, before the tests are started; otherwise a great deal of time may be lost, or one or more tests may have to be abandoned for lack of the proper equipment for making them.

Resistance Measurements*

Hydroelectric generators, except for units of low kilovolt-ampere rating, have very low armature and field winding resistances. Special artifices are often necessary to obtain an accurate measurement of resistance. The voltammeter method is usually employed, as use of the Kelvin bridge is not practicable for field measurements. Battery voltage and low range voltmeter have been found to be satisfactory, with the usual precautions. If the armature winding is two, three, or four circuit, as is frequently the case, each circuit can be measured separately, or all windings in one phase may be connected in series and the voltage drop across each measured. Temperature detectors almost always are specified for the hydroelectric generator, and are used to measure the winding temperature. Care must be taken to have the generator in thermal equilibrium at the time resistance measurements are made. The test current must not be so great that the winding temperature is affected by the copper loss due to the current.

The field resistance at a known temperature is required for the following reasons:

1. To determine accurately the field I^2R loss.

2. To determine the temperature rise of the field.

3. To calibrate the field temperature indicator if such is provided.

The voltammeter method should be used to make this measurement, as the "hot" resistance, of necessity, must be determined by this method. The measurement of temperature of a winding by its change in resistance requires that every source of error be minimized. The cold and hot resistances should be measured with the same instruments, and with deflections on the instruments of the same order of magnitude.

Telephone Interference Factor

Although hydroelectric generators of modern design have a telephone interference factor low enough to prevent disturbance in telephone circuits, it is possible that disturbing harmonics inadvertently may be present in the voltage wave. Conditions at some remote point, where a power and communication circuit are in-

* The sequence of these notes has been made generally the same as in the Test Code for Synchronous Machines.

volved in a parallel may be magnified by the presence of these harmonics. Measurement of the telephone interference factor is recommended where equipment is available to determine this factor, especially if the design of the generator winding is limited in freedom of choice to the point where it becomes difficult to eliminate undesirable harmonics.

Phase Characteristic Curves (V Curves)

These curves offer the best method of determining the excitation values at all loads and power factors. As discussed later under load excitation, the zero power factor saturation curve used with the open circuit saturation curve to obtain the excitation characteristics is always difficult and often impossible to obtain. It is not usually possible to set the voltage, load, and power factor at exactly the value desired when the unit is operating on the system. Small deviations from the desired values, especially in power factor, cause relatively large changes in field current. The phase characteristic curve permits greater accuracy in the determination of excitation under any condition of load, provided the voltage can be held close to normal value.

Line Charging Capacity

This characteristic may be important in the case of hydroelectric generators because the units are usually associated with a transmission network of high-voltage lines. Voltage must be built up on a line for line testing, and the generator should have sufficient line charging capacity to permit this without becoming self-exciting. Self-excitation is an unstable condition, leading to high and uncontrolled voltage on the generator and system being tested. Excitation can be reduced to zero on a hydroelectric generator with safety, and even made slightly negative, with the generator under test connected to the system. Provided the kilovars taken by the generator are not large enough to disturb system conditions, the ability of the generator to supply line charging kilovars thus can be determined exactly.

Load Excitation

It is frequently difficult or impossible to obtain a saturation curve at zero power factor and rated amperes on a hydroelectric generator. The difficulty arises because it is impossible to circulate full load current between one generator and another of equal size, even if both can be synchronized on the same low-voltage bus. It is sometimes possible to synchronize the generator with the system, and obtain one or perhaps two points on the curve at or near normal voltage. A third point is available at zero voltage from the short-circuit impedance curve. Such meager data are insufficient to plot an accurate zero-power-factor saturation curve.

As stated earlier in this paper, the use of the phase characteristic or V curves, which can be determined readily, is recommended.

Sudden Short-Circuit Tests and Synchronous Machine Quantities

The 3-phase sudden short-circuit test at rated voltage should not be omitted on a large machine of new design, as mechanical failures due to inadequate bracing of the stator winding are known to occur. If oscillograms are taken, the transient and subtransient reactances and their time constants can be determined. The determination of these reactances and time constants by test gives valuable information to both designer and user.

Very little information is available on the suitability of the test methods for determining other synchronous machine quantities. Those that have been tried in the field have given only fair results. There is need for an exchange of information among those interested covering the technique to be used. The instructions in the test code appear to be insufficient, and need to be proved in the field. Such tests are in a comparatively new field in testing of hydroelectric generators, although the value of a knowledge of these quantities in estimating the performance of a generator has been appreciated.

Losses

Several methods for measuring generator losses are listed in the Test Code (page 13 and those that follow). Only the retardation method has been found uniformly successful for hydroelectric units. The separate driving motor, calorimeter, cooler method, and input-output method are either impractical or require special facilities and time for execution. The electrical input method has been used, not because it was satisfactory, but because the retardation method had not been developed to the present degree of accuracy. This method requires special low-ratio current transformers, which are often difficult to mount in the leads from the generator, especially if these leads are of cable, brought out to a metal-clad bus structure. It is impossible to prevent hunting between driving and driven units, and great care is necessary to obtain a consistent set of readings. Harmonics are usually present in the current wave, and may increase the error already present from other causes. There is great danger of the units falling out of step if the voltage is lowered to a point where synchronizing power is insufficient. If this condition should develop, a heavy overload is placed on the metering current transformers, and these may burn out before they can be protected by closing their short-circuiting disconnects. The measurement of stray loss by this method is involved, and the accuracy doubtful. One major source of error arises in the use of high-ratio current transformers and low-power-factor current, giving current transformer errors and errors due to small deflections on the wattmeter used. The latter error may be decreased by using a low-power-factor wattmeter. The use of the electrical input method, at least for medium or large units, is not recommended, unless no other method can be used.

The retardation method depends for its accuracy on careful determination of the Wk^2 of the generator, and of the speed-time curve, both of which are essential for the calculation of the loss under any given condition.

A very close approximation of Wk^2 of the generator can be made for the rotor of a water-wheel generator. The weight of each salient pole is known accurately,

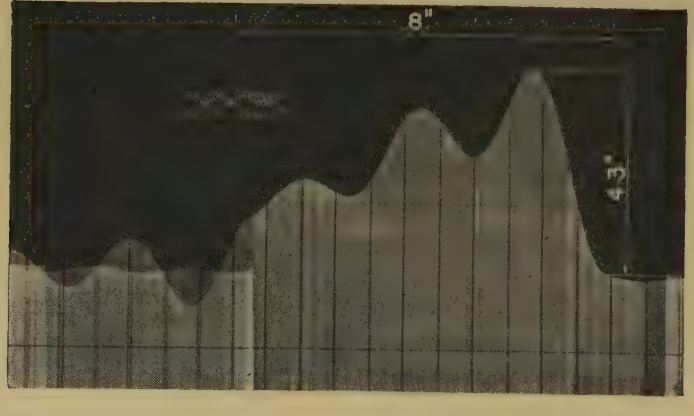


Figure 1. Gibson diagram from differential test of 66,000-horsepower unit

and the weight of the rim is also capable of accurate calculation from drawings. These calculations can be checked by test, using one or more of the methods outlined in the test code.

Use of the d-c generator separately excited, with biased output voltage (see test code, pages 18–19) has proved most successful for measurement of speed. The measurement must be made carefully, and frequent checks made during the progress of the test to prove the constancy of the calibration. This method of speed measurement is given in detail in the test code, and need not be repeated here.

The calorimeter method of determining losses[3] is applicable only to totally enclosed hydroelectric generators. Unless the temperature of the ambient air can be closely controlled, as in the case of the totally enclosed generator, it is extremely difficult to relate the temperature rise of the air to the loss or losses causing it, due to the thermal capacity of the generator. The increase in number of this type of

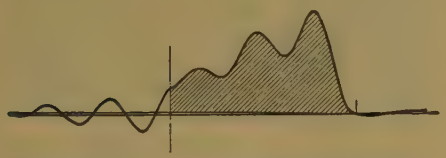


Figure 2. Delineation of area on Gibson diagram measuring impulse

Actual length of hatched area 7.75 inches or 10.6 seconds

Maximum height 4.4 inches, equivalent to 4.80 feet of water

Average height equivalent to 2.65 feet of water

generating unit permits use of this alternative method of loss measurement. Its chief disadvantage is the time required for a complete set of tests. A crosscheck can be obtained on the total losses, by operating the generator at rated load and measuring the temperature rise of the cooling air. The individual losses also can be measured, and windage separated from friction loss.

The segregated generator losses are used to establish the generator efficiency, and also are used to determine generator input on the acceptance test of the prime mover. Their use in this latter respect is discussed in some detail later in this paper.

Hydraulic Tests

This section of the paper deals chiefly with the acceptance tests of the prime mover and the rating test of the hydroelectric generating unit. The acceptance test is that having as its objective the determination of whether or not the unit and its component parts satisfy the guarantees of capacity, efficiency, and reliability made by the manufacturers. The rating test determines the efficiency of the unit as a whole, and the variation in efficiency, in order that the most effective use may be made of it along with other units in the same power plant and with other plants in the same system.

The acceptance test of necessity considers the component parts of the unit separately, that is to say the generator and turbine independently of each other. The discussion will not extend to other parts such as the governing system, and water passages except incidentally. The rating test on the other hand considers the unit as a whole including not only the turbine and generator but conduits and other water passages serving that unit and no other.

For tests of both kinds, three primary quantities must be measured, namely, the power, the flow, and the head. The flow is the same whether one is considering the acceptance or the rating test, but power and head are not. In the acceptance test of the turbine the output power is the same as the input to the generator shaft and therefore includes the generator output and all generator losses while in the rating test the power is the net output of the generator. The head in the acceptance test is determined from measurements made as close to the turbine as practicable. In the rating test the head considered is the difference of elevation of forebay or headpond and tailwater.

Accuracy

At this point the authors would like to comment on certain features of the precision required in test equipment and observations. Insofar as the acceptance test is concerned, test codes of various associations and technical societies define in greater or less detail the method in which various quantities shall be measured and the acceptable degree of precision. No such criteria exist, however, to govern accuracy in rating tests. The responsibility of securing the results required at a cost no greater than is warranted by their value rests with the engineer in charge of the tests. It is the authors' considered opinion that as great accuracy is necessary in the rating tests as in the acceptance test where the representative of the manufacturer carefully scans the details of all arrangements for the test and all observations in order that the final result for efficiency may not fall

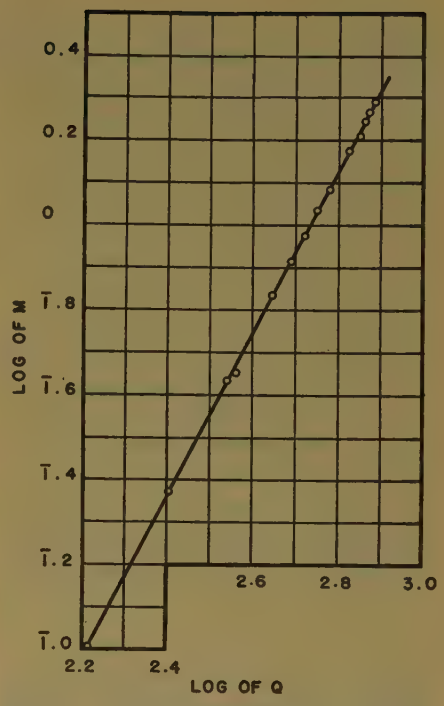


Figure 3. Relation of discharge to pressure differential between piezometers in penstock and scroll case of turbine

M = differential pressure, feet of mercury
Q = discharge, cubic feet per second

so much as a tenth of one per cent below the maximum that can be shown honestly.

Because of their ready availability, there is a tendency to substitute switchboard meters, gauges, or instruments of low grade for test instruments of high precision and accuracy, and to use observers unskilled in tests and investigations of this type. In consequence of this, unreliable or misleading results may be secured and incorrect conclusions reached. The authors call to mind certain specific incidents that justify this criticism.

The acceptance test of the turbine and the rating test of the unit frequently are made at the same time. It is convenient therefore to give a single description of measurements and procedure applying to both. This description will be divided into three parts, each part dealing with one of the three primary quantities to be measured.

Measurement of Power

For the rating test the quantity to be measured is the output of the generator. The authors have been associated in many tests and have used instruments of various types. In general the instrument preferred is a calibrated polyphase wattmeter. Exception may be taken to this instrument and in fact many test codes require that single-phase meters be used. The objection to the use of the polyphase

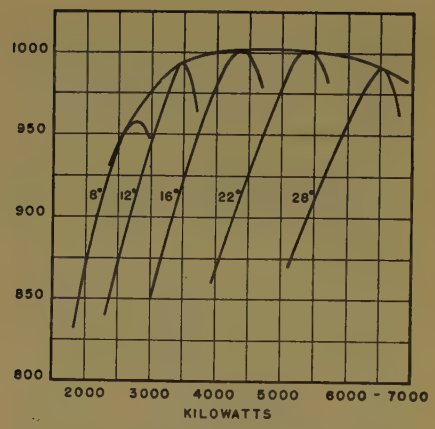


Figure 4. Power efficiency relation from an index test

The variation of efficiency with load and blade angle is found although the absolute value of the efficiency is not known

meter is based in some instances on the type of generator connection and grounding. The objection does not apply in the case of the plants operated by the organization with which the writers are connected and the advantages of using a single instrument are so evident that it is to be preferred wherever it is properly applicable.

In the acceptance test of the turbine, its power output is required. Where the turbine and generator are mounted on the same shaft, the turbine output is the generator output plus the generator losses. The accuracy required makes the method of dividing the generator output by generator efficiency unsatisfactory, although the authors have found it necessary on occasion to do this, on generating units of small size, where insufficient data were available to enable generator losses to be computed.

If generator losses have been measured on the unit under test, readings of generator voltage, stator current and temperature, field current, and exciter outputs, on each test run, will permit an accurate computation of individual losses. These can be added to the measured generator output. The precision of measurement of the losses is very high, compared to the measurement of generator output, so that it is possible to use losses as measured on a duplicate generator, or even to use the generator designer's estimate of losses, without introducing an error large enough to have any noticeable effect on the overall result.

Calibrated portable instruments of high standard should be used for the electrical measurements. The instrument transformers associated with them should have a known ratio of transformation. Otherwise they should be calibrated. In at least one instance a calibration of the instrument transformers requested by the representative of the turbine manufacturer disclosed errors that were quite unsuspected until the calibration had been made.

The importance of this test on occasion may justify duplicate measurement of power by independent observers, using separate instrument transformers and wattmeters calibrated against different laboratory standards.

Measurement of Flow

The accurate measurement of the quantity of water flowing through the turbine is one of great difficulty. Various methods of measurement are available, the choice of method depending on the particular situation in hand. Four of these methods will be described briefly. Complete descriptions of all of these considered herein are available elsewhere; hence descriptions are carried only so far as to make clear the comments on their fields of application and reliability.

The Gibson Method[4]

The Gibson time-pressure method of measurement of flow is an invention of Doctor Norman R. Gibson, and an outcome of his extensive studies of pressure-rise in hydraulic pipe lines. The method, simple in principle and fundamentally sound, is an application of the second law of motion, expressed briefly as

$$Pt = m(v_1 - v_2)$$

When a column of water flowing in the penstock of a hydroelectric unit is brought to rest by closing the turbine gates, a force is impressed on the water column in bringing it to rest. Assuming that the mass of water has its velocity changed to zero during gate closure, the change in momentum effected is the product of the mass of the water in the penstock and the original velocity. This change in momentum is equal to the impulse causing it, that is to say, the mean value of the force acting upon it to bring it to rest multiplied by the time during which it acts. Of these four quantities, force, time, mass and velocity, three can be measured and the fourth, the velocity, computed, it being the only unknown in the equation.

Equipment was devised by Gibson to measure the force or pressure acting on the water column by a mercury U-tube, and to record the pressure variations on a moving film. The equipment, with minor changes, has been used by nearly all, if not all, investigators on this continent. German scientists working mainly with Doctor D. Thoma at Munich built instruments in which pressure changes deflected a mirror through the movement of a spring-controlled piston. A beam of light of high intensity focused in the mirror is reflected through lenses to a photographic paper moving past a narrow slot. Comments on both of these types of equipment will be made later.

The Gibson instrument consists of a camera at the front of which one leg of a mercury U-tube is clamped at a definite distance from the lens. The U-tube is connected to the penstock, and the level of the mercury in it is a measure of the pressure in the penstock. At the rear of the camera is a photographic film on a cylinder which is rotated at a speed suited to the rate of closure of the turbine gate. Between the U-tube and the lens, a pendulum is arranged to cut off the light passing through the U-tube once every second. Illumination for exposure of the film is provided by a bank of photoflood lamps. The instrument is so constructed that no light can reach the film except that passing through the U-tube. As the pressure varies in the penstock corresponding movements take place in the mercury column in the U-tube and these movements are recorded on the film at the rear of the camera.

The procedure, in making a measurement of flow in a penstock, is as follows: The unit under test is loaded to the point at which it is desired to measure the discharge and sufficient time allowed for operating conditions to become satisfactorily steady. On signal from the operator at the Gibson instrument, the turbine gates are closed at a uniform, predetermined rate, during which time, and for a few seconds before and after, the moving film in the camera is exposed recording the rise and fall of the mercury column in the U-tube, and therefore the changes in pressure. From an analysis of the exposed film an area is delineated which measures the impulse bringing the mass of water in the penstock to rest. The measurements are repeated for a series of similar runs covering the whole range of capacity and flow for the turbine.

Originally it was the practice to have a connection to the penstock from one leg only of the U-tube, the other leg being carried to a sufficient height to balance the penstock pressure. The mercury column was often of great height, 20 feet or more in some tests conducted by the authors, which introduced certain difficulties in conducting the tests. It made it necessary also to secure, in synchronism with the Gibson diagram, a graphic record of the variations in headwater level.

It is the practice now, whenever possible, to connect both legs of the U-tube to the penstock at sections so far apart as to secure a diagram of satisfactory area on the film. The test made with a single connection is known as a simple test, that with two connections to the penstock as a differential test.

In Figure 1, a diagram from a differential test is submitted. The dimensions of the original are marked on the figure to give a better idea of the scale. In Figure 2 is shown a copy of this diagram with the area representing the product of pressure and time crosshatched. It is not intended to discuss here the method of determining the lower and left hand limits of the area, but this explanation should be made:

The regular waves following the end of the diagram result from the fact that the mercury column swings up and down in the tube until friction brings it to rest at its final static level. They are not due to pressure variations in the penstock. These after waves enable the end point of the diagram to be determined in most cases. The author has found it necessary for tests of plants with very short supply pipes to have a contact, closed by the servomotor piston at the end of its stroke, complete a circuit which gives an indication in the film of the completion of closure of the turbine gates.

The instruments made by Volkhardt and Deckel and used at Munich, Eitting, and Heidenheim, are much more complicated than the instrument by Gibson. One of the advantages sought in their design is the elimination of effects due to the inertia of the mercury column. This inertia, however, has certain compensating advantages, Thoma points out, enabling a more precise determination of the end point of the diagram, in certain instances, than the instruments with spring controlled pistons. Special provision is made to overcome the effect of friction. Calibration is difficult and liable to change. However, they are instruments of great precision.

Deckel submitted the results of tests by his instrument made at Munich in 1930 in which the average difference from the measurement by a calibrated weir was 0.41 per cent, only 2 runs out of 14 showing errors exceeding one per cent. Deckel's comments on the method are interesting in that other methods of measurement have found greater favor generally in the institution in which his work was done:

"The Gibson measurement process in many cases offers considerable advantages as compared with other measurement methods. These advantages are based on the practical simplicity and good theoretic foundation for the process. It must be provided, of course, that its grade of accuracy is not below that of other processes, that is, the possible error should not exceed one per cent when compared with the highly developed stage of present measuring processes . . . The tests which were carried out will confirm this."

Allen Salt-Velocity Method[5]

Professor C. M. Allen of Worcester, Mass., has, by his research, brought to a high degree of precision the measurement of flow by observations of the time for a charge of brine to pass from one section to another in a penstock. In this method the charge of brine is injected through one or more special valves suitably disposed on the cross section of the penstock and the time for it to move from the point of injection to a cross section further downstream is measured. At the lower cross section a series of electrodes is set up in the penstock and the time of passage from the point of injection to the electrodes is determined by a graphic measurement of the change in conductivity of the water, the time being accurately measured on the chart as well as conductivity. The method is adaptable to situations where the cross-sectional area of the penstock is irregular or where velocities are extremely low and other cases where the Gibson method is not readily applicable. Its disadvantages are that the disposal of the injection valves and the electrodes on the cross sections require considerable experience with this type of test. A more or less prolonged shutdown of the unit is necessary also to install the equipment.

The necessity for experience in the design of the equipment and its disposal on the cross section will be realized when it is remembered that the charge of salt coming through a valve at the center of the penstock moves downstream at a greater velocity than a charge injected at the side of the penstock. It is therefore necessary to design the equipment so that the average time of passage from one cross section to the other will be recorded correctly. The authors have attempted to use the method on one occasion and from the difficulties experienced in securing satisfactory results in that instance have some appreciation of the vast amount of effort that has been put into the perfection of the method by Professor Allen.

The Current Meter[6]

The third method to which reference will be made and one that has been used perhaps more frequently than any other, is the current meter method. The method has been brought to a high degree of accuracy for measurement of discharge of power houses through the work of a large number of investigators in North America commencing with the work of Groat and Nagler in 1912. The method has been preferred above all others for measurements in Europe and a great deal of work on the development of suitable instruments has been carried out there.

The method is simple enough in principle. It consists of the measurement of velocity at a large number of points on a cross section at the intake of the unit and the computations of the discharge by multiplying the average measured velocity by the area of the cross section. The necessity for refinement comes about because the velocities at any section are not at right angles to the cross section. In areas of disturbed flow certain meters have a tendency to over-register, that is to say, they measure a velocity greater than the resolved part of the velocity normal to the measured cross section. Other meters under-register, some to a greater degree than others. By using groups of meters of different types in a test and comparing the results, each with the other, the correct normal velocity may be determined.

The method is readily adaptable to cases where a very short supply pipe leads to the turbine, therefore making it difficult to apply the Gibson or Allen methods. As just indicated the common European practice applies the current meter method in nearly all instances, in fact it has been used frequently in Europe to measure the velocity on the cross section of a penstock

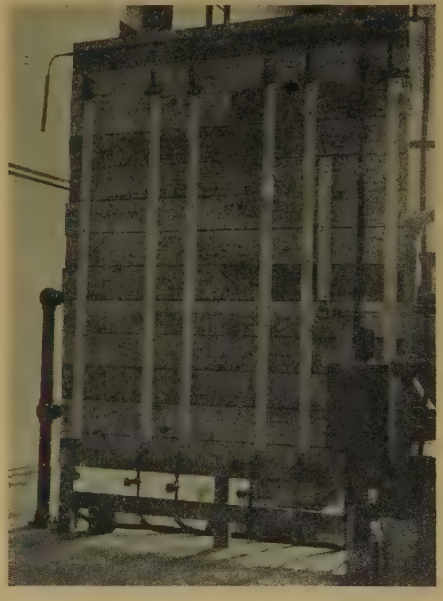


Figure 5. Bank of gauges used for index test

These are simple water columns under compressed air to depress them to the range of the scales

where in North America one of the other methods would be applied.

The Weir

In some instances it is possible to install a weir in the tailrace of the plant. Measurement of discharge by a weir is only possible in cases where the discharge is moderate, that is to say, not more than two or three hundred cubic feet per second and where the reduction in head resulting from the installation of the weir is only a small percentage of the total head.

Measurement of Head

The third of the primary quantities to be measured is the head acting on the turbine or on the plant. There is, of course, a distinction between these, sometimes of considerable magnitude, for example, in the case of a plant having a long penstock. For low-head plants the difference is not so marked. For the purpose of tests, the simpler the equipment, the more satisfactory it is for measurement of water level. In the forebay or tailrace of a plant, simple float gauges are preferred installed in float boxes connecting with the body of water, the surface elevation of which is to be measured, by a small opening in the float box which dampens surges. The usual practice in the rating test of a generating unit is to install at least two of these in the forebay and two in the tailrace, usually in the stop log checks.

In the acceptance test of the turbine unit, however, the head must be measured at the entrance to the turbine casing, and in a plant having a long penstock the head measured at this point will be appreciably different from that measured in the forebay. Bourdon gauges are unsatisfactory for this purpose and a mercury manometer is preferable even though this may be of great height, requiring two observers to read it. A case in point is a plant on which a test was made recently where the operating head was 340 feet and the mercury manometer about 24 feet in height.

In the case of the acceptance test, as indicated previously, the pressure head is measured at the entrance to the turbine casing. To the pressure head, plus elevation head at that point, there must be added the velocity head in the penstock. The net head acting on the turbine is the head at entrance to the casing, expressed as an elevation, minus the sum of tailwater elevation and the velocity head at the section at which the tailwater level is measured. In some instances, however, the velocity head in the tailrace is neglected. In the case of the rating tests of the plant the gross head only is to be considered, that is to say, the difference of level in the water in the forebay and in the tailrace.

Frequently gauges measuring these water levels are installed to give an indication in the control room of the levels, and it is most desirable to check these gauges during the tests, not only for correctness in their indications, but also for the correctness of indication by them of the true forebay or tailrace level. The location of the actuating element of the gauge is frequently such that it is affected by local disturbances and by variation in load on the particular unit near which it is installed. It is the authors' practice to observe the operations of such gauges carefully during the test in addition to making observations on special gauges installed for the test itself.

In addition to the primary measurements dealt with in the three preceding sections, a number of other quantities are observed such as gate opening of the turbine and information that will enable segregation of the hydraulic losses in the water conduits to be made.

Analysis of Data

Having computed the three primary quantities, power, head, and discharge, for each run, these are tabulated and corrected for departure of the test head from the rated head of the unit. In the case of the acceptance test, capacity and efficiency of the turbine will be given by the turbine builder for some specific head. In the tests the actual head will differ from this slightly, and power and discharge for each of the runs will be corrected to that which would have been realized had the test been made at rated head. This correction can be made without impairing the accuracy of the results provided that the test head does not differ by more than three or four per cent from the rated head. The results are then plotted in the form of a power-discharge curve. Two additional curves are plotted also, namely, the power on a base of gate opening, and discharge on a base of gate opening. The three curves are then compared and adjusted until all three are in agreement. From this point on practically all of the results secured regarding capacity and efficiency will be based on the three curves, particularly the power-discharge curve. It is customary to compute the efficiency of the unit from the adjusted power-discharge curve and not from the individual test runs.

A similar set of three curves will also be drawn based on the gross head of the plant and the generator output, these forming the basis of a report on the rating test of the plant.

Rating Discharge Against Differential Pressures

It will be appreciated from the description of the various methods of measuring the quantity of water flowing that this part of the test is difficult and expensive and may involve serious interruptions to operation of the unit. It is desirable therefore to secure records that can later be used to measure the discharge with less inconvenience and expense. The author used such a method some 23 years ago at the Queenston plant on the Niagara River by observing the reduction in head from forebay to a point at the entrance to the casing of the turbine, using a mercury manometer for the purpose. The reduction in pressure head was largely due to the great increase in velocity head at the lower measuring point and was a function of the magnitude of the flow of water in the penstock. The ratings so made in the original tests by the Gibson method were later used in tests which involved simply a measurement of the difference in the pressure head at forebay and scroll case, to determine the flow. It is common practice now to install piezometer connections at suitable points in the penstock and scroll case and to determine, at the time of the original tests when the flow is measured by one of the methods described above, the relation of the discharge to the differential pressure between two of these piezometers.

The results of such a measurement in a turbine test made recently are as shown in Figure 3. The flow was measured by the Gibson method and the differential pressure was read on a differential manometer connected to a piezometer in the speed ring and a ring of four piezometers around the downstream end of the penstock. It is only necessary at any future time to measure the differential pressure to determine discharge from the data submitted in the graph. The relation is unaffected by head, the condition of the turbine runner or other changes beyond the piezometers.

Index Tests

When, for physical or economic reasons, it is unadvisable to make discharge measurements, it is still possible in many instances to secure records of variation of efficiency of a turbine unit by measuring quantities, the variation of which with the discharge is known, approximately, if not exactly. Tests in which such quantity is measured instead of the discharge are known as index tests. From them, the power and head being measured, it is possible to derive efficiency curves which show the variation of efficiency with load but not the absolute value of the efficiency.

To illustrate: In order that the governing mechanism of a Kaplan turbine may be so designed as to secure the highest efficiency at all loads, information must be available as to the variation of efficiency with gate opening, or load, and blade angle. The quantity related to the discharge, which is measured is a pressure differential between two piezometers suitably disposed. The discharge varies approximately with the square root of the differential pressure and the efficiency therefore with the kilowatts divided by the square root of the differential pressure. In Figure 4 such a series of curves derived from a test of a Kaplan runner is shown, each curve being for a specific blade angle.

The envelope of these curves provides the information for the design of the cam which properly correlates gate opening and blade angle. Forty or more separate measurements of discharge would be required to develop the five efficiency curves shown in Figure 4. The gauge, or series of gauges set up for the test, is shown in Figure 5. Readings in this case were taken on water columns depressed by compressed air to a reading range. The various gauge columns are connected to piezometers in penstock and scroll case.

Conclusion

In conclusion, it may be stated that a definite policy of making tests on both generator and prime mover, even if considerable expense and effort is involved, undoubtedly will pay dividends. These tests make quantitative data available, the value of which may not be apparent at the time the tests were made. However, it later may make possible an engineering solution to some difficult problem of operation, or point the way to improvement in performance in the unit tested, or succeeding ones in the same or other stations.

References

1. Test Code for Hydraulic Prime Movers. American Society of Mechanical Engineers, June 1938.

2. AIEE Test Code for Synchronous Machines. Number 503, June 1945.

3. Calorimeter Measurement of Stray Load Losses of 55,000-Kva Generator Having Enclosed System of Ventilation, G. D. Floyd, J. R. Dunbar. AIEE Transactions, volume 51, 1932, pages 12–18.

4. The Gibson Method and Apparatus for Measuring the Flow of Water in Closed Conduits, Norman R. Gibson. American Society of Mechanical Engineers *Transactions*, volume 45, 1923, page 343.

5. The Salt Velocity of Water Measurement, Charles M. Allen, Edwin A. Taylor. American Society of Mechanical Engineers *Transactions*, volume 45, 1923, page 285.

6. Water Gauging for Low Head Units of High Capacity, J. M. Mousson. American Society of Mechanical Engineers *Transactions*, volume 57, 1935, page 303.

Dielectric Recovery by an A-C Arc in an Air Blast

T. E. BROWNE, JR.
MEMBER AIEE

SINCE the extinction of the arc drawn upon opening an a-c switch depends upon a rapid transition of the arc near a normal current zero from a conducting to an insulating state, much study has been given by switch designers to this transition, often referred to as dielectric recovery. However, the published experimental data with regard to the mechanism of this dielectric recovery still are meager and there is no generally agreed upon theory, even for the simpler cases. One simple case, of growing importance in this country, is that of the arc in an air-blast circuit breaker. Perhaps the simplest arrangement is found in the nozzle type of air-blast breaker variously described as radial blast or axial blast. Figure 1 is illustrative of such nozzles, somewhat reduced from practical forms.

Of particular value for the understanding of the arc extinction processes are curves showing the rise of the arcs reignition voltage, or dielectric strength, with time during the first few hundred microseconds following arc failure near a normal current zero. There have been several attempts to predict the course of such curves for the air-blast breaker, of which that by Kesselring and Koppelmann[1] is noteworthy for its completeness. Some direct experimental results defining a single curve and indicating another have been presented by Prince, Henley, and Rankin[2] for a cross-blast or splitter type of breaker at greatly reduced air pressure and unstated current. Also presented by Prince were some very interesting high-speed moving pictures of the arc in a splitter type breaker, but these, like earlier ones presented by Biermanns[3] for the nozzle type breaker, are somewhat inconclusive. These photographs and the theoretical picture of arc interruption in an air blast have been further discussed by Slepian.[4] In the theory of Kesselring and Koppelmann and others a physical cutting and progressive displacement of the permanent arc core is presumed. Slepian, in agreement with earlier discussions by Mayr,[5] has preferred to ascribe the dielectric recovery of the arc space to cooling and ion diffusion, and has pointed out the decisive importance of turbulence of the gas motion in enhancing the diffusive effects.

In the course of an extended experimental study by the writer of the factors influencing arc extinction in models of air-blast orifices like those of Figure 1, a considerable mass of data has been obtained, including 16 more or less complete curves of dielectric recovery with time by the arc space under widely varying conditions. Some of these results will be presented and briefly discussed in the light of existing theories.

Experiments

The nozzle and contact arrangement shown in section in Figure 1A is typical of the earlier forms studied. This sketch shows the location of arc resisting inserts of copper-tungsten and soapstone as generally used, these being omitted in the other sketches for simplicity. In all of the work to be described the orifice diameter was 0.765 inch and the arc was drawn by rapid downward motion of the lower (upstream) contact through the orifice to the open position shown. Compressed air from a storage tank was introduced into the annular space between the supporting fiber plates through a poppet valve, piping, and entrance orifices which reduced the steady-state gauge pressure at the interrupting orifice entrance to between 0.7 and 0.8 of the initially adjusted tank pressure. Beyond the arc space the discharged air passed through openings having $3^1/_3$ times the area of the main orifice, resulting in a pressure elevation on the discharge side of the orifice roughly 1/10 the entrance-side gauge pressure without arcing and up to two or three times this in the presence of a one or two thousand-ampere arc.

Of all the orifice arrangements tried, that of Figure 1B proved to be the most efficient in terms of required air pressure for interruption of low power factor currents up to 2,200 amperes at 13,800 volts

Paper 46-21, recommended by the AIEE committee on protective devices for presentation at the AIEE winter convention, New York, N. Y., January 21–25, 1946. Manuscript submitted November 9, 1945; made available for printing December 13, 1945.

T. E. Browne, Jr., is research engineer in the high-voltage laboratory, Westinghouse Electric Corporation, Trafford, Pa.

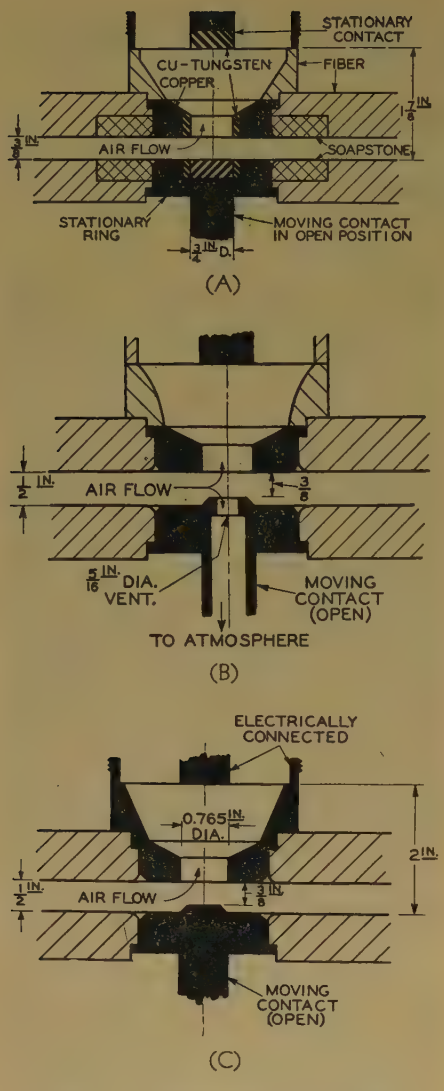


Figure 1. Experimental air-blast orifices

and 4,200 amperes at 6,900 volts, the maximum values available for these tests. Interrupting test results with this orifice are plotted in Figure 2A. The upper broken line is drawn through points representing tests at the maximum gauge pressure in the tank at which a failure to interrupt occurred and the lower line through points of minimum gauge pressure in the tank for a successful interruption. Interruptions were considered successful if not more than one cycle of arcing (at 60 cycles per second) occurred after passage of the electrode tip through the orifice. These limits were always checked by obtaining at least four tests just outside the limits all of which were either successful or unsuccessful. Thus, the region between the lines is one of uncertainty separating regions of high and of low probability of interruption. Figure 2B is a similar plot for the orifice of Figure 1C, which was a much less efficient interrupter, especially at the lower currents. The favorable features combined in the Figure 1B orifice were indicated step by step in a long series of tests leading up to it. They are principally:

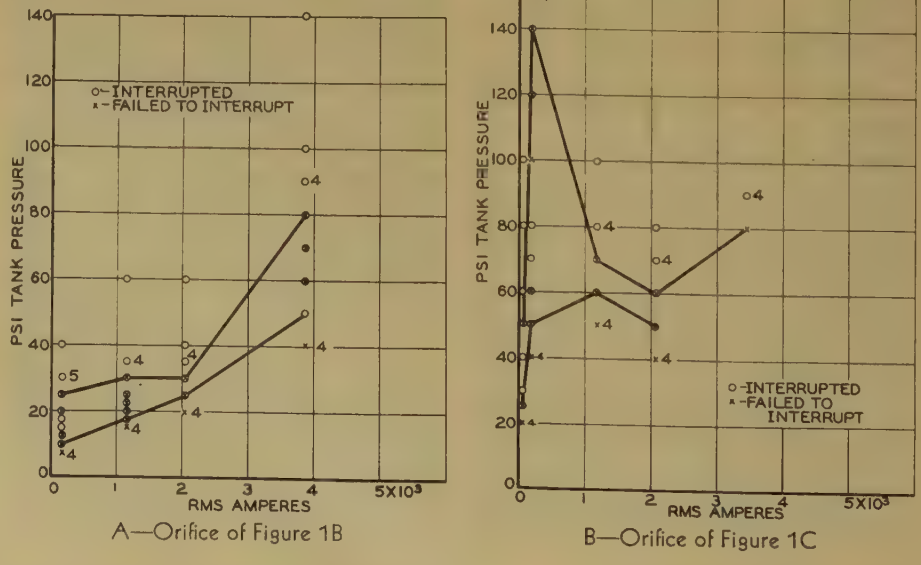
1. Rounding of the edges of the orifice and contact rings to minimize electric stress concentration.
2. Proper spacing of the contacts relative to the orifice.
3. A slight crowning, or beveling of the upstream contact face.
4. Insulation of the metal orifice ring from the downstream contact.
5. Venting to atmosphere of the center of the upstream contact face through a smaller auxiliary orifice.

These features are in close correspondence with those of an orifice-type high-voltage compressed-air circuit interrupting element developed by Ludwig and Baker.[6] The orifice of Figure 1C, lacking only features 4 and 5 of the preceding list, was chosen for an extended study of dielectric recovery with time because its inferior performance permitted it to be tested adequately over a much wider range of pressures and currents than would have been possible with the Figure 1B orifice. Also, the Figure 1C orifice is itself of practical interest, since its simpler construction permits its use in simpler and more compact circuit breakers, especially those for the lower voltages.

Figure 3 shows some of the information leading up to the Figure 1B type of orifice. These data were replotted from families of curves like those of Figure 2, using points from the upper limit curves only. These maximum failure pressures are plotted in Figure 3A as a function of the spacing of the downstream contact, in this case a copper-tungsten tipped 1/4-inch rod, above the open position of the upstream contact face. For convenience in interpretation, the orifice and electrode sections are dotted in to the scale of the spacing co-ordinate with the plane of the upstream contact face at the origin. Smooth curves are drawn through the somewhat scattered points for each of the three currents, 175, 1,100, and 2,000 amperes, all of these tests being at 13,800 volts. It may be deduced from the slopes of these curves that the region near the flow constriction, or "vena contracta," is of most importance at all currents but was practically the only effective interrupting region at the higher currents. At 175 amperes, the axial region beyond the orifice was of lesser but still of considerable importance. Figure 3B is a similar plot of results of tests in which the projection into the orifice region of a 1/4-inch stud from the center of the upstream contact face was the varying parameter. These curves similarly show a more sharply restricted interrupting region for the higher currents. The minimum near 3/16-inch projection for the 175-ampere curve probably also points to the advantage of a somewhat pointed or crowned shape for the upstream contact face.

In all of the work just described the testing circuit was used without modification of its normal transient characteristics, the natural frequencies and decrements of the recovery voltage oscillation components varying with the particular circuit adjustments, particularly with the short-circuit current settings.

Figure 2. Interrupting pressure range as a function of current

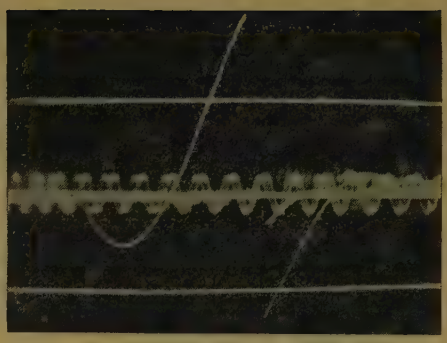


To get direct information about the course of the dielectric recovery in the arc space with time, the natural frequency of the circuit, or its rate of rise of voltage, was controlled by capacitor shunts in parallel with the arc, and the reignition voltages appearing across the arc terminals were measured from cathode-ray oscillograms. Figure 4 shows four samples of such oscillograms, taken by photographing the screen of an RCA 904 cathode-ray tube with a miniature camera. The beam was oscillated magnetically at power frequency with such phase and amplitude that it passed across the screen only during each recurrence of a small time interval embracing each current zero moment. At this time the rate of change of the deflecting magnetic field and so the speed of the beam was nearly constant. Voltage calibration was provided by superimposing the horizontal lines resulting from application of open circuit voltage (these being the positive and negative peaks of the voltage waves), and time calibration by further superimposing a small amplitude trace produced by a calibrated oscillator.

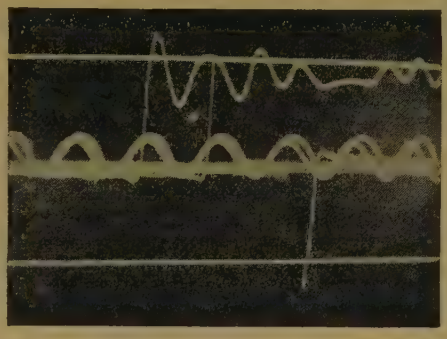
The oscillograms in Figure 4 of tests 12,417 and 12,440 show, successively, the effect on the reignition transients of a 175-ampere arc with 20 pounds per square inch air tank pressure of adding a small (0.035 microfarad) shunting capacitor. Wide variations in reignition voltage and time at successive current zeros are well illustrated by the three reignition traces in test 12,440. The smallest value (of negative polarity) probably occurred before the contacts were fully open. The oscillograms of tests 13,110 and 12,848 each show two arc reignition transients followed by an extinction transient, the currents interrupted being 1,070 amperes and 2,260 amperes, respectively. In test 13,110 the circuit, containing an air-core reactor, was unshunted and in test 12,848 a delaying shunt of 0.102-microfarad capacitance was added.



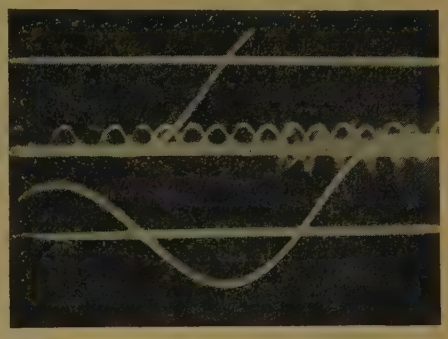
A—175 amperes at 13.8 kv, no shunt, 20 pounds per square inch in the tank, 20-kilocycle timing frequency



B—175 amperes at 13.8 kv, 0.035-microfarad shunt, 20 pounds per square inch in the tank, 20-kilocycle timing frequency



C—1,070 amperes at 13.8 kv, no shunt, 80 pounds per square inch in the tank, 20-kilocycle timing frequency



D—2,260 amperes at 9.2 kv, 0.102-microfarad shunt, 5 pounds per square inch in the tank, 33-kilocycle timing frequency

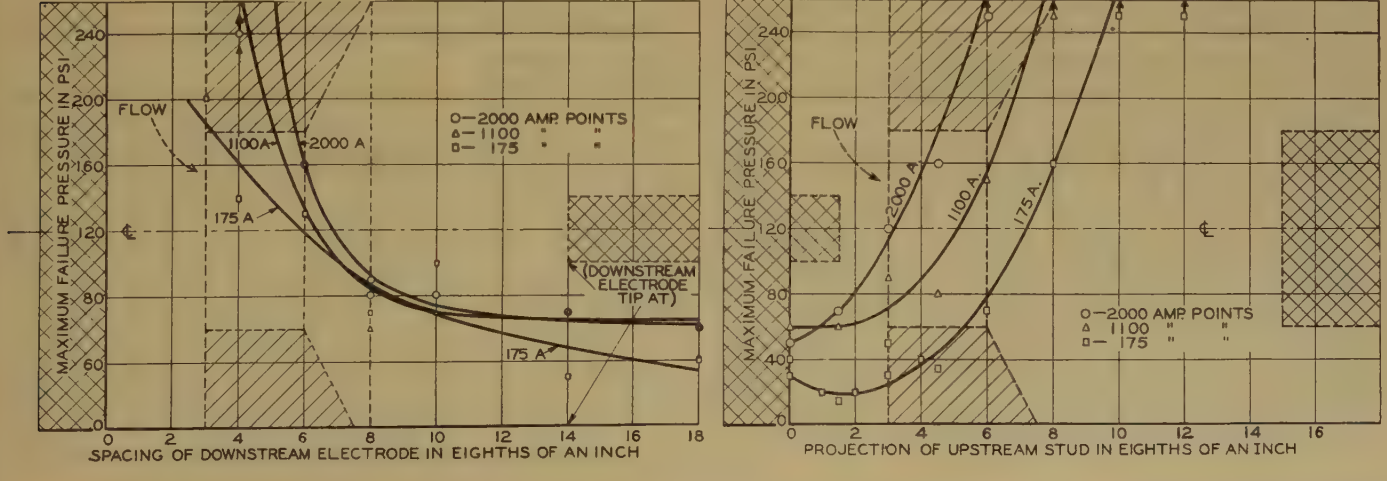
Figure 4. Cathode-ray oscillograms of arc reignition and extinction voltages

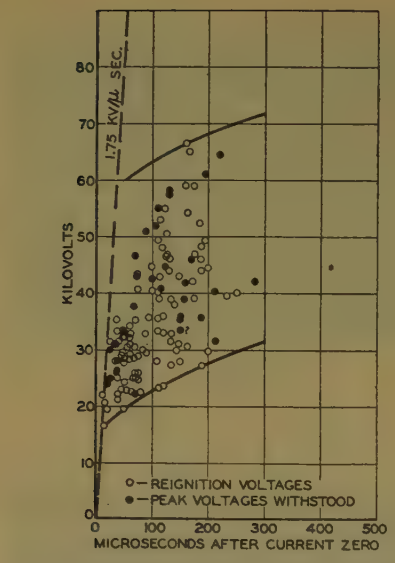
The results of a long series of such oscillographic measurements of tests with the Figure 1C type orifice were plotted and are shown in Figure 5. In addition to the reignition voltage points marked with open circles, in many cases the peaks of recovery voltage transients which did not cause reignition (extinction voltages) were also plotted and marked with solid circles. Where possible, envelopes were drawn enclosing the estimated regions of uncertainty within which most of the breakdowns occurred. Low breakdown points near or outside the envelopes, when indicated by adjacent question marks, were judged probably to indicate breakdowns at less than maximum contact separation. The dotted lines through the origin are lines of a theoretically calculated dielectric recovery to be explained later.

Figure 3. Effect of electrode position on maximum failure pressures at 13.8 kv and various currents for an orifice similar to that of Figure 1A

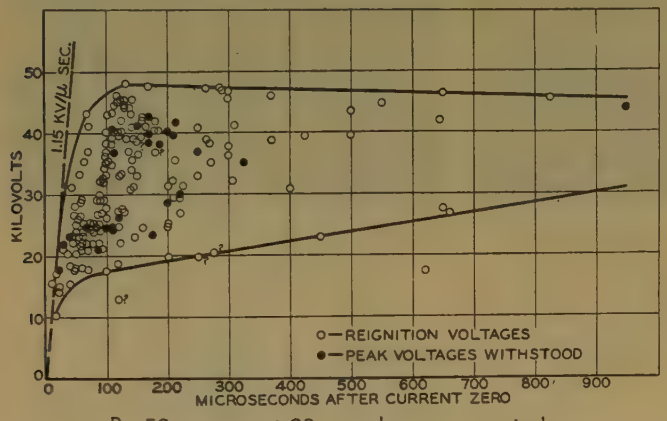
A—(left) Downstream electrode position varied

B—(right) Upstream electrode position varied

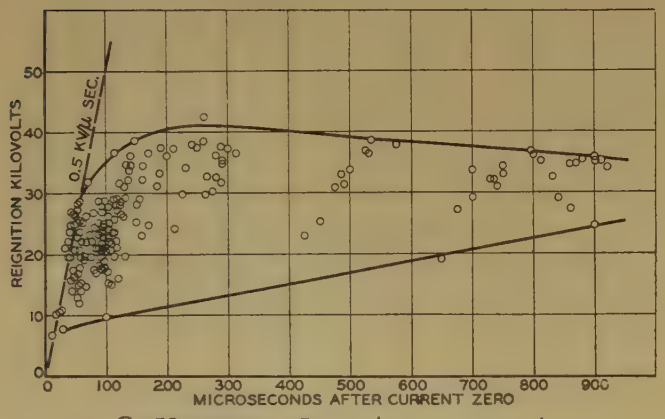




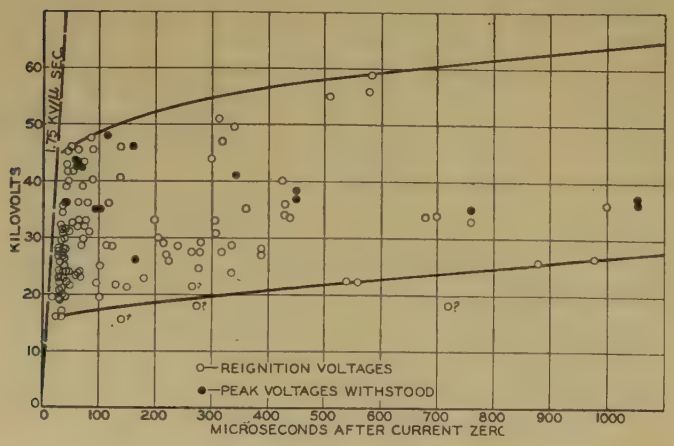
A—50 amperes at 40 pounds per square inch



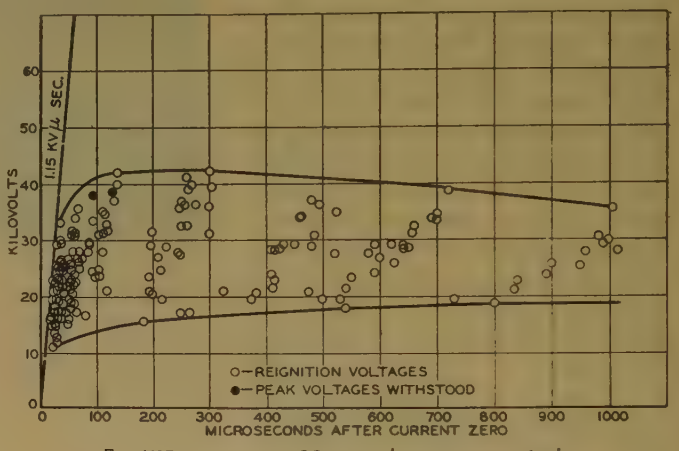
B—50 amperes at 20 pounds per square inch



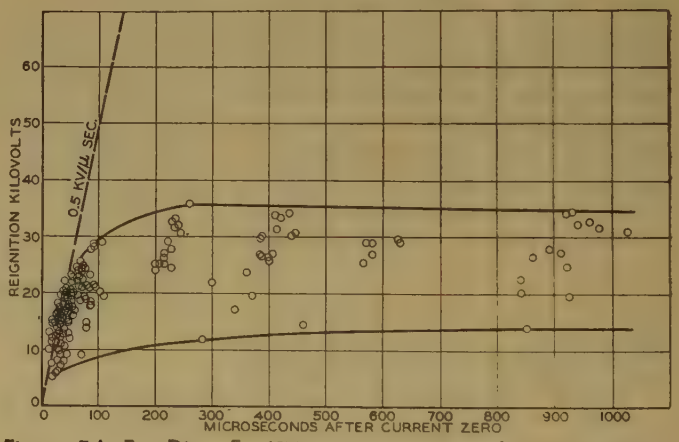
C—50 amperes at 5 pounds per square inch



D—175 amperes at 40 pounds per square inch



E—175 amperes at 20 pounds per square inch



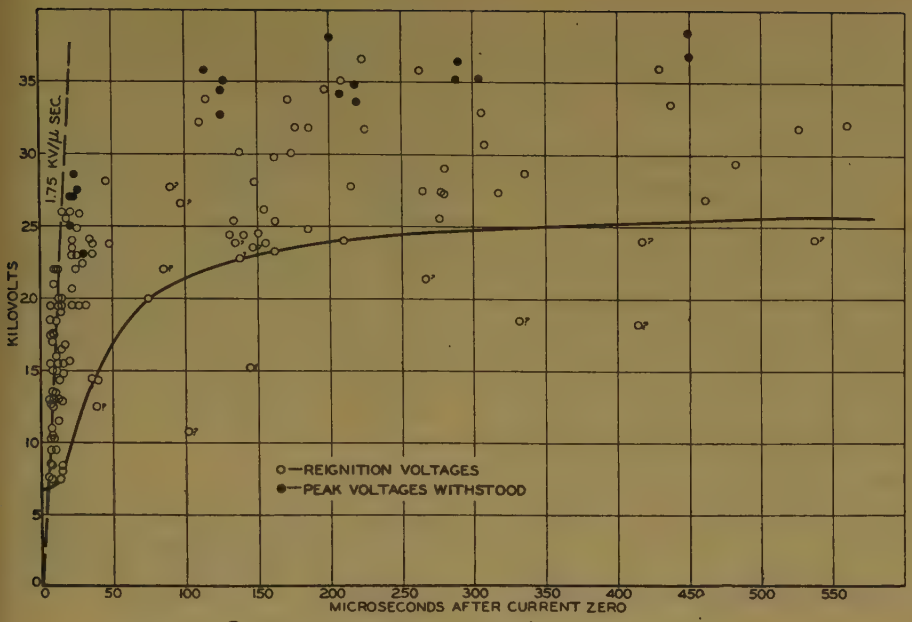
F—175 amperes at 5 pounds per square inch

Figure 5A–F. Dielectric recovery following apparent arc failure at current zero by 60-cycle arcs of various currents in a 0.765-inch solidly connected metal orifice with air flow from the tank at various gauge pressures

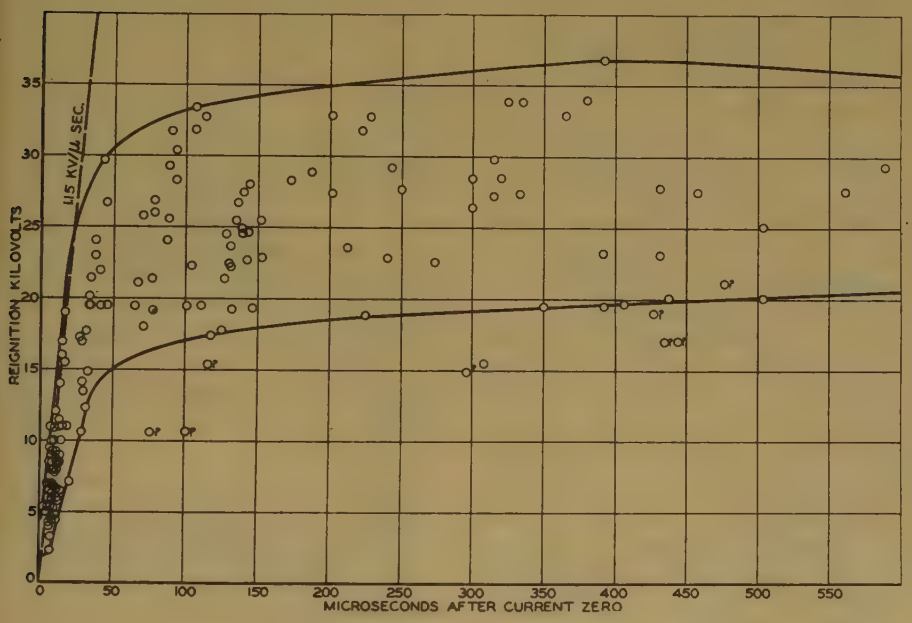
Orifice of Figure 1C

The method of voltage measurement from the oscillograms and of the measurement of the longer times probably involved errors of not more than 10 per cent, but random errors of as much as 50 per cent may easily be present in the measurement of recovery times of the order of 10 or 20 microseconds because of skewing of the oscilloscope axis and uncertainty in locating the often poorly defined arc "current zero" moment. This moment was taken as that at which the course of the arc terminal voltage began to be determined mainly by the circuit rather than by the arc. At low rms currents, this point on the arc terminal voltage record is generally clearly marked by a sudden radical change in slope followed by a smooth oscillation and is believed to be accompanied by a sudden virtual cessation of the arc current, or by an "arc failure." At the higher currents, however, such a transition point becomes much less clear on the oscillograms and also undoubtedly less clear in physical meaning, measurable arc conductivity often persisting up to and beyond the voltage reversal point, which is the only point at which the arc current is certainly known to be zero. It should be kept in mind, therefore, that "time after current zero" plotted in the figures actually means time after apparent arc failure.

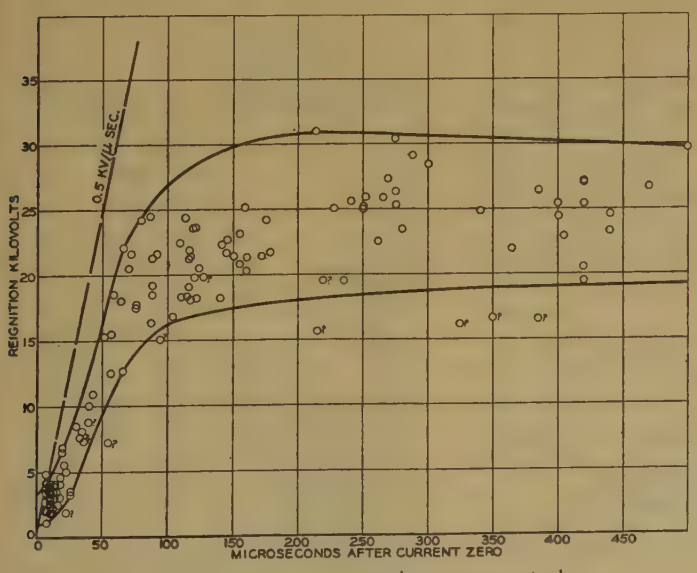
An outstanding feature of all experiments with a-c arcs in general and arcs in an air blast in particular is the very wide and apparently random variation in dielectric recovery, not only between tests but also between successive current zero moments. These are well illustrated by all of the curves in Figures 5 and 6, as well as by the oscillograms of Figure 4. The especially great variability characterizing the reignition of low-current arcs (Figure 5, A–F) probably is due in part to the variability in the currents just preceding arc failure. Similar variations in arc failure current



G—1,200 amperes at 40 pounds per square inch



H—1,200 amperes at 20 pounds per square inch



I—1,200 amperes at 5 pounds per square inch

Figure 5G–I. Dielectric recovery following apparent arc failure at current zero by 60-cycle arcs of various currents in a 0.765-inch solidly connected metal orifice with air flow from the tank at various gauge pressures

Orifice of Figure 1C

were first observed and pointed out by Attwood, Dow, and Krausnick,[7] who also measured and plotted dielectric recovery envelopes similar to those presented here except that they were for low current arcs in still air and in comparatively low voltage circuits.

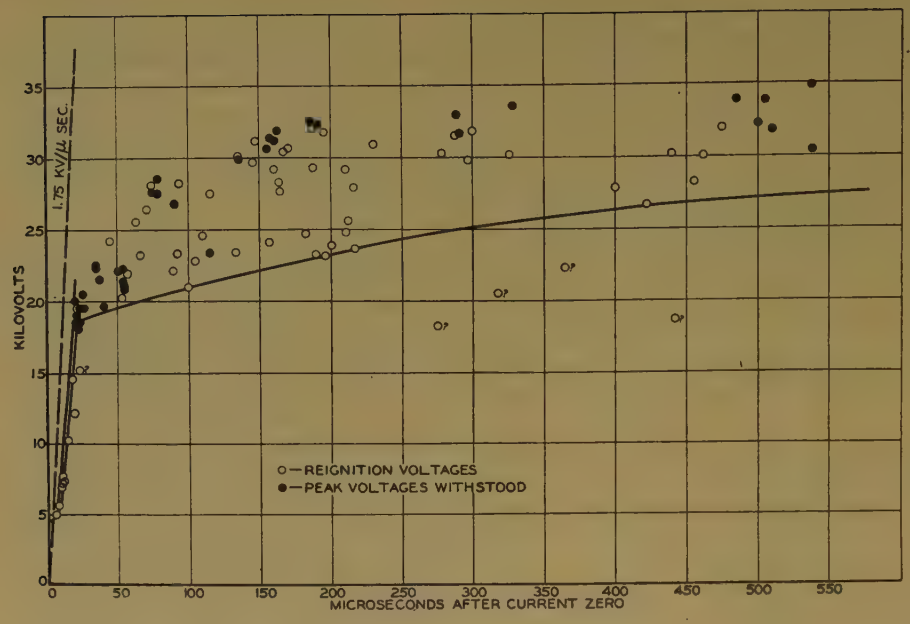
A general survey of the whole array of recovery envelopes and partial envelopes of Figure 5, covering the ranges of currents and pressures: 50, 175, 1,100, 2,200, and 4,200 amperes at 40, 20, and 5 pounds per square inch air tank pressure, reveals certain basic characteristics more or less common to them all. These characteristics are most clearly shown in Figures such as 5I and 5L where a combination of high current and low air pressure resulted in a slower and so more easily followed recovery than in many of the other figures. These envelopes exhibit three separate regions or successive stages of recovery. At very short times (up to 10 or 20 microseconds in these figures) reignition voltages are only moderately higher than the last arc voltages in the preceding half cycle, indicating relatively slight dielectric recovery. After this pause, however, the reignition voltages show a rapid rise with time along loci roughly parallel to the linear rate of rise values indicated by the dotted lines through the origin. This region of rapid recovery at a nearly constant rate is ended, with this orifice, when a rather broad and nearly horizontal breakdown region is reached where the dielectric strength becomes almost independent of time on this few-hundred-microsecond scale. Although showing wide variations and not always so clearly defined, this same pattern seems to characterize the dielectric recovery under all the conditions of current and air pressure covered by these tests. At currents as low as 50 and 175 amperes, the greater natural period of the higher-inductance circuits did not permit exploration of the very short times in which the initial pause might be expected to be evident and so the results are inconclusive with regard to the existence of a delay period at such low currents. Even the rapid-rise portions of the recovery envelopes were largely missed at these currents, especially at the higher pressures. The reignitions at 40 pounds per square inch, for example (Figures 5A and 5D), apparently occurred entirely in the nearly time-independent region. At 1,200 amperes (Figure 5, G–I) most of the early reignitions fell within the rapidly rising recovery region following a possible initial pause. At 2,200 amperes (Figure 5, J–L) and more especially at 4,200

amperes (Figure 5, M–O) reignitions within an initial pause region began to be apparent. At the higher currents and air pressures the upper limits of dielectric strength in the "plateau" regions (see Figures 5G, 5J, and 5K) were above the reach of the transient voltages which the testing circuits could produce and so these limits could not be determined. At 4,200 amperes, the reignition voltages available from the 6,900-volt source were insufficient even to reach the plateau regions.

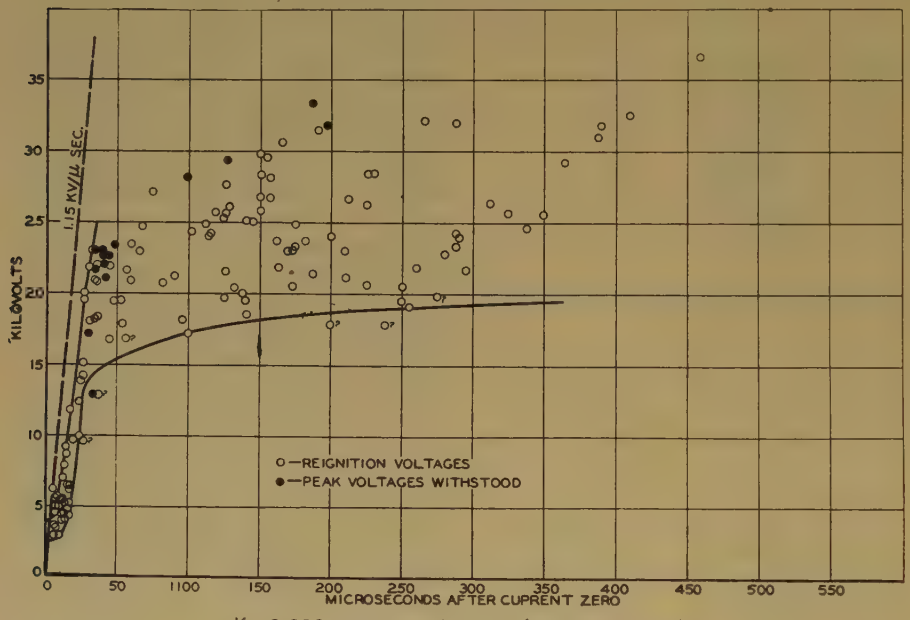
Figure 6 is a plot of a few dielectric

Figure 5J–O. Dielectric recovery following apparent arc failure at current zero by 60-cycle arcs of various currents in a 0.765-inch solidly connected metal orifice with air flow from the tank at various gauge pressures

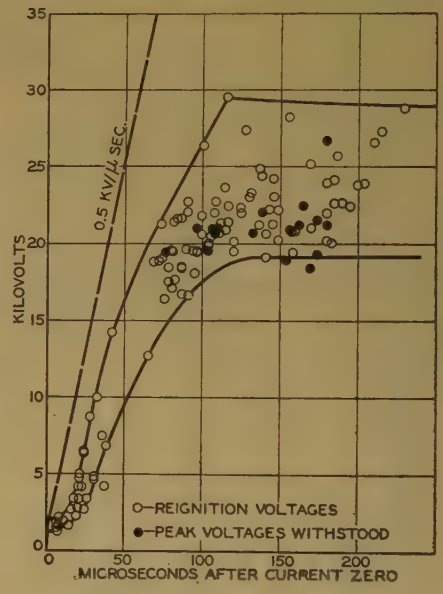
Orifice of Figure 1C



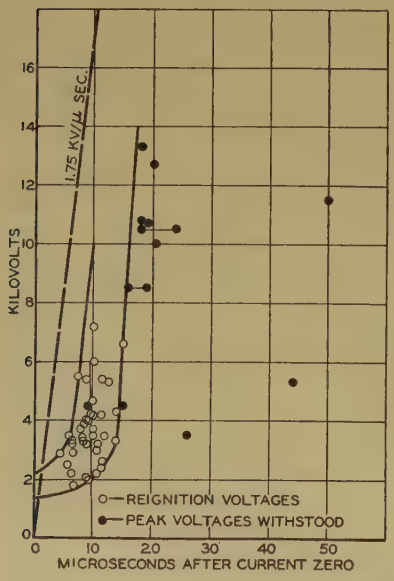
J—2,200 amperes at 40 pounds per square inch



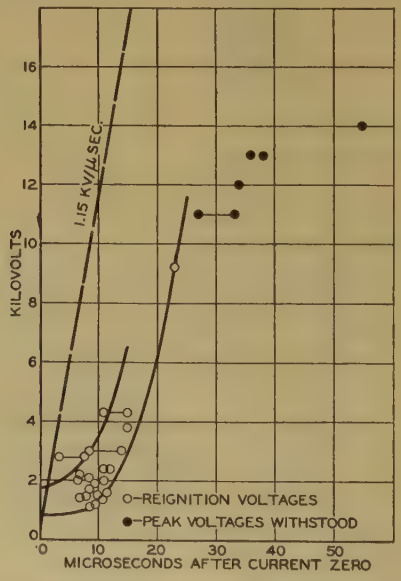
K—2,200 amperes at 20 pounds per square inch



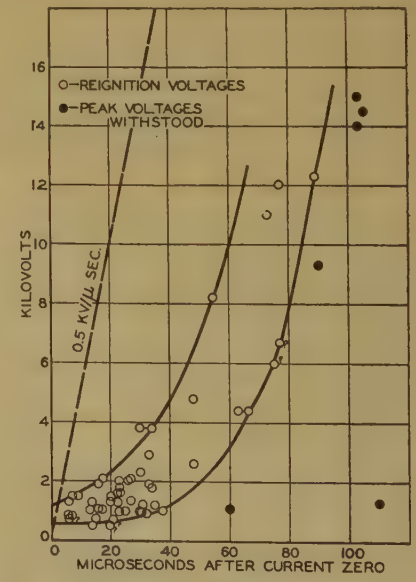
L—2,200 amperes at 5 pounds per square inch



M—4,200 amperes at 40 pounds per square inch



N—4,200 amperes at 20 pounds per square inch



O—4,200 amperes at 5 pounds per square inch

recovery tests with the more efficient insulated and vented orifice arrangement of Figure 1B at the same current and air pressure as the results of Figure 5I for the Figure 1C orifice. The superiority of the Figure 1B orifice is evident in its slightly shorter initial pause, its somewhat more rapid subsequent recovery, and in its much higher plateau voltage limit. This latter is in agreement with the interruption data of Figure 2 where the greatest difference in performance appears at low currents where reignitions occurred only in or near the plateau region.

In conjunction with the dielectric recovery envelopes, the results of Figure 3 now help to locate in space along the orifice axis the different time regions of dielectric recovery. Since the reignitions of the 175-ampere arc in the unshunted test circuit occurred generally in the third, or plateau, time region only, the plateau dielectric strength appears, in Figure 3A, to be fairly well distributed along the flow axis. The early dielectric recovery determining the extinction or reignition of the 1,100- and 2,000-ampere arcs, however, is shown to be quite closely confined to a short portion of the arc channel near the minimum flow section. Figure 3B seems to show that this critical arc length for early dielectric recovery lies nearer to the orifice entrance for the 2,000-ampere arc (faster circuit) than for the 1,100-ampere arc (slower circuit), suggesting that effective dielectric strength makes its first appearance near the entrance and then progresses along the axis in the direction of the flow.

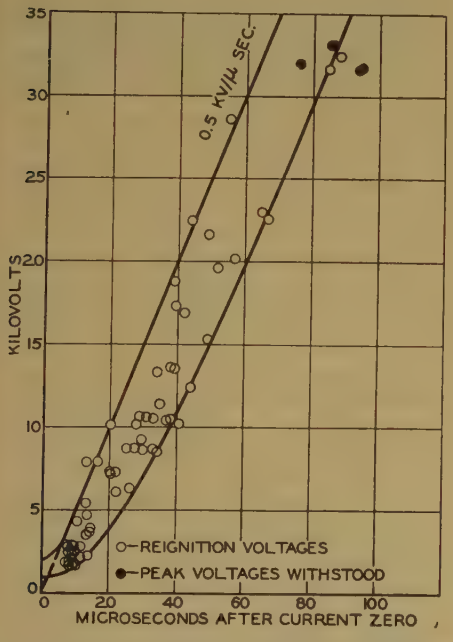


Figure 6. Dielectric recovery following current zero by a 1,100-ampere 60-cycle arc in the Figure 1B insulated metal orifice, lower contact vented, with air flow from the tank at 5 pounds per square inch gauge pressure

Discussion of Results in Terms of Theory

Space limitations do not permit an extended treatment of the various dielectric recovery theories in this paper, but a few possible theoretical interpretations of the foregoing results will be indicated briefly. There still remains so much of vagueness and uncertainty in the physical picture of the rapidly changing a-c arc space near a current zero that precise calculations on the basis of any theory are impossible. Only very broad limits, at best, can be calculated, often so broad as to be valueless in distinguishing between theories.

The apparent initial mean time delays before the beginning of rapid dielectric recovery have been estimated roughly from Figure 5, G–O, and presented in Table I as functions of pressure and rms arc current.

It is possible that these delays, observable only at the higher currents, are, or should be thought of as, mere transition periods of rapidly decreasing but still finite arc conductivity preceding actual arc extinction,[8] which extinction may coincide with the observed upturn in dielectric strength. If, on the other hand, this delay can be thought of as a period when the arc is already essentially out (having negligible conductivity) the delay may be explained in various ways. By analogy with the cooling of an initially uniformly heated solid cylinder, the diffusion theory would predict just such an initial delay preceding a rapid fall of temperature and ion density along the arc axis. Quantitative agreement with the observed time values can also be shown for a one-millimeter arc channel by using Slepian's[4] assumption of a hundred fold or so increase in diffusion rate due to turbulence. If the cooling, and deionization of the last arc filament should be much faster than this, a time delay of the same order can also be calculated to result from the finite rate of acceleration of the surrounding cold and comparatively dense air as it closes in on the low density and so electrically weak arc channel after its temperature and hence its pressure have dropped to a low value. With very rapid cooling, such a momentary associated pressure drop along the arc axis might at least be contributory to the delay in dielectric recovery.

Table I. Time Delays

Pressure		Initial Time Delay in μ sec at Various Currents		
Psi Gauge in the Tank	Abs Atm at Orifice Entrance	1,200 A	2,200 A	4,200 A
5	1.24	13	18	40
20	2.12	6	9	10
40	3.25	5	7	9

The subsequent rapid dielectric recovery also follows from the turbulence enhanced diffusion theory, both qualitatively and quantitatively. After the initial appearance of appreciable dielectric strength, probably at some most favorable point along the arc axis, it may be expected to increase rapidly also by lengthening of the affected region by axial progression of the cooling and recompression process and further by the stretching action of the nonuniform-air velocity near the flow constriction. That such a process may be tied loosely to and so tend to vary with the product of mean air velocity and air pressure (or density) is not surprising. This correspondence is evident in the rather marked agreement (discrepancy two to one or less) between the steep slopes of most of the well defined dielectric recovery envelopes and the slopes of the dotted lines drawn through the origins. These lines were drawn in accordance with the simple displacement theory of Prince[2] on the assumption of a dielectric barrier of sound air formed at "current zero" at the "vena contracta" and growing with the air velocity existing at this point. At first glance, this agreement appears to support the displacement theory, at least in part, but Slepian has shown[4] that the formation of such an assumed sound fluid barrier by simple displacement is physically impossible and the foregoing consideration of the probable diffusion process shows that the agreement can be explained on a basis other than that of simple displacement.

An interesting feature of the plateau dielectric strength values is their relative insensitivity to pressure, especially at the higher currents. The upper and lower limit values at 300 microseconds (well within the plateau region in all cases) have been plotted as a function of the air pressures at the orifice entrance in Figure 7 for different arc current values. The loci of the envelope limits are compared with a dot-and-dash line through the origin representing a linear extrapolation of the observed 60-cycle breakdown voltage at atmospheric pressure with neither air flow nor preliminary arcing. The growing departure with increasing arc current of the plateau breakdown

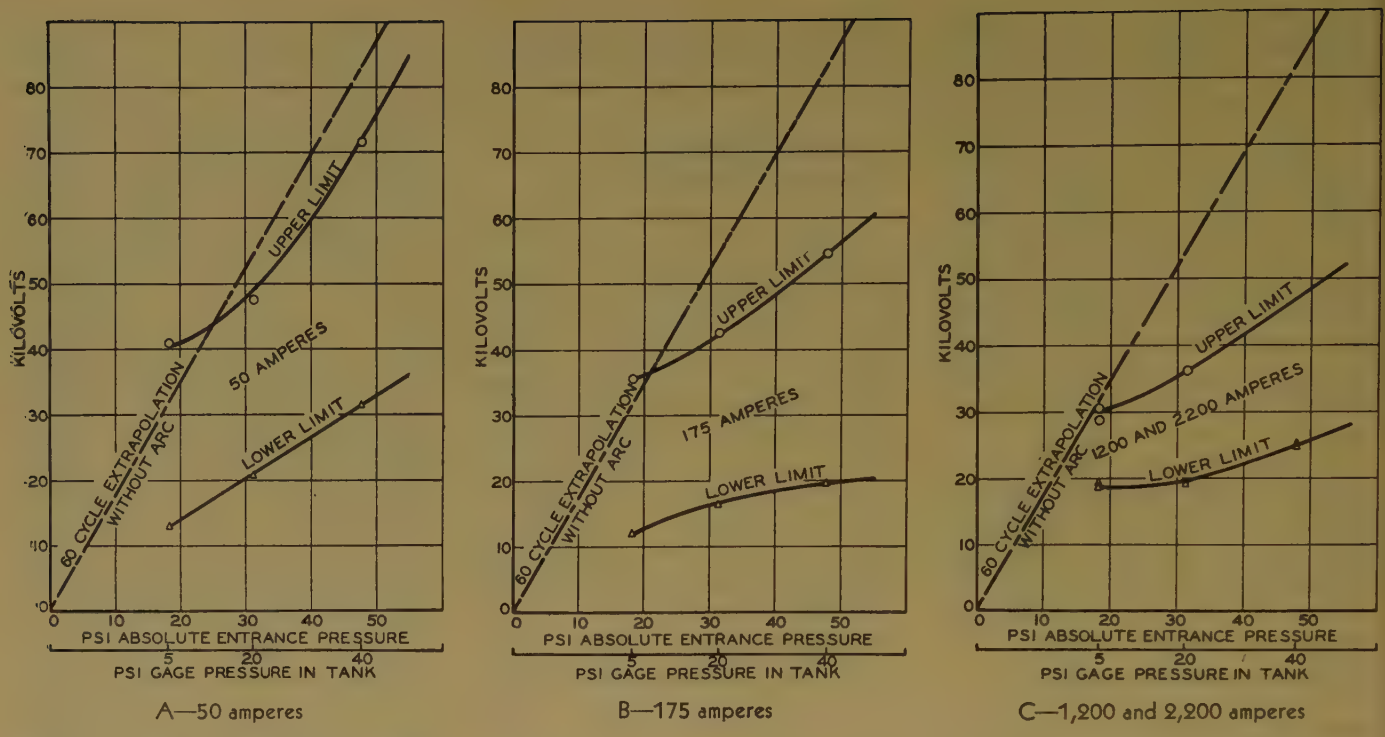


Figure 7. Effect of pressure on dielectric strength recovered 300 microseconds after extinction of arcs of various currents in the Figure 1C orifice

limits from such a no-arc line is particularly hard to explain on the basis of simple displacement of the arc channel by the air flow. It definitely seems to suggest the continuing presence of a still somewhat heated and perhaps partially ionized path along the arc channel after the initially very rapid diffusion has become comparatively slow. The presence in this orifice of a "dead space" of high pressure and low velocity gas at the tip of the upstream contact may be expected to contribute to the slow disappearance of this residual contaminated arc path. The shape of these curves and some incomplete recovery data at higher pressures suggest that these breakdown voltages all increase more rapidly with pressure in the higher pressure range used in practical circuit breakers than they do at the lower pressures covered by these figures.

References

1. Das Schaltproblem der Hochspannungstechnik, III, F. Kesselring, F. Koppelmann. *Archiv. fuer Elektrotechnik*, volume 30, 1936, pages 71–108.

2. The Cross-Air-Blast Circuit Breaker, D. C. Prince, J. A. Henley, W. K. Rankin. AIEE Transactions, volume 59, 1940, September section, pages 510–17.

3. J. Biermanns, Association Suisse des Electriciens *Bulletin*, volume 23, 1932, page 588.

4. Displacement and Diffusion in Fluid-Flow Arc Extinction, J. Slepian. AIEE Transactions, volume 60, 1941, April section, pages 162–7.

5. O. Mayr, *Elektrotechnische Zeitschrift*, volume 53, 1932, pages 75–81, and Association Suisse des Electriciens *Bulletin*, volume 23, 1932, pages 605–10.

6. A Vertical-Flow Outdoor Compressed-Air Breaker, L. R. Ludwig, B. P. Baker. AIEE Transactions, volume 60, 1941, May section, pages 217–22.

7. Reignition of Metallic A-C Arcs in Air, S. S. Attwood, W. C. Dow, W. Krausnick. AIEE Transactions, volume 50, 1931, pages 854–68.

8. The Electric Arc in Circuit Interrupters, J. Slepian. Franklin Institute *Journal*, volume 214, 1932, pages 413–42.

TRANSACTIONS SECTION

Preprint of Corresponding Pages From the Current Annual AIEE Transactions Volume

Applications of Thin Permalloy Tape in Wide-Band Telephone and Pulse Transformers

A. G. GANZ
MEMBER AIEE

THE development of thin permalloy tape and its use in cores have resulted from the increasing need for efficient magnetic structures at high frequencies. For some time for example, the trend in the telephone plant has been to the use of higher frequencies in the longer distance toll circuits. The reason is that these permit the simultaneous transmission of a larger number of telephone conversations over a single conducting circuit. The coaxial transmission system developed before the outbreak of the war, operates over the range of about 64 to 3,200 kilocycles and required transformers for repeater amplifiers and terminals capable of passing this wide band efficiently. Eddy current effects at these frequencies preclude the use in such transformers of magnetic material in conventional thicknesses.

With the advent of radar pulse transformers were needed urgently to transmit high power pulses. The latter are in the order of a microsecond in length and square-shaped with very steep sides. Fourier analysis of the pulses reveals large components of energy at high frequencies. Consequently, here also cores with low eddy current losses are required for the transformers, not only to assure the faithful transmission of the pulse shape, but also to reduce heating to permissible values.

The use of magnetic powder might suggest itself for these high frequency purposes. However, this involves a three dimensional subdivision of the material. The effect of the particle separations in the direction of the flux is equivalent to a large series air gap in the core, and the net permeability, even with the best alloys, is much too low. With punched laminations, as they are made thinner to reduce eddy currents, the number required for a given stack-up increases. Then fabricating, handling, and insulating the thin laminations to form cores become a problem.

There is thus an area of high intrinsic permeability and low eddy current losses which is satisfied neither by powder cores nor, at the other extreme, by practical punched lamination structures. It is here that permalloy cores of tape 2 mils and less in thickness find their field of use. The tape may be insulated and formed into cores in a continuous operation as will be described. The magnetic circuit is essentially closed. For the wide-band application small toroidal cores of one mil tape accordingly were used. For the pulse transformer applications one and two mil permalloy tape in the form of larger rectangular cores found immediate successful use. The excellence of the results obtained in these designs is largely attributable to these materials.

Fabrication

The permalloys are well adapted to use in thin tape cores. They can be rolled to one mil and less with relative ease compared, for example, with silicon iron. Nor are their magnetic properties materially impaired in the process. Of the two permalloys that mainly have been used for such purposes molybdenum permalloy has the higher permeability. It consists of 4 per cent molybdenum, 79 per cent nickel, and the remainder iron. However, 45 permalloy has a higher saturation value. It consists of 45 per cent nickel and 55 per cent iron. Both these alloys are melted in an arc furnace, and, after hot rolling of the thicker sections, the strip is cold rolled to finished size. For the thinnest tapes the final reductions are carried on in a multibacked rolling mill with small work rolls. For some applications the tape is used at 1/4 mil and 1/8 mil thicknesses. The latter is obtained by plating an equal thickness of copper onto the tape and rolling the combination down to 1/4 mil. The copper then is removed by an acid bath, leaving the desired 1/8 mil tape. Cross sections of thin tape are illustrated in Figure 1.

The method of insulation that has been found best is by cataphoresis, that is, the electrodeposition of fine colloidal particles. In this process the tape is passed through a suspension of silicic acid in acetone. The tape is kept at a positive potential of from 5 to 45 volts with reference to the container. The charged particles of the acid powder are attracted to the tape and form a very uniform coating, the thickness of which is under the control of the operator. The tape is dried by means of hot air jets as it leaves the bath and is wound under tension on a mandrel to form the core. The coating so applied is quite adherent. The apparatus that has been developed for this process is illustrated in Figure 2. The insulated core is heat treated in an atmosphere of hydrogen, and when rectangular

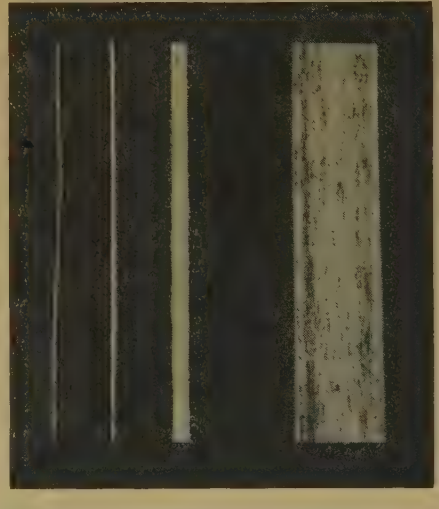


Figure 1. Molybdenum permalloy tape of 1/8 mil, 1/4 mil, and one mil thickness

Thicknesses compared with that of human hair shown at right. Magnification 100×

Paper 46-27, recommended by the AIEE committee on communication and presented at the AIEE winter convention, New York, N. Y., January 21–25, 1946. Manuscript submitted November 23, 1945; made available for printing December 12, 1946.

A. G. GANZ is with Bell Telephone Laboratories, Inc., New York, N. Y.

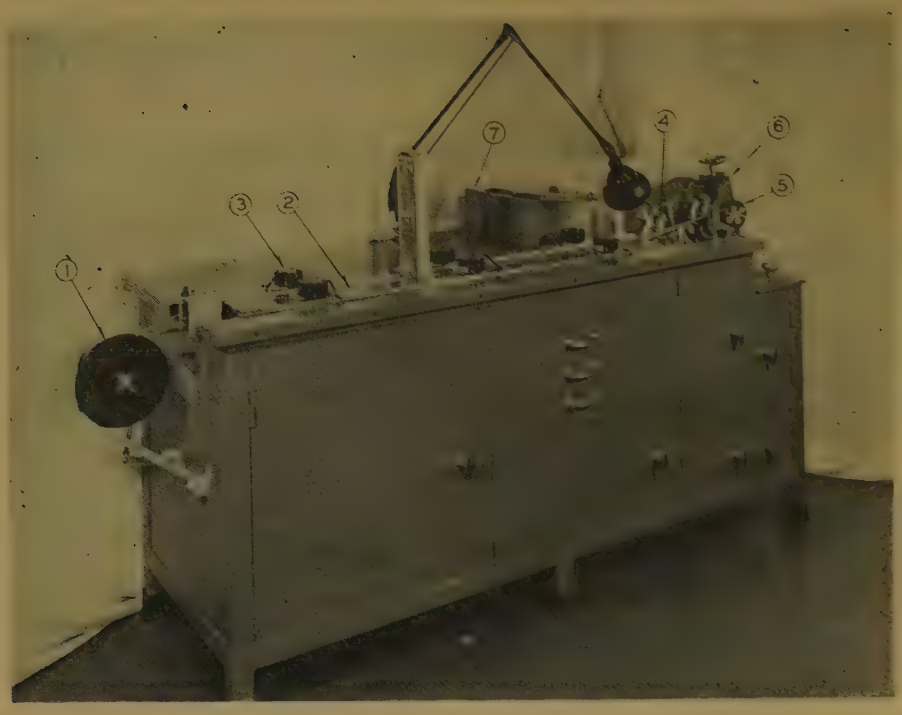


Figure 2. Cataphoresis insulating equipment

1—Tape supply spool and Prony brake
2—Cover for insulating bath
3—Motors for agitating suspension
4—Hot air jets
5—Mandrel on which core is wound
6—Take-up mechanism which winds tape under tension
7—Control panel

shaped it is held in clamps to maintain close dimensional tolerances. At the high temperatures the silicic acid dehydrates to silicon dioxide which provides the final interlaminar insulation. It also prevents welding of adjacent layers of tape during treatment. This process results in a fully adequate insulation and a typical packing factor of 80 per cent for one mil tape.

The cores so made are sufficiently rigid to require no strengthening by impregnation. Windings are applied to the closed cores by winding machines with circular shuttles. For some uses, a very small air gap is advantageous as will be described. The core is cut into halves using a wet rubber-bonded cutoff wheel. The windings are applied directly to the core halves. These are reassembled and the butting surfaces held together under pressure.

Application to Wide Band Transformers

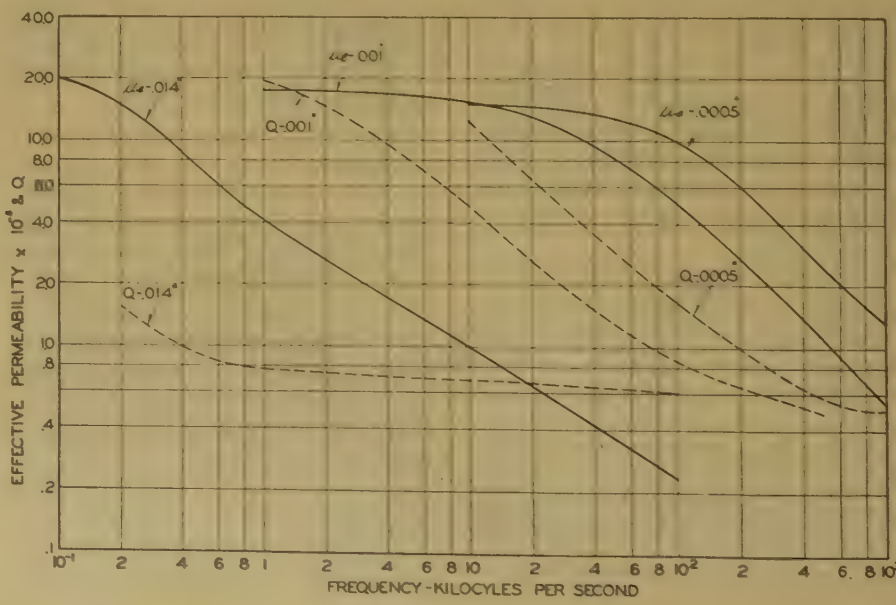
In the design of wide band transformers* for carrier telephone circuits, the problem is to obtain a sufficiently wide transmission band with low attenuation. Leakage inductance is a major factor in limiting this band. Reducing the leakage by closer coupling of the windings usually increases the winding capacitances which also restrict the range. Lower leakage therefore must come from the use of better cores which permit fewer turns without increasing the shunt attenuation. It is for such reasons that magnetic materials having higher permeabilities at frequencies above 50 kilocycles are needed.

Transformers in telephone circuits operate at low alternating voltages, and the flux densities in the cores are correspondingly low, less than 20 gausses. Molybdenum permalloy is characterized by very high permeability at low densities and also by very low hysteresis effects. This latter feature is valuable, since magnetic modulation might otherwise cause objectionable interchannel cross talk and noise. Figure 3 gives the effective permeability and Q of molybdenum permalloy tapes in the form of cores. A curve for 14 mil material also is given for purposes of comparison. As pointed out previously, the windings are applied to these cores with shuttle type winding machines. This permits a continuous magnetic circuit to be used and the high permeability of the tape to be fully retained in the core. The fact that the permeability of thin tape holds up at high frequencies is noteworthy and accounts for the low attenuation of the transformers. Figure 4 shows a typical core of one mil tape together with a transformer in which it is used.

Application in Low Voltage Pulse Transformers

Radar indicator circuits employ transformers passing low amplitude pulses of short duration. The high frequency components of the pulses correspond roughly to those of the wide band transformers and the design considerations requiring a high effective permeability core apply here also. However, the core material then is operated over a different portion of its magnetic characteristics from that for alternating current.

Figure 3. Effective permeability and Q of three thicknesses of 4-79 molybdenum permalloy as a function of frequency



* The design of the amplifiers in which these are used impose many other requirements, the discussion of which is beyond the scope of this paper

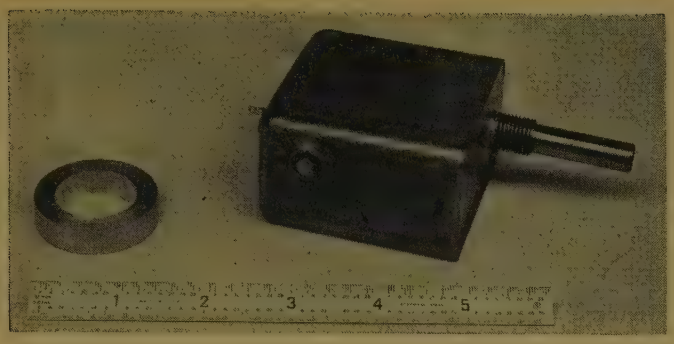


Figure 4. One mil 4-79 molybdenum permalloy core and transformer in which it is used

Operating range 64–3,200 kilocycles

Each unidirectional pulse conditions the material for the succeeding pulse. From the basic relation $e = -K_1NA \times (dB) \div (dt)$ each pulse demands a flux density change $\Delta B = (K_2Et) \div (NA)$, where E is constant during the pulse. For virgin material the initial flux density swing, $O-P_1-B_1$ leaves the material magnetized to the value B_1, as shown in Figure 5, the falling portions of the loop P_1-B_1 representing the decay occurring between pulses. The next cycle leaves the material magnetized to the value B_2, and so on. The steady state condition $B_n-P_n-B_n$ is reached when the falling portion of the loop is equal to the flux density change required by the pulse. The permeability that applies is then the ratio of the change in B to that in H for this cycle. For larger flux changes the loop becomes $B_r-P_r-B_r$ where B_r is near the retentivity of the material. This permeability value is always substantially less than the initial permeability and for molybdenum permalloy is in the order of 4,000 for a 1,000 gausses change. Reverse magnetization between pulses alters the phenomena, and this will be described under high power pulse transformers where it is more likely to occur.

The permeability values as described are of course reduced by eddy currents owing to the rapid change of flux during the pulse. For low density operation the characteristic of the material may be regarded as linear for analytical purposes. The equations for flux distribution, effective permeability, and losses for the linear case are given in the appendix. Ranges of values are given in the graphs of Figures 6 and 7.

These graphs illustrate the extreme variation of flux density which may be caused by eddy currents and the corresponding low permeability which may obtain with pulses of short duration, that is, small values of t. They also illustrate that this loss of permeability may be recovered to any desired extent by using thinner magnetic material, that is, smaller values of α. These considerations have led to the use of thin tape in low voltage as well as in high voltage pulse transformers. In a typical case one mil molybdenum permalloy was required. The core was toroidal and very similar to that illustrated in Figure 4. By this means it was possible in the transformer to transmit one microsecond square pulses with 0.05 microsecond sides without appreciable distortion.

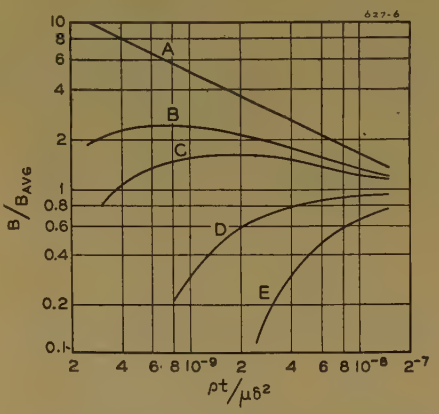


Figure 6. Relative flux density distribution in tape with square pulse voltage excitation

The average flux density B_{av} increases linearly with time

A—$y = \frac{\delta}{2}$ (surface)

B—$y = \frac{5}{12}\delta$

C—$y = \frac{3}{8}\delta$

D—$y = \frac{\delta}{4}$

E—$y = 0$

ρ = resistivity of tape in ohm-centimeters
δ = thickness of tape in inches
t = time in seconds
μ = d-c permeability
y = distance from mid-plane of tape in inches

Application in High Power Pulse Transformers

These transformers are used in the modulator circuits of radar transmitters to impress pulses on magnetrons. Power ranging from 100 to 1,000 kw is carried by these transformers for the duration of each square pulse. The high winding voltages range from 10 to 30 kv. Most uses demand small size and weight in apparatus, especially air-borne equipment. It is thus necessary that transformers for these powers insulated for the high voltages be designed on small core structures; for example, 2 pounds for 300-kw pulses. Further, the magnetrons to which the transformers are connected are voltage

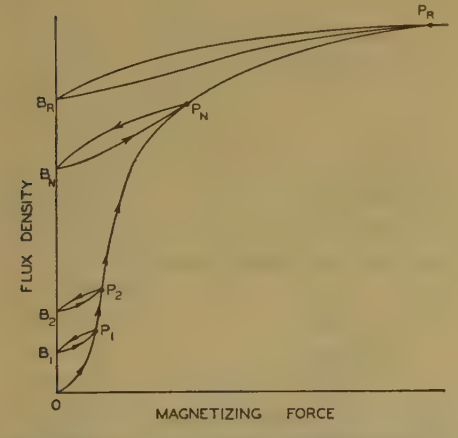


Figure 5. Sequence of flux-density changes with repeated unidirectional pulses, namely, $O-P_1-B_1$, $B_1-P_2-B_2$, $\cdots B_n-P_n-B_n$; larger changes result in $B_r-P_r-B_r$

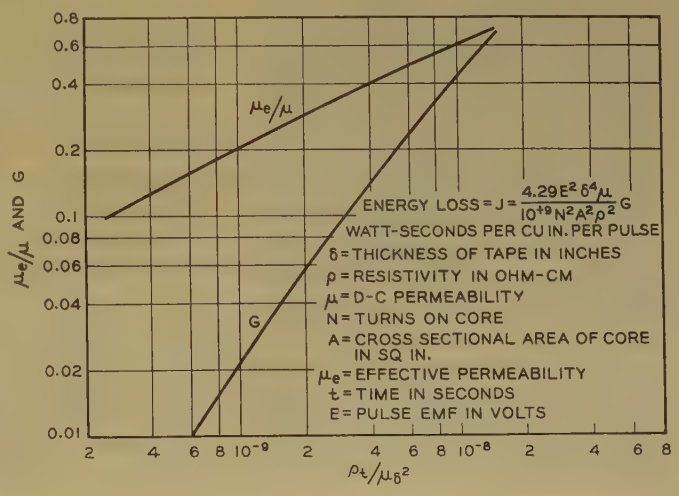


Figure 7. Curves for computing the effective permeability and the eddy current loss in tape with square pulse voltage excitation

When t is taken as the pulse length, J is the total loss during and after the pulse, assuming that the voltage is zero after the end of the pulse

sensitive in their operation. Appreciable magnetizing current being drawn through the source impedance is objectionable as it tends to reduce the voltage applied. All these factors impose severe demands on the core material requiring thin tape of the high quality obtainable in the permalloys.*

Range of Flux Density

The power capability of the transformers obviously is governed by the flux density range in the core material. Where there is simply decay of the flux between pulses, the minor $B-H$ loops traversed are like those shown in Figure 5. The useful flux density range is limited by the difference between saturation and retentivity. Generally speaking, as the magnetic quality of materials is improved and the permeabilities increase, the loops become more nearly square. This is illustrated for the two permalloys in Figures 8 and 9. Consequently, the difference between saturation and retentivity becomes less.

The available flux range can be increased substantially by the addition of an appropriate air gap. This is illustrated by the dotted hysteresis loop of Figure 8 for molybdenum permalloy with a 0.02 per cent air gap. The loop is sheared compared with the normal loop, and the apparent retentivity has been reduced to about 400. The flux density range now is increased to B_s-B_r', approximately 8,100 for the proportions shown in the figure. The maximum permeability, however, has been reduced, which represents some sacrifice in efficiency to obtain the flux range. The principle of adding an air gap for this purpose has found general use where reversal between pulses, as will be described, was not effective.

Reverse Magnetization

If, during the long interval between pulses, the material is magnetized in a reverse direction, an even wider flux range can be obtained. Referring to Figure 9 the peak reverse current between pulses provides a reverse magnetizing force of H_r. This causes the material to traverse the $P-B_r-A-B_n$ section of the loop. The rate is slow enough not to be affected by eddy currents. When the next pulse is applied, the flux can swing from B_n to P.

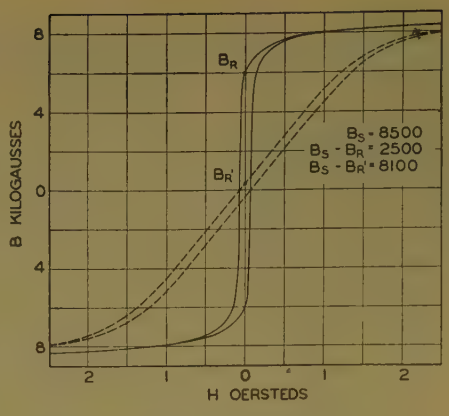


Figure 8. Hysteresis loop of one mil 4-79 molybdenum permalloy obtained on completed core, showing effect of 0.02 per cent air gap

Packing factor 0.8

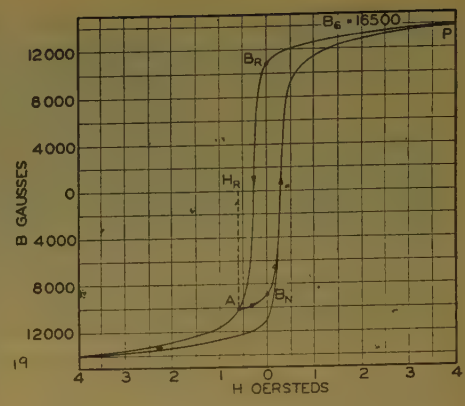


Figure 9. Hysteresis loop of 2 mil 45 permalloy obtained on completed core, showing flux density cycle with reverse magnetizing force

Packing factor 0.9

The material then is being used over the steepest part of the loop where the permeability is upwards of 50,000 over a large part of it (see Figure 9). It is possible with high enough peak reverse current to make available the limiting range from the retentivity below the axis to saturation above, that is, 10,000 + 16,500, or a total swing of 26,500 gausses for 45 permalloy. It is clear from the illustration that the reverse magnetizing force to be very effective must be at least greater than the coercive force of the material. It is also clear from comparing the solid with the dotted loops of Figure 8 that much better results can be obtained with a closed magnetic circuit than with an air gap. A reverse direct current fed to the winding has been used experimentally, raising the limiting flux swing to twice saturation. This has not been found of sufficient advantage in the pulse transformer cases considered to warrant the attendant circuit complications.

Reverse magnetization between pulses has been used very successfully in practice to obtain wide flux swings. The permalloys are especially well adapted to take advantage of this feature by virtue of their low coercive forces, which are 0.05 and 0.3 oersted as illustrated in Figures 8 and 9. These values permit reversal to be effected with minimum magnetizing forces.

High Density Pulse Magnetization

With high power operation the effect of the eddy currents on short pulses is usually to saturate the surface of the tape. This follows from the large differences in flux density within the tape as illustrated in Figure 6. Under these conditions the characteristics of the material are not at all linear, and the equations previously referred to do not directly apply. Unfortunately, the rigorous analysis of the nonlinear case is, at the least, laborious.

The high density behavior may be analyzed readily by making simplifying assumptions appropriate to the high permeability alloys. It will be observed from Figures 8 and 9 that the d-c permeability over most of the range is exceedingly high with a rapid transition to saturation. Accordingly, let infinite d-c permeability but finite saturation be assumed. At the start of the pulse the flux is confined to the surfaces of the tape which saturate. The saturated regions propagate toward the center of the tape until the pulse ends or until the entire lamination is saturated. Equations for permeability and loss for this case are derived in the appendix.

The behavior of actual tape of the best magnetic materials approximates that described. For example, for 1.1-mil tape the computed value of 5,050 for a 2.1-microsecond pulse using these equations is approached by the measured value of 4,000 (see Figure 11). The previous equations for the linear case are also of some use for high densities if a proper averaged value of d-c permeability is assumed. Together the two sets of equations provide a check on empirical data and serve as a guide in design.

Pulse Loops

Magnetic materials and cores are evaluated experimentally by pulse loops. The measuring circuit operates on the same principle as the familiar hysteresograph often used for obtaining 60-cycle loops. A schematic of the pulse circuit

* 4-43 Permalloy, a new alloy, also has been used, to a limited extent. It consists of 4 per cent molybdenum, 43 per cent nickel, and the remainder iron. It is characterized by high resistivity and the core losses are accordingly at least 30 per cent lower than other materials.

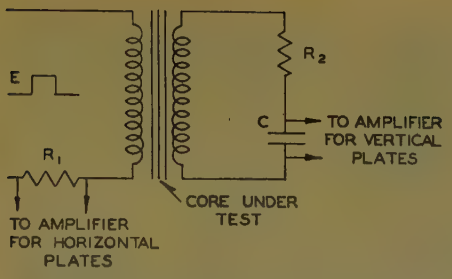


Figure 10. Simplified circuit schematic for presentation of pulse loop on oscilloscope screen

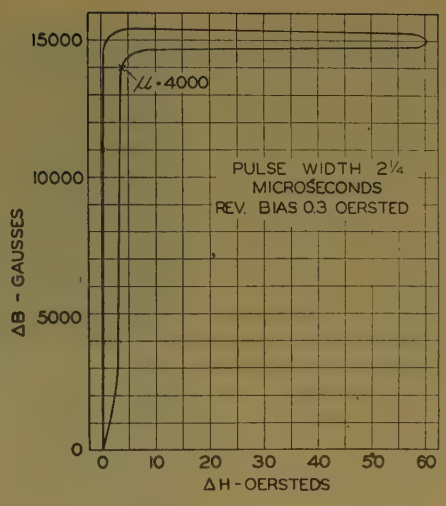


Figure 11. Pulse loop of 1 mil 4-79 molybdenum permalloy with reverse bias obtained on completed core without air gap

Packing factor 0.8

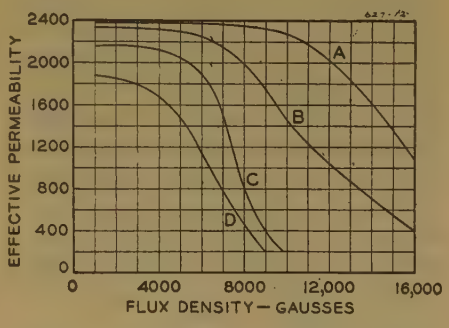


Figure 12. Effective permeability with 5 microsecond pulses obtained in completed core of 2 mil 45 permalloy without air gap

Packing factor 0.9

A—Reverse d-c bias, 0.52 oersted
B—0.28 oersted
C—0.078 oersted
D—No bias

for oscilloscope presentation is shown in Figure 10. The lower portion of the loops obtained defines the material, the return trace varying with circuit conditions. Calorimetric methods are relied upon for accurate loss determinations. Figure 11 shows the pulse loop of one-mil molybdenum permalloy tape in a core with 0.3 oersted reverse bias. The effective permeability is seen to be 4,000 with a flux swing of 14,000 gausses. The loop was taken with a reverse d-c bias instead of peak reversal between pulses, since the measuring circuit is better adapted to the former procedure. Peak reversal yields somewhat less flux swing, in this instance about 12,500 gausses. Figure 12 shows how different reversals affect the pulse permeability of a 45 permalloy core. The data were obtained from pulse loops with varying average flux densities. Figure 13 gives data on the pulse permeability of two thicknesses of molybdenum permalloy with small air gaps.

Figure 14 shows a pulse transformer which has found wide use in air-borne radar equipments. The core shown with it is the one on which the pulse loop of Figure 11 was taken. Figure 15 shows a large pulse transformer with a 45 permalloy core. In contrast there is shown one of the smallest transformers of this type. These illustrate the range of application of the superior magnetic properties of thin permalloy tape.

Application to Nonlinear Coils

It is characteristic of molybdenum permalloy mentioned here that the magnetization curve is very steep, that it has a relatively sharp transition to the saturated condition, and that the permeability there is very low. Valuable use has been made of these features in the generation of groups of harmonics. The basic circuit is shown schematically in Figure 16. The generator provides current of the fundamental frequency to which the series coil and capacitor are resonant. During that part of the cycle where the nonlinear coil has a high inductance, the capacitor C_2 is charged. As the coil begins to saturate its inductance falls and the capacitor discharges through it. This carries the material farther into the saturated region where the permeability is very low. The coil thus acts as a magnetic switch by which a sharply peaked current pulse rich in harmonics is generated. These harmonics pass through appropriate equalizers and filters to supply the carrier currents to multichannel coaxial and other carrier systems. Coils of this type are attractive as modulating devices, as they are stable and have an indefinitely long life compared to vacuum tubes.

The efficiency of the device requires that the inductance during the nonsatu-

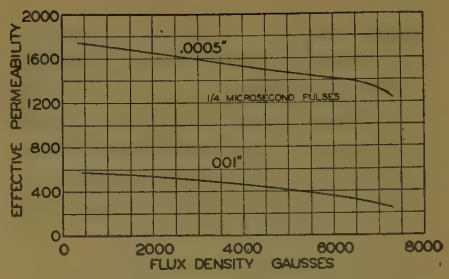


Figure 13. Effective permeability characteristics of 4-79 molybdenum permalloy obtained in completed cores with small air gaps

Packing factor 0.7 for 1/2 mil tape and 0.8 for 1 mil tape

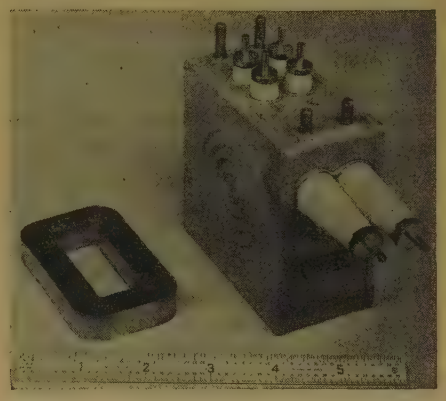


Figure 14. Rectangular core of 1 mil 4-79 molybdenum permalloy and pulse transformer in which it is used

Pulse power 100 kw

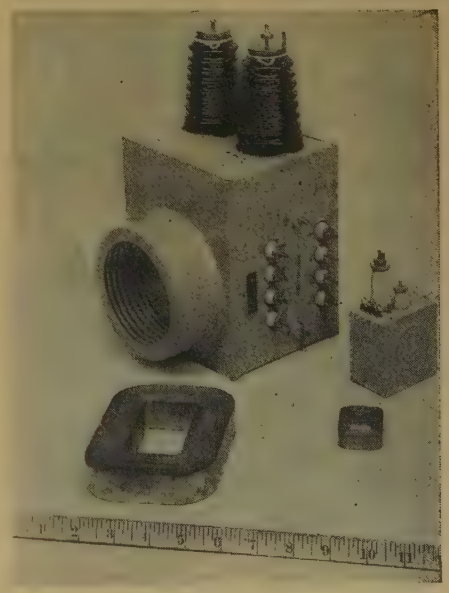


Figure 15. Rectangular core of 2 mil 45 permalloy weighing 3 pounds and 1/4 pound core of one mil 4-79 molybdenum permalloy with the pulse transformers in which they are used

rated interval be very high compared to the saturated interval. For a fundamental of 120 kilocycles the flux swing from negative saturation to positive takes place in less than 4 microseconds. The approach to saturation takes place in tenths of a microsecond. If eddy currents are not minimized, much larger power input is needed to avoid broadening the peaked pulse and so reducing the output of high frequency harmonics. These considerations again dictate a core of very thin molybdenum permalloy tape, in this instance 1/4 mil. This core in a specific case has differential permeability, with eddy currents, over the steep part of the curve of more than 10,000. This is in striking contrast to the value of 3 at the flat portion of the curve, where it is driven by the peak magnetizing force of 20 oersteds. Similar coils have found military uses. In tank communication circuits they provide means for frequency modulation of a desired harmonic of the carrier input. The fundamental frequency there is 400 kilocycles requiring 1/8 mil tape. In order to operate effectively at this frequency and with small power, the cores were designed with a diameter of 0.3 centimeter and weigh only 20 milligrams. Figure 17 illustrates coils of this type.

Nonlinear coils have found further important use as magnetic switches in the generation of high power pulses. These are accompanied by heavy currents up to 100 amperes. Nonlinear coils readily can be designed to carry heavy currents in the saturated condition. They therefore can function as high current switches with the feature that they do not deteriorate with use. Cores of one mil molybdenum permalloy tape for this purpose weigh from 2 to 30 pounds and are illustrated in Figure 18. They are used in radar equipments.

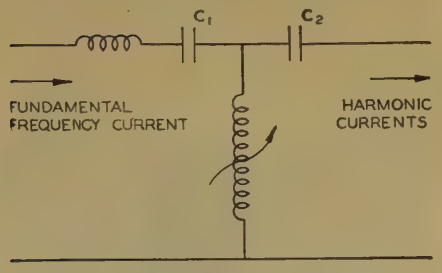


Figure 16. Elementary circuit for harmonic generation by nonlinear coil

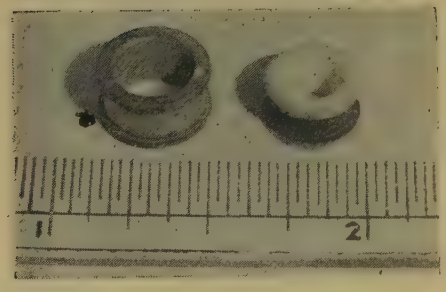


Figure 17. Cores of 1/4 mil and 1/8 mil 4-79 molybdenum permalloy used in harmonic generator coils

Tape is wound on ceramic forms for mechanical support. Weights of metal 60 and 20 milligrams, respectively



Figure 18. Cores of one mil 4-79 molybdenum permalloy tape and partially assembled nonlinear coils in which they are used

Weights of core stacks and pulse powers are as follows: 30 pounds, 1,000 kw; 2 pounds, 100 kw; 1 pound, 50 kw

Appendix

Voltage Pulse Magnetization—Linear Case

The applied voltage is taken as constant for the duration of the pulse which is the usual condition for pulse transformer operation. If a homogeneous material with constant permeability and not saturable is assumed, the following expressions are derived* from Maxwell's equations by straightforward methods. The flux distribution during the pulse after an interval of time t is given by

$$\frac{B}{B_{avg}}=\frac{2.025\mu\delta^2\times10^{-8}}{\rho t}\left[\frac{2y^2}{\delta^2}-\frac{1}{6}+\frac{49.3\rho t}{\mu\delta^2 10^{-6}}-\frac{2}{\pi^2}\sum_{n=1}^{\infty}\frac{(-1)^n}{n^2}\cos\frac{2n\pi y}{\delta}\exp\frac{-487n^2\rho t}{\mu\delta^2 10^{-6}}\right] \quad (1)$$

where the average flux density in the tape is

$$B_{avg}=\frac{15.5Et}{NA}10^{+6}$$

gauss.

The effective permeability, defined for pulses as the ratio of the average flux density in the tape to the magnetomotive force at the surface, at time t during pulse is given by

$$\mu_e=\frac{49.3\rho t}{\delta^2}\times10^{+6}\left[\frac{1}{3}+\frac{49.3\rho t}{\mu\delta^2 10^{-6}}-\frac{2}{\pi^2}\sum_{n=1}^{\infty}n^{-2}\exp\frac{-487n^2\rho t}{\mu\delta^2 10^{-6}}\right]^{-1} \quad (2)$$

The total energy loss due to eddy currents during and after the pulse, assuming that the voltage after the pulse is zero for infinite time, is given by

$$J=\frac{4.29E^2\mu\delta^4}{10^9N^2A^2\rho^2}\left[\frac{49.3\rho T}{\mu\delta^2 10^{-6}}-\frac{1}{15}+\frac{6}{\pi^4}\sum_{n=1}^{\infty}n^{-4}\exp\frac{-487n^2\rho T}{\mu\delta^2 10^{-6}}\right]$$

watt-seconds per cubic inch per pulse (3)

This equation is plotted in Figure 7. The conditions assumed apply to a well-designed pulse transformer in the usual circuit. There the voltage in the relatively long interval between pulses is small, and the total flux decays so slowly that the eddy current losses from this source can be neglected. On the other hand, eddy current losses accompany the rapid transition from a nonuniform to a uniform distribution of the flux within the tape after the pulse, and these losses are included in the foregoing expression.

If the voltage after the pulse is not small, no general expression can be given as the loss then depends on the particular conditions. However, the loss during the pulse itself, which is the major part, is determined and is given by

$$J_T=\frac{2.54E^2\delta^2}{N^2A^2\rho}\left[\frac{T}{12}-\frac{20.8\mu\delta^2}{10^{11}\rho}\sum_{n=1}^{\infty}\times\frac{1-\epsilon^{-\frac{487n^2T\rho}{10^{-6}\mu\delta^2}}}{n^4}+\frac{5.20\mu\delta^2}{10^{11}\rho}\sum_{n=1}^{\infty}\frac{1-\epsilon^{-\frac{974n^2T\rho}{10^{-6}\mu\delta^2}}}{n^4}\right]$$

watt-seconds per cubic inch per pulse (4)

where

* By Doctor L. A. MacColl, Bell Telephone Laboratories, Inc.

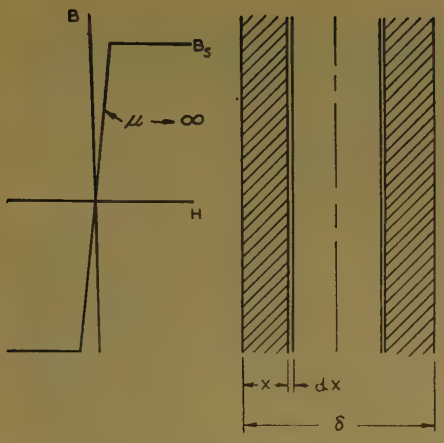


Figure 19

μ = the permeability relative to free space without eddy currents
δ = the thickness of the tape in inches
y = the distance from the mid-section of the tape in inches
ρ = the resistivity in ohm-centimeters
t = the time in seconds
T = pulse length in seconds
A = the cross section of the core in square inches
N = the number of turns in the winding
E = the electromotive force applied to the winding, in volts

Current Pulse Magnetization—Linear Case

The corresponding equations for the current pulse are given for completeness:

$$B=\frac{\mu NI}{2.02l}\left[1-\frac{4}{\pi}\sum_{n=1}^{\infty}n^{-1}\times\left(\sin\frac{n\pi}{2}\right)^2\sin\frac{n\pi y}{\delta}\exp\frac{-122n^2\rho t}{\mu\delta^2 10^{-6}}\right] \text{ gauss} \quad (5)$$

$$\mu_e=\mu\left[1-\frac{8}{\pi^2}\sum_{n=1}^{\infty}n^{-2}\times\left(\sin\frac{n\pi}{2}\right)^4\exp\frac{-122n^2\rho t}{\mu\delta^2 10^{-6}}\right] \quad (6)$$

$$J=\frac{2.58N^2I^2\mu}{10^8 l^2}\sum_{n=1}^{\infty}n^{-2}\left(\sin\frac{n\pi}{2}\right)^4\times\left(1-\exp\frac{-122n^2\rho T}{\mu\delta^2 10^{-6}}\right)$$

watt-seconds per cubic inch per pulse (7)

where l is the length of magnetic circuit in inches, and I is the current in amperes, constant during pulse and zero thereafter. J includes the losses during and after the pulse.

Voltage Pulse Magnetization—Nonlinear Case With Saturation

For this case an idealized magnetization curve as shown in Figure 19 is assumed. With infinite permeability the tape is divided at any instant into surface sections which are saturated and a central section devoid of flux as shown in the figure.

For a section of tape of thickness δ and unit length and width, the eddy current

$$i_e=2\Delta B_s K_1\frac{dx}{dt}\cdot\frac{2.54x}{2\rho} \text{ amperes}$$

where ΔB_s is change in flux density from the initial value to saturation. $\Delta B_s = B_s$ when the material originally is unmagnetized. Since the permeability is infinite, the magnetomotive force at the surface is only that required to maintain the eddy current. Whence, $H=0.495i_e$ oersted. The change in average flux density, $\Delta B_{avg}=(2x\,\Delta B_s)\div\delta$. Whence the effective permeability

$$\mu_e=\frac{\Delta B_{avg}}{H}=\frac{1.59\rho}{K_1\delta\dfrac{dx}{dt}}$$

For the winding

$$E=2\Delta B_s K_1\frac{dx}{dt}\frac{NA}{\delta}$$

By substitution

$$\mu_e=\frac{3.18\rho NA\,\Delta B_s}{\delta^2 E} \quad (8)$$

Since the change in average flux density is linear with time, this also may be written

$$\mu_e=\frac{0.493\rho T_0 10^{+8}}{\delta^2}, \text{ where } T_0=\frac{\Delta B_s}{\Delta B_{avg}}T \quad (9)$$

where T_0 is time in seconds to saturate tape without eddy currents. It is also the time required to saturate the entire cross-section of the tape under the assumed conditions. As before, μ_e is relative to free space, ρ is the resistivity in ohm-centimeters, A is the core area in square inches, δ is the tape thickness in inches, B_s is in gauss, E is in volts, N turns, and T is pulse length in seconds.

Since the effective permeability is constant during the pulse, the loss is proportional to the square of the flux density and may be written

$$\text{loss}=\frac{6.52VF\Delta B_{avg}{}^2 10^{-8}}{\mu_e} \text{ watts} \quad (10)$$

where V is net core volume in inches cubed, F is in pulses per second, ΔB_{avg} is the change in average flux density to end of pulse. Since magnetic energy is proportional to $\int HdB$, there is no storage of energy at any time under the assumed condition of infinite permeability.

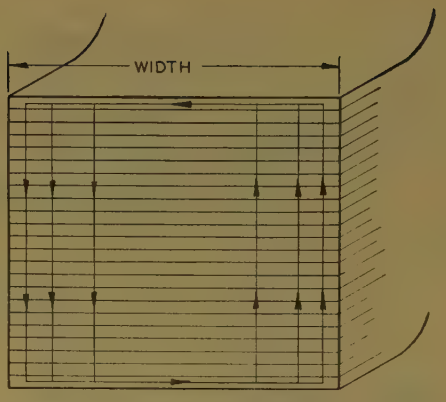


Figure 20. Distribution of intersheet eddy currents in cross section of core

Resistivity across stack ≫ than resistivity of tape. The dimension for the width shown is to be used for the thickness, δ, in the equations when these are applied to the core

Intersheet Eddy Currents

It is worth noting that all the foregoing equations for tape may be employed in dealing with intersheet effects in a core. The resistivity across the stack is ordinarily very high compared to that of the tape The eddy currents then run essentially perpendicular to the tape, and the current loops are completed in the end tapes as illustrated in Figure 20. The distribution of flux and currents in the cross section is then the same as that in a strip having resistivity equal to that across the stack, thickness equal to the stack width, and of indefinite extent in the remaining directions. It is only necessary to substitute the width w for δ in the expressions and graphs. Evidently, when the stack resistivity equals $(\rho w^2)\div\delta^2$, the stack losses are equal to those contributed by the tape.

References

1. Permalloy, H. D. Arnold, G. W. Elmen. *Journal* of the Franklin Institute, volume 195, May 1923.

2. Magnetic Alloys of Iron, Nickel, and Cobalt, G. W. Elmen. *Journal* of the Franklin Institute, volume 207, May 1929, pages 583–617.

3. Improvements in Communication Transformers, A. G. Ganz, A. G. Laird. AIEE Transactions, volume 54, 1935, December section, page 1367–73.

4. Magnetic Generation of a Group of Harmonics, E. Peterson, J. W. Manley, L. R. Wrathall. AIEE Transactions, volume 56, 1937, August section, pages 995–1001.

5. Survey of Magnetic Materials and Applications in the Telephone System, V. E. Legg. *Bell System Technical Journal*, volume 18, July 1939, pages 438–64.

Laboratory Method for Objective Testing of Bone Receivers and Throat Microphones

E. H. GREIBACH
MEMBER AIEE

THE development and testing of inertia-type transducers require equipment similar to the artificial ear used in the testing of air conduction receivers.

The problem of building a reliable artificial ear is relatively simple compared to that of constructing an artificial mastoid for testing bone conduction receivers, or an artificial throat for testing throat microphones. The artificial ear employs an air cavity, which simulates the cavity of the ear and couples the receiver under test to a condenser microphone, in order to measure the pressure produced in the cavity by the receiver. In the case of the bone conduction receiver, the role of the air cavity is played by a layer of skin, coupling the bone conduction receiver to the mastoid bone. A similar situation is encountered in the case of throat microphones, where the larynx is coupled to the throat microphone through an interposed layer of skin. The properties of the layer of skin vary over a very wide range, making it difficult to determine what is the average impedance looking into the human head or throat. There is also a controversy as to whether one should measure the pressure or the velocity transmitted through the layer of skin.

An artificial throat suitable for testing throat microphones must have a vibrating platform capable of imparting a velocity to a throat microphone through a filter simulating the layer of skin. The platform must be large enough to make the microphone response independent of small changes in orientation or locating of the microphone on its surface. The velocity of this platform should have some simple law of distribution over the desired frequency spectrum (preferably a uniform distribution) of approximately 50 to 10,000 cycles. At the same time, the platform must have a sufficiently high mechanical impedance in order for its motion not to be affected by the high impedance of the tested throat microphone at its points of resonance. In the selection of a proper system, consideration was given to a design of platform which would be controlled by one of the three possible parameters, namely: resistance, stiffness, or mass. Resistance control has the advantage of uniform velocity distribution over the frequency range, but it was very difficult to find a physical embodiment of a stable mechanical resistance. Stiffness control is difficult to realize, since in a physical stiffness element there must be some mass present.

A mass controlled platform on the other hand is relatively easy to construct. A platform having a mass of approximately 4,000 grams can be driven with a relatively small expenditure of wattless power. For example, in order to impart an amplitude A of 10^{-7} centimeters at 10,000 cycles (which amplitude is far in excess of the amplitude of vibration actually encountered) to a mass M of 4,000 grams, a wattless power of $\omega^3 MA^2 \times 10^{-7}$ or 0.001 watt, is required.

In an early model of the artificial throat, one end surface of a brass cylinder, approximately $3\frac{1}{4}$ inches in diameter and $3\frac{1}{2}$ inches in length, was used as the driving platform. The opposite end of the cylinder was designed to support a driving "voice" coil. This voice coil moves in the field provided by the cylindrical air gap of a 50 watt loud-speaker structure (Jensen, PM type) (5 in Figure 1).

In order to insure mass-controlled operation, the cylinder is supported and guided by a system of extremely flexible springs, resulting in a natural resonant frequency for the mass and stiffness combination of approximately 1 cycle per second. The power which has to be supplied to the driving coil can be estimated approximately as follows.

The total impedance of the driving coil of N turns and a diameter (D), moving in a magnetic field of intensity H, can be shown to be:

$$Z_t = Z_e + \frac{\pi^2 (NHD)^2 10^{-9}}{Z_m} = Z_e + Z_d$$

In this equation Z_e is the electrical blocked impedance of the magnetic coil, while the second term, which we may call Z_d, is the motional impedance of the coil in the magnetic field. The mechanical impedance, Z_m, in this case is essentially $j\omega M$, since the resonance frequency here is far below the frequency of forced vibrations at which the mass is driven. The motional impedance Z_d is the part of the total impedance which is responsible for the energy transfer from the coil into the mass of the cylinder. We can, therefore, state that the efficiency of the driving system is approximately proportional to $\left| \frac{Z_d}{(Z_e + Z_d)} \right|$, or, since Z_d is in this case negligible in comparison with Z_e, the efficiency is equal to $\left| \frac{Z_d}{Z_e} \right|$. Z_d is approximately equal to 0.025 ohm for actual values of $N = 250$, $D = 2\frac{1}{2}$ inches, and $H = 15{,}000$. Thus, with Z_e equal to approximately 250 ohms at 10,000 cycles, we have an energy transfer efficiency at 10,000 cycles equal to 10^{-4}. Therefore in order to impart to this mass an amplitude of 10^{-7} centimeters at 10,000 cycles, the necessary power input to the coil is 10 watts. The actual amplifier used to drive the artificial throat with a power output capacity of 50 watts was found sufficient to satisfy all requirements encountered in development work and testing.

Figure 1 shows the cross section of the artificial throat described above. The cylinder (1) is supported by four springs (2 and 3), illustrated in Figure 2. These springs serve to guide the cylinder in the axial direction. They are extremely flexible in a direction perpendicular to their plane, while they are very rigid in a radial direction. Two such springs, displaced angularly by 90 degrees to each other, are used near each end of the cylinder. These springs were punched out of thin phosphor bronze sheet, in order to keep the resonant frequencies of their free spring portion S, connecting the inner and outer rings of the springs, considerably below 50 cycles. This is important in order to prevent these springs from reacting upon the motion of the cylinder in the useful frequency range. The weight of the cylinder is supported by four very compliant helical springs

Paper 46-25, recommended by the AIEE committee on communication and technical program for presentation at the AIEE winter convention, New York, N. Y. January 21–25, 1946. Manuscript submitted November 19, 1945; made available for printing December 13, 1945.

E. H. GREIBACH, director of research, Sonotone Corporation, Elmsford, N. Y.

The author acknowledges the co-operation of the Sonotone Corporation in sponsoring the development work on the apparatus described. He desires also to express his appreciation to F. P. Greenwood, M. E. Zaret, and Jack Sobol for their co-operation in the development of the testing equipment and to H. A. Pearson for many valuable discussions during the progress of the work.

(6), which are permitted to be sufficiently extended to support the weight of the cylinder. The position of the helical springs can be adjusted by means of levers mounted in the cylinder (7), thus providing for proper centering of the voice coil (4) in the air gap. The throat microphone under test is shielded both magnetically and electrically by the series of disks shown in Figure 1.

The system of compliant springs maintains the mass of the cylinder effectively floating in air and does not affect its pure mass impedance character. This behavior of the cylinder is, however, disturbed at the frequency at which the cylinder ceases to be a rigid mass and becomes a half wave length transmission line with distributed parameters. This change occurs for a brass cylinder of the dimensions used at a frequency of approximately 17,500 cycles. Therefore, at frequencies whose second and third harmonics are equal to 17,500 cycles, marked resonance effects were observed. This resonance was shifted to a higher frequency by substituting stainless steel for brass, since the velocity of sound in stainless steel is considerably higher than in brass. By using stainless steel cylinders of a shape slightly different from the one shown in Figure 1, it was possible to move this half wave resonant frequency up to 27,000 cycles. In this way, the first resonant effect obtained was in the neighborhood of 9,000 cycles.

In order to obtain a uniform velocity of the platform in the frequency range required, it is necessary to energize the driving coil with a current increasing linearly with frequency. This was accomplished by providing the input of the linear 50-watt amplifier with a simple dividing network, consisting of condensers and resistors. Figure 3 shows the velocity distribution of an artificial throat containing the brass cylinder. Two peaks, one at 5,800 and one at 8,700 cycles are seen in this figure. They are due to a very small amount of second and third harmonics present in the output of the driving amplifier. The peaks are sharp on account of the very high Q of the brass cylinder. In the final design, using a stainless steel cylinder, the velocity distribution turned out to be uniform within ± 2 decibels in the range from 50 to 10,000 cycles.

The velocity calibration was obtained by means of the experimental setup shown in Figure 4. It consists of a second voice coil attached to the moving platform of the artificial throat under test. This coil moves inside a stationary magnetic field provided by a permanent magnet loud speaker field structure *m*. The magnet is suspended from a substantially vibration-proof mounting shown in the figure. This mounting consists of two heavy cylinders connected to each other by means of three very flexible springs and a large oil dash pot to provide damping. The upper of the two cylinders is suspended from the ceiling by means of a set of three chains

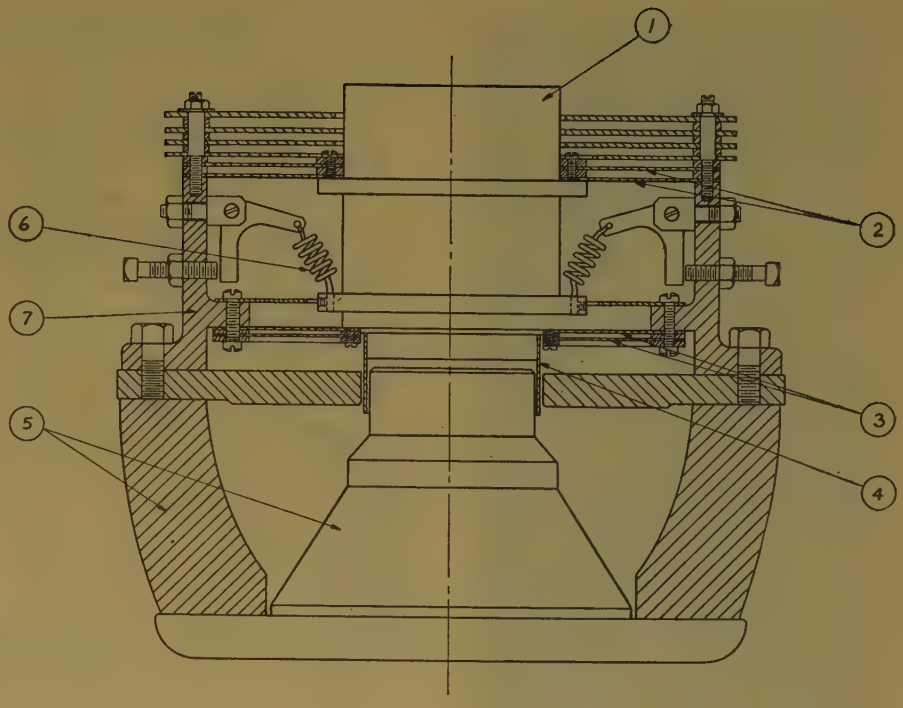


Figure 1. Cross-sectional view of artificial throat

1—Driving mass
2 and 3—Guide springs
4—Driving coil (voice coil)
5—Permanent magnet loudspeaker structure
6—Supporting springs
7—Supporting structure for driving mass

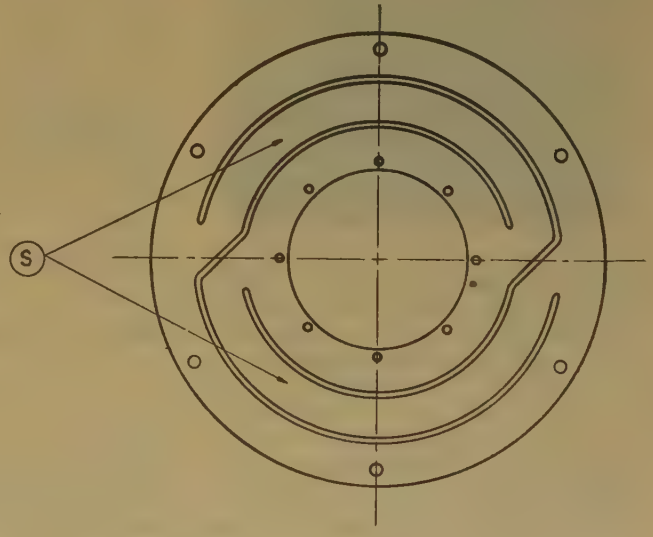


Figure 2. Support springs of artificial throat (2 and 3 in Figure 1)

S—Free spring portion

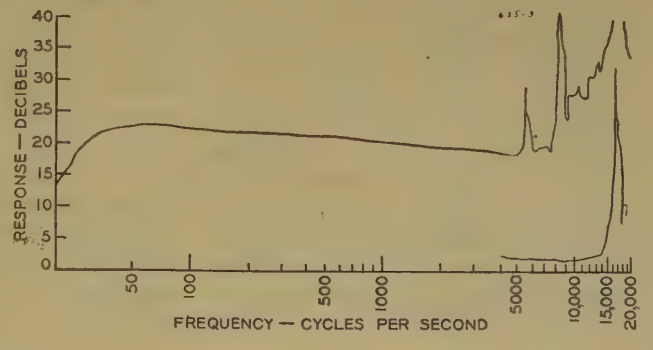


Figure 3. Frequency response curves for 50-watt artificial throat with solid brass driving mass

Upper curve is typical frequency response of artificial throat. Lower curve is 15 decibels lower than upper for location of frequency of upper peak



Figure 4. Artificial throat set up for operation. The system of masses, springs, and dashpot serve to keep magnet *m* stationary for calibration of the equipment

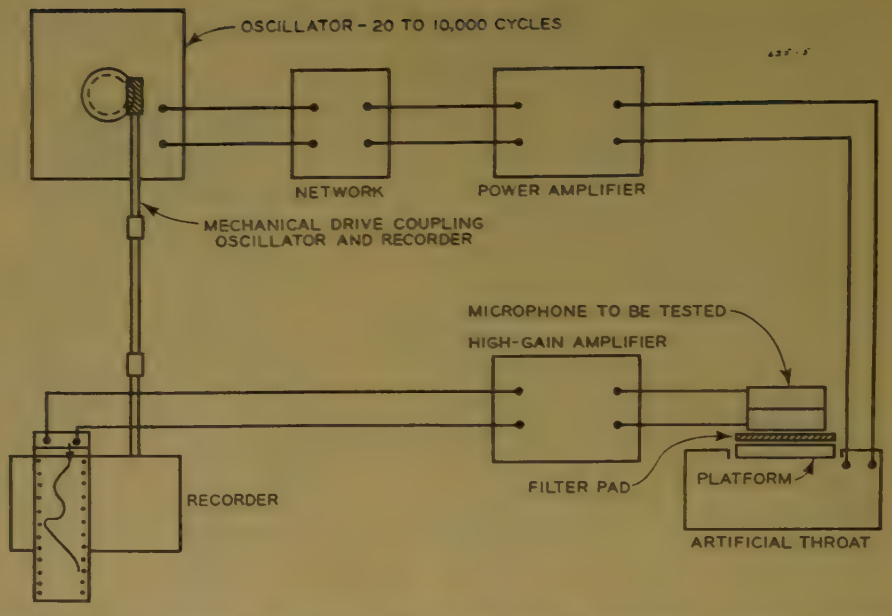


Figure 5. Experimental setup for automatically recording frequency response of throat microphone driven by artificial throat

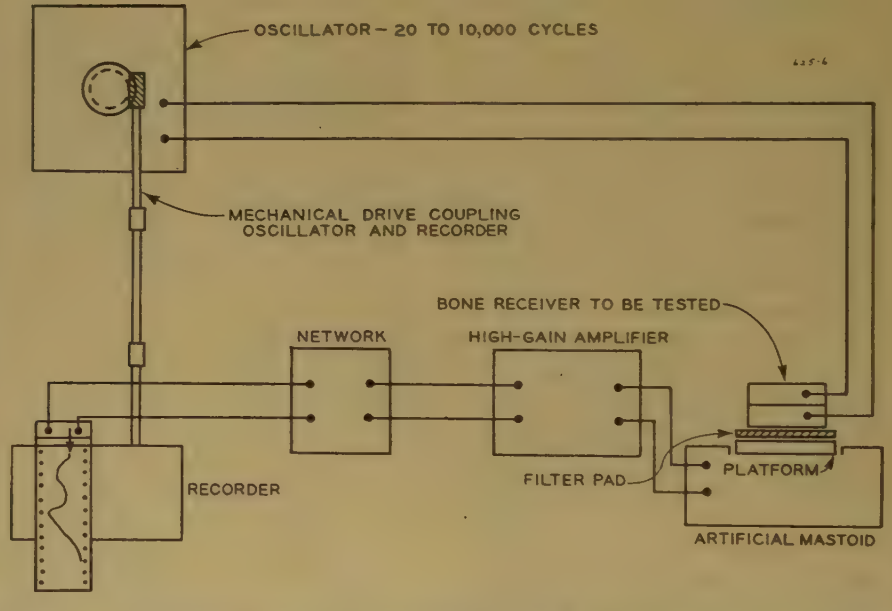


Figure 6. Experimental setup for automatically recording frequency response of bone receiver driving an artificial mastoid

and springs. The artificial throat, as seen in Figure 4, rests on a heavy table. Centering of the calibrating coil in the field of a small suspended magnet is accomplished as seen in the picture by means of an ordinary machine shop cross-feed device. Employing this set-up, it was possible to measure the velocity of the platform with good accuracy and freedom from external influence.

The block diagram of an experimental set-up for automatic recording of frequency responses of throat microphones is shown in Figure 5.[2] A beat frequency oscillator, driven by the motor of the recorder, supplies a voltage to the attenuating network mentioned above, which in turn excites a power amplifier with a voltage increasing linearly with frequency. The output of the power amplifier is fed to the artificial throat which drives a throat microphone (fastened to its platform by means of a compliant elastic band) through an interposed filter pad. The output of the throat microphone is then fed through a linear high gain amplifier to the recorder. The position of the microphone on the platform is not critical and identical response curves are obtained when the microphone is shifted on the platform.

The choice of a proper filter pad is the most difficult part of the problem. A filter pad should simulate the impedance looking into the human throat through the skin (or, in case of bone receivers, into the human head). This impedance has mainly stiffness and loss components. It was found possible to simulate either of the components by means of properly chosen pads. However, to date, serious difficulties have been encountered in constructing a pad that would give faithful reproduction of both parameters and thereby obtaining curves which are a true picture of the sensations received by the

Inertia Throat Microphones

E. H. GREIBACH
MEMBER AIEE

L. G. PACENT
FELLOW AIEE

Synopsis: This paper deals with the theory and design of magnetic inertia throat microphones. Especial attention is given to the treatment of sound power and high articulation throat microphones. The sound power microphones described contain a double frequency, undamped vibrating system, while the high articulation microphones have damping introduced, which reduces the low frequency peak with resultant increase in articulation. Wide range frequency response is obtained from the neighborhood of 100 cycles, extending up to 3,000, 4,000, or 5,000 cycles, as may be desired. These microphones have a band pass filter character with a sharp high frequency cutoff. This cutoff is desirable in order to cut out high frequency noises.

IT IS frequently necessary to send messages from noisy surroundings, such as machine shops, airplanes, and battlefields. For example, although the noise levels found in industrial plants or aircraft are often of the order of 100 or more decibels, communication must be maintained at all times. This creates the need for a discriminating microphone, that is, a microphone which will attenuate substantially the undesired sounds to favor the particular desired message. The throat microphone is such a discriminating microphone, as it is highly sensitive to vibrations transmitted to it by bodily contact with the sound-producing throat while it is quite insensitive to sound waves transmitted by air.

A throat microphone also has the advantage that it produces less discomfort than any other style, is less subject to shifting out of position or getting knocked off because of movements of its wearer. Another advantage is that it permits normal conversation to be carried on unrestricted to a degree not approached by any other form of microphone.

Throat microphones can be built on different principles, according to the method used for the conversion of acoustic into electric energy, such as carbon chambers, crystal microphones, and electromagnetic systems. Of these three kinds of elements, as will be shown, the electromagnetic system is especially well suited to provide a high articulation throat microphone.

Throat microphones reproduce speech by picking up the vibrations of the larynx rather than the sound waves generated in the air by the speaker. High frequency vibrations picked up from the larynx are subject to considerably greater attenuation than low frequency vibrations, since these high speech frequencies generally are produced in the forward portion of the mouth and have to pass over a long path of soft flesh to reach the larynx. In addition, the larynx is covered with a sheath of compliant skin, which attenuates the higher frequencies still further. The throat microphone therefore should be designed to differentiate strongly in favor of the higher frequencies of the vibrations of the larynx.

Because throat microphones operate while pressed against the throat or other portion of the human body, it is necessary to enclose the working mechanism entirely within a rigid housing in order to prevent external forces from affecting the air gap. For the same reason, it also becomes desirable to use the inertia principle in the design of such microphones.*

In short, an electromagnetic throat microphone should favor the higher speech frequencies and be enclosed in a rigid housing, which latter calls for the use of the inertia principle.

The inertia unit consists of an electromagnet L_1 supported by a spring C_1, as represented in Figure 1. The electromagnet L_1 consists of two small Alnico magnets, a central core with a coil wound around it, and a yoke and pole plate. C_1 is an S-shaped spring, supporting the electromagnet and forming the working air gap between its central portion and pole surfaces. This electromagnet struc-

Paper 46-24, recommended by the AIEE committee on communication for presentation at the AIEE winter convention, New York, N. Y., January 21–25, 1946. Manuscript submitted November 19, 1945; made available for printing December 13, 1945.

E. H. GREIBACH is director of research, Sonotone Corporation, Elmsford, N. Y. L. G. PACENT is president, Pacent Engineering Corporation, New York, N. Y.

The authors thank the management of the Sonotone Corporation for its approval of this project. They also are indebted to Mr. H. A. Pearson for many constructive discussions during the development program and to Mr. F. P. Greenwood and Mr. J. A. Kucher for carrying out the experimental work.

* E. H. Greibach, United States patents 2,255,249 and 2,255,250.

---

head in the case of bone conduction, or a true output of the human throat as it affects a throat microphone. While perforated rubber pads were found suitable to simulate the stiffness component of the skin and while pads of damping material, like "Viscoloid," have given a fair approach to the loss component of the skin, it was difficult to find a pad or combination of pads to simulate both stiffness and resistance together and in proper proportion.

It is readily seen that the artificial throat described above can also be used as an artificial mastoid. In the case of the artificial mastoid, the floating cylinder is driven by a bone conduction receiver through a filter pad simulating the skin over the mastoid bone, and the output of the coil mounted on the lower portion of the cylinder (driving coil for the throat) is then amplified and fed into a recorder. When it is desired to obtain response curves representing the force transmitted through the filter pad into the floating cylinder, it is necessary to use a dividing network (similar to the network used with the artificial throat) in the output of the linear high gain amplifier. This network will then deliver a voltage increasing linearly with frequency for a constant input voltage. On the other hand, response curves, representing the velocity transmitted through the filter pad, are obtained by using the linear high gain amplifier without an additional dividing network. Figure 6 shows how the equipment pictured in Figure 5 is rearranged to take frequency response characteristics of inertia bone receivers.

The above described equipment, in spite of some limitations, has proved to be a useful and powerful laboratory tool. The setups shown in Figures 5 and 6 permit the rapid taking of consistently reproducible response curves.

References

1. APPLIED ACOUSTICS (second edition). Olsen Massa. Page 286.

2. INERTIA THROAT MICROPHONES. E. H. Greibach, L. G. Pacent. AIEE TRANSACTIONS, volume 65, 1946, April section, pages 187–91.

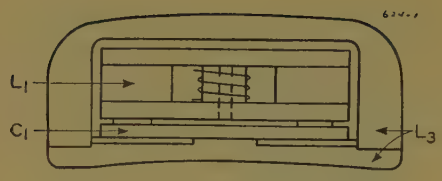


Figure 1. Construction of inertia unit

L_1—electromagnet structure
C_1—spring
L_3—housing

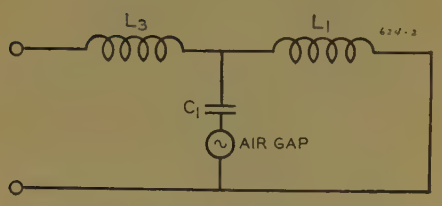


Figure 2. Equivalent electric circuit for structure shown in Figure 1

ture is surrounded by a housing, indicated schematically in Figure 1 as L_3. The equivalent electric circuit is represented in Figure 2, where the same symbols are used as in Figure 1 to designate the respective equivalent components.

The voltage produced across the magnet coil is proportional to the air gap velocity. It can be shown that the velocity I_1 of the air gap bears the following relationship to the velocity, I, imparted to the housing L_3 by external forces:

$$I_1 = Ix \frac{(f/f_o)^2}{1-(f/f_o)^2} \qquad (1)$$

where f_o is the resonant frequency of the vibrating system formed by the spring C_1 and electromagnet L_1, while f is the frequency of the force applied to the housing. For frequencies below resonance where f/f_o is small, the formula then can be written:

$$I_1 = Ix\ (f/f_o)^2 \qquad (2)$$

Equation 2 shows the air gap velocity to be proportional to the square of the applied frequency at frequencies below resonance. Therefore, magnetic or dynamic microphones will have a frequency discrimination of 12 decibels per octave in this range. In contrast, crystal or carbon microphones, in which voltage is proportional to the displacement, will have a frequency discrimination of only 6 decibels per octave. This result illustrates the advantage of the inertia magnetic throat microphone over the other types on account of its greater ability to discriminate against low frequencies.

It thus is seen that the rapidly rising response characteristic of the magnetic inertia throat microphone, below the resonant frequency, effectively compensates for the frequency distortion generated in the throat. In order to obtain satisfactory intelligibility, it is desirable to set the resonant frequency of the microphone at a relatively high value, in the neighborhood of 3,000 to 4,000 cycles. On the other hand, though such high frequency inertia throat microphones give a very good intelligibility when used with standard flat-response amplifiers, their output is low. The output can be increased substantially by lowering the resonant frequency to about 1,000 cycles, but this is accomplished at the expense of intelligibility.

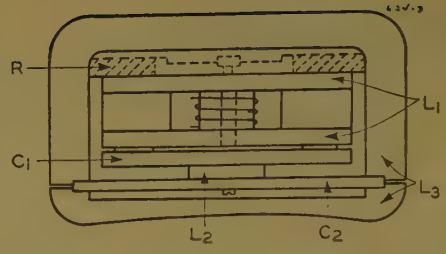


Figure 3. Construction of double resonant inertia unit

L_1—electromagnet structure
L_2—coupler
L_3—housing
C_1—spring of single resonant unit
C_2—spring for second resonance

Despite this difficulty, there are many applications which require that the two conflicting requirements of high sensitivity and high intelligibility be satisfied simultaneously, for example, in the case of sound powered communication systems. Through the addition of a second resonant frequency to a low frequency microphone system (approximately 1,000 cycles) a substantial extension of the sensitivity of the throat microphone can be obtained without loss of intelligibility. This second frequency is obtained by incorporating in its mechanical system a second mass and compliance system, having its resonant frequency somewhere in the range between 2,500 and 4,000 cycles. Such double resonant microphones have then a substantial output over the entire range from 1,000 to 3,000 or 4,000 cycles.

Figure 3 shows a schematic layout of a double resonant electromagnetic inertia system. Here L_1 is the mass of the electromagnet, supported by the spring C_1 in the same fashion as shown in Figure 1. Springs C_1, C_2, and coupler of mass L_2 form the second resonant system. C_2 is connected to the spring C_1 through L_2. All parts shown in Figure 3 also are shown in the exploded Figure 4 and are designated by the same symbols. The spring C_2 is held inside a frame structure, which is necessary to facilitate the mounting of the spring inside the housing. Use of the frame structure also reduces the losses in C_2 and provides means for easy duplication of spring properties in production. Figure 5 represents the equivalent electric circuit and uses the same symbols as in Figures 3 and 4 to designate the respective equivalent components. The electromagnet L_1 is connected to the housing L_3 through a mechanical transmission system, consisting of the springs C_1 and C_2, and the interposed mass L_2. This transmission system transmits the imparted velocity to the air gap formed between L_1 and C_1 with an efficiency which increases with frequency, thus permitting emphasis on the high frequencies at the expense of the low.

Of the two resonant frequencies incorporated in this system, one is represented approximately by the system consisting of the mass L_1 and the spring C_1. The second resonance, that of the system consisting of the two springs C_1 and C_2 and the mass L_2, is considerably higher than the first one. At frequencies above the second resonance most of the velocity imparted into the housing is absorbed by the spring C_1, and only a small fraction of it can be transmitted to the air gap. This results in a relatively sharp cutoff at

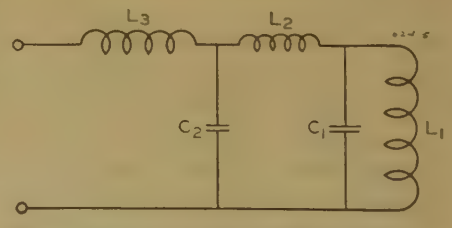


Figure 5. Equivalent electric circuit for structure shown in Figures 3 and 4



Figure 4. Exploded view of parts comprising a double resonant unit

higher frequencies and a band pass character for this type of throat microphone. The sharp cutting off of frequencies outside the range required for intelligibility is desirable, as it prevents transmission of high frequency noises and static and thus contributes to the improvement of intelligibility.

The values of the two resonant frequencies are obtained by solving the characteristic determinant of the equivalent circuit of Figure 5. Equation 3 is the solution for the two resonant frequencies with $\omega = 2\pi f$.

$$\omega^2 = \frac{1}{2}\frac{1}{L_1C_1}\left(\frac{L_1C_1}{L_3C_2}+\frac{L_1C_1}{L_2C_2}+1+\frac{L_1}{L_2}\right) \pm \frac{1}{L_1C_1}\left[\left(\frac{L_1C_1}{L_2C_2}+\frac{L_1C_1}{L_3C_2}-1+\frac{L_1}{L_2}\right)^2 + 4\frac{L_1^2}{L_2^2}\frac{C_1}{C_2}\right]^{1/2} \quad (3)$$

By expanding the square root expression and retaining the first two terms only, the following simplified approximate equations are obtained:

$$\omega_1^2 = \frac{1}{C_1}\left(\frac{1}{L_1}+\frac{1}{L_2}\right) - \delta = \omega_{10}^2 - \delta \quad (4)$$

$$\omega_2^2 = \frac{1}{C_2}\left(\frac{1}{L_2}+\frac{1}{L_3}\right) + \delta = \omega_{20}^2 + \delta \quad (5)$$

where

$$\delta = \frac{1}{L_2^2C_1C_2(\omega_{20}^2-\omega_{10}^2)}$$

The foregoing expansion is valid only when the difference $\omega_{20}^2-\omega_{10}^2$ is large, so that the correction term δ is small compared with both ω_{10}^2 and ω_{20}^2. ω_{10} and ω_{20} correspond roughly to the two resonance frequencies of the system.

For experimental purposes, as well as for different applications, it is desirable to build models having different spreads between the two resonant frequencies. This can be accomplished by changing some or all of the parameters in equations 4 and 5. On the other hand, the values of certain components remain more or less fixed on account of limitations in size, as well as the need to obtain optimum efficiency within a given volume. Among the fixed values are L_1 and C_1, which form the electromagnetic system, as well as the value of L_3, which is the mass of the housing.

Equations 4 and 5 demonstrate that, even if the values L_1, C_1, and L_3 are kept fixed, it is still possible to obtain wide variations in the value of the frequency f_2 by simply changing L_2 and C_2. It is further seen by inspecting equation 3 that the frequencies f_1 and f_2 are functions of

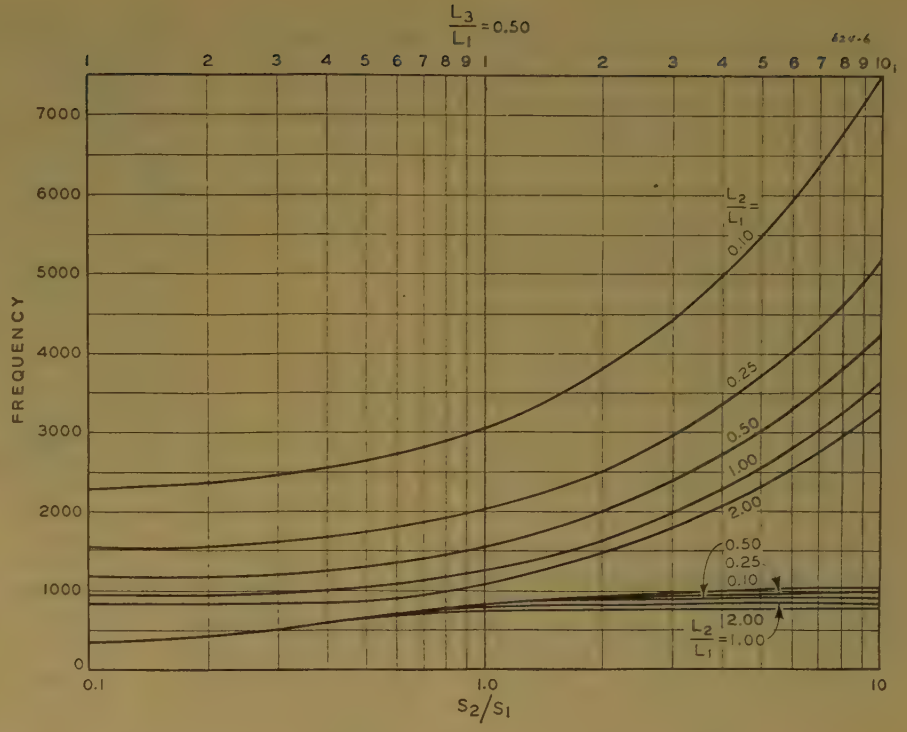


Figure 6. Curves showing relation of frequencies f_1 and f_2 as functions of the ratio $S_2 \div S_1$ plotted for various values of $L_2 \div L_1$

Curves computed for $L_3 \div L_1 = 0.50$

the two ratios: $L_2 \div L_1$ and $C_1 \div C_2$.

It is therefore possible to plot families of curves for the two frequencies as functions, for example, of the ratio C_1/C_2, the different curves corresponding to different values of L_2/L_1. Such curves, as calculated from equation 3, are shown in Figure 6. In this figure, the values for f_1 form the lower family of curves, which fall closely together, as is to be expected from equation 4, where L_1 and C_1 remain fixed. On the other hand the values for f_2 show a wide spread, since as shown in equation 5 both C_2 and L_2 are variables. The curves in Figure 6 therefore can be used to construct throat microphones with different properties. The curves were computed for: $L_3 \div L_1 = 0.50$.

It is desirable sometimes to build electromagnetic transducers having an extremely narrow band of response. For example, in bridge circuits the null position must be determined very sharply for the frequency of the power source to which such a bridge is connected and for the elimination of the disturbing effect of harmonics present in the source due to unavoidable distortion. In this case it is important to have a detector which will be sensitive only to the frequency of the fundamental component of the current wave. Here equations 4 and 5 become invalid, as the difference $\omega_{20}^2-\omega_{10}^2$ becomes very small, hence δ very large.

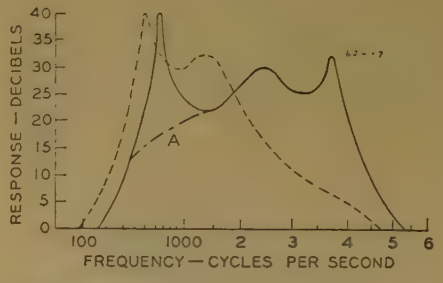


Figure 7. Comparative response curves for single and double resonant units

------ Single resonance unit
——— Double resonance unit
— — — Effect of damping on double resonant unit (high articulation)
A—High articulation unit

The complete equation 3 consequently must be used. For example, by using the values $L_2 \div L_1 = 1$ and $C_1 \div C_2 = 1$, response in the narrow band from approximately 800 to 1,250 cycles is obtained (Figure 6). Such a unit, when used as a detector (receiver), will permit very sharp balancing of a 1,000-cycle bridge.

Throat microphones built with components as illustrated in Figure 4 and having response in the band between 1,000 and 4,000 cycles have given high intelligibility scores when used as a sound powered microphone in conjunction with sound powered receivers.

In Figure 7 comparative response curves of single and double resonant units are shown. The light curve represents the response of a single resonant unit, and the heavy curve represents that of a

double resonant unit, the two units having identical electromagnets. These curves of the throat microphones were obtained by driving the microphones with an artificial throat. The artificial throat used in the preparation of these curves has a platform moving with substantially constant velocity in the frequency range from 50 to 10,000 cycles. A compliant pad, simulating the skin layer over the larynx, was interposed between the platform and the throat microphone under test. The effect of the interposed pad is to introduce an attenuation increasing with frequency and also an additional peak. The extra peak in each case is due to the compliance of the interposed pad coupling the housing to the platform.

The heavy curve in Figure 7 has an appreciable peak on the low frequency end at about 800 cycles. It is desirable for many applications, especially when throat microphones are used with flat response

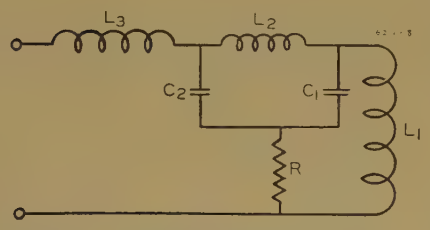


Figure 8. Equivalent electric circuit for damped double resonant unit

amplifying systems, to reduce or eliminate this peak in order to improve still further the intelligibility of such communication systems. This is done by introducing a damping member between the electromagnet L_1 and the housing L_3, as indicated schematically by the dotted lines in Figure 3. The equivalent electric circuit is shown in Figure 8. Placing the resistor R in the position shown in Figure 8 permits a very effective damping of the low frequency peak without affecting essentially the performance of such throat microphones in the neighborhood of the high frequency resonance. This is true since the damping resistance R effectively can suppress oscillations set up in the mesh, consisting of L_1, C_1, and R. On the other hand, high frequency oscillations set up in the mesh L_2, C_1, and C_2 are affected only a little by the energy absorbing resistance R, since any transfer of energy from this mesh must take place through the high impedance path L_1 in order to reach R. The dotted line in Figure 7 represents the response of a damped double resonance throat microphone. The articulation of these microphones is

Figure 9. Completely assembled typical throat microphone of electromagnetic type described in the paper



better than that of undamped throat microphones when used in conjunction with amplifying systems. The suppression of this low peak for sound power application is not important, since sound powered receivers can be built to have a somewhat attenuated response in the range corresponding to the low frequency peak of the throat microphone. The loss of sensitivity caused by the introduction of damping is not serious, as these microphones are used with amplifying systems. Damping can be obtained by using different damping materials introduced into the mechanical system, in the manner indicated in Figure 3. Best results were obtained by using a damping cup containing oil. Oil damping cups have the advantage of containing little stiffness as compared with the amount of resistance they introduce. The introduction of damping reduces to some extent the sharp cutoff characteristic of the undamped unit. The average output of a sound power throat microphone wound for 100-ohm internal impedance is approximately 15 millivolts, whereas the output of a similar high articulation throat microphone is on the average of 2 millivolts.

It is obvious that other parts of the head, such as cheeks, jaw, temple, vibrate under the influence of sounds produced in the mouth cavity and can be used to actuate such contact microphones. Especially good results are obtained when placing the throat microphone on the lips.

Figure 9 is a photograph of a typical throat microphone. This instrument consists of two units, disposed symmetrically on both sides of the throat. They are

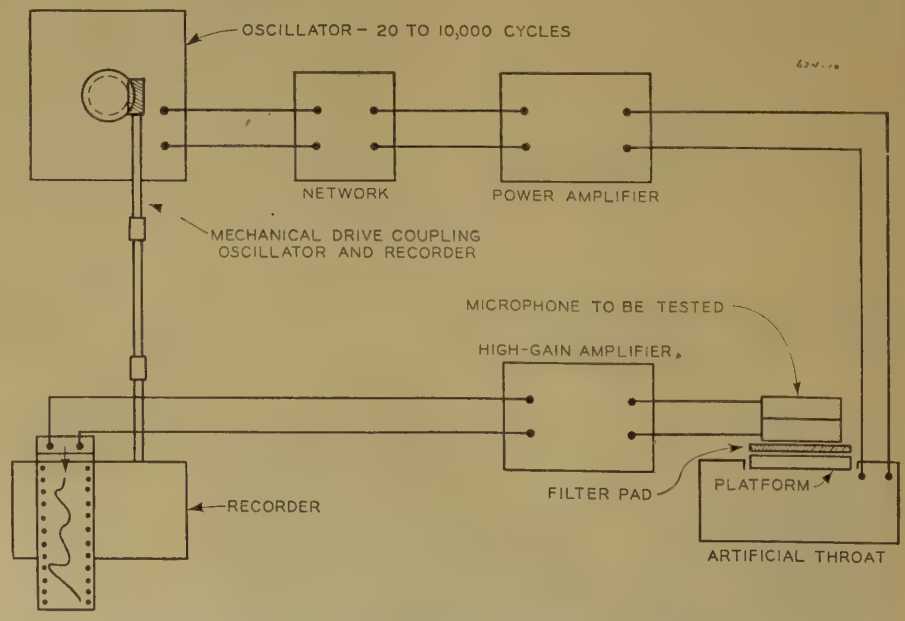


Figure 10. Experimental setup for automatically recording frequency response of throat microphone driven by artificial throat

Performance Calculations on Polyphase Reluctance Motors (Synchronous Motors Without Field Excitation)

P. H. TRICKEY
MEMBER AIEE

IN 1926, Messrs. Doherty and Nickle presented their classic paper on "Synchronous Machines" giving a complete and thorough analysis. Since many fractional horsepower engineers have occasion to design small reluctance motors (synchronous motors without field excitation) and these engineers in general have no need of becoming thoroughly familiar with the great and extensive field of synchronous motor theory, it has seemed advisable to simplify the equations from this famous paper by eliminating the terms having to do with field current and to arrange them in the form of a simple calculation sheet. It also has been found possible by the use of calculated curves to arrange a simple method of calculating the synchronous pull-out torque.

As in the case of induction motors, it is customary also in synchronous motor engineering to divide the work of designing a unit into three parts, first, choosing trial dimensions and windings, second, calculating the motor "constants" such as resistances, reactances, and iron loss and third, calculating the performance of the trial design. If the performance is not satisfactory further trial designs are made and the same procedure followed.

In the case of the first step, the experienced designer can often make the first trial very close to the correct design either from his experience or from making ratios from similar designs. If the designer is inexperienced or if the required design is radically different from any previous machine, sometimes a number of trials may be necessary.

Many papers have been written on the second step, the calculation of motor constants. Reference to some of these papers is given in the bibliography. It is not the purpose of this paper to discuss step one and two, but step three, the calculation of performance from calculated or tested constants.

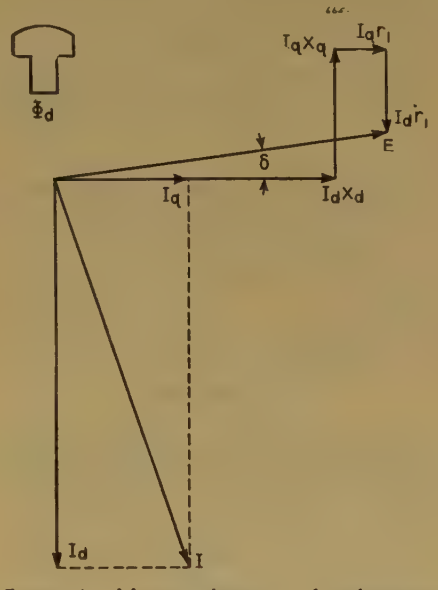


Figure 1. Vector diagram of reluctance motor

In the usual calculations of induction motors, the calculation forms are arranged so that performance is a function of slip, and trials of slip are made until the desired output is obtained. In this case, also, a trial and error method is used. This time the displacement angle is the variable and trials are made until proper output is obtained. On large machines, it is fairly easy to check the torque angle by test. With small motors below one horsepower it often is difficult to obtain the zero angle positon as a reference point. This is not greatly disadvantageous, however, as the performance versus output torque is much more important, and calculated displacement angles are usually sufficient.

Performance Equations

Rearranging Figure 20, page 925 of the reference paper,[1] to omit field excitation, we arrive at the diagram shown in Figure 1 and the equation below.

$$E = I_d X_d + I_q r_1 + j(I_q X_q - I_d r_1)$$

Solving for I_d and I_q,

$$I_d = \frac{E}{X_d} \frac{1}{1+(r_1/X_q)(r_1/X_d)} \times \left(\cos\delta - \frac{r_1}{X_q}\sin\delta\right)$$

$$I_q = \frac{E}{X_d} \frac{1}{1+(r_1/X_q)(r_1/X_d)} \times \left(\frac{1}{X_q/X_d}\sin\delta + \frac{r_1}{X_q}\cos\delta\right)$$

Line current

$$I = \sqrt{I_q^2 + I_d^2}$$

Power input

$$P = ph\,E\,(I_q\cos\delta - I_d\sin\delta)$$

Output

$$\text{Output} = \text{input} - (\text{Iron loss} + \text{friction} + \text{windage} + ph\,I^2 r_1)$$

Torque

$$T = \frac{112.7}{Syn}\,\text{output (in ounce feet)}$$

held on the throat by means of an elastic band, which is adjustable to control the pressure on the throat. As seen in the illustration, the instrument is provided with a standard cord and plug.

Figure 10 is a schematic diagram of the setup used in testing throat microphones. It consists of an oscillator mechanically coupled to a sound level recorder. The oscillator feeds a signal with continuously variable frequency through a network into a linear power amplifier. The power amplifier in turn drives an artificial throat whose platform vibrates with an essentially constant velocity in the frequency range of 50 cycles to 10,000 cycles. The throat microphone is placed on the vibrating platform with a filter pad interposed between the microphone and the platform. The purpose of the filter pad is to simulate as far as possible the layer of skin covering the larynx of an average speaker. The output of the throat microphone is amplified by a high gain amplifier and fed into the sound level recorder. Thus an automatic record is obtained of the variation of the output as a function of the frequency applied to the microphone.

Paper 46-65, recommended by the AIEE committee on electric machinery and technical program for presentation at the AIEE winter convention technical meeting, New York, N. Y., January 21–25, 1946. Manuscript submitted April 12, 1945; made available for printing December 26, 1945.

P. H. TRICKEY is chief engineer, Diehl Manufacturing Company, Somerville, N. J.

Synchronous Pull-Out Torque

The maximum torque that the motor will develop while in synchronism, known as "pull-out" torque, may be obtained as follows:

$T = (112.7/Syn)$ output $= (112.7/Syn)$ (input − losses)

$T = (112.7/Syn)$ [(input − copper loss) − $(Fe+F+W)$]

$T = (112.7/Syn)$ $[P_1 - (Fe+F+W)]$

Since iron loss, friction, and windage are essentially constant at synchronous speed, the maximum synchronous torque will occur when P_1 is at its maximum value. By substituting the current values given above in the equations for input and copper loss, it can be shown that

$$P_1 = ph\frac{E^2}{X_d}\frac{1}{1+(r_1/X_q)(r_1/X_d)}A$$

Where A is a rather cumbersome group of terms containing r_1, X_q, X_d, and δ.

Values of A maximum have been calculated and plotted in Figure 2, so that we find it fairly easy to calculate the synchronous pull-out torque.

$$T_{PO} = \frac{112.7}{Syn}[ph\,E\,M_1\,A_m - (Fe+F+W)]$$

(ounce-feet)

Where $M_1 = \frac{E}{X_d}\frac{1}{1+(r_1/X_q)(r_1/X_d)}$

It can easily be seen from Figure 2 how important it is to keep r_1/X_q and r_1/X_d as small as possible.

Figure 3 shows a form which has been arranged to make these calculations as simple as possible. The displacement angle δ is assumed and the performance values calculated. Items 23 to 27 are only in calculating the pull-out torque.

Since reluctance motors are usually less than one horsepower, Figure 3 has been arranged in terms of actual values of volts, amperes, and ohms, instead of "per unit" values which are seldom used by fractional horsepower motor engineers.

List of Symbols

E = volts per phase
$F+W$ = friction plus windage
Fe = iron loss
I = current per phase
I_d = current in direct axis
I_q = current in quadrature axis
ph = number of phases
P = power input in watts
r_1 = primary resistance per phase
Syn = synchronous rpm
T = torque in ounce-feet
T_{PI} = synchronous pull-in torque
T_{PO} = synchronous pull-out torque

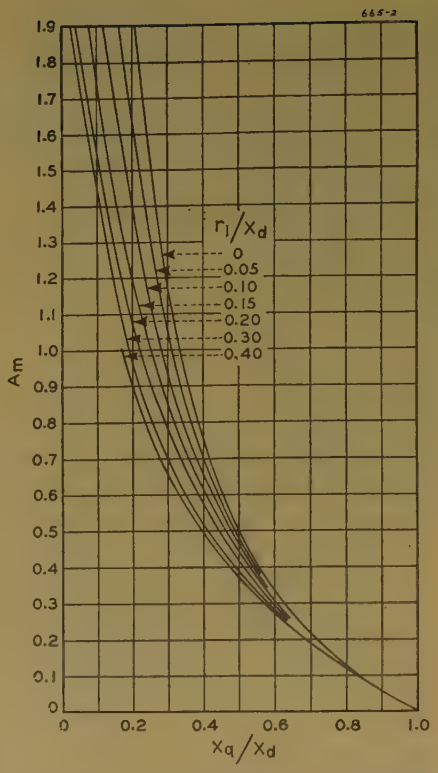


Figure 2. Constant A_m used in calculating pull-out torque

X_d = total direct axis reactance per phase
X_q = total quadrature axis reactance per phase
δ = displacement angle in electrical degrees

Appendix I. Performance Equations

Rearranging Figure 20, page 925 of the reference paper[1] to omit field excitation, we arrive at the diagram shown in Figure 1.

$$E = I_dX_d + I_qr_1 + j(I_qX_q - I_dr_1)$$

$E\cos\delta = I_dX_d + I_qr_1$ and $E\sin\delta = I_qX_q - I_dr_1$

Solving for I_d

$EX_q\cos\delta = I_dX_dX_q + I_qX_qr_1$ and
$Er_1\sin\delta = -I_dr_1^2 + I_qX_qr_1$
$E(X_q\cos\delta - r_1\sin\delta) = I_d(X_qX_d + r_1^2)$

$$I_d = E\frac{1}{r_1^2+X_qX_d}(X_q\cos\delta - r_1\sin\delta) = \frac{E}{X_d}\frac{1}{1+(r_1/X_q)(r_1/X_d)}\left(\cos\delta - \frac{r_1}{X_q}\sin\delta\right)$$

Solving for I_q

$Er_1\cos\delta = I_dX_dr_1 + I_qr_1^2$, and
$EX_d\sin\delta = -I_dX_dr_1 + I_qX_qX_d$
$E(X_d\sin\delta + r_1\cos\delta) = I_q(r_1^2 + X_qX_d)$

$$I_q = E\frac{1}{r_1^2+X_qX_d}X_d\sin\delta + r_1\cos\delta = \frac{E}{X_d}\frac{1}{1+(r_1/X_q)(r_1/X_d)}\left(\frac{\sin\delta}{X_q/X_d} + \frac{r_1}{X_q}\cos\delta\right)$$

Line current $I = \sqrt{I_q^2 + I_d^2}$

	E	127		
	X_d	1.79		
	X_q	51.8		
	r_1	6.76		
	r_1/X_d	0.0378		
	r_1/X_q	0.1306		
	X_q/X_d	0.290		
	$(r_1/X_d)(r_1/X_q)$	0.00494		
	$1+(r_1/X_d)(r_1/X_q)$	1.005		
	$M_1 = \frac{E}{X_d}\frac{1}{1+(r_1/X_d)(r_1/X_q)}$	0.705		
1	δ (IN ELEC. DEG.)	5	15	
2	COS δ	0.996	0.966	
3	(r_1/X_q) SIN δ	0.0114	0.0338	
4	(2) − (3)	0.985	0.932	
5	$I_d = M_1 \times (4)$	0.695	0.657	
6	$[1/(X_q/X_d)]$ SIN δ	0.300	0.893	
7	(r_1/X_q) COS δ	0.130	0.126	
8	(6) + (7)	0.430	1.019	
9	$I_q = M_1 \times (8)$	0.303	0.718	
10	$I = \sqrt{I_d^2 + I_q^2}$	0.758	0.973	
11	I_q COS δ	0.302	0.694	
12	I_d SIN δ	0.061	0.170	
13	(11) − (12)	0.241	0.524	
14	INPUT = ph E (13)	92.0	199	
15	$I^2 r_1$ ph	11.6	19.2	
16	Fe LOSS	21.7	21.7	
17	F + W	5.8	5.8	
18	LOSSES = (15) + (16) + (17)	39.1	46.7	
19	OUTPUT = (14) − (18)	52.9	152.3	
20	TORQUE = $\frac{112.7}{SYN}$ (19)	3.31	9.5	
21	EFF = (19)/(14)	57.5	76.6	
22	P.F. = (13)/(10)	31.8	53.9	
23	HORSEPOWER	0.0708	0.203	
24	Am (FROM FIG. 2)			1.130
25	$P_{I\,MAX} = ph\,E\,M_1\,A_m$			303
26	Fe + F + W = (16) + (17)			28
27	(25) − (26)			275
28	$T_{PO} = \frac{112.7}{SYN}$ (27)			17.2

Figure 3. Calculation sheet for reluctance motors

Power input $P = ph\,E\,I_q\cos\delta - ph\,EI_d\sin\delta$
$P = ph\,E\,(I_q\cos\delta - I_d\sin\delta)$
Total losses $L = Fe + F + W + ph\,I^2r_1$
Output = input − losses
Torque = $(112.7/Syn)$ output (in ounce-feet)
Efficiency = Output/input
Power factor = Input/$ph\,E\,I$

Appendix II. Pull-Out Torque or Maximum Synchronous Torque

$T = (112.7/Syn)$ output $= (112.7/Syn)$ (input − losses)

$T = (112.7/Syn)$ [(input − copper loss) − $(Fe+F+W)$]

$T = (112.7/Syn)$ $[P_1 - (Fe+F+W)]$

Since the iron loss, friction, and windage are essentially constant at synchronous speed, the maximum synchronous torque will occur when P_1 is at its maximum value. Power input in terms of δ power input

$P = ph\,E\,(I_q\cos\delta - I_d\sin\delta)$

$$P = ph\,E\left\{\frac{E}{X_d}\frac{1}{1+(r_1/X_q)(r_1/X_d)}\left(\sin\delta\cos\delta+\frac{r_1}{X_q}\frac{X_q}{X_d}\cos^2\delta\right)-\frac{E}{X_d}\frac{1}{1+(r_1/X_q)(r_1/X_d)}\times\left(\frac{X_q}{X_d}\sin\delta\cos\delta-\frac{r_1}{X_q}\frac{X_q}{X_d}\sin^2\delta\right)\right\}\frac{1}{X_q/X_d}$$

Input $P = ph\dfrac{E^2}{X_d}\dfrac{1}{1+(r_1/X_q)(r_1/X_d)}\times$

$$\left\{\left(1-\frac{X_q}{X_d}\right)\sin\delta\cos\delta+\frac{r_1}{X_q}\frac{X_q}{X_d}\right\}\frac{1}{X_q/X_d}$$

Copper loss in terms of δ

Copper loss $= ph\,I^2 r_1, \quad I^2 = I_d^2 + I_q^2$

Thus,

Copper loss $= ph\,r_1(I_d^2+I_q^2)$

$$\text{Copper loss} = ph\,r_1\left(\frac{E}{X_q}\frac{1}{1+(r_1/X_q)(r_1/X_d)}\right)^2\left\{\left(\frac{X_q}{X_d}\cos\delta-\frac{r_1 X_q}{X_q X_d}\sin\delta\right)^2+\left(\sin\delta+\frac{r' X_q}{X_q X_d}\cos\delta\right)^2\right\}$$

$$\text{Copper loss} = \frac{ph\,E^2}{X_q}\frac{1}{1+(r_1/X_q)(r_1/X_d)}\times\left(\frac{r_1}{X_q}\frac{1}{1+(r_1/X_q)(r_1/X_d)}\right)\left\{\left(\frac{X_q}{X_d}\cos\delta-\frac{r_1 X_q}{X_q X_d}\times\sin\delta\right)^2+\left(\sin\delta+\frac{r_1 X_q}{X_q X_d}\cos\delta\right)^2\right\}$$

$$\text{Copper loss} = \frac{ph\,E^2}{X_q}\frac{1}{1+(r_1/X_q)(r_1/X_d)}\times\left(\frac{r_1}{X_q}\frac{1}{1+(r_1/X_q)(r_1/X_d)}\right)\times\left\{\left(\frac{X_q}{X_d}\right)^2\cos^2\delta-2\frac{r_1}{X_q}\left(\frac{X_q}{X_d}\right)^2\sin\delta\cos\delta+\left(\frac{r_1}{X_q}\right)^2\left(\frac{X_q}{X_d}\right)^2\sin^2\delta+\sin^2\delta+2\times\frac{r_1}{X_q}\frac{X_q}{X_d}\sin\delta\cos\delta+\left(\frac{r_1}{X_q}\frac{X_q}{X_d}\right)^2\cos^2\delta\right\}$$

$$\text{Copper loss} = \frac{ph\,E^2}{X_d}\frac{1}{1+(r_1/X_q)(r_1/X_d)}\times\left(\frac{r_1}{X_q}\frac{1}{1+(r_1/X_q)(r_1/X_d)}\right)\times\left\{\sin^2\delta+\left(\frac{X_q}{X_d}\right)^2\cos^2\delta+\left(\frac{r_1}{X_q}\right)^2\left(\frac{X_q}{X_d}\right)^2+2\frac{r_1}{X_q}\frac{X_q}{X_d}\left(1-\frac{X_q}{X_d}\right)\sin\delta\cos\delta\right\}\frac{1}{X_q/X_d}$$

Power input − copper loss $= P_1$

$$P_1 = \frac{ph\,E^2}{X_d}\frac{1}{1+(r_1/X_q)(r_1/X_d)}\times\left\{\left(1-\frac{X_q}{X_d}\right)\sin\delta\cos\delta+\frac{r_1}{X_q}\frac{X_q}{X_d}-\frac{r_1}{X_q}\frac{1}{1+(r_1/X_q)(r_1/X_d)}\left[\sin^2\delta-\left(\frac{X_q}{X_d}\right)^2\cos^2\delta+\left(\frac{r_1}{X_q}\frac{X_q}{X_d}\right)^2+2\frac{r_1}{X_q}\frac{X_q}{X_d}\left(1-\frac{X}{X_d}\right)\sin\delta\cos\delta\right]\right\}\frac{1}{X_q/X_d}$$

$$P_1 = ph\frac{E^2}{X_d}\frac{1}{1+(r_1/X_q)(r_1/X_d)}A$$

Output = (power input − copper loss) − $(Fe+F+W)$

Output $= P_1 - (Fe+F+W)$

Torque $= (112.7/Syn)\,[P_1-(Fe+F+W)]$

Maximum or pull-out torque will occur when P_1 is maximum. $P_{1\max}$ will occur when A is maximum. Thus

$$T_{PO} = (112.7/Syn)\,[P_{1\max}-(Fe+F+W)]$$

$$P_{1\max} = \frac{ph\,E^2}{X_d}\frac{1}{1+(r_1/X_q)(r_1/X_d)}A_m$$

$$P_{1\max} = ph\,E\,M_1 A_m$$

Where

$$A = \left\{\left(1-\frac{X_q}{X_d}\right)\sin\delta\cos\delta\left[1-\frac{r_1}{X_q}\times\frac{1}{1+(r_1/X_q)(r_1/X_d)}2\frac{r_1}{X_q}\frac{X_q}{X_d}\right]+\frac{r_1}{X_q}\frac{X_q}{X_d}\left[1-\frac{r_1}{X_q}\frac{1}{1+(r_1/X_q)(r_1/X_d)}\frac{r_1}{X_q}\frac{X_q}{X_d}\right]-\frac{r_1}{X_q}\frac{1}{1+(r_1/X_q)(r_1/X_d)}\sin^2\delta-\frac{r_1}{X_q}\frac{1}{1+(r_1/X_q)(r_1/X_d)}\left(\frac{X_q}{X_d}\right)^2\cos^2\delta\right\}\frac{1}{X_q/X_d}$$

or

$$A = \left\{\left(1-\frac{X_q}{X_d}\right)\sin\delta\cos\delta\left[1-2\left(\frac{r_1}{X_d}\right)^2\times\frac{1}{X_q/X_d}\frac{1}{1+(r_1/X_d)^2 1/(X_q/X_d)}\right]+\frac{r_1}{X_d}\left[1-\left(\frac{r_1}{X_d}\right)^2\frac{1}{X_q/X_d}\times\frac{1}{1+(r_1/X_d)^2 1/(X_q/X_d)}\right]-\frac{r_1}{X_d}\frac{1}{X_q/X_d}\times\frac{1}{1+(r_1/X_d)^2 1/(X_q/X_d)}\sin^2\delta-\frac{r_1}{X_d}\frac{X_q}{X_d}\frac{1}{1+(r_1/X_d)^2 1/(X_q/X_d)}\cos^2\delta\right\}\frac{1}{X_q/X_d}$$

Let

$$B = \frac{r_1}{X_d}\frac{1}{X_q/X_d}\frac{1}{1+(r_1/X_d)^2 1/(X_q/X_d)}$$

then

$$A = \left\{\left(1-\frac{X_q}{X_d}\right)\sin\delta\cos\delta\left[1-2\frac{r_1}{X_d}B\right]+\frac{r_1}{X_d}\left[1-\frac{r_1}{X_d}B\right]-B\sin^2\delta-B\left(\frac{X_q}{X_d}\right)^2\cos^2\delta\right\}\frac{1}{X_q/X_d}$$

$$A = \left(1-2\frac{r_1}{X_d}B\right)\frac{1}{X_q/X_d}\times\left(1-\frac{X_q}{X_d}\right)\sin\delta\cos^2\delta-B\left(\frac{1}{X_q/X_d}\sin^2\delta+\frac{X_q}{X_d}\cos^2\delta-1\right)$$

The maximum value of A against δ as the variable has been plotted in Figure 2 for different values of X_q/X_d and r_1/X_d.

References

1. Synchronous Machines, R. E. Doherty C. A. Nickle. AIEE Transactions, volume 45 1926, pages 912–47.

2. The Nonexcited Synchronous Motor, P. H. Trickey. *Electric Journal*, April 1933.

3. Calculation of Synchronous Machine Constants, L. A. Kilgore. AIEE Transactions, volume 50, 1931, pages 1201–14.

4. Determination of Synchronous Machine Constants by Test, S. H. Wright. AIEE Transactions, volume 50, 1931, pages 1331–51.

5. Calculation of Armature Reactance of Synchronous Machines, P. L. Alger. AIEE Transactions, volume 47, 1928, pages 493–513.

6. Graphical Determination of Magnetic Fields, R. W. Wieseman. AIEE Transactions, volume 46, 1927, pages 141–54.

7. End Connection Reactance of Synchronous Machines, Alfred Still. AIEE Journal, volume 49, 1930, pages 535–8.

8. Graphical Flux Mapping, Calvert, Harrison. *Electric Journal*, 1928.

9. Reactances of Synchronous Machines, R. H. Park, B. L. Robertson. AIEE Transactions volume 47, 1928, pages 514–36.

10. No Load Induction Motor Core Losses, Spooner, Kincaid. AIEE Transactions, volume 48, 1929, pages 645–55.

Governor for Variable-Ratio Transmission Used in Developmental 400-Cycle Electric System for Large Aircraft

P. F. DESCH
NONMEMBER AIEE

D. E. GARR
MEMBER AIEE

J. G. HUTTON
NONMEMBER AIEE

Synopsis: A prerequisite for the successful parallel operation of main engine driven a-c generators is a suitable infinitely variable-ratio transmission and high speed governor to control it. This paper describes the development of such a governor and its successful operation on a developmental two-generator 400-cycle a-c system.

THE TREND of certain types of military and civil aircraft toward larger airplanes requiring large amounts of electric power, demanded equally revolutionary thinking in the field of aircraft electrical engineering. Much thought and discussion[1,2] in recent years has been given to an a-c system which would have the generators driven by the main engines and operating in parallel, which with proper controls makes possible improved continuity of service.[3] Flight conditions may demand more than a 3 to 1 speed range of the main engines, and all engines would not necessarily operate at the same speed throughout one flight. With such conditions it is essential that some form of variable ratio transmission be coupled between each prime mover and generator, so that a parallel system at substantially constant frequency is practical. Variation in the ratio of each transmission would have to be automatic, to maintain each generator speed within the range required in spite of high acceleration and wide speed differences of the prime movers. An electric governor which maintained successful parallel operation of the generators and equality of load division under various conditions of acceleration and loading was developed. Design data and performance characteristics of this governor are presented in the following.

Conclusions

Approximately 200 hours of operating experience have been gained on the developmental 400-cycle a-c two-generator system, and governor operation has been satisfactory throughout. Under both steady state and transient conditions the governor and its attendant load-frequency droop circuit have performed their required functions well. Although load division with values of no-load to full-load linear droop of less than 5 per cent was generally satisfactory, the system performance was at times erratic. A linear frequency droop from no-load to full-load of 5 per cent was found to be eminently satisfactory, and this value was adopted for all remaining tests on the two generator system.

The speed of response of the governor was good. With the generators operating in parallel, and one prime mover accelerated or decelerated, the governor responded to begin to restore initial conditions before the end of the acceleration or deceleration period.

In general, movement of the governor servomechanism began 0.008 second after inception by the control coil of the signal demanding governor response. On the equivalent of an unloaded system the effective gear ratio of the variable-ratio transmission was changed from 2:1 to 1.3:1 in 0.18 second and vice versa. Since the speed changes were brought about by a unit function change in signal voltage, the simulated acceleration approached an infinite value.

Tests on a four-generator system have not yet been made, but it is hoped to begin these, together with preliminary flight tests, in the near future.

The weight of the governor pilot valve and solenoid assembly is approximately 8 pounds; the weight of the junction box containing the control and droop circuits is approximately 5 pounds; in an aircraft installation the piston assembly is part of the variable-ratio transmission.

The governor, together with the variable-ratio transmission which it controls, and attendant electric apparatus have combined to make an a-c system with parallel operated generators practical for use on large aircraft of the future. Operation of a developmental two-generator system over a period of several months and under varying conditions has been very satisfactory. It is hoped that in the near future planned flight tests will prove further the value of a-c systems for aircraft auxiliary apparatus.

Paper 46-79, recommended by the AIEE committee on air transportation and presented at the AIEE winter convention, New York, N. Y., January 21–25, 1946. Manuscript submitted November 23, 1945; made available for printing December 13, 1945.

P. F. Desch, D. E. Garr, and J. G. Hutton all are with the general engineering and consulting laboratory, General Electric Company, Schenectady, N. Y.

Governor Requirements

The governor design and performance requirements were set up to meet the most extreme operating conditions thought possible on airplanes which require a-c accessory power. Calculations based upon the application of rated engine torque to the propeller inertia of the engine–propeller combination indicated a possible acceleration at the engine drive pad of 2,150 rpm per second. Though in practice accelerations will probably be less than this, the governor was designed to maintain parallel operation with one engine accelerated at this rate while the speed of the others remained constant. Some of the essential features of the performance requirements are that the governor be designed to operate from sea level to 40,000 feet with ambient temperature variations from −55 degrees centigrade to +60 degrees centigrade, under humid or dusty conditions with specified linear and torsional vibrations. More particularly, requirements affecting the operational design of the governor are set out as in Table I. With these conditions arising from the design of the variable ratio transmission, the governor was required

Table I. Performance Requirements of Governor

Item	Characteristic	Governor Requirement
1.	Input speed range to variable-ratio transmission	2,100–9,000 rpm
2.	Output speed of generator	6,000 rpm
3.	Speed of governor tachometer shaft for generator speed of 6,000 rpm	3,000 rpm
4.	Maximum overdrive ratio of variable-ratio transmission	2.85
5.	Maximum underdrive ratio of variable-ratio transmission	0.67
6.	Total stroke of governor tie rod	1.25 inches
7.	Oil pressure available for governor	250 pounds per square inch
8.	Force on governor tie rod	See Figure 1
9.	Tie rod speed at maximum acceleration (2,150 rpm per second at engine). Maximum overdrive	3.5 inches per second
10.	Tie rod speed at maximum acceleration (2,150 rpm per second at engine). Maximum underdrive	0.5 inch per second
11.	Maximum time for tie rod to reach required velocity	0.03 second

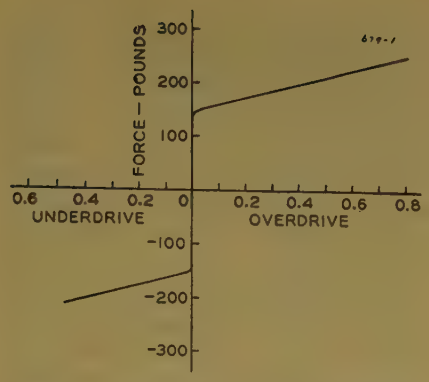


Figure 1. Curve of force on tie rod of governor servomechanism

to permit satisfactory parallel operation of the alternators under specified operating conditions with possible engine accelerations of 2,150 rpm per second. To assist in obtaining successful parallel operation of the generators an electric circuit was required which would admit of a decrease in generator speed with increasing load. Thus over the expected engine speed range of 700 rpm to 3,000 rpm, which with the step-up gear becomes 2,100 rpm to 9,000 rpm at the variable-ratio transmission, the governor was required to hold speed as follows:

Alternator Load, Kw	Speed, Rpm	Tolerance, Per Cent
0	6,300 (105 per cent)	±1
30 (100 per cent)	6,000 (100 per cent)	±1
45 (150 per cent)	5,850 (97.5 per cent)	±1
60 (200 per cent)	5,700 (95 per cent)	±1

In accordance with general aircraft practice the governor and its control circuits were required to be of minimum weight and to occupy a minimum of space in meeting all requirements.

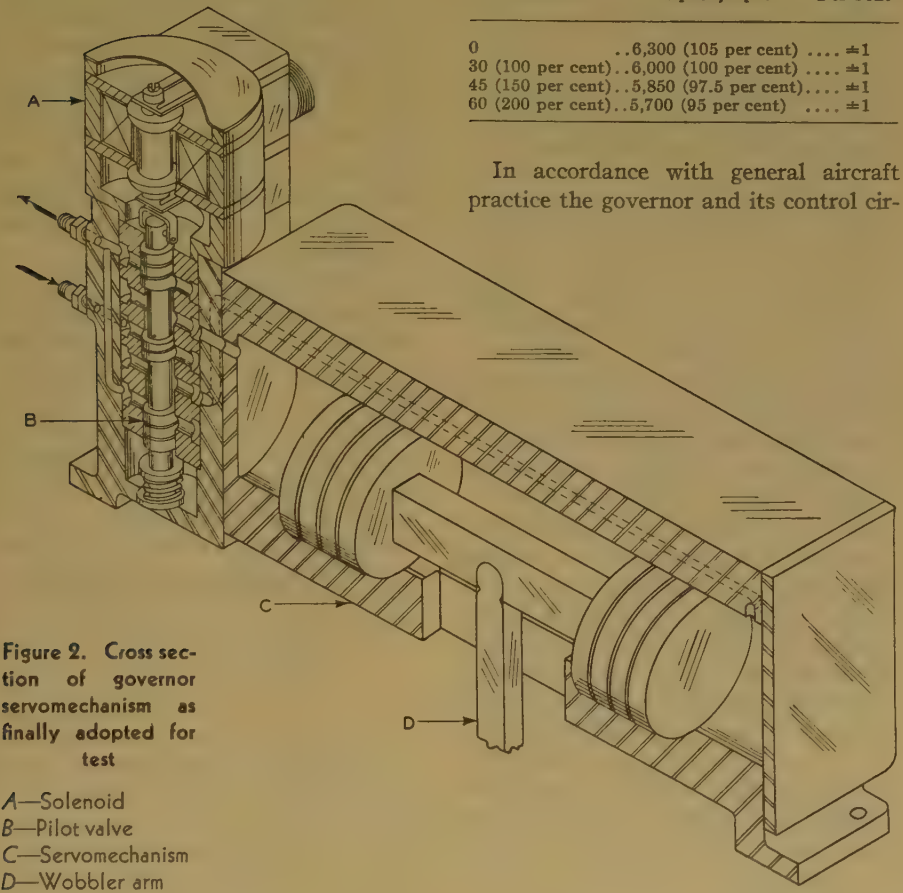


Figure 2. Cross section of governor servomechanism as finally adopted for test

A—Solenoid
B—Pilot valve
C—Servomechanism
D—Wobbler arm

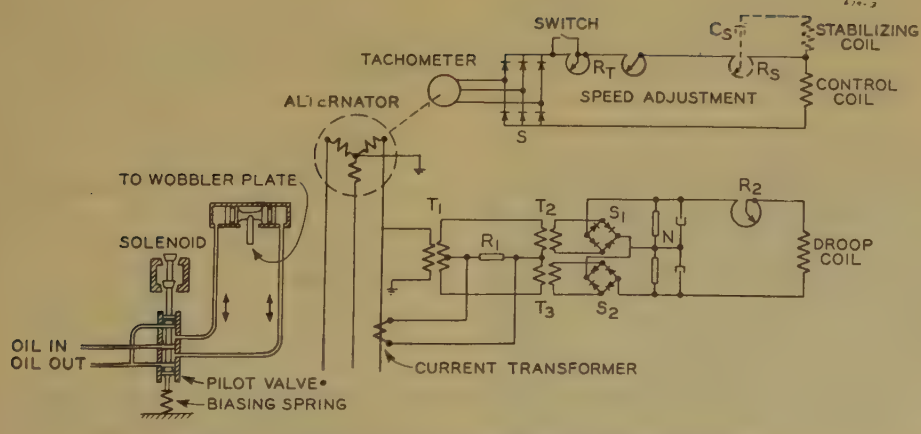


Figure 3. Schematic diagram of governor and control circuits

Design Data for Solenoid and Pilot-Valve Assembly

The governor is essentially a constant speed device. To provide suitable load division among the generators a characteristic is added to each governor which produces a 5 per cent decrease in system frequency when the generators are delivering full load. This droop circuit is independent of the actual governing circuits and therefore need not be considered in the design of the solenoid and pilot-valve assembly.

An isometric view of the governor assembly, as finally adopted for test, is shown in Figure 2 and a schematic diagram in Figure 3. Under steady state conditions the pilot valve is balanced in its mid-position against the force of a solenoid magnet by means of a biasing spring. A momentary change in current to the solenoid (because of a momentary change in output speed of the transmission) results in temporary unbalance, and oil is allowed to flow to the servomechanism until the condition is corrected. This correction must be very rapid to provide reasonably good load division among generators during engine speed transients. The pilot valve therefore must move with small changes of current through the solenoid coil. By use of a magnet with a tapered air gap, force-deflection characteristics such as those shown in Figure 4A are obtained, the various curves being plotted for different numbers of ampere turns X, Y, and Z. However, since the characteristics of the biasing spring are linear (line R^1T^1), the magnet is constrained to move linearly, resulting in an operating characteristic as represented by line RST, Figure 4A. By extrapolating from the line RST, and the curves for different ampere turns, a curve such as LMN in Figure 4B is obtained. In the working range of the governor only small ampere-turn changes are necessary for satisfactory governor operation and therefore only the portion L^1MN^1 of Figure 4B, need be considered: L^1MN^1 is essentially a straight line.

Since the magnet must be responsive to small changes in solenoid current, the required pilot valve travel also must be small. In the governor under consideration the total travel of the pilot valve is 0.1 inch, whereas under normal working conditions a movement of only ±0.010 inch is required for a tie-rod velocity great enough to ensure correct parallel performance. A solenoid force of $1^1/_2$–2

pounds is sufficient to do this, while an oil pressure of 250 pounds per square inch on a piston area of approximately 1.2 square inch is ample for movement of the servomechanism.

Other characteristics of the governor are as follows:

Control coil current	0.4 ampere
Turns on control coil	1,000
Resistance of control coil	16 ohms
Diameter of pilot valve	3/8 inch

Figure 5 shows a view of the completed governor assembly. The accumulator shown mounted on top was found from test to be unnecessary and was not used thereafter.

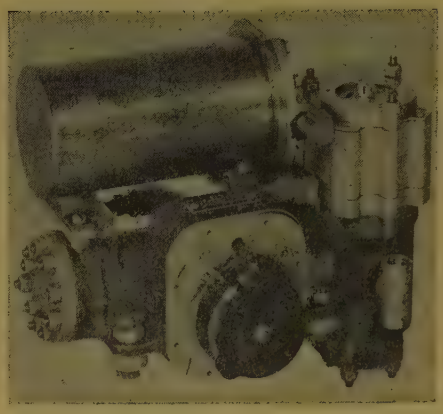
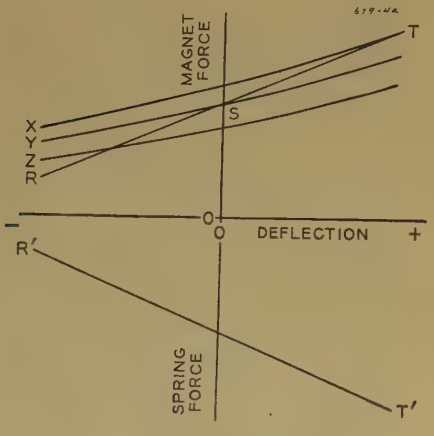


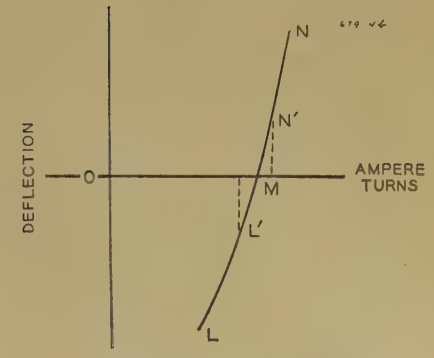
Figure 5. Oblique rear view of an experimental electric governor

Control Circuit

A schematic electrical diagram of the governor control circuit used for test is shown in Figure 3. The output voltage of a small 3-phase a-c tachometer with a permanent magnet field driven at a speed proportional to the output speed of the variable-ratio transmission is rectified by means of the 3-phase full-wave rectifier, S, shown. The output terminals of the rectifier are connected through a variable resistance to the governor control coil.



A. Force versus deflection



B. Deflection versus ampere turns

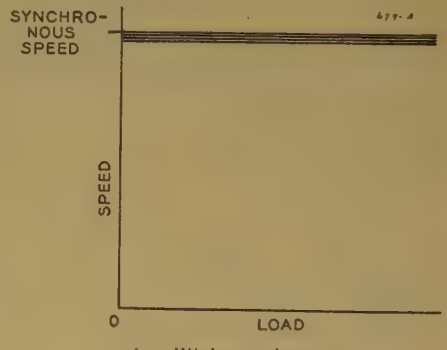
Figure 4. Curves of governor solenoid design characteristics

This control coil operates on a solenoid coupled mechanically to a three-land valve and biasing spring shown also in Figure 2. Under steady state conditions the force of the solenoid is balanced by the spring, and the valve floats in its neutral position. Any change in output speed of the variable-ratio transmission, either because of load variation or input speed changes, results in a momentary increase or decrease in current to the control coil. Balance of the pilot-valve assembly thus is lost temporarily, and oil is allowed to flow to and from the servomechanism controlling the transmission. The force on the servo pistons is such that the effective gear ratio of the drive is changed to restore original speed conditions. As soon as these are obtained, the pilot valve is returned to its neutral position. Steady state speed adjustments may be made by means of the trimming rheostat R_T. On an aircraft installation a rheostat may be mounted on the flight engineer's panel and connected in parallel with R_T to provide remote control of each generator speed. For parallel operated generators this is also an adjustment for load division, should the governor setting deviate during a flight.

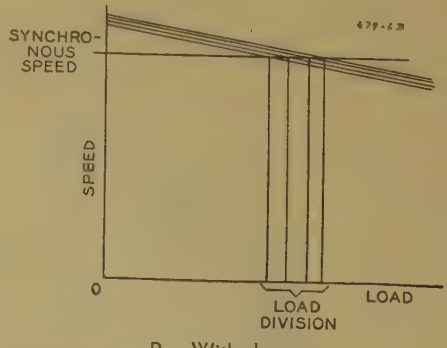
Stabilizing of the governor may be obtained by means of the circuit shown in broken lines above the control coil in Figure 3. The rheostat R_s is geared to a rack on the servo pistons, and therefore movement of the latter will result in a change in the amount of the resistance R_s in the stabilizing circuit. Since the governor control current is essentially constant, movement of R_s results in a change in voltage to the capacitor and stabilizing coil. The capacitor therefore will either charge or discharge, depending on whether the voltage decreases or increases. In either case a current will flow through the stabilizing coil, producing ampere turns in opposition to the change in ampere turns in the control coil. A stabilizing action therefore is produced.

For successful parallel operation the alternators should be controlled, so that their speed decreases with increasing load. In Figure 6A is shown the speed–load characteristics of four alternators without controls to give speed regulation. Prior to synchronizing, the speeds of the machines probably are slightly different one from the other due to inherent instrument and human error. On synchronizing, the machine with the highest initial speed will assume all subsequent load, thus giving a very undesirable condition. In Figure 6B is shown in the same order the speed-load characteristics of the same four alternators, but in this case they have controls to give speed regulation. The same initial speed errors are shown, but, on synchronizing, subsequent load is divided among the machines in proportion to their initial speed errors. The drawing is not to scale, the percentage droop being exaggerated for the purposes of illustration.

The control circuit (load-frequency droop control) giving this desired speed regulation is part of the governing system and is shown in Figure 3. One line to neutral voltage of the alternator is supplied to the primary winding of transformer T_1. The secondary winding of this transformer is midtapped and con-



A. Without droop



B. With droop

Figure 6. Diagram showing how load-frequency droop provides for real power division

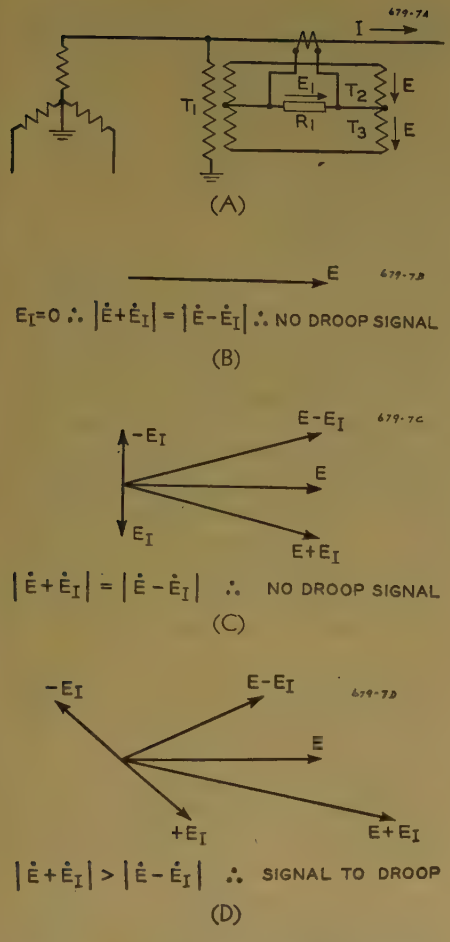


Figure 7. A. Schematic electrical diagram of a-c portion droop circuit
B, C, D. Vector relations in the primary windings of transformers T_2 and T_3 for different load and power factor conditions

B—No load
C—Zero power factor load
D—0.75 power factor load

nected through a resistance, R_1, to the primary windings of the identical transformers T_2 and T_3. The output of each of these transformers is rectified by means of selenium rectifiers S_1 and S_2. By connecting the rectifier outputs subtractive, the difference in d-c signals can be placed on the droop circuit coil connected as shown. On no load the alternator line to neutral voltage produces equal signals in the rectifiers. The resulting two d-c signals being subtractive, there is no signal to the droop circuit coil. The secondary winding of the current transformer, CT, is connected across the resistance R_1. On load, a signal proportional to alternator output current therefore is added vectorially to and subtracted from the voltage signal, thus producing unbalance in the outputs of rectifiers S_1 and S_2. This unbalance results in current flow, smoothed out by means of the capacitor-resistance network, N, shown, through the droop circuit coil. The control and droop coils are wound concentrically, the latter being connected so that on load, the flux produced is in the same direction as that of the control coil. This has the same effect as an increase in output speed of the variable-ratio transmission, and the governor acts accordingly. By means of the variable resistance, R_2, the percentage speed regulation of the alternator can be adjusted to its most effective value. On an actual aircraft installation it is expected that the value of R_2 will be fixed.

Vector relations involved in the load-frequency droop circuit are shown in Figures 7A, B, C, and D.

It is sufficient to consider the absolute magnitudes of the resultant voltages applied to the primary windings of transformers T_2 and T_3, in determining the droop coil signal voltage, since the output of each rectifier is proportional to the respective magnitude of the voltage in the transformer to which it is connected. The rectifiers are connected subtractive, and therefore the net signal to the droop coil is zero whenever the voltages applied to the primary windings of T_2 and T_3 are equal in magnitude.

In Figure 7A is shown the skeleton droop circuit and the voltages contributing to its operation. Since transformers T_2 and T_3 are identical, the voltage components, E, applied to the windings by virtue of the alternator phase to neutral voltage, are equal. Similarly a voltage component, E_I, is applied to transformers T_2 and T_3 by virtue of the drop in the resistor R_1, caused by the flow of load current through the current transformer. The voltages E and E_I therefore will be vectorially additive in one transformer and vectorially subtractive in the other transformer.

In Figure 7B, with no load on the system, the voltage E_I is zero, and consequently there is no signal to the droop coil.

In Figure 7C with zero power factor load the absolute value of the vector sum, $|\boldsymbol{E}+\boldsymbol{E}_I|$, is equal to the absolute value of the vector difference $|\boldsymbol{E}-\boldsymbol{E}_I|$. Again the signal to the droop coil is zero.

In Figure 7D with a load power factor of 75 per cent the absolute value of the vector sum, $|\boldsymbol{E}+\boldsymbol{E}_I|$, is greater than the absolute value of the vector difference, $|\boldsymbol{E}-\boldsymbol{E}_I|$. Consequently, a voltage proportional to the difference between the absolute values is applied to the droop coil circuit, actuating the governor in such a way as to tend to restore load balance. It is clear from the vector relations shown in Figures 7C and 7D, that the droop coil signal is sensitive to real power current and insensitive to reactive power current.

Performance Data

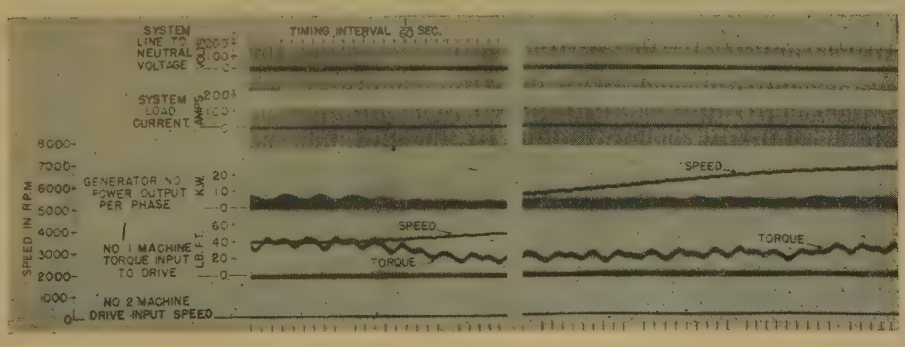
General

Performance data obtained at the time of writing the paper have been confined to a developmental two-generator system. Each prime mover of the system was a 450-horsepower 9-cylinder gasoline engine, coupled through a step-up gear in order to obtain input speeds to the variable-ratio transmission comparable with those expected on an aircraft installation. The gear output shaft was connected through a double universal coupling to the input flange of the variable-ratio transmission. A 3-phase a-c tachometer with a permanent magnet field was driven through a gear at half output speed and provided power for the governor control circuit.

A freewheeling device located between the variable-ratio drive and the alternator allows the alternator to be driven but does not permit it to attempt to drive the prime mover. Loading of the alternators was provided by water-cooled calrod units and air-core reactors, the continuous rating of the alternator being 30 kw, 40 kva, at 400 cycles per second and 208Y–120 volts.

The presence of the freewheeling unit between the drive and alternator made synchronizing of the alternators a simple matter. Successful parallel operation

Figure 8. Oscillogram showing transient division of real power between generators by governor action during acceleration of one engine



was achieved, the generators staying in step during various types of disturbances and dividing load equally under steady state conditions and reasonably well during transient disturbances (see Figure 8). The general performance of the governors was very satisfactory throughout a series of system tests which followed successful parallel operation.

Stabilizing Circuit

A considerable amount of previous development work on governors for gasoline engines used in tanks greatly expedited the development of the governor to control the variable-ratio transmission. Because of the rates of response and the values of inertia involved in controlling the tank engines, stabilizing circuits were required in governors built for this purpose. A variable resistance, R_s, and capacitance, C_s, connected, as shown dotted in Figure 3, to a second solenoid coil enabled this stabilizing to be achieved. In the case of the governor for use on aircraft where a variable-ratio transmission is to be controlled, the slip is relatively small and the speed of response high. Consequently the afore-mentioned type of stabilizing is unnecessary. Tests showed, however, that if an application should occur where stabilizing is required, this could be accomplished readily.

Droop Circuit

The value of the resistance R_2 in the droop circuit (Figure 3) was set arbitrarily to give a 5 per cent frequency decrease linearly from no load to full load on the alternator. Load division under steady state conditions was excellent, each generator taking an equal share of the load. By varying the value of R_2 the percentage droop was decreased. For values less than 4 per cent the load division became less satisfactory and erratic. The value of R_2 therefore was fixed to give a linear frequency droop of 5 per cent with full load on the alternator. With no load frequency of 420 cycles per second, a full load frequency of 400 cycles per second thus was obtained.

Part of the load on a military airplane using the a-c system for electric power may be thyratron controlled gun turrets. When in operation, these control circuits will produce a d-c component of current in the a-c system. This will tend to saturate any current transformers which may be used there. Since a current transformer was an essential part of the droop circuit, tests were performed with a thyratron controlled gun turret load to determine its effect on the operation of the droop circuit. It was found that load division was satisfactory, the saturation of the current transformers used having no noticeable effect on governor action.

Speed of Response

The general speed of response of the governor is illustrated in Figure 8 which shows two sections of an oscillogram taken with the machines operating in parallel and one engine being accelerated. The portion between the two sections of the oscillogram represents a time interval of 0.9 second. The average rate of acceleration at the input shaft to the drive for the total interval is approximately 2,000 rpm per second, the machines staying in step throughout. The left-hand section of Figure 8 shows conditions prior to accelerating. The system is carrying approximately 30 kw of load. The machine being accelerated assumes more load while the other machine takes less load as indicated in the oscillogram. However, before the acceleration is completed the governors have begun to restore conditions, so that the machine not being accelerated begins to assume its share of the load again. This is illustrated in the right-hand section of Figure 8. Other oscillograms were taken showing the effects of acceleration and deceleration when the system was supplying lagging power factor loads. Performance of the system was equally satisfactory under these conditions. However, Figure 8, which depicts the effect of acceleration with a unity power factor load on the system, is presented here, since real power changes are more readily observable in oscillograph power traces when unity power factor loads are used.

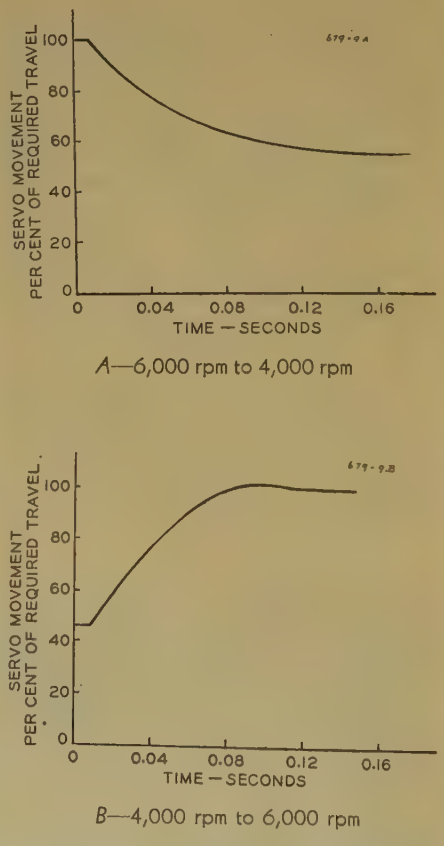


Figure 9. Curves of movement of governor servomechanism after change in electric signal

In order to determine accurately the speed of response of the governor, it was necessary to resort to somewhat artificial means. A switch SW, Figure 3, was connected across the trimming rheostat, R_T. The value of the resistance was adjusted so that by closing SW, the output speed dropped from 6,000 rpm to approximately 4,000 rpm. A battery connected appropriately to R_s, the rheostat formerly used in the stabilizing circuit, enabled movement of the servomechanism to be determined after receipt of the unit function signal by the governor control coil. The tests were performed on one governor, and variable-ratio transmission coupled to a generator but supplying no load.

Figure 9A shows a plot of movement of the governor servomechanism in terms of time after receipt by the control coil of the unit function signal. The output speed of the variable-ratio transmission was reduced from 6,000 rpm to approximately 4,000 rpm. With an input speed of 3,000 rpm this gave a change in drive ratio from 2:1 to 1.3:1.

Figure 9B shows a similar curve obtained by opening the switch S (Figure 3) and thus increasing the output speed from 4,000 rpm to 6,000 rpm. Here there is an overshoot of approximately 2 per cent. This is due to the inherent delay of the moving parts and the oil pressure of the hydraulic system, reaching steady state conditions after completion of the unit function change in electric signal.

The successful operation of the governor over a period of 200 hours under severe conditions brought about by many stops and starts with heavy loads often applied and removed suddenly indicates that a suitable automatic control has been developed for the variable-ratio transmission so necessary in the parallel operation of main engine driven aircraft alternators.

References

1. Why To-morrow's Planes Will Have A-C Electrical Systems, T. B. Holliday. *Electrical Manufacturing*, July 1943.

2. Governor Requirements for Aircraft Alternator Drives, W. K. Boice, L. G. Levoy, Jr. AIEE Transactions, volume 64, 1945, July section, pages 534–40.

3. Basic Consideration in the Selection of Electric Systems for Large Aircraft, W. K. Boice, L. G. Levoy, Jr. AIEE Transactions, volume 63, 1944, June section, pages 279–87.

Field Tests of Interrupting Capacity of 138-Kv Oil Circuit Breakers

W. B. BUCHANAN
MEMBER AIEE

G. D. FLOYD
MEMBER AIEE

Synopsis: The preliminary planning necessary to estimate the amount of current to be interrupted on a large network for staged tests under short-circuit conditions is outlined, also the precautions necessary to keep the applied fault from developing into a total system interruption. The circuit breakers under test are identified, various quantities required for record, and the means of obtaining the same are discussed. The results of a number of tests are given as well as a general discussion as to the conditions of the tests and of results obtained.

THE 25-CYCLE high-voltage network of the Hydro-Electric Power Commission of Ontario extends from the Quebec border to Windsor, with generating sources on the Ottawa, Gatineau, Lievre, and St. Lawrence Rivers in the east and on the Niagara River.[1] Primary transmission from the east is at 230 kv, while the loads located from Toronto to Windsor are supplied from a 115-kv network covering the afore-mentioned area.

The total generating capacity normally interconnected and supplying this network is in the order of 1,750,000 kva. The short circuit kilovolt-amperes on the 115-kv network has increased with system growth, with the result that, although circuit breakers had been provided at many points with the highest interrupting capacity available from time to time, the increase in short-circuit kilovolt-amperes always had to be considered in regrouping lines or paralleling busses. In some cases it has been necessary to sectionalize busses to reduce short-circuit currents, where best operating practice indicated parallel operation. The necessity of operating all generating sources to their capacity during the war also has tended to increase the short-circuit kilovolt-amperes.

When considering the point to which it would be reasonably safe to interconnect the network without inviting failure of the circuit breakers to interrupt faults, the Commission's engineers were required to answer the question, what modifying factor, if any, should be applied to the interrupting capacity of the circuit breaker at 60 cycles, as demonstrated by laboratory and field tests, when this circuit breaker was required to interrupt 25-cycle current. There appeared to be no clear-cut answer to this question. After discussion with manufacturer's engineers, it was decided to make the tests described in this paper on a modern oil circuit breaker, by having this circuit breaker interrupt actual system fault currents up to its rated interrupting capacity and observing the results.

A 138-kv single tank circuit breaker equipped with type BH deion grid, located at Burlington transformer station, having rated interrupting current of 7,950 amperes at 110 kv, was selected, the manufacturer being asked to place this circuit breaker in "factory condition" prior to the test. It also was decided to make a test on a second circuit breaker of the same interrupting capacity by installing in it temporarily an improved interrupting device, known as the type MF grid. This assembly was to be tested at not over 13,200 amperes at 110 kv.

Preliminary Work

Certain preliminary studies are required before tests of this nature can be made. Important studies include:

1. Determination of system required, including departures from normal network and generating capacity.
2. Careful scrutiny of the system and its relay protection, to determine the possibility of loss of tie lines, busses not involved in the fault, frequency changer ties, synchronous loads, and generating capacity and, where it could be done, to prevent their occurrence.
3. Listing of quantities to be measured and providing of equipment for measuring these quantities.

The circuit breaker to be tested also must be conditioned, if the tests on it are to be considered a fair demonstration of its performance.

System Required

The American Standards Association "Standard for Oil Circuit Breakers, C37-4" defines rated interrupting current as the *total* rms current at the time the contacts part. It was agreed that these standards were to apply. One problem in the preliminary work became that of determining the system setup required to produce a short-circuit current, as defined by the ASA Standard, as nearly equal to, but no greater than, the rated interrupting current given by the manufacturer.

The system upon which the fault was to be placed is shown in Figure 1. Burlington transformer substation is located at the heart of the 115-kv network. Although the only sources of short-circuit current close to the point of fault are the two 40,000-kva synchronous condensers at Burlington, there are points of infeed from eastern sources over the 230-kv network and from Niagara River plants over 115-kv lines. Generators in the latter plants, which are on busses separate from the 115-kv subsystem on which the fault was placed, also supply current to the fault by back-feeding through 230-kv transformers at Burlington to the common 230-kv bus.

It had been decided that two preliminary tests would be made, one at approximately 1/4 and one at 1/2 rated interrupting current before the final test on the lower rated circuit breaker, and one preliminary test at not over 7,900 amperes on the higher rated contact assembly. To determine the initial values of symmetrical current, and the system rearrangement required to produce them, the system shown in Figure 1 was placed on the network calculator.

System generation and loads for a normal Saturday were used with the impedance of generating sources represented by their subtransient reactance.

After a number of trials on the calculator one grouping of lines was found such that with the fault located at the distant end of the line whose line circuit breaker would be under test, approximately 1/4 rated current would flow initially, and the same network with fault located at the near end of the same line would produce approximately 1/2 rated current. It should be noted that rather severe restrictions were placed on modifying the system to develop the required values of short-circuit current. Sufficient generation had to be retained to supply the system load, and circuits could not be opened to the point where service security would be threatened seriously.

The system required to give a 3-phase

Paper 46-19, recommended by the AIEE committee on protective devices for presentation at the AIEE winter convention, New York, N. Y., January 21–25, 1946. Manuscript submitted November 19, 1945; made available for printing December 18, 1945.

W. B. BUCHANAN is assistant laboratory engineer and G. D. FLOYD is electrical consultant with the Hydro-Electric Power Commission of Ontario, Toronto, Ontario, Canada.

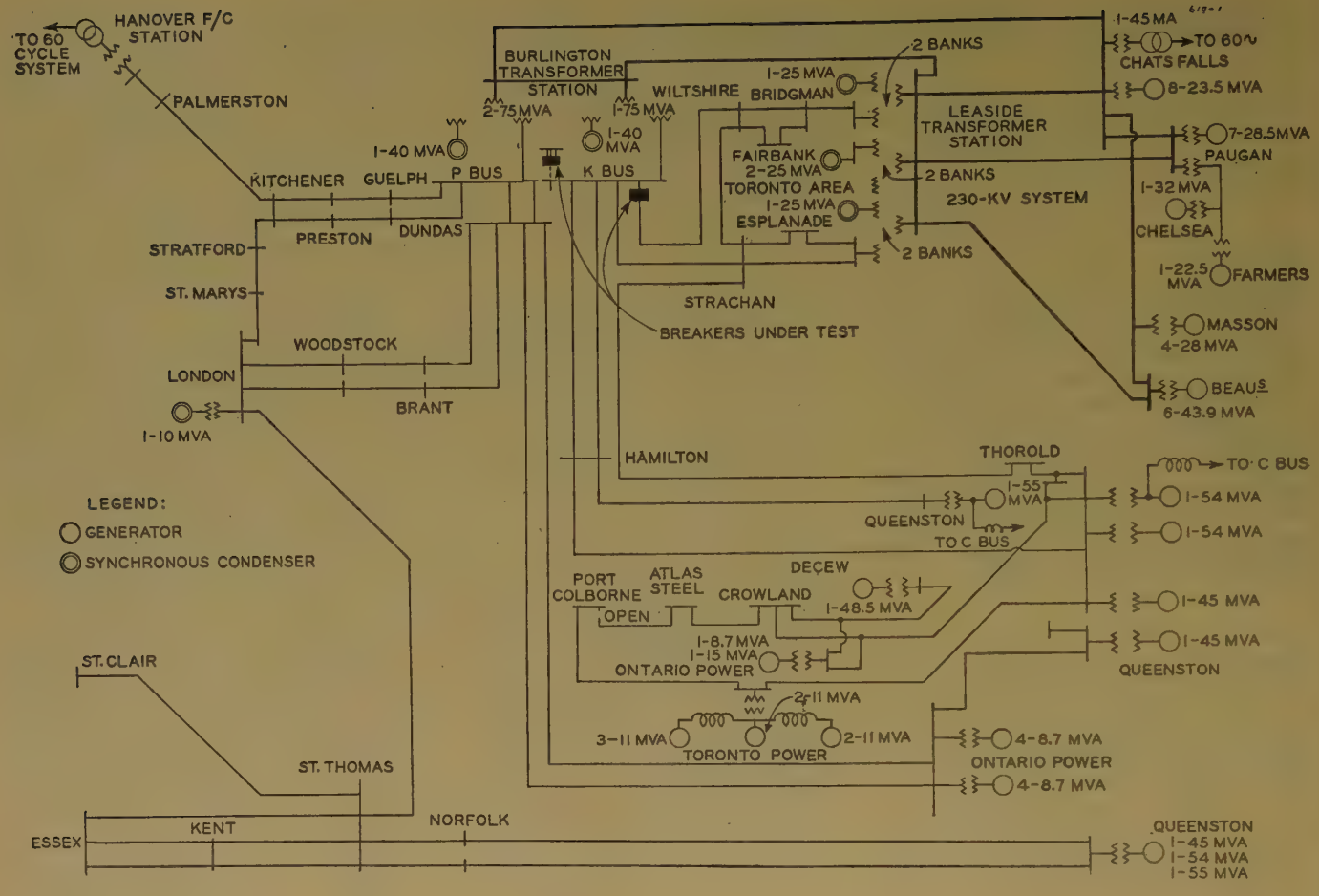


Figure 1. Niagara division transmission network of the Hydro-Electric Power Commission of Ontario

short circuit of 7,900 amperes and that required to produce approximately 13,000 amperes likewise were determined. For the latter the two 115-kv busses at Burlington would be parallelled and both synchronous condensers operating. These condensers could be used to advantage to obtain vernier calibration of the current, as the amount of infeed from each was known from the calculator readings.

Calculator readings give only *the initial symmetrical* current, so that the relation between this current and the *total* current at the time the contacts separated remained to be determined.

The d-c component of total current decreases exponentially according to the formula $i = I_0\epsilon^{-Rt/L}$. The ratio R/L is the ratio of resistance to inductance of the system looking into the system from point of fault. This ratio was determined from measurements on the calculator and found to be 33, giving a time constant of 0.03 second for the d-c component. It, therefore, was concluded that at 3 to 4 cycles (0.12 second to 0.16 second) after beginning of the fault, the d-c component would have disappeared, or at least it would be so small as to have negligible effect on the value of total current.

Standard decrement curves[2] indicated that, when corrected for frequency, the a-c component of total current at 3 to 4 cycles was practically the same as the initial a-c component.

As a result of the foregoing conclusions, the decision was made to use the system setup determined on the calculator, including as nearly as possible the same system generation without modification.

Provision for Service Security

It was of utmost importance that impairment to service should be avoided. The expected behavior of the system and its associated relay protections under severe 3-phase faults were studied to determine points of weakness. As a result of this study it was decided all frequency changer ties would be opened and certain relays on tie lines blocked for the brief test period. Backup protection for the circuit breakers under test was provided, and tested, and arrangements were made to place observers at widely separated key points to block those relays considered necessary and to be available if unforeseen trouble developed. Some loss of synchronous load appeared to be unavoidable and was accepted.

Study of Quantities to Be Measured

The quantities having direct bearing on the behavior of the circuit breaker itself and methods developed and used to obtain them are described later in the paper. Advantage was taken of every opportunity afforded by tests of this nature to obtain information on system and relay behavior. As a result observations quite foreign to those required for the test itself were included in the program, and useful data were obtained. To avoid confusion these data are not included in this paper.

Description of Circuit Breakers and Contacts

The two circuit breakers tested are 138-kv type BQOB oil circuit breakers manufactured by the Canadian Westinghouse Company. The 3 poles are mounted in a single floor-mounted tank. The spacing at the top of the bushings is the same as the minimum spacing for bushings of 3-phase transformers of the same voltage class.

The bushings are standard oil-filled condenser type, with deion grid contacts,

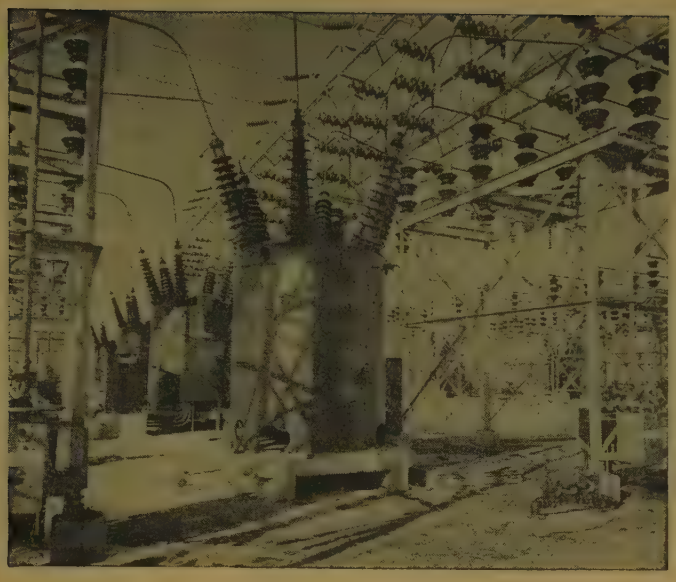


Figure 2. Type BQOB 138-kv oil circuit breakers at Burlington transformer station

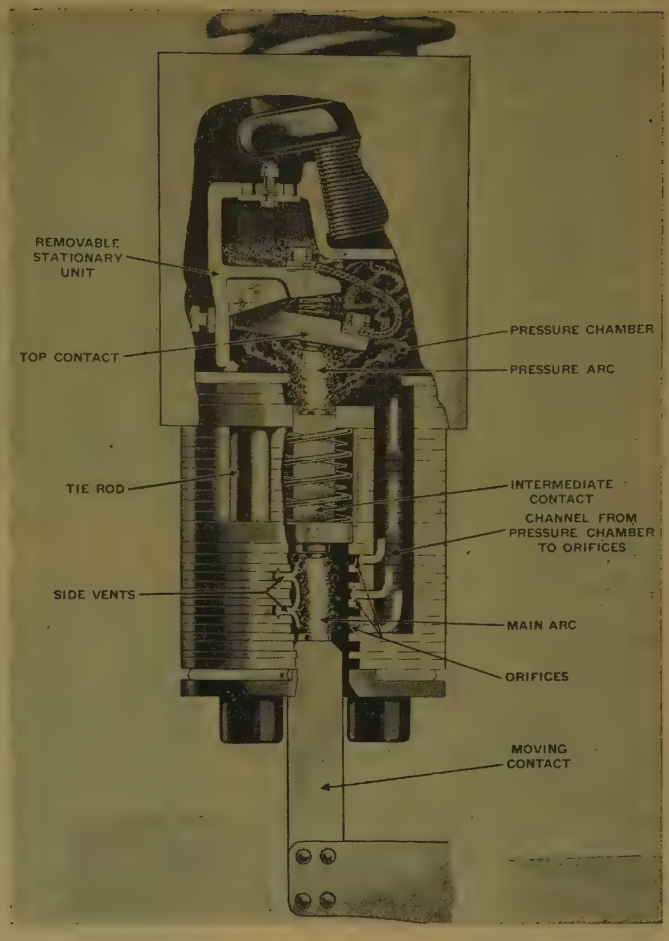


Figure 3 (right). Section through 138-kv type MF contact multiflow 5-cycle Deion grid, 2½ million kva

type BH for the 8-cycle 1,500,000-kva rating, and type MF for the 5-cycle circuit breaker rated at 2,500,000 kva. Each grid is surrounded by a heavy circular insulating tube, which acts as a barrier between phases. Entry to the tank is through a manhole at the side of the tank. Ample space is available between the contacts and the tank for inspection and maintenance.

Figure 2 shows a row of these circuit breakers at Burlington transformer station. Figure 3 shows a section through the type MF contact.

Measuring Equipment

Past experience indicated that high internal pressures could be developed and oil ejected when circuit breakers opened on heavy fault currents. A pressure gauge therefore was installed giving an output suitable for oscillographic records. This gauge consisted of a Crosby steam gauge, in which a slide wire potentiometer had been substituted for the oscillating cylinder and fitted with a 60-pound spring. The gauge was connected to a 1-inch bushing, the latter welded to the tank about 27 inches above the concrete base. The pressures that might occur were quite conjectural, but the choice proved satisfactory for these tests.

Circuit breaker tanks also had been known to shift on their bases, and a detailed study of motions and stresses was suggested. Zenith vibration recorders were mounted, one on each of the four lifting lugs at the top of the tank. These units contain circular clock-driven charts and are very sensitive to vertical displacements that occur at high accelerations.

Other stress indicating devices, such as scratch extensometers and electric units of the strain-resistance type, were attached at the base of the tank and to the holding-down bolts.

A special travel indicator was designed, attached to the indicator arm, and a calibration curve of the relative motion between the vertical lift rod and the indicator arm was obtained. To obtain a continuous accurate record, two slide wires with independent sliding contacts were used in parallel as a potentiometer.

Line to ground voltages were obtained from the secondary windings of three potential transformers, the primary windings of which were connected line to ground on the 115-kv bus.

Currents were measured by inserting Weston multiratio current transformers in the secondary windings of the regular bushing-type current transformers, to provide a further stepdown of current to the oscillograph shunts. An over-all calibration of the oscillograph element circuits was made by circulating alternating current in the primary winding of the Weston current transformers.

The entire group of measurements required the use of 18 and occasionally 20, oscillograph elements plus some mechanical records.

Procedure on Test

Immediately before each test, duly accredited representatives of the manufacturer and of the engineering and operating departments of the Commission were consulted as to final readiness and consent obtained to proceed with the test.

Arrangements previously had been made covering the system required for each test. A request was made through the load supervisor to have this system arrangement established, and at the same time the relay section of the operating department was conferred with for any special checking or blocking of relays to maintain protection without interfering in any way with the test proposed.

Finally, the instrument operators were checked for readiness. The last group of items checked consisted of oscillographs and mechanical recorders, which were automatic in operation.

A public address system is installed in various buildings and in the yard in Burlington transformer station. The oper-

ator in charge announced to all present the test was to take place; communication was established also with operators at Niagara, Dundas, Toronto, London, and other stations, over the private telephone system. A 2-minute warning was given, then at the proper time, 10 seconds, 9, 8, and so on, and on the stroke of zero the circuit breaker was closed on the short circuit.

With one exception the actual time during which the current was maintained was about 1/8 second. In the exceptional case the short circuit was cleared in about 30 cycles by the opening of seven circuit breakers without any major interruption on the system. Data obtained from this test gave more complete information on system transients, permitting analysis of the decrement of short-circuit current.

Results of Tests

A standard operating duty cycle consists of closing the circuit breaker on a short circuit and allowing it to open automatically, then after 15 seconds delay repeating the closing and automatic opening operation. This is designated a CO-15-CO operation. In the tabulated list of results each test as listed indicates a single close–open operation.

Figures 4 and 5 are typical records of

1. The red-phase line-to-ground voltage.
2. The three 115-kv line currents.
3. The trip-coil current.
4. The record of the travel indicator.

The data shown on Table I were obtained from the oscillograms. The current listed for each test is the maximum measured on any one of the 3 phases. Duplicate records taken on another oscillograph provided a satisfactory check on the current values as listed.

The current, arcing time, and total duration of fault current were obtained by the method outlined in the American Standard for "Alternating-Current Power Circuit Breakers 37.4 to 37.9," inclusive.

The results of the electrical tests require very little comment. Close inspection of the oscillograms indicate, in some cases, an erratic variation in resistance of the arc while it was being quenched.

Vertical motion to a maximum of 0.4 inch was recorded by the Zenith recorders at the top of the tank. The precision of the figures does not warrant drawing any elaborate conclusions, but some points are of more than passing interest. Table II shows the record obtained from these instruments.

The mechanical shocks registered on the first three tests seem to be independent of current, as greater motion (approximately twice as much) was recorded on test 2, with current at 4,720 amperes as occurred on test 3-2, when 7,720 amperes were interrupted.

This suggests that the acceleration and deceleration of parts played an important part in the over-all motion of the tank. It may be noted that the vertical motion of the top of the tank of the circuit breaker equipped with the MF grids was substantially less than on that with the BH grids, though the current interrupted was very much greater.

No quantitative results have been obtained from the records of stresses at the base of the tank because of various difficulties in anticipating their performance. It is conclusive, however, that, if stresses of objectionable magnitude had occurred, they would have been detected on the records.

The hydrostatic pressures set up in the tank appeared in the form of waves of decreasing amplitude. The maximum positive pressure was greater on the circuit breaker equipped with BH grids but did not exceed approximately 25 pounds per square inch as recorded. Even this was not a sustained pressure but a pressure-wave reflected back and forth with decreasing amplitude. By dividing the time interval between pulses, the actual time of the event in the circuit breaker contacts which causes the pulse may be estimated and identified.

The pressure gauge records from tests 2, 3, and 5 have been transferred to a single chart (Figure 6) for better comparison. A timing wave for test 2 was not available on the same film, but the action is sufficiently like test 3 for identification.

The small impulse registered first in each case seems to occur at the closing of the contacts; the heavier pressure waves continued for three surge-cycles after the arc was extinguished.

This device would not record negative pressures, so it is not possible to continue the analysis of the pressure waves further, though it is an interesting and unexpected aspect of the problem.

Samples of the insulating oil were taken after each test on the circuit breakers, and later tested for dielectric strength. No deterioration could be detected from the breakdown values, though the oil had become somewhat darker in color.

Comparison of Test Results With Calculator Values of Current

A comparison of values of current obtained on test with network calculator values has been made, to establish the accuracy of the latter in determining circuit breaker interrupting capacity.

The preliminary tests at 1/4 and 1/2 rated current were found to be about 15 per cent higher than given by the calculator, but this was due in part at least to increased and different distribution of generation from that used on the calculator. There was also a slightly different system arrangement. These variations were unavoidable but indicate that the system must be set up as accurately as possible, if close estimates of fault currents are required.

Table I. Tests on 138-Kv Circuit Breakers on 3-Phase Short Circuit

Test	Maximum Current at Parting of Contacts, Amps, Rms	Phase	Type of Grid	Arcing Time, Cycles	Duration of Fault Current, Cycles	Voltage Recovery, Per Cent	Capacity Interrupted, Millions of Kva
1-1	2,730	Blue	BH	1.4	3.4	93.5	0.54
1-2	2,730	Blue	BH	1.7	4.0	92.5	0.54
2	4,720	White	BH	1.7	3.5	85.5	0.91
3-1	7,490	Blue	BH	1.4	3.5	91.0	1.46
3-2	7,720	Blue	BH	1.6	3.4	92.5	1.48
4A	7,250	White	MF	1.0	3.0	91.5	1.37
5-1	13,100	Red	MF	1.2	2.9	88.0	2.58
5-2	13,000	White	MF	1.2	3.0	83.5	2.57

Table II. Record of Zenith Recorders at Top of the Circuit Breaker in Inches

Test	Type of Grid	Recorder 1	Recorder 2	Recorder 3	Recorder 4
1	BH	Up 0.06	0	0	Up 0.16
2	BH	Up 0.33	Up 0.4	Up 0.3	Up 0.2
		Down 0.33	Down 0.4	Down 0.33	
3-1	BH	Up 0.16	Up 0.2	Up 0.33	Up 0.1
3-2	BH	Up 0.13	Up 0.2	0	Up 0.13
		Down 0.13			Down 0.13
4A	MF	0	0	0	0
5	MF	0.2	Up 0.06	Up 0.1	Down 0.06

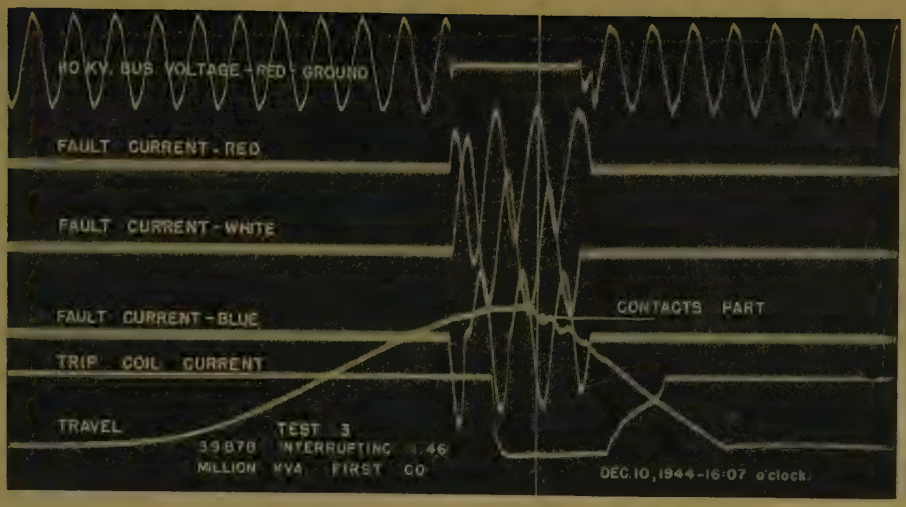


Figure 4. Oscillograph record of current interruption with BH grid

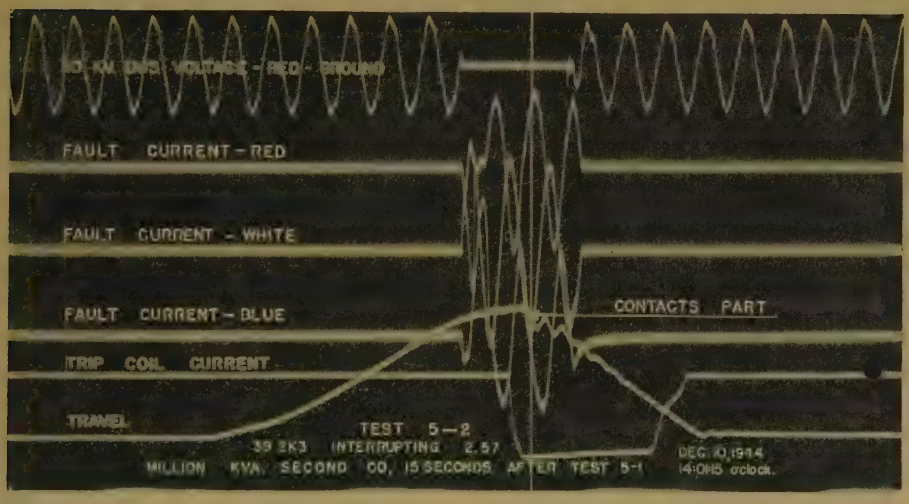


Figure 5. Oscillograph record of current interruption with MF grid

There was 5 per cent variation in fault current as measured on two field tests made with identical system arrangement, including the same generation.

On all tests it was found that the d-c component, although still measurable, added only one or two per cent to the total current. The largest value of this component on any test as measured, was approximately 15 per cent of the total.

On all but one test the duration of fault current was so short that no accurate estimate of decrement could be made. The agreement between calculated and test values of current, the former being initial values of rms symmetrical current, was an indication that for the time periods of interruption obtained on these tests it is safe to assume that no decrease in current occurred. Any error due to this assumption is in favor of the circuit breaker from the point of view of circuit breaker application, as it gives higher currents than the actual currents interrupted.

On one test the current through the circuit breaker existed for 30 cycles, until the fault was cleared by backup relays and system voltage restored to normal. This test, although it was a failure as a test on the circuit breaker, gave very useful data on the behavior of this system under 3-phase short circuit.

The currents recorded have been analyzed with the following results: The d-c component had an average short-circuit time constant of 0.00 second, compared with the 0.03 second obtained from calculator readings.

A comparison of test current (average of three phases) as measured and total current obtained from standard decrement curves, the latter corrected for a 25-cycle system by assuming an average open circuit time constant for this system of 10 seconds indicated close agreement (Figure 7). The decrement curves give values of total current, assuming a totally displaced wave. As no one of the test currents was totally displaced, it was possible to compare only the a-c components.

Condition of Circuit Breakers Following Tests

Circuit Breaker Having BH Grids

The circuit breaker in which the type BH grids were installed was rated at 7,950 amperes and was tested at 2,700 amperes, 4,700 amperes, and 7,700 amperes approximately with inspection following each test. Following the initial test there was only slight discoloration of oil. After the second test inspection showed discoloration of oil and slight pitting on the edge of the moving contacts. After the third test there was con-

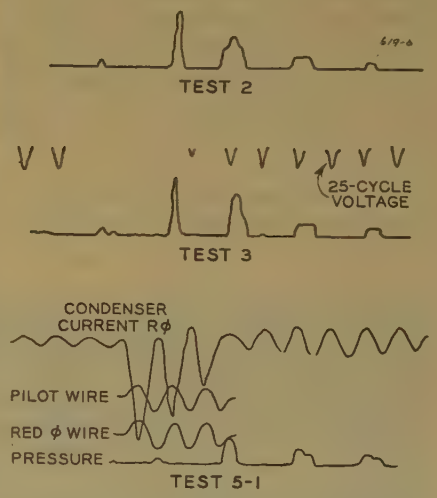


Figure 6. Record of pressures developed in circuit breaker tank on selected tests

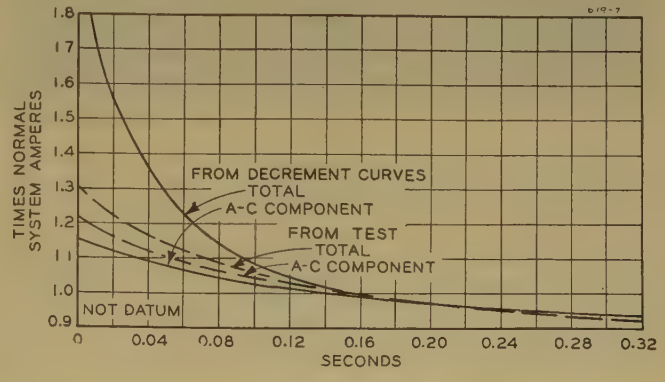


Figure 7. Comparison of test current with that from standard decrement curves



Figure 8. Micarta shield from type BH grid assembly after test at 7,500 amperes, showing crack at bolt hole



Figure 10. Type MF contact assembly and contacts after test at 13,100 amperes



Figure 11. Moving contact assembly type MF after test at 13,100 amperes

siderable discoloration of oil but no decrease in its dielectric strength. The moving contacts were burned slightly on the outside edges. The Micarta shield on one bushing was cracked at a bolt hole (Figure 8). The alignment of lift rods, moving contacts, and grids had not changed.

The Deion grids were removed and disassembled. No permanent damage was discovered, the only evidence of the interruption being a black substance blown through a number of the stacks (Figure 9).

Circuit Breaker Equipped With Type MF Grid

This circuit breaker interrupted 13,100 amperes with very little movement of the tank. The condition of the contact mechanism is shown on Figures 10 and 11. In our opinion the contact mechanism could have interrupted an undetermined further number of short circuits at 2,500,000 kva without overhaul becoming necessary. It therefore fulfills the requirements of the American Standard C37.4 in this regard.

Conclusions

1. It is quite feasible to test circuit breakers by staged tests on a large system, provided suitable precautions are taken, and the necessary preliminary work is done to establish the generation and line arrangement required to produce the specified value of short circuit current. On a large system use of the d-c or a-c calculator to determine the system required is essential.

2. Three-phase short-circuit current values at 25 cycles obtained on the calculator agree with actual system values, at least to the same accuracy as obtained on successive tests (5 per cent), using subtransient values of generator reactance and no decrement, if the circuit breaker time is 3 cycles.

3. The standard decrement curves modified for 25-cycle conditions, agree with actual system behavior within the accuracy of the test itself.

4. The circuit breaker with rated interrupting capacity of 1,500,000 kva is capable of interrupting 7,950 amperes at 110 kv and 25 cycles, within the meaning of the American Standard C37.4.

5. The contact assembly or type MF grid is capable of interrupting 13,100 amperes at 110 kv and 25 cycles, within the meaning of the American Standard C37.4.

6. Comparison of results from this test with those made previously in the high current test laboratory at 60 cycles indicates that the margin between rated and maximum interrupting capacity appears to be reduced for 25-cycle faults.

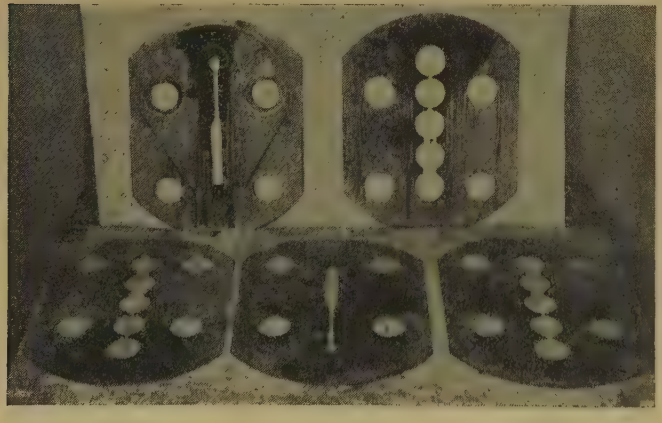


Figure 9. Plates from type BH grid stack after test at 7,500 amperes, showing material blown between plates by the arc

References

1. The 220,000-Volt System of the Hydro-Electric Power Commission of Ontario II, A. H. Frampton, E. M. Wood. AIEE Transactions, volume 60, 1941, pages 1215–21.

2. Standard Decrement Curves, W. C. Hahn, C. F. Wagner. AIEE Transactions, volume 51, 1932, pages 353–61.

Electronically Balanced Recorder for Flight Testing and Spectroscopy

A. J. WILLIAMS, JR. MEMBER AIEE
W. R. CLARK MEMBER AIEE
R. E. TARPLEY ASSOCIATE AIEE

Synopsis: A multiple-point potentiometer recorder for thermocouples is described having a slidewire driven to balance by a small induction motor powered from a 6L6 electron tube. The preamplifier gain is sufficient that the conventional input transformer (voltage step-up type) is not required, and thus a high impedance input circuit is made available. This permits the use of small capacitance values in the *RC* circuits for signal filtering and motor damping. The relation of this to the short balancing time (1.5 seconds) is discussed.

Spectroscopy supplied the incentive for the development of two additional but similar recorders. The first of these is a curve-drawing multiple-range microampere recorder with the smallest range 0.5 microampere, and with a balancing time of less than 1.0 second. The second is a multiple-range current-ratio recorder requiring only about 10 microamperes for the reference current.

IN A PREVIOUS PAPER[1] there was described the application of this recorder in potentiometer form to the measurement of 140 thermocouple temperatures during flight tests of planes. The switching of the thermocouples was described and the need for the short balancing time in the recorder was explained, but a description of the recorder itself was beyond the particular purpose of that paper. Interest in the recorder for other uses, such as wind tunnel testing, turbine checking at sea, and, in modified forms for spectroscopy is the reason for the present paper on the recorder itself.

Potentiometer Recorder

Figure 1 of the multiple-point potentiometer recorder shows the scales, the pointer, a section of the 21-point print wheel (under the pointer), and the perforated strip chart. The print wheel is pressed onto the paper once every 1.63 seconds by mechanical linkage from the same synchronous motor that drives the chart at constant speed. There is a violin string and pulley connection between the print wheel carriage and the slidewire potentiometer. All this is conventional.

Figure 2 shows the basic potentiometer circuit which is used. In operation, if the thermocouple gets hotter, its electromotive force increases above that of the potentiometer. The detector notes the unbalanced voltage and, through the balancing system *A–A*, moves the contact to balance and with it the print wheel and pointer. The current through the potentiometer is standardized by manually moving the battery rheostat, with the switch in the standardizing position, until the potentiometer contact comes within a limited region, as indicated by the pointer coming within a marked region of the scale.

Reference Junction Compensation

The circuit of Figure 3 is used for reference junction compensation. It is unconventional, as the reference junctions are remote from the recorder with plug connectors *X* of uncertain contact resistance in the leads 1, 2, 3, and 4. To minimize the effects of contact resistance and still have the reference junctions remote from the recorder, a complete bridge containing the compensating coils is located at the switch box with large end coil resistors R_A and R_B so the bridge can be supplied from the full 1.2 volts. 1.2 volts is the "end point" voltage for the dry battery with this circuit.

Mechanical Construction

In Figure 4 the door and the chart table are hinged away showing the slidewire, in large pan shaped enclosure, its vertical shaft and its direct gearing to the balancing motor. In the rear of the case, between the motor and slidewire shaft, can be seen one of the tubes in the amplifier, the chassis of which is hidden.

The amplifier and motor make up the balancing system shown as the detector and dotted line *A–A* of Figures 2 and 3.

Amplifier

The amplifier handles the unbalance as a 60 cycles per second a-c signal obtained by conversion from the d-c unbalance. The conversion is accomplished by a vibrator driven synchronously at line frequency as shown in Figure 5A. A blocking capacitor *C* prevents direct current from flowing from the thermocouple circuit to the tube or conversely. Four stages of triode voltage amplifiers are used together with one beam power output stage (6L6) with transformer coupling to one phase of the motor. The other phase of the motor is connected directly to the line. The quadrature phase relation required between the two motor windings is met by a fixed amount of phase shift in the vibrator drive-coil circuit. The mechanical drive from the motor to the slidewire completes the feedback loop. By using direct current on the heaters of the triodes, and by using rubber shock mounting on the low-level tube (first two stages), the total noise is held to less than seven microvolts referred to the first grid.

Filter Circuits

External circuits may produce alternating voltages in the thermocouple circuit as a result of capacitive or inductive coupling. If these voltages reach the detector input circuit, some interfering voltage will appear at the first grid. The vibrator suppresses the fundamental component but, like all modulators, adds components at new frequencies. The 60 cycles per second component is the only one which produces torque in the motor, but the other frequencies are almost as bad because they overload the amplifier. When overloaded at an odd frequency, the amplifier cannot handle the regular 60 cycles per second signal as it should.

All this points to the need for filtering out alternating voltages "picked up" by the thermocouple or its leads. Figure 5A shows the four-section resistance capacitance (*RC*) filter that is used. Inductances were not used for the series elements because of their inherent characteristic of "picking up" voltage from stray fluctuating magnetic flux. To shield such inductances magnetically introduces complications, size, and expense. The *RC* filter never can be built to have the sharp frequency cutoff of the *LC* filter, but it was found that it could be built sufficiently sharp to meet the requirements. The requirements are:

1. Attenuation of 60 cycles per second (and higher frequencies) by a factor of 500 or more (loss of 54 decibels or more).

Paper 46-62, recommended by the AIEE committees on instruments and measurements and electronics and presented at the AIEE winter convention, New York, N. Y., January 21–25, 1946. Manuscript submitted November 23, 1945; made available for printing December 12, 1945.

A. J. Williams, Jr., is chief, electrical division, and W. R. Clark and R. E. Tarpley are supervisory research technologists, all of the research department, Leeds and Northrup Company, Philadelphia, Pa.

The authors are grateful to Mrs. A. H. Springman for calculations on the reference junction compensation, to P. A. Towle for the slidewire on the ratio recorder, to E. W. Yetter and V. J. Porter for building and testing the ratio recorder, and to I. Melville Stein for his encouragement at times when it was most needed.

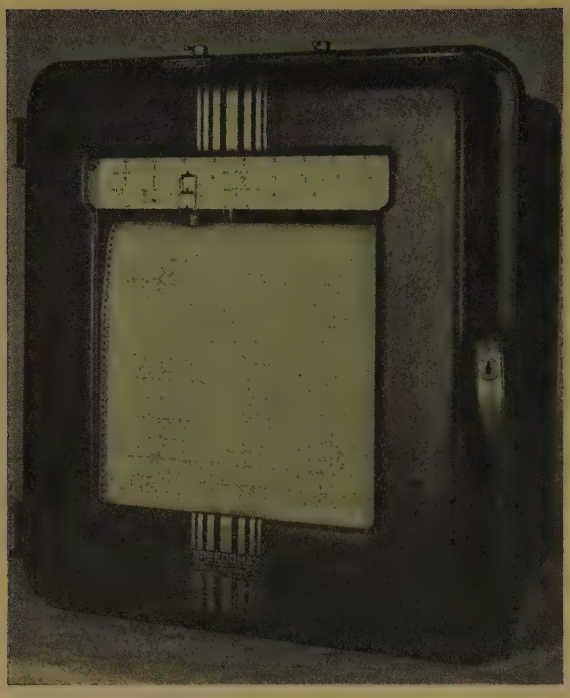


Figure 1. Multiple-point potentiometer recorder

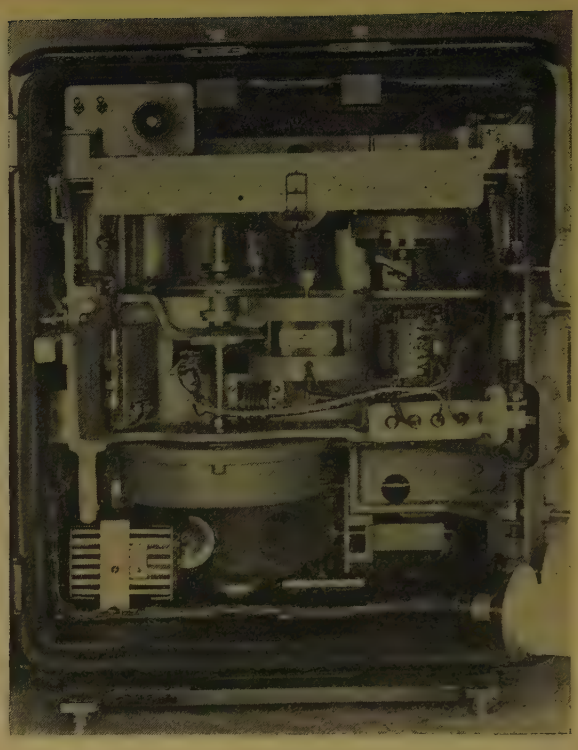


Figure 4. Internal view of recorder

2. Transmission of low frequencies of about one cycle per second and lower to 0.998 or better (loss of 0.016 decibel or less).

Requirement 2 could be stated as follows: After switching from a cold couple (reading at low end) to a hot couple (reading at the high end) the voltage at C_4 shall assume the voltage of the hot couple to within 0.2 per cent in 1.5 seconds or less.

Theoretically, the use of multiple sections in the filter is adequate to meet these conflicting requirements. Experimentally it was found that this was not sufficient. If electrolytic capacitors were used, requirement 2 would not be met. Many samples of electrolytic capacitors of many types and ratings have been tried. A typical result is shown on Figure 6A, which is a recorder response curve made with the chart driven at high speed. A satisfactory result with paper capacitors of the same 60 cycles per second capacitance is shown on curve *B* of the same figure. The reason for the excessive delaying action of the electrolytic capacitors was not investigated further. It may be the result of interfacial polarization inherent in the complex electrolytic film.

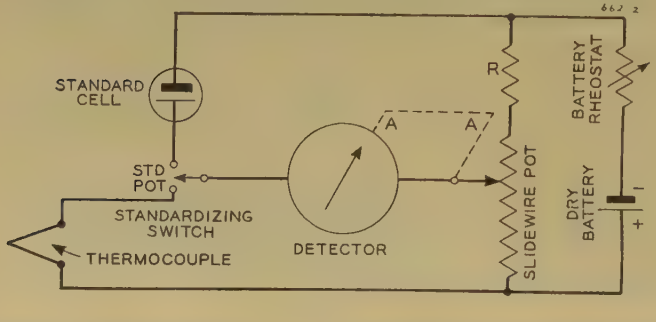
The impedance looking into this filter from the detector side at low frequencies (and direct current) is 20,000 ohms. The impedance of the detector is greater than this so it receives the greater part of any change in thermocouple voltage. Therefore the combination of high impedance detector and multisection *RC* filter using paper capacitors insures that the detector will receive changes in the thermocouple voltage without serious delay or attenuation.

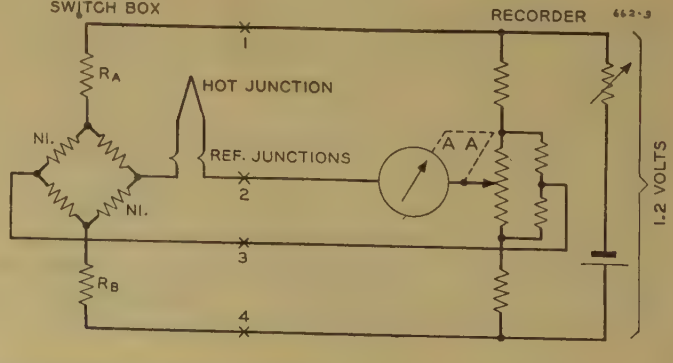
Damping

Because of the inertia of the balancing motor, there is a tendency for it to overshoot the balance point. This is avoided by reversing the torque shortly before the balance point is reached. The torque is reversed by reversing the input to the detector, and this is done by introducing a voltage proportional to the motor velocity.[2] As the slidewire and motor are geared together, the slidewire velocity is proportional to the motor velocity. Figure 5B shows a simple circuit for which the output voltage E_2 is proportional to the rate of change of the input voltage, dE_1/dt, provided only that dE_1/dt has been constant long enough for the transient to have expired. If the circuit of Figure 5B were inserted into Figure 5A at *B–B*, there would be delivered to the detector mesh a voltage proportional to velocity as required. Of course, no voltage proportional to slidewire position would be delivered; however, if the circuit of Figure 5C is used, the voltage E_2 delivered to the detector mesh is exactly one-half the voltage E_1 of the slidewire when the slidewire comes to rest, and the transient has expired. When the slidewire is moving there is a component in E_2 proportional to the velocity. The time constant of the transient is the parallel resistance from

Figure 3. Circuit used for reference junction compensation

Figure 2. Basic potentiometer circuit





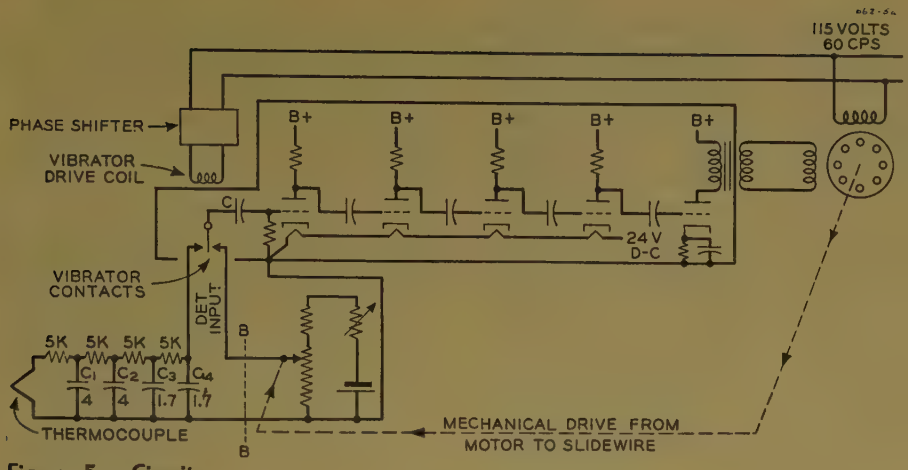
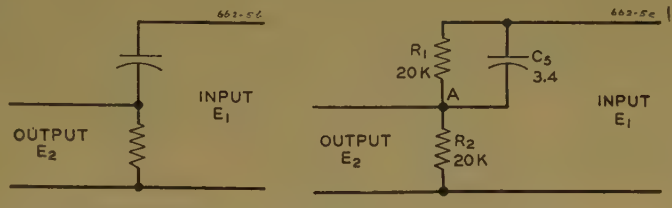


Figure 5. Circuits for balancing, filtering, and damping

A—Circuit without damping network
B—Explanatory network
C—Damping network



Resistor values are given in ohms and capacitor values in microfarads

point A times capacitance $= \frac{R_1 R_2}{R_1 + R_2} C_5 =$ $10{,}000 \times 3.4 \times 10^{-6} = 0.034$ second. This is so small as to have only a secondary effect, and the main object is accomplished, that is, to introduce a voltage proportional to velocity for the purpose of damping. The damping is sufficiently good to permit switching, completing a full scale balance and printing in 1.63 seconds.

It will be noticed that with this circuit some current is drawn from the slidewire even at balance. Quantitatively, however, it would require 40 ohms resistance in the slidewire, and its contact, to introduce an error of 0.1 per cent, and no such resistances ever have been found.

With the filter circuits and damping circuits described in the foregoing, and with the high impedance detector, two things are accomplished:

1. Large unbalances are completed in a minimum time without overshoot.
2. The voltage level at the detector is kept as high as possible, and therefore has the greatest possible margin above stray thermal electromotive forces.

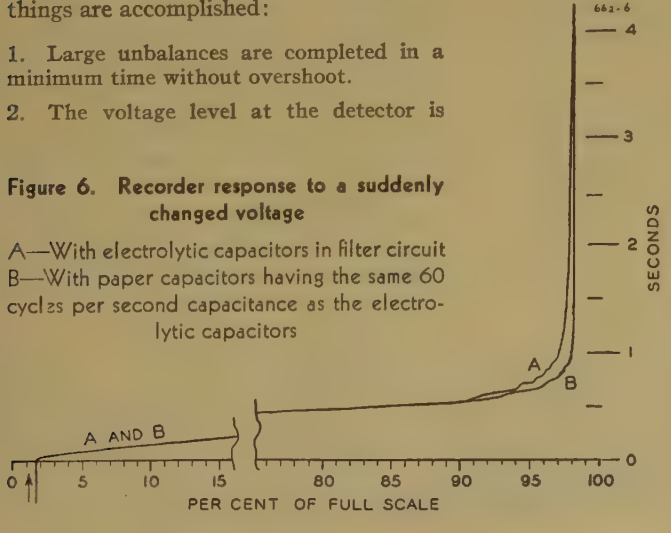


Figure 6. Recorder response to a suddenly changed voltage

A—With electrolytic capacitors in filter circuit
B—With paper capacitors having the same 60 cycles per second capacitance as the electrolytic capacitors

Microampere Recorder

For the recording of thermocouple temperatures, a potentiometer recorder is required because it is the open circuit (zero current) voltage that is the function of the temperature. For the recording of light or other radiation on a barrier layer* photoelectric cell, a current recorder is required because it is the short circuit (zero voltage) current that is the function of the radiation.

Figure 7A shows, in simplified form, how the slidewire type of null recorder can be arranged to present zero voltage to the photoelectric cell at balance. When any appreciable voltage does appear across the photoelectric cell, and hence across the detector, it operates through A–A to move the slidewire and so changes the current through the calibrated resistor until that current equals the current from the photoelectric cell, thus returning to zero the current through the detector and the voltage across the detector and photoelectric cell.

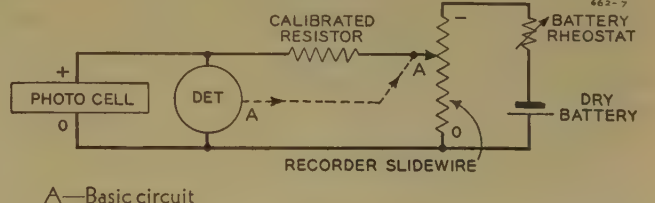
Figure 7B shows how filtering and damping are added. It will be noted that resistance is inserted between the photoelectric cell and detector for the purpose of filtering yet this resistance does not prevent the photoelectric cell and the detector reaching zero voltage at balance, as no direct current flows through this resistance at balance. As the slidewire has a low impedance, all three capacitors contribute to the filtering of alternating current from the photoelectric cell circuit away from the detector.

The damping is provided by capacitor C_3 which gives a component of voltage across the detector proportional to slidewire velocity. Figure 8 shows balancing curves with the chart speeded up in order to show detail. The balance time is approximately 0.8 second extrapolated for a full scale change. Most of the time the motor is running at top speed which is near to synchronous speed. The time lost in getting up to speed is 0.06 second or four cycles, and the time lost in stopping is 0.08 second or five cycles. Good damping is indicated by the fact that the time lost in stopping is nearly as small as the time lost in starting.

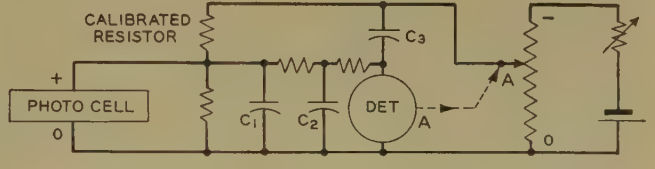
In addition to the null current range of 0.5 microampere, there have been added for convenience other current ranges and several voltage ranges by

* With an emission-type photoelectric cell it is the combination of the cell and its voltage supply which should look into a short circuit (zero voltage).

Figure 7. Circuits for microampere (null current) recorder



A—Basic circuit



B—Circuit with filtering and damping components added

means of shunts and multipliers, respectively.

A microampere recorder of this general type has been found by Dieke to work well with photomultiplier tubes for the direct intensity measurement of spectrum lines.[3] On the lower current ranges of the recorder the dark current of the photomultipliers shows up and should be balanced out or subtracted from the readings, if the use of these low ranges is to be justified.

Ratio Recorder

The microampere recorder is suited well to the study of the intensity of spectrum lines and their variations arising from all causes. For spectrographic analysis, it is desired to measure the variation resulting from change of composition of the specimen being sparked and to suppress variations from all other causes. A big step in this direction is to measure the ratio of the intensity of two spectrum lines.

Figure 9A shows in simplified form how a slidewire type of recorder can be adapted to measuring ratio. If the fixed resistor equals the slidewire, then the ratio I_x/I_s is read directly as the fractional position of the slidewire.

Several experimental recorders have been built using this basic circuit, together with a detector and balancing system about the same as that already described.

Figure 9B shows a more detailed circuit including the photomultipliers. The slidewire resistance is 5,000 ohms so that small currents from S (ten microamperes) yield adequate slidewire voltage and hence good sensitivity. The drop coil R is 25,000 ohms so that the fundamental full scale ratio I_x/I_s is 0.2. Other ratios can be read by switching the "Ayrton" shunt ratio multipliers.

The high valued resistor R_H balances the recorder slightly on scale for $I_x = 0$, which is of value when looking for small amounts of dark current. Conventional methods of doing this were not applicable because of the common terminal at battery + for I_x and I_s.

Filtering for the signal I_x is done as already described. In order that the recorder shall plot a steady ratio for fluctuating currents (of constant ratio I_x/I_s) it is necessary to filter I_s also. Furthermore, it is necessary that the two filters shall have carefully matched frequency responses.

Figure 10A, shows the record given with currents I_x and I_s of constant ratio, but with a reduction of both to one-half value, and then a return to the initial value. Figure 10B, is a record with the same recorder, made after the chart had been rolled back and rerun. The recorder is used here as a straight microammeter on I_x by supplying the slidewire from a battery. The reduction of I_x and its return to its initial value is shown. The effectiveness of the ratio method in ironing out the effect of change in absolute magnitude of the two currents is apparent.

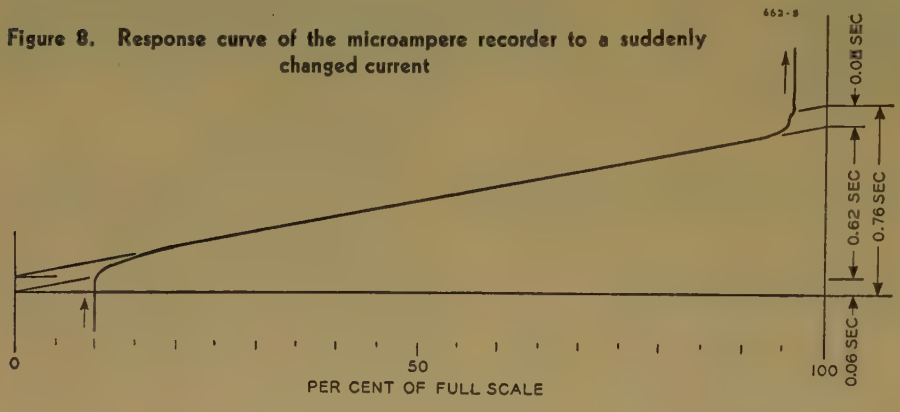


Figure 8. Response curve of the microampere recorder to a suddenly changed current

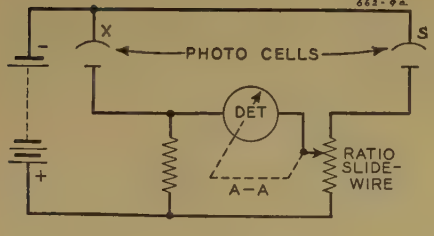
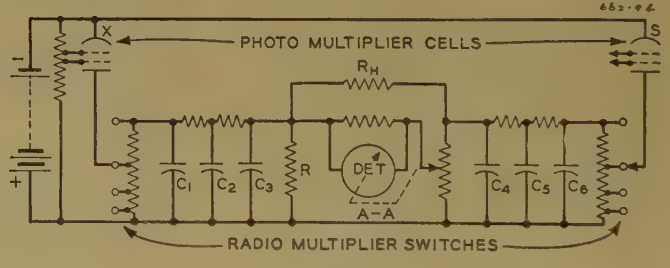


Figure 9. Circuits for the ratio recorder

A—Basic circuit
B—Circuit with filtering and damping components added



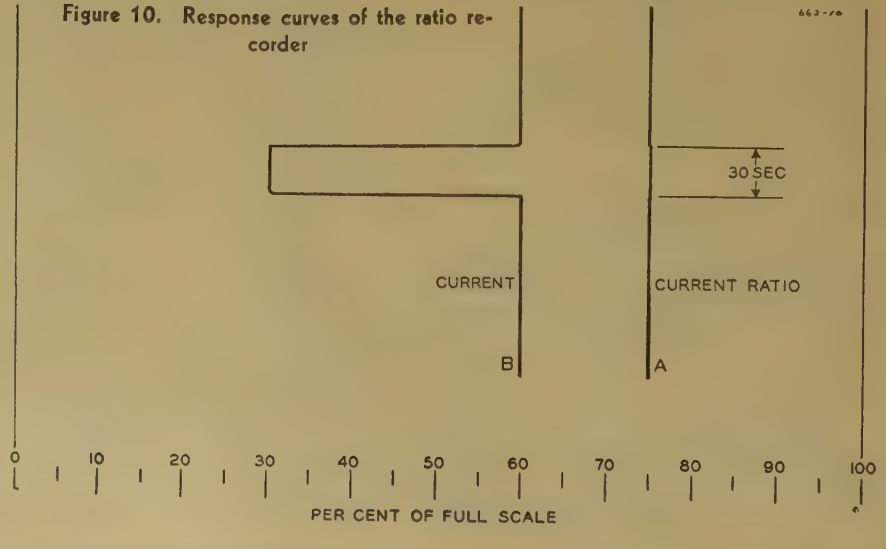


Figure 10. Response curves of the ratio recorder

References

1. High Speed Multiple-Point Potentiometer Recorder for Measuring Thermocouple Temperatures During Test Plane Flights, I. M. Stein, A. J. Williams, Jr., W. R. Clark. *Transactions* of the American Society of Mechanical Engineers, volume 66, number 4, 1944, pages 271–5.

2. Combined Thyratron and Tachometer Speed Control of Small Motors, A. J. Williams, Jr. AIEE Transactions, volume 57, 1938, October section, pages 565–8.

3. Direct Intensity Measurements of Spectrum Lines With Photomultiplier Tubes, G. H. Dieke, H. M. Crosswhite. *Journal* of the Optical Society of America, volume 35, number 7, July 1945, pages 471–80.

Radar Systems Considerations

D. A. QUARLES
FELLOW AIEE

IN the comparatively brief history of its development, the radar art has passed quickly through the general practitioner stage into the stage of many specialists. Today there are a dozen or more highly developed fields of specialization, all essential to the development of a new radar system. Each of these fields has its own basic science foundations and its engineering technology, and as soon as security conditions permit, each will have its own literature. To tie these several fields together calls for systems engineering and planning. The over-all characteristics and performance of a radar system are dependent both on the excellence of the component parts and the nicety with which they are fitted together to perform the desired function. It is the purpose of the present paper to discuss some of these systems engineering considerations, with examples of practical solutions that have been found, leaving to the specialists in the several fields the more detailed and exact exposition of their respective arts.

There have been many technical workers in this broad field, and both in England and this country they have enjoyed full interchange of technical information so that each could use the building blocks of the other as well as those of his own design. This makes it exceedingly difficult to recognize and give credit to the sources of specific contributions, and the present paper will not attempt to do so. Most of the illustrative solutions shown are the product of Bell Telephone Laboratories, but it is freely admitted that many of the basic ideas entering into these designs may have originated elsewhere. In particular, the Bell Laboratories worked very closely in this field first with Army and Navy laboratories and later with the Radiation Laboratory of the Massachusetts Institute of Technology, and in all cases there was the freest interchange of technical material. It is therefore a pleasure for us to recognize and acclaim the splendid research and development work that was done at these laboratories, even though specific recognition of their contributions seems impracticable at this time.

Antenna

The alpha and omega of a radar system are its antenna. This is true in a literal radiation sense. It is also true in the sense that the antenna was usually the first part of the system to be blocked out in plan and the last part to be completely frozen in design. This antenna problem is familiar to radio engineers, but in modern radar where the same antenna is used both to transmit and receive, its characteristics have an even more profound influence on the performance of the system. The simplest radar antenna resembles a searchlight in that it consists of a suitably shaped reflector illuminated by one or more sources of electromagnetic energy. If the reflector is a paraboloid of revolution with the source at its focus, the radiation is of the single lobe or beam variety in which the angular width of the beam is inversely proportional to the diameter of the reflector and directly proportional to the wave length of the radiation. While such a beam antenna has been extensively used, many of the more recent radar systems have demanded more specialized radiation patterns. For example, in airborne search and bombing radars, a fan-shaped beam has come to be considered optimum. At any one position, such an antenna illuminates a narrow wedge of the terrain below, extending, ideally, from the point of the terrain vertically beneath the plane out radially to the maximum effective range of the system. The design objective here is to produce as narrow a beam as possible with a vertical pattern such that substantially equal signals are received at all ground ranges. This requires that the effective voltage be approximately proportional to the square of the cosecant of the vertical angle measured downward from the horizon. A more recent and as yet unpublished study of this problem has indicated that some modification of this cosecant squared

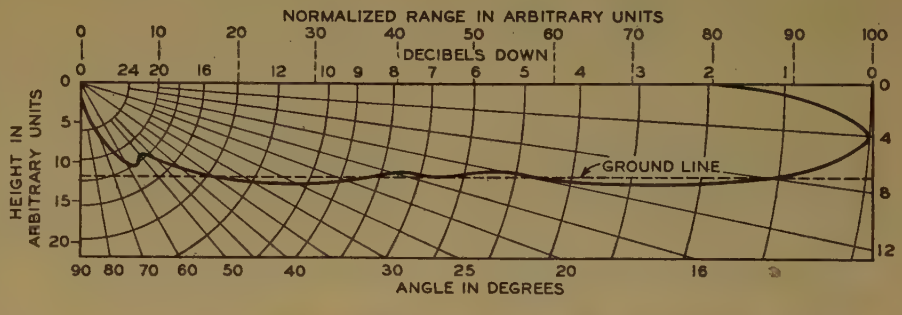


Figure 1 (above). Vertical antenna pattern (airborne radar system)

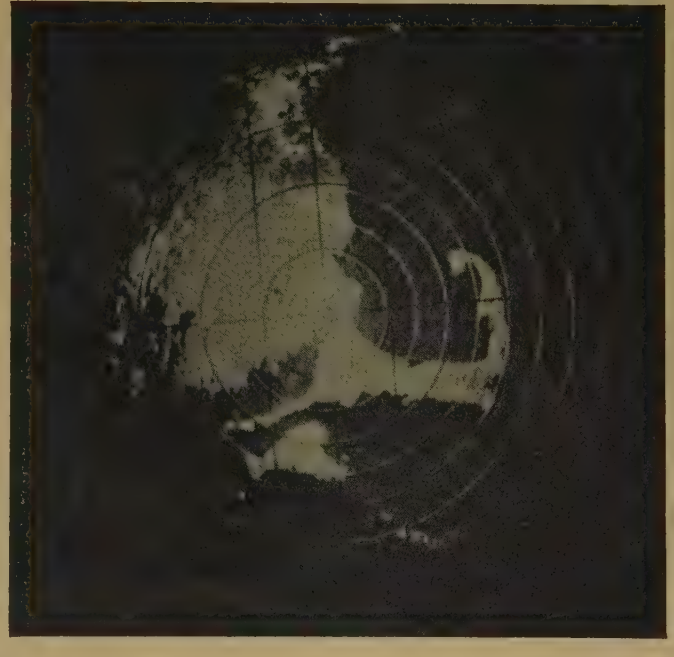


Figure 2. Oscilloscope picture of Cape Cod from 19,000 feet (range circles are spaced at five miles)

Paper 46-46, recommended by the AIEE committee on communication for presentation at the AIEE winter convention, New York, N. Y., January 21–25, 1946. Manuscript submitted December 14, 1945; made available for printing December 27, 1945.

D. A. QUARLES is with Bell Telephone Laboratories, Inc., New York, N. Y.

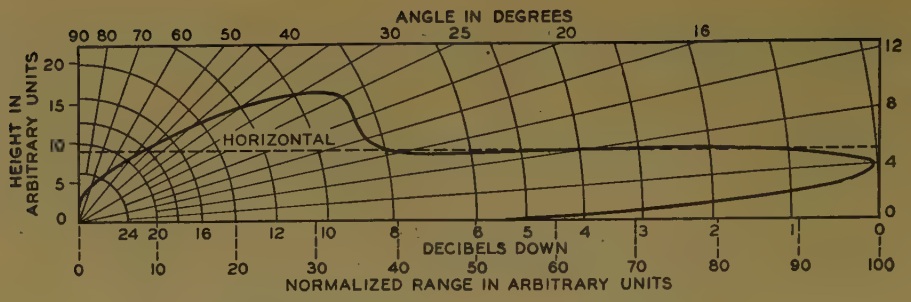


Figure 3. Vertical antenna pattern in free space (land-based search radar system)

formula may be advisable. In any event, the fair approximations to the ideal that it has been possible to achieve in actual design give satisfactorily uniform ground illumination. For example, the vertical pattern of the final stage of antenna evolution of a radar set used for search and bombing purposes in B-29 planes is shown as Figure 1. Figure 2 shows that quite satisfactory uniformity of ground illumination was achieved by this vertical pattern.

Other variations on antenna pattern include beams very much sharper in azimuth than in elevation for airplane search purposes and the reverse for height-finding purposes. One of the latest refinements here is illustrated by a typical vertical antenna pattern of a recent land-based air search antenna, as shown in Figure 3. In this case, in order to get high angle coverage, something approaching the cosecant squared pattern is achieved, the vertical angle being measured upward rather than downward from the horizon.

In general, land- and ship-mounted radar sets used to search the horizon for either ships or planes must take account of the fact that the intervening land or water surfaces reflect that part of the radiation directed below the horizon. Combination of the direct and the reflected waves produces a characteristic interference pattern in the vertical plane, greatly extending the range of the radar system at certain elevation angles and correspondingly reducing it at intermediate angles. A typical vertical performance or coverage chart of a light early-warning system is shown as Figure 4. In this case the beam in free space is fan-shaped with a horizontal width of about 3.5 degrees. The horizontal pattern is not greatly affected by the surface reflection, while the vertical pattern shows the very sharp lobes resulting from direct and reflected wave interference.

Frequency

Since the whole trend of radio development in the past two or three decades has been toward shorter wave length and higher frequency, it is not surprising that the same trend should have characterized radar development. In the case of radar, however, there were considerations over and above those applying to radio, which put a large premium on higher frequency and shorter wave length. This is because radar is essentially a seeing and measuring art, and fineness of vision and precision of measurement are related directly to fineness or shortness of wave. This, of course, comes about from the fact that with an antenna of given physical dimensions, the spread of the beam is proportional to the wave length, other things being equal, so that as the beam sweeps through an angle, its ability to discriminate between two nearby reflecting objects is an inverse function of the beam width. The above assumes that the two objects are at equal range. If, on the other hand, they are on a line with the radar antenna but at unequal range, the ability of the radar set to discriminate between them is an inverse function of the pulse length. It follows from the above broad reasoning that each radar set will be characterized by a figure of confusion in space, the cross-section of which is directly related to the beam height and width and the depth of which is directly related to pulse length. Within this figure, multiple reflectors will appear as one. Reflectors that cannot be encompassed within such a figure of confusion, on the other hand, would be resolved. Actually, certain characteristics must be met in other parts of the radar system, notably in the intermediate-frequency (hereafter referred to as i-f) and video amplification and in the cathode ray tube properties, in order to realize the theoretically possible discrimination provided by the radiation system. It is quite practicable, however, and in fact common practice, to design the rest of the system so that the discrimination of the radiation system is limiting. Since, with fixed antenna size, beam width is directly pro-

Figure 4. Vertical coverage chart (land-based radar system at a low site overlooking water)

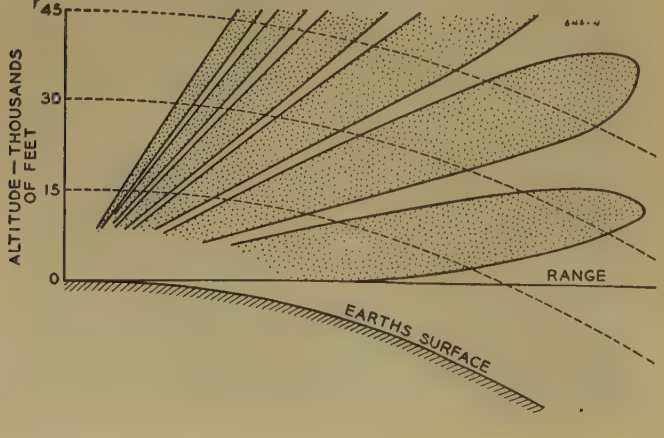
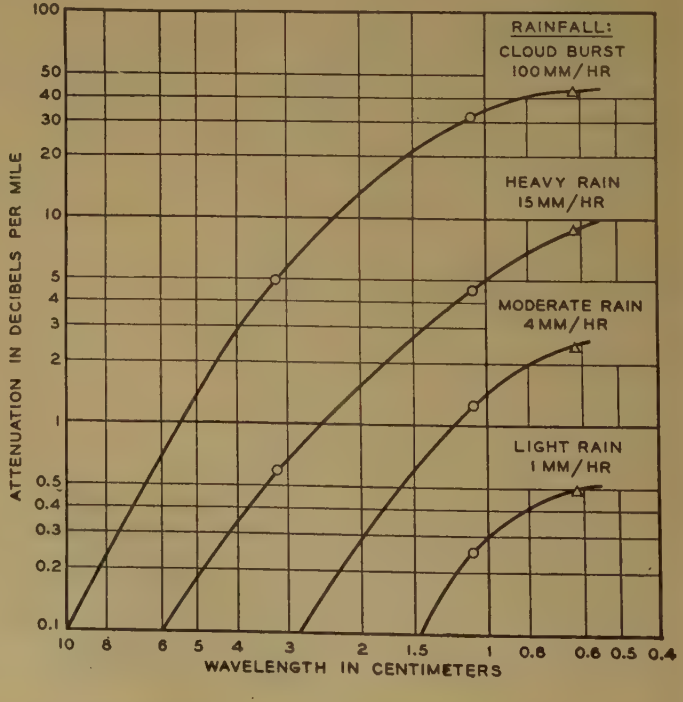


Figure 5. Effect of wave length on attenuation caused by rain



portional to wave length, it follows that to achieve high resolution or high discrimination, radar had a very special reason for seeking higher frequencies and the same reason for preferring shorter pulse lengths even though the latter, in general, meant a sacrifice in range. Actually, early radar sets made the best use of prewar technology and employed wave lengths down to about one meter. In four fairly discrete steps, this wave length was reduced successively to bands in the neighborhood of 40, 10, 3, and 1 centimeter. This change was accompanied by the use of shorter and shorter pulses so that the over-all effect of the development was to decrease the volume of the figure of confusion by about five orders of magnitude, two each for height and width and one for depth. As in so many other trends of this kind, these advantages were not gained without penalties. In fact, in the case of the shortest wave length mentioned, atmospheric absorption and raindrop interference get to be such serious limitations as to appear to restrict this and shorter wave lengths to only very special uses. Figure 5 shows the relation of attenuation to precipitation at different wave lengths, and Figure 6 shows the effect of energy absorption by gaseous components of the atmosphere. If this restriction proves real and permanent, it appears that the useful free space spectrum has now been explored and, in fact, is rapidly being conquered and settled.

Transmitter

The two principal elements of the transmitting system are the radio-frequency oscillating tube and the source of high-voltage pulses, variously called a keyer, modulator, or pulser. It is the function of the latter to deliver to the oscillator tube square-topped spurts or pulses of very high voltage of the order of a microsecond in length and spaced of the order of a millisecond apart, these specific values varying over considerable ranges according to the specific purposes of the radar equipment.

Two basic methods have been used to form the microsecond pulses:

1. Short-circuiting or open-circuiting a charged artificial transmission line, often called a pulse network.
2. Creating large-voltage surges by driving a magnetic circuit into the region of saturation.

In connection with 1, the switches used to open- or short-circuit the charged pulse network have been

1. High-voltage vacuum tubes.
2. A spark-gap discharge either of the open air or enclosed type.
3. The hydrogen filled thyratron.

Since these several forms of modulators will be described in detail by others, suffice it to say here that all of them were applied extensively in operating systems, with recent design tending toward a preference for the hydrogen thyratron.

During the brief interval of the pulse, powers ranging up to the order of a megawatt may be delivered by the pulser. Since the particular combination of current and voltage put out by the pulser may not be that required by the oscillator, it is common to interpose a pulse transformer, the function of which is to step the voltage up or down to the desired level. In some radar systems, a transmission line is required between the pulser and its associated transmitter, in which case pulse transformers may be required at each end of the line. A typical oscillogram of the magnetron input current as a function of time, delivered by a hard tube modulator used extensively in airborne

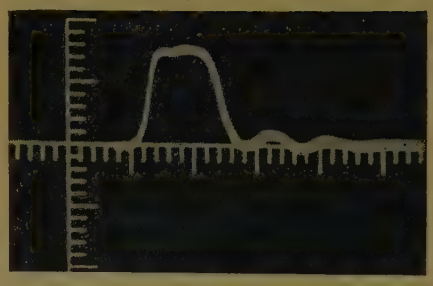


Figure 7. Magnetron input current delivered by hard tube modulator

$^3/_8$ μsec, 800 pulses per second
Magnetron current = 4.5 ma average
= 14 amp peak
Rise time = 0.03 μsec
Pulse width = 0.42 μsec
Pulse scale = 0.07 μsec per division

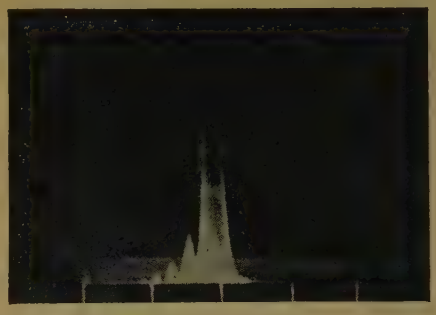
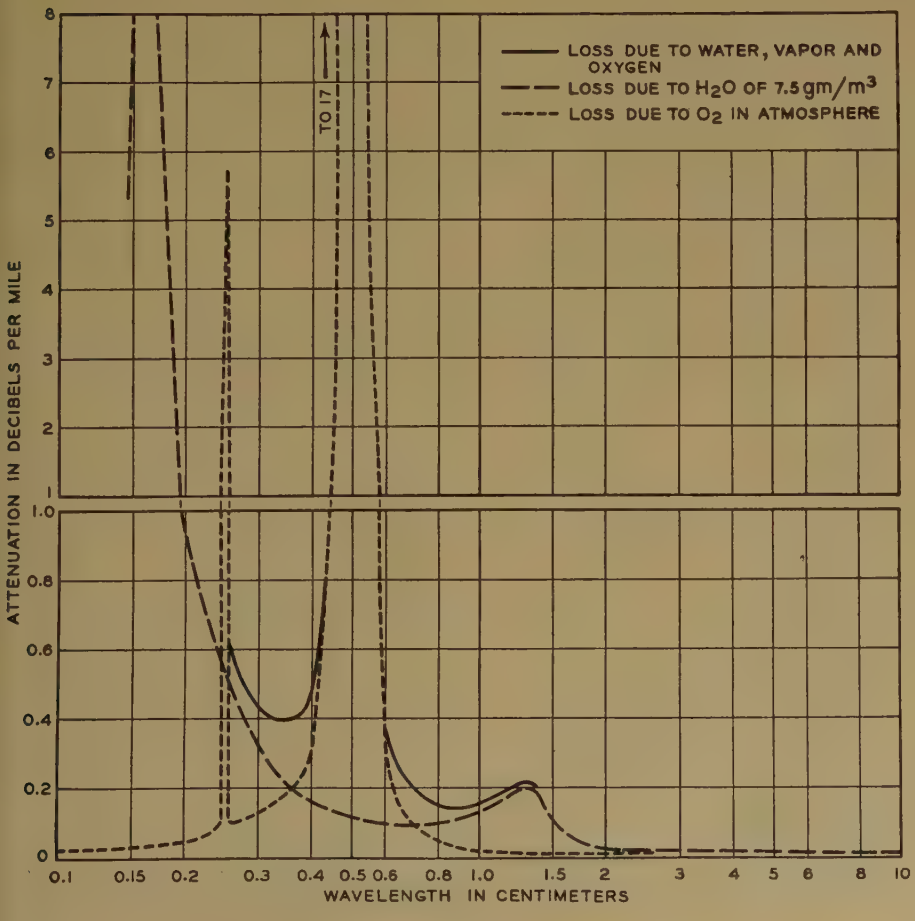


Figure 8. Magnetron frequency spectrum (scale = 10 megacycles per division)

Figure 6. Effect of wave length on attenuation caused by gases in atmosphere



systems, is shown in Figure 7. The frequency spectrum produced by this pulse is shown on Figure 8.

Various forms of more or less conventional triodes found application as transmitting oscillators in the earlier longer wave radar sets. In this class of tube, time of flight of electron from cathode to plate must be short compared with the signal period—an increasingly serious limitation as the art moved into the microwave range. Velocity modulation tubes avoid this limitation in a sense by making use of the electron stream in flight. A particular form of velocity modulation tube, the cavity magnetron, has virtually monopolized the transmitting oscillator role in the more modern systems. In fact, its adaptation to very high power, very short pulse operation, and its very high frequency stability make it ideally suited to this purpose. In earlier forms, the magnetron was a fixed frequency device, but more recently external means of tuning over a moderate range have been devised and applied in practical design. While the frequency of the cavity magnetron is largely controlled by its built-in cavity construction, it is, of course, necessary to couple the oscillations in the internal cavities with the output line, and the reaction on the magnetron of this coupling imposes some neat problems of system design. As the antenna scans, the impedance facing the magnetron varies on account of varying reflections from discontinuities such as rotary joints in the output line to the antenna. These effective impedance changes, reflected back into the magnetron through its output coupling, tend to modulate or pull the frequency of the magnetron. Maximum power output calls for tight coupling between the magnetron and its antenna system, but such tight coupling in turn accentuates this pulling effect. In addition, there is a "long line" effect which causes an impedance irregularity to be more serious the longer the transmission path between it and the magnetron. Practical system design makes it necessary to take all of these factors into account and to tailor the characteristics of the magnetron to the degree of smoothness and excellence it is practicable to achieve in the radio frequency transmission system.

Duplexer

One of the most important practical contributions to radar design was the development of duplexer methods making it possible to use the same antenna for both transmitting and receiving purposes. Since the outgoing radar pulse occupies a very small fraction of the time, characteristically about one-tenth of one per cent, a switch which would associate the transmitter with the antenna during this brief interval and then disconnect the transmitter and connect the receiver during the relatively long silent interval, was called for. Since the total cycle, however, was only of the order of a millisecond, a very fast switch was required. In practical design, a gas-filled "TR" tube was almost universally used for this purpose. It is obvious that the requirements that this tube protect the receiver during the very high power transmitting interval and that it recover rapidly enough to admit echoes from nearby targets and thus achieve the desired minimum range for the system made it a very important element. Figure 9 shows the transmission characteristics of a typical "TR" tube assembly as measured in the transmit and receive paths over one complete pulse cycle.

Receiver

From our present point of view, the most significant elements of the radar receiver in order in the circuit are the beating oscillator, the detector, the i-f amplifier, followed by a second detector and video amplifier, and finally the display system. While each one of these elements has its own peculiar art, there are certain broad systems considerations. For the early long wave length radar sets, beating oscillators were of the more or less conventional triode construction. In fact, one very special triode, the so-called lighthouse tube, has been used as a beating oscillator up into the microwave range. As in the case of transmitting oscillators, velocity modulation has been the key to the design of most of the receiving or beating oscillators used in microwave systems, and for the most part, these have been of the single-cavity built-in type. The earlier forms had fixed or manually tuned cavities and beyond this, were tunable within a fairly narrow range by adjustment of the voltage of the repeller electrode. Not only was this voltage adjustment used for narrow range manual tuning of the receiver to its transmitter output, but automatic frequency-control circuits employing an intermediate frequency-discriminator circuit were devised which regulated the repeller voltage at the proper value for reception of echoes of the transmitted pulse. These automatic frequency-control circuits were not without their difficulties, but various improvements were introduced so that those embodied in most recent systems were quite stable and satisfactory. A typical

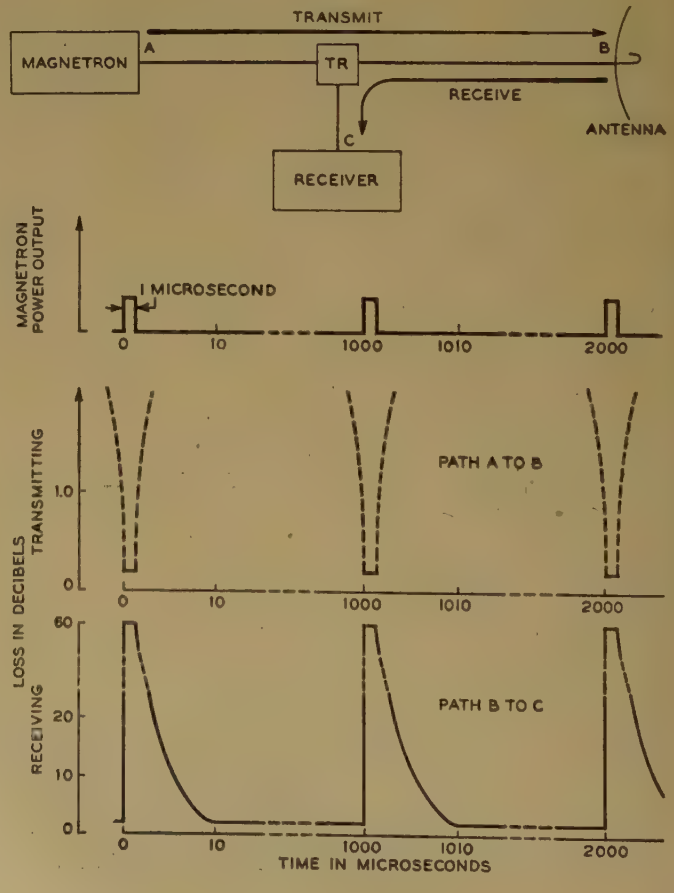


Figure 9. Transmission characteristics of "TR" tube assembly



Figure 10. Typical velocity-modulated beating oscillator

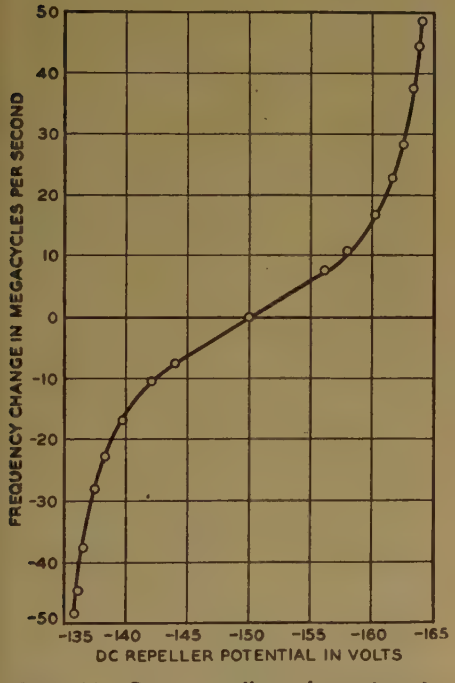


Figure 11. Beating oscillator electronic tuning

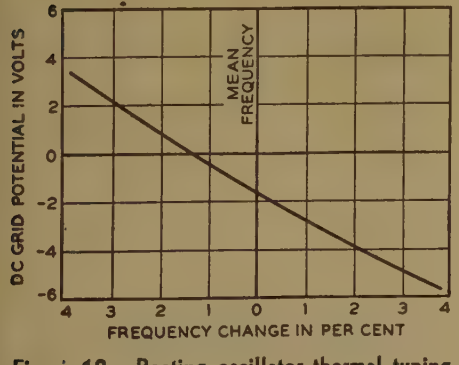


Figure 12. Beating oscillator thermal tuning

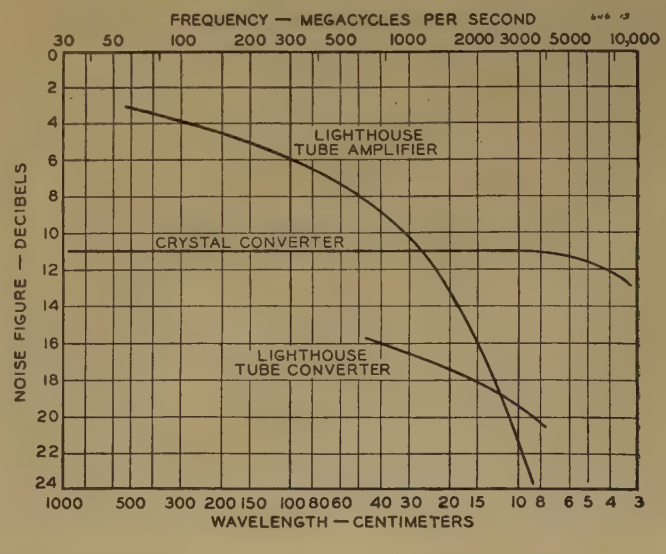
velocity-modulated beating oscillator with built-in cavity is shown as Figure 10, and the relationship between frequency and repeller voltage is shown as Figure 11.

More recently, thermal means of controlling oscillator cavity size have been devised, the heating effect being regulated by a control voltage. A typical relationship between this thermal control voltage and oscillator frequency is shown in Figure 12. Where thermal control of this type is available, automatic frequency control may be built around it rather than resorting to repeller voltage control as in the earlier systems.

First Detector (Converter)

In a radar system, the selection of frequency is based among other things on the noise figure available in the receiver. The input circuit of the receiver is the low-signal level point of the system, and the problem here has been to achieve the greatest possible freedom from noise. The longer wave radar receivers employ a combination of vacuum tube pre-amplifier and detector to achieve the best noise figure. In general, however, crystal detectors of the fixed cat's-whisker-on-silicon type have been almost universally used at wave lengths of about 30 centimeters and less. Figure 13 shows a comparison between the noise values of the lighthouse tube as an amplifier or detector, and the crystal-type detector. A great amount of development work has been done on these crystals, with the result that a uniform product has been achieved within a few decibels of the theoretical resistance noise limit. While the crystal is not strictly frequency-sensitive, optimum design calls for different crystal units for the different frequency bands. Means must be provided in the system to protect the crystal from high-voltage overload which would destroy its sensitivity.

Figure 13. Effect of wave length on receiver noise



Intermediate Frequency

Choice of intermediate frequency rests on a number of factors, including signal-to-noise ratio and band width. About 90 decibels of i-f gain is required with a band width of from one to ten or more megacycles. Since resistance noise (power) is proportional to band width, the early tendency was to make i-f amplifiers as narrow as possible consistent with the pulse length to be accommodated. In more recent systems, there has been a trend toward wider band receivers as a means of sharpening up the picture. While, for example, a one-megacycle i-f system followed up by a one-half-megacycle video system would be expected to give approximately the optimum signal-to-noise ratio for a radar set employing a pulse of about one microsecond, it has been found in certain types of display that considerable advantage can be had by widening the band by a factor of as much as five. In such cases the increased noise is more than offset by the greater sharpness of the signal and by the finer grain structure of the noise.

Actually, most of the i-f amplifiers have been designed around a frequency of either 30 or 60 megacycles, but it would go beyond the scope of the present paper to discuss the relative uses and advantages of these two intermediate frequencies. Great progress has been made in achieving very low noise amplification and in producing the desired gain and gain frequency characteristic with a minimum of tubes and other components. The development of the 6*AK*5 high figure of merit miniature pentode was a great boon to i-f amplifier designers. Figure 14

attached shows an i-f strip employing six 6*AK*5 tubes and giving a gain of 65 decibels at a band width of 13.5 megacycles, centered at 60 megacycles. The design of the second detector and video amplification circuits is closely related to the television art and perhaps deserves no further comment in this paper.

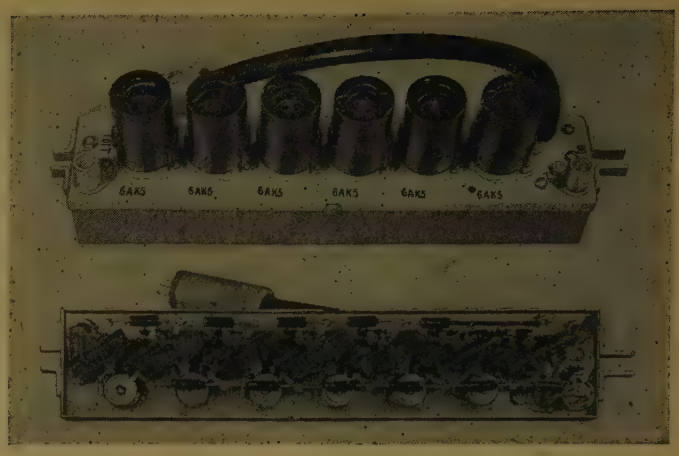


Figure 14. Typical i-f amplifier assembly

Display Circuits

The cathode ray tube has been substantially without a competitor for radar display purposes. A variety of display techniques has been developed, and a variety of cathode ray tubes of several sizes and of several different phosphors has been developed to meet the needs of radar systems. Rather than trying to tabulate these several varieties and their uses, the systems problem will perhaps be best illustrated by taking one of the most important combinations and examining its characteristics in relation to over-all performance. For this purpose, we choose a high-persistence so-called cascade phosphor and operate the tube as a plan-positon indicator in which each sweep is radial from the center to the outer edge and the direction of the sweep rotates like the spoke of a wagon wheel, at any instant the direction corresponding to the direction in space of the scanning antenna. The beam is intensity-modulated by the video signal, and the radial sweep is timed to correspond to the outward sweep in space of the radar pulse. In such a display, therefore, signals are shown on the face of the tube in their plan position relationship in space, the center of the tube normally corresponding to the position in space of the radar set. Here, again, the problem is not unlike that of a television receiver scope except that in the plan-position indicator type of display, a different scanning system is employed. In most recent systems, a permanent magnet focusing mechanism has been employed, the principal advantage being stability of adjustment and economy in the use of rectified power as compared with the earlier electromagnetic focusing scheme. To produce a wagon-spoke rotating beam needed to follow an all-around-looking antenna, best results have been achieved by placing an electromagnetic sweep coil around the neck of the tube and rotating the coil in synchronism with the scanning antenna. Gain, intensity, and focus controls parallel closely those found in television practice. It should be noted here, however, that special features such as facilities for expanding desired portions of the picture or stabilizing the picture against motions of the mother plane or ship have been devised and afford very important improvements in certain display systems. Methods also have been devised for discriminating between fixed and moving targets. These methods are of great importance in search systems where echoes from distant planes tend to be masked by permanent echoes from mountains or other features of the terrain.

Fire Control Radar

The above discussion deals primarily with radar as a search device. Many of its most important military applications, however, go beyond this search or seeing function to the more precise measuring function of fire control. In general, a radar fire control system must perform the following functions:

1. Precise three-co-ordinate location and tracking of the present position of the target.
2. Prediction of the location of the target at some future time, for example, the time at which a projectile would cross its path.
3. Generation of control orders, such as signals, to train and elevate the gun, set the fuse, and, in general, control the fire.
4. Servo systems for carrying out these orders.

When the fire control system is located on a plane or a ship, these problems are greatly complicated by the motions of the mother vehicle, calling in turn for stabilized reference systems and much other gear.

Automatic tracking is achieved by one or another form of lobe switching in which the antenna beam is rapidly switched back and forth between two angular positions and the target is centered between these positions by making the two received echoes equal. In fact, a servo system having as its input the echoes received from the two lobes can then be made to drive the antenna to a position where the two echoes are equal, and thus continuously adjust the antenna to such a position as the source of the echo moves. A variation on lobe switching in which the antenna conically scans, makes it possible to center the antenna in both azimuth and elevation and similarly uses two servo systems to track automatically in both dimensions. Automatic tracking in range involves a different technique. For this purpose, it is necessary to build into the radar a range unit producing a variable range pip or marker which may be compared with the range of the incoming signal. Here again it has been possible to make this range tracking automatic by employing a servo system which drives the range unit up or down under control of a voltage representing the deviation of the indicated range from the actual range. The same servo drive can be used to drive a shaft or potentiometer to give an output angle or voltage proportional to range. By resorting to precision methods, radar sets have been devised which not only track automatically in all three dimensions but which deliver present position information continuously to a computing system to accuracies of a few mils in angle and a few yards in range, this without the target ever being visible and, in fact, without human assistance once the radar equipment is locked on the desired target. The art, based fundamentally on feedback amplifier theory, of producing servo systems that are tight enough to give the desired speed and accuracy of response and at the same time stable over the operating range has been adequately treated elsewhere.

Computers

As it is the purpose of this paper to deal primarily with radar systems, any detailed discussion of computers would be



Figure 15. Computer used with airborne bombing radar

beyond its scope. It is pertinent to point out, however, that association with computers in a fire control system has a profound effect on the requirements to be imposed on the radar system proper. A more detailed consideration of one particular combination of radar and computer would illustrate this point. In a radar bombing system, fire control becomes bombing plane and bomb control. The computer, as before, has as inputs present-position information about the target. It must predict the future position of the target, the time interval being that required for the bomb to fall from the plane to the ground. The fire control orders in this case are directions to the pilot or to the automatic flight control equipment as to the proper course for the bombing plane and directions to the bomb release mechanism as to the instant in the plane's flight at which the bomb should be released. Such a computing mechanism must also be given as inputs the altitude of the plane and the ballistic characteristics of the particular bomb to be dropped. These are either previously known or separately determined and set into the computing mechanism in advance. Here again a great amount of development work has been done to improve the practicability and accuracy of the system and to make the best use of the not too adequate radar data available. The complexity of the problem and of the equipment required to solve it is perhaps best indicated by the photograph, Figure 15, of a bomb sight computer developed and introduced in radar bombing shortly before the termination of hostilities. Without attempting to explain the mechanism, suffice it to say that this computer performs the following operations: In association with a radar system displaying before the bombing operator a plan-position indicator type of "map" of the target terrain, the operator tracks by centering electronic range and azimuth markers on the "target." This tracking process not only feeds present position into the computer but at the same time enables the computer to determine the essential forward and transverse rates of the plane. Into the computer will previously have been set the ballistic constants of the bombs to be dropped. The height of the plane above the terrain will have been determined by a prior range tracking on the nearest ground return which would come from that vertically beneath the plane. Using these input data, the computer will predict the future position of the plane at an interval equal to the time-of-fall of the bomb; it will set up steering orders, either to the pilot or through the automatic flight control equipment, to move the plane into the correct position and heading; and it will give a bomb release order or control signal to operate the release mechanism at the correct instant. In the particular equipment shown, the computations assume level, steady flight, a limitation which it would require considerable additional gear to remove. This computer does, however, afford one very important additional facility, namely that of offset bombing. Because of the coarseness of radar data, information about the terrain is at best not too good. Certain landmarks do stand out sharply, and the geographical relation of these to strategic targets may be known or determined by reconnaissance. The ability to track a radar landmark and bomb a target of known range and azimuth offset from the tracking point greatly increases the flexibility of the equipment. The computer shown provides this feature, so that, having set in known offset co-ordinates, the operator proceeds as though to bomb the aiming point, the computer making the corrections and actually directing the attack against the target.

Radar bombing systems cover a wide range of weight and complexity and require nice judgment to reach a fair balance between such factors as operating facility and precision on the one hand and equipment bulk, reliability, and other "price" factors on the other. Enough progress has already been made to assure that highly flexible and precise radar bombing systems will become available at a "price" that is in reasonable balance with other factors.

Any discussion of radar systems would be incomplete if it failed to touch on the all-important question of testing and test equipment. Actually, the practical success of radar in the field was largely dependent on the provision of adequate specialized test gear. This was an art in itself, the treatment of which is reserved for a companion paper.

This paper will have served its purpose if it gives a technical background for the more detailed exposition of the many-sided art that is modern radar. Security will probably continue to limit workers in this field in the telling of their story, but it will be possible to tell enough to indicate clearly the truly wonderful advances in electronic and related arts that have brought radar to its present stage of development.

A New Wire Recorder Head Design

T. H. LONG
MEMBER AIEE

Synopsis: Certain defects inherent in the usual design of wire recorder heads are pointed out. Some defects are of a practical nature and one is based on theoretical considerations. An improved design is proposed on which a limited amount of experience has been obtained. A natural modification of this design permits level-winding across the record-playback head, thus distributing the wear and resulting in a head that is virtually self cleaning.

WORK with wire recording during the past few years seems to have been confined to two general types of heads for recording, playback, and erase purposes.[5] These are illustrated to a somewhat enlarged scale in Figures 1 and 2. Figure 1 shows two variations of the so-called open type of head in which the recording wire runs over a grooved pole piece, and Figure 2 shows a closed type of head in which the relation between the recording wire and the pole piece is substantially the same as in Figure 1, but in which the exciting coil surrounds both the pole piece and the wire.

Certain combination heads have been developed which combine the functions of record and erase in one structure. These always use separate gaps for the erase and the record operations. Playback is over the record gap. The structural modifications seem obvious and are not shown. The principal difference between a record or playback head and an erase head is that the latter ordinarily uses a gap of about 0.010 inch, and the playback gap for a wire speed of two feet per second is preferably about 0.0015 inch.

Figure 3 shows the relative record-and-playback characteristics for the open and closed type heads. A qualitative analysis of the situation that causes this difference between open and closed type heads has been given by Holmes and Clark.[1] According to this analysis, the so-called stray field is responsible for the irregularities, since the phase relation between the stray field and the main field depends on the frequency and the wire speed. It should be pointed out that a closed head greatly reduces the effect of stray fields, since the leakage flux has to go through the coil to contribute any adverse effect (on playback).

Figure 4 is a photograph of an equipment that has been set up to study experimentally the characteristics of various types of heads. This is arranged so that it can be operated on a continuous loop of wire about 20 or 30 feet long, or so that it can be operated from spool to spool. Provision is included for various speeds from 1.25 to 5 feet per second. The playback head is located a few feet along the wire from the record head so that in listening tests it is possible to get a quick comparison between a few bars of music as recorded and as played back. This almost instantaneous playback is very useful in collecting data, especially when working from spool to spool.

The first heads used on this equipment were of the closed type but in which the operating gap was adjustable. An optical system was used that made it possible to project on the wall of the room a 150-diameter enlargement of the operating gap and the wire traveling through it.

One of the first things discovered with this equipment was that the gummy residue that accumulates on the heads is a magnetic mud that has a shunting effect on the working gap. This seems to be of little consequence at low frequencies, but the effect at 5,000 cycles may be as great as 15 decibels or more, for a two-foot-per-second wire speed.

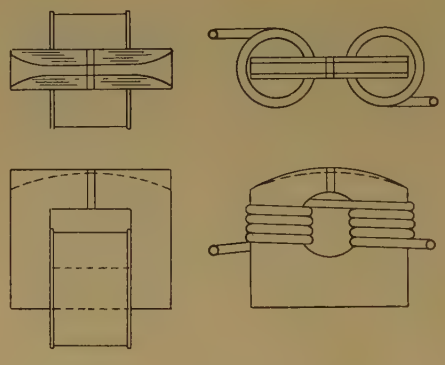


Figure 1. Open type record–playback head

A—High impedance head with laminated magnetic structure

B—Low impedance single lamination head, used with step-up transformer on playback

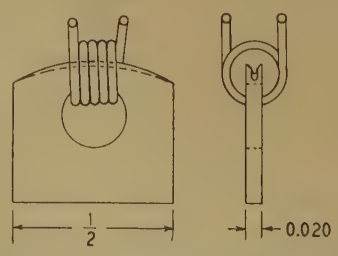


Figure 2. Closed type single lamination record–playback head

Lamination thickness is exaggerated

It was found that by frequent cleaning with carbon tetrachloride, quite consistent results were possible, even at high frequencies. It seemed apparent that in more conventional head designs there would be little trouble from this accumulation of magnetic mud, since the operating gap is filled with solder. The actual event however was contrary to this wishful thinking.

By lifting the wire a little as it moved through the gap and observing the enlarged image on the wall, it was determined that at low frequencies it made no difference where the wire was in the gap until the wire started to leave the region between the sides of the groove. At high frequencies (5,000 cycles), however, the smallest motion perceptible in the enlarged image on the wall, corresponding to about 0.0002 inch at the gap, made a difference in playback of about three decibels. These tests were made at the playback head, since there was no time lag there between cause and effect. Subsequent experiments show that for high frequencies the effect at the record head may be even more pronounced.

It is an unfortunate fact that this magnetic mud frequently will build up underneath the recording wire, even with substantial tension in the wire and working over a small radius such as one-fourth inch. This causes the actual performance of such a system to be rather uncertain above about 2,500 cycles, at least for wire speeds on the order of two feet per second.

By the simple expedient of using sufficient carbon tetrachloride and using it often enough, it is possible to keep the grooved type of heads fairly clean. But this has caused another sort of trouble, since with no lubricant whatever the wire may abrade the head sufficiently to cause a 6- or 7-decibel increase in the noise level. This noise level evidently is due to microphonic action of the head. In such cases a drop of oil on the head will bring the erase noise level down about three decibels in the first minute, and another three

Paper 46-29, recommended by the AIEE committee on communication for presentation at the AIEE winter convention, New York, N. Y., January 21–25, 1946. Manuscript submitted November 8, 1945; made available for printing December 26, 1945.

T. H. LONG is senior research engineer, C. G. Conn, Ltd., Elkhart, Ind.

or four decibels in a few more minutes.

Another minor disaster that may happen with the grooved type of head is that after running for quite a while on wire that is 0.004 inch in diameter some wire may come along that is 0.0042 inch in diameter. The least that will happen is that the wire will bind in the head. This may cause repeated breakage of the wire, and certainly will introduce a pronounced kinkyness on account of cold working one side of the wire

This also may cause a substantial change in the magnetic quality of the wire and the partial loss of any recording then on it. Unless the wire is run with an unusual amount of tension the curliness alone caused by such an accident will preclude further use of that particular section of wire. It is true that such things do not happen often but they are vastly annoying when they do happen.

This raises a question as to the practicability for home or school use of any head that depends for its performance on running the wire at the bottom of a groove, unless some means can be devised to insure intimate contact between the wire and the pole pieces. A suitable method should preclude the possibility of the binding action just described. The tendency of mud to accumulate under the wire is a factor that must be overcome by eliminating the mud or redesigning the head so it will be easy to clean.

Figure 3. Playback characteristic taken with closed type record head

O—Open type playback head
●—Closed type playback head

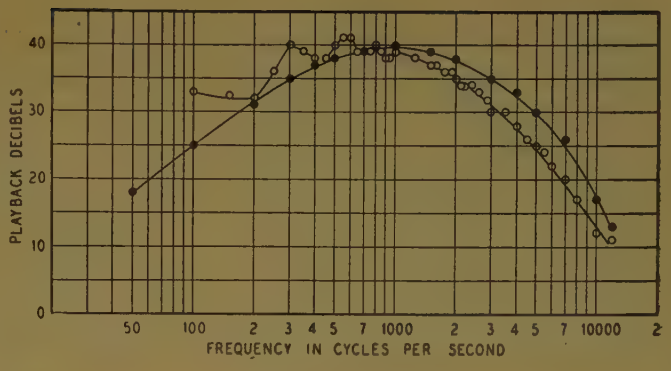
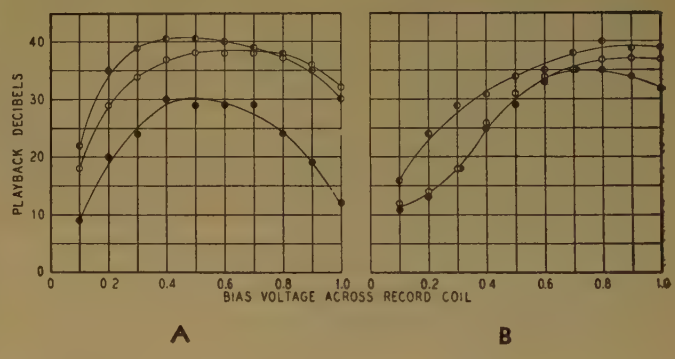


Figure 4. Experimental equipment for record and playback studies



Figure 5. Record–playback characteristic versus high frequency bias voltage, using closed type playback head

A—For closed type record head
B—For new type open record head
O = 500 cycles
◐ = 2,000 cycles
● = 5,000 cycles



Magnetic Considerations

It can be shown (see appendix) that for small values of lamination thickness or cylinder diameter, the flux penetration is less in the lamination. By an extension of the idea that the flux penetration is a function of the curvature of the surface penetrated, it follows that the penetration will be even less into a concave surface than into a plane surface, and this decrease of penetration will be marked particularly when the concave surface has a small radius, such as 0.0025 inch.

These considerations make it appear that the conventional head design in which the recording wire runs at the bottom of a narrow groove is not a good design magnetically, unless the laminations are so thin that skin effect is not appreciable.

Since satisfactory operation requires a biasing magnetomotive force in the record gap having a frequency as high as 20 to 40 kilocycles, the required laminations would be around 0.005 thick if of conventional high permeability alloy, and a design that would be satisfactory from mechanical considerations becomes difficult. An alternative solution would be to use a low permeability alloy or even powdered iron. However, such a step would reduce the playback efficiency somewhat, and it is not clear that there would be any net gain, even if the bottom of the groove could be kept clean.

It is reasonably clear that the magnetic requirements for a good record head are somewhat opposed to those for a good playback head, since in the latter case skin effect in the magnetic structure is of no importance and a material of maximum permeability would be most desirable. In the record head any reduction in permeability without reducing the saturation flux density reduces the skin effect and therefore reduces saturation effects.

There is clear evidence of saturation in the record head at levels below that at which saturation occurs in the wire. This is shown by Figure 5A, which is a plot of the playback response versus record bias at several record frequencies, and on a conventional closed type head. The fact that the bias for maximum response decreases as the frequency increases is a clear indication of saturation in the record head. Without saturation in the record head all record frequencies would show maximum playback at the same value of bias.

Minimum third harmonic distortion is obtained at that bias that gives maximum low-frequency response, and in other frequency response curves given here, the bias has always been set at the lowest value consistent with maximum response at 500 cycles.

New Head Design

As a result of these considerations it seemed worth while to try a head design on the order of that shown in Figure 6.

We were forced to that conclusion while experimenting with a record head of the same general type but with a groove for the wire to run in and a closed type winding. The playback head in this experiment was the conventional type of Figure 2. The results seemed quite erratic, and in running down the cause it was found that at high frequencies the playback response was eight decibels higher when the wire was out of the groove and running across the top of the lamination than when the wire was bottomed properly in the groove. The single lamination used was about 0.060 inch thick, the groove about 0.030 deep including a shallow V at the top, and in operating on a continuous loop the wire frequently would not return to the groove after the knot went past.

It was found by using a head of the type shown in Figure 6 for record purposes, that with either an open or a closed type of winding it substantially duplicated the performance of the conventional closed type head of Figure 2 when used with stainless steel wire of moderate coercive force (around 175 oersteds) and usual retentivity. With this type of head (of Figure 6) there is virtually no difference between the performance with a closed type winding and with an open type winding. The reason for this is evidently the fact that the wire leaves the record head in a direction in which the magnetomotive force gradient is negligible so that it experiences negligible demagnetization except that which necessarily occurs immediately after passing the record gap. When used as a playback head it seems that the so-called stray field is quite negligible since the recording wire is running substantially tangent to a cylinder. See Figure 7A for playback response on closed type head for closed type and new open type record heads compared on the same loop of wire.

In recording with the same head on a wire that had a coercive force of about 250 oersteds, it was found that in the high frequency range the playback response was up to 10 decibels higher than with the head of Figure 2. In fact, it was so good that if the frequency range of interest is limited to 7,000 cycles[3] at the upper end, there is no point in doing much high frequency equalizing. Figure 7B shows the same sort of comparison as Figure 7A, but for wire having a coercive force of 250 oersteds.

It perhaps should be pointed out that this improvement in high frequency response depends on the production of a high coercive force wire. Without this there is no appreciable gain at high frequency except in reliability, and there

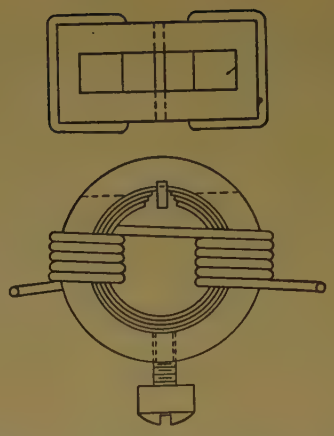


Figure 6. New design of open type head that is easily cleaned and magnetically efficient

may be a net loss of one or two decibels at frequencies on the order of 100 cycles.

The same construction is applicable to erase heads, but in this case it becomes important to use a bakelite receptacle rather than the brass ring shown. The high frequency erase current is sufficient to generate substantial heat in the brass ring.

Practical Considerations

Experience with this new type of head so far has been most instructive. When the record gap is filled with soft copper there is a pronounced tendency for metal to drag across the gap from the pole pieces, and eventually to shunt the gap. There seems also to be a tendency to undercut the copper. These two factors explain the short life occasionally experienced with the grooved type of head in which the working gap is filled with solder as a usual practice.

It would seem desirable to fill the gap with something that would wear away more slowly than the pole pieces, and hardened beryllium copper has been used for this purpose, with satisfactory results to date.

The most significant advance involved in this new type of head is that it is a very simple head to clean and keep clean. Our experience indicates that there is no way to obtain reliable performance at desirable wire speeds without virtually eliminating dirt from the record and playback heads. Eliminating dirt from the erase head is also desirable but not so critical on account of the wider gap (about 0.010 inch).

With a head design in which the operating part of the head is an element of a cylinder the possibility of level-winding across the head naturally suggests itself. This would result in playing the recording wire back and forth along the length of the working gap (the wire crosses the gap at right angles) and this would distribute the wear and at the same time help keep the working surface clean. Figure 8 shows an experimental design of such a

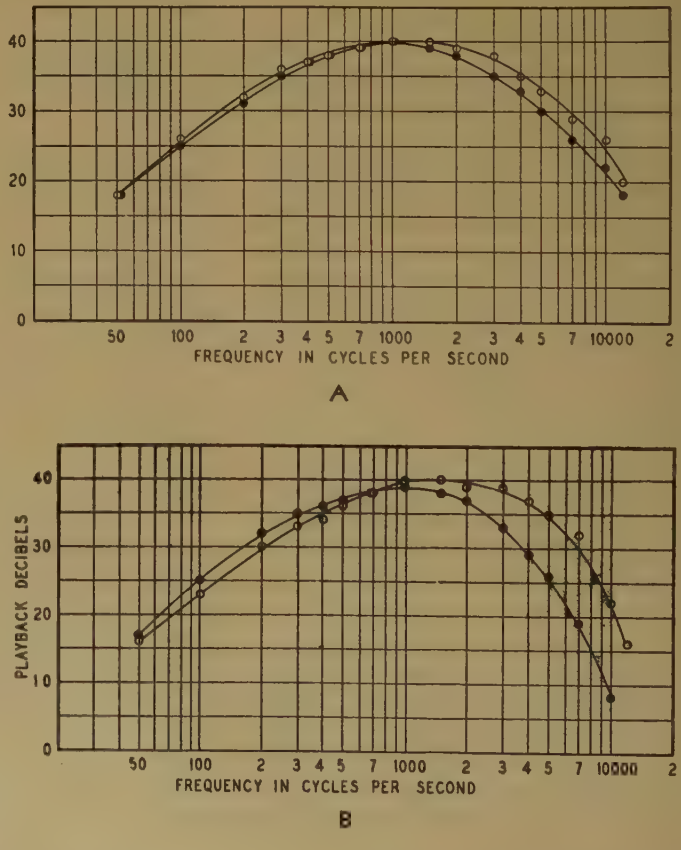


Figure 7. Comparison of closed type and new open type record heads

Playback head was closed type. Wire speed two feet per second

O—New open type head

●—Closed type head

Wire characteristics: A—H_c, 180; B_r, 5,900

Centimeter-gram-second units; B—H_c, 250; B_r, 4,650



Figure 8. Experimental model of level-wind head with open type winding

This has been modified from the design of Figure 6 by lengthening the record gap along the axis of the cylinder

head in which the wire plays back and forth one half inch as the level-wind travels in and out.

Experimental results to date on this level-wind type of head have been completely satisfactory. Response data indicate the same performance as for the head illustrated in Figure 6.

Conclusions

Certain defects of a practical nature have been found in heads of conventional design. These defects seem to be inherent in the design of these heads and the nature of the problem.

Improved designs have been tried experimentally and their performance verified as far as electromagnetic characteristics are concerned.

There has not been time enough for the experience that is required to establish their practical merit beyond any question, but the nature of the change makes their practical merit seem very likely.

On the experimental equipment shown in Figure 4, a maximum range between saturation and erase noise level of 45 decibels is obtained regularly. This corresponds to a usable dynamic range of about 40 decibels. The quality is comparable to vertically cut vinylite records.

It has been shown quite clearly that the new design reduces magnetic saturation effects at the record head. It should therefore reduce cross modulation effects.

In those cases in which the level-wind feature can be sacrificed, the possibility is presented of accomplishing tone control in a very simple manner. It would be necessary only to taper the playback gap from say 0.0015 to 0.003 inch and shift the recording wire to the wider part of the gap to eliminate the higher frequencies in the playback.

Appendix

Practical units and inch dimensions are used in the work that follows, except that ρ is given in microhms per centimeter cube corresponding to usage in tables. Let

r = radius in inches to cylindrical element of radial thickness dr or distance in inches from center plane to plane element of thickness dr

r_1 = outside radius in inches of magnetic cylinder or half thickness in inches of magnetic lamination

μ = relative permeability

f = frequency in cycles per second

ρ = resistivity in microhms per centimeter cube

B = flux density at dr in lines per square inch

B_1 = flux density at r_1 in lines per square inch

ϕ = integrated flux from unit length of periphery to center line or plane

$m = 0.505(\mu f/\rho)^{1/2}$

K = effective flux penetration in inches/$1.4(e/\mu f)^{1/2}$

$x = mr$

$y = mr\sqrt{2}$

$z = 2mr$

It can be shown that the differential equation of alternating magnetic flux distribution into a cylinder is[4]

$$\frac{d^2B}{dr^2}+\frac{1}{r}\frac{dB}{dr}-2jm^2B=0 \qquad (1)$$

if the direction of the magnetic flux is parallel to the axis of the cylinder. The same equation obtains for the penetration into a lamination of flux parallel to the lamination, except that in this case the coefficient $1/r$ of the first order term is zero.

For the solid cylinder the solution is

$$B = B_1(\text{ber } y + j \text{ bei } y)/(\text{ber } y_1 + j \text{ bei } y_1) \qquad (2)$$

For the lamination the solution is

$$B = B_1\frac{(\cosh x \cos x + j \sinh x \sin x)}{\cosh x_1 \cos x_1 + j \sinh x_1 \sin x_1} \qquad (3)$$

The corresponding equations for the integrated flux from unit length of periphery to the center line of the cylinder or to the center plane of the lamination are

$$\phi = \frac{B_1}{2m}\frac{[\sinh z_1+\sin z_1-j(\sinh z_1-\sin z_1)]}{\cosh z_1+\cos z_1} \qquad (4)$$

$$\phi = \frac{B_1}{\sqrt{2}m}\frac{[\text{ber } y_1 \text{ bei}' y_1-\text{bei } y_1 \text{ ber}' y_1-j(\text{ber } y_1 \text{ ber}' y_1+\text{bei } y_1 \text{ bei}' y_1)]}{\text{ber}^2 y_1+\text{bei}^2 y_1} \qquad (5)$$

The equation in Bessel's functions applies of course to the cylinder.

The corresponding average flux densities are

$$B_{ave} = \frac{B_1}{z_1}\frac{[\sinh z_1+\sin z_1-j(\sinh z_1-\sin z_1)]}{\cosh z_1+\cos z_1} \qquad (6)$$

$$B_{ave} = \frac{2B_1}{y_1}\frac{[\text{ber } y_1 \text{ bei}' y_1-\text{bei } y_1 \text{ ber}' y_1-j(\text{ber } y_1 \text{ ber}' y_1+\text{bei } y_1 \text{ bei}' y_1)]}{\text{ber}^2 y_1+\text{bei}^2 y_1} \qquad (7)$$

Equations 6 and 7 may be divided by B_1. Then the absolute value of the right hand sides will be the effective flux penetration as a fraction of half the lamination thickness, or as a fraction of the cylinder area which can be reduced to a radial depth.

Then the right hand side of the equation derived from equation 6 can be multiplied by r_1 to give the effective flux penetration in inches, and this may be divided by 1.4 $(\rho/\mu f)^{1/2}$ to get a factor K which gives the penetration in dimensionless terms. This value used for effective flux penetration in inches into a thick lamination, $1.4(\rho/\mu f)^{1/2}$ is equivalent to the formula for penetration in centimeters, $3.57(\rho/\mu f)^{1/2}$, given by Steinmetz.[2] The net effect of the operations described is to divide the absolute value of the term in hyperbolic and circular functions by $\sqrt{2}$.

By somewhat analogous steps the effective flux penetration into a solid cylinder may be compared to the Steinmetz formula and these comparisons are shown plotted together in Figure 9. For values of $z_1<2$ the skin effect is of little consequence, since penetration is limited by the size of the piece. For $z_1>2$ the penetration into the cylinder is substantially greater than into the lamination.

This difference is due solely to the curvature of the convex cylindrical surface and by an extension of the same idea the penetration into a concave surface would be substantially less than into the plane surface of a lamination.

This reasoning is entirely valid, but it is more satisfactory to approximate the con-

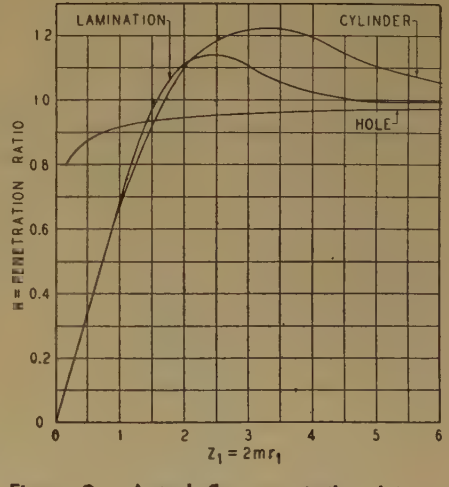


Figure 9. Actual flux penetration into a cylinder or lamination, or radially outward from a round hole in an infinite mass, divided by the Steinmetz formula value and plotted against $z_1(=2mr_1)$. Comparison is based on cylinder diameter = hole diameter = lamination thickness

Size Reduction and Rating Extension of Magnetic Air Circuit Breakers up to 500,000 Kva, 15 Kv

R. C. DICKINSON
MEMBER AIEE

RUSSELL FRINK
ASSOCIATE AIEE

AIR CIRCUIT BREAKERS rapidly are becoming the standard of the industry for voltages up to 15,000 volts and for kilovolt-ampere ratings of 50,000 to 500,000 kva. Their general desirability as compared to oil-type switchgear is now recognized by most users.

As has been previously pointed out before the Institute, the present trend of air circuit breaker development was started by the introduction in 1929 of a 500,000-kva 15,000-volt circuit breaker based on the multiple cold-cathode principle of Slepian.[1, 2] It may be noted that this rating is today, 16 years later, the highest standard rating for self-contained air circuit breakers. The original development was followed by successively producing ratings down to 100,000 kva at 2.5 and 5 kv.

Although large numbers of these multiple cold-cathode-type breakers are still giving excellent service, this principle was found to have certain limitations. Therefore, the magnetic deion principle[3] was developed, and it permitted ratings up to 250,000 kva at 5 kv.

These ratings of magnetic air breakers were smaller and simpler than the previous types of air breakers and created a demand for 7.5- and 15-kv breakers of more compact construction.

The next step in the development of the magnetic air breaker, however, was not a rush to enlarge the interrupters to cover the 7.5- and 15-kv ratings, since these were already covered by other forms of self-contained air breakers. It was instead an earnest attempt through research and development to improve further the interrupting principles so that a breaker of more compact construction and improved characteristics could be offered. These aims have now been fulfilled, and the magnetic air breakers are now available in all ratings up to 15 kv 500,000 kva. The 15-kv 500,000-kva unit, while containing the fundamental features of the original magnetic air breaker as presented to the Institute by Ludwig, Grissinger, and Nau in 1939,[3, 4] has been developed and refined until the interrupting capacity available in a given space has been more than tripled.

Paper 46-55, recommended by the AIEE committee on protective devices for presentation at the AIEE winter convention, New York, N. Y., January 21–25, 1946. Manuscript submitted November 23, 1945; made available for printing December 19, 1945.

R. C. Dickinson is section engineer, air circuit breaker section, and Russell Frink is a member of the protective devices engineering department, Westinghouse Electric Corporation, East Pittsburgh, Pa.

The New Interrupter

It is reasonable to say that if a certain arc chute will interrupt a given voltage, then by doubling the length it will interrupt twice as much voltage. This is generally true on account of momentary current leakage following current zero, giving the effect of a potential divider to equalize voltage over the length of the arc chute. However, consideration shows that increased voltage rating obtained in this way is not economical in floor space. To keep the space requirement within desirable limits, the desirable course of action was to increase the interrupting capacity within a given space.

It was believed that by making a systematic study of all the known factors influencing arc interruption in air, each factor could be emphasized and co-ordinated into an optimum over-all design for a given rating.

From previous experience with the magnetic construction, it was decided that the general idea of multiple arc-resisting plates having V-shaped or tapered slots into which the arc is moved showed the greatest promise of success. The plate type of construction, in general, permits practical manufacture with high grade refractory ceramic material. As is well known, materials of this general class are

---

dition at the bottom of the groove by studying the radially outward penetration of magnetic flux from a hole in an infinite mass. It is assumed that a helical magnetizing coil extends through the hole. The solution of equation 1 is then

$$B = B_1(\ker y + j \operatorname{kei} y)/(\ker y_1 + j \operatorname{kei} y_1) \quad (8)$$

Since[6]

$$\int_0^y y \ker y\, dy = y \operatorname{kei}' y \quad \text{and}$$

$$\int_0^y y \operatorname{kei} y\, dy = -y \ker' y$$

$$\phi = B_1(-\operatorname{kei}' y_1 + j \ker' y_1)/\sqrt{2}m \times (\ker y_1 + j \operatorname{kei} y_1) \quad (9)$$

If we take the absolute values

$$\phi = \frac{B_1}{\sqrt{2}m}\sqrt{\frac{\operatorname{kei}'^2 y_1 + \ker'^2 y_1}{\ker^2 y_1 + \operatorname{kei}^2 y_1}} = \frac{B_1}{\sqrt{2}m} Q \quad (10)$$

If p = depth of penetration in inches, the integrated flux $2\pi r_1\phi$ can be expressed in terms of p and r_1, or in terms of Q and m, so that

$$[(r_1+p)^2 - r_1^2]\pi B_1 = 2\pi r_1 B_1 Q/\sqrt{2}m \quad (11)$$

$$p = r_1(-1 \mp \sqrt{1+2Q/y_1}) \quad (12)$$

Let p_s = flux penetration in inches according to Steinmetz formula $= 1/\sqrt{2}m$; then

$$K = p/p_s = y_1(-1 \mp \sqrt{1+2Q/y_1}) \quad (13)$$

The values of K from this equation have been added to Figure 9 to complete the comparison. Values of the ker and kei functions and their first derivatives have been taken from Savidge's[7] table, which seems to be about the only one in existence. The tabular interval of 0.1 makes possible reasonably precise detail for values of y_1 greater than 0.1, corresponding to z_1 greater than 0.14.

It should be understood, of course, that for large values of mr_1, the actual flux penetration in any case approaches that stated by the Steinmetz formula.

References

1. Supersonic Bias for Magnetic Recording, Holmes, Clark. *Electronics*, July 1945, pages 126–136.

2. Transient Electric Phenomena (book), C. P. Steinmetz. McGraw-Hill Book Company, New York, N. Y. Page 371.

3. Tonal Range and Sound-Intensity Preferences of Broadcast Listeners, Chinn, Eisenberg. IRE *Proceedings*, September 1945, pages 571–81.

4. Calculations for Coreless Induction Furnace, Dwight, Bagai. AIEE Transactions, 1935, pages 312–15.

5. United States patents 2,351,003, 2,351,004, 2,351,006, 2,351,007, Marvin Camras and others.

6. Treatise on Bessel Functions (second edition), Gray, Mathews. Macmillan and Company, New York, N. Y. Page 27.

7. Tables of ker, kei, ker′, kei′, H. G. Savidge. British Association Report, 1915. Pages 36–38.

non-gas forming and are chemically stable even when exposed to arc temperatures. They do not take on appreciable moisture from the atmosphere and are high in dielectric strength. By proper choice of composition, high resistance to thermal shock also can be obtained.

The theory of magnetic deionization has been described before the Institute.[4] Briefly, it consists of moving the arc toward the closed tops of slots in insulating arc-resisting plates. At this position the presence of a strong magnetic field imparts to the electrons an upward velocity. They in turn bombard gas particles and produce an actual blast of gas perpendicular to the arc, which action requires the arc continually to ionize fresh gas in considerable quantities. When current zero is reached, this action continues in a sufficient degree effectively to deionize the plurality of short lengths of arc near the edges of the slots.

This theory would indicate that increased interrupting capacity can be obtained by increased strength of the magnetic field. While this is a factor, it was found that blindly increasing the field strength might be detrimental rather than helpful. Slot shape, plate spacing, and magnetic field strength are interdependent and must be co-ordinated for optimum results. The design of the interrupting unit is most easily approached by blending the proper plate structure with a strong magnetic field.

The theory of magnetic deionization points out that interruption depends upon the rate of deionization at the instant of current zero. If some way could be found to control the field so that it would have appreciable strength at current zero, the interrupting capacity apparently should be increased. In other words, if the field flux was made to lag behind the arc current, it would have some magnitude at arc current zero. On the other hand, an in-phase flux is zero when the arc current is zero and positive driving forces are, therefore, momentarily absent. Tests proved that if the field flux lagged the arc current by the proper phase angle, the voltage limit of a well-designed interrupter was increased considerably.

A phase shift between the magnet flux and arc current may be accomplished by shunting the magnet coil with a resistor. It was not possible to predict mathematically the advantage to be gained by a particular phase shift. Therefore, it was necessary to make numerous tests to find the best value. However, the resistor seemed to be an undesirable appendage, and theory indicated that the same result could be accomplished with a shading coil. Such a coil was calculated to supply the same effect as the previously determined best value of resistance, and confirming tests demonstrated that this shading coil gave a correct phase shift. In the final design, the shading coil consists of a single turn around the magnet yoke adjacent to the magnet coil so that in operation it encloses the total flux.

Slot shape and plate spacing also are important factors in the performance of the interrupter, inasmuch as they control the motion of the arc through fluid friction and restriction. Mathematical analysis is helpful in determining the designs, but it is necessary to rely on empirical data on account of unpredictable factors such as gas temperatures, velocities, etc.

The fundamental theory of the magnetic Deion breaker states that interruption is accomplished by the blast of gas perpendicular to an arc held stationary at the ends of slots. This blast deionizes the arc and establishes dielectric strength. In the development of the new interrupter, it was determined that advantage could be taken of the better field and its phase relationship by elongating the arc exposed to this blast. Therefore, the full value of these factors was utilized by offsetting the ends of the slots in the plates.

Referring to Figure 1, one terminal of the magnet coil is connected to the upper stud. The other terminal is connected to the panel-end horn. The coil is introduced into the circuit by the impingement of the arc on the panel-end horn and the interruption of the short length of arc between the horn and the upper stud. The extra field strength which has been introduced to produce a more efficient interrupter gives rise to a new problem. All the flux across the interrupting space must thread the magnet coil. This means that when short-circuit current is introduced into the coil, a reactance voltage of several hundred volts appears across the terminals of the coil. To introduce the short-circuit current into the coil quickly and positively against this reactance voltage requires that an auxiliary or transfer interrupter be built into the arc chute. This interrupter, although very compact, must perform a duty comparable to that of a high-capacity low-voltage breaker.

Figure 1 is an illustration of an arc chute for a 15-kv 500,000-kva circuit breaker based on the above considerations. The magnetic structure for this unit consists of one coil and one magnet. With this type of construction, the magnet shoes form a support for the arc chute which makes possible the quick and easy removal of the relatively light arc chute for inspection while the heavy magnet remains on the breaker. However, more important is the simplification of insulation problems and the energizing of the field simultaneously over the entire interrupting structure so as to obtain fast uniform arc motion.

The contacts are of conventional design. In an opening operation, the current is transferred from the main current-carrying contacts to secondary contacts and then to the arcing contacts, which are protected by inlays of silver-tungsten alloy. When the arcing contacts part, the current loop in the contact structure causes the arc to expand into the arcing chamber. Suitably placed iron draws the arc into the transfer stack, which interrupts the section of arc between the stationary arcing contact and the panel-end arc horn. The current path is now from the top bushing stud through the magnet coil, into the adjacent arc horn, through the arc in the main interrupting stack, and into the opposite arc horn which is connected to the opposite side of the cir-

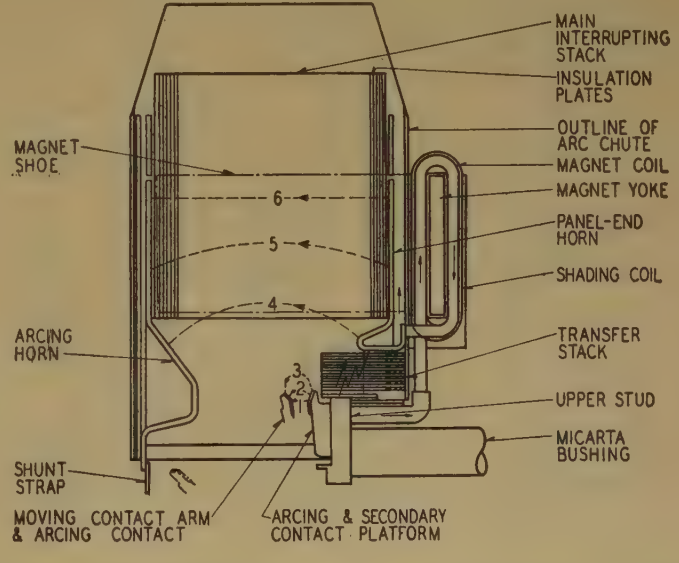


Figure 1. Schematic illustration of a 500,000 kva 15-kv magnetic interrupter

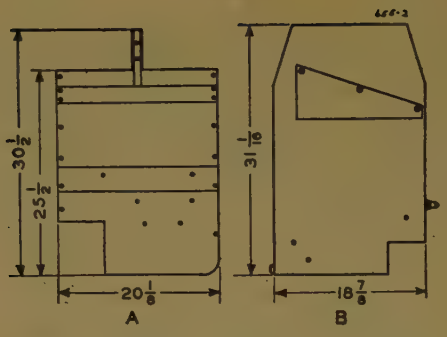


Figure 2. Progress in magnetic interrupter design

A—A 100,000-kva 5-kv arc chute of early design
B—The new 500,000-kva 15-kv arc chute
Both have ceramic interrupting plates of the same width

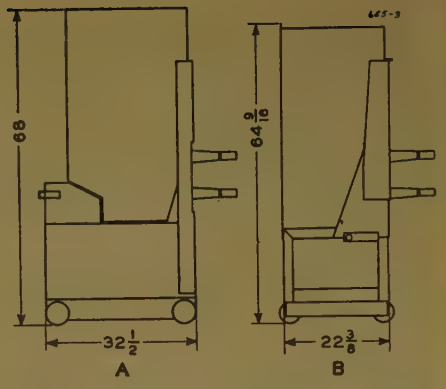


Figure 3. Progress in magnetic air breaker design

A—An early 5-kv 150,000-kva unit
B—The current design
Note smaller depthwise dimensions of the later design. Both units are for 26-inch metal-clad cell width



Figure 5. General view of the new 15-kv 500,000-kva magnetic air breaker for metal-clad horizontal drawout switchgear

cuit. The field is now energized, and interruption takes place at the next current zero.

The proper amount of phase shift between the current and the field is obtained by using a carefully designed shading coil placed around the magnet core adjacent to the coil. This shading coil also eases the duty on the transfer stack by slowing the rate of rise of restored voltage across it when the transfer arc is extinguished.

Figures 2, 3, and 4 illustrate some of the results accomplished by this development. Figure 2 is an outline comparing the 5-kv 100,000-kva arc chute of an earlier design with the new 15-kv 500,000-kva arc chute. Both use ceramic plates of the same width. Figure 3A shows the outline dimensions of the original magnetic air breaker for 5 kv and 150,000 kva, while 3B shows the current design for the same rating, which is also applicable at 2,300 volts. It will be noted that the later design saves considerable depth of floor space. Figures 4A, B, and C show the relative size of the original 5-kv 150,000-kva rating, the 7.5-kv 250,000-kva rating, and the latest developed design, the 15-kv 500,000-kva rating.

Figure 5 shows a general view of a new 15-kv breaker. In line with the present general trend, this unit is designed particularly for metal-clad switchgear and as shown constitutes the complete removable element. In this view it will be noted that the horizontal drawout construction results in an inherently transportable removable unit with self-contained secondary and ground contacts. This permits quick movement to the test position and quick reconnection of control circuits for testing within the cell. It also permits quick interchange of breakers in a cell. The location of the main barrier, arc chute, and contacts also permits easy removal and inspection of those parts.

The arc chute is placed above the contacts, which is the most natural position for it because this position permits the arc to be drawn horizontally and moved vertically upward. With this construction, thermal convection assists in moving low current arcs into the interrupters. An auxiliary air piston may be added to speed up interruption of low currents, but the breaker can interrupt them without its help.

The component parts of the breaker are arranged so that the arc chute compartment can be vented directly to the outside atmosphere, thus completely isolating this compartment from the bus structure. The 19-inch-long arc chute for a 15-kv 500,000-kva breaker is admirably suited for this drawout construction and adds further to its inherent advantages in the economy of floor space required.

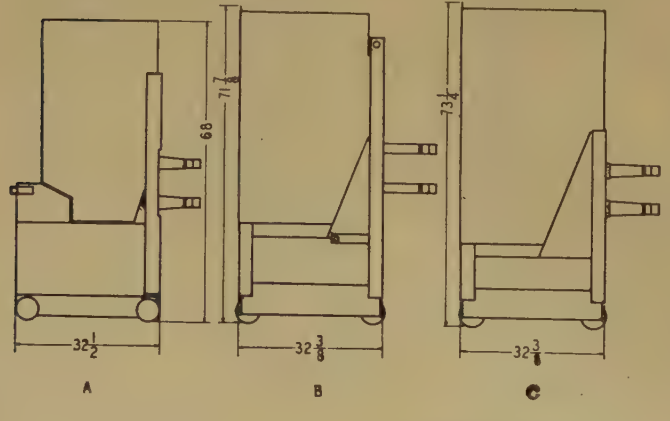


Figure 4. Progress to 15-kv magnetic air breaker

A—The 5-kv 150,000-kva breaker of early design
B—A 7.5-kv 250,000-kva breaker
C—The new 15-kv 500,000-kva magnetic breaker

Tests on the Breakers

In line with present practice, it is almost needless to say that many full power interrupting tests were made in developing the new ratings. These tests again have demonstrated the ability of the ceramic arc chute to withstand repeated interruptions with low deterioration.

The breaker was connected across the terminals of a 60,000-kva star-connected high power laboratory generator, and the short circuit was formed by a copper bar bolted across the load side of the breaker. The generator neutral was grounded through a 7-ohm resistance, while the short-circuiting bar was ungrounded, which is equivalent to a grounded fault on an ungrounded system. Currents were limited by air core reactors.

Typical oscillograms are shown in Figures 6 to 9. Figure 6 shows a 3-phase interruption at 505,000 kva and 13.2 kv. Figure 7 shows an interruption at 163,000 kva and 13.2 kv. Figure 8 is of interest in that it shows a single phase interrup-

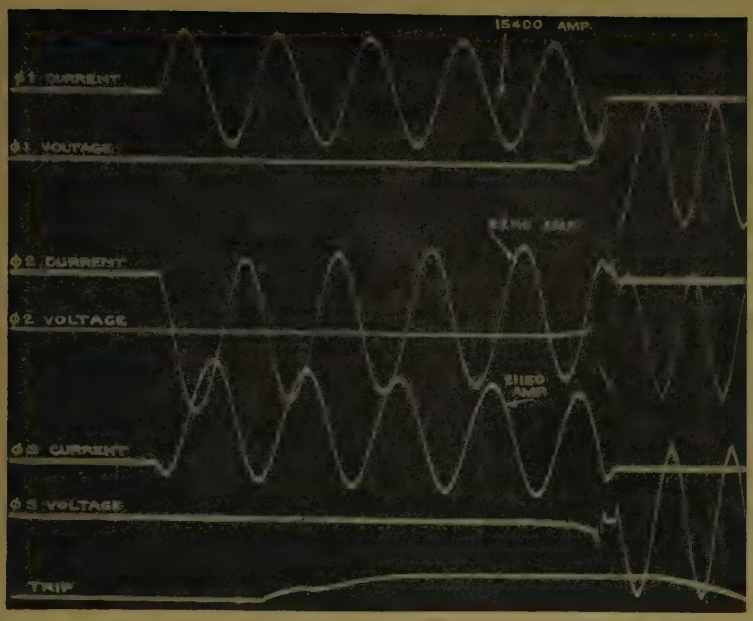


Figure 6. Oscillogram of 3-phase ungrounded short-circuit interrupting test on 15-kv 500,000-kva magnetic air breaker shown in Figure 5

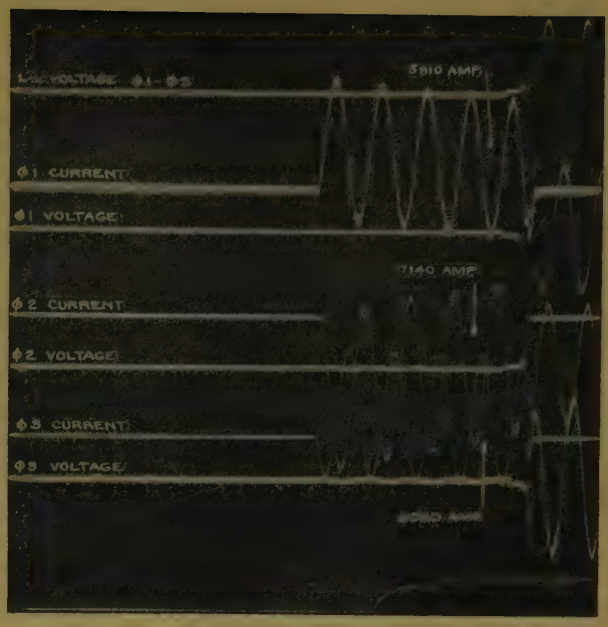


Figure 7. Oscillogram of 3-phase ungrounded fault at 163,000 kva on the 500,000-kva breaker

tion of 7,300 amperes at 13.2 kv across a single pole.

Figure 9 illustrates, by single phase oscillograms, an interesting characteristic of the new types of magnetic interrupters. On all tests except those at very low currents, when the field is energized 30 degrees or more ahead of a current zero, the breaker will interrupt on that zero. On the other hand, the current is not likely to transfer to the coil on the rising part of the current wave, and the arc will remain in the comparatively wide arc box at low arc voltage until the current has gone through its peak value. Coil transfer is then completed, and the strong field drives the arc up to the ends of the slots at extremely high velocity. At the ends of the slots, deionization and interruption is accomplished. As shown in Figure 9A, this type of interruption, with high arc energy released during only a small portion of the half cycle, is characteristic of an interrupter of this type. This produces a minimum of heating and deterioration in the arc chute. As shown in Figure 9B, another type of interruption is possible, and that is where the field is energized fewer than 30 degrees before current zero. On a probability basis, this type of interruption should occur in one out of six interruptions. Insufficient time is available to drive the arc to the top of the slots before current zero, and the arc must remain there for another half cycle. However, the high degree of restriction and the loss of ions from the arc stream on account of the field keep the arc resistance so high that the current reaches only a small magnitude. The arc energy released is not much greater than in the previously described type of interruption. Throughout all the tests made in this development, it was impossible to find any difference in interrupting capacity between the two types of interruptions.



Figure 8. Oscillogram of single-phase interruption at 13.2-kv on single pole of the 15-kv magnetic breaker



Figure 9. Oscillograms illustrating two types of interruption on the new magnetic breaker for 15 kv (see text)

The tests described and the oscillograms shown apply to the 500,000-kva 15-kv breaker. The same principle of interruption has been applied to breakers of other ratings, namely, 150,000 kva and 250,000 kva at 15 kv, and similar test results have been obtained. The same principle of interruption has been found to work equally as well on the currents encountered at 7,500 volts, including 500,000 kva at 6,600 volts and 25 cycles.

Conclusion

The principle of magnetic deionization has been extended to air circuit breakers of the 15-kv class with interrupting ratings up to 500,000 kva. The interrupter has been so refined and improved that the increase in kilovolt-amperes rating of up to 500 per cent has not resulted in undue increase in space requirements. The short arc chute, 19 inches long for a 500,000 kva 15 kv unit, has made possible compact horizontal drawout construction with all its inherent advantages.

References

1. Extinction of an A-C Arc, J. Slepian. AIEE Transactions, volume 47, 1928, pages 1398–1408.

2. Theory of the Deion Circuit-Breaker, J. Slepian. AIEE Transactions, volume 48, 1929, pages 523–527.

3. A New High-Capacity Air Breaker, L. R. Ludwig, G. G. Grissinger. AIEE Transactions, volume 58, 1939, August section, pages 414–20.

4. Magnetic "De-ion" Air Breaker for 2,500–5,000 Volts, L. R. Ludwig, R. H. Nau. AIEE Transactions, volume 59, 1940, September section, pages 518–22.

A New Line of High-Voltage Outdoor Tank-Type Oil Circuit Breakers

W. F. SKEATS
FELLOW AIEE

E. B. RIETZ
ASSOCIATE AIEE

THE TREND of the past few years and studies of future trends indicate an oncoming demand for higher interrupting capacities and decreased interrupting and reclosing times. Today there may be relatively few applications which justify these more severe requirements, but there is every indication that as time passes they will become more and more universal.

A year ago there was described before the Institute[1] a development in tank-type breakers which made possible interruption of short-circuits up to 3,500 megavolt-amperes within three cycles in the voltage range from 115 kv to 161 kv with 20-cycle reclosing. Field tests were also reported[2] substantiating this performance. The present paper describes further developments in these breakers, resulting in reduced over-all dimensions and increased convenience in handling, while maintaining or improving the desirable performance characteristics. These characteristics have also been realized in an interrupter and breaker suitable for operation at 230 kv.

Figure 1 shows the 138-kv breaker.

From both structural and functional standpoints, a discussion of these breakers divides itself naturally into four major parts:

1. The interrupter.
2. The bushing.
3. The tank and top frame.
4. The operating mechanism.

In order to meet the exacting performance requirements of high interrupting capacity, fast interruption, and rapid reclosure, and at the same time to reduce maintenance to a minimum and readily make accessible those parts which require inspection and maintenance, each one of these parts must receive careful attention from the designer. This development has involved significant improvements in all of them. These changes will be discussed under the four corresponding headings.

Paper 46-20, recommended by the AIEE committee on protective devices for presentation at the AIEE winter convention, New York, N. Y., January 21–25, 1946. Manuscript submitted November 26, 1945; made available for printing December 21, 1945.

W. F. Skeats and E. B. Rietz are with the power circuit breaker division, General Electric Company, Philadelphia, Pa.

The authors wish to express their indebtedness to many of their associates who materially assisted in the development of these breakers. In particular, T. R. Coggeshall and J. M. Milne have contributed ideas for the solution of the many problems involved and have been untiring in following the innumerable details which are an indispensable part of such a program.

The Interrupter

As the interrupter is the part primarily responsible for the performance of the distinctive function of the circuit breaker, it is natural that this should receive first consideration.

A cross-sectional view of the interrupter of the earlier breaker is shown in Figure 2, and a similar view of the new interrupter is shown in Figure 3. Figure 4 shows the new interrupter with separate views of the moving system and the resistor. Figure 5 shows two interrupters mounted on bushings with blade, lift rod, and guide in place as when assembled in the tank.

The same general principle of interruption is used in both designs. Interruption is performed by a number of 2-break units, each of which consists of one break whose primary purpose is to generate pressure and a second break so located that the arc drawn there is placed in the path of a blast of oil forced out through properly located ports by the pressure generated by the first arc. For application at voltages from 115 kv to 161 kv, two such units are used in each interrupter. Thus, starting at the lower end, current enters the interrupter on the lower stationary contact, passes through the elkonite contact tips to the bridging contact, and flows from the other end of the bridging contact to the lower end of the intermediate stationary contact. This cycle is repeated in passing from the upper end of the intermediate stationary contact to the upper stationary contact. This path includes four breaks, of which those at the lower stationary contact and the upper end of the intermediate contact are located away from ports and serve principally the function of pressure generation. The other two breaks are immediately adjacent to ports, and the arc there is interrupted by the blast of oil flowing out through the ports.

An appreciable reduction in the arcing time of the new interrupter has been achieved by strengthening the opening springs on the interrupter to increase the speed of its moving parts. The tendency to increased pressure associated with this change in speed was more than counterbalanced by lengthening the arcing plates and by using the pressure control ports shown in Figure 3.

The arcing plates function by shortening the pressure generating arc.

The pressure control ports are located near the pressure-generating arc, but far enough away to be reached by the gas bubble only when interrupting high currents. Their use was suggested by the observation that in operations in which a gas bubble might be expected to be present in the interrupter, as in the second interruption of a reclosing operation, the pressures experienced were found to be much lower than when such a bubble was not present. Thus it appeared desirable to provide the cushioning effect of such a bubble for all conditions, and as the high pressures appeared only towards the end of the arcing period, the most convenient way to accomplish this was to allow the lighter pressure in the early part of the arcing period to force oil out through these ports and thus create additional expansion space for the bubbles already present at the contacts.

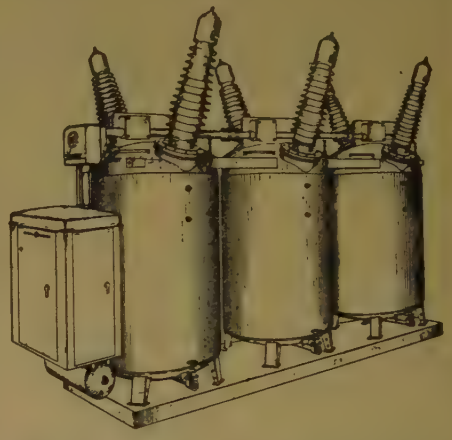


Figure 1. The new 138-kv oil-blast circuit breaker, 3,500-megavolt-ampere interrupting rating, 3-cycle interrupting time rating and 20-cycle reclosing time rating

The effectiveness of this combination in achieving both short arc lengths and low pressures is evident from Figures 6 and 7, in which arc duration and interrupter pressure, respectively, are plotted against current interrupted for both the

new and the superseded interrupter. It will be noted readily that the circled points, representing the new interrupter, show a substantial improvement in both respects, with satisfactory performance at currents well beyond that corresponding to the 3,500-megavolt-ampere standard rating.

The simplification of the present design is obvious from a comparison of Figures 2 and 3. The principal changes are as follows:

1. The ends of the interrupters are secured to the cylindrical herkolite walls by means of metal studs. This has been found to be quite as strong as the earlier construction and results in a very appreciable reduction in the diameter of conducting material. There is also a substantial reduction in weight, which is accentuated by the use of a light alloy for the end pieces.

2. The moving contact assembly has been simplified greatly by placing all of the contact springing immediately below the bridging contacts themselves, thus eliminating the necessity for any additional cushioning springs at the bottom of the interrupter. This has made possible the use of a simple textolite cylinder, which makes an excellent guide bearing, at the point where the moving part passes through the bottom plate of the interrupter. A strong opening spring and a buffer spring are placed around this cylinder, the one insuring that the moving parts of the interrupter move with the breaker crosshead to the limit of the interrupter stroke and the other controlling overtravel of the contacts on the closing stroke.

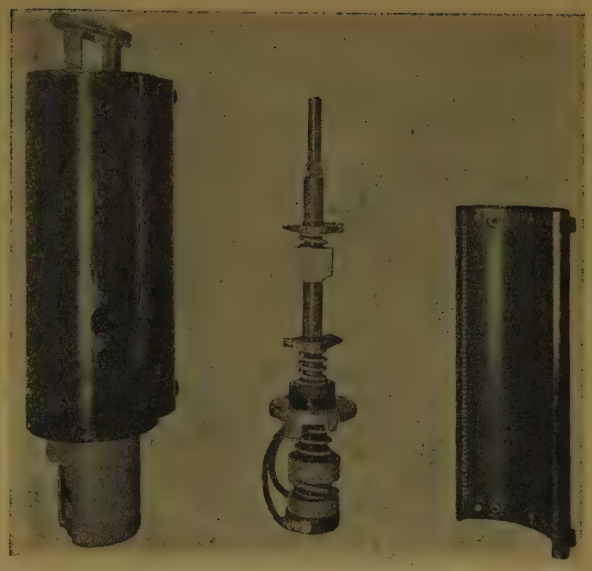


Figure 4. The 115-kv–161-kv interrupter with additional views of the moving part assembly and the resistor

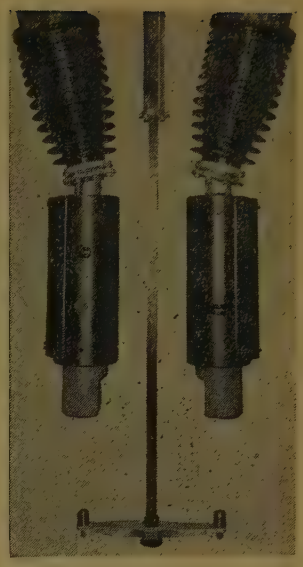


Figure 5. Pole unit assembly of interrupters for the 138-kv breaker

3. Both the new and the superseded interrupter use a parallel resistor for positive control of overvoltages in connection with the interruption of line-charging currents.[3] The new resistor is shown at the right-hand side of Figure 4. It consists of a helix of nichrome wire which is wound on a grooved board that has its short dimension molded into the shape of a circle arc. Protective covers are secured to the board. The resulting assembly conforms to the outside of the interrupting cylinder and thus requires less space than the older resistor.

4. Additional items that will be helpful in facilitating inspection and maintenance are the smaller electrostatic shield at the bottom of the interrupter and the elimination of the upper insulating shield, both made possible by removal of the clamping metal outside the interrupting cylinder.

The interrupter of Figures 3 and 4 is used at voltages from 115 kv to 161 kv. For application at 230 kv, the interrupter shown in Figure 8 is used. This is quite similar in principle to the lower-voltage interrupter but has three pairs of internal

Figure 2. Cutaway view of 115-kv–161-kv interrupter of the superseded design

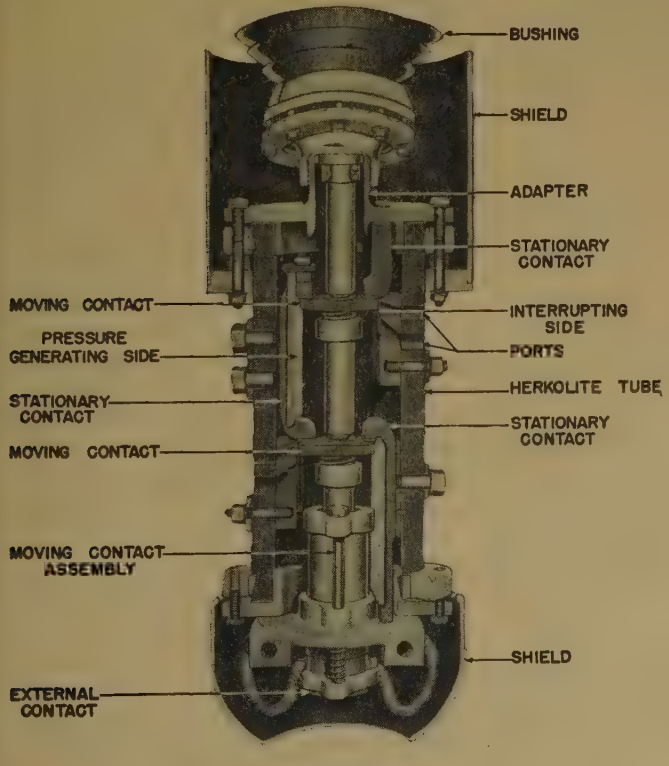
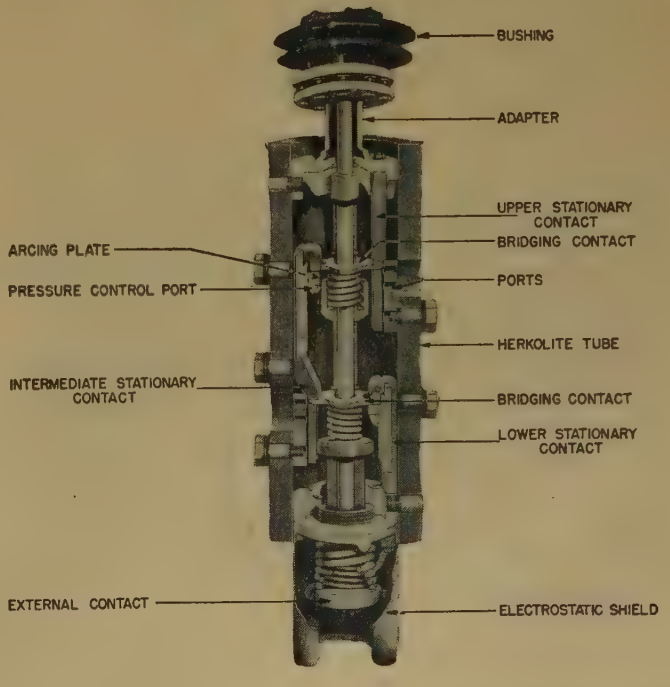


Figure 3. Cutaway view of 115-kv–161-kv interrupter of the new design



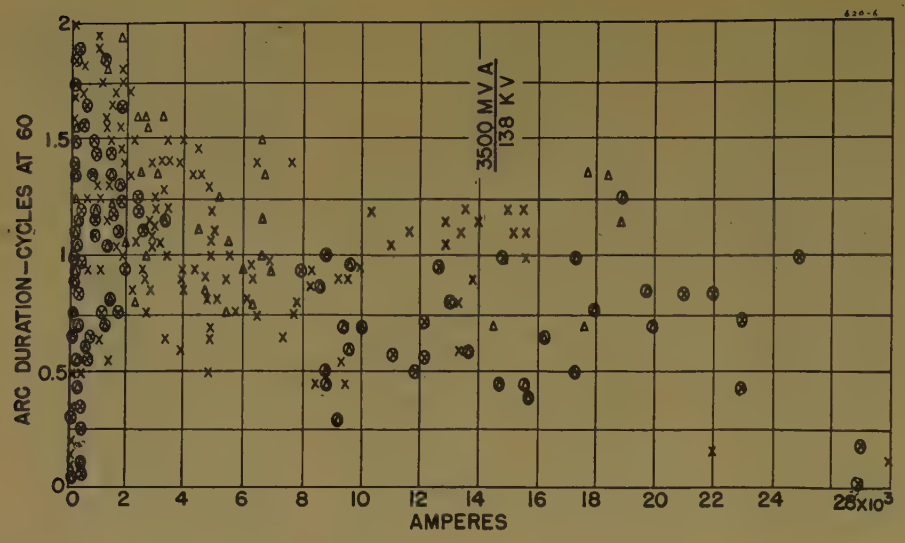


Figure 6. Arc duration as a function of current for 115-kv–161-kv interrupters

×—Superseded interrupter, initial opening operation

△—Superseded interrupter, second opening operation on reclosing duty cycle

The same symbols enclosed in circles represent the new interrupter under the same conditions

Tests made on a pole unit at voltages from 14.5 kv to 132 kv



Figure 8. The 230-kv interrupter

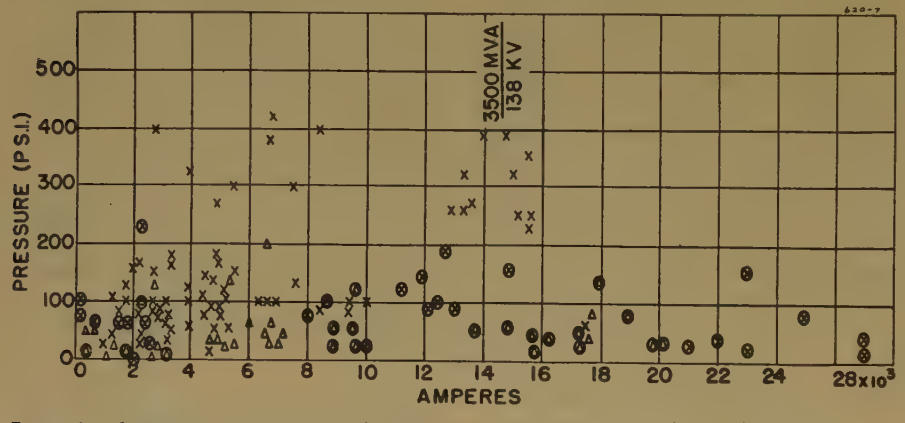


Figure 7. Interrupter pressure as a function of current for 115-kv–161-kv interrupters

×—Superseded interrupter, initial opening operation

△—Superseded interrupter, second opening operation on reclosing duty cycle

The same symbols enclosed in circles represent the new interrupter under the same conditions

Tests made on pole unit at voltages from 14.5 kv to 132 kv

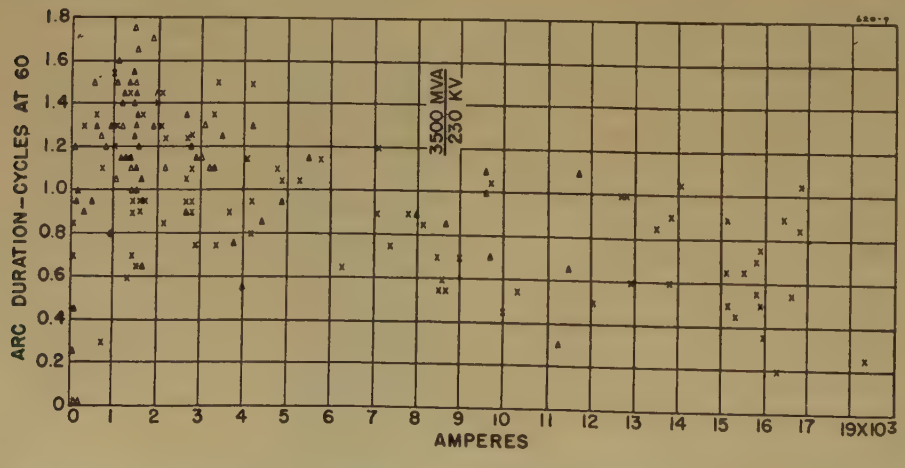


Figure 9. Arc duration as a function of current for the 230-kv interrupter

×—Initial opening operation

△—Second opening operation on reclosing duty cycle

Tests made at voltages of from 8.4 kv per interrupter to 132 kv per interrupter

breaks instead of two. Also, the resistor has somewhat more thermal capacity as required at the higher voltage. The interrupting performance of this interrupter is shown in Figure 9. It will be noted that the arcing time varies from less than 1/2 cycle to $1^1/_2$ cycles at currents above 25 per cent of rating. With a contact-parting time of $1^1/_2$ cycles, this gives a breaker-interrupting time of from two to three cycles, or with the conventional tripping arrangement, a 5-cycle interrupting time is easily realized.

The interrupting performance on line-charging currents is indicated in Table I for the 115-kv–161-kv interrupter and in Table II for the 230-kv interrupter. In each case the tests were made on a single interrupter or half a pole unit, using static capacitors. Since the resistors effectively divide the voltage between the two interrupters of a pole unit, the normal voltage for such a test is half leg voltage or 46 kv for 161-kv application and 66 kv for 230-kv application. In both cases, tests were made at approximately these voltages and also at a voltage from 20 per cent to 33 per cent higher to insure adequate margin to take care of surges introduced by any mutual effect between phases. Performance was entirely satisfactory in all tests, the voltage being limited to twice the crest value before interruption. An oscillogram of one of these tests is shown in Figure 10.

A comment is in order with respect to short-circuit interrupting tests. Under uncontrolled conditions of interruption,

there are two elements subject to rather wide variation. These are:

1. The point on the voltage wave at which the short circuit is initiated.

2. The point on the current wave at which the breaker is tripped.

With the reduction in arcing time that has taken place in recent years, the influence of these variations becomes accentuated to the point where they may be responsible for the difference between four-tenths of a cycle and a complete cycle in arc duration, with a very pronounced difference in interrupter pressure, jar, contact burning, and any other manifestation of severity of duty. To be sure of covering the worst conditions at any voltage and reactance tap, therefore, either a large number of tests must be taken or some control must be exercised over the timing. For over ten years now, the authors and their associates have made extensive use of a special fast-closing breaker with synchronous control to make possible the selection of the point on the voltage wave at which the circuit is closed, and more recently the same type of control has been applied to the tripping of the test breaker. Thus it is now possible to control both the displacement of the short-circuit current wave and the point on the wave at which the contacts separate. It has been the practice first to make exploratory tests over the complete range of variation of these controls and then to concentrate for a number of tests on that condition which appears to be worst. Thus any other random phenomena will have an opportunity to show up at their worst also, and in a reasonably small number of laboratory tests, conditions may be explored which would not appear in many times the corresponding number of field operations or uncontrolled laboratory tests.

Table I. Performance of 115–161-Kv Interrupter on Line-Charging Currents
Tests on One Interrupter

Test No.	Voltage, Kv	Equivalent Miles of Line	Current, Amperes	Arc Duration, Cycles
1	44	190	110	0.3
2	44	190	110	0.3
3	44	190	110	0.0
4	44	190	110	0.1
5	44	190	110	0.1
6	55	190	140	0.1
7	55	190	140	1.6
8	55	190	140	1.6
9	55	190	140	0.0
10	55	190	140	1.4

Table II. Performance of 230-Kv Interrupter on Line-Charging Currents
Tests on One Interrupter

Test No.	Voltage, Kv	Equivalent Miles of Line	Current, Amperes	Arc Duration, Cycles
1	66	190	140	0.7
2	66	190	140	0.2
3	66	190	140	0.7
4	66	190	140	1.0
5	66	190	140	0.9
6	88	110	110	0.9
7	88	110	110	1.2
8	88	110	110	1.1
9	88	110	110	0.9
10	88	110	110	0.6

Bushings

Oil filled bushings for high-voltage oil circuit breakers have an enviable record of performance. While the electrical and mechanical performance of these bushings has been generally satisfactory, numerous improvements have been made for the purpose of reducing maintenance. The sump washer-drain, bell-mouthed breather, amber gauge glass, and thermal seal are the most noteworthy. In recent years it has become obvious that the next step is complete sealing of the bushing against the atmosphere so as to eliminate completely any source of contamination of the filler oil. Numerous designs of sealed bushings have been developed, with the moderate voltage type *L* bushing as one of the first. The experience with over 80,000 of these bushings and varied special applications of sealed oil-filled bushings gave the proper background for developing the completely sealed bushings for the 115–161-kv ratings.

The completely sealed bushing, Figures 11 and 12, uses a general arrangement of insulation similar to that of the original oil-filled bushings, although a number of structural improvements were found desirable. The insulated conductor is surrounded by concentric insulating cylinders of treated paper of high dielectric strength spaced apart so as to give alternate layers of solid insulation and oil. These cylinders are between the live conductor and the grounded support sleeve. Electrostatic shielding is incorporated internally in these cylinders by coating a part of the paper with conducting resin as it is wound. This imbedding of the conducting shield within the cylinder is a distinct improvement over the older method of winding conducting foil on the outside of the cylinders.

Center clamping is used to clamp the bushing parts firmly together. This makes use of the center conductor as a means of clamping the lower porcelain, ground sleeve, upper porcelain, and expansion chamber into an integral unit. Adequate clamping pressure is maintained on the four gasketed joints even with slight differences caused by thermal expansion, by means of short heavy compression springs between the terminal cap fastened to the conductor and the top of the expansion chamber.

Synthetic rubber gaskets impervious to both oil and water are used at all joints. These are confined in appropriate recesses in the metal parts.

Standard circuit breaker or transformer oil is used as a filling liquid. Expansion space for this medium is present in the metal expansion chamber at the top of the bushing. The oil level is registered by a magnetic-type oil gauge incorporated in the expansion chamber and easily visible from the ground, as shown in Figure 13.

The use of center clamping results in a reduction in diameter dimensions because of the omission of the cemented-on clamping rings. This is particularly advantageous at the lower end because it permits smaller current transformers and sim-

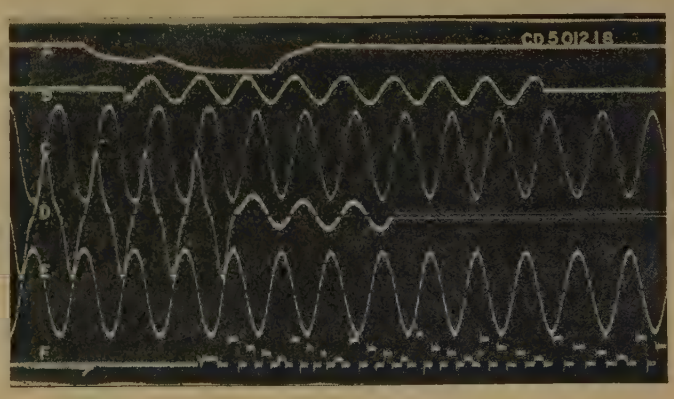


Figure 10. Oscillogram of line-charging current interruption on 115-kv–161-kv interrupter, interrupting 140 amperes at 55 kv across a single interrupter

A—Trip coil current
B—Cathode ray oscillograph control
C—Supply voltage at breaker
D—Current through breaker, showing initial capacitance current, resistor current, and final interruption
E—Alternator voltage
F—Breaker travel: one-half inch per impulse



Figure 11. 115-kv sealed oil-filled circuit breaker bushing with capacitance tap having smaller dimensions resulting from center clamping and removal of cemented-on clamping rings

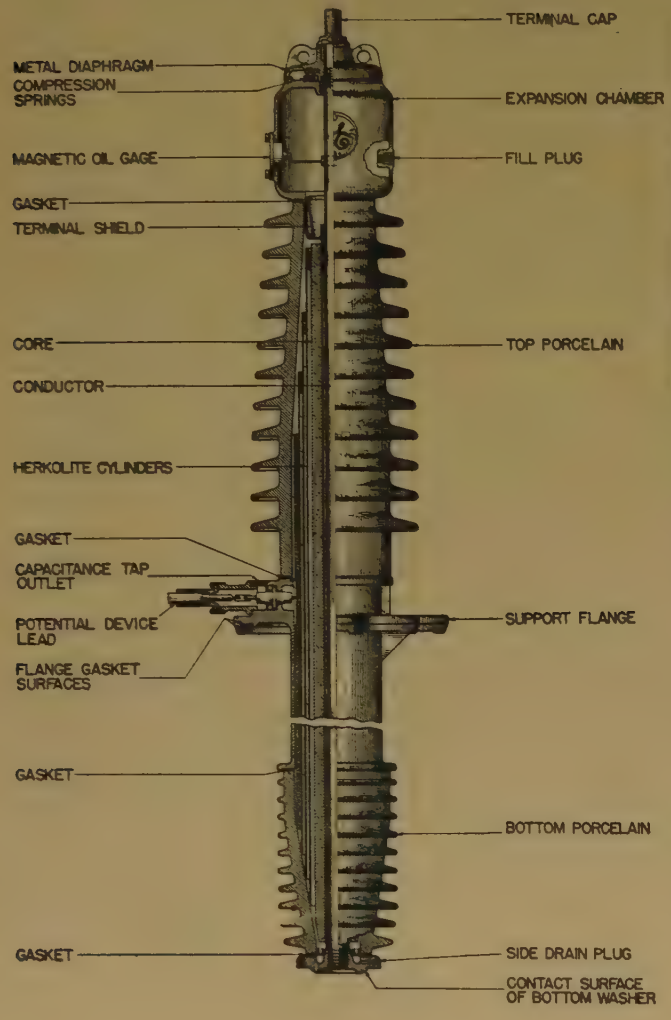


Figure12(left). 115-kv sealed oil-filled circuit breaker bushing in cutaway semisection showing arrangement of porcelains and gaskets



Figure 13 (above). Top of sealed oil-filled circuit breaker bushing showing expansion chamber and magnetic type oil level indicator

plifications in the breaker top frame construction.

Exhaustive tests have been made, not only under static conditions but also under operating conditions such as the loadings that bushings are subjected to during the interruption of heavy short circuits. Every attempt has been made to find failure points under both of these conditions. The interrupting tests unquestionably subjected the bushing to the most severe mechanical loadings. On all tests the bushings gave a remarkably satisfactory performance. Many readers will be interested in a performance comparison between the new and the superseded designs. The new design has turned out to be both electrically and mechanically stronger than the older oil-filled type.

An additional feature of the new bushing is the interchangeability with the old design. A long background of interchangeable breaker bushings dictated that from a user's standpoint, the new bushing fall into the same pattern. Therefore, the mounting bolts and flange gasket locations are identical with those of the older bushings. The elimination of the lower clamping ring has permitted shortening of the bushings by about three inches. For replacements, however, a suitable spacer can be provided to compensate for this shortening, and the new bushing is available as a replacement unit for any oil-filled bushing on older oil circuit breakers.

Table III. Comparison of New and Old Designs Illustrating the Substantial Reduction in Oil Requirements and Loading on Foundations

Breaker Rating	Type New	Type Old
115 Kv		
Tank diam., in.	54	54
Weight, lb	36,600	39,400
Oil, gal	2,300	2,420
138 Kv		
Tank diam, In.	54	60
Weight, lb	38,500	47,800
Oil, gal	2,400	2,970
161 Kv		
Tank diam., in.	60	72
Weight, lb	44,800	64,300
Oil, gal	2,950	4,700
230—196 Kv		
Tank diam, in.	78	108
Weight, lb	85,000	168,500
Oil, gal	7,250	14,000
230 Kv		
Tank diam, in.	84	108
Weight, lb	110,000	180,000
Oil, gal	8,800	15,400

Tank and Top Frame

The pole units of the new breakers have a number of design features resulting from changes in the essential component parts (Figure 14). The smaller-sized interrupters made a reduction in tank dimensions possible. The new sealed bushings with smaller lower end dimensions permitted smaller bushing current transformers and a simplified arrangement of the transformer housing. The increasing demand for more 3-cycle breakers made it advisable to design the pole unit linkage with this objective in mind. Many of the accessories were simplified and relocated to facilitate maintenance.

The smaller size and smooth contours of the new interrupters have permitted substantial reductions in the sizes of the 138-, 161-, and 230-kv breakers and at the same time have improved their overvoltage performance. Table III shows a comparison of the new practice and the old.

The changes in the bushing current transformer housings resulting from the smaller bushings are quite striking as compared with superseded designs. As shown in Figures 1 and 14, the smaller housing fits within the dome outline so that space is available for two current transformers per bushing without a special design. The conduit connections are large enough for the leads of two current transformers so that a second set can be easily installed in the field. The new arrangement also makes it possible to remove the current transformers over the lower end of the bushings. Thus changes can be made without the laborious pro-

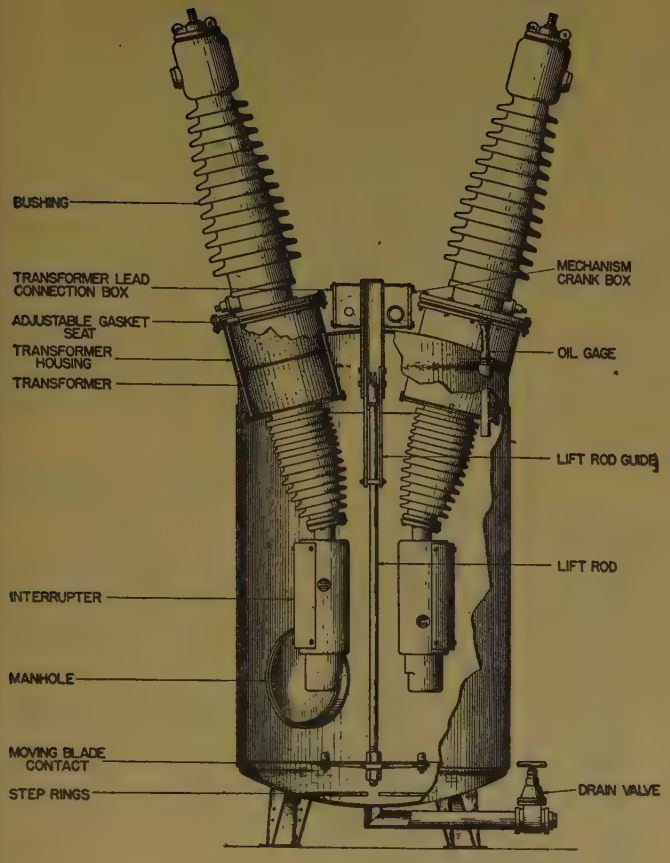


Figure 14. Cross-section of pole unit showing relationship of component parts: interrupters, bushings, tank structure, and bushing current transformers

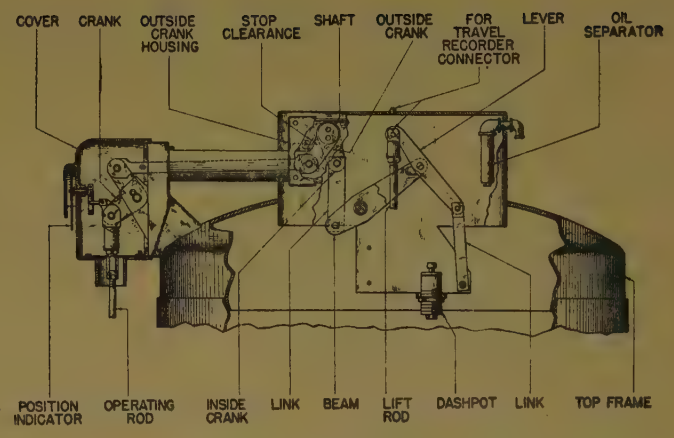


Figure 15. Pole unit breaker mechanism showing straight line linkage and crank housing above operating mechanism

cedure of removing the bushings. The new current transformers have all of the characteristics prescribed by various breaker standards. The current transformers are treated to provide a positive protection against water absorption. The tops of the transformer housings which support the bushings have a special gasket arrangement to permit tilting of the bushing to obtain proper contact alignment.

The increasing demand for 3-cycle breakers has indicated that the mechanical design should be basically suited to such performance. After several arrangements had been reviewed, it was decided to adhere in general to the straight line linkage which has been used successfully in breakers of this type for the past 20 years. But as shown in Figure 15, its size was greatly reduced by taking advantage of the relatively short breaker operating strokes which have resulted from a proper analysis of the clearing distances needed. A feature of this design is the use of low friction bearings which are particularly helpful where high-speed tripping is required. Gas- and oil-tight seals are provided on the main operating shafts by means of close-fitting bearings with splined shafts and cranks for ready assembly. An external indication is provided in the side crank box housing for determining the proper closed position of the linkage. Self-contained oil-filled dashpots absorb the energy of the moving parts at the end of the opening stroke, and their adjustment has been greatly facilitated by providing a threaded assembly with a suitable locking arrangement.

Operating springs are kept to a minimum. Lightweight moving contacts and pneumatic operation make it unnecessary to provide balancing springs for closing to offset the dead weight of the moving members. Buffer springs to limit overtravel are not required, since this function is incorporated in the interrupter contact springs. Opening springs on the rear pole unit keep the interphase connecting pipes in tension for both closing and opening and can be adjusted readily from outside of the breaker to obtain the proper opening speed characteristics.

Tank supports are used to hold the pole unit tanks above the foundation, so that complete drainage can be obtained without any enclosure which would restrict inspection and maintenance of the underside of the tank, as shown in Figure 16. This arrangement permits a reduction of the size of foundation pads. Side manhole openings as shown in Figure 17 give convenient accessibility, and parts for installation in the tanks are easily transferred. The heavy steel manhole covers are supported by hinged joints. Step rings on the outside of the top frame and on the inside of the tank bottom give a firm footing in spite of adverse weather conditions or the presence of an oil film. The oil level is shown by a float-type gauge whose sight glass is easily visible from the ground. Each pole unit has an emergency vent (Figure 18) built into the top frame for protection against permanent damage to the unit when through some unusual circumstances, excessive tank pressure is present. This has a flat copper diaphragm which is designed to rupture at a pressure much less than the tank strength. A semaphore indicator at the front end of the breaker shows the position of the moving contacts at all times. The front crank box cover can be removed for making adjustments at the upper end of the operating rod. The bottom of each pole unit tank is marked to

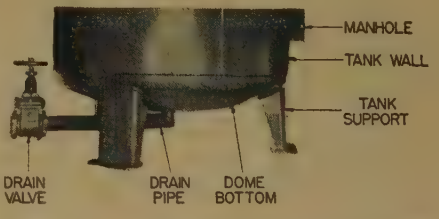


Figure 16. View showing tank supports which give maximum accessibility for maintenance under tank bottom



Figure 17. Maintenance manhole in side of tank provides easy access

indicate quadrant positions so that location on the foundation is facilitated. Likewise, plumb bob reference points can be used for leveling.

Operating Mechanism

The modern high-voltage oil circuit breaker requires for its operation a large amount of power delivered for a relatively short time. The pneumatic type of operation is well suited to this requirement. A self-contained unit on each breaker with its own individual air compressor equipment lends itself readily to application on various ratings of breakers whether they are new or in the process of modernization. The breaker pole unit tank is provided with mounting brackets for the support of the housing and its equipment as shown in Figure 19. Electrical connections are no different from those of other types of electrically operated mechanism. Power requirements are very light, and standard control cables will meet all requirements.

Reclosing times are constantly becoming shorter, and the basic design of the pneumatic operation should be adapted to this requirement. The pneumatically trip-free mechanism is so adapted. It is not handicapped by the relatching time of mechanically trip-free designs or any complicated arrangement to avoid it. With the pneumatically trip-free mechanism, the reclosing time is a matter of the size of the power unit and the operating pressure. It is relatively simple to provide for the minimum reclosing times without special designs.

One of the elements involved in the interrupting time of a breaker is the time required to part contacts. A goodly portion of this is dependent on the unlatching of the mechanism after the trip impulse is received. A 5-cycle breaker requires only a conventional trip coil to obtain the unlatching time commensurate with this breaker rating. A 3-cycle breaker, on the other hand, requires a very short unlatching time, and a special design of high-speed trip is necessary. In other respects, the two operating mechanisms have the same characteristics and are built with common parts.

The power unit is similar to those previously described in references 1 and 4 and is shown in Figure 20. It consists of the mechanism frame with closing and tripping linkage actuated by an air piston. The admission of air to the cylinder is controlled by an electrically operated valve as explained in reference 4. Associated with the power unit is a small compressor unit which maintains pressure in the air receiver located underneath the housing. Electrical and pneumatic controls are assembled on a common panel which is accessible through a hinged side door.

The 5-cycle breaker mechanism uses a conventional trip solenoid, as shown in Figure 21. The 3-cycle breaker mechanism uses a high-speed flux-shifting type trip similar to that described in Reference 1 and shown in Figure 22. An auxiliary air control valve admitting air above the piston also is required to obtain the equivalent time on a trip-free operation. This

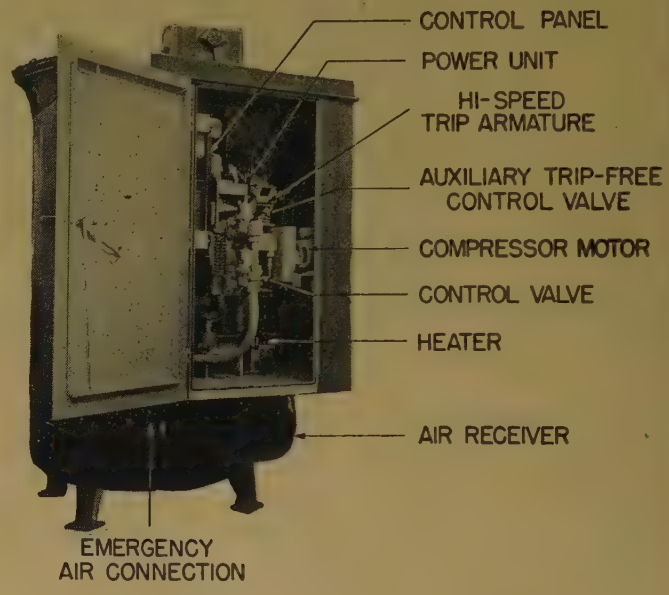


Figure 19. A pneumatic operating mechanism for a 3-cycle, 20 - cycle - reclosing 115–161-kv breaker

The complete unit is mounted on the first pole unit tank

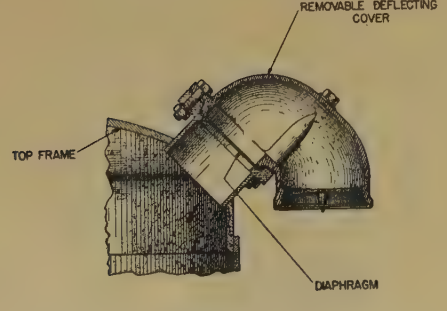


Figure 18. Assembly of emergency vent showing diaphragm which ruptures under excessive pressure and cover to direct discharge to ground

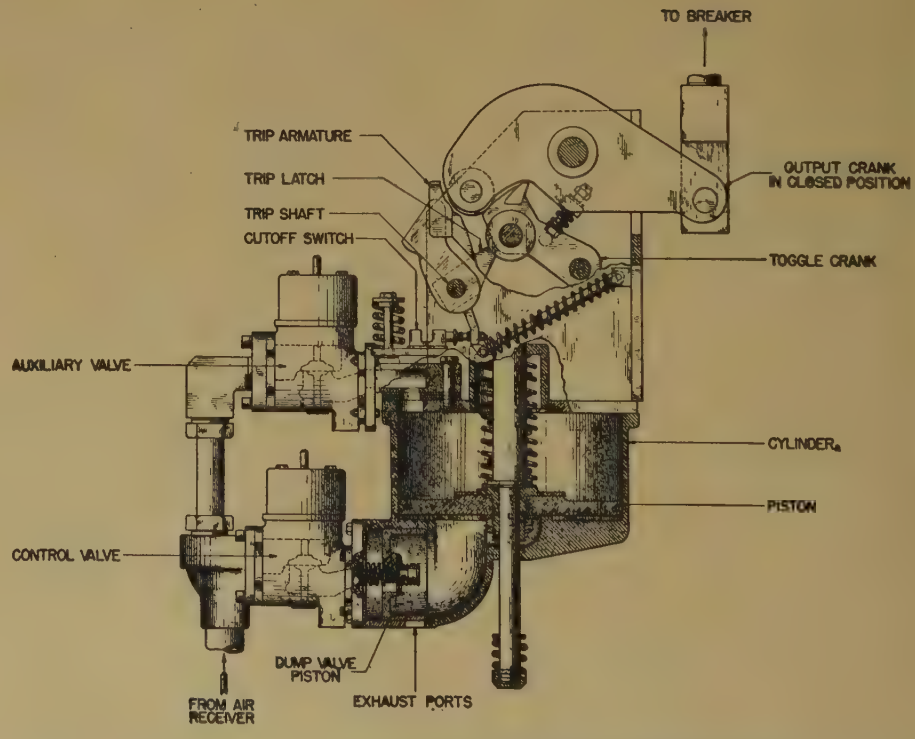


Figure 20. Cross-section of a 3-cycle pneumatic operating mechanism showing the power unit with air control valve and closing and tripping linkages

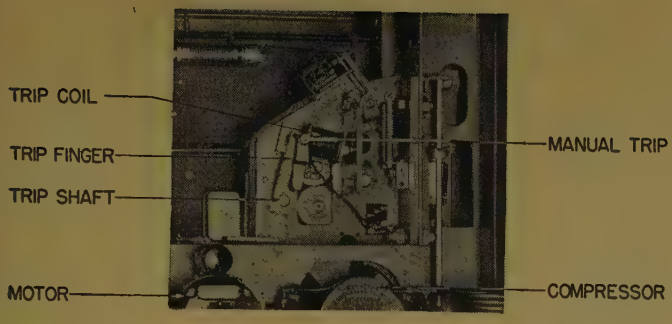


Figure 21. Trip arrangement for a 5-cycle breaker showing parts on frame for adapting high-speed 3-cycle trip



Figure 22. Trip arrangement for a 3-cycle breaker showing flux-shifting trip for high-speed operation

is assembled directly above the main control valve.

Rating Standards

A careful examination and analysis of the breakers described in this paper indicates that there is very little about them that reasonably can be changed in order to produce a breaker with lower interrupting capacity and lower cost but otherwise meeting the high standard of performance of the breaker as described. This suggests the use of only one breaker design and one rating for each voltage. This would reduce the number of ratings listed in the present American Standards Association standards for 115- to 230-kv breakers from 13 to 4. The resulting simplifications eventually would be of benefit to both user and manufacturer.

Conclusions

This paper has described a line of outdoor tank type oil circuit breakers with voltage ratings from 115 kv to 230 kv and capable of handling all standard interrupting ratings at these voltages with liberal margins on a 20-cycle reclosing basis. The breakers can be adapted to either 3-cycle or 5-cycle operation.

These breakers incorporate improved performance, smaller dimensions, and lower weight both of the breaker as a whole and of many of the parts which require handling in inspection and maintenance.

The authors recommend consideration of the reduction of the number of standard breaker ratings in the 115-kv–230-kv voltage range to one rating for each voltage.

References

1. A High-Capacity High-Voltage Three-Cycle Oil Circuit Breaker, H. L. Byrd, E. B. Rietz. AIEE Transactions, volume 64, 1945, April section, pages 160–3.

2. Field Tests and Performance of Heavy-Duty High-Speed 138-Kv Circuit Breakers—Oil and Air-Blast, Philip Sporn, Harry P. St. Clair. AIEE Transactions, volume 64, 1945, pages 401–10.

3. Switching Overvoltage Hazard Eliminated in High-Voltage Oil Circuit Breakers, L. F. Hunt, E. W. Boehne, H. A. Peterson. AIEE Transactions, volume 62, 1943, February section, pages 98–106.

4. A Pneumatic Mechanism for Outdoor Oil Circuit Breakers, L. J. Linde, E. B. Rietz. AIEE Transactions, volume 63, 1944, July section, pages 543–6.

Shoran Precision Radar

STUART WILLIAM SEELEY
NONMEMBER AIEE

Synopsis: Shoran navigational radar is generally credited with being the most precise system of its type devised by man. The history of the conception and development of the principles employed, as well as a description of the physical make-up of the equipment, are of interest. Recent military declassification permits the exposition of both as set forth in this paper.

SHORAN is the common name for Army radar sets AN/APN-3 and AN/CPN-2. The equipment is used for high-precision position-finding in aerial navigation, principally for blind bombing and aerial mapping, although several other practical applications have been suggested. The term Shoran is a contraction of the two words short and range. What might at first appear to be a slightly derogatory title—in view of satisfactory performance out to 250 miles—has a logical explanation in the sequence of events prior to adoption of Shoran as the semiofficial designation. The history of the conception and development of the equipment pre-dates that of Loran, the widely used and now well-known long range navigational system. Development work on the latter was also carried on in RCA Laboratories under contract to the Office of Scientific Research and Development after its original inception by the Radiation Laboratory of the National Defense Research Committee. The Loran range of operation was approximately three times that of Shoran. Thus, while work progressed simultaneously on both in the same laboratory after April of 1942, Loran was the first to be adopted, named, and put into general use by the armed services, and the term Shoran for the shorter-range, higher-precision device followed almost automatically. Actually the two are completely dissimilar in equipment and operation. The only common aspect lies in the fact that each is used for aerial navigation.

History of the Shoran Development

The history of the development of Shoran is the story of a search for extreme accuracy of propagation time measurement coupled with ruggedness and reliability of equipment and simplicity of operation. It can truthfully be said that all of those aims were accomplished without compromising any one of them for another.

So much has transpired since the start of war developments that it is difficult to transport one's thoughts back seven years to the fall of 1938. At that time, war in Europe seemed a possibility but was still a year away. The concept of pulsed transmitters of radiant energy for the purpose of propagation time and distance determinations was not widespread. The term radar was nonexistent, and the only generally conceived applications of radio to war needs were for communication purposes or possible remote control of guided missiles of one sort or another.

At that time, work on television transmission and reception equipment was proceeding in many laboratories throughout the world. One of the knotty problems which vexed every television receiver engineer was that of multipath or "ghost" images which so often marred his otherwise creditable results. The television pictures in the industry service division of RCA Laboratories were no exception. The signals received at 711 Fifth Avenue in New York, N. Y., from the Empire State Building often showed as many as five separate and distinct ghost images when inside (or poorly exposed outside) antennas were used. Analysis of the picture content with particular reference to the horizontal displacement of a particular ghost image and the ratio of that displacement to the length of a complete scanning line gave a good indication of the increased path length of the reflected signal which caused the ghost.

At that time the Radio Manufacturers Association television standards specified a 441-line television picture, of which approximately 400 lines were visible, the other ten per cent being used for the vertical synchronizing action.

The aspect ratio of the pictures was four horizontal to three vertical. Thus, there were approximately 530 picture elements along each line. The time required for the scan of the visible portion of each line was 64 microseconds, and since a ghost image displaced by two picture elements was plainly discernible, it was evident that a reflected signal which arrived as much as one fourth microsecond later than the direct signal was detectable. Such a ghost would be displaced approximately 1/32 of an inch on a 12-inch tube picture, and reference to the velocity of propagation indicated that it had traveled about 250 feet farther than the direct wave. The position of multipath images displaced by as much as one fourth inch or more could often be measured to the nearest 1/64 of an inch, and thus the extra distance traveled could be determined to within ±125 feet.

These findings gave rise to the belief that specially designed equipment built primarily for the purpose of path length determination could give an accuracy of ±50 feet or better, and the considerable thought given to that possibility in the fall of 1938 resulted in the early concept of Shoran as it is today.

Actually it was not known, at first, to what uses a system for accurate transmission path length measurement could be put, but it seemed logical one use might be for blind navigation, particularly of aircraft. Blind bombing suggested itself automatically because of the apparent imminence of war in Europe.

However, if delay times equivalent to tens or even hundreds of miles instead of tens or hundreds of feet were to be measured, it was apparent that two requirements would immediately present themselves. First, a round-trip signal between the two points of distance determination would have to be used. This would call for either an extremely efficient reflector at one end of the path or for retransmission of the original signal at the path terminal. Second, some type of vernier or decimal indication would be necessary in order that the radio "yardstick" could be read to, say, ±100 feet even though the round-trip or total distance was of the order of 2,000,000 feet or 400 miles.

Many experiments were performed in the fall of 1938 and the spring of 1939 to confirm the belief that relatively long distances could be measured with even higher absolute accuracy, and thus perhaps a thousand-fold greater proportional accuracy, than the original television multipath determinations.

One interesting experiment consisted of retransmitting the television pictures from the Empire State Building between

Paper 46-49, recommended by the AIEE committee on communication for presentation at the AIEE winter convention, New York, N. Y., January 21–25, 1946. Manuscript submitted December 19, 1945; made available for printing January 2, 1946.

STUART WILLIAM SEELEY is associated with the Industry Service Division, RCA Laboratories, Radio Corporation of America, New York, N. Y.

two points on Long Island separated in such manner that the relayed picture arrived at a receiver almost exactly one line later than the direct signal. The raster on the cathode ray tube face was synchronized continuously with the direct signal from National Broadcasting Company while the video content was commutated between the direct and relayed pictures. When the relayed signal path length corresponded exactly to one line, the commutation process produced no horizontal jitter of the television image. The signal was, of course, delayed in the relay terminal equipment by the electric inertia of tuned circuits, video amplifiers, and connecting cables. These time intervals had to be taken into account, and those which could not be accurately calculated were measured by a determination of the phase shift characteristics of the modulation components of an r-f signal passing through the equipment. It is interesting to note that the total time elapsed in the relay receiver and transmitter corresponded to a path length of nearly 2,000 feet. But since it could be accurately measured to within 0.01 microsecond by the slope of the phase versus modulation frequency characteristic, errors from that source were not more than ±10 feet. It was necessary to call on the U. S. Coast and Geodetic Survey for accurate ground distance information.

The results of that experiment and others were convincing proof that a radio "yardstick" could be constructed for first-order determination of distances out to the limits of propagation of the radio frequencies used. The latter had to be relatively high to accommodate the rapid modulation necessary for sharp time indications. Amplitude or frequency changes in the radiated wave would have to occur in the order of 1/10 microsecond if measurements with an accuracy of that order were to be possible. This called for a transmission frequency whose fundamental period was not more than 1/50 microsecond or a minimum 50 megacycles.

The transmission of what could be termed single picture elements, one at a time, with the transmitter completely quiescent between those pulses, was chosen as the most practical mode of operation. Such a system would allow relatively high power radiations with relatively low average power consumption. This principle, decided upon in October of 1938 for the original Shoran development work, has been used almost universally in all radar equipments whose function requires operational ranges greater than one or two miles.

It is not meant to imply that this date marked the first concept of pulse type operation. However, the choice of pulse type operation at that early stage of the Shoran work marked the final equipment for success. Attempts to derive the same end results by other systems have proved the wisdom of that choice.

During 1939 many types of possible vernier time measurement devices were conceived, built, tested, and discarded. Since it seemed certain that on occasion multiple pulses, due to reflected waves traveling devious paths, would arrive at the receivers at each terminal of the transmission path, and since, obviously, the first pulse to arrive would be the only one to give an indication of the direct path distance, it seemed clear that a cathode-ray-tube type of data presentation would offer the simplest means of discrimination between the desired or first-arriving information and subsequent indications. It was conceivable that circuit arrangements could be effected whereby the elapsed time could be indicated on meters or transposed to data transmission systems. However, the most straightforward procedure appeared to lie in the use of linear determinations of the position of an alteration in either the intensity or deflection of a cathode ray tube trace.

Here again this early choice of the cathode ray tube as the indicating element has certainly been vindicated by subsequent developments. Much later in the history of Shoran, circuits were developed for transferring the derived information to a data transmission system. This made it available at positions remote from the equipment; but those circuits, which will be described later, are of only secondary importance, and the cathode ray tube remains the prime indicator.

Two further principles, each of which contributed markedly to the success of Shoran, were also adopted early in its history. First, the repetition rate of the transmitted pulses, which could be controlled by quartz crystal oscillators to an accuracy of one part in 1,000,000 if necessary, was selected as the fundamental unit of measurement. Second, an old principle familiar to precision instrument makers in many fields and known as the set-back type of operation was adopted. This principle is exemplified in precision aneroid barometers wherein movement of the bellows caused by varying air pressure is counteracted either by adjustable weights or by adjustable spring tension sufficient to return the bellows distortion to a fixed zero. The weights or the spring adjustment necessary to perform that function then give an indication of the air pressure. While this type of operation seems cumbersome compared to the simpler method of causing the bellows to move a pointer around a calibrated scale, actually the increased precision is well worth the complexity.

As applied to Shoran, this system eliminates the need for the maintenance of exact linearity of the cathode-ray-tube sweep speeds in the presence of varying power line voltages, varying vacuum tube characteristics, and varying circuit parameters. So far as is known to the author, Shoran is the only radar system which adopted the continuous set-back principle. However, the advantages which accrue from its use are not as necessary in equipments which seek less inherent accuracy.

By the summer of 1939, enough experimental and developmental work had been done to indicate the probable practicability of a blind bombing navigational device founded upon the principles enumerated above. Operation would call for an equipment in an airplane which could simultaneously measure its exact distance from two separated and accurately known ground locations in friendly territory while the plane flew over enemy targets. Investigation revealed that all of Europe, together with all of the North American continent, had been sufficiently well mapped so that the distance between any two points within 250 miles of each other in those parts of the earth could be calculated with a probable error of 50 feet or less.

Armed with this information, and fortified with the confidence of many months of satisfying experimental endeavor, the project was presented by Radio Corporation of America to the United States Army Air Forces with the proposal that funds be allocated for the development of operating models of the necessary equipment to test its feasibility. That was in the summer of 1940.

It is an interesting commentary on the thinking of those times that the author felt constrained to write into the specifications of the proposal the suggestion that the probable accuracy of distance measurements would be of the order of ±500 feet. These predictions, definitely pessimistic in view of the favorable experimental results in the laboratory, were made pessimistic principally because it appeared utterly fantastic at those times to presume to achieve even that goal. To have suggested more would have branded

the project as completely unrealistic.

Even with those moderate claims, the apparent unreality of the proposed program hindered the progress and retarded the growth of Shoran up to the very day the first Shoran bombs dropped to destroy a 30-foot-wide enemy-held bridge in northern Italy.

War in Europe had been declared at the time of these first proposals. The pace of preparedness in the United States quickened after the fateful September 1, 1939. More money was allocated to the armed services for development of new devices, and even some of the projects which were felt to be a bit on the fantastic side were given the green light.

Accordingly, a contract was awarded to RCA Laboratories in February of 1941, about nine months before Pearl Harbor. This called for completion by February 1942 of two ground station equipments and one airborne equipment to give simultaneous and continuous distance determinations from each of the ground stations to a plane, out to optical line of sight, with an accuracy not poorer than −500 feet at 100 miles or 0.1 per cent of the distance beyond that point.

The 2 1/2 years of experimental work before the awarding of the contract had allowed the plans for the model to be so well formulated that just four months later the plane equipment and one ground station were completed and ready to operate. With one complete operating chain, many previously unanswered questions could be resolved. One determination which had not been made concerned the possible variations in the propagation velocity of a radio wave at tangency with the earth's surface. It appeared that vegetation and partially conducting soil with a high dielectric constant could well have a marked effect on that all-important characteristic. Also the probable variation caused by changes in the humidity of the air was a possible source of difficulty which could only be crudely calculated. Accordingly, it was decided to place the plane equipment in the tower of the Empire State Building, put the ground station out beyond the optical horizon at Rocky Point, Long Island, and make day-to-day measurements of the distance between the two points. This was done after flight tests from Wings Field near Philadelphia, Pa., to the Rocky Point location had confirmed adequately the predicted range of operation.

Measurements between the Empire State tower and Rocky Point were continued for a period of three months during the summer of 1941. Hundreds of readings were taken and the equipment operated by many different observers. During that time the temperature varied more than 40 degrees Fahrenheit and the humidity ranged from a low of 30 per cent to a high of 100 per cent. An average of all readings indicated a distance of 56.126 miles with a total spread of 0.013 mile. There was no apparent correlation between climatic conditions and the readings. Later the United States Coast and Geodetic Survey gave the measured distance as 56.127 miles, or five feet more than the average of the Shoran readings. Obviously the transmission path to the Rocky Point location, which was 400 feet below optical line of sight, through scrub pines and over sand, was not affecting the velocity of propagation to any marked extent over and above the variations caused by normal sea level air pressure. The latter had been calculated beforehand and introduced into the equipment as a correction to the frequency of the crystal-controlled pulse repetition rate. The agreement between the Shoran and geodetic distance measurements was actually too close for comfort. Had they differed by 200 feet or so, they could have been given to the Aircraft Radio Laboratory as evidence of the potentialities of the system. Under the circumstances, it was decided that it would be best to say nothing about that particular series of measurements and let the contracting agency make its own accuracy determinations.

At the time of Pearl Harbor, the Aircraft Radio Laboratory took delivery of two specially constructed all-metal trailers which they had ordered built to specification to house the Shoran ground stations. Each of these had its own 5-kw gasoline-driven a-c generator in a glass-enclosed gas-tight compartment. These were in turn delivered to the RCA Communications Laboratory at Rocky Point and the Shoran gear installed. Further tests followed with the ground stations operating as complete self-contained mobile units. Then shortly before the contract expiration date, the entire equipment was sent to Wright Field for acceptance tests.

It is well to bear in mind the particular conditions which existed at that time. The United States had been at war for just 2 1/2 months. The mad rush to prepare for the titanic struggle which was already upon us called for emphasis on the most necessary fundamentals first. Communication radio and liaison equipment for a rapidly expanding air force were requisites of prime importance. The Aircraft Radio Laboratory at Wright Field was so completely occupied with the specification and procurement of these necessities that they had neither time nor facilities for acceptance tests of such apparently obtuse devices as Shoran. It was not until six months later, in August of 1942, that the original plane equipment was mounted in a B-17 Flying Fortress and taken to Eglin Field, Fla., for bomb-dropping tests. The mobile ground stations were set up at Montgomery, Ala., and at Tallahassee, Fla. In order to save time, the distances from each ground station to the 30-foot square-base pyramid target in the bay near Eglin Field were determined by flying over the target with a Norden bombsight set to vertical and reading the Shoran distances. This process was repeated several times, but the pitch and roll of the plane, together with the inability of the automatic pilot to do a precise job of following the bomb sight lead, resulted in considerable discrepancy between successive readings. Admittedly the bomb-dropping trials were to be handicapped, not only by the possible Shoran errors but by those of the Norden bombsight and automatic pilot as well. The distances finally determined were 108.297 miles to Tallahassee and 125.431 miles to Montgomery.

Of the first 12 100-pound sand-filled practice bombs dropped from 14,000 feet, the average dispersal from the target was 220 feet. Two of the bombs hit the 30-foot-square wooden target. The results were on a par with those to be expected from a mission dropping the same number of that type of bomb by visual means. The ballistics of sand filled practice bombs are erratic in comparison with those of heavier missiles. Additional tests were made from 20,000 feet and the results were relatively the same. It appeared that Shoran had proved its capabilities as a blind bombing device even before its precision for distance measurements had been evaluated.

The procedures developed for determination of the release point of the bomb on those early test runs are interesting. It would be beside the point to go into all the ramifications of the calculations of bomb trajectories and release points in this paper. Suffice it to say that the vector winds through which the plane was passing were determined by comparing the indicated air speed of the plane with the rate of change of Shoran distances for a given plane heading. Manual release at the proper point was effected by the simple process of pressing a button connected electrically to the bomb rack intervalometer. Human reaction time was not considered a factor because of the

anticipatory knowledge constantly supplied by the Shoran indications. Later production models were equipped with devices which automatically measured the plane speed as well as the vector wind, made the required corrections in the ground path of the plane, and automatically released the bomb at the corrected point on that path. That portion of the equipment was developed primarily by F. J. Hooven in co-operation with engineers of the Harris Seybold Potter Company under contract to the Armament Laboratory of the Air Technical Service Command. It is a marvel of ingenuity and precision, but at this writing, information regarding the details of that device is still restricted.

After the Eglin Field tests, it seemed certain that an immediate request for product designs and production schedules would be forthcoming. Much to the personal disappointment of those who had nurtured the development from its conception, such was not to be the case. Interest in blind bombing devices was at fever heat, but the new microwave techniques were coming on the scene and their freedom from any tie to fixed locations on the ground seemed to offer the only complete answer. Actually it was not until after the close of war in Europe that it was determined that 80 per cent of all strategic missions and almost 100 per cent of all tactical missions flown in that theater were within the Shoran range of operation.

A further deterrent to Shoran progress lay in the fact that by then the British had started development of a somewhat similar system and it was felt inadvisable to carry on two separate product design and procurement programs without coordination. Accordingly, a small group of military personnel headed by Lieutenant Colonel R. R. Brunner, together with two Radio Corporation of America engineers, left for England on December 1, 1942, to exchange information and to resolve the degree to which the two programs could be integrated. However, the work carried on at Telecommunications Radio Establishments under the Air Ministry was based on entirely different principles than those of the Shoran development and there appeared to be no common basis upon which the two programs could be combined.

On the return trip from England, the party split into separate groups. The group consisting of Colonel Brunner and some British military personnel coming to the United States to get a better picture of the Shoran project was lost in flying the South Atlantic Ocean. Viewed in retrospect, it seems certain that this loss was a major factor in keeping Shoran progressing at a snail's pace toward its ultimate conclusion.

Finally in March of 1943 a product design contract was given to RCA and work progressed again at full steam. The contract stated that the ultimate equipment should have an accuracy of distance measurement at least equal to that of the original model which, by then, carried the army designation SCR297-T2. It was realized by all concerned that the ±500 feet specification was so pessimistic as to be meaningless, so no figures were mentioned. Several of the automatic features referred to previously were specified as essential to fulfillment of that contract.

That work was completed in January of 1944. It is a credit to all concerned to say that the faith of the Air Technical Service Command Aircraft Radio Laboratory in the ultimate outcome of that program was such that they recommended, and Radio Corporation of America received, large procurement orders well in advance of its completion. Thus the Shoran radar program acquired the unique distinction of having been conceived, developed, product-designed, and manufactured entirely within one company. This, of course, neglects the auxiliary equipment mentioned above.

After the completion of the design work, and while waiting for production quantities to become available, a six-month program of rigorous flight and field tests was inaugurated at Boca Ratan, Fla., under the auspices of the Aircraft Radio Laboratory. For the first time, a true indication of the accuracy of distance measurements from a plane to a fixed point on the ground was available. This was derived by the use of so-called Zenith cameras located at known control points approximately 100 miles from the Shoran ground stations. The plane was equipped with a gas-filled flash lamp on the under side of the fuselage. As the plane passed over the Zenith camera, the lamp was flashed and the Shoran distance readings recorded. Many nights of such flights with many passages back and forth across each new Zenith camera location gave sufficient data to indicate the probable error of distance measurement as being somewhat less than 50 feet out to the limit of its range. Hundreds of bombs were dropped and many different operators acted as Shoran bombardiers. As a matter of fact, no single individual ever dropped enough bombs to become really proficient in the use of the equipment, but the design was such that it was relatively simple to operate. Thus, human errors, particularly when the operator had had training on a Norden bombsight, were at a minimum.

The extreme accuracy of distance determination attracted the attention of the Army geodetic and mapping groups. As a result of their interest, the equipment is being used today for establishing control points with first-order survey accuracy at very great distances. For this work a ground station is established at each point to be located and a plane flown back and forth across the line between any two such points. The average minimum sum of the distances between the plane and each ground station, as indicated by a photographic recorder for each line crossing, gives the true distance between the points. The comparative simplicity of surveying a line from, say, Chicago to Kansas City to Amarillo, Texas, in only two jumps can be imagined. For a survey of that route, three ground stations would be used, one at each of the three cities, and 10 or 20 flights back and forth across the approximate center of each line would be all that would be required. Except for one consideration, it would be unnecessary for any individual to set foot upon the intervening terrain. Subsequent to the early tests between the Empire State Building and Rocky Point, the true effect of climatic conditions on propagation velocity and on the refraction of the radio waves between plane and ground had been determined. As a result, sounding balloon or other types of atmospheric determinations along the path are considered necessary when the equipment is used for first-order survey work. Nevertheless, the simplicity and rapidity with which unmapped portions of the surface of the earth can be brought into survey control with equipment of this type is little short of amazing.

At the completion of the Boca Ratan tests, the remarkable results achieved became known to the commanders in the fields of operation and requests for equipment began to pour in. In September of 1944, it was decided to test the equipment in actual operation against the enemy. Several personnel from the Aircraft Radio Laboratory and the Armament Laboratory (also at Wright Field) were accompanied to Corsica by three Radio Corporation of America engineers to aid in setting up the equipment and to train ground and air crews in its use over northern Italy. There were many disappointing delays in the arrival of the equipment. Boxes supposed to contain transmitter tubes were found to contain toilet necessities and flashlight batteries.

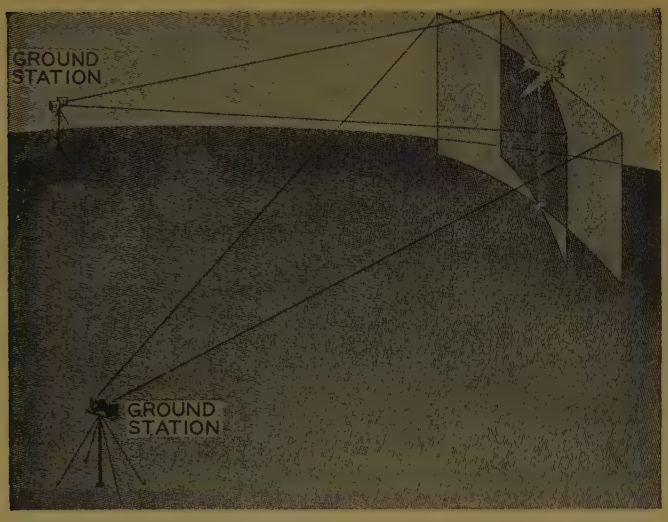


Figure 1. The Principle of Shoran

The Shoran set indicates plane's distance from two ground stations, thus "fixing" it at intersection of the corresponding circular arcs swung around the two stations

More weeks followed during which crews were training and practice bombing. Finally on December 11, 1944, the first Shoran bombs were dropped. From that time on, events moved with rapidity. Operational results were phenomenal. Bridges that had withstood many close misses by visual missions were destroyed on the first Shoran run. Weather was no hindrance to tactical air support with Shoran. By the time the war ended in Europe, the amount of tactical bombing being done in any area was predicated almost entirely upon the availability of Shoran equipment. By the time the war with Japan was brought to a close, the plans of the Army and Navy for the use of Shoran in the Pacific were astounding even to those who knew its potentialities.

The Shoran System

Figure 1 shows the 2-distance "fix" method used by Shoran to locate a position in flight. The airplane equipment transmits a series of short pulses of radio frequency energy to each of a pair of ground stations. These in turn immediately retransmit the received signals to the plane where the round-trip transmission time is measured in terms of distance. In bombing operations the plane flies in either direction on an arc about one of the ground stations. The radius of the arc is equal to the station-to-target distance. Since either ground station may be used as the center of the flight path, four different approach headings are possible when bombing a given target. With normal station-to-target distances, the curvature of the bomb run path is relatively slight. A refined type of pilot direction indicator meter, deriving its information automatically from the equipment, is in front of the pilot. During a bomb run, with the aid of this instrument, it is not difficult to keep the plane on its arc path with deviations less than the span of the plane wings.

It should be noted that no information is passed along the path joining the ground stations. If the geographic locations of those stations, as well as those of all possible targets, are accurately known, as was the case in the European use of Shoran, the geodetic problems connected with Shoran operations are relatively simple of solution. When they are not known, Shoran reconnaissance photography of possible targets will reveal their co-ordinates.

It is highly desirable that a pair of ground stations be able to serve a large number of planes bombing widely separated targets simultaneously. This is possible with Shoran installations, and the means by which it is accomplished without interference will be described later in this article.

Planning of a Shoran mission, with all the geographic distances known, is not as simple as it might at first appear. The great circle path of a plane several thousand feet in the air differs from the great circle path on the earth's surface, often by as much as one tenth mile. Contrary to a widely held belief, radio waves do not travel in a straight line over any appreciable distance, but tend to be refracted into a vertical arc. Radiant energy travels faster at bomber plane altitudes than it does through sea level air pressures. Fortunately, all of these effects are predictable accurately, and all are taken into account in determining Shoran co-ordinates for a given bombing mission. The calculations involved are completed before take-off. In bombing operations, possible corrections indicated by variations in climatic conditions are usually of insufficient magnitude to be significant.

The ruggedness and relative simplicity of operation of the components of a Shoran system, together with the freedom from equipment failures which it provided in combat use, are all remarkable in view of the extreme precision of the results obtained. Details of the individual portions of the equipment are given herewith.

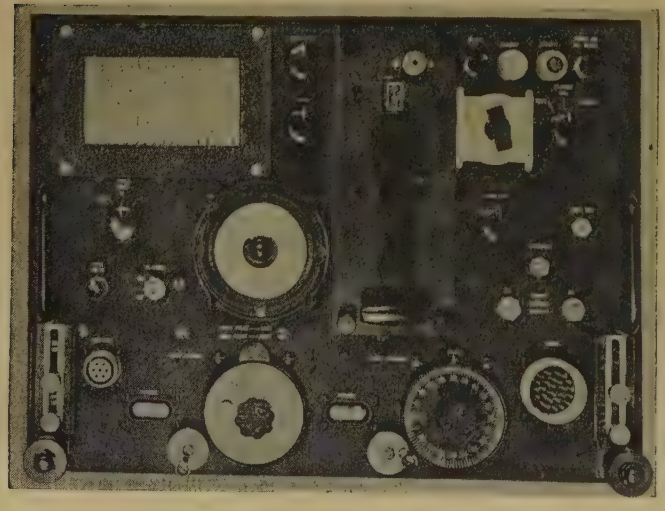


Figure 2. Panel of timing and indicating unit of Shoran plane equipment

Figure 3. The airplane transmitter



The Plane Equipment

The principal units of a Shoran plane equipment are shown in Figures 2 and 3. Figure 2 shows the timing and indicating device which is the most vital part of the Shoran system. This unit permits regulation of the timing of the transmitted pulses in such manner that the signal returned by retransmission from the ground arrives back at the plane receiver and makes its appearance on the screen of the cathode ray tube coincidentally with the fixed, or so-called T_0 marker indication. The adjustment necessary to effect this coincidence is calibrated in miles and decimal portions of a mile. Thus the mileage indications are read from the dial settings rather than from the face of the cathode ray tube, in accordance with the set-back principle referred to previously.

The pulse timing function is duplicated in the indicator unit to allow for simultaneous distance measurements from two ground stations. Reference to Figure 2 will show the two large 100-mile dials at the bottom of the panel. At the left of each dial is a Veeder-type counter, the three digits of which indicate miles, tenths of a mile, and hundredths of a mile. Estimation to the nearest 1/1,000 of a mile is possible. Adjustment of each of the two sets of distance indicators is made by rotation of the small hand wheels to the left and slightly below the large dials. In the case of a plane in motion, continuous rotation, achieved by variable speed motor drive, can be imparted to the shafts carrying the hand wheels, thus keeping the indicated data up to date. It can be readily understood that the rate of rotation necessary to maintain coincidence between the received signal and the T_0 marker is of value in determining the plane's ground speed and in the calculation of bomb release points. Beyond 100 miles the readings are repeated. Thus the readings would be the same for distances of 57, 157, and 257 miles.



Figure 4. The goniometer which determines Shoran timing

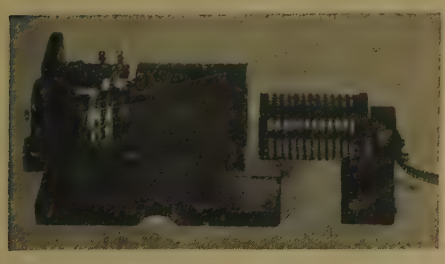
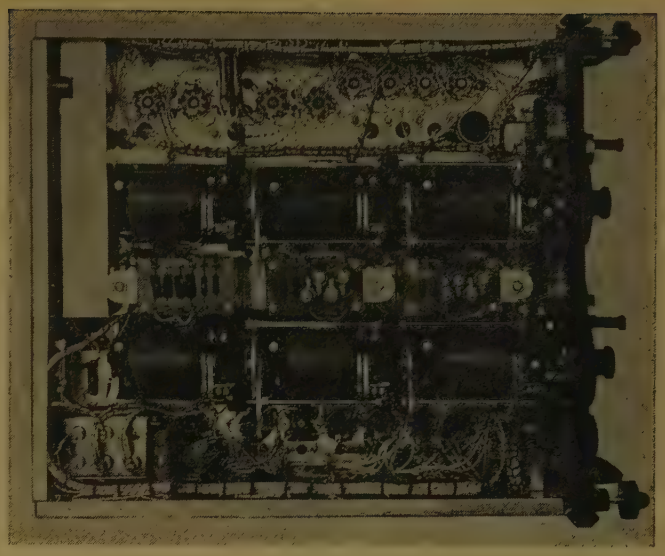


Figure 5. Goniometer with rotor withdrawn

The Faraday screen of copper ribbon covers the crossed windings of the stator

Figure 6. Bottom view of timing and indicating unit

Each goniometer is mechanically connected through reduction gears to the others in the chain



The most interesting portions of the timing and indicating circuits are those which control the timing of the transmitted pulses. The accuracy of that function depends upon the stability of a quartz crystal oscillator operating at 93,109 cycles per second. It should be noted that this figure is exactly one-half of 186,218, which is the number of miles traveled each second by a radio wave passing through sea level air pressure. Thus the period of one cycle of the oscillator is equivalent to the time required for a radiated signal to travel a *round-trip* distance of one mile.

The voltage output from the oscillator is distorted in vacuum tube circuits by clipping and differentiation processes to form a very short pulse, accurately located at a fixed phase of the cycle. This is passed to the cathode ray tube and becomes the T_0 marker on the screen. The output of the 93-kilocycle oscillator is also split into two accurately spaced quadrature components and delivered to the crossed windings of the stator of a goniometer. Pictures of this unit are shown in Figures 4 and 5. The rotor of the goniometer can be turned throughout 360 degrees, and the output potentials, derived by way of the slip rings, have a phase corresponding to the position of the rotor. This potential is likewise clipped and differentiated and produces a pip which then can be timed accurately to any point midway between two marker pips. One degree of rotation of the goniometer corresponds to a round-trip path length of 15 feet. If these adjustable pips were all used to actuate the transmitter, there would be several hundred transmitted impulses stretched out over the round-trip path between the plane and a ground station, and confusion would result. Therefore, it is necessary to select *one* pulse out of each 100 that are developed and discard the others. Accordingly, the 93-kilocycle wave is passed to a 10:1 phase degenerated frequency divider and the new frequency split into quadrature components for a second goniometer. This unit is mechanically connected to the first goniometer through 10:1 reduction gears. The resultant output is used as a gate to select one out of each ten of the developed pips. Again the process is repeated with another 10:1 divider, and a third goniometer is driven by the second through another 10:1 reduction gear. The final output voltage at 931.09 cycles selects one of the ten previously selected pips and thus discards all but one of the original 100 which were developed. The second and third goniometers have no effect on over-all accuracy if the output phase of each is correct within the selection limits of ± 15 degrees. Greater discrepancies would produce errors of exact multiples of one mile or ten miles, depending upon which of the two units was at fault. The circuits which deliver the

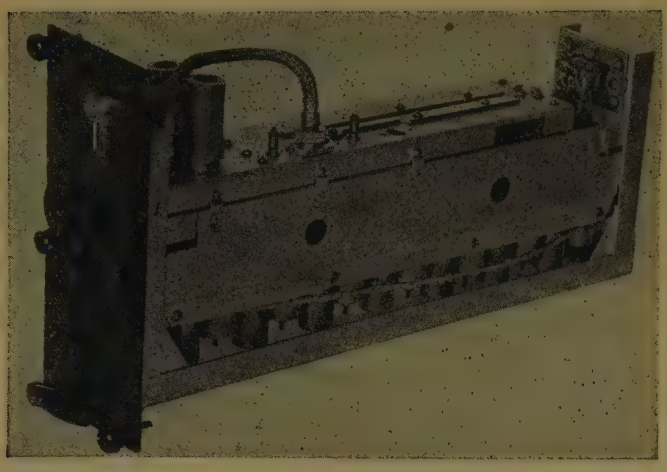


Figure 7. The Shoran receiver used in both plane and ground stations

quadrature currents to the goniometers are unique in one important characteristic. Large changes in the power factor of the stator windings produce no phase variations of the currents which flow through them. Thus temperature compensation is unnecessary, and ambient temperature variations from −70 degrees Fahrenheit to +140 degrees Fahrenheit make no readable change in indications. The complete chain of goniometers, mechanically coupled through reduction gears and supplied with the proper energy from the associated circuits, permits accurate placement of the transmitter pulse to within 1/100 of one degree of any position throughout the 100-mile repetition rate cycle. This is accomplished without excessively close tolerance specifications on any parts of the equipment. The twin rows of goniometers can be seen in the bottom view of the timing and indicating unit chassis in Figure 6.

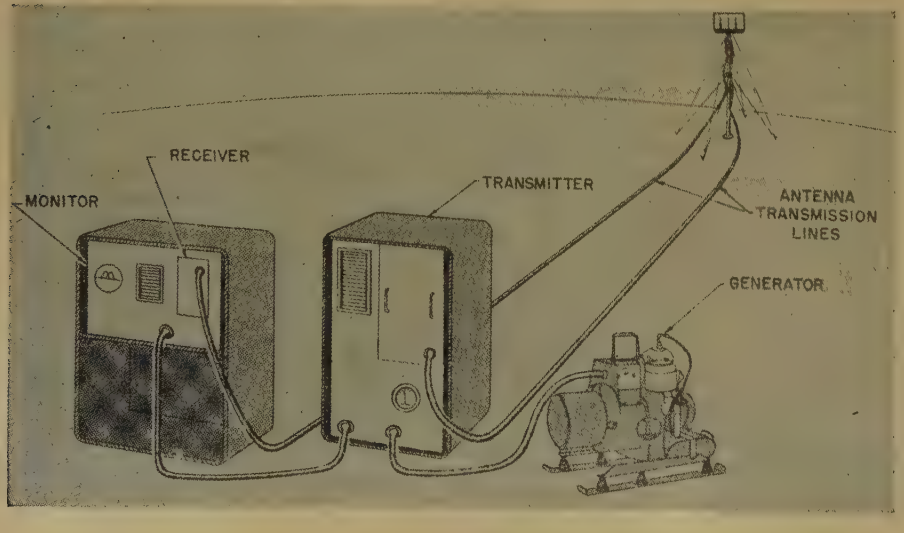
The two timing devices are completely independent of each other, and the transmitter control is commutated between them approximately ten times per second. During the commutation cycle, the frequency of the transmitter is altered so that all pulses sent out in accordance with timing derived from the left-hand control are on one wave length, while those from the right-hand control are on another. Thus each of the two ground station receivers can pick up and retransmit the signals meant for it and discriminate against those intended for the other. The commutation process also switches the gain control function of the plane receiver alternately between two potentiometers, each of which can be adjusted separately. This allows for wide differences between the strengths of signals received at the plane from the two ground transmitters, as is the case when operating close to one but remote from the other.

One other function of importance is performed during the commutation cycle. In order to operate many planes in the air at once and have them all use the same pair of ground stations, it is necessary that transmission from a ground station to one plane not interfere with the proper operation of Shoran equipment in another. Since the repetition rate of Shoran pulses is the precise yardstick in terms of which the distances are measured, all planes utilizing a pair of ground stations simultaneously will be using that same yardstick. Thus it would be possible for the accurately synchronized indications from a ground station, meant for one plane, to be picked up by another and give the second plane crew an erroneous indication of their position. This possibility is obviated by an action of the commutator during a third portion of the one-tenth-second period of its cycle during which *no* transmissions occur. During this time, the repetition rate circuits of the timer are momentarily blocked off and then immediately allowed to resume operation precisely at the previous rate. The result is that no two plane equipments interrogating a common ground station can stay synchronized for more than a small fraction of a second, in spite of the fact that their interrogation rates are precisely the same.

The trace on the cathode ray tube is circular. There were two reasons for this choice. A 3-inch tube will accommodate a $7\frac{1}{2}$-inch circular trace compared to a $2\frac{1}{2}$-inch linear sweep. Also a circular sweep is continuous without breaks in its continuity while the spot returns to its starting position. A throw of a switch changes the deflection rate of the circular pattern from a 1- to a 10- to a 100-mile scale. For navigational purposes, out to the initial point of a bomb run, the 100-mile scale is adequate. The use of this scale allows the operator to effect coincidence of the received and marker pulses to well within the ±5-mile interval over which they are visible on the ten-mile scale. He can then repeat the process and switch to the one-mile scale. Thereafter, if the data are kept up-to-date, he need not return to the 10- or 100-mile scales, since the complete information is constantly available on the mileage dials. All traces on the oscilloscope are blanked out when using the 1- or 10-mile scales except for the particular 1- or 10-mile interval containing the T_0 time. Actually, the T_0 marker is traced on the screen for the 1- and 10-mile scales during an unused portion of the 100-mile repetition rate. Thus, the received pulses, which are outward for the left-hand mileage controls and inward for the right-hand dials, appear to be superimposed upon the marker deflection rather than to mingle with it and thus cause confusion. Matching is correct when the left-hand (leading) edges of all pulses are coincident.

The plane receiver controls are on the separate oblong panel extending upward

Figure 8. Units and cabling of ground station



slightly to the right of center in Figure 2. The receiver can be withdrawn and replaced in a matter of only a few seconds in case of defective operation. All connections, with the exception of the antenna, are made through sliding contacts and are thus automatically broken and reestablished when the unit is removed and replaced. One of the filters for the forced air cooling system can be seen in the upper left-hand corner. Figure 7 shows a receiver withdrawn from its compartment.

Figure 3 shows the plane transmitter which generates the signals radiated under control of the timing and indicating unit. It is usually mounted in some out-of-the-way position in the airplane, since it has no adjustments that need attention while in flight. "Start," "stop," and "standby" operation are remotely controlled by relays actuated in

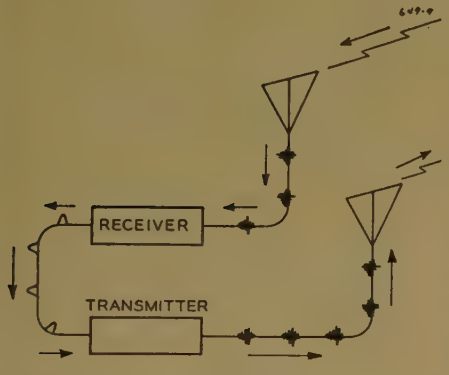


Figure 9. The function of the ground station
Pulses received from the airborne transmitter are amplified and retransmitted to the plane

conjunction with those of the timing and indicating unit.

The peak power input to the transmitter tubes is approximately 50,000 watts, and a plate circuit efficiency of about 30 per cent is realized. The low operating duty cycle results in an average plate power consumption during operating periods of only 30 watts. Positive plate, or B voltages, are not used on the two push-pull self-oscillating transmitter tubes which derived their plate energy entirely from the 5,000-volt positive swing of the secondary of the pulse modulation transformer. The two transmitter frequencies, which are commutated during operation, are adjustable in the region of 220 to 260 megacycles. Usually they are separated by from five to ten megacycles, but they must correspond to the respective ground station receiver frequencies. Commutation of the radiated wave length is made possible by the action of a solenoid-operated vacuum-contact short-circuiting bar on the resonant grid line of the oscillators. The adjustment of the position of that bar and of all other grid and cathode line connections is controlled by screw driver adjustment through the front panel. The plates of the oscillators are at radio frequency ground potential.

The antenna for radiating the transmitter power is of the stub type and is mounted vertically either above or below the fuselage. An attempt is made to produce as nearly an omnidirectional pattern of vertically polarized radiation as possible. The antenna proper is somewhat unconventional. It consists of a center rod extending approximately 1/8 wave length beyond a 1/8-wave grounded concentric sleeve. The entire assembly is about 12 inches in length. In operation the antenna has relatively broad band characteristics and produces a low order of standing wave ratios on the 50-ohm transmission feed line throughout the transmitter frequency range.

The plane receiving antenna is of the same type of construction but is somewhat shorter in over-all length, since it receives signals from ground stations which transmit on approximately 310 megacycles.

Lengths of interconnecting cables between units and between the transmitter and receiver and their respective antennas have an effect on the total time spent by pulse energy in traversing all of the plane equipment circuits. Therefore, each plane installation must be compensated by a process which involves the sending of test signals around the complete loop and making the necessary corrections in the position of the marker pulse. Actually, the adjustment is not made to zero but to a standard negative value of distance which compensates for all of the fixed delays in the ground station as well as for those in the plane. Thus, if the inter-

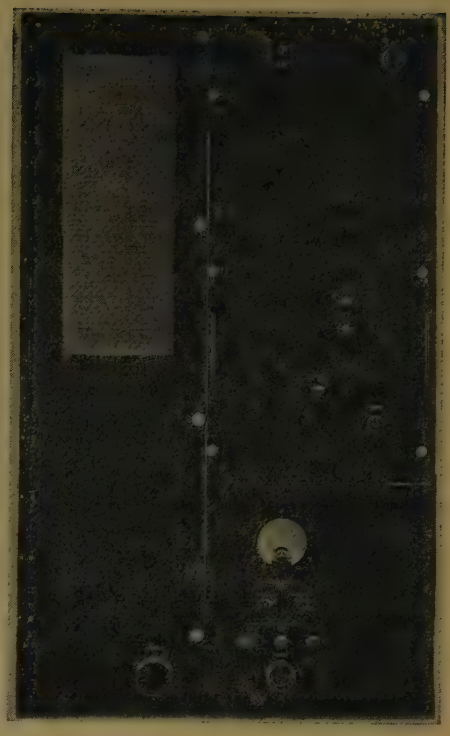


Figure 11. Panel of ground station transmitter

vening path between the plane antennas and those of the ground station were of zero length, a pulse initiated in a timer chain reading zero would pass through the plane transmitter, all the ground equipment, and finally arrive back at the plane receiver in time to appear on the cathode ray tube exactly superimposed upon the T_0 marker. The point which bisects an imaginary line drawn between the plane transmitting and receiving antennas is that from which all measured distances are indicated.

The Ground Station Equipment

A ground installation consists essentially of four principal units. These are the receiver-monitor, the transmitter,

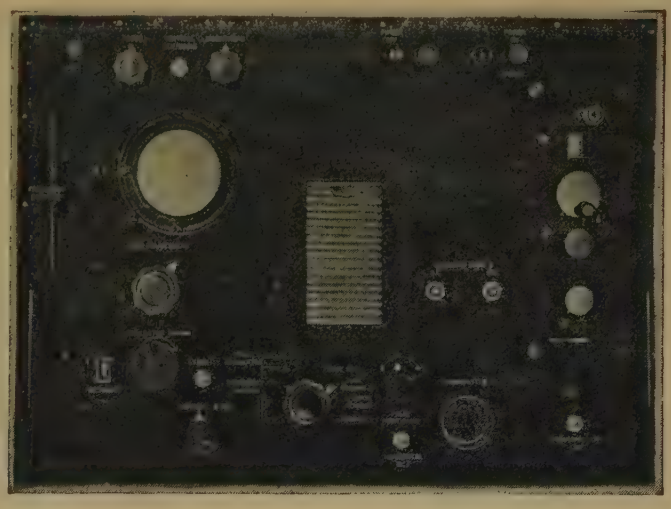


Figure 10. Panel of ground station monitor-receiver

the antenna arrays, and the gasoline-driven power supply. See Figure 8. The complete equipment is air-transportable and can be flown to a known location and put into operation within 90 minutes after arrival.

The primary function of the ground equipment is to receive, reshape, and retransmit all pulses arriving at the location on the particular wave length to which the receiver is tuned. See Figure 9. The elapsed time between the arrival of a signal at the receiving antenna and the radiation of the resultant pulse from the transmitting antenna must be accurately adjusted to a fixed standard time interval. That adjustment, as well as others necessary for proper operation of the installation, is performed with the aid of the monitor portion of the monitor-receiver unit. This is shown in Figure 10.

The oscilloscope in this piece of the equipment facilitates adjustment of frequency dividers which regulate the timing of standard repetition rate radiations independently of any received signals. These are under the control of an extremely accurate 93, 109-cycle temperature-controlled crystal and allow a plane equipment operator to make a slight adjustment in the frequency of his crystal if temperature or other conditions have caused excessive drift. Continuous radiation of standard pulses from the ground also enables the plane operator to tell whether or not he has sufficient altitude to be within range of that station even before he starts transmitting.



Figure 12. Ground station antenna assembly

The adjustment of the total delay interval to the standard value is made by varying the number of delay line sections in the circuit until the loop-delayed pulse matches another which is passed only through a standard delay network.

The receiver, shown on the right-hand side in Figure 10, is identical to, and interchangeable with, the receiver in a plane equipment. It has a continuously adjustable tuning range between 210 and 320 megacycles.

The transmitter, shown in Figure 11, is very similar to that used in a plane. However, it has a much higher duty cycle, when serving a large number of planes, and the modulator circuits are, therefore, made heavier to handle that load. Whereas the average plate power in a plane transmitter is 30 watts during operation, the ground transmitter may be developing as much as 400 watts. Each develops a peak input power of about 50 kw.

The transmitting and receiving antennas are shown in Figure 12. The reflectors give power gain of approximately eight to one in the forward direction with a horizontal coverage angle of about 70 degrees to the half-power points. The whole assembly is supported on a 50-foot sectionalized plywood mast.

The gasoline-driven generator delivers about 1,500 watts at 115 volts, 400 cycles, and approximately 400 watts at 28 volts direct current.

Operational Results

The use of blind Shoran bombing over the battle fields of Europe showed that it was capable of equalling visual bombing in accuracy under normal conditions and surpassing it when the latter suffered from target identification difficulties. On occasion, rolling barrages of fragmentation bombs were laid only a few hundred feet ahead of our own advancing troops. The demoralizing influence of such a barrage, from planes completely hidden in a clouded sky, was tremendous. Such operations with equipment of less precision than Shoran would have been foolhardy.

TRANSACTIONS SECTION

Preprint of Corresponding Pages From the Current Annual AIEE Transactions Volume

Application of the Betatron to Practical Radiography

J. P. GIRARD
ASSOCIATE AIEE

G. D. ADAMS
NONMEMBER AIEE

Synopsis: The development of the betatron, which accelerates electrons by magnetic induction making possible the production of higher energy X rays than is practical by the direct application of the accelerating potential, has extended the range of X rays indefinitely, the only limit being the size of the machine. Tests with the betatron have shown that the best energy for medical and radiographic use is 20 mev (million electron volts). The development of this machine from a physics laboratory instrument to an industrial machine is described, as well as the radiographic properties of the X rays produced.

THE FIRST successful type of betatron, invented by Doctor D. W. Kerst at the University of Illinois, is an induction electron accelerator which means that electrons are accelerated by magnetic induction instead of by direct application of high potential. The result is that the voltage insulation is not the limiting factor in the acceleration of the electrons, and they can be given energies not previously obtainable by any other man-made means.

In the betatron an alternating magnetic field holds the electrons in a stable circular orbit within an evacuated annular chamber called a "donut," and the increasing field produces a force on the electrons which accelerates them to high velocities. A special field contour is necessary to hold the electron in its orbit as its mass changes relativistically with increasing velocity.

Development of the Theory

The idea of acceleration of electrons by magnetic induction was the subject of experiments conducted by many scientists. J. Slepian stated the general principle in his patent[1] issued in 1927, but he apparently did not develop his calculations to the point of producing a satisfactorily workable machine. Wideroe[2] was the first to show that the necessary field condition for a stable equilibrium orbit is $\phi_0 = 2\pi r_0^2 H_0$ where

r_0 = radius of equilibrium orbit
ϕ_0 = flux within orbit
H_0 = field at the orbit

This was verified by Walton[3] and later referred to by Steenbeck[4] as the 1:2 relation as the flux within the orbit is twice as much as would be obtained if the magnetic field were uniform in space. Steenbeck stated that the field in the region of the orbit should be $H \propto 1/r^n$, where $0 < n < 1$. Kerst and Serber[5] verified the calculations of Wideroe and Walton and also developed the equations for transient phenomena in the magnetic field. Kerst[6] was the first to place an injector in the magnetic field for supplying electrons at a substantial initial velocity to the orbit. Several of the earlier investigators had tried to inject electrons from outside the magnetic field tangentially to the orbit but had not been successful. Steenbeck placed a heated filament in the magnetic field, but provided no means of directing the electrons emitted or of giving them an initial velocity. The injector as developed from the one used by Kerst is shown in Figure 1, and consists of a heated filament, grid, and surrounding plate so that the stream of electrons is ejected by a negative pulse applied to the filament (the plate is grounded to prevent its disturbing the orbit by its electrostatic field). The grid is a solid piece of metal used to minimize the electron bombardment of the plate and is connected to one side of the filament.

On the basis of the calculations made by Kerst and Serber, Kerst[6,7,8] was able to construct the first betatron to operate successfully in a practical manner.

Kerst and Serber also calculated the paths of electrons which would oscillate about the equilibrium orbit while the focusing forces are damping the oscillation. From their calculations they could predict the best value for n so that the most electrons would miss the injector on the later revolutions and be focused to the orbit.

The Kerst type of betatron is essentially a three-legged transformer with the accelerating field formed in an air gap by

Paper 46-54, recommended by the AIEE committees on electronics and industrial power applications for presentation at the AIEE winter convention, New York, N. Y., January 21–25, 1946. Manuscript submitted November 21, 1945; made available for printing December 31, 1945.

J. P. GIRARD is application engineer, transformer sales division, Allis-Chalmers Manufacturing Company, Milwaukee, Wis. G. D. ADAMS is assistant professor, department of physics, University of Illinois, Urbana, Ill.

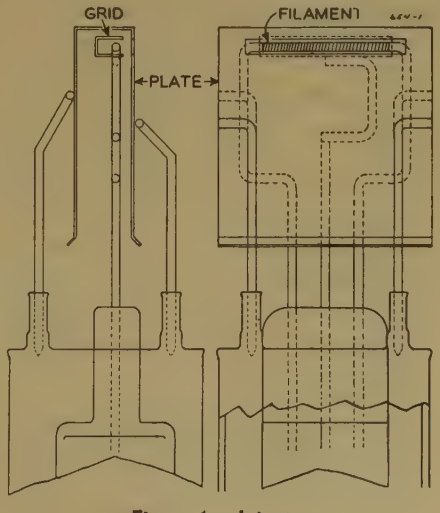
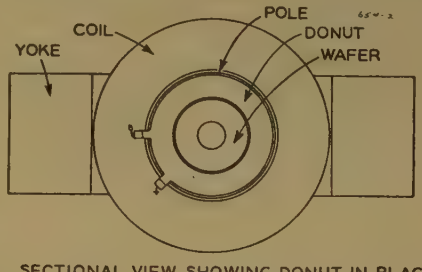
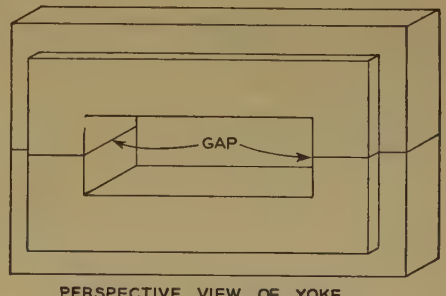


Figure 1. Injector



SECTIONAL VIEW SHOWING DONUT IN PLACE



PERSPECTIVE VIEW OF YOKE

Figure 2. Betatron magnet

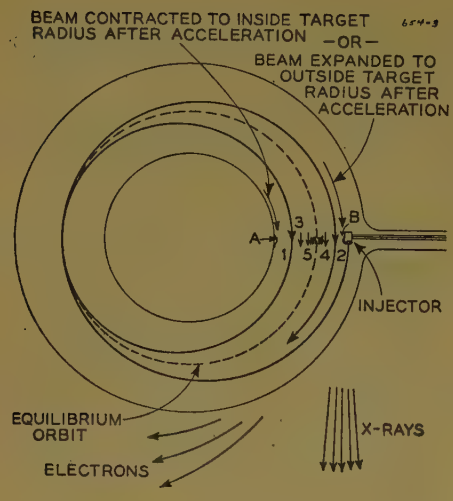


Figure 3. Sectional view of donut showing positions of injector and targets as well as electron paths

radially symmetrical poles in the center leg as shown in Figure 2. Coils shown provide the necessary flux when a voltage is applied to them. In practice a sinusoidal voltage is applied as this is the simplest means of providing the time-increasing field, although only one quarter of each cycle is utilized in the acceleration of the electrons. The donut and injector are shown in position in Figure 3 which also illustrates the various electron paths during focusing, injection, and expansion.

In operation, electrons are injected when the flux wave is at point A as shown in Figure 4. They are accelerated as the flux increases until point B is reached where they are caused to deviate from the equilibrium orbit by either of the two following means: (1) the center of the pole is allowed to saturate with the result that $2H_0$ increases faster than $\phi/\pi r_0^2$ so that r_0 becomes smaller and the electrons spiral in until they strike a target, such as A in Figure 3; or (2) a pulse of current is sent through a turn of wire on each pole face in such a direction that the flux caused so upsets the equilibrium condition

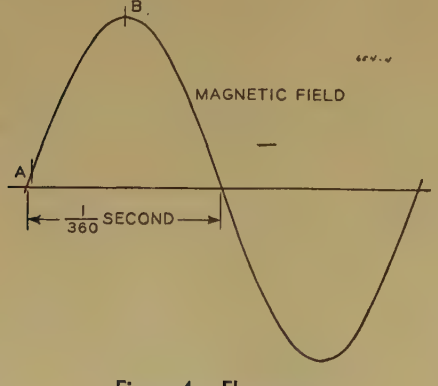


Figure 4. Flux wave

that r_0 becomes larger causing the electrons to spiral out and strike a target (B in Figure 3) mounted on the back of the injector. Kerst, in his original machine, used the first method as it is simpler and does not require a carefully timed electronic tube circuit as does the beam expansion method.

The Production of X Rays

When the high energy electrons strike the target, X rays are produced, the greatest intensity of which emerge from the donut in a narrow cone in the direction which the electrons are traveling at that time. As the conversion of the kinetic energy of the electrons to X rays is higher for high energies than low (theoretically 65 per cent of the electron energy is converted to X rays at 20 million electron volts as compared to a few per cent at

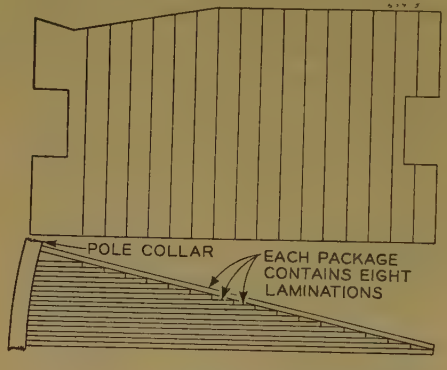


Figure 5. Details of pole laminations

1 million electron volts) very little of the energy is absorbed by the target, so that the target remains relatively cold and does not deteriorate with use.

Development

After successfully operating his first betatron which had a maximum energy of 2.3 million electron volts, Kerst was granted a leave of absence from the University of Illinois to supervise the construction of a 20-million-electron-volt betatron.[9] This betatron was loaned permanently to the University of Illinois for use under his direction. This and subsequent 20-million-electron-volt betatrons used expansion coils to cause the orbit to spiral out as this method results in higher maximum energy and higher X-ray output.

In order to determine whether or not the X radiation produced by the betatron was suitable for industrial use in thick section radiography, the Office of Scientific Research and Development ap-

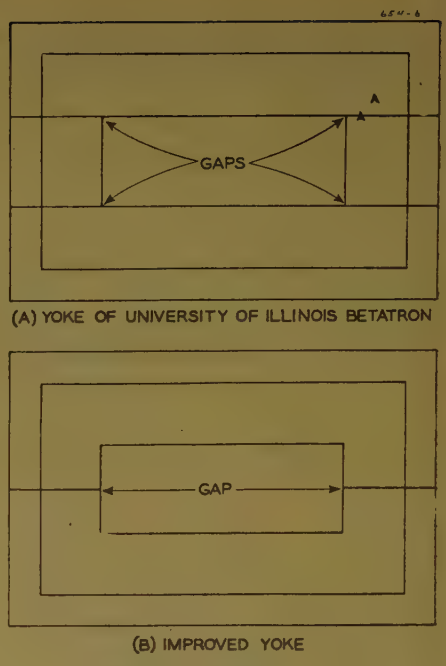


Figure 6. Betatron yoke

pointed Kerst as official investigator and allotted funds for the work. When the investigation showed that the 20-million-electron-volt betatron could be used to great advantage in thick section radiography, OSRD authorized and financed the further work necessary to develop the betatron for industrial use, including the building of one machine. Kerst and his staff from the University of Illinois then obtained the co-operation of the Allis-Chalmers Manufacturing Company in this development in order to make the betatron available to war projects. The general details, such as size of pole and dimensions of yoke, are practically the same as described by Kerst with the major improvement being made in the mechanical construction of the betatron, and in the development of the donut.

One of the major improvements made in this development was in the improved construction of the pole. The simplest way to construct a radially symmetrical pole is by making pie-shaped sectors of various lengths as shown in Figure 5 with several sectors making a complete pole. In the first 20-million-electron-volt betatron, these laminations were held together by a thermal setting resin which proved in operation that it was not strong enough to hold against the magnetic forces present, and gradually the pole developed short circuits until the beam was disrupted and the X-ray yield materially decreased. By careful welding and insulating, a very rigid pole was constructed. One set of these poles has been installed on the University of Illinois machine for over a year, and has been operated as many hours as

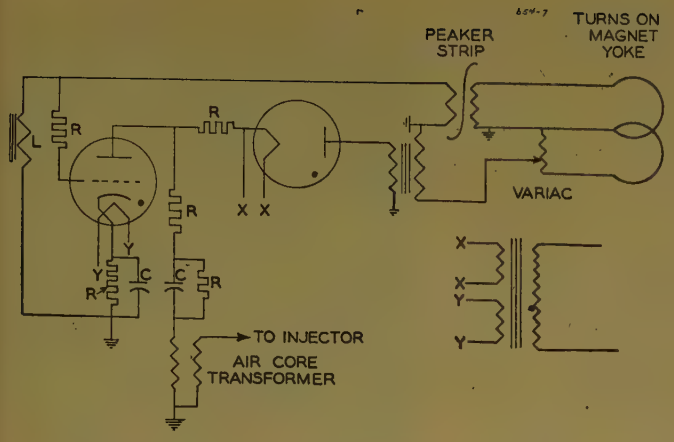


Figure 7. Injector circuit

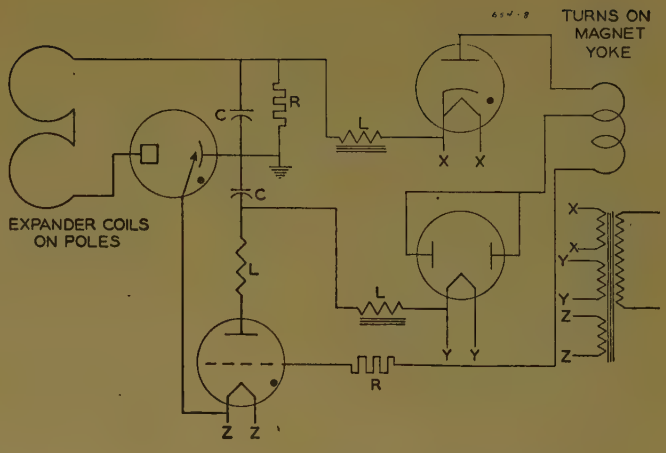


Figure 8. Expander circuit

the original set, but shows no signs of going bad. In fact, the yield is now higher than ever was obtained with the original machine. Also, the pole laminations were cut on a die which assured a very smooth and radially symmetrical pole.

The coils on the commercial machine are held very rigidly in place and air ducts provided to aid in cooling. Because of the high leakage flux caused by the air gap for the accelerating field, the turns must be stranded with each strand insulated from all others by Formvar varnish and all layers wound in the same direction in order to keep induced voltages and eddy currents at a minimum.

The yoke on the University of Illinois machine was made in four pieces as shown in Figure 6A with only the weight of the steel holding them in place. By assembling in two halves as shown in Figure 6B, a much better construction was possible, and by the use of guide rods, the alignment of the poles could be made at the time of assembly with the assurance that the poles could be separated for installation of a donut and the alignment would always be the same. Then, by installing lifting jacks operated by a gear motor with chain and sprocket system the top half of the betatron could be lifted without the use of an auxiliary hoist. The construction of the yoke in two halves also will simplify the clamping necessary to make possible the mounting of the betatron for rotation of the beam should it be desired.

One of the most interesting developments made was in the manufacture of donuts. The first donuts made for the University of Illinois 20-million-electron-volt machine consisted of two short glass cylinders forming the outer and inner wall with two glass washers forming the top and bottom. These glass parts were waxed together with tubes waxed on to hold the injector and for the pump stem. The sections of glass forming the inner surface of the donut had to be sand blasted so that a suitable conducting coating could be applied. The coating was necessary so that the stray electrons not captured by the beam and striking the donut walls would be drained off and would not be allowed to build up static charges which would disturb the beam; and, at the same time, the coat must be of high enough resistance that the eddy currents induced would not disturb the beam or heat the donut too much. The main trouble with the waxed donut was that the tube could not be evacuated and then sealed off, necessitating a pumping system. Also, owing to the heat generated by the injector filament, it was necessary to blow air on the wax close to the injector stem to prevent softening of the wax with resulting leaks.

To solve the donut problems, the Ceramic Engineering Department at the University of Illinois, under a contract with OSRD, was able to develop a porcelain which was capable of having glass sealed to it and was vacuum tight. Moreover, this porcelain donut could be made by coreless casting which resulted in a fairly inexpensive product. Some development was necessary in order to coat the inside of this tube and make the glass seals, but the difficulties were overcome and donuts were produced, evacuated, and sealed-off which have been giving very satisfactory service. This resulted in the elimination of a high-vacuum pumping system on the betatron which would have been the cause of much trouble in the successful operation of betatrons in industrial radiography.

A study was made of the injector and the design and structure were improved

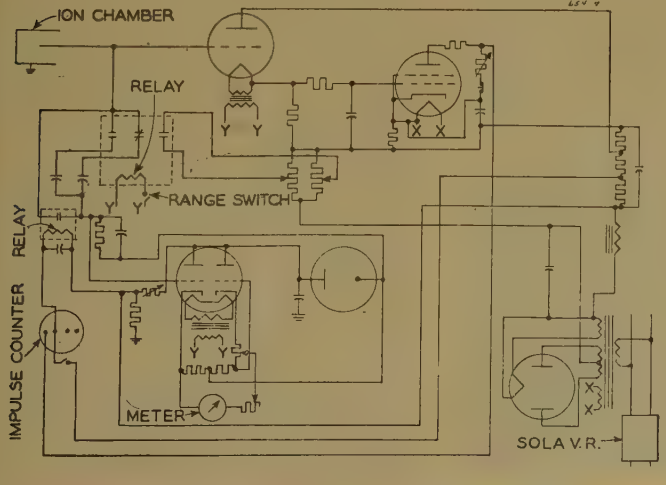


Figure 9. Exposure control circuit

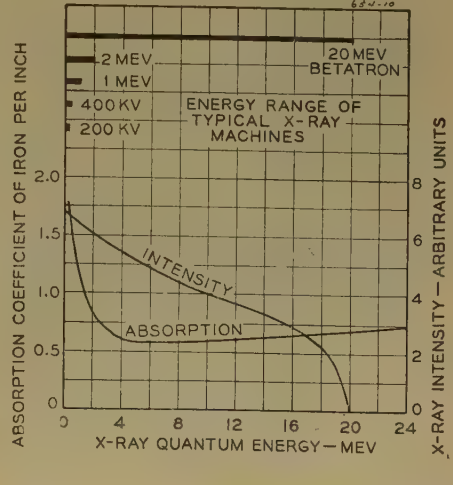


Figure 10 (right). Absorption curve for steel and theoretical X-ray spectrum at 20 million electron volts

so that an increased yield was realized. The injector, which is an electron gun, should not have too large a distance between the filament and the part of the injector closest to the orbit so that as many electrons as possible will miss the injector on successive revolutions, and be captured by the orbit. In addition, the injector must be sufficiently rigid so the vibration caused by the alternating magnetic field will not shake it apart.

The target developed made possible a focal spot of the order of 0.010 inch high. This small focal spot is one of the outstanding features of the successful betatron. If the electrons hit the back of the injector with no special target, the focal spot will be of the order of 0.050 inch high. The width in both cases is so small as not to be measurable. Calculations have been made which show that the difference in successive revolutions of the electrons as they spiral out is of the order of 10^{-4} centimeter so the width of the focal spot should be of the same order.

The circuits of producing the injection and expansion pulses described in Kerst's paper[9] were improved with the idea of providing a more satisfactory unit for industrial use. For example, all batteries were eliminated and tubes were replaced by others having more reliable operating characteristics to reduce to a minimum the variables for obtaining maximum yield. The present injector and expander circuits are shown in Figures 7 and 8, respectively. A very convenient additional circuit is the exposure control circuit (Figure 9) whereby the exposure in Roentgen units can be set on an impulse counter and the betatron will be shut off when it has produced the required amount of X rays.

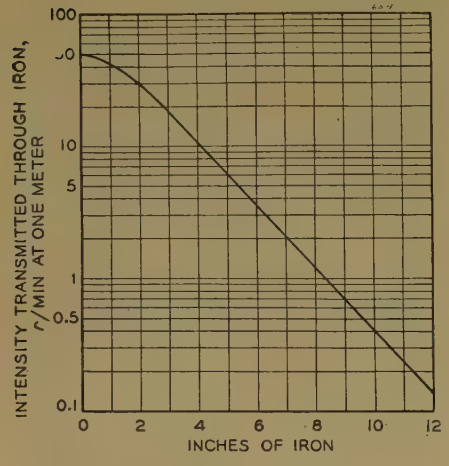


Figure 11. Transmission curve for steel at 20 million electron volts

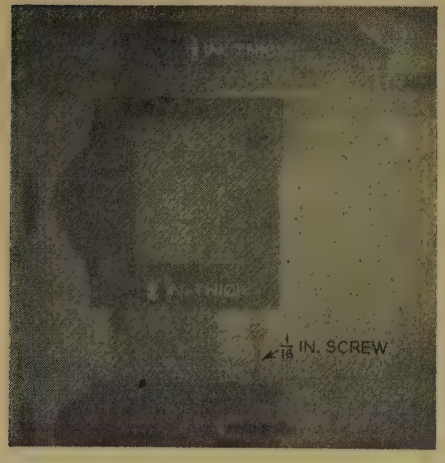


Figure 12. Radiograph of vernier caliper between two one-inch slabs of steel with jaws open 0.010 inch

Enlargement on negative was 3.3

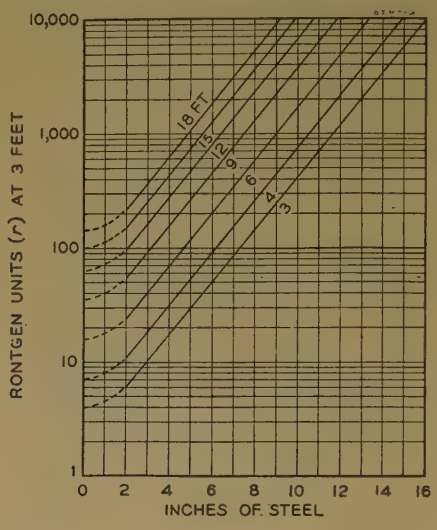


Figure 13. Exposure chart for 20-million-electron-volt X rays with Eastman industrial film, type A, 0.040-inch front lead screen, density of 2

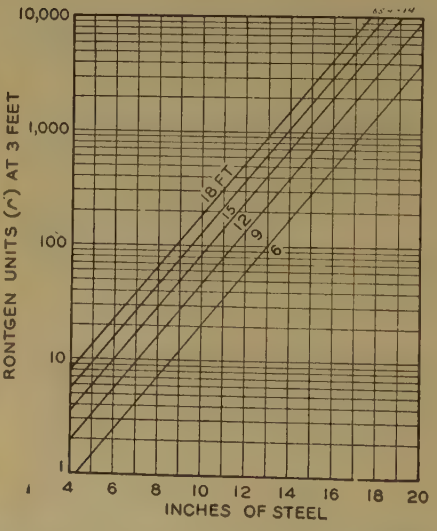


Figure 14. Exposure chart for 20-million-electron-volt X rays with Eastman industrial film, type F, 0.030-inch front lead and special intensifying screens, density of 2

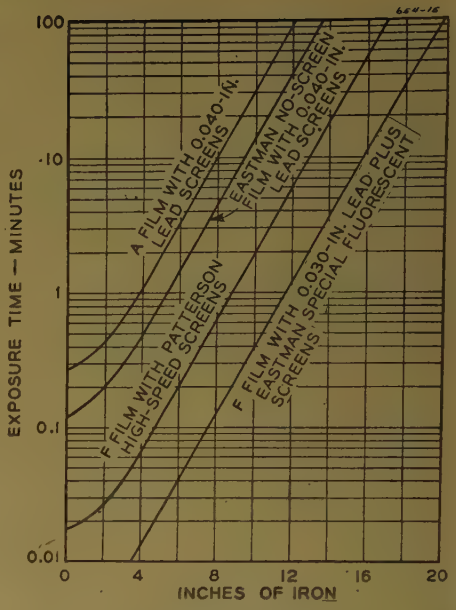


Figure 15. Chart showing comparison of different films and screens

Radiography

The betatron makes possible the radiography of thick section steel, bronze, and other heavy metals. In Figure 10 the absorption coefficient curve for iron is shown together with the theoretical intensity distribution spectrum of X rays produced by the 20-million-electron-volt betatron. From these two curves, one can see that most of the X rays produced are in the region of low absorption of steel (the absorption curves for other heavy metals are similar). In other words, the X rays in the approximate range of from 3 to 20 million electron volts are the most penetrating, and the absorption curve is nearly constant over this range which is the region of most of the X rays produced by the 20-million-electron-volt betatron. This explains the straight line transmission curve shown in Figure 11 after one or two inches of steel.

Another factor influencing the selection of 20 million electron volts as the best energy for thick-section radiography was that by going to higher energies the secondary X rays produced as a result of the absorption of the primary rays would be more penetrating than the primary rays and tend to result in a diffused image. This fact can be explained by an analysis of X-ray absorption. Unfortunately, the absorption of X rays above one million electron volt generally results in the production of electron pairs with each electron of the pair produced having on the

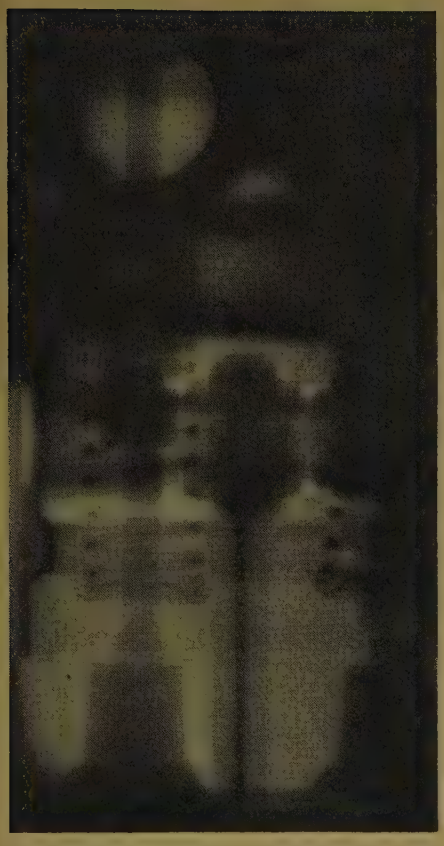


Figure 16. Section of radiograph of Ford model T motor. Note the damaged valve stem

average nearly one half the energy of the primary ray. These high-energy electrons lose their energy with the accompanying production of X rays which, because of the lower energy, may be more penetrating than the primary rays. The secondary rays travel in the general direction of the primary, but there is some divergence which affects the definition on the film. The 20-million-electron-volt betatron tests show that a comparatively small part of the density on the film is caused by secondary rays. With higher energy betatrons, tertiary, and higher order X rays would be produced which would be more divergent and penetrating than the secondary rays and, therefore, would produce a more diffuse image on the film.

The choice of a lower energy betatron was eliminated as the intensity for different energies at the same frequency goes as nearly the fourth power of the energy. At 10 million electron volts and 180 cycles the intensity would be 1/15 that at 20. This would necessitate a much higher frequency which would mean increased heating and higher power requirements. The heating would necessitate liquid cooling and the advantage of a lower weight machine at lower energies partially would be lost. At a lower energy output a smaller percentage of the X rays would be in the region of low absorption so that the exposure would be much longer for the same intensity. Tests at 10 million electron volts show that the fraction of density on the film contributed by the secondary rays is considerably larger than that at 20 million electron volts.

Another advantage of 20-million-electron-volt X rays is that an absolute sensitivity is obtained. This means that the size of minimum detectable flaw is the same regardless of the thickness of steel being radiographed. A 1/32-inch flaw was displayed with equal clarity through various thicknesses of steel from 2 to 12 inches on Eastman type *A* film.

In 20-million-electron-volt radiography, no blocking is necessary for variations in thickness of the specimen or around the outline. In fact, outlines may be less well defined when blocking is used.

Because the large angle of back-scattered radiation is detrimental to the image, no lead is placed behind the film. A thickness of 0.040 inch is used in front of the film for the best results. Thicknesses of from 0.010 to 0.020 inch will result in about 50 per cent more density for a given exposure, but the detail will be less clear so that it is not recommended.

The great penetration of 20-million-electron-volt X rays makes possible the study of great variations of thickness on the same radiograph. Radiographs have been taken on which differences of thickness of over six inches of steel were examined. The penetration of these X rays implies that it is difficult to detect small flaws in specimens of low density or small atomic number.

The small focal spot inherent with the betatron and not with other X-ray machines is nearly the ideal point source. The natural focal spot is 0.050 inch high and less than 0.005 inch wide. By using a special target which was developed, the height is reduced to 0.010 inch. This focal spot makes possible the enlargement of the specimen on the radiograph by increasing the specimen-to-film distance. Figure 12 shows a radiograph of a vernier caliper between two 1-inch slabs of steel with the jaws open to 0.010 inch. With a magnification of 3.3 this opening could be seen.

Figures 13 and 14 show exposure charts based on different films and screens. The exposure is given in Roentgen units *r* and on the basis that the industrial units built have given about 75 *r* per minute, the exposure times can be calculated. Figure 15 gives a comparison between different films and screens.

With the pronounced beaming of the X rays (characteristic of high energy radiation) for full utilization of the film, a good rule in the taking of radiographs is to have the target to film distance at least five times the major dimension of the film.

To show the latitude and detail of 20-million-electron-volt radiographs, Figure 16 is a radiograph of a section of a model T Ford engine. Figure 17 is a radiograph of a steel forging which showed defects that could not be determined otherwise except by very long exposures or machining and testing.

The betatron has increased to at least

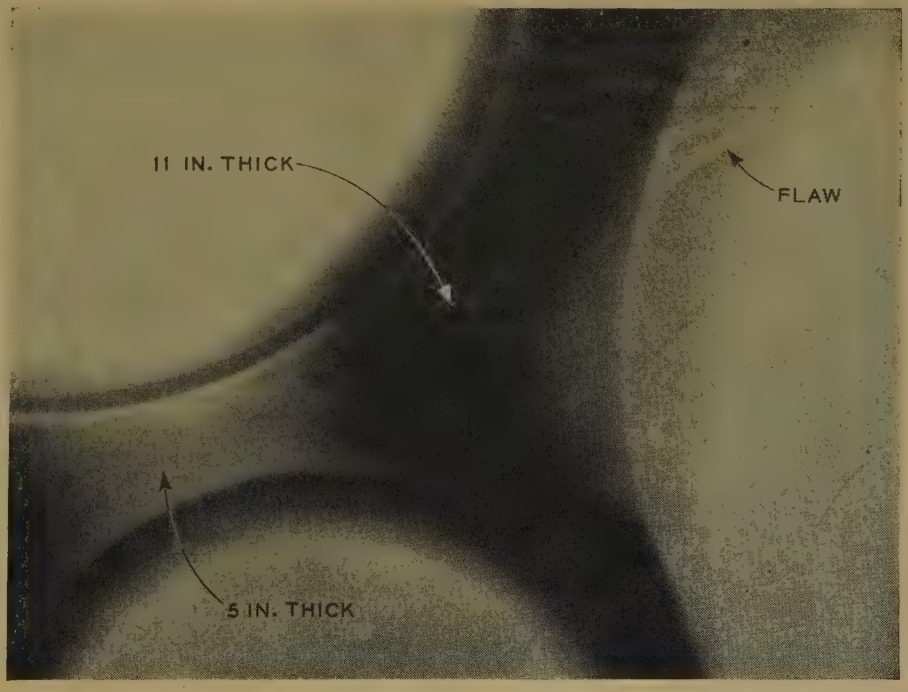


Figure 17. Section of radiograph of steel forging revealing a flaw

Application and Performance of Electronic Exciters for Large A-C Generators

H. A. P. LANGSTAFF
FELLOW AIEE

H. R. VAUGHAN
MEMBER AIEE

R. F. LAWRENCE
ASSOCIATE AIEE

Synopsis: Power rectifiers have proved themselves as efficient and reliable converters of a-c to d-c power for many industrial applications. They also have been used to a limited extent as exciters for synchronous motors and condensers. This paper discusses the requirements of rectifiers when used to excite large a-c generators and presents the results of tests made to determine performance under various operating conditions. The results cover preliminary tests that were made on a laboratory model in addition to extensive and more complete tests on an electronic exciter now installed in the Springdale generating station of the West Penn Power Company. The electronic exciter was designed to serve eventually as the main exciter for an 81,250-kva 3,600-rpm turbine generator just installed, but it is now supplying excitation to a 47,100-kva 1,800-rpm turbine generator. Switching arrangements are provided for exciting either unit from the electronic exciter or from an existing motor-driven exciter.

SINCE the introduction of the metal-tank type of power rectifier, particularly the single-anode type,[1] the application of rectifiers in the field of power conversion has expanded to include practically every type of industry that requires d-c power.[2] Years of experience with many thousands of kilowatts of installed capacity testify to their reliability and efficient performance. With this background of usage, power rectifiers naturally have received consideration as exciters for rotating machines. A limited number have been used to excite synchronous motors, synchronous condensers, and one or two small generators. However, there has been a hesitancy in applying them as exciters for large a-c generators because of a natural reluctance to risk anything that might jeopardize the reliability or performance of a machine as important as a large a-c generator.

Rotating exciters have been used with success for many years, whereas the ability of a power rectifier to meet the exacting requirements of a power station generator has not been demonstrated by operating experience. It is the purpose of this paper, therefore, to discuss the application of electronic exciters to large a-c generators, to present the results of comprehensive tests that were made to demonstrate the performance of an electronic exciter under severe operating conditions, and to describe an actual installation.

Paper 46-74, recommended by the AIEE committee on power generation for presentation at the AIEE winter convention, New York, N. Y., January 21–25, 1946. Manuscript submitted November 21, 1945; made available for printing December 11, 1945.

H. A. P. LANGSTAFF is with West Penn Power Company, Pittsburgh, Pa.; H. R. VAUGHAN and R. F. LAWRENCE are central station engineers with Westinghouse Electric Corporation, East Pittsburgh, Pa.

Requirements

Large generators for power systems are capable of operating and are expected to operate months at a time without shutdown. They must maintain constant supply voltage under varying load conditions and must recover rapidly from disturbances caused by severe load fluctuations or system faults. The degree to which the generator meets these conditions depends in a large measure on the performance of its exciter, which must fulfill the following requirements:

1. It must be dependable and capable of operating without shutdown over long periods of time.
2. It should lend itself to ease of maintenance so that wearing parts can be maintained, tested, or replaced without shutting down the unit.
3. It must be capable of providing the required excitation during system disturbances when the generator may be called upon to supply a high reactive current output.
4. It must be capable of operating over a broad range of d-c voltage, from generator no-load to maximum output. Momentary values of field current considerably greater than full-load magnitude may be required.
5. It must respond rapidly to high excita-

---

20 inches, the thickness of steel and other heavy materials which can be radiographed satisfactorily, the maximum thickness depending on the minimum flaw to be detected or the detail desired.

Other Possible Uses

Any new X-ray machine is considered for its possible application to medical therapy. As the main development has been in producing a machine for industrial radiography, little time has been devoted to studying possible therapeutical application. However, one paper[10] has been published demonstrating the advantages of 20-million-electron-volt X rays and theory indicates that if the electron beam can be brought out of the donut, it would be more useful than the X rays. Both the 20-million-electron-volt X rays and electrons may be powerful weapons for the therapy of deep seated cancer.

From present indication, higher energy betatrons apparently would have no advantages in industrial radiography and their main use would probably be in connection with nuclear research. At the present time, Doctor Kerst is planning the construction of a betatron capable of producing at least 250-million-electron-volt X rays. Such a machine would enable physicists to produce radiation of cosmic ray energies in the laboratory.

References

1. United States patent 1,645,304, J. Slepian. October 11, 1927.

2. R. Wideroe, *Archiv für Elektrotechnik*, volume 21, 1928, page 387.

3. E. T. S. Walton, *Proceedings* of the Cambridge Philosophical Society, volume 25, 1929, page 469.

4. United States patent 2,103,303, M. Steenbeck. December 28, 1937.

5. ELECTRON ORBITS IN INDUCTION ACCELERATOR, D. W. Kerst, R. Serber. *Physical Review*, volume 60, July 1, 1941, pages 53–8.

6. ACCELERATION OF ELECTRONS BY MAGNETIC INDUCTION, D. W. Kerst. *Physical Review*, volume 58, 1940, page 841.

7. D. W. Kerst. *Physical Review*, volume 59, 1941, page 110.

8. ACCELERATION OF ELECTRONS BY MAGNETIC INDUCTION, D. W. Kerst. *Physical Review*, volume 60, July 1, 1941, pages 47–53.

9. 20 MEV BETATRON OR INDUCTION ACCELERATOR, D. W. Kerst. *Review of Scientific Instruments*, volume 13, 1942, pages 387–94.

10. EXPERIMENTAL DEPTH DOSE FOR 5, 10, 15 AND 20-MILLION-VOLT X-RAYS, H. W. Koch, D. W. Kerst, P. Morrison. *Radiology*, volume 40, February 1943, pages 120–6.

tion requirements, particularly where system stability is to be reckoned with.

6. It must be simple in structure and operation so that it does not complicate the over-all operation of the generating unit.

7. The cost, if higher, must be justified by advantages over other available methods of excitation.

Application Problems

An electronic exciter consists essentially of a power rectifier fed from an a-c source of power and provided with the necessary control, protective, and regulating equipment. The co-ordination of these component parts presents certain problems which must be dealt with in meeting the excitation requirements of large a-c generators.

A-C Power Supply

The rectifier may be self-excited, that is, its source of a-c power taken from the terminals of the a-c generator to which it is supplying excitation, or it may be excited separately, with its a-c power supplied from a separate source. Self-excitation makes possible unit operation with no dependence on a separate source of power for excitation. At the same time, it requires no rotating machine. However, it differs from a direct-connected rotating exciter in performance in that its output is affected by voltage dips at the generator caused by disturbances on the a-c system. The d-c ceiling voltage of the electronic exciter would decrease in proportion to the a-c voltage at a time when overexcitation is actually required by the generator. This may be compensated for in two ways. One way is to provide the rectifier with an abnormally high d-c ceiling voltage with full a-c voltage applied so that when the a-c voltage drops, the necessary d-c ceiling voltage still is obtainable. During normal operation, the d-c voltage would be reduced to normal by firing delay in the rectifier. It means a rectifier transformer somewhat larger than normal and a higher angle of firing delay during normal operation of the rectifier.

The second way to compensate for drops in a-c voltage is to provide series compensators to maintain a-c voltage on the rectifier transformer during momentary system disturbances. The primary of each of the compensators would be connected in series with one phase of the generator armature. The secondaries would be connected in series with the leads to the rectifier transformer so as to boost the a-c voltage supplied to the rectifier transformer in proportion to the reactive current fed from the generator. Either method of compensation is practical.

Separate excitation of the electronic exciter requires a reliable source of a-c power such as a separate station auxiliary generator or an auxiliary generator mechanically connected to the shaft of the main generator.

If used to supply power to the electronic exciter only, the shaft generator could be designed to feed the rectifier directly without an interposing rectifier transformer. This scheme would be comparable to a direct-connected exciter from the standpoint of being independent of system disturbances.

If the electronic exciter is self-excited, a means of supplying partial excitation during the starting-up period must be provided to get the machine up to voltage. Tests have shown that a d-c voltage of approximately 15 per cent of rated field voltage at full load applied to the field of the main generator, will start firing of the rectifier and cause it to build up voltage. This primer d-c voltage may be supplied from a small motor-generator set or from a battery connected to the generator field in parallel with the rectifier during the starting period. The motor-generator set or battery may be switched off automatically when the rectifier starts firing, by means of a reverse-current d-c relay set to detect feedback into the motor-generator set or battery.

Co-ordination of Protective Devices

The usual complement of rectifier protective devices should be included with an electronic exciter to protect against arc-back, misfiring, loss of cooling water, and so forth. Anode circuit breakers should be provided to clear an arc back on one or two phases without interrupting the d-c output of the rectifier and also to permit isolating one or more of the anodes for maintenance without interfering with the operation of the others. Three 2-pole anode breakers, one for each pair of diametrically opposite phases of a 6-phase rectifier, normally would fulfill these requirements. The cathode breaker should not have overload protection.

The rectifier transformer normally would be connected to its a-c power source through a circuit breaker or through fuses to protect against an internal short circuit. Whichever device is used must be selected so that it will not operate on heavy exciter overloads or clear ahead of the anode breakers on arc-back.

Regulation

The output voltage of an ignitron can be varied over a broad range by controlling the point on the a-c voltage wave at which firing occurs. This control can be

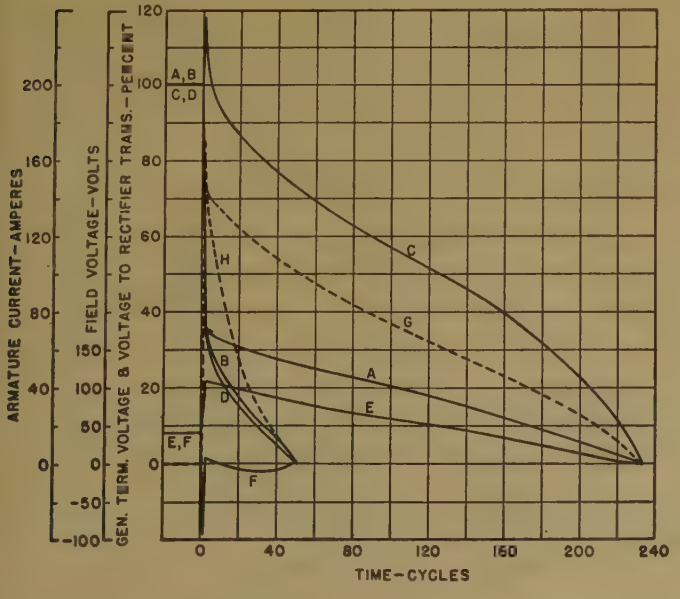


Figure 1. Three-phase fault applied on 100-kva generator through 12 per cent external reactance with generator self-excited

A, B—Terminal voltage, with and without compensator
C, D—Voltage to the rectifier transformer, with and without compensator
E, F—Field voltage, with and without compensator
G, H—Armature current, with and without compensator

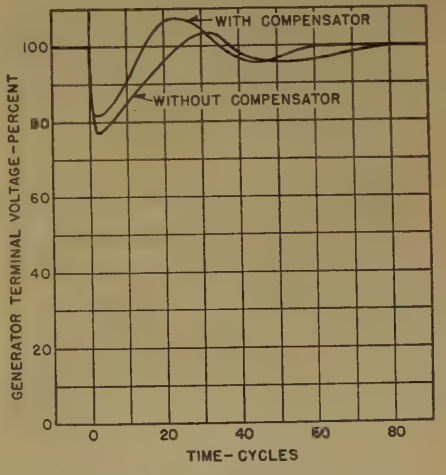


Figure 2. Application of 100 per cent reactive load on 100-kva generator, self-excited, with and without compensator

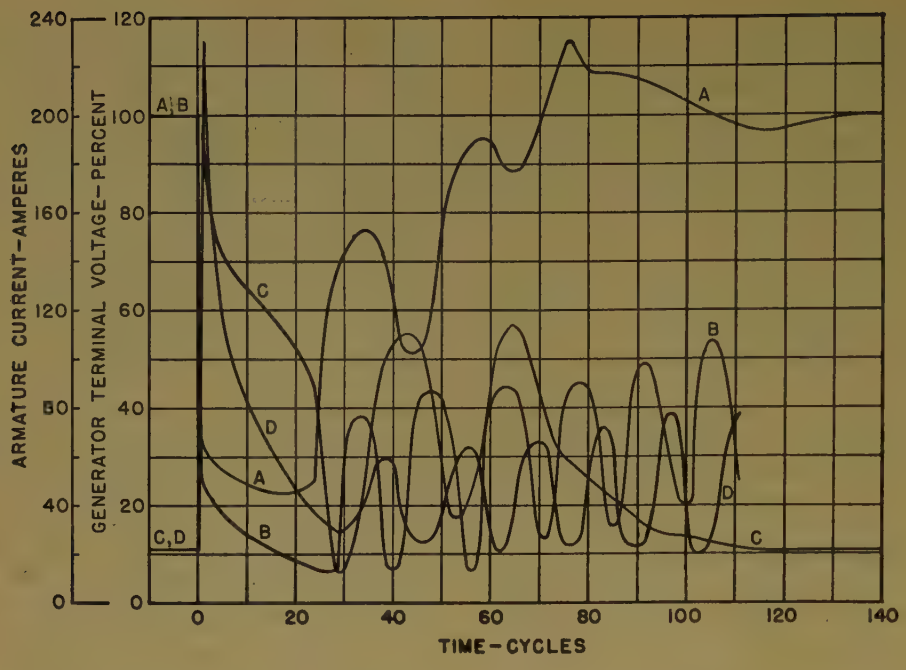


Figure 3. Three-phase fault applied one-third of electrical distance from 100-kva generator to motor, with generator supplying 40 kw at unity power factor through 22.7 reactance between generator and motor

A, B—Terminal voltage, with and without compensator

C, D—Armature current, with and without compensator

made broad enough to cover the full operating range of the generator without the necessity of a generator field rheostat. It can be accomplished automatically with a voltage regulator responsive to the terminal voltage of the a-c generator. Since the regulator controls only the firing circuit, it can be a low-energy device. No large rheostats or resistors are necessary.

The ability of an electronic exciter to build up to its ceiling voltage practically instantaneously makes it well suited where high speed of response excitation is necessary. However, this high rate of response is conducive to regulator hunting, which must be given particular attention in the design of the regulator.

Effect on Fault Current and System Relaying

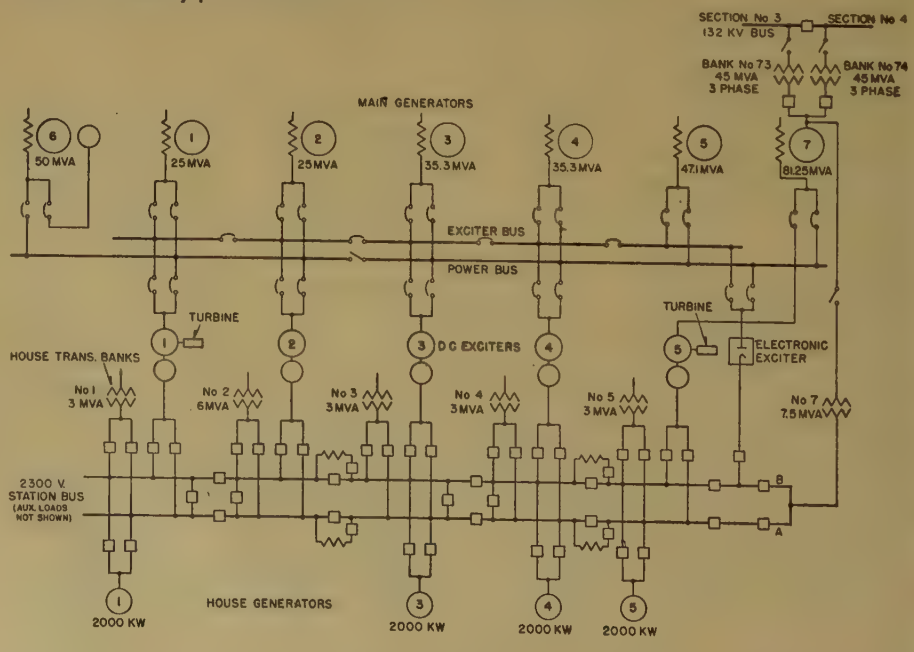
The effect of an electronic exciter on the short-circuit current of an a-c generator depends on the duration of the fault, the impedance to the point of fault, and on how the electronic exciter is excited. The fault current during the subtransient period, about the first three cycles, is the same regardless of the type of exciter that is used. If the electronic exciter is excited separately, the transient fault current and the sustained current are the same as with a rotating exciter for operation without a voltage regulator. For operation with a voltage regulator, the transient current is somewhat higher with the electronic exciter on account of its faster response. The sustained currents would be proportional to the ceiling voltages of the two exciters.

A self-excited electronic exciter with a series compensator designed to maintain a-c voltage on the rectifier during the transient period would result in about the same transient current as a separately excited electronic exciter with or without regulator operation. However, the sustained current would be proportional to the generator terminal voltage and would drop to zero if the fault were close by so that the terminal voltage dropped too low to sustain firing of the rectifier.

A self-excited electronic exciter without a series compensator and without regulator operation would cause the fault current to drop rapidly to zero if the fault impedance were low. With regulator operation and with the exciter provided with a high ceiling voltage to compensate for drop in a-c voltage, the transient current would be essentially the same as with a separately excited electronic exciter or a rotating exciter. The sustained current still would collapse to zero if the fault impedance were low.

From the above, it can be reasoned that an electronic exciter would have little or no effect on modern high-speed relays that operate in the first few cycles following a fault. The decay of fault current for low impedance faults of long duration with a self-excited electronic exciter should be taken into consideration in its effect on relay operation. It is, in general, desirable to boost or at least maintain excitation during a system fault to prevent generator instability and to hasten recovery to normal voltage after the fault is cleared. However, prolonged high excitation is undesirable where the fault is of low impedance and in a location that cannot be cleared, such as an unprotected bus. A self-excited electronic exciter would cause the fault current to collapse following the transient period and thereby make the generator self-protecting. If desired, the generator voltage could be restored after the fault was cleared by automatically applying the primer voltage to the field to start firing of the rectifier.

Figure 4. West Penn Power Company's Springdale Power Station exciter system and auxiliary power sources



Tests on Laboratory Model

A laboratory model of an electronic exciter was built and tested in order to obtain fundamental data which would be a guide in the basic design of a large exciter and also to determine the effectiveness of a series compensator. This exciter consisted essentially of a rectifier transformer, six thyratron tubes, a grid transformer, and a direct-acting voltage regulator. It supplied excitation to a 100-kva 1,150-volt 1,200-rpm 3-phase synchronous generator. An auxiliary transformer was provided to transform the generator voltage to 230 volts for the rectifier transformer, the grid transformer, and the d-c grid bias circuit. The voltage regulator was used to regulate the generator terminal voltage by controlling the d-c grid bias voltage and consequently the firing of the thyratron tubes. This method of voltage control is the same as that used on the large electronic exciter discussed later.

Series compensators were provided, each consisting of three current transformers connected in series per phase with a reactor across the three secondary windings. The primaries of the compensators were connected in series with the generator armature leads; the secondaries were connected in series with the leads to the auxiliary transformer. The compensators were connected to boost the voltage to the auxiliary transformer with lagging reactive current flow from the generator. They were designed to give 100 per cent voltage compensation with 200 amperes in the primary.

Description of Tests

The tests consisted essentially of load changes, application of faults, steady state and transient stability, transfer of excitation, and build-up of generator terminal voltage. All references to "per cent applied load" mean that the load is zero power factor lagging and is expressed as a percentage of full-load kilovolt-ampere rating of the generator. A total of 28 tests was run with oscillograms taken for each test. The generator field current and voltage, armature current, terminal voltage, the voltage to the rectifier transformer, and the d-c grid bias voltage were recorded. Reactive loads ranging from 25 to 200 per cent were applied and dropped. Three-phase and line-to-line faults were applied through approximately 12 per cent reactance on a 100-kva base. Steady-state stability tests were run with the generator connected directly to a synchronous motor load. For transient stability tests, the generator and motor were connected together through 22.7 per cent reactance on a 100-kva base, and 3-phase and line-to-line faults were applied for about one-half second at a point one-third of the electrical distance between the generator and the load. The generator was carrying 40 kw at unity power factor. All of the tests were made with and without the compensator.

Test Results

Meter readings recorded under steady-state conditions show that the compensator boosted the voltage to the rectifier. With no compensator, the voltage to the rectifier transformer was constant for a change in generator load (80 per cent power factor) from zero to 100 per cent; with the compensator in, this voltage was about 87 per cent at no load because of the drop through the compensator. However, with an increase in load, it increased because of the boost from the compensator. At approximately 75 per cent load on the generator, it was 100 per cent and at full load was 106 per cent. At no load the angle of firing delay without the compensator was higher than with the compensator because more voltage was available to the rectifier transformer; at full load the angle of delay without the compensator was lower than with the compensator because less voltage was available to the rectifier transformer. In other words, for a change from no load to full load at a given power factor, the compensator has a regulating effect on the generator voltage with the angle of delay tending to remain more nearly constant than without the compensator.

With the generator self-excited, severe faults of long duration caused the terminal voltage and consequently the excitation to decay to zero. The faults were intentionally not cleared until after the terminal voltage had decayed to zero. As shown in Figure 1, the compensator maintains the terminal voltage approximately five times as long as without it. The compensator boosted the voltage to the rectifier transformer to approximately 113 per cent for a 3-phase fault. With an initial current of 150 amperes at two cycles, the voltage to the rectifier was boosted 77 per cent. This is equivalent to a 103-per-cent boost at 200 amperes. The decay of the armature current during the subtransient period is the same with or without the compensator. From three cycles on, the decay is much more rapid without the compensator.

Figure 2 shows terminal voltage versus time for the application of 100 per cent reactive load with and without the compensator. With the compensator the maximum voltage drop is decreased 4.5 per cent, and the generator terminal voltage is returned to 100 per cent on the first

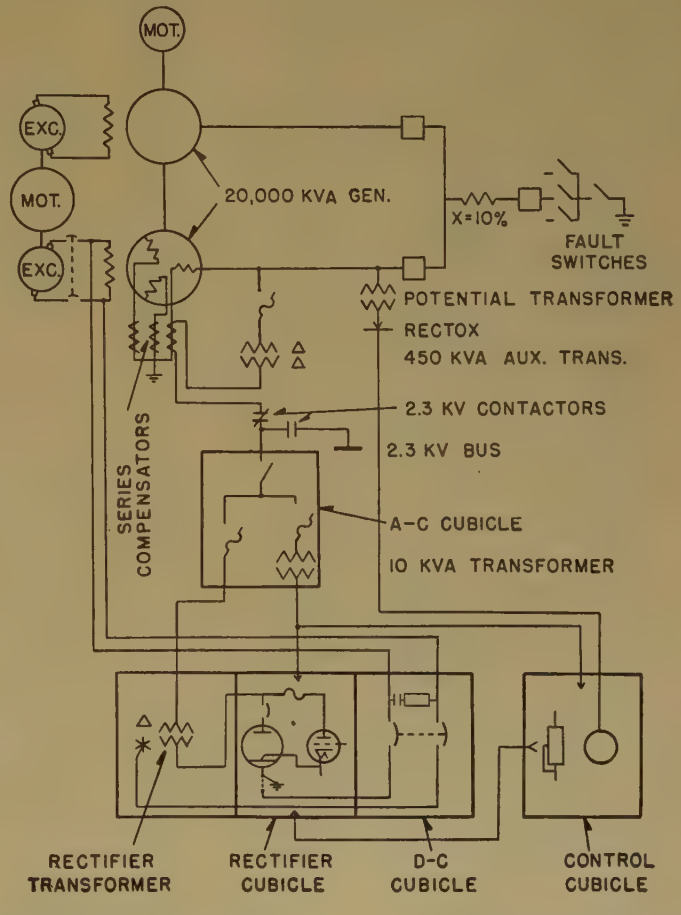


Figure 5. Schematic diagram of electronic exciter test setup in one of the a-c high-power laboratories

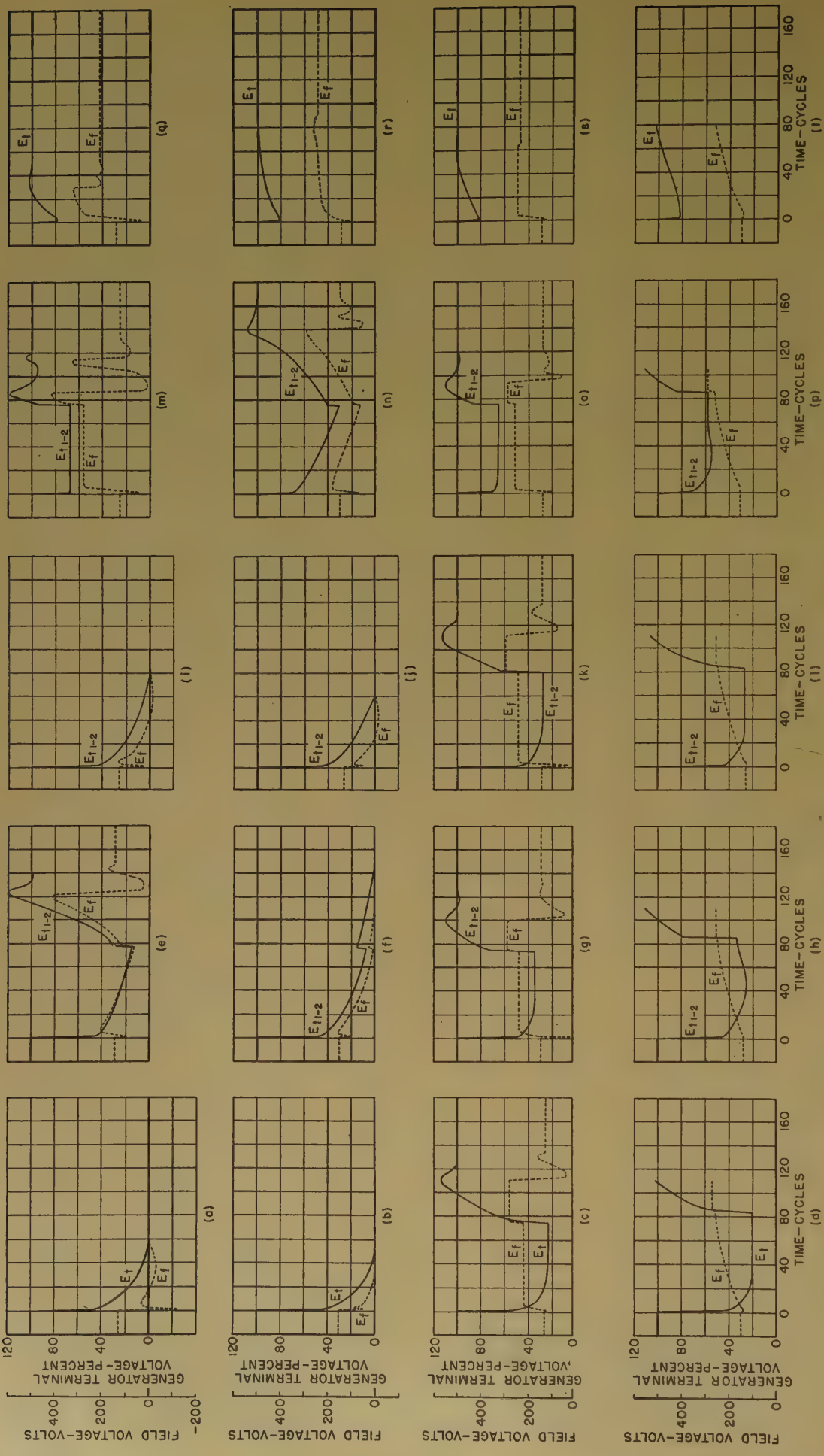


Figure 6. Curves of terminal and field voltage for application of faults through approximately ten per cent external reactance and load changes on 20,000-kva generator

a, b, c, d—Three-phase faults for conditions 1, 2, 3, and 5, respectively
e, f, g, h—Line-to-line faults on phases 1 and 2 for conditions 1, 2, 3, and 5, respectively
i, j, k, l—Double line-to-ground faults on phases 1 and 2 for conditions 1, 2, 3, and 5, respectively
m, n, o, p—Single line-to-ground faults on phase 1 for conditions 1, 2, 3, and 5, respectively
q, r, s, t—Application of 60 per cent reactive load for conditions 1, 2, 3, and 5, respectively

overshoot, ten cycles sooner than without the compensator. The terminal voltage ultimately is returned to normal in about 65 cycles with the compensator, compared with 80 cycles without the compensator.

A comparison of the transient stability characteristics of the generator with and without a series compensator is shown in Figure 3. Without the compensator the generator pulled out of step and did not regain synchronism. However, with the compensator, synchronism was not lost and the terminal voltage returned to a constant value in 111 cycles after the fault was cleared.

Application to West Penn Power Company System

The Springdale generating station includes five 1,800-rpm turbine generators excited from motor and dual-driven exciters with switching for exciting any generator from any exciter through excitation busses. There is one 3,600-rpm 50,000-kva high pressure unit with a direct-connected exciter.

The new number 7 unit, rated 81,250 kva 3,600 rpm, is practically a separate station electrically, with no paralleling of circuits other than at 132 kv. Only a few of the auxiliaries for this unit are supplied from the existing 2,300-volt auxiliary bus. A shutdown would therefore be very costly.

In order to eliminate shutdown because of the possibility of exciter trouble which might require mechanical disconnection from the shaft of the main unit, a separate exciter source was decided upon, and an electronic type was selected. Initially, this exciter supplies excitation to one of the existing generators. The number 5 dual-driven exciter, supplied from either one of the existing 2,300-volt station auxiliary busses, supplies excitation to the number 7 unit. A pilot exciter was added to the shaft of this dual set. This was considered a reliable source of excitation because there has been no outage to these busses or to the dual set over a period of years. After sufficient operating experience is obtained with the electronic exciter on one of the older units, it will serve as the main exciter for the number 7 unit for which it originally was designed. Any one of the older generators can be excited from the electronic exciter or any of the station exciters as shown in Figure 4.

When the electronic exciter is used to excite the number 7 unit, it operates essentially self-excited, subject to drop in the terminal voltage of the generator. A 3-phase fault at the high-voltage terminals of the step-up transformers with the 132-kv bus tie breaker closed would cause the generator terminal voltage to drop instantly to approximately 50 per cent. Faults at other locations on the high-voltage system would result in less voltage drop.

The rectifier transformer was designed to give approximately 400 volts d-c ceiling with full a-c voltage applied, so as to assure excitation during fault periods. It also is provided with an extension to the high-voltage winding to give a ceiling d-c voltage of approximately 300 volts, which would correspond to a normal design to be operated either separately excited without a compensator or self-excited with a compensator. Both schemes of compensation were used in making the laboratory tests to be described later. The series compensators used in the tests proved inadequate for the compensation desired, so the exciter was installed to operate on the high-voltage taps without series compensators. Space is available for future installation of compensation and their connections if proved desirable.

Table I. Characteristics of Generators

	Laboratory Test Generator	Springdale Station No. 7 Generator
Generator rating	20,000 kva	81,250 kva
Normal rated voltage	6,600 volts	11,500 volts
Synchronous reactance, per unit	0.853	1.20
Transient reactance, $X_{d'}$ sat, per unit	0.10	0.117
Negative-sequence reactance, X_2, per unit	0.10	0.073
Zero-sequence reactance, X_0, per unit	0.025	0.067
Open-circuit transient time constant T'_{d0}	3.2 sec	7.56 sec
Field resistance at 75° C.	0.145 ohm	0.234 ohm
No load field current	830 amp	400 amp
Full load 80% power factor field current	1,340 amp	800 amp

Laboratory Tests on West Penn Power Company Exciter

Laboratory tests on the model proved the feasibility of an electronic exciter for excitation of a synchronous generator. They also showed that a series compensator could be designed which would be effective in maintaining voltage to the rectifier transformer during the transient period under fault conditions. In order to obtain complete performance data on the electronic exciter for the West Penn Power Company for operating conditions which might occur in service but which could not readily be staged on the actual installation, extensive tests were made on this exciter at the factory.

Table II. Estimated Maximum Fault Clearing Time to Permit Recovery of Generator Voltage

Type of Fault	Time in Cycles: Condition 1	Condition 2	Condition 4
Three-phase	32	27	28
Line-to-line	78*	56	59
Double line-to-ground	47	34	38
Single line-to-ground	78**	75*	74*
Line-to-line fault with one anode breaker open	78*	49	57

*Fault was cleared at this time.

**Maximum fault clearing time is infinite.

The tests were made in one of the a-c high-power laboratories. A schematic diagram of the electronic exciter and the associated test apparatus is shown in Figure 5. The laboratory consists of a 3,300-horsepower motor driving two 20,000-kva generators which are synchronized mechanically so that their respective voltages are in phase A motor-driven dual exciter set is provided to furnish excitation to each generator. Switching arrangements are such that the two generators can be paralleled or one can be used alone. Facilities are available for applying any type of fault through an external reactance from zero to five ohms. Reactive load can be applied on either generator by paralleling it with the other underexcited.

The electronic exciter consists essentially of an a-c cubicle, an air-cooled rectifier transformer, a rectifier cubicle, a d-c cubicle, and a control cubicle, all shown schematically in Figure 5.

The voltage regulator and firing control circuits of this exciter and the model are the same. The thyratron tubes fire the ignitron tubes, whereas on the model they were used actually to supply power to the field circuit.

A 450-kva transformer bank transformed the generator terminal voltage to 2,300 volts to supply the rectifier transformer. Mechanically and electrically interlocked 2,300-volt contactors were provided so that power for the electronic exciter could be supplied from either the generator terminals or a separate source.

The series compensators, shown in Figure 5, were selected with the idea of boosting the a-c voltage applied to the rectifier transformer 50 per cent (625 volts per phase) with 25,000 amperes through a single-turn primary. This is the value of generator transient current that would result for a 3-phase fault on the high-voltage terminals of the transformers connected to the number 7 unit at Springdale. With the test generator connected

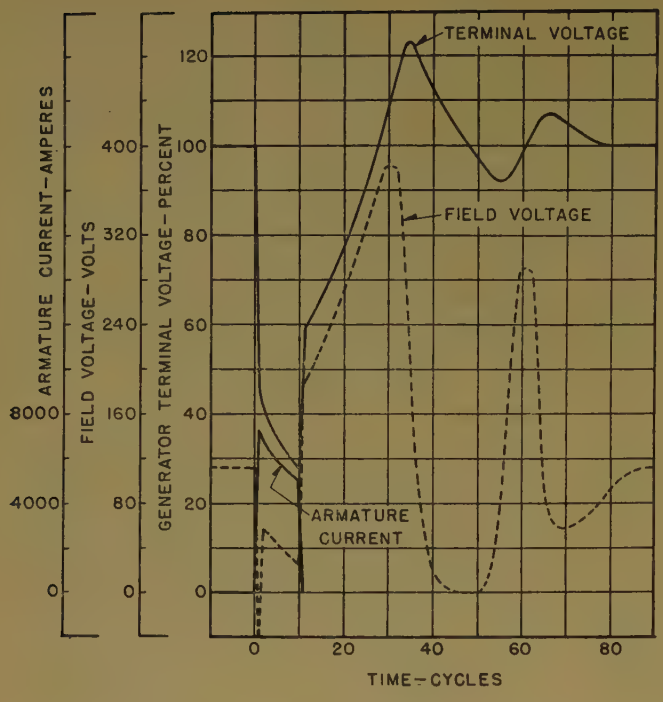


Figure 7. Three-phase 10-cycle fault applied on 20,000-kva generator through ten per cent external reactance. Generator was self-excited and rectifier transformer was on high-voltage tap

for 6,600 volts, line-to-line, the transient current for a 3-phase fault with 10 per cent (20,000-kva base) external reactance between the generator and fault is approximately 8,750 amperes. Therefore, one compensator was connected in the neutral leg of each phase of the generator with three loops through the primary to obtain the equivalent ampere turns of the actual installation. The generator neutral was grounded solidly to permit the application of ground faults.

The electrical characteristics of the test generator and the number 7 generator are compared in Table I. The full-load field voltage of the test generator during tests was about 15 per cent greater than the full-load field voltage on the number 7 generator at normal operating temperature. The full-load field current of the test generator is 1.67 times that of the number 7 generator. This, together with the smaller auxiliary transformer (450 kva compared with 7,500 kva), resulted in a higher d-c voltage regulation of the rectifier in the laboratory tests than in the actual installation. The shorter time constants of the test generator resulted in faster decay of voltages and currents during faults.

Description of Tests

The tests consisted essentially of the application of all types of faults, application and dropping of reactive load, changeover from self-excitation to separate excitation, simulated arc-backs and sympathetic arc-backs, and build-up of generator terminal voltage.

The tests were made under the five following conditions of excitation:

1. The rectifier transformer was connected on the high-voltage tap (approximately 400 volts d-c, no-load ceiling) and the compensators were not connected in the circuit. The generator was self-excited, that is, the supply to the rectifier transformer was taken from the generator terminals.

2. The rectifier transformer was connected on the low-voltage tap (approximately 300 volts d-c, no-load ceiling) and the compensators were not connected in the circuit. The generator was self-excited.

3. The rectifier transformer was connected on the low-voltage tap and the compensators were not connected in the circuit. The generator was excited separately, that is, the supply to the rectifier transformer was taken from a separate a-c source.

4. The rectifier transformer was connected on the low-voltage tap and the compensators were connected. The generator was self-excited.

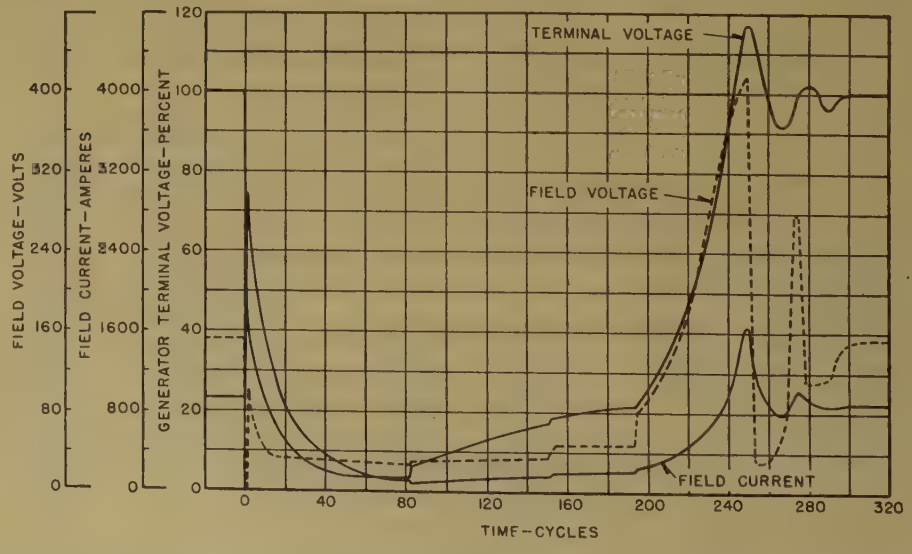
5. The rotating exciter was used to excite the generator field. A high-speed contactor short-circuited the exciter field resistance to assimilate the high-speed field-forcing contactor in a rheostatic type voltage regulator. The output ceiling voltage of the rotating exciter is 270 volts and the response ratio is 0.5.

For each of these conditions, 60 per cent reactive load was applied and dropped, and a 3-phase, a line-to-line, a double line-to-ground, and a single line-to-ground fault was applied. To assimilate faults on the 132-kv bus on the actual installation, all faults were applied through ten per cent external reactance on a 20,000-kva base. Under this condition the initial generator terminal voltage drop was approximately 50 per cent. With the exception of condition 5, a line-to-line fault was applied with each of the anode breakers open. This assimilates a line-to-ground fault on the 132-kv West Penn Power Company system during operation with one rectifier cubicle (two ignitron tubes) out of service for maintenance. The duration of the faults was approximately 1.25 seconds. This was longer than would be expected in normal operation but was desirable in order to determine the performance of the electronic exciter for disturbances of long duration.

For electronic exciter tests on which oscillograms were taken, 24 quantities were recorded simultaneously on three 9-element oscillographs as follows:

3—generator line-to-line terminal voltages
3—generator line currents
1—generator field voltage
1—generator field current
1—thyratron tube d-c grid bias voltage

Figure 8. Severe long-duration fault on 20,000-kva generator with primer voltage applied to return terminal voltage to normal after fault was cleared



3—line-to-line voltage applied to the rectifier transformer
6—anode to cathode voltages
6—anode currents

Only the first eight quantities were recorded for tests involving the rotating exciter.

Test Results

Figure 6 shows curves plotted from oscillograms of generator terminal voltage and field voltage versus time for a 3-phase fault, a line-to-line fault, a double line-to-ground fault, a single line-to-ground fault, and application of 60 per cent reactive load. The results of the tests made under conditions 1, 2, 3, and 5 are shown. Condition 4 is not included because the results were about the same with the compensators as without them. This was primarily because of the high-voltage regulation in the a-c supply circuit to the rectifier, which resulted from the high field current requirements of the test generator. In those cases where the field voltage becomes a negative value, the induced voltage in the field resulting from fault current in the armature is higher than the rectifier output voltage.

Faults of short duration similar to those normally experienced with modern high-speed relays and breakers were also applied. Curves plotted from an oscillogram of a 3-phase 10-cycle fault are shown in Figure 7. The rectifier transformer was connected on the high-voltage tap and the generator was self-excited.

The tests showed that with the generator self-excited and the rectifier transformer on the high-voltage tap, a 3-phase fault must be cleared in approximately 30 cycles to permit the generator terminal voltage to return to normal. The maximum fault clearing times to permit recovery of generator voltage for other types of faults were estimated from the oscillogram and are shown in Table II.

Figure 8 shows how the generator terminal voltage was returned to normal following a long duration 3-phase fault which caused the rectifier to stop firing because of the decay of terminal voltage to zero. About 40 cycles after application of the fault, a 32-volt d-c source was automatically connected to the generator field. This is the lowest voltage which will cause the ignitron tubes to fire and consequently build up the generator voltage. The fault was cleared in 82 cycles and the ignitron tubes started to fire at 152 cycles. At 194 cycles the rectifier voltage was high enough to cause reverse current to flow into the 32-volt d-c supply, which was tripped off by means of a reverse current relay. From 194 cycles to 300 cycles, the curves show the action of the voltage regulator and the build-up of the terminal voltage, which becomes a constant value of 100 per cent at 300 cycles.

During the tests, one arc-back and one sympathetic arc-back occurred which caused the associated anode breaker to open. Both occurred with cold tubes and with the rectifier supplying no load excitation to the generator with operation of the tubes at a high firing delay. Such conditions are known to increase the probability of arc-back and sympathetic arc-back.[3] No oscillograms were obtained because they occurred at a time when no records were being made. Arc-backs were simulated by short-circuiting a rectifier tube. The tests were run with the rectifier transformer separately excited with no load on the rectifier and with the tubes firing at zero degrees delay. Under these conditions the arc-back currents were maximum. Sympathetic arc-backs were simulated by short-circuiting two ignitron tubes connected to adjacent phases of the rectifier transformer. Power to the rectifier was supplied from the generator terminals and the voltage regulator was in service. The anode breakers opened in $2^1/_2$ cycles and the rectifier functioned with four tubes out of service. As shown in an oscillogram of one of the tests, Figure 9, there was no disturbance to the generator terminal voltage.

A total of 43 fault, 7 load change, 14 arc-back, 22 sympathetic arc-back, 1 transfer of excitation, and 3 generator voltage build-up tests was recorded on oscillograms. In addition, a number of tests were made without taking oscillographic records. It is believed that the results of these tests provide valuable information that could not be obtained in actual service even over many years.

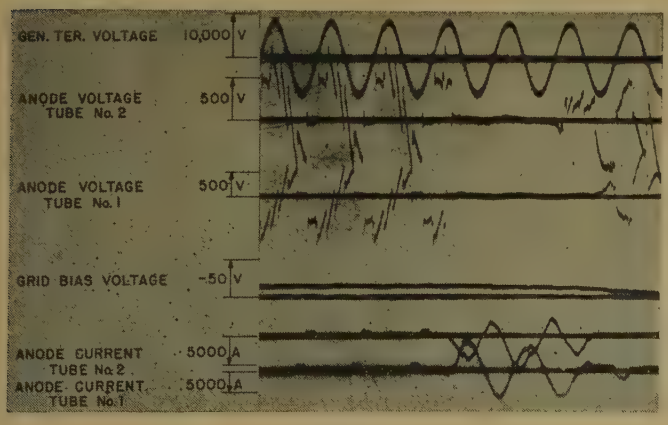


Figure 9. Oscillogram of sympathetic arc-back on ignitron tubes 1 and 2, simulated by short-circuiting each tube simultaneously

Conclusions

1. Extensive laboratory tests based on pessimistic conditions that are unlikely to be matched in service have demonstrated that an electronic exciter can be depended on as a reliable source of excitation for large a-c generators.

2. The type of a-c power supply to the rectifier best suited to the application is dependent on the particular conditions.

3. If self-excited, the electronic exciter should have either a high ceiling voltage or should be provided with series compensators to compensate for drop in a-c voltage during system disturbances. Either method is practical.

4. An electronic exciter may be installed at any desired location in the generating station, it is easy to maintain, it has an inherent high speed of response, and it is adapted easily to generator voltage regulation. Its cost is higher than that of a rotating machine.

5. Modern high-speed relaying would not be affected by using electronic exciters instead of the rotating type. Relays with long time settings, in excess of one second, might be affected if the electronic exciter operates self-excited because of faster decay of short-circuit current.

6. An a-c generator self-excited with an electronic exciter can be operated as an independent unit in an isolated station. A primer excitation for starting can be obtained from a battery or small motor-generator set.

7. The decay of short-circuit current for long-duration low-impedance faults with a self-excited electronic exciter would prevent excessive fault damage. If desired, generator voltage can be restored by automatically applying a primer voltage to the field to start firing of the rectifier.

References

1. A New Method for Initiating the Cathode of an Arc, J. Slepian, L. R. Ludwig. AIEE Transactions, volume 52, 1933, June section, page 693–8.

2. Ignitron Rectifiers in Industry, J. H. Cox, G. F. Jones. AIEE Transactions, volume 61, 1942, October section, pages 713–18.

3. Arc-Backs in Rectifier Circuits Artificial Arc-Back Tests, R. D. Evans, A. J. Maslin. AIEE Transactions, volume 64, 1945, June section, page 303–11.

Peak Voltages Induced by Accelerated Flux Reversal in Reactor Cores Operating Above Saturation Density

THEODORE SPECHT
ASSOCIATE AIEE

E. C. WENTZ
MEMBER AIEE

Synopsis: The existence of peak voltages in the windings of many sorts of series transformers and reactors, when abnormal conditions force the flux density above saturation, has been understood in a qualitative manner for many years. This paper will derive means for calculating these voltages for the various combinations of magnetizing force and rate of variation. The close agreement between test and calculation over a wide range of magnetizing forces indicates the accuracy and general applicability of the method.

THE magnetic flux in a-c apparatus usually varies nearly sinusoidally over a range of flux densities well below the saturation value. However, in certain types of apparatus, notably series apparatus, abnormal conditions will produce magnetizing forces as high as hundreds of times normal, and the flux density will not only reach saturation, but the flux variation will no longer be sinusoidal. The variation of the flux through zero is usually accelerated and induces relatively enormous peak voltages.

Examples of such apparatus are:

1. Current transformers under overcurrent, high burden (or a combination), or open circuit.
2. Preventive autotransformers when a tap change coincides with a line fault.
3. Series transformers for street lighting when a lamp burns out.

The existence of these voltages is well known, but only very approximate methods,[1] limited in application, have been derived for calculation of their values. With recent increases in capacities of systems, the possible voltages are higher and more dangerous than ever. One-ampere secondary current transformers are being used more frequently, and their voltages are five times as high as standard. Hence it has become more necessary to have more generally applicable, more exact, means of calculation of voltage.

Paper 46-68, recommended by the AIEE committee on instruments and measurements for presentation at the AIEE winter convention, New York, N. Y., January 21–25, 1946. Manuscript submitted November 8, 1945; made available for printing December 11, 1945.

THEODORE SPECHT, an electrical design engineer, and E. C. WENTZ, a transformer design engineer, are both with Westinghouse Electric Corporation, Sharon, Pa.

Peak Voltage Phenomenon and Methods of Analysis

The conventional description of the phenomenon is illustrated in Figure 1A. Starting at point *A* on the current wave, the reactor is saturated, and as the current decreases, the flux changes very little and the voltage is nearly zero. As the current decreases to the saturation value near *B*, the flux starts to decrease, and the flux change is accelerated through current zero at *C*, inducing a high-voltage peak.

The high-voltage peak, induced by the high inductance of the saturating reactor near current zero, resists the change in the primary current, the high inductance tending to maintain the current and thus to make the peak voltage itself less than it would be otherwise if the current wave maintained its sinusoidal shape. Analysis of the circuit to determine the effect of the peak voltage on the wave shape of the current and the determination of the resulting peak voltage is the first part of the problem.

The high rate of flux change induces eddy currents in the lamination which are very effective toward maintaining the flux, delaying its change. Analysis of these eddy currents is the second part of the problem.

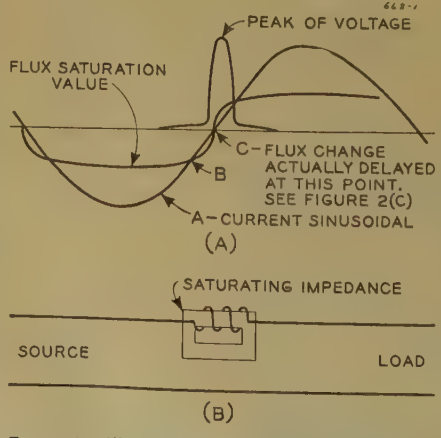


Figure 1. Illustration of the problem with conventional description of mode of flux variation

Compare with Figure 2 and Figure 11

Two methods of analysis of the whole problem have been developed. Method *A* gives a satisfactory solution of the first part of the problem (variation of voltages and currents in the circuit) based on an assumption as to the solution of the second part. Method *B* gives the solution of the second part of the problem (eddy currents and their effect on the flux distribution and voltage) based on an assumption as to the solution of the first part. The use of two methods can be justified by the fact that although neither method gives exactly the correct result, they do give the approximate upper and lower limits of possible peak voltage.

The advantage of method *A*, analysis by the assumption of uniform flux density in the lamination, is that it permits representing the actual reactor by an equivalent perfect reactor in parallel with a resistor, according to Figure 2. This enables the mathematical analysis of the circuit which will be given later.

The classic analysis of eddy currents is based on the assumption of uniform flux density. The loss then is proportional to the square of the rate of flux change or, instantaneously, to the square of the voltage induced in the reactor. Clearly, a resistor shunted across the reactor has a loss varying in the same way, and a resistor *R* in parallel with a perfect reactor *L*, as in Figure 2, will represent the actual reactor.

By method *B* determination of flux distribution in the lamination, the variation of flux is analyzed on the basis that a sine wave of current is maintained through the reactor, and the effect of the eddy currents in forcing the flux to redistribute itself toward the surface of the lamination is determined.

Method *B*, which takes account of the effect of the eddy currents in forcing the flux change to occur first at the surface of the lamination, can be expected to give lower voltages. The analyses to be given show that it gives a voltage about half as great, and the tests show that the actual values are between the two.

Mathematical Analysis

The equivalent reactor (or primary of the series transformer) in method *A* (see Figure 2B) is not a constant quantity; as the flux in the core increases toward saturation, the permeability and effective inductance decrease to a value only a small

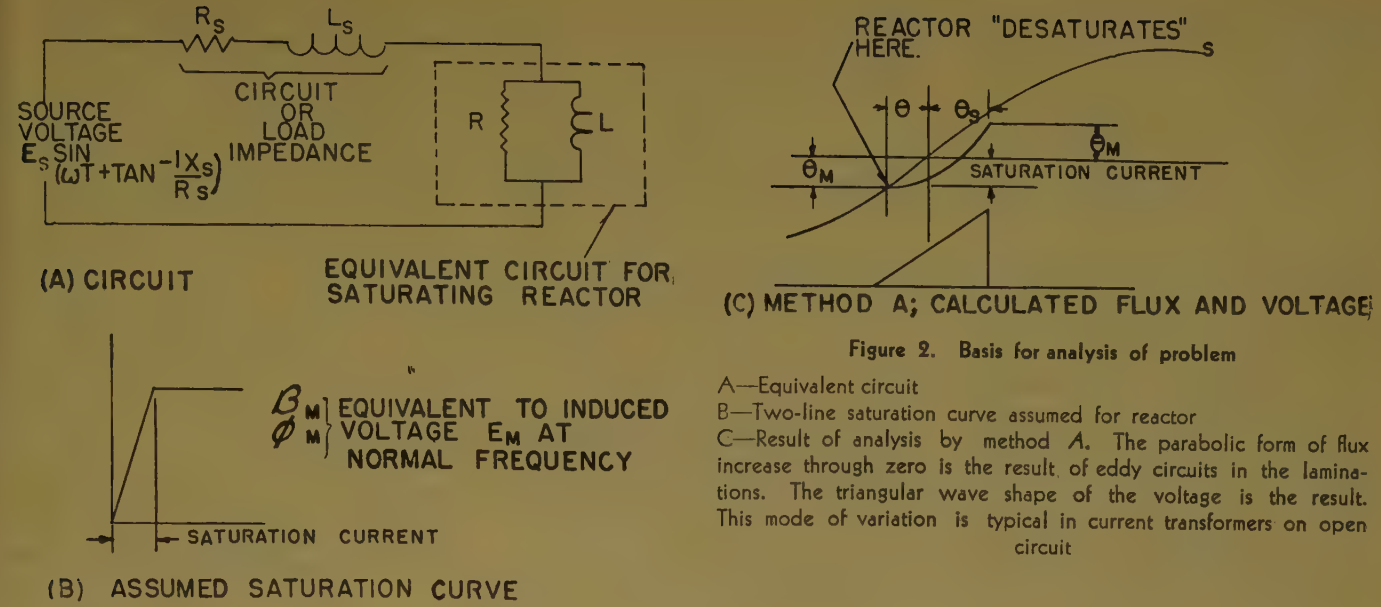


Figure 2. Basis for analysis of problem

A—Equivalent circuit
B—Two-line saturation curve assumed for reactor
C—Result of analysis by method *A*. The parabolic form of flux increase through zero is the result of eddy circuits in the laminations. The triangular wave shape of the voltage is the result. This mode of variation is typical in current transformers on open circuit

fraction of the initial value, and in a complicated manner that cannot be represented by any simple formula. Therefore some simplifying assumptions will have to be made. An obvious device which has been used in similar problems is to assume that the saturation curve is composed of two straight lines, as shown in Figure 2B. The voltage induced by B_m at normal frequency will be E_m; the method of determining E_m from the AC saturation curve of the reactor is given in Appendix I.

The hysteresis loop, by this assumption, is assumed to have zero area. As it will appear later that the permeability of the iron is not too important in determining the peak voltage, the variation of permeability during the hysteresis loop reasonably may be neglected.

Method *A*

Method *A*, as has been shown, is based on analysis of the circuit of Figure 2A. For this circuit we may write the equations

$$\sqrt{2}E_s \sin\left(\omega t + \tan^{-1}\frac{X_s}{R_s}\right) - i_s R_s - L_s\frac{di_s}{dt} - L\frac{di_L}{dt} = 0 \quad (1)$$

The reason for writing in $\tan^{-1} X_s/R_s$ is that the resulting equations are simplified. The current i_s, which would flow in the circuit if the series reactor were not present, is $i_s = (E_s/Z_s)\sin\omega t$. Time = 0 is thus when the current would be zero if the reactor were not in the circuit.

$$L\frac{di_L}{dt} = i_R R = e \quad (2)$$

$$i_s = i_L + i_R \quad (3)$$

A further limitation, inherent in the nature of the reactor, is that $L=0$ if i_L exceeds the saturation value. If we suppose the current to exceed this value initially (at point A, Figure 2C) and to be decreasing sinusoidally toward zero, it all will be flowing in the L branch, none in the R branch, of the equivalent reactor because $L=0$ while the current exceeds the saturation value. At some time $-t_a$ or time angle $-\theta_a$, the current decreases to the value at which the reactor "desaturates" and suddenly regains its inductance L. The flux must remain momentarily at the same value, so that the current in the reactor (i_L) must have an initial value at time angle $-\theta_a$ equal to the saturation value, with zero current in the resistor R and zero voltage across the reactor. The value of $-\theta_a$ is derived in Appendix II.

As the flux in the reactor reverses, the current in the reactor branch L finally reaches the saturation value again at some time t_s (angle θ_s), at which time the inductance L becomes zero, all the current transfers to the L branch, and the circuit carries on until the next half-cycle.

Equations 1, 2, and 3 are obviously very difficult to solve for i_L or i_R.* Some assumptions or simplifications must be made. The solution can be worked out by either of two assumptions.

Solution by Assumption Number 1. Neglect $R_s\{[(\sqrt{2}E_s\omega t)/Z_s] - i_s\}$. The demonstration that the solution is valid for low-power-factor circuits follows.

If we write equation 1 in the form

$$L_s\frac{di_s}{dt} + L\frac{di_L}{dt} = \sqrt{2}E_s \sin \times \left(\omega t + \tan^{-1}\frac{X_s}{R_s}\right) - R_s i_s$$

* This equation can be solved for e because the differential equation

$$\frac{d^2 i_L}{dt^2} + \left(\frac{R_s}{L_s} + \frac{R}{L_s} + \frac{R}{L}\right)\frac{di_L}{dt} + \frac{RR_s}{LL_s} i_L = \frac{Re_s}{LL_s}$$

can be derived from it (e_s = source voltage). The solution is of the form $i_L = K_1\epsilon^{\lambda_1 t} + K_2\epsilon^{\lambda_2 t}$ + steady state current. The initial and final conditions are the same. λ_1 and λ_2 come out to be rather complicated functions of R, R_s, X, X_s, while K_1 and K_2 are still more complicated functions of λ_1, λ_2 and the other variables. The final solution is difficult to work with, and as the more simple solutions give results sufficiently accurate for the purpose (especially in light of the fact that the basic assumption of a constant R introduces some error), only the simple solutions are given in complete form and the calculations will be based on these simple solutions. The values of λ_1, λ_2, K_1, and K_2 are given in Appendix V.

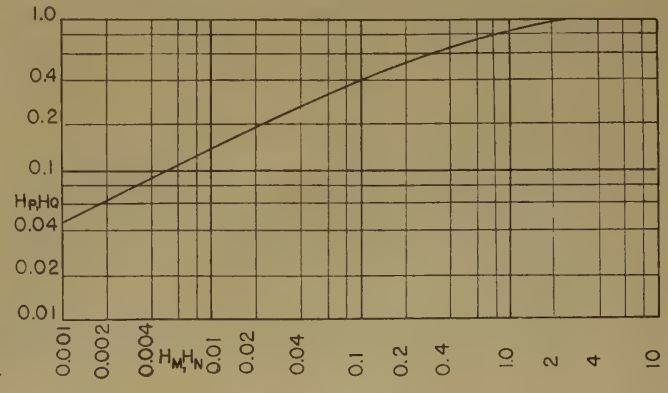


Figure 3. Curve of H_p as a function of H_m (or H_q as a function of H_n)

and if we consider the current reversal to take place in such a short time that $\sin \omega t = \omega t$,

$$L_s\frac{di_s}{dt}+L\frac{di_L}{dt}=\sqrt{2}\frac{E_sX_s}{Z_s}+R_s\left(\sqrt{2}\frac{E_st\omega}{Z_s}-i_s\right) \quad (4)$$

Now this equation can be solved if we can neglect the last term. But if the current variation is sinusoidal so that $i_s=\sqrt{2}(E_s/Z_s)\sin\omega t=\sqrt{2}(E_s/Z_s)t\omega$ the last factor will be zero. If L_s is very large compared with L, the variation will be substantially sinusoidal, the last term will be zero, and the equation can be solved. Of course, if $R_s=0$, the last term will be zero and the calculation will be exact, even if the current wave is not sinusoidal. We can determine the relative magnitude of error by solving the equation for i_s, and determining the relative magnitude of the i_sR part of the last term which has been neglected. This will indicate the approximate amount of error. The ratio of this error to the other term $\sqrt{2}(E_sX_s/Z_s)$ will come out equal to

$$\frac{R_s}{X_s}\left[\frac{X}{X+X_s}\omega(t+t_d)+\left(\frac{X}{X+X_s}\right)^2\times\frac{X_s}{R}\left(1-\epsilon^{-\frac{R(X+X_s)}{XX_s}(t+t_d)}\right)\right]$$

Examples worked out for different circuit constants indicate that the maximum usual error will not exceed 20 per cent. Tests to be given indicate good agreement.

Then we can write for Equation 4

$$\sqrt{2}\frac{E_sX_s}{Z_s}=L_s\frac{di_s}{dt}+L\frac{di_L}{dt} \quad (4a)$$

Eliminating i_s and i_L by Equations 2 and 3,

$$\frac{de}{dt}+\frac{R(L+L_s)}{LL_s}e=\frac{\sqrt{2}E_sR\omega}{Z_s} \quad (5)$$

Solving this equation, using the initial condition that $e=0$ at $\omega t=-\theta_d$,

$$e=\frac{\sqrt{2}E_sXX_s}{Z_s(X+X_s)}\left(1-\epsilon^{-\frac{R(X+X_s)}{XX_s}(\theta+\theta d)}\right) \quad (6)$$

For small values of the exponent,

$$e=\frac{\sqrt{2}E_sR}{Z_s}(\theta+\theta_d) \quad (7)$$

To find the angle of saturation, θ_s, use the relation that $e=N(d\phi/dt)10^{-8}$

$$\int_{-\theta_d}^{\theta_s}ed\theta=\int_{-\phi_m}^{\phi_m}\omega N\frac{d\phi}{dt}10^{-8}dt=2\omega N\phi_m10^{-8}$$

But

$$E_m=\frac{\omega N\phi_m10^{-8}}{\sqrt{2}} \quad \text{(see Figure 2B)}$$

So that

$$\int_{-\theta_d}^{\theta_s}ed\theta=2\sqrt{2}E_m \text{ volts} \quad (8)$$

Integrating equation 6 from $-\theta_d$ to θ_s, equating to $2\sqrt{2}E_m$, and rearranging terms,

$$\frac{2E_mZ_sR}{E_s}\left(\frac{X+X_s}{XX_s}\right)^2=\frac{R(X+X_s)(\theta_s+\theta_d)}{XX_s}+\epsilon^{-\frac{R(X+X_s)(\theta_s+\theta_d)}{XX_s}}-1=H_m \quad (9)$$

From equation 6 it is apparent that the peak voltage occurs at θ_s. Introducing an experience factor k, which will be discussed further under test results, the peak voltage is

$$e_p=k\frac{\sqrt{2}E_sXX_s}{Z_s(X+X_s)}\left(1-\epsilon^{-\frac{R(X+X_s)(\theta_s+\theta_d)}{XX_s}}\right) \quad (10)$$

Let

$$H_p=1-\epsilon^{-\frac{R(X+X_s)(\theta_s+\theta_d)}{XX_s}} \quad (11)$$

Then

$$e_p=k\frac{\sqrt{2}E_sXX_s}{Z_s(X+X_s)}H_p \quad (12)$$

It can be seen from equations 9 and 11 that H_m and H_p are functions of the same parameter. It is then possible to plot H_p directly as a function of H_m. This curve is shown in Figure 3. H_m can be calculated from the first part of equation 9, H_p read from Figure 3, and e_p calculated by equation 12. If the angle $\theta_s+\theta_d$ is desired, it can be found from equation 11 as follows:

$$\theta_s+\theta_d=\frac{1}{k}\frac{XX_s}{R(X+X_s)}\times\log_e\frac{1}{1-H_p}\text{ radians} \quad (13)$$

Here the angle is divided by the experience factor k; for whatever the peak voltage is reduced by, the angle will be increased by, as is apparent from equation 8. For accurate results this angle should be less than one-half radian.

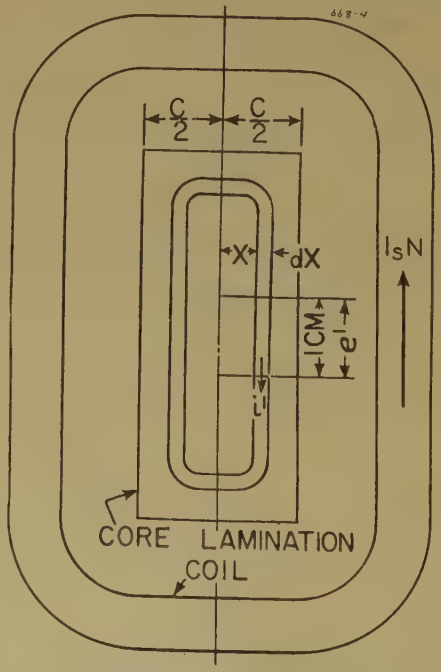


Figure 4. Cross section of a core lamination magnetized by a primary coil

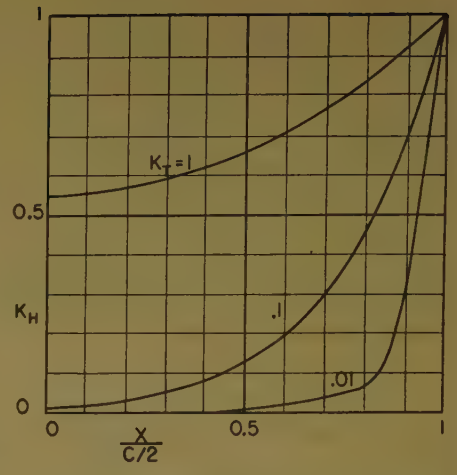


Figure 5. Distribution of flux in a lamination as a function of the distance from the center of the lamination for three values of time

See equation 46

Solution by Assumption Number 2. Neglect $L_s[(\sqrt{2}\omega E_s/Z_s)-(di_s/dt)]$. The demonstration that the solution is valid for high-power-factor circuits follows.

We may also write equation 1 in the form

$$I_sR_s+L\frac{di_L}{dt}=\sqrt{2}E_s\sin\left(\omega t+\tan^{-1}\frac{X_s}{R_s}\right)-L_s\frac{di_s}{dt} \quad (14)$$

or, as before, letting $\sin\omega t=\omega t$

$$i_sR_s+L\frac{di_L}{dt}=\sqrt{2}\frac{E_s}{Z_s}R_s\omega t+L_s\left(\sqrt{2}\frac{E_s}{Z_s}\omega-\frac{di_s}{dt}\right) \quad (15)$$

Again it appears that the equation can be solved if we neglect the last term. Again, if $i_s=\sqrt{2}(E_s/Z_s)\omega t$ so that $di_s/dt=\sqrt{2}(E_s/Z_s)\omega$, the last factor is zero, so that this equation is also valid if the series impedance is so high as to maintain sinusoidal current. And obviously it is valid for $L_s=0$, but not for $R_s=0$, so that the solution will be valid for high-power-factor circuits.

Then we may write equation 15 with-

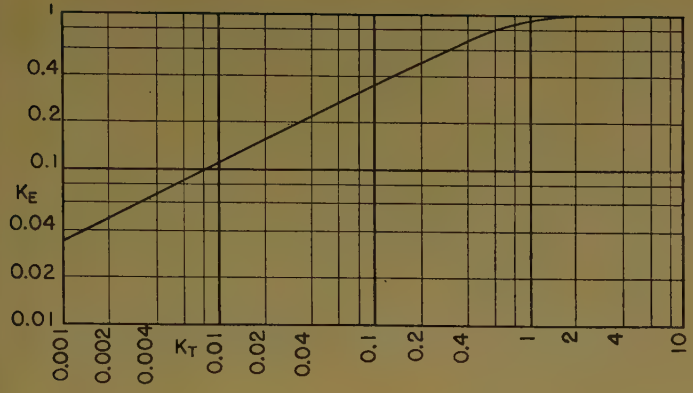


Figure 6. Curve of K_e as a function of K_t

See equation 48

out the last term, and again eliminating i_s and i_L by use of equations 2 and 3, we get

$$\frac{de}{dt}+\frac{RR_s}{(R_s+R)L}e=\frac{\sqrt{2}E_sR_sR\omega}{Z_s(R_s+R)} \quad (16)$$

At $\omega t=-\theta_d$, $e=0$,

$$e=\frac{\sqrt{2}E_sX}{Z_s}\left(1-\epsilon^{-\frac{RR_s(\theta+\theta_d)}{(R_s+R)X}}\right) \quad (17)$$

For small values of the exponent,

$$e=\frac{\sqrt{2}E_sRR_s}{Z_s(R_s+R)}(\theta+\theta_d) \quad (18)$$

Comparing with equation 7, it is seen that the two methods result in the same voltage if R_s is large compared to R. Integrating equation 17 from $-\theta_d$ to θ_s as in equation 8,

$$\frac{2E_mZ_sRR_s}{(R_s+R)X^2E_s}=\frac{RR_s(\theta_s+\theta_d)}{(R_s+R)X}+\epsilon^{-\frac{RR_s(\theta_s+\theta_d)}{(R_s+R)X}}-1=H_n \quad (19)$$

and

$$H_q=1-\epsilon^{-\frac{RR_s(\theta_s+\theta_d)}{(R_s+R)X}} \quad (20)$$

H_n and H_q are of the same form as in equations 9 and 11 but are functions of a different parameter. Introducing the experience factor k, equation 17 becomes

$$e_p=k\frac{\sqrt{2}E_sX}{Z_s}H_q \quad (21)$$

It is evident that Figure 3 also may be used to evaluate H_n and H_q. Method 1 above is exact for R_s equal to zero and method 2 is exact for X_s equal to zero. The calculated voltages for intermediate power factors will be too low by either formula unless the series impedance is high enough to keep the source current sinusoidal. If the peak voltage is calculated by both methods, the larger of the two answers should be correct within a reasonable degree of accuracy.

From Figure 3 it is evident that the straight line relationship

$$H_p=\sqrt{2H_m}\ (\text{or } H_q=\sqrt{2H_n}) \quad (22)$$

is entirely adequate if H_m or H_n is less than one-tenth. That equation 22 is the exact relation for low values of the variables can be demonstrated by expanding the expressions for H_p and H_m from equations 11 and 9 in infinite series, retaining only the lowest-powered term in each, and then eliminating the parameter between the two equations. Substituting the value of H_m from equation 9 into equation 22, and this value of H_p into equation 12, gives

$$e_p=k\left(\frac{8E_sE_mR}{Z_s}\right)^{1/2} \quad (23)$$

It can be shown that this same equation holds for method 2 for a high-power-factor circuit if R_s is large compared with R. From equations 7 or 18, it is evident that the voltage wave shape is essentially triangular.*

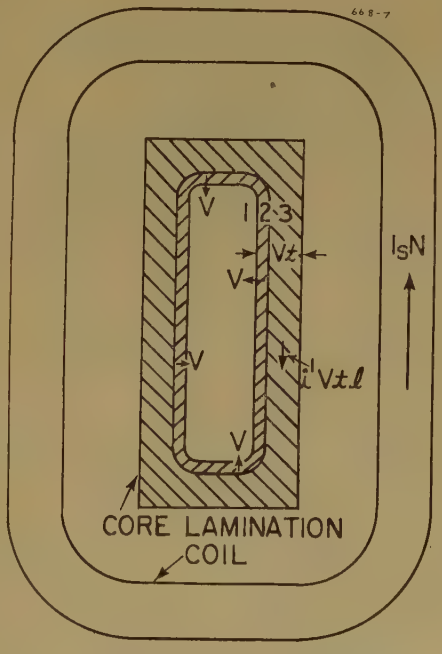


Figure 7. Cross section of a core lamination subjected to very large magnetomotive forces

The flux travels as a wave from the surface to the center. There has been little flux change in the area 1; in the relatively narrow strip 2, the flux is changing; and in the area 3, the iron is completely saturated

To get the root mean square voltage, we can write

$$\int_{-\theta_d}^{\theta_s}ed\theta=\frac{1}{2}\left[k\left(\frac{8E_sE_mR}{Z_s}\right)^{1/2}\right]\times(\theta_s+\theta_d)=2\sqrt{2}E_m \quad (24)$$

$$\theta_s+\theta_d=\frac{2}{k}\left(\frac{E_mZ_s}{E_sR}\right)^{1/2}\text{ radians} \quad (25)$$

The expression for the voltage e can be rewritten as follows, where e_p is the peak value as given by equation 23:

$$e=e_p\frac{\theta+\theta_d}{\theta_s+\theta_d} \quad (26)$$

To find the root mean square value of this voltage, the value of e is substituted in the following formula and evaluated.

$$e_{rms}=\left(\frac{1}{\pi}\int_{-\theta_d}^{\theta_s}e^2d\theta\right)^{1/2} \quad (27)$$

$$=e_p\left(\frac{\theta_s+\theta_d}{3\pi}\right)^{1/2}\text{ volts} \quad (28)$$

The values from equations 23 and 25 can be substituted in equation 28.

$$e_{rms}=\sqrt{k}\frac{4}{\sqrt{3\pi}}\left(\frac{E_sR}{Z_s}\right)^{1/4}E_m^{3/4}\text{ volts} \quad (29)$$

The watts loss in the core would be

$$W=\frac{e_{rms}^2}{R}=k\frac{16}{3\pi}\left(\frac{E_s}{Z_sR}\right)^{1/2}E_m^{3/2}\text{ watts} \quad (30)$$

It is possible to express these equations directly in terms of the material constants. Using the values for E_m and R developed in equations 69 and 74, Appendix I, equations 23, 25, 29, and 30 may be written as follows:

$$\frac{e_p}{NA}=k\,8.25\frac{(\omega B_m\rho)^{1/2}}{c}\left(\frac{NE_s}{lZ_s}\right)^{1/2}\times 10^{-4}\text{ v per turn per sq cm} \quad (31)$$

$$\theta_s+\theta_d=\frac{0.485c\left(\frac{\omega B_m}{\rho}\right)^{1/2}10^{-4}}{k\left(\frac{NE_s}{lZ_s}\right)^{1/2}}\text{ radians} \quad (32)$$

$$\frac{e_{rms}}{NA}=\sqrt{k}1.87\frac{\rho^{1/4}(\omega B_m)^{3/4}}{c^{1/2}}\left(\frac{NE_s}{lZ_s}\right)^{1/4}\times 10^{-6}\text{ v per turn per sq cm} \quad (33)$$

$$\frac{W}{G}=k0.29\frac{(\omega B_m)^{3/2}c}{\rho^{1/2}\delta}\left(\frac{NE_s}{lZ_s}\right)^{1/2}\times 10^{-12}\text{ w per gram} \quad (34)$$

* It is interesting to note that X does not appear in equation 23. This is a consequence of neglecting the additional terms of the form $1/n![(R/X)(\theta_s+\theta_d)]^n$ in the expansion by series to get equation 22. If X were very small, this could not be done. In effect, X has been assumed to be infinite with respect to $R(\theta_s+\theta_d)$, and in many problems this will be true. Therefore the voltage does not depend on X. This means that the change of flux in the core is limited entirely by the eddy currents, the permeability of the iron having a negligible effect.

METHOD B

As was mentioned earlier in this paper, high rates of change of flux in the core cause eddy currents which materially distort the flux distribution in the lamination. It is possible to write exact equations for the flux distribution in the lamination, assuming constant permeability. The condition is actually much different and vastly more complicated by the gradual yet enormous change in permeability. However, this solution will be used if the permeability value is chosen with this limitation in mind. In so doing, the mathematical analysis will be simplified if the flux density throughout the lamination is considered initially to be zero, instead of minus ϕ_m, and to rise from zero to twice its saturation value.

It would be expected that the peak voltage would occur when the surface of the lamination was just saturating. Figure 4 shows a single lamination of steel of thickness c and mean length of flux path l. It is assumed that the laminations are insulated from each other adequately and that the width of each lamination is large compared with its thickness. What occurs in this one lamination occurs in all of the others. This lamination is linked by a primary coil of N turns carrying an effective alternating current of I_s amperes. It is assumed that the transient will occur in a sufficiently short time that the slope of the current wave may be assumed constant and equal to its value at current zero. The equation for the primary coil magnetomotive force will be

$$\frac{0.4\pi\sqrt{2}I_sN\omega t}{l} \text{ oersted} \tag{35}$$

To agree with the change of flux from zero to twice maximum, this magnetomotive force will be assumed to be applied to the core at zero time. Let x be the distance out, measured from the center of the lamination; let H_o be the magnetomotive force at the center of the lamination; and let i' be the eddy current density at any point in the lamination. The magnetomotive force at x is

$$h=H_o+0.4\pi\int_0^x i'\,dx \text{ oersteds} \tag{36}$$

$$\frac{\partial^2 h}{\partial x^2}=0.4\pi\frac{\partial i'}{\partial x} \tag{37}$$

The induced voltage gradient in the lamination at any point x is

$$e'=10^{-8}\int_0^x\frac{\partial B}{\partial t}\,dx \tag{38}$$

$$B=\mu h \tag{39}$$

$$i'=\frac{e'}{\rho}=\frac{10^{-8}\mu}{\rho}\int_0^x\frac{\partial h}{\partial t}\,dx \tag{40}$$

$$\frac{\partial i'}{\partial x}=\frac{10^{-8}\mu}{\rho}\frac{\partial h}{\partial t} \tag{41}$$

Substituting equation 41 in equation 37,

$$\frac{\partial^2 h}{\partial x^2}=\frac{0.4\pi\mu 10^{-8}}{\rho}\frac{\partial h}{\partial t} \tag{42}$$

Since at the surface of the steel there will be no eddy currents to prevent the flow of flux, the magnetomotive force at the surface will be equal directly to that of the coil as given by equation 35. The

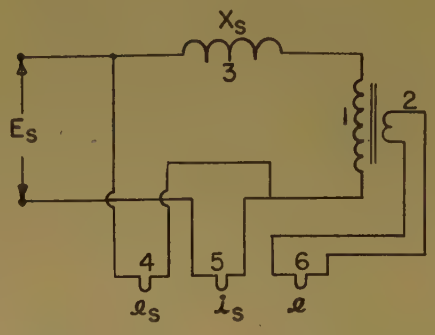


Figure 8. Test circuit for measuring peak voltages

The saturating reactor is 1, on which is wound a search coil, 2. The air-core loading reactor is 3, and 4, 5, and 6 are oscillograph elements

solution of equation 42 for these conditions (see Appendix III) is

$$h=\frac{0.4\pi\sqrt{2}I_sN\omega}{}\left\{t+\sum_{s=1}^{s=\infty}(-1)^s\times\right.$$
$$\frac{16}{(2s-1)^3\pi^3}\frac{0.4\pi\mu 10^{-8}}{\rho}\left(\frac{c}{2}\right)^2\left(\cos\frac{2s-1}{2}\cdot\frac{\pi x}{\frac{c}{2}}\right)\times$$
$$\left.\left(1-\epsilon^{-\frac{(2s-1)^2\pi^2}{4}\frac{\rho}{0.4\pi\mu\,10^{-8}}\frac{t}{(c/2)^2}}\right)\right\} \tag{43}$$

Let

$$K_h=\frac{hl}{0.4\pi\sqrt{2}I_sN\omega t} \tag{44}$$

$$K_t=\frac{\rho}{0.4\pi\mu 10^{-8}}\frac{t}{\left(\frac{c}{2}\right)^2} \tag{45}$$

Rewriting equation 43 using these values,

$$K_h=1+\sum_{s=1}^{s=\infty}(-1)^s\frac{16}{(2s-1)^3\pi^3}\times$$
$$\frac{\cos\frac{(2s-1)}{2}\frac{\pi x}{c/2}}{K_t}\left(1-\epsilon^{-\frac{(2s-1)^2\pi^2}{4}K_t}\right) \tag{46}$$

Figure 5 is a plot of equation 46 for various values of K_t. The total voltage induced in the coil would be

$$e=\frac{AN10^{-8}\mu}{\frac{c}{2}}\int_0^{c/2}\frac{\partial h}{\partial t}\,dx \tag{47}$$

Substituting the value of h from equation 43 and simplifying by substituting X and K_t for their equivalents,

$$K_e=\frac{e}{\sqrt{2}I_sX}=1-\sum_{s=1}^{s=\infty}\frac{8}{(2s-1)^2\pi^2}\times$$
$$\epsilon^{-\frac{(2s-1)^2\pi^2}{4}K_t} \tag{48}$$

Figure 6 is a curve of K_e as a function of K_t. It can be seen that for large values of K_t, $Ke=1$;

$$e=\sqrt{2}I_sX \tag{49}$$

In Appendix IV it is shown and from Figure 6 it can be seen that for small values of the variables,

$$K_e=\frac{2}{\sqrt{\pi}}\sqrt{K_t} \tag{50}$$

If the values for ρ and μ from equations 75 and 72 of Appendix I are substituted in equation 45 and this value of K_t substituted in equation 50,

$$e=I_s\left(\frac{8RX\theta}{3\pi}\right)^{1/2} \tag{51}$$

Comparing this equation with equation 7, this equation is seen to vary as the square root of time whereas equation 7, using the equivalent circuit, varies directly with time.

To find the angle at which the surface saturates, it is evident that the magnetomotive force at the surface is equal to that of the primary coil. From equation 37 then,

$$\mu\frac{0.4\pi\sqrt{2}I_sN\omega t_s}{l}=2B_m \tag{52}$$

Substituting the value of μ and B_m from equations 72 and 70 of Appendix I in equation 52,

$$\theta_s=\frac{2E_m}{I_sX} \tag{53}$$

Substituting this value of θ_s in equation 51,

$$e_p=\left(\frac{16I_sRE_m}{3\pi}\right)^{1/2} \tag{54}$$

Comparing this equation with equation 23 for the equivalent circuit analysis, the form is seen to be identical, except the coefficient, which is only 46 per cent as large.

Equation 54 is valid as long as the value of K_t at the time the surface saturates, or K_{ts}, is less than three-tenths.

the value of t_s from equation 52 is substituted into equation 45,

$$K_{ts}=\frac{5.06\rho B_m 10^{+8}}{\omega(\mu c)^2(NI_s/l)} \qquad (55)$$

All the factors in equation 55 are constant except the permeability μ. This varies over quite a range over the region of operation. K_{ts} is evaluated for the following example, which represents an average low-voltage current transformer, using a relatively low value for the permeability.

$\omega=377$	$\rho=60$ microhms per cm cube
$\mu=1{,}000$	
$B_m=12{,}000$ gausses	$NI_s=1{,}200$ ampere turns
$c=0.033$ cm	
$l=51$ cm	$K_{ts}=37.8$

Solving equation 44 for h, the flux density becomes

$$B=\mu h=\mu.4\pi\sqrt{2}I_s N\omega t\,\frac{K_h}{l}$$

Referring to Figure 5, if K_t exceeds one, the value of K_h will be between 0.55 and 1.0 so that the flux at every point will be at least 55 per cent of the maximum value. Considering that μ usually is not known within a factor of two, B might be considered to be uniform for all practical purposes. Since method A is based on uniform distribution of flux, we can say that when K_t exceeds unity, the flux distribution is sufficiently uniform that method A applies. In the example given, K_t will exceed unity after a very small fraction of the transient time has elapsed, and thus method A will be applicable.

The permeability is, of course, higher than 1,000 over part of the transient; however, it has been found that up to 1,000 ampere turns (rms) per inch, 29-gauge laminations, 60 cycles, the effect of nonuniform distribution of flux is slight and that method A with the 0.85 correction factor is satisfactory. Above this value the correction factor decreases to a minimum of six-tenths at very high ampere turns.

Not included in this paper is the effect of capacity in the windings, which also begins to take effect when the peak of voltage is very short.

Penetration of Flux Into the Lamination. After the surface of the lamination is saturated, the reversal must spread into the center of the lamination in some manner. Figure 5 is a curve drawn to show the flux distribution for various rates of change of flux. It is apparent that the more rapidly the flux changes, the less the penetration of the flux into the center of the lamination. Also, the

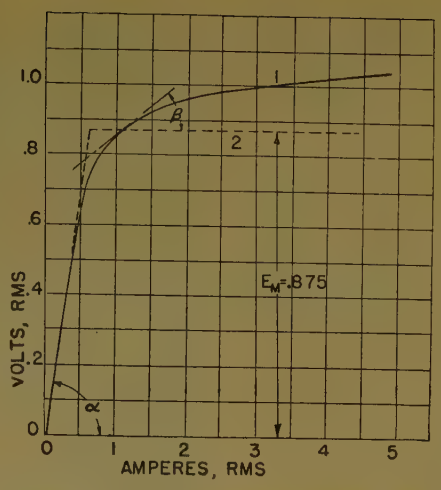


Figure 9. Iron-core reactor excitation curve

The actual curve is 1 and the assumed theoretical curve is 2. For a reactor with no air gaps, E_m is approximately the point of tangency of a line drawn tangent to the knee of the curve such that $\tan\beta=(\tan\alpha)/10$

width of the zone in which the flux is changing becomes smaller the more rapidly the change is made, and as a limit the wave front is almost vertical. As soon as the surface is saturated, the flux wave will start to penetrate the steel.

During this period the material can be divided into three zones: the center where there is little flux, the wave-front zone where the flux is changing, and the outer

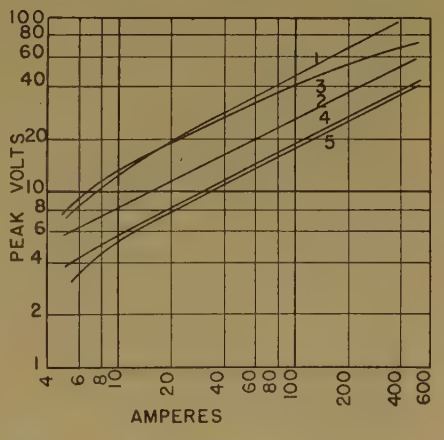


Figure 10. Peak voltage of a saturating reactor

1—Calculated curve for reactor only, using equation 12

2—Calculated curve for reactor only, assuming forcing of flux to surface of lamination, using equation 56

3—Test curve of reactor only which follows calculated curve 1 up to high values of current where it begins to bend over and approach curve 2

4—Calculated curve of reactor shunted by a 0.9-ohm resistor using equations 12 and 68

5—Test curve of reactor shunted by a 0.9-ohm resistor which follows the calculated curve 4 quite well

zone where the iron is saturated. The wave-front zone must travel in from the surface to the center. However, it must travel in with such a speed that it will induce enough voltage in the saturated zone behind it to circulate enough current to nearly balance the ampere turns of the primary coil. Enough ampere turns must be left over, though, to provide the magnetomotive force necessary for the wave-front zone. In the usual case, this will be small, and the generalization can be made that the eddy currents in the saturated zone must balance the primary ampere turns. If the flux travels in with a velocity of v centimeters per second, referring to Figure 7, the flux in the saturated zone in a strip one centimeter wide would be

$$\phi_s=2B_m vt \qquad (56)$$

The voltage gradient in the saturated zone would be

$$e'=(d\phi_s/dt)10^{-8}=2B_m v10^{-8}\text{ volts} \qquad (57)$$

The current density in the saturated zone is

$$i'=e'/\rho\text{ amperes per sq cm} \qquad (58)$$

The total current in the saturated zone is

$$i'vtl=\frac{2B_m v10^{-8}vtl}{\rho} \qquad (59)$$

This is equal to the primary ampere turns

$$\frac{2B_m v^2 10^{-8}tl}{\rho}=\sqrt{2}I_s\omega tN \qquad (60)$$

$$v=\left(\frac{I_s\omega N\rho 10^8}{\sqrt{2}B_m l}\right)^{1/2}\text{ centimeters per second} \qquad (61)$$

The total voltage induced in the primary coil will be

$$e=Ne'\frac{A}{c/2} \qquad (62)$$

If the value of v from equation 61 is substituted in equation 57, and this value of e' from equation 57 substituted in equation 62, and if the values of ρ and B_m from equations 75 and 70 of Appendix I are substituted in this equation for e, the peak voltage becomes.

$$e_p=\left(\frac{4I_s E_m R}{3}\right)^{1/2}\text{ volts} \qquad (63)$$

This is seen to be a value 12 per cent lower than that given by equation 54.

The voltage given by equation 63 is a flat-topped voltage. It is to be expected then that if a direct-current voltage were applied to a reactor, the current drawn would increase linearly with time,

$$i=\sqrt{2}\omega I_s t \qquad (64)$$

Substituting the value of I_s from equation 63,

$$i=\frac{1.06e_p^2\omega t}{E_mR} \text{ amperes} \qquad (65)$$

Shunting of Reactor With a Resistor. The open-circuit voltage of a current transformer can be controlled by connecting a resistor to the secondary terminals. The value of the resistor can be very high relative to any normal burden so that its normal shunting effect is negligible, and yet considerable reduction in voltage may be obtained. Short-circuited bands of resistance metal sometimes used for phase-angle correction have exactly the same effect. The effect can be calculated by considering this resistor to be in parallel with R (see Figure 2). The effective resistance of the burden resistance and the core resistance in parallel is

$$\frac{R_bR}{R_b+R}=\frac{R}{1+\frac{R}{R_b}} \qquad (66)$$

From equation 66 it is seen that the new effective resistance is the core resistance divided by $1+(R/R_b)$.

From equation 23 it is seen that the peak voltage with a shunt resistor is equal to the peak voltage without, divided by the square root of $1+(R/R_b)$.

From equation 29 it is seen that the root mean square voltage with a shunt resistor is equal to the value without a shunt resistor divided by the fourth root of $1+(R/R_b)$.

These formulas are applicable only to method A where the core resistance can be separated out. If a resistor of any size shunts the reactor, it usually will make the formulas of method A even more applicable, as the eddy currents and flux are definitely separated.

Test Data

Tests were made on a small ring-type iron-core reactor on alternating current to determine the peak voltages developed at various values of current. Tests also were made with the reactor shunted by a resistance to determine the effect of the resistor in reducing the peak voltages.

The circuit used is that shown in Figure 8. The series inductance for loading the circuit was an air-core reactor to make certain that it would have linear characteristics. A search coil was wound on the iron-core reactor and connected to an oscillograph element. The resistance of the oscillograph circuit was kept high so that its shunting effect on the peak voltages would be negligible. The line current and voltage also were connected to oscillograph elements. Tests were made on the reactor, measuring the currents and the peak voltages developed. These tests were rerun with a resistance shunted across the test reactor.

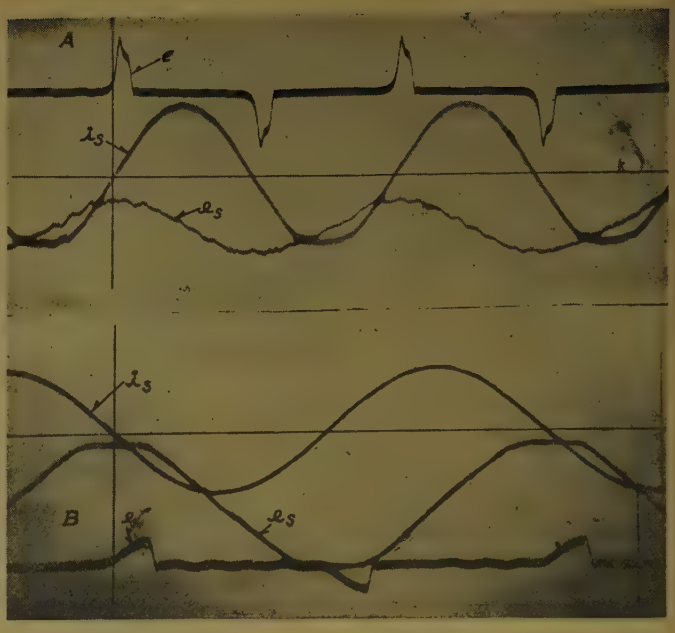


Figure 11. Oscillograms of peak voltage of a saturated reactor

Part *A* is for a reactor only; $I_s=5.8$ amperes root mean square, 60 cycles; and the peak voltage is 9.1 volts

Part *B* is for the reactor shunted by a 0.9-ohm resistor; $I_s=11.75$ amperes root mean square, 60 cycles; and the peak voltage is 5.9 volts. Part *A* shows flattening of the peaks of voltage from initial saturation of the surface and gradual penetration of the flux reversal. The minor peaks of voltage are caused by overtravel in the oscillograph. Part *B* corresponds to Figure 2C

Data for the circuit are as follows:

Power supply: 60 cycles alternating current, 0.2-ohm reactance

Air-core series reactor: 5.5 ohms

Test reactor:

Turns, $N=16$

Losses at 0.483 volts

$VA=0.159$ volt-ampere
W (total) $=0.129$ watt
W (eddy) $=0.049$ watt
$VAR=0.0925$ volt-ampere reactive

Excitation curve per Figure 9

Shunt resistor: 0.9 ohm

The results are given in curve form in Figure 10. Typical oscillograms are shown in Figure 11. It was found that the best correlation was secured between calculated and test data if a factor of 0.85 was used for k.

Calculations

Test reactor constants:

$$R=\frac{E^2}{w_e}=(0.483)^2/0.049=4.77 \text{ ohms}$$

$$X=\frac{E^2}{VAR}=(0.483)^2/0.0925=2.53 \text{ ohms}$$

From Figure 9, $E_m=0.875$ volt

Calculations by sinusoidal voltage, method *A:*

1. $I_s=5.8$ amperes, no shunt resistor

$$H_m=\frac{2E_mZ_sR}{E_s}\left(\frac{X+X_s}{XX_s}\right)^2$$

$$=\frac{2\times0.875\times4.77}{5.8}\left(\frac{2.53+5.7}{2.53\times5.7}\right)^2=0.47$$

From Figure 3, $H_p=0.68$, and using equation 12 for e_p,

$$e_p=k\frac{\sqrt{2}E_sXX_s}{Z_s(X+X_s)}H_p$$

$$e_p=0.85\frac{\sqrt{2}\times5.8\times2.53\times5.7}{2.53+5.7}0.68=8.3 \text{ volts}$$

2. $I_s=11.75$ amperes with 0.9-ohm shunt resistor

$$R'=\frac{RR_b}{R+R_b}=4.77\times0.9/(4.77+0.9)$$

$$=0.755 \text{ ohm}$$

$H_m=0.0366$, $H_p=0.25$

$$e_p=0.85\frac{\sqrt{2}\times11.75\times2.53\times5.7}{2.53+5.7}\times$$

$$0.25=6.2 \text{ volts}$$

Calculations by simplified equation 23:

1. No shunt resistor:

$$e_p=k\sqrt{8I_sE_mR}=0.85\sqrt{8I_s\times0.875\times4.77}$$

$$=4.9\sqrt{I_s} \text{ volts}$$

2. With 0.9-ohm shunt resistor:

$$e_p=\frac{4.9\sqrt{I_s}}{\left(1+\frac{R}{R_b}\right)^{1/2}}=\frac{4.9\sqrt{I_s}}{\left(1+\frac{4.77}{0.9}\right)^{1/2}}$$

$$=1.95\sqrt{I_s} \text{ volts}$$

Calculations by flux distribution, method *B;*

$$e_p=\left(\frac{16I_sE_mR}{3\pi}\right)^{1/2}=2.66\sqrt{I_s}$$

Table I. Peak Secondary Open-Circuit Voltage Developed by Typical Current Transformers With 100 Per Cent Primary Current, Maintained Sinusoidal, 60 Cycles

Type	Voltage Class	Current Ratio	Accuracy Rating	Peak Voltage
WE	600	200/5	0.5-B-0.1, 0.2	175
KO	5,000	5/5–600/5	1.2-B-0.1, 0.5	475
CT-5	5,000	5/5–600/5	0.3-B-0.1, 0.5, 2	1,800
H-5	5,000	2,500/5	0.3-B-0.1, 0.5, 2	11,000
*Ring	46,000	1,200/5	2.5-L-400	6,700
OPC-33	34,500	5/5–800/5	0.3-B-0.1, 0.5, 2	7,300
OPC-66	69,000	5/5–800/5	0.3-B-0.1, 0.5, 2	8,300

* Multiratio bushing type for use on 46-kv bushing.

These calculated curves also are placed on Figure 10.

Conclusions

The curves of Figure 10 which were calculated from method A (assumed uniform flux density in the lamination) show good agreement with the tests except at the higher values of current. At the higher values, the effect of crowding the flux to the surface becomes more noticeable. Presumably, at still higher currents the minimum value which would be calculated by method B, 46 per cent of that given by method A (when $K=1$), would be approached. The oscillograms all indicate a flattening of the top of the wave at higher currents, confirming the fact of a nearly uniform rate of flux change as the reversal travels in from the surface.

When the reactor is shunted by a resistor, accurate calculations are possible. The voltage peaks are nearly true triangles.

The method for fairly exact calculation of peak voltage will permit design of apparatus for minimum values of voltage, as far as possible, and design of proper protection against these voltages. One of the useful results of the method is that the energy available in the voltage peaks can be determined.

Table I lists the maximum open-circuit voltage that can be developed at rated current in certain typical current transformers. The voltage varies approximately as the square root of the current.

Symbols

A = net core area, sq cm
B = instantaneous flux density, gauss
B_m = maximum flux density, gauss (Figure 2)
c = core lamination thickness, cm
e = instantaneous voltage of reactor, volts
e_p = peak induced voltage of reactor, volts
e_{rms} = root mean square value of reactor peak voltage, volts
e' = eddy voltage gradient in lamination, volts/centimeter
E_s = system root mean square voltage, volts
E_m = root mean square voltage reactor will induce, volts, at B_m normal frequency
G = core weight, grams
h = instantaneous magnetomotive force in lamination, oersteds
H_m, H_n = see equation 9 and equation 19, respectively
H_o = instantaneous magnetomotive force at center of lamination, oersteds
H_p, H_q = see equation 11 and equation 20, respectively
i_r = instantaneous current through equivalent R of reactor, amperes
i_L = instantaneous current through equivalent L of reactor, amperes
i_s = instantaneous system current, amperes
i' = eddy current density in lamination, amperes per square centimeters
I_s = system root mean square current, amperes
k = experience factor for peak voltage, about 0.85
K_e = see equation 48
K_h = see equation 44
K_t = see equation 45
K_{ts} = see equation 55
l = mean length of flux path, centimeters
L = equivalent inductance for reactor, henries
L_s = system inductance, henries
N = reactor turns
R = equivalent resistance for reactor, ohms
R_b = resistance of shunt resistor, ohms
R_s = system resistance, ohms
t = time, seconds
v = velocity of flux wave, centimeters per second
W = core loss, watts
W_e = eddy component of core loss, watts
x = distance as measured from center of lamination, centimeters
X = equivalent reactance for reactor, ohms
X_s = system reactance, ohms
Z_s = system impedance, ohms
δ = core density, grams per cubic centimeter
$\theta = \omega t$, radians
θ_d = angle before current zero at which core desaturates, radians
θ_s = angle after current zero at which core saturates, radians
μ = core permeability
ρ = core resistivity, ohms per centimeter cube
ϕ = total flux in core, lines
ϕ_m = maximum total flux in core, lines
$\omega = 2\pi$ frequency, radians per second

Appendix I. Reactor Constants

At low frequencies, the equivalent circuit for the reactor is as shown in Figure 2, with an inductance and resistance in parallel. The primary definition of E_m, the maximum alternating voltage at system frequency that the reactor will induce, will be taken as equation 8. Using this as the definition has the advantage that if any correction must be applied to the theoretical values of the peak voltage, the duration of the pulse will be known to change in the opposite direction approximately the same percentage. This follows from equation 8, for the area under the voltage curve is a constant, regardless of the shape of the voltage curve. It usually will not be convenient to determine E_m in this manner, but from the sample tests it was found that the construction shown in Figure 9 gave a value of E_m that agreed with the oscillograms. Referring to Figure 9, a curve is drawn with the alternating-current voltage as a function of the alternating-current exciting current on rectangular-co-ordinate paper for a core with no air gaps. A line then is drawn tangent to the knee of the curve with a slope one-tenth the slope of the initial straight part of the curve. The point of tangency then gave E_m approximately.

The equivalent reactance X and the eddy-loss resistance, R, of the reactor can be determined from values of I, E, W (total watts loss), and W_e (watts eddy-loss) corresponding to some convenient point on the initial straight part of the excitation curve.

$$X = \frac{1}{\left[\left(\frac{I}{E}\right)^2 - \left(\frac{W}{E^2}\right)^2\right]^{1/2}} \text{ ohms} \qquad (67)$$

$$R = \frac{E^2}{W_e} \text{ ohms} \qquad (68)$$

The values of E_m, X, and R can be calculated from material constants, or the material constants can be calculated from test results by the following formulas:

$$E_m = \frac{\omega N B_m A 10^{-8}}{\sqrt{2}} \text{ volts} \qquad (69)$$

$$B_m = \sqrt{2} E_m / \omega N A \ 10^{-8} \text{ gauss} \qquad (70)$$

$$X = \omega 0.4\pi N^2 \mu A \ 10^{-8}/l \text{ ohms} \qquad (71)$$

$$\mu = Xl/(\omega 0.4\pi N^2 A \ 10^{-8}) \qquad (72)$$

$$W_e = \frac{E^2}{R} = \frac{(\omega N B A \ 10^{-8})^2}{2R}$$

$$= (\delta l A)\left[\frac{\omega^2 B^2 c^2 \ 10^{-16}}{24\delta\rho}\right] \text{ watts} \qquad (73)$$

$$R = 12N^2 A\rho/(lc^2) \text{ ohms} \qquad (74)$$

$$\rho = Rlc^2/(12N^2 A) \text{ ohms per centimeter cube} \qquad (75)$$

Appendix II. Calculation of θ_d

To calculate the angle at which the core starts to desaturate,

$$B_m = 0.4\pi N i \mu / l \qquad (76)$$

For time near current zero, the equation for the line current is approximately

$$i_s = \sqrt{2}\omega I_s t \tag{77}$$

$$\omega t = \theta_d = \frac{B_m l}{0.4\pi N \mu \sqrt{2} I_s} \tag{78}$$

Substituting the values of B_m and μ from equations 70 and 72,

$$\theta_d = \frac{E_m}{I_s X} \text{ radians} \tag{79}$$

Appendix III. Solution of Equation 43

Referring to "Mathematics of Modern Engineering," by Doherty and Keller,[5] page 282, the partial differential equation of a cable with distributed constants of series R and shunt C per unit of length is

$$\frac{\partial^2 e}{\partial x^2} = RC \frac{\partial e}{\partial t} \tag{80}$$

Comparing with equation 42, these are seen to be identical if

$$RC = \frac{0.4\pi\mu\, 10^{-8}}{\rho} \tag{81}$$

Since the terminal conditions are the same, the solution for voltage on a cable may be used for the solution of magnetomotive force for iron if the above substitution for RC is made.

The foregoing reference gives the solution on pages 285–7 for a unit function voltage applied to a cable of finite length with the receiving end open-circuited. The solution desired is that with a voltage which increases uniformly with time. This can be found very simply from the preceding solution by the following method. On page 286, equation 339 is given for the operational solution for voltage:

$$e = \frac{E \cosh nx}{\cosh nl} 1 \tag{82}$$

The solution desired for a voltage that increases linearly with time would be of the form

$$e = \frac{E' t \cosh nx}{\cosh nl} 1 \tag{83}$$

The operational form for t is $1/p$, though

$$e = \frac{E' \cosh nx}{p \cosh nl} 1 \tag{84}$$

The solution of equation 84 is

$$e = E' \int_0^t \left(\frac{\cosh nx}{\cosh nl} 1 \right) dt \tag{85}$$

Hence if the solution on page 287 is integrated from zero to t, it will be the solution for a voltage that increases linearly with time. This leads directly to equation 43.

Appendix IV. Solution of Equation 50

It is not at all evident from an inspection of equation 48 that it does approach equation 50 for low values of t. Letting $z^2 = K_t$ in equation 48,

$$\frac{dK_e}{dz} = \frac{8}{\pi^2} \sum_{s=1}^{s=\infty} \frac{\pi^2 2z}{4} \epsilon^{-\frac{(2s-1)^2 \pi^2 z^2}{4}} \tag{86}$$

If z approaches zero, this can be replaced by the integral

$$\frac{dK_e}{dz} = 4z \int_{s=0}^{s=\infty} \epsilon^{-\frac{(2s+1)^2 \pi^2 z^2}{4}} ds = \frac{4z}{\pi z} \frac{\sqrt{\pi}}{2} \tag{87}$$

$$\frac{dK_e}{dz} = \frac{2}{\sqrt{\pi}} \tag{88}$$

And for values of z near zero,

$$K_e = c_1 + \frac{2z}{\sqrt{\pi}} = c_1 + 2\frac{\sqrt{K_t}}{\sqrt{\pi}} \tag{89}$$

To show that c_1 is equal to zero, substitute in a point on the straight part of the curve of Figure 6.

Appendix V. Complete Solution for i_L

If $e_s = \sqrt{2} E_s \sin(\omega t + \psi)$, and if it is assumed that the line current has returned to its sinusoidal value after the peak during the previous half-cycle, the current through the equivalent inductance L is

$$i_L = K_1 \epsilon^{\lambda_1 t} + K_2 \epsilon^{\lambda_2 t} + \frac{\sqrt{2} E_s}{Z_t} \sin(\omega t + \psi - \beta) \tag{90}$$

$$\psi = \tan^{-1}(X_s/R_s) \tag{91}$$

$$\beta = \tan^{-1} \frac{\frac{R}{X_s} + \frac{R}{X} + \frac{R_s}{X_s}}{\frac{R}{X} \cdot \frac{R_s}{X_s} - 1} \tag{92}$$

$$Z_t = \frac{XX_s}{R} \left[\left(\frac{R}{X_s} + \frac{R}{X} + \frac{R_s}{X_s} \right)^2 + \left(\frac{R}{X} \cdot \frac{R_s}{X_s} - 1 \right)^2 \right]^{1/2} \tag{93}$$

$$\frac{2\lambda_1}{\omega} = -\left(\frac{R}{X_s} + \frac{R}{X} + \frac{R_s}{X_s} \right) - \left[\left(\frac{R}{X_s} + \frac{R}{X} + \frac{R_s}{X_s} \right)^2 - 4\left(\frac{R}{X} \cdot \frac{R_s}{X_s} \right) \right]^{1/2} \tag{94}$$

$$\frac{2\lambda_2}{\omega} = -\left(\frac{R}{X_s} + \frac{R}{X} + \frac{R_s}{X_s} \right) + \left[\left(\frac{R}{X_s} + \frac{R}{X} + \frac{R_s}{X_s} \right)^2 - 4\left(\frac{R}{X} \cdot \frac{R_s}{X_s} \right) \right]^{1/2} \tag{95}$$

$$K_1 = \frac{\sqrt{2} E_s \omega}{\lambda_2 - \lambda_1} \epsilon^{\frac{\lambda_1 \theta_d}{\omega}} \times \left[\frac{\cos(-\theta_d + \psi - \beta)}{Z_t} - \frac{\lambda_2 \sin \theta_d}{\omega Z_s} - \frac{\lambda_2 \sin(-\theta_d + \psi - \beta)}{\omega Z_t} \right] \tag{96}$$

$$K_2 = \frac{\sqrt{2} E_s \omega}{\lambda_1 - \lambda_2} \epsilon^{\frac{\lambda_2 \theta_d}{\omega}} \times \left[\frac{\cos(-\theta_d + \psi - \beta)}{Z_t} - \frac{\lambda_1 \sin \theta_d}{\omega Z_s} - \frac{\lambda_1 \sin(-\theta_d + \psi - \beta)}{\omega Z_t} \right] \tag{97}$$

$$Z_s = (R_s^2 + X_s^2)^{1/2} \tag{98}$$

θ_d is found from equation 79. To use equation 90, the time of saturation, t_s, is found by setting I_L equal to $+\sqrt{2}\, I_s \sin \theta_d$ and solving for t_s. The peak voltage is the value of $L(di_L/dt)$ at t_s. There appears to be no simple manner in which to secure t_s, and the nature of the problem does not warrant the labor as compared with the approximate methods developed in the paper.

References

1. Peak Voltages Across Saturating Reactances, H. Fahnoe, A. J. Maslin. *Electric Journal*, March 1932, page 120.

2. Peak Voltages on Saturating Reactances in Three-Phase Circuits, E. L. Harder. *Electric Journal*, March 1932, pages 124–9.

3. Overvoltage Protection of Current Transformer Secondary Windings and Associated Circuits, R. H. Kaufmann, G. Camilli. AIEE Transactions, volume 62, 1943, July section, pages 467–72.

4. Evolution of Standard Lines of Current Transformers for High Overcurrent Capacity, E. C. Wentz. AIEE Transactions, volume 63, 1944, September section, pages 658–62.

5. Mathematics of Modern Engineering, volume I (book), R. E. Doherty, E. G. Keller. John Wiley and Sons, New York, N. Y., 1936. Pages 282–7.

6. Characteristics of Current Transformers on Open Circuit, W. R. Woodward. *Electric Journal*, February 1918, pages 48–50.

A Tunable Rejection Filter

R. C. TAYLOR
ASSOCIATE AIEE

Synopsis: The theory and design of a tunable bridge-type narrow-band rejection filter are given for the general case, considering elements with dissipation. Range of adjustment and effect of manufacturing variations are discussed with the help of impedance circle diagrams. Approximate attenuation formulas for various levels of attenuation are derived, and a convenient graphical method of studying performance is suggested. A formula for the effective width of a special arrangement of two filters in tandem is derived.

IN COMMUNICATION and allied branches of electrical engineering, it is frequently necessary to use a filter with a narrow stop band to reject a single interfering frequency. It is the purpose of this paper to describe the theory of operation and methods for design and reduction to practice of such a device which has proved to be valuable at frequencies from 1,000 to 20,000 cycles per second. The principles of the device are equally applicable at much lower[1] and at much higher frequencies.

The familiar bridge circuit of Figure 1, frequently employed as a delay circuit, is the basic arrangement for the narrow band rejection filter. An elementary explanation of the device[2] sets forth that each of the bridge arms is resonant at the reject frequency and the inevitable dissipation is such that the four arms become equal resistances at the reject frequency, and the bridge is therefore balanced and the undesired frequency rejected. The impedance circle diagram of Figure 2 illustrates this concept. In the practical case, resistances are functions of frequency, and although the line and circle loci are distorted, the distortion is not enough to destroy the usefulness of the concept, since most of the distortion is in those parts of the loci far from resonance. The circle applies to the parallel resonant arms and the vertical line to the series resonant arms. The familiar half-energy points of the resonance curve are found at the intersections of the 45-degree lines with these loci, which Kennelly has called the quadrantal points.[3] Both loci contain arrowheads to indicate the direction in which the tip of the impedance vector moves as the frequency increases. The narrowness of the stop region near the balance point b is a function of the velocity with which these vector loci are traced as the frequency is varied. Since they are traced most rapidly near resonance, which occurs at b, and particularly since they are traced in opposite directions near the balance point, a very narrow stop band is realized, the width of which is found to vary inversely as the circuit Q. A device of this kind rejecting 1,100 cycles per second has been inserted in a telephone circuit with negligible loss of intelligibility.

The construction of such a device with the line exactly tangent to the circle and the resonance of all arms of the bridge occurring at the same frequency is difficult and unnecessary, since closely similar performance can be realized with the balance condition illustrated in Figure 3. In Figure 3, the balance point does not occur at resonance, and the series and parallel circuits have different resonant points shown at r_1 and r_2. There are two possible balance conditions indicated by the intersection points b_1 and b_2, and either can be obtained by adjusting the resonant frequencies. The impedances of all four bridge arms at balance are equal both in magnitude and angle. This procedure requires much less accurate control of the resistance, which is often less predictable than the reactance, and assures a balance, since a balance is always possible if the line and the circle intersect. If the tangent condition is attempted, any increase in dissipation results in the separation of the two loci, and no balance is possible, although some attenuation can be obtained where the loci are nearest together.

Range of Adjustment

A considerable range of reject frequencies is obtainable with any given set of coils. Consider, for example, a coil that has no dissipation other than d-c resistance. The position of the straight line locus then is independent of frequency. The diameter of the circle locus is proportional to the square of the resonant frequency according to the equation,

$$\text{Resonant resistance} = \omega^2 L^2 / R_{DC}$$

If a rejection filter of this type, operating as shown in Figure 3, is tuned to successively lower frequencies, the circle locus will decrease in size until the tangent condition of Figure 2 is reached. With any further decrease in frequency, the loci will separate and no balance will be possible. If the frequency is increased above that corresponding to Figure 3, the diameter of the circle will increase as the square of the frequency, and the balance points b_1 and b_2 will become farther and farther separated from the resonance r_2. Balance is still possible, since the loci intersect, but it is not usually desirable to use this condition, since it produces an

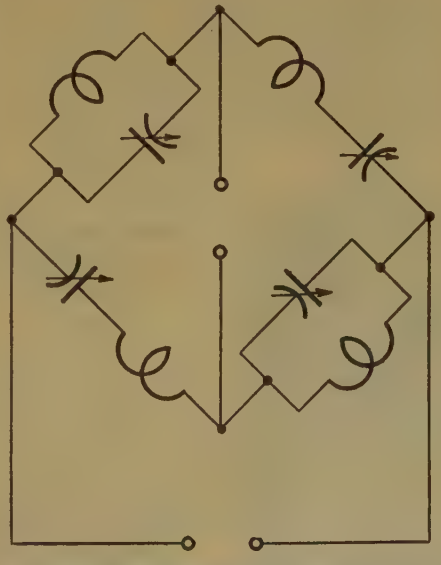


Figure 1. Basic circuit of the rejection filter

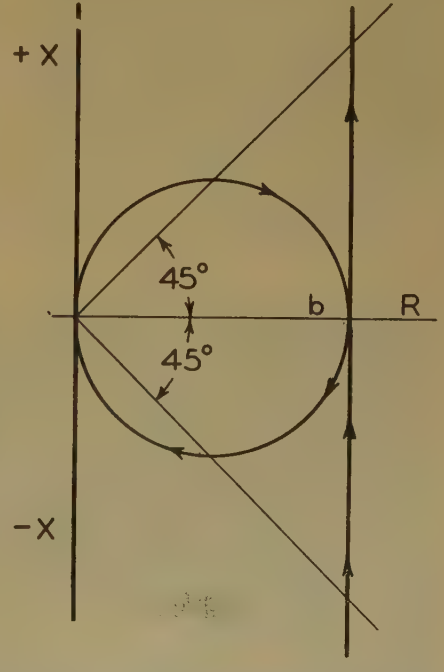


Figure 2. Impedance diagram, limiting case

Paper 46-23, recommended by the AIEE committee on communication for presentation at the AIEE winter convention, New York, N. Y., January 21–25, 1946. Manuscript submitted November 8, 1945; made available for printing December 12, 1945.

R. C. TAYLOR is with the engineering department, Western Union Telegraph Company, New York, N. Y.

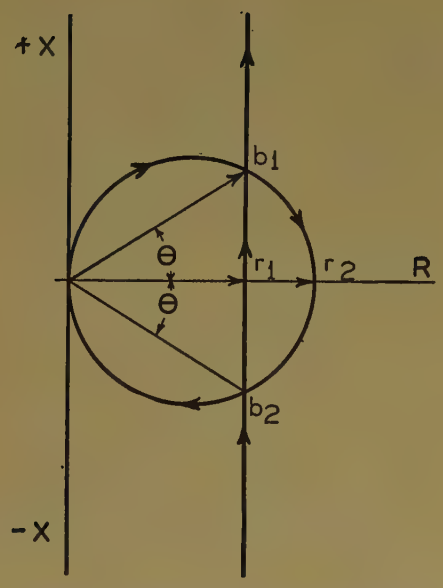


Figure 3. Impedance diagram, general case

effect very similar to reducing the Q. If an arbitrary standard were set up requiring the parallel resonant resistance to be not more than twice the series resonant resistance (line passing through center of circle), then the frequency range of adjustment in this case would be limited to $\sqrt{2}$ to 1. However, as bad a condition as this is seldom met in practice, and a range of adjustment approaching two to one is practicable in most cases. The range realized depends on the variation of dissipation with frequency and on the need for maximum narrowness of stop band.

Theoretically, infinite range of adjustment is obtained when the product of the series resonant and shunt resonant Q's is constant. As an illustration, let the dissipation of the series resonant circuit be a series resistance independent of frequency and the dissipation of the parallel resonant circuit be a shunt resistance independent of frequency and, of course, slightly larger than the series resistance. This results in constant product of the Q's and is also the condition for no distortion of the loci, and resonant resistance independent of frequency. Such a combination could be tuned to reject any frequency with equally good results. Practically, such a combination of properties is seldom available without loss of stability or circuit Q, and one is likely to find the resonant resistance of desirable components varying with the frequency, introducing some distortion of the loci and limiting the range of adjustment to about two to one.

Practical Circuit Arrangement

In practice it is usually preferable to modify the circuit of Figure 1 to that of Figure 5, where inductances with the same letter designations are on the same core. Imperfect coupling between windings is not often serious, the principal effect being the inclusion of a series inductance in the parallel resonant branches. Since at frequencies much greater than balance frequency, the useful frequencies flow to the receiver through the parallel resonant arms of the bridge, the series inductance will limit the high frequency response. In practice this limitation is not severe, since the parallel resonant inductance is a small one if the Q is ten or greater; leakage inductance can easily be made a small fraction of the total; and consequently a wide pass band above the reject frequency will exist. It has been found convenient to select transformation ratios that make the three capacitors marked C of equal capacity.

Since the stop band is very narrow, it is usually desirable to use trimmer capacitors which permit about one per cent adjustment of capacity (Figures 4 and 5). Larger air capacitors with precision mechanical drives are convenient for greater range. Figure 5 shows input and output coupling transformers to match impedance levels.

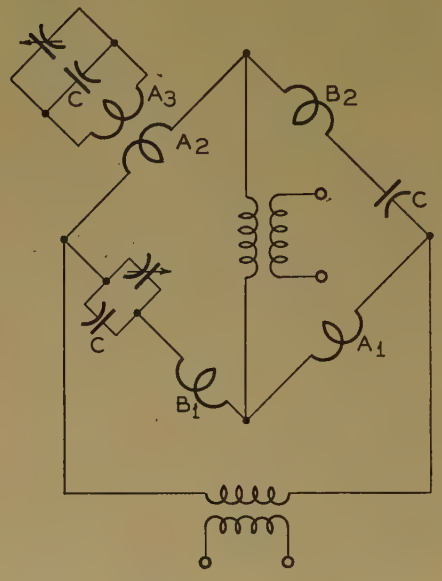


Figure 5. Practical circuit of the rejection filter

Attenuation Formulas and Graphs

The attenuation of all such reject filters is shown as a function of frequency in Figures 6 and 7. These curves can be represented for attenuations greater than ten decibels by the following equation derived in the appendix:

$$\alpha = 20 \log_{10} (K/W) \qquad (1)$$

These curves are universal curves, since the constant K has the same dimensions as the variable W, the width of the stop band on the frequency scale at attentuation α. In other words, the frequency scale may be thought of as plotted in K units as indicated in Figure 7.

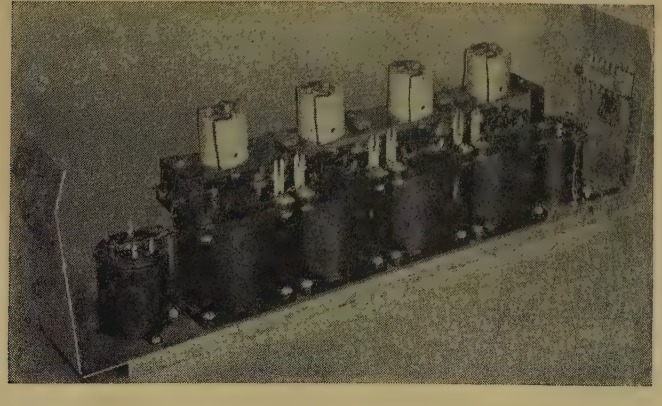


Figure 4 (left). Tandem filter showing trimmer capacitors

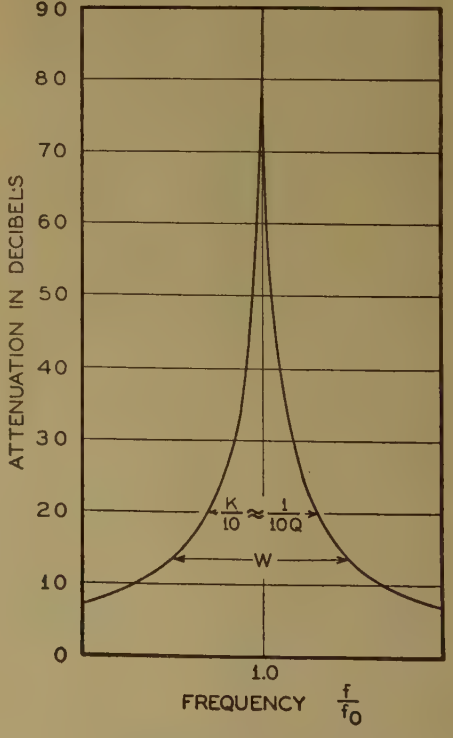


Figure 6 (right). Attenuation of single rejection filter

In Figure 7 the dotted curve at A indicates either an imperfect balance or noise present in the test equipment, and the dotted extension at B indicates a graphical method of determining K. If the data are plotted with width in cycles per second as abscissa instead of K units as abscissa, the intersection of the straight line with the axis gives the actual value of K in cycles per second.

A slightly more complicated empirical equation useful down to three decibels is

$$\alpha = 20 \log_{10} [K/W + 1/(1 + K/W)] \qquad (2)$$

K can be determined graphically from the curves, as indicated, or computed by formula 25. As shown in the appendix, a better approximation for attenuations between one-tenth decibel and three decibels is given by

$$\alpha = 20 \log_{10} [1 + (1/2)(K/W)^2] \qquad (3)$$

The attenuation curve is rather difficult to measure at large attenuations, since either or both low frequency noise and harmonics of the reject frequency tend to reduce the apparent attenuation. Another difficulty is the requirement of very small frequency steps near the reject frequency. A cycles increment dial on a beat frequency oscillator is a convenience for these tests.

Figure 7 suggests the use of two crossed rejection filters as a discriminator in frequency modulation receivers, provided some ten decibels of minimum loss can be tolerated.

Two Reject Filters in Tandem

If a rejection band wider than that provided by one section of this type of filter is required to secure sufficient band width to reject a narrow band of frequencies rather than a single frequency, it may be desirable to widen the stop band by using two or more filters in tandem, each filter rejecting a slightly different frequency. In some cases this arrangement may be found advantageous to preserve the required attenuation if the circuit elements are not sufficiently stable. Two sections result in a characteristic of the type shown in Figure 8. Using equation 1, it can be shown (see appendix) that

$$W_0/W_s = \sqrt{2 \text{ antilog}_{10} (\alpha_0/20)} \qquad (4)$$

where W_s is the width of one filter at the attenuation α_0. The increase in width is shown by Table I, which shows a very large relative increase at high attenuations.

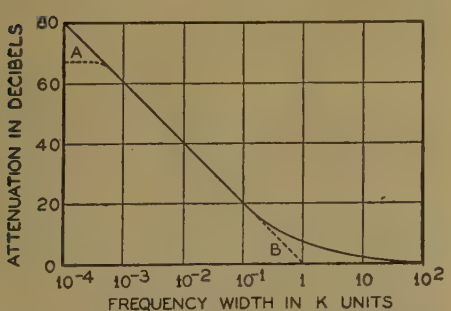


Figure 7. Graphical method of determining K

Stability Measurements

In the construction of these filters, it is essential that all components, including the resistances of the circuit, have good stability with respect to temperature, humidity, and voltage. Silvered-mica capacitors with air trimmers and powdered-iron cores made of Carbonyl E iron have been found to be of satisfactory stability. The final stability coefficient of the rejection frequency and attenuation is a complex function of the separate coefficients of the filter components and also of whichever of the two possible balance points is selected. One model designed to be tunable from 3,000 to 4,800 cycles per second was adjusted to 70 decibels attenuation at 3,600 cycles per second, and subjected to temperatures from 55 to 100 degrees Fahrenheit. The peak attenuation decreased about five decibels and the frequency at which the peak occurred changed less than two cycles per second. In any individual case, the various temperature coefficients can be made to counteract each other if components of both positive and negative coefficients are available.

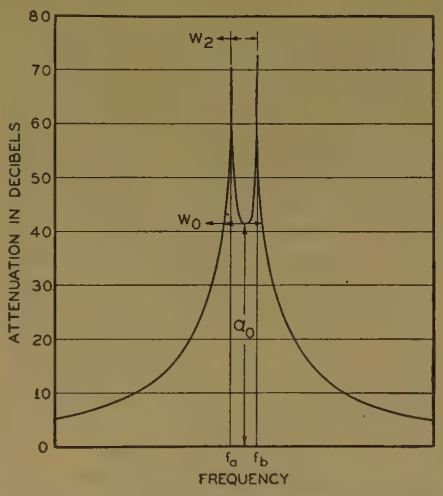


Figure 8. Attenuation characteristic of tandem rejection filters

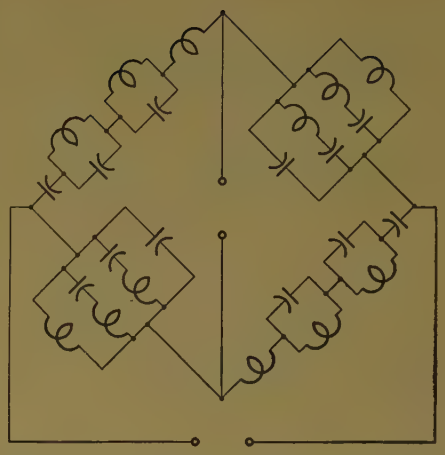


Figure 9. Multiple frequency rejection filter

Relation to Filter Theory

While it is obviously appropriate to call this device a filter, since it has pass and stop frequency regions, the attenuation in the stop band is explained only by the resistances present, while conventional filter theory excludes resistance and deals with reactances. The device illustrated in Figure 1 is an all-pass network with no attenuation at any frequency when considered as a conventional filter. It is only when resistance is considered as in Figures 2 and 3 that the attenuation region appears. If the resonant frequencies of the series tuned and shunt tuned arms are slightly separated, then an attenuation band is predicted by filter theory; but only small attenuations will be realized when reactances of the size given by the design equations are used.

The extension of these principles to multiple reject frequencies in a single section is illustrated in Figure 9. Such a device results in an economy of elements but requires variable inductors as well as capacitors, and the adjustments of various reject frequencies are not independent, so that a more practical solution may be the use of simpler sections in tandem. The bridge arms in Figure 9 are shown in a canonic form.[4]

Coil Design

Since the Q of the circuit determines the narrowness of the rejection band and

Table I. K Units

Db	W_s	W_0	W_0/W_s
20	0.1	0.447	4.47
34	0.02	0.20	10.
40	0.01	0.141	14.1
60	0.001	0.0447	44.7
74	0.0002	0.02	100.

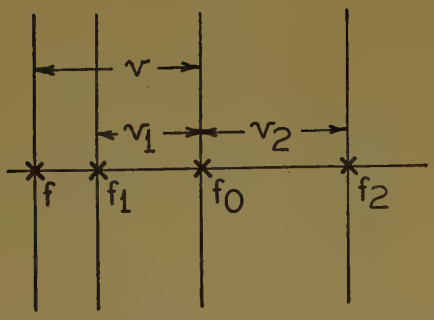


Figure 10. Relation of resonant and balance frequencies

the capacitors are responsible for little of the loss in the circuit, the design of coils with a specified high Q is fundamental. Another important factor results from the large ratio between the inductances of the parallel and series tuned branches. Equation 32 shows this ratio to be approximately Q^2 and therefore may be as high as 100,000 or more. This indirectly determines the impedance level of the bridge, since the series-tuned inductances should not be so large as to lose Q from distributed capacity and leakage effects, and the parallel-tuned inductance should not be so small as to require too small a number of turns, since it is impossible to get close coupling to the tuned winding with less than one turn, and the change of one turn in a small number results in a limited choice of inductance.

Typical windings are illustrated in Figure 11. Notice that in Figure 11A most of the space is allotted to the tuned winding to get maximum Q and consequently minimum width of the reject band.

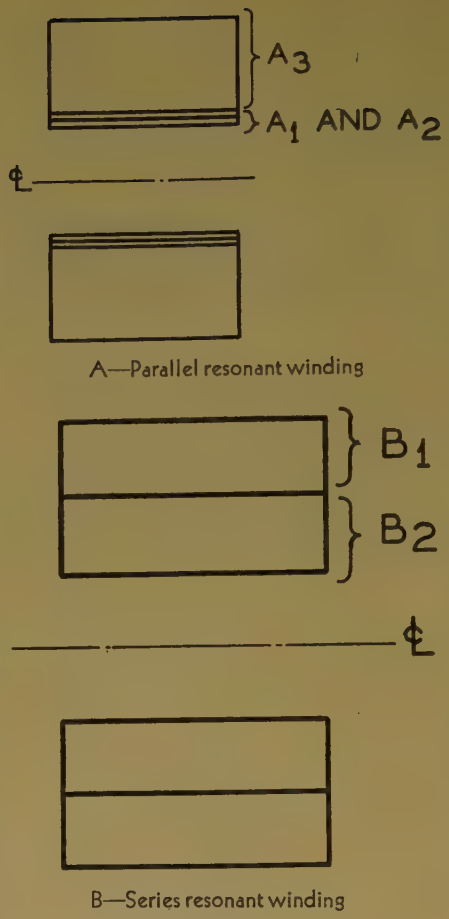


Figure 11

Appendix

Attenuation Formulas

The propagation constant of a bridge or lattice network is given by[4]

$$\alpha = 20 \log_{10} [(\sqrt{ZY}+1)/(\sqrt{ZY}-1)] \quad (5)$$

and balance of the bridge is obtained when $ZY=1+j0$. Two approximate forms of the equation for the propagation constant are of interest in this application. The first is applicable when

$$ZY=1+jT \qquad T \ll 1$$

and results in

$$\alpha = 20 \log_{10} (4/T) \quad (6)$$

The other is applicable when

$$ZY=-S+jT \qquad T \ll S$$

and results in

$$\alpha = 20 \log_{10} (1+T/S^{3/2}) \approx 17.37 T/S^{3/2} \quad (7)$$

The impedance of the series resonant arm is given by

$$Z_1 = -jX_1[(f_1/f)-(f/f_1)+jR/X_1] \quad (8)$$

where

$$X_1 = 2\pi f_1 L_1$$

and the admittance of the parallel resonant arm is given by

$$Y_2 = -jB_2[(f_2/f)-(f/f_2)+jG/B_2] \quad (9)$$

where

$$B_2 = 2\pi f_2 C_2$$

and R, X, G, B, Z, and Y have their usual Ohm's law meaning, and f_1 and f_2 are the resonant frequencies of Z_1 and Y_2 respectively. The appearance of the expressions may be simplified by writing them as

$$Z_1 = -jX_1(m_1+j1/Q_1) \quad (8a)$$

$$Y_2 = -jB_2(m_2+j1/Q_2) \quad (9a)$$

Using equations 8a and 9a,

$$Z_1Y_2 = -X_1B_2[m_1m_2-1/Q_1Q_2+ j(m_1/Q_2+m_2/Q_1)] \quad (10)$$

where

$$X_1B_2 = 4\pi^2 f_1 f_2 L_1 C_2 = f_1L_1/f_2L_2 \quad (11)$$

At balance

$$\sqrt{ZY} = 1+j0 \quad (12)$$

Consequently balance conditions are

$$m_1/Q_2 = m_2/Q_1 = 0 \quad (13)$$

and

$$1/X_1B_2 = 1/(Q_1Q_2)-(m_1m_2) = 1/Q_a^2 \quad (14)$$

Calculation of m_1 and m_2 near balance may be made easier if f/f_1 is written (see Figure 10) as

$$f/f_1 = 1-(v-v_1)/f_1 = 1-a \quad (15)$$

and similarly

$$f/f_2 = 1-(v-v_2)/f_2 = 1-b \quad (16)$$

Then

$$m_1 = 1/(1-a)-(1-a) = 2a+a^2+a^3+\ldots. \quad (17)$$

$$m_2 = 1/(1-b)-(1-b) = 2b+b^2+b^3+\ldots. \quad (18)$$

and

$$m_1m_2 = 4ab+2a^2b+2ab^2+2a^3b+ a^2b^2+2ab^3+\ldots. \quad (19)$$

Near balance,

$$m_1m_2-1/Q_1Q_2 \approx -1/Q_a^2 \quad (20)$$

Since Q_1 and Q_2 vary slowly and $m_1m_2 \ll 1/Q_1Q_2$

$$Z_1Y_2 \approx 1-jQ_a^2(m_1/Q_2+m_2/Q_1) \quad (21)$$

Equation 6 is applicable, giving

$$\alpha = 20 \log_{10} [4/Q_a^2(m_1/Q_2+m_2/Q_1)] \quad (22)$$

Farther from balance, $m_1m_2 \gg 1/Q_1Q_2$ and

$$Z_1Y_2 \approx -Q_a^2m_1m_2-jQ_a^2(m_1/Q_2+m_2/Q_1) \quad (23)$$

Equation 7 is applicable, giving

$$\alpha = 20 \log_{10}\left[1+\frac{Q_a^2(m_1/Q_2+m_2/Q_1}{(Q_a^2\ m_1m_2)^{3/2}}\right] \quad (24)$$

The simplified formulas 1 and 3 can be obtained from 22 and 24 by letting $Q_1=Q_2$, which allows v_1 to be taken equal to v_2. Letting the definition of K be

$$K = 2f_0Q/Q_a^2 \quad (25)$$

Equation 22 becomes

$$\alpha = 20 \log_{10} (2f_0/WQ_a^2) = 20 \log_{10} (K/W) \quad (22a)$$

and equation 24 becomes

$$\alpha = 20 \log_{10} [1+(1/2)(Q_a/Q)^2(K/W)^2] \quad (24a)$$

which is identical with equation 3 when $Q_a=Q$.

Stop Band for Two Filters in Tandem

If a filter rejecting frequency f_a is connected in tandem with a similar one rejecting f_b where $f_b-f_a=W_2$ (Figure 8), the sum of the attenuations will have a minimum α_0 midway between f_a and f_b. If the component attenuations are large enough for formula 1 to apply, we can determine the width W_0 of the reject band having attenuation α_0 by the following process. Let the width at frequency f (less than f_a) of the filter rejecting f_a be called W. Then the

filter rejecting f_b has width $W+2W_2$ at frequency f.

At the central minimum

$$\alpha_s = 20 \log_{10} (K/W_2)^2 \quad (26)$$

Let $f=f_1$ and $W=W_1$ at the edge of the stop band having attenuation α_s. Then

$$\alpha_0 = 20 \log_{10} (K/W_1)[K/(W_1+2W_2)] \quad (27)$$

For a single section with attenuation α_0.

$$\alpha_0 = 20 \log_{10} (K/W_s) \quad (28)$$

Consequently, from equations 26, 27, and 28,

$$W_1(W_1+2W_2) = W_2^2 = KW_s \quad (29)$$

and since

$$W_1 = W_0 - W_2 \quad (30)$$

equation 29 can be rewritten to give

$$W_0/W_s = \sqrt{2K/W_s} = \sqrt{2 \text{ antilog}_{10} (\alpha_0/20)} \quad (31)$$

and

$$W_0/W_2 = \sqrt{2} \quad (31a)$$

Design Equations

Combining equations 11 and 14,

$$L_1/L_2 = f_2 Q_a^2/f_1 \quad (32)$$

The second equation to permit solving for L_1 and L_2 is obtained by setting the quotient of equations 8 and 9 equal to R_0^2, where R_0 is the resistance of generator and load. This results at pass band frequencies in

$$L_1 L_2 = R_0^2/4\pi^2 f_1 f_2 \quad (33)$$

Combining equations 32 and 33, we get

$$L_1 = Q_a R_0/2\pi f_1 \quad (34)$$

and

$$L_2 = R_0/2\pi f_2 Q_a \quad (35)$$

L_1 and L_2 are the inductances actually effective in the bridge arms. If the coupled arrangement of Figure 5 is used, the coupling coefficients increase the inductances as follows:

$$L_1 = (Q_a R_0/2\pi f_1) 2/(1+k_1) \quad (34a)$$

and

$$L_2 = R_0/2\pi f_2 Q_a k_2^2 \quad (35a)$$

where k_1 is the coupling coefficient between windings B in Figure 5 and k_2 is the coupling coefficient between the tuned winding A and either of the A windings included in the bridge arms.

References

1. Control of Inductive Interference to Telegraph Systems, J. W. Milnor. AIEE Transactions, volume 59, 1940, August section, pages 469–74.

2. United States Patent 2,173,722.

3. Electrical Vibration Instruments (book), A. E. Kennelly. Macmillan Company, New York, N. Y., 1923.

4. Electrical Networks, volume II, E. A. Guillemin. John Wiley and Sons, Inc., New York, N. Y., 1935.

Protection of Pilot Wires From Induced Potentials

R. B. KILLEN
ASSOCIATE AIEE

G. G. LAW
ASSOCIATE AIEE

Synopsis: The use of pilot-wire relays for protection of power transmission circuits usually requires a reliable pilot channel which is free of any induced potentials which may cause transient voltages to appear between wires even though they may be of relatively low magnitude. This is particularly true in the case of pilot relays using a sequence network in which a single-phase alternating voltage is applied to the pilot wires. Conventional methods of protection, such as those used on telephone circuits, are not suitable. As a result it frequently has been necessary to install special pilot circuits which are insulated for voltages far in excess of their normal operating voltage to insure reliable operation. This paper describes a method of protection which provides reliable and satisfactory operation of a-c pilot channels through low-voltage telephone-type cable even though the cable may be subject to induced potentials high enough to operate discharge gaps.

PILOT WIRES used for relay protection of 66-kv transmission lines on the system of The Dayton Power and Light Company in several cases parallel 12-kv distribution feeders. Lead-sheathed telephone cable is used. In overhead sections it is installed on the same poles with the 12-kv lines and in underground sections occupies adjacent ducts to 12-kv underground feeders.

Figure 1 is a map of the protected 66-kv circuits and the routes of the pilot wires and their paralleling 12-kv 4-wire feeders. Figures 2 and 3 show typical configurations of the exposures. All cable sheaths, including the pilot-wire cable sheaths, are bonded at every manhole. Power cable sheaths serve as neutral conductors and are grounded at the substation and at all terminals or risers. The pilot-wire cable sheaths are grounded at each terminal, at the dispatcher's office, and at every riser. In overhead sections the power system neutral is multigrounded but not bonded to the telephone cable sheath, except at risers. The 12-kv system neutral is solidly grounded at substations.

A schematic diagram of the pilot relay circuits, as originally installed, is shown in Figure 4. During fault conditions, single-phase alternating potentials are applied to the pilot wires by the positive- and zero-sequence networks in the pilot relays. When unequal currents flow in and out of the line section, unequal voltages are produced by the relay networks and the resultant difference in current flows through the operating coils. During faults external to the protected section, the potentials produced by the relay networks at opposite terminals act in series, circulating current through the restraint coils and pilot wires to prevent tripping.

The condition thus is established that when the voltage between pilot wires is built up to a critical value by reason of unequal currents flowing in and out of the line section, tripping occurs. It is also true that if this critical voltage is exceeded by reason of some extraneous voltage impressed between pilot wires, tripping will occur.

The maximum current and voltage impressed on the pilot wires by the relays is approximately 100 milliamperes and 60 volts. The minimum alternating potential required between pilot wires to cause the relay contacts to close is approximately 15 volts.

Incorrect Operations

Early experience in the operation of the relays disclosed the following types of incorrect operations:

1. Potentials induced by ground faults on 12-kv circuits paralleling the pilot wires caused incorrect tripping of 66-kv breakers. An example of this type of incorrect operation occurred during a 12-kv line-to-ground fault at industrial plant A (see Figure 1). Induced potentials appeared on the paralleling pilot wires, causing operation of the carbon block protectors. The discharge through these protectors, being unequal, resulted in a potential appearing between pilot wires, which caused tripping of all 66-kv circuits supplying Webster substation.

Paper 46-35, recommended by the AIEE committees on protective devices and power transmission and distribution for presentation at the AIEE winter convention, New York, N. Y., January 21–25, 1946. Manuscript submitted October 29, 1945; made available for printing December 18, 1945.

R. B. Killen is planning engineer and G. G. Law is supervisor, testing department, The Dayton Power and Light Company, Dayton, Ohio.

The authors wish to acknowledge the assistance of representatives of the American Telephone and Telegraph Company, General Electric Company, and Westinghouse Electric Corporation.

2. Normal load currents in paralleling 12-kv 4-wire feeders caused induced potentials in the pilot wires which circulated current through the alarm relays and gave incorrect alarms. Potentials of 20 to 30 volts between pilot wires and ground frequently were encountered. This potential caused current to flow through the distributed capacitance of the pilot wires to ground, some of which returned through the grounded mid-point of the supervisory relay transformer. The capacitors connected between mid-points of the insulating transformer and the ground served to by-pass some of this current. However, this did not entirely correct the difficulty.

3. Normal load currents in paralleling 12-kv 4-wire feeders caused induced potentials in the pilot wires, which incorrectly tripped 66-kv breakers if one pilot wire accidentally became grounded. Grounding of one pilot wire causes any induced potential to appear between pilot wires. If the potential exceeds 15 volts, tripping results. Several operations of this type occurred when workmen accidently grounded one of the pilot wires while working on other circuits in the cable.

As a result of these difficulties, a series of investigations was conducted to determine the magnitude of the extraneous potentials appearing on the pilot wires and to devise a suitable means of correcting these troubles.

Field Tests

Field tests were carried out on the underground exposure from Webster to industrial plant *A* and on the overhead exposure from Hoover to industrial plant *B*. These tests were designed to determine the magnitude of the longitudinal voltages with which a protective scheme would have to deal. With the power circuits disconnected from their normal busses, a 230-volt test voltage was applied to cause ground fault current to flow in the exposures. From these tests, mutual impedance values were found as shown in Table I. Applying these factors to calculated values of fault current, the maximum longitudinal pilot-wire voltage was found to be 1,650 volts. With this information, the problem was resolved into designing a protective scheme meeting certain requirements for satisfactory operation of the relays.

Pilot-Wire Protective Scheme

The fundamental requirements of the protective scheme are as follows:

1. The protective scheme should function to discharge properly any extraneous potentials imposed in the pilot wires without resulting in any appreciable potential difference appearing between pilot wires. Any such potential between wires should not exceed 15 volts.

2. The voltage from a pilot wire to ground (or other wires in the cable) must be limited to 700 volts crest value during any system disturbance to avoid exceeding the voltage rating of the cable.

3. The protective scheme should permit normal operation of the pilot relays during periods in which the protective equipment is functioning. This is necessary to insure correct relay operation in case of faults involving both 66-kv and 12-kv circuits simultaneously.

4. The proper functioning of the pilot-wire supervisory relays, which indicate to the operators the presence of open- or short-circuit conditions in the pilot wires, must be maintained.

5. The protective equipment used must automatically restore the circuits to normal after its operation.

With these requirements in mind, it appeared that a solution could be found

Table I. Pilot-Wire Voltages to Ground Resulting From Faults on Paralleling 12-Kv Feeders

	*Underground Exposure	Overhead Exposure
Mutual impedance in ohms per mile (ratio of pilot-wire voltage per mile of exposure to ground fault current in power circuits)	0.096–0.100	0.262–0.265

* Fault current in either or both power cables to industrial plant *A*.

Table II. Laboratory Measurements of Pilot-Wire Currents and Voltages

Current in ground lead of arresters, amp	18.4
Applied longitudinal pilot-wire voltage, v rms	1,500
Voltage from pilot wire to ground at terminals of insulating transformer, v rms	293
Voltage between pilot wires at terminals of insulating transformer, v rms	2.6

Table III. Zero-Phase-Sequence Constants of Underground Cables From Webster to Industrial Plant *A*

	One Cable	Two Cables
Voltage impressed between paralleled phase conductors and ground, v	210	197
Total current, amp	332.8	552
Power input, kw	49	89.6
Length of cable, miles	1.87	1.87
Z_0 in ohms per phase per mile	0.710+*j*0.722	0.472+*j*0.324

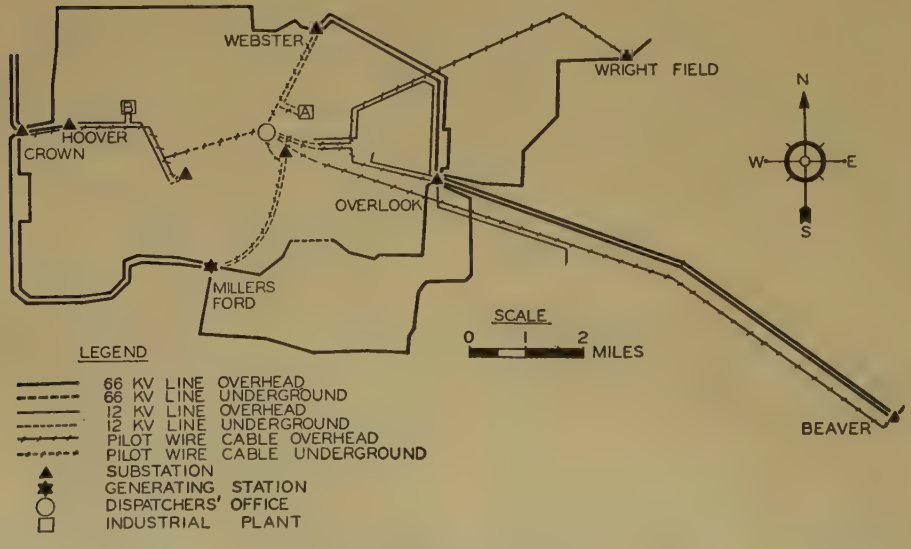


Figure 1. Map of 66-kv lines protected by pilot-wire relaying showing routes of pilot-wire cables and inductive exposures to 12-kv power feeders

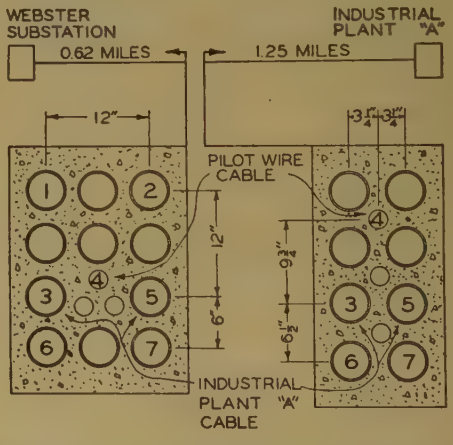


Figure 2. Details of underground ducts between Webster substation and industrial plant *A*

Cables 1, 2, 3, 5, 6, and 7 are 3-conductor 500,000-cir-mil shielded sector-type, with 13/64-inch conductor insulation and 8/64-inch lead sheath. Cable 4 is 51-pair number 19 0.075-inch-lead 0.95-inch-outside-diameter pilot-wire cable

Table IV. Phase Angle of Pilot-Wire Voltages to Ground Resulting From Faults on Paralleling 12-Kv Feeders

	Underground Exposure	Overhead Exposure
Approximate angle the pilot-wire voltage leads the power conductor current, deg	0	31

Table V. Rise in Substation Ground Potential During 12-Kv Faults to Ground

	Webster Substation	Hoover Substation
Type of 12-kv feeder faulted	Underground	Overhead
Rise in substation ground potential in volts per ampere of fault current	0.0064	0.0578
Maximum calculated rise in ground potential for faults near substation, v	130	600

Table VI. Pilot-Wire Voltages to Ground and Rise in Substation Ground Potential for 66-Kv Faults to Ground

	Webster Substation	Crown Substation
Fault current to substation ground bus, amp	1,788	1,460
Pilot-wire voltage to substation ground with opposite end grounded, v	13	174
Rise in substation ground potential, v	130	234

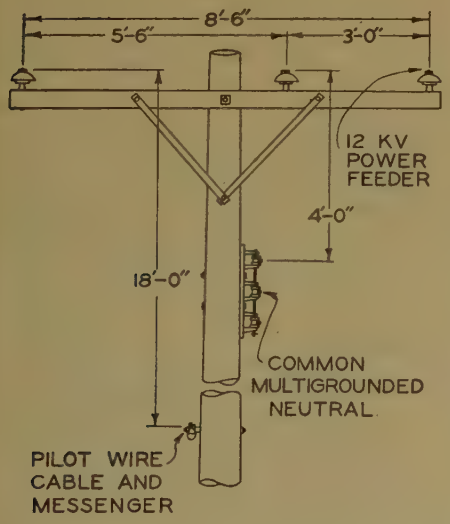


Figure 3. Typical pole top detail showing 12-kv power feeder, secondary, and 51-pair number 19 0.075-inch-lead 0.95-inch-outside-diameter pilot-wire cable, supported by 5/16-inch high-strength galvanized steel messenger

in the application of the principle used in the American Telephone and Telegraph Company's number 223-A retardation coil, used for the reduction of metallic voltages on open-wire carrier lines. It consists simply of modified drainage coils with middle connections isolated from ground by gaps. When the gaps discharge the assembly functions as a drainage coil.

Preliminary laboratory tests were made using coils of various excitation characteristics and several types of discharge gaps.

The connection diagram adopted from these tests is shown in Figure 5. It will be noted that the mutual reactors at the substations are connected to the mid-terminals of the relay insulating transformers instead of across the pilot wires. This connection was adopted in order to cause a minimum change in pilot-wire shunt impedance during discharge. However, if circumstances required connection across the pilot wires or additional protectors between terminals, the shunt impedance could be made high enough to cause only slight decrease in the sensitivity of the pilot relays.

A mutual reactor was selected, each winding of which has an exciting impedance of approximately 11,500 ohms at 200 volts. This value of impedance was considered sufficiently high to result in a negligible change in the sensitivity of the pilot relays during gap discharge. This value of impedance also was considered sufficiently high to insure satisfactory operation of the protector tubes without causing excessive excitation currents in the reactors.

A gas-filled protector tube was selected which had the following characteristics:

A-c rms breakdown voltage, v	300–500
Maximum discharge current for two seconds, amp	50
Average arc drop, v, d-c	20–30

The tube is capable of repeated discharges without material change in characteristics.

Final Laboratory Tests

Equipment was connected in the laboratory as shown in Figure 5. Resistors were used to simulate pilot-wire resistance.

Test Number 1

With protector tubes removed at points *B* and *C* and terminals 2 and 3 connected at *B*, test potential was applied between the mid-point of the mutual reactor at *B* and ground. Oscillograph elements were connected to measure quantities as shown in Table II. This test indicated that with maximum longitudinal voltage induced on the pilot wires, the potential between wires was sufficiently low to prevent incorrect relay operation. Also the voltage between pilot wire and ground was well within its insulation rating.

Test Number 2

This test was made to determine the effect of protector discharges on the sensitivity of the pilot relays.

1. With all protector tubes short-circuited, no appreciable change in the sensitivity of the pilot relays was detected.

2. A similar test was performed with current flowing in the pilot wires and protective equipment simulating discharge currents. This was accomplished by short-circuiting the protector tube at *A* and applying test potential between the mid-point of the mutual reactor at *B* and ground, with terminals 2 and 3 connected. The results of this test indicated no appreciable change in pilot relay sensitivity with currents in each pilot wire up to three amperes.

Field Application

On the basis of the laboratory tests, the 66-kv pilot-relay circuits were equipped

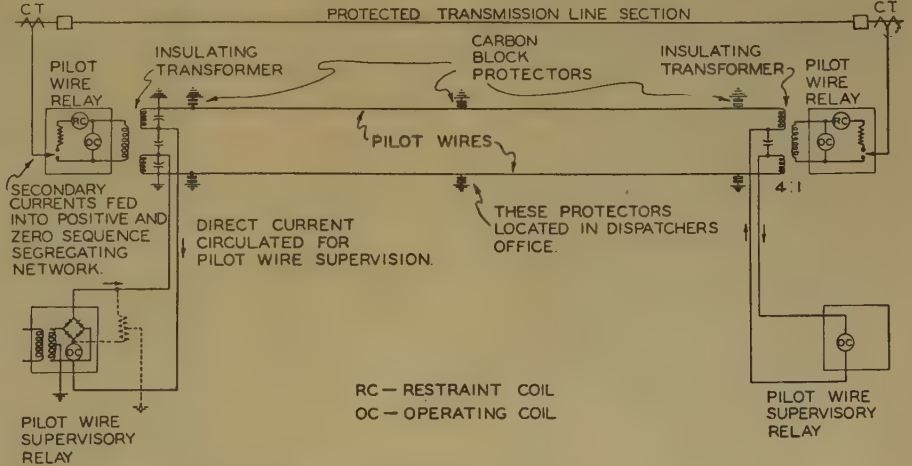


Figure 4. Schematic diagram of pilot-wire relaying as originally installed

Table VII. Substation Ground Resistance

	Webster Sub-station	Crown Sub-station	Hoover Sub-station
Substation ground resistance, ohms	0.14	0.87	0.36

with the new protective devices. The laboratory tests described indicated that this equipment satisfactorily would eliminate incorrect relay operations caused by ground faults on paralleling 12-kv 4-wire feeders.

The second-mentioned difficulty, involving improper operation of the alarm relays, was corrected by the relay manufacturer. A grounding resistor is used with a grounded center tap connected across the output of the rectifier in the alarm relay, instead of grounding the center tap of the transformer supplying the rectifier unit, as shown in Figure 4. This measure prevented induced potentials from causing current to flow through the rectifier and operating coil of the alarm relay.

The foregoing modifications did not eliminate completely potential between pilot wires resulting from normal load currents in paralleling 12-kv 4-wire feeders. This potential appears when a pilot wire becomes accidentally grounded. However, the voltage was reduced below the 15-volt operating level of the relays by the use of the grounding resistor on the alarm relay and the removal of the capacitors connected between the mid-points of the insulating transformer and ground. This resulted in a considerable increase in the impedance between the pilot wires and ground at this point, thereby reducing the potential between pilot wires when one wire becomes grounded. The net result of this change, as determined from field measurements, is a reduction in the potential between pilot wires of approximately 50 per cent for equivalent values of induced potential.

Final Field Tests

The operation of the protective devices was tested by staged ground faults on the 12-kv circuit at the end of the overhead exposure between Hoover substation and industrial plant *B*. Oscillograph measurements were made of the voltage between pilot wires and from pilot wire to ground, and of the fault current. With a fault current of 2,400 amperes, the voltage between pilot wires at Hoover substation was less than two volts, and from pilot wire to ground was 320 volts rms. The calculated longitudinal voltage induced for this value of fault current is approximately 1,000 volts. During the tests, protector tubes discharged, but no pilot-wire relay operations occurred.

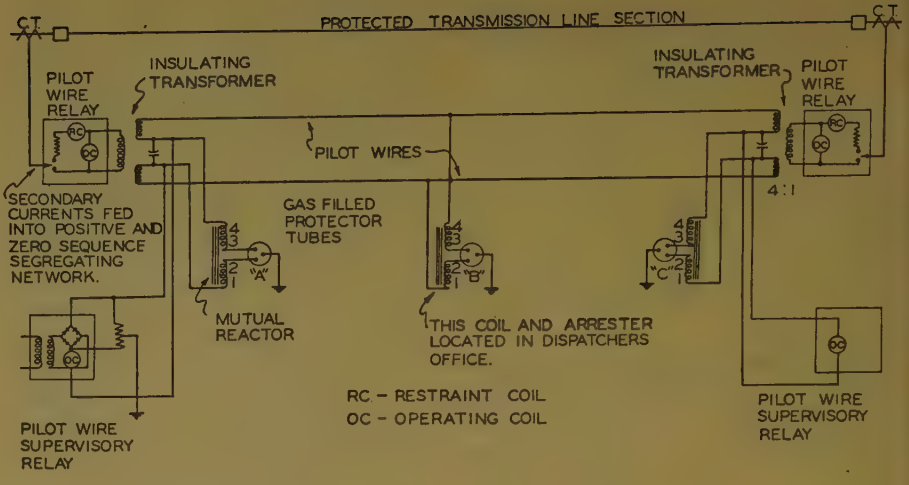


Figure 5. Schematic diagram of pilot-wire relaying equipped with new protective devices

Conclusions

The coils and protector tubes described were obtained from a limited selection of available material, and the laboratory tests were intended to indicate their suitability rather than to determine the most satisfactory design.

Field tests were not conducted on simultaneous 12-kv and 66-kv faults. However, on the basis of the laboratory tests, it is believed that such faults will be relayed correctly.

Since the installation of the protective equipment, several faults have occurred on 12-kv circuits at locations which had formerly caused incorrect operations of the pilot relays. All of these faults were cleared satisfactorily without operation of the 66-kv pilot relays. During this same period, several 66-kv faults occurred, all of which were cleared properly by the pilot relays.

Appendix

During field tests it was convenient to make certain other measurements which did not bear directly on the problem at hand Some of these data are included in the hope that they may add to the knowledge on these subjects.

Table III shows the results of measurements made to determine the zero-phase-sequence impedance of the underground cables from Webster to industrial plant *A*, illustrated in Figure 2. The duct line is removed fairly well from pipe lines or other known underground structures.

Table IV shows the results of measurements made to determine the phase position of the induced potential with reference to the current in the power conductor. These measurements were made by a voltage triangulation method using a high resistance voltmeter. A reference voltage in phase with the power conductor current was obtained by connecting a noninductive resistor to the secondary of the current transformer in the power circuit.

Table V shows the results of measurements made to determine the rise in substation ground potential caused by 12-kv faults to ground. The measurements were made between the substation ground bus and reference grounds driven approximately 1,000 feet from the substation at 90 degrees to the faulted feeder.

Table VI shows the results of measurements made to determine the pilot-wire voltage and the rise in substation ground potential during ground faults on the 66-kv system. Ground faults were applied at Webster and Crown substations to the substation ground bus. The rise in substation ground potential was measured with reference to a remote driven ground located approximately 1,000 feet from the substation and as near 90 degrees to the 66-kv lines as possible.

Table VII shows the results of ground resistance measurements of substation ground busses made with a ground resistance tester using two remote reference grounds.

Marine Radar for Peacetime Use

L. H. LYNN
NONMEMBER AIEE

O. H. WINN
ASSOCIATE AIEE

MILITARY RADAR systems by the score have been developed for such varied purposes as surface search, aircraft detection, height finding, gunfire control, range finding, and other wartime uses not as yet released from the classified categories.

In most of these systems, the prime function was connected in some way with locating the enemy accurately, judging his course, speed, and strength, and getting this knowledge quickly enough to take appropriate counteraction. The sooner such data were accumulated and evaluated, the stronger offensive (or defensive) measures were possible. For this reason, design parameters that affected cost, complexity, or operator skill were less important than those which governed range, accuracy, resistance to gunfire shock, etc.

The relative importance of these factors was reflected necessarily into the space and power requirements of the military equipment, and the very design elements that permitted excellent military radar are often those which make for an unsuitable peacetime radar.

Let us forget, for the moment, the spectacular achievements of radar during the past few years and look ahead to its function as a safety device for civilian use. Among the many jobs that have been envisioned for this branch of electronics, there is perhaps none as important as that of marine radar. From the economic viewpoint alone, the intrinsic value of ships, cargo, and time lost because of poor visibility mounts to enormous proportions. This waste, plus the attendant loss of life, can be reduced to a very small amount by the use of radar equipment properly designed for the job.

Paper 46-47, recommended by the AIEE committee on communication for presentation at the AIEE winter convention, New York, N. Y., January 21–25, 1946. Manuscript submitted December 12, 1945; made available for printing January 1, 1946.

L. H. LYNN and O. H. WINN are with General Electric Company, Schenectady, N. Y.

Design Requirements for Peacetime Radar

The design variables which are controllable include at least the following: reliability, simplicity, accuracy of range and bearing, cost, ease of maintenance, resolving power (on adjacent objects) maximum range, minimum range, appearance, accessibility of components, and size.

In either case, military or civilian, reliability comes first. Cost is a minor point in military designs, a major one in civilian designs. Simplicity of installation and operation is not too important on a battleship where dozens of technically trained men are available. A cargo ship, however, operating in a highly competitive field, must consider any extra personnel from the accountant's viewpoint and use a radar capable of operation by the regular complement of officers.

Maximum ranges of military equipments frequently exceed 100 miles and require appropriate high power for such a range. A passenger ship is concerned much more with an obstacle which may be only several miles away; hence a large equipment is neither justified nor desirable.

The minimum range of a destroyer's radar may well be a mile or two, on the theory that an enemy must be discovered long before he can approach that close. The minimum range of a radar for a cargo ship is required to be less than a ship length—the shorter the better, in order that navigation may be accomplished safely in congested harbors.

And so, all through the whole list of design factors, there must be a new philosophy of design to create suitable radar equipment for our commercial uses. Our peacetime designers must not say, "Who is shooting at my ship from over the horizon?" but rather, "Can this device permit my present complement of personnel to avoid collisions and to obtain fixes from charted landmarks?"

One Design of Commercial Radar

Early in 1943, experiments were conducted on a Great Lakes ore boat, using a modification of a military ship-borne "search radar." From six months' operating data, two outstanding facts stand out:

1. Despite some inherent weaknesses, common to all radar systems, the installation proved to be a highly useful navigational tool.

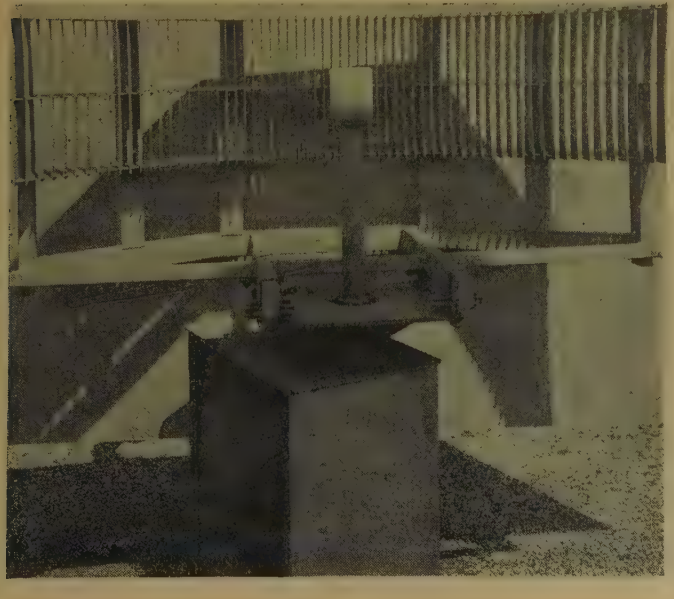


Figure 1 (left). Rotating antenna assembly



Figure 2 (right). Electronic navigator console

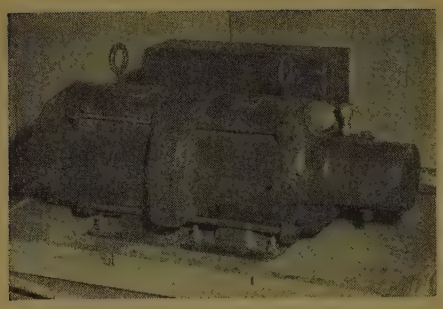


Figure 3 (left). Speed-regulated motor-alternator

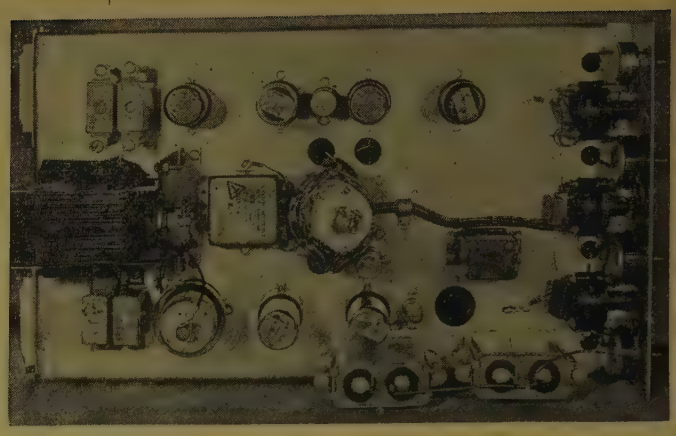


Figure 6 (right). Typical removable chassis of electronic navigator console

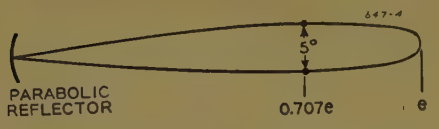


Figure 4. Typical beam pattern in horizontal plane, showing five degrees width at half-power points

2. It was too complex for nontechnical personnel to operate.

From these early experiences, plus a study of several hundred service reports from military installations, the present electronic navigator was evolved. Figures 1, 2, and 3 show the three units of the complete equipment: the antenna system, console, and motor-alternator, respectively.

The antenna system is driven by a gear-motor located in the antenna base, or "pedestal," and the slatted reflector rotates continuously at 10 rpm. The surface of this reflector is a truncated paraboloid of revolution and is proportioned to project a beam 5 degrees wide and 15 degrees high. (A fully parabolic reflector of the same width would project a conical beam 5 degrees wide, with the resultant danger of lost targets when the ship rolled.) Note that these figures do not imply that there is zero radiation outside the angles mentioned; the accepted method of measuring beam width is at the half-power points, as shown in Figure 4.



Figure 5. Electronic navigator console with front cover removed, showing removable chassis

The console, Figure 2, contains the transmitter, receiver, cathode ray tube, sweep circuits, pulsing circuits, rotating field mechanism, appropriate power supplies, and controls. During normal operation, seven controls are available to the operator. Having adjusted the instrument and selected the desired range scale (2, 6, or 30 miles) no further manipulation is required unless it is desired to take a bearing on some specific object. In this case a knob is provided to control a radial bearing line which can be caused to bisect the object in question and thus read its azimuth on a scale around the circumference of the cathode ray tube.

All other controls which are required for initial adjustment during installation are accessible to recognized service personnel only and are covered by a locked panel. Figure 5 shows these controls and also the test jacks and the panels of the various removable chassis. In case of trouble with any chassis, it is possible for the service engineer to substitute an entire chassis in a minute and repair the original one at leisure. Figure 6 illustrates a typical chassis removed from the console.

Figure 7 is a block diagram of the radar circuits and emphasizes the relative simplicity as compared with usual military designs. The pulse generator of Figure 8 is a blocking oscillator whose recurrence rate is determined by a network Z and resistors R_1 and R_2. (Most blocking oscillators employ only a capacitor in place of a network.) The function of the lumped-constant line Z is to provide a delay in the discharge time so that the tube may be allowed to conduct its full saturation current for a definite time interval, as shown in the pulse shape of Figure 9, which depicts the voltage across the primary of transformer T_1. This transformer

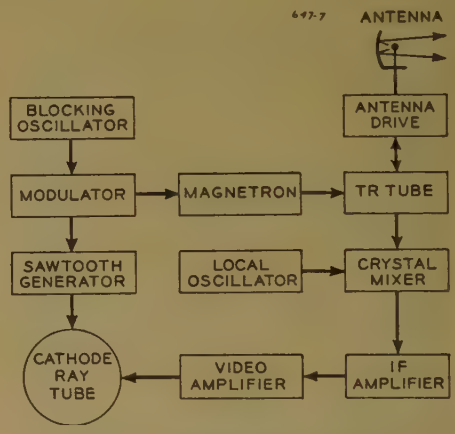


Figure 7. Block diagram of circuits

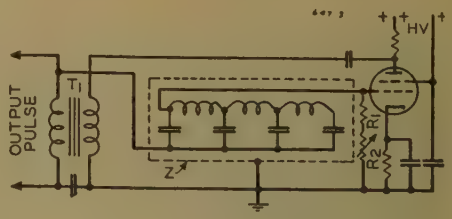


Figure 8. Pulse-forming circuit

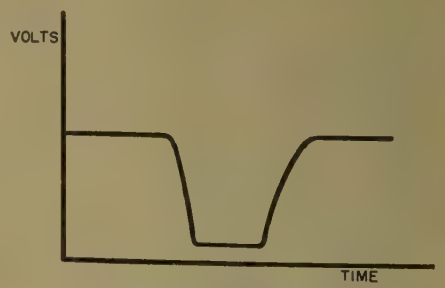


Figure 9. Pulse shape

is so connected as to provide regenerative feedback for the oscillator, and thus the cycle is repetitive and at a rate controlled by variable resistor R_2. The simplicity and reliability of this circuit makes it particularly suitable, for this application. The pulses formed by the blocking oscillator are amplified by a suitable pentode and used to drive the magnetron oscillator which operates in the 10-centimeter region. See Figure 10. The modulation transformer (T_2) permits the magnetron filament to be operated 5,000 volts above ground, for this is the order of magnitude of the amplified pulse voltage. A tap on the modulation transformer allows the modulator tube to be properly loaded.

The pulse is considerably less than one microsecond in length and repeats at about 1,000 cycles per second. Thus the peak power delivered to the magnetron is of the order of kilowatts, though the average power is but a few watts.

Referring again to Figure 7, the output of the magnetron is delivered to the antenna through the transmit-receive (T-R) tube, the function of which is to protect the receiver during transmitter pulses and to close off the path to the magnetron during the receiving time, between pulses.

The returning echo from the "target" is collected by the parabolic reflector, focused on the antenna dipole, and carried through the transmit-receive tube to the receiver circuits. In the crystal mixer the returning signal is caused to beat with the output of a klystron local oscillator, the resultant frequency being about 30 megacycles. This is amplified by a wide-band intermediate-frequency amplifier, detected and further amplified by the video amplifier, and thence applied to the control grid of the cathode ray tube.

In the meantime the antenna assembly has been rotating continuously, and its

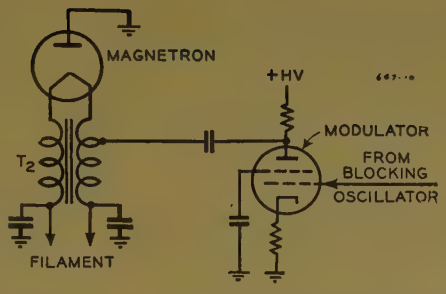


Figure 10. Modulator and magnetron circuits

motion has been transmitted by a very compact and simple Selsyn system to the rotating magnetic deflection coil located around the neck of the cathode ray tube. Impressed across this rotating coil is the sawtooth sweep voltage which provides a linear radial time axis. Time, too, is synchronized with the transmitter, and as both the outgoing pulse and the returning echo travel at the speed of light, this time axis is really a distance measure.

The over-all result is that as the radial time (that is, distance) axis rotates, any returning echo will intensify a portion of this axis as the rotating antenna "beams" on the target. With an ordinary cathode ray screen, the bright flashes of light would indicate the presence of reflecting objects, but the operator would have to remember where the flashes occurred, obviously an undesirable disadvantage.

Hence, a long-persistence screen is used, in which the cathode ray first excites a short-persistence phosphor, which in turn causes a second long-persistence phosphor to glow. This glow persists for a long enough time to "remember" a scene until rekindled by the next rotation of the radial sweep.

Since the resultant illumination is in the form of a plan view of the surrounding area, with one's own ship at the center, the system is commonly termed "plan presentation indicator," or simply "P.P.I."

Figure 11 illustrates such a picture, showing land masses, open water, buoys, and ships in the vicinity of Matinicock Point in Long Island Sound. For comparison, the actual chart of that area is printed beside the radar chart.

There are simpler presentation systems, but they require more skill in interpretation. It was felt that the plan presentation indicator picture "spoke the language" of the navigator better, since it shows him the data in familiar chart form. This has been borne out in actual experience, both with skilled navigators and students in training.

Practical Results

The particular design described above has completed an 8-months' test installation on the United States Maritime training ship, AMERICAN MARINER. During that time, several hundred persons have operated the equipment. This group has included military personnel highly trained in radar principles, captains of cargo ships, shipowners, shipyard executives, tugboat captains, river pilots, navigators, trainees, and even deckhands.

From their varied reactions, it has been possible to create a design well suited for the job, unhampered by excessive gadgeting, and capable of operation by nontechnical personnel. Further, it has been possible to spread the idea that radar is not a cure-all scheduled to usurp the functions of existing instruments; rather it is a very powerful aid to those instruments, performing new duties previously left to guess work or chance.

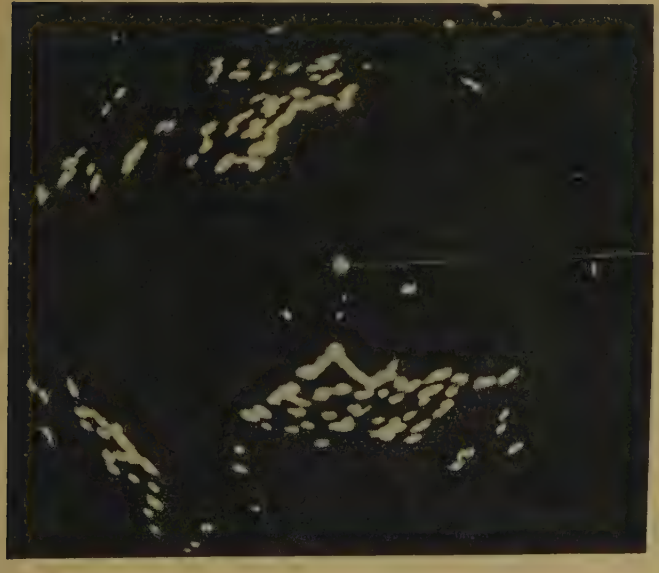




Figure 11. Comparison of radar picture and actual navigation chart

Techniques and Facilities for Microwave Radar Testing

E. I. GREEN
FELLOW AIEE

H. J. FISHER
ASSOCIATE AIEE

J. G. FERGUSON
MEMBER AIEE

Synopsis: Methods and devices are described for testing microwave radar equipment in the radio frequency range from about 500 megacycles to 25,000 megacycles and at associated video frequencies. In general, the same instruments and techniques are applicable also in testing microwave communication systems.

THAT RADAR equipments are marvels of ingenuity has long since become common knowledge. This ingenuity is reflected, however, in complexity of circuits. A rough index of this complexity is found in the number of vacuum tubes, which for a single radar set may range from 50 to 250. Notwithstanding the most careful design, it is easy for the radar performance to become impaired under operating conditions.

Not only is radar complex, but its performance criteria are less tangible than those of conventional communication systems. Ordinary radio is to some extent self-testing in that reception of intelligible speech or signals frequently constitutes a sufficient check of satisfactory performance. With radar, the greater the range coverage and the more accurate the data, the more valuable the information is likely to be. However, the working range may fall to a fraction of the possible maximum, or some other degradation or malfunctioning may occur, with nothing in the operation of the radar equipment to tell that this has happened. Since lack of maximum performance may have serious military results, measurement of performance assumes the utmost importance in radar work.

The new techniques and new frequency ranges employed for radar necessitated the wartime development of a wide variety of new types of test equipment. A large part of this development work was concentrated at Bell Telephone Laboratories and at the National Defense Research Council's Radiation Laboratory at Massachusetts Institute of Technology, working in close co-ordination with one another and with the technical services of the Army and the Navy. In the manufacture of radar test equipment, Western Electric took a major part. This article discusses the techniques of radar testing and describes the types of test gear developed by Bell Laboratories and manufactured by Western Electric. These cover the radio frequency range from about 500 megacycles to 25,000 megacycles, together with associated video frequencies.

Because of its importance during the war, emphasis has been placed on the testing of microwave radar equipment. However, similar methods and instruments also have been employed in the testing of microwave communication systems, and such applications can be expected to increase. In this situation the developers and users of microwave communication systems are fortunate in that almost all of the techniques and devices developed for radar testing are equally applicable to communication systems. This is even true of the video units, which are useful in connection with pulse-modulated telephone systems and amplitude-modulated or frequency-modulated television systems.

So many persons, both within and outside Bell Laboratories, have contributed to the developments described that the authors have reluctantly reached the conclusion that the assignment of individual credit should not be attempted.

Paper 46-40, recommended by the AIEE committee on communication for presentation at the AIEE winter convention, New York, N. Y., January 21–25, 1946. Manuscript submitted December 19, 1945; made available for printing December 28, 1945.

E. I. GREEN is test engineer, transmission development department; H. J. FISHER and J. G. FERGUSON are members of the technical staff, Bell Telephone Laboratories, Inc., New York, N. Y.

Requirements

Subsequent discussion may be simplified by first reviewing briefly the operation of a typical radar set, as shown in Figure 1. Under the control of d-c or so-called video pulses from the modulator, short pulses of radio frequency energy are delivered by the magnetron transmitter to a highly directive antenna, ordinarily arranged to scan a section of space. Energy reflected from an object or "target" in the path of the beam is intercepted by the same antenna. The received pulses or echoes are converted to an intermediate frequency by heterodyning against a local oscillator, the frequency of which may be automatically controlled.

To enable the same antenna to serve for both transmitting and receiving, a transmit-receive tube or transmit-receive switch is usually provided. This consists of a partially evacuated resonant cavity containing a spark gap which breaks down during the transmitted pulse, thus preventing the transmitted power from injuring the sensitive receiver. A receive-transmit (RT) tube, consisting of a similar resonant cavity and spark gap, may be provided to prevent absorption of the received signal by the transmitter. After amplification and detection of the received signal, the resultant video pulses are applied to an indicator which may present information in any of several different ways. Customarily, the direction of the target (determined by antenna orientation) and its range (determined by reflection interval, 10.7 microseconds per mile) are shown. The system may be used merely for searching, or for fire control, bomb direction, or other functions, with additional equipment as required.

Types of Tests and Test Sets

Figure 2 shows an early assemblage of radar test equipment for the 10-centimeter range, initially produced in 1942, which has seen wide usage.

The more important types of tests required in radar work, either at radar operating locations or at centralized service points, are:

1. Over-all performance (range capability).
2. Transmitter power.
3. Receiver sensitivity.
4. Transmitter frequency.
5. Transmitter spectrum.
6. Standing wave ratio.
7. Radio-frequency (RF) envelope.
8. Receiver recovery.
9. Automatic frequency control (AFC) tracking.
10. Intermediate-frequency (IF) alignment.
11. Video wave shapes.
12. Range calibration.
13. Computer calibration.

The principal types of test sets required for carrying out the above are:

1. Signal generators.
2. Echo boxes.
3. Frequency and power meters (separate or combined).
4. Standing wavemeters.

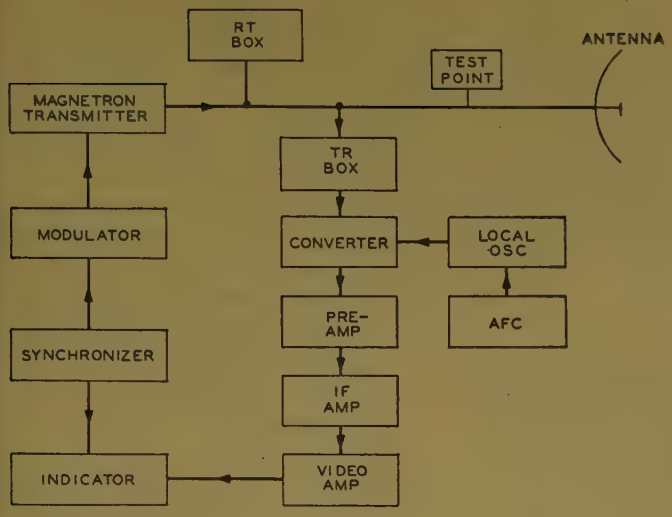


Figure 1. Diagram of typical radar equipment

5. RF loads.
6. Oscilloscopes.
7. Video dividers and loads.
8. Range calibrators.
9. Computer test sets.
10. Spectrum analyzers.

Various auxiliary testing instruments also are employed, including vacuum tube testers, intermediate-frequency signal generators, audio oscillators, flux meters, and so forth. Before discussing the above tests and devices individually, some of the requirements for radar test equipment, especially those requirements resulting from military usage, will be summarized.

Generality of Application

Radar sets perform a great variety of functions, including search and surveillance, gun laying and fire control, bomb direction, and navigation. They are used in the air, on shipboard, and on the ground; in attack and in defense; in combat zones and in rear areas. To realize the advantages of different parts of the frequency spectrum, avoid interference, and keep ahead of enemy countermeasures, it has been necessary for radar to exploit many different frequency bands and sub-bands. These diversities have bred a multiplicity of types of radar, with a corresponding variety of testing problems and requirements.

Maintenance and testing of radar equipment must be performed at many different locations. In the Army these locations, known as echelons, include

1. The operating unit.
2. Central service points, either fixed or mobile, for a number of operating units.
3. Large depots either in the military theaters or in the United States.

Navy maintenance and testing are carried out aboard the fighting ships or auxiliaries and at advance and overhaul bases.

In developing test equipment, an offhand approach might have been to provide specialized equipment for testing each radar set under specific conditions. Since this would have made the total burden of development, manufacture, and field maintenance well-nigh intolerable, a co-ordinated plan was followed whereby (with minor exceptions) each test set was made capable of widespread application in testing as many radar equipments under as varied conditions as possible.

Broadbanding

Generality of application required the designing of test equipment for broad frequency bands, bands as a rule much wider than those of the radar sets themselves. It was necessary, therefore, not only to develop new microwave testing techniques, but to advance the art still further to render the testing components as far as possible insensitive to frequency.

Precision

A radar set itself is an instrument of considerable precision. The test equipment used for checking the radar performance in the field has to have still higher accuracy. It is noteworthy that the measuring accuracy realized throughout the microwave range is comparable with that obtainable at lower frequencies where many years of background exist.

Packaging—Size and Weight

Light weight and compactness are of paramount importance where a test set

Figure 2. Early radar test set for 3,000-megacycle range

It includes signal generator, oscilloscope, power meter, test antenna, and auxiliary units



has to be carried any distance by the maintenance man; where it is used in cramped quarters in a plane, truck, or submarine; or where it has to be taken up ship ladders or through small hatchways. To permit portable use under such conditions, the design objective was established of a weight not exceeding about 30 pounds (exclusive of transit case), combined with a ruggedness adequate for all conditions of use. Through rigorous attention to both mechanical and electrical design, this objective has been realized (in many cases with considerable margin) except for a few sets intended primarily for bench use. Figure 3 illustrates the use of lightweight test equipment in maintaining air-borne radar equipment.



Figure 3. Portable units used in checking air-borne radar sets at Boca Raton, Fla.

Environmental Influences

Military usage requires that the test equipment be capable of efficient operation at any ambient temperature between a minimun of the order of −40 degrees to −55 degees centigrade and a maximum of the order of +65 degrees to +70 degrees centigrade, as well as at any relative humidity up to 95 per cent. In addition, the set must withstand continued exposure to driving rain, dust storms, and all other conditions encountered in tropical, desert, or arctic climates. Often the test set in its transit case must be capable of submergence under water without ill effects. Fungus-proofing with a fungicidal lacquer is a standard requirement.

Simplicity, Reliability, Accessibility

Not only must the functioning of the test set be reliable, stable, and trouble-free, but the set must make minimum demands for special skill or technique on the part of the maintenance man. Access for maintenance purposes, while important in radar test sets, is not as controlling as in the radar equipments themselves and sometimes has to be sacrificed in part for compactness.

Ruggedness

For general application, the test equipment must be capable of withstanding airplane vibration, the shock of heavy guns, depth charges and near misses, and the combinations of shock and vibration connoted by the requirement of "transportation over all types of terrain in any Army vehicle." Test and experience have made it possible to translate these general requirements into two specific requirements, namely, the ability to withstand

1. Vibration at frequencies from 10 to 33 cycles per second, with 1/16 inch excursion for 30 minutes in each of three axes.

2. The shock produced by a 400-pound hammer falling through distances of one, two, and three feet in each of three axes and striking an anvil to which the set is attached.

These requirements have been met without using shock and vibration mounts, which are undesirable in test sets because they increase size and weight.

Range Capability

The range capability of a radar set, like that of any radio system, depends upon three things:

1. The transmitted power.

2. The loss in the medium.

3. The minimum perceptible received signal.

Two of these can be combined by taking the ratio of the radiated signal to the minimum perceptible received signal. This ratio, ordinarily expressed as a level difference in decibels, is variously termed the "system performance," "over-all performance," or merely the "level difference." It may be determined by separate measurement of transmitter power and receiver sensitivity, or by a single over-all measurement. With the powers and sensitivities commonly employed in radar, the level difference is of the order of 150 to 180 decibels.

The actual range that can be spanned for a given performance ratio varies considerably. For a given transmitted power, the echo power received by a radar set theoretically varies inversely as the fourth power of the range. The reason for this is simple. In free space the power intercepted by a target which is small in comparison with the area of the radar beam in its vicinity will vary according to the inverse square of the distance from the radar. Similarly, that fraction of the energy reflected from the target which is intercepted by the receiving antenna will vary as the inverse square law. Since the received power involves the product of these two factors, the relation becomes

$$P_r = K\frac{P_t}{R^4} \text{ or } R = \left(K\frac{P_t}{P_r}\right)^{1/4} \qquad (1)$$

where P_t and P_r represent, respectively, the transmitted and received power; R, the range; and K, a constant determined by antenna design, character of target, and so forth.

Under operating conditions, considerable departure from the above relationship may be experienced, because of such factors as

1. The curvature of the earth.

2. Interference between the direct beam and single or multiple reflections.

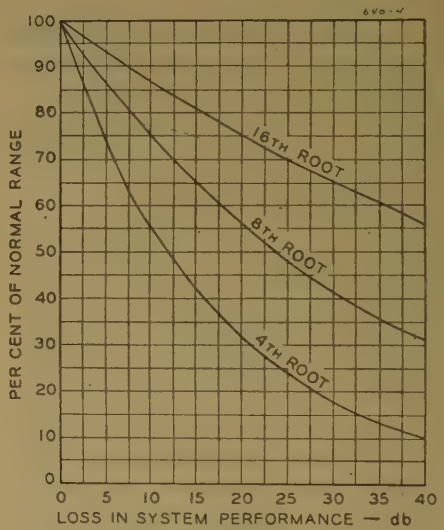


Figure 4. Effect of reduction in system performance on radar range

3. Attenuation caused by atmospheric absorption.

Except under conditions of severe attenuation such as may occur at the very short wave lengths, the received power commonly varies somewhere between the inverse fourth power and the inverse sixteenth power of distance. To state it another way, the change in effective range is somewhere between the fourth and the sixteenth root of the change in system performance. The former condition might hold for high-angle plane-to-ship search in

clear weather, the latter for ship-to-ship search in fog. The loss of range resulting from a given degradation of system performance is shown for fourth, eighth, and sixteenth root laws by the curves of Figure 4. Whatever the propagation law, reduction in performance always means loss of range.

Field surveys have shown that when test equipment is not available or not used, radar sets in the field are likely to give no more than one half to one fourth of the maximum range of which they are capable. Hence it is necessary to know with good accuracy the over-all performance. Known or so-called standard targets have often been used in the field for checking performance. Because of wide variations in transmission caused by many factors, results obtained from such targets are frequently misleading.

Signal Generators

Signal generators for radar work deliver one or more different types of test signals, which may serve a variety of functions. More important among these functions are

1. Tuning or alignment of the radar components (TR and RT boxes, converter, beat oscillator, automatic frequency control, and so forth).
2. Measurement of receiver sensitivity.
3. Check of TR and receiver recovery.
4. Measurement of loss.
5. Detection of frequency pulling.
6. Check of automatic frequency control following.
7. Measurement of intermediate-frequency band width.
8. Check of automatic range tracking.
9. Measurement of standing wave ratio.
10. Check of video "gating" circuits.

Many signal generators include means for measuring the power and frequency of the test signal and also of an incoming signal.

Types of Signals

The test signals delivered by a signal generator may be continuous wave, pulsed, or frequency-modulated. Occasionally, square wave or sine wave modulation is provided.

Pulsed signal generators deliver a succession of single RF pulses or pulse trains, either of these generally synchronous with the pulses of the radar equipment under test. Multivibrator or trigger techniques are used to generate the pulses for modulating the microwave generator. The trigger pulse for synchronizing the pulsing circuits is commonly produced by rectifying RF pulses from the radar transmitter, thus avoiding a separate video connection to the radar. To avoid possible difficulties in video response, the RF test pulses should be of a width comparable with those of the radar set under test. For observing the test signals, either the radar indicator or an auxiliary oscilloscope may be used. With the single pulse method, provision is usually made for varying the delay of the test pulse with respect to the radar pulse. The width of the test pulse may also be adjustable or variable.

If the frequency of the signal generator is swept over a sufficiently wide frequency band, the IF output of the radar set traces the curve of IF selectivity, thus producing a kind of pulse. With a suitable rate of frequency sweep, this pulse becomes comparable in width with the transmitter pulse, and when synchronized with the radar set it can be used for test purposes. Since the pulse is produced in the radar equipment, comparison of the shapes of receiver input and output pulses is not possible. The nominal duration of the pulse in the IF output is

$$T = B/\gamma \qquad (2)$$

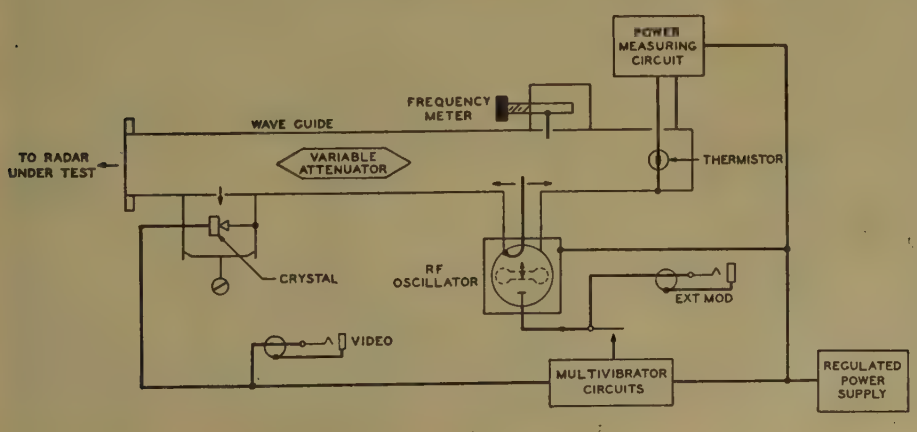
where B is the width of the IF band in cycles per second (for this purpose conveniently measured between six decibel points) and γ is the speed of frequency sweep in cycles per second per second. For best results this nominal width should be similar to the width of the transmitter pulse for which the IF and video circuits are designed. This means that the scanning speed should be in the neighborhood of $B^2/_2$.

A continuous-wave input of the same frequency as the transmitter produces in the output of the IF detector merely a direct current to which the video amplifier and radar indicator do not respond. However, continuous-wave test signals may be utilized by observing on a d-c meter (built into the radar set or separate) the change produced in detector current or converter current.



Figure 6. 1942-model signal generator (left) compared with one produced in 1945

Figure 5. Block diagram of *TS-35A/AP* signal generator



Receiver Sensitivity

Just as in radio, the sensitivity of a radar receiver is defined as the minimum received signal that is perceptible in the presence of set noise.* At microwave frequencies, atmospheric disturbances are usually negligible, so that unless accidental or deliberate interfering signals are present, the operating sensitivity is the same as the intrinsic sensitivity of the receiver.

Receiver sensitivity is commonly stated as the minimum perceptible signal power in decibels referred to a milliwatt (abbreviated as dbm). In practice, the receiver

*The term noise is commonly used even though the disturbances are observed on a cathode-ray screen.

sensitivity depends upon the noise figure of the converter, the conversion loss, and the noise figure of the IF amplifier. If a RF amplifier is used, as is the practice at lower microwave frequencies, its noise figure is likely to be controlling. By noise figure in each case is meant the noise power in comparison with the thermal noise. The thermal noise in watts delivered to a load is kTB, where k is Boltzmann's constant, T is absolute temperature in degrees K, and B is the frequency band width. Thus for a 4-megacycle band at 25 degrees centigrade, the thermal noise is −108 decibel-milliwatts. With good design the over-all receiver noise is of the order of 10 to 15 decibels higher than thermal noise. The minimum detectable signal is usually not equal to the receiver noise but depends on the type of indicator, particularly on whether the presence of an echo is indicated by spot deflection or spot modulation.

With a continuous-wave signal generator, receiver sensitivity is measured by determining the minimum input power necessary to produce a perceptible change in meter reading. This affords a satisfactory relative measure of receiver performance, but since the radar indicator usually permits better visual discrimination against noise, the minimum input as read with the meter ordinarily differs from the minimum pulse input for barely discernible indicator response.

Radio-Frequency Oscillators

Beat oscillator tubes for radar sets deliver (with sufficient decoupling or isolation to prevent undue frequency pulling) a power of the order of milliwatts. This power being adequate for most test purposes, such tubes are well adapted for use as signal generators.

Throughout the greater part of the microwave range, reflex velocity-modulated tubes,[2] both the type with built-in cavity (Pierce-Shepherd) tuned mechanically or thermally, and that with external cavity (McNally) tuned by plugs, vanes, or adjustment of dimensions, have been used. The former is more convenient for general use, but the latter usually permits wider frequency coverage. Oscillation occurs when the repeller voltage is adjusted so that the round trip transit time corresponds to an odd number of quarter wave lengths. Ordinarily there are several different ranges of repeller voltage,

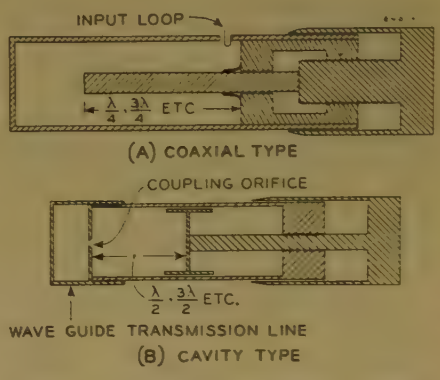


Figure 7. Types of frequency meters

corresponding to different numbers of quarter waves, each of which supports oscillation over a range of frequencies called a mode of oscillation. Pulsing or frequency modulation is accomplished by applying a pulse or sawtooth wave to the repeller.

At the longer microwaves, a triode with closely spaced electrodes, or so-called "lighthouse" tube,[3] has been employed in a tuned-plate tuned-grid oscillator of the positive grid type. Two coaxial lines, conveniently placed one inside the other, provide the tuning, with the feedback through interelectrode capacitances supplemented by loop coupling. The inner cavity (between plate and grid) controls the frequency of oscillation, while the outer cavity (between grid and cathode) provides a suitably high grid impedance. Mechanical arrangements are provided for tracking the tuning of the two cavities over a wide frequency range.

Some Design Principles

Standard signal generators which have been employed in the past for measuring the sensitivity of radio receivers usually deliver a known voltage across a low impedance. This voltage is applied in series with a dummy antenna to the receiver under test. In the microwave range, this technique is inconvenient, and signal generators are designed to deliver test power on a matched impedance basis. Receiver sensitivity is stated in terms of power (decibel-milliwatts) instead of volts.

The components of a signal generator or other test unit are commonly arranged along a microwave transmission line. The wave guide type of line possesses certain advantages over a coaxial line in affording a lower loss, facilitating attenuator design as discussed in a subsequent section, and so forth. Hence the wave guide type of line is used in test equipment for those frequencies where its size is not excessive, that is, from about 4,000 megacycles upwards, and coaxial line for lower frequencies.

A major problem in the design of microwave signal generators is the provision of shielding adequate to reduce leakage signals, caused by unwanted couplings or stray fields, well below the minimum signal required for receiver testing. This minimum level may be as low as −70 or

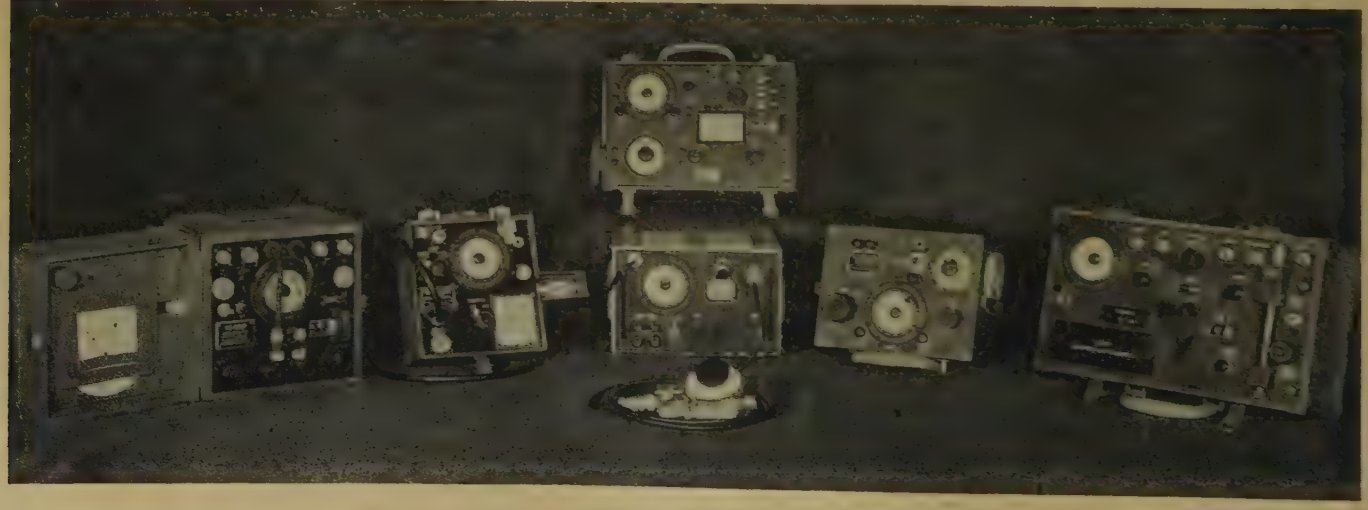


Figure 8. A group of frequency and power meters designed for various bands in the frequency range from 500 to 25,000 megacycles

−80 decibel-milliwatts depending on the coupling loss in the test connection.

Pulsed and Frequency-Modulated Signal Generator

To illustrate the functioning of a signal generator, there is shown in Figure 5 a block schematic of a design (Army-Navy type *TS-35A/AP*) which covers a 12% frequency band in the vicinity of 9,000 megacycles. An RF connection to the radar equipment is established with a wave guide flange coupling. The frequency and power of the radar transmitter are measured by means of a coaxial-type frequency meter and thermistor power-measuring circuit as described in subsequent sections. The attenuator and pad are adjusted to reduce the incoming average power to about one milliwatt, which gives a suitable deflection on the indicating meter. The

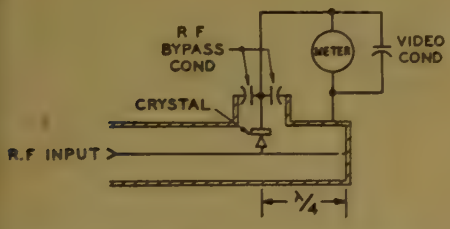


Figure 9. Crystal detector for pulsed RF signals

thermistor is mounted across the wave guide.

An RF pulse train is employed in many tests. To produce this, the RF oscillator output is modulated by a multivibrator which pulses continuously except when being synchronized. Synchronizing pulses are derived by crystal rectification of the RF pulses from the radar transmitter. The result is an initial RF pulse of seven microseconds, followed by an off period of about ten microseconds, followed by a train of RF pulses each two microseconds wide and recurring every eight microseconds until resynchronization occurs at the next radar pulse.

Using the pulse train, the radar system components can be tuned for maximum sensitivity by maximizing the signal on the indicator. To check receiver sensitivity, the continuous-wave power is first adjusted so that a power of one milliwatt is delivered to the pad and attenuator. Then with the set in the pulsed condition, the amplitude of the test signal is adjusted by means of the attenuator and pad until the signal on the radar indicator is barely discernible. It is necessary for this test that the frequency of the test signal be equal to the magnetron frequency. The frequency meter is provided as part of the signal generator for this purpose.

The receiver recovery, that is, the time required by the receiver to recover after disablement by the transmitter pulse, determines the minimum range at which a radar can be used. With this test set, the receiver recovery characteristic is indicated by the amplitude of the test pulses in the interval immediately following the transmitter pulse.

The set also is adapted to serve as a frequency-modulated signal generator. A sawtooth wave applied to the repeller gives a succession of frequency sweeps, each about 20 megacycles wide, and lasting about six microseconds. With this frequency-modulated signal, the width of receiver response may be observed on a class A oscilloscope, that is, one showing signal amplitude versus time. However, with nonadjustable intermediate-frequency strips, such measurement is seldom required. Failure of the radar automatic frequency control to follow frequency changes caused by antenna scanning or other causes is indicated by a change in the indicator presentation. Pulling of the magnetron frequency because of changes in load impedance can be detected by turning off the automatic frequency control.

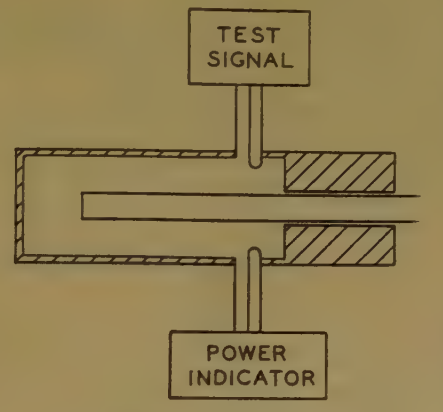


Figure 10 (above). Types of frequency meter circuits

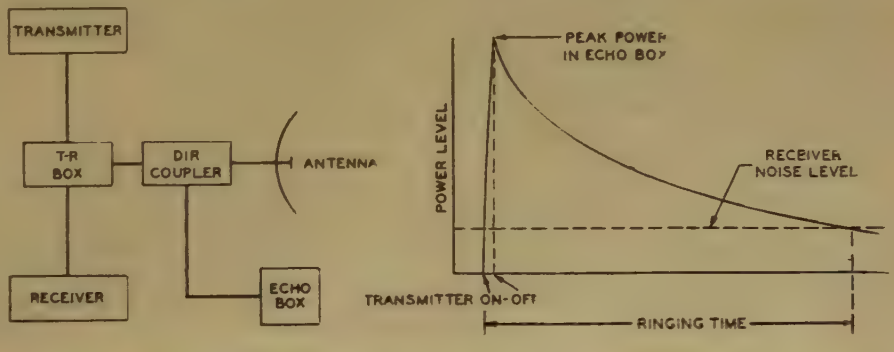
Signal Generator Designs

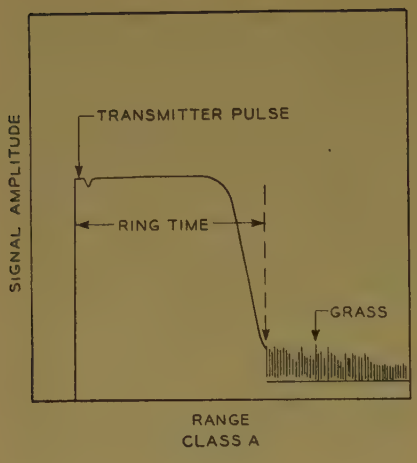
Designs of signal generators developed for the military arms during the war are interesting as landmarks of progress. The signal generator of the *IE30* test set, deliveries of which began in May 1942, delivered pulsed RF signals in the ten-centimeter range, using sine wave synchronization. Following only three months later was the signal generator of the Army *IE57A* and the Navy *LZ* test sets (Figure 6), which covered a then very broad frequency band of 20 per cent in the vicinity of ten centimeters and was designed to be triggered by the incoming RF pulse from the radar set instead of by a separate synchronizing connection. This set and a redesigned version of it have seen wide usage in testing Army, Navy, and Marine Corps radar equipment.

Delivery of a test set for the three-centimeter range, designated *TS-35/AP*, started in the fall of 1943. This set furnished both a train of pulses and a train of frequency-modulated signals, both of which features have proved valuable. It covered a nine per cent frequency band with no tuning adjustment except for the oscillator. An improved design known as *TS-35A* (see Figure 6) covered a 12 per cent band.

Progress in reducing the size and weight of the test units is indicated by the fact that the *IE30* signal generator weighed 121 pounds and *IE57* weighed 74 pounds, whereas *TS-35* and *TS-35A* weigh approximately 30 pounds.

Figure 11 (below). Radar test with echo box





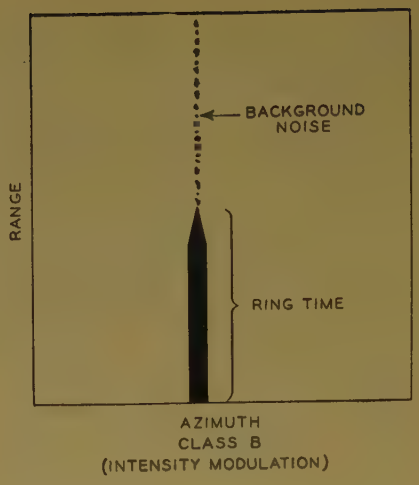




Figure 12. Typical ringtime patterns on radar indicators

Frequency Measurement

Usually a radar set need not operate at a precise frequency. Accurate measurements are required in the field, however, to keep the operating frequency within limits, to set the local oscillator, to check the measuring frequency, and so forth. In the laboratory, accurate frequency measurement is fundamental.

Frequency measurement in the microwave range is ordinarily accomplished by

1. A resonant coaxial line or
2. A resonant cavity, generally cylindrical.

These types are illustrated in Figure 7. Sometimes a combination of the two, referred to as a hybrid or transition type resonator, is employed. The measurement is actually one of wave length, with the scale calibrated in frequency or a conversion chart provided. Some specific designs of frequency meters are shown in Figure 8.

Coaxial Wavemeters

A coaxial wavemeter is formed of a section of coaxial transmission line of small enough diameter so that only the coaxial mode (in wave guide notation, $TM_{0,0,n}$) can exist. Usually the line is short-circuited at one end and open at the other, in which case resonance occurs at the odd quarter wave lengths ($\lambda/4$, $3\lambda/4$, and so forth). The open circuit is obtained merely by terminating the inner coaxial conductor, the continuing outer conductor acting as a wave guide below cutoff. Sometimes the line is short-circuited at both ends, giving resonance at the even quarter wave lengths ($\lambda/2$, λ, and so forth).

Cylindrical Cavity Wavemeters

A cylindrical cavity wavemeter is merely a section of cylindrical wave guide transmission line[4] whose length is varied.

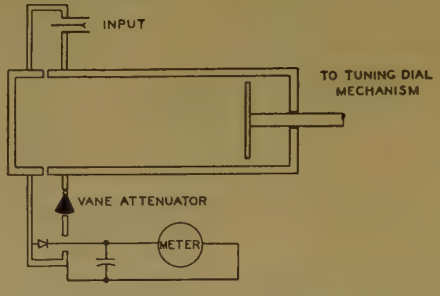


Figure 13. Functional schematic of tuned echo box

In order to avoid confusion with other modes, it is preferable to use the dominant mode (described in wave guide notation, $TE_{1,1,n}$*), that is, the mode with the lowest cutoff frequency. The cutoff wave length (λ_c) of this mode is $1.706D$, where D is the diameter in meters. For a higher Q it may be necessary to use the circular electric mode $TE_{0,1,n}$. The cutoff wave length for this mode is $0.82D$. No useful purpose is served by using modes with l and m subscripts above unity. TM modes are often used for fixed frequency cavities, but for variable cavities TE modes are preferable since these have zero current at the inner wall of the cylinder and thus obviate moving-contact difficulty. If any mode higher than the dominant one is used, suppression of unwanted modes may be required.

The Value of Q

The accuracy of a wavemeter is dependent on its resolving power. This in turn depends upon Q, which is an index of the decrement of the resonant circuit and is equal to $f/\Delta f$, where Δf is the distance between three decibel points on the resonance curve.

In a coaxial wavemeter, maximum Q for a given inner diameter is obtained with a diameter ratio of about 3.6.[5] The basic Q of a coaxial wavemeter, assuming copper of standard conductivity, is roughly[6]

$$Q_o = 0.042D\sqrt{f} \qquad (3)$$

This expression neglects end effects and hence gives somewhat too high a value of Q.

The basic Q's for $TE_{1,1,n}$ and $TE_{0,1,n}$ cylindrical cavity resonators employing copper of standard conductivity are, respectively,

$$Q_o = 0.0937\times10^{10}\frac{A^3}{\sqrt{f}}\times\frac{1}{1+B^2\left(0.826\frac{B}{n}+0.295\right)} \qquad (4)$$

$$Q_o = 0.2762\times10^{10}\frac{A^3}{\sqrt{f}}\times\frac{1}{1+B^2\left(2.439\frac{B}{n}\right)} \qquad (5)$$

where $A = \lambda_c/\lambda$, $B^2 = A^2 - 1$, and f is in cycles per second.

The value of Q which determines accuracy is not the basic Q, but the loaded or working Q, herein designated Q_L.

The resolving power of a wavemeter used for measuring a single frequency can be made considerably better than f/Q_L. With a sensitive meter it is readily possible to detect differences less than one decibel, which corresponds to a frequency interval of $f/2Q_L$.

The required accuracy in a wavemeter is generally absolute rather than a percentage. Hence increasingly large values

*TE and TM represent, respectively, transverse electric and transverse magnetic. The subscripts l, m, n denote, respectively, the number of wave lengths around any concentric circle in the cross section, the number of wave lengths across a diameter, and the number of half wave lengths along the length of the cylinder.

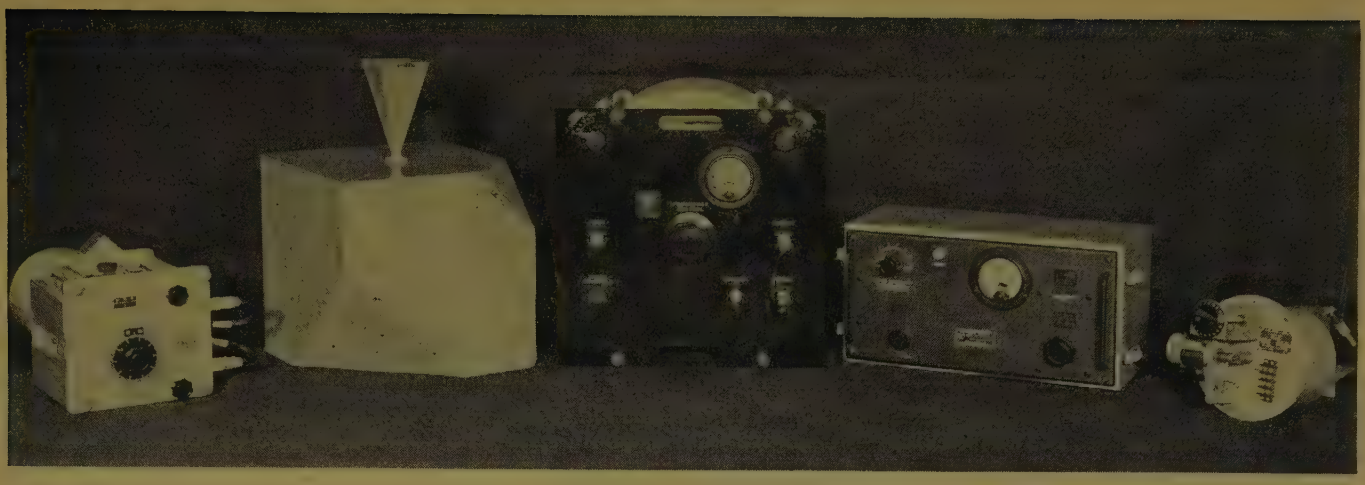


Figure 14. A group of echo boxes of various types

of Q_L are required at the higher frequencies. Thus for a resolution of one megacycle, assuming one decibel discrimination, the values of Q_L required for different frequencies are:

Frequency	Q_L	Frequency	Q_L
1,000 mc.....	500	10,000 mc.....	5,000
3,000 mc.....	1,500	25,000 mc.....	12,500

An unnecessarily high value of Q_L has the disadvantage of making it more difficult to find the desired frequency.

Linearity

The displacement of the coaxial plunger of a coaxial-type wavemeter for resonance is substantially a direct linear function of free space wave length, and if an ordinary centimeter micrometer drive is used, it is possible to read wave length differentials directly. Over band widths less than 20 per cent, displacement versus frequency is also quite linear, which is of considerable advantage for some uses.

For the cavity-type wavemeter, the displacement is a variable function of free space wave length and becomes very nonlinear as the cutoff frequency of the guide or cavity is approached. This is evident from the relation between wave length in the guide, λ_g, wave length in free space, λ, and cutoff wave length, λ_c:

$$\lambda_g = \frac{\lambda}{\sqrt{1 - \frac{\lambda^2}{\lambda_c^2}}} \qquad (6)$$

A cam or mechanical linkage may be employed to obtain a linear scale.

Frequency Coverage

Increasing the length of a wavemeter is desirable because this gives a larger mechanical displacement for a given frequency interval. The permissible increase is limited, however, by ambiguity with the next lower mode in going toward the upper end of the frequency scale and with the next higher mode in going toward the lower end. This means that if ambiguity is to be avoided, the ratio of top to bottom frequency cannot exceed $(n + 2)/n$ for a coaxial line of n quarter-waves. For a cylindrical cavity resonator, the ratio for the 0, 1, n mode must be less than $(n + 1)/n$, the exact limit depending on proximity to cutoff.

Guideposts

The following guideposts are suggested for choosing the type of wavemeter in the microwave range. Where limitations of size and Q permit, the coaxial quarter-wave type should be used because of its greater linearity. If this type is inapplicable, the cavity type with $TE_{1,1,n}$ should be used unless its Q is inadequate, in which case $TE_{0,1,n}$ should be employed.

Couplings

A loop, orifice, or probe may be used for coupling to a wavemeter. Coupling to a coaxial wavemeter is generally effected by a loop placed near a short-circuited end so as to be in the maximum magnetic field. For coupling to a cylindrical cavity wavemeter, an orifice in or near the base of the cavity is usually employed. The coupling to the wavemeter is kept small enough to avoid serious reduction of loaded Q.

Types of Detectors

Various types of detectors may be associated with a wavemeter, the most commonly used being (1) a crystal rectifier and microammeter and (2) a thermistor bolometer. When a crystal rectifier is employed with a cavity or coaxial wavemeter, a circuit similar to that shown in Figure 9 is used. Important items in such a circuit are the RF by-pass capacitor, and the video capacitor. The latter, by providing a low impedance path to the video signals, improves rectification efficiency when the input signal is pulsed. The quarter-wave stub shown in the figure is used when the input or coupling circuit does not provide d-c and video paths. When the signal is pulsed at a low-duty cycle, high peak currents through the crystal are obtained even though the average current through the meter is small, and it is possible to impair or burn out the crystal unless extreme care is taken. The use of a thermistor, which is self-protecting for large overloads, avoids this danger. Another expedient is to limit the crystal current to a small value and employ a video amplifier and oscilloscope.

Methods of Use

A wavemeter may be used as either a transmission or a reaction instrument. In the former case (Figure 10A), it is inserted directly in the transmission path, so that substantially no through transmission occurs except at resonance. In the latter case (Figure 10B), the wavemeter is coupled to the transmission path or a branch circuit. When the meter is tuned off resonance, it presents such a high impedance to the main path that its effect is negligible. At resonance, however, it offers a lower impedance which reflects energy in the main line so that less power reaches the detector and a dip in the reading occurs. For most applications the reaction arrangement is preferable, since the power transmitted when the wavemeter is off tune may serve various purposes. For analysis of frequency spectrum the transmission method is necessary. This method requires two couplings to the wavemeter, which lowers the Q as compared with the reaction type.

Drive and Scale

A direct drive with a precision lead screw of the micrometer type is frequently used. Accuracy of reading is insured by spring loading to minimize backlash and by specifying close tolerances for threads and for concentricity of plunger and cavity. The scale on a wavemeter must be fine enough to permit utilization of the resolving power. The conventional micrometer type of scale sometimes makes accurate reading difficult in a small compact meter. Scale mechanisms which have been used include counter types, clock face, or expanded drum types with gearing between vernier and coarse scales, and a single direct reading scale with divisions arranged in a spiral for compactness.

Effect of Temperature and Humidity

To minimize the effects of temperature on the accuracy of readings, invar has been employed for elements whose dimensions affect the wave length. For accurate work, the scale reading must be corrected for temperature. A rough approximation is that the scale reading varies in accordance with the coefficient of expansion of the metal.

Water vapor included in the air dielectric of a wavemeter has an appreciable effect on the dielectric constant and hence on the resonant frequency.[7] Thus, for example, in going at sea level from 25 degrees centigrade and 60 per cent humidity to 50 degrees centigrade and 90 per cent humidity, the scale reading should be reduced by 0.03 per cent. Correction can be made by means of a chart, a convenient form of which has been prepared by Radiation Laboratory.

Calibration

Frequency meters are calibrated against sub-standards which in turn are calibrated against a multiplier from lower frequencies for which a high order of accuracy can be obtained. Such multipliers have been made available at Radiation Laboratory and the National Bureau of Standards. The accuracy obtained at interpolation frequencies is of course less than at exact multiples of the base frequency. In the microwave range, the accuracy is believed to be of the order of one part in 100,000.

Power Measurement

There are two needs for power measurement in radar maintenance, namely, in evaluating transmitter performance and in standardizing test signals. Power output is, of course, only one factor in transmitter performance, others being (a) frequency and (b) spectral distribution or shape of RF envelope. Ability to measure absolute power is desirable to permit interchangeable use of sets in the field.

Measurement of Pulse Power

The transmitter power as used in formula 1 is the average power during the pulse. The relationship of pulse to (long) average power is

$$\frac{P_t \text{ avg}}{P_t \text{ pulse}} = Tf_r \qquad (7)$$

T is the pulse duration in seconds and f_r is the pulse recurrence frequency (P.R.F.) in cycles per second. The product Tf_r is the duty cycle. (Sometimes the reciprocal of this number is referred to as the duty cycle. The magnitude is usually such that no ambiguity arises.)

During the early days of radar, it was the practice to measure pulse power. The test equipment was coupled to the radar set by a path of known loss. The RF envelope was derived by means of a crystal rectifier and applied to an oscilloscope. With the aid of an RF attenuator, the level applied to the crystal rectifier and oscilloscope was held constant. Calibration was obtained by using a signal generator whose output was standardized, prior to pulsing, with an averaging type of power meter. The procedure was rather involved, with several sources of possible error. Since it is much simpler to measure average power, field measurement of pulse power soon was abandoned. Though the pulse power can be computed from average power if the pulse width, pulse shape, and repetition rate are known, it soon became the practice to specify field performance requirements in terms of average power.

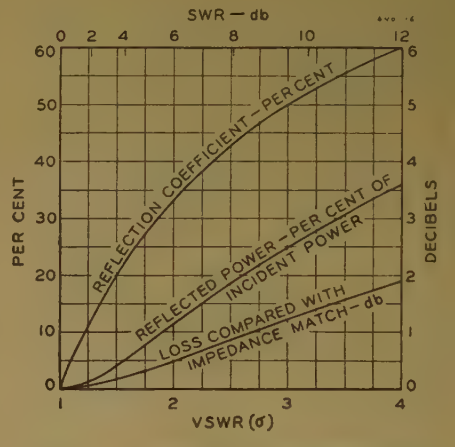


Figure 16. Relations in mismatched transmission lines

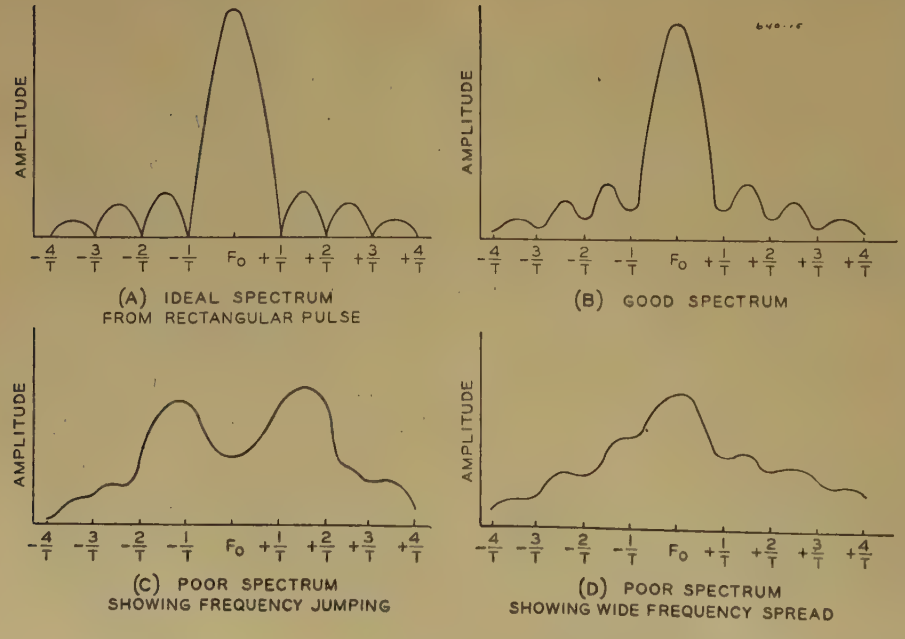


Figure 15. Radar spectrum analysis with echo box

Thermistor Power Meters

A number of devices have been used for measuring average power in the microwave range. Those suitable for handling the small amounts of power normally involved in field tests include thermistors, platinum wires, and thermocouples. In each case the RF power to be measured is absorbed in the measuring element. The measurement consists in observing the resistance change in the thermistor or platinum wire, or the thermoelectric voltage from the thermocouple. By analogy with devices used for measuring minute quantities of radiant heat, either a therm-

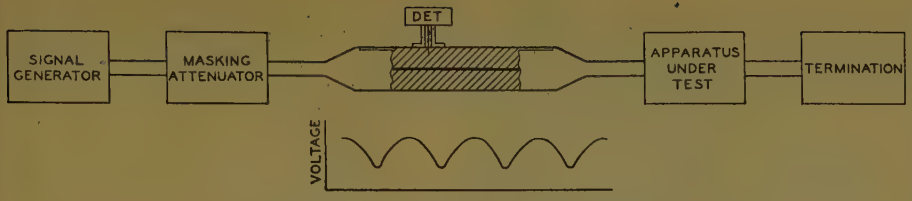


Figure 17. Standing wave measurement

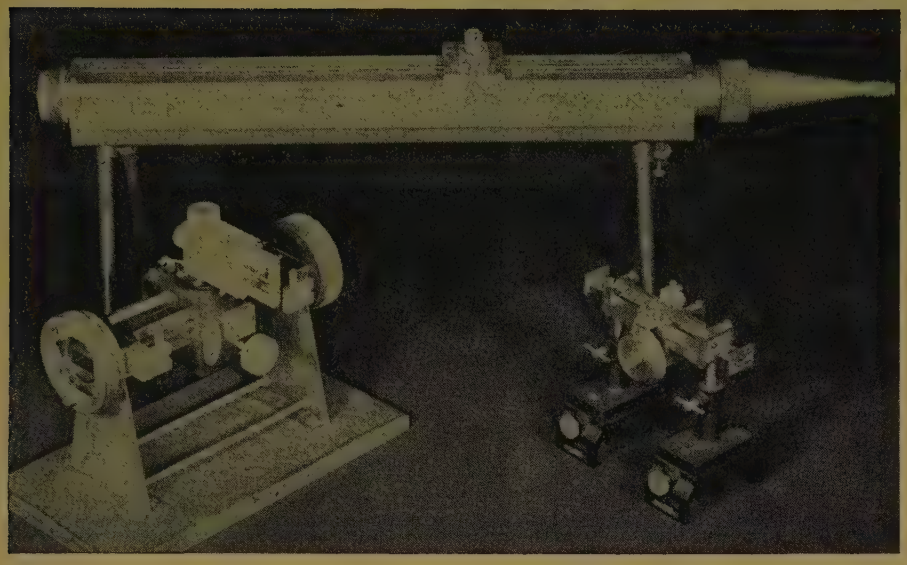


Figure 18. Standing wave detectors used on coaxial and wave guide transmission lines

istor or a platinum wire instrument is sometimes referred to as a bolometer. The platinum wire device has also been termed a barretter.

A thermistor for microwave power measurement is a tiny bead (about five mils in diameter) composed of a mixture of oxides of manganese, cobalt, nickel, and copper, constituting a resistor with a very high negative temperature coefficient.[8]

The thermistor has a number of advantages for microwave work, namely:

1. Resistance is highly sensitive to change of heating power, which obviates any need for amplification or a super-sensitive meter and makes it possible to use a rugged d-c meter.

2. Reactance is low compared with RF resistance, which makes it possible to incorporate the thermistor in a power-absorbing termination which matches the impedance of a microwave transmission line over a wide band.

3. Resistance change is the same function of electrical heating power at any frequency, which permits direct comparison of the unknown microwave power with easily measurable d-c power.

4. Sensitivity to damage and burn-out is inherently low, and added protection results from impedance mismatch during overload.

Because of these characteristics, thermistors have been far more widely used than other detectors for microwave power measurement. Broadband thermistor mounts have been designed to match both wave guide and coaxial transmission lines, the latter not only in the microwave range but also down to low frequencies. Some of the test sets specifically intended for power measurement or for combined power and frequency measurement are shown in Figure 8.

The change in the thermistor resistance caused by radio-frequency heating current is determined by placing the thermistor in one arm of a d-c bridge. By noting the d-c power necessary to balance the bridge with and without RF power in the thermistor, the magnitude of the RF power may be determined. For most purposes, however, a direct-reading power meter is preferable. This can be obtained over a moderate range of power levels by employing an unbalanced bridge. The bridge is balanced for direct current only, and the measurement consists in noting the meter deflection when radio-frequency power is added.

The resistance of a thermistor is a highly sensitive function not only of electrical heating power but also of ambient temperature. For convenient field measurement, the effect of ambient temperature must be cancelled out in the indicator circuit so that the indication depends only on RF power.

Water Loads

A method which has been used in the laboratory and the factory for measuring high level microwave power consists in terminating the RF transmission line in a water load arranged as a continuous flow calorimeter. This method can be made quite accurate but is cumbersome. More recent practice is to terminate the RF line in a solid load of a type described later in this article and to couple a thermistor power meter to the line by means of a directional coupler (described below) of known loss. Very close correlations have been obtained between the two methods over the entire microwave band.

Echo Boxes

A device unique to radar testing is a high Q resonant cavity, known as an echo box or ring box. The cavity is coupled to the radar transmission line or antenna as indicated in Figure 11. During the transmitted pulse, microwave energy is stored in the cavity. In the period immediately thereafter, energy is returned to the radar over the same path, producing a signal on the radar indicator. The energy in the cavity builds up exponentially to an amplitude dependent on the radar power. At the end of the pulse, the returned energy decays exponentially, disappearing into the noise at a point determined by receiver sensitivity. The time interval between the end of the transmitted pulse and the point where the signal on the radar indicator disappears into the background noise, called the ringtime, therefore measures the over-all performance of the radar set.

An echo box is a particularly useful instrument for radar testing because

1. It measures over-all performance directly

2. It permits a rapid tune-up.

3. It utilizes the radar transmitter as its only source of power and therefore can be made extremely portable.

Figure 12 shows typical ringtime patterns on different types of indicators. In actual practice the ringtime is read in miles on the radar range scale and hence is measured from the beginning of the transmitted pulse rather than the end. The difference is unimportant, however, since standard and limiting values of ringtime are established for operating conditions. It will be noted that the echo box does not return a true echo to the radar, so that the name "echo box" is not entirely appropriate.

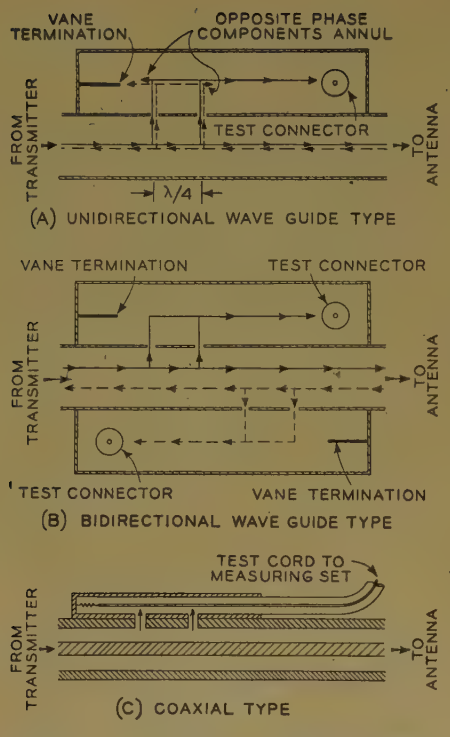


Figure 19. Directional coupler arrangement

Types and Uses

Echo boxes are of two general types, tuned and untuned. A tuned echo box is designed to resonate in a single mode adjustable over the operating frequency range. An untuned echo box is a fixed cavity of a size sufficient to support a very large number of modes within the working range. Tuned echo boxes are more versatile and more widely used than untuned boxes.

The most common type of tuned echo box is designed for hand tuning. While other shapes are possible, the most convenient one is a right cylinder whose length is adjusted by a movable piston. The $TE_{0,1,n}$ mode gives maximum Q for a given volume and minimizes the number of unwanted modes present within the desired band. The value of n is determined by the desired value of Q (see formula 5). Unwanted modes can be partially avoided by choice of design parameters. However, for high values of Q, and especially for broad frequency bands, the suppression of unwanted modes involves design problems of the highest order.

As indicated in Figure 13, a tuned echo box cavity is usually provided with two couplings. One of these is to the radar pick-up; the other is to an attenuating device, crystal rectifier, and meter, which serve for tuning the cavity and for other purposes. With such an instrument, not only can the radar be tuned up and its over-all performance determined, but many other tests can be made, to wit:

1. The setting of the plunger at resonance indicates the transmitter frequency or wave length.

2. Calibration of the crystal affords a rough measure of output power.

3. Since the Q required for adequate ringtime is so high that the cavity selects only a narrow segment of the transmitter spectrum, a spectrum analysis can be made by plotting frequency versus crystal current reading.

4. Slow recovery of TR box and receiver after the transmitted pulse can be detected by noting the behavior of the ringtime pattern at short ranges as the echo box is detuned.

5. Inability of the receiver to recover promptly after a strong signal (the result of imperfect d-c reinsertion in the video amplifier or of overloading of the IF amplifier) is indicated by a blank following the end of the ring.

6. Improper pulsing (for example, double moding or misfiring) can be determined with a class A oscilloscope.

7. The frequency and power of the local oscillator can be measured.

In tuned echo boxes, requirements for extreme fineness of tuning control and precise resettability have given rise to interesting problems in the design of the mechanical drive and indicating mechanism.

In another type of echo box, hand tuning is supplemented by motor-driven tuning or so-called "wobbling" over a frequency range wide enough to embrace expected variations in transmitter frequency. Operation is controlled by a single push-button which energizes the motor and actuates the cavity coupling. Such an instrument may be permanently installed in a plane and used to check the radar during flight.

For an untuned or multiresonant echo box, rectangular shape is convenient. The box should be large enough to make it highly probable that over the operating band, one or more modes will be present within any frequency interval of width equal to the main concentration of the transmitter spectrum. For a given rectangular volume, a cube gives the largest number of modes. The total number of modes up to a frequency of wave length λ_0 is

$$N_M = 8.38 V/\lambda_0^3 \qquad (8)$$

where V is the volume. However, because of the cubical shape, many different modes tend to coincide in wave length, a condition referred to as degeneracy. To spread out the modes, the box is made slightly off cube and one or more corners sliced off. At the longer microwaves, the size of box is determined by the number of modes, and the size becomes quite awkward. For the shorter microwaves, the size is determined by the required value of Q. Hence the use of untuned echo boxes has been limited to the frequency range from about 9,000 megacycles upwards, with sizes of the order of from 12 to 24 inches on a side. Even with an extraordinarily high probability of finding modes within the radar band, substantial differences in response are found for relatively small changes in frequency. Accordingly, untuned echo boxes are more useful for rough tune-up than for precise measurement.

A number of specific designs of echo boxes for different microwave bands are shown in Figure 14.

Q and Ringtime

For satisfactory measurement the ringtime must extend beyond nearby echoes which would obscure the test signal. For most radars a ringtime of 20 to 30 microseconds (about two to three miles) has been found satisfactory, although considerably higher values have sometimes been provided. Even apart from echoes, a long ringtime is desirable since this gives a lower decay rate and a more sensitive measurement.

Computation will show that an extremely high value of Q is necessary to obtain the desired ringtime. For maximum ringtime the cavity coupling should be such as to make the working Q (Q_L) about 90 per cent of the nonloaded Q. Values of working Q which have been provided in different frequency ranges are approximately as follows:

Frequency	Q_L	Frequency	Q_L
1,000 mc	70,000*	10,000 mc	100,000
3,000 mc	40,000	24,000 mc	200,000

*In this case a higher Q was needed for a long range ground search system.

The difference in performance corresponding to a given change in ringtime can be determined from the decay rate, which is

$$d = 27.3 f/Q_L \text{ decibels per microsecond} \qquad (9)$$

For a given frequency, the ringtime is directly proportional, and the decay rate inversely proportional, to Q. For a given ringtime, the required Q is directly proportional to frequency.

Accurate measurement of extremely high Q's is essential in echo box work. A decrement method, in which a pulsed radio-frequency oscillator and oscillo-

scope are used to determine the loss corresponding to a known time interval, has proved most satisfactory.

Spectrum Analysis

The frequency components of a non-repetitive rectangular d-c pulse may be determined by well-known methods using Fourier integral analysis. The envelope of amplitudes is of the form $(\sin x)/x$, where $x = \pi fT$. This envelope is shown by the right-hand side of the curve of Figure 15a, f_0 being assumed to represent zero frequency. The first zero occurs at the frequency $f = 1/T$.

Similarly, the envelope of the spectrum of a rectangular a-c pulse is given by the complete curve of Figure 15A, f_0 in this case being the carrier frequency. For a non-repetitive pulse, all frequencies are present in amplitude as shown by the envelope. When a stable carrier frequency is pulsed at uniform intervals and in precise phase relation, only harmonics of the repetition frequency are present under the envelope. In radar practice, conditions are, as a rule, not sufficiently stable for this to occur.

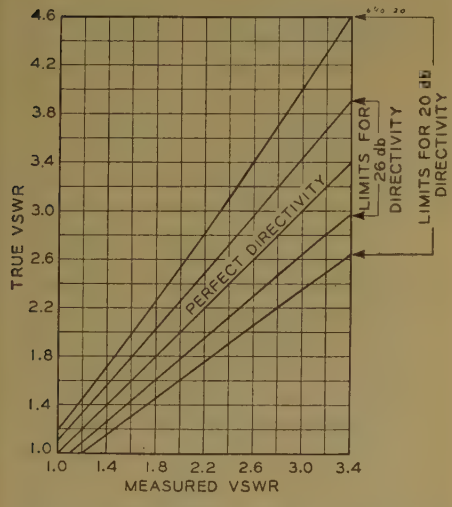


Figure 20. Error in standing wave measurements caused by directivity of directional coupler

Because of its band width, an echo box cannot reproduce the ideal spectrum envelope of Figure 15A. Instead, the curve for a good spectrum may resemble that of Figure 15B, while spectrum irregularities detrimental to radar performance may be revealed by curves such as those of Figure 15C and 15D. Broadening of the spectrum is undesirable because less energy falls within the receiver band. Energy removed from the main concentration may result from double moding

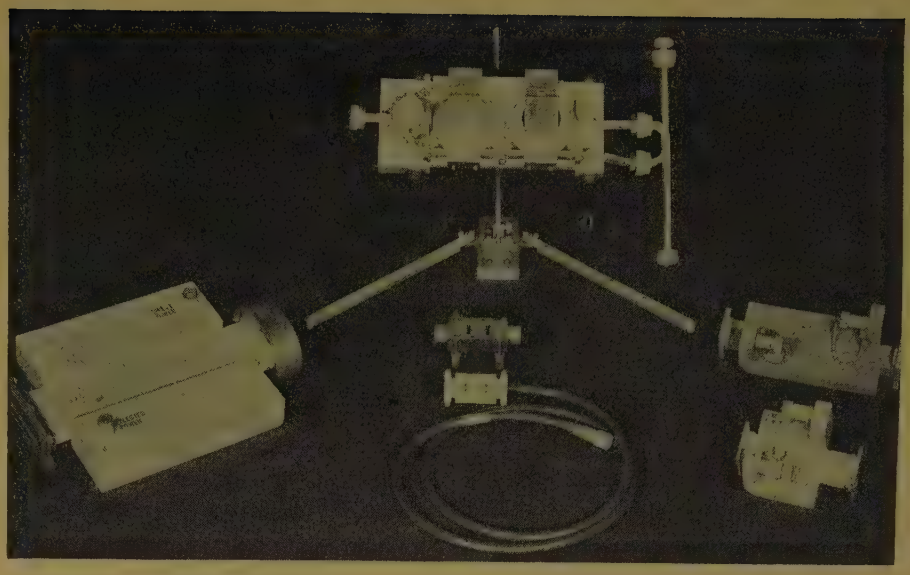


Figure 21. A group of microwave directional couplers together with a directional coupler test set

or from the occurrence of a different frequency during the rise or fall of the pulse. Frequency modulation caused by a sloping or spiked input pulse produces a non-symmetrical spectrum, not infrequently characterized by a high side lobe. Frequency jump in the middle of the pulse, resulting from line reflection, may produce two distinct maxima.

Standing Wave Measurements

The expression for the distribution of current or voltage along a misterminated line of appreciable electrical length yields two terms which may be considered as representing two waves transmitted in opposite directions, one (the incident wave) from the generator toward the load, the other (the reflected wave) from the load toward the generator. The summation is a standing wave pattern. The standing wave ratio (SWR) is defined as the ratio of the wave amplitude at a maximum point (anti-node) to that at a minimum point (node). If the standing wave ratio is stated as a numeric, it is necessary to specify whether it applies to voltage (VSWR) or power (PSWR). Possibility of ambiguity is avoided by stating the ratio in decibels.

The ratio of the reflected current to the incident current is the reflection coefficient, here designated as ρ. The value of the reflection coefficient is given both in magnitude and phase by

$$\rho = \frac{Z_0 - Z}{Z_0 + Z} \qquad (10)$$

where Z_0 is the characteristic impedance of the line and Z is the load impedance. The reflection coefficient is related to the standing wave ratio as follows:

$$\text{VSWR} = \sigma = \frac{1+\rho}{1-\rho}, \text{ or, } \rho = \frac{\sigma - 1}{\sigma + 1} \qquad (11)$$

Plots of the relationships are shown in Figure 16.

The reduction of radiated power because of reflection losses in a radar transmission line, while important, is usually less serious than other effects of impedance irregularities. Since the load impedance reacts on the oscillator circuit, the frequency and the output of most transmitter tubes are quite sensitive to load impedance. If the line is electrically long, so that its impedance varies rapidly with frequency, marked instability of oscillator frequency may occur, a condition referred to as "long line effect."

Since radar transmission lines contain many potential sources of impedance discontinuity, including not only the antenna but a variety of couplings, bends, wobble joints, rotating joints, switches, and so forth, measurements of standing wave ratio are frequently required. The need for such measurements depends in part on whether the line is "preplumbed" or is provided with field adjustments.

Devices

Standing waves may be detected and measured by several different types of devices, including

1. A slotted line.
2. A squeeze section.
3. A directional coupler.
4. A hybrid T.

All of these furnish information on the magnitude of the standing wave ratio. In some cases, phase information may be obtained also, which information permits determination of impedance,[9] but this

knowledge, while useful in the laboratory, seldom is required in field work.

A block diagram of an arrangement employing a slotted line for measuring standing waves is shown in Figure 17. The oscillator source is commonly followed by a pad or attenuator to prevent frequency pulling. The slotted section may be either a coaxial or a wave guide line employing a mode which is not disturbed by the presence of the slot (for example, normal coaxial mode, $TE_{1,0}$ in rectangular wave guide, $TM_{0,1}$ in round wave guide). A traveling pick-up probe or loop projects through the slot and couples energy from the line into a detector which delivers direct current or audio frequency to the indicator. The probe is moved longitudinally to find points of maximum and minimum field strength. To avoid distortion of the field within the line, the probe should be small and should project only a short distance inside the slot. For accurate results, extreme care must be exercised in design and construction to avoid variation in depth of immersion as the probe is moved. Several slotted lines employed for standing wave measurements are shown in Figure 18.

A squeeze section consists of a section of rectangular guide with slots milled in the center of both broad faces so that the width of the guide can be varied by external deforming means. This changes the wave length in the guide, so that maximum and minimum values may be determined by a fixed probe and indicator.

The use of a directional coupler for standing wave measurement is discussed in the following section.

Another useful device for standing wave measurement is the hybrid T or magic T. This is a sort of microwave bridge, consisting of a main wave guide to which an E plane branch and an H plane branch are joined in the same physical plane. With matched terminations of the two ends of the main guide, the two branches are conjugate. Terminating one end of the main guide in the unknown impedance and the other in a matched termination, the degree of impedance mismatch of the unknown is indicated by the magnitude of the reflected wave which appears in one branch when energy is fed into the other.

Directional Couplers

Accurate measurement of transmitter power and receiver sensitivity requires a coupling path of known loss between the radar set and the test set. The first method employed for this was to place a portable test antenna (see Figure 2) in the field of the radar antenna. Depending on the frequency range, this test antenna took the form of a dipole,[10] with or without a small reflector, or an electromagnetic horn.[11] With this method, it was necessary to calibrate the loss of the space coupling path between the two antennas. Since it proved difficult to locate the test antenna at exactly the same point and to be sure that the main antenna pattern remained the same, a separate calibration of the coupling loss was usually required whenever a measurement was made.

An alternative method was to place a single probe in the radar transmission line. This introduced another sort of difficulty. Accuracy of measurement was vitiated by the presence of standing waves which rendered the probe pick-up a function of frequency and of location with respect to the irregularities. A highly satisfactory answer to the entire problem was found in a device which is called a directional coupler because it couples only to the wave propagated in one direction. In its simplest form, a directional coupler consists of two couplings to the main transmission line, which add for one direction of transmission and cancel for the other. Thus, for example, Figure 10A shows a form of directional coupler for wave guide which is placed in the radar transmission line at the point indicated schematically in Figure 1. An auxiliary wave guide is coupled to the main guide through two identical orifices spaced $\lambda g/4$ between centers (or more generally $n\lambda g/4$, where n is an odd integer). Assuming the incident and reflected waves in the main guide to be directed as shown and the auxiliary guide to be terminated on one end, a test circuit connected to the other end will be coupled to the incident wave, while theoretically the two couplings to the reflected wave will differ by $\lambda/2$ and therefore cancel one another.

With such a device, measurements may be made of the characteristics of the incident wave independently of reflections.

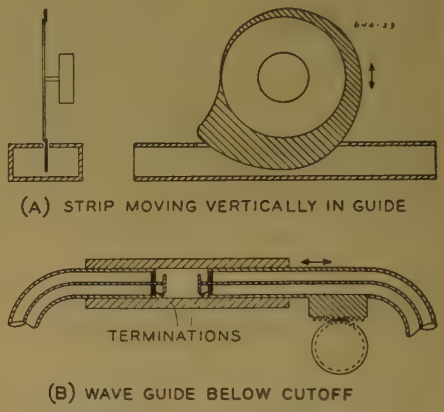


Figure 23. Microwave attenuators

If the coupling to the main line is not too close, there is no appreciable effect on the incident wave, and continuous monitoring can be had. Conversely, test signals applied through the directional coupler will travel in the main guide in the proper direction for testing the radar receiver.

If the locations of the termination and the test connection point in Figure 19A are reversed, the couplings to the main transmission line also are reversed. Such an arrangement therefore permits measurement of the reflected power, which in turn makes it possible to adjust for minimum reflected power and hence for minimum standing wave ratio. Comparison of the reflected power with the direct power determines the standing wave ratio. For convenience in measurement, two directional couplers pointed in opposite directions are frequently used, the combination being referred to as a bidirectional coupler (Figure 19B). One advantage of this arrangement is that the ability to measure the reflected power from the antenna and that part of trans-

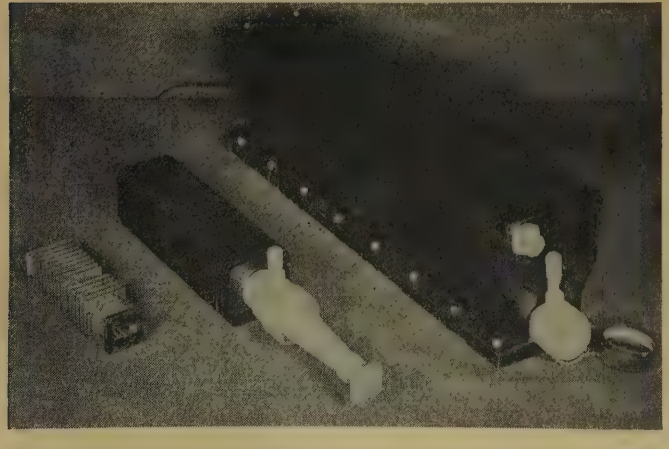


Figure 22. RF loads for different bands in the microwave frequency range

mission line beyond the coupler provides means for detecting trouble in that part of the system. Directional couplers may be applied to any type of transmission line. Figure 19C shows a simple form of directional coupler for a coaxial line.

One characteristic of importance in a directional coupler is the coupling loss. A small value of coupling loss affords increased sensitivity of measurement, while a sizable value is desirable to minimize reaction on the main transmission line, as well as for other reasons. A loss of around 20 decibels has usually been found a good compromise. It is now the practice to incorporate a directional coupler in every radar set to obtain a test connection point.

Because of unavoidable imperfections, a directional coupler never gives complete cancellation for the undesired direction of transmission. The departure from ideality is indicated by the directivity (also referred to as front-to-back ratio), which is defined as the scalar ratio of the two powers measured at the test connection point when the same amount of power is applied to the main guide, first in one direction and then in the other. For measurements of the direct wave and of receiver characteristics, a moderate directivity, of the order of 15 decibels or better is sufficient. In measuring reflected power, however, the directivity determines the amount of direct power which appears at the point of measurement, and therefore controls accuracy. The chart of Figure 20 will facilitate determination of the maximum error that may occur in measuring different values of the standing wave ratio with various assumed directivities.

With a simple two-hole coupler, the directivity deteriorates rapidly as the frequency departs from that corresponding to quarter-wave spacing. By providing additional couplings suitably spaced, the residuals from different sets of couplings also can be cancelled against one another and the directivity versus frequency characteristic can be broadened materially. With multiple hole couplings, a minimum directivity of 26 to 30 decibels over a frequency band of 10 to 20 per cent is readily practicable in quantity production, and much better values are obtained in the laboratory. Some of the numerous designs of directional couplers developed for association with operating radar equipment are shown in Figure 21.

Because they are more convenient than slotted lines and can be made more accurate, directional couplers have been extensively used for standing wave ratio measurement in the laboratory. A number of special arrangements have been devised to improve both accuracy and convenience. A directional coupler arrangement which has been provided for field measurement of standing wave ratio in the vicinity of 25,000 megacycles also is illustrated in Figure 21. In this the direct power is brought to equality with the reflected power by an attenuator whose dial is calibrated directly in standing wave ratio. A wave-guide switch facilitates the power comparison.

Auxiliaries and Components

An RF load (or dummy antenna) which will absorb the radar power in an impedance which matches the transmission line is very useful in radar work. Such a device permits testing the radar set in operating condition without actual radiation which might give information to the enemy or interfere with other radar equipment. It also makes it possible to test the radar set in locations where reflections from the ground or nearby objects otherwise would hamper or prevent a test. RF loads for microwave work usually consist of a section of transmission line (either coaxial or wave guide, depending on wave length) containing a high-loss dielectric. The impedance of such a load is necessarily low and must be matched to the radar line by tapering the dielectric over a distance of several wave lengths.[10] Moreover, if the line is to handle high power, tapering over a considerable length is necessary to distribute the heat.

A coaxial load preferably is tapered from outer conductor to inner conductor, since this both reduces the voltage gradient and facilitates heat dissipation. A dielectric consisting of a mixture of bakelite, silica, and graphite, molded in place, has been found satisfactory. For wave guides, a ceramic containing carbon may be preformed, with taper in one or two dimensions, and cemented in place.

Figure 22 shows a number of RF loads developed for different frequency bands. One of these, *TS-235/UP*, provides an excellent impedance match over the frequency range from 500 megacycles to above 3,000 megacycles. When equipped with a blower designed for uniform transverse ventilation, it will handle a peak power of the order of 750 kw with a duty cycle of about 0.001.

Microwave Attenuators and Pads

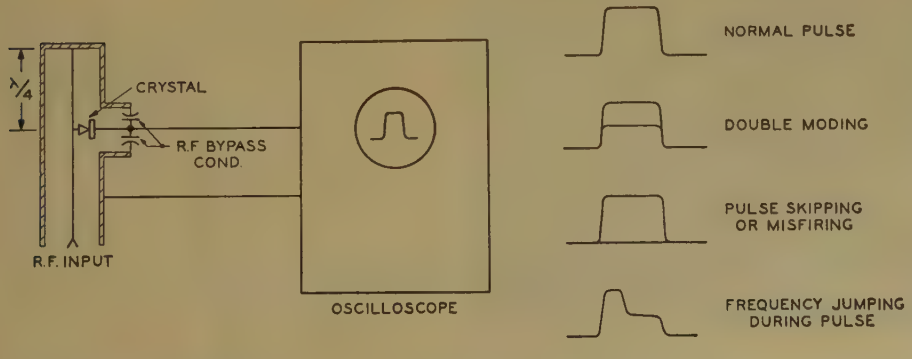
RF attenuators and pads are cornerstones of microwave testing. Attenuators are used to adjust unknown signals to levels suitable for measurement and to obtain the minute test signals required for measuring receiver characteristics. Pads serve to change levels and to prevent interaction between testing components. Microwave attenuators and pads are of two general types:

1. Those which employ dissipative elements to absorb power.
2. Nondissipative devices which introduce propagation or coupling loss.

For the shorter microwaves, the most convenient form of attenuator is of the dissipative type, employing a strip or vane of dielectric coated with a resistance material, as for example, carbon-coated bakelite. This is placed in rectangular wave guide with its plane paralleling the side of the guide. The attenuation is varied by varying the depth to which the vane is inserted in the guide (Figure 23A) or by changing its position in the guide. A valuable feature of such attenuators is that the minimum loss can be made substantially zero. For good impedance match, the strip must be tapered. By using two strips, the over-all length of the attenuator can be reduced. Extremely satisfactory attenuators of this type covering a frequency range of 8 to 12 per cent, with loss variable from 0 to 35 or 40 decibels, have been obtained in the frequency range 4,000 to 24,000 megacycles.

For the longer microwaves, where wave guides are inconveniently large, attenuators of the wave guide-below-cutoff type are very useful. These consist of a

Figure 24. Radar pulse envelopes



section of round wave guide the diameter of which is small compared with wave length and whose length is adjusted by telescoping. (See Figure 23B.) The $TM_{0,1}$ mode has been found very satisfactory, and $TE_{1,1}$ has also been used. Connection is made to the attenuator by a coaxial circuit at each end, with disk excitation for the $TM_{0,1}$ mode and loop coupling for $TE_{1,1}$. The attenuation formulas are[12]

$$TM_{0,1}. \quad A = \frac{41.8}{D}\sqrt{1-\left(\frac{1.31D}{\lambda}\right)^2} \text{ decibels per meter} \quad (12)$$

$$TE_{1,1}. \quad A = \frac{32.0}{D}\sqrt{1-\left(\frac{1.71D}{\lambda}\right)^2} \text{ decibels per meter} \quad (13)$$

where D = diameter of wave guide in meters. Because of the effect of other modes when the coupling is close, a minimum loss of 20 to 30 decibels is required before the attenuation becomes linear with displacement. The attenuation differentials are substantially independent of frequency. Attenuators of this type present a large impedance mismatch at either end, the effect of which may be alleviated by padding or by a termination.

Types of pads employed in microwave work include the following:

1. Flexible coaxial cable, usually with high resistance inner conductor.
2. Coaxial π with carbon-coated rod and disks.
3. Coaxial with carbon-coated rod as inner conductor.
4. Resistance strip in wave guide.
5. Directional coupler.

In calibrating microwave attenuators and pads, comparison with an accurately calibrated IF attenuator, using a heterodyne test set, has been found to give excellent results.

RF Cables and Connectors

Flexible radio-frequency cables for connecting test equipment to equipment under test are an important adjunct of field testing. At frequencies of 10,000 megacycles and below, flexible coaxial cables of about 0.4-inch over-all diameter with solid or stranded inner conductor, solid low loss dielectric (polyethylene) and braided outer conductor have been used satisfactorily, although in the upper part of this range special measures have been necessary to prevent attenuation change caused by flexure and aging. Over most of this range, coaxial jack and plug connections have been found satisfactory, but wave guide connectors are preferable at the upper end. In the range above 10,000 megacycles, coaxial cables of requisite stability have not yet been obtained, and rubber-covered wave guide with soldered articulated joints is the best form of flexible cable now available.

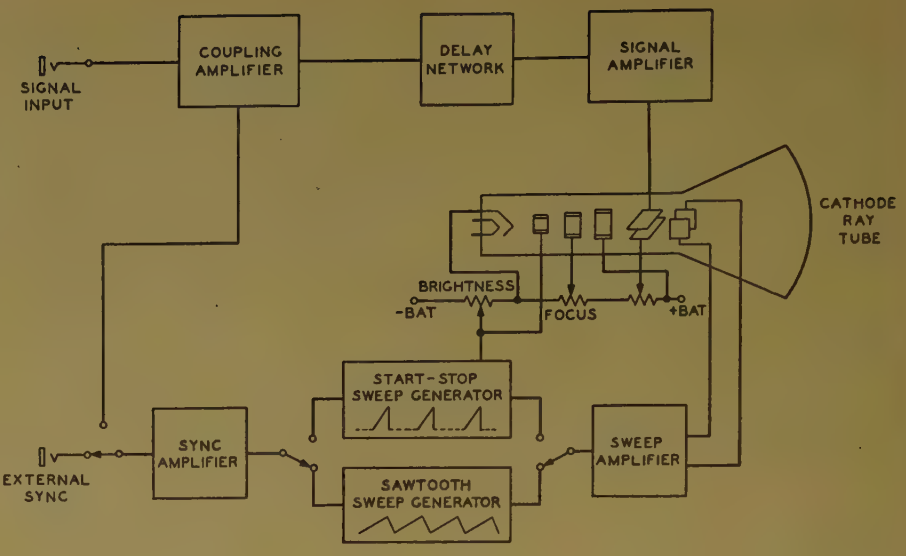


Figure 26. Block diagram of *TS-34/AP* and *TS-34A/AP* oscilloscopes

Oscilloscopes

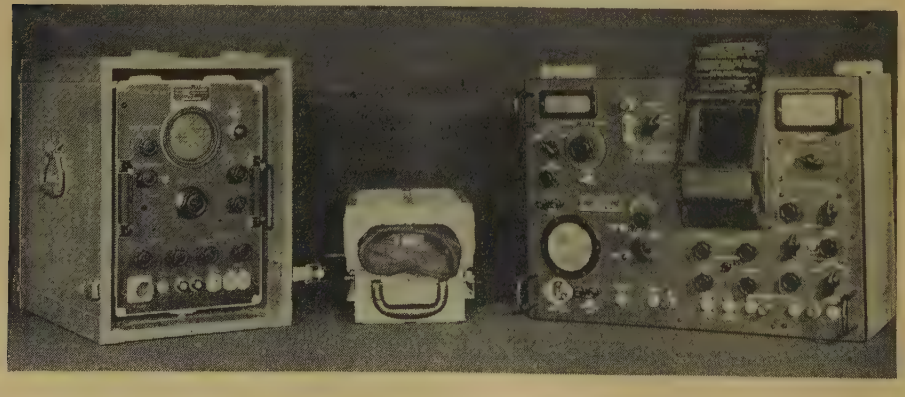
Oscilloscopes are used extensively in radar maintenance for examination of video waves and for viewing RF envelopes. Satisfactory radar performance depends on a variety of video wave shapes, which may include trapezoidal or triangular pulses, sawtooth waves, square waves, or combinations of these. Observation of these wave shapes, supplemented if necessary by measurements of amplitude and duration, helps in diagnosing many troubles.

Examination of the envelope of the RF pulse is a convenient but less informative alternative to spectrum analysis. The envelope should be a clean, single trace of good shape. Figure 24 shows traces sometimes experienced. Double modding, that is, oscillating at different frequencies on different pulses, is shown by a double trace. Frequency-jumping during a pulse is shown by a break in the envelope. Misfiring gives a base line under the envelope. Other abnormalities in the RF envelope may result from incorrect video wave shape. Observation of the RF envelope requires a rectifier, usually a crystal, together with a suitable video amplifier. Since limitation of the oscilloscope to video functions permits general application to radar sets of all frequencies, the rectifier generally is provided externally.

The oscilloscopes available before the war did not meet the requirements of radar. Fast sweeps were necessary to permit viewing of pulses ranging from several microseconds to a fraction of a microsecond. Amplifiers were required for such pulses with low phase and amplitude distortion over a broad frequency band. Existing methods of synchronizing and phasing sweeps were also inadequate. The progress of the oscilloscope

Figure 25. Test oscilloscopes for viewing wave forms in radar equipments

Left to right: *BC-910-A* (1942), *TS-34A/AP* (1944), and *TS-239/UP* (1945)



art during the war is illustrated in the successive designs of field test oscilloscopes shown in Figure 25.

The *BC*910*A* oscilloscope, gotten out as a stop gap not long after the attack on Pearl Harbor, incorporates fast sweeps and broad-band amplification. Following close upon this was the *BC*1087*A* (Navy code *CW*60*AAY*), which replaced sine-wave synchronization by a start-stop sweep triggered by the incoming pulses. This feature made it possible to superpose the erratic pulses produced by spark wheel and similar pulsers and at the same time avoided external synchronizing connections. A valuable feature conjoined with the start-stop sweep was a delay network in the main transmission path which gave the sweep time to start before the pulse reached the cathode-ray tube. This oscilloscope in original and modified form has seen wide service in all theaters. However, its weight of more than 60 pounds was a handicap for many uses.

Further advances in oscilloscope circuitry and in weight limitation resulted in *TS*-34/*AP*, weighing only 25 pounds. This combined the short-pulse features of the previous design with those of the conventional oscilloscope for viewing slower waves. A schematic diagram is shown in Figure 26. A redesign, coded as *TS*-34*A*/*AP*, incorporated variable start-stop sweeps and improved mechanical design. These two oscilloscopes, *TS*-34 and *TS*-34*A*, were produced to a total of some 12,000 and were used universally by all branches of the service for both radar and radio testing. Toward the end of the war the trend toward shorter pulses, coupled with the need for precise measurement of wave amplitude and duration, led to a new design, *TS*-239/*UP*, which embodied wide advances over *TS*-34*A* in performance and versatility but with an increase in weight.

In association with different oscilloscopes, other video devices have been employed. The amplitude of pulse applied to the magnetron is thousands of volts. To derive a voltage suitable for application to the oscilloscope, a voltage divider of the capacitor type is used (*TS*-89/*AP*). Suitable video terminations, dividers, and loads, sometimes of high voltage and power capacity, are required to obtain proper test conditions and provide convenient test points (*TS*-98/*AP*, *TS*-390/-*TPM*-4, *TS*-90/*AP*, *TS*-234/*UP*). Originally a high impedance connection to the oscilloscope was effected by a single-stage amplifier unit (*BC*1167*A*), but a simple divider-type of probe was later found more satisfactory for this purpose.

Range Calibration

Types of timing circuits used for radar range determination include multivibrators, coil and capacitor oscillators (generally without but sometimes with temperature control), and occasionally quartz crystal oscillators. The first two depend for their accuracy on capacitors, resistances, coils and other elements which are subject to error due to aging, temperature, humidity, mechanical damage, and the like. Nor is the quartz crystal oscillator wholly immune to error. Consequently, portable range calibrators are required for field maintenance.

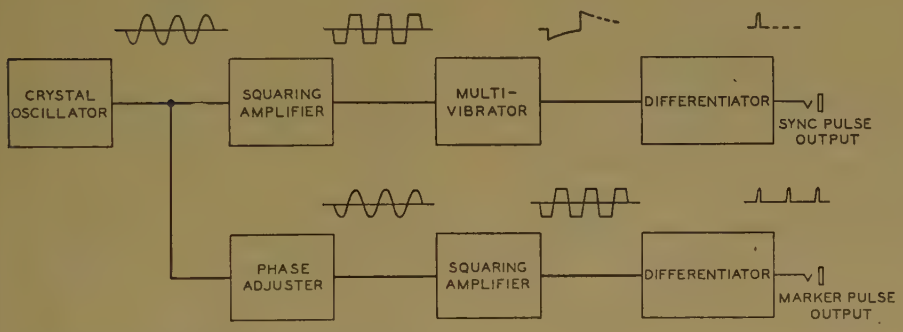


Figure 27. Block diagram of *TS*-102/*AP* and *TS*-102*A*/*AP* range calibrators

TS-102*A*/*AP* (Figure 27) and its predecessors, *TS*-102 and *TS*-19, are precision calibrators which have been extensively used for checking a large number of different air-borne bombing and gun-laying radar equipments, and ship-borne fire control and search radar equipments. These sets deliver accurately spaced marker pulses, derived from a quartz crystal oscillator, for checking the radar range pulses. A trigger pulse derived from a multivibrator synchronized with the quartz oscillator is also provided for actuating the radar timing circuits. With certain radars the calibration procedure requires an oscilloscope as well. Extreme stability of marker pulses, better than ± 0.02 microsecond, is obtained. A stop watch is included in these sets for checking rate of change in range.

Less precision is required in range calibration of search radar sets. For this purpose the *TS*-5/*AP* calibrator provides marker pulses of one-quarter, one, five, or ten nautical or statute miles, derived from a coil and capacitor oscillator with closely controlled temperature coefficients. This calibrator is designed to be triggered by the radar or some other external source.

Computer Test Sets

A number of radar sets are equipped with computers which receive the data on location of target and its direction and rate of change, together with essential related information on such factors as wind velocity, ground speed, altitude, and so forth, and deliver the solution of the ballistic problem in the form of a voltage which releases bombs, points the guns, or serves other purposes. Means for checking the accuracy of these computing devices are generally required. The type of test set needed depends upon the computer design, which has taken different forms according to the nature of the problem and the state of the art.

Two types of computer test sets are

Figure 28. Two test sets for checking the computers used in bombsight and fire control radar sets



shown in Figure 28. *TS-158/AP*, designed for use with certain air-borne bombing radars, furnishes to the computer a signal representing a target approaching at known speed and checks the accuracy of bomb release. *TS-434/UP*, designed for several air-borne and ground radars is an accurate instrument for determining the voltage ratios at various points in a computer and thus checking its performance.

Conclusion

More than 200 different designs of test sets were developed during the war by Bell Laboratories to meet the exacting requirements of radar field maintenance. These differed radically from previous art. Outstanding features were portability, precision, and generality of application. The large number of designs are caused partly by the varied functions of radar and the varied conditions of use. Largely, however, it results from the fact that the frequency band that can be handled in any one set is limited, whereas many frequency ranges and subranges had to be covered in all.

Altogether, more than 75,000 radar test sets were manufactured by Western Electric Company, and these were used in all theaters of war by the United Nations forces. The production rate at the end of the war exceeded 5,000 test sets a month. In numerous cases, moreover, small preproduction quantities of test equipment were built on a "crash" basis for special missions and for training purposes. The test equipment produced for the field had to be more precise than the radar sets, and the equipment used in the factory and the laboratory to test the field test equipment had to be still more precise.

Trends of development at war's end were toward

1. Further broadbanding, simplification, and precising.
2. Coverage of new frequency ranges.

References

1. Ultra-High Frequency Techniques (book), J. G. Brainard, G. Koehler, H. J. Reich, L. F. Woodruff. D. Van Nostrand Company, Inc., New York, N. Y., 1942.

2. Reflex Oscillators, J. R. Pierce. *Proceedings of the Institute of Radio Engineers*, volume 33, February 1945, page 112.

3. The Lighthouse Tube, E. D. McArthur, E. F. Peterson. *Proceedings of National Electronics Conference*, volume I, 1944, page 38.

4. Electromagnetic Waves (book), S. A. Schelkunoff. D. Van Nostrand Company, Inc., New York, N. Y., 1943.

5. The Proportioning of Shielded Circuits, E. I. Green, F. A. Leibe, H. E. Curtis. *Bell System Technical Journal*, volume 15, April 1936, page 248.

6. Resonant Lines in Radio Circuits, F. E. Terman. AIEE Transactions, volume 53, July 1934, pages 1046–53.

7. Ultra-Short-Wave Transmission Phenomena, C. R. Englund, H. T. Crawford, W. W. Mumford. *Bell System Technical Journal*, volume 14, July 1935, page 369.

8. Thermistors in Electronic Circuits, R. R. Batcher. *Electronic Industries*, volume 4, January 1945, page 76.

9. An Impedance Transmission Line Calculator, P. H. Smith. *Electronics*, January 1944.

10. Microwave Transmission (book), J. C. Slater. McGraw-Hill Book Company, New York, N. Y., 1942.

11. Theory of the Electromagnetic Horn, W. L. Barrow, L. J. Chu. *Proceedings of the Institute of Radio Engineers*, volume 27, January 1939, page 51.

12. Attenuation of Electromagnetic Fields in Pipes Smaller Than Critical Size, E. G. Lindner. *Proceedings of the Institute of Radio Engineers*, volume 30, December 1942, page 554.

Motor-Driven Exciters for Turbine Alternators

R. B. BODINE, MEMBER AIEE
S. B. CRARY, FELLOW AIEE
A. W. RANKIN, MEMBER AIEE

THIS PAPER presents a study of the performance of a motor-driven excitation set designed for large turbine alternators connected to modern power systems. This excitation set has been so designed that its performance, both steady state and transient, is essentially comparable with the usual direct-connected (shaft-driven) exciter even when the driving motor is receiving its voltage from the alternator to which the generator is supplying excitation.

A significant trend to the unit type of generating station,[1,2] with each generator connected by its high-voltage transformer to the transmission system, has been evolving during the last 20 years. This trend has been the result of the ability to operate largeinter-connected systems with a high degree of reliability. Important factors in this evolution have been the development of high-speed high-interrupting-capacity circuit breakers, the application of quick relaying, and the experience to analyze and design systems for both normal and abnormal operating conditions. In this type of system, each generating element is a small part of the total capacity, and complete reliance on its operation is not so essential as is the reliable performance of the major transmission system. Transmission line links are required to carry blocks of power of greater magnitude than the output of individual generating units. The system is accordingly able to withstand the loss of any single unit of generation more easily than the loss of important line capacity. An element of generation may be quickly disconnected as a unit because of out-of-step operation or any other trouble. In this way the disturbance is localized and more easily cleared. Serious system disturbances, resulting in load interruptions, usually involve more than one generating element or station and are the result of failure to localize the initial trouble.

For the type of station and system where the loss of an individual generating unit is important to the system reliability, the essential auxiliaries may be driven from a separate supply such as a house alternator. Such an arrangement does not place severe requirements on the motor-driven exciter, if used, and therefore is not considered in this paper. The necessity for this type of station design will decrease in the future for even the larger capacity generating units.

With this trend in station and system design, it is natural that the essential auxiliaries of a generating element should more and more obtain their power from an auxiliary bus connected by a transformer to the alternator terminals. This practice has found considerable favor, with the possible exception of the exciter of the main generating unit. The exciter is one of the most important essential auxiliaries, and since its output is usually increased several times at the time of a system disturbance or low system voltage, it is understandable that direct-connected exciters should continue to be used in-

Paper 46-77, recommended by the AIEE committee on power generation for presentation at the AIEE winter convention, New York, N. Y., January 21–25, 1946. Manuscript submitted November 7, 1945; made available for printing December 17, 1945.

R. B. Bodine and S. B. Crary are with central station engineering division, and A. W. Rankin with turbine engineering division, General Electric Company, Schenectady, N. Y.

The authors wish to acknowledge the suggestions and co-operation of the engineers of the Dayton Power and Light Company and of L. W. Thompson, E. H. Bancker, and J. B. McClure, of General Electric Company.

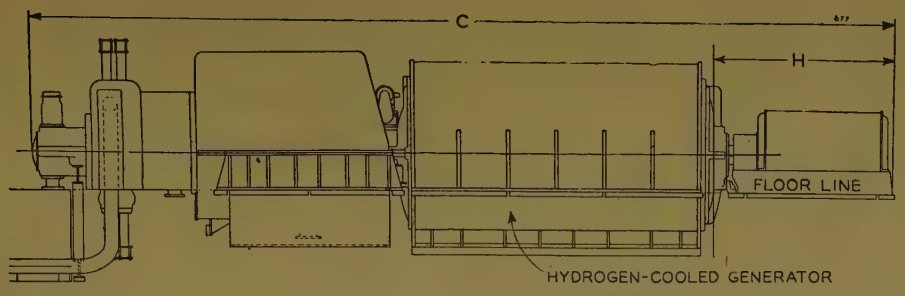


Figure 1. Outline of typical 30,000-kw 3,600-rpm turbine alternator showing comparative over-all dimensions for three types of excitation systems

Excitation system:	C	H
Direct drive, 3,600 rpm	50 ft 4 1/4 in	9 ft 4 in
Gear drive, 1,776 rpm	52 ft 11 7/8 in	11 ft 11 5/8 in
Motor drive	44 ft 2 1/4 in	3 ft 2 in*

Dimensions of motor-driven exciter set:
Length—10 ft 11 in
Width—3 ft 10 1/4 in
Height—4 ft 3/4 in
* Length to end of alternator shaft.

stead of the more flexible separately driven exciters. However, with these modern systems it is now possible, as will be shown in this paper, to design a motor-driven exciter set which will have a reliability comparable with that of the other essential auxiliary drives.

Motor-driven exciters for turbine-alternators have the following, rather self-evident, advantages over the conventional high-speed exciters which are direct-driven from the shaft of the main alternator:

1. A motor-driven excitation set can be of unit construction, and it can be installed in locations less expensive than those required by a direct-driven exciter.

2. The motor-driven exciter can be designed without gearing for a lower and more satisfactory speed for a d-c generator of its rating.

3. The design and construction of the main alternator unit is simplified.[3,4]

In Figure 1 is shown an outline drawing of a typical 30,000-kw turbine-alternator set, and on this are given the over-all lengths when each of the three major types of excitation systems is used: direct-drive, gear-drive, and motor-drive. Note that the over-all length of the turbine-alternator set using the motor-driven exciter is almost nine feet less than the over-all length of the turbine-alternator set using the gear-driven exciter. The principal dimensions of a special motor-driven 1,200-rpm exciter of co-ordinated design for a typical 30,000-kw turbine-alternator are shown in Figure 2.

Reasons for the former poor reputation of motor-driven exciters, and the modern developments which have tended to minimize the importance of these reasons, may be summarized as follows:

1. Before the use of modern switches and relays, the motor-driven exciter connected to the main system was not capable of maintaining the alternator excitation at the high values demanded during loss of synchronism and resulting periods of prolonged low voltage. This requirement, however, largely has been eliminated by better system design and modern apparatus.

2. During a period of low system frequency and consequently low motor speed, motor-driven exciters, when operated under manual control of excitation, are likely to reduce the excitation to a point where generator instability can result. This tendency was increased at such periods by the speed governor's trying to increase the kilowatt load of the alternator. With the use of modern voltage regulators, however, the desirability or necessity for operating under manual control has been eliminated. Also, the frequency change during a system emergency is now generally less as a result of the increased inter-connected system capacity.

Because of the developments outlined in the foregoing, it becomes desirable to re-evaluate the field of application for the motor-driven exciter. To fulfill the requirements of a reliable excitation source, a motor-driven exciter must be designed to meet the following performance specifications. These specifications should be met even with the driving motor receiving its voltage from the alternator to which the generator is supplying excitation so as to conform with the trend toward the simplified unit type of generator station design:

1. Maintain and develop excitation equal to that of a direct-connected exciter for alternator terminal voltages down to 70 per cent of normal for sustained periods.

2. Provide excitation equal to that of a direct-connected exciter through the most severe fault that the alternator itself can withstand without losing synchronism when operating at full rated steam flow.

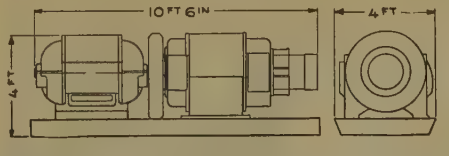


Figure 2. Outline of motor-driven excitation set of co-ordinated design for 30,000-kw turbine alternator

The above requirements, as will be demonstrated, can be obtained by the following three design features:

1. Co-ordinated design of turbine alternator, exciter, and voltage regulator.

2. Induction motor designed with sufficient torque margin to meet the condition of ceiling excitation voltage with 70 per cent alternator terminal voltage (requirement 1 preceding).

3. Sufficient additional flywheel effect for the exciter set so that reasonably rapid excitation can be applied for fault duration and severity which are not quite sufficient to cause loss of synchronism of the turbine alternator at full output (requirement 2 preceding).

Determination of Characteristics

The following is a discussion of the basis for the selection and design of a motor-driven exciter to meet the two previously defined performance requirements, that is, prolonged low system voltage and severe system faults. A motor-driven exciter set for a 30,000-kw turbine alternator built to these general system requirements was furnished the Dayton Power and Light Company. See Figures 3 and 4.

Low System Voltage Requirement

System disturbances may occur in which the system voltage may become comparatively low for relatively prolonged periods of time. A lower system design limit for this condition may be taken as 70 per cent voltage existing for a period of about three minutes.

For a system voltage of this magnitude and duration, difficulty will begin to be experienced with the other essential auxiliaries of the station; the system loads may begin to show a cumulative increase in reactive current requirement because of stalling of induction motors; and the heavily loaded system ties will tend to open because of loss of synchronism. This value of voltage and duration, therefore, seems reasonable as a design value for a motor-driven exciter. Up to these limits the turbine alternator should be capable of making a full contribution to the restoration of normal system conditions in order to prevent and reduce the possibility of such a cumulative breakdown of system interconnection and interruption of system loads. Dif-

ferent limits may, in some cases, be deemed necessary to meet a particular system condition. Operating experience and oscillographic records may indicate that more or less severe limits may be needed as the design values for the set. The important point is that the characteristics of the motor-driven exciter need not be haphazardly selected but can be designed to meet the requirements of the system.

In determining the pullout or maximum torque for which the motor should be designed, the low-voltage condition is the determining factor rather than any of the requirements for transient stability of the alternator. With the motor size determined by the low-voltage condition, a study of the duration and magnitude of this voltage, together with the probable alternator and exciter temperatures at which this condition occurs, must be made in order to obtain an excitation system with the best compromise among size, cost, losses, and pullout power. For instance, an induction motor which must furnish ceiling excitation with 60 per cent voltage at its terminals and with the alternator in the cold (25 degrees centigrade) condition will be about three times as large as one for which it is felt adequate to design for 80 per cent voltage in the hot (125 degrees centigrade) condition, and is about 1.7 times as large as a motor designed for 70 per cent voltage with the alternator and exciter temperatures midway between the hot and cold conditions.

The motor-driven excitation set for the Dayton Power and Light Company was designed for 60 per cent voltage at the motor terminals with the alternator and exciter at 75 degrees centigrade; the thermal capacity of the motor is sufficient to carry this load for isolated intervals of three minutes duration each.

Figure 3. 30,000-kw 3,600-rpm turbine alternator of Dayton Power and Light Company, designed for use with motor-driven exciter of Figure 4

Fault Requirement

The second requirement of being able to supply an excitation equal to that of a standard direct-connected exciter through the most severe fault with a duration corresponding to that which is critical for the turbine generator at full output, requires a consideration of the transient performance of the main unit and of the motor-driven exciter.

In Figure 5 is given the hypothetical system on which transient stability calculations were made to determine the operating performance of an alternator with a motor-driven excitation set. The alternator is connected to an infinite system through a step-up transformer of 10 per cent reactance and a tie-line of 25 per cent reactance. A 3-phase fault through zero impedance is assumed to occur on a stub feeder located immediately on the high side of the alternator transformer. Based on constant flux linkages, the critical switching time for this system is 0.27 second; for the calculations of Appendix I, which include the effect of flux decay, a switching time of 0.25 second is assumed. The induction motor driving the excitation set is supplied through a transformer whose high side is connected directly to the generator terminals.

This time of 0.25 second or 15 cycles for a severe 3-phase fault will be recognized as typical for the critical time of a 3-phase fault for turbine generators. Most modern systems have fault clearing times at least as low as this at and near their important generating stations, particularly when it is important for the maintenance of stability of the generating capacity.

Based on these considerations, the motor-driven exciter designed for the Dayton Power and Light Company was built having the following characteristics:

1. Exciter: 4.0* per unit ceiling exciter voltage at motor synchronous speed; 2.0 per unit (American Standards Association definition) response at motor synchronous speed.

2. Motor: Maximum shaft power with normal voltage equal to 34 per unit.** Slip at maximum power equal to nine per cent.

3. Inertia: Motor, exciter, and flywheel; $H=32$*** ($H\cong 5.0$ based on exciter nameplate kilowatt rating).

A comparison of the performance of this exciter with one of less inertia and pullout power and also with a direct-driven exciter is summarized by Figure 6,



Figure 4. Motor-driven exciter for 30,000-kw turbine alternator of Dayton Power and Light Company of Figure 3

which shows the variation in alternator terminal voltage following the application and clearing of a 3-phase fault. A more complete explanation of the basis for these results, with a more detailed comparison, is given in Appendix I. It will be noted that for the case of a 3-phase high-voltage fault lasting for 0.25 second, a motor-driven exciter of proper design can be as effective as a direct-driven exciter in returning the voltage to normal and preventing loss of alternator synchronism. On the other hand, a motor-driven exciter without adequate motor power or inertia may result in loss of synchronism and, in general, in poorer performance than the conventional direct-driven exciter. This shows the importance of co-ordinating the motor and exciter design with the alternator and system characteristics.



General Design Principles

In order to insure that adequate inertia, pullout, and over-all reliability are built

* Unit exciter voltage is the exciter voltage necessary to provide normal no-load alternator voltage on the air gap line with the alternator field at 75 degrees centigrade.

** Unit field power is the power supplied to the alternator field (75 degrees centigrade) with the alternator at no-load, normal voltage on the air gap line; unit field power is approximately one-sixth of the exciter nameplate rating.

*** The inertia constant, H, is based upon unit power as defined directly above and the total inertia of the entire excitation set.

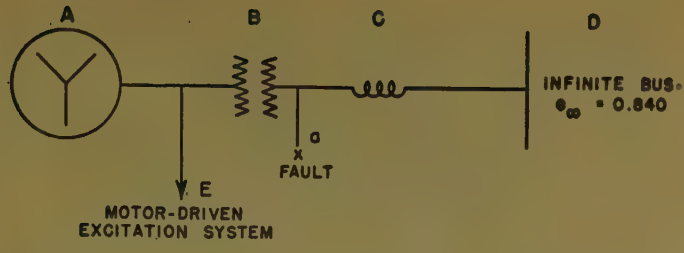


Figure 5A (above). Assumed typical system

A—Alternator
B—Line transformer
C—Line reactance
D—Infinite bus
E—Supply to motor-driven excitation system
a—Stub feed on which fault occurs

Alternator: $x_d=1.25$; $x_q=1.19$; $x'_d=0.13$; $T'_{do}=5.25$ seconds; $H=5.40$ (turbine and generator)
Line transformer: $x=0.10$
Line: $x=0.25$
Fault: 3-phase fault on stub-feeder at *a*; fault cleared in 0.25 seconds

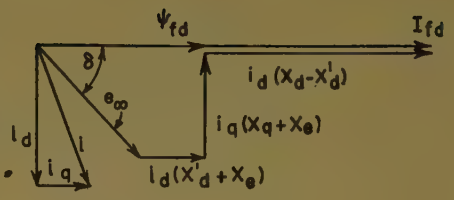


Figure 5B (right). Vector diagram of assumed system. Line and transformer are grouped together in the above diagram as x_e; saturation and resistance are neglected

into the motor-driven excitation set, the following design principles must be taken into consideration:

1. During severe faults, the induced alternator field currents cause the maximum exciter power to reach values of the order of 3.5 times the exciter nameplate rating. Subsequent to the clearing of the fault, the alternator swings coupled with the action of the voltage regulator will cause exciter loads of the order of three times the exciter nameplate rating.

2. The loads discussed in the preceding paragraph must not in any way cause collapse of the exciter voltage, since the primary duty of an exciter during system disturbances is to furnish sufficient excitation voltage to arrest and reverse, as quickly as possible, the flux decay in the alternator caused by the high induced field currents.

3. The exciter must be capable of handling, without failure, the large field currents which are induced during alternator terminal faults. These currents may reach values of the order of 5 times the exciter nameplate rating.

4. During any prolonged low-voltage period, the exciter will go to its ceiling excitation and remain there for the duration of the low voltage. During this period the alternator field current will be determined approximately by the alternator field resistance and the exciter voltage, as the induced field currents will not have a major effect.

5. During low-voltage periods of the type described in the preceding paragraph, the maximum exciter load will occur with the alternator and exciter in the cold (25 degrees centigrade) condition. If the exciter ceiling voltage with a cold exciter is ten per cent greater than the ceiling with a hot exciter, the exciter load with both alternator and exciter in the cold condition is 170 per cent of the exciter load when the alternator (125 degrees centigrade) and exciter are in the hot condition.

6. Transformers and other apparatus between the motor terminals and the alternator lines will cause the motor voltage to be lower than the alternator voltage during system disturbances.

7. During high-voltage transmission system faults for a unit type of generating station, a practical lower limit of the motor voltage will be about 30 per cent. Sufficient inertia must be built into the excitation set to carry it through this fault period without its speed decreasing to values so low as to cause collapse of the exciter voltage.

8. The main exciter and pilot exciter themselves must be designed so that the main exciter voltage will not collapse when the speed drops to the maximum slip for which the excitation set was designed.

9. The motor pullout must be high enough to prevent exciter voltage collapse during any prolonged low-voltage condition. In particular, the motor must be capable of maintaining excitation during low-voltage periods even with the alternator and exciter in the cold condition.

10. The exciter ceiling voltage must be high enough so that even with the maximum motor slip the ceiling voltage is equal to that of a conventional direct-driven exciter. An upper design limit, however, must be placed on the maximum ceiling voltage which occurs with the exciter in the cold condition, since too high a ceiling voltage at this point may produce pullout of the induction motor.

11. In order to provide the maximum reliability of operation, it is necessary to have the alternator under automatic voltage regulator control; otherwise a system disturbance results in reduction of alternator field excitation. Greater reliance can be placed on the voltage regulator when it is provided with a lower limit of excitation which is varied with valve position or steam flow. This was accomplished in the Dayton Power and Light Company's installation by using a new type of direct-acting voltage regulator with a simple type of variable lower limit. See Figure 7 for a schematic diagram of the excitation system and Figure 8 for a photograph of the regulator.

Voltage Regulator

The automatic voltage regulator used in the Dayton Power and Light Company's installation is a sturdy mechanical device consisting essentially of a torque motor and a simple spring-mounted contact system connected to taps on the regulating resistor. The design of the device is as simple mechanically as is consistent with the desired accuracy of regulation. The arrangement of parts is apparent from Figure 8.

The torque-motor, excited from the alternator terminal voltage through suitable transformers, resistors, and rectifiers, operates silver contacts by means of the lever, varying resistance in the exciter field circuit to maintain alternator terminal voltage at the desired value. An equalizing reactor in combination with a current transformer is provided to assure proper division of reactive kilovolt-amperes where two or more similar equipments are used on machines in parallel. A lower limit on excitation which varies with steam flow is obtained by a rheostat attached to the control valve cam shaft. The rheostat, connected in parallel with the regulating resistance of the voltage regulator as shown in Figure 7, determines as a function of steam flow the maximum resistance which can be inserted in the main exciter field circuit. This lower limit is effective for either manual or automatic control of excitation.

This direct-acting voltage regulator provides, in a simple mechanical device:

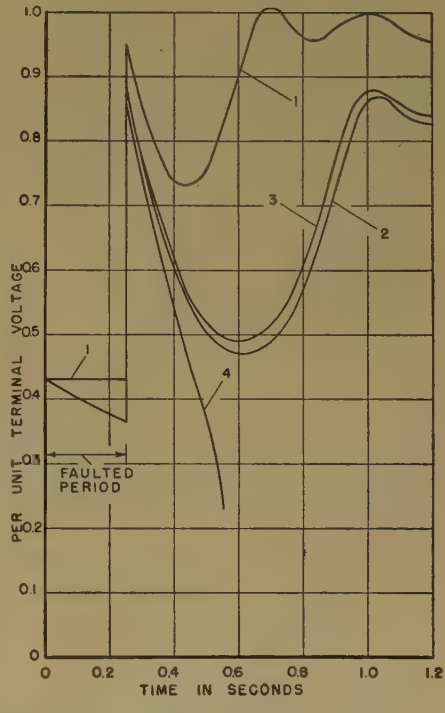
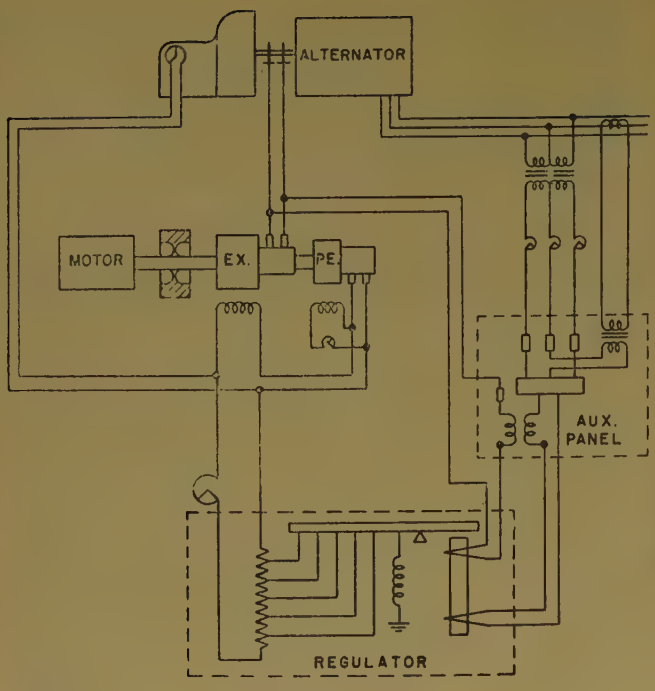


Figure 6. Alternator terminal voltage (see Appendix II)

1—Constant alternator field flux linkages
2—Conventional direct-driven exciter
3—Adequate motor-driven exciter
4—Inadequate motor-driven exciter



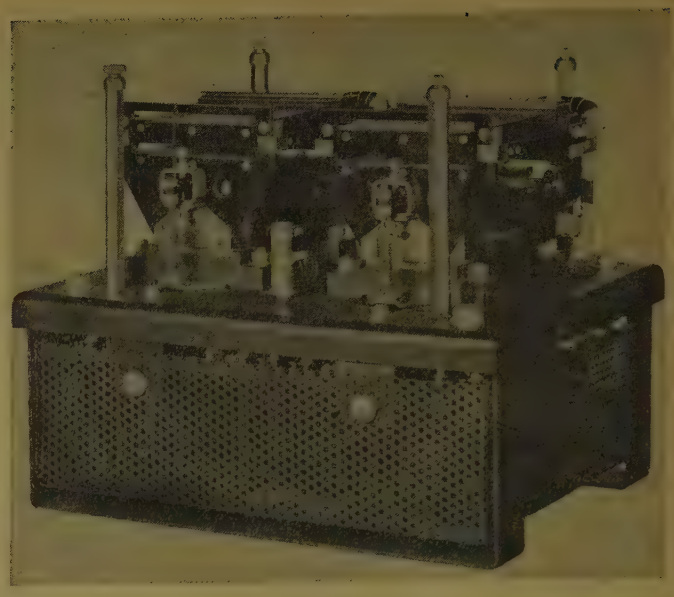


Figure 7 (left). Schematic diagram of connections for motor-driven exciter set and voltage regulator

Figure 8 (above). Direct acting voltage regulator for 30,000-kw turbine alternator of Dayton Power and Light Company

1. A smooth fast-acting accurate voltage control.
2. A lower limit on excitation which is varied with load on the turbine.
3. Proper division of reactive kilovolt-amperes between generators operating in parallel.

Losses

The losses of the competing excitation systems are not of major importance, since their magnitudes are each less than one tenth of one per cent of the total generation, with the motor-driven set being only 0.01 of one per cent of the total generation greater than the direct-driven exciter.

Conclusions

The following conclusions are drawn from the results of the study:

1. A motor-driven exciter of co-ordinated design which meets the reliability requirements of modern systems is entirely competitive and offers several advantages over the direct-connected exciter for the majority of steam stations.

2. This greater field of application results largely from the following developments:

(*a*). Quicker system fault clearing times.

(*b*). High voltage transmission line interconnections.

(*c*). Use of unit type of station arrangement.

(*d*). Development of new and improved automatic voltage regulators with variable lower limits controlled by steam flow.

(*e*). Ability to predict and analyze system requirements during emergency conditions.

3. Systems using modern equipment and design practices can readily take advantage of the possibility of using motor-driven exciters.

4. Because of the inherent advantages of the motor-driven exciter, it is expected more and more to replace direct-connected exciters in the future, particularly for the larger 3,600-rpm units.

References

1. Power Systems for Auxiliary Drives in Steam Electric Stations, J. B. McClure, S. J. Whittlesey. AIEE Transactions, volume 64, 1945, December section, pages 844–51.

2. Electric Drives for Steam-Electric Generating-Station Auxiliaries, W. R. Brownlee, S. A. Elzi. AIEE Transactions, volume 64, 1945, November section, pages 741–5.

3. Progress in Power Apparatus Development, A. C. Monteith. *Edison Electric Institute Bulletin*, June 1945, pages 169–72.

4. Standardization and Design of A-C Turbo-Type Generators, G. A. Juhlin. *The Journal of the Institute of Electrical Engineers*, volume 92, part II, April 1945, pages 147–64.

5. Two-Reaction Theory of Synchronous Machines—Part I, R. H. Park. AIEE Transactions volume 48, 1929, July section, pages 716–27.

Appendix I. Analysis of System Stability

The stability analysis of this paper is based on the representative system shown in Figure 5. Step-by-step calculations on this system were used to determine the comparative transient stability of an alternator excited by a motor-driven exciter.

Saturation effects and resistances (except the alternator field resistance) were not included in this analysis, but the alternator saliency effects were included. Step-by-step calculations were necessary in order to include the effects of alternator swings, field decrements, exciter response, and deceleration of the motor-driven excitation set.

The critical switching time for the system of Figure 5 is 0.27 second when based on constant flux linkages, and for this paper a switching time of 0.25 second was assumed. The assumed switching time is so close to the critical switching time that the flux decrement has a very pronounced effect. A diminution of alternator flux causes the synchronizing torque to decrease considerably and produces an appreciable lengthening of the alternator swings, which in turn imposes a severe load on the exciter for a relatively prolonged period.

Shorter switching times, or a stiffer tie with the infinite bus, or a partial fault instead of the assumed 3-phase fault, will all result in less severe duty on the excitation set. In addition, the resistance present in any actual system will decrease the alternator swings during the fault period, and the saturation present in any actual machine will retard the alternator flux decrement; both of these effects will therefore lessen the duty on the excitation set. It is evident from these considerations that the results given in this paper will err on the conservative side.

Constants

Alternator: $x_d = 1.25$, $x_q = 1.19$, $x'_d = 0.13$, $T'_{do} = 5.25$ seconds, $R_{fd} = 0.513$ ohm at 125 degrees centigrade. The inertia constant (turbine + generator) $= H = 5.40$. With 1.0 voltage, 1.0 current, 1.0 kva, 0.80 power factor at the alternator terminals, the initial angle between the alternator excitation axis and the infinite bus is 48.4 degrees.

Tie line: Line $x = 0.25$, transformer $x = 0.10$, voltage of infinite bus $= 0.84$.

Exciter: Ceiling voltage $= 4.00$ (400 volts) at 1,200 rpm, response $= 2.0$ at 1,200 rpm. The main exciter is separately excited from the compound-wound pilot exciter; the main exciter voltage is assumed to vary as the cube of the exciter speed down to 85 per cent of the synchronous (1,200 rpm) speed,

and is assumed then to collapse completely. (The exciter for the direct-driven set is assumed to have a 3.0 ceiling voltage and a 1.0 response.)

Induction motor: The power-slip curve of the induction motor has a maximum power of 34 per unit at nine per cent slip, with a transformer reactance of three per cent (on a 200-kva base) between the motor and the alternator terminals. Unit motor power is defined as the power supplied to the field of the alternator with the latter at open circuit, normal voltage, on the air gap line. The H constant for the entire excitation set (motor, exciter, and flywheel) is 32 based on unit power to the alternator field.

Fault: The 3-phase fault on the stub feeder is located on the line side of the generator transformer. The fault is cleared in 0.25 second.

Critical switching time: The critical switching time, based on constant flux linkage, for a 3-phase fault as given above is 0.27 second.

Method

The vector diagram of Figure 5B can be obtained for the system of Figure 5A by using the infinite-bus voltage as a reference, and by grouping together the line, transformer, and alternator reactances.

Using the nonreciprocal unit system of Park,[5] the d-axis equations are as follows:

$$\psi_d = I_{fd} - x_d i_d$$
$$\psi_{fd} = I_{fd} - (x_d - x'_d) i_d$$
$$E_{fd} = I_{fd} + T'_{do} p \psi_{fd}$$

From Figure 5B the following are self-evident:

$$\psi'_d = e_\infty \cos\delta + i_d (x'_d + x_e) = \psi_{fd}$$
$$0 = e_\infty \sin\delta - i_q (x_q + x_e)$$
$$P = i_d e_\infty \sin\delta + i_q e_\infty \cos\delta$$

Therefore

$$P = \frac{\psi_d e_\infty \sin\delta}{(x'_q + x_e)} - \frac{(x_q - x'_d) e_\infty^2 \sin 2\delta}{2 (x_q + x_e)(x'_d + x_e)}$$

The above expression for power is also the expression for torque, since alternator speed variations are assumed negligible.

Alternator field current I_{fd}, and alternator terminal voltage e_t, are obtained as follows:

$$\psi_{fd} = \psi_{fd} + (x_d - x'_d) i_d$$

or

$$I_{fd} = e_\infty \cos\delta + (x_d + x_e) i_d$$
$$e_{td} = I_{fd} - 1.25 i_d$$
$$e_{tq} = 1.19 i_q$$

($1.25 = x_d$ of alternator; $1.19 = x_q$ of alternator; $0.35 = x_e$ of external system: transformer plus tie line.)

$$e_t = \sqrt{e_{td}^2 + e_{tq}^2}$$

The decrement of $\psi_d' (= \psi_{fd})$ is obtained from the machine equations:

$$E_{fd} = I_{fd} + T'_{do} p \psi_{fd}$$

$$\Delta\psi_{fd} = \frac{E_{fd} - I_{fd}}{T'_{do}} \Delta t = \Delta\psi'_d$$

The above is the decrement in the alternator field linkages during the interval Δt. The field flux at any time t_n can be obtained by subtracting from the initial value of ψ_{fd} the sum of all the decrements $\Delta\psi_{fd}$ prior to the time t_n.

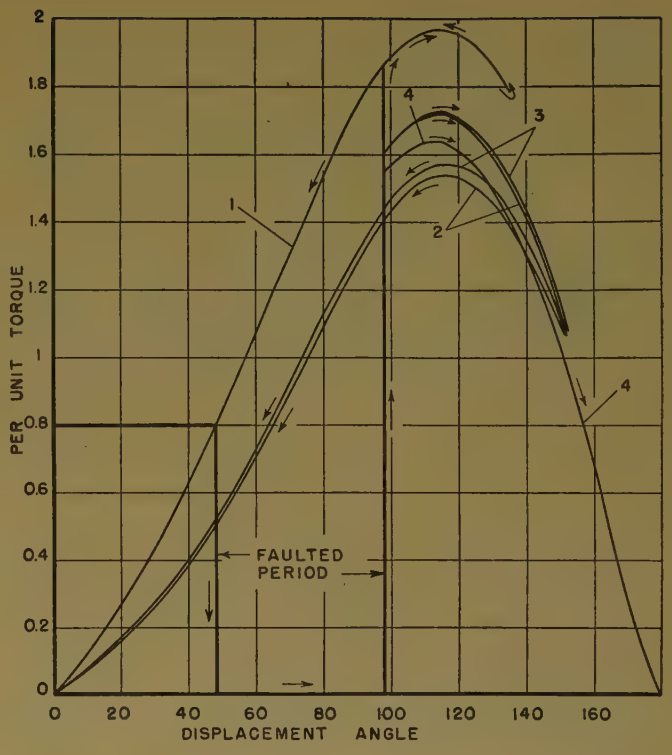


Figure 9. Torque angle curves

1—Constant alternator field flux linkages
2—Conventional direct-driven exciter
3—Adequate motor-driven exciter
4—Inadequate motor-driven exciter

Results

Based upon the analysis given above, the step-by-step calculations in Appendixes III and IV were organized. The transient performance of both the alternator and motor-driven excitation set can be obtained from these tables. The curves given in Figure 6 and Figures 9 to 14, inclusive, show the results obtained for a specific motor-driven excitation set designed for a typical 30,000-kw alternator, as well as for the other cases defined in Appendix II.

Case 1 is the ideal case usually assumed in swing curve calculations and assumes that the exciter response is sufficiently rapid to prevent any flux decrement. For the present study, this assumption is too ideal, and case 1 is of interest only in furnishing a basis for the study of the other cases.

Cases 2 and 3 are direct comparisons of the alternator performance with well-designed direct-driven and motor-driven exciters respectively. As mentioned above, the motor-driven exciter has been designed with a faster response than that of the direct-driven exciter. Figure 9 shows the alternator torque-angle curves—the alternator torque with the motor-driven exciter is always greater than the alternator torque with the direct-driven exciter. Figure 10, which shows the alternator displacement angle, shows that the alternator with the motor-driven exciter swings less than the alternator with the direct-driven exciter. Figure 11 shows that the flux linkages in the alternator excited from the motor-driven exciter are always greater than in the alternator excited from the conventional direct-driven exciter. Figure 12 shows the slip-time curves of the driving motor and shows how adequate inertia will prevent the motor slip from exceeding the slip (15 per cent) at which the exciter voltage will collapse. Figure 6 gives alternator terminal voltage versus time and shows that the

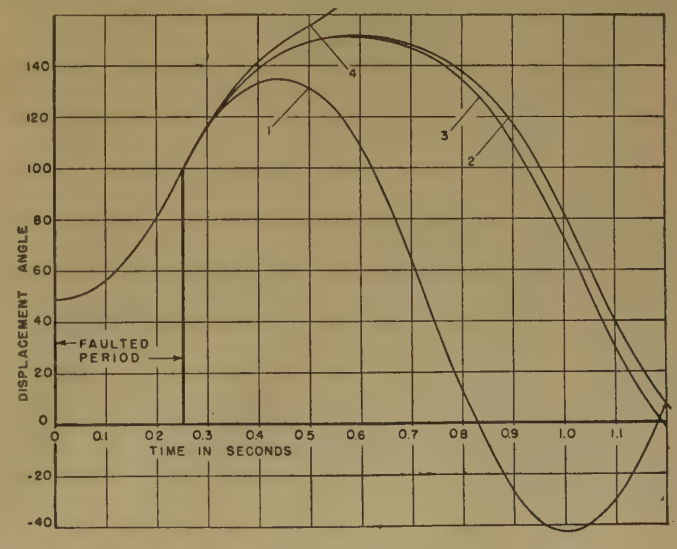


Figure 10. Alternator displacement angle

1—Constant alternator field flux linkages
2—Conventional direct-driven exciter
3—Adequate motor-driven exciter
4—Inadequate motor-driven exciter

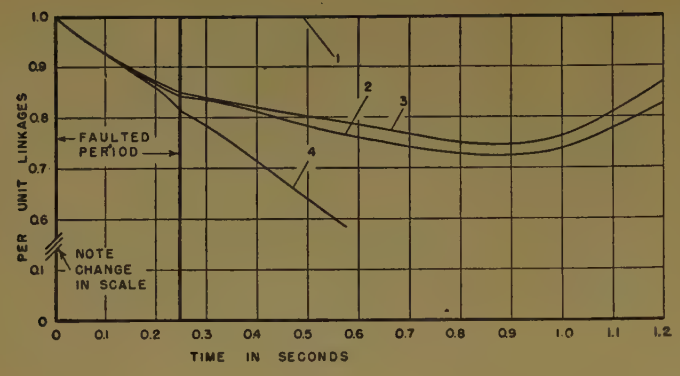


Figure 11. Alternator field flux linkages

1—Constant alternator field flux linkages
2—Conventional direct-driven exciter
3—Adequate motor-driven exciter
4—Inadequate motor-driven exciter

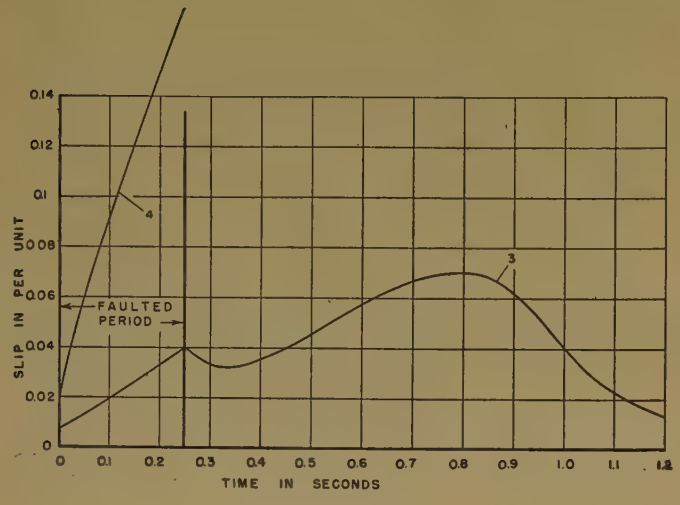


Figure 12. Slip curves

1—Constant alternator field flux linkages
2—Conventional direct-driven exciter
3—Adequate motor-driven exciter
4—Inadequate motor-driven exciter

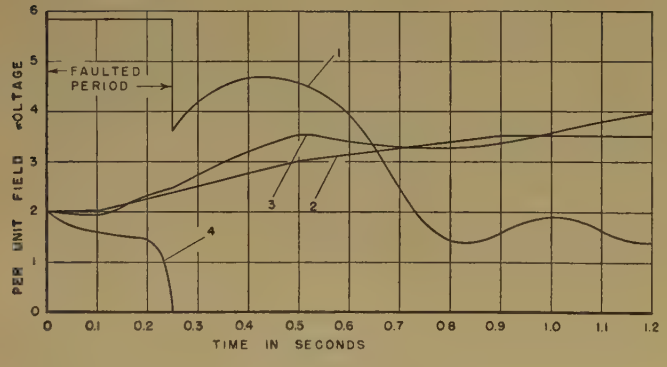


Figure 13. Alternator field voltage

1—Constant alternator field flux linkages
2—Conventional direct-driven exciter
3—Adequate motor-driven exciter
4—Inadequate motor-driven exciter

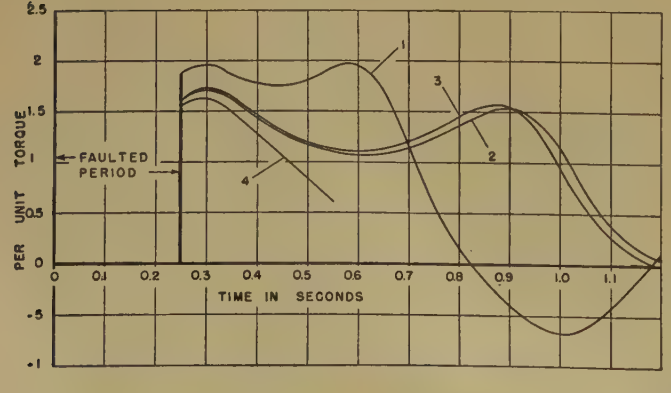


Figure 14. Alternator torque

1—Constant alternator field flux linkages
2—Conventional direct-driven exciter
3—Adequate motor-driven exciter
4—Inadequate motor-driven exciter

motor-driven exciter maintains higher alternator voltage than the direct-driven exciter for the conditions of this comparison. On Figure 13 are shown the exciter voltage curves, and the motor-driven exciter voltage is higher than the direct-driven exciter voltage for almost the entire period. On Figure 14 are shown the alternator torque curves; the motor-driven exciter maintains a higher alternator torque than the direct-driven exciter except around one second when the torque of case 3 becomes lower than that of case 2 because the alternator is swinging back past the initial angle, and the swing with the motor-driven exciter is less than the swing with the direct-driven exciter, thereby indicating a greater stability margin with the motor-driven exciter.

Case 4 is of particular practical interest as it shows the alternator instability which may develop if the motor-driven excitation set is not designed with sufficient inertia and pullout. Figure 10 shows how the alternator displacement angle increases without limit. Figure 12 shows how the driving motor begins to stall, and Figure 6 shows how the alternator voltage decreases toward zero.

These results show that with the quick switching times of modern systems, it is possible to build motor-driven exciters whose performance is comparable with that of the direct-driven exciter.

Appendix II. Comparative Characteristics of Excitation Systems

The comparative transient performance of a turbine-generator excited by various excitation systems is given by the following figures. (Details pertaining to the calculation of the curves of these figures are given in Appendix I.)

Figure 6—Terminal voltage versus time.
Figure 9—Torque-angle curves.
Figure 10—Displacement angle versus time.
Figure 11—Field flux linkages versus time.
Figure 12—Motor slip versus time.
Figure 13—Field voltages versus time.
Figure 14—Torque versus time.

The numbers on the curves of the above figures refer to the various excitation systems and are defined as follows:

1. Constant alternator field flux linkages.

2. Conventional direct-driven exciter (direct-driven from shaft of turbine-generator); 3.0 ceiling; 1.0 response.

3. Motor-driven exciter with adequate inertia and motor power. Exciter: 4.0 ceiling at motor synchronous speed; 2.0 response at motor synchronous speed. Motor: maximum shaft power $(1.0e) = 34$ per unit;* slip at maximum power = 9 per cent; inertia: motor, exciter, and flywheel; $H = 32$.**

4. Motor-driven exciter with inadequate inertia and motor power. Exciter: 3.0 ceiling at motor synchronous speed; 1.0 response at motor synchronous speed. Motor: maximum shaft power $(1.0e) = 12$ per unit;* slip at maximum power = 10 per cent. Inertia: motor and exciter (no flywheel); $H = 6$.**

* Unit field power is the power supplied to the alternator field with the alternator at no-load, normal voltage on the air-gap line; unit field power is approximately one-sixth of the exciter nameplate rating.

** The inertia constant H is based upon unit power as defined directly above, and the total inertia of the entire excitation set.

Appendix III. Alternator Calculation

1.	Time in seconds at center of interval	t	n
2.	Displacement angle from swing sheet	δ	n
3.	d-axis field-winding flux	ψ_{fd}	n
4.	$e_\infty \cos \delta$	$e_\infty \cos \delta$	n
5.	$(x'_d+x_e)i_d=\psi_{fd}-e_\infty \cos \delta$ (3–4)	$(x'_d+x_e)i_d$	n
6.	i_d	i_d	n
7.	$(x_q+x_e)i_q=e_\infty \sin \delta$	$e_\infty \sin \delta$	n
8.	i_q	i_q	n
9.	$i_d e_\infty \sin \delta$ (6×7)	$i_d e_\infty \sin \delta$	n
10.	$i_q e_\infty \cos \delta$ (8×4)	$i_d e_\infty \cos \delta$	n
11.	$i_d e_\infty \sin \delta+i_q e_\infty \cos \delta=T$	T	n
12.	$(x_d+x_e)i_d$	$(x_d+x_e)i_d$	n
13.	$e_\infty \cos \delta$	$e_\infty \cos \delta$	n
14.	$I_{fd}=(x_d+x_e)i_d+e_\infty \cos \delta$(12+13)	I_{fd}	n
15.	E_{fd} from g of Appendix IV	E_{fd}	n
16.	$T'_{do}p\psi_{fd}=E_{fd}-I_{fd}$(15–14)	$E_{fd}-I_{fd}$	n
17.	$\frac{E_{fd}-I_{fd}}{T'_{do}}=\frac{\Delta\psi_{fd}}{\Delta t}$	$\frac{\Delta\psi_{fd}}{\Delta t}$	n
18.	$\frac{\Delta\psi_{fd}}{\Delta t}\times\Delta t$ with $\Delta t=0.05$ second. ($\Delta t=0.025$ second for discontinuous points)	$\Delta\psi_{fd}$	n
19.	ψ_{fd} of preceding interval and $\Delta\psi_{fd}$	ψ_{fd}	$n+1/2$
20.	Time at end of interval	t	$n+1/2$
21a.	I_{fd} (14)	I_{fd}	n
21b.	$x_d i_d$	$x_d i_d$	n
21c.	$e_{td}=I_{fd}-x_d i_d$ (21a–21b)	e_{td}	n
22.	$e_{tq}=x_q i_q$	e_{tq}	n
23.	$e_t=\sqrt{e^2_{td}+e^2_{tq}}$	e_t	n

Appendix IV. Induction Motor Calculation

(a).	Time in seconds at center of interval	t	n
(b).	e_t from 23 of Appendix III	e_t	n
(c).	Slip at time t	s	n
(d).	kw_m=input to induction motor=Pe_t^2. (P at slip s is obtained from power slip curve)	kw_m	n
(e).	Exciter response for zero slip	$\Delta E_{fd}(s=0)$	n
(f).	Exciter voltage for zero slip $E_{fd}(s=0)$ of preceding interval plus $\Delta E_{fd}(s=0)$	$E_{fd}(s=0)$	n
(g).	Actual exciter voltage=$(1-s)^3 E_{fd}(s=0)$	E_{fd}	n
(h).	I_{fd} from 14 of Appendix III	I_{fd}	n
(i).	Kilowatts delivered to alternator field=$E_{fd}\times I_{fd}$	kw_g	n
(j).	$kw_m-kw_g(d-i)$	Δkw	n
(k).	Δkw of $j\times\Delta t$ with $\Delta t=0.05$ second ($\Delta t=0.025$ second for discontinuous points)	Δkw seconds	n
(l).	kw seconds of preceding interval plus Δkw seconds	kw seconds	$n+1/2$
(m).	$\sqrt{\frac{kw \text{ sec of } 1}{H \text{ of excitation system}}}$=speed	δ	$n+1/2$
(n).	Slip at end of interval=$1-s$	s	$n+1/2$
(o).	Time at end of interval	t	$n+1/2$

Arcing Ground Tests on a Normally Ungrounded 13-Kv 3-Phase Bus

J. E. ALLEN
MEMBER AIEE

S. K. WALDORF
MEMBER AIEE

THE BUSSES and connected equipment in electric power stations sometimes are operated ungrounded. When a single insulation fault to ground occurs on a system of this type, the fault current is relatively small, the arc damage usually slight, and the faulted equipment in nearly all cases can be removed from service without relay action or service disturbance of any kind. However, in April 1942, faults developed simultaneously at two points 300 feet apart on the ungrounded 60-cycle 13.2-kv bus in the Holtwood station of the Pennsylvania Water and Power Company. This trouble resulted in severe arcing and damage to the bus structure before the faults were isolated.

It is unlikely that two insulators at a distance from each other would fail simultaneously without some electrical disturbance initiated by the failure of one causing the failure of the other. Numerous studies of ungrounded electric systems have been published which show that overvoltages as high as six to eight times normal theoretically can occur when a ground fault produces an arc.[1,2,3,7] This paper describes an experimental determination of the magnitude of overvoltages produced by several types of arcing grounds on the Holtwood bus, and complementary tests and analyses to determine the nature of the phenomena responsible for the insulation failures and the forced outage. The investigation differed from those previously described in technical literature in that experimental work was done with actual high voltage arcs to ground on a 13-kv station bus rather than on a high-voltage transmission line or a low-voltage theoretically equivalent circuit.

Because the work reported here was done only with arcing grounds on a 13-kv normally ungrounded station bus, conclusions are limited to only this class of service and do not include high-voltage transmission line phenomena or effects of switching surges.

Scope of Investigation

The investigation involved the following steps:

1. As an introduction to arcing ground phenomena on a 3-phase bus, a study was made of the electrical vector relationships involved.

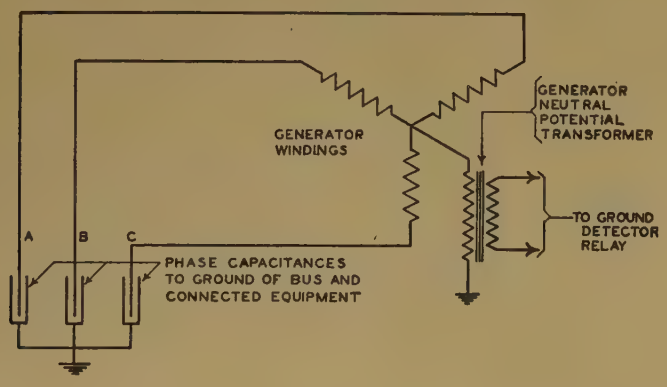


Figure 1. Simplified equivalent circuit of Holtwood 60-cycle bus

2. A study of the high-frequency characteristics of the bus and connected equipment was made to determine whether standing waves could have contributed to the generation of very high voltages on the Holtwood bus.

3. The characteristics of arcs under simulated arcing ground conditions were studied on a laboratory scale. Arc gaps were developed which had, as nearly as practicable, the characteristics theoretically required for the production of high voltages by arcing grounds.

4. Arcing grounds at high voltages were placed on the Holtwood bus under progressively more severe conditions, to determine if high overvoltages could be produced by any arcing ground condition likely to occur in service.

5. An analysis was made to determine whether the neutral voltage fault detecting method installed on the Holtwood bus can warn of impaired insulation to ground before the insulation is completely broken down. The analysis is included as an appendix to this paper. Curves were developed which can be used to determine easily the sensitivity of this type of detector to reduced insulation resistance in any similar installation.

The Vector Relationships on an Ungrounded 3-Phase Bus

An ungrounded bus system has distributed capacitances between each phase conductor and ground whose charges supply the current through a ground fault. When examining the vector relationships of the voltages and currents involved, the phase-to-ground capacitances can be considered as three equal lumped constants connected as shown in Figure 1.

In normal operation, the capacitances have the phase-to-neutral voltages E_{OA}, $E_O{}^b$, and E_{OC}, shown in Figure 2A, impressed upon them. The simplest type

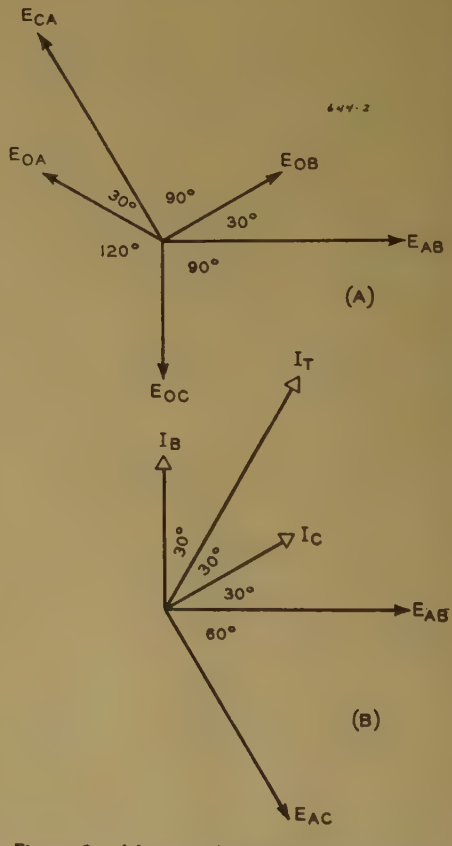


Figure 2. Vector relationships on a 3-phase bus.

A—Voltage vectors

B—Voltage and charging current vectors with A-phase grounded

Paper 46-44, recommended by the AIEE committees on protective devices and power transmission and distribution for presentation at the AIEE winter convention, New York, N. Y., January 21–25, 1946. Manuscript submitted November 21, 1945; made available for printing December 20, 1945.

J. E. ALLEN is chief of tests and S. K. WALDORF is senior test engineer, Pennsylvania Water and Power Company, Baltimore, Md.

of ground fault to examine is a solid connection through an ammeter connected as indicated in Figure 3. With the solid ground, the phase A capacitance is short-circuited, the voltage on phase B capacitance becomes $E_A{}^b$ and that on phase C capacitance becomes E_{AC}, shown in Figure 2B. The power voltage to ground on the unfaulted phase capacitances

Table I. Frequencies at Which Resonance Phenomena Appear on Representative 60-Cycle Units in Holtwood Station

Unit	Rating	Resonant Frequencies, Kc
No. 15 transformer	3 phase, 13.2 to 73 kv with taps, 33,750 kva	16, 18, 46, 55, 60
No. 12 transformer	3 phase, 13.2 to 73 kv with taps, 20,000 kva	15.5, 21.5, 26
No. 10 waterwheel generator	3 phase, 13.2 kv, 94.7 rpm, 15,000 kva	1.6, 10
No. 15 steam turbine generator	3 phase, 13.2 kv, 1,800 rpm, 12,500 kva	3.8, 33, 62
No. 62 frequency changer	3 phase, 60-cycle, 13.2 kv, 300 rpm, 7,140 kva	4.2, 21.2, 50

thus becomes phase-to-phase voltage or 1.73 times the normal phase-to-neutral voltage.

When one conductor is grounded, the neutrals of Y-connected equipment on the bus are no longer at ground potential. In the case considered, the voltage between the equipment neutrals and ground becomes E_{OA}. By the connection of generator neutral potential transformers as shown in Figure 1, the appearance of a neutral voltage to ground is used at Holtwood to detect the presence of a ground fault. In the majority of cases, the operation of the ground detector relay is the only indication to the station operator that something is wrong, because the equipment continues to function otherwise in a normal manner. The characteristics of this type of fault detector are analyzed in Appendix II.

If insulation should fail on phase A, it probably will occur when E_{OA} is at or near its peak value. Phase A capacitance will be short-circuited, its charge sending a surge through the fault. The voltages on the two unfaulted phase capacitances suddenly change from the respective phase-to-neutral values to the higher phase-to-phase values. These capacitances are charged through the fault by the higher voltages. The magnitude of the surge through the fault depends upon the system operating voltage and the value of the phase capacitances. It is therefore important, when investigating arcing grounds, to know the system voltage, which can be measured directly, and the phase-to-ground capacitances or capacitive reactances. A method for measuring the latter is given in Appendix I.

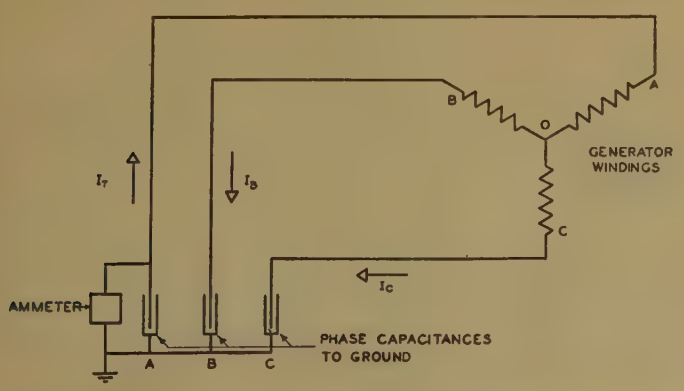
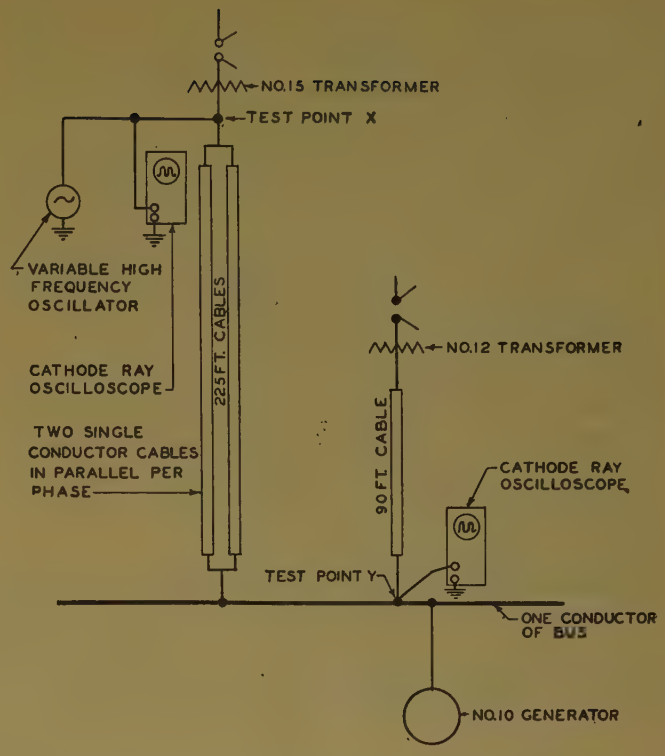


Figure 3. Circuit conditions when A-phase bus conductor is grounded through an ammeter

Figure 4. Connections for high-frequency measurements on bus

Distance between test points X and Y is about 300 circuit feet



Standing Wave Characteristics of Operating Equipment

A station bus and its connected equipment do not have concentrated capacitances to ground as shown in the simplified equivalent circuit of Figure 1. Each element of bus and equipment has its inherent distributed capacitance and inductance with consequent characteristic frequencies at which resonance phenomena can occur. With the individual components of the system connected in parallel for operation, there are a number of such resonance frequencies at which oscillations might be initiated by an arcing ground. The phenomena are of interest because standing waves at the resonance frequencies can cause uneven distribution of voltage to ground along the bus system. A study of standing waves on such a system gives some insight into the way in which wave phenomena can cause overvoltages.

Standing waves on the Holtwood bus were investigated by observing changes of impedance of each type of equipment, singly and in combination, as the frequency of a voltage applied between one phase conductor and ground was varied between 100 and 100,000 cycles per second. Except for the high-frequency voltage, the equipment was not energized. The work was done expeditiously by utilizing a chart-drawing transmission line fault locator.[11] The fault locator charts were obtained quickly and on them the resonance frequencies were at once apparent.

The frequency characteristic of one unit of each type of 60-cycle equipment normally connected to the Holtwood bus was measured. The resonance frequencies and equipment ratings are indicated in Table I. The bus structure used in the tests apparently has no effect in the frequency range covered.

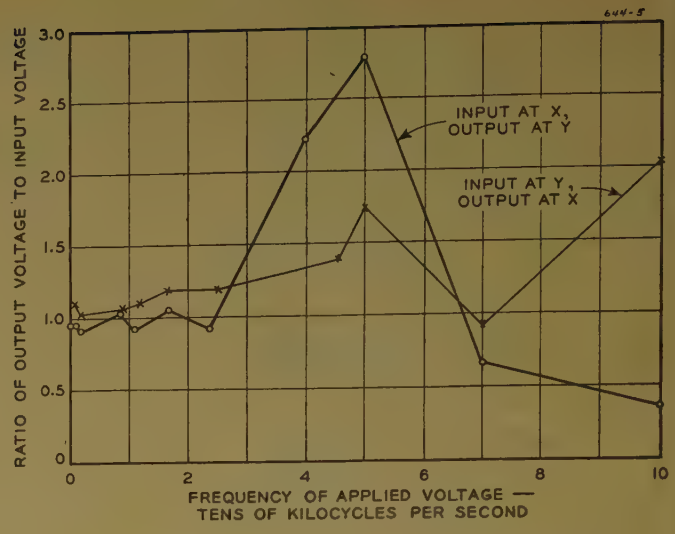
More directly bearing on a study of overvoltage production is the behavior of a combination of station operating units when a voltage of varying frequency is applied. The combination of equipment shown in Figure 4 was connected and energized only by the variable frequency oscillator connected in turn at test points *X* and *Y*. *X* and *Y* were chosen as test locations because it was at these points, separated by about 300 feet of lead covered cable, that the faults occurred causing the disturbance of April 1942.

The two cathode ray oscilloscopes were used as voltmeters, one at the oscillator and the other at the other test point. The ratio of the instrument indications was a measure of the voltage rise due to standing waves.

Figure 5 shows that voltage multiplication up to $2^3/_4$ times was measured with the test arrangement. The resonance frequencies for the combination were those of the connected individual units. It should be noted that the maximum voltage multiplication within the measurement range occurs at the relatively high frequencies of 50,000 and 100,000 cycles per second. These tests indicate that no voltage higher than three times normal is to be expected from standing waves at any natural frequency of the system, a point substantiated by the arcing tests described later.

Figure 5. Voltage multiplication in test circuit of preceding figure

X and *Y* are test locations indicated in Figure 4



Characteristics of Arc Gaps

The ways in which overvoltages can be developed on an ungrounded system have been described in great detail in the technical literature. A few of the many papers on the subject are listed in the references of this paper. Simply stated, overvoltages can be built up by an arcing ground if the arc is made to restrike each half cycle at progressively higher voltages. If this restriking can be made to occur at the natural period of the system, the resulting voltages theoretically will be higher than if the restriking phenomenon occurs at power frequency.[1]

Before the arcing tests on the Holtwood bus were undertaken, it was necessary to study the characteristics of various types of arc gaps and to develop one having as nearly as possible the behavior which theory indicates should produce high overvoltages. While making the development, highly artificial methods were avoided such as are employed in high speed circuit breaker practice to obtain progressively higher dielectric strength in the arc gap at each restrike, because such conditions are unlikely to occur in the field.

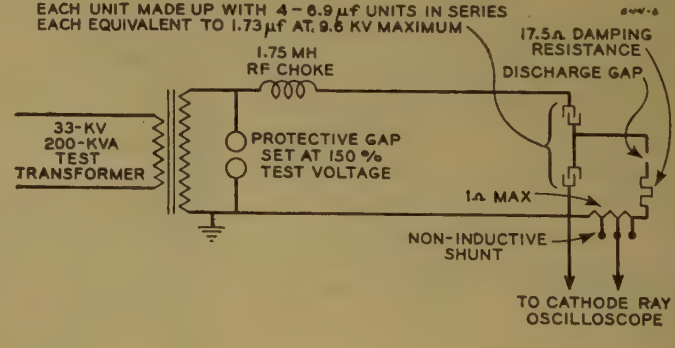
Three-phase equipment was not available for the developmental work to supply the same arc voltage and current as would be produced in the field. However, conditions were approximated quite well with the single phase circuit shown in Figure 6. The maximum voltage that could be used was limited to 9.6 kv by the rating of the capacitors, as compared to 13.2 kv on the tested bus. The breakdown of the tested gaps during the developmental period could not exceed $^1/_2$ of 9.6 kv = 4.8 kv because of the capacitor limitation. This compares with 13.2/1.73 = 7.6 kv, the voltage initially across any fault that might develop on the actual bus.

In the circuit of Figure 6, two other elements for the protection of equipment were added besides the protective gap. The 17.5-ohm resistor in series with the arc gap was included to damp out high frequency oscillations which overheated conductors in the early stages of the work. The choke coil was placed to keep stray high frequency currents from the transformer. The noninductive shunt of straight carbon rod provided the voltage drop for making the wave form of the arc current appear on the oscilloscope. Besides being used for the gap development, the circuit of Figure 6 was used to ensure that the instrument transformers used in the field tests correctly reproduced wave forms within the frequency capabilities of the oscilloscopes and oscillograph used.

The first type of gap studied was a simple air gap of the form shown in Figure 7. It was tested in the circuit of Figure 6 where it exhibited a restriking characteristic. Each half cycle the voltage on the gap rose and then dropped abruptly as the gap broke down. The wave form of the arc current also showed that the arc was out for an appreciable fraction of each half-cycle.

The initial breakdown of the gap was always at a voltage higher than subsequent breakdowns, a characteristic common to all open, fixed-length arcs in still air, and which is unfavorable for overvoltage production. A strong blast of

Figure 6. Arrangement for preliminary tests of discharge gaps, oscillograph shunt, and instrument transformers used in the arcing ground tests



air blown across the gap maintained the breakdown at its high initial value and also caused several restrikes each half cycle. Since this artificial condition is not normal in the field, the air blast was not used for any bus tests.

The next type of gap tested is shown in Figure 8 and consists of a porcelain enclosed and filled gap designed to produce in a controlled way an arcing breakdown similar to that occurring when a porcelain insulator fails. The large electrodes, 1-inch diameter, were used to simulate the large metal cap and pin of an insulator which do not overheat quickly when an arc is formed. The length of this enclosed gap was set by trial to give the desired breakdown value with the gap space filled with porcelain granules. While this adjustment was being made, a high resistance was connected in series with the gap to limit the current to a small value. When the gap was placed in the test circuit of Figure 6, the arc was erratic, sometimes restriking a number of times each half-cycle. After a few cycles the porcelain granules fused and the gap practically short-circuited. The number of cycles that the arc persisted depended upon the power liberated in the arc. This gap, like the simple open gap, did not restrike at progressively higher voltages but acted more as a voltage limiter.

A third type of gap which was thought to produce more severe test conditions was constructed by converting the simple gap of Figure 7 into a self-lengthening gap. One of the cap screw electrodes was drilled axially to hold a small fusible electrode, a number 22 gauge wire. The position of the wire was adjusted with respect to the undrilled electrode, and held fast with a set screw, to give any desired initial breakdown. After an arc formed on the self-lengthening gap, the burning of the wire during each half-cycle of power current increased the length of the arc gap, permitting the restrike voltage to rise progressively. Figure 9 shows the appearance of the self-lengthening gap, before and after a test. As described later, this type of gap produced higher voltages than the fixed length gaps when used for arcing grounds on the Holtwood bus, but still the voltages were not nearly as high as published theory indicates.

The final design of gap, which produced the most severe arcing conditions in the bus tests, was an enclosed self-lengthening gap obtained by modifying the enclosed gap of Figure 8. The porcelain tube having 1-inch inside diameter was replaced with one having 3/16-inch bore. Iron electrodes were gasket-sealed into this tube. The air gap was made self-lengthening by providing one of the iron electrodes with a projecting small copper wire to be burned away by the arc. The small sealed space occupied by the arc and the progressive arc lengthening were especially favorable to overvoltage production.

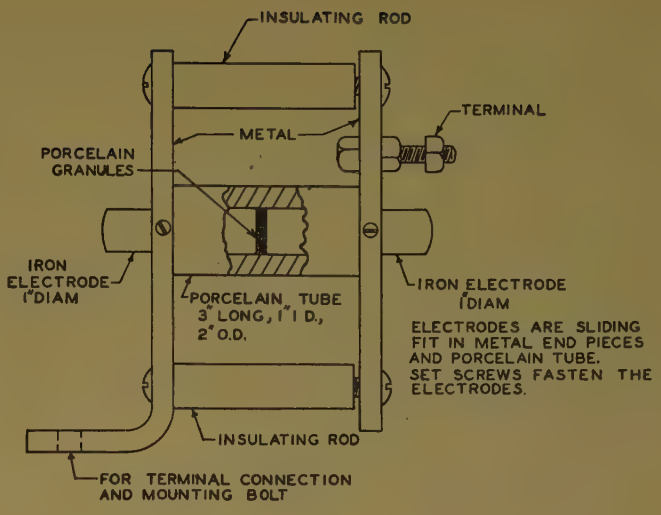


Figure 8. Porcelain enclosed and filled arc gap

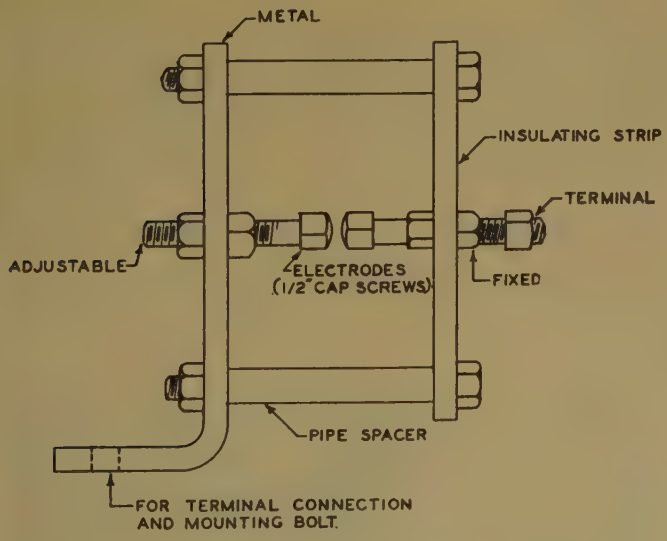


Figure 7. Open arc gap

Method of Making Arcing Ground Tests on the Station Bus

The station equipment which was used for the high frequency measurements was also used for the high voltage arcing ground tests. Due to system operating conditions, number 9 generator was substituted for number 10 generator in the latter tests; the two machines are essentially duplicates. Figure 10 gives the connections for the arcing ground tests. This test arrangement produced a charging current of 2.5 amperes through a solid ground as compared to a current of about 9.1 amperes produced by the entire bus system used in normal operation. The capacitive reactance to ground of one phase conductor of the test arrangement was thus about $9.1/2.5 \times 2{,}500 = 9{,}100$ ohms as compared to 2,500 ohms for operating conditions.

The section of the bus indicated in Figure 10 was that on which occurred one of the faults of April 1942 and power transformer $T1$ was number 15 transformer where the other fault occurred. The fuse and gaps shown in the arc gap circuit of Figure 10 were included as safety precautions. Another safety measure was the insulating transformer between the oscillograph and the arc gap circuit. It was especially developed for the work, tested and modified until it had insulation adequate to protect the oscillograph operator against mishaps and it reproduced complex wave forms faithfully on the oscillograph.

The klydonograph, a photographic surge crest voltage recorder producing Lichtenberg figures, was connected to the bus through a 3-pole capacitive poten-

tiometer. The klydonograph–potentiometer combination was calibrated as a unit with 60-cycle voltage.

The test potential transformers *PT*1 and *PT*2 had a rating of 34.5 kv, 4½ times the normal bus voltage to ground, to ensure the proper recording of any power frequency overvoltages. The klydonograph was relied upon to record any high frequency or surge overvoltages beyond the range of the magnetic oscillograph. The potential transformers *PT*3 and *PT*4, measuring the generator neutral-to-ground voltage and the phase *A*-to-phase *B* voltage, respectively, were regularly used station equipment.

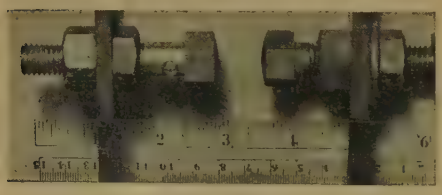
Because more station equipment is normally connected to the bus than was the case during the tests, one of the tests was performed with a 3-phase Y-connected neutral-grounded bank of capacitors connected to the bus at test location *Y*. Each of the three legs of the bank had a nominal rating of 7.2 kv, 2.3 microfarads. This capacitance, with the capacitance to ground of 0.29 microfarad per phase of the station equipment, gave a phase-to-ground capacitance of around 2.6 microfarads for the test. This value is more than twice as much as the 1.06 microfarad of the equipment normally connected.

Arcing Test Procedure

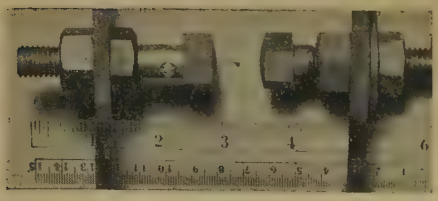
Preliminary to each test, the arc gap for the test was adjusted and tested in a laboratory low-current circuit to have the desired initial breakdown value.

After the equipment was connected for a test as shown in Figure 10, the disconnecting switch in the arc gap circuit was left open and the generator voltage was then set at the chosen test value. Following this, the generator was left running at normal speed without field excitation. The disconnecting switch was then closed, connecting the arc gap circuit to the phase *A* conductor. The gap in each case was previously adjusted to 90 per cent of the preset generator phase-to-neutral voltage.

When the recording instruments were ready, the field switch of the generator was closed. This operation, in addition to exciting the generator field, also lit a small lamp, signaling the oscillograph operator to start that instrument. The generator required about 2 or 3 seconds to attain its preset voltage. When the arc gap flashed over, the voltmeter shown in Figure 10 connected to the generator neutral potential transformer, deflected. When making tests with the fixed length gaps, this was a signal to the generator operator to open the generator field breaker to extinguish the arc. When using the self-lengthening gaps, the operator delayed opening the field breaker for a few seconds after the neutral voltmeter first deflected to allow time for the arc to extinguish itself by lengthening the gap. This method of circuit control was used to ensure that any overvoltage produced during a test was due to the arcing ground alone and not due to any switching surges.



A—Before test



B—After test

Figure 9. High-speed self-lengthening arc gap

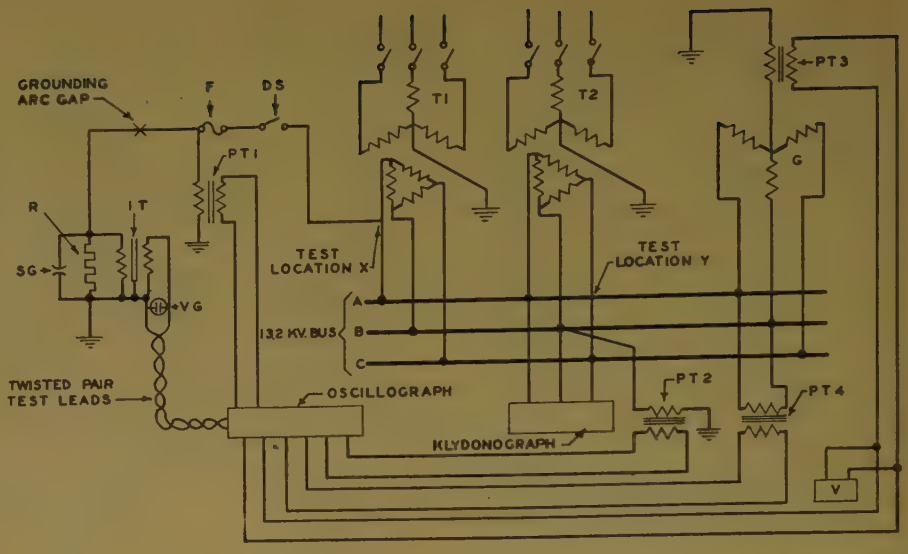


Figure 10. Connections for arcing ground tests on Holtwood 60-cycle bus

SG = 1/32-inch spill gap
R = 0.3-ohm rod resistor
IT = insulating transformer
VG = safety vacuum gap
PT1, PT2 = 34,500- to 115-volt instrument transformers
PT3, PT4 = 13,200- to 110-volt instrument transformers
F = 15,000-volt 100-ampere fuse
DS = disconnect switch
T1, T2 = power transformers
G = water wheel generator
V = generator neutral voltmeter

Results of Arcing Tests With Fixed Length Gaps

Because of the widespread belief that an arcing ground quite easily will produce dangerously high overvoltages on an ungrounded bus system, the tests on the Holtwood bus were begun with reduced bus voltage and a simple open fixed-length gap. As shown in Table II, test 1, very high voltages were not produced. The maximum did not exceed 2.3 times normal. The bus voltage was then raised in two steps to its rated value, but still the voltage to ground on the unfaulted phases was little more than can be predicted from the 3-phase power voltage relationship (Table II, tests 2, 3, and 6). The oscillogram from test 1, Table II, when the test voltage was only 50 per cent of the normal operating value, showed that the arc restruck regularly each half-cycle at almost the initial breakdown value. The oscillograms from tests 3 and 6, Table II, when the test voltage was the full operating value, showed that the arc always restruck at a voltage substantially less than the initial breakdown value. The change in the restriking phenomenon with increase of test voltage was probably due to the greater arc energy in the latter tests making the gap more difficult to deionize.

Tests 4 and 5 with the porcelain filled gap showed that an arcing ground produced by the failure of a porcelain insulator is not likely to produce high transient overvoltages. The oscillograms

Table II. Voltages Produced by Arcing Grounds With Fixed Length Gaps

Test	Generator Voltage Setting (Per Cent Normal)	Gap Type	Maximum Phase-to-Ground Voltages (Per Cent Phase-to-Neutral Voltage) From Oscillograph B Phase	From Klydonograph B Phase	From Klydonograph C Phase	Total Duration of Arcing, Sec
1	50	Open	212	226	177	1.5
2	75	Open	186	190	176	1.2
3	100	Open	183	180	150	1.43
4	75	Porcelain filled	187	156	145	0.01−
5	100	Porcelain filled	200	233	168	0.01−
6*	100	Open	192	190	190	1.42

*20 ohms on secondary of neutral potential transformer.

Arc was extinguished in these tests by opening generator field circuit.

Table III. Voltages Produced by Arcing Grounds With Self-Lengthening Gaps

Test	Generator Voltage Setting (Per Cent Normal)	Gap Type	Wire in Fusible Electrode	Maximum Phase-to-Ground Voltages (Per Cent Phase-to-Neutral Voltage) From Oscillograph B Phase	From Klydonograph B Phase	From Klydonograph C Phase	Total Duration of Arc, Sec
1	50	Open	No. 22 Nichrome	227	224	268	0.8+
2	50	Open	No. 22 copper	232	209	145	2.25
3	50	Enclosed	No. 22 copper	282	220	189	1.05
4	50	Enclosed	No. 30 copper	279	232	212	0.08
5*	40	Open	No. 22 copper	301	280	256	0.11

*2.3-microfarad capacitor added between each phase conductor and ground.

Arc extinguished itself in these tests, because of elongation of gap, before the generator field circuit was opened.

showed that the voltage across the gap was very low after the initial strike.

For each of the tests in this group, the fixed length of the gap acted as a limiter to prevent the recovery voltage across the gap from rising above the initial breakdown value. Consequently, the voltages from the unfaulted phases to ground did not much exceed 1.73 times the normal phase-to-neutral voltage in any of these tests.

Results of Arcing Tests With Self-Lengthening Gaps

After showing that high overvoltages do not accompany arcing grounds on gaps having fixed length, due to the limiting effect of the gap on the recovery voltage, further testing was done with self-lengthening gaps. The results of these latter tests are given in Table III.

Nichrome wire, size 22, was used in the first test of this group to ensure that the arc would persist long enough for overvoltage to build up, if there were any such tendency present. No very high overvoltage developed. The second test, using faster fusing copper wire, gave about the same value of overvoltage as the first test, with a total arcing time of about $2\frac{1}{4}$ seconds. Both tests were made with open gaps.

Tests 3 and 4, where the enclosed self-lengthening gap was used, showed higher overvoltages than the preceding tests, but not more than about 2.8 times normal phase-to-neutral voltage. The type of gap used for this test probably produced as severe an arcing condition as is likely to occur on the station bus under operating conditions. Most likely, an arcing ground on the bus will be formed across a gap having fixed length, where the voltage to ground will not rise much above two times normal due to the limiting action of the gap.

Figure 11 is the oscillogram obtained during test 4 of Table III for which an enclosed self-lengthening gap was used. The oscillogram shows that the arcing ground persisted for only a fraction of each cycle of power frequency, but that each strike produced a highly damped train of oscillations having a frequency of about 1,140 cycles per second. Table I shows that the lowest natural frequency for any equipment on the unenergized bus is 1,600 cycles per second, which is for the waterwheel generator with no field excitation. It is probable that the lower natural frequency obtained under arcing conditions is due to generator field excitation, which changes the inductance of the generator windings.

In test 4 the arc struck only 11 times because of the small size (number 30) of the fusible electrode used in the gap; the behavior is typical except that the arc struck more frequently during the other tests of this group.

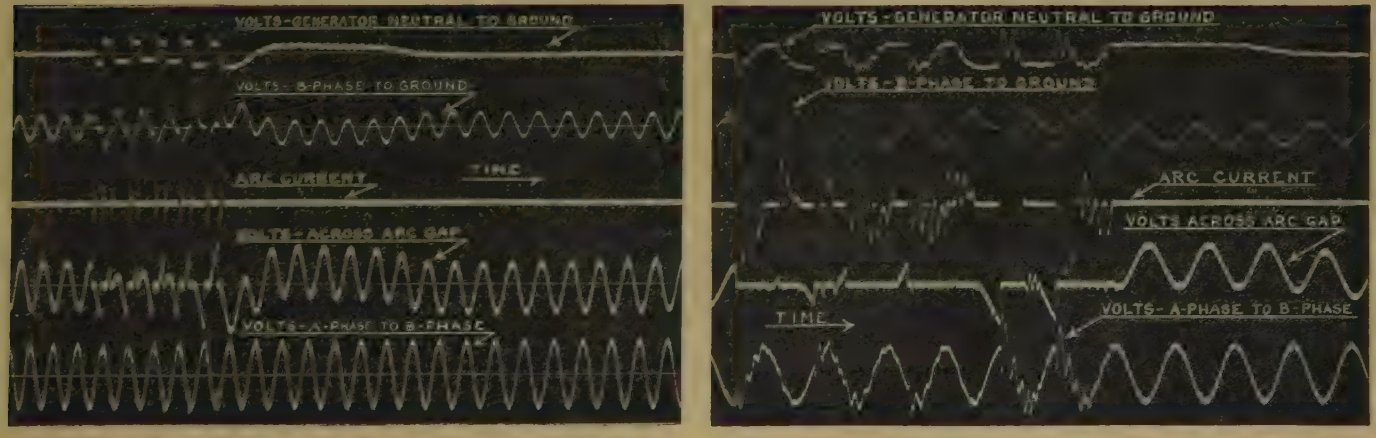
The highest instantaneous value of

Figure 11. Oscillogram from test with enclosed self-lengthening gap

Test 4, Table III

Figure 12. Test with capacitors connected to bus

Oscillogram from test 5, Table III



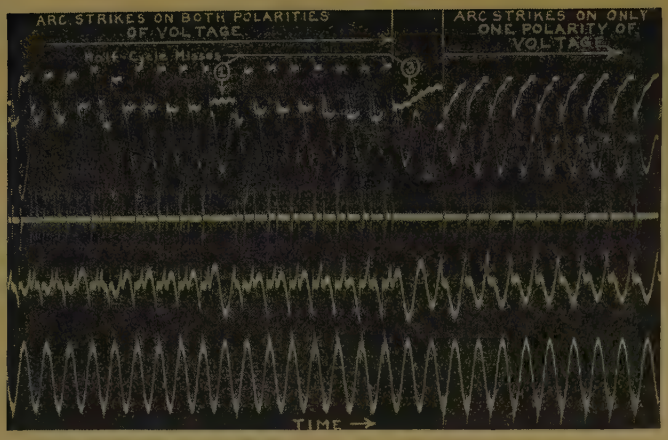


Figure 13. Arc strikes on only one polarity of voltage

Section of oscillogram from test 2, Table III

arc current recorded on the oscillogram of Figure 11 is 44 amperes, which occurred during the next to last arc strike.

The frequency of oscillations in the arc current and in the several recorded voltages was mostly between 1,080 and 1,200 cycles per second, sometimes around 1,600 cycles per second. In test 5, Table III, a capacitance of 2.3 microfarads was added between each phase conductor and ground. During this test the oscillations had four distinct frequencies, being about 460, 2,700, 4,200 and 6,780 cycles per second. Figure 12 is the oscillogram obtained during this test.

Discussion

Figure 11 shows the characteristic behavior of the 60-cycle voltages to ground after the arc remained extinguished: the almost completely displaced wave, producing a recovery voltage two times normal, and its slow return to normal. The phenomenon is caused by the relatively slow re-establishment of normal charge distribution on the three bus capacitances to ground shown in Figure 1. It is the retention of charge by these capacitances, added to the dynamic power voltages, that causes the recovery voltage wave to be two times normal by being completely displaced. Theoretically this can produce overvoltages to ground on the unfaulted phases as high as 2.73 times normal, because at the time of arc extinction, the unfaulted phase capacitances can remain charged to 1.73 times the normal phase-to-neutral voltage, to which may add the generated system phase-to-neutral voltage. By comparison, in the tests with the fixed length gaps, the recovery voltage across the arc gap was always limited to the normal crest phase-to-neutral value or less and the voltages measured on the unfaulted phases did not greatly exceed 1.73 times normal phase-to-neutral voltage.

Superimposed on the power frequency effects just described are the natural frequency transients, of which those shown in Figure 11 are typical. In addition to raising the *B* phase to ground voltage, they also raised the phase-to-phase voltage as shown in the bottom record of Figure 11. In this case the *A*-phase to *B*-phase voltage was raised a maximum of 1.56 times its normal value.

Figure 13 is a section of the oscillogram obtained during test 2 of Table III. It shows a very interesting phenomenon. The arc was quite unsteady, missing a few cycles occasionally as shown in Figure 13, then it restruck regularly on only one polarity of voltage. The single polarity arcing continued for 51 cycles, then missed a cycle and finally struck one more time. This phenomenon might have been caused by the rounded shape of one electrode of the arc gap and pointed form of the other. However, this explanation is not entirely satisfactory because none of the other tests with the self-lengthening gaps exhibited this effect even though the electrode shapes were practically the same in all tests. Repeated restriking of an arcing ground on only one polarity of voltage has not been previously reported in any of the technical literature consulted, although P. A. Jeanne[9] has reported a similar phenomenon of a few cycles of arcing at one polarity, changing to a few cycles of arcing at opposite polarity.

In the arc current record of Figure 12 there is evidence of arc extinction and restriking at the lowest natural frequency of the system, about 460 cycles per second. However, it is significant that the voltage across the arc gap did not rise appreciably prior to each restrike, apparently due to the short time available for deionization, It is doubtful if an arcing ground, either open or confined, on an actual bus will be subjected to high speed deionization, because highly artificial means, such as air or oil blast, must be employed for high speed circuit interruption. It thus appears that restriking of an arcing ground at progressively higher voltages and at resonant frequency is highly improbable on an actual bus system.

Within the frequency limitations of the electromagnetic oscillograph, that is, for voltages having a frequency less than about 3,500 cycles per second, the oscillograph is a more accurate instrument than the klydonograph. The klydonograph excels where the voltages are of high frequency or steep wave front. It will be noted in Tables II and III that the oscillograph usually indicated a higher overvoltage than did the klydonograph. This is interpreted to mean that steep-front surge voltages and voltages with a frequency above 3,500 cycles per second play no appreciable part in the production of overvoltage under the test conditions.

The klydonograph measurements in Tables II and III show that the maximum voltage to ground on the two unfaulted phases of the bus consistently are not equal when an arcing ground exists. The reason for this is indicated on the oscillogram of Figure 11, which can be taken as typical, where the arcing persists at most for only a third of a 60-cycle half wave. In this figure and also in the bottom trace of Figure 13, it will be seen that the voltage oscillations produced by the arc begin before or at the peak of *A*-phase to *B*-phase voltage. When *A* phase is grounded by an arc, the *A*-phase to *B*-phase voltage is the same as *B*-phase to ground voltage except for the arc drop, which is comparatively small. Figure 2 shows the phase relationships when *A*-phase bus conductor is grounded. With respect to the grounded conductor (*A* phase), voltage E_{AB} leads E_{AC} by 60°. Figure 14 shows the appearance of two sinusoidal half waves of power voltage having this relationship. If the arcing

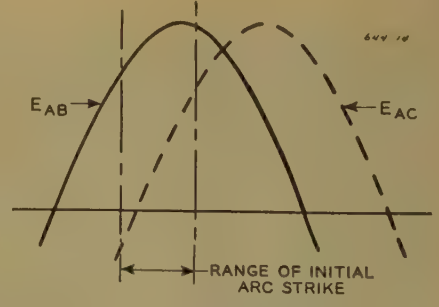


Figure 14. Period during which arcing transients begin on the phase-to-ground voltages of the unfaulted phases

Current and voltage relations when *A*-phase bus is grounded

transient occurs anywhere in the range indicated on Figure 14, it will be superimposed simultaneously on an instantaneous value of E_{AB} higher than the corresponding instantaneous value of E_{AC}. This usually makes the voltage to ground on B-phase conductor higher than that on C phase, although erratic arc strikes at other phase positions may alter this relationship. Such an unusual condition occurred in test 2 (Table III), where the highest transient voltages during the test occurred when the arc struck for voltages of only one polarity.

Summary and Conclusions

As stated previously, the following apply only to arcing grounds on normally ungrounded station busses and not to switching phenomena or effects of surges on extensive systems.

1. Arcing grounds on the tested station bus did not produce voltages to ground exceeding three times the normal crest phase-to-neutral voltage. Higher overvoltages did not materialize even though conditions in some of the tests were as severe as any likely to occur under operating conditions.

2. It has been shown in previously published literature that extremely high voltages can be produced by arcing grounds when the arcs quench and restrike at progressively higher voltages and at system natural frequency. It has been suggested that a ground fault in a pothead, cable, or other arc confining piece of equipment might provide especially favorable conditions.[12] As far as is known, build-up of voltage in excess of about three times the normal phase-to-neutral value has yet to be measured on an actual bus system operating at 13 kv or less. The study of arc gaps described in this report and operating experience published elsewhere, show that very rapid quenching of an arcing ground is not likely to be accomplished by any combination of circumstances which might occur on a station bus and associated equipment.

3. The maximum voltages to ground on the unfaulted phases of a three-phase bus are not equal under most arcing ground conditions.

4. Arcing grounds occur sometimes on only one polarity of voltage.

5. The tests revealed arcing transients which raise the phase-to-phase bus voltages as high as 1.74 times normal. The frequency of these transients was found to be as high as 6,780 cycles per second. Transients of this character may cause abnormal voltage stresses on the turn insulation of machines.

6. The faults of April 1942 on the ungrounded Holtwood bus very probably were caused by failure of defective porcelain insulators in quick succession because very careful inspection of the bus after the disturbance disclosed a number of them with minute cracks in the porcelain. It is probable that the trouble was initiated by the failure of one porcelain insulator, causing bus voltages to ground on the other phases between 1.73 and 3 times normal. This overvoltage then probably caused failure of one or more additional defective insulators. On an ungrounded bus system, it is particularly important that the insulation of the bus and of associated equipment be maintained at its initial strength and be tested periodically with the most sensitive means available for detecting defects. It is believed that many insulation breakdowns on ungrounded busses which have been attributed to voltage build-up, were probably caused by reduced insulation which might have been found by modern testing means.

7. Insulation should be provided on ungrounded busses and connected equipment capable of withstanding voltages to ground in excess of three times the normal phase-to-neutral value. Also, the turn insulation on machine windings must withstand high frequency voltages which accompany arcing grounds. How severe these latter voltages are, has not been determined. With these conditions met, advantage can be taken of the operating features which an ungrounded bus provides, and it is believed that no great concern need be felt that unlimited high voltages will be produced by an occasional ground fault.

8. A device for warning of impaired insulation on an ungrounded bus system and operated by the appearance of neutral-to-ground voltage is often inoperative until the insulation is broken down completely. In spite of this limitation, the device has proved useful in operation. A method is included in the paper for easily determining the sensitivity of a neutral voltage ground detector in any given installation.

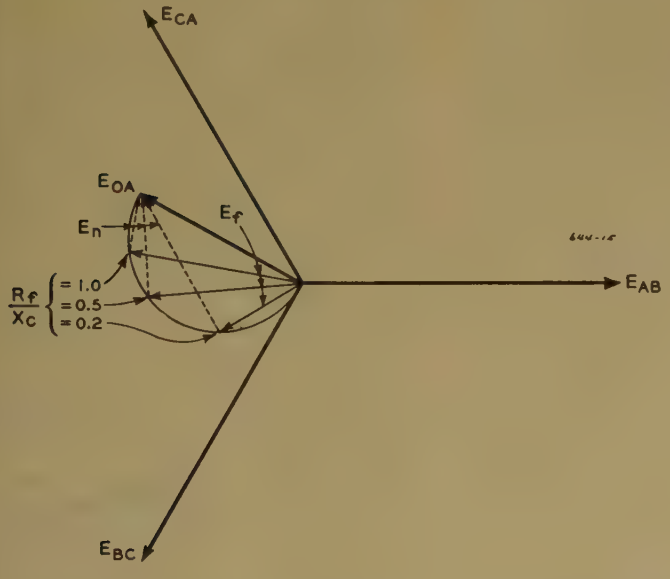


Figure 15. Vector relation between voltage across fault E_f and generator neutral voltage to ground E_n for three ratios of R_f/X_c

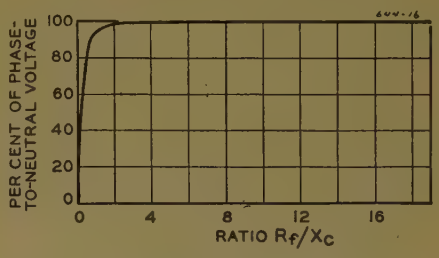


Figure 16. Variation of voltage across fault E_f for various ratios of R_f/X_c

Appendix I. Determination of Phase-to-Ground Capacitance of an Ungrounded 3-Phase Bus

The equivalent circuit of an ungrounded bus and connected apparatus is shown in Figure 1. Each item of equipment connected to the bus system, whether transformer, cable, bus, or rotating machine, contributes its share to the admittance of each phase conductor to ground. When insulation is unimpaired, the corresponding impedances are almost pure capacitive reactances which can be taken as lumped constants for purposes of analysis.

The capacitive reactances to ground of the bus system can be measured in the field by solidly grounding one phase of the system through an ammeter. When this is done, one of the bus-to-ground capacitances is short-circuited and the two ungrounded capacitances pass current through the ammeter as shown in Figure 3. With the directions of current flow as assumed in Figure 3, the vector relations of the currents are as shown in Figure 2B.

$$I_T = I_B \cos 30° + I_C \cos 30°$$

The charging currents of phase-B and phase-C bus conductors are numerically equal:

$$I_{xc} = I_B = I_C$$

Therefore

$$I_T = I_{xc} \cos 30° + I_{xc} \cos 30°$$

$$= 2I_{xc} \times 0.866 = 1.73 I_{xc}$$

or

$$I_{xc} = \frac{I_T}{1.73}$$

The capacitive reactance of one phase conductor to ground is found from the phase-

to-phase voltage E and the grounding ammeter reading I_T:

$$X_c = \frac{E}{I_{xc}} = \frac{E}{I_T/1.73} = \frac{1.73E}{I_T}$$

The capacitance can then be found by solving for C in the equation

$$X_c = \frac{1}{2\pi fC} \text{ or } C = \frac{1}{2\pi fX_c}$$

where f is the power system frequency.

Appendix II. Effect of Ground Fault Resistance on the Neutral-to-Ground Voltage of an Ungrounded 3-Phase Bus

Fault detection with a generator neutral potential transformer requires a shift in the neutral potential for its indications. An impairment of bus or equipment insulation to ground is equivalent to a shunt across the capacitance-to-ground of the phase conductor affected. A ground fault with a given resistance will have more effect on neutral potential shift if the capacitance to ground is small than if it is large. Or expressed in a more practical way, because the capacitive reactance is the quantity determined directly from a grounding ammeter test, the greater the capacitive reactance to ground of a system, the more effect a given value of fault resistance will have on neutral shift. The analysis has been made on a unit basis to

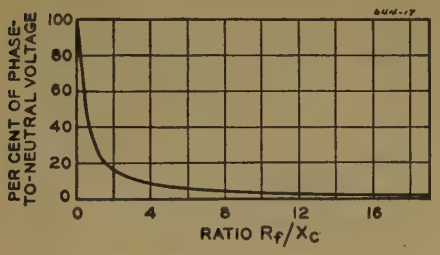


Figure 17. Variation of generator neutral voltage to ground E_n for various ratios of R_f/X_c

make the results applicable to any field condition where the capacitive reactance to ground of the bus can be measured. The steps in the analysis are as follows:

(*a*). The currents and voltages in Figures 2 and 3 are directly proportional to the system phase-to-phase voltage. In the calculations, 1,000 volts was used as the unit base for this voltage. Under these conditions, the phase-to-neutral voltage is 1,000/-1.73 = 577 volts.

(*b*). On a unit basis, the capacitive reactance to ground of each phase conductor was taken as X_c = 1,000 ohms.

(*c*). A bus insulation fault is equivalent to a resistance shunting the capacitive reactance to ground of the faulted phase conductor. Different values of fault resistance R_f were assumed in succession, ranging from one megohm to zero. This gave ratios of R_f/X_c ranging from 1,000 to zero. Each of the following steps was carried through separately for each assumed value of R_f faulting the phase-*A* bus conductor.

(*d*). The parallel circuit of the fault resistance R_f shunting the phase-to-ground capacitive reactance X_c was transformed into its equivalent series circuit, giving Z_e.

(*e*). The current through the X_c of each unfaulted phase is the corresponding phase voltage divided by $X_c + Z_e$, giving I_B and I_C, calculated separately.

(*f*). The current in the circuit composed of the faulted phase capacitance and fault resistance in parallel is $I_T = I_B + I_C$.

(*g*). The voltage across the fault is $E_f = I_T Z_e$ (Figures 15, 16).

(*h*). The generator neutral voltage to ground, E_n, is the phase-to-neutral voltage of the faulted phase minus the fault voltage or

$$E_n = E_{OA} - E_f \text{ (Figures 15, 17)}$$

(*i*). The power dissipated in the fault is

$$P_f = \frac{E_f^2}{R_f}$$

The results of the calculations are summarized in Figures 15, 16, and 17. The computations were checked in the laboratory with equivalent circuits having several values of X_c. The effect of the generator neutral potential transformers and their secondary burdens has been neglected in the computation because the impedance of each is quite high, varying from one to two megohms, depending upon the applied voltage.

Discussion

To avoid forced outages and interruption of central station electric service, it is very desirable to obtain notice of any bus insulation defect as soon as possible. At Holtwood the neutral voltage ground detector shown in Figure 1 is used. The alarm did not operate before the flashovers of April 1942 occurred. However, the relay targets were found to have operated after the trouble. Because the alarm did not give an indication until the trouble occurred, the foregoing analysis was made to determine how low the resistance of a fault must be to operate the alarm.

The capacitive reactance to ground of one phase of the Holtwood station bus is about 2,500 ohms. The relay connected to the secondary of a neutral potential transformer must be set to operate at no less than about 30 per cent of the phase-to-neutral voltage to avoid false indications during normal switching. By referring to Figure 17, it is found that about 30 per cent of phase-to-neutral voltage is obtained when the ratio of fault resistance to the phase-to-ground capacitive reactance is unity. For the Holtwood bus, this voltage is obtained when the fault resistance is 2,500 ohms. Before the fault resistance falls to 2,500 ohms, it can be seen in Figure 18 that considerable power is dissipated in the fault. The power is sufficient to cause noticeable heating of any of the usual types of incipient faults. For instance, when the fault resistance is 0.25 megohm, the power in the fault is 230 watts. The relatively large power dissipation leads to extremely rapid heating of the fault and consequent rapid lowering of fault resistance. The very rapid transition from high to low resistance in the fault explains the failure of a neutral voltage fault detector to give warning of impending insulation trouble, and also the general experience of relatively little burning of equipment when faults occur on systems with an ungrounded neutral. In the first case, when rapid heating and failure of the fault begins, the generator neutral voltage is only a few per cent of the value required to trip the fault detector; in the second case, the extremely short time required for complete breakdown of the fault limits the liberated energy to a relatively small value, even though the power level is high for a short interval.

Analysis thus reveals that a neutral voltage relay can detect impaired insulation in a large installation only when the insulation is broken down completely. Because its sensitivity to insulation resistance varies with the amount of equipment in service,

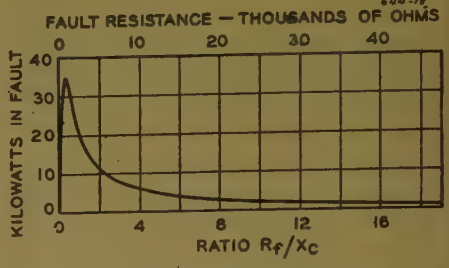


Figure 18. Variation of power dissipated in a fault with fault resistance for X_c = 2,500 ohms

the device might warn of impaired insulation prior to complete failure on a small bus system if the bus capacitance to ground and the bus voltage were sufficiently low. It must be recognized that the Holtwood fault detecting devices, even though insensitive to early stages of insulation failure, have proved valuable in service, indicating insulation failures to ground that otherwise would not have been detected promptly.

References

1. Voltages Induced by Arcing Grounds, J. F. Peters, J. Slepian. AIEE Transactions, volume 42, 1923, pages 478–89.

2. Power-System Transients Caused by Switching and Faults, R. D. Evans, A. C. Monteith, R. L. Witzke. AIEE Transactions, volume 58, 1939, August section, pages 386–94. Discussion, pages 394–7.

3. Overvoltages During Power-System Faults, E. Clarke, S. B. Crary, H. A. Peterson. AIEE Transactions, volume 58, 1939, August section, pages 377–85.

4. Critical Analysis of Rotating Machine Grounding Practice, H. A. Peterson. *General Electric Review*, April 1942, pages 215–20.

5. Merits and Methods of Generator Grounding, S. B. Griscom. *Westinghouse Engineer*, February 1943, pages 33–9.

6. How to Apply Neutral Grounding Devices, A. A. Johnson. *Westinghouse Engineer*, May 1943, pages 66–9.

7. Correlation of System Overvoltages and System-Grounding Impedance, AIEE committee on protective devices. AIEE Transactions, volume 62, 1943, January section, pages 17–24.

8. Arcing Faults in Power Systems, C. Concordia, H. A. Peterson. AIEE Transactions, volume 60, 1941, pages 340–6.

9. Discussion of reference 8, P. A. Jeanne. AIEE Transactions, volume 60, 1941, pages 614–16.

10. Overvoltages on Transmission Lines Due to Ground Faults as Affected by Neutral Impedance, Engineering Report Number 30, Joint Subcommittee on Development and Research, Edison Electric Institute and Bell Telephone System, November 15, 1934. EEI publication number D-14, 1936, pages 105–37.

11. Accurate Line Fault Location, J. E. Allen, G. J. Gross. *Electrical World*, July 20, 1935, pages 23–5.

12. Discussion by C. L. Gilkeson. AIEE Transactions, volume 58, 1939, August section, page 395.

Air-borne Radar for Navigation and Obstacle Detection

R. C. JENSEN
NONMEMBER AIEE

R. A. ARNETT
ASSOCIATE AIEE

Synopsis: The grim uses of radar in war are giving way now to a peacetime role in navigation and obstacle detection. This article discusses the results obtained with military airborne radar as a basis for understanding both the possibilities and the limitations in the application of radar to reduce aviation hazards.

RADAR has been given a great deal of publicity during recent months, and many uses for military operations have been disclosed in technical magazines and newspapers. These publications often included pictures obtained with cathode-ray tube indicators during flight over large American cities and also displayed presentations of enemy territory as viewed on bombing missions. As a result of this publicity and the predictions that have been made for the commercial use of radar, there is probably no single application that catches the public imagination as much as its possible use for navigational aid and obstacle detection in aircraft. Discussions and public expressions of opinions promoting safer navigation are stimulated by aviation accidents such as the Empire State Building disaster and others that have occurred during attempts to land under conditions of obscured vision. Possibly these accidents could have been averted by proper utilization of radar equipment designed to meet obstacle detection requirements. However, there are limitations to present radar performance in that it fails to give the pilot an ideal picture of the area being scanned in its true perspective. But in spite of these limitations, if capable technical effort is applied to the engineering problems involved and these problems are based upon realistic operating requirements and performance, there is every reason to feel that radar will contribute toward safer aircraft navigation and justify the weight of the equipment to be carried.

Paper 46-48, recommended by the AIEE committee on communication for presentation at the AIEE winter convention, New York, N. Y., January 21–25, 1946. Manuscript submitted December 17, 1945; made available for printing January 3, 1946.

R. C. JENSEN is with General Electric Company, Schenectady, N. Y., and R. A. ARNETT is with Geotechnical Corporation, Dallas, Tex.

The authors wish to express their gratitude for the courtesy extended by the National Defense Research Council Radiation Laboratory at Massachusetts Institute of Technology in permitting the use of the radar photographs appearing in this article.

Basic Radar Concepts

The simplest kind of blind navigation system has long been used by pilots of boats operating in rivers and harbors, for they have achieved some measure of success in obstacle detection by using a series of short whistle blasts and then listening for the direction and timing of the echoes.

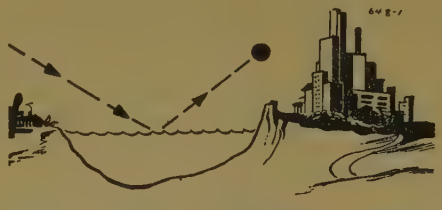


Figure 1. Energy reflected from a smooth surface



Figure 2. Energy return from a shore line

This example in the detection of reflected energy illustrates the basic principle of radar. For the benefit of the reader who is not familiar with radar, a brief outline of the fundamentals may be helpful.

The purpose of radar is to transmit radio-frequency energy in pulses of high intensity and then to measure the round trip travel time of the reflected energy with sufficient accuracy to establish the range to the obstacle. Following each pulse the transmitter is idle for a relatively long time while a receiving unit is ready to receive the echoes from the preceding pulse. Generally the same antenna is used both for transmission and reception. The finite velocity of electromagnetic waves makes it possible to measure the elapsed time from the transmitted pulse to the received echo as a direct measure of range. This elapsed time is approximately six microseconds for each 1,000 yards of range.

The measurement of range is only a part of the information obtainable with a radar system. Azimuth and elevation angles also can be determined for complete location of a target. This is accomplished by using an antenna that directs the pulsed energy in a narrow beam which may be five degrees wide or less at the half-power points. The position of the target then is determined by the direction of the antenna beam. In the cases where only the bearing angle is of importance, the pattern is narrow in the horizontal plane but broad in the vertical plane for wider angle coverage.

The received signals are displayed on a cathode-ray tube whose sweep is timed from the transmitted pulse, and targets appear as deflections of the sweep or as intensity spots. This display is not like television where an actual picture appears, but the results are interpretable to a trained operator.

To illustrate the types of echo responses from ground targets, consider a source of radio frequency energy radiated in a narrow beam from an aircraft as shown in Figures 1 through 4. If the beam is directed toward the ground at a forward angle, the reflection will be a function of the aspect of the target. The energy which strikes the smooth surface of the lake is reflected away from the source and leaves a dark region on the indicator tube. A shore line, buildings, and normal

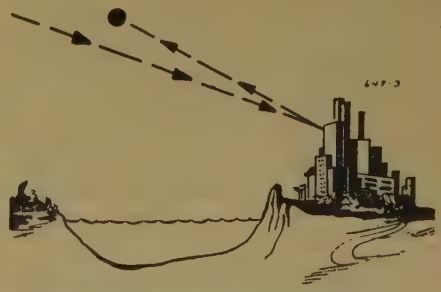


Figure 3. Energy return from structures



Figure 4. Altitude determination by normal incidence

incidence on the terrain directly below the plane will each provide a strong target echo. A wide beam of uniform intensity directed from the aircraft results in ground illumination and echo response as shown in Figures 5 and 6 respectively. These figures also illustrate how it is possible to correlate a radar picture with a relief map of the area.

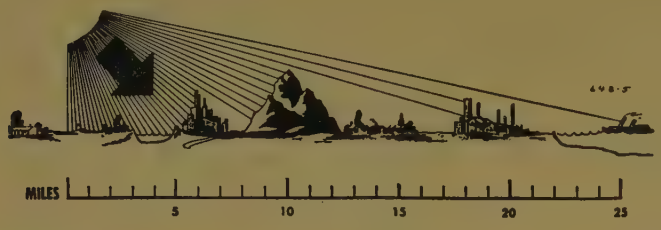


Figure 5. Illumination of generalized topography

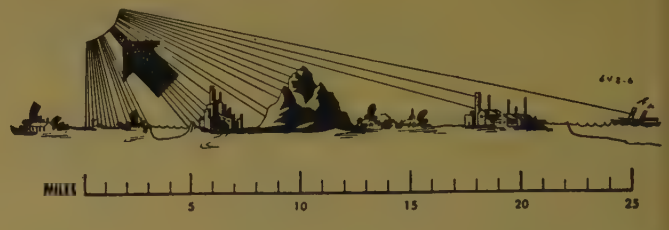


Figure 6. Energy return from ground targets

Navigation Systems

Navigation systems require that large ground areas be scanned, so antenna patterns of the shape shown in Figure 7 are used to an advantage. Note that the beam is narrow in the horizontal plane in order to obtain azimuth accuracy, while in the vertical plane the beam is broadened to sweep a large area but with a corresponding loss in elevation accuracy. The beam intensity is purposely decreased at angles below the main lobe to obtain uniform signal return at the aircraft for equivalent targets for all ranges to be covered. The shape of the beam is designed to compensate for the inverse square law decrease of the power density for both the incident and reflected energy. This type of antenna beam is known as a cosecant squared pattern because it simulates a plot of this function. One method of obtaining such a radiation pattern is to modify a conventional parabolic reflector so that part of the radiated energy is directed downward below the axis of the major lobe. In practice such patterns were obtained only after considerable experimentation with reflector shapes and types of antenna feeds. An actual plot of a cosecant squared pattern is shown in Figure 8, which indicates that with the peak of the beam tilted down 2.5 degrees and the aircraft at 6,500 feet, the radar coverage for uniform signal return extends from 2 to 20 miles.

All the material so far presented serves to show the character of ground echoes and the method of getting uniform ground illumination. If the beam is rotated or sector scanned and also synchronized with the cathode-ray tube trace of an indicator, a map of the ground relief is presented on the fluorescent screen. Rivers, lakes, shore line, valleys, and mountains will appear in relative direction and range with respect to the aircraft. This type of presentation was used to good advantage during the war on bombing missions when such targets as ships, bridges, and industrial areas were located and destroyed entirely with radar navigation. An example of this type of presentation can be observed in Figure 9, in which the coastal outline and promontories of land are spotted easily. Note how readily this picture can be correlated with the aeronautical chart of the same area shown in Figure 10. The L-shaped promontory at Plymouth is identified clearly, and the tip of Cape Cod is appearing just at the right. The circular rings are 2-mile range marks, and the inner bright ring is the start of the radial sweeps on the scope. The second bright ring is the signal return from the bay directly below and so indicates the height of the plane. If targets appear within the altitude ring, it indicates the presence of aircraft at ranges less than the height of the plane. For aircraft beyond the range of the altitude ring, the return signals are obscured fairly well by ground echoes except possibly over water, though even water may have a serious masking effect. A point of importance here is that an illumination and display which is suitable for navigation would have very little use for obstacle detection.

Figure 10 was taken with the aid of a lightweight low power radar system known as *AN/APS*-10. The essential units of this system are shown in Figure 11, and Figure 12 is a suggested arrangement for installation in a transport plane. The antenna with its parabolic reflector is mounted in a protective housing below the skin-line of the plane to permit complete vision. This housing is built of low loss materials designed for maximum transparency to microwave radio frequencies.

Higher power systems are used to get greater ranges and improved coverage as illustrated by Figures 13 and 14. In the latter figure, the circles are 100-mile marks, and the inlaid map indicates how faithfully the topography is portrayed. Note the shaded portion along the Hudson River caused by the screening hills, and the strong response from the mountainous region beyond.

The technical characteristics of radar sets vary over a wide range depending upon the application. The following tabulation has been prepared to indicate the order of magnitude of the operating characteristics employed in systems such as those used to obtain the preceding scope photographs:

Carrier frequency	3,000–10,000 megacycles
Peak power	10–1,000 kw
Pulse frequency	300–1,000 cycles per second
Pulse width	0.25–2 microseconds
Duty cycle	0.0001—0.001
Maximum range	50–200 miles
Range accuracy	40–4,000 yards
Range resolution	75–400 yards
Azimuth accuracy	0.5–1 degree
Azimuth resolution	3–6 degrees
Receiver	Superheterodyne
Intermediate frequency	30 megacycles
Intermediate-frequency band width	0.5–5 megacycles
Minimum detectable signal	1–10 micromicrowatts

Obstacle Detection

It has been stated that a cosecant-squared pattern is unsatisfactory for differentiating between aircraft and ground reflections. This difficulty arises because

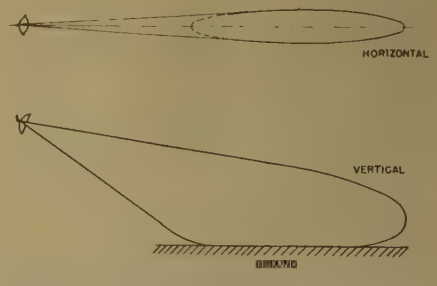


Figure 7. Conventional antenna pattern for navigation radar

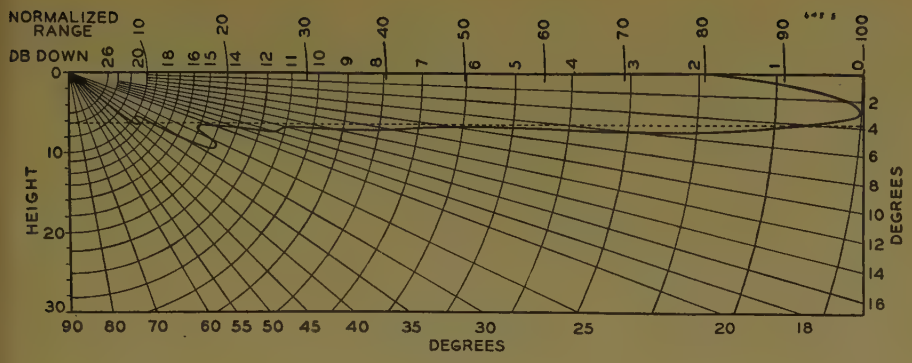


Figure 8. Actual antenna pattern for navigation radar

all targets at equivalent range and bearing appear at the same spot in the display whether at ground level or above. The display shows slant ranges from the plane, not actual ground range. Furthermore, the necessarily wide lobe in the vertical direction fails to indicate elevation even though a plane appears in the beam. There is no way for determining elevation unless the beam pattern has essentially the same configuration in the vertical plane as indicated in Figure 7 for the horizontal plane. This requirement demands considerably more performance from the antenna scanning system if the same solid angle is to be illuminated in a given interval of time. The cosecant squared antenna for a system such as *AN/APS*-10 rotates at 30 rpm, while a uniform lobe antenna must scan at many times that speed and simultaneously nod in the vertical plane in order to illuminate the same area. Such systems have been used to obtain a crude television picture of 10 or 12 lines on an indicator that presents azimuth and elevation information. As the antenna rotates, the cathode-ray tube trace sweeps horizontally and also progresses vertically in synchronism with the antenna position.

A second method for scanning a large area with a narrow beam is known as the Palmer Scan. This system employs a pattern which is narrow in both planes. The axis of the reflector is moved in a rectangular path, for example, through a horizontal angle of 75 degrees and a vertical angle of 45 degrees. During this motion the lobe is made to rotate in a rapid conical sweep such that the apex cone angle formed by the axis of the beam is as many as eight times the beam width. This results in illuminating a circular shell around a blank center region, but as the antenna system moves in its rectangular path, the entire area is filled in. A 6-degree beam which scans 21 degrees off the axis of the reflector thus can cover an area of 120 degrees by 90 degrees, while the axis of the reflector follows the borders of a rectangle 45 degrees by 75 degrees.

A third design for wide angle viewing utilizes a spiraling motion of the antenna beam. The angle of advance for the spiral is small enough so that no blank regions appear in the over-all illumination. A solid angle of coverage may be as much as 120 degrees with a lobe width of 5 degrees.

Present Limitations

These various types of antennas have been discussed briefly to indicate the problems associated with the requirement that enables the system to spot aircraft targets or tall structures and also cover a large area of scanning. They are mechanically complex and require driving mechanisms to spin or slew them at rapid rates so that the scanned area is covered in a few seconds. This is essential if the pilot is to receive scope information comparable with the speed of modern aircraft and avoid collisions. Furthermore, the complexity and fast scanning rates contribute materially toward increased weight of the equipment. In addition, it has been found that beam widths in the order of five degrees are too wide to obtain satisfactory resolution. Lobes of one and two degrees or less are necessary. This demands even faster scanning to cover a given area in a selected interval of time. The point may then be reached where the beam remains on the target for an insufficient length of time to get adequate signal return, and the object is not observed on the indicator. This limit is accepted generally as five pulses on the target during the time of one beam-width

Figure 9. Radar map of Cape Cod area

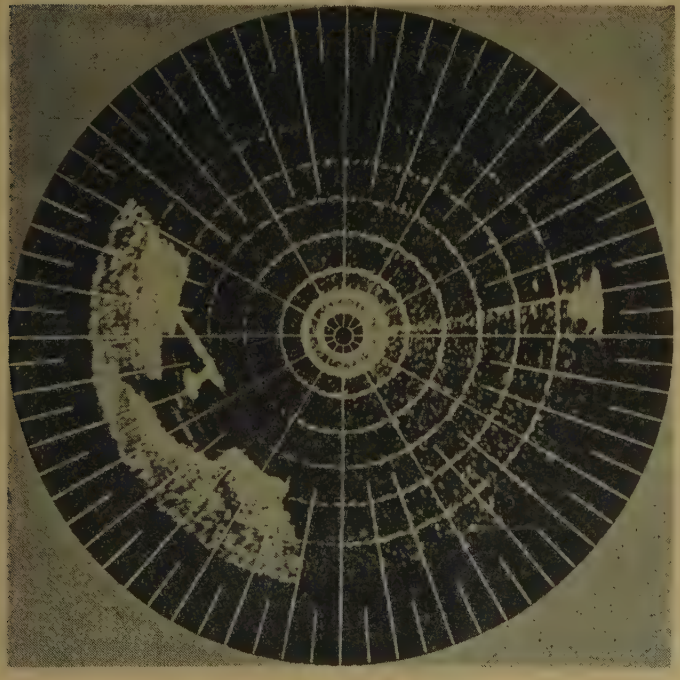


Figure 10. Chart of Cape Cod area



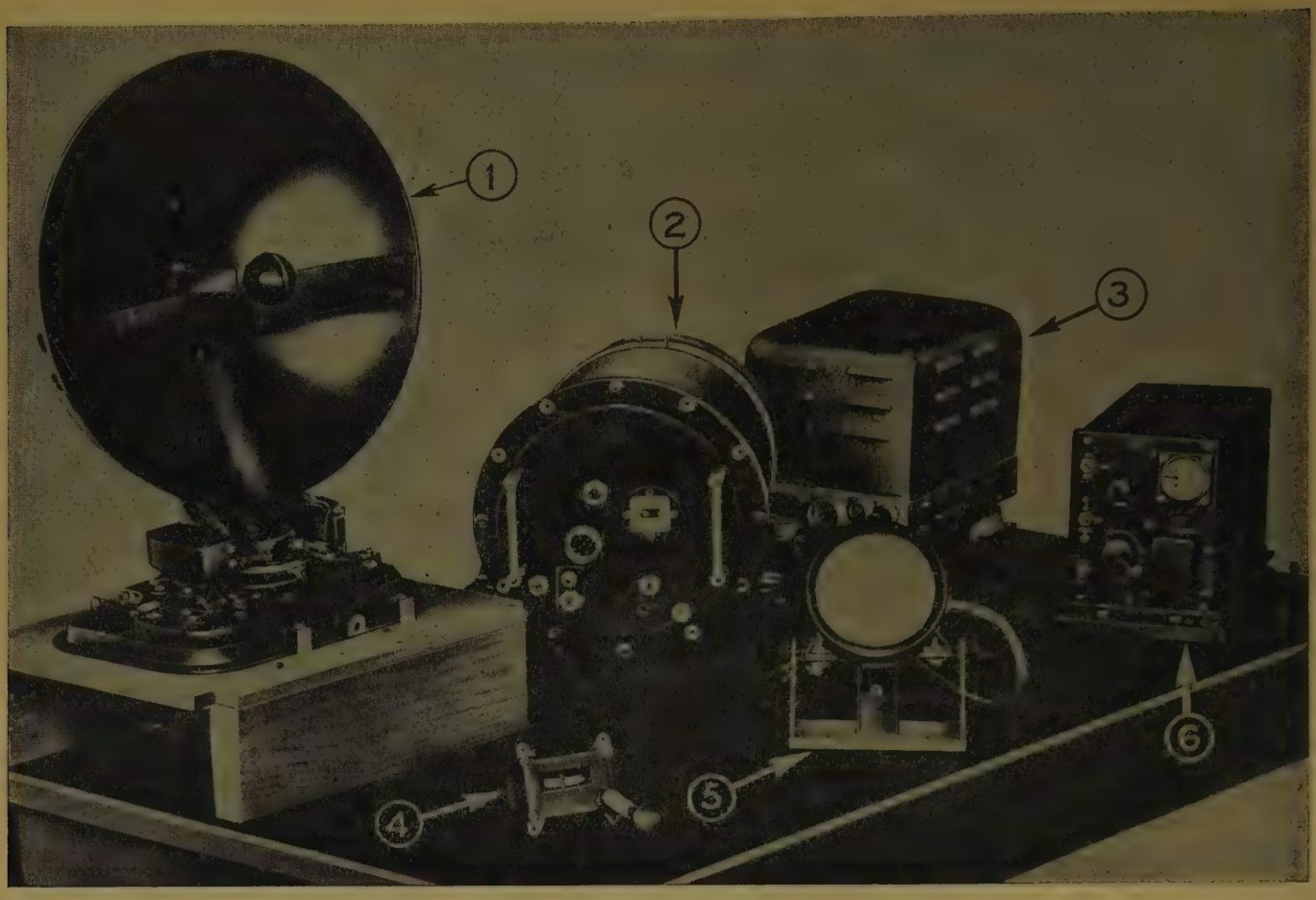


Figure 11. Air-borne radar system

1. Antenna Assembly (*AS-154/APS-10*). The antenna or "spinner" may be mounted in a nacelle on the belly of the plane where it revolves in operation to give 360-degree scanning. It can be tilted up and down for critical coverage

2. Transmitter-Receiver (*RT-69/APS-10*). This sealed can is the heart of *AN/APS-10*. In it are the complete self-contained transmitter and receiver. It is pressurized for operation at altitudes up to 30,000 feet

3. Rectifier Power Unit (*PP-111/APS-10*). This compact box is usually mounted out of the way. It converts 115 volts to six different levels of voltage for various functions. They vary from 4,000 volts down to less than 7 volts

4. Trim Control Box (*C-226/APS-10*). This mechanical unit is always mounted near the radar operator. As its name suggests, it is used to adjust the trim of the antenna to compensate for change in the flight altitude of the plane

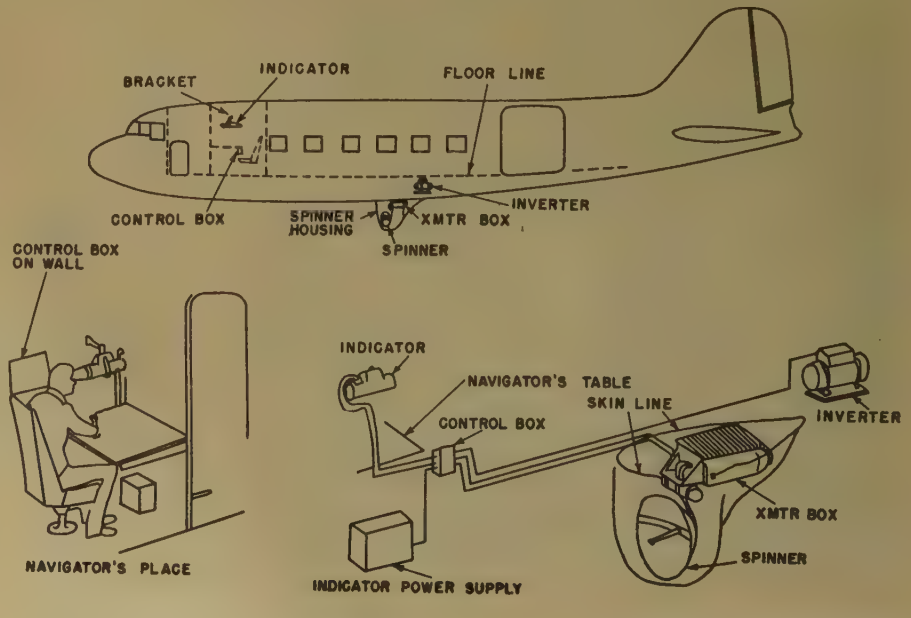
5. Indicator (*ID-99/APS-10*). Here is where the radar information appears. The indicator (PPI) is mounted where it can be studied easily and adjusted quickly. Another one showing identical information may be mounted with the pilot or elsewhere

6. Synchronizer (*SN-17/APS-10*). This small box has most of the manual controls for operation of *AN/APS-10*. It is one of three components in the set which are always mounted within easy reach of the operator

scan. Increasing the pulse rate is the obvious solution, but the pulse repetition rate is dependent upon the maximum operating range, since the return signals should be received before the next pulse is transmitted. Otherwise there would be a confusing indication of targets on the osilloscope. There is also the important consideration of increased average power as pulse rates are accelerated because of the resultant increase in weight with greater power requirements.

The alternative requirement is to reduce the scanned area, thus confining observation to small angles for continuous rapid coverage with the option of selecting other directions for intermittent viewing. The normal operating position would be about the center line of the nose of the airplane.

Figure 12. Typical installation of air-borne radar



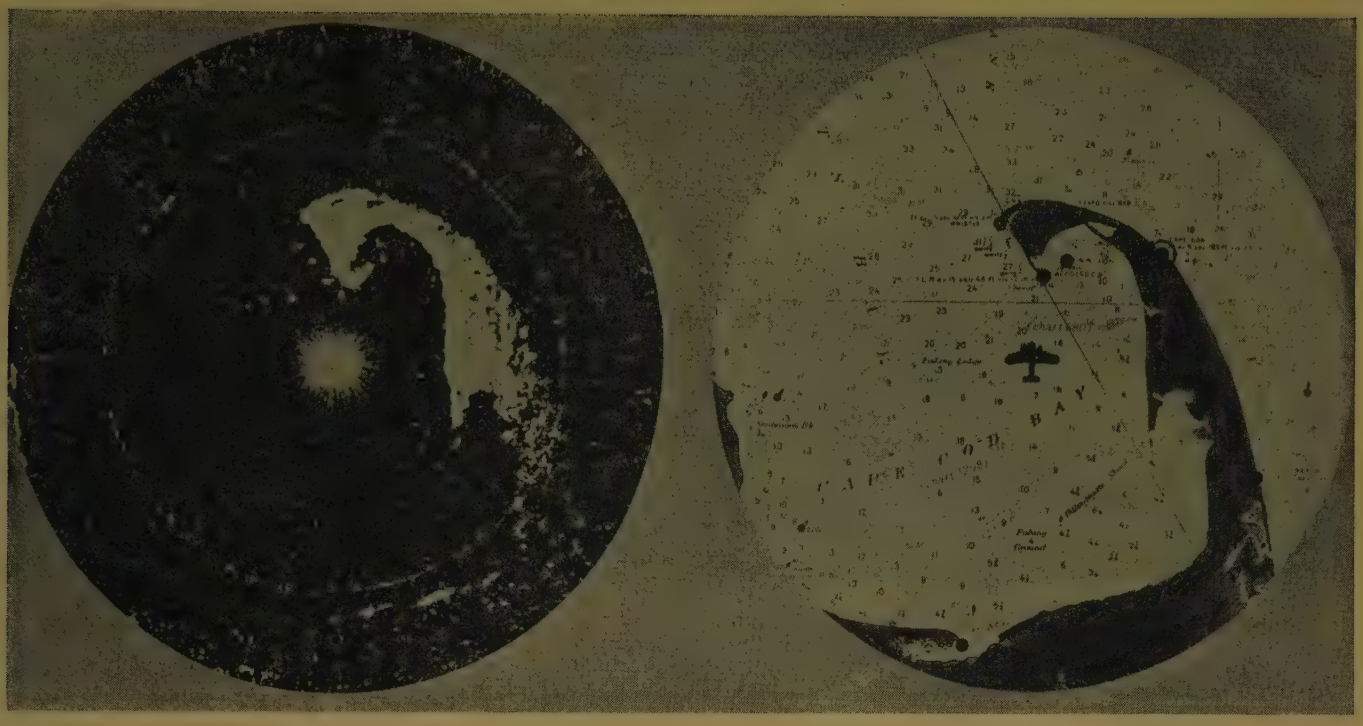


Figure 13. Correlation of radar map with chart

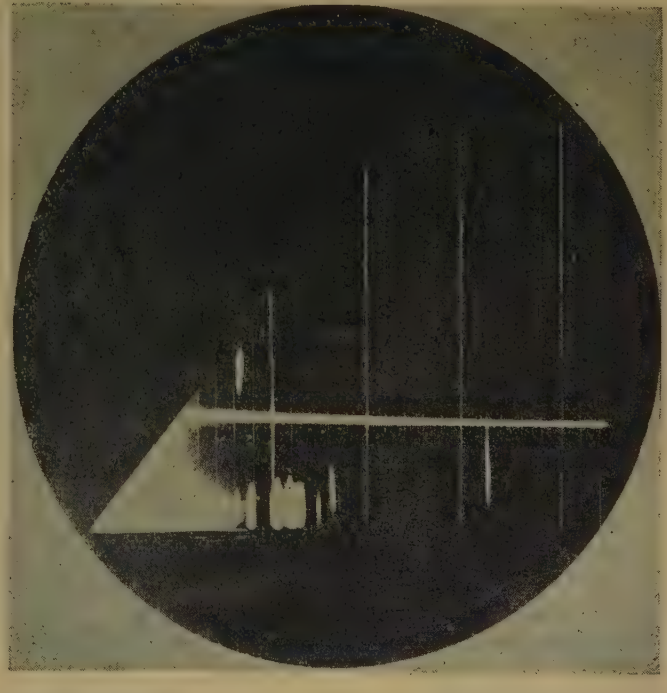
An example of the type of indication that is achieved with a rapid vertical scan antenna using a narrow beam is shown in Figure 15, which plots range against elevation angle. The vertical lines are 2- and 10-mile range marks, while the heavy horizontal trace is an electronic height marker which may be moved by means of a control to line up with a target to indicate elevation. This picture is not indicative of air-borne system performance because it was taken from a high power ground radar; however, it does illustrate the means of presenting target information to obtain height indications. Several aircraft are visible: two at 17 miles and 16,000 feet, very close in range, and a single plane at about 40 miles and 5,000 feet. Two more planes can be observed at about 26 miles. If the picture had been obtained from an air-borne system, the usable range would be reduced considerably because of lower power output. Instead of displaying 50 miles, possibly 20 miles might be the full-scale indication and the ground clutter undoubtedly would extend to the full range. Azimuth information must be read, of course, from a second scope that plots range and azimuth angle, or from a selsyn system that indicates the azimuth position of the antenna. The position of each target would be fixed then with respect to the aircraft.

An interesting photograph that con-

Figure 15. Radar indication of range versus elevation angle

Figure 14. Inlaid radar map of Northeastern States





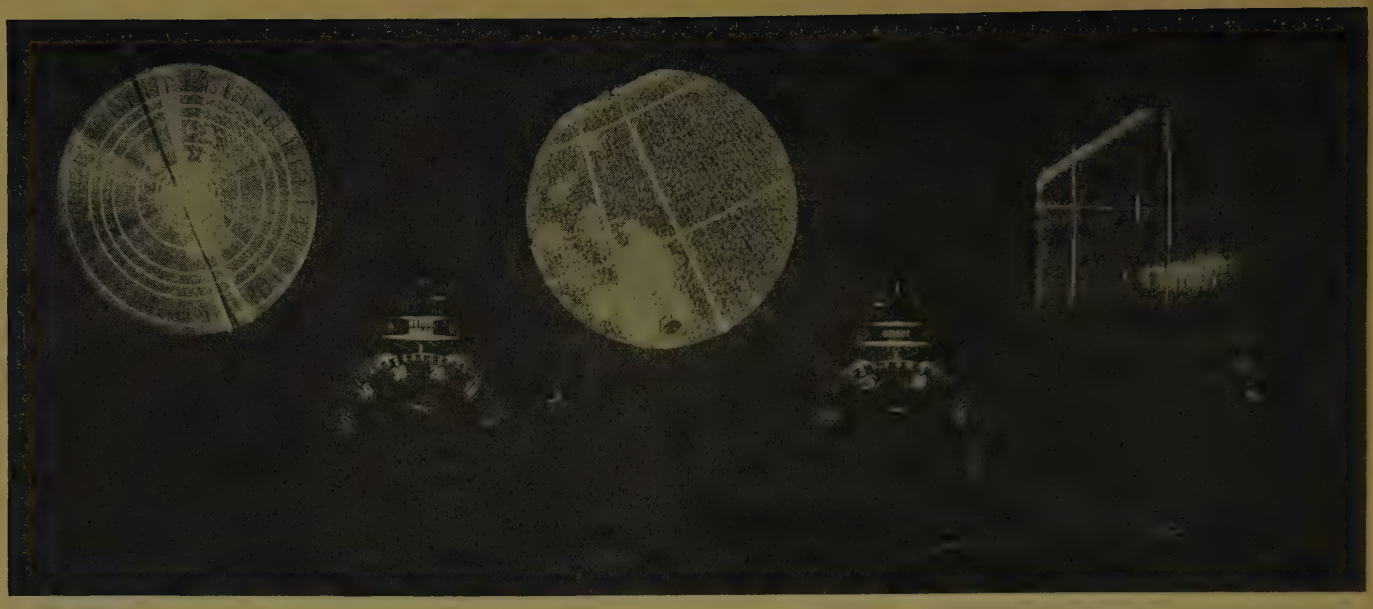


Figure 16. Radar presentation with polar plot, sector polar plot, and range elevation angle

tains both azimuth and elevation information for the same targets is shown in Figure 16. In addition to spotting aircraft, this picture demonstrates the ability of radar to give warning of storm areas. It is apparent that a storm cloud appears at the right and below the target plane in the elevation scope picture, and also can be located in the azimuth presentation.

It should be pointed out that a system which scans only a small sector in the direction of travel to avoid collisions also could obtain navigational information from supplementary land-based equipment. An example of this supplementary equipment is a radar beacon which consists of a transmitter that radiates a coded pulse when properly interrogated by an airborne system. This coded pulse appearing on the radar indicator enables range and bearing to be determined to the known location of the beacon. Such a system has a decided advantage when navigating over water where recognizable targets on a radar map are scarce. Furthermore, it aids in extending the operating range of the equipment beyond the target-response indication because of the higher power signals from the beacon. Since the high frequencies involved propagate only in straight lines, the range generally is limited to line of sight conditions.

Future Developments

The elevation scope pictures illustrate the performance that is obtainable now with ground radar equipment, and in time, equivalent resolution and satisfactory ranges will be achieved with lightweight air-borne systems. However, there are many engineering problems, both electrical and mechanical, to be overcome before an ideal design is evolved that meets the strict limitations imposed upon air-borne apparatus. Not the least of these is the problem of presenting the radar information in a manner that requires little effort on the part of the observer for quick interpretation. Azimuth and elevation data should be combined to provide the pilot with continuous infor-

Figure 17. Radar map of Greater New York



mation on all obstacles within the danger area.

The photograph in Figure 17 illustrates the definition obtainable when using a very narrow beam system. The individual docks on the Manhattan water front, the bridges across the East River, and the railroad tracks in Jersey City are clearly visible. It may well be that eventually radar will approach the equivalent of visual or television presentation in a scope picture so that a similar view of New York City and adjacent areas will enable the pilot to perceive the height of objects with the same resolution that can be observed here for range and bearing. This goal may not be achieved for some time, if ever, but in the meantime, useful radar systems can be designed which will remove many of the hazards of modern air travel.

References

1. Radar, a Report on Science at War (pamphlet), distributed by Office of War Information.

2. Aviation Communication System, D. W. Rentzel. Electrical Engineering, volume 64, November 1945, pages 387–91.

Differential Leakage of a Fractional-Slot Winding

M. M. LIWSCHITZ
MEMBER AIEE

IN a previous paper,[1] the differential (harmonic) leakage of an integral-slot winding and squirrel cage winding was treated. It was shown that a squirrel cage rotor reduces the harmonics and thus the differential leakage of the stator. The influence of the number of stator and rotor slots, as well as of the pitch factor of the stator winding on the damping of the stator harmonics, was discussed. Also, it was shown that skewing of the rotor reduces the damping of the stator harmonics and, therefore increases the differential leakage of the stator. The investigation was made under the following assumptions:

1. The saturation of the leakage paths is negligible.
2. The influence of slot-openings for all harmonics is the same as for the synchronous wave. That is, all harmonic fluxes are reduced by the slot-openings in the ratio of one to K_c, where K_c is the total Carter factor.
3. The magnetomotive force curve has a stepped shape.

The saturation of the leakage paths will be neglected in this paper also. The influence of slot-openings on the individual harmonics and the influence of the shape of the magnetomotive force curve on the differential leakage are treated in appendixes I and II. It follows from these appendixes that the assumptions made with respect to the slot-openings and the shape of the magnetomotive force curve are not entirely correct, but they are justified by the simplification of calculation of the differential leakage to which they lead.

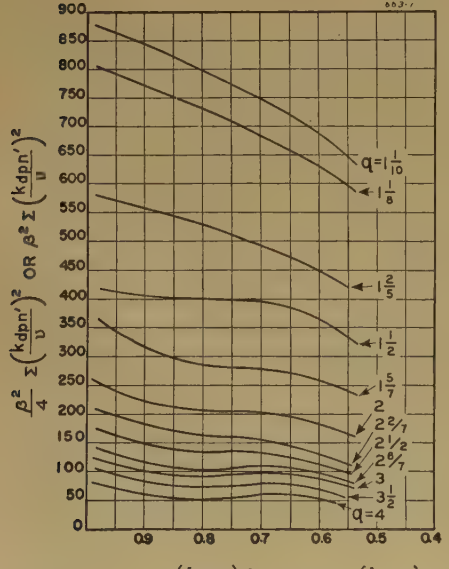


Figure 1. $\frac{\beta^2}{4}\sum_{\nu\neq\frac{\beta}{2}}\left(\frac{k_{dpn'}}{\nu}\right)^2$ and $\beta^2\sum_{\nu\neq\beta}\left(\frac{k_{dpn'}}{\nu}\right)^2$ for fractional-slot 3-phase windings

Actual Harmonics of Fractional-Slot 3-Phase Winding: Their Distribution Factors and Pitch Factors

If the number of slots per pole per phase of the fractional-slot winding is written

$$q=\frac{N}{\beta} \tag{1}$$

where N and β have no common divisor, the actual harmonics of a 3-phase winding are (for symbols see Nomenclature):

$$n'=\frac{2p}{\beta}\nu \qquad \nu=1, 2, 4, 5, 7 \ldots \tag{2}$$

when β is an even number, and

$$n'=\frac{p}{\beta}\nu \qquad \nu=1, 5, 7, 11, 13 \ldots \tag{3}$$

when β is an odd number.

For the synchronous wave, $\nu_s = \beta/2$ when β is an even number, or $\nu_s=\beta$ when β is an odd number. The number of subharmonics is equal to $(\beta-2)/2$ when β is an even number or to $(\beta-1)/2$ when β is an odd number (including those which are a multiple of three and usually do not exist in a 3-phase machine).

The absolute value of the distribution factor of the n'-th harmonic is

$$k_{dn'}=\frac{0.5}{N\sin\alpha_{n'}/2} \tag{4}$$

If P is the smallest integer which makes d an integer in the equation,

$$d=\frac{3NP+1}{\beta} \tag{5}$$

then it is true that when β is an even number

$$\alpha_{n'}=2d\alpha_m\nu+180 \tag{6}$$

and when β is an odd number

$$\alpha_{n'}=d\alpha_m\nu$$

if P is an even number and

$$\alpha_{n'}=d\alpha_m\nu+180 \tag{7}$$

if P is an odd number where

$$\alpha_m=\frac{180}{3N} \tag{8}$$

The pitch factor of the n'-th harmonic is

$$k_{pn'}=\sin\left(\frac{W}{\tau}\frac{180}{\beta}\nu\right) \tag{9a}$$

when β is an even number and

$$k_{pn'}=\sin\left(\frac{W}{\tau}\frac{180}{2\beta}\nu\right) \tag{9b}$$

when β is an odd number.

Harmonic Leakage Reactance of 3-Phase Winding

First the case will be considered where there is no damping, that is, the stator winding of a wound rotor induction motor or the stator winding of a salient pole synchronous machine without a damper winding.

The amplitude of the magnetomotive force of the wave with the length $2\beta\tau$ is

$$F_\beta=\frac{\sqrt{2}}{\pi}mNn_ck_{dp\beta}I \tag{10}$$

and therefore the amplitude of the fundamental wave with the length $2p\tau$ is

$$F_f=\frac{\sqrt{2}}{\pi}mNn_ck_{dpf}I\times\frac{p}{\beta} \tag{11}$$

The amplitude of the n'-th harmonic of the magnetomotive force is thus

$$F_{n'}=\frac{F_f}{n'}\frac{k_{dpn'}}{k_{dpf}}=\frac{\sqrt{2}}{\pi}mNn_c\frac{p}{\beta}\frac{k_{dpn'}}{n'}I \tag{12}$$

If the assumption is made that all harmonics are reduced by the slot-openings in the ratio of one to K_c, then the amplitude of the n'-th field harmonic is

$$B_{n'}=\frac{3.19}{gK_cK_s}F_{n'} \tag{13}$$

and the flux produced by the n'-th field harmonic is

$$\Phi_{n'}=\frac{2}{\pi}\tau_{n'}l_iB_{n'} \tag{14}$$

Paper 46-63, recommended by the AIEE committee on electric machinery for presentation at the AIEE winter convention, New York, N. Y., January 21-25, 1946. Manuscript submitted August 27, 1945; made available for printing December 11, 1945.

M. M. LIWSCHITZ is a consulting engineer to Westinghouse Electric Corporation and is with the Polytechnic Institute of Brooklyn, Brooklyn, N. Y.

The author is grateful to B. Limes for assistance in calculating the data contained in Table I.

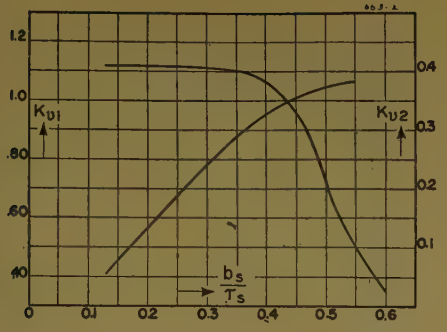


Figure 2. Factors K_{v1} and K_{v2} as functions of ratio between slot opening and slot pitch

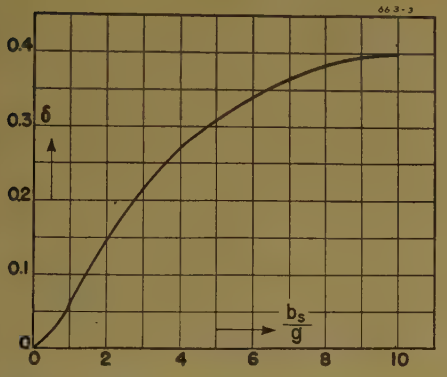


Figure 3. Factor δ as function of ratio between slot opening and air gap

The flux interlinkage caused by the flux $\Phi_{n'}$ is

$$\Psi_{n'}=\Phi_{n'}N_{ph}k_{dpn'} \tag{15}$$

Hence, the harmonic leakage reactance

$$x_h=2\pi f_1\frac{1}{\sqrt{2}I}\sum\Psi_{n'}\times10^{-8}\text{ ohms/phase}$$

$$x_h=\frac{4}{\pi^2}mf_1N_{ph}^2\frac{\tau l_i}{pgK_cK_s}10^{-7}\times\left[\frac{p}{\tau}\sum\left(\frac{\tau_{n'}}{n'}k^2_{dpn'}\right)\right]\text{ ohms/phase} \tag{16}$$

where

$$\tau_{n'}=\frac{p\tau}{n'}$$

Therefore, corresponding to equations 2 and 3,

$$\frac{p}{\tau}\sum\left(\frac{\tau_{n'}}{n'}k^2_{dpn'}\right)=\frac{\beta^2}{4}\sum_{\nu\neq\frac{\beta}{2}}\left(\frac{k_{dpn'}}{\nu}\right)^2 \qquad \nu=1,\ 2,\ 4,\ 5,\ 7\ \ldots \tag{17}$$

when β is an even number and

$$\frac{p}{\tau}\sum\left(\frac{\tau_{n'}}{n'}k^2_{dpn'}\right)=\beta^2\sum_{\nu\neq\beta}\left(\frac{k_{dpn'}}{\nu}\right)^2 \qquad \nu=1,\ 5,\ 7,\ 11\ \ldots \tag{18}$$

when β is an odd number.

The evaluation of the sums of equation 17 and equation 18 is not as simple as for an integral-slot winding. The reactance equation based upon the magnetic energy in the gap and used for the calculation of the harmonic leakage of the integral-slot winding also can be applied here, but the Goerges diagram of the magnetomotive forces of a fractional-slot winding becomes complicated, and the derivation of general formulas becomes tedious.

For this reason the direct summation of the terms $(k_{dpn'}/\nu)^2$ has been used in order to determine the sum of equations 17 and 18. As for the integral-slot windings, only a part of the harmonics of order lower than the slot harmonics of first order, and all slot harmonics, have to be taken into account.

The slot harmonics are:

$$n'_{sl}=\mp kQ+p \tag{19}$$

Thus

$$\nu_{sl}=\frac{\beta}{2}(\mp6kq+1) \tag{20}$$

when β is an even number

$$\nu_{sl}=\beta(\mp6kq+1) \tag{21}$$

when β is an odd number.

When $k>2$, the term $+1$ in the parentheses of equations 20 and 21 can be neglected. Then

$$\sum_{\nu=\nu_{sl}}\left(\frac{k_{dpn'}}{\nu}\right)^2=\frac{4}{\beta^2}k^2_{dp(n'=p)}\left[\frac{1}{(-6q+1)^2}+\frac{1}{(6q+1)^2}+\frac{1}{(-12q+1)^2}+\frac{1}{(12q+1)^2}+\frac{0.786}{(6q)^2}\right] \tag{22}$$

when β is an even number and

$$\sum_{\nu=\nu_{sl}}\left(\frac{k_{dpn'}}{\nu}\right)^2=\frac{1}{\beta^2}k^2_{dp(n'=p)}\times\left[\frac{1}{(-6q+1)^2}+\frac{1}{(6q+1)^2}+\frac{1}{(-12q+1)^2}+\frac{1}{(12q+1)^2}+\frac{0.786}{(6q)^2}\right] \tag{23}$$

when β is an odd number. Here is

$$k_{d(n'=p)}=\frac{\sin 30°}{N\sin\frac{30°}{N}} \tag{24}$$

and

$$k_{p(n'=p)}=\sin\frac{Z}{mq}\frac{\pi}{2}=\sin\frac{Z}{q}30° \tag{25}$$

Z is the coil width in slot pitches.

For the harmonics of lower order than the slot harmonics of first order, formulas 4 to 7 and also Calvert's Tables[3] have been used.

The results for the more frequently used numbers of slots per pole per phase are given in Table I. The third column does not include the subharmonics; however, the fourth column does.

It has been shown that the harmonics of lower order are damped by a squirrel cage more than the harmonics of higher order. This is especially true of the subharmonics; a squirrel cage winding in the induction motor or a damper winding in the synchronous machine damps out these harmonics practically entirely. Because of the high speed of the subharmonics, they are damped considerably by parasitic currents even when there is no squirrel cage or damper winding in the rotor. For the calculation of the harmonic leakage reactance, the subharmonics therefore can be omitted. This is also in agreement with the tests.

Figure 1 gives the sums of equations 17 and 18 without the subharmonics as function of the throw W/τ. The values for $q=2$, 3, and 4 are taken from Figure 1 of reference 1. It can be seen that the curves for fractional-slot windings have the same characteristics as those for integral-slot windings. The ratio between the sums for the same value of W/τ approximately is equal to the inverse ratio of the square of q, and so Figure 1 of reference 1 can be used in order to determine the sum for fractional-slot windings with $q>3\frac{1}{2}$.

Damping of Harmonics by Squirrel Cage Winding

The case of an induction motor with squirrel cage rotor or of a salient pole synchronous machine with damper winding will be considered now. Here the rotor harmonics which correspond to $K_2=0$ (see reference 1) damp the corresponding stator harmonics, thus reducing the leakage reactance. It has been shown there that the damping factor of the n'-th harmonic is

$$\dot{D}_{n'}=1-\frac{js_{n'}X_{mn'}}{r_{2n'}+js_{n'}X_{mn'}(1+\tau_{2n'})} \tag{26}$$

or

$$\dot{D}_{n'}=1-\dot{C}_{n'}\underline{/\theta} \tag{27}$$

where

$$C_{n'}=\frac{\sqrt{[(s_{n'}X_{mn'})^2(1+\tau_{2n'})]^2+(s_{n'}X_{mn'}r_{2n'})^2}}{r_{2n'}{}^2+[s_{n'}X_{mn'}(1+\tau_{2n'})]^2} \tag{28}$$

and

$$\tan\theta=\frac{r_{2n'}}{s_{n'}X_{mn'}(1+\tau_{2n'})} \tag{29}$$

The absolute value of $D_{n'}$ is

$$D_{n'}=\sqrt{(1-C_{n'}\cos\theta)^2+(C_{n'}\sin\theta)^2} \tag{30}$$

Table I

q	W/τ	$\beta^2\sum\left(\frac{k_{dnp'}}{\nu}\right)^2_{\nu\neq\frac{\beta}{2}}$ Without Subharmonics	$\beta^2\sum\left(\frac{k_{dpn'}}{\nu}\right)^2_{\nu\neq\frac{\beta}{2}}$ Including Subharmonics
1 1/2	0.890	0.0403	0.0426
	0.667	0.0397	0.0392
2 1/2	0.933	0.0153	0.0153
	0.800	0.0139	0.0139
1 3/4	0.953	0.0314	0.0488
	0.760	0.0264	0.0383
2 1/4	0.890	0.0175	0.0283
	0.740	0.0158	0.0237
2 3/4	0.969	0.0139	0.0212
	0.850	0.0114	0.0174
1 7/8	0.890	0.0263	0.0447
	0.712	0.0246	0.0366
2 3/8	0.983	0.0207	0.0253
	0.842	0.0184	0.0221
2 7/8	0.928	0.0124	0.0208
	0.812	0.0120	0.0187
1 2/5	0.954	0.0570	0.0680
	0.714	0.0495	0.0529
1 4/5	0.926	0.0297	0.0474
	0.742	0.0256	0.0372
2 1/5	0.910	0.0188	0.0308
	0.758	0.0167	0.0251
1 5/7	0.972	0.0354	0.0522
	0.778	0.0281	0.0402
2 2/7	0.874	0.0175	0.0272
	0.730	0.0164	0.0237
2 6/7	0.933	0.0119	0.0201
	0.817	0.0105	0.0172
1 7/11	0.815	0.0299	0.0369
	0.612	0.0240	0.0283
2 1/11	0.958	0.0255	0.0399
	0.798	0.0320	0.0347
2 7/11	0.885	0.0155	0.0186
	0.760	0.0138	0.0152
1 11/13	0.903	0.0271	0.0452
	0.723	0.0245	0.0371
2 4/13	0.867	0.0173	0.0260
	0.723	0.0156	0.0223
2 10/13	0.964	0.0135	0.0216
	0.842	0.0112	0.0177

It has been shown in reference 1 that there will not be a sensible error when equation 30 is used instead of equation 26.

When $r_{2n'}$ can be neglected,

$$D_{n'}=1-\frac{1}{1+\tau_{2n'}} \tag{31}$$

and when, besides $r_{2n'}$, the slot leakage and the end-winding leakage also can be neglected comparatively with harmonic leakage,

$$D_{n'}=1-(\xi_{2n'}\eta_{2n'})^2 \tag{32}$$

where $\xi_{2n'}$ is the coupling factor of the rotor with respect to the n'-th harmonic and $\eta_{2n'}$ is the skew factor.

As an example, a 350-horsepower 60-cycle, 3-phase synchronous motor with 28 poles will be considered. $Q_1=144$, $q_1=1^5/_7$, $Q_2=5\times28=140$, $W/\tau=0.788$. The damper winding consists of five round bars per pole, three of them of copper, two of bronze with the resistivity two. The poles are not skewed. The motor will be considered at standstill ($s=s_{n'}=1$) and running with normal speed ($s=0_1$ $s_{n'}=$variable).

Table II gives the values of the rotor constants as well as of $C_{n'}$, tan θ, and $D_{n'}$ for standstill ($s_{n'}=1$). Table II gives the same values for synchronous speed ($s_{n'}$ variable). The skin-effect has been neglected and thus both tables have the same values for $r_{2n'}$ and $\tau_{(s+\epsilon)n'}$.

The examination of the tables shows that they have the same character as those for integral slot windings[1] and that the influence of the resistance is small.

A comparison between the last two columns shows that the slot leakage and the end-winding leakage cannot be neglected despite the fact that the harmonic leakage is relatively large here because of the small number of slots per pole of the rotor.

The total damping factor is

$$D_t=\frac{\frac{\beta^2}{4}\sum\left(\frac{k_{dpn'}}{\nu}\right)^2 D_{n'}}{\frac{\beta_2}{4}\sum\left(\frac{k_{dpn'}}{\nu}\right)^2} \qquad \nu\neq\frac{\beta}{2} \tag{33}$$

when β is an even number and

$$D_t=\frac{\beta^2\sum\left(\frac{k_{dpn'}}{\nu}\right)^2 D_{n'}}{\beta^2\sum\left(\frac{k_{dpn'}}{\nu}\right)^2} \qquad \nu\neq\beta \tag{34}$$

when β is an odd number. The denominators of these equations are given in Table I and Figure 1.

The evaluation of equation 34 for the example considered above gives the same value for standstill and for running with synchronous speed, namely, $D_t=0.92$. For the slot harmonics of first order, the factors $D_{n'}$, from Tables II and III have been used. For higher slot harmonics, it has been assumed that $D_{n'}$ equals one and equations 22 and 23 have been applied.

The motor in question has a throw equal to 0.788. The factor D_t has been determined for the throw 0.972 also and has been found to be practically the same as for the throw 0.788. This is in accordance with the results obtained for the integral-slot windings with $q=2$. Also, there the chording has little influence on the damping.

Influence of Slot Openings and Shape of Magnetomotive Force Curve on Harmonic Leakage

The previous considerations are based upon the assumption that the slot-openings reduce all field harmonics in the ratio of one to K_c. It is shown in Appen-

Table II. Standstill

ν	n'	$s_{n'}$	$X_{mn'}$	$r_{2n'}$	$\tau_{(s+\epsilon)n'}$	$\tau_{hn'}$	$\tau_{2n'}$	tan θ	$C_{n'}$	$D_{n'}$	$D_{n'}$ for $r_{2n'}=0$	$D_{n'}$ for $r_{2n'}=0$ and $\tau_{(s+\epsilon)n'}=0$
1	+ 2	1	1,304×10⁻⁴	9.01×10⁻⁴	0.0082	0.005	0.0132	0.0068	0.988	0.0138	0.013	0.005
5	− 10	1	52.	1.66	0.0715	0.02	0.0915	0.0293	0.920	0.090	0.0837	0.0196
11	− 22	1	10.72	1.43	0.332	0.047	0.379	0.0967	0.723	0.288	0.275	0.045
13	+ 26	1	7.68	1.41	0.46	0.064	0.524	0.120	0.652	0.361	0.344	0.060
17	− 34	1	4.49	1.39	0.785	0.111	0.896	0.164	0.523	0.49	0.472	0.10
19	+ 38	1	3.6	1.39	0.975	0.156	1.131	0.181	0.468	0.556	0.531	0.135
23	− 46	1	2.46	1.38	1.43	0.196	1.626	0.214	0.377	0.635	0.619	0.164
25	+ 50	1	2.08	1.38	1.69	0.235	1.925	0.226	0.336	0.675	0.658	0.191
35	− 70	1	1.06	1.375	3.3	0.535	3.83	0.269	0.200	0.81	0.794	0.359
49	+ 98	1	0.541	1.37	6.48	1.47	7.95	0.283	0.109	0.895	0.889	0.595
65	−130	1	0.307	1.375	11.42	4.55	15.97	0.265	0.057	0.945	0.941	0.82
75	+150	1	0.208	1.38	16.92	17.86	34.78	0.187	0.0272	0.972	0.971	0.947

dix I that this assumption is not true of the slot-harmonics. Depending upon the number of slots per pole and the coil pitch, one of the slot-harmonics of first or second order may be increased by the slot-openings while the other slot-harmonic of the same pair is decreased. It is even possible that both slot-harmonics of the first or second order are increased by the slot-openings. Further, the influence of the slot-openings on the slot-harmonics of higher order than two is negligible. This shows that the division of all harmonics by the Carter factor (equation 13) leads to too small a value of the harmonic leakage, the error being larger the larger the ratio of slot-opening to slot pitch and of slot-opening to air gap, that is, the error being larger for open slots than for semiopen slots.

On the other hand, it is shown in Appendix II that the calculation with the stepped magnetomotive force curve, based upon the assumption that the ampere conductors of each slot are concentrated in the middle of the slot, leads to too large amplitudes of the slot-harmonics and, therefore, to a too large value of the harmonic leakage, the error being again larger the larger the slot-opening.

The error caused by the division of all harmonics by the Carter factor and the error caused by the assumption of the stepped shape for the magnetomotive force curve are thus of opposite sense, one decreasing the slot harmonics and the harmonic leakage, the other increasing them.

Conclusion

Experience shows that Figure 1 (as well as Figure 1 of reference 1) yields good practical results for the differential (harmonic) leakage, that is, results which agree with tests. Since these figures do not take into account the damping of the harmonics by the rotor and are based upon the assumptions that the slot-openings reduce equally all harmonics and that the magnetomotive force curve has a stepped shape, their good agreement with tests means that the error caused by the division of all harmonics by the Carter factor is approximately equal and opposite to the errors caused by the neglect of damping and the assumption of the stepped magnetomotive force curve.

Since the differential (harmonic) leakage constitutes only a part of the total leakage, the use of a simple, although not entirely exact method of calculation of this leakage, is justified.

Appendix I. Influence of the Slot Openings on the Differential Leakage

The stator of an induction motor will be considered. The results obtained apply also to the rotor.

The n'-th harmonic of the magnetomotive force curve is

$$f_{n'} = F_{n'} \sin\left(\omega t - n'\frac{\pi}{p_\tau}x\right) \tag{35}$$

$$F_{n'} = \frac{\sqrt{2}}{\pi} m_1 N_1 \frac{k_{dpn'}}{n'} I_1 \tag{36}$$

The n'-th field harmonic has been derived from this (see equation 13) by multiplying with

$$\frac{3.19}{gK_{c1}K_{c2}K_s}$$

where the Carter factors K_{c1} and K_{c2} have to take care of the influence of the slot-openings of stator and rotor. This yields for n'-th field harmonic

$$b_{n'} = \frac{3.19}{gK_{c1}K_{c2}K_s} F_{n'} \sin\left(\omega t - n'\frac{\pi}{p_\tau}x\right) \tag{37}$$

In order to determine more accurately the influence of the slot-openings, the gap permeance will be introduced[4] in accordance with the assumption that the fundamental has two poles, as

$$\left(\frac{1}{g}\right)_{eff} = \frac{1}{g}\left[1 + \epsilon_1 \cos Q_1\frac{\pi}{p_\tau}x + \epsilon_2 \times \cos 2Q_1\frac{\pi}{p_\tau}x + \dots\right] \tag{38}$$

The n'-th field harmonic becomes

$$b_{n'} = \frac{3.19}{gK_s} F_{n'} \sin\left(\omega t - n'\frac{\pi}{p_\tau}x\right) \times \left[1 + \epsilon_1 \cos Q_1\frac{\pi}{p_\tau}x + \epsilon_2 \cos 2Q_1\frac{\pi}{p_\tau}x + \dots\right] \tag{39}$$

With the abbreviation

$$\frac{3.19}{gK_s} F_{n'} = A_{n'} \tag{40}$$

there is

$$b_{n'} = A_{n'} \sin\left(\omega t - n'\frac{\pi}{p_\tau}x\right) + A_{n'}\sum_{c=1,2,3\dots}\epsilon_c \times \cos\left(cQ_1\frac{\pi}{p_\tau}x\right) \times \sin\left(\omega t - n'\frac{\pi}{p_\tau}x\right)$$

or

$$b_{n'} = A_{n'} \sin\left(\omega t - n'\frac{\pi}{p_\tau}x\right) + A_{n'}\sum_{c=1,2,3\dots}\frac{\epsilon_c}{2} \times \left\{\sin\left[\omega t + (cQ_1 - n')\frac{\pi}{p_\tau}x\right] + \sin\left[\omega t - (cQ_1 + n')\frac{\pi}{p_\tau}x\right]\right\} \tag{41}$$

Thus, because of the slot-openings of the stator, the n'-th stator harmonic produces a series of pairs of traveling waves. One wave of each pair travels in the direction of rotation, the other in opposite direction. Their respective velocities with regard to the stator are

$$\frac{p}{cQ_1 + n'}\frac{\tau}{\pi}\omega \text{ and } \frac{p}{cQ_1 - n'}\frac{\tau}{\pi}\omega \qquad c = 1, 2, 3\dots \tag{42}$$

These slot-opening waves may influence considerably those field harmonics with respect to which they are at standstill. Their influence on all other harmonics will be relatively small and can be taken care of by introducing the Carter factor, that is, by introducing in the denominator of equation 40 the factor K_{c1}.

The latter statement applies also to the influence of the rotor slot-openings on the stator harmonics, since the waves produced by them move with respect to the stator harmonics. Therefore, considering the stator

Table III. Synchronous Speed

p	n'	$s_{n'}$	$X_{mn'}$	$r_{2n'}$	$r_{(s+e)n'}$	$r_{hn'}$	$r_{2n'}$	tan θ	$C_{n'}$	$D_{n'}$	$D_{n'}$ for $r_{2n'}=0$	$D_{n'}$ for $r_{2n'}=0$ and $x_{(s+e)n'}=0$
1	+ 2	+ 0.857	1,304×10⁻⁴	9.01×10⁻⁴	0.0082	0.005	0.0132	0.0079	0.986	0.016	0.0128	0.005
5	− 10	+ 1.715	52.	1.66	0.0715	0.02	0.0915	0.0171	0.915	0.085	0.0837	0.0196
11	− 22	+ 2.57	10.72	1.43	0.332	0.047	0.379	0.376	0.727	0.276	0.275	0.045
13	+ 26	− 0.86	7.68	1.41	0.46	0.064	0.524	0.14	0.654	0.354	0.344	0.060
17	− 34	+ 3.43	4.49	1.39	0.785	0.111	0.896	0.0467	0.530	0.475	0.472	0.10
19	+ 38	− 1.72	3.6	1.39	0.975	0.156	1.131	0.105	0.470	0.535	0.531	0.135
23	− 46	+ 4.29	2.46	1.38	1.43	0.196	1.626	0.0496	0.377	0.624	0.619	0.164
25	+ 50	− 2.57	2.08	1.38	1.69	0.235	1.925	0.085	0.345	0.658	0.658	0.191
35	− 70	+ 6.0	1.06	1.375	3.3	0.535	3.83	0.0448	0.207	0.794	0.794	0.359
49	+ 98	− 6.0	0.541	1.37	6.48	1.47	7.95	0.047	0.111	0.889	0.889	0.595
65	−130	+10.3	0.307	1.375	11.42	4.55	15.97	0.0257	0.059	0.941	0.941	0.82
75	+150	−10.3	0.208	1.38	16.92	17.86	34.78	0.0182	0.028	0.971	0.971	0.947

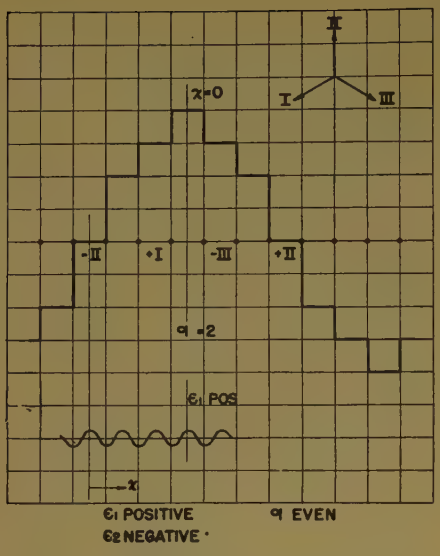


Figure 4. Determination of the signs of ϵ_1 and ϵ_2 for q = even number

harmonics, the factor K_{c2} has to be introduced in equation 40.

Now the stator field harmonics have to be determined, the velocities of which are given by equation 42. These stator field harmonics will be increased or reduced considerably by the slot-opening waves.

The n'-th stator harmonic has with respect to the stator the speed

$$v_{n'}=\frac{p}{n'}\frac{\tau}{\pi}\omega \tag{43}$$

Since the order of the stator slot-harmonics is given by the equation

$$n'_{sl}=\mp kQ_1+p \tag{44}$$

it follows that the slot-opening waves produced by the synchronous wave ($n'=p$) are at standstill with respect to the slot-harmonics and these are the only waves which are at standstill with respect to each other. It follows further from equations 42 and 44 that the slot-opening wave of the order $c=1$ is at standstill with respect to the slot-harmonic of first order ($k=1$), that the slot-opening wave of the order $c=2$ is at standstill with respect to the slot-harmonic of second order ($k=2$), and so on.

Usually only the slot-opening waves of the orders $c=1$ and $c=2$ have to be taken into account. From equation 41

$$b'_{so}=A_{(n'=p)}\frac{\epsilon_c}{2}\sin\left[\omega t-(cQ_1+p)\frac{\pi}{p\tau}x-\psi\right]\frac{I_m}{I_1} \tag{45}$$

and

$$b''_{so}=A_{(n'=p)}\frac{\epsilon_c}{2}\sin\left[\omega t+(cQ_1-p)\frac{\pi}{p\tau}x+\psi\right]\frac{I_m}{I_1} \tag{46}$$

where I_m is the magnetizing current. $A_{(n'=p)}$ is proportional to the primary current I_1. The factor I_m/I_1 takes into account the fact that the amplitude of the slot-opening waves is proportional to the resultant synchronous wave, that is, to the synchronous wave produced by the primary and secondary magnetomotive force together (I_m). The angle has to be introduced because I_m is not in phase with I_1.

The slot harmonics are

$$b'_{sl}=A_{(n'=cQ_1+p)}\sin\left[\omega t-(cQ_1+p)\frac{\pi}{p\tau}x\right] \tag{47}$$

$$b''_{sl}=A_{(n'=-cQ_1+p)}\sin\left[\omega t+(cQ_1-p)\frac{\pi}{p\tau}x\right] \tag{48}$$

The ratio between the amplitudes of the two waves which travel in the direction of rotation is

$$r'=\frac{A_{(n'=p)}}{A_{(n'=cQ_1+p)}}\frac{I_m}{I_1}\frac{\epsilon_c}{2}=\left[\frac{k_{d(n'=p)}}{k_{d(n'=cQ_1+p)}}\right]\left[\frac{k_{p(n'=p)}}{k_{p(n'=cQ_1+p)}}\right]\times\frac{cQ_1+p}{p}\frac{I_m}{I_1}\frac{\epsilon_c}{2} \tag{49}$$

and the ratio between the amplitudes of the two waves which travel opposite to the direction of rotation is

$$r''=\frac{A_{(n'=p)}}{A_{(n'=-cQ_1+p)}}\frac{I_m}{I_1}\frac{\epsilon_c}{2}=\left[\frac{k_{d(n'=p)}}{k_{d(n'=-cQ_1+p)}}\right]\left[\frac{k_{p(n'=p)}}{k_{p(n'=-cQ_1+p)}}\right]\times\frac{cQ_1-p}{p}\frac{I_m}{I_1}\frac{\epsilon_c}{2} \tag{50}$$

The ratio I_m/I_1 as well as the angle ψ depend on the speed of the machine. For the induction motor it is approximately

$$\left.\begin{aligned}&\frac{I_m}{I_1}=0.08\text{ to }0.2\\&\psi=15^\circ\text{ to }25^\circ\end{aligned}\right\}\text{ at standstill} \tag{51}$$

$$\left.\begin{aligned}&\frac{I_m}{I_1}=0.22\text{ to }0.6\\&\psi=78^\circ\text{ to }55^\circ\end{aligned}\right\}\text{ at high speed} \tag{52}$$

The first value refers to machines with a low number of poles, the second to machines with a high number of poles. For the synchronous motor, $I_m/I_1\backsimeq 0.35$ at standstill and $I_m/I_1\backsimeq 0.8$ to 1.1 at high speed; ψ is for both cases approximately 25 degrees.

Further, for integral-slot windings

$$\left.\begin{aligned}&\frac{k_{d(n'=p)}}{k_{d('n=\pm cQ_1+p)}}=\begin{matrix}-1(c=1)\\+1(c=2)\end{matrix}\\&\text{when } q \text{ is even}\\&\frac{k_{d(n'=p)}}{k_{d(n'=\pm cQ_1+p)}}=\begin{matrix}+1(c=1)\\+1(c=2)\end{matrix}\\&\text{when } q \text{ is odd}\end{aligned}\right\} \tag{53}$$

and for fractional-slot windings[2]

$$\left.\begin{aligned}&\frac{k_{d(n'=p)}}{k_{d(n'=\pm cQ_1+p)}}=\begin{matrix}+1(c=1)\\-1(c=2)\end{matrix}\\&\text{when } P \text{ is even}\\&\frac{k_{d(n'=p)}}{k_{d(n'=\pm cQ_1+p)}}=\begin{matrix}+1(c=1)\\+1(c=2)\end{matrix}\\&\text{when } P \text{ is odd and } \beta \text{ is even}\\&\frac{k_{d(n'p=p)}}{k_{d(n'=\pm cQ_1+p)}}=\begin{matrix}-1(c=1)\\+1(c=2)\end{matrix}\\&\text{when } P \text{ is odd and } \beta \text{ is odd}\end{aligned}\right\} \tag{54}$$

For the ratio of the pitch factors,

$$\frac{k_{p(n'=p)}}{k_{p(n'=\pm cQ_1+p)}}=\pm 1\text{ or }\mp 1 \tag{55}$$

that is, when one slot-harmonic has the plus sign, the other slot-harmonic of the same pair has the minus sign.

The magnitude of ϵ_1 depends upon the ratio between slot-opening and slot pitch and upon the ratio between slot-opening and gap. There is[5]

$$\epsilon=K_\nu\delta K_c \tag{56}$$

The factor K_ν takes into account the ratio between slot-opening and slot pitch; its value for $c=1$ and $c=2$ is given in Figure 2. δ takes into account the ratio between slot-opening and air gap; its value is given in Figure 3. $K_c=K_{c1}K_{c2}$ is the Carter factor. For open slots, $\epsilon_1=0.5$ to 0.7 and ϵ_2 is negligible; for semi-open slots $\epsilon_1=0.05$ to 0.25 and $\epsilon_2=0.05$ to 0.15.

In order to find the sign of ϵ_1 with respect to the synchronous wave, consider Figures 4 and 5, which relate to integral-slot windings with $q=2$ and $q=3$. It can be seen that ϵ_1 is positive for even and negative for odd values of q, while ϵ_2 is negative for even as well as odd values of q.

Because of the slot-opening waves produced by the synchronous wave ($n'=p$), one slot-harmonic of a pair may be decreased and the other increased, or both slot-harmonics of the pair may be decreased or increased. Whether the harmonic is decreased or increased depends upon the number of slots per pole and upon the coil pitch, that is, upon the sign of the pitch factor.

Equations 51 and 52 show further that the influence of the slot-openings depends upon the speed of the machine. The harmonic (differential) leakage is therefore not a constant; it changes with the speed of the machine.

As example the stator harmonics of an 800-horsepower 8-pole induction motor with open slots will be considered.

For this machine

$$\frac{b_s}{g}=\frac{0.415}{0.055}=7.49$$

$$\frac{b_s}{\tau_s}=\frac{0.415}{0.789}=0.527$$

From Figures 2 and 3,

$$K_{\nu_1}=1.06\qquad K_{\nu_2}=0.14\qquad \delta=0.37$$

The Carter factor is equal to 1.46. Therefore,

$$\frac{\epsilon_1}{2}=1.06\times 0.37\times 1.46\times 0.5=0.286$$

Further,

$$\frac{I_m}{I_1}=0.239\text{ at full speed}$$

$$\frac{I_m}{I_1}=0.06\text{ at standstill}$$

For the machine under consideration,

$$q=5\qquad \frac{W}{\tau}=0.733$$

Hence,

$$\frac{k_{d(n'=p)}}{k_{d(n'=\pm q_1+p)}}=+1$$

and

$$\frac{k_{p(n'=p)}}{k_{p(n'=q_1+p)}}=-1 \qquad \frac{k_{p(n'=p)}}{k_{p(n'=-q_1+p)}}=+1$$

It follows from equations 39 and 40 for the slot harmonics of first order,

$$r'=(+1)(-1)\frac{120+4}{4}\times 0.239\times(-0.286)=+2.12 \text{ at full speed}$$

$$r''=(+1)(+1)\frac{120-4}{4}\times 0.239\times(-0.286)=-1.98 \text{ at full speed}$$

$$r'=+2.12\frac{0.06}{0.239}=+0.532 \text{ at standstill}$$

$$r''=-1.98\frac{0.06}{0.239}=-0.497 \text{ at standstill}$$

From the two waves of first order produced by the slot-openings, one, which travels with the rotation, has a sign opposite to the corresponding slot-harmonic, while the other, which travels opposite to the direction of rotation, has the same sign as the corresponding slot-harmonic. At standstill, the slot-harmonic that has the same direction of rotation as the synchronous wave is reduced by approximately 50 per cent while the other slot-harmonic is increased by approximately the same amount. The influence of the slot-openings on the slot-harmonics of second order is small here because of the open slots. It should be noted that the influence of the slot-openings on the slot-harmonics of first order is much smaller than in the considered example when the slots are semi-closed. However, in this case the slot-harmonics of second order are more influenced than in the case of open slots.

In the calculation of the harmonic (differential) leakage (equation 13), the influence of the slot-openings has been taken care of by dividing the amplitudes of the harmonics by the Carter factor, that is, by calculating with an increased gap. It follows from the results obtained above that the division by the Carter factor is correct only for the harmonics of lower order but not for the slot-harmonics.

Appendix II. Influence of the Shape of the Magnetomotive Force Curve

The foregoing considerations are based on the assumption that the magnetomotive force has the stepped shape, that is, that the magnetomotive force of a single coil is a rectangle and that the magnetomotive force changes in the center of each slot abruptly. This assumption is not correct. Flux maps indicate that it would be more correct to assume that, because of the slot-opening, the magnetomotive force of each single coil is not a rectangle but a trapezoid, as shown in Figure 6. This yields for the n'-th harmonic of an unchorded 3-phase integral-slot winding[6]

$$f_{n'}=\frac{3\sqrt{2}}{\pi}N_{ph}I\frac{k_{dn'}}{n'}\frac{\sin n'\alpha/2}{n'\alpha/2}\times \sin\left(\omega t\mp n'\frac{\pi}{p\tau}x\right) \quad (57)$$

where

$$\alpha=\frac{b_s}{p\tau}\pi \quad (58)$$

For the rectangular shape (equations 35 and 36)

$$f_{n'}=\frac{3\sqrt{2}}{\pi}N_{ph}I\frac{k_{dn'}}{n'}\sin\left(\omega t\mp n'\frac{\pi}{p\tau}x\right) \quad (59)$$

Thus, the assumption of a trapezoidal shape introduces the factor

$$k_0=\frac{\sin n'\alpha/2}{n'\alpha/2} \quad (60)$$

Since α is a small angle, this factor will not influence the harmonics of lower order, but it will reduce the slot harmonics considerably, especially those of higher order. The harmonic (differential) leakage reactance that is built up by the sum of the leakage reactances of all harmonics, therefore, will be reduced also. The reduction caused by the trapezoid shape of the magnetomotive force will be larger the smaller the number of slots per pole per phase q, since $n'\alpha$ increases with decreasing q.

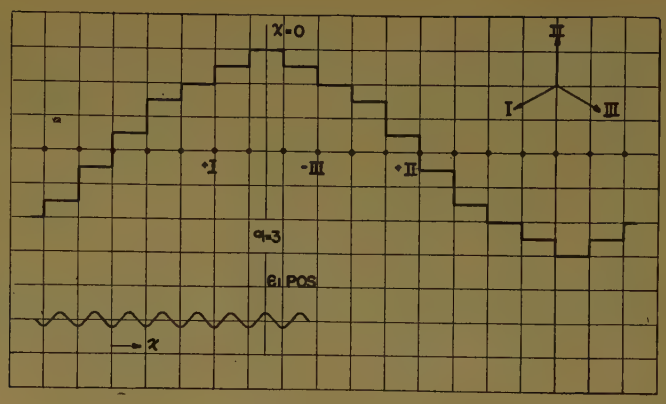


Figure 5. Determination of signs of ϵ_1 and ϵ_2 for q = odd number

ϵ_1 negative
ϵ_2 negative

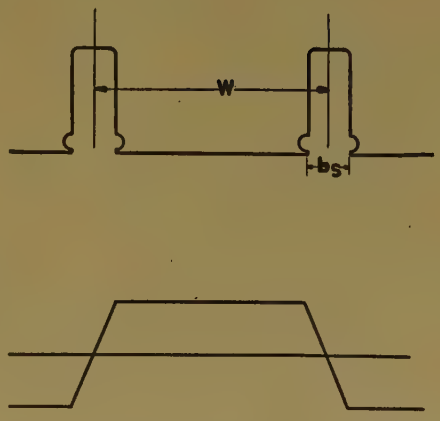


Figure 6. Shape of the magnetomotive force of a single coil in open slots

On the basis of equation 57, the harmonic leakage reactance of an unchorded 3-phase integral-slot winding becomes

$$x_h=\frac{4}{\pi^2}mN_{ph}^2pf_1l\times 10^{-7}\sum\left(\frac{k_{dn'}}{n'}\right)^2\times \frac{\sin n'\alpha/2}{p\alpha/2}\coth\left(n'\frac{\pi g}{p\tau}\right) \quad (61)$$

For the rectangular shape of the magnetomotive force

$$x_h=\frac{4}{\pi^2}m\frac{N_{ph}^2}{p}f_1l_i\frac{\tau}{gK_cK_s}10^{-7}\sum\left(\frac{k_{dn'}}{n'}\right)^2 \quad (62)$$

While the evaluation of the sum in equation 61 is very tedious, the sum in equation 62 can be expressed by a simple formula. For this reason the calculation with the step-shaped magnetomotive force is preferred.

In the specific case of equation 61, that is, for unchorded 3-phase integral-slot windings, the following approximate formula applies:

$$x_h=4.0\frac{N_{ph}^2}{p}f_1l10^{-7}\frac{\frac{\tau}{g'}+4q}{1{,}000}\left(0.6+\frac{b_i}{\tau_s}\frac{6.5-0.6q}{q-1.2}\right) \quad (63)$$

g' is equal to the gap, g, times the Carter factor of the opposite slot.

The results obtained from equations 62 and 63 will be compared for two machines with different numbers of slots per pole per phase.

1. Six-hundred-horsepower induction motor considered in Appendix I: For this machine

$m=3$ $N_{ph}=80$ $p=4$ $f_1=60$ $\tau=11.81$
$l=11$ $l_i=10$ $\tau_s=0.789$ $b_s=0.415$
$g=0.055$ $K_{c1}=1.464$ $K_{c2}=1.047$
$K_s\backsimeq 1.05$ $q=5$ $\sum\left(\frac{k_{dn}}{n}\right)^2=0.0059$

$\left(\text{for } \frac{W}{\tau}=1\right)$

It follows from equation 62

$$x_h=\frac{4}{\pi^2}3\frac{80^2}{4}60\times 10\times \frac{11.81}{0.055\times 1.464\times 1.047\times 1.05}\times 0.0059\times 10^{-7}=0.0873 \text{ ohm/phase}$$

and from equation 63

$$x_h = 4\frac{80^2}{4}60\times11\frac{\dfrac{11.81}{0.055\times1.047}+4\times5}{1{,}000}\times\left(0.6+\frac{0.374}{0.789}\frac{6.5-0.6\times5}{5-1.2}\right)10^{-7}$$

$$=0.098 \text{ ohm/phase}$$

2. Twelve-hundred-horsepower 26-pole induction motor with open slots: For this motor

$m=3 \quad N_{ph}=195 \quad p=13 \quad f_1=60 \quad \tau=8.12$
$l=24 \quad l_i=21 \quad \tau_s=0.901 \quad b_s=0.47 \quad g=0.065$
$K_{c1}=1.447 \quad K_{c2}=1.025 \quad K_s\backsimeq1.05 \quad q=3$

$$\sum\left(\frac{k_{dn}}{n}\right)^2=0.0129\left(\text{for } \frac{W}{\tau}=1\right)$$

It follows from equation 62

$$x_h=\frac{4}{\pi^2}3\frac{150^2}{13}60\times21\times\frac{8.12}{0.065\times1.447\times1.025\times1.05}\times0.0129\times10^{-7}=0.275 \text{ ohm/phase}$$

and from equation 63

$$x_h=4\frac{150^2}{13}60\times24\frac{\dfrac{8.12}{0.065\times1.025}+4\times3}{1{,}000}\times\left(0.6+\frac{0.431}{0.901}\frac{6.5-0.6\times3}{3-1.2}\right)10^{-7}$$

$$=0.247 \text{ ohm/phase}$$

The values of the harmonic leakage obtained from equation 62, that is, on the basis of the stepped shape of the magnetomotive force curve, are about 10 to 15 per cent higher than those obtained from equation 63, that is, on the basis of the trapezoidal shape of the magnetomotive force curve. In the considered examples, q is equal to three and five, respectively. The difference between the results yielded by equations 62 and 63 becomes larger for values of q smaller than three; further, it is smaller for semi-open slots than for open slots; but in all cases the harmonic leakage obtained on the basis of the stepped shape of the magnetomotive force curve is larger than its real value.

Nomenclature

b_s = slot width at the gap
b_t = tooth width at the gap
c = order of the slot-opening wave
D = damping factor
f_1 = line frequency
f = magnetomotive force, instantaneous value
F = magnetomotive force, amplitude
g = air gap
I = current
k_d = distribution factor
k_p = pitch factor
K_c = Carter factor
K_s = saturation factor
k = order of the slot-harmonic
l_i = ideal core length
l = total core length
m = number of phases
n' = order of stator harmonics with respect to a fundamental whose wave length is equal to the circumference of the armature
$\left(n=\frac{n'}{p}\right)$ = order of the stator harmonic with respect to the synchronous wave
n'_{sl} = order of the slot harmonics
n_c = number of conductors in series per slot
N = numerator of the fraction $q=N/\beta$, that is, number of slots per phase in β poles
N_{ph} or N_1 = number of turns per phase
p = number of pole pairs
P = smallest integer which makes d in the equation $d=(3NP+1)/\beta$ an integer
Q = total number of slots
$\left(q=\frac{N}{\beta}\right)$ = number of slots per phase per pole
r_2 = resistance of the rotor per bar
s = slip of the rotor with respect to the synchronous wave
$s_{n'}$ = slip of the rotor with respect to the n'-th stator harmonic
W = coil width (in units of the pole pitch)
X_m = reactance due to the main flux
x_h = differential (harmonic) leakage reactance per phase
Z = coil width in slot pitches
β = denominator of the fraction $q=N/\beta$
ϵ = amplitude of the slot-opening wave
η = skew factor
ξ = coupling factor of the squirrel cage rotor
τ = pole pitch of the synchronous wave
$\tau_{n'}$ = pole pitch of the n'-th harmonic
τ_s = slot pitch
τ_2 = total leakage coefficient of the rotor
$\tau_{(s+e)}$ = slot and end-winding leakage coefficient of the rotor
τ_h = differential leakage coefficient of the rotor
$\omega=2\pi f_1$

References

1. Differential Leakage With Respect to the Fundamental Wave and to the Harmonics, **M. M. Liwschitz.** AIEE Transactions, volume 63, 1944, October section, pages 1139–50. See also the bibliography to this paper containing 42 publications on the subject.

2. Distribution Factors and Pitch Factors of the Harmonics of a Fractional-Slot Winding, **M. M. Liwschitz.** AIEE Transactions, volume 62, 1943, October section, pages 664–6.

3. Amplitudes of Magnetomotive Force Harmonics for Fractional-Slot Windings of Three-Phase Machines, **J. F. Calvert.** *Iowa Engineering Experiment Station, Bulletin* 142, 1939.

4. The Theory of the Induction Motor With Squirrel Cage Rotor, **L. Dreyfus.** *Handlingar Number 34, Ingeniors Vedenskaps Akademiens* (Stockholm, Sweden), 1924.

5. Additional Losses in the Squirrel Cage Windings of Induction Motors and Synchronous Machines, **M. M. Liwschitz, H. Raymund.** *Scientific Publications of the Siemens Concern*, volume 14, 1935, page 16.

6. The Field in the Air Gap of Three-Phase Machines, **W. Putz.** *Institute of Technology*, (Berlin, Germany), 1933.

TRANSACTIONS SECTION

Preprint of Corresponding Pages From the Current Annual AIEE Transactions Volume

The Polyphase Commutator Regulator for Speed Control

A. G. CONRAD
MEMBER AIEE

F. E. BROOKS, JR.
ASSOCIATE AIEE

R. G. FELLERS
ASSOCIATE AIEE

Synopsis: This paper presents an explanation of the theory and explains the characteristics of an a-c adjustable-speed drive obtained by using a polyphase commutator regulator mechanically coupled to the shaft of a wound-rotor induction motor and electrically connected to its slip rings. The theoretical loci of the system current vectors with respect to the voltage vectors of the induction motor are developed in terms of the constants of the machines and the applied voltage. A method of determining the characteristics of the drive from no-load tests or from design data is presented. The characteristics predicted on these bases are in excellent agreement with those obtained experimentally.

SEVERAL methods have been employed to provide an a-c drive of large capacity with suitable adjustable-speed characteristics. The choice of the method used usually is dependent on the characteristics required by the load. One of the most satisfactory of these systems from the standpoint of speed control is obtained by supplying the primary of an induction motor from a balanced polyphase system and connecting its slip rings to a shunt-connected polyphase commutator regulator (see Figure 1).

The electrical circuit of the rotor of this regulating machine is similar to that of a d-c armature. It usually is designed for low voltage in order to obtain good commutation of the alternating currents supplied to it from the brushes. The spacing of the brushes on the commutator is determined by the number of phases on the motor rotor, that is on a 3-phase machine the angle between brushes is 120 electrical degrees. The stator or field winding of the regulator may be a normal distributed polyphase winding such as that found on a polyphase induction motor. However, for good commutation the main field windings usually are placed on salient poles between which interpoles can be provided. A compensating winding usually is placed on the stator and connected in series with the rotor or armature. The field may be designed for operation either in series or in shunt with the armature. The drive using the shunt connection is the more common and is the one which is discussed here. This connection is shown diagrammatically in Figure 1. A transformer bank normally is provided to control the voltage applied to the field winding and thereby control the speed. Excellent speed regulation can be obtained when shunt excitation of the regulator is employed. This drive is a constant horsepower device. For a given power input the torque available at the shaft is increased as the speed is adjusted to lower values.

The object of this paper is

(*a*). To develop the theory of operation of the adjustable-speed drive consisting of a wound-rotor induction motor and a shunt-connected polyphase commutator regulator.

(*b*). To obtain the expression for the primary current of the induction motor as a function of the phase voltage, the machine constants, and the slip.

(*c*). To present a method of predicting the characteristics of the drive from no-load readings taken experimentally on the machines, or from the design data of the machines employed.

Theory

When the stator, or field, winding of the polyphase commutator regulator is connected to a balanced polyphase supply, a rotating magnetic field is set up which induces a voltage in this winding which is essentially equal and opposite to the applied voltage. A voltage is induced in the conductors of the rotor also, unless it is rotating at synchronous speed in the same direction as the magnetic field. If the rotor is stationary the voltages in these conductors can be measured between brushes placed on the commutator. By proper distribution of these brushes on the commutator, these voltages can be made to form a balanced polyphase system of any desired number of phases. If the brushes are all shifted in one direction in unison, the voltages between them are unchanged in magnitude, but the time phase of these voltages with respect to the field voltage will be changed. In this way the time phase of the brush voltages may be so shifted that they directly oppose the voltages supplying the field, or the voltages normally supplied to the brushes. This is referred to as the zero

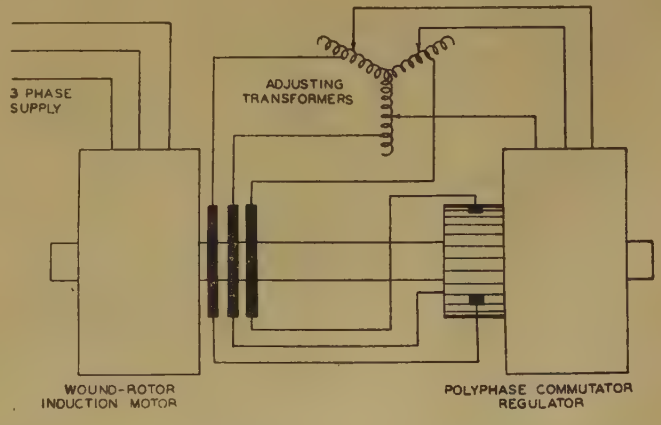


Figure 1. Complete circuit diagram of adjustable-speed drive

Paper 46-59, recommended by the AIEE committee on electric machinery for presentation at the AIEE winter convention, New York, N. Y., January 21–25, 1946. Manuscript submitted August 21, 1945; made available for printing December 4, 1945.

A. G. CONRAD is chairman, department of electrical engineering, Yale University, New Haven, Conn. F. E. BROOKS, JR., is assistant professor, department of electrical engineering, University of Texas, Austin, Tex. R. G. FELLERS is radio research engineer, Naval Research Laboratory, Washington, D. C.

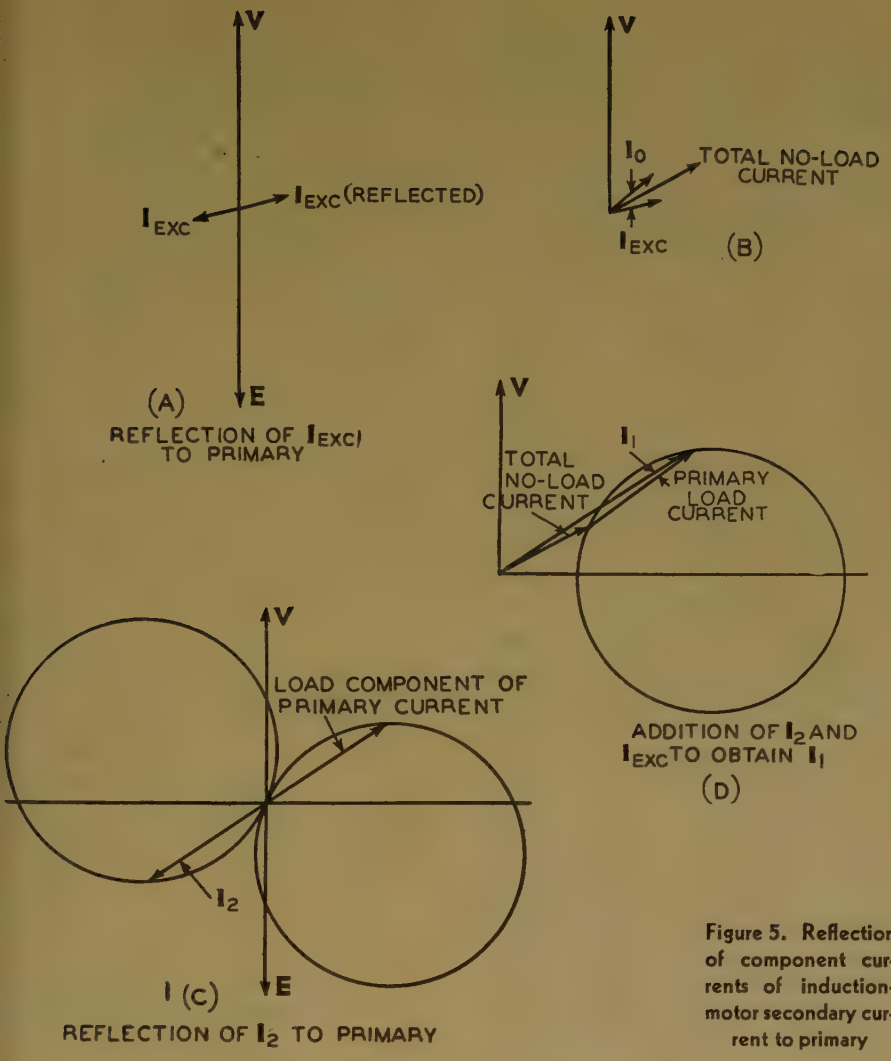


Figure 5. Reflection of component currents of induction-motor secondary current to primary

E_2 represents the voltage induced in one phase of the secondary of the induction motor. E_s is the voltage induced in one phase of the regulator field winding and it is proportional to the value of flux in the air gap and the frequency of the applied voltage. This applied voltage is of slip frequency, since it is the slip-ring voltage of the induction motor. Therefore, $E_s = k\phi s$, where s is the slip of the induction motor, ϕ is the air-gap flux of the polyphase commutator regulator, and k is a constant involving the number of turns, winding, and other factors, of the commutator regulator. The same flux generates the voltage in the armature, and if the armature is assumed to possess the same number of turns as the shunt field, the only difference between the expression for E_a, the armature circuit induced voltage, and E_s is in the manner in which slip occurs. It has been mentioned previously that the voltage appearing at the armature terminals is directly proportional to the speed of the machine, and therefore, $E_a = k\phi(1 - s)$.

By neglecting the effect of exciting current of the commutator machine flowing through the induction-motor secondary, making $Z_2 = R_2 + jsX_2$, $Z_a = R_a + jsX_a$, and letting a be the turns ratio of the transformer in the field circuit, the following circuit equations are obtained:

$$\boldsymbol{E}_2 - \boldsymbol{I}_2(Z_2 + Z_a) = (1-s)k\phi \qquad (1)$$

$$\boldsymbol{E}_2 - \boldsymbol{I}_2 Z_2 = ask\phi \qquad (2)$$

If the voltage induced in one phase of the induction-motor rotor at standstill is E, then E_2 is equal to sE and:

$$\boldsymbol{I}_2 = \frac{s^2(a+1)\boldsymbol{E} - s\boldsymbol{E}}{(a+1)sZ_2 - Z_2 + asZ_a} \qquad (3)$$

If the load component of the secondary current of the induction motor is calculated according to equation 3 for different values of slip, the locus of the extremity of the current vector with respect to the voltage $\boldsymbol{E}$ is of the form indicated by the curve in Figure 3. The operating range as a motor is indicated by the segment *ob* of the inner loop, where *o* represents the no-load point and *b* the standstill point. Although theoretically correct, this locus possesses the disadvantage that all of the constants of both the induction motor and the commutator machine must be known in order to calculate it, and this computation must be carried out point by point as the locus is not a simple geometric figure.

If the voltage drop caused by the current flowing through the resistance of the secondary circuit of the induction motor is neglected when setting up the voltage equation for the stator circuit of the regulating machine, a circle locus defining the vector $\boldsymbol{I}_2$ may be obtained which is a very good approximation of the theoretical curve in the operating range. When this assumption is made the voltage equations for the motor secondary take the following form:

$$\boldsymbol{E}_2 - \boldsymbol{I}_2(Z_2 + Z_a) = (1-s)k\phi \qquad (4)$$

$$\boldsymbol{E}_2 - j\boldsymbol{I}_2 sX_2 = ask\phi \qquad (5)$$

When $s\boldsymbol{E}$ is substituted for $\boldsymbol{E}_2$ and the two equations are solved for $\boldsymbol{I}_2$, the following result is obtained:

$$\boldsymbol{I}_2 = \frac{(a+1)s\boldsymbol{E} - \boldsymbol{E}}{a(R_2 + R_a) + jsa(X_2 + X_a) + jsX_2 - jX_2} \qquad (6)$$

For convenience, let $R_3 = a(R_2 + R_a)$ and $X_3 = a(X_2 + X_a) + X_2$. Then

$$\boldsymbol{I}_2 = \frac{s(a+1)\boldsymbol{E} - \boldsymbol{E}}{R_3 + j(sX_3 - X_2)}$$

By making use of the principle of superposition, the following component currents are obtained:

$$\boldsymbol{I}_2 = \boldsymbol{I}_x + \boldsymbol{I}_y \qquad (7)$$

In which

$$\boldsymbol{I}_x = \frac{s(a+1)\boldsymbol{E}}{R_3 + j(sX_3 - X_2)}$$

and

$$\boldsymbol{I}_y = \frac{-\boldsymbol{E}}{R_3 + j(sX_3 - X_2)}$$

The currents $\boldsymbol{I}_x$ and $\boldsymbol{I}_y$ are always in time phase opposition. They may be considered as currents flowing in the impedance, $R_3 + j(sX_3 - X_2)$, caused by voltages $s(a + 1)\boldsymbol{E}$ and $-\boldsymbol{E}$ which are in time phase opposition. The locus of the extremity of the current vector $\boldsymbol{I}_y$ referred to the voltage $\boldsymbol{E}$ for varying slip is a circle as shown in Figure 4A. Its diameter is vertical and has a magnitude $\boldsymbol{E}/R_3$. The locus of the extremity of the current vector $\boldsymbol{I}_x$ is also a circle as indicated in Figure 4A. Its diameter is

$$\frac{(a+1)\boldsymbol{E}}{X_3} \quad \frac{\sqrt{R_3^2 + X_2^2}}{R_3}$$

at an angle $\tan^{-1}(R_3/X_2)$ with the volt-

age vector E. The derivation of magnitude and position of these circles is given in Appendix I. The locus of the extremity of the vector I_2 obtained from equation 7 also is found to be a circle as illustrated in Figure 4B. The proof that it has a circle locus is presented in Appendix II.

All of this analysis has been carried out neglecting the exciting current of the polyphase commutator regulator and its associated transformer, which flows in the induction-motor secondary. This exciting current is directly proportional to the voltage applied to the field winding and inversely proportional to the frequency of this voltage. As the machines slow down due to increase in load, the slip increases and the frequency of the voltage applied to the regulator field increases proportionally. The voltage across the field winding increases also, though to a lesser degree because of the voltage drop I_2Z_2 in the secondary of the induction motor. Since the speed changes only slightly with load, the voltage and frequency applied to the field of the commutator machine are essentially unchanged. The changes which do occur produce tendencies in opposite directions. Therefore, for a given setting of the regulating transformer, the exciting current of the commutator machine remains substantially constant. It is assumed to remain entirely so in the analysis presented here.

The total secondary current of the induction motor is made up of the exciting current and the current I_2 just obtained. The magnitude and direction of the current in the primary winding of the induction motor resulting from these two secondary currents can be determined by reflecting them separately as vectors to the primary vector diagram. This procedure is indicated in Figure 5. The exciting current is reflected first and combined with the exciting current of the induction motor itself to give the total exciting current of the drive as shown in Figure 5B. The load component I_2, of the secondary current when reflected to the primary winding produces a primary load component of current having a circle locus differing in magnitude from the secondary circle locus by the turns ratio of the motor as indicated in Figure 5C. Thus the primary current is the sum of the three components and is defined by a circle locus also. This is illustrated in Figures 5D and 6.

The characteristics of the drive may be predicted from the circle diagram of the input current.

The speed of the drive can be obtained from relations of slip to the current I_x in the following equation in which the resistance and leakage reactance of the induction motor primary are included.

$$I_x = \frac{V}{R_1 + \frac{R_2}{(a+1)s} + jX_1 + \frac{jX_2}{(a+1)} - \frac{jX_2}{(a+1)s}} \tag{8}$$

For the sake of convenience, let

$$\frac{R_2}{(a+1)} = R_0, \quad \frac{X_2}{(a+1)} = X_0, \text{ and}$$

$$X_1 + \frac{X_2}{(a+1)} = X_4$$

Then

$$I_x = \frac{V}{\frac{R_0}{s} + R_1 + jX_4 - \frac{jX_0}{s}} \tag{9}$$

The slip can now be obtained as follows. For a given current oe, as represented on Figure 7, the phase angle with respect to the voltage is

$$\tan^{-1}\theta = \frac{(sX_4 - X_0)}{(sR_1 + R_0)}$$

For infinite slip tan $\theta = X_4/R_1$. An arbitrary point on the vertical axis, such as a in Figure 7 is selected. The line ab is drawn at the angle γ with the horizontal such that tan $\gamma = R_1/X_4$. The I_x vector is tangent to its circle for the condition of zero slip. This line is extended to give the point d, and the standstill value of I_x is also extended until it intersects ab at f. The length db is then directly proportional to the slip. The line segment df is divided into 100 parts. Slip corresponding to any load current may be obtained by extending the corresponding I_x vector until it intersects this line and reading the slip directly. Proof of the validity of this procedure is found in Appendix III.

The power loss associated with the no-load current is assumed to remain constant for all values of load, just as is done in the treatment of the 2-element induction motor. This power loss is represented by the product of the in-phase component of the no-load current and the phase voltage.

Having determined the slip and the corresponding speed from the construction shown in Figure 7, the other characteristics may be determined by constructing the diagram for the motor shown in Figure 6. In this diagram (Figure 6) the load component of primary current is ob, and the copper loss for the current ob = (loss for oc)$(ob/oc)^2$, where oc is the load component of primary current for the blocked rotor condition. If the loss

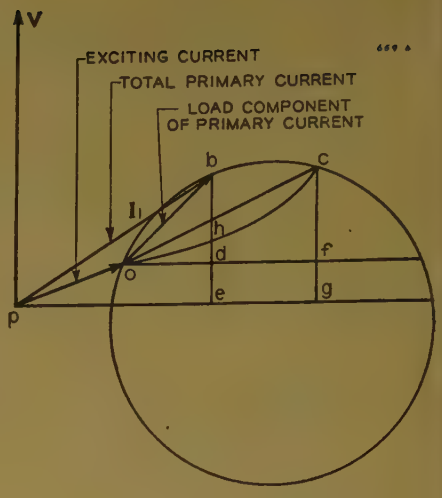


Figure 6. Locus of primary current

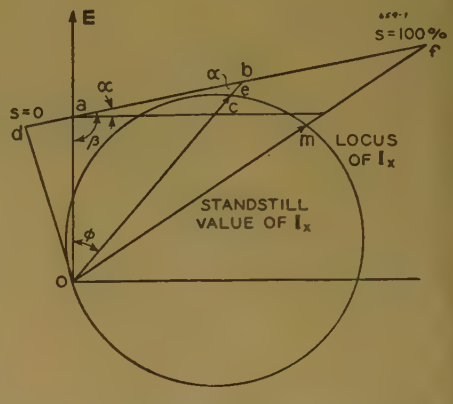


Figure 7. Determination of speed from circle diagram

for oc is known, the copper loss of the drive can be evaluated for all values of the load component of the current I_1, and the curve ohc constructed such that the current dh when multiplied by the voltage, V, gives the copper loss caused by the current ob. Similarly other points on the curve can be obtained for different values of input current.

The different quantities for the drive now can be obtained corresponding to any value of current I_1.

1. Input = $(be)V$ watts per phase
2. Output = $(bh)V$ watts per phase
3. Iron loss, friction, and windage = $(de)V$ watts per phase
4. Copper loss = $(hd)V$ watts per phase
5. Efficiency = $\frac{(bh)}{(be)} \times 100$ per cent
6. Power factor = $\frac{(be)}{(pb)} \times 100$ per cent

All of these letters refer to Figure 6. The slip may be obtained from Figure 7.

7. Slip = $\left(\frac{db}{df}\right) \times 100$ per cent

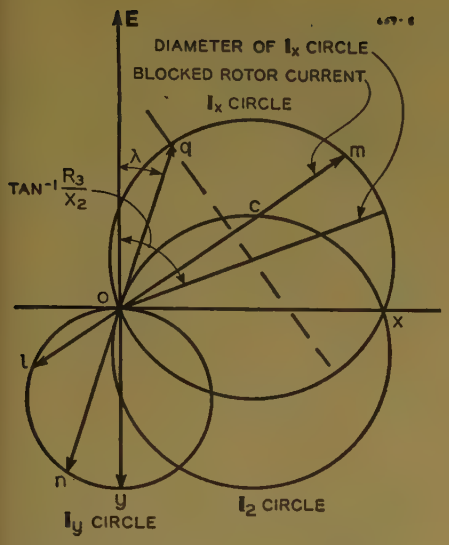


Figure 8. Construction of approximate circle current locus

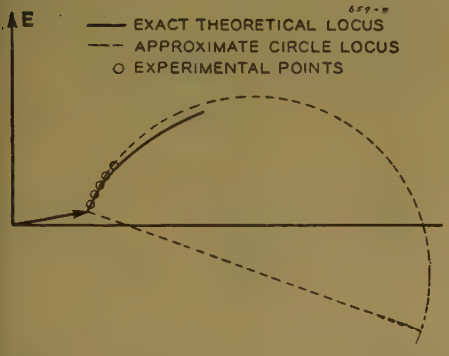


Figure 9. Input current loci of the drive according to both exact and approximate theories, and experimental points

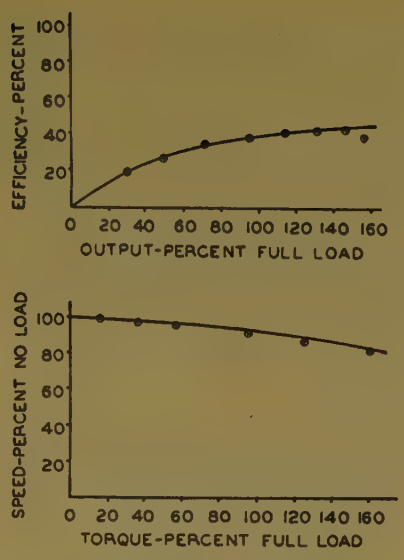
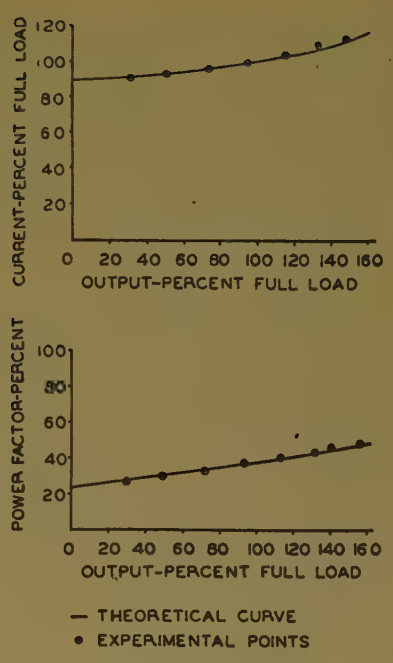


Figure 10. Operating characteristics of the adjustable-speed drive



8. $\text{Speed} = \left(1 - \frac{db}{df}\right) \times \text{synchronous speed}$

9. $\text{Torque} = (\text{horsepower output}) \times \frac{33{,}000}{2\pi N}$

On the basis of these expressions a complete set of characteristics can be predicted.

Experimental Results

In order to verify the theory thus far presented a complete set of tests was made upon a drive consisting of a 4-pole 5-horsepower wound-rotor induction motor and a polyphase commutator regulator of approximately 2-horsepower rating. The brushes of the regulator were so adjusted that the voltage appearing between them was directly opposed to the voltage applied to the primary of the adjustable transformer in its field circuit.

The method employed to obtain the locus of primary current involves a determination of (*a*) no-load voltage, current, and power input to the induction motor, (*b*) the blocked-rotor current, voltage, and input power taken both in the primary of the induction motor and in the armature circuit of the commutator machine, and (*c*) the determination of the voltage ratio *a*. Reduced voltages can be used to obtain data for determining blocked-rotor inputs at rated voltage. By making use of equation 7 for the standstill condition, and the experimentally determined value of *a*, the blocked-rotor current *om* of the I_x circle may be calculated from the blocked-rotor current *oc* of the primary current locus (see Figure 8). Likewise the blocked-rotor current *ol* of the I_y circle is determined.

The slip for which the component currents I_x and I_y are equal in magnitude can be obtained from equation 7. This value is found to be

$$s = \frac{1}{a+1}$$

Substituting this value of slip into the expression for I_x, it is then found that these two currents are equal when

$$I_x = \frac{E}{R_3 + j\left(\frac{X_3}{a+1} - X_3\right)}$$

Substituting the real value for X_3 (see list of symbols), it is found that this current has a power factor angle λ with respect to the stator voltage E such that

$$\tan \lambda = \frac{aX_a}{(a+1)R_3}$$

Since the diameter of I_y circle is determined in direction and the point *l* is now known, the I_y circle can be constructed. The diameter of this circle is E/R_3 in length. The resistance R_3 is equal to E divided by the current *oy*. The value of X_a is obtained from the blocked-rotor readings taken on the regulator. These values can be used to determine the angle λ. This angle and the I_y circle determine the direction and magnitude of the current *on* which was specified as being equal to and opposite to a current vector *oq* having its extremity on the I_x circle. The points *o*, *q*, and *m* determine the I_x circle. The intersection of the I_x circle with the horizontal axis at *x* is a point on the I_2 circle. The points *o*, *c*, and *x* determine the location of the I_2 circle.

The theoretically accurate locus, the approximate circle, and the experimental points are shown in Figure 9. Complete

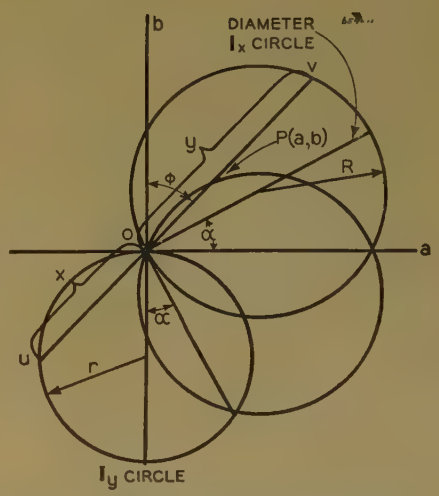


Figure 11. Proof that the terminus of the I_2 vector has a circle locus

characteristics were predicted on the basis of this circle, making use of the method devised in the discussion of the theory. These calculated results were in quite good agreement with the experimentally measured points. Characteristics are shown in Figure 10.

Conclusions

From the current loci it is evident that the power factor of experimental points is slightly higher than that of the theoretical locus. The explanation for this is as follows. It was assumed that the exciting current of the commutator machine was constant. Actually, it decreases with load because the frequency of the voltage impressed on the regulator field increases, thereby increasing the field reactance as the drive slows down. The field voltage, however, was found to be substantially constant with change in speed because of the effect of the voltage drop due to the impedance in the induction-motor secondary winding. This would cause the exciting current of the regulator to be slightly smaller than was originally assumed.

Reference to equations 3 and 7 shows that the impedance used in the approximate theory has a slightly higher power factor than that of the exact expression. This explains why the theoretically less accurate curve is in better agreement with experimental results than that obtained from the more exact theory.

Other errors present in the theory here presented are the statements that the loss associated with the no-load current is constant, regardless of load, and that the machine impedances are constant, independent of current. Both of these errors are inherent in normal induction motor theory.

The polyphase commutator regulator was of considerably lower power rating than the induction motor and hence possessed a higher armature resistance than was desirable. In order to load the induction motor fully, it was necessary to send currents through the armature of this machine considerably in excess of its normal current capacity. This resulted in abnormally high copper loss and the correspondingly low efficiencies observed.

It will be observed that the voltage impressed on the commutator machine is only a fraction of the voltage rating of the induction motor secondary, this fraction being the per cent slip at full load. The current capacity of the regulator, however, should be equal to that of the induction motor secondary winding, and therefore its kilovolt-ampere rating is the product of full-load slip and the rating of the induction motor. A drive designed to operate between synchronous speed and 50 per cent slip would require a commutator machine twice as large as one operating between synchronous speed and 25 per cent slip. For this reason the drive normally employed is a double-range system operating between plus 25 per cent slip and minus 25 per cent slip, rather than between synchronous speed and plus 50 per cent slip. This requires an ohmic drop exciter for passing through synchronism.

The excellent agreement of experimental results with those based on the theory presented in this paper indicates the theory to be sound. The method presented here may be used to obtain from no-load tests or design data the operating characteristics of the drive employing the polyphase commutator regulator. Results have shown the accuracy achieved to be high.

Appendix I. Derivation of Position and Magnitude of the Circle Locus of I_x for the Compensated Commutator Machine

$$I_x=\frac{s(a+1)E}{R_3+j(sX_3-X_2)}=\frac{s(a+1)E}{\sqrt{R_3^2+(sX_3-X_2)^2}}$$

This is readily recognized as the equation of a circle when it is written

$$I_x=\frac{(a+1)E}{\frac{R_3}{s}+j\left(X_3-\frac{X_2}{s}\right)}$$

The diameter of the circle is the maximum value which I_x attains. In order to obtain the value of slip for which I_x is a maximum, this expression is differentiated with respect to s and equated to zero.

$$\frac{dI_x}{ds}=\frac{\left[\sqrt{R_3^2+(sX_3-X_2)^2}(a+1)E-s(a+1)\times E[R_3^2+(sX_3-X_2)^2]^{-1/2}(sX_3-X_2)X_3\right]}{R_3^2+(sX_3-X_2)^2}$$

Multiplying through by

$$[R_3^2+(sX_3-X_2)^2]^{1/2}$$

and clearing fractions gives

$$R_3^2+(sX_3-X_2)^2-sX_3(sX_3-X_2)=0$$

Simplifying and solving for s yields

$$s=\frac{R_3^2+X_2^2}{X_3X_2}$$

Substitute this in the expression for I_x.

$$\text{Max } I_x=\frac{R_3^2+X_2^2}{X_3X_2}\cdot\frac{(a+1)E}{\sqrt{R_3^2+\left(\frac{R_3^2+X_2^2}{X_2}-X_2\right)^2}}$$

Multiply through by X_2 and simplify.

$$\text{Max } I_x=\frac{(a+1)E}{X_3}\cdot\frac{\sqrt{R_3^2+X_2^2}}{R_3}$$

The tangent of the angle which the diameter makes with the voltage is obtained from the following expression:

$$\tan\psi=\frac{sX_3-X_2}{R_3}$$

Substitute in the value of s for maximum I_x.

$$\tan\psi=\frac{\frac{R_3^2+X_2^2}{X_2}-X_2}{R_3}=\frac{R_3}{X_2}$$

Appendix II. Proof That the Combination of the I_x and I_y Circles Is Also a Circle

Employ a as the horizontal co-ordinate and b as the vertical co-ordinate in Figure 11.

Point P is obtained by extending the chord ov of the I_x circle until it intersects the I_y circle at u. The distance $uo=x$ is laid off from v along ov to obtain P. The locus of P is to be proved a circle.

α = angle which diameter of I_x circle makes with horizontal
r = radius of I_y circle
R = radius of I_x circle
d = diameter of I_y circle
D = diameter of I_x circle

From the figure for point P:

$$a=(y-x)\sin\theta$$
$$b=(y-x)\cos\theta$$
$$x=d\cos\theta$$
$$y=D(\sin\theta\cos\alpha+\cos\theta\sin\alpha)$$
$$y-x=D\sin\theta\cos\alpha+\cos\theta(D\sin\alpha-d)$$

Substitute in the expression for a and b the value of $y-x$. This yields:

$$a=D\sin^2\theta\cos\alpha+\sin\theta\cos\theta(D\sin\alpha-d) \quad (10)$$

$$b=D\sin\theta\cos\theta\cos\alpha+\cos^2\theta(D\sin\alpha-d) \quad (11)$$

Let:

$$D\sin\alpha-d=m$$

From equation 10

$$\sin\theta\cos\theta=\frac{a-D\sin^2\theta\cos\alpha}{m}$$

Substitute this into equation 11.

$$b=\frac{Da}{m}\cos\alpha-\frac{D^2}{m}\cos^2\alpha\sin^2\theta+m\cos^2\theta$$

Now

$$\cos^2\theta=1-\sin^2\theta$$

$$b=\frac{Da}{m}\cos\alpha-\left(\frac{D^2\cos^2\alpha+m^2}{m}\right)\sin^2\theta+m$$

$$\sin^2\theta=\frac{\frac{Da\cos\alpha}{m}+m-b}{\frac{D^2\cos^2\alpha}{m}+m}=n^2 \quad (12)$$

letting $n=\sin\theta$. Rewriting equation 10 gives

$$a=D\sin^2\theta\cos\alpha+m\sin\theta\sqrt{1-\sin^2\theta}$$

Substitute $n=\sin\theta$.

$$a=Dn^2\cos\alpha+nm\sqrt{1-n^2}$$

$$\sqrt{1-n^2}=\frac{a-Dn^2\cos\alpha}{mn}=\frac{a}{mn}-\frac{Dn}{m}\cos\alpha$$

Eliminate the square root.

$$0=-m^2(1-n^2)+\frac{a^2}{n^2}+D^2n^2\times\cos^2\alpha-2aD\cos\alpha$$

Substitute for n^2 from equation 12.

$$\frac{\frac{Da\cos\alpha}{m}+m-b}{\frac{D^2\cos^2\alpha}{m}+m}$$

Then

$$-m^2\frac{\frac{D^2\cos^2\alpha}{m}-\frac{Da\cos\alpha}{m}+b}{\frac{D^2\cos^2\alpha}{m}+m}+$$

$$a^2\frac{\frac{D^2\cos^2\alpha}{m}+m}{\frac{Da\cos\alpha}{m}+m-b}+$$

$$\frac{D^2\cos^2\alpha\left(\frac{Da\cos\alpha}{m}+m-b\right)}{\frac{D^2\cos^2\alpha}{m}+m}-2aD\cos\alpha=0$$

And

$$\frac{\left[\begin{array}{l}-D^2m^2\cos^2\alpha+aDm^2\cos\alpha-bm^3+\\ aD^3\cos^3\alpha+D^2m^2\cos^2\alpha-bD^2m\cos^2\alpha\end{array}\right]}{D^2\cos^2\alpha+m^2}+$$

$$\frac{a^2D^2\cos^2\alpha+a^2m^2}{aD\cos\alpha+m^2-bm}-2aD\cos\alpha=0$$

Clear fractions:

$$\begin{array}{l}a^2D^2m^2\cos^2\alpha-abDm^3\cos\alpha+a^2D^4\times\\ \cos^4\alpha-abD^3m\cos^3\alpha+aDm^4\times\\ \cos\alpha-bm^5+aD^3m^2\cos^3\alpha-bD^2m^3\times\\ \cos^2\alpha-abDm^3\cos\alpha+b^2m^4-abD^3m\times\\ \cos^3\alpha+b^2D^2m^2\cos^2\alpha+a^2D^4\times\\ \cos^4\alpha+a^2D^2m^2\cos^2\alpha+a^2D^2m^2\times\\ \cos^2\alpha+a^2m^4-2a^2D^4\cos^4\alpha-2aD^3m^2\times\\ \cos^3\alpha+2abD^2m\cos^3\alpha-2a^2D^2m^2\times\\ \cos^2\alpha-2aDm^4\cos\alpha+2abDm^3\times\\ \cos\alpha=0\end{array}$$

$$\begin{array}{l}a^2(D^2m^2\cos^2\alpha+m^4)-a(D^3m^2\cos^3\alpha+Dm^4\times\\ \cos\alpha)+b^2(D^2m^2\cos^2\alpha+m^4)-b\times\\ (D^2m^3\cos^2\alpha+m^5)=0\end{array}$$

$$a^2-a\left[\frac{D\cos\alpha(D^2\cos^2\alpha+m^2)}{D^2\cos^2\alpha+m^2}\right]+$$

$$b^2-b\left[\frac{m(D^2\cos^2\alpha+m^2)}{D^2\cos^2\alpha+m^2}\right]=0$$

$$\left(a^2-aD\cos\alpha+\frac{D^2}{4}\cos^2\alpha\right)+\left(b^2-bm+\frac{m^2}{4}\right)=\frac{D^2}{4}\cos^2\alpha+\frac{m^2}{4}$$

This is

$$\left(a-\frac{D}{2}\cos\alpha\right)^2+\left(b-\frac{m}{2}\right)^2=\frac{D^2\cos^2\alpha+m^2}{4}$$

This is the equation of a circle with center at $D\cos\alpha/2$, $m/2$.

Appendix III. Proof That the Line *db* of Figure 7 Is Proportional to Slip

The line ab of Figure 7 is drawn at an angle γ with the horizontal such that $\tan\gamma=R_1/X_4$. Point b is the intersection of the I_x vector with the line making the angle γ with the horizontal. Using the notation of Figure 7, the following equality may be written:

By the law of sines

$$\frac{ab}{\sin\theta}=\frac{ao}{\sin\alpha_1}$$

$\alpha_1=\angle abo$

$\beta=\angle oab$

$\alpha_1=180°-(\beta+\theta)$

$\sin[180°-(\beta+\theta)]=\sin(\beta+\theta)$

$$ab=\frac{ao\sin\theta}{\sin(\beta+\theta)}=\frac{ao\sin\theta}{\sin\theta\cos\beta+\cos\theta\sin\beta}$$

Divide through by $\cos\theta$

$$ab=ao\tan\theta\frac{1}{\tan\theta\cos\beta+\sin\beta}$$

Now

$$\cos\beta=-\sin\gamma,\quad \sin\beta=\cos\gamma$$

$$ab=ao\tan\theta\frac{1}{-\tan\theta\sin\gamma+\cos\gamma}$$

The functions of theta and gamma are

$$\tan\theta=\frac{X_4-\frac{X_0}{s}}{R_1+\frac{R_0}{s}}\qquad \sin\gamma=\frac{R_1}{\sqrt{R_1^2+X_4^2}}$$

$$\tan\gamma=\frac{R_1}{X_4}\qquad \cos\gamma=\frac{X_4}{\sqrt{R_1^2+X_4^2}}$$

When these values are substituted in the expression for ab, the following result is obtained:

$$ab=ao\frac{X_4-\frac{X_o}{s}}{R_1+\frac{R_o}{s}}\times\frac{1}{\frac{X_4-\frac{X_0}{s}}{R_1+\frac{R_o}{s}}\cdot\frac{(-R_1)}{\sqrt{R_1^2+X_4^2}}+\frac{X_4}{\sqrt{R_1^2+X_4^2}}}$$

Clearing fractions yields

$$ab=ao(sX_4-X_o)\frac{\sqrt{R_1^2+X_4^2}}{R_1X_o+X_4R_o}$$

At zero slip ob of Figure 7 is tangent to the I_x circle. Under these conditions ab is equal to ad. The magnitude of ab for zero slip is

$$ab=ad=aoX_o\frac{\sqrt{R_1^2+X_4^2}}{R_1X_o+X_4R_o}$$

Now

$$db=ab+da=ao(sX_a-X_o+X_o)\frac{\sqrt{R_1^2+X_4^2}}{R_1X_o+X_4R_o}$$

$$db=ao(sX_4)\frac{\sqrt{R_1^2+X_4^2}}{R_1X_o+X_4R_o}$$

The length db, then, is directly proportional to the slip.

Appendix IV. List of Symbols

a = ratio of number of turns in primary to number of turns in secondary of adjusting transformer in field circuit of polyphase commutator regulator

$\boldsymbol{E}$ = the voltage induced in one phase of the induction motor secondary by the mutual flux at standstill

$\boldsymbol{E}_1$ = the voltage induced in one phase of the armature winding of the compensated commutator regulator by the mutual flux

$\boldsymbol{E}_2$ = the voltage induced in one phase of the induction motor secondary by the mutual flux. It is $s\boldsymbol{E}$ where s is the slip

$\boldsymbol{E}_e$ = the effective generated voltage per phase appearing at the terminals of the armature and compensating winding together for the compensated commutator machine. It is $\boldsymbol{E}_1-\boldsymbol{E}_c=k\phi(1-s)$

$\boldsymbol{E}_c$ = the voltage induced in one phase of the compensating winding of the commutator machine by the mutual flux

$\boldsymbol{E}_s$ = the voltage induced in one phase of the stator winding of the commutator machine by the mutual flux. $\boldsymbol{E}_s=k\phi s$

I_1 = total primary current of induction motor

I_2 = total load component of secondary current of induction motor

I_e = armature current of polyphase commutator regulator

I_{exe} = exciting current of polyphase commutator regulator

I_o = no-load current of induction motor alone

I_x = component of I_2 due to $s(a+1)\boldsymbol{E}$ for the compensated drive

I_y = component of I_2 due to $-\boldsymbol{E}$ for the compensated drive

N = speed of drive in revolutions per minute

N_o = no-load speed of drive in revolutions per minute

N_s = synchronous speed of drive in revolutions per minute

Formulas for the Inductance of Coaxial Busses Comprised of Square Tubular Conductors

HENRY PETER MESSINGER
ASSOCIATE AIEE

THOMAS JAMES HIGGINS
ASSOCIATE AIEE

BY virtue of its axial symmetric geometry, the coaxial tubular bus possesses certain very desirable electrical and mechanical characteristics. Low inductance contributes to good voltage regulation. Reduced skin and proximity effects minimize line losses and average temperature rise under load. Axial-symmetric distribution of skin and proximity effects reduces current density distortion and attendant hot-spot concentrations, hence enables a greater current rating for a specified maximum copper temperature. As electromagnetic forces between conductors are eliminated largely, mechanical bracing against short-circuit forces correspondingly can be reduced. The nested conductors require less space for installation and a smaller supporting structure than they would if arranged side by side.

Yet, despite these desirable characteristics, the paucity of published descriptions of actual installations[1,2,3] indicates that few coaxial busses have been constructed to date. However, until recently factory distribution loads at frequencies greater than 60 cycles were uncommon. Again, most heavy 60-cycle loads were supplied over relatively short distances. As these conditions are such that satisfactory 60-cycle operation can be obtained with the more conventional, though less electrically effective, construction of conductors placed side by side, this limited use of coaxial busses is not surprising. Now, however, by virtue of manufacturing procedures and techniques developed during the war, the bus designer is faced with the necessity of designing heavy distribution busses which are not only long but also are to operate at frequencies of several hundred cycles and higher. But, the electrical characteristics of the coaxial bus are such that it is especially suited to satisfactory operation under either or both of these conditions. Hence it is to be expected that in the near future coaxial busses will find greater use than they have hitherto.

At present, coaxial busses are constructed of circular tubular conductor, of square tubular conductor, and of structural tubular conductor comprised of two slightly separated channels or angles placed flange to flange. To predetermine the operating characteristics of these busses requires knowledge of the a-c resistance, the a-c inductance, the copper temperature under load, and the mechanical forces exerted during short-circuit. Formulas[4] for calculating all four of these quantities are available for busses comprised of a circular tubular conductor. But for a square or structural tubular conductor, though formulas are available for calculating the a-c resistance,[5,6] the copper temperature,[6] and the short-circuit forces,[4] formulas for calculating the a-c inductance, often the determining factor in the design of the bus, are not available.

Such formulas are derived in this paper, it being assumed that the conductors are nonmagnetic, of such lengths that end effects are negligible, of uniform thickness, right-cornered, and carry currents distributed uniformly over their cross sections. Of these five conditions, the first three are satisfied in practice. The fourth, however, though essential to tractable analysis, is usually not true in practice. Square tubes, channels, and angles, drawn, rolled, bent, or otherwise formed in one piece, have rounded edges, but the error introduced by neglecting the rounded edges is small. Commonly, the result obtained, though a bit low, is yet sufficiently accurate for the work in hand. In any case, the incremental inductance associated with the rounded edges can be approximated closely by a simple semi-empirical formula derived by Dwight and Wang.[7] Finally, though skin and proximity effects render the current density over the cross sections of the conductors slightly nonuniform, the analysis in "Corrections for Rounded Edges and for Skin and Proximity Effects," later in this paper, indicates that at power frequencies the a-c inductance is practically identical with the d-c inductance.

Inasmuch as these five postulates are granted as consistent with practice, derivations of the desired formulas, though lengthy, are not difficult. The

R_1 = primary resistance per phase of induction motor

R_2 = secondary resistance per phase of induction motor

$R_3 = a(R_2 + R_a)$

$R_o = \dfrac{R_3}{(a+1)}$

s = slip measured from zero at synchronous speed

X_1 = primary leakage reactance per phase of induction motor at standstill

X_2 = secondary leakage reactance per phase of induction motor at standstill

$X_3 = a(X_2 + X_a) + X_2$

$X_4 = \dfrac{X_3}{(a+1)} + X_1$

X_a = leakage reactance per phase of armature of polyphase commutator regulator with drive at standstill

$X_o = \dfrac{X_2}{(a+1)}$

V = applied voltage per phase of induction motor

Z_3 = impedance per phase of induction motor secondary

Z_a = impedance per phase of armature of polyphase commutator regulator

α = angle which line tangent to I_x circle at origin makes with voltage vector

$\beta = \tan^{-1} - \dfrac{X_4}{R_1}$

$\gamma = \tan^{-1} \dfrac{R_1}{X_4}$

ϕ = total air-gap flux of polyphase commutator regulator

ψ = angle which the diameter of the I_x circle makes with the voltage vector = $\tan^{-1} \dfrac{R_3}{X_3}$

$\lambda = \tan^{-1} = \dfrac{aXa}{(a+1)R_3}$

Paper 46-37, recommended by the AIEE committee on basic sciences for presentation at the AIEE winter convention, New York, N. Y., January 21–25, 1946. Manuscript submitted September 18, 1945; made available for printing December 10, 1945.

HENRY PETER MESSINGER is an electrical engineer in the cyclotron laboratory, Massachusetts Institute of Technology, Cambridge, Mass. THOMAS JAMES HIGGINS is an associate professor of electrical engineering, Illinois Institute of Technology, Chicago, Ill.

This paper is based upon a thesis supervised by Professor Higgins and submitted by Mr. Messinger to the faculty of the Illinois Institute of Technology in February 1946 in partial fulfillment of the requirements for the degree of master of science in electrical engineering.

conductor cross sections can be considered in various fashions as combinations of parallel-sided square areas. By virtue of geometric mean distance theory, the inductance can be expressed in terms of the self and mutual geometric mean distances of these square areas. These geometric mean distances can be calculated from known formulas. Accordingly, determination of the inductance as a function of the parameters defining the geometry of the bus reduces, essentially, to specific determination of the geometric mean distances involved and substitution of them in the general equation for the inductance.

The general formula comprises 36 terms. A simple approximate formula similarly derived, but on the assumption that the conductors can be considered as being indefinitely thin and hence having cross sections comprised of line segments, affords values sufficiently accurate for many design purposes. As a further convenience to numerical computation, this formula is epitomized in a single curve. Conductors which are indefinitely thin are limiting cases of conductors of finite thickness, a physical consideration which indicates that the approximate formula can be considered as a limiting case of the general formula. Analytical confirmation of this deduction provides a simultaneous check of the correctness of the general and approximate formulas.

The desired formulas, having been obtained and checked, are used as illustrated by calculation of the inductance of typical busses constructed of square tubular conductors. Changes in inductance resulting from rounded corners on the conductors and from skin and proximity effects are discussed in detail. Procedures for calculating the inductance of coaxial busses, constructed of channels or angles, are advanced. Illustratively, the inductance of a bus constructed of channels is calculated and found to be in good agreement with the experimentally determined value. Finally, procedure for calculating the inductance of polyphase coaxial busses, comprised of square tubular conductors, is outlined.

General Relationships

From well-known theory,[8,9] the inductance of a bus comprised of two long parallel cylindrical nonmagnetic conductors, each of an arbitrary cross section, is

$$L = 2 \log D_{ab}^2 / D_{aa} D_{bb} \text{ abhenrys per centimeter of bus length} \quad (1)$$

where D_{aa} and D_{bb} are the self geometric mean distances, and D_{ab} is the mutual geometric mean distance of the conductor cross sections.

If each of the two conductors is constructed of several subconductors connected in parallel, m composing the conductor of a cross section S_a and n that of a cross section S_b, equation 1 can be written

$$L = -(2/I^2) \sum_{i=1}^{m+n} \sum_{j=1}^{m+n} w_i w_j S_i S_j \log D_{ij} \quad (2)$$

where I is the bus current; w_i the current density in the ith subconductor of the sectional area S_i, taken positive for current flow in one direction and negative for current flow in the opposite direction; and $D_{ij} \equiv D_{ji}$ is the geometric mean distance between areas S_i and S_j.

If $S_i = RS$ and $S_j = R'S'$ are two arbitrarily located parallel-sided rectangular areas (Figure 1), the mutual geometric mean distance is

$$S_i S_j \log D_{ij} = -(25/12) S_i S_j - (1/24) \times \sum_{p=1}^{4} \sum_{q=1}^{4} (-1)^{p+q} K(A_p, B_q) \quad (3)$$

where

$$K(A_p, B_q) = (A_p^4 - 6A_p^2 B_q^2 + B_q^4) \times \log (A_p^2 + B_q^2)^{1/2} - 4A_p B_q^3 \times \tan^{-1} (A_p/B_q) - 4A_p^3 B_q \tan^{-1} (B_q/A_p) \quad (4)$$

and

$$A_1 = |D+R+R'|, \; A_2 = |D+R,| \; A_3 = |D|, \; A_4 = |D+R'| \quad (5)$$

$$B_1 = |P+S+S'|, \; B_2 = |P+S|, \; B_3 = |P|, \; B_4 = |P+S'| \quad (6)$$

Derivation of the General Formula

Consider a bus comprised of two coaxial square tubular conductors (Figure 2). Each of the conductors can be considered as constructed of two subconductors: one of a full square cross section wherein current exists in the same direction as in the tubular conductor, the other of a smaller full square cross section having current in the opposite direction. Hence $m = n = 4$, and from equation 2

$$L = -(2/I^2) \sum_{i=1}^{4} \sum_{j=1}^{4} w_i w_j S_i S_j \log D_{ij} \quad (7)$$

By definition, $D_{ij} \equiv D_{ji}$. By inspection of Figure 2, $w_1 = -w_2 = I/(a^2 - b^2)$ and $w_3 = -w_4 = -I/(c^2 - d^2)$. Utilizing these relationships in equation 7 yields

$$L = [-2/(a^2-b^2)^2][S_1^2 \log D_{11} + S_2^2 \log D_{22} - 2S_1 S_2 \log D_{12}] + [-2/(c^2-d^2)^2] \times [S_3^2 \log D_{33} + S_4^2 \log D_{44} - 2S_3 S_4 \times \log D_{34}] + [4/(a^2-b^2)(c^2-d^2)] \times [S_1 S_3 \log D_{13} - S_1 S_4 \log D_{14} - S_2 S_3 \times \log D_{23} + S_2 S_4 \log D_{24}] \quad (8)$$

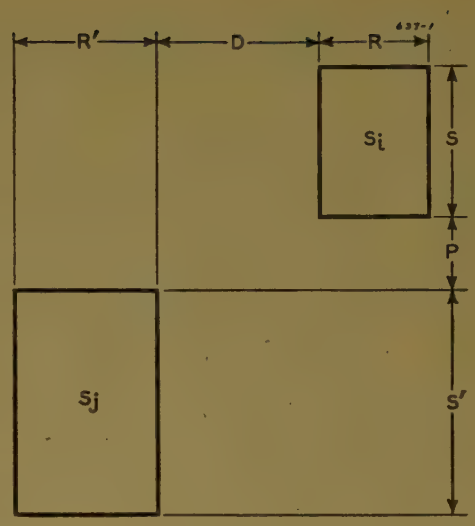


Figure 1

Determining the ten geometric mean distances in the right-hand member of equation 8 by use of equations 3 to 6, substituting appropriately in equation 8, and collecting terms (a detailed analysis appears in Appendix I) yields

$$\begin{aligned} L = {} & \{[-1/6(a^2-b^2)^2][12a^4 \log a + 12b^4 \times \log b - (a-b)^4 \log (a-b) - (a+b)^4 \times \log (a+b) + (a^4 - 6a^2b^2 + b^4) \times \log (a^2+b^2) + 10(a^4+b^4) \log 2 + 8ab \times (a^2-b^2) \tan^{-1} (a-b)/(a+b) + \pi \times (a^2-b^2)(a-b)^2]\} + \{[-1/6(c^2-d^2)^2] \times [12c^4 \log c + 12d^4 \log d - (c-d)^4 \times \log (c-d) - (c+d)^4 \log (c+d) + (c^4 - 6c^2d^2 + d^4) \log (c^2+d^2) + 10(c^4+d^4) \log 2 + 8cd(c^2-d^2) \times \tan^{-1} (c-d)/(c+d) + \pi(c^2-d^2) \times (c-d)^2]\} + \{[-1/6(a^2-b^2) \times (c^2-d^2)][(a-d)^4 \log (a-d) + (a+d)^4 \log (a+d) - (a^4 - 6a^2d^2 + d^4) \times \log (a^2+d^2) - (b-d)^4 \log (b-d) - (b+d)^4 \log (b+d) + (b^4 - 6b^2d^2 + d^4) \times \log (b^2+d^2) - (a-c)^4 \log (a-c) - (a+c)^4 \log (a+c) + (a^4 - 6a^2c^2 + c^4) \times \log (a^2+c^2) + (b-c)^4 \log (b-c) + (b+c)^4 \log (b+c) - (b^4 - 6b^2c^2 + c^4) \times \log (b^2+c^2) - 8ad(a^2-d^2) \times \tan^{-1} (a-d)/(a+d) + 8bd(b^2-d^2) \times \tan^{-1} (b-d)/(b+d) + 8ac(a^2-c^2) \times \tan^{-1} (a-c)/(a+c) - 8bc(b^2-c^2) \times \tan^{-1} (b-c)/(b+c) - \pi(a^2-d^2) \times (a-d)^2 + \pi(b^2-d^2)(b-d)^2 + \pi(a^2-c^2)(a-c)^2 - \pi(b^2-c^2)(b-c)^2]\} \end{aligned} \quad (9)$$

This is the desired formula for the inductance of a single phase bus. Further, it enables calculation of the inductance of a polyphase bus as outlined in "Polyphase Coaxial Busses."

Corroboration of Equation 9

In yet another fashion, each square tubular conductor can be assumed as constructed of four subconductors, each of a rectangular cross section and having

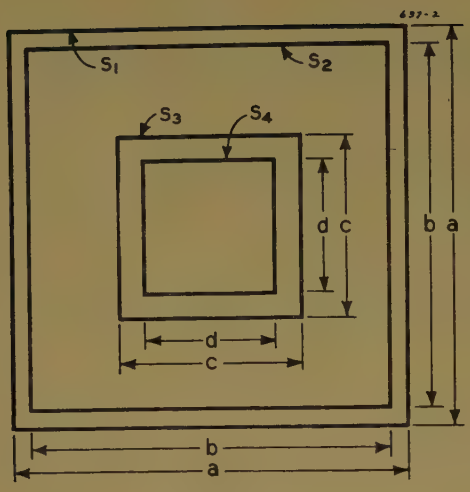


Figure 2

current in the same direction as in the tubular conductor (Figure 3). Hence $m=n=8$, and from equation 2

$$L=-(2/I^2)\sum_{i=1}^{8}\sum_{j=1}^{8}w_iw_jS_iS_j\log D_{ij} \qquad (10)$$

By definition, $D_{ij}\equiv D_{ji}$. By virtue of the geometric symmetries apparent in Figure 3, $D_{11}=D_{33}$, $D_{22}=D_{44}$, $D_{55}=D_{77}$, $D_{66}=D_{88}$, $D_{12}=D_{14}=D_{23}=D_{34}$, $D_{56}=D_{58}=D_{67}=D_{78}$, $D_{15}=D_{37}$, $D_{26}=D_{48}$, $D_{17}=D_{35}$, $D_{28}=D_{46}$, $D_{16}=D_{18}=D_{36}=D_{38}$, and $D_{25}=D_{27}=D_{45}=D_{47}$. Further, $S_1=S_3$, $S_2=S_4$, $S_5=S_7$, $S_6=S_8$; $w_1=w_2=w_3=w_4=I/-(a^2-b^2)$, and $w_5=w_6=w_7=w_8=-I/-(c^2-d^2)$. Utilizing these relationships in equation 10 yields

$$\begin{aligned}L=4\{&[-1/(a^2-b^2)^2][S_1^2(\log D_{11}+\log D_{13})+S_2^2(\log D_{22}+\log D_{24})+4S_1S_2\log D_{12}]+[-1/(c^2-d^2)^2]\times\\&[S_5^2(\log D_{55}+\log D_{57})+S_6^2(\log D_{66}+\log D_{68})+4S_5S_6\log D_{56}]+[2/(a^2-b^2)\times(c^2-d^2)][S_1S_5(\log D_{15}+\log D_{17})+S_2S_6(\log D_{26}+\log D_{28})+2S_1S_6\times\\&\log D_{16}+2S_2S_5\log D_{25}]\} \qquad (11)\end{aligned}$$

Determining the 16 geometric mean distances in the right-hand member of equation 11 as detailed in Appendix II, substituting appropriately in equation 11, and collecting terms yields, corroboratively, equation 9.

Obviously, this corroboration can be interpreted as a check of the correctness of the expressions, derived in Appendixes I and II, for the geometric mean distances indicated in equations 8 and 11.

Approximations to General Formula

The general formula for the inductance comprises 36 terms: 22 logarithmic, 6 arctangentic, and 8 algebraic. But by use of the proper tools (an electric calculating machine and the 15-place Work Projects Administration tables[10] of natural logarithms and arctangents), the computation incident to the calculation of the inductance of a given bus can be effected without difficulty. The computation, however, will be fairly lengthy. For this reason it is most desirable to have approximate formulas which enable rapid determination of values accurate enough for much (in some instances, all) of the computation incident to the final design of a bus.

A means of deriving such formulas stems from an earlier investigation[11] of the inductance of a coplanar bus comprised of rectangular tubular conductors. Therein, values of inductance calculated from the general formula were found to be in excellent agreement with values of inductance calculated from much simpler formulas derived by Dwight and Wang,[7] on the basis that the conductors are indefinitely thin. That is, they have cross sections comprised of line segments.

Consider, then, the cross section of each conductor as constructed of four line segments (Figure 4). Hence $m=n=8$, and from equation 8

$$L=-(2/I^2)\sum_{i=1}^{8}\sum_{j=1}^{8}w_iw_jS_iS_j\log D_{ij} \qquad (12)$$

By definition, $D_{ij}\equiv D_{ji}$. By virtue of the geometric symmetries apparent in Figure 4, $D_{11}=D_{22}=D_{33}=D_{44}$, $D_{55}=D_{66}=D_{77}=D_{88}$, $D_{12}=D_{14}=D_{23}=D_{34}$, $D_{56}=D_{58}=D_{67}=D_{78}$, $D_{13}=D_{24}$, $D_{57}=D_{68}$, $D_{15}=D_{26}=D_{37}=D_{48}$, $D_{17}=D_{28}=D_{35}=D_{46}$, and $D_{16}=D_{18}=D_{25}=D_{27}=D_{36}=D_{38}=D_{45}=D_{47}$. Further, $S_1=S_3$, $S_2=S_4$, $S_5=S_7$, $S_6=S_8$; $w_1=w_2=w_3=w_4=I/4a$, and $w_5=w_6=w_7=w_8=-I/4c$. Utilizing these relationships in equation 12 yields

$$\begin{aligned}L=&(-1/2)[\log D_{11}+2\log D_{12}+\log D_{13}]+(-1/2)[\log D_{55}+2\log D_{56}+\log D_{57}]+[\log D_{15}+2\log D_{16}+\\&\log D_{17}] \qquad (13)\end{aligned}$$

Determining the nine geometric mean distances in the right-hand member of equation 13 as detailed in Appendix III, substituting appropriately in equation 13, and collecting terms yields

$$\begin{aligned}L=&[(a+c)^2/2ac]\log(a+c)-[(a-c)^2/2ac]\times\log(a-c)-\log[(ac)^2/(a^2+c^2)]-[(a^2-c^2)/ac]\tan^{-1}[(a-c)/(a+c)]+\\&\pi(a^2-c^2)/4ac-3\log 2 \qquad (14)\end{aligned}$$

Simple algebraic manipulation of the logarithmic terms of equation 14 yields alternative formulas especially convenient to numerical computation. Thus

$$\begin{aligned}L=&\log[(r^{-1}+r)(r^{-1}-r)]-1/2(r^{-1}+r)\times\log[(1-r)/(1+r)]+(r^{-1}-r)\times[\pi/4-\tan^{-1}(1-r)/(1+r)]-3\log 2\\&(15)\end{aligned}$$

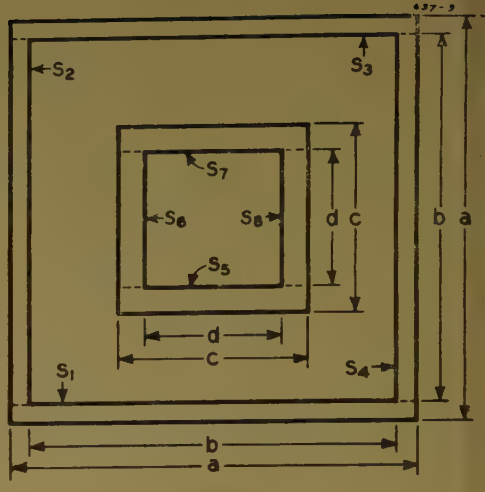


Figure 3

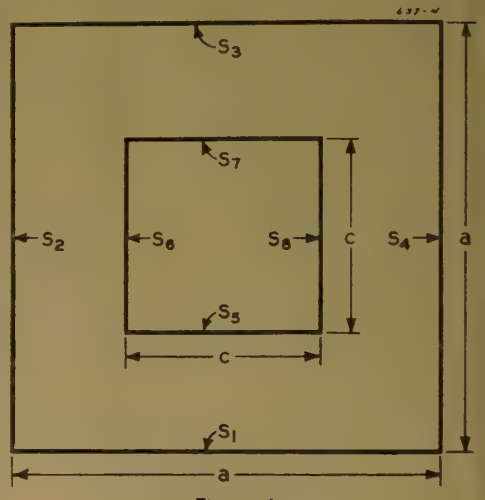


Figure 4

where $r=c/a$. Again

$$L=\log(1+A^2)-2\log(1-A^2)-(1/2r)\times(1-r)^2\log A+(r^{-1}-r)\times(\pi/4-\tan^{-1}A) \qquad (16)$$

where $A=(1-r)/(1+r)$.

For purposes of computation, these approximate formulas possess considerable advantage over the general formula. The latter comprises 36 terms, the former only a few terms. Moreover, the coefficients and arguments of these few terms are quite simple. Therefore, by virtue of the fewness and simplicity of the terms comprising the approximate formulas, they afford rapid computation. In fact, slide rule calculation is quite feasible; commonly, a 20-inch rule will afford values correct to a number of digits sufficient for most design work. But even slide rule calculation can be dispensed with in much work. The curves of Figure 5, plotted from equation 16, afford sufficiently accurate values. For actual use, of course, Figure 5 is too small, but the designer can plot his own curves from the co-ordinates tabulated in Appendix IV.

For use in "Corrections for Rounded

Edges and for Skin and Proximity Effects" in this paper, Figure 5 illustrates curves for the inductance of busses, comprised of indefinitely thin circular tubular conductor. It is interesting to note that these curves evidence the inductance of a bus comprised of thin square tubular conductors to be less than that of a bus comprised of thin circular tubular conductors having diameters equal to the sides of the corresponding square conductors.

Corroboration of the Approximate Equation

As a minor check on the correctness of equation 14, we note that if $a=c$ the conductors of Figure 4 are superimposed. As they carry equal currents in opposite directions, the bus vanishes electrically. Corroboratively, it is evident that $\lim_{a\to c}$ of the right-hand member of equation 14 is zero. A major simultaneous check on both equations 9 and 14 stems from noting that if in Figure 2 $b\to a$ and $d\to c$, we obtain a line-segment cross section as in Figure 4. Corroboratively, as detailed in Appendix V, $\lim_{d\to c}\lim_{b\to a}$ of the right-hand member of equation 9 yields the right-hand member of equation 14.

Inasmuch as the arguments and coefficients of the terms of right-hand members of equations 9, 14, 15, and 16 are without dimension, we note that in substituting in these equations, a, b, c, and d can be expressed in any like unit of length. But otherwise, the units of all quantities mentioned to this point are in the absolute system: bus dimensions in centimeters, current I in abamperes, and inductance L in abhenrys per centimeter of bus length. Multiplying abhenrys per centimeter by 3.048×10^{-5} yields millihenrys per foot of bus length; multiplying by 11.48×10^{-6} yields 60-cycle reactance in ohms per foot of bus length.

Some Illustrative Examples

To illustrate the use of the general formula and to gain knowledge of the accuracy to be expected of values calculated with the approximate formulas, we consider the following examples.

In example 1, the problem is to calculate the inductance of a coaxial bus comprised of two square tubular copper conductors: outer conductor, 6 inches square and 1/8 inch thick; inner conductor, 4 inches square and 3/16 inch thick.

Thus $a=6$, $b=23/4$, $c=4$, and $d=29/8$ inches. Substituting these values in equation 9, collecting and rearranging terms, obtaining values of the logarithmic and arctangentic terms from the Work Projects Administration tables, and effecting all calculations on a 10-row electric calculating machine yields*

$$L=0.75846_2 \text{ abhenry per centimeter of bus length} \quad (17)$$

Obviously, as by virtue of the assumptions underlying derivation of the general formula, it is unlikely that L represents the inductance of the bus to more than plus or minus several in the third decimal place, the last several digits have no physical significance. They are given to emphasize that, insofar as the numerical computation is concerned, the value of L is correct to the number of places indicated. For all logarithmic and arctangentic terms were taken to nine decimal places; values stemming from consequent arithmetic manipulations were held to the same number of decimals.

Inasmuch as the value given in the preceding equation stems from a final algebraic addition of some 32 terms, the largest of which approximates 300,000,000 and the smallest 89, it is essential that some such degree of preciseness be held. But, since the resulting value of L is significant to only two or three decimal places, it is not unlikely that a study of the number of decimal places to be held in the various stages of computation would reveal that a smaller number than actually used still would be satisfactory. However, inasmuch, as 15-place tables were employed and the calculation was performed on a 10-row electric calculating machine, the added labor is negligible, and there is no uncertainty as to the effect of cumulative errors on the accuracy of the first several digits of L.

In example 2, the problem is to calculate the inductance of a bus comprised of line-segment conductors having (1) the external, (2) the mean, and (3) the internal dimensions of the conductors of example 1:

1. $a=6.0$ inches, $c=4.0$ inches, $c/a=0.667$

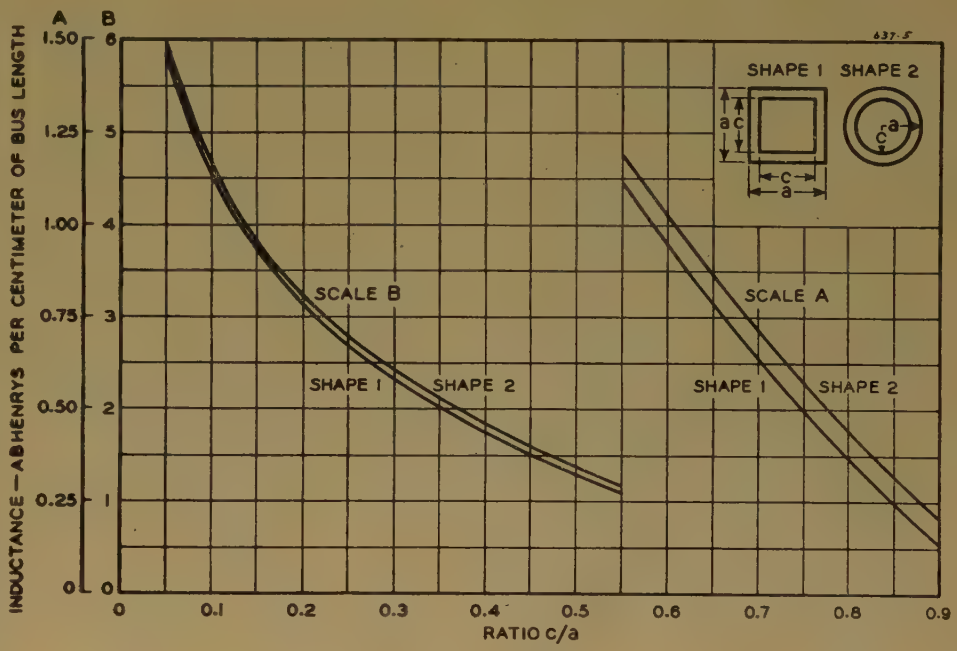


Figure 5

2. $a=47/8$ inches, $c=61/16$ inches, $c/a=0.648$

3. $a=23/4$ inches, $c=29/8$ inches, $c/a=0.631$

For these values of c/a, we obtain from Figure 5:

1. $L_e=0.74$ abhenry per centimeter of bus length.

2. $L_m=0.80$ abhenry per centimeter of bus length.

3. $L_i=0.85$ abhenry per centimeter of bus length.

We note that the value 0.74, corresponding to the use of the external dimensions, and the value 0.758, calculated in example 1 by the use of the general formula, differ by only 2.4 per cent. This close agreement indicates that for the conditions which occur in practice (small conductor thicknesses, and ratio c/a not too near one) values of inductance sufficiently accurate for most design work can be calculated from the approximate formula by use of the external dimensions of the conductors. But since the approximate formula is epitomized in the

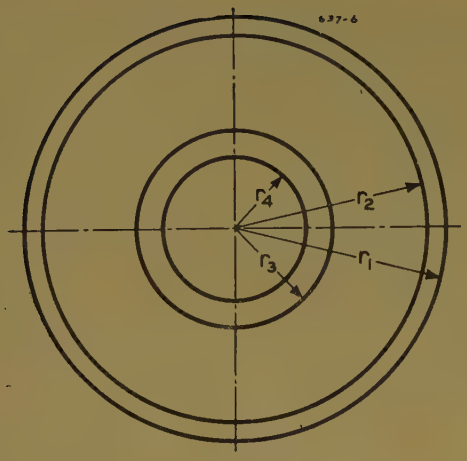


Figure 6

curves of Figure 5, from it we may obtain the inductance we need, only having to calculate the ratio c/a from the specified bus dimensions.

In consequence, considerable advantage with respect to time and labor accrues to the designer. To calculate the inductance from the curves of Figure 5 requires only several minutes, whereas several hours would be required to calculate the inductance from equation 9. Again, the values of example 2 indicate that small changes in bus dimensions result in relatively large changes in bus inductance. In that minimum inductance (hence minimum reactance and correspondingly better voltage regulation) is a desideratum of design, it behooves the designer to investigate all possible combinations of conductors (that are otherwise satisfactory) for the purpose of selecting that combination which possesses minimum inductance. But if the inductances of very many combinations had to be calculated from equation 9, the time, labor, and tedium involved would be considerable; on the other hand, the curves of Figure 5 enable evaluation in almost as many minutes as there are combinations to study.

Corrections for Rounded Edges and for Skin and Proximity Effects

Rounded Edges

To eliminate excessive edge heating caused by skin effect, square tubular conductors of commercial manufacture have rounded edges. Thus square tubular conductors of the sizes specified in example 1 have rounded edges of outer, inner, and mean radius indicated as follows:[12]

$a=6$ inches; $t=a-b=1/8$ inch; $r_o=3/4$ inch, $r_i=5/8$ inch, $r_m=11/16$ inch.

$c=4$ inches; $t'=c-d=3/16$ inch; $r_o=1/2$ inch, $r_i=5/16$ inch, $r_m=13/32$ inch.

Dwight and Wang[7] have derived, semi-empirically, that the approximate increase in inductance ΔL caused by rounding the edges of a conductor of square cross section is

$$\Delta L=2[k^2 \log k^{-1}+0.716k^2+0.5k^3+\ldots] \text{ abhenrys per centimeter of conductor length} \quad (18)$$

where $k=0.463r/s$, r is the mean radius of the rounded edge, s the mean side of the square cross section, and r is small compared with s, the accuracy increasing as $r/s \rightarrow 0$.

For the outer conductor, $s=a-t=47/8$ inches, and $r=11/16$ inch. Hence $k=0.0542$, and $\Delta L=0.022$. For the inner conductor, $s=c-t'=61/16$ inches, and $r=13/32$ inch. Hence $k=0.0494$, and $\Delta L=0.018$. Accordingly, the increase in bus inductance because of the rounded edges is 0.04 abhenry per centimeter of bus length. The corrected value, then, is 0.798 abhenry per centimeter of bus length.

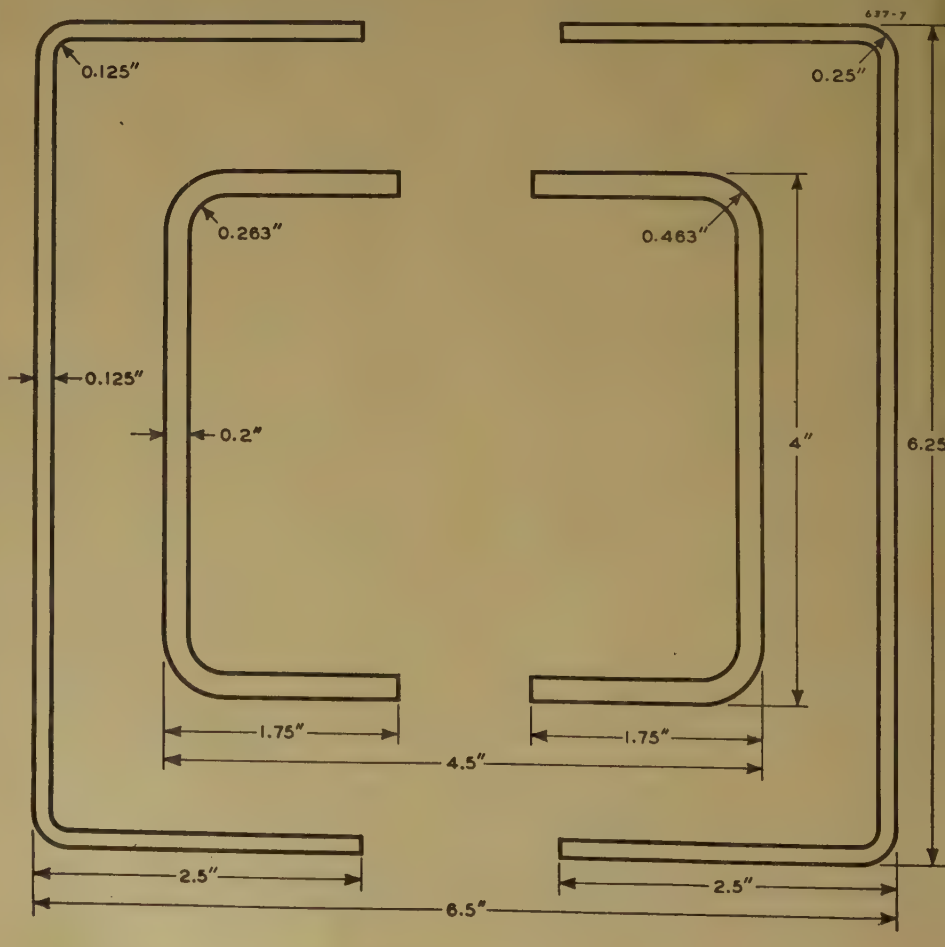
The facts that rounding the corners will result in an increase of inductance and that the increase just calculated from equation 18 is of the correct order of magnitude are confirmed by the following consideration of the coaxial bus with a cross section as shown in Figure 6. As derived in Appendix VI, the d-c inductance of this bus is

$$L=\{(r_3^2-3r_4^2)/2(r_3^2-r_4^2)+[2r_4^4/(r_3^2-r_4^2)^2]\log r_3/r_4\}+\{(r_2^2-3r_1^2)/2\times(r_1^2-r_2^2)+[2r_1^4/(r_1^2-r_2^2)^2]\times\log r_1/r_2\}+[2\log r_2/r_3] \text{ abhenrys per centimeter of bus length} \quad (19)$$

where the first and second braced terms stem, respectively, from the flux-current linkages in the regions $r_4 \leq r \leq r_3$, and $r_2 \leq r \leq r_1$ (hence they are the so-called internal inductances of the inner and outer conductors) and the third braced term stems from the flux-current linkages in the region $r_3 \leq r \leq r_2$ (hence it is the so-called intra-inductance of the conductors). Let the conductors have (1) the same thicknesses and (2) external diameters equal to the external dimensions of the corresponding conductors of example 1. Thus $r_1=3$ inches, $r_2=23/8$ inches, $r_3=2$ inches, and $r_4=29/16$ inches. Substituting these values in equation 19 and performing the indicated computation yields

$$L=0.062+0.029+0.726$$
$$=0.817 \text{ abhenry per centimeter of bus length} \quad (20)$$

Figure 7



This value is a bit greater than the corrected value of 0.798 for rounded square conductors, which is to be expected. For as the radii of rounding increase, the coaxial square tubular bus approaches the coaxial circular tubular bus as a geometrical limit. Again, the magnitudes of the corrections for rounding increase with the radii of rounding. Hence it follows that the inductance of the square tubular bus approaches the inductance of the circular tubular bus as a limit and that the approach is from below.

In conclusion, it is to be noted that rounding of the edges, even if considerable, results in a relatively small increase in inductance, no matter what the sizes may be of the conductors comprising the bus. For a circular tubular conductor can be considered as the extreme case of a rounded square tubular conductor, its side being equal to the diameter of the circular conductor. Yet for all values of the independent variable of Figure 5, corresponding ordinates of the curves for the square and circular conductors differ by only a few per cent.

Skin and Proximity Effects

As the frequency increases from zero to a specified value, the currents in the inner and outer conductors of a coaxial circular tubular conductor tend to concentrate in thin surface strata on the adjacent surfaces of the two conductors. This phenomenon results in a decrease of the flux-current linkages in the regions $r_4 \leq r \leq r_3$, and $r_2 \leq r \leq r_1$. The flux-current linkages in the region $r_3 \leq r \leq r_2$ are, however, unchanged. The net result of the decrease in the internal inductances and of the constancy of the intra-inductance of the conductors is a decrease in the sum of the three, the total inductance of the bus. But, as in practical busses, the sum of the d-c internal inductances is, as evidenced in equation 20, only a few per cent of the total inductance, and as at 60-cycles the decrease in the internal inductances is only a fraction of one per cent of their d-c values, it follows that the actual change in total inductance caused by 60-cycle skin and proximity effects is negligible. Confirmatively, the authors have calculated the actual 60-cycle inductance of the circular tubular bus in a foregoing section ("Rounded Edges") and find it to be identical (to several places of decimals) with the d-c value cited in equation 20.

In view of the negligible change in the inductance of this coaxial circular tubular bus, the small two-per-cent difference between the inductance of this bus and the one of the coaxial rounded square tubular bus of example 1, and the general geometric similarity between these two busses, we conclude that in the bus of example 1, and in practical dimensioned rounded square tubular busses in general, 60-cycle skin and proximity effects are negligible insofar as the inductance of the bus is concerned. This conclusion is in accord with the results of analytic and experimental investigations of the inductance of coplanar busses comprised of square[7] tubular or rectangular[13] conductor.

Busses Comprised of Structural Tubular Conductor

A conductor comprised of two slightly separated channels or angles, placed flange to flange, usually is not of a square cross section. If, however, the cross section does not differ too greatly from a square cross section, and commonly this is the case in practice, it is to be expected that a fairly good approximation to the actual inductance of the bus can be effected by judicious use of the formulas for the square cross section. Thus for the bus dimensioned[2,3] as in Figure 7, consider an equivalent square tubular bus with conductors having the same external

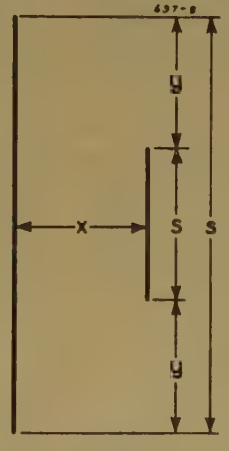


Figure 8

perimeters (rounded edges aside) as the ones in Figure 7. Then, as detailed in Appendix VII, the inductance of this equivalent bus is 0.755 abhenry per centimeter of bus length. Against this value we have the inductance, calculated (in Appendix VII) from the measured load impedance, as 0.837 abhenry per centimeter of bus length. The difference in the two values is approximately 10 per cent of the measured value. On the other hand, if we assume an equivalent bus having square conductors with sides equal to the webs of the given conductors, we obtain an inductance of 0.849 abhenry per centimeter of bus length. This value differs from the measured value by only 1.4 per cent. In general, we infer that selecting an equivalent bus on one or the other of the bases mentioned will yield an approximate value of inductance within a few per cent of the actual value, which is all that is required for most design purposes.

Polyphase Coaxial Busses

To calculate the performance of polyphase busses requires knowledge of the reactance drops on the individual conductors. The general equations for determining these reactance drops have been developed elsewhere.[8] It suffices here to mention that these equations express the reactance drops in terms of the self and mutual geometric mean distances of the cross sections of the square tubular conductors comprising the bus, and that these geometric mean distances are furnished by equation 8. For, as a comparison of equations 1 and 8 makes clear, in the right-hand member of equation 8 the first term is minus twice the logarithm

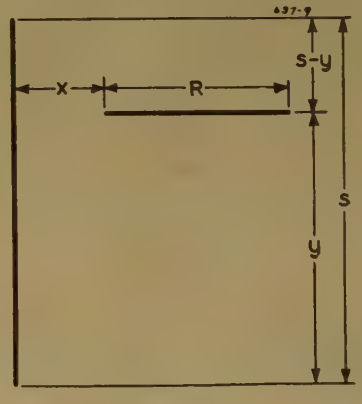


Figure 9

of the self geometric mean distance of the outer hollow square of Figure 2, the second is minus twice the logarithm of the self geometric mean distance of the inner hollow square, and the third is four times the logarithm of the mutual geometric mean distance of the two hollow squares. Hence as a, b, c, and d are arbitrary, we have general formulas for the self and mutual geometric mean distances of two concentric parallel-sided hollow rectangles of arbitrary dimensions. In essence, therefore, calculation of the reactance drops on the conductors of a specified

polyphase bus reduces to determination of the numerical values of the required geometric mean distances from the just-mentioned formulas and substitution of these values in the general equations (which are typified by equation 28 of reference 8).

Appendix I

The geometric mean distances indicated in equation 8 follow from equation 3 by substitution therein of the following values of the parameters A_p and B_q, these values being obtained from equations 5 and 6 through inspection of Figure 2:

$\log D_{11}$: $A_1=A_3=B_1=B_3=a$; $A_2=A_4=B_2=B_4=0$

$\log D_{22}$: $A_1=A_3=B_1=B_3=b$; $A_2=A_4=B_2=B_4=0$

$\log D_{33}$: $A_1=A_3=B_1=B_3=c$; $A_2=A_4=B_2=B_4=0$

$\log D_{44}$: $A_1=A_3=B_1=B_3=d$; $A_2=A_4=B_2=B_4=0$

$\log D_{12}$: $A_1=A_3=B_1=B_4=(a+b)/2$; $A_2=A_4=B_2=B_4=(a-b)/2$

$\log D_{13}$: $A_1=A_3=B_1=B_3=(a+c)/2$; $A_2=A_4=B_2=B_4=(a-c)/2$

$\log D_{14}$: $A_1=A_3=B_1=B_3=(a+d)/2$; $A_2=A_4=B_2=B_4=(a-d)/2$

$\log D_{14}$: $A_1=A_3=B_1=B_3=(b+c)/2$; $A_2=A_4=B_2=B_4=(b-c)/2$

$\log D_{24}$: $A_1=A_3=B_1=B_3=(b+d)/2$; $A_2=A_4=B_2=B_4=(b-d)/2$

$\log D_{34}$: $A_1=A_3=B_1=B_3=(c+d)/2$; $A_2=A_4=B_2=B_4=(c-d)/2$

Utilizing these parameters in equation 3 yields

$$S_1^2 \log D_{11} = -(25/12)S_1^2-(1/6)[K(a,a)+K(0,0)-2K(a,0)] \quad (21)$$

$$S_1S_2 \log D_{12} = -(25/12)S_1S_2-(1/6)\times\{K[(a+b)/2,(a+b)/2]+K[(a-b)/2,(a-b)/2]-2K[(a+b)/2,(a-b)/2]\} \quad (22)$$

and similar obvious equations are obtained for the other eight geometric mean distances.

Substituting appropriately in equation 8 and collecting corresponding terms in K yield

$$\begin{aligned}L=&[-1/3(a^2-b^2)^2]\{2K[(a+b)/2,(a+b)/2]+2K[(a-b)/2,(a-b)/2]-4K[(a+b)/2,(a-b)/2]-K(a,a)-K(b,b)+2K(a,0)+2K(b,0)\}+\\&[-1/3(c^2-d^2)^2]\{2K[(c+d)/2,(c+d)/2]+2K[(c-d)/2,(c-d)/2]-4K[(c+d)/2,(c-d)/2]-K(c,c)-K(d,d)+2K(c,0)+2K(d,0)\}+\\&[2/3(a^2-b^2)(c^2-d^2)]\{K[(a+d)/2,(a+d)/2]+K[(a-d)/2,(a-d)/2]-2K[(a+d)/2,(a-d)/2]-K[(b+d)/2,(b+d)/2]-K[(b-d)/2,(b-d)/2]+2K[(b+d)/2,(b-d)/2]-K[(a+c)/2,(a+c)/2]-K[(a-c)/2,(a-c)/2]+2K[(a+c)/2,(a-c)/2]+K[(b+c)/2,(b+c)/2]+K[(b-c)/2,(b-c)/2]-2K[(b+c)/2,(b-c)/2]\}\end{aligned} \quad (23)$$

Evaluating the various terms through the use of equation 4 yields equation 9.

As already discussed in an earlier part of this paper ("Polyphase Coaxial Busses"), the terms of the right-hand members of equation 9, and thus of equation 23, can be interpreted in terms of the self and mutual geometric mean distances of the two hollow rectangles of Figure 2.

Appendix II

The geometric mean distances indicated in equation 11 follow from equation 3 by substitution therein of the following values of the parameters A_p and B_q, these values being obtained from equations 5 and 6 through inspection of Figure 3:

$\log D_{11}$: $A_1=A_3=a$, $A_2=A_4=0$; $B_1=B_3=(a-b)/2$, $B_2=B_4=0$

$\log D_{22}$: $A_1=A_3=(a-b)/2$, $A_2=A_4=0$; $B_1=B_3=b$, $B_2=B_4=0$

$\log D_{55}$: $A_1=A_3=c$, $A_2=A_4=0$; $B_1=B_3=(c-d)/2$, $B_2=B_4=0$

$\log D_{66}$: $A_1=A_3=(c-d)/2$, $A_2=A_4=0$; $B_1=B_3=d$, $B_2=B_4=0$

$\log D_{12}$: $A_1=(a-b)/2$, $A_2=0$, $A_3=a$, $A_4=(a+b)/2$; $B_1=(a+b)/2$, $B_2=b$, $B_3=0$, $B_4=(a-b)/2$

$\log D_{13}$: $A_1=A_3=a$, $A_2=A_4=0$; $B_1=a$, $B_2=B_4=(a+b)/2$, $B_3=b$

$\log D_{15}$: $A_1=A_3=(a+c)/2$, $A_2=A_4=(a-c)/2$; $B_1=(a-d)/2$, $B_2=(b-d)/2$, $B_3=(b-c)/2$, $B_4=(a-c)/2$

$\log D_{16}$: $A_1=(a-d)/2$, $A_2=(a+d)/2$, $A_3=(a+c)/2$, $A_4=(a-c)/2$; $B_1=(a+d)/2$, $B_2=(b+d)/2$, $B_3=(b-d)/2$, $B_4=(a-d)/2$

$\log D_{17}$: $A_1=A_3=(a+c)/2$, $A_2=A_4=(a-c)/2$; $B_1=(a+c)/2$, $B_2=(b+c)/2$, $B_3=(b+d)/2$, $B_4=(a+d)/2$

$\log D_{24}$: $A_1=a$, $A_2=A_4=(a+b)/2$, $A_3=b$; $B_1=B_3=b$, $B_2=B_4=0$

$\log D_{25}$: $A_1=(a+c)/2$, $A_2=(b+c)/2$, $A_3=(b-c)/2$, $A_4=(a-c)/2$; $B_1=(b-d)/2$, $B_2=(b+d)/2$, $B_3=(b+c)/2$, $B_4=(b-c)/2$

$\log D_{26}$: $A_1=(a-d)/2$, $A_2=(b-d)/2$, $A_3=(b-c)/2$, $A_4=(a-c)/2$; $B_1=B_3=(b+d)/2$, $B_2=B_4=(b-d)/2$

$\log D_{28}$: $A_1=(a+c)/2$, $A_2=(b+c)/2$, $A_3=(b+d)/2$, $A_4=(a+d)/2$; $B_1=B_3=(b+d)/2$, $B_2=B_4=(b-d)/2$

$\log D_{56}$: $A_1=(c-d)/2$, $A_2=(c+d)/2$, $A_3=c$, $A_4=0$; $B_1=(c+d)/2$, $B_2=d$, $B_3=0$, $B_4(c-d)/2$

$\log D_{57}$: $A_1=A_3=c$, $A_2=A_4=0$; $B_1=c$, $B_2=B_4=(c+d)/2$, $B_3=d$

$\log D_{68}$: $A_1=c$, $A_2=A_4=(c+d)/2$, $A_3=d$; $B_1=B_3=d$, $B_2=B_4=0$

Substituting these parameters in equation 3 yields, in terms of K, the desired expressions for the geometric mean distances (which have been omitted here because of the space required). Substituting these expressions in equation 11 and collecting like terms yields equation 23 and hence, corroboratively, equation 9.

Appendix III

The geometric mean distance between two line segments, located as illustrated in Figure 8, is given by equation 11 of reference 9:

$$\begin{aligned}Ss \log D=(1/2)\{&-[x^2-(S+y)^2]\times\log[x^2+(S+y)^2]+(x^2-y^2)\times\log(x^2+y^2)+4x(S+y)\times\tan^{-1}[(S+y)/x]-4xy\times\tan^{-1}(y/x)-3Ss\}\end{aligned} \quad (24)$$

The geometric mean distance between two line segments, located as illustrated in Figure 9, is given by equation 15 of reference 9:

$$Rs \log D = I(R+x,s-y)-I(x,s-y)+I(R+x,y)-I(x,y)-3Rs/2 \quad (25)$$

wherein, typically,

$$I(x,y)=(1/2)[xy\log(x^2+y^2)+x^2\times\tan^{-1}(y/x)+y^2\tan^{-1}(x/y)] \quad (26)$$

The geometric mean distances indicated in equation 13 are obtained by substitution in equation 24 of the first six, and in equation 25 of the last three, of the following sets of values of the parameters x, y, R, and S, these values being obtained by inspection of Figures 4, 8, and 9:

$\log D_{11}$: $x=0$, $y=0$, $S=s=a$

$\log D_{55}$: $x=0$, $y=0$, $S=s=c$

$\log D_{13}$: $x=a$, $y=0$, $S=s=a$

$\log D_{57}$: $x=c$, $y=0$, $S=s=c$

$\log D_{15}$: $x=y=(a-c)/2$, $S=c$, $s=a$

$\log D_{17}$: $x=(a+c)/2$, $y=(a-c)/2$, $S=c$, $s=a$

$\log D_{12}$: $x=0$, $y=0$, $R=s=a$

$\log D_{66}$: $x=0$, $y=0$, $R=S=c$

$\log D_{16}$: $x=(a-c)/2$, $y=(a+c)/2$, $R=c$, $s=a$

Utilizing these parameters in equations 24 and 25 as stated yields

$\log D_{11}=\log a-3/2$

$\log D_{55}=\log c-3/2$

$\log D_{12}=\log a+(1/2)\log 2+\pi/4-3/2$

$\log D_{56}=\log c+(1/2)\log 2+\pi/4-3/2$

$\log D_{13}=\log a+\pi/2-3/2$

$\log D_{57}=\log c+\pi/2-3/2$

$\log D_{15}=(1/2)\{\log(a^2+c^2)+[(a^2-c^2)/ac]\times\tan^{-1}[(a+c)/(a-c)]-\pi(a-c)^2/4ac-3\}$

$\log D_{16}=(1/4)\{[(a+c)^2/ac]\log(a+c)-[(a-c)^2/ac]\log(a-c)-2\log 2+\pi-6\}$

$\log D_{17}=(1/2)1\{\text{og}(a^2+c^2)-[(a^2-c^2)/ac]\times\tan^{-1}[(a-c)/(a+c)]+\pi(a+c)^2/4ac-\log 2-3\}$

Appendix IV

The co-ordinates used for plotting the curves of Figure 5 for the square tubular conductors are obtained by substituting the indicated values of A in equation 16, obtaining the values of the logarithmic and arctangentic terms from the Work Projects Administration tables, and performing all computation on a 10-row electric calculating machine. To avoid cumulative errors all

computation was effected to eight significant figures. For actual plotting, however, the inductance need only be known to the three or four significant figures given in Table I.

Table I

A	r=c/a	L	A	r=c/a	L
0	1	0	0.6	1/4	2.693
0.1	9/11	0.354	0.7	3/17	3.389
0.2	2/3	0.744	0.8	1/9	4.315
0.3	7/13	1.164	0.9	1/19	5.809
0.4	3/7	1.617	1.0	0	∞
0.5	1/3	2.117			

The inductance of a coaxial bus comprised of indefinitely thin circular tubular conductors, dimensioned as in shape 1 of Figure 5, is $L=-2\log(c/a)$. Hence the co-ordinates of the curves of Figure 5 for shape 1 are as shown in Table II.

Table II

c/a	L	c/a	L	c/a	L
0	∞	0.4	1.833	0.8	0.373
0.1	4.605	0.5	1.386	0.9	0.193
0.2	3.219	0.6	1.022	1.0	0
0.3	2.408	0.7	0.728		

Appendix V

Equation 23 for the inductance of a bus, with a cross section as illustrated in Figure 2 is valid for conductors of arbitrary thickness. Accordingly, the inductance of a bus with a cross section comprised of line segments as shown in Figure 4 can be obtained by determining the limit of the inductance of the bus in Figure 2 as the thicknesses of the conductors comprising the bus approach zero.

To effect this determination, we require, as will be seen below, knowledge of the following derivatives: $\partial^2K(u,u)/\partial x^2$, $\partial^2K(v,v)/\partial y^2$, $\partial^2K(u,v)/\partial x\partial y$, wherein $u=(x+y)/2$, and $v=(x-y)/2$. From equation 4 we have

$$K(u,u)=-4u^4\log u-2u^4\log 2-2u^4\pi \quad (27)$$

Substituting from equation 27 into the identity

$$\frac{\partial^2K(u,u)}{\partial y\partial x}=\frac{\partial}{\partial u}\left[\frac{\partial K}{\partial u}\frac{\partial u}{\partial x}\right]\frac{\partial u}{\partial y} \quad (28)$$

and performing the indicated differentiations yield

$$\partial^2K(u,u)/\partial y\partial x=-u^2(12\log u+6\log 2+6\pi+7) \quad (29)$$

Hence

$$\partial^2K[(x+y)/2,\ (x+y)/2]/\partial y\partial x=-[(x+y)^2/4][12\log(x+y)-6\log 2+6\pi+7] \quad (30)$$

Similarly,

$$\partial^2K[(x-y)/2,\ (x-y)/2]/\partial y\partial x=[(x-y)^2/4][12\log(x-y)-6\log 2+6\pi+7] \quad (31)$$

To evaluate $\partial^2K(u,v)/\partial x\partial y$ we note that the real part of the complex function

$$W(w)\equiv W(u+iv)=U(u,v)+iV(u,v)=w^4\log w \quad (32)$$

is

$$Re(W)=U(u,v)=K(u,v)+2\pi uv^3 \quad (33)$$

This identity is easily established by separating $w^4\log w$ into its real and imaginary parts and using the identity $\tan^{-1}u/v+\tan^{-1}v/u=\pi/2$. Now

$$\frac{\partial^2U}{\partial x\partial y}=\frac{\partial^2U}{\partial u^2}\frac{\partial u}{\partial x}\frac{\partial u}{\partial y}+\frac{\partial^2U}{\partial v^2}\frac{\partial v}{\partial x}\frac{\partial v}{\partial y}+\frac{\partial^2U}{\partial u\partial v}\left[\frac{\partial v}{\partial x}\frac{\partial u}{\partial y}+\frac{\partial u}{\partial x}\frac{\partial v}{\partial y}\right]+\frac{\partial U}{\partial u}\frac{\partial^2u}{\partial x\partial y}+\frac{\partial U}{\partial v}\frac{\partial^2v}{\partial x\partial y} \quad (34)$$

Inasmuch as

$$d^2W/dw^2=\partial^2U/\partial u^2+i\partial^2V/\partial u^2=-\partial^2U/\partial v^2-i\partial^2V/\partial v^2 \quad (35)$$

we have $\partial^2U/\partial u^2=-\partial^2U/\partial v^2=Re(d^2W/dw^2)$. Accordingly, substituting appropriately in equation 34 and performing the indicated differentiations with respect to x and y gives

$$\partial^2U/\partial x\partial y=(1/4)[Re(d^2W/dw^2)+Re(d^2W/dw^2)+0+0+0]={}^1/_2Re(d^2W/dw^2) \quad (36)$$

Substituting from equation 32 in equation 36 and performing the indicated differentiation yields

$$\partial^2U/\partial x\partial y=Re(6w^2\log w+7w^2/2)=Re[6(u^2-v^2+2iuv)\log(u+iv)+7(u^2-v^2+2iuv)/2]=3(u^2-v^2)\log(u^2+v^2)-12uv\times\tan^{-1}v/u+7(u^2-v^2)/2 \quad (37)$$

Since, from equation 33,

$$\partial^2K/\partial x\partial y=\partial^2U/\partial x\partial y-2\pi\partial^2(uv^3)/\partial x\partial y \quad (38)$$

we obtain, on substitution in equation 38 from equation 37 and expressing u and v in terms of x and y,

$$\partial^2K[(x+y)/2,\ (x-y)/2]/\partial x\partial y=3xy\times\log(x^2+y^2)-3xy\log 2-3(x^2-y^2)\times\tan^{-1}[(x-y)/(x+y)]+7xy/2+3\pi(x^2-y^2)/4 \quad (39)$$

With these identities obtained, we are prepared to consider the limiting process. For convenience, equation 9 is written in the form

$$L=(-1/3)L_1(a,b)/(a^2-b^2)^2-(1/3)L_2\times(c,d)/(c^2-d^2)^2+(2/3)L_3(a,b,c,d)\div(a^2-b^2)(c^2-d^2) \quad (40)$$

First, let $b\to a$. In the limit the outer conductor of Figure 2 is comprised of line segments. The inductance of the resulting bus is

$$\lim_{b\to a}L=(-1/3)\lim_{b\to a}L_1(a,b)/(a^2-b^2)^2-(1/3)L_2(c,d)/(c^2-d^2)^2+(2/3)\lim_{b\to a}L_3(a,b,c,d)/(a^2-b^2)\times(c^2-d^2) \quad (41)$$

Now $[L_1(a,b)/(a^2-b^2)^2]_{b=a}=0/0$; similarly $[L_3(a,b,c,d)/(a^2-b^2)(c^2-d^2)]_{b=a}=0/0$. Accordingly, the limits in the right-hand member of equation 41 are to be determined by applying L'Hospital's rule for evaluating indeterminate expressions of the form 0/0. Applying this rule to the first limit yields

$$\lim_{b\to a}L_1(a,b)/(a^2-b^2)^2=\{[\partial^2L_1(a,b)/\partial^2b]\div[\partial^2(a^2-b^2)/\partial^2b]\}_{b=a} \quad (42)$$

A second differentiation of numerator and denominator is necessary because the ratio of the first derivatives (for $b=a$) is also of the form 0/0. Performing the differentiations and substitutions indicated gives

$$(1/3)\lim_{b\to a}L_1(a,b)/(a^2-b^2)^2=2\log a+(1/2)\log 2+\pi/2+7/6 \quad (43)$$

For the second limit, L'Hospital's rule yields

$$\lim_{b\to a}L_3(a,b,c,d)/(a^2-b^2)(c^2-d^2)=\{[\partial L_3(a,b,c,d)/\partial b]/[\partial(a^2-b^2)\times(c^2-d^2)/\partial b]\}_{b=a} \quad (44)$$

Effecting the differentiations and substitutions indicated gives

$$\lim_{b\to a}L_3(a,b,c,d)/(a^2-b^2)(c^2-d^2)=L'_3(a,c,d)/(-2a)(c^2-d^2) \quad (45)$$

wherein

$$L'_3(a,c,d)=[\partial\{-K[(a+d)/2,\ (a+d)/2]-K[(a-d)/2,\ (a-d)/2]+2K[(a+d)/2,\ (a-d)/2]+K[(a+c)/2,\ (a+c)/2]+K[(a-c)/2,\ (a-c)/2]-2K[(a+c)/2,\ (a-c)/2]\}/\partial b]_{b=a} \quad (46)$$

Secondly, let $d\to c$. In the limit the inner conductor of Figure 2 is comprised of line segments, hence the cross section is now that of Figure 4. From equations 41, 43, and 45, the inductance of this line segment bus is

$$\lim_{d\to c}\lim_{a\to b}L=-[2\log a+(1/2)\log 2+\pi/2+7/6]-(1/3)\lim_{d\to c}L_2(c,d)\div(c^2-d^2)^2+(2/3)\lim_{d\to c}L'_3(a,c,d)\div(-2a)(c^2-d^2) \quad (47)$$

Except for the interchange of a and b with c and d, the second term in the right-hand member of equation 47 is identical with the first term in the right-hand member of equation 41. Hence from equation 43, we have

$$(1/3)\lim_{d\to c}L_2(c,d)/(c^2-d^2)^2=2\log c+(1/2)\log 2+\pi/2+7/6 \quad (48)$$

Now

$$[L'_3(a,c,d)/(-2a)(c^2-d^2)]_{c=d}=0/0$$

Accordingly, L'Hospital's rule yields

$$\lim_{d\to c}L'_3(a,c,d)/(-2a)(c^2-d^2)=\{[\partial L'_3(a,c,d)/\partial d]/[\partial(-2a)\times(c^2-d^2)/\partial d]\}_{d=c}=L''_3(a,c)/4ac \quad (49)$$

wherein

$$L''_3(a,c)=[\partial^2\{-K[(b+d)/2,\ (b+d)/2]-K[(b-d)/2,(b-d)/2]+2K[(b+d)/2,\ (b-d)/2]\}/\partial d\partial b]_{\substack{b=a\\d=c}} \quad (50)$$

Performing the differentiations by use of equations 30, 31, and 39 and substituting as indicated yields

$$(1/3)L''_3(a,c)/4ac = -(a/4c)\log[(a-c)\div(a+c)] - (c/4a)\log[(a-c)/(a+c)] + (1/2)\log[(a^2-c^2)(a^2+c^2)] - [(a^2-c^2)/2ac]\tan^{-1}[(a-c)\div(a+c)] + \pi(a^2-c^2)/8ac - \log 2 + \pi/2 + 7/6 \quad (51)$$

Finally, substituting from equations 48 and 49 in equation 47 and collecting terms yields, corroboratively, equation 14.

Appendix VI

By virtue of the fundamental definition of the inductance of a circuit, $L = W/2I^2$, wherein W is the energy in the magnetic field produced by the circuit current I, and the calculation of L reduces to the calculation of W. Because of the circular symmetry of the coaxial circular tubular bus with a cross section as illustrated in Figure 6, W easily is calculated from the well-known relation $W = 1/2$ (summation of the flux-current linkages associated with the circuit). Accordingly, $L =$ (summation of the flux-current linkages)$/I^2$.

In that a circular tubular conductor produces no field in the cylindrical space bounded by its internal surface, the flux density B, and thus the flux-current linkage, in the region $0 \geq r \geq r_4$ is zero.

In the region $r_4 \geq r \geq r_3$, we have $B = 2\mu I(r)/r$, wherein $I(r) = I(r^2-r_4^2)/(r_3^2-r_4^2)$ is the current in the region $r_4 \geq r \geq r$. Accordingly, the flux contained in a thin tube of unit length and of thickness dr is $[2\mu I(r)dr/r]$. Hence the total flux-current linkages per unit length are

$$[2\mu I^2/(r_3^2-r_4^2)^2]\int_{r_4}^{r_3}[(r^2-r_4^2)/r]dr = [2\mu I^2/(r_3^2-r_4^2)^2][(r_3^2-r_4^2)\times(r_3^2-3r_4^2)/4 + r_4^4\log(r_3/r_4)] \quad (52)$$

In the region $r_3 \leq r \leq r_2$, the flux density is $B = 2\mu I/r$, the flux contained in a thin tube of unit length and of thickness dr is $(2\mu I/r)dr$, and the current encompassed by this flux is I. Hence the total flux-current linkages are

$$2\mu I^2\int_{r_3}^{r_2}(1/r)dr = 2\mu I^2\log(r_2/r_3) \quad (53)$$

In the region $r_2 \leq r \leq r_1$, we have $B = 2\mu I(r)/r$; hence the flux contained in a thin tube of unit length and of thickness dr is $2\mu I(r)/dr$. The current encompassed by this flux is $I(r) = I - I(r^2-r_2^2)/(r_1^2-r_2^2) = I(r_1^2-r^2)/(r_1^2-r_2^2)$. Thus the total flux linkages are

$$[2\mu I^2/(r_1^2-r_2^2)^2]\int_{r_2}^{r_1}[(r_1^2-r^2)/r]dr = [2\mu I^2/(r_1^2-r_2^2)^2][(r_1^2-r_2^2)\times(r_2^2-3r_1^2)/4 + r_1^4\log(r_1/r_2)] \quad (54)$$

The total of the flux-current linkages is the sum of the right-hand members of equations 52, 53, and 54. Dividing this sum by I^2 and taking $\mu = 1$ yield the right-hand member of equation 19.

Appendix VII

The external perimeters of the cross sections of the outer and inner conductors of Figure 7 are encompassed by rectangles respectively 25.5 inches and 17 inches in perimeter. Consider equivalent conductors of square cross section, of external perimeters equal to these values, and of the same thicknesses as the given conductors. The external, mean, and internal ratios of c/a are, respectively, 0.667, 0.648, and 0.629. From Figure 5 we obtain, respectively, 0.74, 0.80, and 0.855 abhenry per centimeter of bus length. Again, $r_o = 0.1875$ and $r_i = 0.363$, thus $k_e = 0.0134$ and $k_i = 0.0415$. Hence from equation 18, we obtain respectively 0.0019 and 0.0134 abhenry per centimeter of bus length as corrections for the rounding of the edges of the outer and inner conductors. Accordingly, the total inductance of the equivalent bus, depending on the dimensions used, is

$$L_e = 0.755;\ L_m = 0.815;\ L_i = 0.87 \text{ abhenry per centimeter of bus length} \quad (55)$$

On the other hand, if we assume the equivalent bus to be comprised of conductors with sides of 6.25 inches and 4 inches, the dimensions of the webs of the corresponding given conductors, the corresponding ratios of c/a are 0.641, 0.621, and 0.600. From Figure 5 we obtain respectively 0.825, 0.885, and 0.938 abhenry per centimeter of bus length. Again, $k_o = 0.0142$ and $k_i = 0.0442$, hence from equation 18 we obtain respectively 0.002 and 0.015 abhenry per centimeter of bus length as corrections for the rounding of the edges of the outer and inner conductors. Accordingly, the total inductance of the equivalent bus, depending on the dimensions used, is

$$L_e = 0.842;\ L_m = 0.902;\ L_i = 0.950 \text{ abhenry per centimeter of bus length} \quad (56)$$

Though for comparison values of L_e, L_m, and L_i are displayed, the results in the previous section "Some Illustrative Examples" indicate that the external value would be used for actual computation. In such case, calculation of edge corrections is simplified by use of the external rather than the mean dimensions indicated in equation 18. Proceeding thus for the bus equivalent on the basis of webs yields 0.024 rather than 0.017. The difference in these two values is negligible in comparison with the total inductance. Further, as the correction increases, the calculation is on the safe side.

The a-c resistance of the actual bus is

$$R = \rho(A_o^{-1} + A_i^{-1})K_s \text{ ohms per foot of bus length} \quad (57)$$

wherein ρ is the resistivity (in ohms-circular mils per foot) of the copper at operating temperature, A_o and A_i are the areas (in circular mils) of the cross sections of the outer and inner conductors, and K_s is the skin effect factor of the conductors.

In the absence of stated experimental values, we assume conventional values of 50 degrees centigrade for the operating temperature and 98 per cent conductivity for the bus copper. Then the resistivity is $\rho = (10.37/0.98)[1 + 0.00393(50-20)] = 11.82$ ohms-circular mils per foot. The outer conductor, constructed of two rectangular strips bent into shape, is of area $A_o = 2(10.75\times0.125) = 2.69$ square inches, thus 3,430,000 circular mils. The inner conductor, comprised of stock channels, is of area $A = 2[2(1.75-0.463)0.2 + (4-2\times0.463)0.2 + \pi(0.463^2-0.263^2)/2] = 2.72$ square inches, thus 3,460,000 circular mils. The skin-effect factor[12] for a range of square tubular conductors, which encompasses those approximating the shapes of the given conductors, is $K_s = 1.04$.

Substituting these values in equation 57 yields a resistance of 7.18 micro-ohms per foot of bus length. The measured impedance is 12 micro-ohms per foot of bus length. From this value we find the inductance to be $L = (144-51.3)^{1/2}/377 = 2.55$ microhenrys, or in centimeter-gram-second units, 0.837 abhenry per centimeter of bus length.

References

1. Resistance Welder Feed Has Low Resistance Drop, L. R. Bogardus. *Electrical World*, volume 110, 1938, pages 702–04.

2. Concentric Bus for Resistance Welders, W. Specht. *Electrical World*, volume 114, 1940, page 558.

3. A Concentric Channel Bus for Resistance Welders, W. Specht. *Welding Engineer*, volume 26, June 1941, pages 31–2.

4. The Design of Bus-Bar Industrial Distribution Systems: an Epitomization of Available Data, T. J. Higgins. AIEE Transactions, volume 64, 1945, pages 385–400; discussion, pages 486–8.

5. The Alternating-Current Resistance of Hollow Square Conductors, A. H. M. Arnold. *Journal*, Institution of Electrical Engineers (London, England), volume 82, 1938, pages 537–45.

6. Temperature Rise of Bus Bars, H. B. Dwight, G. W. Andrew, H. W. Tileston. *General Electric Review*, volume 43, 1940, pages 213–16.

7. Reactance of Square Tubular Bus Bars, H. B. Dwight, T. K. Wang. AIEE Transactions, volume 57, 1938, pages 762–5; discussion, pages 765–6.

8. Formulas for the Calculation of the Inductance of Linear Conductors of Structural Shape, T. J. Higgins. AIEE Transactions, volume 62, 1943, February section, pages 53–8.

9. Formulas for the Geometric Mean Distances of Rectangular Areas and of Line Segments, T. J. Higgins. *Journal of Applied Physics*, volume 14, 1943, pages 188–95.

10. Tables of Natural Logarithms (book), Work Projects Administration. Columbia University Press, New York, N. Y.

11. Tables of Arctangents (book), Work Projects Administration. Columbia University Press, New York, N. Y.

12. Formulas for the Inductance of Rectangular Tubular Conductors, T. J. Higgins. AIEE Transactions, volume 60, 1941, December section, pages 1046–50.

13. Chase Electrical Handbook (book). Chase Brass and Copper Company, Inc., Waterbury, Conn., 1941. Pages 80–1.

14. The Inductance of Linear Conductors of Rectangular Section, A. H. M. Arnold. *Journal*, Institution of Electrical Engineers (London, England), volume 70, 1931–32, pages 579–86.

Supervisory Control of 30,000-Kva Hydroelectric Plant

C. W. BOHNER
MEMBER AIEE

A. P. MANESS
ASSOCIATE AIEE

Synopsis: Ocoee 3, a 1-unit 30,000-kva supervisory-controlled generating station of the Tennessee Valley Authority, has been in operation since April 30, 1943. An underground cable was selected for the control and telemetering channel, and neutralizing transformers were installed to protect against voltage rise resulting from transmission line faults. Instrumentation, controls, and station auxiliaries were designed particularly to safeguard the unattended equipment. Maintenance includes two or three inspections per week. The cost of supervision, operation, and maintenance is as low as $0.101 per 1,000 kilowatt-hours.

THE AUTOMATIC and supervisory control features of Ocoee 3 hydroelectric plant of the Tennessee Valley Authority are of special interest because of the size and importance of the equipment controlled. The 30,000-kva generator is one of the large units in the United States operating completely unattended, and the outdoor switchyard with its 74,000-kva 161/69/13.8-kv tap-changing-under-load transformer bank serves as a switching center for the 154- and 66-kv transmission lines in the area. The entire plant is supervisory-controlled from Ocoee 2 hydroelectric plant located five miles downstream.

The geographical location and transmission line connections of Ocoee 3 plant are shown in Figure 1. The 154-kv line to Apalachia serves as a tie between the main 154-kv transmission system and the local 66-kv transmission system in the Ocoee River area. The installed generating capacities of Ocoee 2 and Blue Ridge hydroelectric plants, which are connected to the 66-kv system, are 19,900 and 20,000 kw respectively.

Ocoee 3 Dam is located 2.5 miles upstream from the powerhouse, and a connecting tunnel terminates in a surge tank at the upper end of the penstock. A butterfly valve is provided in the penstock near the surge tank. A view of the surge tank, valve house, penstock, powerhouse, and switchyard is shown in Figure 2.

A single-line diagram of the Ocoee 3 main electrical connections and the principal metering and relaying connections is shown in Figure 3. No additional generating units are to be installed in the future, but provision is made in the design for an ultimate of two 154-kv lines and four 66-kv lines.

From the system operating standpoint, it would be preferable to have Ocoee 2 plant supervisory-controlled from Ocoee 3, but this was impractical because of the unsuitability for automatic operation of the equipment in Ocoee 2 plant, which was built in 1913. It was felt that for successful remote operation without undue interruptions for minor troubles, all control features of the major equipment should be selected specially for nonattended operation, and this dictated that Ocoee 3 plant should be the controlled plant with the dispatcher's board located at Ocoee 2.

Control and Telemetering Channels

In selecting the type of channels to be used for the control and metering circuits between Ocoee 3 and Ocoee 2, three possibilities were explored: leased wire from the local telephone company, carrier current, and an overhead or underground cable between the two plants. All forms of open-wire construction were rejected as not being sufficiently reliable, and this decision eliminated the use of leased-wire facilities since only open-wire lines were available from the local telephone company. Carrier channels, while probably somewhat less expensive than an underground cable installation, were rejected because of the limited number of channels obtainable without undue complication and the feeling that at the present state of the art there would be some sacrifice in reliability and increase in maintenance with the use of carrier. The length of the channel, only six miles, was just short enough that the attractive economies of carrier channels over metallic wire channels could not be realized unless the number of channels was reduced to the absolute minimum. Overhead armored cable was considered seriously but decided against. It would have been necessary to follow the highway to avoid rough mountain terrain, and with the highway route, the hazard of malicious damage, rock slides, and traffic accidents made this scheme undesirable. Underground cable was selected finally because it was expected that it would provide practically trouble-free service with the minimum of maintenance and the maximum number of completely independent channels.

The underground cable installed consists of a 51-pair number 19-American-wire-gauge double-paper-insulated lead-covered tape-armored telephone cable with jute covering for subterranean service. The cable is similar to standard telephone cable except that the withstanding voltage from conductors to sheath is 3,500 volts, 60 cycles for 20 seconds, this being approximately double the voltage rating ordinarily used for telephone service. The cable is buried along the edge of the state highway between the plants, with manholes at each splice point spaced approximately 3,000 feet apart. The cable is gas-filled and maintained under 8-pound pressure to prevent the entrance of moisture. Pressure switches are installed in the cable at every third manhole and connected to one of the cable pairs to operate an annunciator at Ocoee 2 in the event of a break in the cable sheath and consequent loss of gas pressure. The allocation of cable pairs is shown in Table I.

Table I

No. of Pairs	Service
2	Supervisory control
23	Metering
4	Direct-wire control and pilot-wire relaying
1	Printing annunciator
8	Communication (includes TVA system communication other than for Ocoee 3)
13	Spare
51	Total

Control Cable Protection

Experience with remote-control and communication cables at a number of TVA plants had demonstrated that extraneous voltages appear on the cable conductors during phase-to-ground faults on the transmission system. With the cables enclosed in metallic sheaths and buried underground, induced voltages are avoided, but serious voltages do result from a rise of station ground potential above remote ground potential. They ap-

Paper 46-71, recommended by the AIEE committee on power generation for presentation at the AIEE winter convention, New York, N. Y., January 21-25, 1946. Manuscript submitted November 21, 1945; made available for printing December 18, 1945.

C. W. BOHNER was formerly principal electrical engineer, design department, Tennessee Valley Authority, Knoxville, Tenn., and is now with International General Electric Company, Schenectady, N. Y. A. P. MANESS is assistant production engineer, power operations department, Tennessee Valley Authority, Chattanooga, Tenn.

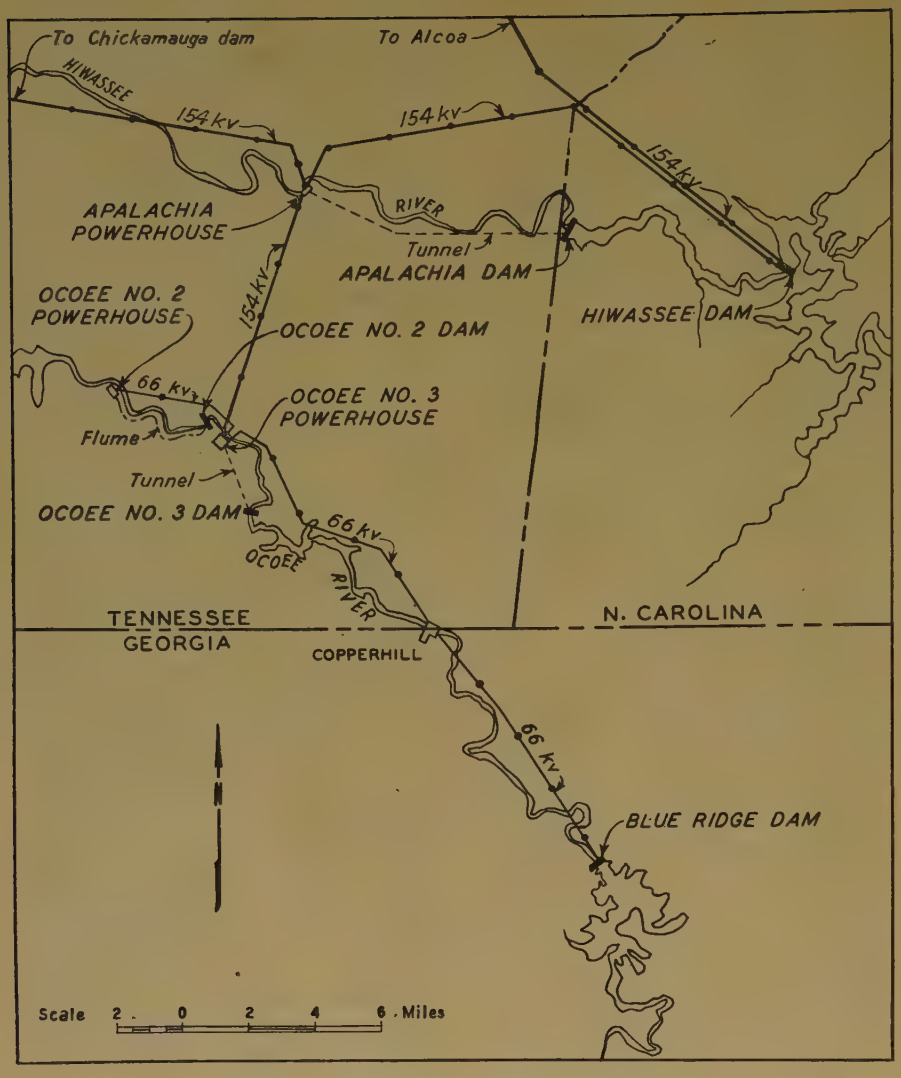


Figure 1. Location and transmission connections

pear across the cable insulation and across the protector gaps at the cable terminals. At plants where large neutral currents are allowed to flow, the extraneous voltages may become excessive and render the circuits inoperative at a time when they are most needed.

Investigation indicated that at the Ocoee plants, excessive voltages caused by the rise of station ground potential were a probability. Although one of the most effective methods of reducing the rise of station ground potential is to reduce the station ground resistance, low ground resistance was extremely difficult to obtain at the Ocoee plants because both plants are located in a mountainous region with deep rock formations underlying a comparatively thin layer of topsoil. The final tested ground resistance at Ocoee 3 was 0.5 ohm, while at Ocoee 2 the lowest value which it was practicable to obtain was 1.4 ohms. With these values of ground resistance, the calculated rise of station ground potential above remote ground for maximum ground fault current in the transformer bank neutrals was considerably in excess of the rating of the protectors. Special measures therefore had to be taken at both plants either to limit or to compensate for the rise in station ground potential.

At Ocoee 3 a 5.5-ohm grounding reactor was installed in the 66-kv neutral of the transformer bank to reduce the maximum neutral short-circuit current. The reactor is of the outdoor oil-insulated type. It reduces the maximum 66-kv neutral fault current from 4,300 to 2,600 amperes, with a corresponding reduction in the rise of the Ocoee 3 ground potential.

A similar solution could not be used at Ocoee 2 because the insulation of the old transformers at this plant is suitable for solidly grounded operation only. The protective measures adopted consisted of installing neutralizing transformers to compensate for the difference in ground potentials. The neutralizing transformers are of the 3-winding type, with the two secondaries of each transformer connected in the conductors of a cable pair and the primary connected between the cable sheath and ground. By keeping the cable sheath at remote ground potential, the difference in ground potential is impressed on the primary winding, thus introducing a compensating voltage in the conductors so that the conductors on the cable side of the neutralizing transformers are at remote ground or sheath potential while on the station side of the neutralizing transformers the conductors are at station ground potential. Obviously, it was necessary to keep the cable sheath and armor free from the influence of the Ocoee 2 station ground potential. To accomplish this, it was not considered practicable to provide an insulating covering over the sheath and armor which would not be subject to rather rapid deterioration; therefore, the cable was brought out of the ground at a point approximately 500 feet from the Ocoee 2 powerhouse and run overhead on poles to the neutralizing transformers.

The neutralizing transformers are indoor-type rated 4,000 volts and are installed in a weatherproof box mounted on a pole structure near Ocoee 2 powerhouse.

Supervisory Control Equipment

The selection of a multiconductor cable for the control channels between the plants permitted an unrestricted choice of the several types of supervisory control equipment available, since it was not necessary to keep the number of conductors required for the control channel to an absolute minimum. Had it been necessary to limit the control channel to two wires, the selection of supervisory control equipment would have been restricted to the type in which all operations are performed by coded impulsing. While this type has been successfully used in smaller installations on the TVA system, it was felt that the large amount and variety of complicated controls involved at Ocoee 3 justified utilizing any simplification which could be obtained in the supervisory control equipment itself.

Accordingly, a type of supervisory system requiring four instead of two line wires was selected. This equipment is essentially a direct-wire system of control and indication with step-type selector relays which transfer the line wires from one circuit to another. After the transfer is made, all operation of the equipment is done directly through auxiliary relays without further impulsing. Two standard 23-point units are installed, of which 30 points are used initially and the remaining

Table II

No. of Supervisory Points	Type of Service	Description
5	Control and indication	13.8-, 66-, and 154-kv oil circuit breaker control
5	Control and indication	13.8-, 66-, and 154-kv motor-operated disconnecting switch control
3	Control and indication	Automatic - manual selection for transformer tap-changing, generator voltage regulator, and generator for starting and stopping
8	Control and indication	Metering selection
2	Control and indication	Generating unit automatic start-stop and penstock butterfly valve emergency close
5	Control only	Raise-lower control for gate limit adjustment, transformer tap-changing, generator voltage adjusting rheostat, and exciter field rheostat and potentiometer telemetering calibration
2	Indication only	Lock-out relay position and generator breaker tripping bus indication
16		Spare
46		Total

16 points are for future expansion. Allocation of the supervisory points is given in Table II.

Telemetering

Continuously telemetered indicators with individual transmitters and receivers are provided for all important quantities to be metered. Intermittently telemetered indicators are provided for the less important quantities, with one transmitter and receiver provided for two or more quantities, with selection by supervisory control. The telemetering provided is shown in Table III.

It was recognized that fewer telemetered indicators could be used, since if abnormal conditions should develop, there is little that the operator at Ocoee 2 could do to correct the trouble, and the automatic protective devices would have to be relied upon to shut down the faulty equipment. It was felt, however, that the additional telemeters were justified because abnormal operation of the equipment may show up on the instruments just before shutdown, and the information obtained may be of value in locating the trouble.

Torque-balance-type telemeters are used for metering amperes, kilowatts, and kilovars. Individual instruments are provided for these quantities for the generator and for transformer 154- and 69-kv amperes. A common instrument is provided for transformer 154-kv kilowatts

Table III

No. of Transmitters and Receivers	Type	Service
3	Torque balance	Generator amperes, kilowatts, and kilovars
4	Torque balance	Transformer 154- and 66-kv amperes, kilowatts, and kilovars
2	Torque balance	66-kv line amperes, kilowatts, and kilovars
3	Potentiometer	Turbine gate position, gate limit and speed adjustment setting, and transformer tap position
2	Direct wire	Generator voltage and speed indicator
5	Direct wire	Synchroscope, incoming and receiving voltage, and frequency

and kilovars, transformer 69-kv kilowatts and kilovars, 69-kv line amperes, and 69-kv line kilowatts and kilovars. Selection between kilowatts and kilovars and between lines can be made by supervisory control.

Potentiometer-type telemetering is used for turbine gate position, gate limit and speed adjustment setting, and main transformer tap position. It consists of small potentiometers, mechanically connected to the device whose position is being telemetered, and milliammeter receivers with appropriate scales. The potentiometers are connected to the Ocoee 3 250-volt control battery. To provide calibration of the receivers for change in battery voltage and line wire resistance, a rheostat is provided in one of the line wires of each receiver, and a supervisory point simultaneously connects the three receivers directly to the Ocoee 3 battery supply.

Generator voltmeter and synchroscope and associated voltmeters and frequency meters are operated directly over the line wires without telemetering transmitters, as is also the turbine speed indicator which is operated from a magneto-generator geared to the main unit shaft.

A recording voltmeter with milliammeter element is operated from a rectifier current transmitter with supervisory control selection of the voltage to be recorded. A station load recorder is operated from a thermoverter. A reservoir level recorder of the impulse type is provided with float-operated transmitter located at the dam. For this latter recorder, the line wires are run overhead on poles between the dam and Ocoee 3 powerhouse and thence through the underground cable to Ocoee 2.

Main Control Switchboards

The main control switchboards at Ocoee 3 are divided into three sections: the control and instrument board section, which is installed in one of the generator room walls and faces into the generator room; the relay board section, which is installed back-to-back to the control and instrument board; and the remote control board, which faces the relay board. Figure 4 shows a floor plan layout of the generator and switchboard rooms.

A complete set of controls and instruments is provided at Ocoee 3 for local control of the plant if desired for maintenance and when the supervisory control is out of service. A view of the control and instrument board is shown in Figure 5. The local controls are similar to the manual controls provided for other TVA plants except for several additional con-

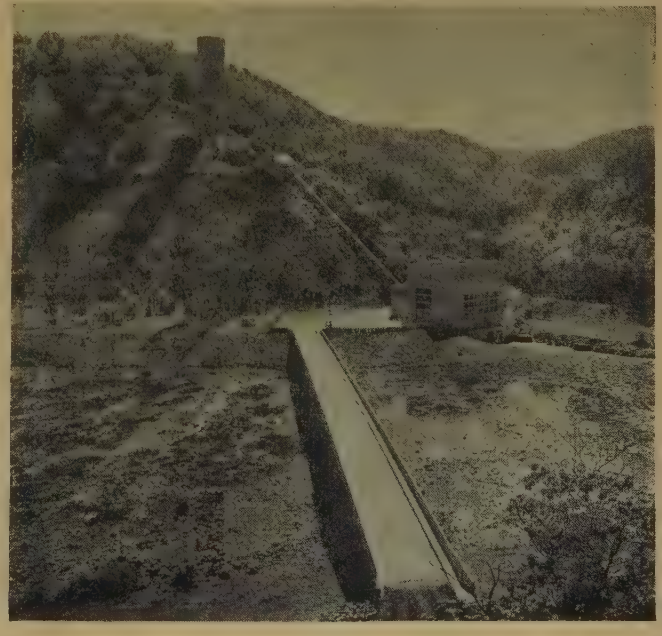


Figure 2. Surge tank, valve house, penstock, powerhouse, and switchyard

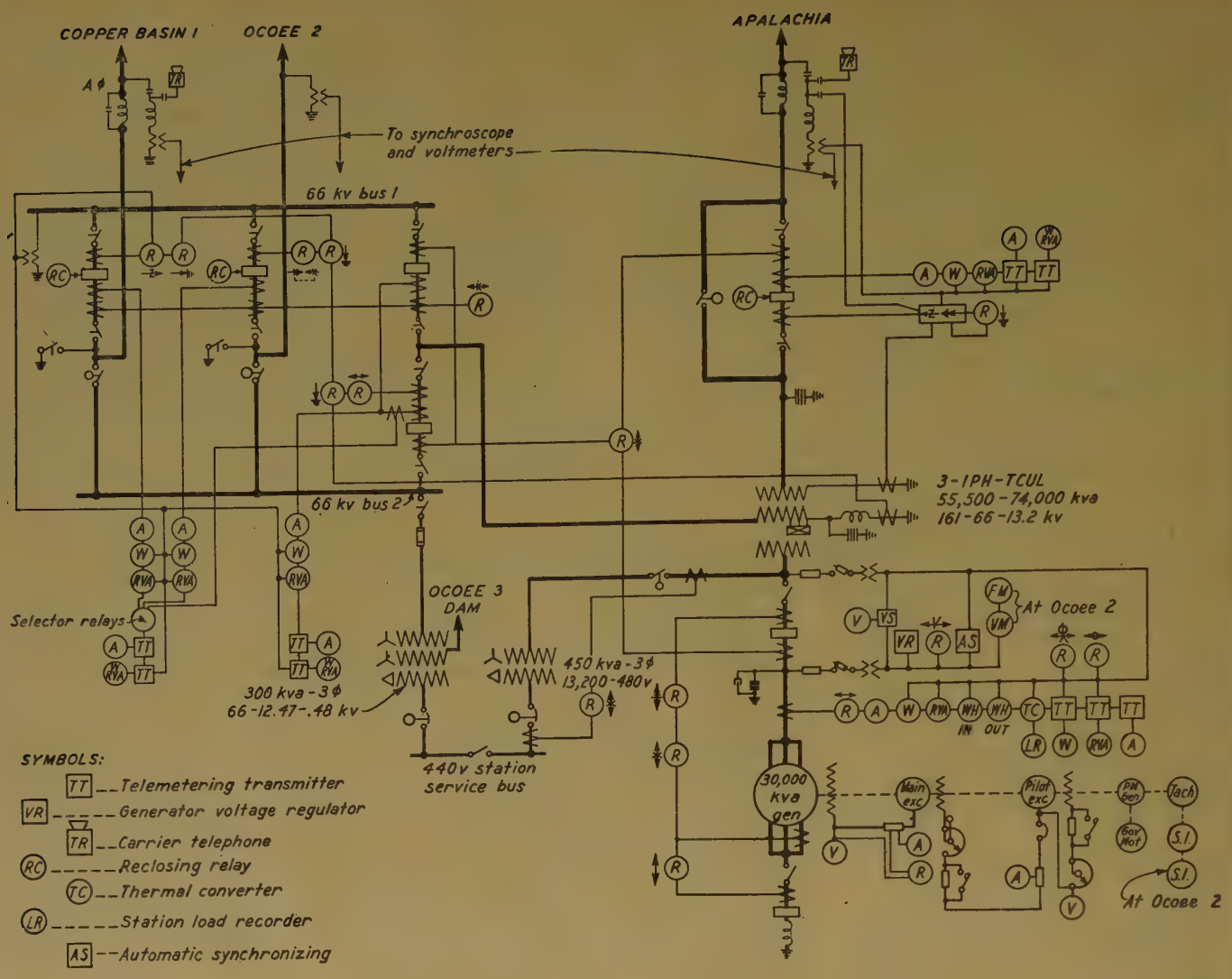


Figure 3. Single-line diagram of main connections and the principal metering and relaying

trol features required because of automatic and supervisory control operations. A switch is provided on each panel for transferring the controls on that panel to either local or supervisory control. On the generator panel a switch is provided to select either manual or automatic starting and synchronizing of the generating unit. A switch also is provided for selecting automatic synchronizing of the unit for manual starting when all auxiliaries are already in operation and it is not desired to go through the entire automatic starting sequence.

All of the main protective and automatic control relays for the generating unit, main transformer bank, and transmission lines are mounted on the relay board. Primary relays are of the withdrawal type with built-in test facilities. Differential relays are of the percentage-differential induction type. An automatic oscillograph is installed on the relay board, and facilities are provided to permit connecting the elements in the more important current and potential circuits for analysis of relay performance.

The supervisory control equipment, the telemetering transmitters, the battery charger controls, and the battery distribution equipment are located on the remote control board.

Dispatcher's Board at Ocoee 2

The dispatcher's board, consisting of a 2-panel completely enclosed cubicle, is installed at the left end of the Ocoee 2 main switchboard. A view of this board is shown in Figure 6. The recording voltmeter, generator-load recorder printing annunciator, and water-level recorder are mounted on one panel, and the indicating telemeter receivers and supervisory controls are mounted on the other panel. The supervisory controls and associated position-indicating lamps are grouped according to function, and mimic busses are provided so as to present a single-line diagram arrangement. The printing annunciator is of the impulse type and automatically prints on a paper chart all abnormal operations of the equipment at Ocoee 3 and also all opening and closing operations of the main circuit breakers.

Generating Unit and Governor

The generating unit consists of a 40,000-horsepower 200-rpm vertical-shaft Francis-type turbine direct-connected to a 30,000-kva 13.8-kv 0.9-power factor generator. The generator is totally enclosed, with Kingsbury-type thrust bearing located below the rotor and with direct-connected main and pilot exciters. The governor is of the actuator type with motor-driven governor head driven by a permanent magnet generator direct-connected to the main unit shaft.

The control and protective features of the main generating unit do not differ materially from those customarily provided for large manually operated units. The turbine guide bearing is lubricated normally by an a-c motor-driven oil pump with pressure switch control arranged to transfer on loss of pressure to an emergency battery-driven pump. An automatic control is provided for the wicket

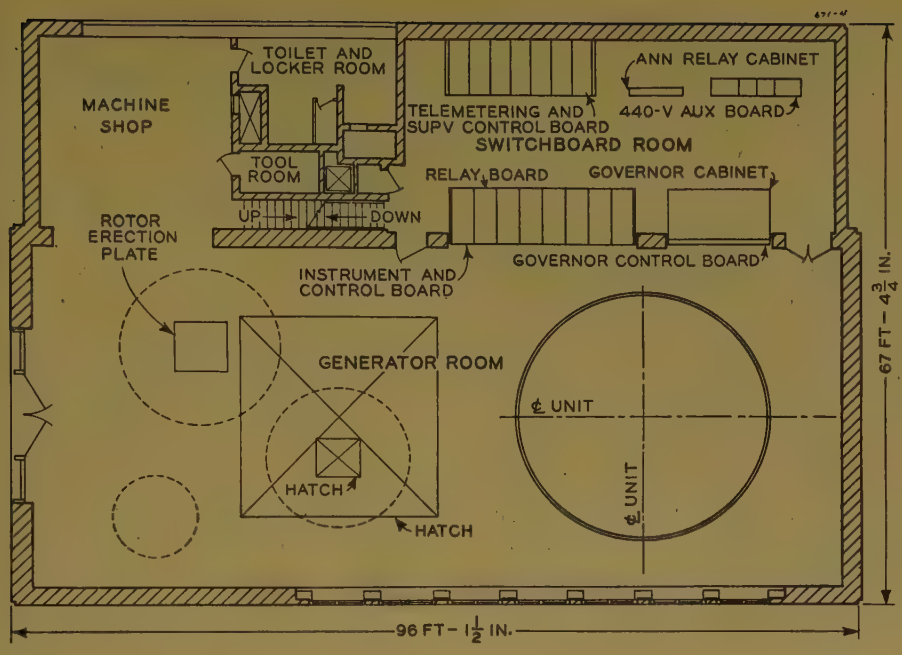


Figure 4. Main floor plan

gates to close and lock them in the closed position upon loss of governor oil pressure. The oil in the generator thrust bearing is self-circulating and no pumps are required. A float switch is provided to operate an annunciator for low thrust-bearing oil level. Temperature detectors are provided in the turbine guide bearing and generator thrust bearing for annunciation and for operation of a bearing temperature recorder mounted on the governor cabinet. An overspeed switch geared to the main shaft is arranged to energize the governor shut-down solenoid and operate an annunciator upon overspeed of the unit but does not close the butterfly valve. If the unit should run away, the operator at Ocoee 2 would be informed through the operation of the annunciator and the tachometer reading on the dispatcher's board and will close the butterfly valve by supervisory control.

Figure 5. Generator room showing generator and main control and instrument board, with governor control board beyond

The governor is of the conventional cabinet actuator type, with two motor-driven oil pumps and governing mechanism mounted on the sump tank. Both pumps are under pressure-switch control, and the control provides for the operation of one pump normally to maintain governor oil pressure. If this pump fails to maintain pressure, the second pump is started automatically. The governor manual controls, the penstock, scroll case, and cooling-water pressure gauges, the bearing "thermoverters," and the tachometer are mounted on the front of the governor cabinet.

The synchronizing and load-limit devices are motor-operated to permit operation of these devices by supervisory control and to permit automatic synchronizing by the automatic speed-matching and synchronizing relays on the main switchboard.

An automatic device is provided on the governor which, when the unit is started, allows the gates to open quickly to the speed-no-load position and then introduces a time delay to permit the governor flyballs to take control and the generator voltage to build up before the gates can be opened further for loading of the unit.

Automatically operated air brakes are provided to stop rotation of the unit after shutdown. Control is by an electrically operated pendulum timer which, after a time delay to allow the speed of the unit to drop to approximately 50 per cent of normal, applies the brakes intermittently until the unit is stopped. The control is interlocked through auxiliary switches to allow application of the brakes only if the wicket gates are completely closed and the generator breaker is open.

Generator Unit Protection

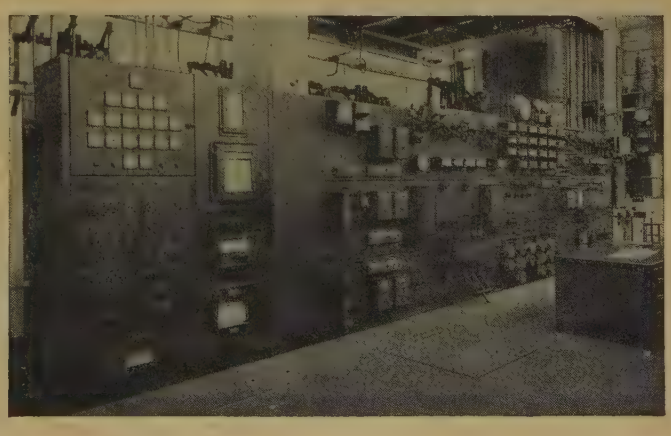
Protective equipment is provided to prevent starting of the unit if any of the following abnormal conditions exist:

1. Overspeed device contacts closed.
2. System voltage below normal.
3. Incorrect phase sequence.
4. Generator thermal relay contacts closed.
5. Exciter field rheostat not at normal voltage no-load position.
6. Main butterfly valve not fully open.
7. Generator neutral breaker not closed.
8. Main exciter field breaker not closed.
9. Lock-out relay not reset.

The following protective devices trip the generator breaker and shut down and



Figure 6. Dispatcher's board at left end of existing control board in Ocoee 2 plant



lock out the unit when abnormal conditions occur:

1. Generator differential and neutral overcurrent relays.
2. Generator thermal and phase overcurrent relays.
3. Generator a-c overvoltage relay.
4. Generator overvoltage relay for sustained overvoltage.

The following protective devices also trip and lock out the unit when abnormal conditions occur, but to prevent overspeeding, the generator breaker is not tripped until the wicket gates are closed to the no-load position.

1. Reverse-phase and unbalanced-phase current relays.
2. Field-failure relay.
3. Flow switches for low flow of turbine seal water, generator bearing water, and air cooling water.
4. Pressure switches for low governor oil pressure.
5. Float switch for low turbine-bearing oil level.
6. Temperature detectors for high turbine- and generator-bearing temperatures.
7. Incomplete starting sequence relay.

Station Service Supply

Normal auxiliary power is obtained from a 450-kva 3-phase 13.8/460-volt transformer connected to the main transformer delta bus through a motor-operated disconnecting switch. Emergency station service power is obtained from a 300-kva 3-winding 3-phase 69,000/12,450/460-volt transformer connected to the 69-kv transfer bus. The 12.45-kv winding supplies power to the dam over a 2.5-mile overhead line. Both transformers normally are kept energized, and automatic transfer control is provided to close the emergency supply 440-volt breaker if the normal supply fails.

Two 10-kw diverter-pole motor generator sets are provided for control-battery charging. One of the sets operates on floating charge at all times, and automatic transfer is provided to start the other set in the event the first set trips off for any reason. A selector switch is provided to permit selecting the set which is to operate normally.

Initial Power Operation

The operation of the reservoir for this plant is co-ordinated to provide storage in advance of floods, to fluctuate the pool elevations to aid in malaria control, and to store water on small stream flow increases for later use for power generation.

During the period from November 1942 to April 19, 1943, the sluice gates at the Ocoee 3 Dam were operated to regulate the downstream flow for power requirements at the Ocoee 1 and 2 plants and to meet the need of construction activities at the Ocoee 3 project. The gates were closed initially for the impounding of water to fill the reservoir on April 19, 1943. From this date on, the entire inflow, except that needed for the operation of the downstream Ocoee plants, was stored. The maximum reservoir elevation was reached on April 24, and the plant went into operation on April 30.

No attendants of any kind are stationed at the powerhouse or the dam. The necessary supervision and operation functions of the Ocoee 3 project are performed by the employees of the Ocoee 2 hydroelectric plant. A maintenance employee and an operating employee visit the plant two or three times a week to check batteries and lamps, test oil, inspect auxiliary equipment, clean switchboard panels, lubricate equipment, and inspect water plant. They stay from four to eight hours, depending on the work involved.

The cost of supervision, operation, and maintenance at Ocoee 3 for the first 20 months of operation is shown in Table IV.

Table IV

	First 8 Months 4/30 to 12/31 1943	Next 6 Months 1/1 to 6/30 1944	Next 6 Months 7/1 to 12/31 1944
Supervision			
Labor	$ 2,017	$ 1,410	$ 738
Material	612	384	168
Operation			
Labor	7,929	3,288	4,662
Material	2,152	612	528
Maintenance			
Labor	2,482	2,640	2,172
Material	536	804	636
Total cost	$15,728	$9,138	$8,904
Gross generation, kwhr	125,368,000	90,561,000	83,221,000
Cost per 1,000 kwhr	$0.125	$0.101	$0.107

The labor costs of supervision and operation are set up as 50 per cent of the salaries of the supervising, clerical, and operating employees. The material costs of supervision and operation and the entire cost of maintenance are charged 100 per cent to the plant.

Ocoee 3 is the first of the Tennessee Valley Authority's generating stations to be operated by supervisory control. Its excellent performance and low operation cost have encouraged an extension of this type of operation. Supervisory control is expected to be used for two other generating stations of larger capacity now under design and is being considered for a number of substations.

Signal and Noise Levels in Magnetic Tape Recording

D. E. WOOLDRIDGE
NONMEMBER AIEE

Synopsis: The primary object of the work described here was to determine what properties of the tape and associated magnetic elements are responsible for the noise and signal output levels of magnetic recordings and, if possible, to display in specific equations the pertinent relationships connecting noise and signal levels with the physical properties of the tape and polepieces. In the course of the study, methods appeared for decreasing the noise and increasing the useful signal reproduced from magnetic tape. These methods and some of the use that Bell Telephone Laboratories and Western Electric have made of them are mentioned in the discussion. While some of the work described in this paper has implications for more than one type of magnetic recording process, perpendicular recording on tape[1] is the actual subject matter dealt with. In every case discussed, the record medium was 0.050 inch wide and 0.0022 inch thick. Except where otherwise noted, a chrome-steel tape was used at a speed of 16 inches per second.

Noise Levels in Magnetic Tape Recording

Noise in Demagnetized Tape

In the experimental work on noise, the polepiece construction was as shown in Figure 1, where the active portion of each polepiece consisted of a sheet of soft magnetic material (for example permalloy) 0.0015 inch thick and 0.040 inch wide, held against the tape by a light spring tension with the narrow dimension parallel to the tape travel, the two polepieces exactly aligned with each other on opposite sides. When a piece of tape from which previous recordings have been erased by a demagnetizing process is passed between such polepieces, the signal picked up by the coils contains energy in a wide band of frequencies. This suggests that the noise may be caused by a large number of small magnetic irregularities in the tape. Therefore it is sensible to start by a quantitative consideration of the noise frequency spectrum that would be produced by such irregularities.

For concreteness, first suppose the tape is completely demagnetized except for one inclusion of magnetized material of dimensions small compared with the polepiece width (0.0015 inch). As the tape moves along, the flux passing into the polepieces must vary with time in some such way as that shown in Figure 2. The width of the flat top must be certainly less than the time required for the tape to travel one polepiece width (0.0015 inch); it may be substantially less than this. The portion of the tape that is so near the polepieces that an appreciable fraction of the flux of a magnetized inclusion gets into them will be called the region of influence of the polepieces in this paper. The curve of Figure 2 may be translated into a relative flux versus distance curve and plotted as in Figure 3; this curve $f(x)$ may be said to have the shape of the region of influence.* The course with time of the flux that links the windings is then given by

$$\Phi(t) = KMf[V(t-t_0)] \tag{1}$$

where V is tape speed, t_0 is the instant when the magnetized inclusion passes the center line of the polepieces, M is the magnetic moment of the inclusion, and K is a constant for the present considerations.

The voltage induced in the reproducing coils that surround the polepiece is

$$e(t) = KMnV \cdot 10^{-8} \frac{df}{dx} \tag{2}$$

where n is the number of turns on the coils. Figure 4 shows the shape of the voltage pulse $e(t)$ corresponding to the shape of the region of influence of Figure 3.

We are interested in the total power developed in the frequency range $\Delta\nu$ by the combined effects of N voltage pulses such as the above scattered at random throughout every time interval T. This problem is treated in Appendix I. The result is shown to be

$$P_N(\nu)d\nu = \frac{2(Kn\times10^{-8})^2}{R} M^2 \left(\frac{N}{T}\right) S(\nu)^2 d\nu \tag{3}$$

where

$$S(\nu) = \int_{-\infty}^{+\infty} \frac{df}{dx} \sin \frac{2\pi\nu x}{V} dx \tag{4}$$

* Dependence of $f(x)$ on the depth of the inclusion in the 0.002-inch tape is taken account of only insofar as the $f(x)$ finally derived is thought of as a value averaged over the tape thickness.

R is the impedance of the reproducing coil circuit, which is assumed to be a pure resistance independent of frequency. (Experimentally, this condition is met by connecting the reproducing coils to a high resistance.)

At this point it is possible to test whether the simple theory under investigation properly accounts for the observed shape of the noise frequency distribution. A complete test would involve computing $f(x)$ from the magnetic and geometric properties of the system and comparing the shape of the resulting $S(\nu)^2$ curve with noise measurements. It is not easy to compute $f(x)$ in more than an approximate manner. Therefore the reverse procedure has been employed. By trial and error an attempt has been made to draw an $f(x)$ curve that, employed in equation 3, leads to a noise frequency distribution that fits the observed facts. The result is shown in Figure 5, where the theoretically derived curve is superposed over the experimental noise measurements. The shape of the region of influence used in the derivation is shown in Figure 6. A study of the x-scale of this figure will show it to be reasonable for polepieces 0.0015 inch wide and tape 0.0022 inch thick.

The approximate agreement between theory and experiment that just has been established justifies some confidence in the validity of the methods and the theory under test. A somewhat more quantitative test may be obtained by comparing the noise frequency distribution and the signal frequency response characteristic. This method is developed in the following paragraphs.

In Appendix II it is shown that the power that is dissipated in the output load R when a sine wave signal of frequency ν is reproduced from the tape is

$$P_s(\nu) = \frac{1}{2} \frac{(Kn\times10^{-8})^2}{R} (I_o ah)^2 V^2 T(\nu)^2 \tag{5}$$

where

$$T(\nu) = \int_{-\infty}^{+\infty} \frac{d}{dx}[f(x)g(x)] \sin \frac{2\pi\nu x}{V} dx \tag{6}$$

In these equations, I_o is the half-amplitude of the tape magnetization, measured when the tape is well away from the region of influence of the polepieces, while $g(x)$ is the factor by which the remanent magnetization of the free tape is enhanced

Paper 46-31, recommended by the AIEE committee on communication for presentation at the AIEE winter convention, New York, N. Y., January 21–25, 1946. Manuscript submitted November 7, 1945; made available for printing December 12, 1945.

D. E. Wooldridge is with the Bell Telephone Laboratories, Inc., New York, N. Y.

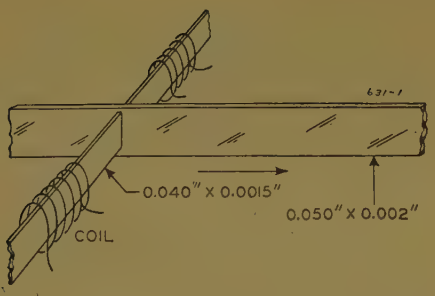


Figure 1. Dimensions of active portion of polepieces used in noise and signal level studies

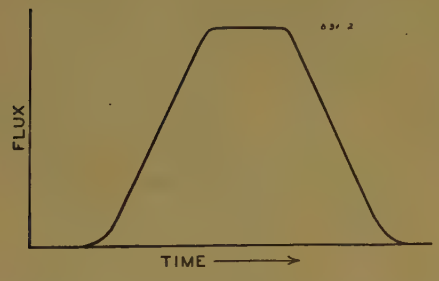


Figure 2. Time variation of flux in polepieces caused by a single small magnetized region in demagnetized tape

by the partial removal of the strong demagnetizing field brought about by the proximity of the reproducing polepieces. Letters a and h are the thickness of the tape and the polepiece height, respectively.

This expression for the reproduced power depends on frequency only through I_o^2 and $T(\nu)^2$. Moreover, I_o is practically independent of frequency if the same current is sent through the recording coils for all frequencies. For frequencies so low that the recording current remains substantially constant during the passage of an element of tape through the region of influence of the polepieces, it is obvious that this should be the case. But even for considerably higher frequencies, wherein the recording current changes appreciably while a tape element is near the polepieces, the amplitude of the recorded wave remains almost unchanged. This is because each tape element "remembers" the *highest* value of magnetizing field to which it is subjected, and not the last or even the average value. Actually, simple theory predicts a loss in I_o of two or three decibels at around 5,000 cycles, but this is opposed by a gain of roughly similar magnitude because of the decrease with decreasing wave length of the demagnetizing factor of perpendicular recording. Therefore we may take I_o to be independent of frequency and consider equation 5 to represent the over-all record-reproduce

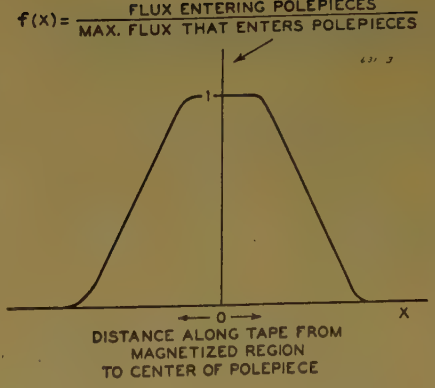


Figure 3. Qualitative shape of region of influence of polepieces

This curve is copied from one derived later and displayed in Figure 6. The sloping sides are actually curved, as indicated by the derivative curve of Figure 4. This curvature is not evident on such a small-scale figure

frequency response characteristic for constant recording current and a high impedance output circuit.

A comparison of equations 3 and 5 shows that

$$\frac{P_N(\nu)}{P_S(\nu)} = C \cdot \frac{S(\nu)^2}{T(\nu)^2} \qquad (7)$$

where C is a constant that is of no immediate interest. Moreover, $S(\nu)$ and $T(\nu)$ will be identical if $g(x)$ is a constant, that is, if the junction of the polepieces with the tape causes an inappreciable increase in the intensity of magnetization. Conversely, if the tape magnetization increases greatly because of the proximity of the polepieces, $g(x)$ will be a strongly peaked function similar to $f(x)$, and their product will be still more strongly peaked. In the first case, we should expect the noise and signal frequency characteristics to be the same; in the second case, the signal response should hold up to higher frequencies than the noise.

The conclusions of the preceding paragraph are valid only if the theory of noise on which equation 3 was derived is true, that is, that the noise is caused by many random magnetic irregularities less than 0.0015 inch in dimension. If the noise is attributable to any sort of mechanical vibration of the tape or polepieces, its frequency spectrum must be peaked at the vibration frequency or frequencies; the curve would bear little resemblance to that yielded by equation 3. If the noise is caused by many random irregularities in the tape which are *not* small in dimension compared to 0.0015 inch, the noise spectrum must be enhanced for wave lengths of the order of the irregularity dimensions. In such a case, the noise spectrum must have relatively less high frequency content than $S(\nu)$ and, therefore, less than $T(\nu)$, whether or not $g(x)$ is nearly constant.

On Figure 7 are replotted the noise measurements and the theoretical curve of Figure 5 together with signal output voltage measurements. The two sets of points have been shifted vertically along the logarithmic scale so that the low frequency 6-decibel-per-octave portions of the curves coincide. Figure 7 shows no concentration of noise at isolated frequencies, corresponding to vibration. Further, the high frequency content of the noise is definitely not lower than that of the signal response characteristic. In the light of the preceding discussions, this requires three conclusions:

1. **The noise is produced by the passage between the polepieces of many randomly distributed magnetic irregularities.**
2. **The noise producing irregularities are smaller than 0.0015 inch in size.**
3. **$g(x)$ is not a strongly peaked function**

While the data seem adequate to justify these conclusions, they do not explain how the noise characteristic can actually have *more* high frequency content than the response characteristic. However, the simple theory given here neglects a number of secondary effects and should not pretend to high accuracy in its predictions.

The conclusion that has been established is as important because of the noise producing mechanisms it proves negligible as for any positive contribution it may make to the theory of tape noise. For example, the noise cannot be caused by mechanical vibration of the tape or associated magnetic structures; it cannot be caused by variations in the magnetic properties of the tape because of mechanical eccentricities in the rolling mill; it cannot be caused by any kind of inclusion or grain size effect unless the dimensions of the irregularities are less than 0.0015 inch.

An obvious possible source of small magnetic irregularities in nominally demagnetized tape is found in the finite size of the magnetic domains that are believed to make up any permanent magnet. If a "demagnetized" tape is made up of many small magnetically saturated regions, oriented so as to cancel one another's field, there must be local imperfections in the cancellation process that result at any instant in the passage into the polepieces of a net flux different from zero. Statistical variations of this leakage flux along the tape must give rise to noise. In Appendix III a cal-

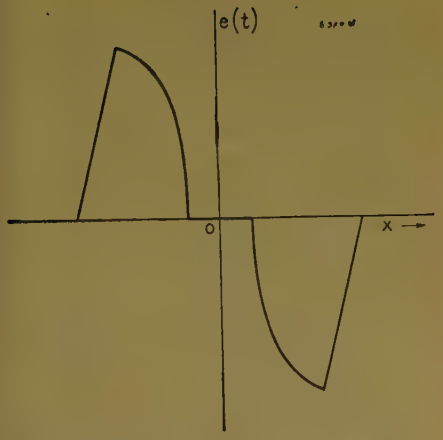


Figure 4. Voltage pulse corresponding to the region of influence shown in Figure 3

culation is carried out which leads to an expression for the open-circuit mean-square-noise voltage that should be measured if the tape consisted of saturated domains of volume v, with completely random directions of magnetization. The expression obtained is

$$E_N^2 = 3 \times 10^4 v \text{ volt}^2 \qquad (8)$$

Now, if the domain theory of the noise of demagnetized tape is an adequate one, equation 8 should predict a noise voltage considerably higher than that actually observed. This is because it is known that mutual interaction among the domains goes a long way toward cancelling out their resultant fields; the leakage flux must be only a fraction of that implied by random orientation, which was assumed in the derivation.

Measurements by various investigators [2,3] lead to values of v for most magnetic materials of the order of 10^{-9} to 10^{-8} centimeters.[3] For tape that is only 0.005 centimeter thick, there may be some reason to reject the higher figure, which corresponds to a linear dimension half as great as the tape thickness. Use of a value for v of 10^{-9} centimeters[3] in equation 8 leads to a noise voltage

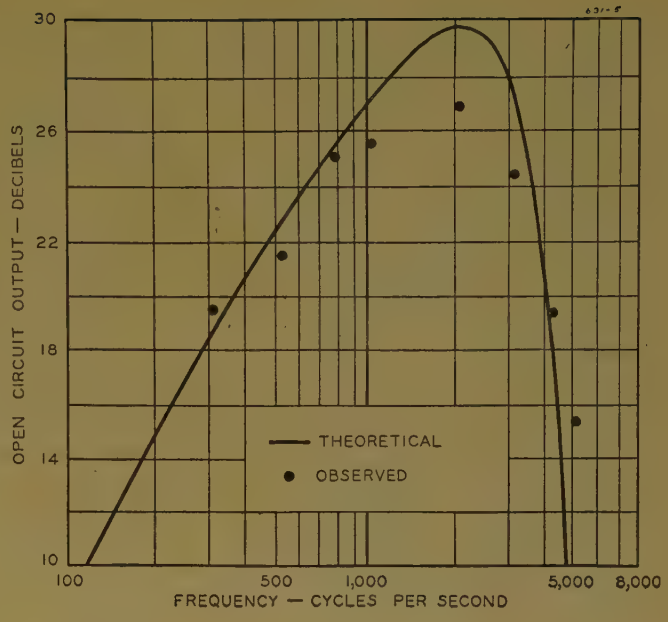
$$E_N^2 \sim 3 \times 10^{-5} \text{ volt}^2$$

The experimentally measured value, for the conditions dealt with, is 2×10^{-11} volt.[2]

Obviously, the domain theory passes the first test of adequacy. From the derivation of Appendix III, it is clear that the observed noise can be accounted for even though the domains cancel all but 1/1,000th of one another's fields. It seems reasonable to conclude that the noise produced when demagnetized tape passes between the polepieces probably is caused by statistical variations in the flux

Figure 5. Comparison between observed noise spectrum of demagnetized tape and theoretical distribution based on region of influence of Figure 6

Tape speed = 16 inches per second. Polepiece width = 0.0015 inch



leaving the tape owing to imperfect cancellation of the domain fields.

Noise in Saturated Tape

When tape from which previous signals have been erased by a saturation process is led through the polepieces, the noise produced in the output circuit is from 10 to 20 decibels higher than that of demagnetized tape, depending on the tape material, but it has the same frequency distribution. As in the case of demagnetized tape noise, this points to small magnetic irregularities as the likely source of the noise.

Since the tape is magnetized, nonmagnetic inclusions or variations in the coercive force or remanence would produce noise, where such irregularities would be ineffective in demagnetized tape. Steel tape is known to contain inclusions of carbon, whereas the coercive force and remanence, measured in the direction of tape magnetization, must vary with the orientation of the tiny crystals that make up the tape. Both these possible sources of noise have been investigated. Tape sections were etched and microphotographs made to reveal carbon particles and crystal boundaries. Measurements were made of the carbon particle sizes and numbers and of the crystal sizes. From such data, order of magnitude calculations of the resulting noise were made in a manner similar to the domain calculation of Appendix III. In both cases the predicted noise was far too low. Although there were probably some nonmagnetic inclusions in the tape that were not revealed by the etching processes used (austenite, for example), it seems unlikely that these inclusions could be numerous enough to account for

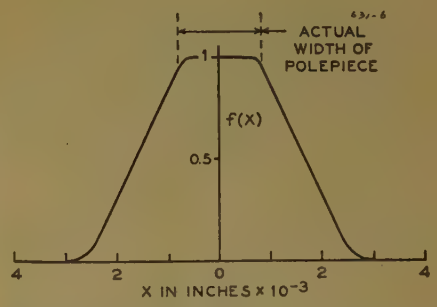


Figure 6. Shape of region of influence of polepieces assumed in deriving curve of Figure 5

the observed noise of magnetized tape.

As a result of these measurements and calculations, it has been concluded that the cause of noise in magnetized tape is probably rather similar to the cause of the lower noise of demagnetized tape. To account for the increased level, it is simply necessary to postulate that the process of saturating the tape and then decreasing its flux nearly to zero by its own demagnetizing field (see the section on signal levels) results in a greater degree of local disorder among the domains, whereby larger variations occur from point to point in the amount of flux leaving the tape surface.

Signal Levels in Magnetic Tape Recording

Equations 5 and 6 constitute a formal expression for the power output of a tape recording, but in greater detail than is needed for signal level considerations. For the present purposes, we may note that for an undistorted sine wave reproduction,

$$\Phi = \Phi_0 \sin 2\pi\nu t$$

where Φ is the flux linking the reproducing windings, and Φ_0 is an amplitude. The rms induced (open-circuit) voltage is therefore

$$e = \sqrt{2}\pi n \Phi_0 \nu \times 10^{-8}$$

It will be convenient to deal with the flux that enters the polepieces rather than the fraction of it that links the coils. Recalling (as stated in Appendix III) that the ratio of these quantities, for the magnetic structures in question, is $2\,1/2$ to 1, we may write

$$e = \frac{\sqrt{2}\pi}{2.5} n \Phi_{REP} \nu \times 10^{-8}$$

where Φ_{REP} is the maximum flux that enters the polepieces during the sine wave reproduction. Substitution of n = 1,500 in this equation gives

$$e = 2.6 \times 10^{-5} \Phi_{REP} \nu \qquad (9)$$

where e is in volts if Φ_{REP} is in maxwells and ν is in cycles per second.

The consideration given in the preceding section to the shape of the signal frequency response characteristic can be interpreted as an exploration of the dependence of Φ_{REP} on frequency and the reasons therefor. In the present section the aim will be to reconcile the observed absolute magnitude of signal output voltage with the physical constants of the tape-polepiece structure. It is both adequate and convenient to deal only with frequencies for which the wave length is so long compared with the region of influence of the polepieces that Φ_{REP} is independent of ν. Frequencies lying along the straight, 6-decibel-per-octave portion of the response curve of Figure 7 meet this requirement. Much of the data to be quoted will pertain to ν = 300 cycles, for which equation 9 becomes

$$e_{300} = 8.0 \times 10^{-3} \Phi_{REP} \qquad (10)$$

Before it is possible to obtain from equations 9 or 10 a figure for the output voltage that should be gotten from a magnetic tape recording, it is necessary to determine the value of Φ_{REP}. The development has implied clearly that the intensity of magnetization in an element of tape when it lies between the reproducing polepieces differs from the intensity in the same element when away from the influence of the polepieces, which in turn differs from the intensity that existed in the element when it lay between the recording polepieces. It is now necessary to examine in detail the hysteresis processes to which an element of tape is subjected during the erase-record-reproduce cycle.

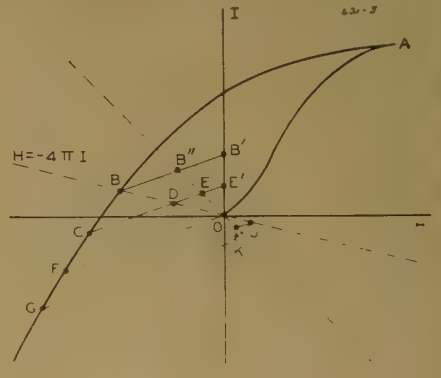
Hysteresis Processes in the Erase-Record-Reproduce Cycle

Two methods of recording will be discussed. The first method erases previous recordings by bringing every element of the tape to magnetic saturation (perpendicular to the tape surface), and then, in the recording process, superposes a d-c biasing field on the fields produced in the polepieces by the signals being recorded. The second method erases previous recordings by demagnetizing the tape; in the recording process an a-c biasing field is superposed on the signal fields.

Saturation Erase; D-C Bias Record. Figure 8 displays the manner in which H and I (perpendicular to the tape surface) vary throughout the erase-record-reproduce cycle. When an element of tape passes between the erasing polepieces, its resulting magnetic state is represented by the point A. As the element of tape leaves the erasing polepieces, its intensity of magnetization drops. If there were no demagnetizing effect, the intensity of magnetization would take on the value given by the intersection of the hysteresis loop with the ordinate axis, that is, the remanence of the magnetic material. However, the tape is so thin compared with its other dimensions that the presence of perpendicular magnetization gives rise to a strong demagnetizing field that tends to diminish this magnetization. For the dimensions of the tape used, the demagnetizing factor is about 95 per cent of that which would be exhibited by an infinitely thin plane. For the purposes of this discussion, it is sufficiently accurate to take the demagnetizing factor as equal to that of the thin plane: 4π. Consequently, when the element of tape under consideration passes out of the influence of the erasing polepieces, its magnetization drops along the hysteresis curve until it intersects the straight line $H = -4\pi I$. Accordingly, B represents the magnetic condition of the element of tape while it is passing from the erasing to the recording polepieces. When this element of tape comes between the recording polepieces, it is subjected to two distinct influences. Because of the junction of the polepieces with the thin tape, the demagnetizing field is diminished so that the point representing the magnetic state of the element of tape tends to move along the line BB' towards higher values of magnetization. This increase in I either is augmented or retarded by the influence of the field that is momentarily produced by the currents in the recording and biasing coils. If these currents sum to zero, the magnetization in the element of tape moves up to a value B'', where the point B'' lies on another straight line that passes through the origin but which has a

Figure 8. Magnetic history of a tape element

Saturation erase; d-c bias record



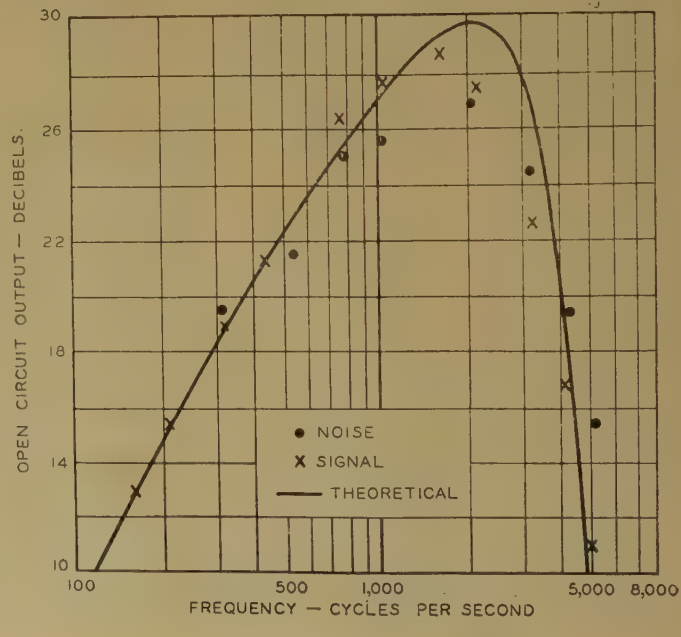


Figure 7. Comparison of noise and signal frequency characteristics

Theoretical curve and noise data copied from Figure 5

slope steeper than that of the line $H=-4\pi I$. The exact value of this slope depends upon the extent to which the demagnetizing field of the thin tape is removed by the junction of the polepieces. If the net field produced by the speech and biasing currents is positive at the instant in question, the point representing the magnetic state of the element will lie to the right of B''. If the field is negative, the representative point will lie to the left of B''. Now it is necessary to take account of an important property of most permanent magnet materials[4]; the hysteresis curve $BB''\ B'$ is nearly a straight line and is nearly reversible. This means that if the point representing the magnetic state of the element of tape while between the recording polepieces lies *anywhere* along the line BB', then the point which represents the magnetic state of that element after it leaves the recording polepieces will lie very close to B. (The representative point for an element of tape which is not in the vicinity of polepieces must always lie somewhere along the line $H=-4\pi I$.) This means that all values of recording fields that produce magnetic states in the tape represented by points lying between B and B' are nearly equivalent as far as the magnetization that they leave in the tape is concerned. It is evident, then, that when this method of recording is used, it is necessary to employ a negative biasing field so that all points representing the magnetic states of elements of tape while between the recording polepieces will lie somewhere along the hysteresis curve to the left of B. When this is done, the magnetic state of an element of tape while between the recording polepieces is represented by some such point at C. When that element of tape leaves the recording polepieces, its magnetization increases along the nearly straight line CE until the point D is reached. When the element of tape comes between the polepieces again for reproducing the magnetization moves up to the still higher value represented by the point E, as the demagnetizing field is diminished by the junction of the polepieces. Since over a limited range the curves whose intersections determine the positions of the points D and E are nearly straight, as is the hysteresis curve BC, the magnetization induced in the reproducing polepieces (at E) is linearly related to the recording current (at C).

The processes just described are shown in the curves of Figure 9, which have been plotted from tracings made on the screen of a cathode ray oscilloscope. The electrical circuit employed in these measurements was so arranged that the voltage supplied to the vertical plates of the oscilloscope was at every instant proportional to the flux density in the element of tape lying between the reproducing polepieces. (This was done by the use of low frequency sine wave recordings on the tape and an appropriate output integrating circuit); the voltage supplied to the horizontal plates was proportional to the recording current that had been used when this particular element was originally magnetized. (The fundamental of the reproduced signal, properly phase-adjusted, supplied this voltage.) In Figure 9, (a) corresponds to the case in which no biasing field was used on recording; in the case of (b), a small negative biasing field was used; in curve (c) a somewhat larger field, and so forth. The sine wave recording current was kept the same for all the curves. It is evident from these pictures that the phenomena described in the preceding paragraph have taken place. When the biasing field was small, as in (a) and (b), a large portion of the recording sine wave was nearly ineffective; when the biasing field became so large that the point representing the magnetic condition of the element of tape while between the recording polepieces always lay to the left of B (Figure 8), the reproduced signal was large and free from distortion, as in (c). When the biasing field became too great, the recording began to get into the overload region of the hysteresis curve, and as a result weak, distorted signals began to appear, as in (d) and (e). When the biasing field was positive, as in (b′) and (c′), the reproduced signals were weak and distorted, as was to be expected.

It has been seen that there is a sharp upper limit to the recording fields that can be employed, and that this limit is the field corresponding to the point B in Figure 8. There is also a lower limit. The lowest recording field which may be used without high distortion is the field corresponding to the point F. This is because the curves $BB''\ B'$, CDE, FO, and so forth begin to diverge markedly from straight lines if they are prolonged beyond the I axis. Consequently, the process GJK, which corresponds to a strong negative recording current, results in a reproduced negative intensity of magnetization I_K which is smaller than it should be if distortionless recording were to be done. This effect is shown in Figure 10. The measurements plotted on this figure were made on a rod of one of the materials from which our magnetic tape is made (vicalloy[5]), which had been heat treated so as to have approximately the same magnetic properties as the tape. (X-ray measurements on vicalloy tape show little preferred orientation of the crystals; hence the longitudinal properties of the rod and the perpendicular properties of the tape should be similar.) The rod was magnetized, demagnetized, and remagnetized in such a way as to

Figure 9. Oscillograms showing reproduced flux density as a function of recording current

Saturation erase; d-c bias record

a, b, c—Correspond to increasingly negative biasing fields

a, b′, c′—Correspond to increasingly positive biasing fields

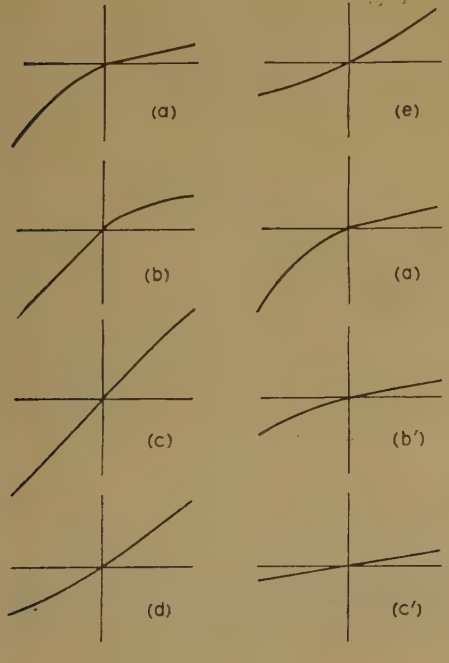
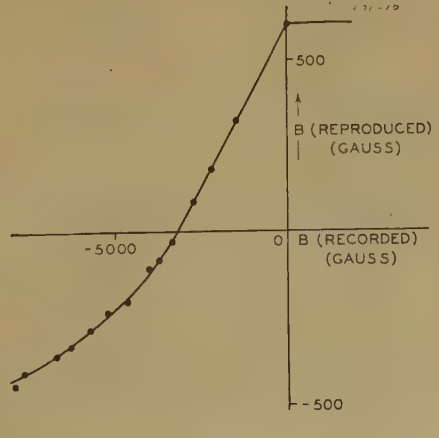


Figure 10. Plot of measurements on vicalloy rod when subjected to the hysteresis processes of the erase-record-reproduce cycle

Demagnetizing field assumed between record and reproduce $=-4\pi I$; at reproduce, $-(1/3)4\pi I$



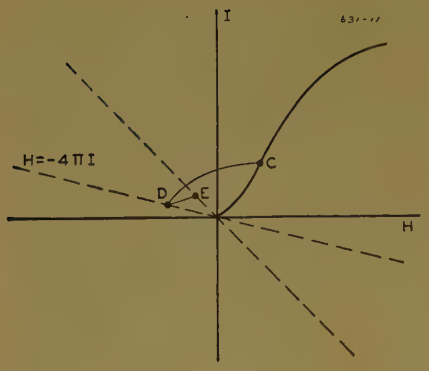


Figure 11. Magnetic history of a tape element

Demagnetization erase; no bias record

trace out curves of the type *ACDE* (Figure 8). For the relation between H and I characteristic of point E, a demagnetizing factor for the tape polepiece combination of amount $(1/3)4\pi$ was used. In later paragraphs it will be shown that a figure of $(1/2)4\pi$ might have been better, but the difference should not affect the conclusions drawn. From experimental determinations of the flux densities at various corresponding points C and E, the curve of Figure 10 was plotted, where the ordinate represents the flux density in the tape when in the reproducing position and the abscissa is proportional to the recording field which originally magnetized the tape. From Figure 10 it is evident that a linear relation between output flux and input field ceases to exist when the reproduced flux becomes negative.

Thus it is clear that this method of recording can employ only the recording currents that correspond to points on the line segment BF. The double amplitude of the maximum flux density that can be reproduced without high distortion is $B_{B''}$. This is only half the amplitude of the overload signal output. Therefore the conclusion: The maximum undistorted volume range of the magnetic tape for this type of recording is at least six decibels less than the maximum distorted range. This is an important practical result which always has been found to be true.

Demagnetization Erase; AC Bias Record. In the section on noise, it has been pointed out that demagnetized tape is 10 to 20 decibels less noisy than tape that has been saturated. Obviously it would be desirable to record on demagnetized tape. But if recording is done directly, without any biasing field, the reproduced signal is highly distorted. This is a natural consequence of the hysteresis cycle through which a tape element goes. In Figure 11, the letters C, D, and E have the same significance as in Figure 8, that is, they represent the state of the tape element while between the recording polepieces, while away from the polepieces, and while between the reproducing polepieces, respectively. Since the magnetization characteristic of a permanent magnet material is strongly curved near the origin, the reproduced intensity of magnetization at E could not be expected to have a linear relation to the magnetizing field at C. Such a linear relation can be achieved by the use of a d-c biasing field that causes recording to be done on the straight portion of the magnetization curve. However, the field required is so high that it restores the noise level practically to the value characteristic of saturated tape.

There is a method whereby the magnetization curve can be effectively straightened out and distortionless recordings thereby made on demagnetized tape. This result, which is achieved by the simple expedient of superposing on the recording fields a moderate field of supersonic frequency, is now well known in the art and will not be gone into here.* For the present purposes, it is sufficient to observe that the effects of the a-c biasing field are properly deduced if it is thought of as simply eliminating the curvature of the magnetization characteristic through the origin. Figure 12 shows the resulting hysteresis cycle through which an element of tape is taken. The curved path CD, which varies with the recorded signal strength is a feature of the hysteresis cycle that is not present in the other method of recording; it is conceivable that this might introduce nonlinearity in the relation between the reproduced magnetization and the recording flux density. In actual practice, however, this is found not to be the case; high quality recordings are produced by this method.

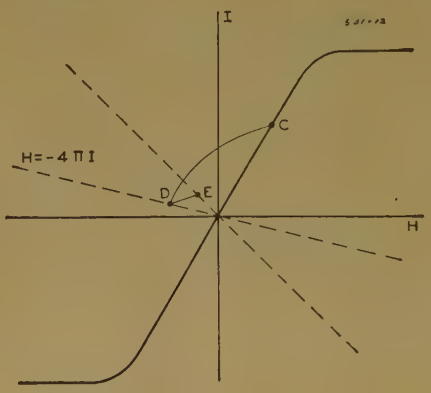


Figure 12. Magnetic history of a tape element

Demagnetization erase; a-c bias record

If the magnetization curve of Figure 12 were perfectly straight up to the saturation value of I, where it overloaded sharply, the double amplitude of the maximum distortionless reproduced flux density would be $2B_{B''}$ (see Figure 8). In such a case this method of recording would be capable of useful output levels six decibels higher than the method previously discussed. In practice the gradual nature of the overload reduces this gain to about four decibels.

Let us now return to the problem of calculating the level of the maximum useful signal that can be reproduced from the tape. Actually, let us deal with the saturation signal, from which we may deduce the maximum signal having comparatively low distortion.

We may start with equation 10, which now becomes

$$e_{\substack{800 \\ EAT}} = 8.0 \times 10^{-8} \Phi_{B''} \qquad (11)$$

The problem now is to obtain a value for $\Phi_{B''}$, the maximum flux that enters the polepieces during the reproduction of an overload sine wave signal.

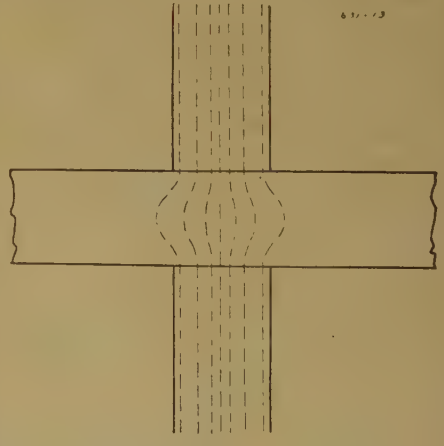


Figure 13. Configuration of lines of force during reproduction

Permeability of tape and polepieces $\gg 1$. Intimate contact between tape and polepieces

* Credit for the discovery of this recording method apparently belongs to W. L. Carlson and G. W. Carpenter, who filed a patent application on it in 1921 (United States patent 1,640,881, issued on August 30, 1927). The first commercial use of the method is believed to have been the audience-participation stereophonic recording display of the Bell System exhibit in the New York World's Fair, 1939–40. Some new techniques for handling the high frequency erasing and biasing problems are disclosed in United States patent 2,235,132, issued to D. E. Wooldridge on March 18, 1941. See also United States Patent 2,351,004, filed by Marvin Camras on December 22, 1941.

Evaluation of $\Phi_{B''}$

Figure 13 shows qualitatively the configuration of the lines of force in the vicinity of the reproducing polepieces. Although a large part of the flux leaks out of the side of a polepiece, through the air to the other polepiece, and back to the tape without linking the windings of the reproducing coils, this leakage is not shown on the drawing. Calculations of the reluctances of the leakage paths involved and search coil measurements agree in establishing that this leakage occurs well away from the pole tips, in a low reluctance portion of the magnetic circuit, and is properly taken account of by the factor of 0.4 that has been used in relating Φ_g and Φ_{REP}. All reluctances that are important in determining the amount of flux entering the polepieces are associated with the portion of the magnetic circuit shown on the figure.

The flux configuration depicted in Figure 13 is appropriate if the permeability of tape and polepieces is high and if intimate contact exists between them. In such a case, nearly all the flux enters the polepiece face, as shown.

The flux that passes into the polepieces may be determined from simple magnetic circuit considerations to be

$$\Phi = \frac{H_c a}{R} \tag{12}$$

where H_c is the value of H when $B=0$, which, for the pertinent hysteresis line $BB''B'$ (Figure 8), is simply the coercive force of the material; R is the reluctance of the complete magnetic circuit, including the tape, polepieces, and connecting yoke.

The reluctance of the circuit was measured directly. A single turn of fine wire was fitted snugly around the very tip of the polepiece lamination, and the voltage induced in it was measured when a small known 1,000-cycle current was sent through the 1,500-turn windings. A vicalloy tape that had been erased by saturation lay between the polepieces. In an obvious way the reluctance of the magnetic circuit was computed. Since there is no question that the reluctance of the circuit lies almost entirely in the pole tip tape region, both for this measurement and for the conditions during reproduction of a signal, this measurement should yield a value of reluctance approximately the same as that called for by equation 12. The measured value was 9.0 centimeter-gram-second units.

Substitution of $R=9.0$ in equation 12, together with the measured coercive force of 250 oersteds and the tape thickness of 0.0022 inch, gives $\Phi_{B'}=0.16$ maxwell. This value of $\Phi_{B''}$, when set into equation 11, predicts a 300-cycle-overload open-circuit reproduced signal of 1.3×10^{-3} volts. The value measured experimentally is 1.6×10^{-3} volts. The discrepancy lies within experimental limits.

Therefore it is possible to conclude that the reproduced signal levels are satisfactorily accounted for by the simple theory that has been given, wherein a detailed study of the hysteresis cycle through which a tape element travels has led to the conclusion that the maximum signal should be determined by the coercive force of the tape and the reluctance of the complete magnetic circuit.

If the theory is to be wholly satisfactory, it must meet the need of the analysis of the frequency characteristics of noise and signal, wherein it was pointed out that the similarity of the curves seemed to require that the magnetization of the tape element should not increase by a very large factor as it comes between the reproducing polepieces. The value of $\Phi_{B''}$ that has just been deduced, 0.16 maxwell, corresponds to a flux density of 180 gausses at the center of the polepieces, if $g(x)$ is *assumed* to be a constant and the flux therefore leaves the tape in accordance with the $f(x)$ shown in Figure 6. From the known relation between H and I, and therefore between B and I, given by the magnetic data that specify the hysteresis line $BB''B'$ of Figure 8 ($H_c=250$ oersteds, $B_{B'}=1{,}500$ gausses), this value of flux density can be computed to correspond to

$$4\pi I_{REP} = 400 \text{ gausses}^*$$

The value before the tape element comes between the polepieces is $4\pi I=250$ gausses. Therefore the assumption that $g(x)$ is constant leads to a result that is consistent with $g(x)$ varying by less than a factor of two, from $x=0$ to $x=\infty$ Replacement of the $f(x)$ used in this calculation by $f(x)\ g(x)$ for such a slowly varying $g(x)$ results in a trivial increase in the derived I_{REP} (about six per cent). It is clear that the correct figure for $4\pi I_{REP}$ at the center of the polepiece is not greatly higher than the value that has been calculated above, and that $g(x)$, as required by the frequency analysis, is such a slowly varying function that its replacement by a constant should produce only a slight change in the shape of the derived response characteristic.

* Thus $\frac{-H}{4\pi I}\sim 1/2$, under the assumptions used. That is, the demagnetizing factor in the presence of the polepieces is half as great as for free tape

The analysis of signal levels is not complete without an inquiry into the reasonableness of the value of 9.0 centimeter-gram-second units that has been measured to be the reluctance of the magnetic circuit. The reluctance of the circuit is made up of two parts, that of the polepieces and connecting yoke, and the reluctance of the tape element itself. For the structures used, the polepiece-yoke reluctance is easily computed to have a value of about 0.2 centimeter-gram-second units. Use has been made already of the fact that this is a negligible part of the total reluctance. The reluctance of the tape element cannot be accurately computed without a detailed knowledge of the flux configuration, but an upper limit can be set by assuming no bending of the flux between the polepieces. When the appropriate permeability value (obtained from measurements of $B_{B'}$ and H_c for vicalloy) and dimensions are set in the obvious equations, a maximum reluctance of 2.2 centimeter-gram-second units is predicted for the tape. Thus the computations predict a reluctance for the magnetic circuit of no more than 2.4 centimeter-gram-second units, as contrasted with the value of 9.0 which was measured, and which properly accounts for the observed signal strength!

It seems likely that the high reluctance of the circuit is caused by a region of low permeability at the tip of each polepiece. This may be thought of as introducing an effective air gap between each pole tip and the tape. The measured reluctance corresponds to a width of 0.0005 inch for each of these air gaps. The existence of an effective air gap of this order of magnitude between the surfaces of soft magnetic materials when pressed together is a common phenomenon in magnetics.[6] The effective air gap is attributed primarily to the pole tips and not to the tape because the reluctance of the circuit was found to be affected but slightly when the tape was removed and the pole tips allowed to touch one another.

Practical Applications

Up to this point the method of procedure has been simply to subject some of the principal features of perpendicular magnetic tape recording to simple analysis in order to arrive at an improved understanding of the physical processes involved. This section is devoted to a discussion of some of the practical implications of the results of the preceding two sections.

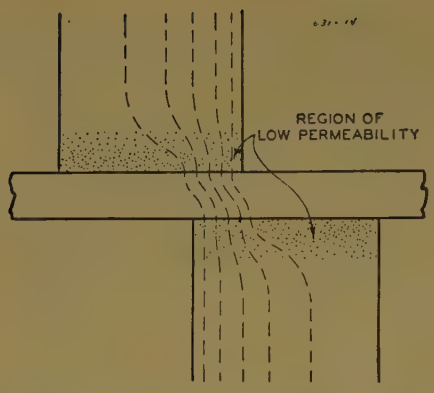


Figure 14. Action of wide offset polepieces

Reluctance of region of low permeability is decreased by increased cross section of the flux path. Region of influence is characteristic of the small overlap length and is not increased by wide polepieces

Increased Signal-to-Noise Level

If the conclusions reached in the first section are correct, a low noise level requires a tape material having a small magnetic domain size and/or a high degree of exactness in the mutual cancellation of the domain fields. The present state of magnetic domain theory does not permit the correlation of tape noise with any measurable magnetic properties. Empirical experiments on various kinds of tape have revealed no such correlation. The only useful generalization that can be drawn about tape noise is that demagnetized tape is always quieter than tape that has been saturated.

From the second section of this paper, a high signal level should be produced by a tape having a high coercive force. This principle guided Bell Telephone Laboratories in the development of vicalloy tape, which has a coercive force of 200 to 250, compared with the value of 40 or 50 characteristic of the chrome steel alloy formerly used. The signal output level is higher than that of the chrome steel tape, but the noise level is not enhanced. When recording is done on demagnetized vicalloy tape by the method that employs a supersonic field superposed on the recording field to straighten out the magnetization characteristic, a volume range (to overload) of 55 decibels is obtained. This signal-to-noise ratio is obtained in a system equalized from 100 to 8,000 cycles, at a tape speed of 16 inches per second. The equalization is done in the output circuit only. Under these circumstances the volume range is practically independent of frequency.* The useful volume range depends on the harmonic content that can be tolerated but is several decibels fewer than 55.

This combination of vicalloy tape and the superposed high frequency method of recording first was used commercially in the audience-participation stereophonic recording display of the Bell System exhibit in the New York World's Fair, 1939–40.

Simplified and Improved Polepiece Structure

When it was discovered that the output signal level was being limited largely by a region of high reluctance in the tips of the polepieces, a search was instigated for polepiece material that would exhibit lower tip reluctance than the molybdenum permalloy in use. The search succeeded in turning up a few other materials as good as the molybdenum permalloy but none better. The resultant directing of attention to other ways of decreasing this reluctance led to the idea of replacing the thin exactly aligned polepiece laminations by wide offset polepieces such as those pictured in Figure 14. The hope was that the region of influence of the polepieces would be controlled by the small overlap so that high frequency sensitivity would not be lost, but that the flux would be able to spread out in the region of low permeability, thus decreasing the reluctance and increasing the output signal level. On Figure 15 are replotted from Figure 7 the output signals obtained from the usual record-reproduce unit, in which the magnetic part of the pole faces consists of a 0.0015 inch by 0.040 inch lamination. In addition are plotted measurements on a unit in which the polepieces consist of molybdenum permalloy rod 0.041 inch by 0.040 inch, the leading edge of one polepiece being exactly opposite the following edge of the other (no overlap in Figure 14). The vertical difference between the two curves is adjusted for the measured difference in flux loss from pole tips to coils for the two units. The two curves correspond to recorded levels the same distance below saturation. Figure 15 shows a general increase in the output level that may be attributed to the expected decrease in pole tip reluctance. The shape of the high frequency portion of the curve is somewhat different for the new unit, but there is no evidence of an increase in the effective polepiece width. The upward bulge in the response of the new unit at low frequency is caused by a longitudinal component of magnetization, which, for the polepiece dimensions used, has a maximum at 200 cycles. This is all to the good, of course, since it reduces the amount of equalization needed. The position of this bulge is controlled by the width of the polepieces. This is the principal reason for the use of pieces 0.041 inch wide. The over-all signal level and moderate-to-high frequency response are just as high for 0.020-inch pieces, for example.

The wide, offset polepieces are also more efficient on recording, about eight decibels fewer ampere turns being required to saturate the tape than with the old unit. Furthermore, the 0.041-inch tip is sturdy and self-supporting. Its use permits a much simpler and cheaper record-reproduce unit design than that associated with the thin laminations, which had to be incorporated in a supporting structure of bakelite and brass and provided with a fairly complicated framework containing guides and yokes. The mechanics of the thick polepiece structure also permit a coil design that recovers practically all of the reproduced

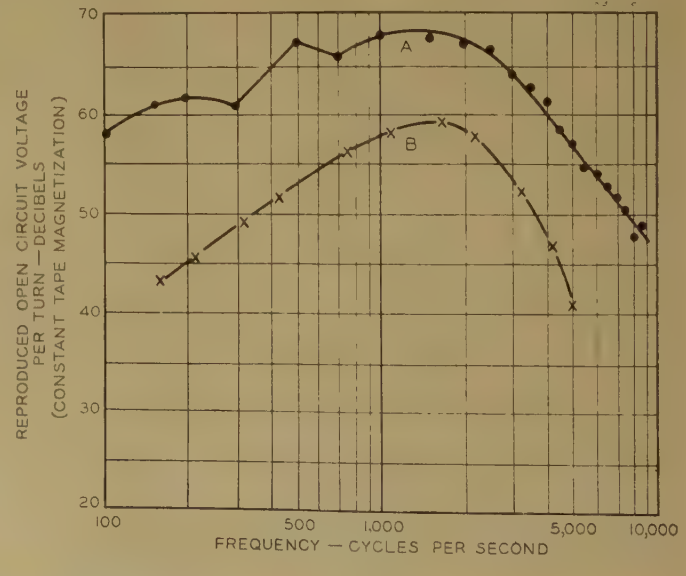


Figure 15. Comparison of output efficiencies of narrow aligned polepieces and wide offset polepieces

Curve *A*—Polepiece dimensions, 0.041 inch by 0.040 inch
Curve *B*—Polepiece dimensions, 0.0015 inch by 0.040 inch
Tape speed = 16 inches per second

* This is a consequence of the similarity between the noise and signal frequency characteristics.

flux that in the older structures leaked out of the polepieces without linking the windings. This adds another eight decibels to the relative efficiency of the new unit. As a result of all these gains, the new unit has an over-all record-reproduce transfer loss twenty-six decibels fewer than that of the old unit at 1,000 cycles. The complete comparison of the efficiencies of the two units is given in Figure 16.

Figure 17 shows the record-reproduce unit used in the Western Electric Mirrophone. The unit contains two polepiece-coil structures, one for erasing, the other for recording and reproducing.

Summary

In the first section of this paper, it was shown that the shape of the noise frequency distribution curve of both magnetized and demagnetized tape can be semi-quantitatively accounted for if it is assumed that the noise is caused by many random magnetic irregularities in the tape, of average dimension smaller than 0.0015 inch. An incidental result of the treatment was a derivation of the shape of the signal frequency response characteristic and an explanation of its similarity to the noise frequency distribution. Various possible sources of noise were examined. The only source found to be qualitatively and quantitatively acceptable consisted of statistical variations in the net flux entering the polepieces because of the finite size of the magnetic domains of the tape material.

In the section on signal levels, detailed consideration was given to the hysteresis processes through which an element of tape travels in the erase-record-reproduce cycle. Both the saturation erase d-c bias record and the demagnetization erase a-c bias record systems were considered. It was shown that the latter system not only is less noisy than the former, but also is capable of somewhat higher level high quality recordings. The magnitude of the overload signal was predicted in terms of the coercive force of the tape material and the reluctance of the magnetic circuit. The signal level prediction was shown to be in satisfactory agreement with experiment. The measured reluctance of the magnetic circuit was found to be so high that it required the existence of an effective air gap of about 0.0005 inch between each pole tip and the tape surface.

In the last section of the paper, it was shown how the search for a tape material having the characteristics that the theory indicated should give a high signal output, resulted in the development by the Bell Telephone Laboratories magnetic and metallurgical groups of a vicalloy tape having a markedly higher signal-to-noise ratio than had previously been obtainable. Attempts to diminish the pole tip reluctance that had been concluded to be a limiting factor in output signal strength were shown to have led to the development of a new type of record-reproduce unit with an improved frequency response, increased efficiency, and greatly simplified design. By a combination of vicalloy tape, the superposed high frequency method of recording, and the new unit design, high quality recordings equalized from 100 to 8,000 cycles with a useful volume range of more than 50 decibels can be made. A tape speed of only 16 inches per second is required, and the erase-record-reproduce unit combines simplicity of construction with low transfer loss.

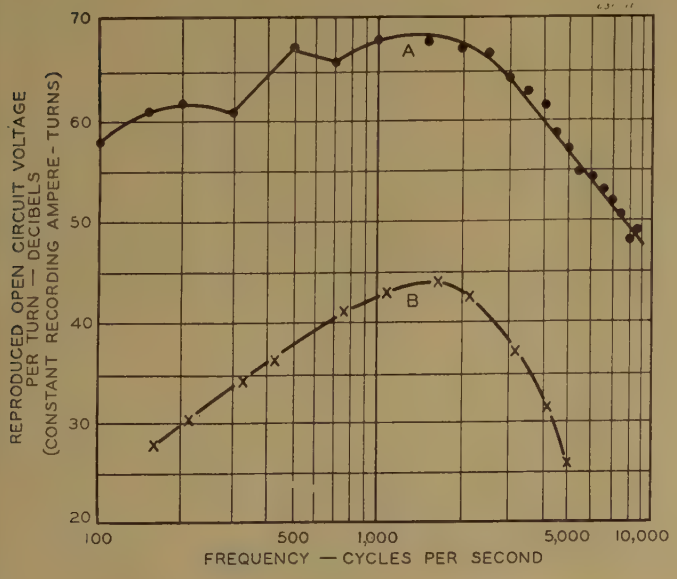


Figure 16. Comparison of over-all record-reproduce efficiencies of new (A) and old (B) units

Recording ampere turns the same for all measurements. Tape speed = 16 inches per second



Figure 17. Illustration of erase-record-reproduce unit used in Western Electric Mirrophone

Tape guides and dust cover removed

Appendix I. Frequency Distribution of Noise Power Caused by Random Small-Voltage Pulses

The Fourier expansion of the $e(t)$ of equation 2 over a time interval T which includes the pulse in question is

$$e(t) = \sum_{m=1}^{\infty} B_m \sin\left(\frac{2\pi mt}{T} + \Phi_m\right) \qquad (13)$$

where

$$B_m = 2KMn \times 10^{-8} \cdot \frac{1}{T}\int_{-\infty}^{+\infty} \frac{df}{dx} \sin\frac{2\pi mx}{VT}\, dx \qquad (14)$$

In equation 13 the phase Φ_m depends on the position of the pulse in the time interval chosen for the expansion. Extension of the limits of integration to $\pm\infty$ is permissible since the integral is zero outside of the small interval occupied by the pulse.

The power developed in the frequency range $\Delta\nu$ by the combined effects of N voltage pulses, such as the above scattered at random throughout every time interval T (large compared with the pulse duration), is

$$P_n(\nu)\Delta\nu = \frac{1}{R}\sum_{m_1}^{m_2} E_m^2 \qquad (15)$$

where the reproducing coil circuit is assumed to have a resistance R for all frequencies, and the range $m_2 - m_1$ is related to $\Delta\nu$ through the equation

$$\frac{m_2 - m_1}{T} = \Delta\nu \qquad (16)$$

E_m^2 is the mean square noise voltage at frequency m/T and is

$$E_m^2 = 1/2NB_m^2 \qquad (17)$$

In equation 17 the 1/2 is caused by the usual relation between average power and voltage amplitude. NB_m^2 is the square of the amplitude of the noise voltage of frequency m/T, caused by N voltage pulses of identical size and shape scattered at random throughout the interval. (In the case of random phases of the elementary pulses, the squares of the amplitude add directly.) Combinations of equations 14, 15, 16, and 17 give, for the noise power in the range $d\nu$ at frequency ν,

$$P_n(\nu)d\nu = \frac{2(Kn\times 10^{-8})^2}{R} M^2\left(\frac{N}{T}\right) S(\nu)^2 d\nu \tag{18}$$

where

$$S(\nu) = \int_{-\infty}^{+\infty} \frac{df}{dx} \sin \frac{2\pi\nu x}{V}\, dx \tag{19}$$

Appendix II. Frequency Response Characteristic of Tape Recording

The problem to be considered is the following: For a given sine wave intensity of magnetization on the tape before it passes between the reproducing polepieces, how does the mean square reproduced signal power depend upon frequency?

At any instant the flux that enters the polepieces from an element of tape of length dx a distance x from the center line of the polepieces is

$$d\Phi = KdMf(x) \tag{20}$$

where dM represents the magnetic moment of the specified element of tape and the other quantities have the same meaning as in equation 1. For dM we may write

$$dM = ahI(x)dx \tag{21}$$

where a = tape thickness (0.0022 inch), h = polepiece height (0.040 inch), and $I(x)$ = intensity of magnetization of the tape a distance x from the center line of the polepieces. $I(x)$, in turn, may be expressed as

$$I(x) = g(x)I_o \sin \frac{2\pi\nu}{V}(x - Vt) \tag{22}$$

where $I_o \sin \frac{2\pi\nu}{V}(x-Vt)$ describes the variation with x and t of the magnetization that would exist if the reproducing polepieces were removed from the tape, while $g(x)$ is the factor by which the remanent magnetization of the free tape is multiplied by the partial removal of the strong demagnetizing field brought about by the proximity of the reproducing polepieces.*

* The hysteresis processes involved are discussed in the section on signal levels.

Equations 20, 21, and 22 give

$$\Phi = KahI_o \int_{-\infty}^{+\infty} f(x)g(x) \sin \frac{2\pi\nu}{V}(x - Vt)dx \tag{23}$$

Employment of the conditions $f(+x)\ g(+x) = f(-x)\ g(-x)$ and $f(\infty)g\ (\infty) = 0$ permits simplification to

$$\Phi = \frac{V}{2\pi\nu} KahI_o \sin 2\pi\nu t T(\nu) \tag{24}$$

where

$$T(\nu) = \int_{-\infty}^{+\infty} \frac{d}{dx}[f(x)g(x)] \sin \frac{2\pi\nu x}{V} dx \tag{25}$$

The reproduced signal power is

$$P_s(\nu) = \frac{1}{2} \frac{\left(10^{-8} n \frac{d\Phi}{dt}\right)^2_{\max}}{R}$$

of

$$P_s(\nu) = \frac{1}{2} \frac{(Kn\times 10^{-8})^2}{R} (I_o ah)^2 V^2 T(\nu)^2 \tag{26}$$

Appendix III. Tape Noise Caused by Saturated Domains of Random Orientation

The calculation must start with an evaluation of the constant K, of equation 18. K is the amount of flux that links the windings of the reproducing coils because of an element of unit magnetic moment lying directly between the polepieces. For the magnetic structures used in these tests, only about 40 per cent of the flux that entered the poletips succeeded in linking the windings. The exact value of the flux that enters the polepieces because of a magnetized region between them depends in a complicated way on the depth of the region in the tape and on the magnetic and geometric properties of the tape-polepiece structure. However, the correct answer can be shown to lie within a factor of three or four of $4\pi\frac{M}{a}$. This is accurate enough for the purpose at hand. Thus

$$K \sim \frac{4}{2.5} \frac{\pi}{a} \sim \frac{4}{a} \tag{27}$$

For evaluating $S(\nu)^2$, the $f(x)$ of Figure 6 may be used. A graphical integration gives

$$\int_o^{5{,}000 \text{ cycles}} S(\nu)^2 d\nu = 5{,}500 \text{ sec}^{-1} \tag{28}$$

Therefore, from equations 18, 27, and 28,

$$E_N^2 = R \int_o^{5{,}000 \text{ cycles}} P_N(\nu)d\nu$$

$$= 1.76\times 10^{-11} n^2 \frac{M^2}{a^2}\left(\frac{N}{T}\right) \tag{29}$$

where E_N^2 is the mean square open-circuit noise voltage, measured in a circuit covering the frequency range 0–5,000 cycles, and M, a, and T are in centimeter-gram-second units. For the reproducing coils used, n = 1,500 turns, whereas the tape thickness was about 0.005 centimeter. Therefore equation 29 becomes

$$E_N^2 = 1.58 M^2\left(\frac{N}{T}\right) \text{ volt}^2 \tag{30}$$

Both M and N/T depend on the domain size. If we consider it to have a volume v,

$$M = vI_{SAT}$$

where I_{SAT} is the saturation intensity of magnetization of the tape. For the materials used, $B_{SAT} \sim 15{,}000$ gausses, or $I_{SAT} \sim 1{,}000$ centimeter-gram-second units.

$$M \sim v \times 1{,}000 \tag{31}$$

For the number of domains per second that pass by the polepieces,

$$\left(\frac{N}{T}\right) = \frac{Vha}{v}$$

Substitution of the values $V = 16$ inches per second, $h = 0.040$ inch, $a = 0.002$ inch, gives

$$\left(\frac{N}{T}\right) = \frac{0.021 \text{ cm}^3 \text{ sec}^{-1}}{v} \tag{32}$$

Equations 30, 31, and 32 give

$$E_N^2 = 3.3\times 10^4 v \text{ volt}^2 \tag{33}$$

References

1. Sound Recording on Magnetic Tape, C. N. Hickman. *Bell System Technical Journal*, volume 16, April 1937, pages 165–78.

2. Barkhausen Effect II. Determination of the Average Size of the Discontinuities in Magnetization, R. M. Bozorth, J. F. Dillinger. *Physical Review*, volume 35, April 1, 1930, pages 733–52.

3. The Magnetic Structure of Iron Crystals, W. C. Elmore. *Physical Review*, volume 62, November 1942, pages 486–93.

4. Werkstoffe fur Dauermagnete, H. Neumann. *Archiv fur Technisches Messen*, number 69, March 1937, pages T38–42.

5. Vicalloy, a New Permanent Magnet Material, E. A. Nesbitt, G. A. Kelsall. *Physical Review*, volume 58, July 15, 1940, page 203.

6. Magnetic Core Materials Practice (booklet), Allegheny Steel Company, Brackenridge, Pa., 1937, page 89.

The Mho Distance Relay

R. M. HUTCHINSON
ASSOCIATE AIEE

THE NEED for more adequate discrimination by means of distance relays, between fault conditions and power swings has been heightened in recent years by the construction of longer transmission lines and by the transmission of larger amounts of energy over existing lines.

Several recent papers[1,2,3] have described the inadequacy of the impedance- and reactance-type directional distance relays to fulfill this need without the addition of auxiliary operating units. Auxiliary units always introduce additional sources of trouble, increase the need for maintenance, and make the maintenance more difficult. R. E. Cordray and A. R. van C. Warrington have described the use of a relay which measures a constant component of admittance for providing this discrimination, in addition to providing correct directional action and accurate distance measurement, all in one unit.[4] This characteristic has been named a mho characteristic.

Figure 2, which has been taken from their paper, illustrates how a relay at A, with a mho characteristic set to protect 90 per cent of the line to B, will operate over a smaller band of power swing conditions than the impedance or reactance-type relays. The line AB is the locus of impedance seen by the relay for metallic faults along the line. The mho distance relay operates for impedances within its circle. The impedance-type relay operates for impedances which lie within its circle of constant impedance and which are above and to the right of the straight-line characteristic of the directional element. The reactance-type relay operates for impedances which lie below its constant reactance locus and which are within the circular characteristic of the starting unit. It has been shown that a relay with the mho characteristic will provide instantaneous tripping during a power swing only if the electrical center of the system is within the section of the line protected by the relay and only if the voltages at the ends of the section become approximately 90 degrees out of phase. Such a condition usually indicates loss of synchronism, and it is usually desirable to sever the system at its electrical center.

It is the purpose of this paper to describe a 3-step distance relay operating on the mho principle. It has three independent units, each capable of providing a complete mho characteristic, thus approaching the ultimate in relaying simplicity—one contact in the trip circuit. Three mho distance relays (type GCY), with an auxiliary timing relay, provide 3-step distance phase protection to one terminal of 3-phase line. This relay also can be used as part of a distance pilot carrier-current relaying terminal.

Every high-speed distance relay has a tendency to trip on faults beyond its ohmic setting when the fault current has a large d-c offset. The induction cylinder-type mho relay has reduced this transient overreach to a few per cent, even for highly lagging transmission line circuits.

Another unique characteristic of the mho unit is its "memory action," which provides a strong polarizing flux for even a zero voltage fault. This condition causes the relay to operate fastest for nearby faults.

Arrangement

The general arrangement is shown in Figure 3, and the ohmic characteristics in Figure 4A. Each mho distance relay has three units providing 3-step directional distance protection for faults between two phases of a 3-phase line.

The first or instantaneous tripping zone is provided by the M_1 unit, which is usually set to operate for faults within the first 90 per cent of the protected section AB. The M_2 unit operates through contacts with a slight time delay to clear faults in the neighborhood of the next bus at B. The conventional third zone, providing time delay backup for faults beyond B, is provided by the offset mho unit, OM_3. The offset, resulting in an ohmic characteristic which encircles the origin, provides a strong steady torque for faults in the vicinity of the relay bus. As a by-product, it provides time delay backup for nearby faults in the reverse direction. It can be used with no offset if desired.

It is possible to reverse the polarity of the OM_3 unit to obtain the reversed OM_3 connection shown in Figure 4B. This provides time delay backup for faults between A and the bus behind it at D. The merits of the reversed OM_3 connection are discussed in a companion paper.[5]

One mho distance relay of drawout construction which affords ease of maintenance and testing is illustrated in Figure 1. The relay occupies approximately 6 by 20 inches of panel space.

Three mho distance relays combine with a common timing relay to give directional distance protection from one end of a 3-phase line. An elementary diagram for the relays at one terminal is shown in Figure 5. For clarity, the d-c connections to two of the mho distance relays are indicated by light lines because they parallel the connections of the third relay.

Figure 1. The mho distance relay



Paper 46-39, recommended by the AIEE committee on protective devices for presentation at the AIEE winter convention, New York, N. Y., January 21–25, 1946. Manuscript submitted November 23, 1945; made available for printing December 18, 1945.

R. M. HUTCHINSON is a project engineer with the Brown Instrument Company, Philadelphia, Pa.

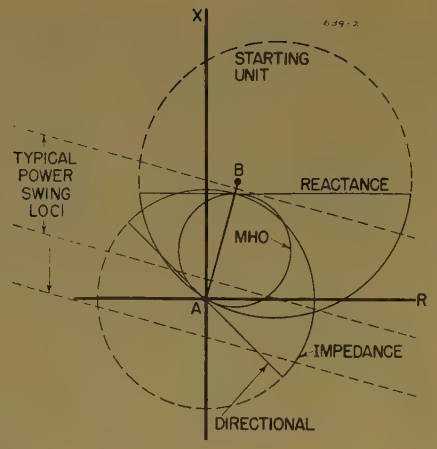


Figure 2. Impedance diagram illustrating tripping zones for impedance, reactance, and mho-type directional distance relays at *A* set to protect 90 per cent of the line *AB*

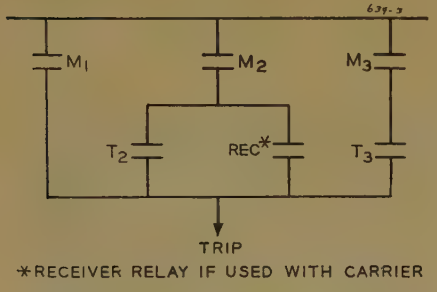


Figure 3. Fundamental trip circuit

The seal-in unit in each mho distance relay gives a target indication to show which phases are affected, while the targets mounted in the timing relay indicate which distance zone has operated.

Construction of the Mho Units

The mechanical construction of the mho unit is shown in Figure 6. Four laminated poles encircle a stationary core or inner stator with a small annular air gap between. Within the annular gap there turns an aluminum induction cylinder supporting a lightweight moving contact structure. The contacts are fine silver cylinders at right angles to provide the ideal point contact and are protected from excessive pressures by means of a clutch. This clutch is adjusted by means of a helical spring on the rotating shaft. The lead-in spiral for the contacts acts as a light control spring to give the contacts a positive position when the relay is de-energized. A lower jewel bearing with a highly polished pivot at the bottom of the shaft and a highly polished guide pin engaging a phosphor bronze bushing in the top of the shaft reduce friction to an almost imperceptible amount.

The arrangement of the coils on a unit which operates for faults between phases 1 and 2 is shown schematically in Figure 7A. The unit is polarized by the same potential that provides the restraining torque and derives its operating torque from double current windings, providing flux proportional to the difference of the currents in the two phases involved. This condition provides the same reach for 3-phase, phase-to-phase, or double phase-to-ground faults.

The two side poles carry the polarizing windings, which are tuned by the capacitor C_2 to have a slightly leading current. This condition causes the natural frequency of the polarizing circuit to be very close to 60 cycles. Therefore, when the terminal voltage drops to almost zero during bus faults, the polarizing flux continues for a period long enough to cause most rapid operation of the unit. See Figures 13, 14, and 15.

Figure 8 illustrates a cathode-ray oscilloscope screen with a recurrent sweep showing the current in the polarizing coils before and during a zero-voltage fault. The accuracy required of the M_1 unit during transient conditions makes the tuning of this circuit critical, so that the tuning reactor X_2 is used in this unit only. In the past, memory action has been incorporated into units which had a primarily directional function. For this purpose, phase resonance[6] was used and proved satisfactory, but to obtain accurate distance measurement also, it is necessary to tune to period resonance. Tuning a circuit for phase resonance produces current at unity power factor, which is the condition generally considered as resonance. Tuning for period resonance produces a circuit whose natural frequency is equal to the frequency of the applied voltage. When resistance is present, there is a difference between these two types of tuning.

Returning to Figure 7A, the restraining flux in the rear pole is supplied by two coils on the rear of the magnetic structure. The size of the ohmic characteristic is adjusted by means of taps on an autotransformer. The resistor R_1 is provided for a factory adjustment of the maximum restraint setting. The capacitor C_1 provides a certain amount of memory action to the restraining circuit of the M_1 unit to aid in preventing false operation of the unit during transient conditions at the inception of a fault, either caused by unsymmetrical currents or the result of mechanical rebound caused by spring in the lightweight rotating structure upon a sudden loss of restraining torque.

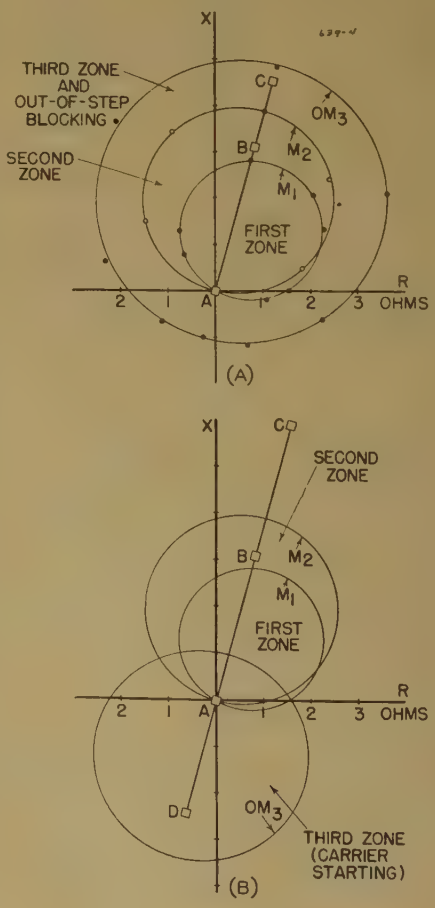
The current coils for providing operating flux to the front pole are wound on top of flux shifting windings on the two front legs of the magnetic structure.

With the accurate tuning of the polarizing circuit of the M_1 unit, no phase shift of the operating flux is necessary to obtain maximum operating torque at 75 degrees lag, because the circuit constants are such that tuning for maximum torque at 75 degrees and natural frequency at 60 cycles occur at the same point. Therefore the flux shifting coils are open-circuited for the 75-degree setting. Use is made of the flux shifting coils in order to obtain two other values of the angle of maximum torque, 60 degrees and 45 degrees. Using capacitive circuits to complete the circuit in the M_1 unit aids in reducing transient operating torques caused by d-c components in the current waves. The angle of maximum torque of the M_1 unit is selected by means of leads on a connection block.

The connections of Figure 7A for the M_2 unit are schematic in that the circuit of the flux shifting coils is completed permanently through R_2 instead of being brought out to a connection block. Ad-

Figure 4

A. Typical setting of mho distance relay for conventional 3-step protection
B. Typical setting of mho distance relay using the reversed OM_3 connection



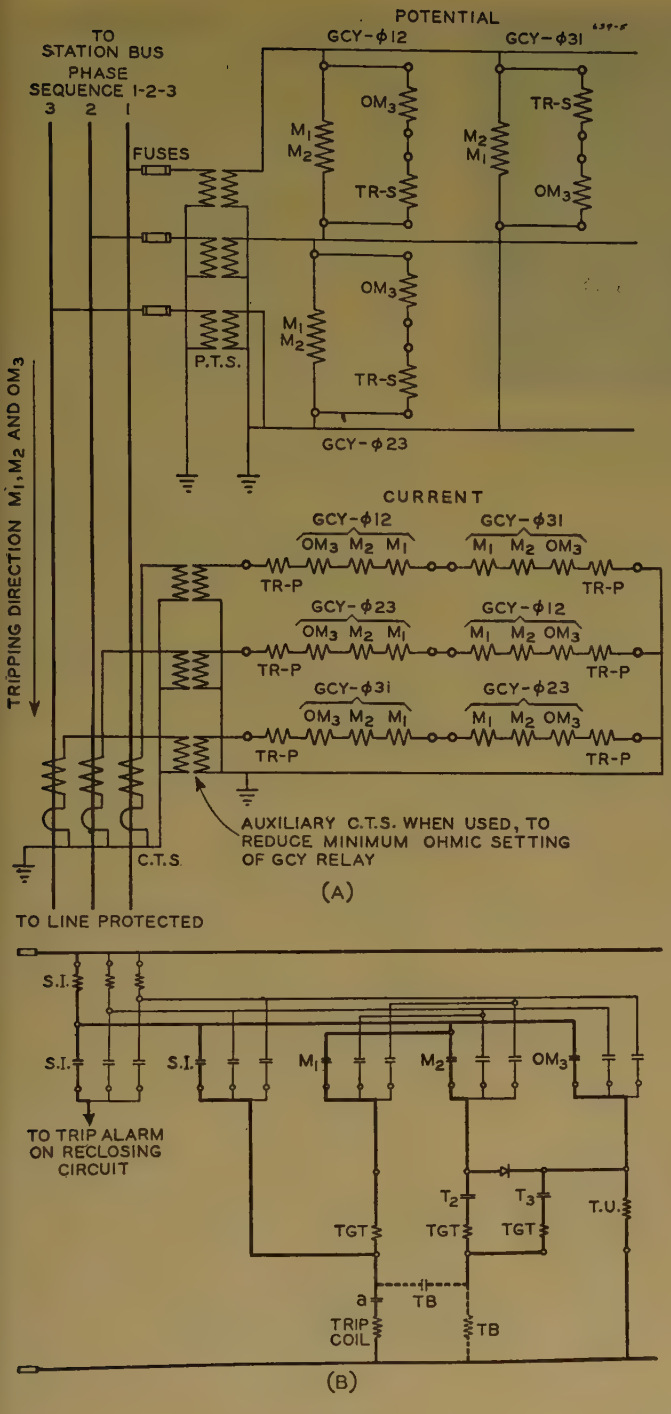
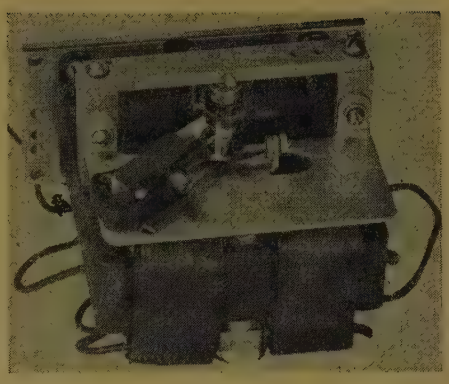


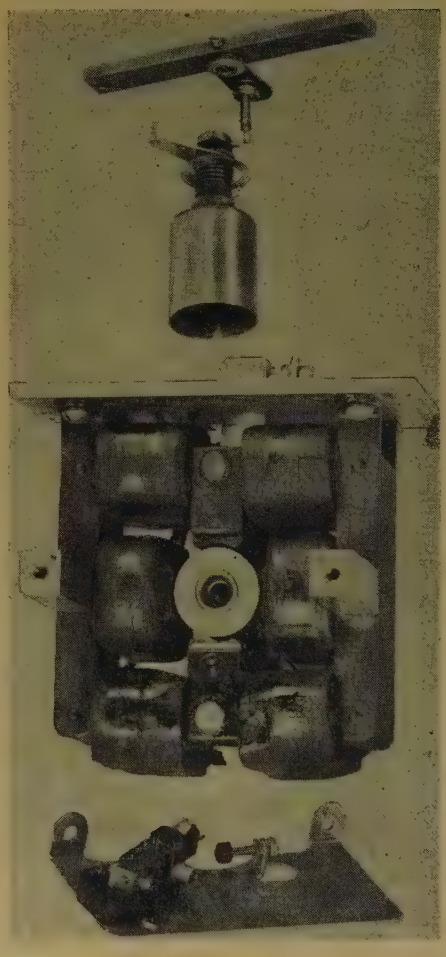
Figure 5. Elementary diagram of connections for one 3-phase terminal

A. A-c circuits
B. D-c circuits

M_1 = mho unit, first zone
M_2 = mho unit, second zone
OM_3 = offset mho unit, third zone
TR-P = transactor primary
TR-S = transactor secondary
S.I. = seal-in unit
T.U. = timing relay operating circuit
T_2 = zone 2 contact of *T.U.*
T_3 = zone 3 contact of *T.U.*
TGT = target
TB = relay for blocking instantaneous reclosing after time delay trip. Omit *TB* if this feature is not required, and connect lower terminals of all three targets
a = auxiliary switch closed when breaker is closed



A. A single mho unit



B. Exploded view of mho unit

Figure 6

justment of the R_2 will provide a continuous range from 60 degrees to 75 degrees for the angle of maximum torque.

The restraining torque of the M_1 and M_2 units is given by the expression $K_1E_{pol}E_{rest}$, where K_1 includes the sine of the angle between the two fluxes and the restraint transformer tap setting. The operating torque expression is $K_2E_{pol}I\cos(\phi-\theta)$, where θ is the phase angle of the relay characteristic, depending upon the phase angle of the polarizing circuit and the phase shift of the operating flux by the flux shifting circuit, and ϕ is the phase angle of the fault current ($I=I_1-I_2$). Therefore the relay torques are balanced when $E_{pol}\ (I\cos(\phi-\theta)-(K_1/K_2)E_{rest})=0$. E_{pol} can be cancelled out of the preceding equation because it is not zero, even for zero voltage faults, because of memory action, leaving

$$\frac{E_{rest}}{I\cos(\phi-\theta)}=\frac{K_2}{K_1}$$

At the angle of maximum torque, $\phi=\theta$ and $E_{rest}/I=Z=K_1/K_2$.

With the closest manufacturing tolerances attainable, it is impossible to eliminate very minor mechanical, and consequently magnetic, dissymmetries from the unit. These introduce spurious torques proportional to the current squared which become strong enough under short-circuit conditions of high current and low voltage to overcome the torques produced by interaction with the polarizing flux.

These torques are reduced to negligible magnitudes by two means. The current coils are connected in parallel in order that the induced voltages in each of a pair of windings will be as nearly equal as possible, thereby producing equal fluxes. Any further adjustment that is

necessary is made by a slight shift in the position of the inner stator by means of a fine screw shown at the rear of the unit in Figure 6B.

The operating unit of OM_3 is identical with the M_2 unit. In order to produce the offset characteristic shown in Figure 4, a transactor is used as shown in Figure 7B. Transactor is the name that has been given to a reactor which has a secondary winding for a voltage several times that corresponding to the impedance drop produced in the transactor's primary winding, without increasing the burden.

The transactor in the OM_3 unit has double current winding, as does the operating unit, so that the voltage induced in its secondary winding is proportional to $I=I_1-I_2$ and leads I by 90 degrees. By connecting the proper amount of resistance R_4 across the transactor's secondary winding, the secondary voltage can be made to lead the primary current, I, by 75 degrees. The addition of this secondary voltage from the transactor in series with the potential transformer secondary

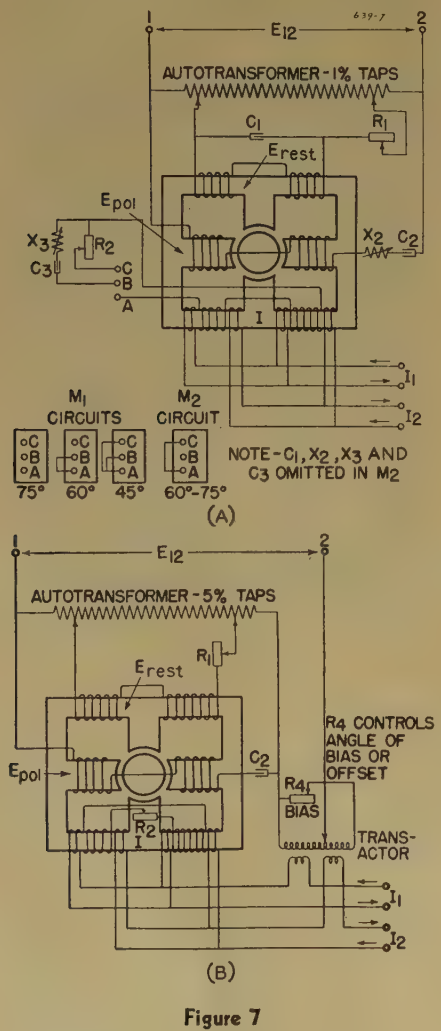


Figure 7

A. Diagrammatic wiring of M_1 and M_2 units
B. Diagrammatic wiring of OM_3 unit

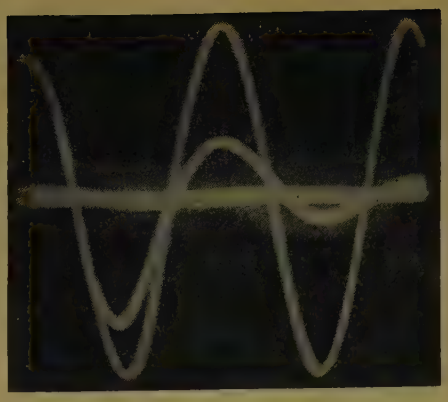


Figure 8. Current in polarizing winding of M_1 unit during zero-voltage fault

voltage, which is applied to the relay terminals, results in a shift of the unit's ohmic circle so that it no longer passes through the origin. This shift, or offset, is a distance corresponding to (transactor secondary voltage)/(I_1-I_2) ohms at a 75-degree phase angle.

Adjustment of R_4 can be made to cause the offset to be along any angle between 75 degrees and 60 degrees to match the angular setting of the operating unit. The magnitude of the offset is governed by taps on the transactor secondary winding.

Characteristics

Each unit has been designed to meet the requirements of its use in either a purely distance relaying scheme or a directional carrier current scheme.

The M_1 unit is purely a directional distance unit. It has been designed to operate for faults out to 90 per cent of the line section and for swing conditions which cause the voltages near the two ends of its protected section to be 90 degrees out of phase. It is provided with connections for setting the angle of maximum torque on 75 degrees, 60 degrees, or 45 degrees. In order to operate properly in the presence of resistance added by arcing faults (Figure 9) it is expected that the 60-degree setting will be used most frequently. This setting is discussed more fully in a companion paper.[5] The 75-degree setting is intended for longer lines, the 45-degree setting for short lines.

The plotted points shown in Figure 4A illustrate the negligible deviation of the operating characteristics of the units in a typical relay from the theoretical mho circle, when rated voltage is applied. This circular characteristic is a result of the steady torque produced in an induction cylinder unit. Units whose operating forces are pulsating throughout a cycle do not produce a true circle, thus adding difficulty to the calculation of settings for obtaining accurate relaying during power swings.

As is common with distance relays, the accuracy falls off at low values of current (and voltage). Figure 10 shows that the contacts of an M_1 or M_2 unit will close under steady state conditions for any fault in the correct direction from zero ohms up to the setting of the unit, so long as the current is greater than the vicinity of seven amperes. At two amperes the contacts will fail to remain closed under steady state conditions for faults within the first five per cent or the last five per cent of the relay's setting. That is, the ohmic circle maintains a constant center, but becomes smaller. This change occurs because the torques caused by the control spring and friction are no longer negligible with respect to the electrical torques in the unit.

The curve in Figure 10 is valid for an M_1 or an M_2 unit on its minimum distance setting. For other settings the accuracy is approximately the same for the same value of relay voltage.

Figure 10 represents accuracy under steady state conditions. With a rapid seal-in unit, the tripping area for fault conditions will be expanded by contact closure caused by transient torques. For faults at the relay bus, the memory action produces a strong torque in the correct direction for currents down to five amperes. For faults a short distance beyond the setting of the M_1 unit, its contacts may close because of a phenomenon known as transient overreach. For this reason the M_1 unit is set to cover 90 per cent of the line section under steady state conditions, allowing ten per cent for such errors. The minimum reach of the M_1 unit for faults near the end of its setting is as shown in Figure 10, but the maximum reach will be approximately ten per cent

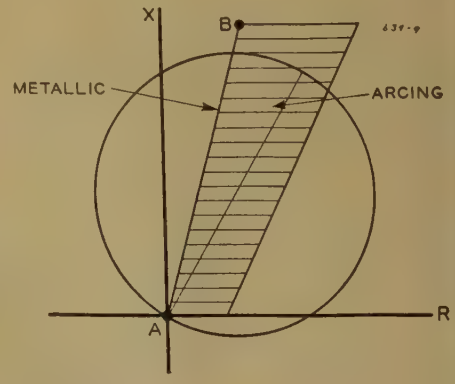
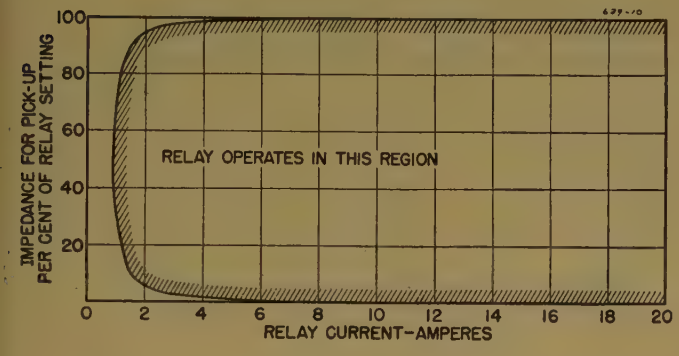


Figure 9. Effect of arcing fault

more. See "Transient Overreach" later in this paper.

The M_1 unit has correct directional discrimination for currents as low as 1.5 amperes at one volt and operates correctly for a period long enough to cause tripping when necessary for currents as low as five amperes on zero-voltage faults.

Figure 10. Steady state accuracy of M_1 and M_2 units



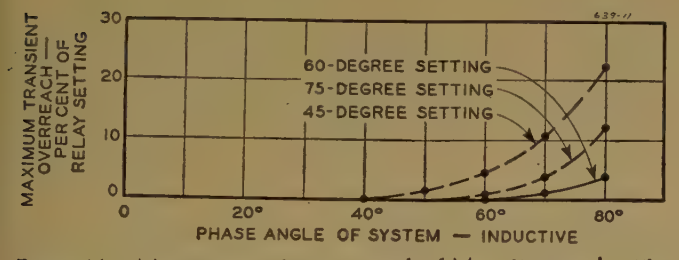


Figure 11. Maximum transient overreach of M_1 unit, normal setting is 60 degrees

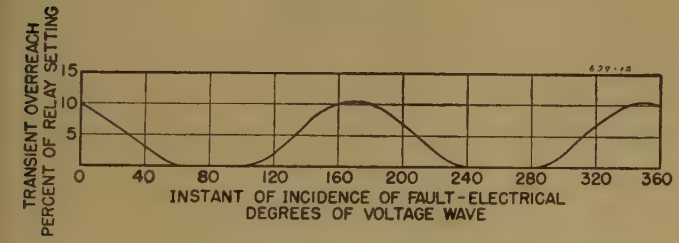


Figure 12. Variation of transient overreach in M_1 unit with instant of incidence of fault

The very small amount of transient overreach for this type of unit has been obtained at the sacrifice of some speed. Operating times of the M_1 unit are shown in Figure 13.

The M_2 unit is used with a short time delay in the timing relay to give the second zone of a distance relay setting, or it can be used as the directional relay to cause tripping in a carrier current relaying system. A large amount of transient overreach can be tolerated for either of these functions. Speed is important for the second function. Therefore the operating times have been made as short as possible (Figure 14), disregarding the transient overreach. The accuracy under steady conditions is the same as that of the M_1 unit, as well as the memory action at zero voltage.

If the OM_3 unit were used without using the transactor to obtain offset, it would operate exactly like an M_2 unit. In addition to the transactor, it has had a normally closed contact added.

The OM_3 unit is designed for use as a time-delay backup unit, for which accuracy is not important, and for use as a fault detector to start the carrier signal when carrier-current relaying is used. For this latter function, speed is very important. The normally closed contacts open in one-half of a cycle (60-cycle basis) for most fault conditions. In order to maintain them in their open position after the initial torque has disappeared for bus faults, it is necessary to use some offset.

Figure 15 shows typical operating times for the OM_3 unit. There are other conditions of distance setting and ohmic offset, but these same curves are approximately correct for the other conditions. Actual curves for the conditions not illustrated would show faster operating times.

The OM_3 unit's setting for the data shown in Figure 15 was three ohms with 1-ohm offset. This means that the ohmic circle has a diameter of three ohms, offset one ohm from the origin. Therefore the reach is two ohms in the unit's forward direction and one ohm in the offset direction.

The effect of the offsetting transactor is to introduce an operating torque proportional to the square of the current. In the offset direction, this I^2 torque has to overcome the torque caused by memory action, resulting in the increased operating times for faults in this direction. For this reason, it is necessary to use the reversed OM_3 connection whenever the OM_3 unit is used for starting a carrier-current signal.

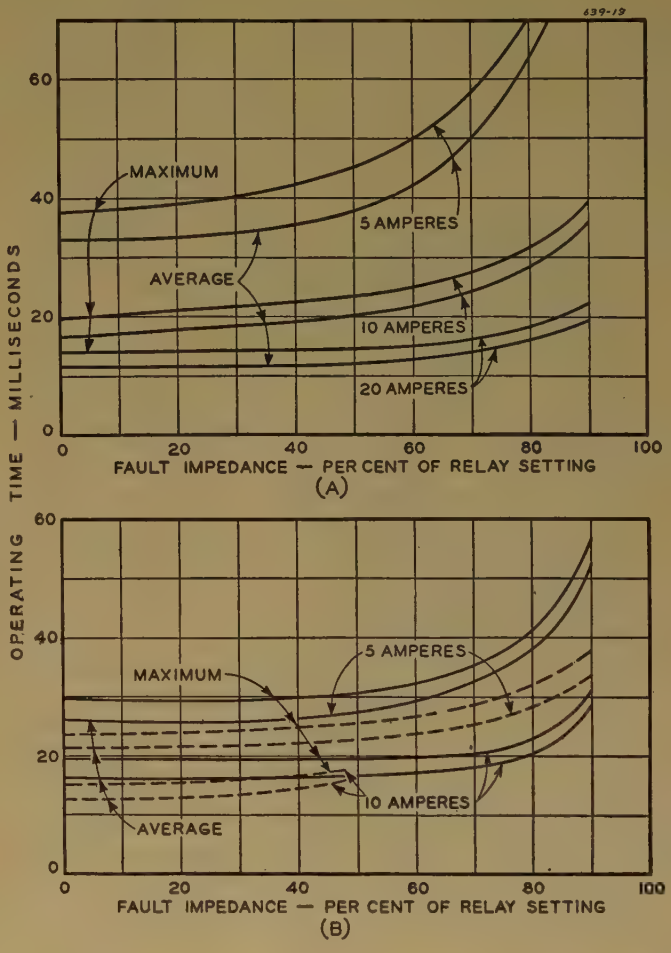


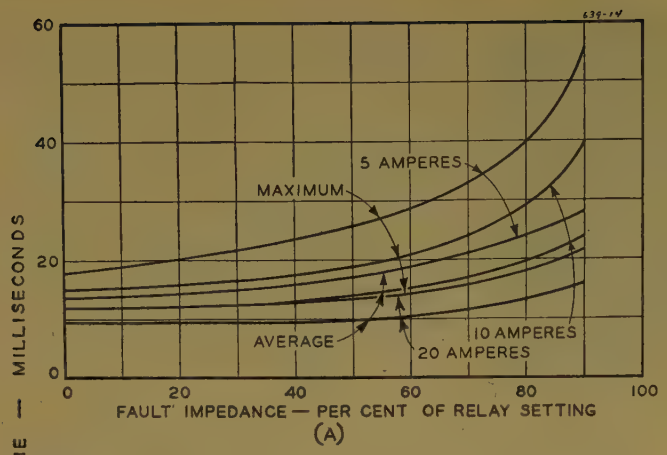
Figure 13

A. Operating times of M_1 unit with 3-ohm setting

B. Operating times of M_1 unit

Solid line—6-ohm setting

Broken line—12-ohm setting



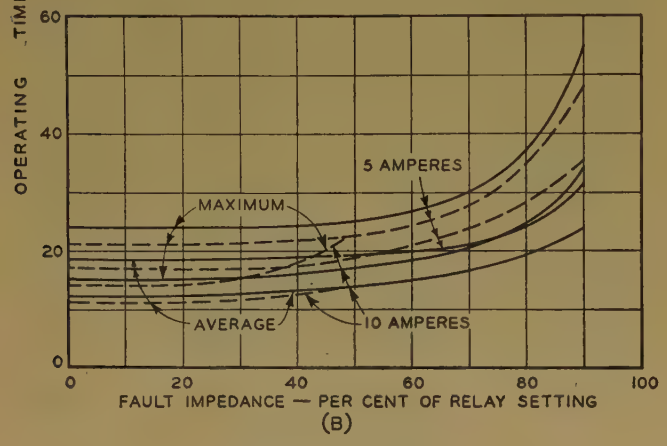
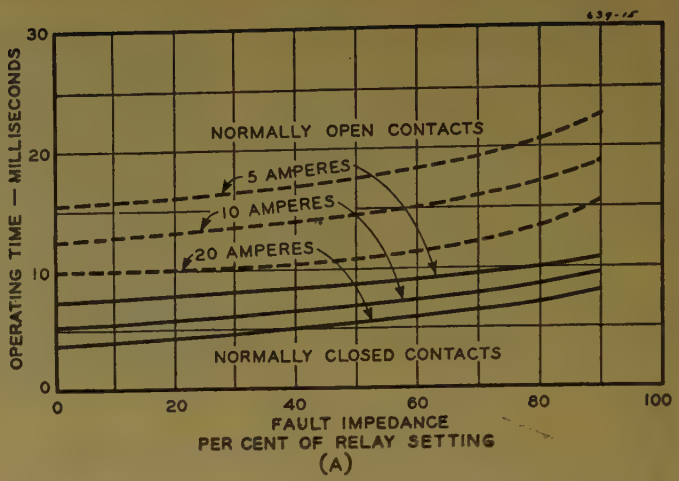
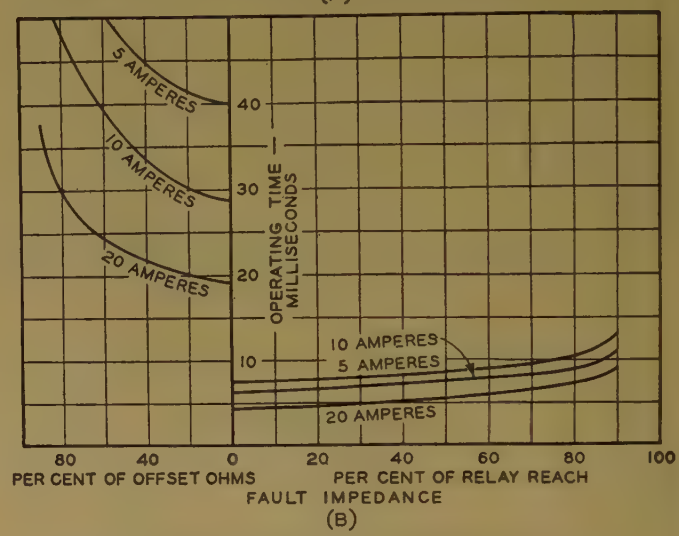


Figure 14 (above)

A. Operating times of M_2 unit with 3-ohm setting
B. Operating times of M_2 unit
Solid line—6-ohm setting
Broken line—12-ohm setting





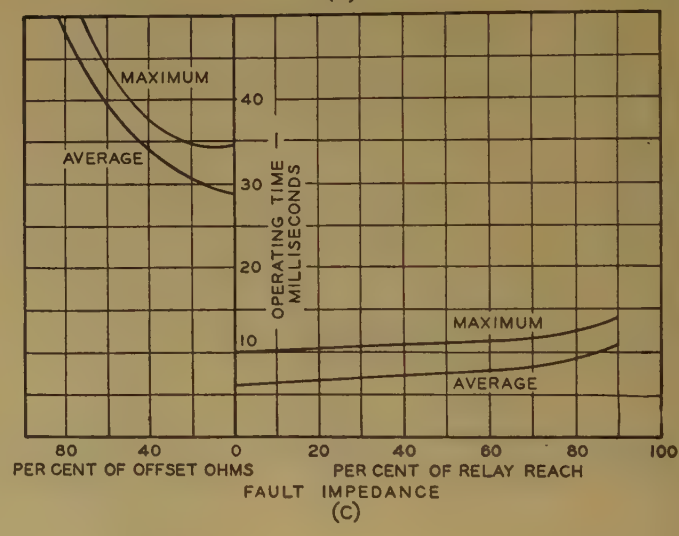


Figure 15 (right)

A. Average operating times of OM_3 unit with 3-ohm setting, zero offset
B. Average operating times of OM_3 unit with 3-ohm setting, 1-ohm offset
C. Operating times of OM_3 unit at ten amperes with 3-ohm setting, 1-ohm offset

Transient Overreach

The transient overreach of the M_1 unit mentioned under "Characteristics" is caused by transient conditions at the inception of a fault. These transient conditions may produce torque in the contact-opening direction, which will result in long operating times for faults within the setting of the unit. When the transient torque is in the contact-closing direction, the operating time is fast, and the contacts will close momentarily for faults a short distance beyond the setting of the relay.

The transients have been minimized in the potential circuits by the use of tuned circuits. The transients in the current circuit have been reduced for the 60-degree setting by the use of a capacitive flux shifting circuit. This reduction is illustrated by the small amount of overreach for the 60-degree setting in Figure 11.

Maximum transient overreach coincides with maximum d-c offset in the current wave. Thus in Figure 11, the higher the phase angle of the system, the greater the possible overreach. Figure 12 shows that for each half-cycle, faults initiated during the period which yields maximum d-c offset are most subject to overreaching.

This d-c offset can become quite large. For example, the equation for the short-circuit current of a fault occurring at the instant which produces the maximum d-c offset can be written

$$i = I(\epsilon^{-(R/\omega L)\omega t} - \cos \omega t)$$

where I is the peak value of steady state current and the shunt capacitance is

neglected. For a 60-cycle system whose ratio $R/\omega L$ produces an 80-degree phase angle, this fault must occur at an instant corresponding to ten degrees before the zero of the voltage wave, and the current becomes

$$i = I(\epsilon^{-66.5t} - \cos 377t)$$

The first current maximum occurs at 0.0081 second and has a magnitude of $1.58I$.

Good current transformers reproduce transients accurately during the first half cycle so that this maximum value is transmitted to the relay. Some types of distance relays have operating forces proportional to the square of the current, thereby multiplying the transient operating force by a factor of 2.5 without a compensating increase in the restraining force.

A d-c offset in the current wave of such magnitude can introduce additional errors when an impedance characteristic is offset into a mho characteristic by using the current to reduce the restraining force.

Ratings

The relay is rated for 115 volts and 5 amperes. In order to achieve the utmost reliability, the mho unit was designed to have the greatest possible torque. Not only was memory action employed, but the input to the relay is as high as thermal conditions will permit.

The maximum burdens for a practical setting of the mho distance relays at one terminal for 5 amperes and 115 volts are approximately 40 watts per phase at 95 per cent lagging power factor in the potential circuits, and 17 volt-amperes per phase at 60 per cent lagging power factor in the current circuits.

The basic ohmic setting of the three units, M_1, M_2, and OM_3, is 3 to 30 ohms phase to neutral at the relay terminals. Where shorter settings are required, auxiliary current transformers with a tap providing a three-to-one or a two-to-one ratio are used to obtain ranges of 1.0 to 10 or 1.5 to 15 ohms respectively. This enables the relays to be readily interchangeable and at the same time permits a high setting of restraining torque on all relays and the utilization of the maximum torque permitted by thermal limits. The connections to these auxiliary current transformers are shown in Figure 5.

The current sensitivity decreases in direct proportion to the ratio of the auxiliary current transformer. For this reason the relay is not applicable to short lines with small short-circuit currents. All characteristics have been presented for the relay without the auxiliary current transformers.

The ohmic offset of the OM_3 unit can be set for zero, one, two, three, or four ohms, phase to neutral. When the auxiliary current transformers are used, these values are reduced to 0, 0.33, 0.67, 1.0, or 1.33 for the 1.0- to 10-ohm range, or 0, 0.5, 1.0, 1.5, or 2 for the 1.5- to 15-ohm range.

Although the relay is designed principally for angular settings of 60 degrees for the M_1 unit and 75 degrees for the M_2 and OM_3 units, provisions have been made for setting the M_1 unit on 75 degrees or 45 degrees, and the M_2 and OM_3 units along with the transactor between 60 degrees and 75 degrees. Changes in the angular setting change the ohmic ranges of the units, with the minimum values as illustrated in Table I, the maximum remaining at ten times the minimum.

Application Limits

There are two limitations on the applicability of the mho distance relay. On systems where a fault near the end of the M_1 unit's setting can result in a small value of current, the unit will be slow, or possibly fail to operate and delay tripping until the time for the second zone. On very short lines, there is a possibility that the resistance added by arcing faults will place the impedance, measured by the relay for a fault which is actually in zone one, to be outside the zone-two setting of the relay. These limitations are discussed in a companion paper.[5]

In some cases, the M_1 unit can be set on 45 degrees to allow for the effect of arc resistance. If this is done on a system whose phase angle under fault conditions is greater than 70 degrees, the transient overreach of the M_1 unit requires that it be set to protect less than 90 per cent of the line section.

Setting of the GCY Relay

The angular setting of the M_1 unit is by means of leads on a connection block as illustrated in Figure 7A. If the angular settings of M_2 and OM_3 are to be changed, they must be changed by test.

The procedure for setting the diameters of the ohmic circles is the same as the one which has been in use for the well established type GCX reactance relay. The output tap settings of the two autotransformers shown in Figure 7 are chosen according to the following formula (the M_1 and M_2 units use the same transformer):

$$\text{Percentage output tap setting} = \frac{\text{unit's minimum ohms} \times 100}{\text{desired ohms}}.$$

The ohmic offset of the OM_3 unit can be adjusted by means of a lead on another connection block. The ohmic reach has to be increased by an amount equal to the ohmic offset to obtain the "desired ohms" in the formula.

Out-of-Step Blocking

As can be seen from Figure 4A, when the OM_3 unit is set to include the M_2 unit's setting, it will pick up on power swings before the M_2 unit. This characteristic can be utilized to recognize an out-of-step condition by the addition of a time delay relay such as *TB* in Figure 5. If the OM_3 unit operates at least four cycles, for example, before the M_2 unit, *TB* operates and can be used to open the tripping circuit. However, the mho unit's inherent characteristic of tripping at the electrical center of the system usually makes it advantageous to permit tripping and to use *TB* to prevent automatic reclosure after tripping caused by out-of-step conditions.

Table I. Change in Minimum Ohmic Setting at 115 Volts Versus Change in Angular Setting of Unit

Angular Setting	Minimum Ohmic Setting M_1	Minimum Ohmic Setting M_2 and OM_3
75°	2.23–2.44	2.94–3.06
70°		2.82–2.97
65°		2.64–2.87
60°	2.94–3.06	2.37–2.78
45°	2.10–2.20	

Conclusions

1. A high-speed directional distance relay has been designed using a unit of the induction cylinder type so that it has an inherent directional characteristic and distance measuring accuracy, permitting one contact to protect 90 per cent of a line section.

2. A modification permitting transient overreach provides speed acceptable for use as a directional relay in carrier-current application.

3. The use of a transactor provides a quasi-impedance unit suitbale for starting a carrier signal and providing time delay backup protection.

4. A combination of the three units with a timing relay provides 3-step distance protection.

Metal-Clad Unit-Type Switchgear for 33-Kv Service

C. H. KREGER
MEMBER AIEE

Synopsis: The experience of the Public Service Company of Northern Illinois with metal-clad switchgear has been outstanding, both from the standpoint of reliability of operation and safety to personnel, two of the principal objectives sought by the engineers of the company when they pioneered this type of equipment. This equipment has been applicable not only to the voltage classes up to and including 15,000 volts, but also in the 33,000-volt class, of which the company has seven major installations which have been in service from 13 to 16 years. This report of experience with 33-kv metal-clad switchgear is offered as proof that development and use should be resumed and continued in what is undoubtedly a fertile field for the application of principles which are now generally accepted. It is not a detailed discussion of the design and construction of metal-clad equipment, but rather a factual record of progress already made and proved by 13 years of operating experience. Conclusions drawn from this report are that the main objectives sought after in the development of metal-clad type of switchgear have been obtained satisfactorily. Experience has demonstrated clearly its outstanding operating reliability as compared with the conventional open type, and its perfect safety record for operating and maintenance personnel has been made possible by the inherent safety features which are practical only in metal-clad equipment. If these and other factors which cannot be evaluated precisely are taken into consideration and if the further exploitation in the post-war period of materials and methods developed during the war is kept in mind, it would appear that there is no question about the continued development of metal-clad type of switchgear in all voltage classes. Repetitive manufacturing, standardization, and prefabrication are some of the most potent means of combating the continually rising cost of electrical station and substation installations. The electrical equipment manufacturers are applying these principles to a growing extent and are promoting their use throughout the industry. The principles, of course, are not new, the present movement being directed mainly toward a more intensive and wide-spread application. Neither the manufacturer nor the utilities can afford to neglect any application of these principles that can be justified economically.

IN the initial use of metal-clad equipment, the engineers of the Public Service Company of Northern Illinois had certain definite objectives in view. Subsequent operating experience has shown that very substantial advances had been made toward these objectives before progress was interrupted about 1931 by economic conditions. This experience indicates that development and use of this equipment should be extended to higher voltages.

The outstanding characteristics of the installations of all voltages made by the Public Service Company of Northern Illinois were complete enclosure in metal, maximum practical factory assembly, and the filling of all space in the enclosing structure with an insulating medium other than air. Various terms were applied to such equipment, the one in most general use being "metal-clad gear." The equipment of this nature now being manufactured and used is enclosed in metal and factory assembled but, with possibly a few exceptions, is not filled with an insulating medium. It also is designated by various terms, including "metal-clad." Complete enclosure and maximum factory assembly are fundamental, but the filling or nonfilling of the housing can be considered a matter of design keeping in view the objectives.

Objectives

Broadly speaking, the objectives of advantages to be obtained from metal-clad construction are Safety, Reliability, and Economy. The first two can be obtained without the third; the third cannot be obtained without the first two.

Safety of personnel is fundamental and needs no explanation.

Reliability can be considered as the quality of being available at all times for the service for which it was designed and rendering that service continually.

Economy is more involved than the other two main objectives and includes both, because no installation can be truly economical if it is not safe and reliable. Safety and reliability in themselves, however, are of sufficient importance to warrant special consideration. They do have a very real and substantial monetary worth, but it is impractical to assign a definite dollar value to it. Economy, therefore, is considered herein as the actual dollar expenditure in rendering service from a given installation. To obtain fair comparisons, economy must include the following cost factors:

1. First cost (manufacturer's cost to user).
2. Engineering, supervision, and overhead (user's).
3. Installation and transportation.
4. Maintenance and repair.
5. Operation.
6. Durability (life expectancy).
7. Space occupancy and appearance.
8. Salvage value.

History and Progress

For the purpose of determining what progress has been made in the attainment of the objectives, we can consider the history of the 33-kv installations as a group in reference to each objective.

5. The unit which causes instantaneous tripping for faults in the first zone can provide correct tripping during out-of-step conditions on most systems without auxiliary blocking relays.

References

1. PROTECTIVE RELAYING FOR LONG TRANSMISSION LINES, **A. R. van C. Warrington.** AIEE TRANSACTIONS, volume 62, 1943, June section, pages 261–8.

2. PERFORMANCE REQUIREMENTS FOR RELAYS ON UNUSUALLY LONG TRANSMISSION LINES, **F. C. Poage, C. A. Streifus, D. M. MacGregor, E. E. George.** AIEE TRANSACTIONS, volume 62, 1943, June section, pages 275–83.

3. IMPEDANCES SEEN BY RELAYS DURING POWER SWINGS WITH AND WITHOUT FAULTS, **Edith Clarke.** AIEE TRANSACTIONS, volume 64, 1945, pages 372–84.

4. THE MHO-CARRIER RELAYING SCHEME, **R. E. Cordray, A. R. van C. Warrington.** AIEE TRANSACTIONS, volume 63, 1944, May section, pages 228–35.

5. APPLICATION OF THE OHM AND MHO PRINCIPLES TO PROTECTIVE RELAYS, **A. R. van C. Warrington.** AIEE TRANSACTIONS, volume 65, 1946, June section, pages 378–86.

6. AMERICAN STANDARD DEFINITIONS OF ELECTRICAL TERMS, C42-1941. American Standards Association, New York, N. Y., 1941. Section 05.05.401.

Paper 46-43, recommended by the AIEE committees on protective devices and power transmission and distribution for presentation at the AIEE winter convention, New York, N. Y., January 21–25, 1946. Manuscript submitted October 29, 1945; made available for printing December 19, 1945.

C. H. KREGER is engineer, electric station and substation design, for the Public Service Company of Northern Illinois, Chicago, Ill.



Figure 1. Typical 33-kv open-type structure
This shows installation used for cost comparison

Safety

There can be no doubt that working conditions are immeasurably safer on all of these installations than on conventional open-type installations. The safety factor is self-evident when it is considered that all current-carrying parts are enclosed in grounded metal and interlocks provided to prevent wrong operations and exposure of energized parts. Interlocking on metal-clad gear is entirely practical to an extent beyond possibility on open-type.

The prevention of inadvertent contact with energized parts can be accepted on the basis of the design. The proof, however, is negative because incidents occurring while working on metal-clad equipment, which would have caused an accident if the equipment had been open-type, are not recorded for the simple reason that there was no accident. An example of this is shown in the routine maintenance work of painting. Since 1928 there have been two accidents on 33-kv open-type structures, one resulting in a fatality and the other in an injury, definitely attributable to painting. These accidents could not have happened on metal-clad equipment. There is no record, of course, of painting in the wrong place on metal-clad because it can be painted while energized.

Since 1928, when the first 33-kv metal-clad gear was installed, to date there have been no accidents caused by inadvertent contact with energized equipment. This is also true of the lower voltage equipment, of which there are many installations on the system of the Public Service Company of Northern Illinois. Only one accident resulting in injury was recorded in this period. This accident was caused by burning oil from a ruptured box housing an oil-immersed disconnect switch. The switch blade fell into a ground clip because of the failure of an operating rod in one of the earliest installations. The failure definitely was caused by a defect in design which has been corrected.

During the same period, three fatalities and four injuries have occurred on open-type 33-kv equipment, all of which, except two of the injury cases, were caused by contact with energized conductors. One of the latter resulted from the failure of a bushing, and the other was the result of falling porcelain from an insulator which had failed mechanically.

Experience has shown that the metal-clad installations have a distinct advantage in reduction of nonelectrical accidents also, mainly by the elimination of the necessity of temporary staging and ladders or the climbing of complicated structures. When necessary, permanent ladders, platforms, and railings are provided easily.

Reliability

The same major characteristic which provides safety in metal-clad gear, that is, the enclosure of all current carrying parts, also gives it an inherent quality of reliability, since it excludes practically all foreign elements which interfere with normal operation, such as weather, animals, birds, deleterious gases, dirt, and solid objects. There is no need to cite the instances of outage or damage to open-type equipment from these causes; they are all too familiar. Two outstanding examples might be mentioned, however. One metal-clad installation is immediately adjacent to a railroad right-of-way, and, in addition to normal heavy traffic, locomotives stand for extended periods on a side track within 20 feet of the structure, which is sometimes obscured in smoke. It is doubtful if an open-type installation could be kept in service at this location. Just recently the Public Service Company of Northern Illinois was forced to remove an open-type 33-kv switching structure on account of many insulator flashovers caused by contamination of the air by an industrial plant one-fourth of a mile distant. It might be well to mention birds particularly, which are a source of trouble and expense in open steel structures. They build nests in enclosed structures also, but there they are merely an annoyance and not a hazard to service.

All of the 33-kv metal-clad installations made by the Public Service Company of Northern Illinois are still in operation and giving reliable service. There were, of course, operating difficulties at the start which are to be expected in any newly designed equipment, particularly in a radical departure such as 33-kv metal-clad was at that time.

Electrical Difficulties

The most serious of the problems arose in connection with the shell bushings which were mounted over openings in the bottom of the metal boxes or housing of the gear and served as the sockets for plugging in the oil circuit breaker. Thus, the inside surface of the shell itself was exposed to air while the outside was exposed to the oil in the box or compartment. The first 33-kv gear was installed in April 1928, and the first failure of a shell bushing occurred in March 1929 with others following. The fact that the failures usually occurred during a rising



Figure 2. Metal-clad installation used for cost comparison

atmospheric temperature or high humidity indicated that condensation on the surface of the shell bushings in the circular space between the shell and the breaker bushing was a contributing factor. This condensation was pronounced because the temperature of the mass of the gear lagged behind the rising ambient temperature. In some of the installations, the lower end of the shell bushing orifice was not closed entirely when the breaker was in place. In the other installations, the orifice was closed by a soft gasket on the base of the breaker bushing when the breaker was raised to operating position. As the shells which were open at the bottom gave by far the most trouble, it was supposed at first that dirt on the surface combined with the moisture from condensation was the cause of flashover, and a cleaning program was instituted.

It soon was noted that severe corona discharges were taking place within shells previous to failure, even to the extent of being audible and visible. It also was noted that these discharges started very soon after cleaning in some cases, particularly during a rapid rise in atmospheric temperature.

Investigation and tests were continued and led to certain conclusions. The bushings, although open to the air (breathing occurred through the gaskets even in those closed at the bottom), were not exposed to the cleaning action of the elements as were ordinary outdoor bushings. This condition was conducive to corona and surface leakage from the energized metal parts at the top and the formation of nitric acid when condensation supplied the water. Conducting paths thus were established, and the process was cumulative until breakdown occurred over the surface of the porcelain. A contributing factor was metal salts from the corrosion of caps and contacts at the top of the shell. As the deposits on the porcelain did not yield readily to ordinary cleaning, special methods involving the use of carbon tetrachloride, alcohol, and certain dilute acids were tried.

Actual failure from this cause occurred at the original installation only, although corona discharge was observed at other locations. The cleaning program prevented the discharges from extending to the point of failure.

The bushing assemblies in the various makes of switchgear differed considerably in detail, and these were studied further in an attempt to eliminate or at least reduce the cleaning required.

As mentioned before, it was assumed at first that the closing of the shells at the bottom would eliminate or at least materially reduce the trouble, and this was the first step taken. The manufacturer was reluctant but later agreed, and that change was completed on the first installation about September 1930.

The closing of the bottom of the shells, of course, was a question of exclusion of deposits from the atmosphere, and leaving them open was to allow circulation of air to reduce condensation. Neither result was accomplished, however. It was impractical to seal the opening tight enough to prevent breathing; and, although actual dirt might be excluded, air usually contains certain acids such as sulphur dioxide, particularly in cities or industrial centers. The circulation of air in the bushings left open was practically nil, as the only opening was at the bottom, and this was very restricted. Some shells are still open, others closed.

This all indicated that the opening or closing of the shell opening was not the answer to the problem. Accelerated time tests in the laboratory indicated all shells were subject to the formation of nitric acid and metallic salts from the slight corrosion of the metal parts at the top. To prevent the corrosion, lead gaskets were eliminated and plating of copper parts experimented with. Chrome plating was tried but was not entirely satisfactory, owing to the difficulty of getting a perfect homogeneous coating on the odd-shaped parts. Tinning all but contact surfaces, which were silvered, finally was adopted for the installations giving the most trouble. There still remained some defective porcelain in one installation and the short leakage distance and inability to clean entirely at

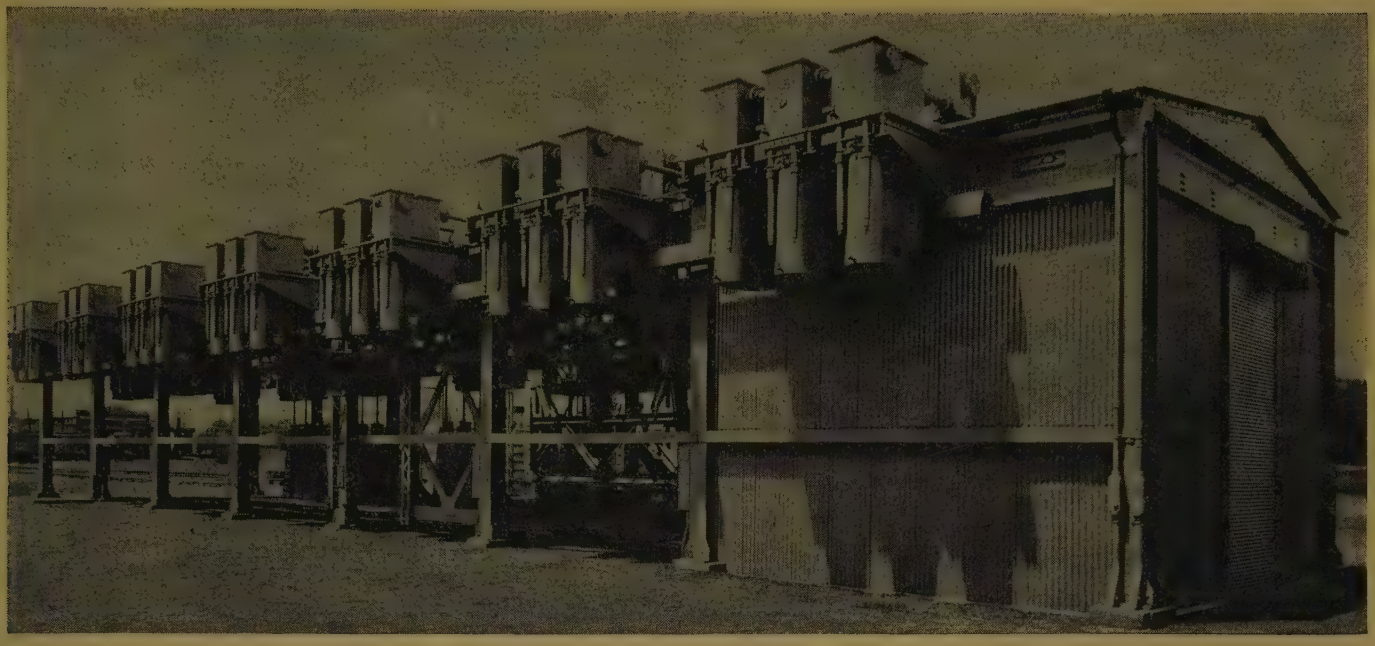


Figure 3. First installation of 33-kv metal-clad switchgear, showing overhanging removable potential transformers

another. These shells all were replaced finally with smooth instead of corrugated porcelain and redesigned contacts and corona shields.

While the changes stated have not eliminated the problem, they have provided shells with better characteristics and have lengthened the interval between cleanings. At present all 33-kv shells are cleaned each fall and spring with a weak solution of muriatic acid followed by thorough washing with a cleaning compound. This program has been followed for the past ten years with no further trouble.

Other than the shell bushings, only one electrical weakness affecting reliability developed. This also was in the first installation and resulted in two cases of bus failure to ground. The bus in all the installations is copper tubing insulated with machine-wound impregnated paper or fabric and supported at intervals centrally in an outer copper pipe by spools of insulating material. The space in the outer pipe around the conductor is filled with oil. The spools at first were turned from a laminous material of pressed paper; later spools were of porcelain or paper wound directly on the conductor insulation. The first theory was that minute drops of water from condensation had collected at the bottom of the bus pipe under the spool, concentrating the electrical stresses and forming creepage paths that resulted in final failure. The manufacturer recommended circulating the oil and heating at intervals to remove moisture, and this was done for a short period. The process was rather expensive and critical, however, as it was necessary to maintain the oil temperature within rather close limits, that is, high enough to remove moisture but not high enough to cause sludging. After the second failure, notice was taken of the fact that although the spools were in halves held around the conductor by cord, the failure was not at the junction of the halves but directly through the spool and parallel to the laminations where they were radial. As previously stated, these spools were turned from a laminated material. This indicated that creepage started between the laminations, and the spools were replaced with a non-laminated material. There have been no failures since, and circulation of oil was discontinued.

It should be noted that neither of these failures caused any damage beyond a small hole in the insulation and outer copper tube and loss of oil in one bus section. There was no fire in either case. The failure was direct to ground. The bus was protected by bus fault relays.

The only actual failure since the early ones mentioned occurred in 1939, and the indications were that it originated with the oil circuit-breaker bushing. In this respect the failure was similar to those occurring in open-type gear. As the breaker was mounted in metal-clad gear, however, the effects must be noted. The failure was in the annular space between the oil circuit-breaker bushing and the shell on the bus side of a line position. Both shell and bushing were fused and burned, severely, typical of an external flashover. The shell was cracked severely but remained in place. The cracking, however, permitted oil to flow into the annular air space between bushing and shell, where it was ignited by the arc and blown out of the shell orifice at the bottom across the top of the breaker, forming an external oil fire which continued after the arc was extinguished. Since the oil burned as it flowed down the wall of the inspection bay before it was extinguished by the gravel bed at the ground level, the fire was more spectacular than damaging. The loss was limited to the breaker bushing, the porcelain shell, the escaped oil, and scorched paint. There was no internal damage to the gear or breaker.

The weather was clear, warm, and dry, which eliminated excessive condensation as a contributing factor as in the earlier troubles.

It was difficult to determine definitely whether the failure originated across the shell or the bushing. There was some evidence of a very slight oil leak at the top of the shell through a defective gasket which formed an oil film on the surface of the shell to which air-borne particles might have adhered and gradually decreased the creepage distance to ground. On the other hand, the particular type of bushing used had been the source of trouble in open-type equipment. The pertinent question for this discussion, however, is whether the failure was the result of or indicated any inherent weakness in the basic hypothesis of the type of installation. Neither the faulty gasket nor the faulty bushing would indicate this. They were both representative of the occasional freaks encountered at

times in any type of construction. Preventive measures against recurrence are the same in this case as for conventional open-type equipment, that is, greater care in fabrication, inspection, and testing and faster relaying to limit fault duration.

It also should be noted that only features peculiar to the type of installation are considered here. For example, there were certain troubles with oil circuit breakers, but these were of the type common to both metal-clad and open-type construction.

Mechanical Difficulties

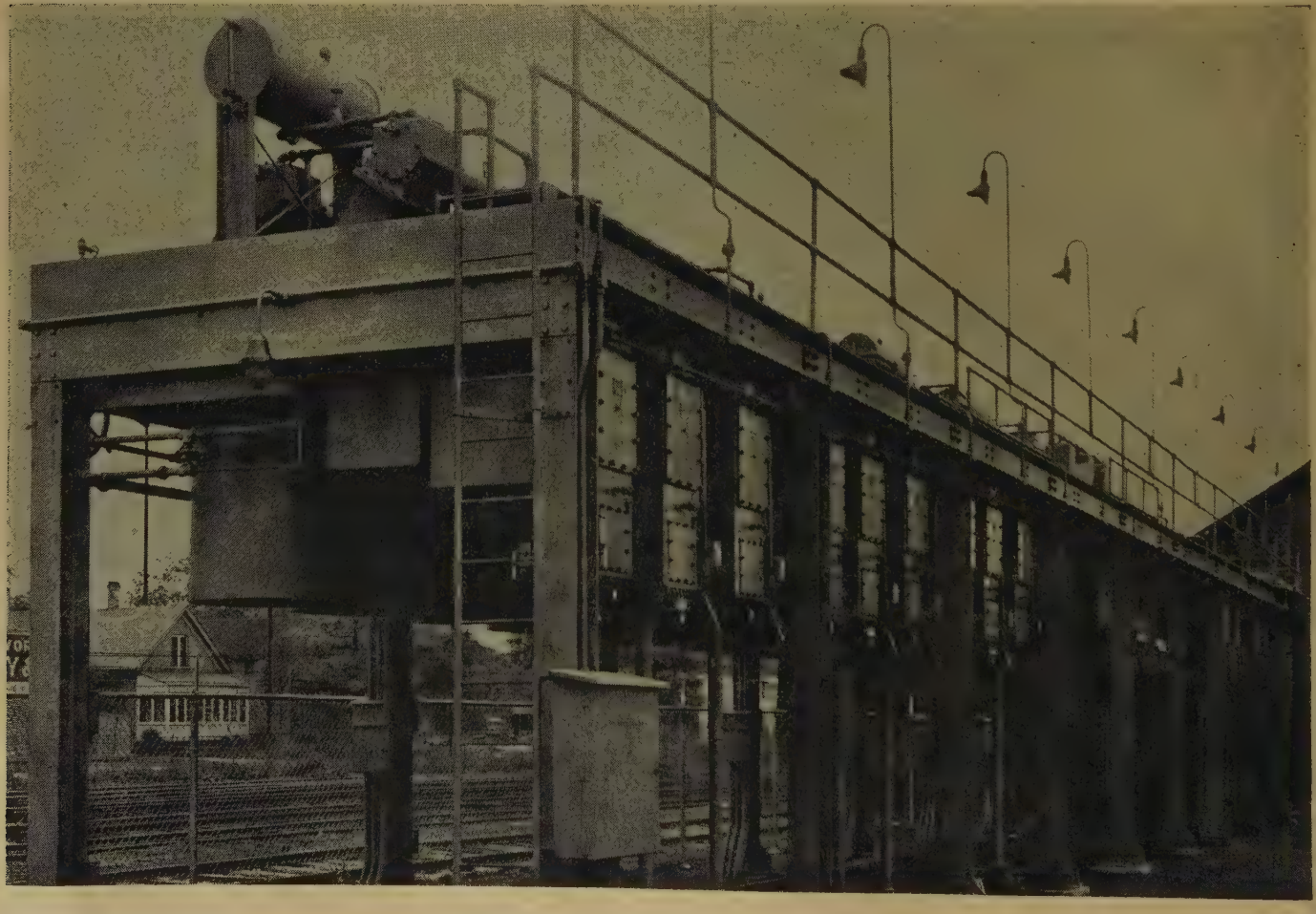
Early experience with the first installations naturally disclosed certain mechanical features which were undesirable or troublesome. None of these was an insurmountable difficulty, nor did the remedy force any basic changes in design.

Soon after the first installation was made, some shell bushings developed circumferential cracks at or close to the upper edge of the bottom metal mounting ring which was cemented to the outside of the porcelain. This had no bearing on the electrical failures and was purely a mechanical problem. The metal mounting flange and cement, of course, were on the outside (oil side) of the shell, so the ring gasket was placed under the lower edge of the porcelain. As the bolt circle was outside of this gasket, a cantilever strain was imposed on the porcelain which was enhanced by slight inequality in tightening the bolts. A very slight shock or misalignment at the top of the shell then could easily cause the crack. The condition was remedied in the new shells by making the relation between the lower edge of the porcelain and the mounting surface such that there was metal-to-metal contact between the mounting flange and the mounting surface. This equalized and limited the strain on the porcelain. This condition existed at certain installations only, as the shells in the other installations were mounted with the flange below the mounting plate.

The only mechanical failure that was at all serious in its results was the breakage of the operating rod on an oil-immersed disconnect switch mentioned previously. As stated, this was remedied by proper design.

Some difficulty was encountered at first in preventing leakage of oil. The various boxes and enclosures in the first installation were of welded steel plate with flat covers and flat cork gaskets. It was soon evident that these gaskets, if not confined, would spread and set, permitting seepage of oil. Further tightening of bolts was only a temporary cure and soon reached its limit. After trials of other gaskets, it was found that a cork gasket confined in a groove and compressed by a tongue gave satisfactory results, and gaskets in later gear were so designed. To change the original flat gaskets to the confined type, however, was impractical and further trials were made ending in the use of a cork or other soft gasket with a thin soft metal sheath. The original gear was equipped with this type several years ago, and oil leaks and seepage have ceased. There was also some oil seepage through welds on boxes and directly through the metal of cast boxes used on the later installations. Tinning of the inside of welds and the inner surface of cast boxes prevented this seepage. Improved welding and the use of different material for cast boxes made tinning unnecessary. This matter of oil leaks and seepage is largely a question of appearance, as in no case was it sufficient to reduce the amount of oil in the gear to any appreciable extent over a very considerable period.

Figure 4. Installation of 33-kv metal-clad switchgear with main and transfer bus



The availability factor of reliability is influenced materially by ordinary routine maintenance requirements. In open-type installations, it is necessary to take out of service major portions or even an entire structure for such work as cleaning or replacement of insulators, painting, and lubrication of moving parts. Frequently busses or lines not being worked on must be de-energized to provide proper safe working clearances. This class of maintenance, with the exception of the semiannual washing of shell bushings mentioned previously, requires no outage of metal-clad equipment. Even an outage for cleaning is reduced to only the particular line or bay directly concerned.

Economy

First Cost. First cost, of course, is a manufacturing problem involving design, fabrication, and assembly. This factory assembly is of major importance. It increases first cost of metal-clad above equipment for a comparative open-type installation but reduces field installation costs, and we are considering over-all economy, as mentioned before. The seven installations made by the Public Service Company of Northern Illinois covered a period of only about three years and were fabricated by three different manufacturers. Naturally, first cost was somewhat high because of development charges and because effort was concentrated on design for safety and reliability rather than cost of manufacture. There was considerable variation also in price among different manufacturers and among different installations by the same manufacturer because there was no background of experience on which to base manufacturing costs.

Each of the installations made was an individual development and did not approach even the first phase of being on a production basis. Two manufacturers built two installations each and one manufacturer built three, and naturally any part or feature developed for the first was used wherever possible in the second. This possibility was exceedingly limited, however, owing to changes in detail design. There were only two major changes in design made during the period which might affect first cost. One was the manner of connecting and mounting potential transformers, and the other was the use of cast boxes or compartments in place of welded plate. In the original installation, connection boxes overhung the structure and were provided with shell bushings permitting the potential transformers to be raised into place or lowered the same as the oil circuit breakers by means of a special traveling elevator on the structure. In all subsequent installations, the potential transformers were connected solidly and mounted in boxes as an integral part of the gear with an arrangement for replacing fuses. This eliminated many shells and bushings as well as an elevator. The use of cast boxes not only affected the cost of the boxes themselves but provided round cover flanges and covers into which it was cheaper to machine grooves for confined gaskets.

A major factor in the cost of any installation is the bus and switching arrangement. Two common variations are complete double bus with two oil circuit breakers per circuit and main and transfer bus with one circuit breaker per circuit. In the latter a breaker is usually provided for energizing the transfer bus from the main bus with section breakers or disconnect switches in the main bus on each side of this feed to permit taking part of the bus out of service for maintenance or keeping part in service in case of bus failure.

The first installation was a double bus arrangement, however; only one circuit breaker was provided for each of two transformer circuits. This possibility of reducing cost and still retaining the advantage of a double bus because the breakers were movable from one bus position to another, a condition which does not exist in conventional open-type construction.

The installation which followed was a main and transfer bus arrangement. There were two reasons for this: first, the available space was limited in width, and only one breaker per bay resulted in a narrower structure; second, it provided a practical trial of that particular bus and switching arrangement as applied to that type of equipment. This required the development and use of enclosed oil-immersed disconnect switches, which present certain problems. While this arrangement reduced the cost per bay, the total cost was not reduced materially because of the provision of two bus section breakers and the transfer bus feed breaker. As equivalent operating facilities at little additional cost could be provided by a double bus arrangement with only one breaker per circuit in some cases, all subsequent installations were built according to this arrangement. The moving of a breaker of any line or transformer position by means of the motor-driven elevator from one bus to the other is comparable to the operating of disconnect switches for connecting a line or



Figure 5. One of the later installations in a residential district

Ornamental brick wall enclosing property is shown

transformer to a transfer bus in open-type structures.

Engineering. The engineering ordinarily considered as preliminary, such as determination of necessity, number, capacity, and location of lines, feeders, and equipment, can be considered as equal in cost for both types of equipment if we forget for the moment an advantage of metal-clad equipment in the matter of location. What might be termed construction engineering follows. For an open-type installation, this consists of considering, specifying, counting, ordering, listing, and delivering to the job various pieces of major equipment and innumerable items for connecting and mounting. Construction specifications and many drawings must be prepared for the assembly of all these parts into a satisfactory structure. For metal-clad equipment the user need specify but one piece of equipment, and very few drawings are needed for installation, thus reducing his engineering costs materially.

It is true that much of the user's engineering cost is transferred to the manufacturer and must be included in first cost because the manufacturer must design and assemble the various parts of the unit. These costs should be considerably less, however, when this work is done by the manufacturer because he is designing and assembling many units, while the user must design each unit for himself. Factory assembly is inherently cheaper than field assembly for several reasons, freedom from weather interference being one.

This, of course, assumes a certain degree of standardization, and metal-clad equipment lends itself to this standardization to a far greater extent than open-type. Standardization in conventional design more usually is limited to component parts.

Installation. Field installation is where metal-clad equipment must show the greatest reduction in cost as compared with open-type. Again consider the innumerable small pieces of an open-type structure which must be assembled piecemeal contrasted with the very few large parts of metal-clad. Here again design plays a major role.

When the first installation was purchased, the goal of unit assembly was in the minds of those concerned. Experience had been had with lower voltage gear, and design changes had brought this to the point where even complete bus sections were shipped and installed as a unit. At that time, to assemble even one bay of a 33-kv structure into a single unit which would be within railroad clearances appeared impossible, at least to the manufacturer, and the first gear was shipped in many parts which were assembled on the job. The installation cost was the highest of any of the installations. As a result of much consultation with manufacturers, a design was worked out which enabled the next installation, which was a main and transfer bus arrangement, to be assembled at the factory and shipped in units of one bay as were all subsequent installations. The component parts as shipped from the factory were the main bay assembly (containing busses, instrument transformers, cable terminals for outgoing circuits, and all connections), the supporting columns on which the bay assembly was mounted, the circuit breakers, and the traveling elevator for raising and lowering breakers.

The next installation having a double bus was shipped assembled, and the complete cost of installation per bay was slightly under 25 per cent of the cost of the first installation.

Transportation of large pieces in carload lots from one point of shipment is more economical than many pieces from many different points for equal distances and total weight. Note also must be taken of the increased cost of following and co-ordinating the receipt of numerous items of equipment required for an open-type structure as compared with factory-assembled units.

An element of cost exists in many installations which does not appear in the cost records. This is elapsed time as distinct from man-hours. There frequently is a very definite saving in meeting a service date or a definite loss in not doing so which is distinct from the actual dollar cost of the installation. Metal-clad equipment has a definite advantage here which will be enhanced by more extensive use and standardization.

As an indication of what was done and what experience was obtained, some of the design features which made unit assembly possible should be mentioned. The unit-type principle must be in mind at all times in design. Considerable study was required so to design the various boxes and compartments comprising the main section as to permit an arrangement compact and rigid enough to make shipment by rail practical. These assemblies or units were shipped complete and filled with oil. The breakers were shipped separately, as they would be removed from their operating position in any case for test and inspection before being placed in service.

The busses presented another problem, as they, of course, extended the length of the structure to form a continuous conductor across all bays. In the first installation, the busses were received entirely separate from any other part and not even complete in themselves. The insulated tubing was in lengths which did not coincide with the width of bay. For subsequent installation, a satisfactory joint was developed for both bus conductor and enclosing tube that could be used at the junction of any bay, a development which permitted all complete busses to be mounted on each bay in the factory ready for connection to busses of an adjacent bay. These joints and other parts were so designed that all mechanical erection could be completed before any electrical work was necessary. Even control and secondary wiring was in place and brought to terminals for connection to the wiring from the control board.

Maintenance and Repair. Maintenance and repair were discussed under the preceding subjects of safety and reliability, and the same factors in metal-clad equipment which increase safety and reliability over that of open-type decrease the direct cost of maintenance and repair. Practically all ordinary routine maintenance such as painting, cleaning, and lubricating, can be performed on metal-clad without removing any part from service. This is seldom true on open-type, and for this reason much of this work is done at night or on Sundays or holidays when lighter load conditions are such that equipment can be taken out of service. This involves overtime which greatly increases the cost.

Repairs are necessary as a result of failure, deterioration, or wear. It is obvious that cost of repair decreases in proportion to increase of reliability.

Operation. If the presence of operators is required at a given substation, these costs will be equal for both types of installations. Metal-clad equipment, however, is more adaptable to control from remote points because of the absence of open disconnect switches and complete protection from interference by the elements.

Durability. The life expectancy of metal-clad equipment is much greater than open-type. The only part exposed to the weather is the enclosing metal structure. Organic insulation, if used on conductors, is not even exposed to the air. All of the 33-kv gear installed by the Public Service Company of Northern Illinois is oil-filled and equipped with

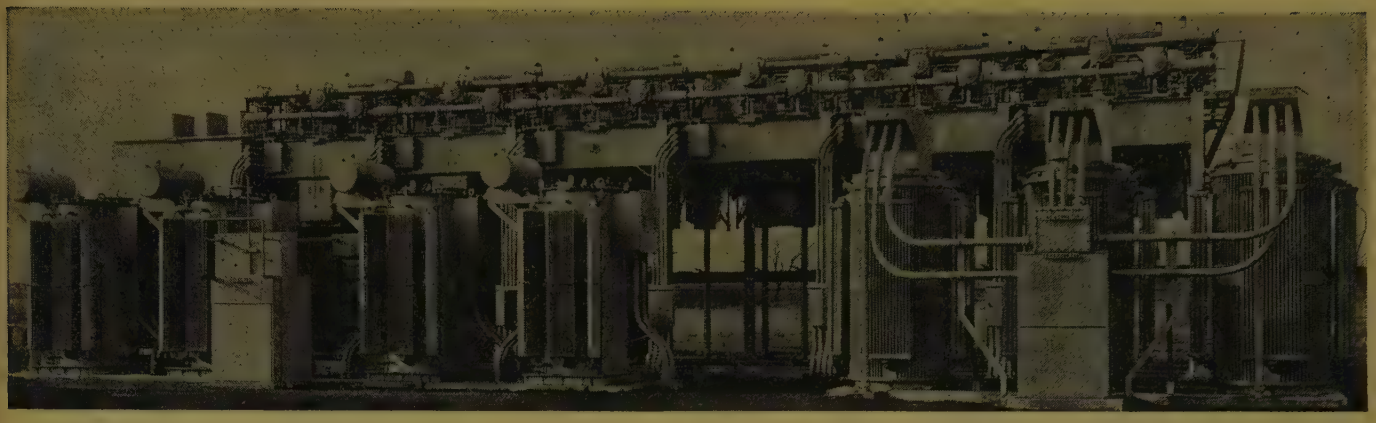


Figure 6. One of the later installations, showing method of enclosing transformer connections

conservator tanks similar to those commonly used on transformers. Experience has shown that oil deterioration is not a problem, as practically all of the original oil is still in service in the gear. There has been no filtering or treatment of any of this oil except that following the failure of the bus insulators mentioned previously, and as stated, that was unnecessary. This of course refers only to the oil used primarily as an insulating and filling medium in the various bus tubes and connection compartments. This oil is far less subject to factors causing deterioration than oil as ordinarily used in transformers or circuit breakers.

After from 13 to 16 years of service, all seven installations can be considered practically in the same condition as when new.

Space Occupancy and Appearance. Here again metal-clad has a very definite advantage, and if space is at a premium, the savings could be considerable. One of the installations, for example, could not have been made at its present location as an open-type structure. It was an old substation site very close to the center of town, bounded on one side by a steam railway and on the other by an electric railway. An open-type 33-kv structure would have required a new location at some distance, involving large costs for new property and building and also new transmission and distribution facilities.

At one location two metal-clad bays were added as an extension to an existing open-type structure and afford a striking comparison. The bays in the open structure occupy 729 square feet each, while the bays in the metal-clad structure occupy 605 square feet each, a saving of about 17 per cent. The height of the open structure is exactly 27 feet; that of the metal-clad is exactly 22 feet. This is not the entire story, however, as there are open disconnects and wiring on the outside of the open structure which require proper clearance and operating space. At one of the installations, there are six double bus bays and an inspection bay, and the structure from the center line to the center line of columns is exactly 90 feet long by 20 feet 8 inches wide. An enclosing fence placed three feet from the center line of columns would give ample space for all operation and inspection. (It could be on the columns if necessary.) Using the 3-foot space, however, gives an enclosed area of exactly 96 feet by 26 feet 8 inches, or 2,560 square feet. An open structure for controlling the same number of circuits would be exactly 108 feet long by exactly 36 feet wide based on the bay size of existing structures, and an enclosing fence should be at least ten feet from the center line of columns (usually it is more). This gives an enclosed area of 7,168 square feet, 2.8 times that required for metal-clad including the inspection bay.

Appearance has a definite economic value in public relations and also an indirect value similar to the space factor by permitting installations at locations where an open structure would be objected to by adjacent property owners. A metal-clad structure does not have the raw and unfinished appearance of an open structure, and if necessary can be camouflaged much more easily by architectural features or landscaping.

Salvage Value. Substation and equipment replacements in a great majority of cases are required by inadequate capacity because of load and system growth or changes. Retirement charges are high unless equipment for which the duty has become too great can be reused where the demand is smaller. This involves removal and reinstallation, and with an open-type structure, the same factors which cause high labor costs in installation also cause high cost of removal. An open-type structure must be dismantled completely to be relocated; and while the major items of equipment can be moved without loss, there is usually considerable retirement in connection with such items as structure, conductors, supports, control conduit, and wiring. A unit-type installation is moved in complete units as at first installed, with no retirement of material or equipment as far as the structure itself is concerned. The retirement of connecting cables and foundations would obtain in either case.

Comparison of Costs. A detailed study of the actual installed costs of one of the metal-clad installations and a comparable contemporary open-type structure gives the following percentage costs for the metal-clad, the cost of each item of conventional open-type being considered as 100 per cent:

Material cost per bay	145.4%
Labor cost per bay (including engineering)	62.6%
Foundations per bay	60.6%
Total installed cost	131.5%

This comparison is made on the actual dollar expenditure only and includes only the first three factors of over-all economy heretofore mentioned. Any reasonable evaluation of the remaining factors should more than offset the additional dollar cost of the metal-clad installation. In addition it must receive a very substantial credit for the high degree of safety and reliability in order to arrive at true over-all economy.

Future Development

In the foregoing discussion, the difficulties and faults of the present 33-kv metal-clad installations are covered in some detail in order to show that these difficulties and faults were overcome and eliminated. There is some accent on the

original installation because it was the first developed and furnished the experience for improvements in those which followed. The possibilities for further improvement, however, are by no means exhausted, particularly in the field of economy.

In future design the possibility of eliminating all shell bushings should be considered. All present installations are arranged with what might be termed removable or plug-in circuit breakers with a rather expensive motor-operated carriage elevator for raising, lowering, and moving them to an enclosed bay at the end of the structure. It is questionable if this is necessary. If the breakers are underhung as an integral part of the structure with a device for lowering tanks only, practically all maintenance and repairs could be accomplished. The gear structure would afford far more protection from the weather than is obtained for breakers in open structures unless temporary enclosures are built. If necessary, it would be a relatively small matter to provide a temporary enclosure on the sides of a metal-clad structure. If desired, this enclosure might be made permanent and enclose the entire lower part of the structure. This also will eliminate the inspection bay and reduce materially the cost of the transfer carriage.

If the breakers are in a fixed position, it will be necessary to provide means for entirely disconnecting them while they are being worked on. The first thought for this is an oil-immersed or enclosed disconnect switch, which is not difficult in itself but which presents certain problems in safety and operation. Being enclosed, the actual opening in the circuit cannot be observed and checked, and reliance must be placed on the operating mechanism or some other indicator. Indicators can be devised which are independent of the operating mechanism and in case of failure or breakage will not give a safety signal. Glass windows have been tried to provide direct view of the disconnecting device but are not always practical, particularly when looking into an oil-filled compartment. There may be a possibility in some of the new plastics in this connection. Even though the break will be visible, there is still the question of possible breakdown across the gap in a disconnect of this sort. A metal (grounded) barrier across the gap may be a solution.

The use of standard forms of cable for busses and connections should be considered as a possible means of reducing the cost and the amount of oil if oil is used.

The means for replacement of potential-transformer fuses can be studied to good advantage, as they are rather complicated and expensive. The reliability of present-day potential transformers suggests that primary fuses might be omitted, a factor which would be a major simplification.

The question of the necessity of an external terminal for testing, phase flashing, and so forth, should be considered. Such a terminal was provided on one of the installations, but in order to maintain the highest degree of safety, rather complicated interlocking on the various disconnect and grounding switches was involved. It must be remembered that as soon as exposed terminals which can be energized are introduced, the high degree of safety provided by entirely-enclosed metal-clad gear is lowered.

Recent development in the production of light metals opens up possibilities of reduction of weight and lowering of handling and installation costs.

Experience with gaskets enclosed in soft metal indicates that recessed gaskets may be eliminated.

Conclusions

From this discussion and the experience which it records, certain definite conclusions may be drawn:

1. Totally enclosed metal-clad construction provides the maximum degree of safety for personnel in the operation of electrical equipment.

2. The reliability of totally enclosed metal-clad equipment is far greater than conventional open-type.

3. While over-all economy of totally enclosed metal-clad equipment has been obtained, there are many possibilities for further advancement toward this objective.

4. Thirteen years of operating experience with seven different installations confirms the above conclusions.

5. A great advancement toward the objectives of safety and reliability in electrical equipment having been made, the research, engineering, and labor expended in making that advancement should be further exploited by continuing the development and use of totally enclosed equipment for voltages of 33 kv and above.

6. The present use of factory-assembled enclosed units indicates that the manufacturers have accepted the principles involved. The lack of development for higher voltages apparently is caused by the high first cost.

7. Metal-clad unit-type factory-assembled equipment for 33 kv is highly adaptable to standardized quantity production, and proper development will reduce first cost as well as over-all cost.

8. This development offers a definite possibility of combating the steadily rising cost of conventional construction.

9. The above possibility warrants earnest co-operation between manufacturer and user.

Induction Heating of Long Cylindrical Charges

HERBERT F. STORM
ASSOCIATE AIEE

Synopsis: With the remarkable expansion of induction heating applications during recent years, a growing number of persons is being involved in the design and operation of induction heating equipment. While the general principle of induction heating is obvious to most, the concepts of certain important peculiarities such as skin effect, including its bearing on the intensity of heat generation, are not as widely understood. One reason for this state lies in the classic approach by partial differential equations[1,2] involving operations with which many engineers interested in induction heating are not familiar. A previous paper by the author offered a new approach for the analysis of the induction heating effect by using concepts commonly applied to a-c engineering and not involving differential equations.[3] A limitation of that paper consisted in the assumption that the radius of the charge will be very large in comparison with the so-called depth of penetration. It is the object of this paper to cast off this limitation and hence provide an analysis which is valid for any size of the radius of the charge and the depth of penetration. The generated heat is expressed in terms of rapidly converging series. The analysis is applied finally to the case where the charge is subdivided into a number of cylindrical rods. It is shown that for one certain radius of the individual rods, the inductor efficiency reaches a maximum. While in the case of a single (not subdivided) charge, the inductor efficiency cannot increase over a certain limit depending on the material of the charge, the subdivision of the charge removes such limitation, and inductor efficiencies can approach asymptotically 100 per cent for any material.

THE BODY to be heated is called the charge and is exposed to an alternating magnetic flux produced by an inductor, for instance a solenoid, which is energized from an a-c generator of suitable frequency (Figure 1). The alternating magnetic flux induces voltages within the charge. As a result, currents, the so-called eddy currents, flow through the charge and produce I^2R heat. Because the heating effect is originated by voltages generated by induction, it is called heating by induction, or induction heating. Heat also may be produced by hysteresis in the case of ferromagnetic materials at temperatures below the Curie point. For a large majority of practical applications of induction heating, the hysteresis loss is negligible and will be disregarded in the following.

Viewing the calculation of the generated heat as the final objective, the first step will be to compute the intensity of the eddy currents and their distribution within the charge.

For a cylindrical charge, the direction of the induced electric field intensity is perpendicular to the radius r, hence the eddy currents follow circles, whose centers coincide with the axis of the charge (Figure 2). The circles are positioned in planes perpendicular to the axis; if the ratio of length to diameter of inductor and charge approach infinity, the magnetic field intensity produced by the current in the inductor is uniform inside the inductor, while the magnetic field intensity on the outside of the inductor is zero.[4] Voltages and eddy currents will be the same along lines parallel to the axis. It follows that a slice cut out of the charge perpendicular to its axis is representative of the state of the entire charge.

Since the voltages and the eddy currents follow concentric circles, and thus have no radial components, a subdivision of the slice into a number of sleeves all telescoped into each other will not change the state of the slice, even if the sleeves were insulated from each other. In order to obtain uniformity of induced voltage and eddy current over the cross-section of the sleeve, its radial thickness is assumed infinitely small; consequently the number of sleeves is infinitely large. The charge thus is reduced to a (infinite) number of electric circuits amenable to quantitative circuit analysis.

Because of the resulting simplification in the analysis, the ratio of length to diameter of inductor and charge will be assumed approaching infinity. A very simple relation between magnetic intensity and ampere-turns per centimeter then results. In practical cases where the ratio of length to diameter of inductor and charge is finite, the spreading of the flux at the ends of the inductor results in a weakening of the induction, hence the formulas derived for the infinite case will give too high values for the generated heat.[5,6,7] However, as the ratio of length to diameter increases, the deviation from the infinite case becomes less and approaches zero asymptotically.

The analysis utilizes two different methods of approach, depending on the ratio between the radius a of the charge and the depth of penetration p. Each method has its special usefulness in its region of application, the border line between the two cases being at a ratio of $a/p = 3$. The results obtained by these methods are identical with the power

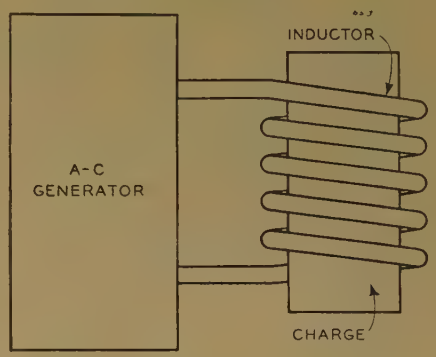


Figure 1. Arrangement of inductor and charge

series of Bessel functions, obtained as solution from an analysis based on partial differential equations.[2]

Case a/p<3

For this case the eddy currents in the charge are calculated by a method of successive approximations. As previously explained, the charge can be reduced to a number of electric circuits. Suppose the charge is now slotted radially from the surface to the axis. All circuits in the slice become open. When such a fictitious charge is inserted into an energized inductor, open circuit voltages will appear across the slots of the various sleeves; the slots, however, prevent eddy currents from circulating through the sleeves.

Suppose the slots are now closed. Eddy currents start to flow through the sleeves, and it will be assumed as a first approximation that the eddy currents are given by the open circuit voltages of the various sleeves, divided by the electrical resistance of the respective sleeves.

Paper 46-53, recommended by the AIEE committee on industrial power applications and the subcommittee on induction and dielectric heating for presentation at the AIEE winter convention, New York, N. Y., January 21–25, 1946. Manuscript submitted October 29, 1945; made available for printing December 21, 1945.

HERBERT F. STORM is with the General Electric Company, Schenectady, N. Y.

The actual eddy currents will differ from those thus obtained for two reasons:

1. According to Lenz's law, the eddy currents tend to weaken the magnetic field produced by the inductor, resulting in a reduction of the open circuit voltages.

2. Voltages of mutual reactance are induced in the various sleeves by eddy currents circulating in other sleeves.

In order to obtain a second approximation, the magnetic field distribution as determined by the first approximation is calculated. A new group of voltages is induced in the charge, which, in combination with the resistance of the sleeves, cause a new set of eddy currents to circulate through the sleeves. These voltages and eddy currents obtained by the second approximation are much smaller in magnitude than those obtained by the first approximation. The total eddy currents in the charge, thus far considered, consist of the sum of the eddy currents of first and second approximation. The actual eddy currents again will differ from those thus far obtained because the eddy currents of second approximation will weaken the previous magnetic field; moreover, voltages of mutual reactance are induced in the various sleeves by the eddy currents of second approximation, circulating in other sleeves. It will be noted, however, that the weakening of the magnetic field by the eddy currents of second approximation is of far lesser degree than previously encountered by the eddy currents of first approximation. Equally reduced in magnitude are the voltages of mutual reactance as a result of the eddy currents of second approximation, compared with the voltages of mutual reactance as a result of the eddy currents of first approximation. Further approximations can be obtained by proceeding in analogous fashion. This process leads to a power series which will be found to be rapidly convergent.

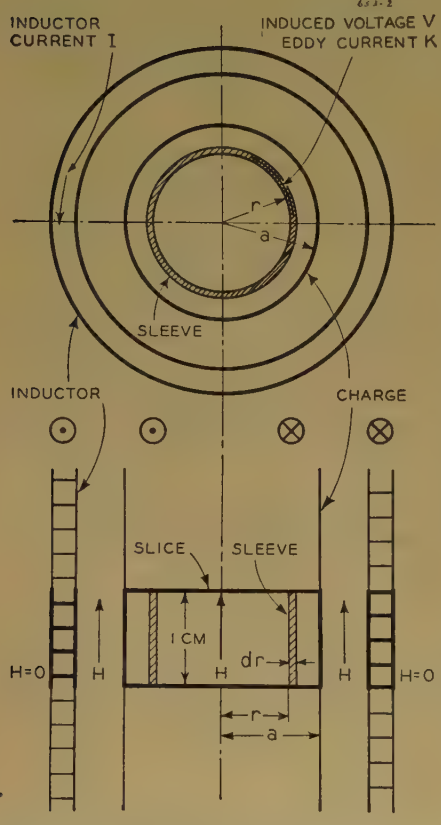


Figure 2. Sectional view of inductor and charge

Positive directions were assigned to the magnetic field intensity H and to the current I in the inductor. They are shown (Figure 2) by arrows parallel to the axis of the inductor and by the head and tail symbols, respectively, indicating a right-hand system. For alternating magnetic intensities and currents, the arrows show the direction of the instantaneous values, provided the latter appear positive in their respective vector diagrams. For a charge inserted into the inductor, the same positive directions are retained for the magnetic intensities H and currents K in the charge.

The magnetic-field intensity, henceforth abbreviated magnetic intensity, follows for an empty inductor from

$$H_o = 0.4\pi I_o n \tag{1}$$

A cylindrical charge is now inserted into the inductor. The induction B_o in the charge (caused by the inductor field) equals

$$B_o = \mu H_o \tag{2}$$

The magnetic flux Φ_o, which is surrounded by a sleeve with the radius r, equals

$$\Phi_o = r^2\pi B_o \tag{3}$$

As a result of Φ_o, voltages V_o, and hence eddy currents K_o, are produced in the charge. The eddy currents, however, produce magnetomotive forces of their own, resulting in the weakening of the original flux Φ_o, and in the induction of voltages in the various sleeves by mutual inductance. These effects of the eddy currents are nullified by introducing a so-called compensating current in the inductor, which is to offset the weakening action of the eddy currents with respect to the flux Φ_o, and furthermore by introducing compensating voltages in the sleeves. The latter voltages are connected in series with each sleeve and develop a voltage equal in magnitude and opposite in sign with respect to the voltage induced in the sleeve by the eddy currents in the charge and by the compensating current in the inductor. Under these assumptions the current I_o in the inductor produces a flux Φ_o (equation 3) which in turn induces a voltage V_o in the sleeve, as expressed conventionally by

$$V_o = -j\omega\Phi_o 10^{-8} \tag{4}$$

where

$$\omega = 2\pi f \tag{5}$$

Utilizing equations 1 to 5, V_o follows as

$$V_o = -j8\pi^2 10^{-9}(\mu f)(I_o n)r^2 \tag{6}$$

It is apparent that the radial distribution of the induced voltage V_o is parabolic. The slice is shown in Figure 3, looking in the axial direction. The magnitude of V_o as a function of the radius is shown by the graph superimposed on the view of the slice.

Before analyzing the implications of equation 6, it will be well to remember that the flux Φ_o also will induce a voltage in the inductor. If the object is to determine the voltage induced in the inductor by the entire flux inside of the charge, the variable radius r in equation 6 is replaced by the outside radius a of the charge. The voltage per turn of the inductor, caused by only the flux within the charge, follows from equation 6

$$E_o/n = -j8\pi^2 10^{-9}(\mu f)(I_o n)a^2 \tag{7}$$

and the voltage E_o per centimeter axial length of inductor is

$$E_o = -j8\pi^2 10^{-9}(\mu f)(I_o n)a^2 \tag{8}$$

It should be observed that other voltages are induced additionally in the inductor. There are the voltages resulting from the magnetic field within the inductor conductor and caused by the magnetic field in the air space between inductor and charge. Furthermore, an ohmic voltage component exists because of the copper loss in the inductor. The current in the inductor, multiplied by the various voltages listed, indicates the true and reactive power spent in the various parts such as the inductor proper, the air gap between the inductor and the charge, and the charge itself. Since this discussion is concerned only with the power requirements introduced by the charge itself, voltages induced in the inductor by parts other than the charge do not require further attention.

Returning to the voltage V_o (equation 6), currents, the so-called eddy currents, will flow in the sleeves as a result. The magnitude and phase of the eddy currents

are controlled by the voltage V_o, the resistance of the individual sleeve and the voltages induced in the sleeve by self inductance and mutual inductance.

While the voltage of self inductance is zero because the infinitely small cross-section of the sleeve multiplied by a finite current density (amperes/centimeter²) results in a current (in amperes) of zero magnitude, the effect of the voltages caused by mutual inductance has been eliminated temporarily by the inception of sources called compensating currents and voltages, as previously indicated.

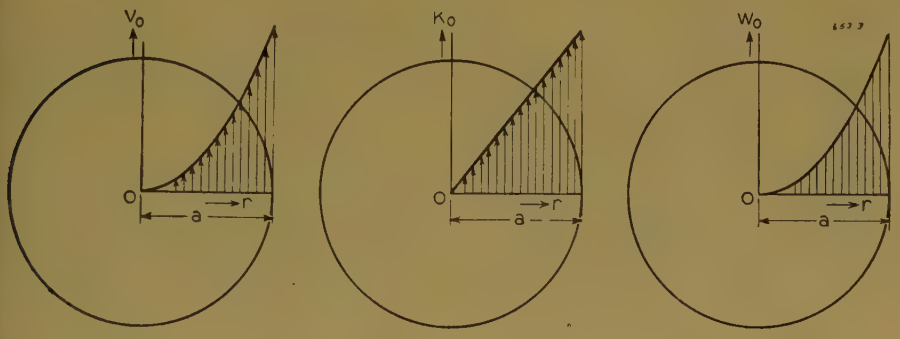


Figure 3. Radial distribution of induced voltage V_o, eddy current density K_o, and generated heat W_o

The eddy current is now solely a function of V_o and the resistance of the sleeve.

If the slice has a height of one centimeter, the resistance of a sleeve of infinitesimal thickness dr is then

$$R=2r\pi\rho/dr \tag{9}$$

and the eddy current density K_o will equal

$$K_o=V_o/2r\pi\rho \tag{10}$$

From equations 6, 7, and 8, one obtains for K_o

$$K_o=-j4\pi^2 10^{-9}(\mu f/\rho)(I_o n)r \tag{11}$$

Finally, the I^2R heat generated by induction is, per cubic centimeter,

$$W_o=K_o^2\rho/2=8\pi^4 10^{-18}(\mu^2 f^2/\rho)\times (I_o n)^2 r^2 \tag{12}$$

where W_o is average value and K_o is peak value.

At this point it is worthwhile to pause for a moment in the further development and to focus our attention on the interpretation of equations 11 and 12. It will be recognized that the generated heat is controlled by the ampere-turns and frequency of the inductor current, by the electrical resistivity and magnetic permeability[8] of the charge, and furthermore by the distance from the axis. The permeability of a number of ferromagnetic materials varies with the magnetic intensity and with the temperature. When the temperature of the charge has reached the Curie point, the permeability drops to unity with an attendant drop in heat generation.

A further inspection of equations 11 and 12 reveals the important facts that the density of the eddy currents K_o is zero at the center of the charge and increases as a linear function of the radius toward the surface (Figure 3). Since the rate of heat generation W_o per unit volume of the charge is proportional to the square of the current density (equation 12), it is obvious that the rate of heating W_o is also zero at the center of the charge, but increases with the square of the radius toward the surface of the charge. The greatest concentration of heat generation thus occurs in the surface layer (Figure 3). This concentration of heat generation toward the surface makes induction heating suitable for surface hardening applications. Although most of the heat is generated in the surface layer, the entire body of the charge can be heated if so desired; this is done simply by continued application of power, the heat being conducted thermally to the interior.

Such, briefly sketched, are the conclusions reached from an inspection of equations 11 and 12. These equations were obtained by disregarding the effect of mutual inductance. The validity of the conclusions, therefore, has to be limited to the region in which the effect of mutual inductance remains negligible. It is the object of the following to demarcate this region and to investigate what modifications the foregoing conclusions have to undergo when the effect of mutual inductance becomes pronounced.

Eddy currents K_o flowing in the charge create a magnetic flux Φ_1, which is interlinked with the sleeves and with the inductor. The flux Φ_1 is a function of the magnetic intensity H_1 which follows from Ampere's law

$$\oint_l H_1 dl=0.4\pi\int\int_s K_o ds \tag{13}$$

Remembering that H_1 has no radial component and equals zero at the outside of the charge, the line integral on the left hand side of equation 13 simplifies for a slice of the height of one centimeter to H_1 (Figure 4). The surface integral on the right hand side also simplifies somewhat, resulting in

$$H_1=0.4\pi\int_r^a K_o dr \tag{14}$$

Simplifying the expressions for K_o by introducing a new parameter p, where

$$p=\frac{1}{2\pi}\sqrt{\frac{\rho 10^9}{2\mu f}} \tag{15}$$

one obtains

$$K_o=-j(1/2p^2)(I_o n)r \tag{16}$$

Substituting equation 16 into equation 14 and integrating, one obtains finally

$$H_1=(-ja^2/8p^2)\cdot 0.8\pi(I_o n)[1-(r/a)^2] \tag{17}$$

The radial distribution of H_1 is parabolic. The induction B_1 follows as

$$B_1=\mu H_1 \tag{18}$$

and is shown in Figure 5.

The magnetic flux Φ_1 will be obtained from

$$\Phi_1=\int_o^r B_1\cdot 2r\pi\cdot dr \tag{19}$$

The following method of splitting the induction B_1 into two components $B_{1,m}$ and $B_{1,n}$ will greatly simplify the further analysis:

$$B_1=B_{1,m}+B_{1,n} \tag{20}$$

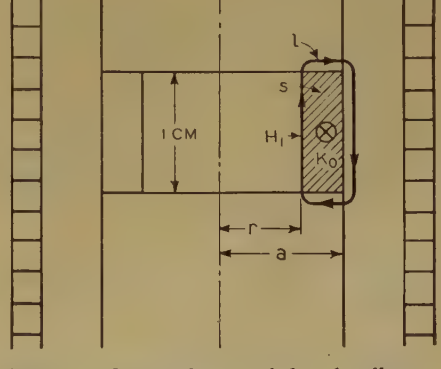


Figure 4. Sectional view of slice for illustration of Ampere's circuital law

Component $B_{1,n}$ shall have such radial distribution that the resulting flux $\Phi_{1,n}$ is not interlinked with the inductor:

$$\Phi_{1,n}\Big|_0^a = \int_0^a B_{1,n}\cdot 2r\pi\cdot dr = 0 \qquad (21)$$

Integrating equation 20 and substituting from equation 21, one obtains an integral equation for $B_{1,m}$:

$$\int_0^a B_1\cdot 2r\pi\cdot dr = \int_0^a B_{1,m}\cdot 2r\pi\cdot dr \qquad (22)$$

The simplest radial distribution which can be assigned to $B_{1,m}$ is to be constant:

$$B_{1,m} = \text{constant} \qquad (23)$$

Applying equation 23 to equation 22, we have

$$\int_0^a B_1\cdot 2r\pi\cdot dr = B_{1,m}\int_0^a 2r\pi\cdot dr \qquad (24)$$

and

$$B_{1,m} = \frac{1}{a^2\pi}\int_0^a B_1\cdot 2r\pi\cdot dr \qquad (25)$$

Utilizing equations 17 and 18, the integration of equation 25 results in

$$B_{1,m} = (-ja^2/8p^2)\cdot 0.4\pi\mu(I_o n) \qquad (26)$$

The other component $B_{1,n}$ follows from equations 17, 18, 20, and 26:

$$B_{1,n} = (-ja^2/8p^2)\cdot 0.4\pi\rho(I_o n)\times [1-2(r/a)^2] \qquad (27)$$

Both components $B_{1,m}$ and $B_{1,n}$, whose radial distributions are illustrated in Figure 5, form together the flux Φ_1. This flux therefore can be considered as consisting of two components: $\Phi_{1,m}$, which has a constant density $B_{1,m}$ throughout the charge, and $\Phi_{1,n}$, which is not interlinked with the inductor.

When considering the effect of the eddy currents K_o and hence of flux Φ_1 on the inductor, only the component $\Phi_{1,m}$ requires attention because the interlinkage of the other component $\Phi_{1,n}$ with the inductor is zero.

It was stated previously that the weakening effect of the eddy currents K_o with respect to the inductor field can be nullified by the introduction of a compensating current I_1 into the inductor, which easily can be determined now. Current I_1 has to produce an induction $B'_{1,m}$ which nullifies $B_{1,m}$.

$$B'_{1,m} = -B_{1,m} \qquad (28)$$

From equations 1, 2, and 28,

$$0.4\pi\mu(I_1 n) = B'_{1,m} = -B_{1,m} \qquad (29)$$

Applying equation 26, one obtains for the compensating current I_1 in the inductor

$$I_1 = -(-ja^2/8p^2)I_o \qquad (30)$$

If this current I_1 is added to the original inductor current I_o, as it will be assumed, the magnetic action of the eddy currents K_o, as far as flux $\Phi_{1,m}$ is concerned, is completely cancelled. After the introduction of current I_1, the flux $\Phi_{1,m}$ ceases to exist and hence does not require any further attention. The only modification of the original eddy current

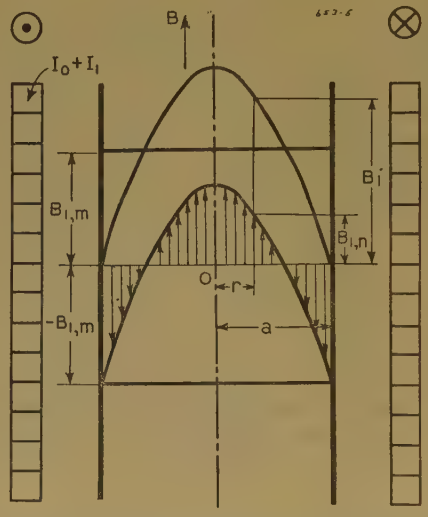


Figure 5. Longitudinal section, illustrating the distribution of induction B_1 caused by eddy currents K_o

distribution as expressed in equations 11 and 12 will be caused by induction $B_{1,n}$ (Figure 5).

In addition to cancelling part of the eddy current field, current I_1 reflects into the inductor the I^2R loss, which occurs in the charge caused by the eddy currents K_o. The current I_1 is in phase with the voltage E_o and thus expresses true power consumption by the inductor (Figure 6). It can be proved that this power P_o expressed in terms of I_1 and E_o (equations 8 and 30) equals the energy dissipated in the charge by the eddy current K_o (equations 11 and 12):

$$P_o = E_o I_1/2 = \pi(a/2p)^4\rho(I_o n)^2 \equiv \int_0^a (K_o^2\rho/2)\cdot 2r\pi\cdot dr \qquad (31)$$

Returning to induction $B_{1,n}$, the corresponding flux $\Phi_{1,n}$ follows in analogy to equation 3:

$$\Phi_{1,n} = \int_0^r B_{1,n}\cdot 2r\pi\cdot dr \qquad (32)$$

The induced voltage V_1 in the charge, caused by flux $\Phi_{1,n}$, is

$$V_1 = -j\omega\Phi_{1,n}10^{-8} \qquad (33)$$

Substituting from equations 27 and 32, one obtains

$$V_1 = [(-ja^2/p^2)\pi\rho(I_o n)r^2/a^2]\times [(-ja^2/8p^2)(1-r^2/a^2)] \qquad (34)$$

These voltages V_1 are induced in the charge by the flux $\Phi_{1,n}$ and previously have been disregarded after compensating voltages were introduced. Actually such compensating voltages do not exist and hence the voltages V_1 will be acting on the charge. Summarizing the reasoning thus far, it can be stated that the inductor carries the currents I_o and I_1, while the charge carries the eddy currents K_o. In addition, free residual voltages V_1 exist in the charge.

At this point an examination of the relative magnitudes of V_1 with respect to V_o is in order. Since the voltages V_1 will cause the flow of eddy currents K_1, just as V_o caused the flow of the eddy currents K_o, the relative magnitude of V_1 with respect to V_o will indicate whether the expression for the heat generation in the charge (equation 31) is sufficiently accurate or whether the effect of the voltages V_1 has to be taken into account.

Recasting the expression for V_o by using equations 6 and 15,

$$E_o = (-ja^2/p^2)\pi\rho(I_o n)r^2/a^2 \qquad (35)$$

The ratio V_1/V_o becomes (equations 34 and 35)

$$V_1/V_o = (-ja^2/8p^2)(1-r^2/a^2) \qquad (36)$$

For a ratio of $a/p<1$, the ratio of the voltages V_1/V_o, and consequently of the eddy currents K_1/K_o, becomes small. Since the generated heat is proportional to K_o^2, and respectively K_1^2, the heat generated by the eddy currents K_1 is then negligible with respect to the heat generated by the eddy currents K_o, and the expression for the heat generation (equation 31) applies.

The current I in the inductor is

$$I = I_o + I_1 = I_o[1+j(a^2/8p^2)] \qquad (37)$$

Solving for I_o,

$$I_o^2 = I^2/[1+j(a^2/8p^2)]^2 \qquad (38)$$

Introducing I_o^2 into equation 31 and remembering that equation 31 is valid only for $a/p<1$, I_o^2 can be approximated very closely by the inductor current I. Since the effective value of the inductor current

$$I_{\text{eff}} = I/\sqrt{2} \qquad (39)$$

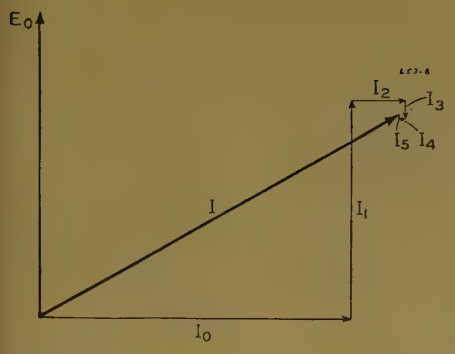


Figure 6. Vector diagram of currents in inductor

the heat generated in the charge can now be expressed as follows:

$$P_o = 2\pi(a/2p)^4 p(I_{eff}n)^2 \quad \text{for } a/p \leq 1 \tag{40}$$

If, however, $a/p > 1$, the effect of V_1 has to be investigated. Just as the voltage V_o produces the eddy current K_o, the voltage V_1 produces a new eddy current K_1, as fully explained in Appendix I. The effect of the eddy currents K_1 can be resolved in an additional current I_2 in the inductor (Figure 6) and free voltages V_2 as follows:

$$K_1 = \left(-j\frac{a^2}{8p^2}\right)^2 \frac{4}{a}(I_o n)\frac{r}{a}\left(1-\frac{r^2}{a^2}\right) \tag{42}$$

$$I_2 = -\left(-j\frac{a^2}{8p^2}\right)^2 I_o \cdot \frac{1}{3} \tag{50}$$

$$V_2 = \left(-j\frac{a^2}{8p^2}\right) V_1 \left(\frac{2}{3}-\frac{r^2}{3a^2}\right) \tag{53}$$

Thus the current in the inductor consists of the vector sum of I_o, I_1, I_2, while the eddy currents consist of the vector sum of K_o, K_1. In addition, free residual voltages V_2 exist in the charge.

With the new eddy currents K_2 (in analogy to equation 42),

$$K_2 = \left(-j\frac{a^2}{8p^2}\right)^2 K_o \left(-\frac{2}{3}+\frac{r^2}{a^2}-\frac{r^4}{3a^4}\right) \tag{54}$$

flowing in the charge, it can be seen that

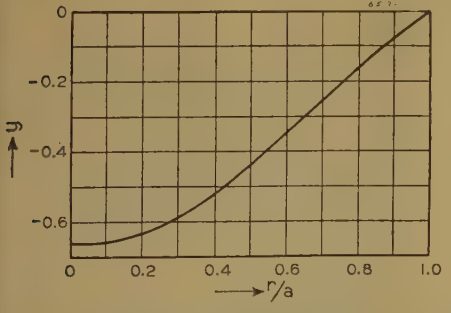


Figure 7. Function y indicates the progressive reduction of eddy current density toward the axis of charge

K_2 is in counterphase with eddy currents K_o, and hence K_2 can be algebraically subtracted from K_o in order to obtain the total nonquadrature eddy current thus far derived. The charge also carries the eddy current K_1. This current K_1 is, however, in phase quadrature with K_o, and its effect on K_o will be neglected for reasons of simplicity. Under this assumption K_2 expresses the amount by which the original intensity K_o of the eddy currents (equation 16) will be modified if the voltages V_1 and V_2 are not negligible.

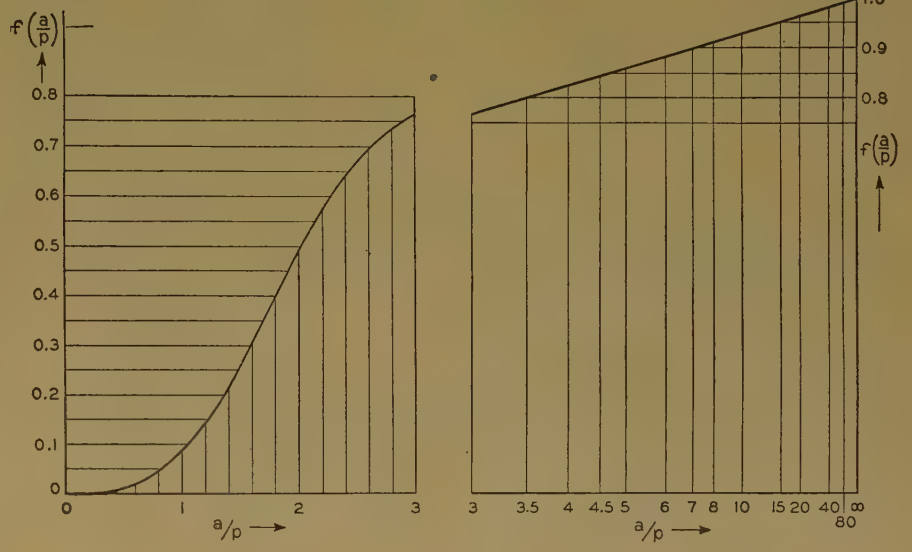


Figure 8. Graph for f(a/p) (from equations 71 and 81)

In order to compare the new eddy current K_2 with the original eddy current K_o, the first is expressed in terms of the latter as shown in equation 55:

$$K_2/K_o = \left(-j\frac{a^2}{8p^2}\right)^2\left(-\frac{2}{3}+\frac{r^2}{a^2}-\frac{r^4}{3a^4}\right) = y \tag{55}$$

Aside from the term $(-ja^2/8p^2)^2$, the new eddy current K_2 equals the original eddy current K_o times a function y. For better illustration, the function y is plotted in Figure 7. This figure reveals:

1. In the interior of the charge the new eddy current K_2 is opposed to the original eddy current K_o at every point, resulting in a smaller eddy current density than expressed in equation 16, and therefore resulting in less heat generation than expressed in equation 12.

2. The eddy current density, and hence heat generation, is progressively reduced toward the center of the charge.

3. The relative reduction of eddy current density and heat generation in the interior is a function of the ratio a/p.

As pointed out in the preceding paragraphs, the generated heat decreases toward the axis at a higher rate than expressed by equation 12. The result is a preponderance of heat generation in the surface layer, called the skin of the charge which effect is called skin effect. If the ratio a/p is increased, the reduction of heat generation toward the axis of the charge is intensified resulting in a still greater preponderance of heat generation in the surface layer of the charge. Besides frequency, resistivity, and permeability, the radius a of the charge is an additional controlling factor for the skin effect. The skin effect may be produced equally in the case of a higher frequency and a charge of smaller diameter, as in the case of a lower frequency and a charge of larger diameter.

After this discussion of skin effect, the attack on the main problem, namely the computation of heat generation, will be resumed. The eddy currents K_2 lead to magnetic intensities H_3 which, in turn, are resolved in a current I_3 in the inductor and free voltages V_3 in the charge. If this method is repeated, further currents I_4, I_5, I_6 are obtained for the inductor:

$$I_1 = -(-ja^2/8p^2)I_o \tag{30}$$
$$I_2 = -(-ja^2/8p^2)^2 I_o \cdot 1/3 \tag{50}$$
$$I_3 = -(-ja^2/8p^2)^3 I_o \cdot 1/6 \tag{56}$$
$$I_4 = -(-ja^2/8p^2)^4 I_o \cdot 4/45 \tag{57}$$
$$I_5 = -(-ja^2/8p^2)^5 I_o \cdot 13/270 \tag{58}$$

The current components in Figure 6 are shown for $a/p = 2.4$. It is evident from Figure 6 that the current components converge rapidly and hence the current represented by I is a very close approximation for the actual current in the inductor. For decreasing ratios of

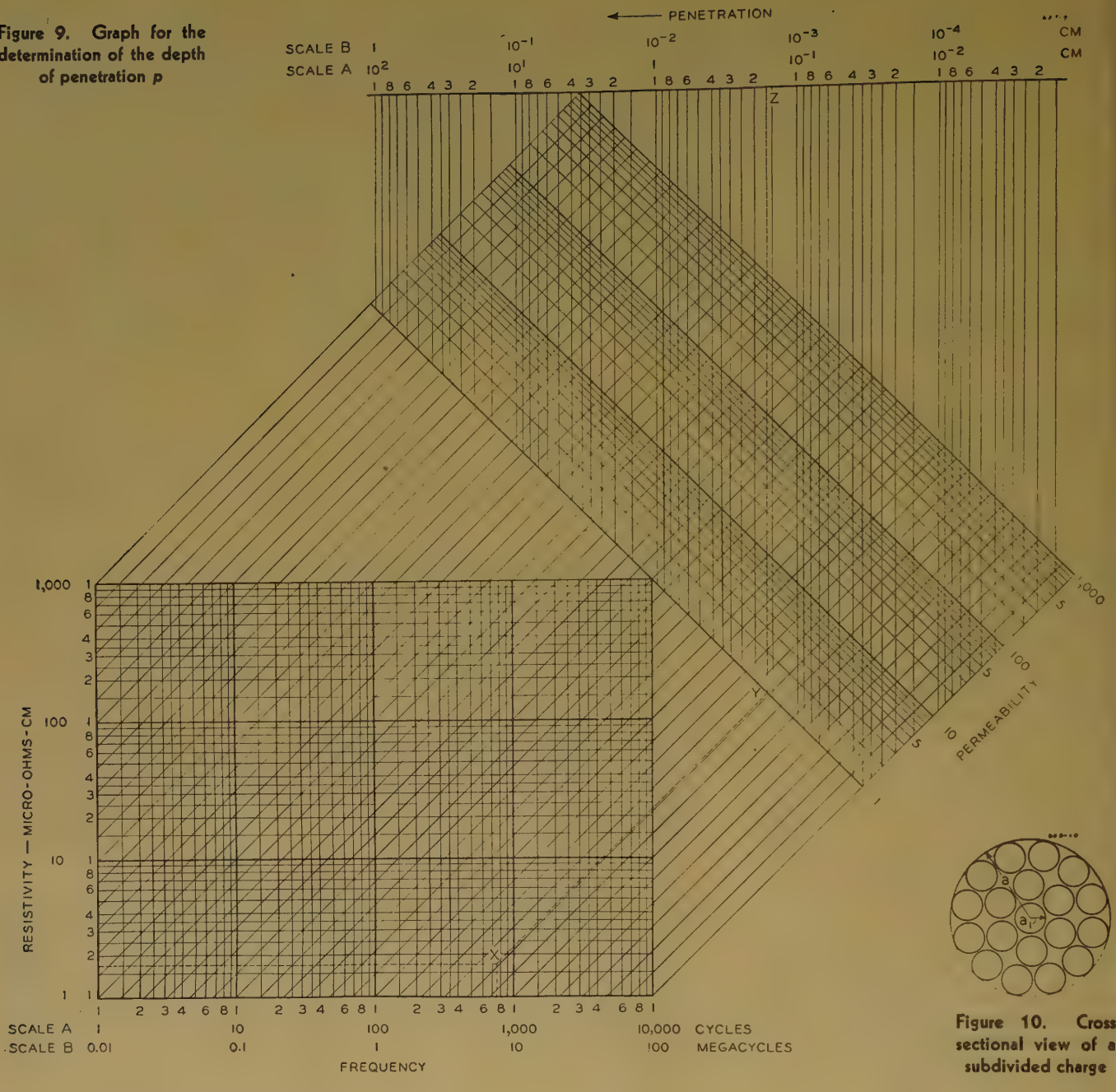


Figure 9. Graph for the determination of the depth of penetration p

Figure 10. Cross sectional view of a subdivided charge

a/p, the convergence is more rapid yet and hence the approximation is still closer.

When the true components I_1, I_3, I_5 are multiplied with the inductor voltage E_o, the true power P dissipated in the charge is obtained. This is shown in Appendix II, resulting in

$$P = 2\pi\rho \frac{\frac{1}{16}\left(\frac{a}{p}\right)^4}{1+\frac{11}{384}\left(\frac{a}{p}\right)^4-\frac{77}{2{,}211{,}840}\left(\frac{a}{p}\right)^8}(I_{eff}n)^2$$

for $a/p<3$ (69)

Thus the generated heat has been determined in the form of a series, as a function of radius, resistivity, permeability of the charge, and the ampere-turns and frequency of the inductor current. For $a/p = 3$ the accuracy of the series is within 1.1 per cent. For smaller ratios of a/p the error rapidly approaches zero. The convergence of the series is so rapid that for a ratio of $a/p \leqslant 2.2$, the third term in the denominator of equation 69 can be neglected without introducing an error of more than 1.2 per cent. The remaining series is still very rapidly converging for decreasing ratios of a/p. If $a/p = 0.8$, the second term in the denominator can be neglected without causing an error of more than 1.2 per cent, which error rapidly decreases for decreasing ratios of a/p.

The formulation of generated heat by means of a sharply converging series introduces a new tool for the analytical attack of various theoretical problems. For practical rapid determination of the heat, equation 60 is split into 2 parts:

$$P = P_\infty \cdot f\left(\frac{a}{p}\right) \tag{70}$$

where

$$f\left(\frac{a}{p}\right) = \frac{\frac{\sqrt{2}}{16}\left(\frac{a}{p}\right)^3}{1+\frac{11}{384}\left(\frac{a}{p}\right)^4-\frac{77}{2{,}211{,}840}\left(\frac{a}{p}\right)^8} \tag{71}$$

for $a/p<3$

$$P_\infty = \pi\sqrt{2}\rho\frac{a}{p}(I_{eff}n)^2 \tag{72}$$

While function $f\ (a/p)$ is plotted in Figure 8, a graph shown in Figure 9, and

explained later in the text, facilitates the rapid determination of p.

Case $a/p \geq 3$

It can be shown[3] that for a magnitude of p which is negligible with respect to the radius a, the heat generation W per unit volume at a radial distance d from the surface of the charge, can be expressed by

$$W=\frac{1}{2}\left(\frac{In}{p}\right)^2 \rho\epsilon \frac{-d\sqrt{2}}{p} \quad (73)$$

where

$$d=a-r \quad (74)$$

The heat generated in a slice of one centimeter height is

$$P=\int_o^a W\cdot 2r\pi\cdot dr \quad (75)$$

If this integral is evaluated as shown in Appendix III, the following expression for the generated heat is obtained as follows:

$$P=\pi\sqrt{2}\rho\frac{a}{p}\left(1-\frac{1}{\frac{a\sqrt{2}}{p}}\right)(I_{eff}n)^2 \quad (80)$$

for $a/p \geq 3$

Equation 80 is accurate within 0.1 per cent for $a/p = 3$. For larger ratios of a/p, the error rapidly approaches zero.

It will be recognized that the application of equation 72 leads to

$$P=P_\infty\cdot f\left(\frac{a}{p}\right) \quad (70)$$

where

$$f\left(\frac{a}{p}\right)=1-\frac{1}{\frac{a\sqrt{2}}{p}} \quad (81)$$

for $a/p \geq 3$

and

$$P_\infty=\pi\sqrt{2}\rho\frac{a}{p}(I_{eff}n)^2 \quad (72)$$

The function $f(a/p)$ (equation 81) can be plotted very rapidly as a straight line, using a hyperbolic scale for the abscissa axis, as shown in Figure 8.

Graph for the Determination of the Depth of Penetration

Every one of the important equations in the preceding analysis contained the factor p (equation 15). For a radius of the charge which is very large compared to p, the magnetic intensity declines exponentially from the surface toward the interior of the charge.[3] At a distance of $p\sqrt{2}$ from the surface, the magnetic intensity and hence the eddy currents are $1/\epsilon$ of their respective values at the surface. The decay of the magnetic intensity as a function of its penetration into the charge can thus be expressed in terms of p, and hence p is often referred to as depth of the magnetic field penetration.

For rapid determination of p, the graph in Figure 9 is recommended. Suppose the penetration should be determined for copper at room temperature ($\rho = 1.7\cdot10^{-6}$ ohm-centimeters, $\mu = 1$) and a frequency of 750 cycles. Erect verticals on the frequency and resistivity axes at the required points, as shown by dotted lines, and intersect at point X. Draw a line through X under 45 degrees until intersection is made with the permeability system at the desired permeability (point Y). Erect a vertical line on Y and intersect penetration axis at point Z. If scale A has been used for frequency, use scale A for penetration; if scale B has been used for frequency, use scale B for penetration. For the foregoing example the solution is 0.17 centimeter.

Subdivided Charge

Thus far the charge consisted of one cylinder with the radius a. When induction heating is applied to melting operations, the charge with which the heating process is started may consist of a multitude of solid pieces of metal, so-called scrap whose upper range of size is limited by the inside diameter of the crucible. As far as the geometry of the crucible is concerned, there is no lower limit for the size of the scrap. It has been observed, however, that the time for melting the same weight of scrap depends upon the size of the scrap, other conditions such as magnitude and frequency of the inductor current remaining the same. Under these assumptions the energy spent on copper losses in the inductor is merely a function of the time during which the current is applied. If various sizes of scrap require various amounts of time for melting, although the weight of scrap remains the same, it is obvious that the size of the scrap influences the efficiency of heating.

In order to analyze the effect of scrap size, it will be assumed that the charge consists of a number of solid, identical, round bars which fill the interior of the crucible as shown in Figure 10. Singling out one bar with the radius a_i, the generated heat can be computed, as previously shown in equation 70, substituting a_i for a. Since the charge, in this case the bar, does not create a magnetic field outside its contours, the space around the bar remains at the same magnetic intensity whether the bar is present or not. This means that the state within one bar is unaffected by the presence of other bars within the same inductor. If, however, the bars touch each other, a current can be transferred across the common surface making the bars interdependent. It will be assumed in the following that the bars do not touch each other, or that oxides are present at the surface of the bars which are sufficiently insulating to make the current transfer betwen bars negligible.

As in the preceding (equation 70), the heat generated per centimeter length of one bar equals

$$P_i=P_{\infty i}\cdot f\left(\frac{a_i}{p}\right) \quad (82)$$

where

$$P_{\infty i}=\pi\sqrt{2}\rho\frac{a_i}{p}(I_{eff}\cdot n)^2 \quad (83)$$

If the number of rods is i, the total area A of the cross sections of the rods equals

$$A=ia_i^2\pi \quad (84)$$

The total heat generated in all bars per centimeter length follows from Appendix IV:

$$P=A\cdot(\mu f10^{-9})\cdot\varphi\left(\frac{a_i}{p}\right)\cdot(I_{eff}n)^2 \quad (90)$$

The function of $\varphi(a_i/p)$ (equations 88 and 89) has been plotted in the graph, as shown in Figure 11. The most striking feature of the function is its maximum. It means that for a certain ratio of a_i/p, the generated heat is a maximum. Since the magnitude and frequency of the current in the inductor are assumed constant, the losses in the inductor are also constant, and hence maximum heat generation means maximum efficiency. In order to find the maximum, the conventional approach of differentiating function $\varphi(a_i/p)$ (equation 88) is applied. The solution is

$$\left[\varphi\left(\frac{a_i}{p}\right)\right]_{max}=29.86 \quad (91)$$

for $a_i=2.53p$

For a given material and frequency, there is one certain radius at which maximum heat generation is achieved. It should, however, be borne in mind, that most metals increase their resistivity with increasing temperature. The penetration p at lower temperature is smaller (equation 15) than at higher temperature. If the radius $a_i = 2.53\ p$ has been determined for the low temperature, the heat generation will be at maximum at

the outset of heating. As the heating process goes on, the temperature of the charge will rise and its resistivity increases. The factor p will also increase, resulting in a decreasing (a_i/p). It is obvious from Figure 11 that a reduction of heat generation will occur. The thermal losses of the charge, however, increase with the temperature, while the generated heat decreases. It is therefore possible that a temperature equilibrium establishes itself below the desired temperature.

In order to avoid this limitation of temperature, the radius a_i of the charge has to be computed from a penetration p, which is based on a resistivity of higher value than at room temperature. If p is based on the resistivity of the metal at its highest temperature, the generated heat also will reach its maximum at the highest temperature.

The maximum heat generation follows from equations 90 and 91:

$$P_{max}=29.86A(\mu f10^{-9})(I_{eff}n)^2 \qquad (92)$$

From the point of view of efficiency of induction heating, equation 92 is very significant. If the charge is not subdivided, and provided $a \gg p$, the generated heat P is given by equation 70. The heat generation P is proportional to the radius of the charge, and the copper losses in the inductor are in proportion to the radius of the inductor. If the radius of the charge is increased, the radius of the inductor has to be increased by a proportional amount. The result is that the ratio between heat generation and inductor loss remains constant, which in turn means that the efficiency is limited to a constant amount depending on the resistivity and permeability of the charge.

For a subdivided charge no such limitation exists. While the loss in the inductor increases linearly with its radius, the area A of the total cross-section of the bars increases approximately with the square of the radius. The result is that by increasing the radius of the inductor, the heat generation in the charge increases much faster than the losses in the inductor, hence the efficiency approaches asymptotically 100 per cent.

Appendix I

The voltage V_1 will cause the flow of new eddy currents of the density K_1. The magnitude and phase of these new eddy currents is controlled by V_1, the resistance of the sleeves, and the voltages V_2 induced in the sleeves by the eddy currents K_1 caused by mutual reactance. A compensating current I_2 is introduced in the inductor to counteract the weakening action of the eddy currents K_1. Furthermore, a compensating voltage $-V_2$ is introduced in series with each sleeve, developing a voltage equal in magnitude and opposite in sign with respect to the voltage induced in the sleeve by the eddy currents K_1 in the charge, and the compensating current I_2 in the inductor, thus nullifying the voltages of mutual reactance. The eddy current K_1 is now only a function of V_1 and the resistance of the sleeve (equation 10):

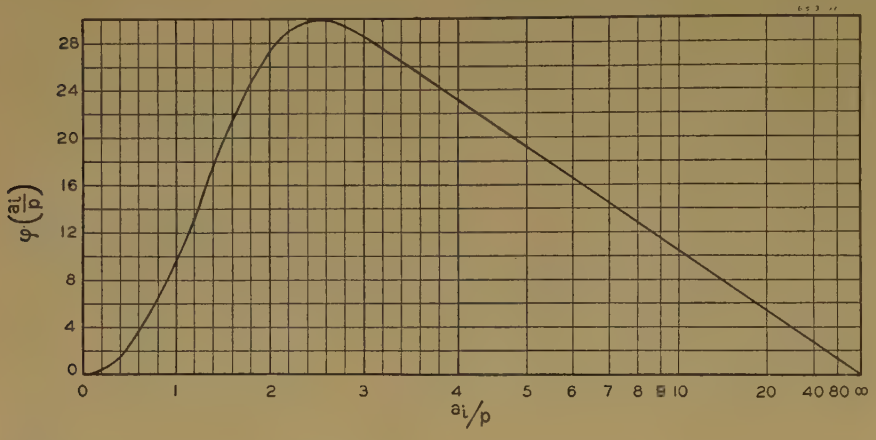


Figure 11. Graph for $\varphi(a_i/p)$ (from equations 88 and 89)

$$K_1=E_1/2r\pi\rho \qquad (41)$$

Taking V_1 from equation 34, one obtains

$$K_1=\left(-j\frac{a^2}{8p^2}\right)^2\frac{4}{a}(I_o n)\frac{r}{a}\left(1-\frac{r^2}{a^2}\right) \qquad (42)$$

The magnetic intensity H_2 results in analogy to equation 14:

$$H_2=0.4\pi\int_r^a K_1 dr \qquad (43)$$

and integrating equation 42,

$$H_2=\left(-j\frac{a^2}{8p^2}\right)^2\cdot 0.4\pi(I_o n)\left(1-2\frac{r^2}{a^2}+\frac{r^4}{a^4}\right) \qquad (44)$$

Again, the resulting induction B_2 is split into two components similar to equation 20:

$$B_2=B_{2,m}+B_{2,n} \qquad (45)$$

Stipulating the same requirements for $B_{2,m}$ and $B_{2,n}$, as previously for $B_{1,m}$ and $B_{1,n}$, respectively,

$$B_{2m}=\left(-j\frac{a^2}{8p^2}\right)^2\cdot 0.4\pi\mu(I_o n)\cdot\frac{1}{3} \qquad (46)$$

The other component $B_{2,n}$ follows from equations 44 and 46:

$$B_{2,n}=\left(-j\frac{a^2}{8p^2}\right)^2\cdot 0.4\pi\mu(I_o n)\left(\frac{2}{3}-2\frac{r^2}{a^2}+\frac{r^4}{a^4}\right) \qquad (47)$$

In order to cancel the effect of $B_{2,m}$, a compensating current I_2 has to flow through the inductor which produces an induction

$$B'_{2,m}=-B_{2,m} \qquad (48)$$

From equations 1, 2, and 48

$$0.4\pi\mu(I_2 n)=B'_{2,m}=-B_{2,m} \qquad (49)$$

Applying equation 46 one obtains the compensating current I_2:

$$I_2=-\left(-j\frac{a^2}{8p^2}\right)^2 I_o\cdot\frac{1}{3} \qquad (50)$$

Only the component $B_{2,n}$ can be effective in inducing voltages V_2 in the sleeves. The corresponding flux

$$\Phi_{2,n}=\int_o^r B_{2,n}\cdot 2r\pi\cdot dr \qquad (51)$$

which, in turn, induces voltages V_2 in the charge

$$V_2=-j\omega\phi_{2,n}10^{-8} \qquad (52)$$

Substituting for $\Phi_{2,n}$ in equation 52 results in an expression for V_2 as follows:

$$V_2=\left(-j\frac{a^2}{8p^2}\right)V_1\left(\frac{2}{3}-\frac{r^2}{3a^2}\right) \qquad (53)$$

Appendix II

The inductor current I has two components: the resistive component I_R in phase with the voltage E_o and the inductive component I_x lagging 90 degrees behind.

$$I=I_R+I_x \qquad (59)$$

The resistive component I_R follows from

$$I_R=I_1+I_3+I_5 \qquad (60)$$

and the inductive component I_x equals

$$I_x=I_o+I_2+I_4 \qquad (61)$$

The resistive component I_R follows from equations 30, 56, 58, and 60:

$$I_R=jI_o\left\{\frac{a^2}{8p^2}\left[1-\frac{1}{6}\left(\frac{a^2}{8p^2}\right)^2+\frac{13}{270}\left(\frac{a^2}{8p^2}\right)^4\right]\right\} \qquad (62)$$

and the inductive component follows from equations 50, 57, and 61

$$I_x = I_o\left[1+\frac{1}{3}\left(\frac{a^2}{8p^2}\right)^2-\frac{4}{45}\left(\frac{a^2}{8p^2}\right)^4\right] \qquad (63)$$

The absolute value of the inductor current I (equation 59) is

$$I=\sqrt{I_R{}^2+I_x{}^2} \qquad (64)$$

Substituting for equations 62 and 63 in equation 64 and neglecting terms of sixth power and up, one obtains for the current I

$$I=I_o\sqrt{1+\frac{5}{3}\left(\frac{a^2}{8p^2}\right)^2-\frac{2}{5}\left(\frac{a^2}{8p^2}\right)^4+\ldots} \qquad (65)$$

The heat generated by eddy currents is taken from the line in the form of the resistive component I_R of inductor current I. The average value of generated heat therefore can be expressed as

$$P=E_oI_R/2 \qquad (66)$$

where E_o and I_R are peak values.

The resistive component I_R is obtained from equations 62 and 65:

$$I_R=I\left(\frac{a^2}{8p^2}\right)\cdot\frac{1-\frac{1}{6}\left(\frac{a^2}{8p^2}\right)^2+\frac{13}{270}\left(\frac{a^2}{8p^2}\right)^4}{\sqrt{1+\frac{5}{3}\left(\frac{a^2}{8p^2}\right)^2-\frac{2}{5}\left(\frac{a^2}{8p^2}\right)^4}} \qquad (67)$$

This expression can be used in equation 66, and by further reference to equations 8 and 67 one obtains for the average power

$$P=4\pi\rho\left(\frac{a^2}{8p^2}\right)^2\times\frac{1-\frac{1}{6}\left(\frac{a^2}{8p^2}\right)^2+\frac{13}{270}\left(\frac{a^2}{8p^2}\right)^4}{1+\frac{5}{3}\left(\frac{a^2}{8p^2}\right)^2-\frac{2}{5}\left(\frac{a^2}{8p^2}\right)^4}(In)^2 \qquad (68)$$

Dividing the denominator by the numerator and neglecting terms of sixth and higher powers, equation 68 simplifies to

$$P=2\pi\rho\frac{\frac{1}{16}\left(\frac{a}{p}\right)^4}{1+\frac{11}{384}\left(\frac{a}{p}\right)^4-\frac{77}{2{,}211{,}840}\left(\frac{a}{p}\right)^8}(I_{\text{eff}}n)^2 \qquad (69)$$

for $a/p<3$

Appendix III

Applying the expression for W (equation 73) to equation 75 and integrating between the limits $r = 0$ and $r = a$ results in the following operations:

$$P=\frac{1}{2}\left(\frac{In}{p}\right)^2\rho 2\pi\int_o^a r\cdot\epsilon^{-\frac{(a-r)\sqrt{2}}{p}}\cdot dr$$

$$=\frac{1}{2}\left(\frac{In}{p}\right)\rho 2\pi\cdot\epsilon^{-\frac{a\sqrt{2}}{p}}\int_o^a r\cdot\epsilon^{\frac{r\sqrt{2}}{p}}\cdot dr \qquad (76)$$

$$\int_o^a r\cdot\epsilon^{\frac{r\sqrt{2}}{p}}\cdot dr=\frac{p^2}{2}\left(\frac{r\sqrt{2}}{p}-1\right)\epsilon^{\frac{r\sqrt{2}}{p}}\Bigg|_o^a$$

$$=\frac{p^2}{2}\left[\left(\frac{a\sqrt{2}}{p}-1\right)\epsilon^{\frac{a\sqrt{2}}{p}}+1\right] \qquad (77)$$

Using the results of equation 77 in equation 76 leads to

$$P=\frac{1}{2}\left(\frac{In}{p}\right)^2 2\pi\rho\frac{p^2}{2}\left(\frac{a\sqrt{2}}{p}-1+\epsilon^{-\frac{a\sqrt{2}}{p}}\right) \qquad (78)$$

$$\epsilon^{-\frac{a\sqrt{2}}{p}}\ll\frac{a\sqrt{2}}{p}-1 \qquad \text{for } a/p\geq 3 \qquad (79)$$

The exponential term in equation 78 thus can be neglected and the generated heat per one centimeter height of the charge is

$$P=\pi\sqrt{2}\rho\frac{a}{p}\left(1-\frac{1}{\frac{a\sqrt{2}}{p}}\right)(I_{\text{eff}}n)^2 \qquad (80)$$

for $a/p\geq 3$

Appendix IV

From equations 70, 82, 83, and 84,

$$P=A\sqrt{2}\frac{1}{a_ip}\cdot\rho\cdot f\left(\frac{a_i}{p}\right)(I_{\text{eff}}n)^2 \qquad (85)$$

Recasting equation 85 and substituting from equation 15 for p,

$$P=A\sqrt{2}\cdot 8\pi^2(\mu f10^{-9}/\rho)\times\left\{\left[f\left(\frac{a_i}{p}\right)\right]\Big/\left(\frac{a_i}{p}\right)\right\}(I_{\text{eff}}n)^2 \qquad (86)$$

Introducing

$$\varphi\left(\frac{a_i}{p}\right)=8\pi^2\sqrt{2}\left[f\left(\frac{a_i}{p}\right)\right]\Big/\frac{a_i}{p} \qquad (87)$$

for $a_i/p<3$ the function $\varphi\left(\frac{a_i}{p}\right)$ follows from equation 71:

$$\varphi\left(\frac{a_i}{p}\right)=\pi^2\frac{\left(\frac{a_i}{p}\right)^2}{1+\frac{11}{384}\left(\frac{a_i}{p}\right)^4-\frac{77}{2{,}211{,}840}\left(\frac{a_i}{p}\right)^8}$$

$$a_i/p<3 \qquad (88)$$

And for $a_i/p\geq 3$ the function $\varphi\left(\frac{a_i}{p}\right)$ follows from equation 81:

$$\varphi\left(\frac{a_i}{p}\right)=8\sqrt{2}\pi^2\left(1-\frac{1}{\frac{a_i\sqrt{2}}{p}}\right)\Big/\frac{a_i}{p} \qquad (89)$$

$$\frac{a_i}{p}\geq 3$$

Returning to the heat generation it can be expressed as

$$P_{\max}=29.86A(\mu f10^{-9})(I_{\text{eff}}n)^2 \qquad (92)$$

Appendix V. Definitions of Symbols

A = total area of subdivided charge, in square centimeters
a = radius of nonsubdivided charge, centimeters
a_i = radius of bars in subdivided charge, centimeters
B = induction, peak value of sinusoid, gausses
d = distance of a point inside of charge to surface, centimeters
E = voltage, peak value of sinusoid, volts
f = frequency of inductor current, cycles per second
$f(a/p)$ = a function of (a/p)
H = magnetic intensity, peak value of sinusoid, oersteds
I = current, peak value of sinusoid, amperes
I_{eff} = current, rms value, amperes
i = number of bars in subdivided charge
$j=\sqrt{-1}$
K = current density of eddy currents, peak value of sinusoid, amperes per square centimeter
l = length of line over which integral is taken
n = number of turns of inductor per centimeter axial length
P = power, average value, watts
p = penetration, centimeters
s = surface over which integral is taken, square centimeters
t = time, seconds
V = induced voltage in charge, peak value of sinusoid, volts
W = generated heat, average value, watts per cubic centimeter
ϵ = base of natural logarithms, 2.71828
μ = permeability, unity
π = 3.14159
Φ = magnetic flux, peak value of sinusoid, maxwells
$\varphi(a_i/p)$ = a function of a_i/p
ρ = resistivity, ohm-centimeters
ω = angular velocity, radians per second

References

1. The Induction of Currents in Cores, O. Heaviside. *Electrician* (London, England), volume 12, May 3, 1884, page 533.

2. A Treatise on the Theory of Alternating Currents (book), A. Russell. Cambridge University Press, 1904. Volume 1, page 368.

3. Surface Heating by Induction, H. F. Storm. AIEE Transactions, volume 63, 1944, October section, pages 749–55.

4. Electric Circuits (book), Staff, Massachusetts Institute of Technology. John Wiley and Sons, Inc., New York, N. Y., 1944. Page 37.

5. Industrial Electric Heating, N. R. Stansel. *General Electric Review*, volume 39, number 9, September 1936, page 440.

6. Efficiency of Induction Heating Coils, G. H. Brown. *Electronics*, volume 17, number 8, August 1944, page 124.

7. Design of Induction-Heating Coils for Cylindrical Nonmagnetic Loads, J. T. Vaughan, J. W. Williamson. AIEE Transactions, volume 64, 1945, August section, pages 587–92.

8. Induction Heating of Moving Magnetic Strip, R. M. Baker. AIEE Transactions, volume 64, 1945, April section, pages 184–9.

Application of the Ohm and Mho Principles to Protective Relays

A. R. van C. WARRINGTON
MEMBER AIEE

THE mho relay unit was first used 15 years ago as the directional unit for an early-type reactance relay. Thus it can be said that "mho" applied to relays is a new term applied to an old principle. The mathematical justification for the term has been given in a paper[1] describing the use of the mho unit in a carrier-current relaying scheme. The mho unit in its present form is a directional impedance unit whose accuracy is comparable with that of the reactance ohm unit used in a distance relay.

The mho characteristic (Figure 1C) is suited ideally for protecting long or heavily loaded transmission lines because it is much less likely to trip on power swings than the conventional reactance or impedance relays. Another desirable feature is that a relay for phase faults should operate only on faults involving the phase pair with which the relay is associated; all other faults or system conditions should not affect it. In Figures 1A and 1B, the large tripping area of the impedance characteristics of the impedance and reactance relays shows that these relays are susceptible to power swings and faults in other phases (denoted by asterisks), whereas the snug fit of the mho circle around the fault area in Figure 1C indicates that the mho relay effectively prevents tripping for power swings and for any faults but those for which the relay is set to trip.

The fact that the mho unit combines sensitive directional action with accurate ohmic measurement means that one mho unit does what two conventional units did before. This not only eliminates the contact races that can occur between the directional element and the measuring element but obviously simplifies the circuits to which the relay is applied.

With these advantages it might appear that the mho unit should be used universally for all applications involving distance measurement. This is generally true, but there is a lower limit of impedance for which it can be set for reasons discussed later. Lines too short for the mho unit still must be protected by the reactance ohm unit.

Several new relays will be described, some of which use ohm units and mho units to perform existing relay functions more efficiently and others to perform some new functions. In order to understand the operation of these new relays, it may be helpful first to consider briefly their operation and to compare their pickup characteristics on the impedance diagram.

Relation Between Ohm and Mho Units

First of all, it should be understood that ohm units and mho units are merely refinements of the straight impedance relay. All distance relays measure the distance to a fault by comparing the current in the faulted circuit with the potential across it. In the impedance relay, this is done by opposing the torques of two electromagnets, one having a current winding and the other a potential winding (Figure 2A). The impedance measured by such a relay is not always a true measurement of distance, however. On short lines the additional potential drop in an arcing fault tends to prevent the impedance relay from operating, and on long lines, the current may be high enough under load or power swing conditions relative to the voltage to present to the relay an impedance as low as that of a fault and cause undesirable tripping.

This difficulty can be overcome largely by the use of the product-type relay whose torques are not proportional to current and voltage alone but to the products of I and E with a third quantity which, being common to both, does not affect the ratio balance E/I but provides phase-angle discrimination. This is shown schematically in Figures 2B and 2C.

The flux from the additional pair of poles (shown vertically in Figures 2B and 2C) acts in much the same way as the current or potential polarizing flux in a directional ground relay, and for want of a better name it will be referred to in the following as a polarizing flux.

The current polarizing flux in Figure 2B goes from the upper I pole through the induction cylinder and the central core iron stacking to the lower I pole and induces a current in the cylinder which flows perpendicular to the plane of the paper up and down the sides of the cup opposite the other two poles. The current opposite the operating pole I reacts with the flux from that pole to produce an I^2 torque tending to close the relay contacts, and the current in the cylinder near the E pole reacts with the flux from that pole producing an EI torque tending to keep the contact open.

In the following paragraphs, it will be shown that the provision of what we have called polarizing poles not only overcomes the above difficulties of distance measurement but provides some interesting new applications. Figure 3 shows the general construction of a high-speed product-type unit, the 4-pole induction cylinder unit.

Current Polarization (Ohm Units)

The torque is the product of the current polarizing flux times the fluxes from the opposed I and E poles. Hence the equation for the operating point, which determines the pickup characteristic, is

$$I[KI - E\cos(\phi - \theta)] = 0 \qquad (1)$$

where K is a winding constant, ϕ is the phase angle of the protected circuit, and θ is the angle of the relay characteristic.

Dividing through by I^2 and rearranging the terms, the equation becomes $Z\cos(\phi - \theta) = K$. Thus the current polarizing winding makes the relay respond to impedance only at a particular angle which is determined by the phase angle of the potential circuit of the relay. For example, a simple 4-pole induction cylinder unit with a current polarizing winding, reacting with a current operating pole and a potential restraining pole, operates on a component of impedance 20 degrees more leading than resistance. Such a relay (Figure 4) has been used as a blinder[2] for preventing other protective relays from tripping during very severe power swings. Two such ohm units, polarized in opposite directions, can be connected through auxiliary relays so as to detect an out-of-step condition after the first half swing period.

Adding a capacitor to make the potential circuit of the aforementioned unit at unity power-factor makes $\theta = 90$ degrees in the pickup equation, which becomes $(E/I)\sin\phi = K$ or $X = K$. In other words, the relay operates on reactance (Figure 5).

The reactance relay is used where the

Paper 46-38, recommended by the AIEE committee on protective devices for presentation at the AIEE winter convention, New York, N. Y., January 21–25, 1946. Manuscript submitted November 26, 1945; made available for printing December 18, 1945.

A. R. VAN C. WARRINGTON is in charge of application of protective relays, General Electric Company, Philadelphia, Pa.

arc resistance is likely to be comparable with the impedance of the protected section and hence likely to interfere with the operation of the impedance relay. The reactance relay ignores the arc resistance and hence is indispensable for short lines and for protecting against ground faults.

Potential Polarization (Mho Units)

With potential polarization, the torque is the product of the potential-polarizing flux times the fluxes from the opposed I and E poles. Hence the equation for pickup is

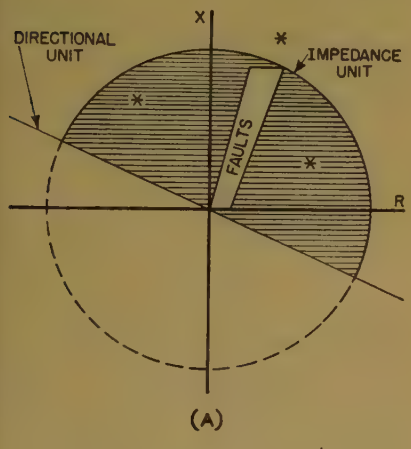
$$E[I\cos(\phi-\theta)-K'E]=0 \qquad (2)$$

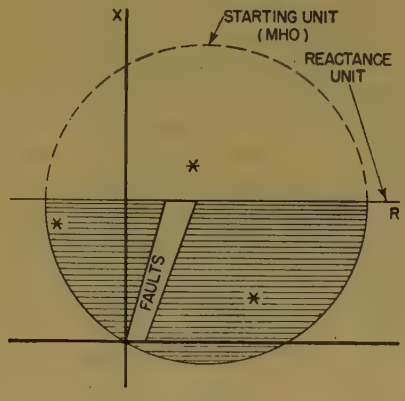
or $-K'E^2+EI\cos(\phi-\theta)=0$. Dividing through by E^2 and putting the K' term on the right, we get $Y\cos(\phi-\theta)=K'$, which is a straight line on an admittance diagram and thus represents a constant component of admittance, that is, the relay will pick up at a constant value of mhos at a certain angle and therefore has been called a mho unit. This is parallel to the case of the ohm unit which picks up at a constant component of impedance, as shown in the impedance diagram of Figure 4A.

It is generally more convenient to plot distance-relay characteristics on an impedance diagram. The impedance equation of the mho unit is obtained by putting the EI term on the right side of the equation and dividing through by $K'EI$, which gives $Z=(1/K')\cos(\phi-\theta)$.

This is the equation of a circle, of diameter $1/K'$, which passes through the origin (Figure 6A). The impedance characteristic of a mho relay is therefore a circle passing through the origin.

The fact that the characteristic passes through the origin means that the unit is inherently directional. The phase angle of the relay characteristic is the angle θ between the diameter of the impedance circle and the R axis. By making θ equal to or a little less lagging than ϕ, the phase angle of the line, the circle is made to fit very closely around the fault area so that the relay is less sensitive to power swings and hence valuable for the protection of long or heavily loaded lines.





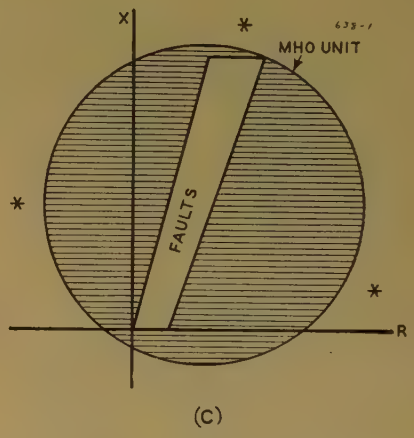


Figure 1. Tripping characteristics

A. Impedance unit
B. Reactance unit
C. Mho unit

The relays trip in the shaded area. Crosses are conditions for which tripping is undesirable

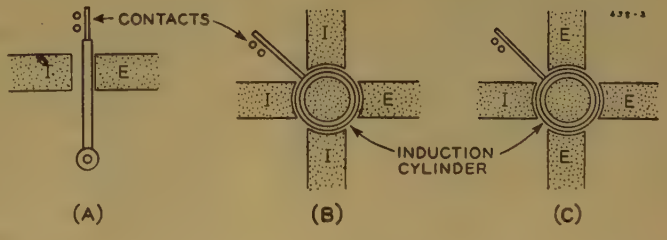


Figure 2. Schematic diagrams

A. Impedance unit
B. Ohm unit
C. Mho unit

Offset Mho Circle

Since both the terms of the equation of the mho relay contain E, it would appear that the relay has zero torque when the potential is zero, as for a bus fault. This shortcoming is avoided in an instantaneous mho relay by providing memory action in the polarizing circuit which maintains the relay polarizing voltage E_{pol} for a few cycles after the line voltage has disappeared, but does not affect the ohmic characteristic. This will be apparent from the torque equation

$$E_{pol}[I\cos(\phi-\theta)-K'E]=0 \qquad (3)$$

Memory action cannot be made to last long enough for the time-delay backup step, but the torque can be maintained in this case by adding torque caused by current alone. The functions of the third step of a distance relay are usually to start carrier blocking and to control the backup time-delay trip. Memory action is used to provide initially high torque to ensure starting carrier very promptly and the contacts are held closed after the expiry of the memory action by the current torque. The introduction of the current torque puts the KI^2 term back into the equation of the mho unit, thus making it the general equation

$$KI^2-K'E^2+EI\cos(\phi-\theta)=0$$

(See Appendix I.)

The offset is secured by adding to the

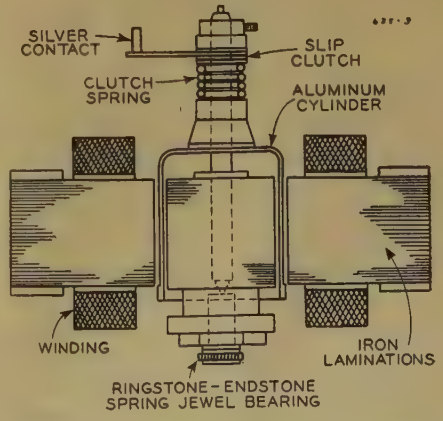


Figure 3. Schematic diagram of 4-pole induction cylinder unit

line potential a biasing potential, IZ_b, proportional to the current, which has the effect of moving the characteristic impedance circle bodily by an amount Z_b. Substituting $E+IZ_b$ for E in the equation for the mho relay, we get

$$-K'(E+IZ_b)^2+(E+IZ_b)I\cos(\phi-\theta)=0 \quad (4)$$

Dividing through by I^2, the equation becomes

$$-K'(Z+Z_b)^2+(Z+Z_b)\cos(\phi-\theta)=0$$

or

$$Z=\frac{\cos(\phi-\theta)}{K'}-Z_b \quad (5)$$

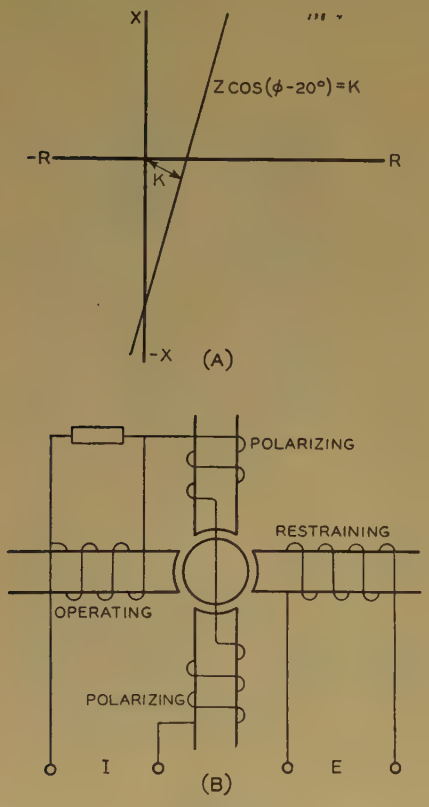


Figure 4

A. Characteristic of ohm unit (blinder)
B. Schematic connections of ohm unit

This shows that the characteristic circle is the same as before except moved through an impedance Z_b (see Figure 7A).

Figure 7B shows how the offset of the mho unit is obtained by introducing, in series with the supply potential, a biasing potential that is obtained from a reactor in the current circuit. Every point on the impedance characteristic of the unit thereby is moved through an impedance equal to that of the reactor. In order to reduce the burden imposed on the current transformers by the reactor, it is provided with two windings. The primary winding with few turns is in the current circuit, and the secondary winding with many turns is in the potential circuit. It is thus a contraction of a transformer and a reactor and is called a transactor.

This offset characteristic is particularly useful for out-of-step blocking because, with the opening of circuit breakers after a fault and hunting between two or more groups of machines, the impedance "seen by the relay" may approach the relay characteristic at almost any angle. Hence the only sure way of initiating out-of-step blocking is by a relay whose characteristic entirely surrounds the characteristic of the tripping relay as shown in Figure 8A.

Relays Using Polarized Impedance Units

A typical form of the polarized impedance unit is the 4-pole induction cylinder unit, which is illustrated in Figure 3 and has been used for ten years in the type GCX reactance relay. The front and back poles are respectively the current operating and potential restraining. The fluxes from these poles produce torque on the induction cylinder by reacting with the currents induced in the cylinder by the flux from the side poles which have the polarizing windings. Another sinusoidal torque is produced by the flux from the polarizing poles reacting with the currents in the cylinder induced by the operating and restraining poles. The second torque is equal to the first and displaced 90 degrees from it in time so that the total torque is not sinusoidal but continuous. This is one of the most valuable features of the induction cylinder and induction disc units and is an advantage not enjoyed by any other relay units. The pickup and dropout of induction cylinder units are practically the same, and their characteristic circles are very close to geometrical perfection.

These units are available in three forms: the current polarized (ohm) unit, the potential polarized (mho) unit, and the offset mho unit in which the potential is biased from the current circuit. In the following paragraphs, uses of these units will be discussed.

Applications of the Mho Unit

One-Step Distance Relay

The simplest application requires a single-step mho relay, type CEY, one per phase. The mho units trip instantaneously and are usually set to cover 90 per cent of the protected section. Backup protection for the neighborhood of the next bus can be provided by the mho type IBCV directional overcurrent relay to be described.

The instantaneous tripping zone provided by the single-step mho relay is superior to that of instantaneous overcurrent or single-step impedance protection because:

1. It is inherently directional, so that only a single contact appears between the battery and the trip coil, which is the ultimate in simplicity and reliability.

2. It is insensitive to offset waves; hence it can be set to cover more of the protected section without risk of overreaching.

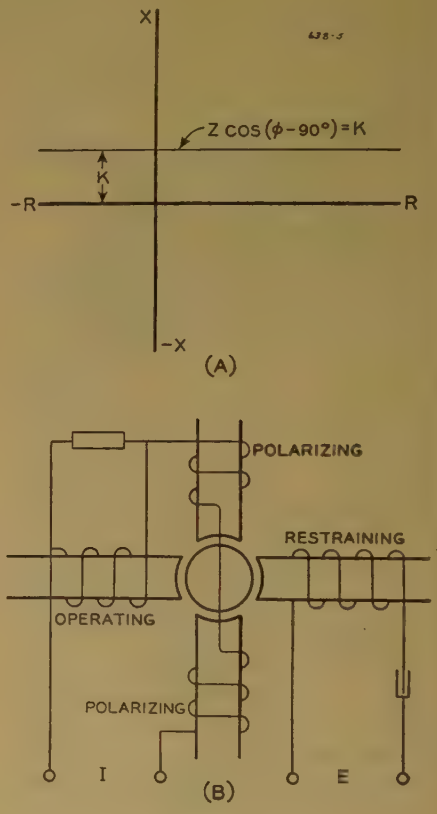


Figure 5

A. Characteristic of reactance unit
B. Schematic connections of reactance unit

3. Its distance reach is not affected by variation in generation as an overcurrent relay would be.

4. It is relatively insensitive to power swings.

Directional Time Overcurrent Relay

Conventional overcurrent relays will not clear faults during periods of minimum generation if the short-circuit current then is less than the maximum load current with maximum generation, unless the settings of the overcurrent relays are changed between maximum and minimum conditions.

The substitution of a mho unit for the conventional directional unit solves this difficulty by permitting overcurrent settings of less than normal load to be used all the time. In other words, if the directional relay has a voltage restraint, it becomes a mho unit and will not operate nor, with the usual directional control arrangement, permit the overcurrent unit to operate unless the impedance presented to the relay falls sufficiently to indicate a fault on the line.

A widely used type of directional overcurrent relay has an induction cylinder directional unit with alternate potential and current coils around the cylinder. It

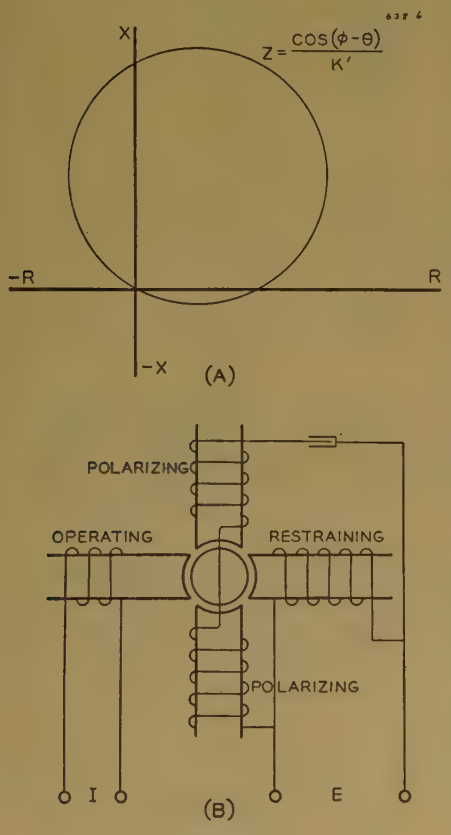


Figure 6

A. Characteristic of mho unit
B. Schematic connections of mho unit

is necessary only to replace some of the current coils with potential coils to provide an E^2 restraining torque, while the remaining coils provide the EI directional torque and thus, change the directional unit into a mho unit.

The directional overcurrent relay with this mho characteristic can be provided with current taps from $1^1/_2$ to 6 amperes on the overcurrent unit instead of the usual 4- to 16-ampere taps. The more sensitive overcurrent settings permit operation on low-current faults, and faster operation can be obtained on heavy faults.

Three-Step Distance Relay

The conventional distance relay consists of a directional unit, a timing unit, and one or more distance measuring units. An instantaneous step and two time-delay steps are usually provided, the three steps being controlled in distance reach either by three distance measuring units (reactance, impedance, or mho) or by one unit whose distance reach is increased in steps by the timing unit.

The first zone unit is used for instantaneous tripping of faults up to 10 per cent from the remote end of the protected section. The second zone unit clears faults in the neighborhood of the next bus in a delayed time, and the third zone provides backup protection for the relays and breaker in the next section beyond.

Reactance Distance Relay

A typical 3-step reactance relay, type GCX, has essentially a mho unit for the directional unit so that it provides the third step of measurement. The normal setting of the reactance unit controls the first step. If the fault is beyond the range of the first step, the timing unit changes the setting of the ohm unit after a time delay to increase its reach and provide a second step.

Mho Distance Relay

A typical 3-step mho relay, type GCY, is described in a companion paper.[3] It has three mho units per phase, M_1, M_2, and OM_3, for measuring the three zones and employs a separate timing unit. No directional unit is necessary because each mho unit is inherently directional. This factor provides more effective backup than where all the units depend upon a common directional unit; it also simplifies the circuit and reduces the number of contacts in the trip circuit. Figure 9 shows schematically the d-c tripping connections for one phase. It can be seen that the zone 1 mho unit, M_1, trips directly so that only a single relay contact is required between the battery and trip coil, which is the ultimate in simplicity and reliability.

The third-step mho unit, OM_3, of the GCY relay has a transactor which can offset its impedance characteristic so that it overlaps the origin, as shown in Figure 7. If polarized in the same direction as the first and second steps, M_1 and M_2, the OM_3 unit can be used for out-of-step detection as well as for time-delay backup protection on lines in which the electrical center of the system is located. The out-of-step condition is detected by making the OM_3 impedance characteristic concentric with the M_2 characteristic, as shown in Figure 8, and somewhat larger, so that the changing impedance seen by the relays during a power swing will always operate the OM_3 unit before the M_2 unit. The OM_3 unit then is arranged to pick up an auxiliary relay with a small time delay; blocking is prevented on faults because the M_2 unit de-energizes the auxiliary relay if the OM_3 does not operate first by the margin of the pickup time of the auxiliary relay. The auxiliary relay generally is arranged to pre-

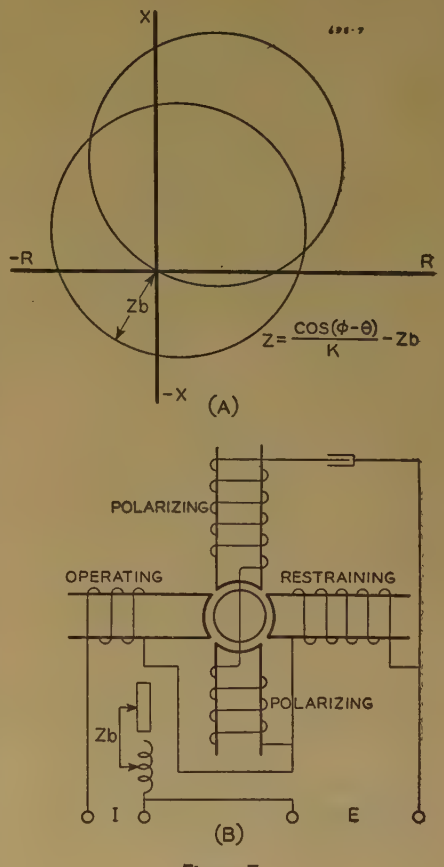


Figure 7

A. Offset mho characteristic
B. Schematic connections of offset mho unit

vent automatic reclosing after a trip on out-of-step conditions but can be used to prevent tripping. It should be remembered, however, that this is necessary only if the relay characteristic circle includes the electrical center of the system, because a mho unit will not trip on out-of-step unless its characteristic is cut by the power swing locus.

In the application of distance relays the first two zones are primarily intended to operate for faults in the protected line section only. Hence they are required to be directional and to operate only for

fault current flowing into the protected line.

The third zone of the distance relay is used for backup protection. As such, it operates only in cases of failure to isolate a fault on some other line section than the one covered by zone 1 and zone 2. Past practice has been to set the third zone element at A of the relays on line AB so that it would operate for a fault at C (see Figure 10A). This meant that the ohmic setting has to equal the line ohms from A to C plus the apparent increase in ohms caused by any fault current fed in at B. Where the line AB is long in terms of secondary ohms, this often resulted in

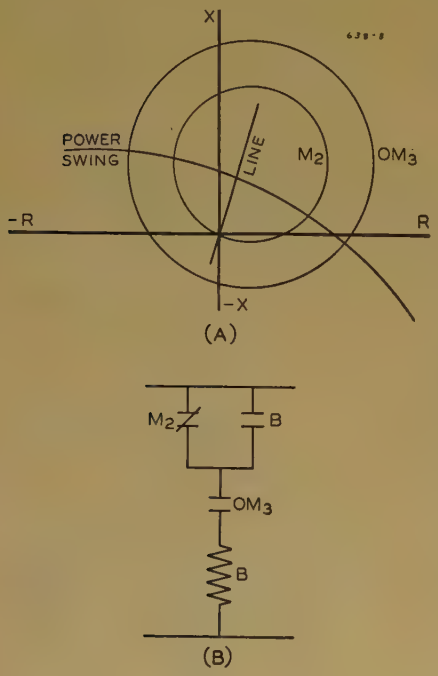


Figure 8

A. Out-of-step blocking with offset mho unit
B. D-c connections of blocking unit

an ohmic setting that would not permit emergency loads to be carried.

With mho relays, since each unit is inherently directional, the third zone tripping direction may be the same as or opposite to that of zone 1 and zone 2. Hence where a third zone setting would be too high in ohms if set in the same direction as zone 1 and zone 2, considerably better settings can be obtained by reversing zone 3. When this is done, the zone 3 element at B on line AB is set to operate for faults at C. The setting in ohms of each zone-3 element is decreased by the impedance of line AB by this reversal, while the over-all protective coverage remains the same. There is no loss of backup protection, since in either case, faults in lines BC or AD result in opening line AB if these faults last for the duration of zone 3 time. In one case, a fault near C opens the breaker at A; in the other case, the breaker at B opens.

It will be seen from Figure 10B that with backup provided by the relay nearest the fault, tap lines in the unfaulted sections will remain in service, whereas with the conventional method of backup, they are lost. On the other hand, it must be understood that failure of the d-c supply or the a-c potential supply could, if it remained undetected, prevent the backup relay from operating, but the conventional backup from the next station would not be affected by this condition. The degree of possibility of such a condition must be weighed against the advantage of improved backup operation when the d-c supply and a-c potential are available.

To summarize, with long lines, adequate backup coverage of the next section often requires such a high ohmic setting for zone 3 in the conventional direction that it may operate on power swings and emergency overload conditions. Hence it is generally advantageous to reverse the zone 3 unit for long lines, especially where some of the sections have tap lines.

Also, where the mho relay is used with carrier, the OM_3 unit must be polarized in the reverse direction from the M_1 and M_2 units because carrier blocking is required only for external faults.

In the case of no tapped lines and no carrier, a check can be made graphically to determine whether the OM_3 unit may operate on power swings and hence whether it is necessary to reverse it. This procedure is described in Appendix II. In such cases a separate offset mho unit is required for out-of-step detection.

Offset Mho Relay

The single-step mho relay can be given an offset characteristic by providing it with a transactor, as described under the heading "Offset Mho Circle." It can be used for out-of-step blocking or backup protection in the same way as has been described for the OM_3 unit of the GCY 3-step distance relay.

When line-to-line faults are not cleared promptly, a power swing may start, and until the fault is cleared, there will be an asymmetrical condition wherein the impedance presented to the relays will be different in each phase. This impedance is a combination of the single-phase impedance of the fault and the balanced 3-phase impedance of the swing. If the relay happens to be connected in the faulted pair of phases, it will measure only the impedance to the fault because the power swing components of current cancel out in the faulted phase pair because of the double current windings of the mho unit. In one of the two remaining phase pairs, the fault current adds to the power swing current and in the other it subtracts from it, so that the impedances measured will be different.

When a power swing follows a fault that has been cleared promptly, it presents a balanced 3-phase condition almost at its inception and certainly before it can operate any out-of-step blocking relays.

For these reasons only one out-of-step blocking relay is required when the system is protected by high-speed relays and breakers, and it can be connected in any phase pair. On the other hand, on systems protected by slow-speed relays and breakers, it is advisable to connect an offset mho unit in each phase so as to ensure recognition of the out-of-step condition and to initiate the blocking as early as possible.

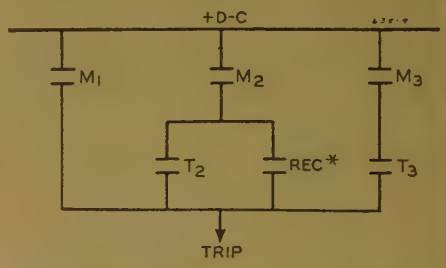


Figure 9

D-c connections of 3-step distance relay

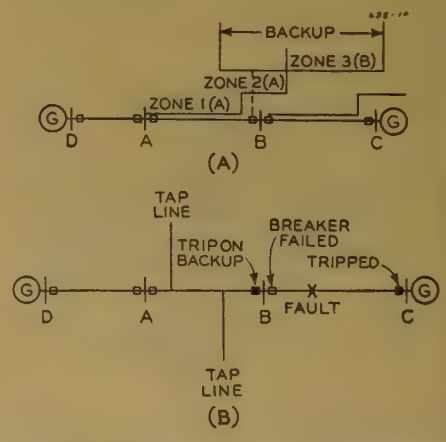


Figure 10. The reversed backup characteristic

A. The time zones
B. Tap lines saved

Applications of the Ohm Unit

Bus Protection

Where a bus section is separated from other circuits by reactors, as shown in Figure 11A, reactance ohm units have

been used to provide protection for the generators and for the bus. Each generator has a reactance ohm unit set to reach into, but not beyond, any of the bus-tie or feeder reactors. A fault in a generator will be cleared immediately because its ohm unit will measure reactance in the reversed direction. A fault on the bus will disconnect all the generators because it will be within the ohm settings of their ohm units.

The main difficulty of conventional differential bus protection is the balancing of the current transformers in all the circuits around the bus to ensure that there is no current to operate the relay during an external fault. This difficulty does not appear with the ohm units because they are connected only to the current transformers in the generator leads.

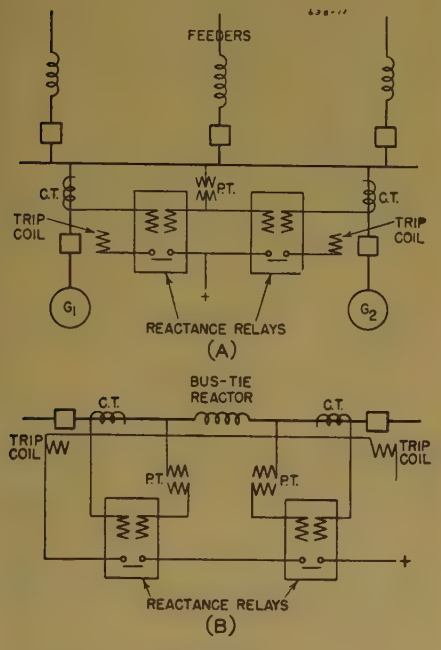


Figure 11

A. Ohm units protecting a bus and generators

B. Ohm units protecting a bus and bus-tie reactor

This form of protection also has been used for bus-tie reactors. Each reactor is protected by two reactance ohm units (Figure 11B) with their contacts in series. The ohm units are polarized away from the reactor so that a fault in the reactor is in the reverse direction for both of them and causes them both to trip and isolate the reactor. A fault on the bus also causes them both to trip and isolate the reactor. In addition, a fault on the bus causes both ohm units to operate, one because it is within its ohmic setting and the other because the fault appears to it in the reverse direction.

Blinders

One application of the ohm unit is to extremely long lines where even the mho unit is not immune to tripping on power swings because the mho circle has to be large in order to cover the long line. In such a case, the straight line characteristic of the ohm unit may be arranged parallel with the line impedance vector so as to cut off one or both sides of the tripping characteristic (Figure 12A) and confine the tripping zone to a strip wide enough to permit tripping on arc resistance.

This scheme was the first attack on the problem of relaying long or heavily loaded lines[2] and is applicable to any form of relay including overcurrent relays. In most applications only one blinder is necessary because the major flow of power generally is in one direction. It is only on interconnections where the maximum power flow is the same in either direction, that two blinders are necessary.

Out-of-Step Tripping

When synchronism is lost, the impedance measured by a relay will pass through the line impedance vector from right to left if the relay is located at the leading or fast end of the system and from left to right if at the lagging end. Two blinders are arranged to operate an auxiliary relay if the impedance crosses the characteristic of one of them before the other, in either direction. This auxiliary relay can be arranged to operate an alarm, trip a breaker, or initiate some form of control.

The advantages of this form of out-of-step relay are:

1. Its operation is not affected by variation in the location of the electrical center of the system.

2. It will not trip under any fault conditions.

3. It trips instantly after the first half cycle of system oscillation. Existing relays require the machine to slip several poles before they will operate.

4. Distinction can be made between speeding up and slowing down of the local generation.

A single-phase relay is adequate for tripping on out-of-step because the regular protective relays will trip during a fault. If the swing continues after the fault has been cleared or if the swing was caused by switching of load or generation without a fault, only a single-phase out-of-step relay is required for tripping because all three phases act similarly.

Reclosing

By means of auxiliary relays, reclosing is prevented after a time-delay trip and after a trip on loss of synchronism. The first is accomplished by an auxiliary relay whose coil is energized whenever the tripping circuit is completed through the timing unit contacts and whose contacts open the reclosing circuit; the connections of this relay are shown in Figure 5 of the companion paper.[5] The second is accomplished by an offset mho unit in a manner already explained earlier in this paper under the heading "Mho Distance Relay."

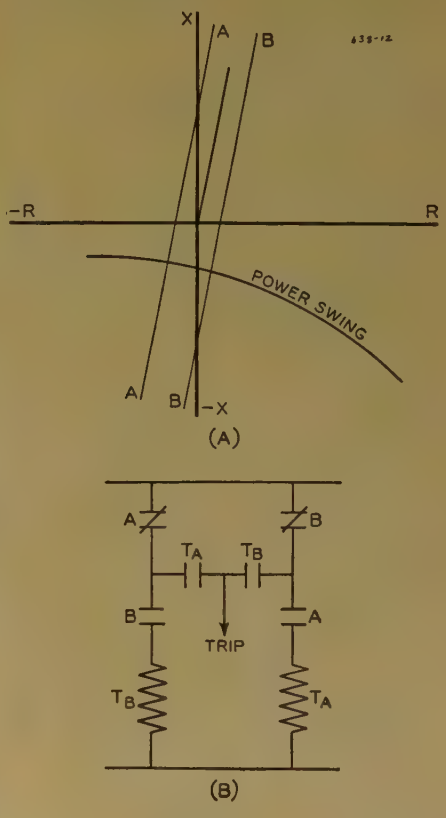


Figure 12. Characteristics of a pair of ohm units for out-of-step tripping

Carrier Relaying

The application of ohm relays to carrier has been discussed in previous papers. The use of mho relays for carrier is the same in function, but the self-contained directional and power swing blocking features of the mho unit simplify the d-c circuits very considerably (Figure 9) and minimize the possibility of sneak circuits.

Mho carrier alone was described in an earlier paper. When carrier is added to mho distance relays, it is necessary only to add two relays containing ground directional and carrier auxiliary elements. The

chief difference between the addition of carrier to mho distance relays and to impedance or reactance relays is the use of the reversed offset mho unit instead of the impedance unit for starting carrier. Figure 13 shows how the QM_3 unit of the 3-step mho distance relay can provide the necessary blocking on external faults with the minimum tendency to operate on power swings and heavy loads.

The OM_3 unit is extremely fast for an induction-type unit. Its minimum time is one-fourth cycle. The time with an average fault is about one-half cycle. This provides a considerable margin of safety between the starting of carrier by the OM_3 unit and tripping for an external fault by the M_2 unit of the relay facing the fault.

Limitations of Ohm Units and Mho Units

For distance-relay applications, the phase angle of the ohm relay is adjusted to make it measure reactance and ignore the resistance component, and, hence, make it indispensable for very short lines where the arc resistance may be comparable with the line impedance. Like the impedance relay, the reactance relay requires a directional unit; this unit is usually of the mho type and also serves as a backup for remote faults. The reactance relay is applicable to lines not subject to overload or power swing conditions which present an impedance low enough to cross the relay characteristic. Whether this will occur can be found only by calculation of the swing impedance. If the system arrangement can be simplified to a 2-machine problem, Appendix II describes a simple construction for plotting the swing impedance.

The phase angle of the mho relay can be adjusted to be approximately the same as that of the line. This ensures the smallest reach at right angles to the line impedance vector, and hence the least tendency to operate on power swings that may be expected on long lines and on heavily loaded lines of medium length. The potential polarizing winding of the mho relay limits its application to long lines because, even with memory action, the torque is likely to be low on very short lines during second zone fault, after the memory action has expired.

Arc resistance also places a limit on the shortness of a line to which the mho unit can be applied. Arc resistance increases as the current decreases and becomes more effective on shorter lines. This is in the same direction as the other limitation of minimum voltage to provide adequate

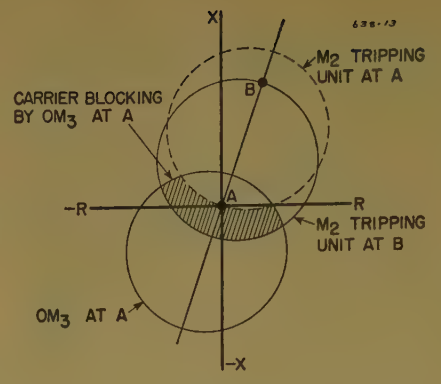


Figure 13. Carrier blocking with offset mho unit

torque. Since the arc resistance limitation is more severe, we shall consider it in detail.

Minimum Length of Line

From the ohmic characteristics in the companion paper[3] on the "Mho Distance Relay," it will be seen that the accuracy of the GCY relay is within ten per cent variation down to eight volts at the relay terminals. This means that if the instantaneous zone is set to cover 90 per cent of the protected section, it may cover only 81 per cent of the section if the section is so short or the fault current is so small that the IZ drop is only eight volts secondary. Although in many cases a greater variation may be permissible, this value will be taken for the purpose of establishing a limit. It should be realized, however that this value has no relation to the ability of the relay to operate reliably on faults within the protected zone because the actual pickup of the relay is around $1\frac{1}{2}$ volts.

Hence for accurate operation, IZ equals eight volts at the relay terminals for a fault at the ohmic setting of the M_1 unit. From this fact, we can determine the minimum line length and fault current for which the relay can be set. Changing to primary phase to neutral values, we have $IZ = 8R_p/\sqrt{3}$, where I is the minimum fault current, Z the ohmic setting of M_1, and R_p is the ratio of the potential transformers. If M_1 is set to cover 90 per cent of the protected section, which is L miles long and has an impedance of 0.9 ohm per mile, then

$$I \times 0.9 \times 0.9L = \frac{8{,}000 \text{ kv}}{115\sqrt{3}}$$

or

$$L = \frac{50 \text{ kv}}{I} \text{ miles}$$

In other words, the relay is applicable to lines down to a minimum length of 50 kv/I miles, where I is the minimum fault current, and kv is line-to-line voltage in kilovolts.

Arc Resistance

The presence of arc resistance will reduce the reach of the mho relay. A small reduction of the instantaneous zone is acceptable, but the intermediate zone always must reach beyond the next bus, that is, faults within the section must not trip in zone 3 time, or selectivity between stations will not be possible.

In Figure 14A, R is the arc resistance, Z is the impedance of the protected section, ϕ is its phase angle ($\tan^{-1} X/R$), and K is the fraction of Z by which the second zone mho unit M_2 reaches beyond the end of the section. It is assumed that the mho unit characteristic is given the same angle ϕ as the line.

The circle in Figure 14A is the characteristic of a mho unit used for the second distance step and is assumed to reach a short distance beyond the end of the protected section. It is noted that

$$a^2 + b^2 = (\text{diameter})^2$$

therefore,

$$R^2 + K^2Z^2 - 2KZR\cos\phi + R^2 + Z^2 + 2ZR\cos\phi = (Z + KZ)^2$$

$$2R^2 - 2KZ^2 + 2RZ(1-K)\cos\phi = 0$$

$$R = \frac{Z}{2}\left[\sqrt{\cos^2\phi(1-K)^2 + 4K} - (1-K)\cos\phi\right]$$

which equals maximum arc resistance to permit zone 2 time or less for all faults within the section.

If M_2 is set for 20 per cent beyond the next bus, $K = 0.2$. Assuming $\phi = 60$ degrees, then, from the formula, $R = 0.29Z$ or $Z = 3.45R$.

The initial arc resistance, assuming 16 kv per foot of insulator string and 440 volts per foot of arc,[4] is

$$R_{arc} = \frac{440}{I_{pri}} \times \frac{\text{kv}}{16\sqrt{3}} \times \frac{115\ C.T.}{1{,}000 \text{ kv}}$$

$$= \frac{1.83}{I_{sec}} \text{ ohms phase-to-neutral}$$

With a fault drawing five amperes secondary, $R_{arc} = 1.83/5 = 0.36$ ohm phase-to-neutral. Since $Z = 3.45R$, from a preceding formula, $Z = 1.24$ ohms for the minimum secondary impedance of a line section that can be protected safely with mho relays.

Where the line impedance is less than 1.24 ohms secondary, each case should be examined individually. If there is a heavy short-circuit current, the arc voltage will be less than 440 volts per foot.

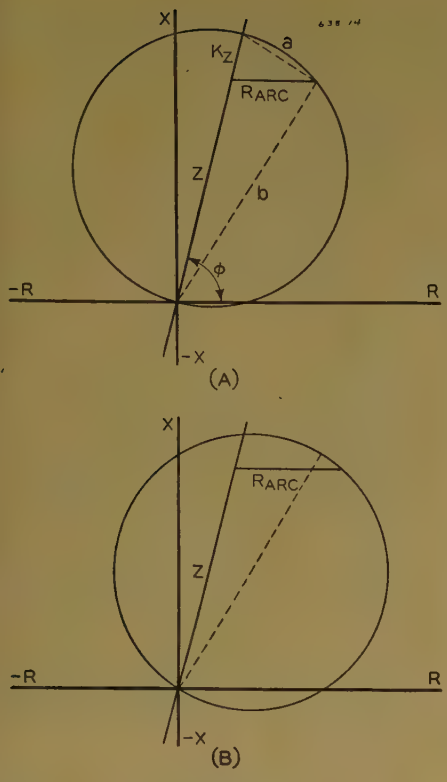


Figure 14

A. Arc resistance shortens reach of mho unit
B. Effect of arc resistance reduced by leading mho characteristic

On the other hand, if the fault occurs near the station, the number of insulators may be higher and the arc resistance proportionately increased; furthermore, at low short-circuit currents, the volts per foot may increase to 600 or 1,000 and should be checked from the formula $R_{arc}=8{,}750L/I^{1.4}$ ohms, where L is the arc length in feet.

If the arc resistance is too high for a reasonable application, some leeway can be obtained on highly lagging lines by setting the mho relay characteristic at a less lagging phase angle than that of the line impedance. This permits more arc resistance anywhere in the section before the relay will fail to pick up (see Figure 14B) or permits the normal application down to one ohm impedance.

Conclusions

The product-type impedance unit is a very useful relay tool whose flexibility enables it to cover the entire field of transmission line protection with simpler circuits and better characteristics than heretofore.

The only limitations to the application of current and potential polarized units are those which prevent either from covering the whole range alone. The natural field for current polarized distance relays is short lines and ground fault protection; interphase faults on long or heavily loaded lines require potential polarized (mho) distance relays.

Appendix I

The characteristic of any ohmic relay on an impedance diagram is a circle. This is because the torque from any form of electromagnetic drive is proportional to the square of the flux or to the product of two fluxes, and the fluxes in turn are proportional to the currents or potentials. The torque[5] of a relay having current and potential windings must therefore be of the form

$$KI^2-K'E^2+EI\cos(\phi-\theta)$$

where K and K' are winding constants, ϕ is the phase angle of the protected circuit, and θ is the angle of the relay characteristic. At the balance point of the relay, the torque is zero and the equation for balance is

$$KI^2-K'E^2+EI\cos(\phi-\theta)=0$$

This general equation of a relay has the two main variables E and I, which can be reduced to one by changing it to an impedance diagram.

Dividing the equation through by $K'I^2$, we get

$$\frac{K}{K'}-Z^2+\frac{Z\cos(\phi-\theta)}{K'}=0$$

Transferring K/K' to the right-hand side and adding $(1/2K')^2$ to both sides, this equation becomes

$$Z^2-\frac{Z\cos(\phi-\theta)}{K'}+\left(\frac{1}{2K'}\right)^2=\frac{1+4KK'}{(2K')^2}$$

This is the equation of a circle of radius $\sqrt{1+4KK'}/2K$, whose center is $1/2K'$ from the origin at an angle θ from the reference vector R (see Figure 15).

The constants K and K' are functions of the turns, and so forth, of the current and potential windings respectively. These constants can be determined from the impedance circle by solving for K and K' in the expressions for the radius and the location of the center. For instance, a 4-ohm circle at 60 degrees with one ohm offset in the direction of the origin has a radius of two and its center is one from the origin. $1/2K'=1$, or $K'=1/2$, and substituting this value in the expression for the radius, $\sqrt{1+4KK'}/2K'$, we get $\sqrt{1+2K}=2$, or $K=3/2$. Hence the equation is

$$\frac{3}{2}I^2-E^2+EI\cos(\phi-60^\circ)=0$$

This equation is typical of the offset mho characteristic in Figure 7A.

Appendix II. Power Swing Check

A simple geometrical construction can be used to determine whether a relay will operate during a swing condition. This method assumes that the system can be simplified to an equivalent system of two machines separated by impedance. It determines the angle between the machines at which the relay will operate. Thus, it can be used to determine whether a reactance or impedance relay should be replaced by a mho relay, whether to reverse the third zone or not, or whether a blinder is needed to prevent the M_1 and M_2 units from tripping on a very severe power swing.

Referring to Figure 16, AB is the impedance of the protected section, SA is the

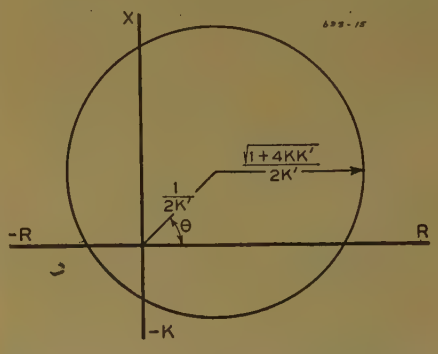


Figure 15. Impedance characteristic corresponding to general relay equation $KI^2-K'E^2+EI\cos(\phi-\theta)=0$

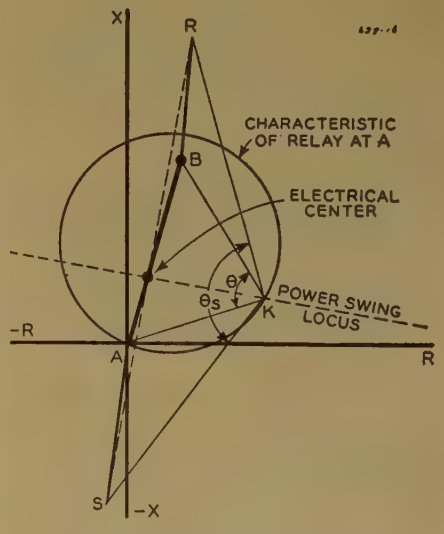


Figure 16. Construction for checking operating point of relay on a power swing

system impedance beyond terminal A, and BR is the system impedance beyond terminal B.

Draw a perpendicular through the midpoint of RS. From the point K where it cuts the relay characteristic, draw lines to R, S, A, and B. RKS is the angle θ_s between the generated electromotive forces at R and S at which the relay at RA will trip. BKA is the angle θ between the terminal voltages at A and B at which the relay at A will trip, and AK is the impedance it sees.

The power swing locus is shown as a straight line. This implies equal generated

The Development, Design, and Performance of Magnetic-Type Power Circuit Breakers

L. J. LINDE
MEMBER AIEE

B. W. WYMAN
ASSOCIATE AIEE

Synopsis: Power circuit breakers for voltage services of 2,300 volts and above use either of two basic principles to complete circuit interruption. The more familiar types, oil breakers or compressed air breakers, complete their operation by maintaining a low resistance arc until the final current zero where interruption is completed. Magnetic air circuit breakers establish a high resistance arc prior to circuit interruptions which modifies the circuit constants before recovery voltage is established. The "Magne-blast" breaker falls in this second class of breakers. The treatment of the arc in this breaker to obtain a high arc resistance is explained in some detail. Also, design practices and operating characteristics of the final magnetic type breaker are reviewed.

IN studying the various types of circuit interrupters in power circuit breakers and the principles on which they operate, it becomes apparent that these interrupters can be placed in one or the other of two classes:

1. Low-arc-resistance interrupters whose arc resistance is maintained low until current zero and then is transformed suddenly into or replaced by a high-resistance dielectric.

2. High-arc-resistance interrupters whose arc resistance is increased gradually to such a high value prior to current zero that arc re-establishment is made impossible following current zero.

Low-Arc-Resistance Interrupters

Power circuit breakers rated 2,300 volts and above generally have functioned as low-arc-resistance interrupters. They are recognized as oil blast breakers, impulse breakers, air blast breakers, and so forth. These breakers interrupt the circuit by drawing a short low-resistance arc in some type of control chamber where a blast of insulating fluid is directed at it. To complete the interruption at current zero, the low resistance of the arc gap must be replaced abruptly by a high-resistance dielectric. This type of interruption can be understood best by reference to the typical oscillograms of a short-circuit interruption shown in Figure 1. In this oscillogram the breaker contacts part at t_0 and the short-circuit current I is interrupted at t_1. During the arcing period $(t_0 - t_1)$, the arc resistance remains so small that the arc-resistance voltage drop e_a at no time rises to more than a few per cent of the generated voltage (shown dotted). The introduction of this low-arc-resistance voltage drop into the circuit does not affect appreciably either the magnitude or the phase angle of the short-circuit current.*

For the circuit to be interrupted as the current passes through zero at t_1, the fluid blast suddenly must increase the low resistance across the contact gap by cooling or displacing the hot ionized arc products to prevent arc re-ignition as the system recovery voltage rises following current zero.

Immediately following current zero at t_1, the voltage across the contacts begins to rise to the system-generated voltage, which at this instant is at its crest (zero power-factor fault). Because of the energy stored in the circuit, the actual voltage appearing across the contacts will rise above the system voltage crest and oscillate about it, as can be seen on the oscillogram in Figure 1, immediately following the current interruption. Figure 2 shows this recovery voltage extended to a microsecond time scale. For the simple single frequency circuit, shown in Figure 3, this frequency is equal to

$$f = \frac{1}{2\pi\sqrt{LC}}$$

The high frequency transient recovery voltage-oscillation superimposed upon the 60-cycle crest voltage causes the total voltage appearing across the contact gap to approach two times the normal crest voltage on the first oscillation. A tangent erected to the first oscillation crest, as shown in Figure 2, determines the rate of rise of recovery voltage. On the highest frequency circuits, this rate-of-rise tangent may equal several thousand volts per microsecond.

The fluid blast in the low-arc-resistance type of interrupter must increase the insulation strength between its contacts immediately following current zero fast enough to withstand this rate of rise of recovery voltage to prevent arc re-establishment after current zero. As the actual rate of rise of recovery voltage encountered in practical applications varies between wide limits, various configurations of low-arc-resistance interrupters have been designed to insure the required fluid velocity to interrupt the highest recovery-rate circuits.

In many breakers using low-arc-resistance interrupters in which the high-velocity fluid blast bodily displaces the low resistance-arc gases, the resistance of the arc gap rises abruptly at current zero to substantially infinity immediately following current zero. These breakers are capable of withstanding rates of rise of recovery voltage higher than any which can be encountered in service and can be duplicated only in the laboratory.

In other breakers using low-arc-resistance interrupters, an auxiliary resistor is inserted into the circuit following the current zero to limit the rate of rise of recovery voltage. Such resistors, shunted into the circuit in parallel with some portion of the contact break, absorb the energy of the transient voltage-oscillations. Applications as now practiced are

---

electromotive forces and no line capacitance. These assumptions simplify the construction and have negligible effect on the angles θ and θ_s at which the relay operates.

References

1. THE MHO CARRIER RELAYING SCHEME, R. E. Cordray, A. R. van C. Warrington. AIEE TRANSACTIONS, volume 63, 1944, May section, pages 228–35.

2. PROTECTIVE RELAYING FOR LONG TRANSMISSION LINES, A. R. van C. Warrington. AIEE TRANSACTIONS, volume 62, 1943, June section, pages 261–8.

3. THE MHO DISTANCE RELAY, R. M. Hutchinson. AIEE TRANSACTIONS, volume 65, 1946, June section, pages 353–60.

4. INTERESTING FACTS ABOUT POWER ARCS, A. R. van C. Warrington. *General Electric Company Relaying News*, January 1941.

5. A CONDENSATION OF THE THEORY OF RELAYS, A. R. van C. Warrington. *General Electric Review*, volume 43, number 9, September 1940.

Paper 46-42, recommended by the AIEE committee on protective devices for presentation at the AIEE winter convention, January 21–25, 1946. Manuscript submitted November 23, 1945; made available for printing December 27, 1945.

L. J. LINDE is with the A. B. Chance Company, Centralia, Mo.; B. W. WYMAN is with the power circuit-breaker division, General Electric Company, Philadelphia, Pa.

*The actual instantaneous values of arc resistance r_a are proportional to the arc length and are an inverse function of arc current because the arc diameter increases and decreases with current. As the short-circuit current approaches zero, r_a will increase proportionately, but the voltage drop in the arc e_a, which equals $i_a r_a$, will remain low.

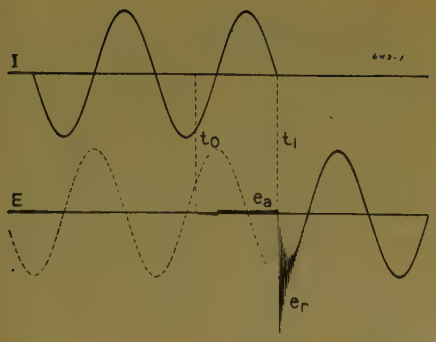


Figure 1. Typical short-circuit interruption by low-arc-resistance type of interrupter (fluid blast) showing high-frequency transient immediately following interruption

E = generator voltage
I = short-circuit current
e_a = arc voltage drop (small on account of low arc resistance)
e_r = transient recovery voltage appearing across contacts of breaker immediately following interruption
t_0 = instant of contact parting
t_1 = instant of circuit interruption

successful in holding the rate of rise of recovery voltage to moderate values, definitely limit the severity of circuit transients, and reduce the rate at which gap resistance must be built up across the contacts.

Such resistors also have proved of value when interrupting faulted circuits to stabilize the clearing of transmission lines, discharging the capacitance charge remaining on the line faster than the generated voltage reverses and thereby preventing possible restriking at the breaker contacts because of excessive overvoltage stresses.[12]

High-Arc-Resistance Interrupters

The high-arc-resistance interrupter, as contrasted with the low-arc-resistance interrupter, builds up a high arc resistance prior to current zero, thereby modifying the circuit current and achieving an early interruption by advancing the current zero to, or near, the recovery voltage zero. The rate of rise of recovery voltage also is held to very low values, a factor which permits the build-up of insulation across the electrodes at the moderate rates achieved by rapid cooling of the arc column. The more successful interrupters of this type are recognized as magnetic-type circuit breakers.

With any magnetic-type air circuit breaker, the arc magnetically is forced to loop away from the contacts and may travel out on diverging arc runners where its length is further increased many times.

As the arc is lengthened and cooled, its resistance increases rapidly so that the resultant resistance voltage drop in the arc column becomes an appreciable percentage of the total circuit voltage. This high-resistance-arc drop has a two-fold effect on the short-circuit current:

1. It reduces the magnitude of the short-circuit current to a fraction of its previous value.

2. It improves the power factor of the circuit bringing the current more nearly into phase with generated voltage, causing the current zero to occur near a voltage zero rather than its normal 90-degree lagging or crest position.

These effects can be seen best by reference to the typical interruption with a magne-blast breaker shown in Figure 4. Here the voltage drop in the arc column rises at a rate of several thousand volts per half-cycle so that the short-circuit current in the last half-cycle is reduced to approximately half its original value. Moreover, the introduction of the arc resistance into the circuit has advanced the current zero from the normal crest point on the generated voltage wave, in this case to approximately one-half crest voltage.

As the instantaneous system voltage at the point of current zero has been reduced greatly, the amplitude of the high-frequency oscillation is reduced correspondingly. This reduction in amplitude of the high-frequency oscillation will reduce the circuit rate of rise of recovery voltage in direct proportion even if the resistance of the arc column were raised to infinity immediately following current zero.

In this type of breaker, however, it has been found that the long hot gaseous post-arc stream between the arc runners im-

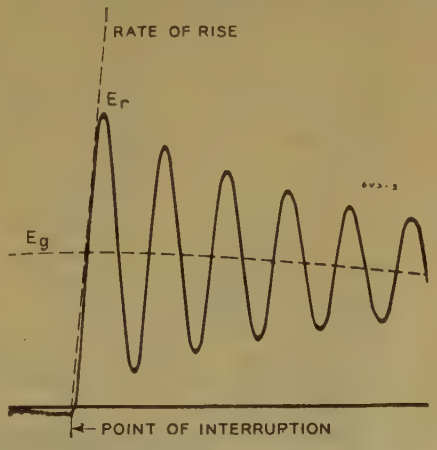
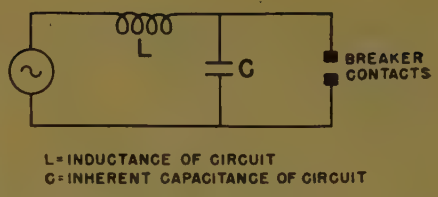


Figure 2. Transient recovery voltage across contacts of low resistance breaker following interruption.

The dotted line tangent to the first oscillation is the rate of rise of recovery voltage



L = INDUCTANCE OF CIRCUIT
C = INHERENT CAPACITANCE OF CIRCUIT

Figure 3. Simple single-frequency test-circuit

$$\text{Oscillating frequency} = f = \frac{1}{2\pi\sqrt{LC}}$$

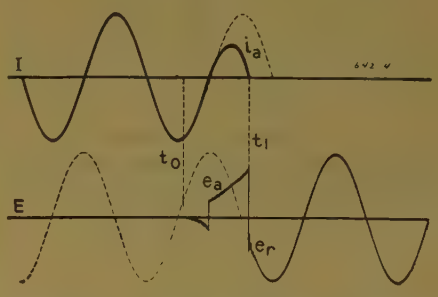


Figure 4. Typical short-circuit interruption by high-arc-resistance type of interrupter (magne-blast) showing high-arc-resistance voltage drop during arcing period which results in marked reduction in both short-circuit current and transient recovery voltage

E = generator voltage
I = short-circuit current
e_a = arc voltage drop (high on account of high arc resistance)
e_r = transient recovery voltage
t_0 = instant of contact parting
t_1 = instant of circuit interruption

mediately following current zero affords an excellent resistor further to damp out recovery voltage-oscillations. Although the resistance of this cooling column of arc gases r_a increases to infinity in a few hundred microseconds after current zero, it is a recovery-rate-limiting resistor just after current zero, fully as effective as the auxiliary resistor used with some types of low-arc-resistance interrupters. The manner in which the pre-current zero arc resistance varies during the current-zero period as plotted from a typical interruption is shown in Figure 5A.

The resistance r_a, of this cooling gaseous column immediately following current zero will vary with

1. The design of the arc chute, which determines the rate of cooling of the hot gases.

2. The magnitude of the current being interrupted, which determines the cross section of the hot gas column.

The initial resistance of this hot gaseous column varies inversely with the short-circuit current being interrupted. This means that the maximum rate of rise of recovery voltage which can appear across the breaker terminals will decrease as the value of short-circuit current is increased. Figure 5B shows how this resistance r_a

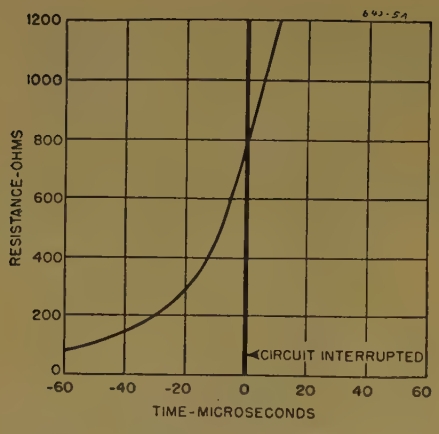


Figure 5A. Increase in resistance of arc column during instant of current zero on an actual interruption by a magne-blast breaker

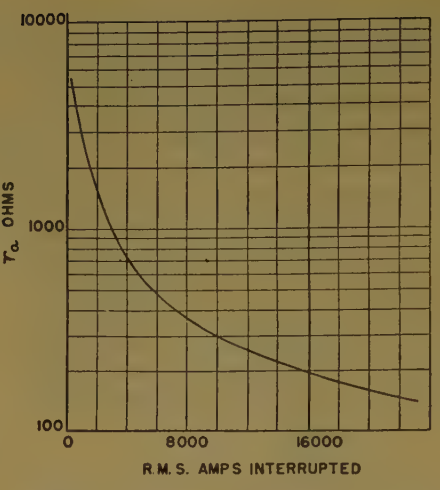


Figure 5B. Variation of arc column resistance r_a following interrupting current zero versus short-circuit current being interrupted

immediately following current zero varies in a 5-kv 100,000-kva breaker.

On circuits having very low inherent capacitance C and high natural rates of rise of recovery voltage, the resistance of this cooling arc column r_a will damp out entirely the oscillating frequency. To do this, the ohmic value of r_a must be less than the critical damping resistance of the circuit, or $r_a < 2\sqrt{L/C}$.

The total effect of the high-resistance-arc type of breaker on the rate of rise of recovery voltage appearing across its terminals may be seen by reference to Figure 6. Here is shown the rise of recovery voltage following an interruption with a magne-blast breaker extended to microsecond scale. For comparison, the dotted curve shows the recovery oscillation which occurs with a low arc resistance interrupting the same circuit at a crest voltage point and without benefit of arc resistance following current zero. Besides the radical reduction in the rate of rise of recovery voltage shown with the magnetic breaker, the first peak of transient recovery voltage-oscillation is reduced from 1.9 times normal crest to 0.35 times normal crest.

The magne-blast breaker has proved that the operation of magnetic air breakers, when properly designed, is independent entirely of natural oscillating frequency or inherent rate of rise of circuit recovery voltage.

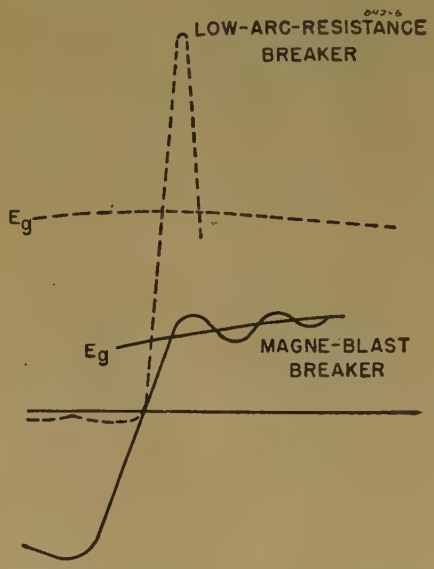


Figure 6. Transient recovery voltage obtained with high-arc-resistance breaker (magne-blast breaker) shown full as compared with transient recovery voltage of low-arc-resistance breaker (fluid blast) shown dotted

Development of High-Arc-Resistance Interrupter Designs

There have been many interesting attempts to develop pure resistance interrupters that might function with little or no arcing. Several years ago the authors made and tested a resistance interrupter designed to interrupt high values of alternating or direct current at 600 volts and to do this with no appreciable arcing. This interrupter (Figure 7) consisted of a stack of graduated wafer-like compound resistances whose composition varied from pure copper, through copper carbon mixes to carbon clays, to a final wafer of fired clay. It was to function much the same as a large rheostat being turned into the circuit. Although the tests on this device demonstrated the need for much improved commutation before arcing could be eliminated at high currents, they did confirm the value of resistance as an interrupter. In a later investigation the arc itself was used as a suitable commutating "brush" to insert a series of ceramic resistance rods into the circuit. These resistance rods were U-shaped and were so arranged that a series of arcs would travel up between them to insert their resistances into the circuit being interrupted, as shown in Figure 8. The separate series arcs were moved up these electrodes by concentrated magnetic fields. This arrangement was acceptable in its performance up to 100,000 kva at 5,000 volts. A careful analysis of its operating characteristics, however, showed that the series arcs were contributing the major portion of the resistance required for successful interruptions and that the complex ceramic resistance rods hardly were justified. This was true particularly if the arcs were controlled properly. Successful air breakers have been built using resistance arc runners, but even in these designs the arc contributed much more resistance than did the runners.

These early studies firmly established the value of a controlled and confined arc

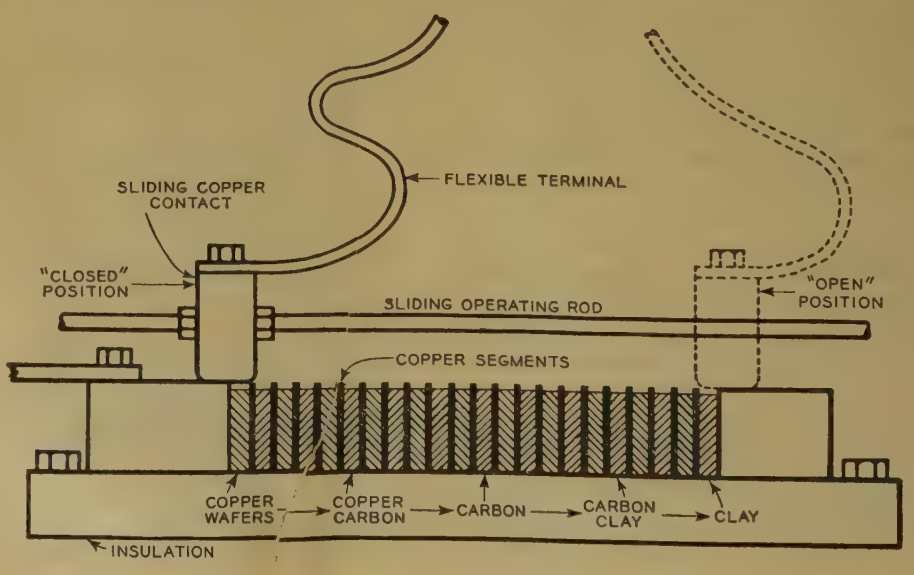


Figure 7. Graduated resistor breaker made up of gradually increasing resistance elements



Figure 8. Disassembled arc chute of high voltage breaker using U-shaped resistor rods inserted in circuit by short arcs

The photograph was taken after high-current tests

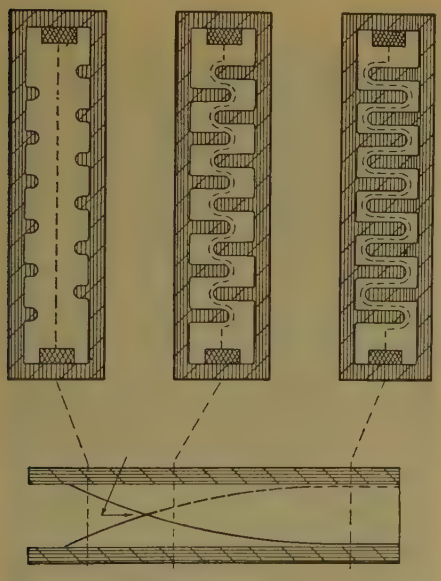


Figure 9. Interleaving fin type of arc chute obtaining arc lengthening in more than one plane by serpentine configuration

in air as a controllable resistor for the interrupters of power circuit breakers. A study then was initiated to determine the most effective way of controlling and confining the arc to establish the proper high-resistance characteristics.

There is a history of successful low-voltage air breakers (600 volts and below) that operate as high-arc-resistance interrupters. The most common arrangement is recognized as the plain break low-voltage circuit breakers where the arc is established between separating electrodes and is cooled and extinguished in open air. Although such circuit breakers are satisfactory interrupters, given sufficient space and time, they are limited in their physical applications because of the long arc in open air required to establish sufficient resistance.

More modern breakers of this low-voltage class, which can be classed as high-arc-resistance interrupters, increase the resistance of the arc per unit length by increasing the arc-cooling by either one of two methods:

1. Forcing the arc into a series of cold metallic pins or plates which cool it and break it into several shorter arcs.

2. Forcing the arc between closely spaced sidewalls of cool ceramic insulation.

When attempting to cool the arcs of a breaker for higher service voltages (2,300 to 15,000 volts) to extinction, it soon became apparent that the necessary arc length in a metallic pin or plate-type arc chute requires greater physical dimensions than the compact design of switchgear equipment for these voltages now affords. Neither can insulating-plate types of arc chutes for these voltages be accommodated to obtain sufficiently high arc resistance in the allowable spacing of modern metal-enclosed equipment if all

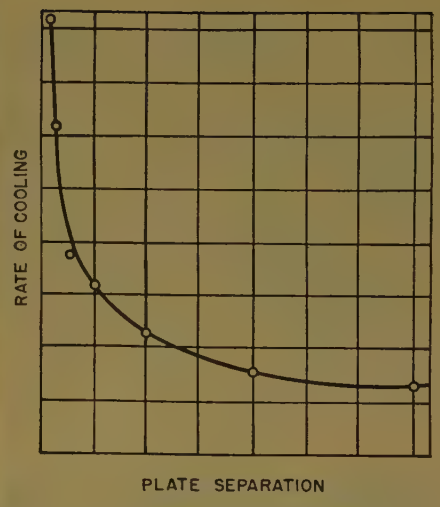


Figure 10. Variation in arc cooling with spacing between insulating plates

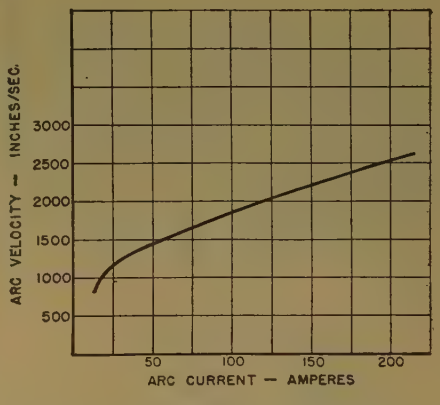


Figure 11A. Variation in arc velocity with arc current in constant transverse magnetic field of 400 gausses

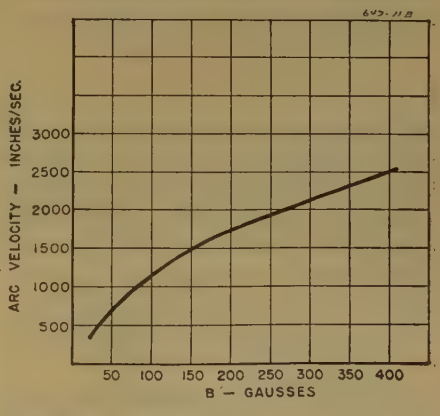


Figure 11B. Variation of arc velocity with transverse magnetic-field strength of 200-ampere arc between parallel arc runners

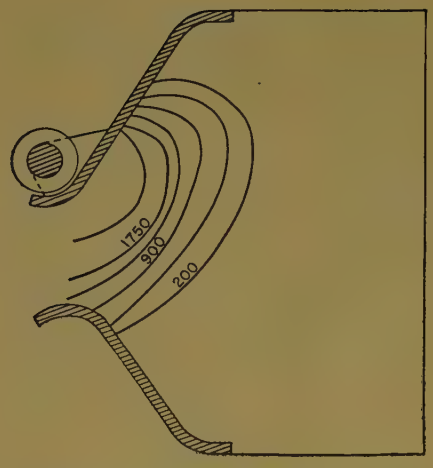


Figure 12A. Poor transverse magnetic-field distribution over area of arc chute resulting from use of single strong magnetic blowout coil

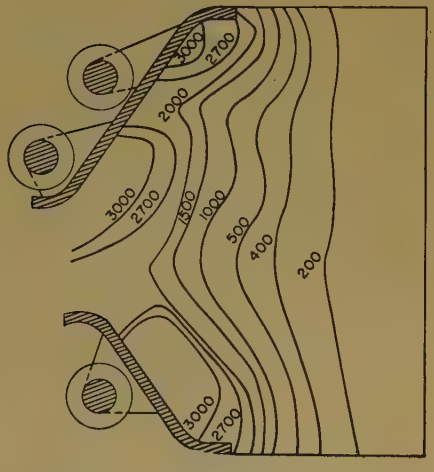


Figure 12B. Improved transverse magnetic-field distribution over area of arc chute with three magnetic blowout coils distributed along arc runners

arc lengthening is performed in one plane. When attempts were made to elongate and confine the arc between closely spaced insulating plates in more than one plane, it soon was realized that a high-arc-resistance type of interrupter could be practical for power circuit breakers. The final arrangement established an arc between electrodes at the throat of a specially constructed arc chute that would force the arc up between interleaving fins of ceramic insulation. This arc movement forced it into a closely confined serpentine pattern of considerable length.

In 1939 the first magne-blast breaker for voltages up to 5,000 volts was presented before the Institute.[3] It used a specially designed arc chute with tapered insulating fins alternately spaced from the inner sidewalls to form an interleaving path for the arc column. As the arc column is forced magnetically into this chute, it is folded back and forth between these fins to extend its length to many times the longitudinal distance between the arc runners, as is shown in Figure 9.

By this construction, an arc chute with a one-foot spacing between arc runner tips creates an arc path several feet in length, depending on the length and amount of overlapping of the interleaving ceramic fins in the chute between the runners. Besides greatly increasing the length of the arc, these closely spaced fins come into very intimate contact with the arc column, flattening it out of its naturally circular cross section. The intimate contact thus effected between the high-temperature arc column and the cool surfaces of the fins extracts heat from the boundary layers of the arc column at a rapid rate, giving a high arc-resistance per unit length. Suits has shown the rate of cooling in an arc column to increase as fins are brought closer together in accordance with the curve shown in Figure 10.

The cooling rate of the arc by the closely spaced fins determines the voltage drop per unit length e_1 in the arc column. The total voltage drop in the arc column e_a is equal to

$$e_a = e_1 l$$

where

e_a = total resistance voltage drop in arc column
e_1 = resistance voltage drop per unit length
l = total length of arc

The total arc-resistance voltage drop e_a required for circuit interruption of a given current is directly proportional to the system voltage E_m. This may be demonstrated easily by connecting two arc chutes in series and noting the double voltage which may be interrupted. If the fin spacing which determines e_1 is held constant, it is then necessary to increase the total arc length l in direct proportion to the circuit voltage. As the number of fins determines the total interleaving arc length, the number of fins required in the arc chute in the magne-blast breaker is proportional to the rated voltage of the breaker

Magne-Blast Design

The Interrupter

The material from which these fins are made is a highly heat-resistant dielectric developed specially for magnetic-breaker arc chutes. As the temperature of the arc column is several thousand degrees centigrade, it loses its heat to the fins by forming a thin molten glaze on the fin surfaces. Immediately following the passage of the arc, this glaze solidifies and its heat passes into the body of the chute. The relatively great mass of the chute provides sufficient thermal storage to accept repeated operations far beyond any service requirement. Because this phenomenon is one entirely of thermal conductance, there is no physical change in the arc chute. As the same thickness of glaze becomes molten and solidifies on each operation, no deterioration in the materials of the arc chute is apparent during the life of a circuit breaker.



Figure 13. Test setup of magne-blast breaker with small quartz rods projecting into side of arc chute to serve as windows for taking high-speed photographs



Figure 14. Actual photographs taken with Rankin high-speed camera showing arc behind windows

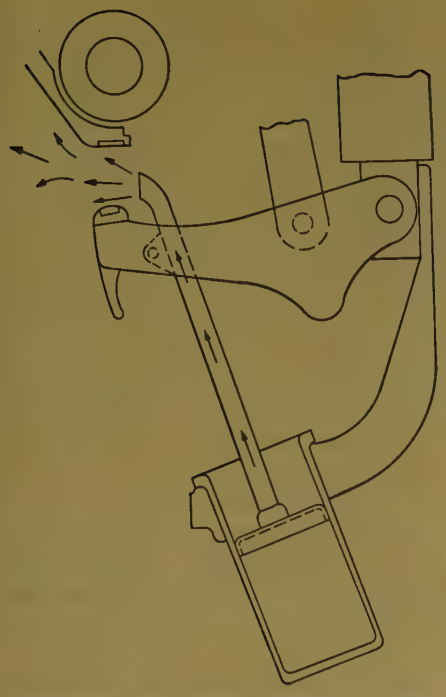


Figure 15. Cross section of piston air booster and movable contact

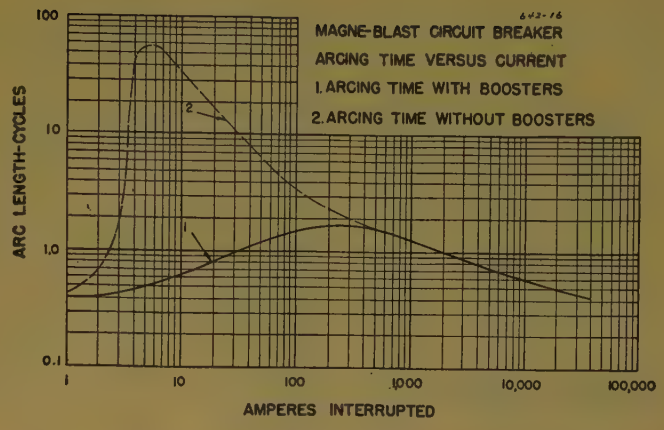


Figure 16. Curve of arcing time versus current of arc chute with piston booster (solid curve) as compared to arcing time without piston booster (dotted curve), showing drastic reduction in arcing time at lower values of short circuit in magnetic air breaker

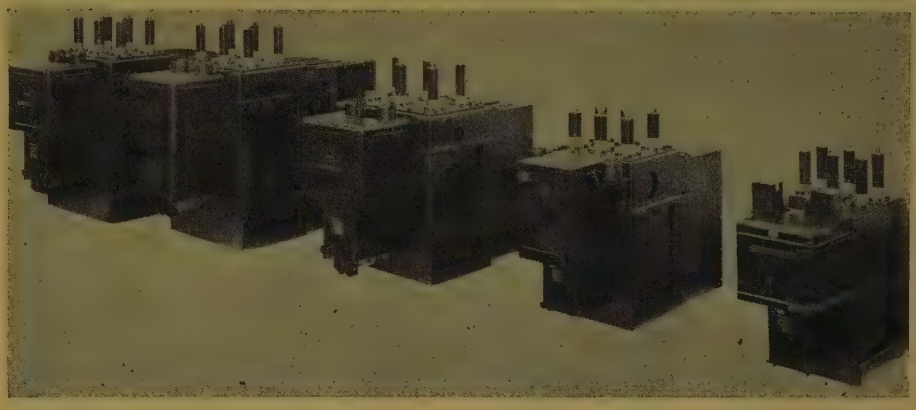


Figure 17. Complete line of magne-blast breakers rated 50,000 to 500,000 kva for use in vertical lift metal-clad switchgear

The faster the arc is moved over these fins of the arc chute, the cooler the fin surfaces will remain and the greater is its cooling effect on the arc. This arc speed is a function of both the current flowing in the arc column and the strength of the transverse magnetic field. Figure 11A shows the variation in velocity of an arc in free air when only the current is varied, while Figure 11B shows the velocity variations of an arc in free air when the transverse magnetic field is the only variable.

It is apparent that a strong uniform magnetic field must be established over the entire working area of the arc chute for maximum arc-chute efficiency. To obtain maximum field-strength uniformity in the larger arc chutes for the higher voltage breakers, it is necessary to use several blowout coils distributed along the arc runners. Several small blowout coils have proved much more effective than a single powerful coil because the magnetic field strength decreases rapidly with the distance away from the coil as a result of leakage flux. This can be seen by reference to Figure 12A which shows the poor field-strength distribution which is obtained over an 18-inch arc chute with a single strong blowout coil. The low flux density reduces materially the arc speed at the extremities of the chute. This would cause arc slowing or arc lingering near the chute extremities, resulting in high local heating and poor arc cooling. The addition of two more blowout coils, as shown in Figure 12B, improves this distribution considerably and maintains a high arc speed over the entire working area of the arc chute.

To study better the effects of localized magnetic blowout coils on arc speed, a special high-speed motion-picture camera developed by Mr. Rankin was used to photograph the movement of the arc through the chute. The extreme speed of this camera (120,000 frames per second maximum) is capable of recording the position of the arc as it passes by tiny quartz windows scattered across the chute sidewalls. Figure 13 pictures the set-up of a magne-blast circuit breaker used for this investigation. The windows are 5/16-inch-diameter quartz rods which project through the magnetic side plates, insulation, and arc-chute side and are flush with the inner ceramic surface. Actual photographs showing this recorded arc travel are shown in Figure 14.

The faster the arc moves into the arc chute, the more rapidly its resistance will increase, resulting in a more rapidly increasing arc-resistance voltage drop e_a. The more rapidly e_a rises, the greater will be the reduction of short-circuit current i_a and the shorter the arc duration $t_0 - t_1$. For very high rates of increase in arc

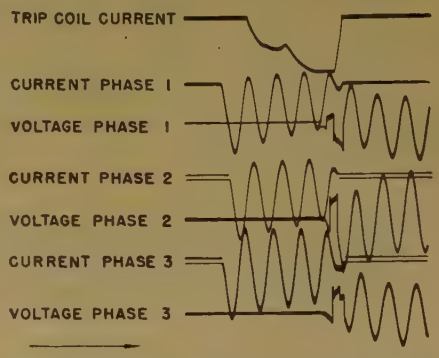


Figure 18A. Oscillogram of 3-phase short-circuit interruption at 560,000 kva, 13,000 volts, showing large reduction in last loop of short-circuit current prior to interruption

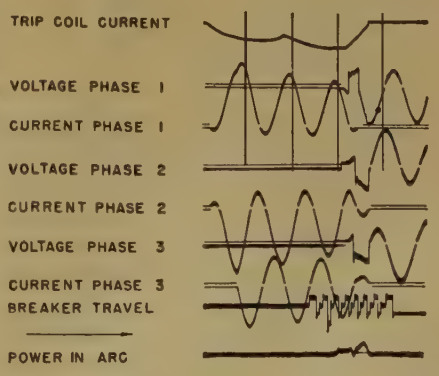


Figure 18B. Oscillogram of 3-phase short-circuit interruption at 550,000 kva, 14,500 volts

Table I. Performance Characteristics of Magne-Blast Circuit Breakers*

Type of Test	Circuit Voltage	Maximum Peak Amperes	Maximum Rms Amperes	Maximum Rms Amperes in Arc	Cycle Arc Duration	Cycles Trip to Interruption	3-Phase Kilovolt-Amperes
500,000-Kva Breaker, 15 Kv							
O	14,500	2,800	1,660	1,580	1.8	4.5	40,000
O	14,500	4,900	2,900	2,900	1.2	3.9	73,000
O	14,500	13,000	8,100	7,500	1.1	3.8	190,000
O	14,500	22,000	13,300	10,200	0.8	3.4	260,000
O	14,500	30,000	18,200	15,800	0.8	3.4	400,000
O	14,500	55,000	33,000	22,000	1.0	3.5	550,000
O	13,000	66,000	40,000	22,000	0.8	3.2	500,000
O	6,500	111,000	70,000	46,000	0.5	2.8	520,000
CO	6,500	110,000	70,000	44,000	0.5	2.8	500,000
250,000-Kva Breaker, 15 Kv							
O	14,500	5,500	3,200	3,000	1.8	4.2	75,000
O	14,500	14,500	7,000	7,000	1.1	3.5	175,000
O	14,500	22,000	13,000	11,000	0.9	3.3	280,000
O	11,000	42,000	26,000	16,200	0.8	3.2	310,000
O	6,600	46,000	27,000	22,000	0.8	3.2	260,000
CO	11,000	40,000	22,000	13,100	0.8	3.2	250,000
CO	6,600	48,000	27,000	23,000	0.8	3.2	260,000
250,000-Kva Breaker, 5 Kv							
O	5,000	5,400	3,200	2,300	1.6	3.6	20,000
O	5,000	24,000	14,400	11,600	1.0	3.0	100,000
O	5,000	47,000	28,000	23,000	0.9	2.9	200,000
O	5,000	65,000	38,000	34,000	0.6	2.6	290,000
CO	4,200	84,000	50,000	34,000	0.7	3.7	250,000
150,000-Kva Breaker, 5 Kv							
O	5,000	1,200	720	610	2.4	4.5	5,300
O	5,000	13,500	7,800	6,600	1.1	3.1	57,000
O	5,000	29,000	17,000	14,400	0.8	2.8	130,000
O	5,000	46,000	27,000	21,000	0.9	2.9	180,000
CO	5,000	63,000	37,000	20,000	1.0	3.0	170,000
CO	2,300	80,000	49,000	38,000	0.7	2.7	150,000
100,000-Kva Breaker, 5 Kv							
O	5,000	1,560	940	940	2.4	4.4	8,100
O	5,000	13,300	7,700	6,700	0.8	2.8	49,000
O	5,000	29,000	17,000	14,400	0.8	2.8	130,000
CO	5,000	28,000	16,700	15,600	0.7	2.7	110,000
CO	2,300	55,000	33,000	25,000	0.7	2.7	100,000
50,000-Kva Breaker, 5 Kv							
O	5,000	1,350	810	690	2.0	4.4	6,000
O	5,000	5,000	2,900	2,300	1.0	3.4	20,000
O	5,000	15,700	9,400	6,300	1.2	3.6	55,000
O	2,300	32,000	17,500	13,200	0.8	3.2	53,000
CO	4,200	14,600	8,800	7,200	1.0	3.4	54,000
CO	2,300	32,000	19,200	13,800	1.1	3.1	55,000

*The above table is a tabulation of actual test data on various ratings of magne-blast breakers.

voltage, as obtained in the magne-blast breaker with its strong uniform magnetic field, the total energy liberated is kept low and the over-all temperature rise of the arc chute is limited to a few degrees.

The total energy liberated in the arc chute during an interruption is equal to

$$\text{Total energy} = \int_{t_0}^{t_1} e_a i_a dt$$

where

e_a = instantaneous arc-voltage drop
i_a = instantaneous arc current
t_0 = time of arc initiation (contact parting)
t_1 = time of arc interruption

At low currents, however, the magnetic field strength from the series blowout coils is very weak, which would result in low arc speeds and long arc durations if this magnetic field were the only driving force. Magne-blast breaker contacts are equipped with simple air-piston boosters to supplement the magnetic field with a blast of air as the contacts part. On light currents the arc, therefore, is carried into the interleaving arc chute with approximately the same speed as on heavy currents. Figure 15 shows the construction of the contact-assembly piston booster on a 15-kv breaker.

The total arcing time of a typical magne-blast breaker with air booster for all values of current is shown in Figure 16. Tests have shown this arcing time to be entirely independent of the direction in which the arc chute is pointing, whether this direction is upward, downward, or in a horizontal plane. The air-piston booster therefore encourages extreme flexibility in breaker design by permitting the arc chute to exhaust either horizontally, downward, or upward, thereby simplifying the design of this breaker for modern vertical-lift metal-clad equipment. Without the air booster, the arcing time at very light currents would be considerably longer, as shown by the dotted line at the top of the figure. The shape of this dotted curve is generally characteristic of all magnetic air breakers without boosters, regardless of the direction of arc-chute exhaust.

Early studies showed that the incandescent gases exhausted from the chute when interrupting high short-circuit currents in closed metal enclosures occasionally would cause flashover if these exhaust gases were not cooled properly before being released from the chute. To cool these exhaust gases, alternate plates of fiber and corrugated metal are assembled as a muffler and successfully cool exhaust gases to a low value before releasing them to the atmosphere. By cooling these exhaust gases and reducing their volume before releasing them to the atmosphere, the audible report also is reduced to a fraction of its unmuffled value.

The Breaker

A proper combination of arc elongation, arc cooling, and arc movement has provided a circuit interrupter that satisfies all of the requirements and benefits of a high arc-resistance interrupter. Arc elongation is achieved by its movement in three planes to form a serpentine path. Arc cooling results by squeezing the arc between ceramic walls and moving it rapidly across these cooling surfaces. Arc movement is established and controlled by directing the circuit currents through multiple blowout coils designed to maintain a strong uniform magnetic-field transverse to the major plane of the arc chute. As accessories to this magnetic field, air boosters assist arc movement at light currents, and a muffler cools the exhaust gases of exceptionally high currents.

The development of an interrupter, however, does not mark the completion of a circuit-breaker design. Contacts, operating means, insulation, conductors, and accessories are all a vital part of the complete device. The magne-blast breaker, adapted for vertical lift metal-enclosed equipments, uses a heavy-duty solenoid mechanism to operate its contacts. These contacts use fine silver primaries to carry load currents with minimum loss and to carry the inrush currents of a heavy fault. As the breaker trips open the current is transferred to an intermediate contact in a parallel circuit. This intermediate contact handles the small arc that is established as the reactance of the first blowout coil is shunted into the circuit through the arc-resistant alloy arcing contacts. The final interrupting arc then is drawn when the arcing contacts part and is carried, by the moving arc contact, to the lower arc runner where a second blowout coil assists in moving the arc along the diverging arc runners and into the arc chute. As the arc travels along these runners, supplemental blowout coils are shunted into the circuit to extend the

magnetic field over the working area of the chute.

The circuit breaker is well insulated by using conventional compound bushings around the conducting studs and by enclosing each phase in a removable housing of insulation. This construction emphasizes accessibility with increased reliability. All operating parts may be exposed readily by removing these subassembled box barriers. The conventional construction of the operating mechanism, accessory devices, and general problems of application have profited by the experience of engineers responsible for the design of the many other varieties of power circuit breakers manufactured.

A complete line of these breakers rated from 50,000 kva to 500,000 kva for use in modern vertical lift metal-clad switchgear is shown in Figure 17. Figures 18A and 18B are two typical oscillograms of the 500,000-kva breaker interrupting in excess of 500,000 kva at 13,000 and 14,500 volts respectively and illustrating the marked reduction in the last loop of short-circuit current caused by the high arc resistance even at these voltages.

It is fortunate that this type of high-arc-resistance breaker conforms to the general pattern and size of correspondingly rated oil circuit breakers while it offers the advantages of no oil. Its application to the same type of metal-clad equipments which have proved their worth for oil circuit breakers is therefore comparatively simple.

References

1. Air-Break Magnetic Blowouts, **J. F. Tritle.** AIEE Transactions, volume 41, 1922, page 262.

2. Magne-Blast Air Circuit Breaker for 5,000-Volt Service, **E. W. Boehne, L. J. Linde.** AIEE Transactions, volume 59, 1940, April section, pages 202–08.

3. The Oil Blast Circuit Breaker, **D. C. Prince, W. F. Skeats.** AIEE Transactions, volume 50, 1931, pages 506–12.

4. Determination of Circuit Recovery Rates, **E. W. Boehne.** AIEE Transactions, volume 54, 1935, pages 530–9.

5. Geometry of Arc Interruption, **E. W. Boehne.** AIEE Transactions, volume 60, 1941. pages 524–32.

6. High Speed Circuit Breakers, **J. W. McNairy.** AIEE Transactions, volume 47, 1928, pages 1276–84.

7. Heat Transfer in Arc Interruption, **Dr. C. G. Suits.** *General Electric Review*, volume 42, October issue, 1939.

8. Magnetic-Type Air Circuit Breaker for 15,000-Volt Services, **L. J. Linde, B. W. Wyman.** AIEE Transactions, volume 63, 1944, March section, pages 140–4.

9. Solenoid Mechanism for Magne-Blast Breakers, **B. W. Wyman, J. H. Keagy.** AIEE Transactions, volume 64, 1945, May section, pages 268–74.

10. Arcing Phenomena of Circuit Interruption, **S. Horikosi.** *ETJ*, January 1940, pages 17–21.

11. Cross Air Blast Circuit Breaker, **D. C. Prince, J. A. Henley, W. K. Rankin.** AIEE Transactions, volume 59, 1940, September section, pages 510–17.

12. Switching Overvoltage Hazard Eliminated in High-Voltage Oil Circuit Breakers, **Lloyd F. Hunt, E. W. Boehne, H. A. Peterson.** AIEE Transactions, volume 62, 1943, February section, pages 98–106.

The Short-Circuit Characteristics of D-C Generators

G. E. FROST
ASSOCIATE AIEE

KNOWLEDGE of the short-circuit characteristics of d-c machines is an essential factor in the design of d-c electric systems having a large low-voltage machine capacity concentrated in a small area. This information is particularly important in the design of systems such as those encountered aboard ship where circuit breakers, fuses, relays, and other protective equipment must be so applied and co-ordinated as to provide a high degree of reliability and service continuity. Available information relative to d-c short-circuit currents has been limited to theoretical analyses based on formal solution of the differential equations of current flow and the machine inductance and resistance values. As a tool in the routine design of d-c systems, this information has not been adequate, particularly when estimates must be made of the effect of fault resistance, choice of machine construction, and so forth.

For some years, the design of a-c systems has been facilitated by the use of the transient and subtransient reactances and the corresponding time constants of synchronous machines. These constants, based on application of the theorem of constant flux linkages to the a-c machine, represent to practical accuracy the performance of that machine under rapidly varying conditions such as those existing during short circuits. Relatively simple tests can be made to determine the various reactance values for a particular machine and form a basis upon which machine and system design requirements may be developed. With the aid of this theory, it has been possible to conduct extensive calculations of short-circuit current flow on a-c systems under a wide variety of conditions of external resistance, external reactance, and so forth, without the formal differential equations which otherwise would be required. The availability of this theory has contributed in no small measure to the high standard of performance which has been obtained on a-c electric systems.

An analysis has been made of d-c machine characteristics with the purpose of deriving a group of machine constants similar to those now applied to a-c machines. It has been found that the effect of magnetic saturation is very large in the short-circuited d-c machine and must be taken into account if a useful analysis is to be made. However, this condition has not prevented derivation of a group of machine constants directly analogous to corresponding a-c machine constants which can be applied practically to d-c system design calculations. In addition, these constants provide a convenient method of describing the effect of series and compensating windings on d-c machine performance. It is the purpose of this paper to describe this analysis. Although the calculation and application of machine constants is illustrated for the particular case of a 60-kw 250-volt shunt wound generator, tests have shown the theory to be applicable to machines of other types and sizes.

Equations for the short-circuit current of a shunt wound d-c machine having negligible armature circuit inductance are derived from the differential equations of current flow in Appendix I. Similar equations are derived for the compound wound machine in Appendix II. The assumption of negligible armature inductance permits armature current to rise practically instantaneously, thereby making the theorem of constant flux linkages applicable. Inasmuch as this theorem is understood more readily than the differential equations and furnishes a useful physical interpretation of the machine constants, the results of the analysis will be described in terms of constant flux linkages.

Paper 46-66, recommended by the AIEE committee on electric machinery for presentation at the AIEE winter convention, New York, N. Y., January 21–25, 1946. Manuscript submitted September 8, 1945; made available for printing December 20, 1945.

G. E. Frost is a patent attorney with the General Electric Company, Schenectady, N. Y.

The author desires to extend his appreciation to C. J. Werner, of the Delco Products Division, General Motors Corporation, for conducting tests required for this study, and to P. N. Ross, central station engineer, Westinghouse Electric Corporation, for his suggestions in the conduct of the analysis.

Short Circuit of the Shunt Wound D-C Machine

Curves of armature and field current taken from an oscillogram of short circuit of a typical 60-kw 240-volt shunt wound d-c generator are shown in Figure 1. The construction of this machine is shown in Figure 2. The current changes following short circuit may be divided into two distinct periods: (1) a period of rapidly increasing armature and field current (*O-A*, Figure 1) and (2) a period of slowly decaying armature and field current (*A-B*, Figure 1). During the former period, total flux linkages in the shunt field winding are maintained nearly constant by current change in that winding, and the machine air-gap voltage changes only to the extent permitted by armature and field leakage flux. Current rise from zero to the peak value takes place at a rate determined by armature circuit inductance and the machine air-gap voltage. Shunt field current increases as required to maintain nearly constant the total effective shunt field flux linkages. The latter period consists of a slow current decay during which shunt field flux linkages, and consequently armature and field currents, are reduced from the value at the peak current point to the final steady short-circuit value. Current change during this period is so slow that armature circuit inductance has a negligible effect, and the rate of field and armature current decay is determined by the field circuit time constant corresponding to the peak value of field current attained.

It is evident from this discussion that the short-circuit characteristics of a d-c machine are closely analogous to those of an a-c machine. In each machine increased armature current associated with the short circuit has a demagnetizing effect on the field winding, which causes the field current to increase as required to maintain nearly constant the total effective field flux linkages. Likewise, after the peak value of armature current is reached (rms current in an a-c machine), the armature current decays to a steady state value at a rate determined by the field circuit time constant. Furthermore, the d-c machine of Figure 1 reaches a steady state short-circuit current value of

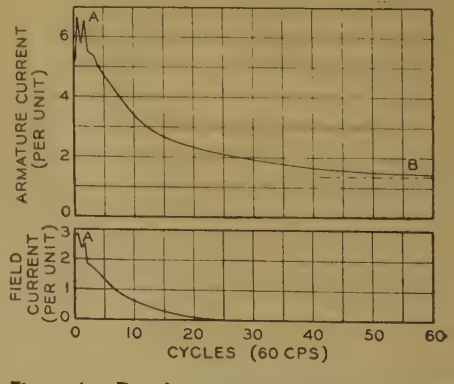


Figure 1. D-c short-circuit transient (no brush shift)

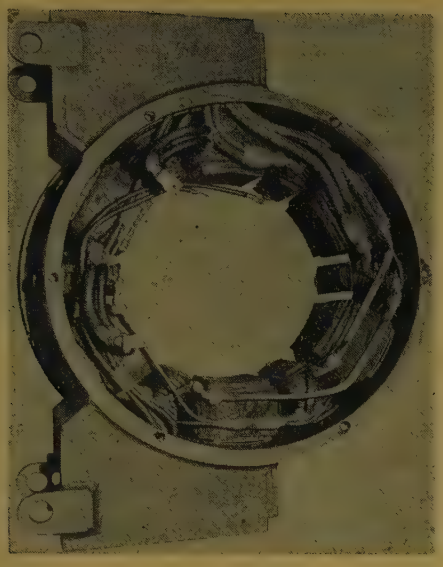


Figure 2. D-c machine typical of those tested

about 1.3 per unit, a value not greatly different from the steady state short-circuit currents encountered on a-c machines.

Magnetizing Effects

Analysis of magnetizing effects during short circuit of a d-c machine can be made most conveniently by considering the machine to have two sets of axes, as shown in Figure 3. The first set of axes, the direct and quadrature field axes, correspond to the actual field structure of the machine. Flux in the direct field axis links only the main field poles, whereas flux in the quadrature field axis links only the interpoles. Since the shunt field winding is on the direct field axis, the flux linkages maintained constant by that winding are the direct field axis flux linkages. The second set of axes, the brush axis and the quadrature brush axis, determines the actual generated voltage within the machine and the direction of armature magnetomotive force. Flux in the quadrature brush axis is effective in producing generated voltage, whereas flux in the brush axis gives no generated voltage. The magnetomotive force produced by the armature, however, is entirely along the brush axis. It is evident that when the brushes are located on the quadrature field axis (the so-called neutral axis), there is no distinction between the pole position and the brush position, and the two sets of axes coincide.

Figure 4 shows the steady state characteristics of a typical separately excited shunt wound d-c machine in terms of total field ampere turns, armature current, and quadrature-brush-axis air-gap flux. The latter quantity represents the machine flux in the quadrature brush axis, and hence the effective flux generating armature voltage. The machine terminal voltage in per unit equals the quadrature-brush-axis air-gap flux in per unit less the per unit voltage drop caused by machine resistance. In the case of a zero resistance fault, there can be no terminal voltage, and the per unit quadrature-brush-axis air-gap flux must equal the machine resistance drop in per unit. Operation therefore must be at some point along the machine *IR* drop line of Figure 4. Since armature inductance effects are negligible during the current decay period (*A-B*, Figure 1), the current changes during this period can be considered to follow the *IR* drop line of Figure 4 as a locus, the rate of motion being determined by the rate of shunt field current decay.

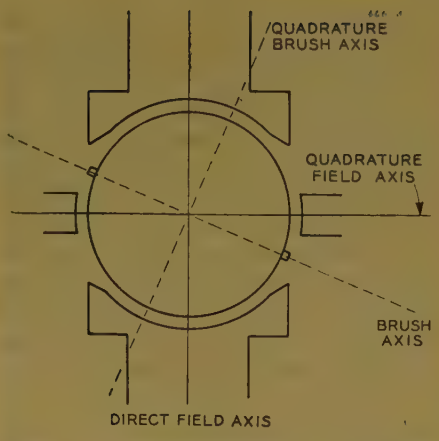


Figure 3. Magnetic structure of d-c machine

The curve of Figure 4 shows that with constant field current, quadrature-brush-axis air-gap flux decreases as armature current is increased. This change is caused by two demagnetizing components: (1) direct-field-axis armature magnetomotive force and (2) apparent direct-field-axis armature magnetomotive force associated with the quadrature-field-axis armature magnetomotive force. The first component is the result of actual direct-axis armature ampere turns and is proportional to the sine of the angle of brush displacement. The second component results from pole face and armature tooth saturation associated with cross flux from the quadrature axis armature magnetomotive force. As shown in Figure 5, the magnetomotive force added on one side of the main pole by quadrature-field-axis ampere turns is equal to that subtracted on the other side, but saturation causes the flux added to be less than the flux subtracted. Hence a lower value of average flux results. Tests show that, for the values of brush shift normally encountered in d-c machines, the effect of direct-field-axis armature ampere turns is small compared to the apparent magnetomotive force caused by the saturating effect of quadrature-field-axis armature ampere turns.

The effect of armature magnetomotive force just discussed is directly analogous to armature demagnetizing action in the a-c machine. There is one vital difference, however, for the armature demagnetizing action in an a-c machine is nearly proportional to the reactive component of armature current, whereas the armature

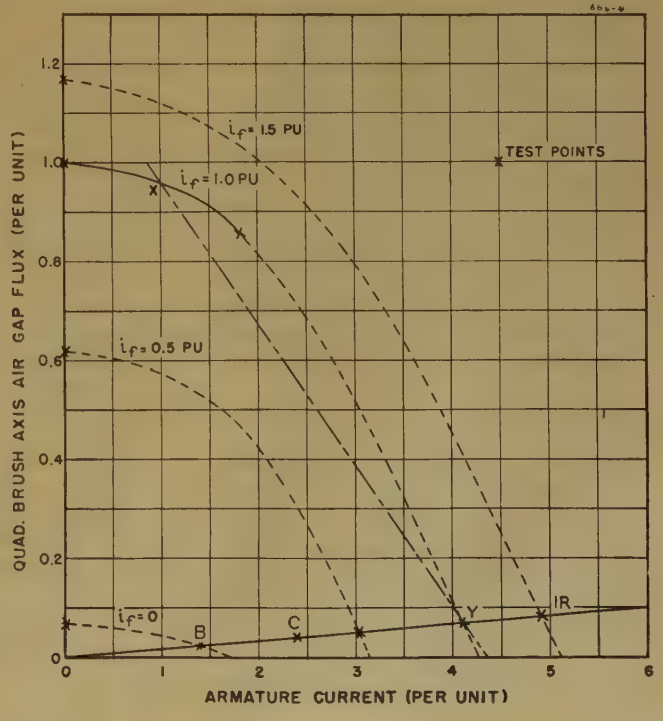


Figure 4. Steady state characteristics of a d-c machine (no brush shift)

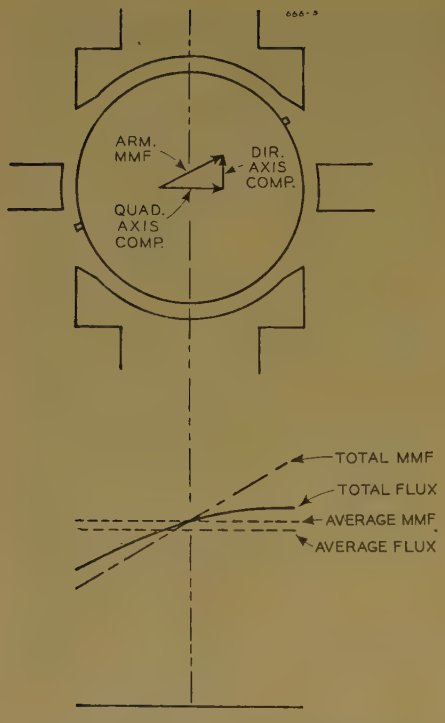


Figure 5. Armature demagnetizing effect in a d-c machine

demagnetization in a d-c machine largely results from magnetic saturation and is not directly proportional to armature current. In the a-c machine, the combined effect of reduced air-gap flux caused by demagnetization and internal voltage drop resulting from leakage reactance is lumped in the machine constant of synchronous reactance. A similar synchronous resistance may be used as a d-c machine characteristic. However, any single value of this resistance is effective only between specific values of armature current, and some error is involved even if these values are relatively close together. In the case of the machine of Figure 4, for instance, synchronous resistance based on the line X-Y may be used at armature currents in excess of one per unit. This line corresponds to one per unit generated voltage (quadrature-brush-axis flux) drop for 3.49 per unit current or an apparent resistance of 0.29 per unit. Adding 0.02 per unit ohmic resistance drop, a total synchronous resistance of 0.31 results.

Steady Current

Figure 4 shows that quadrature-brush-axis air-gap flux exists in a d-c machine even though no field current is flowing. This flux is the combination of two components: (1) residual flux in the direct field axis and (2) the quadrature-brush-axis component of interpole flux. The latter flux is determined by the angle of brush shift, being approximately proportional to the sine of that angle. In the case of a generator, brush shift against rotation results in a positive voltage from interpole flux, whereas brush shift with rotation results in a negative voltage. The residual flux in the direct field axis is the result of previous magnetization of the field poles and is relatively independent of the brush position. Figure 6 shows the variation in quadrature-brush-axis air-gap flux at no field excitation when brush position is changed. It is evident from the figure that the principal source of this flux, within the brush angles shown, is the residual direct-field-axis flux.

Peak Current

In passing from the condition of normal quadrature-brush-axis air-gap flux (Figure 4, point X) to the final short-circuit condition of 0.03 per unit quadrature-brush-axis air-gap flux (Figure 4, point B), the direct-field-axis flux is reduced substantially. In making this transition, however, there can be no instantaneous change in shunt field flux linkages as the infinite

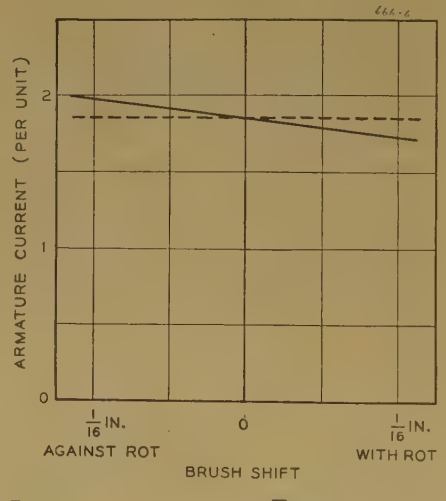


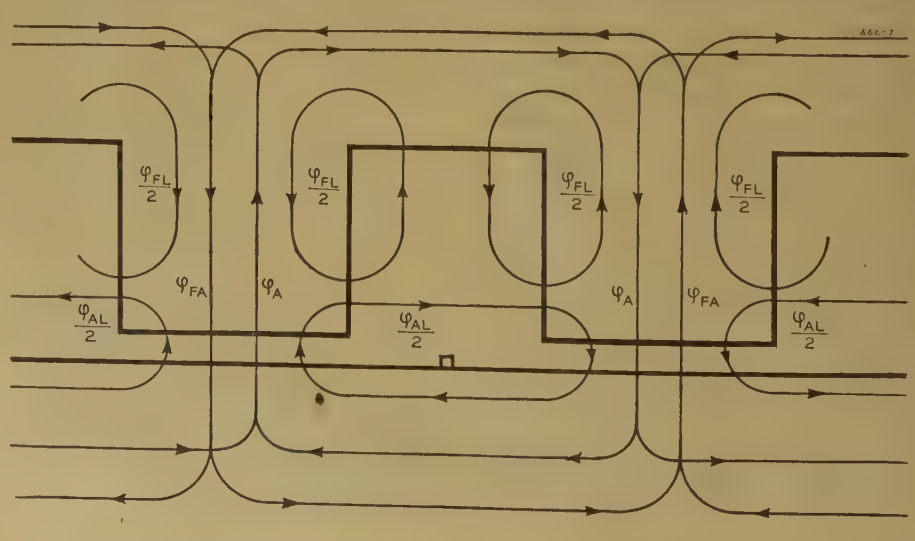
Figure 6. Effect of brush shift on steady state short-circuit current

voltages required to make such change are not available in the shunt field circuit. Accordingly, shunt field current rises to a value sufficient to give constant total flux linkages. At this point the flux linking the shunt field winding differs from the net quadrature-brush-axis air-gap flux by the field and armature leakage fluxes.

Figure 7 shows approximately the paths of armature and field flux components within a short-circuited d-c machine. Field flux consists of two components: (1) flux linking both the field and air gap, φ_{FA} (Figure 7), and (2) flux linking the field winding but not the air gap, φ_{FL}. Armature demagnetizing effects may be considered to produce two flux components, oppositely directed with respect to the main field flux. The first of these components, φ_A, links both the air-gap and the shunt field winding, whereas the second component, φ_{AL}, links only the air-gap. Since the armature leakage flux φ_{AL} does not link the field winding, it can change instantaneously. The combined effects of armature leakage flux and field leakage flux may be lumped in a total effective leakage coefficient which may be used to represent the over-all performance of the machine.

Figure 8 shows the results of a test to determine the magnitude of armature leakage flux. A short circuit was placed on the machine used in the test of Figure 1 and suddenly opened one-fifth second later. Since the shunt field flux linkages were nearly the same value after opening the short circuit as before, the value of terminal voltage following opening indicates the magnitude of armature leakage. The value of armature voltage during short circuit indicated in Figure 8 represents the actual quadrature-brush-axis flux computed from the product of arma-

Figure 7. Basic flux paths in the d-c machine



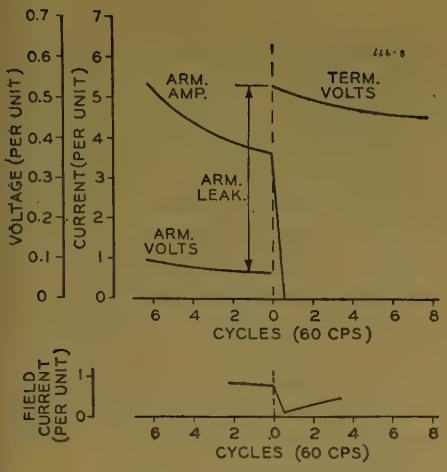


Figure 8. Interruption of a d-c short circuit

ture resistance and armature current. The field current before opening the fault was about 0.8 per unit, giving a value of φ_{FA} of 0.8 per unit (neglecting saturation). Since the net air-gap flux is equal to $\varphi_{FA}-\varphi_A-\varphi_{AL}$ (Figure 7) and is shown on the armature voltage curve to be 0.08, the sum of armature flux φ_A and armature leakage flux φ_{AL} is 0.72 per unit. The net shunt field flux is equal to $\varphi_{FA}+\varphi_{FL}-\varphi_A$ and is held constant by field current change. From the figure this value after opening the short circuit is 0.53 per unit. Assuming 0.2 per unit field leakage flux at one per unit field current, the field leakage flux component becomes 0.16 per unit at the 0.8 per unit field current prior to opening. Substituting this value of field leakage flux and field air-gap flux (0.8 per unit before the opening), the value of armature flux φ_A is 0.43 per unit. Since the sum of armature flux and armature leakage flux is 0.72 per unit, the value of armature leakage flux φ_{AL} is 0.29 and the armature leakage coefficient $[n_a=\varphi_{AL}/\varphi_A]$ is 0.67. Substituting this value of armature leakage flux and a value of 0.2 for the field leakage flux coefficient in equation 13, Appendix I, the value of apparent field leakage coefficient becomes unity.

Analysis of the cause of armature leakage flux in the d-c machine is complicated by the varying degrees of magnetic saturation existing throughout the magnetic circuit. However, a qualitative indication of the origin of this flux may be gained from consideration of Figure 9, which shows an equivalent electric circuit for the simplified magnetic structure of a 2-pole machine. In the figure batteries represent magnetomotive force values, and resistances represent reluctance. The two groups of four parallel resistance–battery combinations represent the four armature teeth assumed to be located under each main pole. In order to represent the effects of saturation, the reluctance values corresponding to the more saturated armature teeth and pole face areas are made larger than those corresponding to the less saturated portions of the magnetic circuit. From the figure it is evident that a substantial armature leakage flux exists in the circuit. If tooth and pole face saturation is neglected, this leakage flux becomes zero. Evidently this effect accounts for the high value of armature leakage flux shown in the tests.

From this analysis, it is evident that the peak armature current of a short-circuited d-c machine equals the value determined on the basis of synchronous resistance plus a current increment taking into account the increased field current required to maintain constant field flux

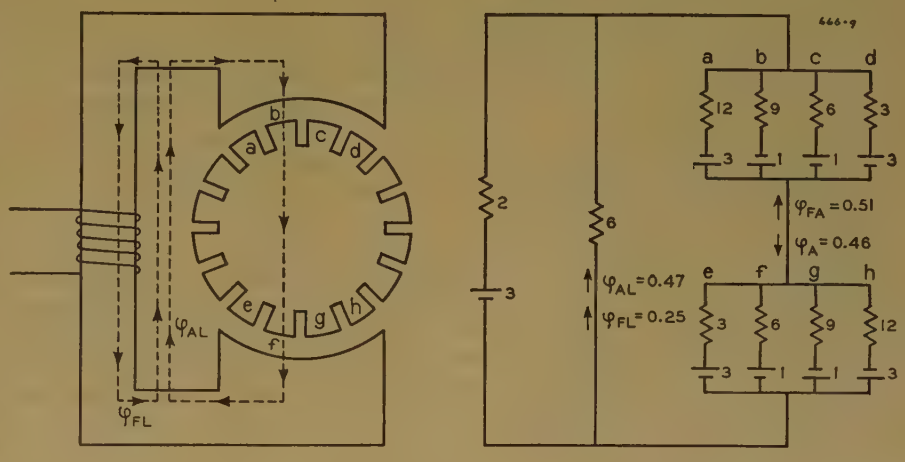


Figure 9. Equivalent magnetic circuit of a d-c machine

linkages. This current may be computed directly by regarding the d-c machine as having a transient resistance similar to direct axis transient reactance of an a-c machine. In Appendix I it is shown that the value of this transient resistance is $R_A+(n/1+n)R_e$, where R_A is the armature ohmic resistance, n is the total effective field leakage flux coefficient, and R_e is the equivalent armature resistance corresponding to the line X-Y, Figure 4. Designating transient resistance by R'_e, the peak short-circuit current from full voltage, full load is

$$i_{peak}=\frac{1+R'_e}{R_z+R'_e}\text{ per unit} \qquad (1)$$

where R_z is the fault resistance.

Equation 1 is directly analogous to the equation of peak transient short-circuit current for an a-c machine. The numerator of the equation can be considered to represent the voltage behind the transient resistance or the flux remaining constant during the short-circuit interval. In the case of the a-c machine, this flux actually exists across the air gap, whereas in the case of the d-c machine it is a purely fictitious flux since equation 1 is derived on the basis that armature demagnetizing effect does not commence until armature current reaches one per unit. The denominator of equation 1 represents the total effective circuit resistance retarding short-circuit current flow.

As shown in Figure 4, a reasonably accurate approximation of the demagnetizing effect of armature current in a d-c machine may be made by neglecting all armature demagnetizing effects for armature currents less than one per unit. Equation 1 is derived on this basis with

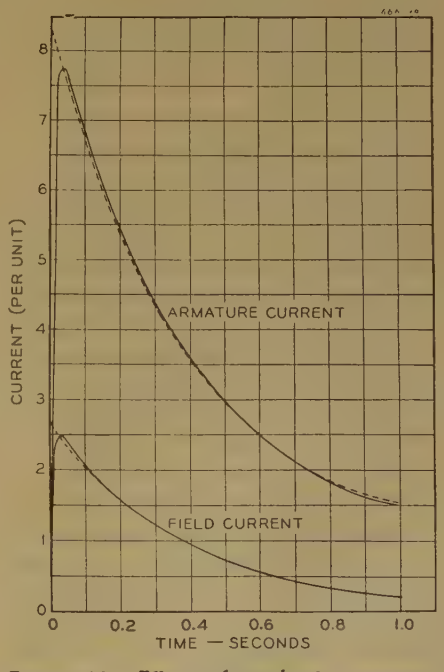


Figure 10. Effect of neglecting armature inductance

———Including armature inductance
– – – –Neglecting armature inductance

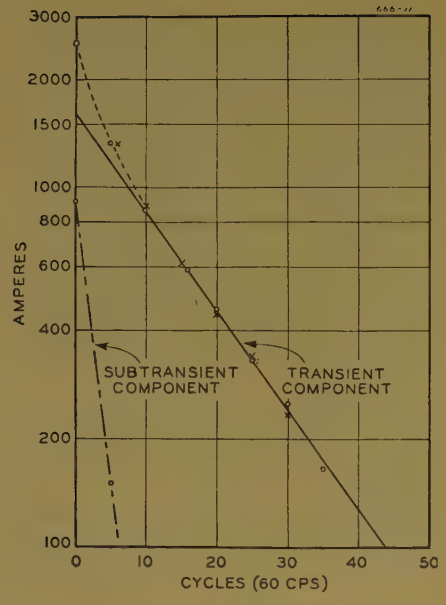


Figure 11. Current decay in d-c machine

o—One-sixteenth-inch brush shift with rotation

x—One-sixteenth-inch brush shift against rotation

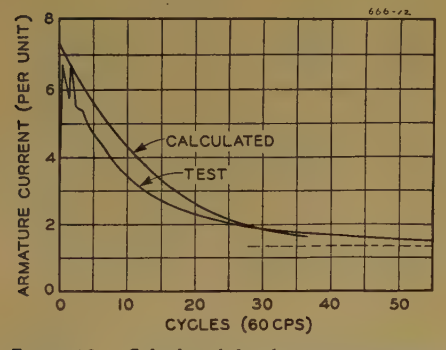


Figure 12. Calculated d-c short-circuit current

the further provision that initial armature current is one per unit. Inasmuch as the initial value of air-gap flux varies only to the extent required by armature resistance as initial armature current is changed from zero to one per unit, there is a very slight change in initial field flux linkages when armature current is changed within this range. Accordingly, equation 1 applies very nearly to all short circuits from initial armature currents between zero and one per unit.

Current Rise

Armature, interpole, and other armature circuit inductances prevent the short-circuit current of a d-c machine from instantaneously reaching the peak value determined by transient resistance. The character of this current rise is exponential if the armature demagnetizing effect behaves as a pure resistance and the armature circuit inductances do not saturate.

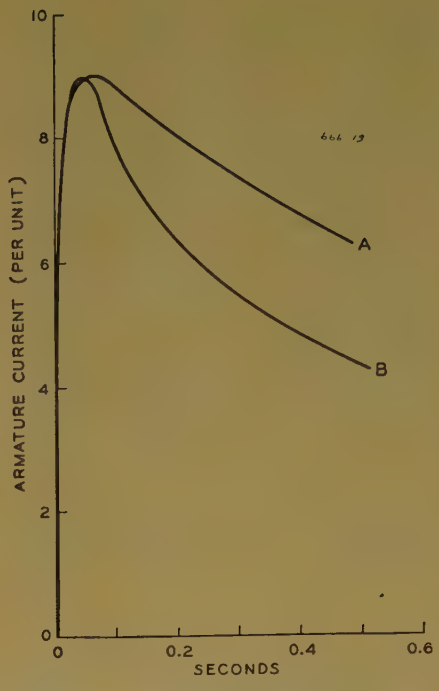


Figure 13. Effect of series field on d-c short-circuit current (300 kw machine)

A—Cumulative field

B—Differential field

Inasmuch as this does not represent the true condition, the current rise deviates from an exponential to some extent. Tests show that initial short-circuit current rise in small d-c generators (60–300-kw) is extremely rapid, varying from 500 to over 1,000 per unit per second. In fact, this current rise has been so rapid that it has been impossible to determine the exact shape of the current rise curve from test data.

Figure 10 shows the effect of the finite value of current rise on the calculated armature current following short circuit. The solid curve is the result of a computation based on the assumptions of Appendix I, but taking into account armature and interpole inductance. It was assumed in this calculation that armature circuit inductance gave an initial current rise of 800 per unit per second. From the figure it is evident that the curves correspond in all respects, except for the peak value and rate of rise of armature and field current. In the peak values, an error of eight per cent is involved, a small error in view of the approximations used in the analysis.

Current Decay

Armature current decays from the value associated with transient resistance to the final steady value at a rate dependent on the field circuit time constant of the machine. In the absence of saturation, this decay is an exponential curve which becomes a straight line when plotted on semi-log paper. Figure 11 shows a curve of this type for two short circuits of a 100-kw 1,200-rpm shunt-wound machine, one with the brushes leading and the other with the brushes lagging. With the exception of the first ten cycles, the decay is very nearly exponential, having a time constant of about 15 cycles. The effect of brush shift on current during the decay period is so small that negligible effect is shown in the figure.

It is shown in Appendix I that the time constant of decay for a zero resistance fault may be computed from

$$T = \frac{R'_e}{R_s} T_{FO} \qquad (2)$$

where T_{FO} is the field time constant at full load, full voltage and R_s the synchronous resistance. This relation is directly analogous to the equation for the transient short-circuit time constant of an a-c machine.

Subtransient Effects

Figure 11 is typical of several tests which have shown that current during the first few cycles following short circuit of a d-c machine exceeds the value based on transient resistance. This evidently is the effect of pole iron, bolts, welded sections, and so forth, in maintaining flux for a short period of time, thus giving the d-c machine a subtransient resistance analogous to the subtransient reactance of an a-c machine. From Figure 11 the approximate value of this resistance is 12 per cent and the time constant three cycles (0.05 second). These values are consistent with subtransient reactance and time constant values encountered on a-c machines of similar size.

Accuracy

To check the above theory, a calculation has been made of the transient short-circuit armature current of the machine used to obtain the data of Figures 1, 4, 8, and the equations of Appendix I. Values of synchronous resistance, effective field leakage coefficient, and open-circuit transient-time constant were taken as 0.31 per unit, 1, and 0.5 second respectively. The corresponding transient resistance is 0.16 per unit. Armature resistance was assumed to be 0.02 per unit. The results of the calculation are shown in Figure 12. It is evident that the computation checks in order of magnitude the actual short-circuit current transient obtained, all that can be expected in view of the assumptions used in deriving the equations of the appendix.

Compounding and Compensation

Figure 13 shows the short-circuit current of a d-c generator for two series field connections, one cumulative and the other differential. The peak armature current is practically the same value in each case, for the shunt field current maintained the same value of total field flux linkages nearly constant during the period of current buildup. That is the same air-gap flux, and therefore shunt field flux linkages, existed in the machine prior to each short circuit, and the same increase in total field magnetomotive force was required to maintain constant these flux linkages. Since the maximum value of total field magnetomotive force is the same in each case, the peak short-circuit currents are identical. However, the rate of current decay following the peak current value for the differential field connection is greater than for the cumulative field connection because the shunt field current required to maintain constant shunt field flux linkages in the former case is substantially greater than in the latter. This condition results because of the influence of the series field in supplying field magnetomotive force, aiding the shunt field in the cumulative wound machine, and opposing the shunt field magnetomotive force in the differential wound machine.

In addition to determining the rate of decay following peak short-circuit current, the presence of a series field alters the steady state short-circuit current value. The magnitude of this effect may be estimated from the curves shown in Figure 8 If a cumulative series field gives 0.1 per unit magnetomotive force at full load, for instance, there will be an added contribution of 0.1 per unit field magnetomotive force for every one per unit armature current. Hence for the case of Figure 4, point *B* will be moved along the line *IR* until the total field magnetomotive force in per unit corresponds to ten per cent of the armature current value, thereby placing point *B* in a position corresponding to 2.4 per unit armature current (point *C*, Figure 4).

The short-circuit curves of Figure 13 are based on two series field connections for a particular generator. If a machine is designed to give a particular value of voltage regulation, the series field winding may be used in lieu of other design changes to achieve this regulation. In particular, a large value of synchronous resistance may be used with a relatively strong cumulative series field to give the same voltage regulation as with a low synchronous resistance and no series field.

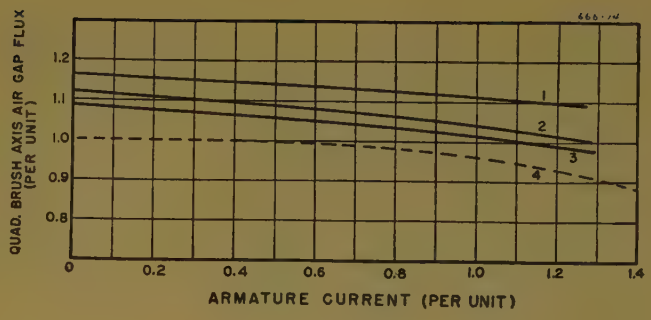


Figure 14. Steady state characteristic of compensated generators (no brush shift)

Curves 1, 2, and 3—1,100 kw 416-volt compensated generators

Curve 4—60-kw 240-volt uncompensated generator

In this case a smaller peak armature current on short circuit will be obtained than with the machine designed to achieve the same voltage regulation with only a shunt field winding. Tests show, however, that this effect is small with machines of 60 to 300 kw capacity, and that these machines have substantially the same peak short-circuit current, whether designed as shunt machines or series machines meeting the same voltage regulation requirements.

Compensating windings are provided in the pole face structure of d-c machines to reduce the magnetizing effects of armature current, thereby limiting saturation caused by quadrature axis armature magnetomotive force and decreasing the value of machine synchronous resistance. A corresponding reduction in transient resistance can be expected. If the compensation secured is perfect, the demagnetizing effects of armature current are reduced to zero and, with the brushes on the neutral axis, the short-circuit current will rise to a value limited only by armature resistance. On large machines this value may exceed 50 times normal current. Actually it does not appear that currents of this magnitude are to be expected, for actual compensation falls far short of the theoretically perfect compensating winding. This condition is evident in Figure 14 which shows a plot of the variation of quadrature-brush-axis air-gap flux with armature current for three 1,100-kw 416-volt compensated generators. By comparison with the curve of the machine of Figure 4, it appears that these particular compensated machines probably have synchronous resistance values comparable to the uncompensated machine of Figure 4.

Fault Resistance

The influence of fault resistance on peak short-circuit current of a d-c generator may be calculated from equation 1. A plot of calculated peak short-circuit current as a function of fault resistance for a particular machine is shown in Figure 15. The two test points indicate that the relation of equation 1 gives approximately correct results.

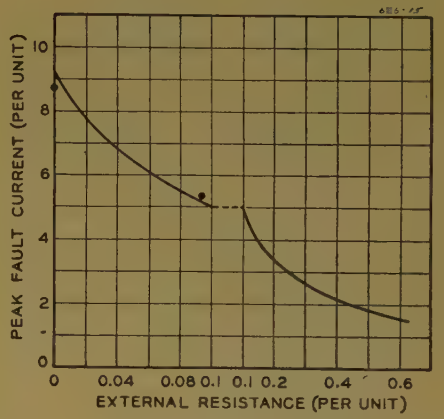


Figure 15. Effect of fault resistance on d-c short-circuit current

●—Test points

The influence of fault resistance on steady state short-circuit current may be estimated from the steady state machine short-circuit characteristics shown in Figure 4. In this case, a new *IR* drop line corresponding to the new total armature circuit resistance is constructed and the steady value of short-circuit current read from that curve.

Commutator Flashover

It generally is assumed that commutator flashover on short-circuited d-c machines can be prevented only by the use of circuit breakers having a combination of high operating speed and low trip setting which prevents buildup of armature current to the full short-circuit current value. A considerable number of tests on d-c machines of the shunt, stabilized shunt, and compound types varying from 60 to 300 kw, 240 volts, and having peak currents from 6 to 11 per unit have failed to produce a flashover. Although the tests were made under controlled conditions, they are considered to show that the probability of flashover has been exaggerated somewhat. In fact, it appears that generators in this range may be constructed economically to have a relatively low prob-

ability of flashover on short circuit, even after a period of service.

If the machine is designed to withstand short-circuit current, or the probability of flashover is considered remote, there appears little need for circuit breakers having the high operating speeds and low trip settings normally used. The entire short-circuit curve of Figure 1 then becomes available for use in establishing circuit-breaker settings, and co-ordination of circuit breakers may be obtained readily. Furthermore, if the circuit breaker is capable of withstanding the peak short-circuit current, an actual reduction in circuit-breaker duty may be achieved by intentional time delay. Inasmuch as the curve of Figure 1 is very similar to the short-circuit-current curve of an a-c machine of equivalent size, the same principles used in establishing circuit breaker settings in a-c systems may be applied to d-c systems of equivalent size, thereby simplifying the design and construction of the d-c system and taking full advantage of a-c developments.

Conclusions

Calculations of the short-circuit current of d-c machines may be conducted by the use of machine constants of synchronous resistance, transient resistance, subtransient resistance, and the corresponding time constants. These values are directly analogous to the constants which have been applied to a-c machine calculations. The principal difference between the application of these constants to a d-c machine and the application of analogous constants to an a-c machine lies in the necessarily approximate method which must be used to represent the effect of machine saturation. This approximation does not, however, prevent reaching useful results.

The value of transient resistance for d-c machines is influenced to a considerable degree by the high value of armature leakage flux. This flux, apparently caused by the saturating effect of flux in the armature teeth, has given armature leakage flux coefficients of the order of 0.7 and corresponding total apparent field leakage flux coefficients of unity. These high values, as compared with the effective field leakage flux coefficient of from 0.2 to 0.4 on a-c machines, constitute an important distinction between the performance of the two types of machines under transient conditions.

The presence of a compound field winding has no influence on the peak value of short-circuit current attained by a d-c machine. However, a winding of this type is of considerable importance in determining the rate of armature current decay from the peak to the final steady value and the value of the final steady current reached. Compensating windings, which theoretically should result in extremely high values of transient resistance, do not appear sufficiently effective to produce this result, and there is little reason to believe that the high values of short-circuit current sometimes assigned to these machines actually will be reached. Further test data on these machines, however, will be required before definite conclusions can be reached.

In the case of small d-c machines, the probability of commutator flashover under short circuit appears to be somewhat exaggerated, and it is believed possible to establish circuit-breaker settings taking advantage of the probability that flashover will not occur. In this case the effective short current transient is very similar to that of equivalent a-c machine, and the methods developed for the design of a-c systems may be applied.

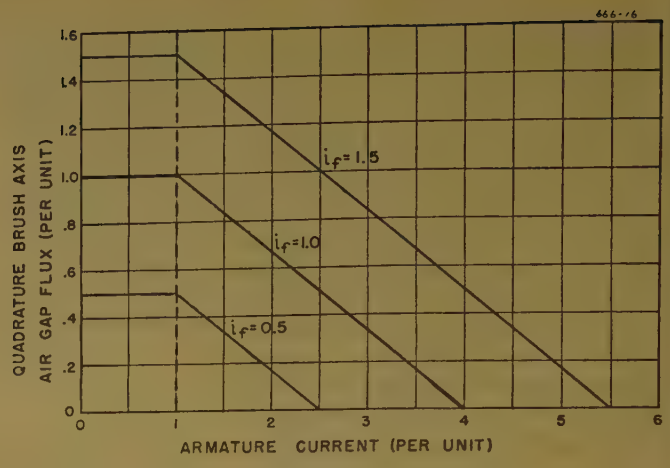


Figure 16. Assumed d-c generator characteristic

Appendix I. Short Circuit of a Shunt Machine—Mathematical Analysis

This analysis is based on the following assumptions:

1. Generated voltage (quadrature-brush-axis air-gap flux) may be represented by the following two components:

(*a*). A positive component proportional to field current, representing the magnetizing effect of field magnetomotive force.

(*b*). A negative component proportional to the excess of armature current over full load armature current, representing the demagnetizing effect of armature magnetomotive force (including saturation of the pole faces caused by quadrature axis flux).

This assumption amounts to representing the machine characteristics by the straight lines in Figure 16.

2. Field current (in amperes) is negligible as compared with armature current (in amperes).

3. The short circuit takes place from an initial condition of rated armature current and rated voltage.

4. Armature and interpole inductance is negligible. From Figure 10 it is evident that no significant error in peak current or current during the decay period results from this assumption.

Subject to these assumptions, the machine circuit equations may be written:

$$E_t = i_f - R_e(i_a - i_1) - R_a i_a \tag{3}$$

$$E_t = R_f i_f + L_f \frac{di_f}{dt} - M\frac{d}{dt}(i_a - i_1) \tag{4}$$

$$E_t = R_x i_a \tag{5}$$

where

E_t = terminal voltage in per unit

i_f = field current in per unit (based on the field current for rated armature voltage at no load)

R_a = armature ohmic resistance in per unit

i_a = armature current in per unit

R_e = equivalent armature resistance corresponding to the demagnetizing effect of armature current in per unit

i_1 = current value above which R_e is measured in per unit (one per unit this analysis)

R_f = field resistance in per unit (based on the units of i_f and E_t)

L_f = field inductance in per unit (per unit field voltage induced by one per unit field current change per second)

M = coefficient of mutual inductance representing the shunt field voltage in per unit corresponding to one per unit armature current change per second

R_x = short-circuit resistance

It is convenient to base the calculation of M on the conventional system of units. Then

$$M_A = \frac{N_f \varphi_f}{i_a} \cdot 10^{-8} \tag{6}$$

where

M_A = value of M in henries

i_A = armature current change in amperes required to produce a change in shunt field flux linkages of $N_f\varphi_f$ maxwell turns

From Figure 16 it is evident that an armature current increase (above one per unit) equal to $1/R_e$ per unit causes the quadrature-axis air-gap flux to be reduced one per unit. The corresponding change in shunt field flux linkages can be shown to be $1/1+n_a$ per unit, where n_a is the ratio φ_{AL}/φ_A (Figure 7). Inasmuch as $1/R_e$ per unit current change produces $1/1+n_a$ per unit change in shunt field flux linkages, the current change required to make a one per unit change in shunt field flux linkages is $(1+n_a)/R_e$.

It is convenient to use as a basis of substitution in equation 6 the shunt field flux linkages upon which the shunt field inductance at no load, full voltage, is based. This value of flux is one per unit plus the shunt field leakage flux. If the shunt field leakage coefficient n_f is equal to $\varphi_{FL}/\varphi_{FA}$ (Figure 6), the shunt field flux at no load, full voltage is $(1+n_f)$ per unit. Since armature current must change $(1+n_a)/R_e$ per unit to give a one per unit change in shunt field flux linkages, an armature current change of $(1+n_a)(1+n_f)/R_e$ per unit is required to give a shunt field flux linkage change corresponding to the value of shunt field flux linkages at no load, full voltage. The value of this current in amperes is

$$i_A=\frac{i_{Au}(1+n_a)(1+n_f)}{R_e} \tag{7}$$

where i_{Au} is the rated armature current in amperes.

The value of $N_f\varphi_f$ at no load, full voltage is the value upon which the open circuit field time constant is based. If L_f is the shunt field circuit inductance (in henries) corresponding to this time constant, the value of $N_f\varphi_f$ is

$$N_f\varphi_f=L_f i_{fu}\cdot 10^8 \tag{8}$$

where i_{fu} is the shunt field current in amperes at no load, full voltage (base field current).

Then

$$M_A=\frac{L_f R_e i_{fu}}{(1+n_a)(1+n_f)i_{au}} \tag{9}$$

The values of M_A and L_f in per unit notation are

$$M=\frac{M_A i_{Au}}{V} \tag{10}$$

$$L_f=\frac{L_f i_{fu}}{V} \tag{11}$$

where V is rated armature voltage. Hence

$$M=\frac{L_f R_e}{(1+n_a)(1+n_f)} \tag{12}$$

It is convenient to consider the operation of the machine in terms of an equivalent shunt field leakage coefficient which combines the effects of field and armature leakage. This leakage coefficient may be defined by

$$(1+n)=(1+n_a)(1+n_f)$$

or

$$n=(1+n_a)(1+n_f)-1 \tag{13}$$

For small values of n_a and n_f, the value of n is nearly equal to n_a+n_f. Then

$$M=\frac{L_f R_e}{1+n} \tag{14}$$

Substituting equation 13 in equations 3, 4, and 5 and eliminating, it follows that

$$\left.\begin{aligned} -i_f+(R_a+R_x+R_e)i_a&=R_e i_1\\ R_f i_f+L_f\frac{di_f}{dt}-R_x i_a-\frac{L_f R_e}{1+n}\frac{di_a}{dt}&=0\end{aligned}\right\} \tag{15}$$

The Laplace transform of equation 15 is[4]

$$\left.\begin{aligned} -i_f(s)+(R_a+R_e+R_x)i_a(s)&=\frac{R_e i_1}{s}\\ (R_f+L_f s)i_f(s)-\left[R_x+\frac{L_f R_e s}{1+n}\right]i_a(s)&\\ =L_f i_{fo}-\frac{L_f R_e}{1+n}i_{ao}&\end{aligned}\right\} \tag{16}$$

where i_{fo} and i_{ao} are the initial field and armature current, respectively, and T_o is the open circuit time constant of the field circuit.

Assuming the fault to take place from an initial condition of full voltage, full load, the constants of equation 15 become

$$R_f=\frac{1}{1+R_a},\ i_{fo}=1+R_a,\ L_f=T_o,\ i_{ao}=1$$

The value of i_1 has been taken previously as one per unit and therefore

$$\left.\begin{aligned} -i_f(s)+(R_a+R_x+R_e)i_a(s)&=\frac{R_e}{s}\\ \left[\frac{1}{1+R_a}+T_o s\right]i_f(s)-\left[R_x+\frac{T_o R_e s}{1+n}\right]\times&\\ i_a(s)=T_o(1+R_a)-\frac{T_o R_e}{1+n}&\end{aligned}\right\} \tag{17}$$

Solving

$$\left.\begin{aligned} i_a(s)&=\frac{1}{sD}\left[\frac{R_e}{1+R_a}+sT_o\left(1+R_a+R_e\frac{n}{1+n}\right)\right]\\ i_f(s)&=\frac{1}{sD}\left[R_x R_e+sT_o\left((1+R_a)(R_a+R_e+R_x)-\frac{R_e}{1+n}(R_x+R_a)\right)\right]\\ D(s)&=\frac{R_a(1-R_x)+R_e}{1+R_a}+sT_o\left(R_a+R_x+R_e\frac{n}{1+n}\right)\end{aligned}\right\} \tag{18}$$

The inverse transformation of equation 17 gives

$$\left.\begin{aligned} i_a&=A+(B-A)\epsilon^{-t/T}\\ i_f&=C+(D-C)\epsilon^{-t/T}\end{aligned}\right\} \tag{19}$$

where

A = steady value of armature current
B = peak value of armature current
C = steady value of field current
D = peak value of field current
T = time constant of decay

and

$$A=\frac{R_e}{R_a(1-R_x)+R_e} \tag{20a}$$

$$B=\frac{1+R_a+R_e\frac{n}{1+n}}{R_a+R_x+R_e\frac{n}{1+n}} \tag{20b}$$

$$C=\frac{R_e R_x(1+R_a)}{[R_a(1-R_x)+R_e]} \tag{20c}$$

$$D=\frac{(R_e+R_a+R_x)(1+R_a)-(R_x+R_a)\ \frac{R_e}{1+n}}{R_a+R_x+\frac{n}{1+n}R_e} \tag{20d}$$

$$T=\frac{(R_a+R_x+\frac{n}{1+n}R_e)(1+R_a)T_o}{R_a(1-R_x)+R_e} \tag{20e}$$

The time constant equation 20e may be simplified to

$$T=T_o\frac{(R_e'+R_x)(1+R_a)}{R_s-R_a R_x} \tag{21}$$

where R_s is the synchronous resistance, and R_e' is the transient resistance. If full load field time constant $T_o(1+R_a)$ is designated T_{FO}, and fault resistance is negligible, then

$$T=T_{FO}\frac{R_e'}{R_s} \tag{22}$$

Appendix II. Short Circuit of Compound Machine

In the series machine, armature current contributes to direct axis magnetomotive force. If the ratio of series field magnetomotive force to shunt field magnetomotive force at full load is k, then equations 3, 4, and 5 become

$$E_t=(i_f+ki_a)-R_a i_a-R_e(i_a-i_1) \tag{23}$$

$$E_t=R_f i_f+L_f\frac{di_f}{dt}-M\frac{d}{dt}(i_a-i_1) \tag{24}$$

$$E_t=R_x i_a \tag{25}$$

In addition to this change, the value of M must be altered to take into account the increased mutual inductance associated with the presence of the series field. The total mutual inductance can be considered as comprising two components: (1) that resulting from R_e and (2) that resulting from the series field. From equation 14 the mutual inductance attributable to R_e is $(L_f R_e)/(1+n)$. From a similar derivation, using the series field current required to produce a change in shunt field flux linkages equal to the no load full voltage linkages, it can be shown that the series field contribution to mutual inductance is $-L_f k$ (neglecting leakage flux between the shunt and series fields). The value of M then becomes $L_f[(R_e/1+n)-k]$.

In the compound wound machine, the initial value of field current must reflect the series field magnetomotive force contribution. For full voltage, full load, the shunt field current is $(1+R_a-k)$ per unit and the corresponding field resistance $1/(1+R_a-k)$ per unit.

Substituting and solving as in the case of

shunt machine, the constants A, B, C, D, and T of equation 18 become

$$\left.\begin{aligned}
A &= \frac{R_e}{(R_a-k)(1-R_x)+R_e} \\
B &= \frac{1+R_o+R_e\dfrac{n}{1+n}}{R_x+R_a+\dfrac{n}{1+n}R_e} \\
C &= \frac{R_xR_e(1+R_a-k)}{(R_a-k)(1+R_x)+R_e} \\
D &= \frac{\left[(R_a+R_e+R_x-k)(1-R_a)-\dfrac{R_e}{1+n}(R_a+R_x+kn)\right]}{R_x+R_a+R_e\dfrac{n}{1+n}} \\
T &= \frac{\left(R_x+R_a+\dfrac{n}{1+n}R_e\right)(1+R_a-k)}{(R_a-k)(1-R_x)+R_e}T_o
\end{aligned}\right\} \quad (26)$$

The peak armature current obtained by use of the values of equation 23 is

$$\frac{1+R_a+\dfrac{n}{1+n}R_e}{R_x+R_a+R_e\dfrac{n}{1+n}}$$

or the same value as obtained from the values for the shunt machine given in equation 19.

Appendix III

The equations derived in Appendix I and Appendix II disregard effects of residual flux, saturation, and armature inductance. It is convenient to have empirical relations taking these effects into account. These relations can be obtained by using the peak current values and time constants from Appendix II and the initial rate of rise and final steady current from other data. The complete equation for armature current then becomes

$$i_a = I_s + (I_p - I_s)\epsilon^{-t/T} - I_p\epsilon^{-t/T} \quad (27)$$

where

I_s = steady current value following short circuit

I_p = peak current value following short circuit from equation 26,

$$\left[\frac{1+R_a+R_e\dfrac{n}{1+n}}{R_x+R_a+R_e\dfrac{n}{1+n}}\right]$$

T = time constant of current decay from equation 26

$$\frac{\left(R_x+R_a+\dfrac{n}{1+n}R_e\right)(1+R_a-k)}{(R_a-k)(1-R_x)+R_e}T_o$$

T' = time constant corresponding to the initial rate of current rise. If i' is the initial rate of current rise in per unit per second, then $T' = \dfrac{I_p - I_s}{i'}$

References

1. Electrical Transmission and Distribution Reference Book, Westinghouse Manufacturing Company, 1943, page 135.

2. Protection of Large D-C Machines by Means of High-Speed Circuit Breakers, **J. E. Housley, O. Jensen.** AIEE Transactions, volume 63, 1944, September section, pages 637–40.

3. Present D-C Aircraft Electric Supply Systems, **H. C. Anderson, S. B. Crary, N. R. Schultz.** AIEE Transactions, volume 63, 1944, June section, pages 265–72.

4. Transients in Linear Systems (book), **Gardner, Barnes.** J. Wiley, Inc., New York, N. Y., 1942.

5. D-C Machine Flashover and Bus Short-Circuit Protection, **T. B. Montgomery, J. F. Sellers.** AIEE Transactions, volume 60, 1941, pages 1168–73.

6. Short Circuit Current and Protection of Large Direct Current Generators, **H. Hess.** *Archiv fuer Elektrotechnik*, volume 27, 1933, page 467.

7. Transients in Arc Welding Generators, **A. R. Miller.** AIEE Transactions, volume 52, March section, 1933, pages 260–7.

8. Principles of Direct-Current Machines (book), **A. S. Langsdorf.** Mc Graw-Hill Book Company, New York, N. Y. Fourth edition, 1931. Page 214.

9. Synchronous Machines—IV, **R. E. Doherty, C. A. Nickle.** AIEE Transactions, volume 47, 1928, April section, pages 457–87.

10. Three-Phase Short Circuit Synchronous Machines—V, **R. E. Doherty, C. A. Nickle.** AIEE Transactions, volume 49, 1930, April section, pages 700–14.



Time

Time is the measure of all things. Few of man's inventions can stand its merciless judgment. Yet Kerite for over 90 years has thrived and spread and gained renown. Time, indeed, gives Kerite its unqualified recommendation.



THE KERITE COMPANY

NEW YORK CHICAGO SAN FRANCISCO

PIONEERS IN CABLE ENGINEERING

First Choice on every count

Permanently Insulated ROCKBESTOS A.V.C.

There are 9 good reasons why you should wire circuits that are exposed to severe operating conditions with Rockbestos A.V.C. wires, cables and cords . . . and they all combine to *insure* you against failures and practically eliminate expensive circuit maintenance.

You won't have to pull out and replace power, control and lighting circuits that are failing too often . . . and then do the same thing all over again . . . if you rewire with *asbestos insulated* Rockbestos A.V.C. Its felted asbestos walls, impregnated with heat, flame and moisture resisting compounds, are built to give you the *extra* protection needed to withstand conditions that ruin wire. They make an installation *permanent*, protect circuit operation and save the cost of repeated replacement.

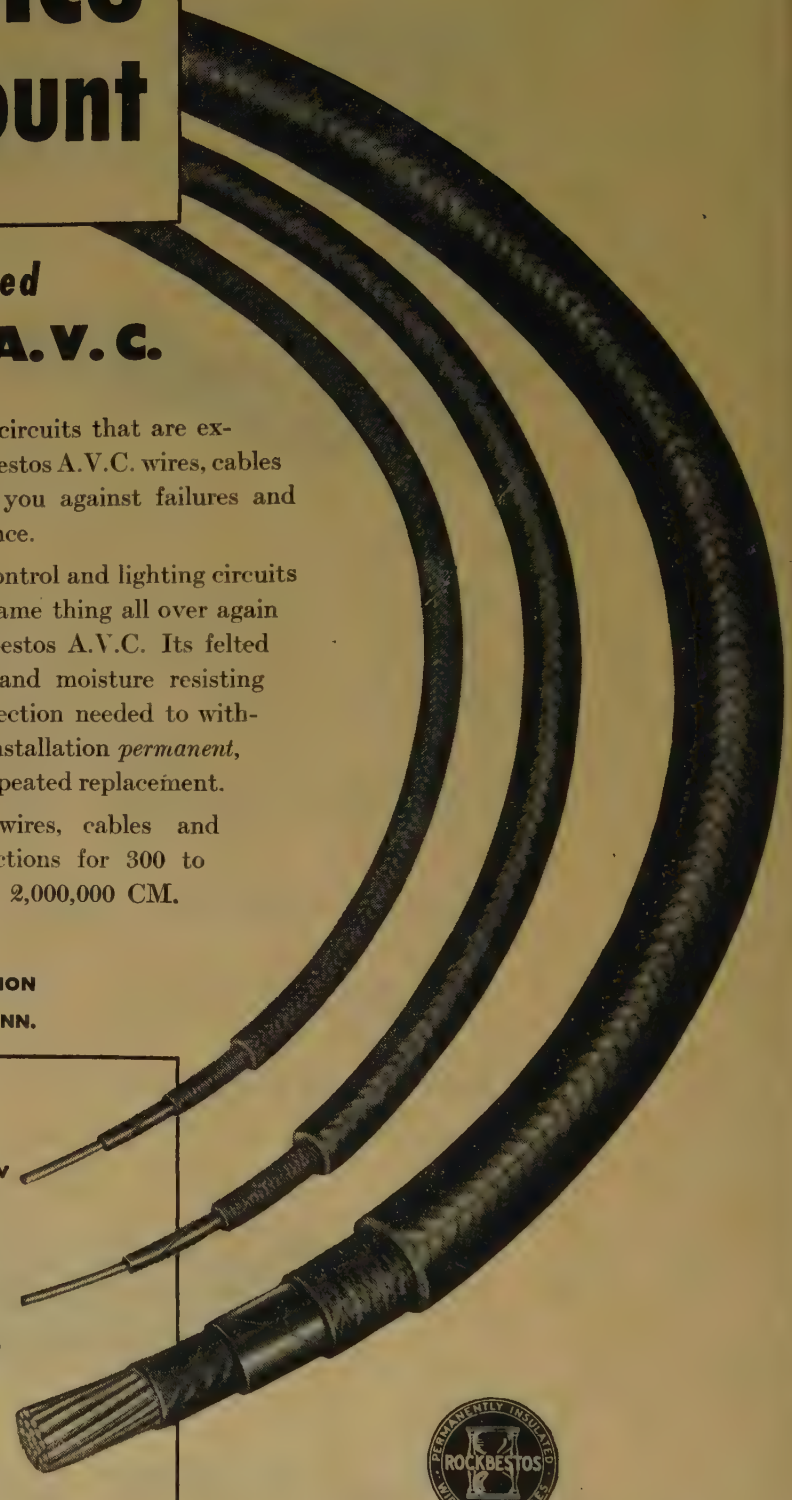
These *permanently insulated* money-saving wires, cables and cords are made in a wide variety of constructions for 300 to 5000 volt service . . . in sizes No. 18 AWG to 2,000,000 CM. For complete data write for a catalog.

ROCKBESTOS PRODUCTS CORPORATION
142 NICOLL ST., NEW HAVEN 4, CONN.

1. **Won't age or deteriorate**
2. **Won't bake brittle, crack or flow under heat**
3. **Won't burn or carry flame**
4. **Corrosive fumes won't rot it**
5. **Remains permanently flexible**
6. **Resists oil, grease and moisture**
7. **Withstands conductor-heating overloads**
8. **Gives greater current carrying capacity**
9. **Reduces circuit maintenance expense**

These characteristics are built into 125 Rockbestos constructions including the wires illustrated:

Rockbestos A.V.C. 600 Volt Switchboard Wire.
Rockbestos A.V.C. 600 Volt Boiler Room Wire.
Rockbestos A.V.C. 600 Volt Power Cable.



ROCKBESTOS A.V.C.
The Wire with Permanent Insulation

NEW YORK BUFFALO CLEVELAND CHICAGO
PITTSBURGH ST. LOUIS LOS ANGELES
SAN FRANCICSO SEATTLE PORTLAND, ORE.

SERVING YOU THROUGH SCIENCE

NEW CODE CHANGES SHOW PROGRESS IN BRANCH CIRCUIT WIRING

		R	RH	RW	RU	T (Formerly SN)	TW
Maximum Operating Temperature	1940	50 C	75 C	50 C	60 C	60 C	
	1946	60 C	75 C	60 C	60 C	60 C	60 C
Insulation Wall Thickness	1940	3/64"—#14, 12, 10 AWG 4/64"—#8—2 AWG 5/64"—#1—4/0 AWG	3/64"—#14, 12, 10 AWG 4/64"—#8—2 AWG 5/64"—#1—4/0 AWG	3/64"—#14, 12, 10 AWG 4/64"—#8—2 AWG 5/64"—#1—4/0 AWG	18 Mils (1.15/64) #14, 12, 10 AWG	2/64"—#14, 12, 10 AWG 3/64"—#8 AWG 4/64"—#6—2 AWG 5/64"—#1—4/0 AWG	
	1946	2/64"—#14, 12 AWG 3/64"—#10 AWG 4/64"—#8—2 AWG 5/64"—#1—4/0 AWG	2/64"—#14, 12 AWG 3/64"—#10 AWG 4/64"—#8—2 AWG 5/64"—#1—4/0 AWG	3/64"—#14, 12, 10 AWG 4/64"—#8—2 AWG 5/64"—#1—4/0 AWG	18 Mils (1.15/64) #14, 12, 10 AWG 25 Mils (1.6/64) #8, 6 AWG	2/64"—#14, 12, 10 AWG 3/64"—#8 AWG 4/64"—#6—2 AWG 5/64"—#1—4/0 AWG	2/64"—#14, 12, 10 AWG 3/64"—#8 AWG 4/64"—#6—2 AWG 5/64"—#1—4/0 AWG
Uses (Under National Electrical Code)	1940	General Use	General Use	General Use or in Wet Locations	Rewiring Only	Rewiring Only	
	1946	General Use	General Use	General Use or in Wet Locations	General Use May be used in Non-Metallic Sheathed Cable	#14—4/0 AWG General #14—2000 MCM Open Work	#14—4/0 AWG General #14—2000 MCM Open Work
Sizes (Under National Electrical Code)	1940	#14—2000 MCM	#14—2000 MCM	#14—2000 MCM	#14, 12, 10 AWG	#14—4/0 AWG	
	1946	#14—2000 MCM	#14—2000 MCM	#14—2000 MCM	Now Approved in Sizes #14—6 AWG	#14—4/0 AWG General #14—2000 MCM Open Work	#14—4/0 AWG General #14—2000 MCM Open Work

Current Carrying Capacity (In Amperes)

	R			RH			RW			RU			T (Formerly SN)			TW		
	Size	Conduit*	Open Wiring	Size	Conduit*	Open Wiring	Size	Conduit*	Open Wiring	Size	Conduit*	Open Wiring	Size	Conduit*	Open Wiring	Size	Conduit*	Open Wiring
1940	14	15	20	14	22	29	14	15		14	18		14	18				
	12	20	26	12	27	37	12	20		12	23		12	23				
	10	25	35	10	37	50	10	25		10	31		10	31				
	8	35	48	8	49	69	8	35					8	41				
	6	45	65	6	65	94	6	45					6	54				
	4	60	87	4	86	125	4	60					4	72				
	2	80	118	2	115	170	2	80					2	96				
1946	14	15	20	14	15	20	14	15	20	14	15	20	14	15	20	14	15	20
	12	20	25	12	20	25	12	20	25	12	20	25	12	20	25	12	20	25
	10	30	40	10	30	40	10	30	40	10	30	40	10	30	40	10	30	40
	8	40	55	8	45	65	8	40	55	8	40	55	8	40	55	8	40	55
	6	55	80	6	65	95	6	55	80	6	55	80	6	55	80	6	55	80
	4	70	105	4	85	125	4	70	105	4			4	70	105	4	70	105
	2	95	140	2	115	170	2	95	140				2	95	140	2	95	140

*Not more than 3 conductors in conduit, raceway or cable. For more than three conductors in conduit, raceway or cable, reduce current carrying capacity in accordance with 1946 Code.

NOTE: According to Underwriters Laboratories; 1946 Code—R, RH and RW—may be labeled after April 1, 1946. Manufacturers need not produce until November 1. When production does start, Underwriters' labels must be applied and tags must be marked: "1946 Code."

1940 Code—R, RH, RW—may be labeled until November 1, 1946. Stocks in inventory after November 1 may be used until supply is exhausted.

Laytex (RU) is America's smallest diameter, lightest weight rubber insulated branch circuit wire. Laminated construction and perfectly centered conductors insure electrical safety.

Write for new wall hanger soon available. In meantime, use this chart

UNITED STATES RUBBER COMPANY

1230 AVENUE OF THE AMERICAS • ROCKEFELLER CENTER • NEW YORK 20, N. Y.



KEPT BOMBERS ON THE BEAM

● Plastics materials are so versatile that molding compounds can be developed to meet special conditions. Often the success of a plastics application depends upon the development of special molding compound.

An example is the Loop Antenna Housing manufactured by General Electric for bombers during the war. When early models were tested, they stood up under wind, rain, ice, sun, and extremes of temperature. But the plastics material used gave unforeseen trouble.

It released ammonia that corroded the metal fittings. And it did not give sufficient safeguard against the building up of static electricity. Too much static would interfere seriously with radio reception.

G-E engineers corrected the corrosion condition by replacing the two-stage phenolic resin with an ammonia-free one-stage resin in the molding compound.

Then it was found that the addition of graphite to the molding compound would give the degree of conductivity necessary to prevent hazardous static build-up in the molded plastics parts.

The fabric filler used in this ammonia-free, graphite-added molding compound were cuttings of fine cotton twill uniform shirts supplied by military tailors. These "shirttails" had to be carefully selected, because textile which had been waterproofed for tropical use failed to absorb resin.

This special molding compound made the plastics Loop Antenna Housing acceptable—and General Electric supplied tens of thousands of them for our bombers.



WHY G. E. USED "DEEP-THROAT" MOLDS FOR ANTENNA HOUSING. **Cross-section split of teardrop design gave alignment to the two sections—facilitated their assembly—minimized shrinkage and warpage factors.**

G. E. employs all available plastics materials in the development of molding compounds. That is why you can be sure of an unbiased material specification when you bring your plastics problem to General Electric—the world's largest manufacturer of finished plastics products. "*Designing Molded Plastics Parts,*" *a helpful booklet, will be sent to you upon request.* Section E-4, Plastics Divisions, Chemical Department, General Electric Company, 1 Plastics Avenue, Pittsfield, Mass.

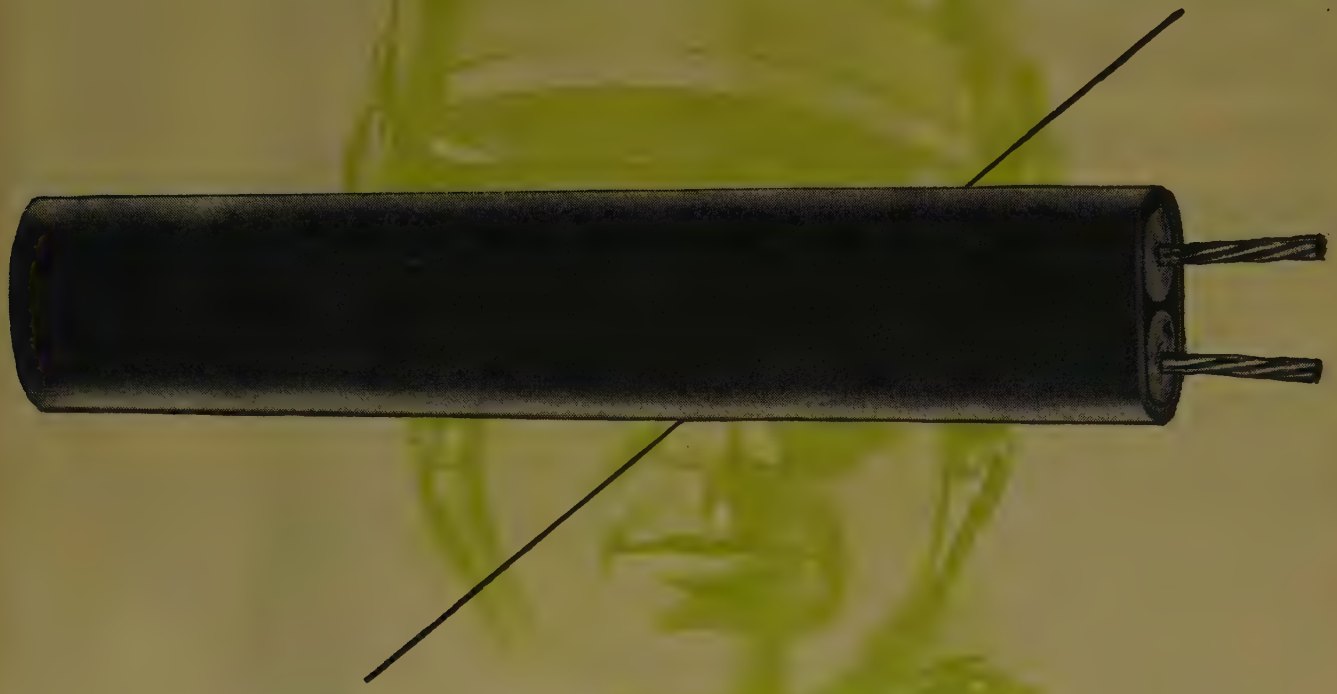
GENERAL ELECTRIC

CD46-H2

EVERYTHING IN PLASTICS

Surer even than a pilot's eyes

. . . the high-freauency cable that makes **RADAR** *possible*



is insulated with

Du Pont POLYTHENE



CUT-BACK SECTION of a modern twin coaxial cable for use in direction-finding equipment at ultra-high frequencies (400 to 10,000 megacycles). JAN-C-17 designation RG-23/U; made by Anaconda Wire & Cable Co. The insulation, about 140-150 mils thick, is Du Pont polythene.

Radar and associated electronic developments, born in stress of war, have important peacetime uses immediately ahead. Ships and planes which, without radar, might be hopelessly lost in foul weather or fog, may now soon be located . . . come safely to harbor or airport . . . thanks to one or several of the four main types of radar.

In this important work Du Pont polythene plays an indispensable part. For radar depends on ultra-high frequencies —anywhere from 2 to 10,000 megacycles! The cables that carry these currents must have an insulating material of low electrical losses—which at the same time is flexible at low temperatures. *Du Pont polythene meets both these requirements.*

Other properties of Du Pont polythene: outstanding chemical inertness, light weight (specific gravity 0.92), low moisture permeability, flexibility in thin sections, rigidity in thick. For complete data sheet, write to E. I. du Pont de Nemours & Co. (Inc.), Plastics Dept., Room 166, Arlington, N. J.

Du Pont manufactures polythene molding powder.

Commercial extruders convert polythene into the forms of



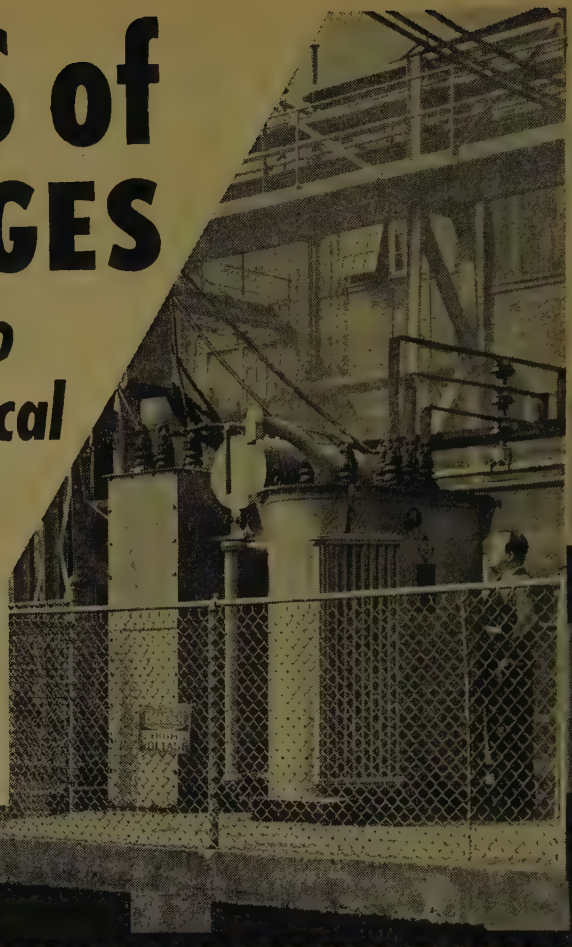
DU PONT
Plastics

ACRES of VOLTAGES

distributed to critical chemical processes

by

AMERTRAN TRANSFORMERS





Three 150 KVA single phase AmerTran Power Transformers. 2300-440 V.

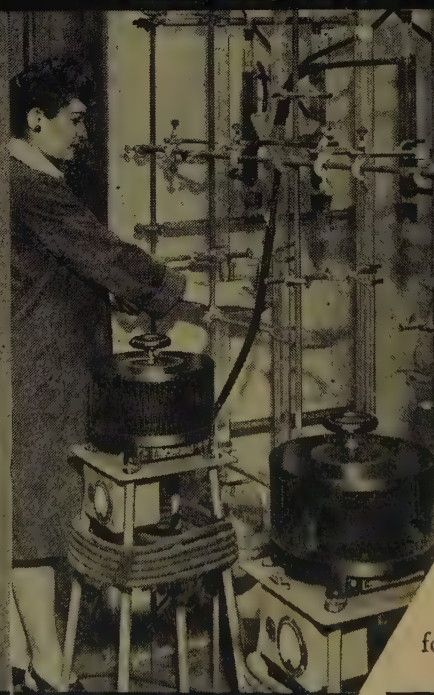


600 KVA O.I.S.C. AmerTran Power Transformer. 3 phase, 2300-440 V.

GENERAL ANILINE AND FILM CORPORATION
GRASSELLI, NEW JERSEY



Three AmerTran Dry Type Transformers, used in load balance circuit. Single phase, 440-220 110 V., 25 KVA. Other AmerTran Dry Type units are used for lighting and at-the-load power.



Two heavy Duty AmerTran Transtats, providing precise AC voltage control for laboratory processes. (There are many more Transtats in this plant.)

Miles of distribution lines cover the many acres of plant operations at the huge Grasselli, New Jersey works of this corporation. The first AmerTran installation went into service many years ago. It is on the job today, supported by many other AmerTrans throughout the property. These units range from the main power transformers down through the various ratings of distribution types—to the compact, troublefree, "at-the-load" dry type AmerTrans.

If continued buying means satisfaction, we'd say that AmerTrans are doing a pretty satisfactory job for this busy company. In fact, they told us so!

AMERTRAN

REG U. S. PAT. OFF.

MANUFACTURING SINCE 1901 AT NEWARK, N. J.

AMERICAN TRANSFORMER CO. 178 Emmet St., Newark 5, N. J.

Pioneer Manufacturers of Transformers, Reactors and Rectifiers for Electronics and Power Transmission

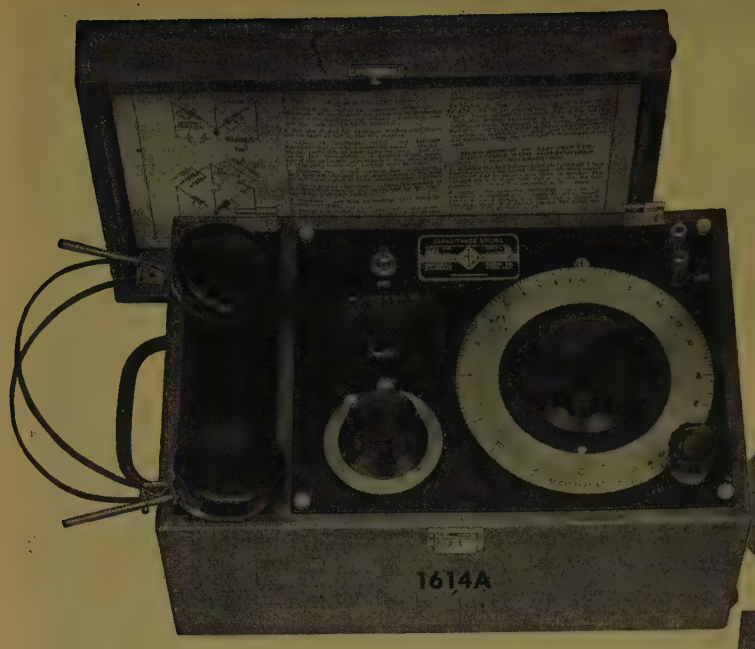
AMER TRAN

BURNDY
Scrulugs



NOW AVAILABLE IN
SIZES UP TO 500 MCM

BURNDY ENGINEERING CO., INC., 107E BRUCKNER BLVD., N. Y. 54, N. Y.





for Rapid Measurements of CAPACITANCE and INDUCTANCE

THESE two portable, self-contained bridges are designed for use in the laboratory, in production testing and in industrial plants. Their accuracy is sufficient for a large majority of routine measurements. Their usefulness is increased considerably by their being portable, self-contained, battery operated, and complete and ready to use at all times. They are both housed in walnut cabinets with removable cover and are supplied with the 6-volt dry battery and headset required for each.

TYPE 1614-A CAPACITANCE BRIDGE

RANGE for Capacitance: 10 micromicrofarads to 100 microfarads in three steps; 10 micromicrofarads to 10,000 micromicrofarads; 0.01 microfarad to 1.0 microfarad and 1.0 microfarad to 100 microfarads. **ACCURACY:** ±2% except on lowest range where, after zero of 9 microfarads is subtracted, accuracy is ±2 microfarads +2% of dial reading. **DIAL CALIBRATION:** approximately logarithmic over two main decades, with compressed lower decade used for measurements below 100 microfarads. **RANGE** for Dissipation Factor: 0 to 45%. **FREQUENCY:** 1000 cycles ±5% from internal oscillator. **ACCESSORIES REQUIRED:** if a d-c polarizing voltage is used a 2 microfarad blocking condenser is required. Space is provided in the cabinet for such a condenser, not supplied with the instrument. **Price: $105.00**

TYPE 1631-A INDUCTANCE BRIDGE

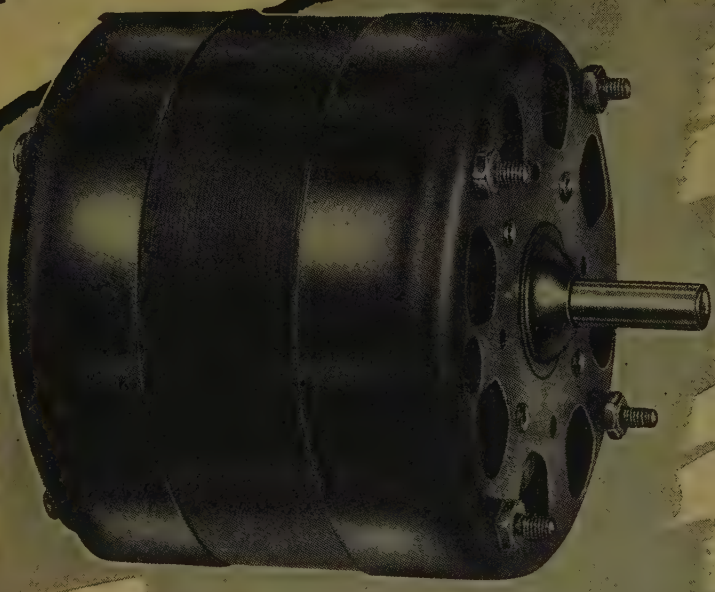
RANGE for Inductance: 10 microhenries to 100 henries in 3 steps of 10 microhenries to 10,000 microhenries; 0.1 henry to 1 henry and 1 henry to 100 henries. **ACCURACY:** ±2.5% of dial reading between 100 microhenries and 10 henries Below 100 microhenries the error varies inversely as the magnitude of the unknown. **DIAL CALIBRATION:** approximately logarithmic over two main decades with a compressed lower decade for measurements below 100 microhenries. **RANGE** for Q (storage factor): 1 to 45. Other specifications are the same as those for the Type 1614-A Capacitance Bridge. **Price: $115.00**

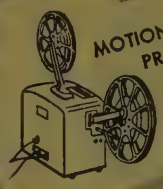
DELIVERIES PROBABLY FROM STOCK. ORDER NOW!

GENERAL RADIO COMPANY Cambridge 39, Massachusetts

90 West St., New York 6 — 920 S. Michigan Ave., Chicago 5 — 950 N. Highland Ave., Los Angeles 38

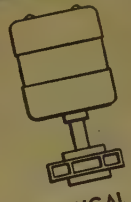
Lower product costs, improve performance through ENGINEERED ADAPTABILITY

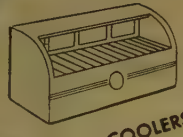


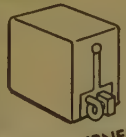

MOTION PICTURE PROJECTORS

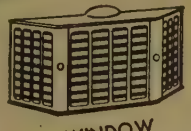

BLOWERS

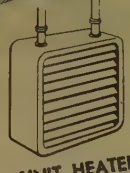

HAIR DRIERS


CENTRIFUGAL PUMPS


DISPLAY COOLERS


OIL BURNERS


WINDOW VENTILATORS


UNIT HEATERS

THE difference between adaptability and *engineered* adaptability may add definite performance and cost advantages to your product. Consult with our engineers NOW if you plan to use production-run quantities of small motors (1/500 to 1/15 H.P.) in your 1947 products. A skilled experienced factory engineer will meet with your engineers in your own plant. He'll make a thorough study of your product design and probably recommend a motor of standard type. *But,* he'll *engineer* the physical and electrical characteristics of the motor—varying them to adapt the motor *specifically* to your product. Write today, describing briefly your product design plans.

F. A. SMITH MANUFACTURING CO., INC.
450 DAVIS STREET ROCHESTER 2, N. Y.

FASCO

Pilot Fractional H.P. MOTORS & BLOWERS

TRUMBULL

RAYMERSION INFRA-RED OVEN

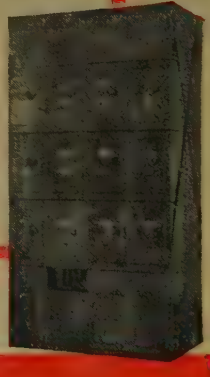
in any size



TRUMBULL
L.V.D. BUSS-WA



TRUMBULL
CONTROL CENTER



NOT ONLY THE OVEN.....BUT ITS ELECTRICAL DISTRIBUTION SYSTEM, AS WELL

Trumbull's long experience in the manufacture of equipment for Distribution and Control of Electrical energy is the "extra dividend" paid to purchasers of Raymersion Infrared Ovens. You may have a complete installation from power source to lamps . . . with assurance that all components have been time tested and proven.

STANDARDIZED, PREFABRICATED

Standardized parts permit the widest range of utility in oven sizes for any type of product, any shape, any mass, any handling method. Temperatures to 500° F. can be obtained, often in seconds, for baking, drying, preheating, expanding or evaporation. Swing-out heater panels facilitate lamp replacement and positioning. Fully insulated from detrimental drafts and heat losses.

FROM POWER SOURCE TO LAMPS

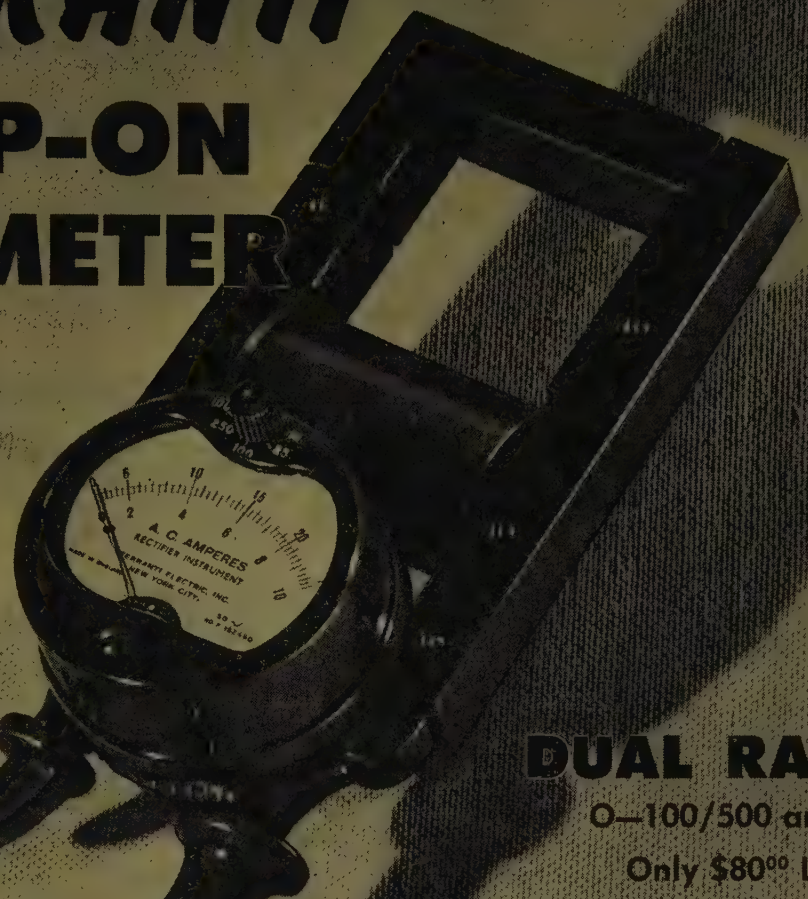
THE TRUMBULL ELECTRIC MANUFACTURING CO.

PLAINVILLE, CONNECTICUT

OTHER FACTORIES AT

WORWOOD, OHIO — LOS ANGELES — SAN FRANCISCO — SEATTLE

FERRANTI
CLIP-ON AMMETER



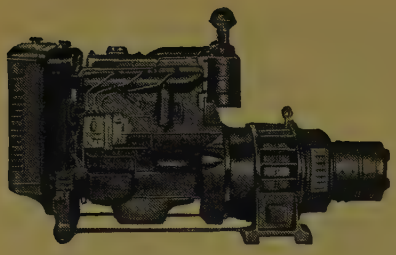
DUAL RANGE
O—100/500 amps.
Only $80.00 List

MULTI-RANGE
O—10/25/100/250/1000 amps.
Only $120.00 List
Case $15.00 List

Free Trial Offer!

FERRANTI ELECTRIC, INC. • RCA BUILDING • NEW YORK 20, N. Y.
Please send me without any obligation: (attach this Coupon to your letterhead)
☐ 1—Dual Range Clip-On Ammeter and Case ☐ 1—Multi-Range Clip-On Ammeter and Case FOR 2 WEEKS' FREE TRIAL

Name .....
Company .....
Address .....



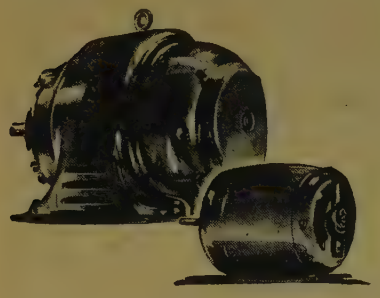
GENERATORS

If unit power generation is your problem, it will pay you to check our large lists of this type of equipment. We have gasoline, steam, Diesel and electric driven generators—(and generators without prime movers) in a wide range of load and voltage characteristics, in both a-c and d-c.



WIRE & CABLE

Our inventory includes an innumerable variety of wire and cable in sizes and insulations usable in industry. Many types conform to underwriters' specifications—others were made for special purposes but are adaptable to industrial and commercial applications.



MOTORS

We have a large supply of electric motors, both a-c and d-c, in unusual speeds, voltages and loads. If you have applications in which these motors can be adapted, inquire at your nearest Regional Office for full particulars and prices.



SWITCH GEAR

Special items in this category are now available if you can use them. Check your requirements and avail yourself of this opportunity to purchase switch gear at considerable savings. Consult your nearest W. A. A. office for description, location and prices.

STANDARD AND SPECIAL ELECTRICAL EQUIPMENT

FOR SALE

priced for immediate disposal

The War Assets Administration offers you government-owned surplus electrical machinery and equipment for your reconversion program at *substantially reduced prices.*

The offer includes wire and cable, generator sets, transformers, switch gear, wiring devices, sub-station power conversion and protective equipment. Much of it is special but adaptable to a large variety of uses.

It has been *priced to sell* and represents attractive bargains to the alert and resourceful industrialist engaging in speedy reconversion.

(Cut out and send to the nearest WAA office listed below)

War Assets Administration: I am interested in the following checked items:

- ☐ WIRE & CABLE
- ☐ GENERATORS
- ☐ SWITCH GEAR
- ☐ SPECIAL ELECTRIC MOTORS
- ☐ WIRING DEVICES
- ☐ POWER CONVERSION EQUIPMENT
- ☐ SUB-STATION EQUIPMENT
- ☐ PROTECTIVE EQUIPMENT

Name..... Tel. No.....

Firm.....

Address.....

City..... State..... 319-1

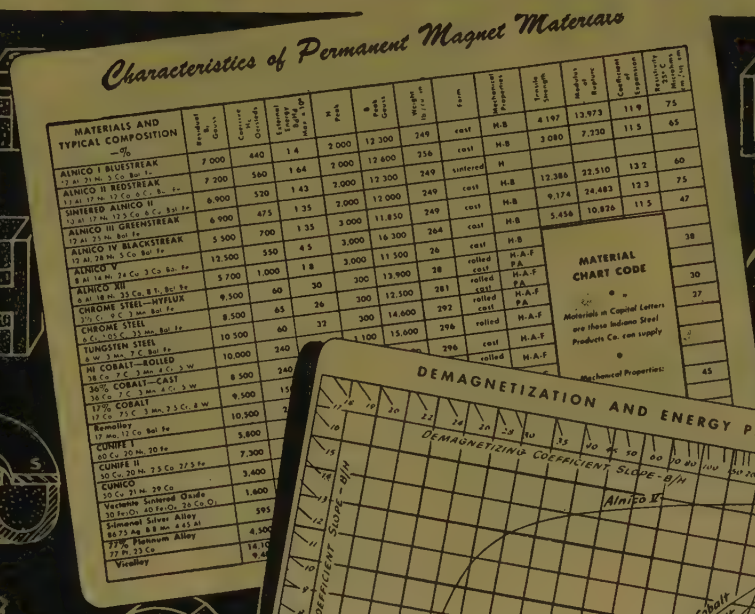
WAR ASSETS ADMINISTRATION

OFFICES LISTED BELOW ARE TEMPORARILY IN RECONSTRUCTION FINANCE CORPORATION AGENCIES

Offices located at: Atlanta • Birmingham • Boston • Charlotte • Chicago • Cleveland • Dallas • Denver Detroit • Helena • Houston • Jacksonville • Kansas City, Mo. • Little Rock • Los Angeles • Louisville Minneapolis • Nashville • New Orleans • New York • Oklahoma City • Omaha • Philadelphia Portland, Ore. • Richmond • St. Louis • Salt Lake City • San Antonio • San Francisco • Seattle • Spokane Cincinnati • Fort Worth (Telephone 3-5381)

VETERANS OF WORLD WAR II: To help you purchase surplus property, a veterans' unit has been established in each WAA office.

PERMANENT MAGNETS MAY DO IT BETTER



Helpful Reference Data for Use of "PACKAGED ENERGY"

Of special interest to engineers and product designers—here are two helpful reference charts, shown in reduced size above, on the *energy product* and *physical characteristics* of permanent magnets featured in the latest "Permanent Magnet Manual", prepared by *Indiana Steel Products Company.*

This manual contains valuable technical data on uses and applications of permanent magnets; modern materials and methods of fabrication—including complete information on the facilities of the Indiana Steel Products Co., the world's largest producer of "Packaged Energy". Ready for prompt mailing to any firm or individual considering commercial magnet application, this manual is available without cost.

More than 24,000 applications of "Packaged Energy" have been developed by our engineers. They are intimately acquainted with all grades of permanent magnet materials and problems of design and application. You are invited to consult with them without obligation.

Write for your free copy of "Permanent Magnet Manual No. 3" today!

***Producers of* Packaged Energy**

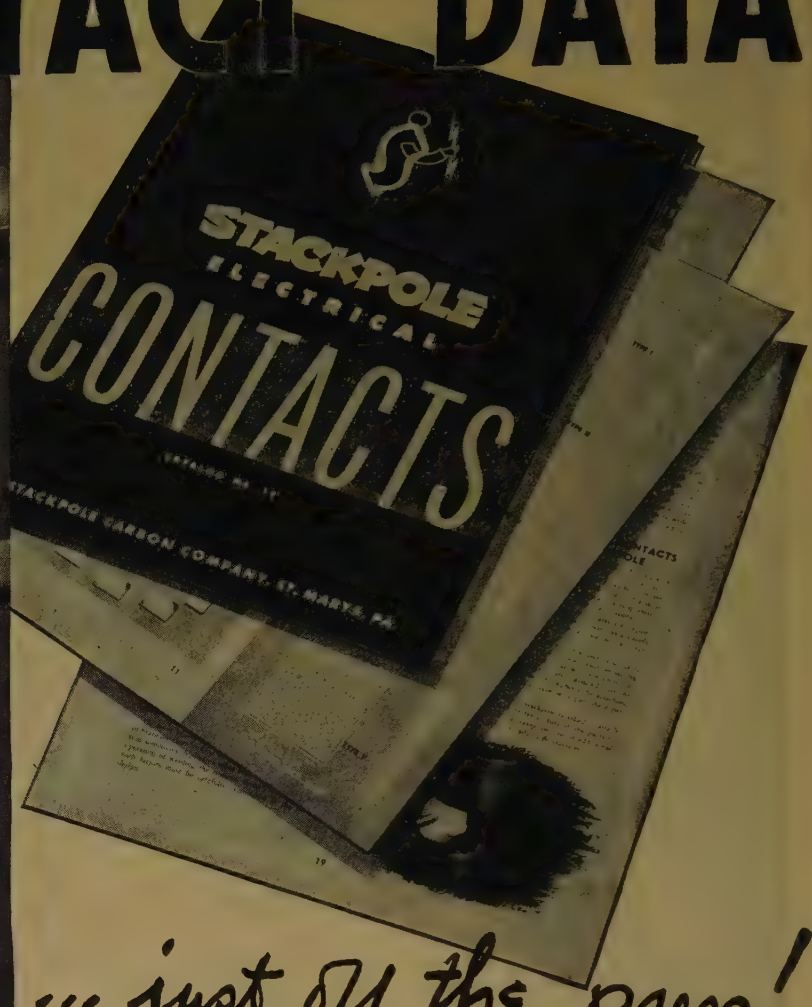
★ ★ ★ **THE INDIANA STEEL PRODUCTS COMPANY** ★ ★ ★

6 NORTH MICHIGAN AVENUE, CHICAGO, 2 ILLINOIS

Copr. 1946, The Indiana Steel Products Co.

SPECIALISTS IN PERMANENT MAGNETS SINCE 1910

CONTACT DATA



... just off the press!

If your product uses contacts you'll find in this new Stackpole Contact Catalog a wealth of information designed to help you select units for maximum service under all conditions of use. New contact developments described will prove highly important in the design of smaller, better post-war electrical equipment. Write today!

STACKPOLE CARBON COMPANY, ST. MARYS, PA.

WRITE FOR YOUR COPY TODAY!

STACKPOLE

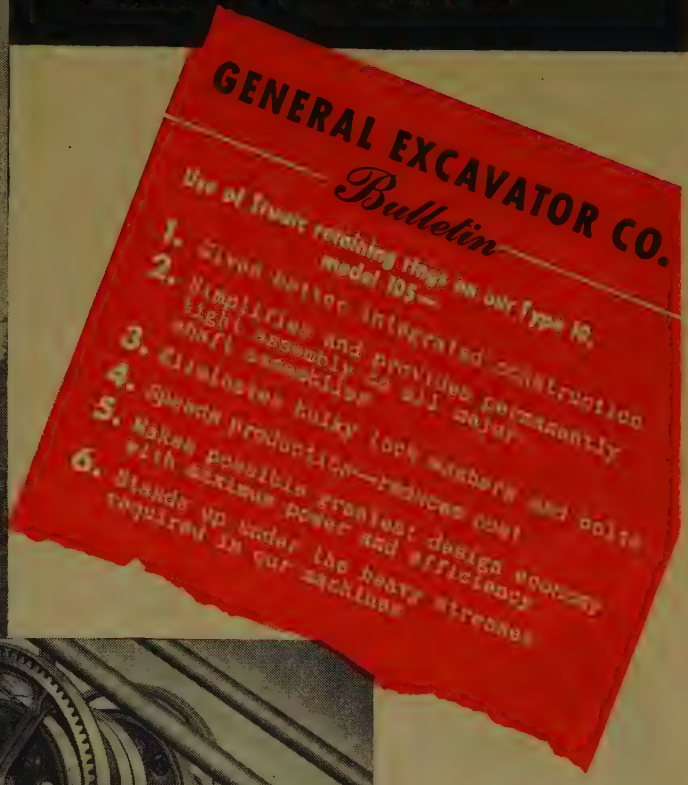
BRUSHES and CONTACTS *(All carbon, graphite, metal and composition types)*
RARE METAL CONTACTS • IRON CORES • WELDING CARBON PRODUCTS
PACKING, PISTON AND SEAL RINGS • RHEOSTAT PLATES AND DISCS
BATTERY CARBONS • POWER TUBE ANODES • CARBON PIPE, ETC.

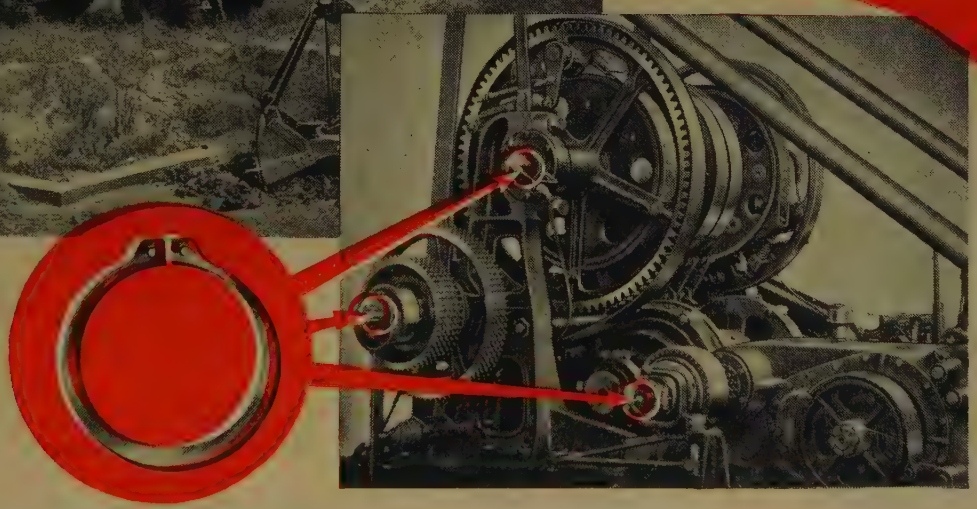
6 WAYS WALDES TRUARC RETAINING RINGS IMPROVED GENERAL EXCAVATOR'S FAMOUS "TYPE 10"



GENERAL EXCAVATOR'S TYPE 10 IN ACTION

An amazing time saving money saving machine. "Type 10" is *precision* equipment—a revolutionary development in excavating machinery. It's one of many products—large and small that have the design economy and greater work efficiency of Truarc rings.

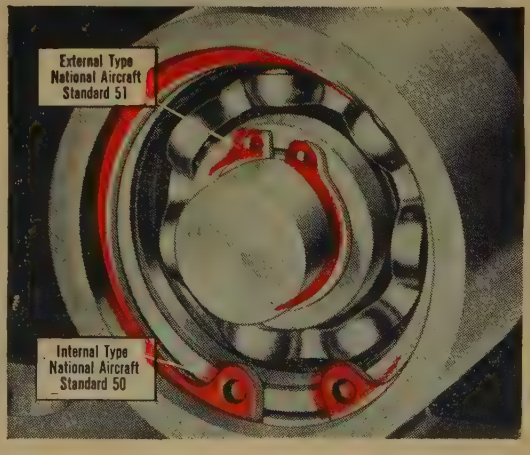




FREE! See how Truarc can improve your products—cut production and maintenance costs. Write today for Truarc booklet showing applications and design sketches. Specify Booklet 16C

NOW YOUR MACHINES CAN HAVE THE DESIGN ECONOMY of retaining rings regardless of load, stress or accuracy involved. Waldes TRUARC high precision retaining rings do the job of nuts, shoulders, collars, pins and snap rings. Yet they allow lighter, more compact units—make assembly and disassembly quicker, easier. TRUARC retaining rings give *better, more dependable retention* because their mathematical precision means perfect circularity—insures an unfailing grip. There's a Truarc ring for every mechanical purpose.

U.S. PAT. RE. 18,144



WALDES TRUARC RETAINING RINGS

TRADE MARK

WALDES KOHINOOR INC., LONG ISLAND CITY 1, N. Y.

CANADIAN REPRESENTATIVE: PRENCO PROGRESS AND ENGINEERING CORPORATION, LTD., 72-74 STAFFORD STREET, TORONTO

Good News!...

INTER-OFFICE MEMO

To: Harry A. Ehle, Vice-pres., Sales
Date: 4/20/46

Production capacity on all types and ranges of All-Metal Rheostats has now been increased to provide additional production for scheduling during last week of May and following months, as per your request of 2/20/46.

From: O. J. Greenway, Works Manager

IRC

All Metal RHEOSTATS

. . . Increased Quantities Now Available on Short Delivery Cycle!



PR-25

TYPE PR-25—25-watt rating. Temperature rise, 140°C. Standard resistance values, 1 ohm to 5,000 ohms. Diameter, 1 21/32". Depth behind panel, 31/32".



PR-50

TYPE PR-50—50-watt rating. Temperature rise, 170°C. Standard resistance values, 0.5 ohm to 10,000 ohms. Diameter, 2 23/32". Depth behind panel, 1 3/8".



PRT (AN3155)

TYPE PRT-25—(AN3155-25). 25-watt rating. Fulfills AN3155 specifications. Totally enclosed. Heat-radiating black finish. Rear terminals. Standard values, 10 ohms to 200 ohms. To 5,000 ohms on special order. Temp. rise, 140°C.

TYPE PRT-50—(AN3155-50). 50-watt rating. Same construction as PRT-25, to AN3155 specifications. Standard values, 5 ohms to 200 ohms. To 10,000 ohms on special order. Temp. rise, 170°C.

All IRC Rheostats operate at about half the temperature rise of equivalent units and can be operated at full load on as little as 25% of the winding with only a slight increase in temperature rise.

CONTACT YOUR IRC REPRESENTATIVE FOR COMPLETE DETAILS

PREFERRED FOR PERFORMANCE · IRC · FIXED & VARIABLE RESISTORS

INTERNATIONAL RESISTANCE CO.

401 N. BROAD ST., PHILADELPHIA 8, PA.

Canadian Licensee: International Resistance Co., Ltd., Toronto

WATCH FOR IT!

DU MONT'S *new* 5-INCH OSCILLOGRAPH

The Type 274

Designed to meet the demand for an inexpensive general-purpose instrument



COMPARES FREQUENCIES • ANALYZES PERFORMANCE • SHOWS CIRCUIT FUNCTIONS

In engineering the new Du Mont Type 274 Oscillograph, the emphasis has been on "quality at a price" —and not price alone. The result: the finest laboratory instrument ever offered for less than one hundred dollars. Available soon—and *it's worth waiting for!*

only

$99.50

© ALLEN B. DU MONT LABORATORIES, INC

DUMONT *Precision Electronics & Television*

ALLEN B DuMONT LABORATORIES, INC., PASSAIC, NEW JERSEY • CABLE ADDRESS: ALBEEDU PASSAIC N. J. U. S. A.

Announcing

THE NEW ROWAN OIL IMMERSED

TYPE 800

LIGHTING SWITCH



Industrial demand for a rugged Lighting Switch which provides safety, dependability, minimum maintenance and positive operation for use in locations where atmospheric conditions are adverse, has been met by Rowan engineers with the new type 800, oil immersed Lighting Switch. These switches are now available in 6- and 12-gang single circuit panels of 125/250 Volt A.C., 3 wire main.

Short circuit and overload protection is provided by use of the time-tested Rowan Air-seal fuses. All electrical operating parts are completely oil immersed thereby eliminating undue heating and oxidation of the fuse clips.

Accelerated tests of over 3,000,000 operations without failure assure you of dependable performance and minimum maintenance.

Descriptive circular available upon request.



Sectional view of the Rowan time-tested Air-seal fuse.

ROWAN CONTROL

THE ROWAN CONTROLLER CO., BALTIMORE, MD.

MOLONEY

Constant Current

TRANSFORMERS

For closer regulation through all ranges of load...less attention...lower maintenance cost! The superior features of Moloney Transformers coupled with soundness of mechanical design is your assurance of years of trouble-free service under the most severe operating conditions.





"TWO MOVING COIL" TYPE . . . BOTH COILS MOVE!

Upon changes in load or on primary surges, normal secondary current is more quickly attained because each coil moves only *half the distance* that the single coil would move on an ordinary regulator. Throughout the operation the coils are kept in parallel position thus securing closer regulation of secondary current.

SHORT CIRCUIT SHOCKS MINIMIZED!

Another feature of Moloney double-moving coil design is the lowered kinetic energy of the coils which practically eliminates force on the bumpers during a short circuit. By eliminating direct metallic contact between the core frames and tank, the usual transformer hum is practically eliminated. Moloney Constant Current Transformers give you these operating features: Automatic and instantaneous regulation . . . no taps or adjustments necessary to maintain constant current from full load to short circuit, when primary voltage is between 5% plus or minus of normal rated voltage.



External View, Type SLB Constant Current Transformer

MOLONEY ELECTRIC CO. ☆ ST. LOUIS 20, MO.

BRANCH OFFICES IN ALL PRINCIPAL CITIES



Cooler Cables in Transite Ducts Carry Heavier Loads

Increases of as much as 15% in current carrying capacity have been measured in cables sheathed in Transite Ducts!

The figures in the test case illustrated, made by Johns-Manville Research Engineers in collaboration with several leading cable engineers, apply to a single Transite Duct compared with an organic duct.

Transite Ducts have been proved to dissipate I^2R losses 13% faster than other ductways tested, thus keeping cables cooler. Higher load capacity, reduced copper losses and increased cable insulation life are the results.

Made of asbestos and cement, Transite Ducts are strong, immune to rust and rot. They are incombustible and unaffected by electrolysis or galvanic action. A permanently smooth bore makes possible long cable pulls and easy replacements. Long, lightweight lengths can be quickly and economically installed. In addition, a full line of fittings simplifies even the most complicated installations.

HOW TRANSITE DUCTS INCREASE CABLE CARRYING CAPACITIES

Tests made on a lead-sheathed 500,000 CM cable insulated with ½" paper and placed inside a single duct encased in concrete.

Sheath Temperature, 145° F.
Ambient Air Temperature, 90° F.

CURRENT CARRYING CAPACITY

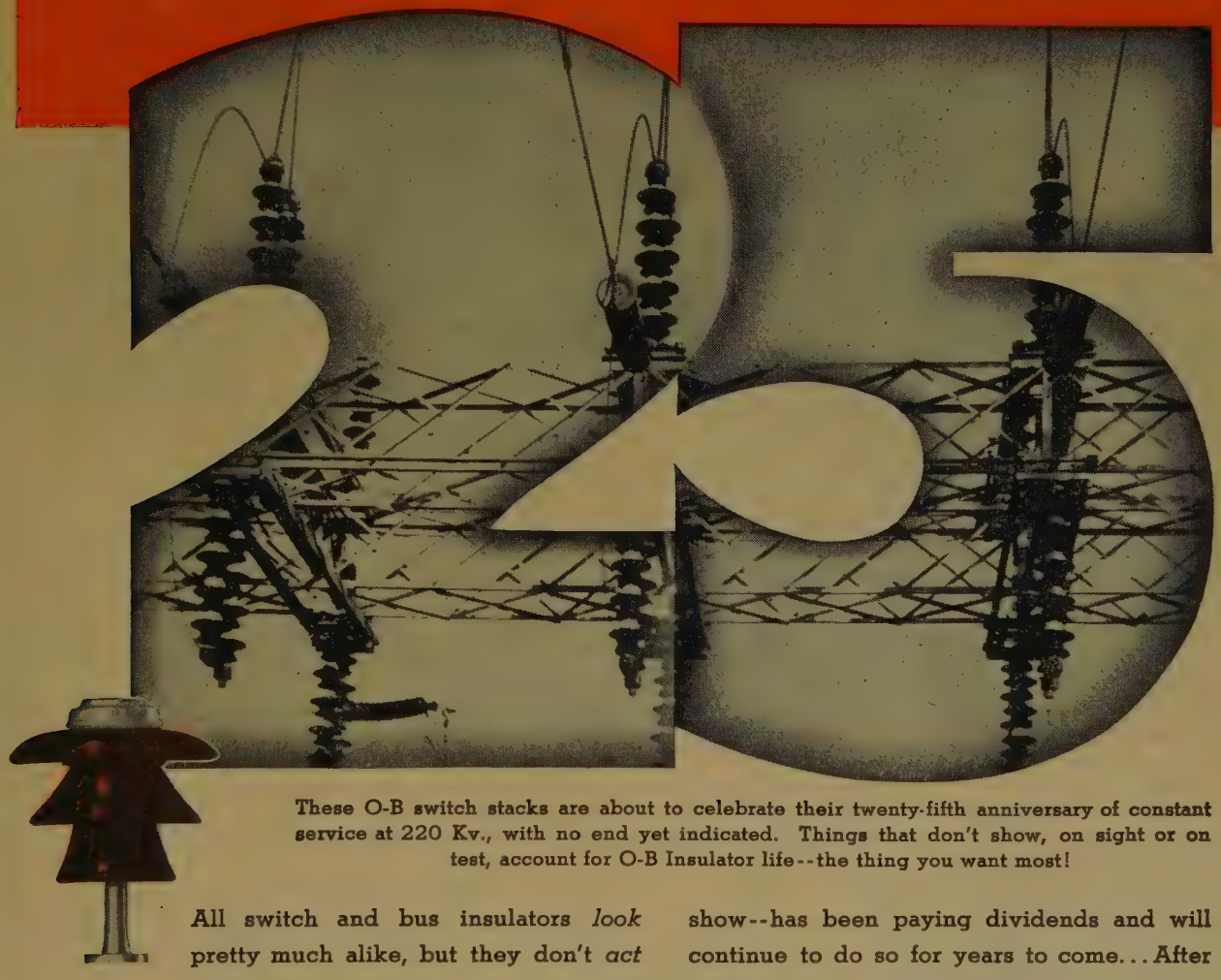
Transite Duct	796 amperes
Organic Duct	691 amperes
Difference	105 amperes

(Figures are results of tests conducted in the J-M Laboratory in collaboration with several leading cable engineers.)

For full information on Transite Ducts, write for Data Book DS-410. Johns-Manville, Box 290, New York 16, New York.

Johns-Manville **TRANSITE DUCTS**
CONDUIT for use without concrete
KORDUCT for concreting in

THE "SILVER ANNIVERSARY" OF A SOUND DECISION



These O-B switch stacks are about to celebrate their twenty-fifth anniversary of constant service at 220 Kv., with no end yet indicated. Things that don't show, on sight or on test, account for O-B Insulator life--the thing you want most!

All switch and bus insulators *look* pretty much alike, but they don't *act* alike! When new, there isn't much difference, but they don't stay new! It's one thing to meet standard specifications with a unit fresh from stock, but it's something entirely different to continue meeting every *service requirement* for a quarter-century or more, with the end nowhere in sight... Many thousands of O-B switch and bus insulators have passed their "Silver Anniversary" of faultless performance. The ruggedness that was there when they were new--but didn't show--has been paying dividends and will continue to do so for years to come... After all, isn't this what you *really want* in an insulator? Then buy O-B!

Ohio Brass

MANSFIELD, OHIO

CANADIAN OHIO BRASS CO., LTD.,
NIAGARA FALLS, ONT.

HEADQUARTERS FOR PORCELAIN INSULATORS

2648-H



A New Data Sheet, richly illustrated, has been issued giving new information about Simplex-PLASTEX insulated wire. It contains important information that will help you to select the right type of wire for your work. It contains engineering information which illustrates why no one plastic compound is satisfactory for all wire and cable uses and lends weight to our statement that to get best results, plastic insulation, like rubber compounds, must be designed for the job in hand.

A copy of this Data Sheet will gladly be sent without obligation. Write for your copy of Data Sheet #114 today.

SIMPLEX WIRES & CABLES

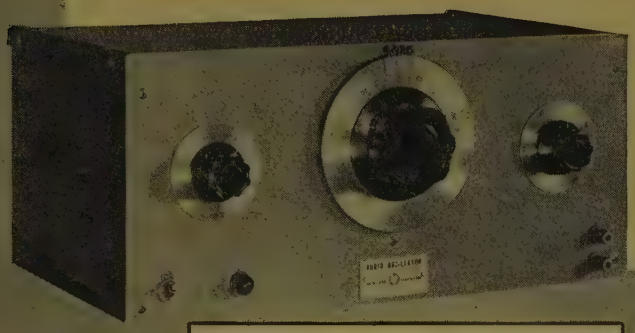
SIMPLEX WIRE & CABLE CO.,
79 SIDNEY ST., CAMBRIDGE 39, MASS.

LABORATORY INSTRUMENTS FOR SPEED AND ACCURACY

BASIC EQUIPMENT FOR AUDIO MEASUREMENTS



VACUUM TUBE VOLTMETER (MODEL 400A)
Full-scale sensitivity from .03 volts to 300 volts in 9 ranges. Input impedance 1 megohm in parallel with 16 mmf. Frequency response—10 cps to 1 mc.



RESISTANCE TUNED OSCILLATORS
Available in 7 models; frequency ranges between 2 cps and 200 kc. No zero setting. Constant output. Low distortion.



AUDIO SIGNAL GENERATOR (MODEL 205AG)
Frequency range 20 cps to 20 kc. 5 watts output with less than 1% distortion. Output impedances of 50, 200, 500, and 5000 ohms, center-tapped. Output attenuator provides 110 db attenuation in 1 db steps.

Wherever audio-frequency and supersonic measurements are made, whether in an electronics laboratory, a broadcast station, or on a production line, -*hp*- equipment will speed the job and guarantee the accuracy of the results. Measurements of frequency response, gain, power, and voltage level throughout the audio-frequency and supersonic range can be made with -*hp*- Resistance Tuned Oscillators, Audio Signal Generators, and Vacuum Tube Voltmeters. Total distortion, hum, and noise are conveniently measured with -*hp*- Distortion Analyzers, and individual components of complex waves may be studied with the -*hp*- Model 300A Wave Analyzer. Frequency measurements are readily made with the Model 100B Secondary Frequency Standard or the Model 500A Electronic Frequency Meter. For more data on -*hp*- measurement equipment, write direct to factory.



HARMONIC ANALYZER (MODEL 300A)
Measures individual components of a complex wave. Frequency range 30 cps to 16 kc. Variable selectivity. Full-scale sensitivity from 1 millivolt to 500 volts.

HEWLETT-PACKARD COMPANY

BOX 1222 B • STATION A • PALO ALTO, CALIFORNIA

Audio Frequency Oscillators *Signal Generators* *Vacuum Tube Voltmeters*
Noise and Distortion Analyzers *Wave Analyzers* *Frequency Meters*
Square Wave Generators *Frequency Standards* *Attenuators* *Electronic Tachometers*

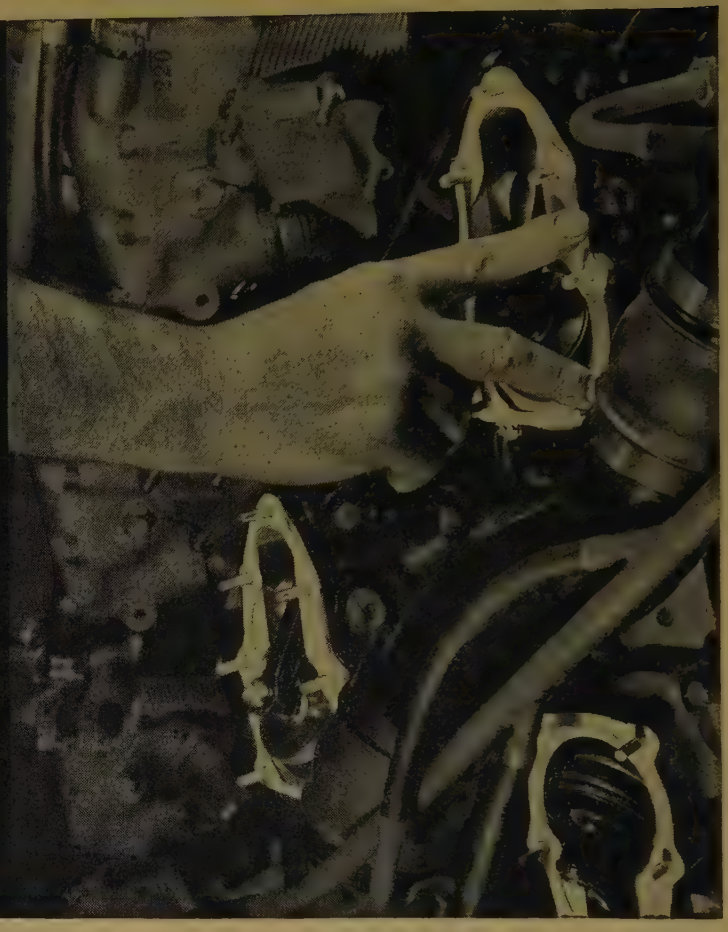
DC
DOW CORNING
SILICONES

SILASTIC
FLUIDS
VARNISHES
RESINS
GREASES

withstand heat
resist oxidation
exclude moisture

SILASTIC* GASKETS

for the
most powerful aircraft
engine ever built!



chosen best among all gasket materials tested for service at 450°F.

"NOTHING BUT THE BEST!" That's the policy followed by Pratt & Whitney in selecting materials for the powerful new 28-cylinder, 3650 h.p. Wasp Major.

That's why Silastic was chosen for these rocker box gaskets. Factors in the choice were Silastic's resiliency at the 450°F. operating temperature, resistance to the hot oil, and convenience in handling.

Silastic will fly with the Wasp Major in such giant new airliners as the Boeing Stratocruiser, Douglas Globemaster, Martin Mars, and Republic Rainbow.

If you need a rubber-like material that's resilient up to 500°F. and flexible down to −70°F., call for "Silastic Facts" No. 1A—and *TRY SILASTIC!*

*Trade Mark, Dow Corning Corporation



Silastic gaskets fabricated from Dow Corning silicone rubber by the Connecticut Hard Rubber Co. seal 56 rocker boxes of the 28-cylinder Pratt & Whitney Wasp Major.

Dow Corning
FIRST IN SILICONES

DOW CORNING CORPORATION • MIDLAND, MICHIGAN

Chicago Office: Builders' Building Cleveland Office: Terminal Tower
New York Office: Empire State Building
In Canada: Dow Corning Products Distributed by Fiberglas Canada, Ltd., Toronto

OVER A THOUSAND DIFFERENT

STOCK Rheostats, Resistors, Tap Switches

AT

OHMITE

Offers a Quick Answer to Resistance Control Needs



Send for Stock-Unit Catalog No. 18

Write for this quick, helpful reference. Gives valuable data and information on the wide variety of Ohmite Stock Units

THE Ohmite stock of power rheostats, resistors and tap switches is the largest and most complete in existence . . . in variety and number!

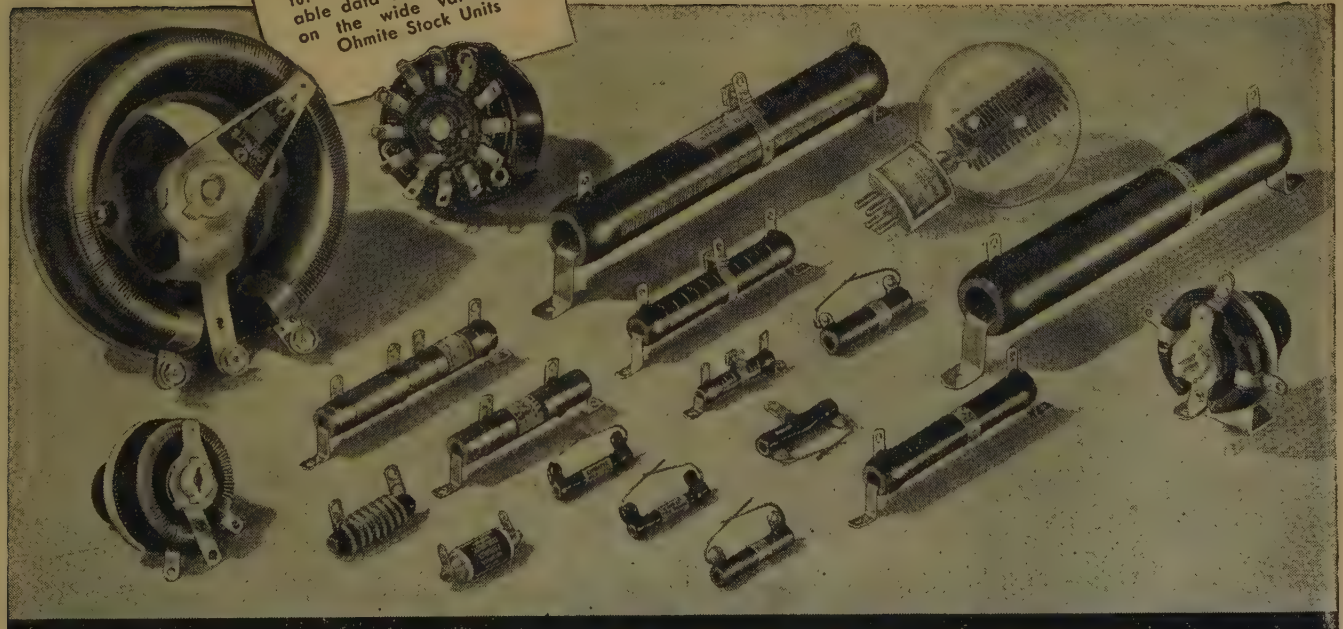
Stock model rheostats are available in six different sizes from 25 to 500 watts . . . each size carried in more than a score of different resistance values . . . some as low as 0.5 ohm and others as high as 10,000 ohms.

Among the stock resistors are eight sizes of wire-wound fixed resistors rated at 1, 10, 20, 25, 50, 100, 160 and 200 watts. Also seven sizes of "Dividohm" adjustable resistors rated at 10, 25, 50, 75, 100, 160 and 200 watts. All sizes are available in scores of resistance values, some less than 1 ohm, others as high as 250,000 ohms.

There are also three series of stock tapped resistors (ten-section "Multivolts"), three series of non-inductive resistors, two series of glass-enclosed non-inductive resistors, five series of "Riteohm" precision resistors, seven series of tap switches, nine series of radio frequency chokes, and many other units.

So great is the variety of Ohmite stock units that a combination of them can be used to obtain an endless number of resistances and wattage capacities. Special units engineered and produced to your specifications.

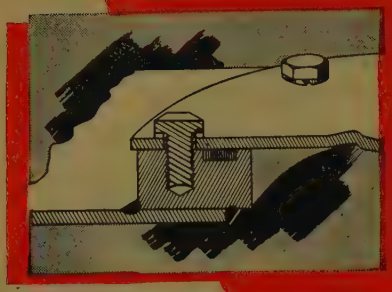
OHMITE MANUFACTURING COMPANY
4803 FLOURNOY STREET, CHICAGO 44, U.S.A.



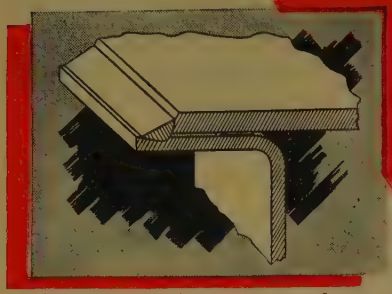
Be Right with **OHMITE**

RHEOSTATS • RESISTORS • TAP SWITCHES

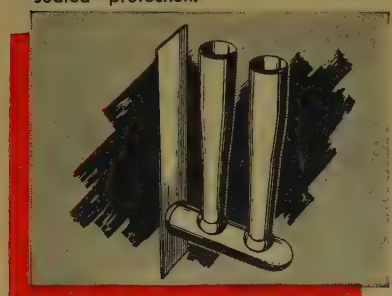
Maintenance Savings Begin with Design of the *tank* of a G-E TRANSFORMER



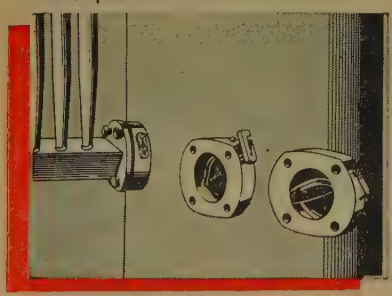
Synthetic rubber gasket, plus metal-to-metal bolting gives weatherproof, liquid-tight joint on transformers rated above 2000 kva.



Welded cover for power transformers of 501 to 2000 kva provides "factory-sealed" protection.



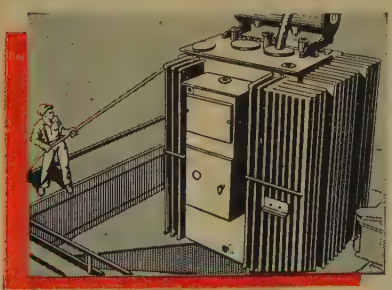
Tubes are swaged at ends for extra thickness and strength at point of welds. This also gives more room for cleaning and inspection.



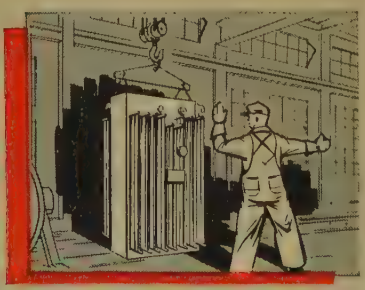
Larger tanks have detachable radiators. Radiator valves permit removal without draining the tank.

IN a G-E power transformer tank there is no such thing as a "minor detail." From the laboratory controlled selection of open-hearth steel plate, down to the 3 baked-on coatings of Glyptal paint, these tanks are built to give utmost protection to core and coils—*with a minimum of inspection and maintenance.*

Efficient protection of the insulating liquid from leakage, moisture absorption and oxidation is essential to trouble-free service. In the manufacture and design of G-E tanks, no effort is spared to provide oil tightness and moisture-proof construction. At the same time, all precautions are taken to assure that the unit will retain these maintenance-reducing qualities through many years of service under all weather conditions. Advanced welding methods, pressure-



Three coats of Glyptal paint, applied on a clean, smooth, shot-blasted surface offer maximum resistance to weather.



Cover can be taken off and core and coils removed without completely draining tank.



Radiators are fabricated and thoroughly tested prior to their installation on the transformer tank.

These G-E tank-construction features keep maintenance costs low

1. Conveniently located filter press connections and oil sampling valve enable easy testing and conditioning of oil.
2. Welds which hold liquid are made externally for accessibility.
3. Tubes are braced against vibration.
4. Glyptal paint, applied over clean, shot-blasted surface inhibits corrosion.
5. Tubes are sturdy, swaged at ends to increase thickness at point of welding, and to reduce strains.
6. Tank is open-hearth steel, checked for carbon content to insure good welding qualities.
7. Properly compressed synthetic rubber gaskets or non-porous welds seal all tank joints.
8. Tube and header construction contributes to oil tightness by radically reducing the number of openings in the tank wall.



The tank is an integral part of a G-E transformer. Strength, shape of housing, liquid tightness, resistance to weather have all been considered. The result is a tank that is **durable**; that requires only a **minimum** of maintenance throughout the life of the transformer.

g of welds, the use of synthetic rubber gaskets, uniform
ainting—all are major factors in the construction of
anks.

s detailed forethought in the design of the tank typifies
esign of every element of a G-E transformer. First-hand
ience with field maintenance conditions, an outstanding
edge of electrical design, and testing with the most up-
te facilities have anticipated every feature that will cut
e costs and keep your transformer in continuous, efficient
tion.

ou are in the process of selecting a transformer, look
ese features that will result in tangible savings in instal-
and maintenance costs. For information call your nearest
epresentative, or write to *Apparatus Dept., General*
c Company, Schenectady 5, N. Y.

POWER TRANSFORMERS

GENERAL ELECTRIC

401-32-5155



Yes, or alike as two telephone handsets made by the same process. Yet, pins or handsets — no two could ever be made exactly alike. Dimensions, weight, performance — all vary every time due to variables in manufacture. How can these variables be *controlled?*

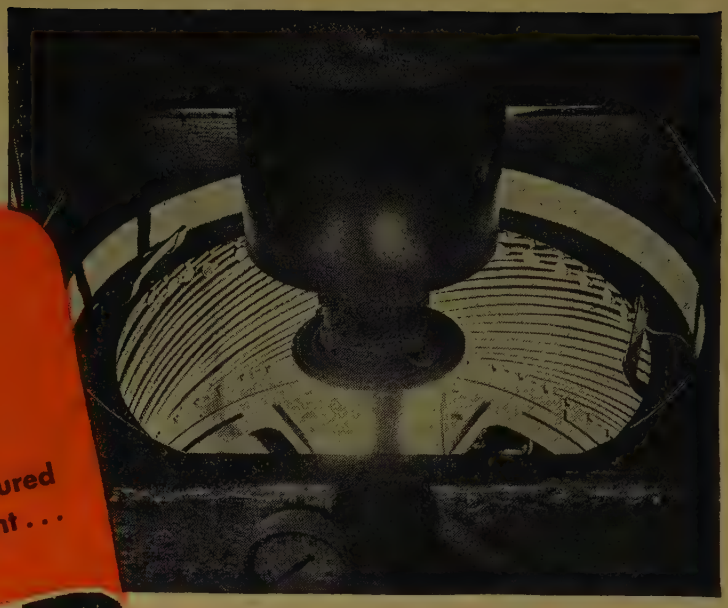
Back in 1924, Bell Laboratories' mathematicians and engineers teamed up to find out, forming the first group of quality-control specialists in history. They invented the now familiar Quality Control Chart, designed inspection tables for scientific sampling. They discovered that test data mathematically charted in the light of probability theory were talking a language that could be read for the benefit of all industry. Western Electric, manufacturing branch of the Bell System, applied the new science to its large-scale production. In war, it was used by industrial and government agencies of the United Nations in establishing and maintaining standards for military matériel. A Quality Assurance Department, a novelty back in the nineteen-twenties, has come to be indispensable to almost every important manufacturer.

Scientific quality control is one of many Bell Laboratories' ideas that have born fruit in the Bell System. The application of mathematics to production helps good management all over the industrial world — and furthers the cause of good telephone service.

BELL TELEPHONE LABORATORIES

EXPLORING AND INVENTING, DEVISING AND PERFECTING FOR CONTINUED IMPROVEMENTS AND ECONOMIES IN TELEPHONE SERVICE.

In the Weather-Ometer, Weatherproof coverings are subjected to the accelerated aging effects of sunlight, wetting and drying, freezing and thawing, simulating rain, sleet and searing sun.



THE PAST...

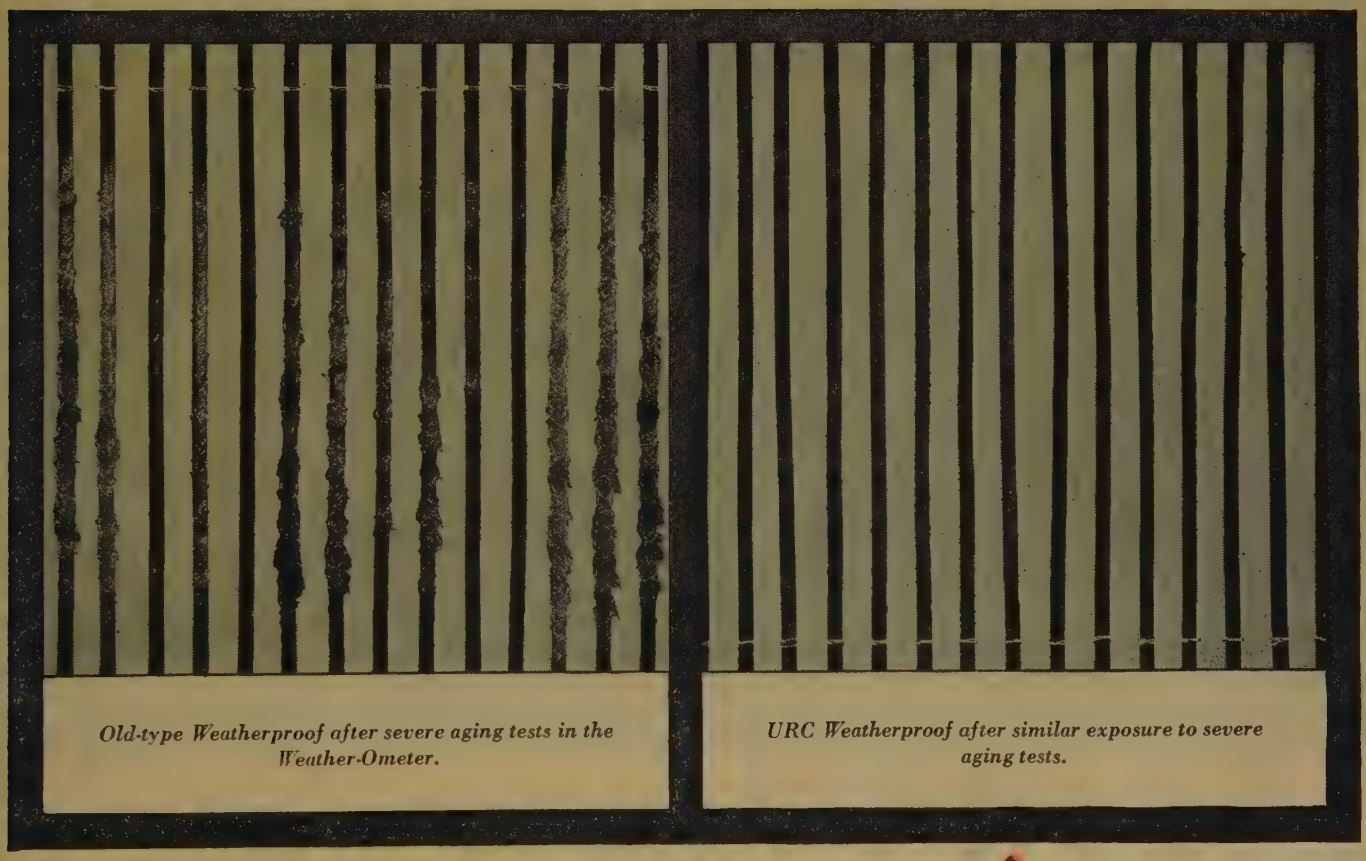
"Festooning" was not unusual . . .

THE PRESENT...

Today, lasting Weatherproof is assured by URC research and development . . .

For Continuity of Service... Anaconda Triple Braid or Duraline URC

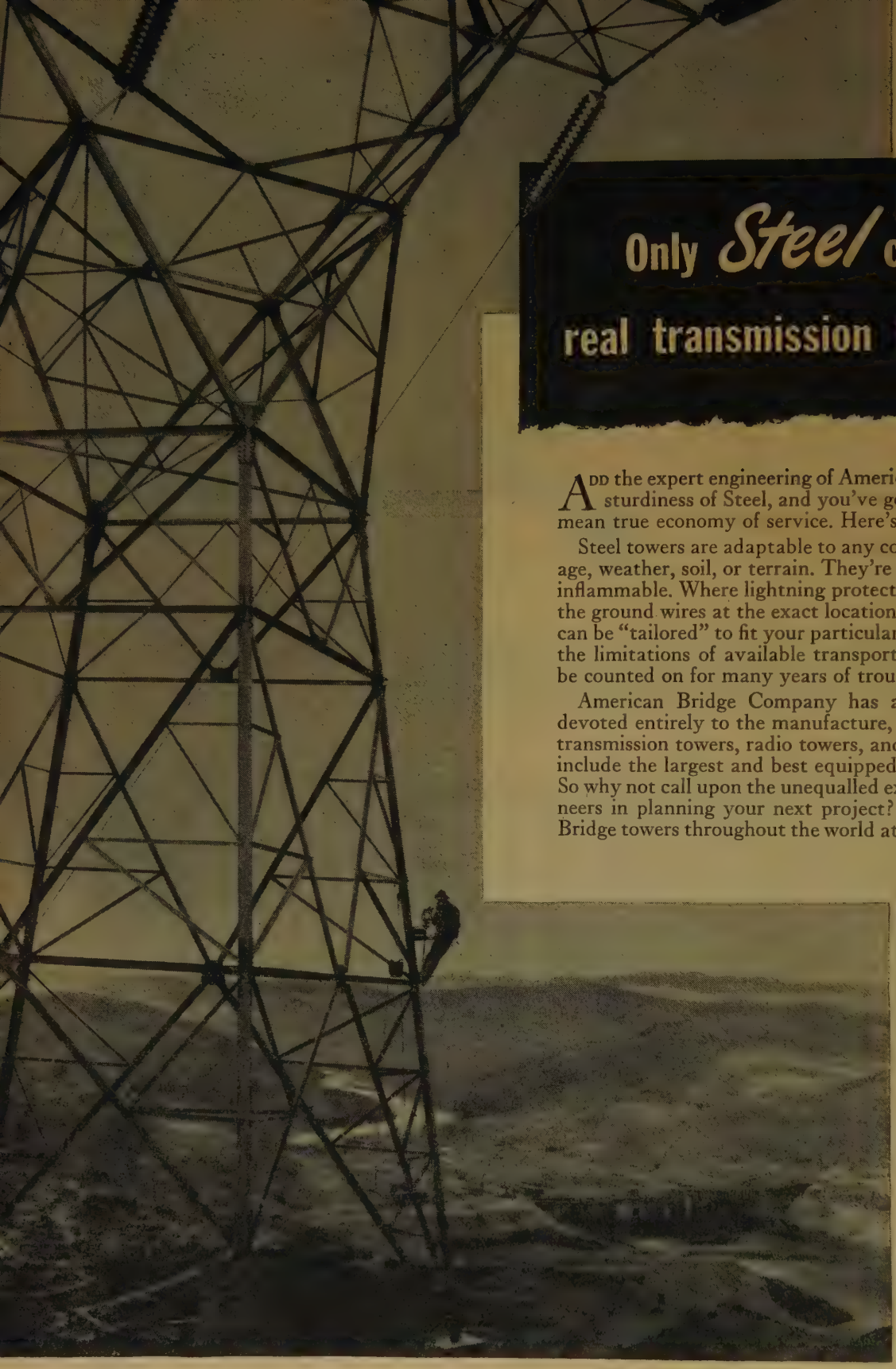
• The long field service expectancy of URC Weatherproof is proven by exhaustive tests on materials and finished wire and cable. These data, plus actual field experience, indicate URC Weatherproof will last for years and years. 46299



Old-type Weatherproof after severe aging tests in the Weather-Ometer.

URC Weatherproof after similar exposure to severe aging tests.

LOOK TO *Anaconda* ANACONDA from mine to consumer **FOR WEATHERPROOF THAT LASTS!**



Only *Steel* can give you real transmission tower economy

ADD the expert engineering of American Bridge Company to the sturdiness of Steel, and you've got transmission towers that mean true economy of service. Here's why:

Steel towers are adaptable to any condition—regardless of voltage, weather, soil, or terrain. They're verminproof. They're noninflammable. Where lightning protection is needed, they support the ground wires at the exact location to do the most good. They can be "tailored" to fit your particular requirements, and to meet the limitations of available transportation. Above all, they can be counted on for many years of trouble-free service.

American Bridge Company has a complete, modern plant devoted entirely to the manufacture, galvanizing, and testing of transmission towers, radio towers, and substations. Our facilities include the largest and best equipped test frame in the country. So why not call upon the unequalled experience of our tower engineers in planning your next project? Sixty thousand American Bridge towers throughout the world attest their success on the job.



AMERICAN BRIDGE COMPANY

General Offices: Frick Building, Pittsburgh, Pa.

District Offices in: Baltimore · Boston · Chicago · Cincinnati · Cleveland · Denver · Detroit
Duluth · Minneapolis · New York · Philadelphia · St. Louis

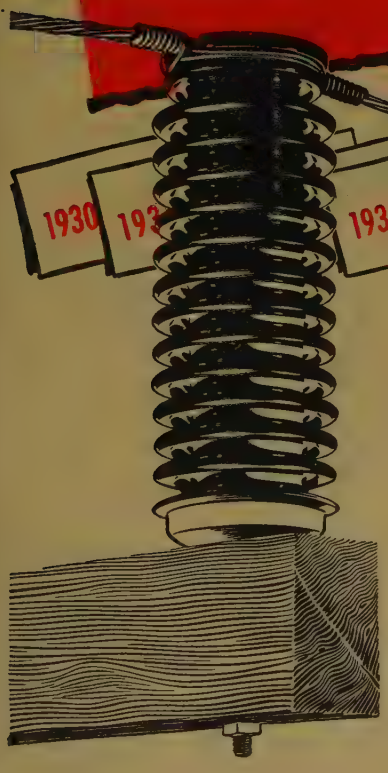
Columbia Steel Company, San Francisco, *Pacific Coast Distributors*
United States Steel Export Company, New York

UNITED STATES STEEL

LINE POST LINES ARE PERMANENTLY RADIO-FREE

In the days when complaints of radio interference constituted the number-one headache to Customer Relations and Transmission Engineering departments, the Lapp Post series of insulators offered the first completely satisfying answer. Radio-free by design—corona cannot form at rated operating voltages and well beyond —Line Posts and Station Posts provide permanent and complete elimination of insulator-generated radio noise.







LAPP LINE POSTS HAVE A 15-YEAR SERVICE RECORD

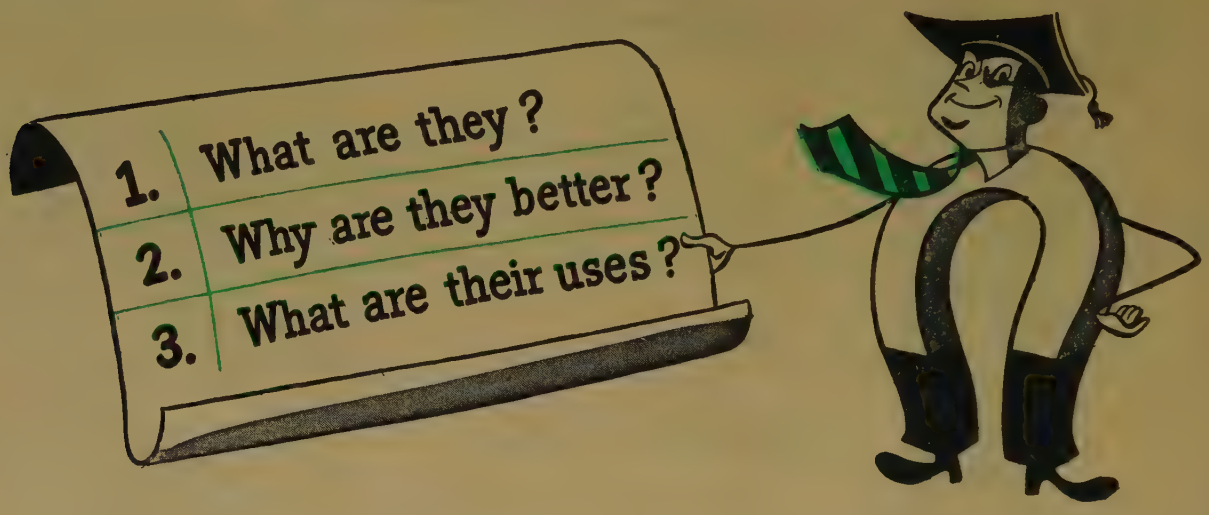
The first shipment of Lapp Line Posts went into service 15 years ago. The installation was the one which had inspired The Line Post design—a particularly bad, and previously unsolved, dirt condition. Since then, hundreds of thousands of Lapp Posts have gone up, in many cases a desperation answer to a difficult service problem—dirt condition, mechanical attack, radio noise, arcover failure. And the 15-year service record of these insulators shows them to stand up better, with fewer line outages, and lower replacement ratio, than any other insulator now in use.



Lapp

LAPP INSULATOR COMPANY, INC., LE ROY, N. Y.

The 3 "most-asked" questions about Carbonyl Iron Powders



For wartime uses, design engineers asked these three questions.

In peacetime, as design engineers plan for peacetime equipment, the same questions are asked.

"What are they?"

G.A.F. Carbonyl Iron Powders are obtained by thermal decomposition of iron penta-carbonyl. There are five different grades in production, designated as "L," "C," "E," "TH," and "SF" Powder. Each of these five types of iron powder is obtained by special processing methods and has its special field of application.

The particles making up the powders "E," "TH," and "SF" are spherical with a characteristic structure of concentric shells. The particles of "L" and "C" are made up of homogeneous spheres and agglomerates.

Their weight-average diameter, their total iron contents, and their carbon contents are given in the table at upper right.

"Why are they better?"

Carbonyl Iron Powders are better because of their unique spherical shape, shell structure, particle size distribution, high degree of purity and freedom from stress.

Their stability against magnetic shock, temperature changes, and time (aging) is of the highest order.

Permeabilities range up to 70 with low eddy-current losses. Q values are the highest obtainable because of extremely small eddy-current and hysteresis losses.

Carbonyl Iron Powders are better as electromagnetic material over the entire communication frequency spectrum.

A set of relative Q values for the five powder grades is given in the graph on the other page to show the conventional frequency range for each grade.

"What are their uses?"

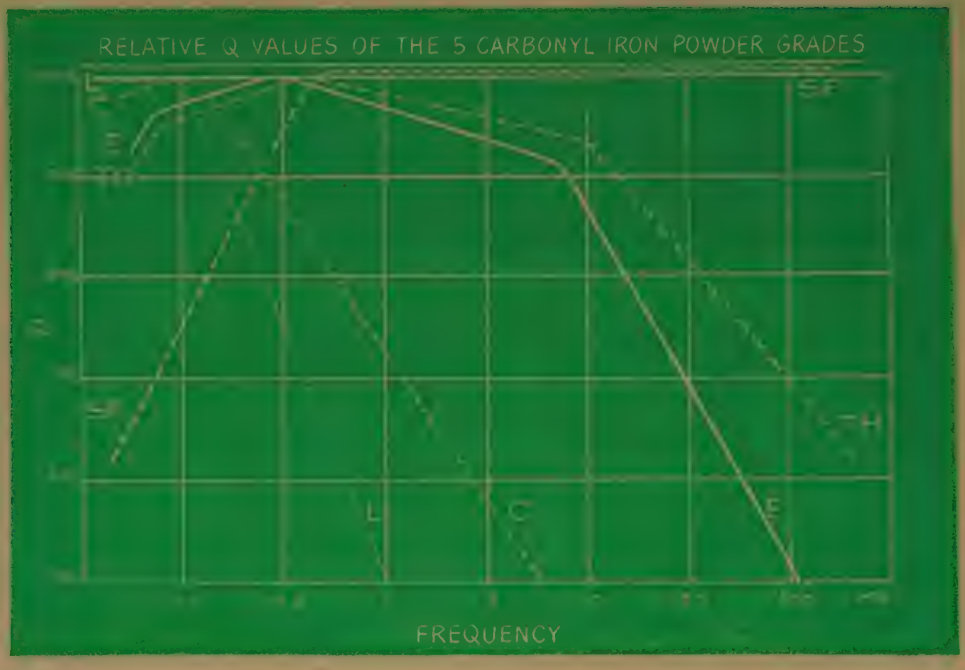
Carbonyl Iron Powders are used for electromagnetic cores and structures for widely different purposes. Five typical applications are shown on the chart at bottom of other page.

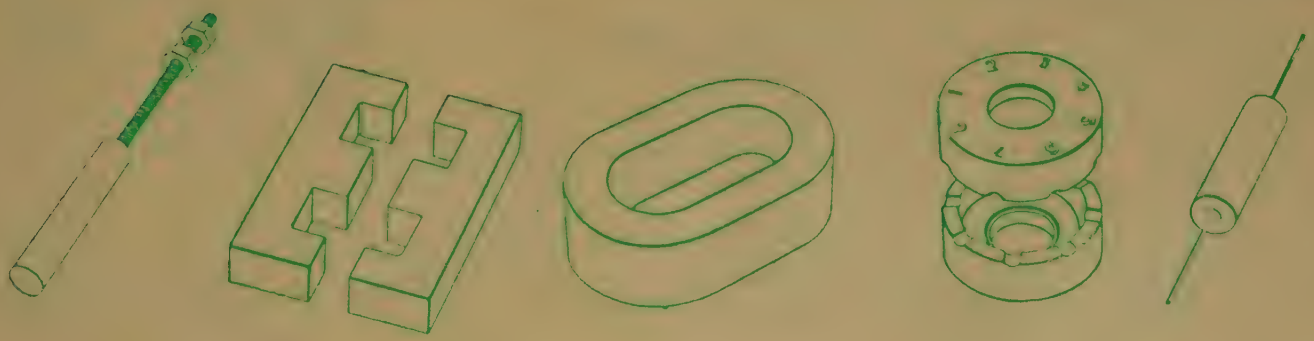
"L" and "C" powders are also used as powder metallurgical material because of their low sintering temperatures, high tensile strengths, and other very desirable qualities. Sintering begins below 500°C and tensile strengths reach 150,000 psi. Compacts can be made having regular pronounced porosity to function as a spongy mass. Compacts can also be made of highest density for excellent magnetic properties.

Further information can be obtained from the Special Products Sales Dept., General Aniline & Film Corporation, 270 Park Avenue, New York 17, N. Y.

Diameters and Chemical Composition of the 5 Carbonyl Iron Powder Grades

Carbonyl Iron Grade	Weight-Average Diameter Microns	Total Fe Content %	Total Carbon Content %
L	20	99.7-99.9	0.005-0.03
C	10	99.5-99.8	0.03 -0.12
E	8	97.9-98.3	0.65 -0.80
TH	5	98.1-98.5	0.5 -0.6
SF	3	98.0-98.3	0.5 -0.6





"L" Type Powder used in cores for permeability tuning.

"C" Type Powder for E-cores in filter coils.

For antenna coils, "E" Type Powder used in cores.

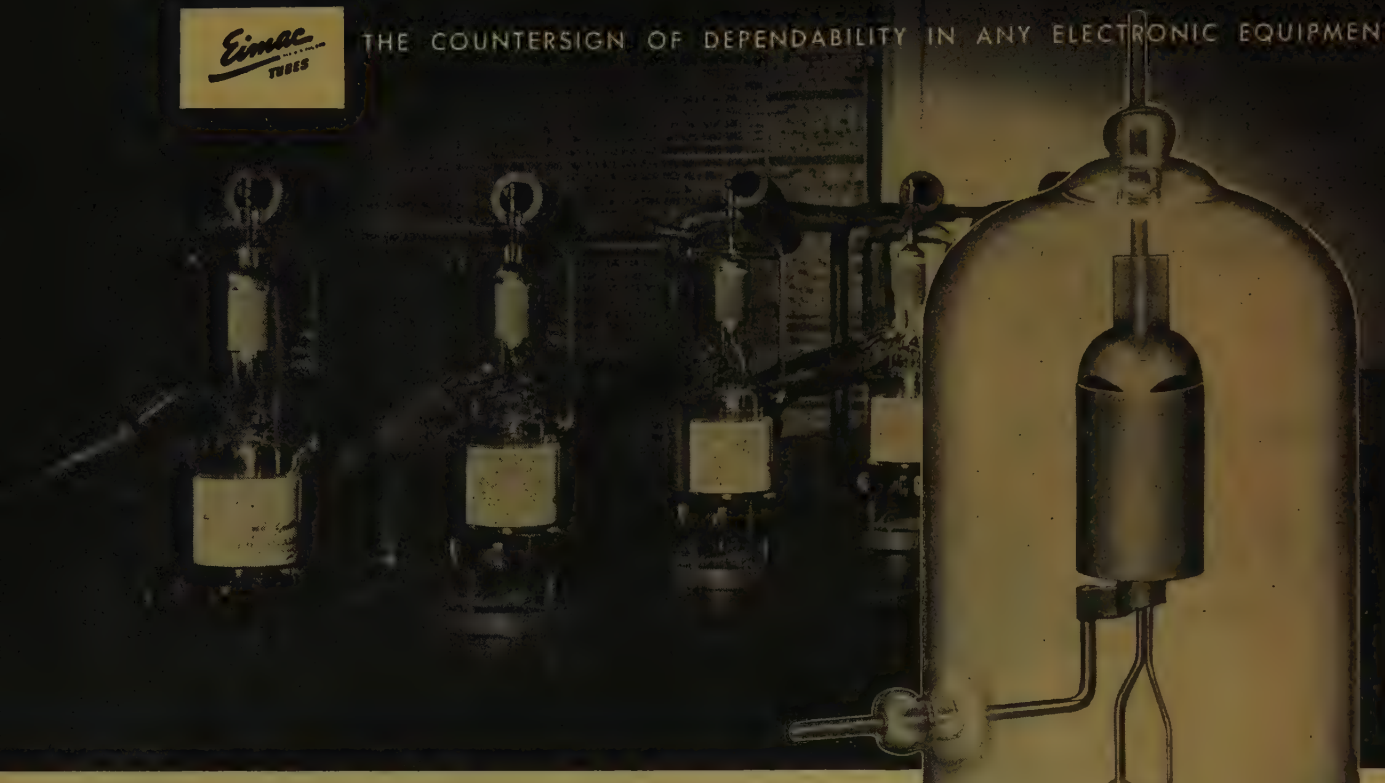
"TH" Type Powder is employed for cup shields in coils.

One use of "SF" Type Powder is in high frequency choke cores (with sealed-in leads).

G.A.F. CARBONYL IRON POWDERS

Eimac TUBES

THE COUNTERSIGN OF DEPENDABILITY IN ANY ELECTRONIC EQUIPMENT



EIMAC 35TG POWER TRIODE

A BETTER 35TG

The famous Eimac 35TG VHF tube, with its low interelectrode capacitances, its logical terminal arrangement, its lack of internal hardware, *is further improved.* It now has a non-emitting grid, an improved filament, and a cooler operating plate. These improved elements, the result of wartime developments in manufacturing technique, are being incorporated in many Eimac tubes and are consistently resulting in vastly increased life.

The 35TG is a power triode of wide applicability. It will function as a Class-C oscillator or amplifier, or as a Class-B audio or supersonic amplifier, and in such service will give excellent performance, due to its stability and low driving-power requirements.

Longer operating life is but one of the many advantages afforded by Eimac tubes. It will pay you to keep informed... see your nearest Eimac representative today, or write direct.

ELECTRICAL CHARACTERISTICS

Filament: Thoriated tungsten	
Voltage	5.0 volts
Current	4.0 amperes
Amplification Factor (Average)	39
Direct Interelectrode Capacitances (Average)	
Grid-Plate	1.8 uuf
Grid-Filament	2.5 uuf
Plate-Filament	0.4 uuf
Transconductance (i_b = 100 ma., E_b = 2000 V., E_c = −30 V.)	2850 umhos
Frequency for Maximum Ratings	100 mc

Follow the leaders to

Eimac TUBES REG. U. S. PAT. OFF.

EITEL-McCULLOUGH, INC.
1229R San Mateo Ave., San Bruno, Calif.
Plant located at: San Bruno, California
Export Agents: Frazar and Hansen, 301 Clay Street, San Francisco 11, California, U. S. A.

CALL IN AN EIMAC REPRESENTATIVE FOR INFORMATION

ROYAL J. HIGGINS (W9AIO), 600 S. Michigan Ave., Room 818, Chicago 5, Illinois. Phone: Harrison 5948.

VERNER O. JENSEN, CO., 2616 Second Ave., Seattle 1, Washington. Phone: Elliott 6871.

M. B. PATTERSON (W5CI), 1124 Irwin-Keasler Bldg., Dallas 1, Texas. Phone: Central 5764.

ADOLPH SCHWARTZ (W2CN), 220 Broadway, Room 2210, New York 7, N. Y. Phone: Cortland 7-0011.

HERB BECKER (W6QD), 1406 S. Grand Ave., Los Angeles 15, California. Phone: Richmond 6191.

TIM COAKLEY (W1KKP), 11 Beacon Street, Boston 8, Massachusetts. Phone: Capitol 0050.



THE NEW Fibron #5373

FLEXIBLE PLASTIC TUBING

Test Data

Tensile Strength.....3000 P.S.I.
Dielectric Strength (.020" wall) Wet.....1000 VPM
Dry.....1000 VPM
Life at 105° C.....2000 Hrs.
Chemical Resistance (room temperature)
50% Sulfuric Acid and
30% Sodium Hydroxide.....Unaffected
Does not support combustion
Low Temperature Flexibility
I.V.I. Pinch test.....—40°C.
Bell test.....—30°C.
Heat Endurance (.166" ID tubing, .016" wall) ASTM-D350-43T): 7 days @ 125°C.—No crack when bent 180° around ¼" mandrel—Retains flexibility when varnished and baked 22 hours at 260°F.—No flow or drip during 8 hours at 300°F.

This Irvington formulation provides new advantages, new cost-saving features, for many plastic tubing applications. For example: Transformer leads of #5373 remain flexible even after varnishing and baking . . . Underwriters' Laboratories approved #5373 insulation on applications involving continuous operating temperatures up to 75 deg. C. and intermittent temperatures as high as 85 deg. C. In addition, #5373 possesses the excellent electrical, mechanical and chemical properties which distinguish all Fibron tubings.

Tubings of Fibron #5373 are available in all standard colors and sizes, and in heavy wall thicknesses—in 36" lengths, continuous coils, or cut pieces. For full details and generous samples, write Dept. 36. Irvington Varnish and Insulator Co., Irvington 11, New Jersey.

IRVINGTON

Varnish and Insulator Company
IRVINGTON 11, NEW JERSEY, U.S.A.



MODEL 2405

Volt•Ohm•Milliammeter

25,000 OHMS PER VOLT D.C.

STANDARDS ARE SET BY TRIPLETT

SPECIFICATIONS

NEW "SQUARE LINE" metal case, attractive tan "hammered" baked-on enamel, brown trim.

- PLUG-IN RECTIFIER—replacement in case of overloading is as simple as changing radio tube.
- READABILITY—the most readable of all Volt-Ohm-Milliameter scales —5.6 inches long at top arc.
- RED•DOT LIFETIME GUARANTEE on 6" instrument protects against defects in workmanship and material.

NEW ENGINEERING • NEW DESIGN • NEW RANGES
30 RANGES

Voltage: 5 D.C. 0-10-50-250-500-1000 at 25000 ohms per volt.
5 A.C. 0-10-50-250-500-1000 at 1000 ohms per volt.
Current: 4 A.C. 0-.5-1-5-10 amp.
6 D.C. 0-50 microamperes — 0-1-10-50-250 milliamperes—0-10 amperes.
4 Resistance 0-4000-40,000 ohms—4-40 megohms.
6 Decibel -10 to +15, +29, +43, +49, +55
Output Condenser in series with A.C. volt ranges.

Model 2400 is similar but has D.C. volts Ranges at 5000 ohms per volt.

Write for complete description

Triplett
ELECTRICAL INSTRUMENT CO.
BLUFFTON OHIO.

Recommended Practice for

ELECTRIC INSTALLATIONS ON SHIPBOARD:—

The latest edition of the "Marine Rules" is now available. These Rules serve as a guide for the equipment of merchant vessels with electric apparatus for lighting, signaling, communication, power and propulsion. This edition includes all items contained in 45A (war time supplement to the 1940 edition now withdrawn from use) which it has been agreed should be recommended as standard construction.

Price: $2.00 per copy—50% discount to AIEE member on single copies.

ELECTRIC POWER DISTRIBUTION for Industrial Plants:—

This report outlines sound engineering principles in the design of electric power distribution systems for industrial plants and in the selection of equipment for these systems from the point of entrance of the power company service or the plant generating bus to the terminals of the utilization devices.

Price: $1.00 per copy—No discounts allowable

American Institute of Electrical Engineers — 33 W. 39th St., New York 18



"Copperweld" means copper-covered steel wire made by the PROVED MOLTEN-WELDING PROCESS

For more than 30 years, the name "Copperweld" has been the mark of copper-covered steel wire made by Copperweld Steel Company's exclusive Molten-Welding process. And—because Copperweld products have proved their dependability and economy throughout this long period—the following facts are vitally important to you:

1. COPPERWELD is the only wire made by the Molten-Welding process—in which a thick covering of protective copper is permanently and continuously welded to a core of strong alloy steel. The perfect interlocking of these two metals, accomplished only by molten-welding, provides rugged strength, high conductivity, rust-resistance and long life.

2. The name COPPERWELD is a registered trademark of the Copperweld Steel Company.

3. Only Copperweld Steel Company makes COPPERWELD. Only Copperweld Steel Company sells and licenses others to fabricate and sell Copperweld-Copper composite conductors. These licensees are Anaconda Wire & Cable Company, Kennecott Wire & Cable Company, Phelps Dodge Copper Products Corporation, and John A. Roebling's Sons Company.

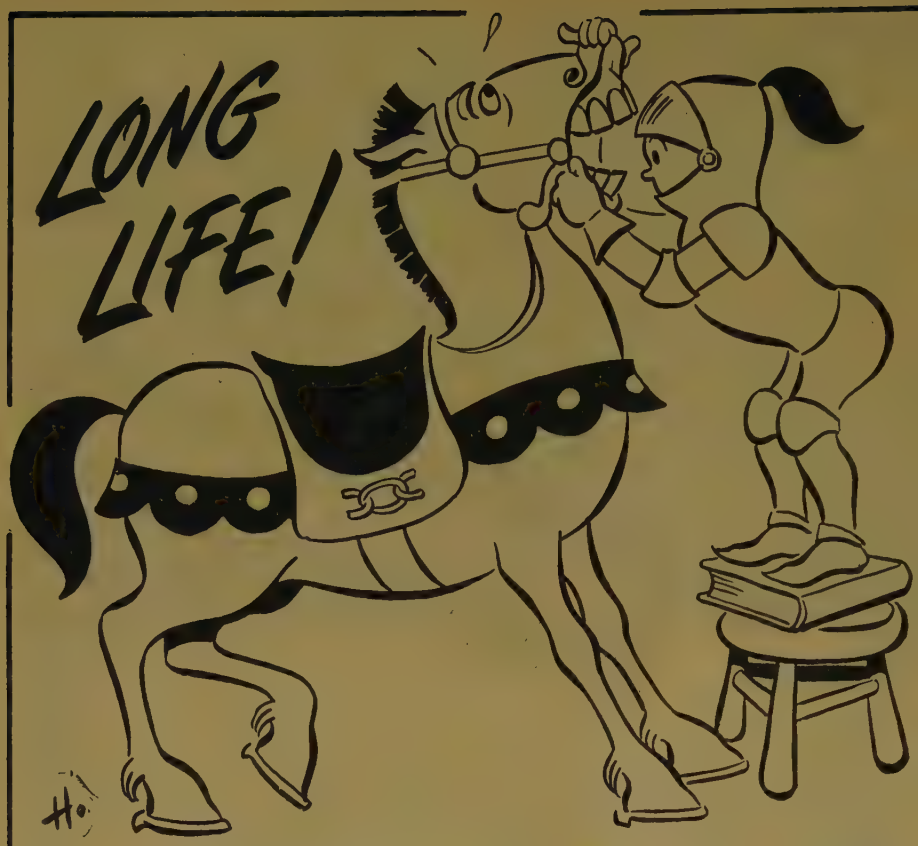
4. The name COPPERWELD should be used only when referring to copper-covered steel wire made by the Molten-Welding process.

5. The name COPPERWELD should never be used when referring to any other type of copper-covered steel wire—for example—wire having copper merely plated on steel.

All those familiar with the many unique advantages which only Copperweld can offer, will see in these statements our sincere desire to protect every user. When your specifications or purchase orders call for Copperweld, make certain that you get Copperweld quality by actually seeing the name "Copperweld" on the product itself or on the tag accompanying every coil and reel.



COPPERWELD STEEL COMPANY
GLASSPORT, PA.
SALES OFFICES IN PRINCIPAL CITIES





Long life in a commutator or ring, as well as long brush life, means lower maintenance costs. Morganite grades are designed to give long brush life with a minimum of commutator and ring wear.

Morganite

CARBON BRUSHES

1629 Telegraph Ave. Oakland 12, Cal. Tel. GLencourt 5838

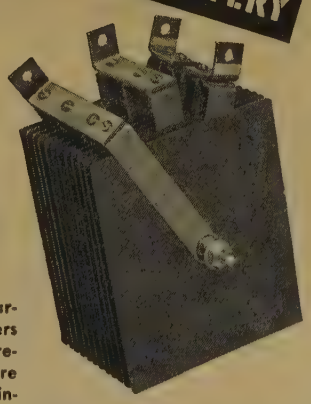
453 So. Spring St. Los Angeles 13, Cal. Tel. MUtual 3824

343 So. Dearborn St. Room 802, Chicago 4, Ill. Tel. WEbster 4936

MORGANITE BRUSH COMPANY, INC., LONG ISLAND CITY 1, N. Y.



If you need DC, get the facts on Selenium Rectifiers. Selenium Rectifiers are available in a wide range of ratings and sizes, each designed to perform an exact and vital function in all rectifier applications. Selenium Rectifiers are small in size, light weight, efficient, economical and adaptable to all mechanical arrangements. Selenium Rectifiers have no moving parts and require no maintenance. They are simple, rugged and provide instantaneous and silent operation.



46-3

SELENIUM CORPORATION OF AMERICA

Affiliate of VICKERS, Incorporated

1719 WEST PICO BOULEVARD • LOS ANGELES 15, CALIFORNIA

Export Division: Frazar & Hansen, 301 Clay Street, San Francisco 11, Calif.

In Canada: Canadian Line Materials, Ltd., Toronto 3, Canada

ELECTRIC SERVICE CONTROL, INC.

We are in a position to pass on years of extensive war experience to the electrical industry on the manufacturing of switchboard and distribution equipment, regardless of how complicated its operation might be.

ELECTRIC SERVICE ESCO CONTROL Incorporated

Our experience in packing for the Navy and Maritime Commission puts us in a favorable position to pack for export.



We solicit the requirements of

UTILITIES
INDUSTRIALS
CONTRACTORS
ENGINEERS
ARCHITECTS
GOV'T AGENCIES OF ALL COUNTRIES
EXPORTERS

Engineering, Estimating and Consulting Service Available on Request

ELECTRIC SERVICE CONTROL, INC.

205 NORTH 12th ST. NEWARK 7, N. J.

FEDERAL'S INDUSTRIAL POWER TUBES ... Built to perform better and last longer

... in industrial electronic equipment such as this 5KW dielectric heating unit

FEDERAL'S 7C25 is *especially* designed for hard working conditions. It withstands not only the abuse of extreme load variations in electronic heating operations ... but mechanical deterioration as well.

Widely spaced, unusually tough filament and grid elements, positioned without ceramic insulators, resist shocks and constant vibration from adjacent machinery. In addition, electrical ratings are conservative, with a wide margin of safety ... insuring still further the long, trouble-free service you can expect from this tube.

In 37 years of Federal tube making and research, longer tube life has always been a prime objective. Federal's success in the 7C25, as well as in a broad line of rectifying and transmitting tubes, means lower tube costs to you. Write for your copy of Federal's 68-page Handbook of Tube Operation.

5KW Dielectric Heating Unit manufactured by Illinois Tool Works, Chicago. Two Federal 7C25 Tubes are more than ample to produce the rated output of this unit.



TECHNICAL DATA FOR TYPE 7C25

Filament Voltage	11.0 volts
Filament Current	27.5 amps.

Maximum Ratings for Maximum Frequency of 50 Mcs

DC Plate Voltage	4500 volts
DC Plate Current	1.25 amp.
Plate Dissipation	2500 watts
Overall Height	App. 7 inches
Maximum Diameter	3½ inches

Supplied with 6" flexible copper leads, 2 on each terminal.

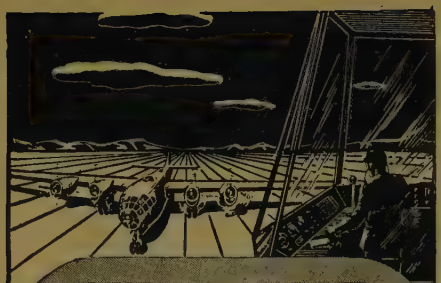
Type of Cooling ..... Forced-air

Federal Telephone and Radio Corporation

Newark 1, New Jersey

Export Distributors:
International Standard Electric Corporation

AN IT&T ASSOCIATE — FEDERAL TELEPHONE & RADIO — FTR



An invitation to all electrical designers to

TRY SILVER GRAPHALLOY

FOR RELAYS • MOTORS • CONTROLS • ELECTRONICS

GRAPHALLOY

FOR BRUSHES

High current density, low contact drop, low electrical noise, and self-lubrication are characteristics of this silver-impregnated molded graphite that may be the answer to your electrical brush problems.

FOR CONTACTS

Low contact resistance and non-welding when breaking surge currents are inherent properties of this unique combination of conductive silver and self-lubricating graphite.



SLIP-RING AND COMMUTATOR



BRUSHES AND CONTACTS

SAMPLES of Silver Graphalloy will be gladly furnished for test on your applications. Silver Graphalloy is usually silver plated to permit easy soldering to leaf springs or holders. Why not WRITE NOW for your test samples?

ALWAYS SPECIFY GRAPHALLOY TRADE MARK REG. U. S. PAT. OFF.

GRAPHITE METALLIZING CORPORATION

1053 NEPPERHAN AVE • YONKERS, NEW YORK

STANDARDS

Steam Turbine Generators

(Large 3600-rpm, 3-phase, 60-cycle condensing)

Preferred Standards—No. 601

Standard Specifications—No. 602

(Published as one pamphlet)

30 cents per copy

Members discount of 50% on single copies

Test Code for Synchronous Machines

Instructions for conducting the more generally applicable and acceptable tests to determine the performance characteristics of synchronous machines. Includes performance tests for synchronous generators, synchronous motors (larger than fractional horsepower), synchronous condensers, frequency changers and rotary phase advancers.

60 cents per copy

Members discount of 50% on single copies

A-C Power Circuit Breakers

C37.4 to C37.9

A new American Standard, approved May 16, 1945. Supersedes the 1941 edition of the proposed American Standard bearing the same number and the interim AIEE Standard No. 19 of 1943.

$1.25 per copy net

Aircraft D-C Apparatus Voltage Ratings—No. 700

Report on a proposed AIEE Standard, giving recommended standard voltages for all types of aircraft d-c electric apparatus.

No charge

American Institute of Electrical Engineers

33 West 39th Street
New York 18, N. Y.



WHAT TYPE OF *Jewel Assembly* DO YOU NEED?

No matter what type or size of Jewel Light Assembly you need, chances are we can produce it for you quickly, more satisfactorily, *and at lower cost!* Here, every facility is available for high speed quantity production . . speedy, efficient, economical service. Drake *patented features* add greatly to the value and dependability of our products.

You'll like the friendly, intelligent cooperation of our engineers. Let them help you with signal or illumination problems. Suggestions, sketches, cost estimates or asking for our newest catalog incur no obligation.

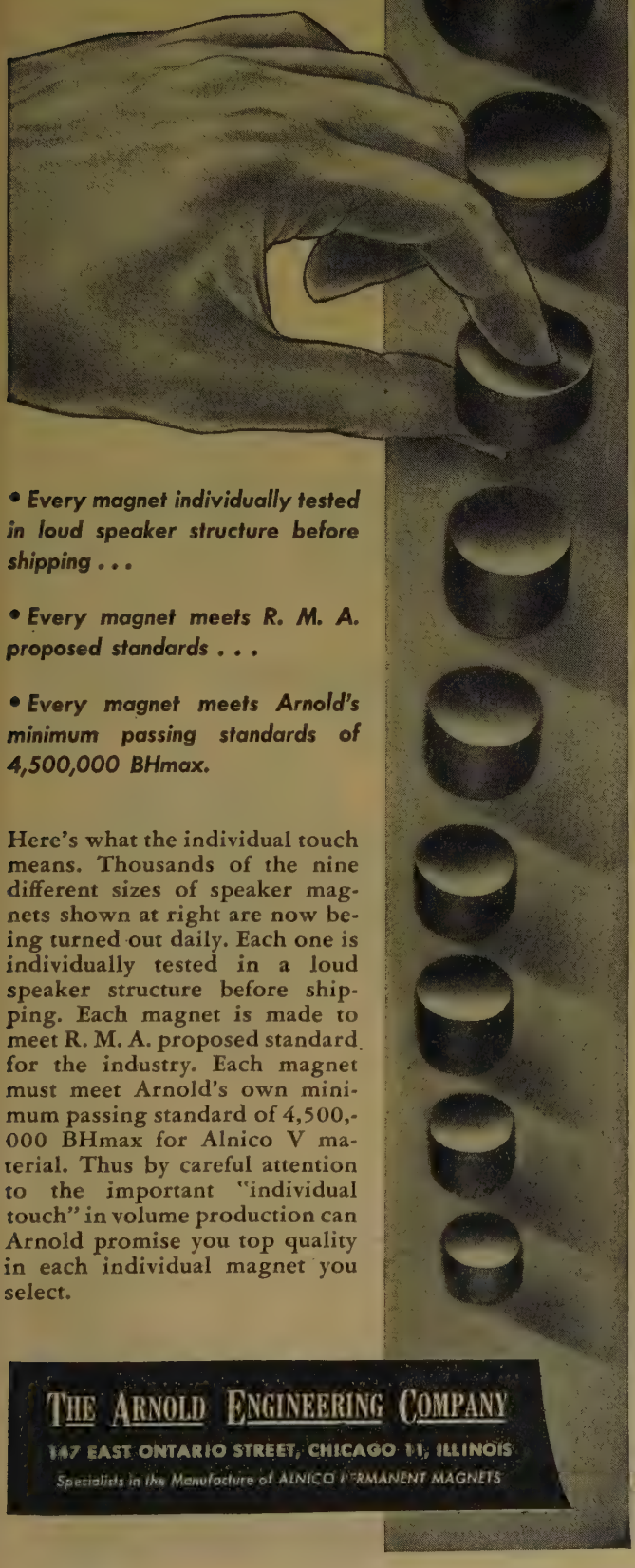
DRAKE

SOCKET AND JEWEL LIGHT ASSEMBLIES

DRAKE MANUFACTURING CO.

1713 W HUBBARD ST CHICAGO 22, ILL.

THE *Individual* TOUCH



- *Every magnet individually tested in loud speaker structure before shipping . . .*
- *Every magnet meets R. M. A. proposed standards . . .*
- *Every magnet meets Arnold's minimum passing standards of 4,500,000 BHmax.*

Here's what the individual touch means. Thousands of the nine different sizes of speaker magnets shown at right are now being turned out daily. Each one is individually tested in a loud speaker structure before shipping. Each magnet is made to meet R. M. A. proposed standard for the industry. Each magnet must meet Arnold's own minimum passing standard of 4,500,000 BHmax for Alnico V material. Thus by careful attention to the important "individual touch" in volume production can Arnold promise you top quality in each individual magnet you select.

THE ARNOLD ENGINEERING COMPANY
147 EAST ONTARIO STREET, CHICAGO 11, ILLINOIS
Specialists in the Manufacture of ALNICO PERMANENT MAGNETS

INDUCTANCE CALCULATIONS SIMPLIFIED

At last, inductance calculations—so important to power, communication, electrical engineers and those in related fields—have been reduced to simple, *slide-rule* computation.

INDUCTANCE CALCULATIONS

Working Formulas and Tables
By Frederick Warren Grover, Ph.D.

Professor of Electrical Engineering, Union College
Formerly Consulting Physicist, National Bureau of Standards

In this brand-new book all problems in inductance calculation are made easy and direct. The best single formula (or two for checking) has been chosen for every type of element or coil; and factors corresponding to dimensions of particular elements or coils are provided, so you can find the exact theoretical (not empirical) value by the most simple computations.

Included are tables that save the vast amounts of computation, often with complex mathematical functions, which hitherto have been necessary. Now all problems in inductance calculations can be computed by the use of interpolated values of constants, and even with the more complicated arrangements of conductors, a straight-forward procedure can be outlined.

CHAPTER HEADINGS

General Principles; Geometric Mean Distances; Construction of and Method of Using The Collection of Working Formulas. CIRCUITS WHOSE ELEMENTS ARE STRAIGHT FILAMENTS. Parallel Elements of Equal Length; Mutual Inductance of Unequal Parallel Filaments; Mutual Inductance of Filaments Inclined at an Angle to Each Other; Circuits Composed of Combinations of Straight Wires; Mutual Inductance of Equal, Parallel, Coaxial Polygons of Wire; Inductance of Single-Layer Coils on Rectangular Winding Forms. COILS AND OTHER CIRCUITS COMPOSED OF CIRCULAR ELEMENTS. Mutual Inductance of Coaxial Circular Filaments. Mutual Inductance of Coaxial Circular Coils; Self-Inductance of Circular Coils of Rectangular Cross Section; Mutual Inductance of a Solenoid and a Coaxial Circular Filament; Mutual Inductance of Coaxial Single-Layer Coils; Single-Layer Coils on Cylindrical Winding Forms; Special Types of Single-Layer Coil; Mutual Inductance of Circular Elements with Parallel Axes; Mutual Inductance of Circular Filaments Whose Axes are Inclined to One Another; Mutual Inductance of Solenoids with Inclined Axes, and Solenoids and Circular Coils with Inclined Axes; Circuit Elements of Larger Cross Sections with Parallel Axes; Auxiliary Tables for Calculations with Formulas Involving Zonal Harmonic Functions; Formulas for the Calculation of the Magnetic Force Between Coils; High Frequency Formulas.

Durable cloth binding 6 × 9 295 pages $5.75

SEND FOR YOUR COPY NOW

Use the convenient order form at right to obtain your copy of this important new book.

MAIL THIS COUPON

D. VAN NOSTRAND COMPANY, INC.
250 Fourth Avenue
New York 3, New York

Gentlemen:

Please send me.....copies of INDUCTANCE CALCULATIONS.

Signed.....

Address.....

City.....Zone.....State.....

EE-6/46

At right: Aerovox Series 20 Hyvol impregnated and filled capacitors in ratings up to 50,000 v. Below: Aerovox Series 26 stack-mounting Hyvol impregnated and filled capacitors in ratings up to 150,000 v.



● For those extra-severe-service applications of the largest capacitors, as well as others, Aerovox units have that extra stamina that makes them last. Decades of specialization provide an experience background second to none in solving all kinds of capacitor problems; unexcelled production facilities assure QUALITY as well as quantity.

Aerovox capacitors are liberally engineered for their individual applications. Special multi-layer capacitor tissues . . . long-life, non-inflammable Hyvol impregnant and fill . . . constant filtration as regular production routine . . . thorough evacuation and impregnation . . . positive hermetic sealing—these facts of Aerovox craftsmanship spell long, trouble-free service.

Aerovox capacitors in daily use speak for themselves. No finer capacitors are built. Aerovox engineers stand ready to meet your most severe requirements.

● *Submit your capacitor problem. The tougher the better! Write for literature.*

AEROVOX capacitors

FOR RADIO-ELECTRONIC AND INDUSTRIAL APPLICATIONS

AEROVOX CORP., NEW BEDFORD, MASS., U. S. A.

SALES OFFICES IN ALL PRINCIPAL CITIES • EXPORT: 13 E. 40th ST., NEW YORK 16, N. Y.

Cable: 'ARLAB' • In Canada: AEROVOX CANADA LTD., HAMILTON, ONT.

AMPERITE

THERMOSTATIC METAL TYPE

DELAY RELAYS

PROVIDE DELAYS RANGING FROM 1 TO 120 SECONDS

Other important features include:

1. Compensated for ambient temperature changes from —40° to 110°F.
2. Contact ratings up to 115V-10a AC.
3. Hermetically sealed — not affected by altitude, moisture or other climate changes . . . Explosion-proof.
4. Octal radio base permits easy replacement.
5. Compact, light, rugged, inexpensive.
6. Circuits available: SPST Normally Open; SPST Normally Closed.

WHAT'S YOUR PROBLEM? Send for "Special Problem Sheet" . . . and Descriptive Bulletin.

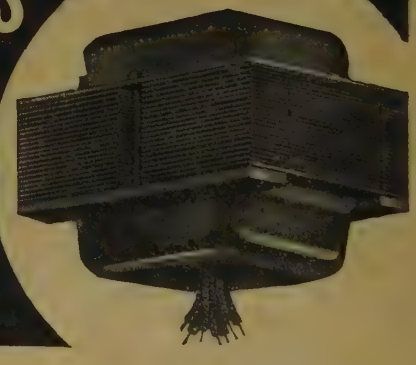


with porcelain heater

with heater wound directly on blade

AMPERITE CO.
561 BROADWAY
NEW YORK 12, N. Y.
Canada: Atlas Radio Corp. Ltd.
560 King St. W. Toronto

THIS IS MOUNTING TYPE 130

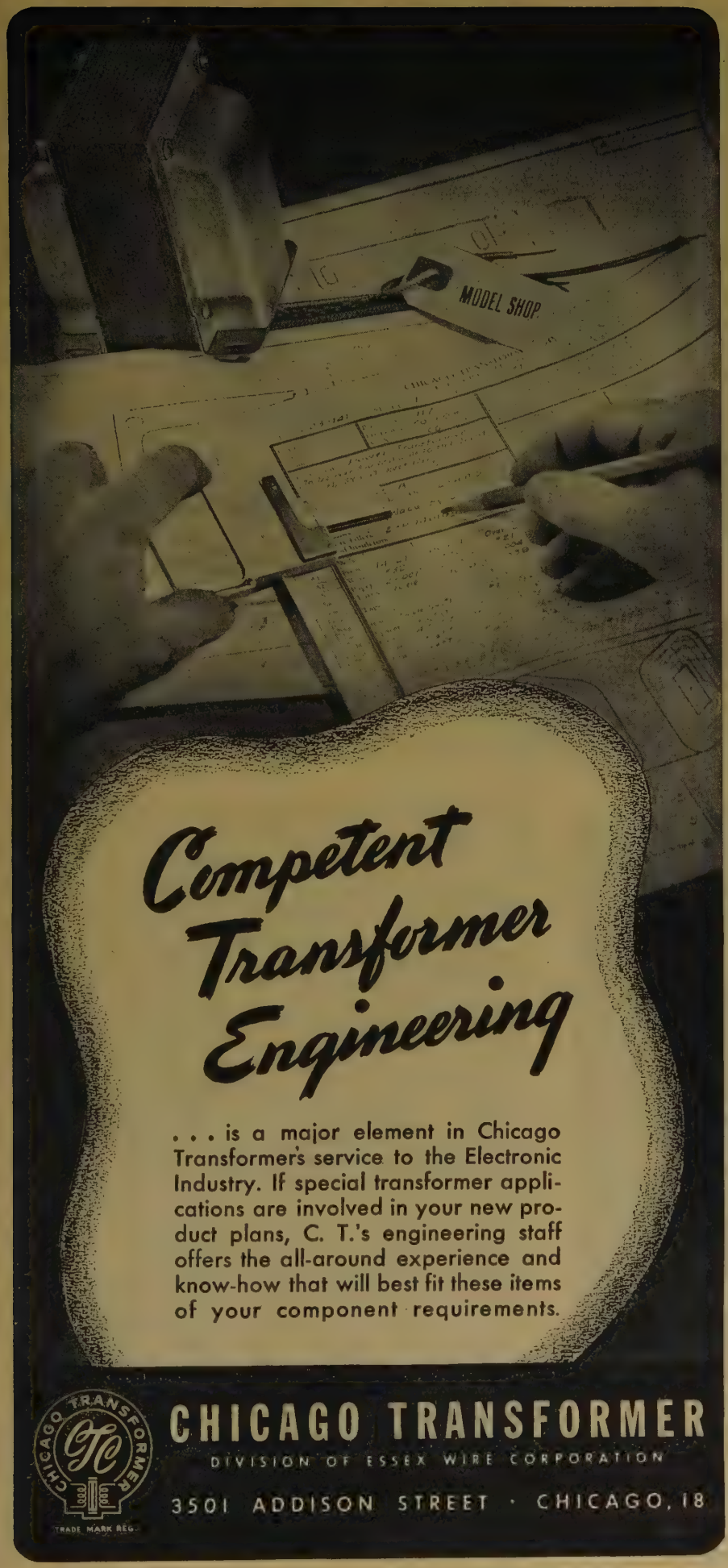


This transformer (series 130) has many desirable features for installation as an integral part of electrical equipment. Two-hole horizontal mounting cuts assembly time of your product. Lead holes can be provided on bottom, top or side of shell. Can be supplied to your specifications in a range of sizes from 15 VA to 100 VA. Overall mounting space 2-11/32" x 2-13/32" to 3-1/8" x 3-3/4".

Write for Bulletin 168.

THE ACME ELECTRIC & MFG. CO.
22 WATER ST. CUBA, N. Y.

Acme ACME Electric



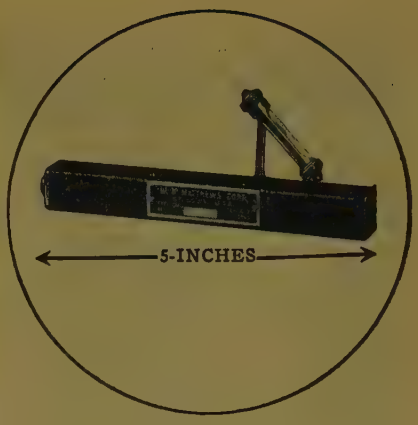
Competent Transformer Engineering

. . . is a major element in Chicago Transformer's service to the Electronic Industry. If special transformer applications are involved in your new product plans, C. T.'s engineering staff offers the all-around experience and know-how that will best fit these items of your component requirements.

CHICAGO TRANSFORMER

DIVISION OF ESSEX WIRE CORPORATION

3501 ADDISON STREET · CHICAGO, 18



No Fallacious Guesses.

There is no guessing with a Matthews Teleheight. Any lineman can be taught to use it and get any height within an inch or so. He can learn in five minutes.

The extra cost of just one wrong guess will pay for one or two Matthews Teleheights. Hundreds of them are saving lots of money for their owners all over the country. Many are being used for quickly figuring the cubical contents of buildings, the clearance of bridges, highlines, etc.

Matthews Teleheight is only five inches long. Has no moving parts. It is furnished with a leather carrying case that will fit in the vest pocket. The drawing below shows how simple are the directions for using it.

Great for Appraisal Jobs.

Try one at our risk of your approval.

W. N. MATTHEWS CORPORATION

ST. LOUIS, U. S. A.





COORS
U.S.A.

COORS
ZIRCON INSULATORS

Suitable for uses at high voltages, high frequencies, high temperatures, now available to the electrical industry at large.

Composition and manufacturing methods are the same as those employed in our production of insulators for the Manhattan District, Oak Ridge, Tennessee.

COORS PORCELAIN COMPANY
GOLDEN, COLORADO

Large capacity—prompt delivery.
Inquiries solicited.



. . . an example of an intricately designed insulator produced in quantity by Universal. Universal porcelain insulators have a high dielectric factor, high compressive strength. They are unaffected by arcing, heat, cold or fumes. They will not corrode, carbonize or oxidize. You can depend on Universal insulators to provide long life and satisfactory performance in your electrical equipment.

THE UNIVERSAL CLAY PRODUCTS CO.
1560 FIRST STREET SANDUSKY, OHIO



Professional Engineering Directory

BLACK & VEATCH
Consulting Engineers
Water, Steam and Electric Power Investigations, Design, Supervision of Constructions, Valuation and Tests
4706 Broadway KANSAS CITY, MO.

FRANK LEDERMANN, E.E.
Registered Patent Attorney
154 Nassau Street New York 7, N. Y.
Telephone: BEekman 3-2936

SARGENT & LUNDY
ENGINEERS
140 South Dearborn Street
CHICAGO, ILLINOIS

REG. 1911 MEM. AIEE
CHRISTIAN E. BROWN
Mechanical and Electrical Engineer
DESIGNS—SPECIFICATIONS—REPORTS
Tel. 7046 MANCHESTER, CONN.

Roland R. Miner, Member AIEE — Lottye E. Miner, Associate AIEE
MINER & MINER
Consulting Engineers
Design - Development - Investigations
Valuations
Experience in the utility, industrial and appliance manufacturing fields
1825 Tenth Avenue Greeley, Colorado

GEORGE H. STUMPF, E.E.
ELECTROMAGNETIC CONTROLS
SOLENOIDS, LIFTING MAGNETS
DESIGNS & SPECIFICATIONS
Reg. P. E. 18901 PLEASANTVILLE, N. Y.

Member AIEE
JULIEN H. DAVIS
Consulting Engineer
Industrial
Utility—Electrical—Mechanical
1730 West Slauson Ave.,
Los Angeles 44, Calif.

Z. H. POLACHEK
Reg. Patent Attorney
Professional Engineer
PATENTS OBTAINED & SEARCHED
for any invention in U. S. Pat. Off.
1234 Broadway (At 31 St.) NEW YORK
Phone LOngacre 5-3088

WESTCOTT & MAPES, INC.
Architects & Engineers
Power Plants Public Utilities
Industrial Plants
New Haven, Conn.

HODGSON & ASSOCIATES
Physics, Mathematics, Research
Development and Patent Consultants
Satisfaction guaranteed or no charge.
Submit your problem for a free preliminary survey.
Box 874 SHERMAN OAKS, California

GEORGE E. QUINN CO.
MANAGEMENT CONSULTANTS
Industrial - Electrical Engineering
3224 Grand Concourse
NEW YORK 58, N. Y.

THE J. G. WHITE Engineering Corporation
Design—Construction—Reports—Appraisals
80 BROAD STREET NEW YORK

JACKSON & MORELAND
Engineers
Public Utilities—Industrials
Railroad Electrification
Designs and Supervision—Valuations
Economic and Operating Reports
BOSTON NEW YORK

SANDERSON & PORTER
ENGINEERS
AND
CONSTRUCTORS

J. G. WRAY & CO.
Engineers
Utilities and Industrial Properties
Appraisals Construction Rate Surveys
Plans Organizations Estimates
Financial Investigations Management
231 South La Salle Street, Chicago

CORRECTION

"Recommended Practice for Electric Installations on Shipboard" AIEE No. 45

ERRATA—Standard 45, Pages 30 and 31
Sections 18.65, 67, 69, 81, 83 and 85
In "Third" change "0.136 in." to "0.115 in."

Errata sheets for insertion in the 1945 edition can be obtained by writing to
AMERICAN INSTITUTE OF ELECTRICAL ENGINEERS - 33 W. 39th St., New York 18, N. Y.

New! Complete!
FREE CONCORD Radio Catalog



RADIO SETS
AMPLIFIERS
RADIO PARTS
Electronic Equipment

For the newest, the latest, and the best in radio sets, parts, amateur kits, test equipment, tools, books . . . mail coupon for your free copy of Concord's first post-war Catalog. Contains huge storehouse of thousands of top-quality, standard line items . . . ready for same-day shipment from CHICAGO or ATLANTA. Includes most-talked-about line of exclusive Concord Multiamp ADD-A-UNIT Amplifiers in America—new-design throughout, offering startling innovations in flexibility, fidelity, power, and economy . . . new high standards of performance almost beyond belief. Mail coupon below for full details . . . and for "everything that's new in radio and electronics."

CONCORD
RADIO CORPORATION
LAFAYETTE RADIO CORPORATION
CHICAGO 7 ★ ATLANTA 3
901 W. JACKSON BLVD. 265 PEACHTREE ST.

Concord Radio Corporation, Dept. C-66
901 W. Jackson Blvd., Chicago 7, Ill.

Yes, rush FREE COPY of the comprehensive new Concord Radio Catalog.

Name.....

Address.....

City..... State.....

Engineering Societies Personnel Service, Inc.

New York 8 West 40th St. | Chicago 211 West Wacker Dr. | Detroit 100 Farnsworth Ave. | San Francisco 57 Post St.

In applying for positions advertised by the Service, the applicant agrees, if actually placed in a position through the Service as a result of these advertisements to pay a placement fee in accordance with the rates as listed by the Service. These rates have been established in order to maintain an efficient, non-profit personnel service and are available upon request. This also applies to registrants whose notices are placed in these columns.

All replies should be addressed to the key numbers indicated and mailed to the New York Office.

Men Available

TELEPHONE ENGR, B.S. in E.E.; age 28; veteran; married, no children; 5½ yrs exper outside plant planning, des, layout and constr supervision. Also Central office layouts. Desires pos with future. Location immaterial. E-214.

ELEC ENGR; 51, married; General Electric test, public util engg, switchgear sales and specifications, and insurance inspections. Desires perm pos. Available two weeks. E-215.

QUALITY CONTROL ENGR, E.E. grad; 32, single; 4 yrs quality control exper with U.S. Signal Corps; 7yrs total inspection exper. Desires responsible pos in eastern U.S. Would consider consulting basis. Available immediately. E-216.

ELEC MAINT SUPT, indus plants, public bldgs, hotels; 25 yrs exper elec mech maint. Prefers south midwest or west coast. E-217.

GRAD ELEC ENGR: licensed, Pa; 41 married; 17 yrs exper, testing and high voltage research, transformers, insulation and protective eqpt; 3 yrs Asst Prof elec engg and high voltage research. E-218.

ELEC ENGR, R.P.I.; 13 yrs prod des, devpmt, application. Outstanding record personal initiative and results. Excellent admin background. Broad exper customer relations. Desires exec pos product-application engg, or similar. East preferred. E-219.

ENGR, M.S. in E.E., 1940; Navy veteran; 34, married; 2½ yrs exper in lamp manufacturing, 3½ yrs in electronics. Desires project engg with small manufacturer. Location, east or west coast. E-220.

ELECTRONICS ENGR. B.S. in E.E., 1942; 26, single; 2 yrs tech work and supervision elec pwr drafting; 3 yrs Naval Electronics Officer. Desires engg pos with future. Location secondary. E-221-465-C-4 San Francisco.

EXEC DESIGNING ENGR; age 49; long record elec, mech, arch and constr work; desires pos South America, contract basis. Spanish spoken. Active alert leadership. E-222-2203-Chicago.

Positions Available

HYDRO-ELECTRIC DESIGN ENGINEER who is qualified by experience to take charge of the design of hydro-electric stations with unit capacities of 25,000 KW and larger. Permanent. Salary open. Location, Pennsylvania. W-6516(b).

EXECUTIVE ENGINEERS, 2, 35–45, electrical or mechanical graduates of recognized colleges with at least five years' experience in industry in executive capacity. Will be responsible for efficient, business-like operations of a medium sized engineering department, completely staffed technically. Salaries, $7500–$8000 a year. Locations: one for truck assembly plant in south central New York; this applicant must have had extensive experience in truck engineering design; the other for communications equipment plant in Connecticut. W-6958.

PRODUCT ENGINEERS, electrical, mechanical or chemical graduates, preferably with two years' experience in product engineering work, for work on technical glass products, including choice of glass composition, design to meet customers requirements supervising manufacturing drawings and specifications. Salary, $3000–$4500 a year. Location, upstate New York. W-7065.

ELECTRICAL ENGINEERS with training and experience in electronics. Salary, $2320–$5180 a year. Location, Virginia. W-7073.

ENGINEERS. (a) Development Engineer, electrical graduate, with at least ten years' experience in research and development of radio and telephone communication equipment, to assist in circuit development program. (b) Model Makers, junior and senior, with four to five years' radio experience, to produce test items from sketches and verbal instructions. Salaries: (a) $4800–$6000; (b) $3300 a year. Location, New York, N. Y. W-7125.

ENGINEERS. (a) Engineer experienced in electrical wiring materials and prices gained through years of contact with electrical wholesalers of such materials. Must know prices. (b) Electrical Engineer familiar with local utility engineering practices and having had some sales experience. Must have, or obtain, New York State Professional License. (c) Electrical Engineer, graduate, to learn electrical construction designing. Location, New York, N. Y. W-7140.

ENGINEERS, to 45, electrical graduates or equivalent. (a) Development Engineer with experience in the design and development of telephone and signalling equipment and components. Salary, $4420 a year. (b) Product Designer with experience in mechanical design pertaining to electro-mechanical devices. Thorough knowledge of mechanical motions, gearing, etc., essential. Salary, $3900 a year. Location, Connecticut. W-7150.

INSTRUCTORS of electrical engineering. (a) Assistant Professor with some teaching experience. (b) Instructor with or without experience, but with an interest in teaching. Salaries open. Location, Massachusetts. W-7158.

INSTRUCTOR to teach electrical measurements laboratory, service courses based on such texts as Blalock and Fitzgerald, and a major course at sophomore level based on Timbie and Bush with emphasis on problem material. Salary, $2000–$2500. Position starts September 1946. Location, Maine. W-7199.

INSTRUCTORS AND ASSISTANT PROFESSORS of electrical engineering, engineering mechanics or engineering drawing. Bachelor's degree required for Instructor; Master's for Assistant Professor. One year of teaching required for Instructor and five or more for Assistant Professor. Appointments for fall term of 1946. Salaries approximately $2300–$3500. Location, Michigan. W-7215-D-2868.

ELECTRICAL ENGINEER, graduate, not over 30, for standardization work. Salary, $4000 a year. Location, New York, N. Y. W-7236.

CLASSIFIED ADVERTISEMENTS

RATES: Sixty cents per line; minimum charge based on use of five lines; maximum space not to exceed thirty-five lines. Copy is due on the 18th of the month preceding publication date.

ELECTRICAL ENGINEER—31—10 years experience in engineering field—6 years as supervising Welding Engineer in progressive laboratory on research and production problems. Well acquainted with all types of welding material and apparatus. Good working knowledge of metallurgy and nondestructive material inspection methods. Experienced in electrical instrumentation. Desire position in production field or in sales engineering where future is restricted only by ability. Address, Box 377, Electrical Engineering, 33 West 39th Street, New York 18, N. Y.

BSEE 1942, Kansas State College. 4 years experience in design, development and research in radio for a naval laboratory. Specialty directive antenna systems, broad band and match amplifiers, and cathode ray tube indicator circuits of all types. Desires position *with a future* in research and development of radio equipment. West Coast area preferred; any location in U. S. considered. Address, Box 378, Electrical Engineering, 33 West 39th Street, New York 18, N. Y.

WANTED — ELECTRICAL ENGINEER — for power plant design, must have public utility experience. WESTCOTT & MAPES, Inc., New Haven, Connecticut.

WANTED—Copies of the (November 1945) issues of Electrical Engineering. Please mail (parcel post) to American Institute of Electrical Engineers, 33 W. 39th St., New York City (18), printing your name and address upon the enclosed wrapper. Twenty-five cents plus postage, will be paid for each copy returned.

Fairchild Aerial Surveys, Inc.

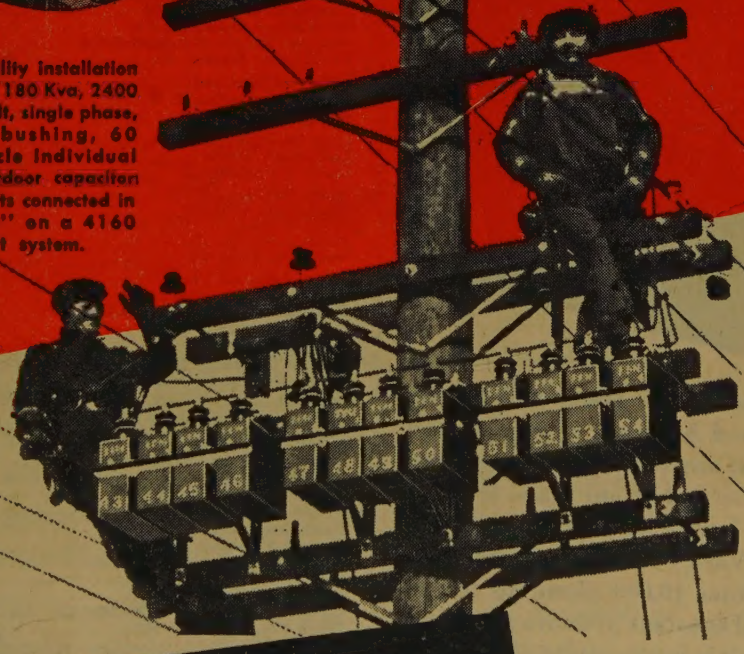
more capacity on-the-spot...





WITH YEARS OF MAINTENANCE-FREE SERVICE

Utility installation of 180 Kva, 2400 volt, single phase, 2 bushing, 60 cycle individual outdoor capacitor units connected in "y" on a 4160 volt system.

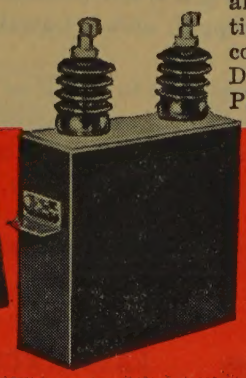


C-D capacitors provide the simplest and most flexible method for boosting power load at critical spots without the addition of costly equipment, lines, and maintenance. Pole-mounted or arranged in banks for large blocks of reactive kva, they adapt power distribution systems for any present or future load shifts. C-D capacitors can be shunted easily from the banks and quickly installed at critical load points. Each unit is weather-sealed against corrosion and discharges in accordance with NEMA requirements for complete handling safety.

Cornell-Dubilier offers prompt service from its large range of Capacitors in all sizes and types for utility applications. Our field engineers will be glad to consult with you. Or write to Cornell-Dubilier Electric Corporation, South Plainfield, New Jersey.

CORNELL-DUBILIER CAPACITORS

FOR POWER-FACTOR IMPROVEMENT
CARRIER-CURRENT COUPLING



A PERFECT CASE FOR C-D CAPACITORS

Heavy metal case hermetically seals components and protects them against the abuse of frequent shifting. 10 to 15 years of effective life is a conservative estimate for C-D capacitors.

Everything you need . . .

FOR ELECTRICAL RESISTANCE MEASUREMENT

From .01 ohm to 200 megohms - IN ONE "MEGGER"* UNIT



The "BRIDGE-MEG" Resistance Tester

HERE is a combined "Megger" Insulation Tester and Wheatstone Bridge that has been proved by years of service, and that can be used to measure almost any resistance encountered in electrical equipment—anywhere and at any time. It measures conductor resistance from as low as .01 ohm up to 999,900 ohms, and can be supplied withVarley loop test facilities. It measures insulation resistance from 10,000 ohms up to 200 megohms. Having a self-contained constant pressure generator rated at 250, 500 or 1000 volts d-c, it is independent of batteries or outside source of power supply, and is portable, compact and simple to operate.

To all who have electrical equipment to install or to maintain, and who appreciate the advantages of one superior instrument for all resistance measurements, we recommend and offer the "Bridge-Meg" Resistance Tester. Weight 14 lbs. Dimensions 7" x 8¾" x 12".

For complete description write for Bulletin 1615-EE.

* Trade Mark Reg. U. S. Pat. Off.

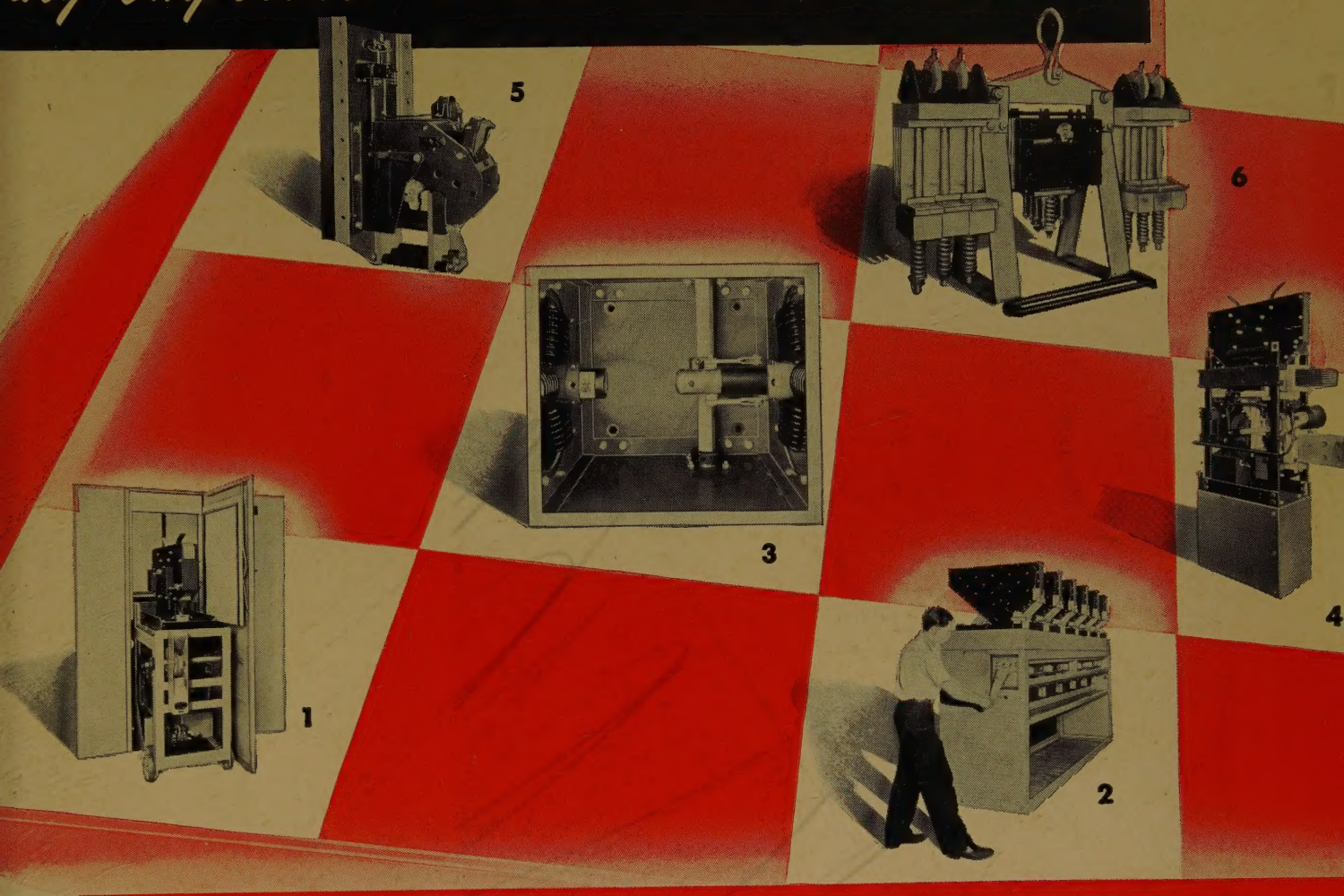
JAMES G. BIDDLE CO. • 1316 ARCH STREET PHILADELPHIA 7, PA.

ADVERTISERS

	Page
Acme Electric Co.	50
Aerovox Corp.	50
Allis-Chalmers Mfg. Co.	*
Aluminum Company of America	6
American Bridge Co.	38
American Lava Corp.	8
American Steel & Wire Co.	*
American Transformer Co.	14
Amperite Co.	50
Anaconda Copper Mining Co.	37
Arnold Engineering Co.	49
Belden Mfg. Co.	*
Bell Telephone Laboratories	36
Bethlehem Steel Co., Inc.	*
Biddle Co., James G.	56
Black & Veatch	53
Brown, Christian E.	53
Brush Development Co.	4
Burndy Engineering Co.	15
Chicago Transformer Co.	51
Classified Advertisements	54
Concord Radio Corp.	54
Coors Porcelain Co.	52
Copperweld Steel Co.	45
Cornell-Dubilier Electric Corp.	55
Corning Glass Works	*
Davis, Julien H.	53
Dolph Co., John C.	*
Dow-Corning Corp.	32
Drake Mfg. Co.	48
Dumont Laboratories, Allen B.	25
Dunn Co., Struthers	*
du Pont de Nemours & Co., E. I.	13
Eitel McCullough, Inc.	42
Electrical Reactance Corp.	*
Electric Service Control Co.	46
Engineering Soc. Personnel Service	54
Federal Tel. & Radio Corp.	47
Ferranti Electric, Inc.	19
General Aniline & Film Corp.	40, 41
General Electric Co.	7, 12, 34, 35
General Radio Co.	16
Graphite Metallizing Corp.	48
Harvey Wells Electronics Inc.	*
Hewlett-Packard Co.	31
Hodgson & Associates	53
Indiana Steel Products Co.	21
International Resistance Co.	24
Irvington Varnish & Insulation Co.	43
I-T-E Circuit Breaker Co.	3rd Cover
Jackson & Moreland	53
Johns-Manville Co., H. W.	28
Kerite Company, The	9
Lapp Insulator Co.	39
Ledermann, Frank	53
Leeds & Northrup Co.	2
Matthews Corp., W. N.	51
Measurements Corp.	*
Miner & Miner	53
Moloney Electric Co.	27
Morganite Brush Co.	46
National Carbon Co.	*
National Electric Coil Co.	*
National Varnished Products Corp.	*
Ohio Brass Co.	29
Ohmite Mfg. Co.	33
Okonite Company, The	5
Owens-Corning Fiberglas Corp.	*
Polachek, Z. H.	53
Professional Engineering Directory	53
Quinn Co., George E.	53
Radio Corporation of America	*
Raytheon Mfg. Co.	*
Rockbestos Products Corp.	10
Rowan Controller Co., The	26
Sanderson & Porter	53
Sargent & Lundy	53
Schweitzer & Conrad, Inc.	*
Selenium Corp.	46
Shallcross Mfg. Co.	*
Simplex Wire & Cable Co.	30
Smith Mfg. Co., F. A., Inc.	17
Sola Electric Co.	2nd Cover
Solar Mfg. Co.	4th Cover
Sprague Electric Co.	*
Square D Company	*
Stackpole Carbon Co.	22
Standard Electric Time Co.	*
Standards—AIEE	44, 48, 53
Stumpf, George H.	53
Superior Electric Co.	*
Triplett Electrical Instrument Co.	44
Trumbull Electric Mfg. Co.	18
U. S. Rubber Co.	11
U. S. Steel Corp.	38
United Transformer Co.	52
Universal Clay Products Co.	52
D. Van Nostrand Co., Inc.	49
Waldes-Kohinoor Inc.	23
War Assets Administration	20
Westcott & Mapes, Inc.	53
Westinghouse Electric Corp.	*
Weston Electrical Instrument Corp.	*
White, J. G., Engineering Corp.	53
Wiley, John & Sons	*
Wray, I. G.	53

** See previous issues.*

...ving "Impossible" Circuit Breaker Problems



...Improves Standard I-T-E Equipment

I-T-E has found the answer to many unusual circuit breaker problems . . . some of which were given up by others as unsolvable. Those illustrated, together with many others, cover a wide range of electrical applications and each meets unique requirements according to rigid standards.

The experience accumulated by I-T-E in developing special circuit breakers is an invaluable aid to the policy of constantly improving the standard I-T-E line. Having pioneered the airbreak principle and specialized in the manufacture of circuit breakers and switchgear for over 60 years, you can be sure of extra dividends in circuit protection when you specify I-T-E.

Get in touch with I-T-E regarding your circuit breaker requirements. An I-T-E application engineer is anxious to help you. I-T-E Circuit Breaker Co., 19th & Hamilton Sts., Philadelphia 30, Pa.

1 One of a group of fifteen 2000 ampere, 750 volt, d-c enclosed drawout automatic reclosing circuit breakers supplied a large city transportation company.

2 A six pole Klamptite disconnect switch arranged for use with an anode circuit breaker protecting a large 600 volt, d-c rectifier.

3 A 1200 ampere, 15,000 volt Klamptite switch arranged for operation in isolated phase bus for a western utility company.

4 A 7500 ampere, 600 volt, d-c high speed circuit breaker having an opening speed of 2/5 of a cycle on a 60 cycle basis.

5 A 570 volt, d-c "circuit maker" capable of closing a 200,000 ampere circuit.

6 A portable, crane operated switch for shunting current around the pot connections for a large metal reduction company.

I-T-E

HIGH SPEED CIRCUIT BREAKERS • SWITCHGEAR
BUS STRUCTURES • SUBSTATION UNITS
AUTOMATIC RECLOSING CIRCUIT BREAKERS

Representatives in Principal Cities

Always Specify-

I-T-E AIR SWITCHGEAR

THE WINNER!



WANTED: 200,000 STARTS

TEST SPECIFICATIONS

CAPACITOR RATING: 130-157 MF, 110 V. A-C, 60 cycles

LINE VOLTAGE: 132 V. A-C, 60 cycles*

MOTOR TEST CYCLE: 120 2 second starts/hour

AMBIENT TEMPERATURE: 65°C

* *Results in actual application of 150 volts to capacitors for about ¼ second before starting switch opens.*

DELIVERED: 1,237,660 STARTS!

. . . and Still running!



"Set your own test specifications for our Solar A-C Electrolytic Motor-Starting Capacitors", said Solar to a very, very large manufacturer of refrigerator motors. "Make them as stiff as you want and name your own test laboratory."

We sent the motor manufacturer's laboratory 8 Solar type DX capacitors, right off the production line. Eight—so there'd be no question of freak performance!

The specification test started. At *400,000* starts eyebrows raised, at the *million* mark, surprise changed to open-mouthed amazement. 1,237,660 starts were recorded for each capacitor when they let us see the test results after 14 months of continuous starting service. No wonder the motor manufacturer's engineers say, "We're convinced Solar *is* BEST for us".

In the Solar line, there's a capacitor that's best for your use, too—one that will take the toughest punishment and come out THE WINNER!

Call on Solar for your capacitor needs for Motors, Fluorescent Lamps, Electronic Heating and Industrial Control Equipment.

SOLAR CAPACITORS

SOLAR MANUFACTURING CORPORATION

285 MADISON AVENUE • NEW YORK 17, N. Y.